Bulletin of the American Physical Society Atlanta GA DPP 2009 Vol. 54, No. 15 November 2009

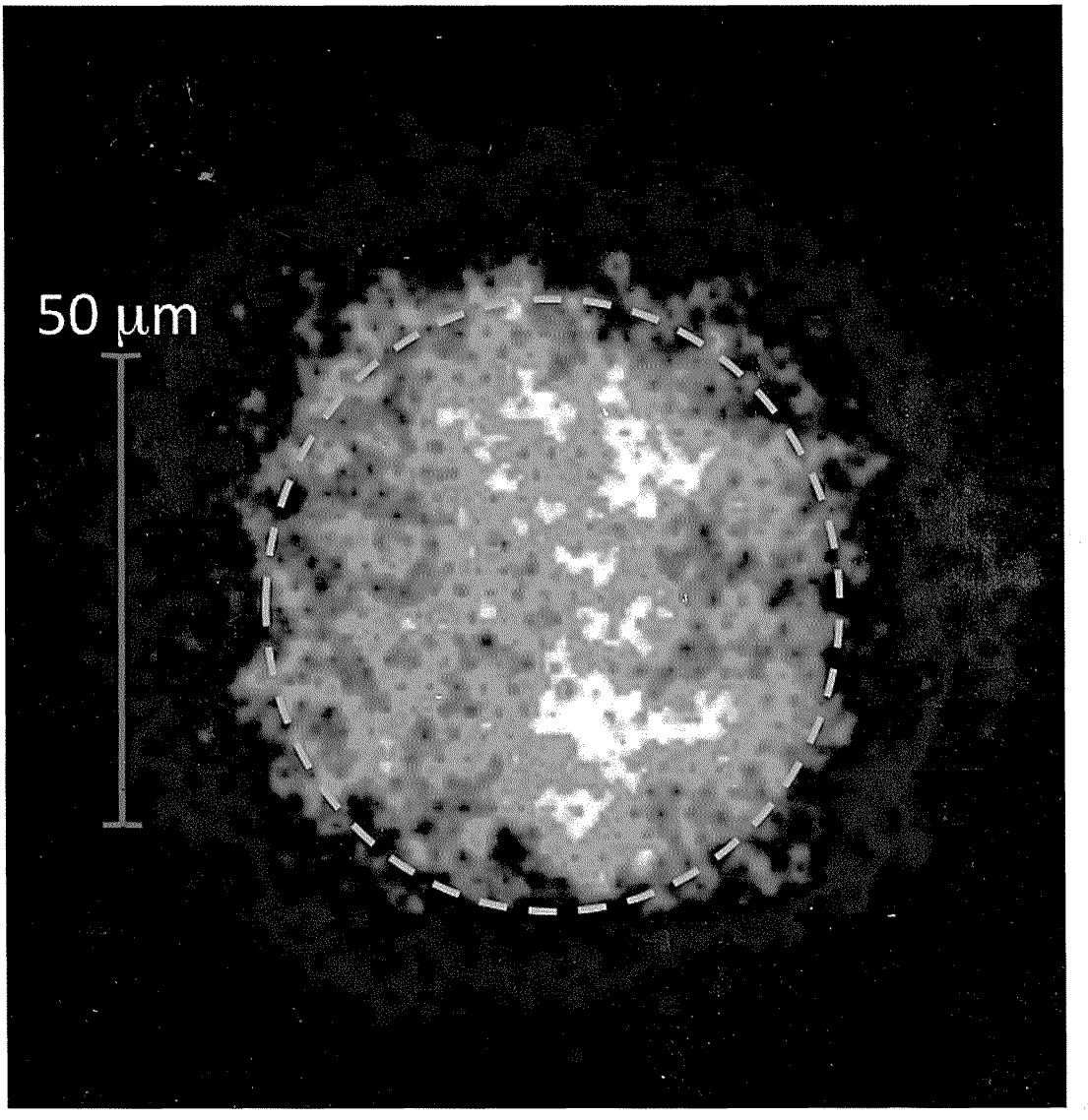
BULLETIN

OF THE AMERICAN PHYSICAL SOCIETY

51st Annual Meeting of the Division of Plasma Physics

November 2–6, 2009

Atlanta, Georgia



IFS Library copy

November 2009

Volume 54, No. 15

APS physics

BULLETIN
OF THE AMERICAN PHYSICAL SOCIETY

Coden BAPSA6 ISSN: 0003-0503
Series II, Vol. 54, No. 15 **November 2009**
Copyright 2009 by the American Physical Society

APS COUNCIL 2009

President
Cherry A. Murray,* *Lawrence Livermore National Laboratory*

President-Elect
Curtis G. Callan, Jr.,* *Princeton University*

Vice President
Barry C. Barish,* *California Institute of Technology*

Executive Officer
Judy R. Franz,* *University of Alabama, Huntsville (on leave)*

Treasurer
Joseph W. Serene,* *Georgetown University*

Editor-in-Chief
Gene D. Sprouse,* *State University of New York, Stony Brook (on leave)*

Past-President
Arthur Bienenstock,* *Stanford University*

General Councillors
Robert Austin, Christina Back,* Marcela Carena, Elizabeth Beise,* Katherine Freese, Wendell Hill,* Nergis Mavalvala, Jorge Pullin

Division, Forum and Section Councillors
Charles Dermer (*Astrophysics*), P. Julienne (*Atomic, Molecular & Optical Physics*), Mark Reeves (*Biological*), Nancy Levinger (*Chemical*), Arthur Epstein (*Condensed Matter Physics*), David Landau (*Computational*), James Brassuer* (*Fluid Dynamics*), Gay Stewart (*Forum on Education*), Amber Stuver (*Forum on Graduate Student Affairs*), Roger Stuewer (*Forum on History of Physics*), Stefan Zolner (*Forum on Industrial and Applied Physics*), David Ernst* (*Forum on International Physics*), Philip "Bo" Hammer (*Forum on Physics and Society*), Steven Rolston (*Laser Science*), Ted Einstein (*Materials*), Akif Balantekin* (*Nuclear*), Janet Conrad (*Particles & Fields*), Ronald Ruth (*Physics of Beams*), David Hammer* (*Plasma*), Scott Milner (*Polymer Physics*), Heather Galloway* (*Texas Section*), Bruce Barrett (*Four Corners Section*)

Members of the APS Executive Board

Scientific Program Coordinator:
Vinaya K. Sathyasheelappa

APS MEETINGS DEPARTMENT
One Physics Ellipse
College Park, MD 20740-3844
Telephone: (301) 209-3286
Fax: (301) 209-0866
Email: meetings@aps.org
Donna Baudrau, *Director of Meetings & Conventions*
Terri Gaier, *Assistant Director of Meetings & Conventions*
Don Wise, *Registrar*
Christine Lenihan, *Meetings Program Coordinator*

International Councillor
Sabayasachi Bhattacharya

Chair, Nominating Committee
Angela Olinto

Chair, Panel on Public Affairs
Duncan Moore

ADVISORS

Representatives from other Societies
Fred Dylla, *AIP*; Alexander Dickison, *AAPT*

International Advisors
Louis Felipe Rodriguez Jorge, *Mexican Physical Society*; Robert Mann, *Canadian Association of Physicists*

Staff Representatives
Alan Chodos, *Associate Executive Officer*; Amy Flatten, *Director of International Affairs*; Ted Hodapp, *Director of Education and Outreach*; Michael Lubell, *Director, Public Affairs*; Dan Kulp, *Editorial Director*; Christine Giaccone, *Director, Journal Operations*; Michael Stephens, *Controller and Assistant Treasurer*

Administrator for Governing Committees
Ken Cole

Please Note: APS has made every effort to provide accurate and complete information in this *Bulletin*. However, changes or corrections may occasionally be necessary and may be made without notice after the date of publication. To ensure that you receive the most up-to-date information, please check the meeting Corrigenda distributed with this *Bulletin*.

BULLETIN
OF THE AMERICAN PHYSICAL SOCIETY

Vol. 54, No. 15, November 2009
Division of Plasma Physics Meeting 2009

TABLE OF CONTENTS

Acknowledgments 3
Program Organization 3
DPP Program Committee 3
Local Arrangements 3
Meeting Staff 3

Program Overview 3
Session Numbering Scheme 3
Review Presentations 4
Invited Talks 4
Invited and Review Paper Publication in Physics of Plasmas 4
Tutorial Talks 4
Contributed Papers - Oral 5
Contributed Papers - Posters 5

Guidelines for Scientific Presentations 5

Abstract Policy 5

Mini-Conferences 5

Prizes and Awards 6

Science Education and Outreach Activities 6
Science Teachers' Day 7
Plasma Sciences Expo 7

Volunteer Opportunities 7

Other Activities of Interest 7
Companions Breakfast 7

Job Fair 8
Women in Plasma Physics Luncheon 8
Panel Discussion 8
University Fusion Association General Meeting, including Town Meeting on DOE Research Needs Workshops 8
Town Hall Meeting on the High Energy Density Laboratory Plasma Research Needs Workshop 9
Concerns of Junior Scientists Town Meeting 9
Meet the Editors of the APS Journals 9
Student Appreciation Reception 9
Conversation with Dr. Steven Koonin 9
Division of Plasma Physics Business Meeting 9
DPP Banquet 9
General Information 10
APS and DPP Membership 10
Registration Hours and Fees 10
Email Pavilion and Wireless Access 10
Messages 10
Coffee and Refreshment Breaks 10
Audio-Visual Equipment 11
Housing Information 11
Please Note 11
Room Key 12
Poster Session Breakdown 13
Epitome 14
Main Text 19
Monday, November 2 19
Tuesday, November 3 92
Wednesday, November 4 178
Thursday, November 5 252
Friday, November 6 342
Author Index 359
Floor Plans ..... **End of Issue**

51st Annual Meeting of the Division of Plasma Physics
November 2–6, 2009
Atlanta, Georgia

Welcome to the 51st Annual Meeting of the Division of Plasma Physics (DPP) of The American Physical Society (APS). All technical sessions, including the Mini-Conferences, will be held in the Hyatt Regency Atlanta Hotel, which also serves as the Conference Hotel. We hope you find the meeting enjoyable, informative, and productive.

ACKNOWLEDGMENTS

PROGRAM ORGANIZATION

We extend our thanks to the DPP Program Committee for the outstanding program they have assembled.

DPP PROGRAM COMMITTEE

Thomas Antonsen, (Chair), Steve Allen, Andre Anders, Lee Berry, Amitava Bhattacharjee, Paul Bonoli, Dylan Brennan, Paul Chu, Ronald Cohen, Alan Costley, Richard Dendy, Daniel J. Den Hartog, Michael Desjarlais, Robert Dewar, Russell Doerner, Kevin Felch, Jill Foley, Eric Fredrickson, Gurudas Ganguli, Andrea Garofalo, Cameron Geddes, Mark Gilmore, Gail Glendinning, Siegfried Glenzer, Nikolai Gorelenkov, Robert Granetz, Houyang Guo, Satoshi Hamaguchi, James Hanson, William Heidbrink, Gregory Howes, Amy Keesee, John Kline, Rick Lee, Yu Lin, Roberto Mancini, Darlene Markevich, Chuang Ren, Adam Sefkow, Michael Shay, Matthew Stoneking, Edward Thomas, Ronald Waltz, Heather Wilkins

We also thank Tom Simonen for organizing a Mini-Conference on Innovative Magnetic Mirror Concepts and Applications, and Tom Intrator for organizing a Mini-Conference on Unsteady Reconnection in Laboratory and Nature.

LOCAL ARRANGEMENTS

A special thanks goes to Lee Berry, Oak Ridge National Laboratory, for overseeing the local arrangements for the DPP 2009 annual meeting.

MEETING STAFF

The DPP wishes to express its appreciation to the APS Meetings Department staff members for their efforts in coordinating the scientific program and meeting logistics: Donna Baudrau, Terri Gaier, Steven Mon, Vinaya Sathyasheelappa, and Donald Wise. We also thank Lee Warren and the AVMG crew.

A special thanks to DPP Administrator, Saralyn Stewart, University of Texas, for her assistance.

PROGRAM OVERVIEW

The program committee has organized a program consisting of four invited review papers, 92 invited papers, five postdeadline invited papers, and three tutorial invited papers (chosen from approximately 200 nominations). The total number of submitted papers is approximately 1,661. On Thursday morning Professor Miklos Porkolab, Massachusetts Institute of Technology, will give the Maxwell Prize Address.

SESSION NUMBERING SCHEME

Each session has a code consisting of two letters and a number. The first letter indicates the time slot for that session, the second letter indicates the type of session, and the number indicates the room location. The numbering scheme is driven by requirements of the APS meeting database system.

First Letter in Session Code = Time slot designation

A, F, M, S, W = 8:00 a.m. Review Time Slot

B, G, N, T, X = 9:30 a.m. Morning Time Slot

C, J, P, U = 2:00 p.m. Afternoon Time Slot

D, E, H, K, L, Q, R, V, Y = Other Afternoon and Evening Time Slots

Session Type		Room Location
R	Review	1 Centennial I-II
I	Invited	2 Centennial I
I/T	Invited/Tutorial	3 Centennial II
O	Oral contributed	4 Regency VI
O	Oral contributed	5 Hanover CDE
O	Oral contributed	6 Hanover FG
O	Oral contributed	7 Regency VII
P	Poster contributed	8 Grand Hall East
M	Mini-Conference	9 The Learning Center/ Regency V
E	Special Session	
Plasma Expo Exhibits (Thursday/Friday)		Grand Hall West

Number in Session Code = Room location at the Hyatt Regency Hotel.

For example: BO4 = Monday, 9:30 a.m., oral contributed, in Regency VI.

REVIEW PRESENTATIONS

All review papers (except the Maxwell Prize address) are 50 minutes long, followed by 10 minutes for questions and answers, and will be presented each morning at 8:00 a.m., Monday through Wednesday, and Friday in the Centennial I-II of the Hyatt Regency Hotel. LCD computer projectors will be used in all oral sessions at the expense of DPP.

Monday: Timothy Luce, General Atomics, *Realizing Steady State Tokamak Operation for Fusion Energy*

Tuesday: Karl Krushelnick, University of Michigan, *Ion Acceleration Using Ultra-high Intensity Lasers*

Wednesday: John Sarff, University of Wisconsin, *Physics Progress of Reversed Field Pinch Magnetic Confinement*

Friday: Gregory Rochau, Sandia National Laboratories, *Applied Spectroscopy in Pulsed Power Plasmas*

On Thursday morning, Miklos Porkolab will give the James Clerk Maxwell Prize for Plasma Physics address in the Centennial I-II, in a review session. The address will be 50 minutes long followed by 10 minutes for questions and answers. The title of the address is: *Taming Magnetically Confined Plasmas with RF Waves: A Historical Perspective.*

INVITED TALKS

Each invited paper is 25 minutes plus 5 minutes for discussion. Invited presentations will be held morning and afternoon in the Centennial I and Centennial II in the Hyatt Regency Hotel. Poster versions of review, invited, and tutorial talks are optional and are scheduled Monday through Friday, in the following half-day session, in a designated area of Grand Hall East. For example, the Monday morning review and invited talks may also be presented as posters in the Monday afternoon poster session. This option will be available on Monday morning for invited papers scheduled on Friday morning. LCD projectors will be used in all oral sessions at the expense of DPP.

INVITED AND REVIEW PAPER PUBLICATION IN PHYSICS OF PLASMAS

Arrangements have been made to publish the invited papers in the Twenty-First Annual Special Issue of Physics of Plasmas. This year's guest editor is Tom Antonsen, chair of the 2009 Program Committee. All submissions of DPP papers will be made via PXP, the journal's online submission and peer review system. Invited speakers have received submission instructions, but should remember that submissions must be identified as a DPP paper by selecting one of the DPP options as the manuscript type. The deadline for submission of the papers is Friday, November 20, two weeks after the end of the DPP Annual Meeting. Early submissions are always encouraged. Sandy Schmidt, Assistant Editor, will be available to answer questions at the Physics of Plasmas booth inside Grand Hall Prefunction, Monday through Thursday of the Meeting, or she can be contacted at sschmidt@pppl.gov.

TUTORIAL TALKS

Tutorial presentations have proven to be a valuable addition to the program and have helped foster the cross-fertilization of ideas. Three tutorials will be offered this year. The duration of each is 50 minutes plus 10 minutes for discussion, and each one is the first talk in an afternoon invited talk session, Monday through Wednesday. The goal of a tutorial talk is to explain basic principles to those not working in an area and to convey an appreciation of the accomplishments, issues, and objectives of that area. The tutorial presentations assume an audience with a graduate level understanding of basic plasma physics, but no familiarity with the particular research area that is the subject of the tutorial. In contrast, the traditional invited presentations are intended to expand upon the latest research within a subfield. LCD projectors will be used in all oral sessions at the expense of DPP.

CONTRIBUTED PAPERS - ORAL

Oral presentations are 10 minutes long plus 2 minutes of discussion, and will be held Monday through Thursday morning at 9:30 a.m., afternoon oral presentations will begin at 2:00 p.m. More than 25 of the scientific program are oral presentations. They will take place in Regency VI, Hanover CDE, Hanover FG, and Regency VII of the Hyatt Regency Hotel. Every effort will be made to adhere to the 12-minute schedule for contributed oral presentations. If speakers are not present at the appointed time, the presiding chair will call for a 12-minute break to maintain the schedule. Likewise, the chair should adhere to the 12-minute limit for each contributed talk. Presiding chairs are expected to enforce the Society's rule that a presenter attempting to deliver a second oral paper in the same session will have that presentation placed at the end of the session, to be given if time permits at the discretion of the presiding chair. LCD projectors will be used in all oral sessions at the expense of DPP.

CONTRIBUTED PAPERS - POSTER

More than 1,127 papers will be presented as posters. Poster sessions will be held in Grand Hall East, Monday through Friday morning 9:30 a.m. to 12:30 p.m., and Monday through Thursday afternoon 2:00 p.m. to 5:00 p.m. Poster boards are 8 feet (wide) x 4 feet (high). Pushpins will be provided. It is recommended that each poster include a title and list of authors in large letters and a large-type copy of the abstract for casual observers, leaving more time to discuss the details with those who are particularly interested in the work, and that attention be paid to the production of effective visuals. Poster presentations should be arranged so that a number of people may view them at one time. Handouts of printed material and a sign-up sheet for correspondence are often helpful. If you leave your assigned board, write a note indicating when you will return. Please clear the poster board promptly at the end of your session. DPP is not responsible for papers left on and around boards beyond the allotted poster session time.

GUIDELINES FOR SCIENTIFIC PRESENTATIONS

Our colleague, James Callen, University of Wisconsin, has developed some useful materials for preparing effective scientific presentations. The Program Committee urges all participants to prepare clear and effective presentations. James Callen's website, entitled *Materials for Preparing Effective Scientific Talks, Posters* is available online as pdf documents at http://homepages.cae.wisc.edu/~callen/talks.html

ABSTRACT POLICY

Contributed abstracts have been arranged according to APS rules, which stipulate that the first author is expected to present the paper and that an author can be listed as first author on only one abstract in the regular program. Additional abstracts by the same first author have been assigned to the Supplemental Poster Session, Friday, November 6, 9:30 a.m. to 12:30 p.m. in Grand Hall East. Abstracts received after the regular deadline of July 17 but before September 15 have been assigned to the Postdeadline Poster Session.

Authors of abstracts not submitted by September 15 may still present their paper as a poster in the Friday morning Postdeadline Poster Session. The contributor must bring a copy of the abstract to the meeting for display on a designated bulletin board in Grand Hall East. Please contact Saralyn Stewart at the DPP Registration Desk for a poster board assignment for the Friday morning session, or contact Vinaya Sathyasheelappa at the DPP Information Booth.

MINI-CONFERENCES

Two mini-conferences are scheduled Monday through Wednesday to be held at the Hyatt Regency Hotel. Check the Epitome for the speaker start times.

MINI-CONFERENCE ON INNOVATIVE MAGNETIC MIRROR CONCEPTS AND APPLICATIONS

The Learning Center

Monday, November 2 at 9:30 a.m. to 12:30 p.m. and 2:00 to 5:00 p.m.

Organizers: Tom Simonen (University of California, Berkeley) and Xianzhu Tang (Los Alamos National Laboratory)

Description: New directions of research and new results in foreign labs have rekindled interest in mirror confined plasmas. This new work opens up the attractive possibility of a mirror system based 14 MeV neutron source for materials testing or even as a fusion-fission hybrid. The goals of this mini-conference are to highlight these new results, identify key physics issues

and applications, and to bring together U.S. and international scientists for information exchange and possible collaboration.

MINI-CONFERENCE ON UNSTEADY RECONNECTION IN LABORATORY AND NATURE

Co-sponsored by the APS Topical Group on Plasma Astrophysics and the Center for Magnetic Self-Organization

Regency V

Tuesday, November 3 at 9:30 a.m. to 12:30 p.m. and 2:00 to 5:00 p.m.

Wednesday, November 4 at 9:30 a.m. to 12:30 p.m. and 2:00 to 5:00 p.m.

Organizer: Tom Intrator (Los Alamos National Laboratory)

Description: Magnetic reconnection underlies magnetic activity in both space and laboratory contexts. Much theoretical, computational and experimental work has been devoted to the study of steady reconnection, but in both nature and the laboratory reconnection is free to develop along quasi-static, intermittent, or even turbulent paths. The goal of this mini-conference is to gather the interests and competences of the experts in space, astrophysical, and laboratory reconnection to review the current theoretical, experimental, and computational understanding of the conditions leading to unsteady reconnection. The organizers invite meeting attendees to submit oral and poster contributed abstracts.

These mini-conferences are organized with several talks and time for questions and discussion. They will employ a question-orientated format to stimulate discussion and interaction amongst the participants.

PRIZES AND AWARDS

Awards will be presented at the banquet on Wednesday, November 4.

JAMES CLERK MAXWELL PRIZE FOR PLASMA PHYSICS

Recipient: Miklos Porkolab, Massachusetts Institute of Technology

Maxwell Prize Address: Centennial I-II

Thursday, November 5, 8:00 a.m.

The 2009 Maxwell Prize Address will be given in Thursday's review session. The prize citation reads: "For pioneering investigations of linear and nonlinear plasma waves and wave-particle interactions; fundamental contributions to the development of plasma heating, current drive and diagnostics; and leadership in promoting plasma science education and domestic and international collaborations."

The John Dawson Award for Excellence in Plasma Physics Research recipient is Yitzhak Maron, Weizmann Institute of Science, Israel. The citation reads: "For revolutionary, non-invasive spectroscopic techniques to measure magnetic fields in dense plasmas and for resolving in detail in space and time the implosion phase of the Z pinch."

The Marshall N. Rosenbluth Outstanding Doctoral Thesis Award recipient is Anne White, General Atomics. The Award was established to recognize exceptional young scientists who have performed original doctoral thesis work of outstanding scientific quality and achievement in the area of plasma physics. Anne White's Ph.D. thesis advisors were Professor Troy Carter and Drs. Tony Peebles and Lothar Schmitz at the University of California, Los Angeles. The citation reads: "For the first simultaneous measurements of long-wavelength electron temperature and density fluctuations in the core of a high-performance tokamak plasma, demonstrating larger than expected temperature fluctuations; and for comparison of this data with nonlinear gyrokinetic simulations."

SCIENCE EDUCATION AND OUTREACH ACTIVITIES

For the past two decades, the Division of Plasma Physics (DPP) annual meeting has featured Science Teachers Day and the Plasma Sciences Expo, to help inspire the next generation of plasma scientists, with activities increasing in scope and popularity each year. In 2009, DPP expects to draw approximately 125 teachers, nearly 2,000 students, and a large number of public participants.

The DPP recognizes that no cost events like these are invaluable resources to local schools, particularly during tough economic times. With help from Atlanta teachers, the 2009 education ad hoc committee has developed an outstanding set of interactive events for middle and high school students and teachers, DPP participants and the general public.

SCIENCE TEACHERS' DAY

Science Teachers' Day includes workshops on topical areas of plasma and fusion sciences along with technology applications, and the opportunity to discuss plasma physics with poster presenters, during the Tuesday afternoon poster session. The 2009 workshops align with national science standards and the Georgia Performance Science Standards. The day also includes continental breakfast, a lunch with plasma scientists and raffle prizes. Teachers leave the day with tools created in the workshops that they can take back to their classroom and use as instructional aides.

Sciences Teachers' Day will be held on Tuesday, November 3 from 7:30 a.m. to 4:00 p.m., with general sessions in Regency VII, workshops on the Atlanta Conference Center level and poster session highlights (Session JP8) in the Grand Hall East. The DPP also invites participating teachers to attend any part of the DPP meeting. DPP meeting participants are invited to attend the Science Teachers' Day opening session and listen to the University of California, Berkley Physics Professor Joel Fajans' presentation *Angels and Demons: The Science Revealed and Why Physicists Would Love to Trap Antihydrogen, but the Vatican Need Not Fear*, from 8:00 to 8:45 a.m., in Regency VII Ballroom.

PLASMA SCIENCES EXPO

The Plasma Sciences Expo offers middle and high school students, teachers, parents and the public an opportunity to talk with scientists while visiting a variety of exhibits and interactive displays, which include making arcs of lightning, manipulating plasma with magnets, observing fluctuating body temperature, playing fusion video games, and exploring optics using a laser. Exhibitor booths are hosted by U.S. Department of Energy (DOE) national labs, industry, and universities from across the country.

The Plasma Science Expo for students and teachers will be held in the Grand Hall West on Thursday and Friday, November 5 and 6, from 8 a.m. to 2 p.m. The general public is invited to the expo evening session on Thursday, November 5, from 6 to 8 p.m. DPP meeting participants are invited to attend any session that fits their schedule.

EVENT SPONSORS

The American Physical Society Office of Education, the DPP, U.S. DOE Office of Fusion Energy Science, and DPP member/institutional contributions sponsor Science Teachers Day and the Plasma Sciences Expo.

The DPP education ad hoc committee includes members from Massachusetts Institute of Technology; Contemporary Physics Education Project; Oak Ridge National Laboratory; Princeton Plasma Physics Laboratory; General Atomics; Lawrence Livermore National Laboratory; University of California, San Diego; University of Texas; the U.S. Department of Energy; and various other universities and industrial organizations.

VOLUNTEER OPPORTUNITIES

To learn about how you can start an outreach program in your community, work with colleagues on existing outreach programs, or support the DPP education activities, please contact Rick Lee via email at leer@fusion.gat.com

OTHER ACTIVITIES OF INTEREST

(Listed in chronological order and held at the Hyatt Regency Hotel.)

COMPANIONS BREAKFAST

Greenbriar

Monday, November 2, 8:30-11:00 a.m.

Join other companions for a DPP-sponsored complimentary continental breakfast at the Hyatt Regency Hotel. You will have an opportunity to meet other companions and reacquaint with friends from past meetings. A representative from the Convention Bureau will be at the breakfast to talk about tours offered in the Atlanta area.

CONTACT CONGRESS

Sponsored by APS Washington DC Office

Grand Hall Prefunction

Monday-Wednesday, November 2-4,

9:00 a.m.-5:00 p.m.

Stop by the Contact Congress booth to sign letters to your Congressional delegation on the importance of federal funding for basic research. It takes only a minute. By doing so, you are making your voice heard in Washington and helping to influence the funding lev-

els for physics research and education. To amplify the impact, the APS Washington DC Office follows up each letter with a call or visit to congressional staff. The strongest and most persuasive advocates on Capitol Hill come from a Senator or Representative's constituents. That means you! If you live in the United States, you are qualified to write to your members of Congress.

If you have any questions about what is happening in Washington, just stop by the Contact Congress desk to ask the experts.

JOB FAIR

Sponsored by APS-DPP

Hanover AB

(Interviews to be held in Edgewood, Atlanta Conference Center Level)

Monday, November 2, 10:00 a.m.-5:00 p.m.

Tuesday, November 3, 10:00 a.m.-4:00 p.m.

The Job Fair is the best place to connect with employers and job seekers from all areas of plasma physics, beams and coherent radiation, inertial confinement and high-energy-density plasmas, and more.

Attendees are encouraged to visit the Job Fair to take advantage of our many recruiting services:

Showcase your company with a Recruitment Exhibit

Search our high-powered job and resume database

Network and interview with companies and job-candidates onsite

Create alerts to inform you of new resumes and jobs

Manage your interview calendar online

For additional information visit our website: www.aps.org/careers/employment/jobfairs.cfm or contact Alix Brice at 301-209-3187, or email Alix at abrice@aip.org

WOMEN IN PLASMA PHYSICS LUNCHEON

Dunwoody

Monday, November 2, 12:30-2:45 p.m.

To attend please check the appropriate space on the meeting registration form to register for the luncheon. The cost for lunch is $25; graduate and undergraduate students will pay $10. Both costs are partially supported by the DPP. Discussions on issues of interest to women in plasma physics will be encouraged at each table.

PANEL DISCUSSION: TOOLS NEEDED TO SURVIVE IN SCIENCE

Sponsored by Committee on Women in Plasma Physics and Committee on Concerns of Junior Scientists

Regency VI

Monday, November 2, 5:30-7:30 p.m.

Plan to attend a panel discussion focused on career strategies for junior scientists. The two person panel, comprised of Peter Feibelman, author of *A Ph.D. is not Enough: A Guide to Survival in Science* and Tudor Johnston, co-author of *Survival Skills for Scientists* will answer questions posed by a moderator as well as questions from the audience. The panel discussion will be of interest not only to graduate students and early career scientists, but also to mentors and advisors, as well as mid-career and senior scientists who can reflect on the obstacles faced early in their careers and strategies that worked to enhance their careers.

Peter Feibelman is a solid state physicist at Sandia National Laboratories. Tudor Johnston is a plasma physicist at the INRS Center for Energy, Materials, and Telecommunications at the University of Quebec in Varennes, Canada.

UNIVERSITY FUSION ASSOCIATION GENERAL MEETING, INCLUDING TOWN MEETING ON DOE RESEARCH NEEDS WORKSHOPS

Hanover CDE

Monday, November 2, 7:00-9:00 p.m.

The UFA will hold its annual general meeting Monday night during the APS-DPP annual meeting in Atlanta. The UFA general meeting typically discusses issues of relevance to fusion science research in U.S. universities and the status of the U.S. fusion program. This year, Dr. Edmund Synakowski, Associate Director of Fusion Energy Sciences at DOE OFES, will review the status of the program and discuss directions of the U.S. fusion program in the burning plasma era. In addition, there will be brief presentations on the MFE, Fission-Fusion Hybrid, and HEDLP ReNeW efforts, followed by an open question and answer session. The UFA meeting is open to members of the community and all conference attendees.

TOWN HALL MEETING ON THE HIGH ENERGY DENSITY LABORATORY PLASMA RESEARCH NEEDS WORKSHOP

Hanover FG

Monday, November 2, 9:00-10:00 p.m.

There will be a town meeting on the HEDLP ReNeW at the APS-DPP annual meeting in Atlanta, at which the goals and methods of the workshop will be discussed and many panelists will be present to receive your suggestions and hear your comments. The town meeting is scheduled immediately following the University Fusion Association General Meeting.

TOWN MEETING ON CONCERNS OF JUNIOR SCIENTISTS

The Learning Center

Tuesday, November 3, 1:00-2:00 p.m.

The DPP Committee on Concerns of Junior Scientists is pleased to announce a Town Meeting on outreach and policy. Several speakers will discuss the impact that educational outreach and scientific policy activities such as Fusion Day can have. This meeting will provide an opportunity to show junior scientists how they can become involved in these activities and help influence the public perception of the plasma physics community. Please join us for this event.

MEET THE EDITORS OF THE AMERICAN PHYSICAL SOCIETY JOURNALS

Courtland

Tuesday, November 3, 5:00-7:00 p.m.

The Editors of the APS Journals cordially invite you to join them for conversation and refreshments. Your questions, suggestions, compliments and complaints about the journals are welcome. We hope you are able to join us.

STUDENT APPRECIATION RECEPTION

Fairlie

Tuesday, November 3, 6:00-7:00 p.m.

Please plan to attend a complimentary reception in honor of the student participants of the 2009 DPP annual meeting. Students and student advisors are particularly encouraged to attend. Punch and an assortment of cookies will be served. Professor Amitava Bhattacharjee, DPP Chair, cordially welcomes all DPP meeting participants to this reception, and encourages their open discussion on topics of interest to students of plasma physics.

TOWN MEETING: A CONVERSATION WITH DR. STEVEN KOONIN (UNDER-SECRETARY FOR SCIENCE, U.S. DOE)

Centennial I

Tuesday, November 3, 7:30-9:30 p.m.

Dr. Koonin will give a talk on the topic: "How can we Accelerate Scientific Progress Towards Fusion Energy?" and take questions from the audience.

BUSINESS MEETING OF THE DIVISION OF PLASMA PHYSICS

Hanover FG

Wednesday, November 4, 5:15-6:15 p.m.

The business meeting of the Division of Plasma Physics will include reports of actions undertaken by DPP on issues important to our membership. New items of business will be considered in the following order: (1) Written motions, together with any supporting arguments, received by the Secretary-Treasurer, Dr. William Heidbrink, at the DPP Registration Desk, Hyatt Regency Hotel, before noon on Monday, November 2, or which were emailed to Dr. Heidbrink by noon on Friday, October 23, 2009. Copies of such material will be displayed on a bulletin board near the DPP registration area in order to give members reasonable notice in case they wish to participate in the discussion and vote on such motions. (2) Written motions submitted to the Secretary-Treasurer prior to the start of the business meeting. (3) Other new business not included in (1) or (2).

DPP BANQUET

Wednesday, November 4

Reception: Centennial Prefunction, 6:30 p.m.

Dinner: Centennial III-IV, 7:30 p.m.

The official banquet of the DPP will be held on Wednesday evening. A cash-bar reception preceding the evening banquet at 6:30 p.m. will be held in the Centennial Prefunction area. A subsidized banquet ticket can be purchased for $40 with preregistration or at the registration desk Monday, November 2 up to 5:00 p.m. Tickets will be sold on a space-available basis and are non-refundable. Tickets must be presented for admission at the door to the banquet room. Tickets will not be

sold at the door. The banquet program will include presentation of the James Clerk Maxwell Prize, the John Dawson Award for Excellence in Plasma Physics Research, the Marshall N. Rosenbluth Outstanding Doctoral Thesis Award in Plasma Physics, and newly elected APS Fellows. The after-dinner entertainment will be the Spelman College Glee Club, based in Atlanta.

GENERAL INFORMATION

All technical sessions, satellite meetings, the DPP Business Meeting, and the Reception/Banquet will be held at the Hyatt Regency Atlanta Hotel. Consult the schedule of satellite meetings on the Satellite Meetings board near the DPP Registration Desk.

APS AND DPP MEMBERSHIP BOOTH AND STORE

The APS Membership Department staff will be on hand to answer questions about APS and DPP membership in the Grand Hall Prefunction area at the Hyatt Regency Hotel. Stop by for information on how to become a member, receive journal subscriptions, and purchase fun and practical items in the souvenir store. By becoming a member you will receive timely and detailed information about DPP activities and discounted meeting fees. The booth and store will be staffed Monday through Wednesday 8:00 a.m. to 5:00 p.m.

REGISTRATION HOURS

The meeting registration desk will be located in the Grand Hall Prefunction area, of the Hyatt Regency Hotel. (See Hyatt Regency Atlanta floor plan at the end of this Bulletin.)

Registration hours are as follows:

Sunday, November 1	3:00 p.m. to 7:00 p.m.
Monday, November 2	7:00 a.m. to 5:00 p.m.
Tuesday, November 3	7:00 a.m. to 4:00 p.m.
Wednesday, November 4	7:00 a.m. to 3:00 p.m.
Thursday, November 5	7:00 a.m. to 3:00 p.m.
Friday, November 6	7:00 a.m. to 10:00 a.m.

REGISTRATION FEES

Preregistration fees before October 2 are:

APS Member $385

Nonmember $505

Retired/Unemployed APS Member $125

Student member $75

One-Day APS Member $190

One-Day Nonmember $250

On-site registration fees after October 2 are:

APS Member $435

Nonmember $555

Retired/Unemployed APS Member $135

Student member $125

One-Day APS Member $215

One-Day Nonmember $275

Members of international physics societies having an official reciprocal relationship with the APS can register at member rates.

EMAIL PAVILION

Computer and Internet service will be available for use by participants. Desktop computers, as well as Ethernet ports for laptops, allowing web and email access will be available in Centennial Prefunction during the following hours:

Sunday, November 1	3:00 p.m. to 8:00 p.m.
Monday, November 2	7:00 a.m. to 6:00 p.m.
Tuesday, November 3	7:00 a.m. to 6:00 p.m.
Wednesday, November 4	7:00 a.m. to 6:00 p.m.
Thursday, November 5	7:00 a.m. to 6:00 p.m.
Friday, November 6	7:00 a.m. to 1:00 p.m.

WIRELESS ACCESS

Wireless access will be available for DPP attendees in Grand Hall East until 10:00 pm. Wireless will be available continuously in the foyer outside the Centennial Ballroom.

Note: DPP offers wireless and email access to participants as a complimentary service.

MESSAGES

Message boards will be located near the DPP Registration Desk and in Grand Hall East where the Poster Sessions are held.

COFFEE AND REFRESHMENT BREAKS

Coffee breaks will be served in two locations, the Grand Hall Prefunction and the Centennial Prefunction. Morning coffee service will be Monday through Friday at 9:00 a.m. to 9:30 a.m., and afternoon coffee service will be Monday through Thursday from 3:00 p.m. to 3:30 p.m. Coffee and hot tea will be provided at the

morning breaks. In the afternoons, coffee, hot tea, and soft drinks will be available. Each break throughout the week will offer beverages on a limited basis and will not be replenished.

AUDIO VISUAL EQUIPMENT FOR SESSIONS

Speaker Ready Room: Chicago AB

All oral sessions will be equipped with one LCD projector, one Windows-based PC laptop, one high intensity overhead projector, one screen, lavaliere microphone, and one laser pointer. It is not necessary to bring your laptop if your presentation has been downloaded to a memory stick or a CD, you will be able to use the laptop provided. However, whichever mechanism you utilize you must first visit the Speaker Ready Room to test your presentation with a technician to ensure successful connectivity in your session for your presentation. This will ensure the sessions run smoothly. Speakers using LCD projectors may wish to bring back-up transparencies in case of a technical problem. Presenters are not allowed to use personal projectors at the annual meeting.

Speaker Ready Room Hours:

Sunday, November 1	3:00 p.m. to 8:00 p.m.
Monday, November 2	7:00 a.m. to 5:00 p.m.
Tuesday, November 3	7:00 a.m. to 5:00 p.m.
Wednesday, November 4	7:00 a.m. to 5:00 p.m.
Thursday, November 5	7:00 a.m. to 5:00 p.m.
Friday, November 6	7:00 a.m. to 11:00 a.m.

HOUSING INFORMATION

Hyatt Regency Atlanta

265 Peachtree Street NE

Atlanta, Georgia 30303

404-577-1234

Note: If you cancel your hotel reservation, you must do so 24 hours prior to arrival to avoid paying one night's hotel rate. Your date of departure will be confirmed upon check-in at the hotel. There may be a charge for early departure once you confirm your departure date.

Non-Government Rates:

$176 single, $176 double, plus 15% tax

Government Rates: (These rates will be the prevailing rate at the time of check-in at the Hyatt.)

$140 single, $140 double, plus 15% tax

NOTE

The APS-DPP has made every effort to provide accurate and complete information in this Bulletin. However, changes or corrections may occasionally be necessary and may be made without notice after the date of publication. To ensure that you receive the most up-to-date information, please check the corrigenda distributed with this Bulletin.

ROOM KEY

The label for each session begins with a letter that indicates the time of the session: A for the first session on Monday, through Z for the last session on Friday. The second letter in the label indicates the type of session: R for plenary, I for invited, O for contributed oral, M for mini-conference, P for contributed poster, E for special event. The last number in each session ID corresponds with a particular room. See the key below for locations.

One tutorial talk (50 minutes plus 10 minutes for discussion) is scheduled as the first presentation in one of the afternoon invited sessions each day, Monday through Thursday. At any given time, there are two simultaneous invited sessions (I1 and I2), two or three simultaneous oral contributed sessions (O3, O4 and O5), and one mini-conference (beginning Wednesday morning). There is one poster session each morning and each afternoon, but it is partitioned into plenary, invited, and tutorial talk posters, and contributed posters covering several subject areas. (See Poster Session Breakdown on the following page.) All technical sessions, including mini-conferences, will be held in the Hyatt Regency Hotel. The location of a session is specified by its label, as follows:

Session	Content	Rooms at Hyatt
R	Plenary	1 Centennial I-II
I	Invited	2 Centennial I
I/T	Invited/Tutorial	3 Centennial II
O	Oral contributed	4 Regency VI
O	Oral contributed	5 Hanover CDE
O	Oral contributed	6 Hanover FG
O	Oral contributed	7 Regency VII
P	Poster contributed	8 Grand Hall East
M	Mini-Conference	9 The Learning Center or Regency V
E	Special Session	
Plasma Expo Exhibits (Thursday/Friday)		Grand Hall West

All Review papers (except the Maxwell Prize address) are 30 minutes long, followed by 6 minutes for questions and answers, and will be presented each morning at 8:00 a.m. **Each tutorial is scheduled for a 50-minute presentation followed by 10 minutes for discussion**, and invited presentations are scheduled for 25 minutes with 5 minutes for discussion. All tutorial talks are in the afternoon sessions, and all invited talks begin on either the hour or the half hour. Oral contributed presentations are 10 minutes followed by 2 minutes for discussion. The names in italics below each session title in the Epitome are those of plenary, tutorial and invited speakers.

POSTER SESSION BREAKDOWN

Listed below are the topics to be presented in each poster session. Authors are required to be in attendance at the times posted below. Please remove your poster materials as soon as your session is over. The APS/DPP will not be responsible for poster materials that are left on poster boards after the session is over. All poster sessions will take place in Grand Hall East.

Session BP8: Poster Session I
Monday morning, November 2
9:45 am–12:45 pm
1-15 Plasma Sources and Boundaries
16-62 Gyrokinetics and Turbulence
63-111 Complex, Non-neutral and Other Novel Plasmas

Session CP8: Poster Session II
Monday afternoon, November 2
2:00–5:00 pm
1-35 Diagnostics, Heating, Current Drive
36-114 Diagnostics, Laser Plasma Interactions, and Fast Ignition

Session GP8: Poster Session III
Tuesday morning, November 3
9:45 am–12:45 pm
1-73 ITER, General Tokamak, Simulation and Modeling
74-102 MHD, Linear and Nonlinear Phenomena
103-153 Waves and Instabilities in Basic Plasmas

Session JP8: Poster Session IV
Tuesday afternoon, November 3
2:00–5:00 pm
1-6 Education and Outreach
7-78 Undergraduate and High School Research
79-117 DIII-D Tokamak II
118-152 Laser and Plasma Based Accelerators

Session NP8: Poster Session V
Wednesday morning, November 4
9:45 am–12:45 pm
1-33 Electron and Ion Beams and Radiation Generation
34-57 Low Temperature Plasmas
58-110 Pinches, Equation of State, and Simulations
111-131 Edge

Session PP8: Poster Session VI
Wednesday afternoon, November 4
2:00–5:00 pm
1-32 C-MOD
33-102 NSTX and General Spherical Torus
103-125 Simulation and Modeling of Basic Plasma Phenomena

Session TP8: Poster Session VII
Thursday morning, November 5
9:45 am–12:45 pm
1-39 DIII-D Tokamak III
40-108 MST, RFP, and Stellarator
109-141 Magnetic Reconnection
142-162 Magneto-Inertial-Fusion

Session UP8: Poster Session VIII
Thursday afternoon, November 5
2:00–5:00 pm
1-61 Alternates
62-106 Turbulence, Transport, and Stability
107-157 Space and Astrophysical Plasmas

Session XP8: Poster Session IX
Friday morning, November 6
9:45 am–12:45 pm
1-36 Supplementary Abstracts
37-70 Post-deadline Abstracts

Epitome of the 2009 Annual Meeting of the Division of Plasma Physics of the American Physical Society

8:00 MONDAY MORNING 2 NOVEMBER 2009

AR1 **Review: Realizing Steady State Tokamak Operation for Fusion Energy**
T.C. Luce
Centennial I-II

9:30 MONDAY MORNING 2 NOVEMBER 2009

BI2 **Reconnection in Laboratory and Space**
Yi-Min Huang, Eric Lawrence, Vadim Roytershteyn, Ari Le, Gennady Fiksel, Tim Gray
Centennial I

BI3 **Advances in Tokamaks: Core and Edge Physics**
Nobuhiko Hayashi, Wojciech Fundamenski, Jiangang Li, Jerry Hughes, Istvan Cziegler, Natalia Krasheninnikova
Centennial II

BO4 **Magnetic Confinement Theory, Simulation and Modeling**
Regency VI

BO5 **Hohlraum Physics**
Hanover CDE

BO6 **Microwaves, Compton Scattering and Accelerator Physics**
Hanover FG

BP8 **Poster Session I: Plasma Sources and Boundaries; Gyrokinetics and Turbulence; Complex, Non-neutral and Other Novel Plasmas**
Grand Hall East

BM9 **Mini-Conference on Innovative Magnetic Mirror Concepts and Applications I**
The Learning Center

14:00 MONDAY AFTERNOON 2 NOVEMBER 2009

CI2 **Accelerators, Beam Dynamics and Radiation**
Alex Friedman, Igor Kaganovich, Erik Gilson, Diktys Stratakis, Alexander Vlasov, Gregory Werner
Centennial I

CT3 **Tutorial: Flow driven MHD Instabilities in Weakly Magnetized Laboratory Experiments: Dynamos and MRI**
Cary Forest
Centennial II

CO4 **DIII-D Tokamak**
Regency VI

CO5 **Equation of State, Strength, and Hydrodynamics**
Hanover CDE

CO6 **Magnetic Reconnection and Turbulence**
Hanover FG

CO7 **Low Temperature Plasmas I**
Regency VII

CP8 **Poster Session II: Diagnostics, Heating, Current Drive; Diagnostics, Laser Plasma Interactions, and Fast Ignition**
Grand Hall East

CM9 **Mini-Conference on Innovative Magnetic Mirror Concepts and Applications II**
The Learning Center

15:00 MONDAY AFTERNOON 2 NOVEMBER 2009

DI3 **Gyrokinetic Theory and Simulation**
Michael Barnes, J. Candy, Felix I. Parra, Andris Dimits
Centennial II

17:30 MONDAY EVENING
2 NOVEMBER 2009

EE1 **Panel Discussion: Tools Needed to Survive in Science**
Regency VI

19:00 MONDAY EVENING
2 NOVEMBER 2009

EE2 **University Fusion Association General Meeting, including Town Meeting on DOE Research Needs Workshops**
Hanover CDE

21:00 MONDAY EVENING
2 NOVEMBER 2009

EE3 **Town Hall Meeting on the High Energy Density Laboratory Plasma Research Needs Workshop**
Hanover FG

8:00 TUESDAY MORNING
3 NOVEMBER 2009

FR1 **Review: Ion Acceleration using Ultra-high Intensity Lasers**
Karl Krushelnick
Centennial I-II

9:30 TUESDAY MORNING
3 NOVEMBER 2009

GI2 **Micro and Low-temperature Plasmas**
Osamu Sakai, Dmytro Sydorenko, Scott D. Baalrud, Jeffrey Hopwood, T.R. Weber, Michael Keidar
Centennial I

GI3 **Islands, Kinks and Sawteeth**
A.D. Turnbull, Jonathan Graves, R.J. La Haye, Hillary Stephens, John W. Berkery, L.J. Zheng
Centennial II

GO4 **C MOD Tokamak**
Regency VI

GO5 **Z-pinches, X-pinches, and Dense Plasma Focus**
Hanover CDE

GO6 **Laser Acceleration and Transport; Radiation and FELs**
Hanover FG

GP8 **Poster Session III: ITER, General Tokamak, Simulation and Modeling; MHD, Linear and Nonlinear Phenomena; Waves and Instabilities in Basic Plasmas**
Grand Hall East

GM9 **Mini-Conference on Unsteady Reconnection in Laboratory and Nature I: Reconnection Rate and Dynamics**
Regency V

13:00 TUESDAY AFTERNOON
3 NOVEMBER 2009

HE1 **Town Meeting on Concerns of Junior Scientists**
The Learning Center

14:00 TUESDAY AFTERNOON
3 NOVEMBER 2009

JI2 **ICF Compression, Equations of State and Z-pinches**
Marcus Knudson, M.A. Barrios, Sebastien Lepape, Christopher Jennings, Max Karasik, Stephen Slutz
Centennial I

JT3 **Tutorial: Verification and Validation for Magnetic Fusion: Moving Toward Predictive Capability**
Martin Greenwald
Centennial II

JO4 **NSTX Spherical Torus**
Regency VI

JO5 **Laser-plasma Coupling at Long Scale Lengths**
Hanover CDE

JO6 **Waves, Turbulence, and Boundary Effects in Laboratory and Space Plasmas I**
Hanover FG

JP8 **Poster Session IV: Education and Outreach; Undergraduate and High School Research; DIII-D Tokamak II; Laser and Plasma Based Accelerators**
Grand Hall East

JM9 **Mini-Conference on Unsteady Reconnection in Laboratory and Nature II: Impulsive Reconnection and Onset**
Regency V

15:00 TUESDAY AFTERNOON 3 NOVEMBER 2009

KI3 **Turbulent Transport Measurement and Modeling**
A.E. White, Liang Lin, J.C. DeBoo, David L. Brower
Centennial II

19:30 TUESDAY EVENING 3 NOVEMBER 2009

LE1 **Town Meeting: A Conversation with Dr. Steven Koonin, Undersecretary for Science, Department of Energy**
Centennial I

8:00 WEDNESDAY MORNING 4 NOVEMBER 2009

MR1 **Review: Physics Progress of Reversed Field Pinch Magnetic Confinement**
John S. Sarff
Centennial I-II

9:30 WEDNESDAY MORNING 4 NOVEMBER 2009

NI2 **ICF Capsules and Rayleigh-Taylor Instability**
Otto Landen, T.C. Sangster, Kelly Vaughan, Johan Frenje, Hye-Sook Park, Eric Loomis
Centennial I

NI3 **Plasma Rotation and Helical Equilibria**
J.D. Callen, W.M. Solomon, R.E. Bell, Michael Zarnstorff, Piero Martin, Jeremy Lore
Centennial II

NO4 **International Tokamak Research and ITER**
Regency VI

NO5 **Fast Ignition**
Hanover CDE

NO6 **Complex Plasmas**
Hanover FG

NP8 **Poster Session V: Electron and Ion Beams and Radiation Generation; Low Temperature Plasmas; Pinches, Equations of State, and Simulations; Edge**
Grand Hall East

NM9 **Mini-Conference on Unsteady Reconnection in Laboratory and Nature III: 3D Reconnection and Diffusion Region**
Regency V

14:00 WEDNESDAY AFTERNOON 4 NOVEMBER 2009

PI2 **Tokamak Physics: Edge, Scrape-off Layer and Wall**
Linda E. Sugiyama, Elena de la Luna, Rajesh Maingi, Masahiro Kobayashi, Adam McLean, Dennis Whyte
Centennial I

PT3 **Tutorial: ICF Ignition: The Lawson Criterion, and Comparison with MFE Ignition**
R. Betti
Centennial II

PO5 **High-intensity Short-pulse Laser Plasma Interactions**
Hanover CDE

PO6 **Waves, Turbulence, and Boundary Effects in Laboratory and Space Plasmas II**
Hanover FG

PP8 **Poster Session VI: C-Mod; NSTX and General Spherical Torus; Simulation and Modeling of Basic Plasma Phenomena**
Grand Hall East

PM9 **Mini-Conference on Unsteady Reconnection in Laboratory and Nature IV: Turbulence and Multiple Reconnections**
Regency V

15:00 WEDNESDAY AFTERNOON 4 NOVEMBER 2009

QI3 **ICF and Ignition**
Nathan Meezan, Dustin Froula, Pierre Michel, Klaus Widmann
Centennial II

17:15 WEDNESDAY EVENING 4 NOVEMBER 2009

RE1 **DPP Business Meeting**
Hanover FG

18:30 WEDNESDAY EVENING 4 NOVEMBER 2009

RE2 **Reception and Banquet**
Centennial III/IV

8:00 THURSDAY MORNING 5 NOVEMBER 2009

SR1 **Maxwell Prize Address: Taming Magnetically Confined Plasmas with RF Waves: A Historical Perspective**
Miklos Porkolab
Centennial I-II

9:30 THURSDAY MORNING 5 NOVEMBER 2009

TI2 **Flows and Turbulence in Laboratory and Space**
Ian H. Hutchinson, Alfred Wong, Earl Scime, Jean C. Perez, Troy Carter, P.H. Diamond
Centennial I

TI3 **RF in Tokamaks and ITER**
M. Choi, Gary Taylor, Syun'ichi Shiraiwa, G.L. Jackson, Andrei Smolyakov
Centennial II

TO4 **Laser Wakefield Accelerators and Radiation Sources**
Regency VI

TO5 **ICF Simulations and Target Fabrications**
Hanover CDE

TO6 **Laboratory Astrophysics**
Hanover FG

TO7 **Shock Ignition, Diagnostics, and X-ray Sources**
Regency VII

TP8 **Poster Session VII: DIII-D Tokamak III; MST, RFP, and Stellarator; Magnetic Reconnection; Magneto-Inertial-Fusion**
Grand Hall East

14:00 THURSDAY AFTERNOON 5 NOVEMBER 2009

UI2 **Laser Wakefield Acceleration and Solid Target Interactions**
Anthony Gonsalves, Joseph Ralph, Samuel Martins, Alec Thomas, Farhat Beg, Andreas Kemp
Centennial I

UI3 **Basic Plasmas: Novel Plasmas in Laboratory and Space**
C. Fred Driscoll, Michael Drewsen, Jon Eggert, Bruno Coppi, David Ampleford, David Speirs
Centennial II

UO4 **Research In Support of ITER**
Regency VI

UO5 **Compression and Burn**
Hanover CDE

UO6 **Basic Plasma Phenomena: Theory and Simulation**
Hanover FG

UO7 **Magneto Inertial Fusion and Neutron Generation**
Regency VII

UP8 **Poster Session VIII: Alternates; Turbulence, Transport, and Stability; Space and Astrophysical Plasmas**
Grand Hall East

8:00 FRIDAY MORNING 6 NOVEMBER 2009

WR1 **Review: Applied Spectroscopy in Pulsed Power Plasmas**
Gregory Rochau
Centennial I-II

9:30 FRIDAY MORNING 6 NOVEMBER 2009

XI2 **High Energy Density Physics and High Performance Capsule Implosions**
J.P. Knauer, E.C. Harding, Hideaki Habara, Harry F. Robey
Centennial I

XI3 **Energetic Particles**
Herbert Berk, E.M. Bass, W.L. Zhang, E.M. Hollmann, Roscoe White, Christopher Cothran
Centennial II

XP8 **Poster Session IX: Supplemental and Post-Deadline Posters**
Grand Hall East

12:35 FRIDAY AFTERNOON 6 NOVEMBER 2009

YR1 **Door Prize Drawing**
Centennial I

SESSION AR1: REVIEW: REALIZING STEADY STATE TOKAMAK OPERATION FOR FUSION ENERGY
Monday Morning, 2 November 2009; Centennial I-II at 8:00; Steven Allen, LLNL/General Atomics, presiding

8:00
AR1 1 Realizing Steady State Tokamak Operation for Fusion Energy.*
T.C. LUCE, *General Atomics*

Continuous operation of a tokamak for fusion energy has obvious engineering advantages, but also presents physics challenges beyond the achievement of conditions needed for a burning plasma. The power from fusion reactions and external sources must support both the pressure and the current equilibrium without inductive current drive, leading to demands on stability, confinement, current drive, and plasma-wall interactions that exceed those for pulsed tokamaks. These conditions have been met individually in the present generation of tokamaks, and significant progress has been made in the last decade to realize scenarios where the required conditions are obtained simultaneously. Tokamaks are now operated routinely without disruptions close to the ideal MHD pressure limit, as needed for steady-state operation. Scenarios that project to high fusion gain have been demonstrated where more than half of the current is supplied by the "bootstrap" current generated by the pressure gradient in the plasma. Fully noninductive sustainment has been obtained for about a resistive time (the longest intrinsic time scale in the confined plasma) with normalized pressure and confinement approaching those needed for demonstration of steady-state conditions in ITER. One key challenge remaining to be addressed is how to handle the demanding heat and particle fluxes expected in a steady-state tokamak without compromising the high level of core plasma performance. Rather than attempt a comprehensive historical survey, this review will start from the plasma requirements of a steady-state tokamak powerplant, illustrate with examples the progress made in both experimental and theoretical understanding, and point to the remaining physics challenges.

*Supported by US DOE under DE-FC02-04ER54698.

SESSION BI2: RECONNECTION IN LABORATORY AND SPACE
Monday Morning, 2 November 2009; Hantao Ji, Princeton Plasma Physics Laboratory, presiding

9:30
BI2 1 Effects of Line-tying on Magnetohydrodynamic Instabilities and Current Sheet Formation.*
YI-MIN HUANG, *Center for Integrated Computation and Analysis of Reconnection and Turbulence, University of New Hampshire*

The effects of line-tying on magnetohydrodynamic instabilities are an important issue for astrophysical plasmas, such as the solar corona or astrophysical jets, where magnetic field lines are deeply anchored at a dense medium. Recently, several laboratory experiments aimed at studying line-tying effects have been initiated. In this talk, the effects of line-tying on the ideal kink mode and resistive tearing mode will be presented. In general, line-tying has a stabilizing effect on the linear instability, and it also smooths out the internal layer of the linear eigenfunction. What is more interesting, however, is the nonlinear evolution of the unstable modes. It is well known that the ideal internal kink mode and ideal coalescence instability evolve nonlinearly into tangential discontinuities, or current sheets, in the absence of line-tying. Whether the same result remains true in the presence of the line-tying remains an open question. Current sheet formation in line-tied systems is essential in Parker's scenario of coronal heating. New theoretical results on nonlinear current sheet formation will be presented.

*In collaboration with A. Bhattacharjee and Ellen G. Zweibel.

10:00
BI2 2 Experimental measurement of quasi-separatrix layers in magnetic flux ropes.*
ERIC LAWRENCE, *University of California, Los Angeles*

A quasi-separatrix layer (QSL) is a region in a magnetic configuration where there are strong spatial gradients in the field line connectivity, and are thought to be favorable sites for 3D magnetic reconnection. Solar physicists have used QSLs extensively to identify reconnection sites in the complicated 3D magnetic configurations in solar flares, but we present the the first use of the technique in an experimental setting. In this experiment, performed in the Large Plasma Device (LAPD) at UCLA, two lanthanum hexaboride cathodes produce current channels initially parallel to the background

magnetic field. The current channels create twisted helical structures, or flux ropes, in the magnetic field. The flux ropes rotate about their central axes, which causes them to periodically collide. Three dimensional magnetic measurements at 20000 spatial locations make the QSL calculation possible. During these collisions, QSLs, as well as reverse current sheets, are observed to form between the flux ropes. The structure of these QSLs is very similar to those seen in MHD simulations of merging currents.

*Research is conducted at the Basic Plasma Science Facility at UCLA, and is supported by the National Science Foundation and the Department of Energy.

10:30
BI2 3 Influence of Coulomb Collisions on the Dynamics of Magnetic Reconnection in Space and Laboratory Plasmas.
VADIM ROYTERSHTEYN,* *Los Alamos National Laboratory*

Magnetic reconnection is the process of a rapid change in the magnetic field topology, frequently associated with a conversion of magnetic energy into various forms of plasma kinetic energy. Many systems of interest, such as the solar corona and laboratory experiments, operate in the parameter regimes inaccessible to both collisionless and fluid models, where the collisional mean free path is comparable to the characteristic scale lengths of interest and/or the reconnection electric field is of the order of the runaway field. In this work, fully kinetic simulations with a Monte-Carlo treatment of Landau collision integral are used to analyze two problems in reconnection under such conditions. Made practical by the recent progress in computing capabilities, this powerful simulation technique allows a seamless transition from collisionless to fully collisional regimes. First, we present simulations with boundary conditions [1] mimicking the Magnetic Reconnection eXperiment (MRX). A thorough comparison of the structure of the electron reconnection layer between the experiment and the simulations allows the relative roles of the collisional dissipation and that of the collisionless effects in MRX to be quantified. Ultimately, this provides important insights into a possible role of 3D current-aligned instabilities and helps bridge the gap between a small laboratory experiment and much larger systems in Nature. As a second example, we discuss the transition between the collisional and the kinetic reconnection regimes. In relatively short systems with Lundquist number below $S \sim 10^3$ the transition, signified by a rapid increase in the reconnection rate, occurs at the temperature that corresponds to the width of the Sweet-Parker current sheet $\delta_{SP} \sim d_i$, where d_i is the ion inertial length. In larger systems $S > 10^3$, the transition is observed at significantly lower temperatures than are expected from a simple criterion $\delta_{SP} \sim d_i$. In particular, the Sweet-Parker current sheet is found to be unstable against a tearing-like instability that leads to a significant modulation of the current sheet thickness [2]. The transition is achieved when the *minimum* thickness of the current sheet falls below d_i. These results may have strong implications for reconnection in the solar corona, since many of the existing models are based on the premise that the Sweet-Parker scaling is relevant at practically important $S \sim 10^{12}$ and neglect the influence of secondary islands in estimating the transition to kinetic scales. [1] S. Dorfman et al. Phys. Plasmas **15**, 102107 (2008) [2] W. Daughton et al. *"Transition from Collisional to Kinetic Regimes in Large-Scale Reconnection Layers"*, to appear in Phys. Rev. Letters

*In collaboration with W. Daughton, L. Yin, B.J. Albright, K.J. Bowers (LANL), S. Dorfman, H. Ji, M. Yamada (PPPL), H. Karimabadi (UCSD)

11:00
BI2 4 Equations of State in Collisionless Reconnection.
ARI LE, *MIT*

Wind and Cluster spacecraft measurements of reconnecting current sheets in the Earth's magnetosphere show strong electron temperature anisotropy. This anisotropy is accounted for in a solution of the Vlasov equation recently derived for general reconnection geometries with magnetized electrons in the limit of fast transit time [1]. A necessary ingredient is an ion-scale parallel electric field, which maintains quasi-neutrality by regulating the electron density, traps a large fraction of thermal electrons, and heats electrons in the parallel direction. Based on the expression for the electron phase space density, equations of state provide a fluid closure that relates the parallel and perpendicular pressures to the density and magnetic field strength [2]. The resulting fluid model agrees well with fully kinetic simulations of guide-field reconnection, where the parallel electron temperature becomes several times greater than the perpendicular temperature. In addition, the equations of state relate features of the electron diffusion region that develop during anti-parallel reconnection to the upstream electron beta. They impose strong constraints on the electron Hall currents and magnetic fields. The equations of state are suitable for implementation in two-fluid or hybrid codes. Such codes could retain important electron kinetic effects in numerical models of large-scale collisionless plasmas, which lie beyond current computational limits in kinetic simulation. [1] J. Egedal, W. Fox, N. Katz, et al., J. Geophys. Res. 113, A12207 (2008). [2] A. Le, J. Egedal, et al., Phys. Rev. Lett. 102, 085001 (2009).

11:30
BI2 5 Investigation of ion heating due to reconnection in the MST reversed-field pinch.*
GENNADY FIKSEL, *University of Wisconsin-Madison and Center for Magnetic Self-Organization in Laboratory and Astrophysical Plasmas*

Anomalous ion heating in laboratory and astrophysical plasmas is not well understood. In the Madison Symmetric Torus (MST) reversed-field pinch experiment, ions are heated rapidly during impulsive reconnection, attaining temperatures exceeding hundreds of eV, often well in excess of the electron temperature. The energy source for this heating is the equilibrium magnetic field energy released during reconnection, but the means by which magnetic energy is converted to ion thermal energy has not yet been established. The results and diagnostic techniques reported here aim to test several distinct theoretical models that could describe the energy conversion is both laboratory and space plasmas: viscous damping of tearing flows, ion cyclotron heating, and stochastic heating. Neutral-beam-based diagnostics are used for ion temperature measurements. Rutherford scattering monitors the majority ions, while charge-exchange- recombination spectroscopy monitors the minority ions. The high spatial (several centimeters) and temporal (tens of microseconds) resolution of these diagnostics allows for detailed comparison of the dynamics of the ion heating with theoretical predictions. The energy budget of the ion heating and its mass scaling in hydrogen, deuterium, and helium plasmas was determined by measuring the fraction of the released magnetic energy converted to ion thermal energy. The fraction ranges from about 10-30% and increases approximately as the square root of the ion mass. Ion heating increasing with ion mass agrees with observations in other laboratory experiments as well as in the solar corona. In addition, a recent upgrade of the charge-exchange diagnostic now allows simultaneous measurement of the perpendicular and parallel ion temperature, facilitating still further discrimination among the proposed heating mechanisms.

*Work supported by the USDOE and NSF.

12:00
BI2 6 Evolution to a minimum energy Taylor state in multiple flux conserving boundaries in SSX.*
TIM GRAY, *Swarthmore College*

Dynamical evolution and final MHD states are measured and analyzed in four different flux conserving boundaries in SSX. Oblate (L/R = 1.2), slightly prolate (L/R = 2.0), prolate (L/R = 3.0), and super prolate (L/R = 10) geometries are studied. The flux conserving boundaries are provided by highly conducting copper walls. In each case, dynamics are initiated by injecting small, dense spheromaks into each end of the flux conserver. The helicity of the spheromaks can be individually chosen, allowing for both counter and co-helicity merging, both of which have been tried. During the merging process, complex behavior is observed; interpenetrating, two component flows are measured with a high resolution ion Doppler spectrometer (IDS), as well as dynamic activity of the magnetic fields. After the merging phase, complex activity subsides and a minimum energy Taylor state with constant helicity is reached. This state is measured and compared to the lowest energy eigenmode predicted by $\nabla \times B = \lambda B$. Eigenmodes for the various flux conserver geometries are calculated by PSI-TET. Ion temperatures are monitored throughout the process by the IDS system. Between 48 and 288 separate magnetic probes have been employed to characterize the magnetic structure of the plasma. Typical parameters of the merged low beta plasmas are $B = 0.1$ T, $n_e = 1 - 5 \times 10^{20}$ m^{-3}, $T_i = 20$ eV, and $\beta = 0.1$.

*Supported by US DOE and NSF.

SESSION BI3: ADVANCES IN TOKAMAKS: CORE AND EDGE PHYSICS
Monday Morning, 2 November 2009; Centennial II at 9:30; Robert Granetz, Massachusetts Institute of Technology, presiding

9:30
BI3 1 Advanced Tokamak Research with Integrated Modeling in JT-60U.
NOBUHIKO HAYASHI, *Japan Atomic Energy Agency, Fusion Research and Development Directorate*

Researches on advanced tokamak (AT) characterized by high normalized beta, high bootstrap current fraction and high confinement have been progressed in JT-60U with integrated modeling. In AT, simultaneous achievement of high performances is important, because physical factors are strongly coupled with each other, resulting in complexity and autonomy. Edge pedestal has coupling physics of core plasma and SOL-divertor-wall characteristics. Its coupling is further enhanced by ELMs. The linkage among them has been systematically clarified in JT-60U experiments [1], in which a plasma rotation also affected the linkage. Although plasma performances may be controlled by the rotation, the rotation was varied not only by an external input but also by the intrinsic mechanism due to plasma itself. To predict and control these complex and autonomous plasmas and to achieve simultaneously high performances, new models are constructed and integrated based on JT-60U experimental analyses. In this paper, we report researches of JT-60U

experiments with integrated models of core, pedestal, SOL-divertor-wall, which are important for AT and have coupling physics. It is found that a toroidal rotation with perpendicularly-injected NB is caused by fast ion orbit and driven most efficiently by horizontal injection. This indicates the possibility of producing and controlling an intrinsic rotation in AT. Steeping a pressure gradient in the core beyond the pedestal is found to enhance the ELM energy loss. The pressure gradient optimization is required for AT with high beta and low ELM energy loss. 2D SOL-divertor-wall integrated code is developed and further integrated with 1.5D core-pedestal transport code for understanding the whole coupling physics.
[1] N. Oyama and the JT-60U team., "Overview of JT-60U results toward establishment of advanced tokamak operation," Nucl. Fusion, in print (2009).

10:00
BI3 2 Power and particle exhaust: recent progress on JET and implications for ITER.*
WOJCIECH FUNDAMENSKI, *Euratom/UKAEA Fusion Association*

Fusion burn, on the one hand, and particle and power exhaust, on the other, impose different constraints on plasma scenarios – the former requiring sufficient levels of fuelling, heating, and confinement to achieve and maintain ignition, the latter for the helium ash, impurity ions and total power to be removed without undue damage to the plasma facing components (PFCs). Recent experiments on JET have significantly progressed our understanding of tokamak exhaust physics, specifically the steady-state and transient heat loads on divertor and main chamber PFCs, as well as first wall material migration and hydrogenic fuel retention. As part of these experiments, various strategies of reducing plasma loads onto PFCs have been investigated. The reduction of steady-state heat loads was achieved by a combination of fuelling and extrinsic impurity (nitrogen and neon) seeding, thereby increasing the energy radiated from the plasma edge, cooling the divertor/SOL plasma and facilitating its 'detachment' from the divertor target PFCs. Transient heat loads associated with edge localized modes (ELMs) were reduced by increasing the frequency (reducing the size) of ELM events, by fuelling, seeding and active techniques, while those associated with plasma termination (disruption) were partly mitigated by massive gas injection (mixtures of deuterium, argon and neon). Finally, a series of dedicated, day-long experiments were performed to measure the fuel retention under various plasma conditions. In this contribution, the results of the recent JET experiments are summarized and their implications for ITER are discussed.

*Work partly funded by the UK EPSRC and EURATOM under conducted under EFDA.

10:30
BI3 3 Recent Progress on EAST Superconducting Tokamak.
JIANGANG LI, *Institute of Plasma Physics,CAS*

EAST is the first fully superconducting tokamak with divertor configurations starting operation since 2006. It has now been upgraded from initial full metal wall to actively cooled graphite plasma facing components (PFC) and bakable to 350 [r]C. Stable double null (DN) divertor plasma discharges over 60 seconds have been achieved with the actively cooled graphite PFCs and the new internal divertor cryo-pump. Plasma current up to 600 kA, electron density $\sim 5\text{x}10^{19}\text{m}^{-3}$, electron temperature $\sim$ 2.5keV have been obtained with lower hybrid current drive (LHCD) and auxiliary heating. Low loop voltage breakdown at 0.15V/m and plasma ramping rate between 0.1MA/s and 0.5MA/s have been obtained with assistance of LHCD. Various start-up scenarios have been explored for operating PF superconducting coils with a large safety margin. Up to 1.2MW LHCD power has been coupled to both SN (single null) and DN plasmas. Divertor performance under long pulse operating conditions has been assessed for both SN and DN configurations. DN operation led to stronger asymmetry in power loading, favoring the outer divertor. Novel wall conditioning techniques, including RF wall conditioning and high frequency RF wall conditioning in the presence of toroidal magnetic fields have also been successfully tested. The details of these recent advances are presented.

11:00
BI3 4 Pedestal regulation techniques for enhanced confinement regimes on Alcator C Mod.*
JERRY HUGHES, *MIT PSFC*

Recent research on Alcator C-Mod has achieved greater leverage on global confinement through both optimization and active modification of the edge pedestal. Pedestal scalings that are quite robust in typical H-mode operation can be broken, and particle and thermal transport in the edge barrier can be decoupled substantially. In H-mode, pedestal parameters show a striking sensitivity to the ion $B \times \nabla B$ drift direction, relative to the active x-point position, with considerable variability observed when the distance between separatrices is on the order of the pedestal width ($\approx$ 5mm) or less, *i.e.* very near double null (DN). Near DN H-modes can have improved confinement factors ($H_{98} > 1$) as a result of elevated pedestal temperature (T_{ped}), with the edge regulated by benign small ELMs or continuous modes, regimes desirable for ITER and other future devices. Operating with a single null and with ∇B drift away from the x-point allows the formation of discharges with L-mode-like particle confinement, yet with excellent energy confinement. This enhanced confinement regime has demonstrated $H_{98} \approx 1$, $T_{ped} \approx$ 1keV, and can be maintained steady-state with no ELMs by operating with high current and strong shaping, while holding input power below the L-H threshold to suppress particle barrier formation. Additional pedestal modification has also been obtained in H-modes by application of lower hybrid (LH) waves. Strong relaxation of the density pedestal is observed and accompanied by increases in T_{ped}, providing a

substantial reduction in overall collisionality and somewhat improved confinement. Direct interaction of the LHRF with the edge plasma appears to play a role in enhancing the pedestal particle transport, which conveniently relaxes the discharge to a less dense and hotter state, one more conducive to core LH penetration and damping. In all cases, strongly modified pedestals affect core properties, often including surprising effects on core rotation.

*Supported by USDoE award DE-FC02-99-ER54512.

11:30
BI3 5 Turbulence Structures and Velocities in the Edge of Alcator C-Mod.*
ISTVAN CZIEGLER, *MIT PSFC*

The work to be presented describes the velocity fields and scale structure of the turbulent edge regions in Alcator C-Mod plasmas. Strong turbulence phenomena are routinely observed in the plasma edge and Scrape-Off-Layer regardless of the quality of global confinement. These turbulence layers have been characterized using Gas-Puff-Imaging measurements. Observations of short ($\sim$ 10 μs) timescale features and variations of the velocity fields will be presented for plasmas with a range of n_e,I_p, in both L and H-mode regimes. Radial profiles of poloidal propagation velocities have been constructed using direct Fourier methods. The observed experimental dispersion relations show a clear radial structure with turbulence propagating in the ion-diamagnetic direction (1.5 $-$ 2 km/s) around and outside the separatrix, and moving in the electron-diamagnetic direction (3.5 $-$ 4 km/s) around and inside the separatrix. In the crossover region around the separatrix two counter-propagating velocities are registered as long as the observation duration is $>$ 1 ms. However for observation durations ($\sim$ 100μs) coinciding with the characteristic time for the ejection of coherent features (blobs), rapid changes in the propagation direction are revealed, while the speed of propagation in the two regions remains largely invariant. Data obtained from both classical and spatio-temporal wavelet analysis on the statistical behavior of the propagation velocities and spectral characteristics will also be presented. These results suggest a view of the plasma edge qualitatively different from the one previously considered. Possible interpretations and implications will be discussed in relation to the formation of blobs and the structure of the high-shear region.

*Supported by USDoE award DE-FC02-99ER54512.

12:00
BI3 6 Kinetic simulations of plasma sheath with parallel to the wall magnetic field.*
NATALIA KRASHENINNIKOVA, *LANL*

Plasma-wall interactions can play an important role in plasma transport and confinement. The sheath serves as a boundary between the interior quasi-neutral plasma and the wall's surface and can impact the energy and particles fluxes striking the vessel, and consequently can influence the choice for the wall material. As hotter and denser plasmas are confined by almost parallel to the wall magnetic field in current fusion experiments, the need to understand this particular type of plasma sheath is apparent. For example, in magnetized target fusion the confining B field remains mostly parallel to the converging liner surface, while on ITER, the magnetic field intercepts the main chamber and the divertor plates at no more than a couple degrees. The physics of such plasma sheath is fundamentally different from the conventional one, as it is the ions that are positively charging the wall due to their large Larmor radii. Detailed 1D and 2D kinetic simulations using VPIC[1] suggest that the particles' distribution functions in the sheath significantly deviate from a local Maxwellian (contrary to common assumption in analytical theory[2]). The anomalies in the distribution functions are quantified by analyzing the particles drift velocities and the roles of different parts that make up the sheath force balance, such as electric field, Lorentz force, pressure gradient, and viscosity tensor. Scanning of plasma parameters yields a scaling of the sheath width with magnetic field and electron and ion temperatures that differs from conventional Debye-length scaling. The instabilities due to non-Maxwellian particles distribution functions, pressure gradient, and sheared ExB flow are also considered and compared with the observed dynamical fluctuations in both 1D and higher dimensional simulations. [1] K. J. Bowers, et al. Phys. Plasmas 15, 055703 (2008). [2] U. Daybelge, et al. Phys. Fluids 24 (6) (1981).

*Work supported by OFES and LANL LDRD.

SESSION BO4: MAGNETIC CONFINEMENT THEORY, SIMULATION AND MODELING
Monday Morning, 2 November 2009
Regency VI at 9:30
Don Batchelor, Oak Ridge National Laboratory, presiding

9:30
BO4 1 System size and shear flow effects on ion temperature gradient turbulence BEN McMILLAN, JOLLIET SEBASTIEN, TRACH-MINH TRAN, *CRPP, Ecole Polytechnique Federale de Lausanne* BOTTINO ALBERTO, *Max Planck Institut fur Plasmaphysik, IPP-EURATOM Association, Garching* VILLARD LAURENT, *CRPP, Ecole Polytechnique Federale de Lausanne* We explore the role of system size (ρ^* scaling) and shear flow levels on ion temperature gradient (ITG) turbulence in gyrokinetic simulations. Firstly, the scaling of heat flux level versus system size in plasmas with zero initial flow shear is reexamined. Averages over an ensemble of simulations are made to quantify errors in the mean flux estimate. Our scaling results are compared with others in light of this error. Secondly, the effect of poloidal shear flow on ITG turbulence is examined. Turbulence levels are suppressed when the flow shearing rate is similar to the ITG growth rate. Even at flow levels many times smaller than the supression threshold, nonlinear turbulence is only seen in the simulation if the initial perturbation is large: the system manifests subcritical turbulence. Inward or outward propagating avalanches and inward and outward shifted diffusivity profiles are seen according to the sign of the flow shear. In cases with strong flow shear almost all the flux is associated with avalanches, which propagate across the entire region with strong pressure gradient. The non-local and non-diffusive physics are explored by performing a second scan in system size.

9:42
BO4 2 Gyrokinetic Particle Simulations of Toroidal Momentum Transport in Plasma with Kinetic Electrons* I. HOLOD, Z. LIN, *UCI* Large scale gyrokinetic particle simulations find that momentum transport driven by microturbulence in magnetized plasmas includes both diffusive and off-diagonal (pinch and residual stress) components. Primitive separation of these momentum fluxes in toroidal plasma requires running simulations with a zero background rotation, a rigid rotation, and a sheared rotation, which give rise to the residual stress term, the pinch-like flux, and the diffusive flux, respectively. We have performed global gyrokinetic particle simulations using GTC code for the toroidal momentum transport in driftwave turbulence. Both ions and electrons are treated kinetically. We observe significant radial redistribution of toroidal momentum in cases with constant angular velocity (rigid rotation), which is the manifestation of residual stress and pinch fluxes. Momentum pinch is found to be enhanced by kinetic electrons. Using obtained off-diagonal fluxes we were able to subtract them from total flux in the sheared rotation case, getting as the result the diffusive flux. The ratio of momentum to heat diffusivity (Prandtl number) is found to be in good agreement with quasilinear estimates. The origin of off-diagonal fluxes has been studies through symmetry breaking mechanisms associated with zonal flow generation.

*The work was supported by SciDAC GPS and GSEP Centers.

9:54
BO4 3 Collision methods for particle simulations* F.L. HINTON, *UCSD* C.S. CHANG, *NYU* E.S. YOON, *PPPL* Particle-in-cell simulations of magnetically confined plasmas require a method for incorporating the effects of Coulomb collisions, especially near the plasma edge, where these are especially important. We compare two possible types of methods: (1) Langevin, or Monte-Carlo, methods, which scatter the velocities of the particles, and (2) methods which change only the particle weights as a result of collisions. The weight-changing methods which we discuss use grid-based solutions of the Fokker-Planck equation, with interpolation between the grid and the particle velocities. For the Langevin methods, the errors in momentum and energy conservation are due to time-discretization, and accumulate in time. The weight-changing methods we discuss conserve momentum and energy exactly, assuming certain properties of the velocity-space shape functions for the particles. The details of these methods and their conservation laws will be presented. Also of interest are the effects of noise due to finite numbers of particles per grid cell. These are being investigated, and the results will be presented.

*Supported by U.S.D.O.E. Office of Fusion Energy Science and Office of Advanced Scientific Computing Research.

10:06
BO4 4 Kinetic integrated modeling of tokamak plasmas by TASK3G* A. FUKUYAMA, S. MURAKAMI, A. WAKASA, H. NUGA, T. OKAMOTO, *Kyoto University* Deviation of momentum distribution function from the Maxwellian is unavoidable in tokamak plasmas under heating and current drive. The deviation may affect transport, global stability, diagnostics and fusion reaction rate of burning plasmas. In order to describe the time evolution of the momentum distribution functions of plasma species self-consistently, we have developed a kinetic version of the integrated tokamak modeling code TASK3G as the third generation of the TASK code. Transport, heating and current drive are described by the bounce averaged Fokker-Planck equation. The calculated momentum distribution function is used for the analyses of wave propagation and absorption, global stability, and diagnostics. The bounce-averaged Fokker-Planck equation includes nonlinear Coulomb collision, quasi-linear wave interaction, neoclassical and turbulent-driven radial transport and particle source/sink. A typical example of TASK3G result for ITER burning plasma will be presented.

*This work is supported by Grant-in-Aid for Scientific Research (S) (20226017) from JSPS.

10:18
BO4 5 Progress in the Development of an Integrated Modeling Tool to Support DIII-D and EAST* Q. REN, *ASIPP* L.L. LAO, M.S. CHU, H.E. ST. JOHN, G. ABLA, A. COLLIER, R. PRATER, *GA* J.M. PARK, *ORNL* G. LI, W. GUO, C. PAN, *ASIPP* R. SRINIVASAN, *IPR* M. WORRALL, *Colorado School of Mines* Recent progress in the development of the IMFIT Integrated modeling tool is presented. The goal of IMFIT is to develop a modern and efficient integrated modeling platform to support DIII-D and EAST research, including the capability to simulate the behavior of tokamak discharges. Recent progress includes user-friendly and Python-based GUIs with multi-links to equilibrium, transport, and stability codes to facilitate modeling and analysis, and EFIT F90 upgrade with dynamic memory allocation and MPI option to support multiple devices and grid sizes. Through the GUI, straight-

forward analysis for kinetic EFIT reconstruction is made available. Ongoing developments include design of efficient algorithms to support interactions among physics modules such as EFIT/ONETWO/TGLF coupling for scenario development and transport flux analysis and EFIT/PEST3/TORAY coupling for modeling of tearing mode stability. Details will be presented.

*Work supported in part by the US DOE under DE-FG03-95ER54309 and DE-AC05-00OR22725.

10:30

BO4 6 Model Data Fusion: developing Bayesian inversion to constrain equilibrium and stability theory* MATTHEW HOLE, *Australian National University* J. SVENSSON, *Max-Planck-Institute for Plasmaphysics* L.C. APPEL, *Euratom/UKAEA Fusion* G. VON NESSI, R.L. DEWAR, J. BERTRAM, B.D. BLACKWELL, J. HOWARD, *Australian National University* Recently, a new probabilistic "data fusion" framework based on Bayesian principles has been developed on JET and W7-AS. The Bayesian analysis framework folds in uncertainties and interdependencies in the diagnostic data and signal forward-models, together with prior knowledge of the state of the plasma, to yield predictions of internal magnetic structure. A feature of the framework, known as Minerva (J. Svensson, A. Werner, Plasma Physics and Controlled Fusion 50, 085022, 2008), is the inference of magnetic flux surfaces without the use of a force balance model. We discuss results from a new project to develop Bayesian inversion tools that aim to (1) distinguish between competing equilibrium theories, which capture different physics, using the MAST spherical tokamak; and (2) test the predictions of MHD theory, particularly mode structure, using the H-1 Heliac. A novel spin-off application is development of a Tikhonov cross- validation method, that sequentially removes "anomalous" diagnostic data until the change in the inferred toroidal current is minimised.

*Supported by International Science Linkages Grant CG130047.

10:42

BO4 7 Collisional-radiative modeling of EBIT spectra from highly-charged high-Z ions of relevance to magnetic fusion* YURI RALCHENKO, ILIJA N. DRAGANIĆ, JOHN D. GILLASPY, JOSEPH READER, JOSEPH N. TAN, JOSHUA M. POMEROY, SAMUEL M. BREWER, *NIST* Electron Beam Ion Traps (EBITs) are currently the primary source of spectroscopic information on highly-charged ions of heavy elements, e.g. tungsten, that are important for diagnostics of magnetic confinement fusion devices such as ITER. We will present some results on collisional-radiative (CR) modeling of low-density non-Maxwellian plasmas of EBITs and discuss how various physical processes affect spectral emission and ionization balance. Special attention will be given to the accuracy of radiative and collisional data used for the CR modeling. The simulated spectra will be compared with our recently measured x-ray and extreme-ultraviolet spectra of highly-charged (ion charge z=35-68) Hf, Ta, W, and Au.

*Supported in part by the Office of Fusion Energy Sciences of the U.S. Department of Energy.

10:54

BO4 8 Gauging MRI* ISON HERRON, *Rensselaer Polytechnic Institute* JEREMY GOODMAN, *Princeton University* Axisymmetric stability of viscous resistive magnetized Couette flow is re-examined, with emphasis on flows that would be hydrodynamically stable according to Rayleigh's criterion: opposing gradients of angular velocity and specific angular momentum. A uniform axial magnetic field permeates the fluid. In this regime, magnetorotational instability (MRI) may occur. It is proved that MRI is suppressed, in fact no instability at all occurs, with insulating boundary conditions, when the magnetic resistivity is sufficiently large. This shows conclusively that small magnetic dissipation is a feature of this instability for all magnetic Prandtl numbers. A criterion is provided for the onset of MRI.

*This material is based upon work supported in part by the U. S. Department of Energy under Grant No. DE-FG02-05ER25666 (to I. H.) and by NSF award PHY-0821899 "Center for Magnetic Self-Organization in Laboratory and Astrophysical Plasmas" (to J. G.).

11:06

BO4 9 Kinetic Theory of Ballooning Modes in High Beta Plasmas C.Z. CHENG, *Plasma and Space Science Center, National Cheng Kung University* N.N. GORELENKOV, *PPPL, Princeton University* S. ZAHARIA, *LANL* High-β plasmas in fusion or laboratory plasma devices usually have plasma beta less than unity. But, in space plasmas beta can be much larger than unity. Based on MHD theory ballooning modes in high-β plasmas can be destabilized when the free energy associated with the combined effect of plasma pressure gradient in bad magnetic field curvature overcomes the stabilizing effect of magnetic field line tension. However, when there is a large fraction of magnetically trapped particles, trapped particle dynamics and finite ion gyroradius effect can produce a large parallel electric field and hence a parallel current that greatly enhances the stabilizing field line tension to stabilize the MHD ballooning modes. However, in even higher plasma beta regime, a weaker kinetic ballooning instability can occur due to wave-particle magnetic drift resonances. To demonstrate the resonance kinetic ballooning instability we will present numerical solutions using self-consistent equilibrium solutions for magnetospheric plasmas.

11:18

BO4 10 Results from an International MHD Data Mining Collaboration B.D. BLACKWELL, D.G. PRETTY, *Australian National University* S. YAMAMOTO, K. NAGASAKI, *Institute of Advanced Energy, Kyoto University, Japan* E. ASCASIBAR, R. JIMENEZ-GOMEZ, *Laboratorio Nacional de Fusion, EURATOM-CIEMAT, Spain* S. SAKAKIBARA, *National Institute for Fusion Science, Japan* F. DETERING, *Diversity Arrays Technology P/L, Canberra, Australia* New data mining techniques have been successfully applied to MHD data on H-1, TJ-II and Heliotron-J, and are being implemented on LHD and W-7AS data. The motivation for automated mining of fusion databases is to distil and classify data for inclusion in fusion physics databases, and to highlight physically-interesting, previously unnoticed modes. We present results from data mining of more than 10,000 shots from H-1, TJ-II and Heliotron J, showing a range of Alfvénic and non-Alfvénic modes, many with well-defined poloidal mode structure and clear relation to heating configuration and plasma geometry. In the case of H-1, the dispersion relations for several of these modes have been examined in detail exploiting H-1's high resolution in rotational transform. Examples of use of this relation

to provide information about rotational transform (a form of Alfven spectroscopy) are given. We also discuss possible real-time application of the cluster technique to preliminary mode identification as data is being acquired, and some initial work on application of image processing techniques to MHD spectrogram analysis.

11:30

BO4 11 Hiro currents, current spikes and forces in tokamak disruptions* LEONID E. ZAKHAROV, *Princeton University, PPPL* The talk gives resolution of the oldest (known since 1963) puzzle in tokamak physics, related to such bright phenomena as the positive current spike (negative voltage spike) in tokamak disruptions. It is shown that the electric contact between plasma and the wall plays crucial role in tokamak disruptions. When the safety factor q at the plasma boundary crosses the resonant value and a kink mode is excited, two effects follows. One is the generation of the surface, called "Hiro," current at the plasma boundary, unrelated to the resonant character of q-value. Another is the excitation of the stabilizing eddy currents in the wall, negligible when q is resonant. The kink mode starts its development as a fast, invisible magnetically ideal mode with no wall effect present. As soon as plasma touches the wall, the surface Hiro currents from the plasma will be driven through the wall. This stops fast instability and convertw it into a slower resistive mode. The Hiro currents are always opposite to the plasma current. This is consistent with toroidal asymmetry in the plasma current measurements on JET due to m/n=1/1 kink mode. The same Hiro currents, generated by $m > 1$ modes are responsible for positive plasma current spikes (and negative voltage spikes) in conventional disruptions.

*Supported by US DoE contract No.DE–AC020–76–CHO–3073

11:42

BO4 12 Resonant Field Amplification in JET Advanced Regimes* MIKHAIL GRYAZNEVICH, *UKAEA-EURATOM Fusion Association, Culham, UK* T.C. HENDER, Y. LIU, I.T. CHAPMAN, D. HOWELL, C.D. CHALLIS, *UKAEA-EURATOM Fusion Association* E. JOFFRIN, R. KOSLOWSKI, *JET-EFDA, Cilham* P. BURATTI, *EURATOM-ENEA Fusion Association and JET-EFDA contributors* Resonant Field Amplification (RFA) has been systematically measured on JET, in two domains favourable for ITER steady-state operations: broad q-profiles with qmin 1 and qmin 2. MARS-F code modelling reproduces RFA data at low and high beta and suggests a new method of how the RFA data should be used to determine the no-wall limit experimentally. Although there is no strong evidence of a beta-limit connected with the RWM even at betaN 4 and performance was limited by internal n=1 modes, the observed (using RFA data) decrease in the no-wall limit with the increase in qmin is in agreement with the same dependence of the experimentally achieved highest beta values.

*Funded by the United Kingdom Engineering and Physical Sciences Research Council and by the European Communities under the contract of Association between EURATOM and UKAEA.

SESSION BO5: HOHLRAUM PHYSICS
Monday Morning, 2 November 2009
Hanover CDE at 9:30
Mordecai Rosen, Lawrence Livermore National Laboratory, presiding

9:30

BO5 1 Lasnex Calculations of NIF Vacuum Hohlraum Experiments* R.E. OLSON, *SNL* L.J. SUTER, *LLNL* J.L. KLINE, *LANL* E.A. WILLIAMS, S.H. GLENZER, K. WIDMANN, D.A. CALLAHAN, N.B. MEEZAN, S.H. LANGER, *LLNL* Lasnex calculations will be described and the results compared with experimental data for a series of NIF vacuum hohlraum experiments that were among the first targets shot on NIF as part of the facility commissioning. The pre-shot calculations predicted that the 6.40 mm long, 3.55 mm diameter hohlraums would be heated to peak radiation temperatures in the range of 225-275 eV using a 96 beam subset of the NIF laser beams (up to 350 kJ total on-target), and to a peak radiation temperature of 330 eV using all 192 NIF laser beams (700 kJ total). These 2 ns sq pulse, 3w drive energies are 10-20x the on-target energies used in previous hohlraum experiments at the Nova and Omega laser facilities. The new NIF hohlraum calculations and experimental data will be compared with previous (Omega/Nova) hohlraum calculations and data. This data will allow us to validate the Lasnex code and associated physics packages at the increased size and energy regimes now available for hohlraum experiments at the NIF.

*Sandia is a multiprogram laboratory operated by the Sandia Corporation, a Lockheed Martin Company, for the U.S. Department of Energy under Contract No. DE-AC04-94AL85000.

9:42

BO5 2 The Hohlraum Energetics experimental campaign on the National Ignition Facility* S. GLENZER, J. ATHERTON, R. BERGER, E. DEWALD, L. DIVOL, S. DIXIT, E. DZENITIS, D. HINKEL, D. CALLAHAN, D. KALANTAR, *LLNL* J. KLINE, G. KYRALLA, *LANL* O. LANDEN, S. LEPAPE, B. MacGOWAN, N. MEEZAN, P. MICHEL, J. MOODY, E. MOSES, L. SUTER, R. WALLACE, K. WIDMANN, *LLNL* NIC EXPERIMENTAL TEAM, NIC TARGET FABRICATION TEAM, We will review progress in performing the hohlraum energetics experiments on the National Ignition Facility. The experiments are designed to first activate target diagnostics and to demonstrate target experiments with cryogenic targets. In particular, a series of hohlraum and gas-filled target shots will be fielded to demonstrate performance of the absolutely calibrated soft x-ray spectrometer, Dante, the laser backscatter suite of diagnostics, i.e., the full aperture backscatter station (FABS) and Near Backscatter Imager (NBI) on two cones of the 48 quads of beams, and the absolutely calibrated hard x-ray bremsstrahlung detector, FFLEX. The campaign is designed to demonstrate laser beam intensity and laser conditioning to efficiently heat ignition hohlraums to radiation temperatures required to drive ignition capsules with laser energies in the range of 1-1.5 MJ. In this talk, we will discuss progress towards fielding this campaign on the National Ignition Facility and describe our approach for selecting the radiation temperature for ignition hohlraums.

*This was work performed under the auspices of the U.S. Department of Energy by Lawrence Livermore National Laboratory under Contract DE-AC52-07NA27344.

9:54

BO5 3 Vacuum Hohlraum energetic experiments on the National Ignition Facility* JOHN KLINE, *LANL* S. GLENZER, *LLNL* K. WIDMANN, R. OLSON, *SNL* D. HINKEL, *LLNL* E. WILLIAMS, L. SUTER, J. CELESTE, E. DEWALD, S. DIXIT, W. HSING, O. LANDEN, B. MacGOWAN, A. WARRICK, J. ATHERTON, R. BERGER, D. CALLAHAN, L. DIVOL, C. HAYNAM, D. KALANTAR, J. KILKENNY, *GA* S. LE PAPE, *LLNL* D. LARSON, N. MEEZAN, M. SCHNEIDER, Results from vacuum hohlraum energetics experiments on the National Ignition Facility using a subset of NIF's 192 beams are presented. In these experiments, the scaling of radiation temperature for conventional gold hohlraums as well as gold hohlraums lined with a thin gold-boron liner was measured. These experiments are the first test of hohlraum drive scaling at ~ 70% of full-NIF scale. We show how these results compare with scalings developed on predecessor facilities at a fraction of the laser energy being used here. In NIF ignition hohlraums, one of the mitigation strategies for SBS is to mix boron into the inner 0.6 μm of the Au hohlraum wall. These experiments also test if, as predicted by simulations, there is no anomalous degradation of the radiation temperature due to the gold-boron liner.

*This work performed under the auspices of the U.S. DOE by LANL under contract DE-AC52-06NA25396, by LLNL under Contract DE-AC52-07NA27344, and by SNL under contract DE-AC04-94AL85000.

10:06

BO5 4 High Resolution Integrated Hohlraum-Capsule Simulations for Virtual NIF Ignition Campaign* O.S. JONES, M.M. MARINAK, C.J. CERJAN, D.S. CLARK, M.J. EDWARDS, S.W. HAAN, S.H. LANGER, J.D. SALMONSON, *LLNL* We have undertaken a virtual campaign to assess the viability of the sequence of NIF experiments planned for 2010 that will experimentally tune the shock timing, symmetry, and ablator thickness of a cryogenic ignition capsule prior to the first ignition attempt. The virtual campaign consists of two teams. The "red team" creates realistic simulated diagnostic data for a given experiment from the output of a detailed radiation hydrodynamics calculation that has physics models that have been altered in a way that is consistent with probable physics uncertainties. The "blue team" executes a series of virtual experiments and interprets the simulated diagnostic data from those virtual experiments. To support this effort we have developed a capability to do very high spatial resolution integrated hohlraum-capsule simulations using the Hydra code. Surface perturbations for all ablator layer surfaces and the DT ice layer are calculated explicitly through mode 30. The effects of the fill tube, cracks in the ice layer, and defects in the ablator are included in models extracted from higher resolution calculations. Very high wave number mix is included through a mix model. We will show results from these calculations in the context of the ongoing virtual campaign.

*Prepared by LLNL under Contract DE-AC52-07NA27344.

10:18

BO5 5 NIF Ignition Hohlraum Designs With and Without Laser Entrance Hole Liners* DEBRA CALLAHAN, DENISE HINKEL, SIEGFRIED GLENZER, JOHN LINDL, NATHAN MEEZAN, PIERRE MICHEL, RICHARD TOWN, LARRY SUTER, *Lawrence Livermore National Laboratory* The laser entrance hole (LEH) of the NIF ignition hohlraum has typically been lined with a thin (~ 30 micron) plastic liner. The purpose of this liner is to tamp the motion of the gold blow-off from the LEH lip. This simplifies symmetry optimization but increases the LEH plasma density. Single beam calculations of the expected laser-plasma interactions (LPI) show little gain in this region. However, multiple beam effects may amplify the single beam backscatter in the LEH. Reducing LEH plasma density by removing the liner reduces the multiple beam effects. To compensate for the LEH closure, the initial LEH is larger without the liner. This results in an increase in the laser power and energy required to drive the same capsule. In this talk, we will discuss designs with and without an LEH liner and how we will optimize the design based on the early hohlraum experiments on NIF.

*This work was performed under the auspices of the U.S. Department of Energy by Lawrence Livermore National Laboratory under contract DE-AC52-07NA27344.

10:30

BO5 6 Tuning Implosion Symmetry on the National Ignition Facility* S.V. WEBER, D. CALLAHAN, M.J. EDWARDS, N. MEEZAN, B. SPEARS, *LLNL* G. KYRALA, D.C. WILSON, *LANL* Implosion symmetry on the National Ignition Facility (NIF) will be achieved though experiments employing a series of surrogate capsules of increasing fidelity to the ignition target. Initial tuning will employ gas-filled symmetry capsules (SymCaps) of reduced size from the ignition targets. These are tuned to minimize asymmetry of the imploded core x-ray emission by varying hohlraum length, relative powers of the laser beam cones, and cone frequency difference. Later experiments, still at smaller scale, employ dudded-fuel capsules with reduced-deuterium THD ice layers, which are closer surrogates of the ignition capsule. The modest neutron yields of these targets are compatible with our full suite of x-ray diagnostics. Finally, full-size THD capsules will be tested, preparing us for ignition attempts with live DT fuel. Single parameter sensitivity studies have been used to set fabrication tolerances.

*Prepared by LLNL under Contract DE-AC52-07NA27344.

10:42

BO5 7 The Use of Symcaps for Symmetry Tuning of Ignition Capsules* GEORGE KYRALA, S.H. GLENZER, N.B. MEEZAN, S.V. WEBER, L.J. SUTER, N. IZUMI, D.A. CALLAHAN, M.J. EDWARDS, O.L. LANDEN, *LLNL* Symmetry tuning of the ICF imploding capsule has a great impact on the performance of capsule to eventually reach ignition. We will discuss the technique of using symcap capsules to measure the symmetry. In symcaps the DT is replaced by an equivalent ablator mass, are calculated to mimic the hydrodynamic behavior of the ignition capsule, and their x-ray emission signature correlates well with an ignition capsules' core shape. Due to their low convergence, symcaps have lower sensitivity to irradiation symmetry than ignition capsules. But, they still allow, initially, tuning the symmetry of an ignition capsule, without the complications of yield or cryogenics. We will describe the initial use of symcaps in NIF hohraums to measure the sensitivity of their shape to variations in the fraction of energy in each cone of the incident laser beams, and their use to tune the symmetry of the implosion.

*Work performed by Los Alamos National Laboratory and Livermore National Laboratory under contracts DE-AC52-06NA25396,and DE-AC52-07NA27344, for the National Nuclear Security Administration of the U.S. Department of Energy.

10:54

BO5 8 First re-emit experiments on the National Ignition Facility for early time symmetry tuning of indirect drive ignition implosions* EDUARD DEWALD, JOSE MILOVICH, CLIFF THOMAS, STEVEN GLENN, *LLNL* JOHN KLINE, *LANL* RAHUL PRASAD, OTTO LANDEN, *LLNL* In indirect drive ignition experiments on the National Ignition Facility (NIF), the symmetry of the hohlraum radiation drive for the first 2 ns is tuned using the re-emit technique [1] which measures the instantaneous x-ray drive asymmetry based on soft (600-1200 eV) x-ray imaging of the re-emission of a high-Z sphere surrogate capsule. We performed multi-view re-emit symmetry experiments in 90% scale NIF ignition vacuum hohlraums at 90-110 eV NIF foot radiation temperatures at the Omega facility. Compared to [1] these experiments use a less perturbing off-axis stalk rather than a thin CH tent to hold the capsule and have an azimuthal laser beam illumination similar to NIF. We measured radiation symmetry sensitivity to inner/outer beams power balance and we assessed the residual radiation asymmetry of the patched diagnostic holes and missing laser beams. We will also report on the first re-emit experiments performed recently on the National Ignition Facility in full ignition scale gas filled hohlraums. These experiments assess the effects on radiation symmetry and expected uncertainties of the technique due to the additional effects given by the hohlraum gas fill. [1] E.L. Dewald, *et. al.*, Rev. Sci. Instrum. 79, 10E903, 2008.

**This work was performed under the auspices of the U.S. DOE by LLNL under Contract DE-AC52-07NA27344.

11:06

BO5 9 3D studies of the NIF symmetry tuning targets* J. MILOVICH, O. JONES, M. EDWARDS, S. WEBER, E. DEWALD, O. LANDEN, M. MARINAK, *LLNL* Minimizing radiation drive asymmetries is necessary for a successful ignition campaign. Since the ignition capsule symmetry is most sensitive to the foot (first 2 ns) and the peak of the laser pulse, two different targets will be fielded on the NIF: re-emit and symmetry capsules (Sym-Caps). The first measures the incoming flux asymmetries during the foot by observing the re-radiated flux of a high-Z ball in place of the ignition capsule. The Sym-Caps resemble the ignition target with the frozen DT layer replaced by an equivalent mass of ablator material, thus preserving the hydrodynamic implosion properties. By measuring the x-ray self-emission near peak compression the ignition capsule core shape can be tuned. Simulations with 2D radiation-hydrodynamic simulations codes omit 3D effects in the hohlraum such as diagnostic holes, capsule roughness, shot-to-shot variations caused by laser beam power imbalances and pointing errors. We study these effects by performing 3D simulations using HYDRA and found that tuning the laser pulse using a finite number of shots is not substantially compromised.

*Prepared by LLNL under Contract DE-AC52-07NA27344.

11:18

BO5 10 3-D simulations for assessment of NIF shock timing techniques* H.F. ROBEY, *LLNL* R.E. OLSON, *Sandia National Laboratories* O.S. JONES, J.L. MILOVICH, S.M. SEPKE, *LLNL* Capsule implosions planned for the National Ignition Facility (NIF) require a series of shocks, which propagate through the ablator and DT ice shell. The strength and timing of these shocks is critical for maintaining the DT fuel on a low adiabat. To meet the requirements, tuning experiments are being planned to measure and adjust the shock timing. These experiments use a modified target geometry that employs a re-entrant Au cone to provide optical access to the shocks in capsule interior. This modified geometry introduces some additional uncertainties, which are intrinsically three-dimensional in nature. Examples of 3D uncertainties include beam-to-beam power balance, pointing, and 3D fabrication features, all of which may have a greater impact on these localized shock timing measurements than they will have on the overall drive symmetry in the hohlraum. In order to assess the effect of these uncertainties, 3D simulations using HYDRA have been performed to test the robustness of the shock timing measurements.

*Prepared by LLNL under Contract DE-AC52-07NA27344.

11:30

BO5 11 Optimizing implosion yields using rugby-shaped hohlraums* HYE-SOOK PARK, H. ROBEY, P. AMENDT, *LLNL* F. PHILIPPE, A. CASNER, T. CAILLAUD, J.-L. BOURGADE, O. LANDOAS, *CEA* C.K. LI, R. PETRASSO, F. SEGUIN, M. ROSENBERG, *MIT* V. YU. GLEBOV, *LLE* We present the first experimental results on optimizing capsule implosion experiments by using rugby-shaped hohlraums [1] on the Omega laser, University of Rochester. This campaign compared D_2-filled capsule performance between standard cylindrical Au hohlraums and rugby-shaped hohlraums for demonstrating the energetics advantages of the rugby geometry. Not only did the rugby-shaped hohlraums show nearly 20% more x-ray drive energy over the cylindrical hohlraums, but also the high-performance design of the capsules provided nearly 20 times more DD neutrons than in any previous Omega hohlraum campaigns, thereby enabling use of neutron temporal diagnostics. Comparison with simulations on neutron burn histories, x-ray core imaging, backscattered laser light and radiation temperature are presented. [1] P. Amendt *et al.*, Phys. Plasmas 15, 012702 (2008)

*This work was performed under the auspices of the Lawrence Livermore National Security, LLC, (LLNS) under Contract No. DE-AC52-07NA27344.

11:42

BO5 12 What measurements of proton self emission tell us about hohlraum fields and yield anomalies* R. PETRASSO, C. LI, F. SEGUIN, J. FRENJE, M. ROSENBERG, H. RINDERKNECHT, *MIT* F. PHILIPPE, A. CASNER, T. CAILLAUD, O. LANDOAS, J.-L. BOURGADE, *CEA* P. AMENDT, N. IZUMI, J. KOCH, O. LANDEN, J. MILOVICH, H. PARK, H. ROBEY, R. ROBEY, R. TOWN, *LLNL* A. NIKROO, J. KILKENNY, *GA* Measurements have been made of 14.7-MeV self-emission protons, from reactions of D-3He fuel, for a variety of hohlraums - scale 1 and scale ^{5}ker$n$ $-$ $.1em$/ker$n$ $-$ $.15em_{.25}$, gold and cocktail hohlraums, vacuum and gas-filled hohlraums, cylindrical and rugby geometries, drive with and without phase plates, drive with different numbers of beams, and implosions with different capsule parameters. The picture that emerges is quite consistent: large anisotropies in the proton fluence pattern are generally observed out the LEH but little if any variations through the hohlraum equator. In addition, we examine whether the scaling of yields from pure D2 to D-3He mixtures is found to deviate from the expected density scaling (i.e. the Rygg Effect), as reported recently for directly driven capsules (1). (1) H. Herrmann *et al.*, PoP **16,** 056312(2009)

*Work supported in part by DOE, LLNL, and CEA.

11:54

BO5 13 Filamentation in the coronae of imploding ICF capsules F.H. SEGUIN, C.K. LI, M. MANUEL, J.R. RYGG,*J.A. FRENJE, R.D. PETRASSO, *MIT* R. BETTI, F.J. MARSHALL, D.D. MEYERHOFER, *LLE* Electromagnetic fields associated with filamentary structures in the coronae of directly-driven ICF capsules have been studied with charged-particle radiography at the OMEGA laser facility. The time evolution and structures of the fields, including identification of field type, will be described on the basis of complementary radiographs recorded with several particle types as well as Monte-Carlo simulations. The particles include monoenergetic species (15-MeV protons, 3-MeV protons, and 3.6-MeV alpha particles, from laser-driven, imploding-pusher capsules with D^3He fill) as well as protons with exponential spectra (produced from short-pulse OMEGA-EP laser beams incident on a foil). Possible connections with specific hydrodynamic and/or laser-plasma-interaction instabilities, and implications for implosion physics, will be discussed. This work was performed at the LLE NLUF, and was supported in part by the FSC at U. of R., US DoE, LLNL, and LLE.

*Currently at LLNL

12:06

BO5 14 Electromagnetic Fields and Plasma Flow in Laser-Irradiated Hohlraums at OMEGA C.K. LI, F.H. SEGUIN, J.A. FRENJE, M.J. ROSENBERG, R.D. PETRASSO, *MIT* P.A. AMENDT, R.P.J. TOWN, O.L. LANDEN, J.L. MILOVICH, J.R. RYGG, *LLNL* R. BETTI, J. KNAUER, D.D. MEYERHOFER, J.M. SOURES, *LLE* C.A. BACK, J.D. KILKENNY, A. NIKROO, *GA* We report on the first proton radiography of laser-irradiated hohlraums and of indirectly-driven capsule implosions in inertial confinement fusion (ICF). These experiments resulted in observations of self-generated electric and magnetic fields. Peak values are $\sim 10^9$ V m^{-1} and $\sim 10^6$ gauss. Time-gated radiographs of monoenergetic protons with discrete energies (15.0 and 3.3 MeV) reveal dynamic pictures of field structures and plasma flow. Near the end of the 1-ns laser drive, a stagnating Au plasma ($\sim$ 10 mg cm^{-3}) forms at the center of the hohlraum. This is a consequence of supersonic, radially directed Au jets ($\sim$ 1000 μm ns^{-1}, $\sim$ Mach 4) formed as laser-driven plasma bubbles approach one another. Experimental details will be presented and the physics will be discussed. This work was performed at the LLE NLUF, and was supported in part by the FSC at U. of R., US DoE, LLNL, LLE, and GA.

SESSION BO6: MICROWAVES, COMPTON SCATTERING AND ACCELERATOR PHYSICS
Monday Morning, 2 November 2009
Hanover FG at 9:30
Kevin Felch, CPI, presiding

9:30

BO6 1 Physics of Frequency Step-tuning in Terahertz Traveling Wave Tube Regenerative Oscillators* JOHN BOOSKE, *University of Wisconsin, Madison* PENG GAO, *University of Wisconsin, Madison and University of Electronic Science and Technology of China, Chengdu* Efficient generation (higher than 0.3 percent) of terahertz regime radiation was recently demonstrated with a traveling wave tube (TWT) regenerative oscillator using a folded waveguide (FWG) slow wave circuit [1]. By varying the beam voltage between 9.2 and 10 kV, the oscillation frequency was observed between 607-675 GHz. However, step-tuning rather than the expected smooth variation of frequency was observed. Theoretical analyses show that constructive phase interference between the passive backward wave and the recirculated feedback wave leads to step tuning. Results will be presented, including the effects of circuit loss. [1] J. Tucek, et al, Conf. Digest, 2007 IEEE Intl Vac. Elec. Conf., pp. 219-220 (IEEE Cat. No. 07EX1526).

*This work was supported in part by A.F.O.S.R.

9:42

BO6 2 Remote sensing of an elevated level of background ionization with a 1 THz, 1 kW Gyro-BWO* VICTOR GRANATSTEIN, GREGORY NUSINOVICH, *IREAP, University of Maryland, College Park* One application of the THz gyro- BWO under development at the University of Maryland is remote sensing of an elevated level of background ionization in air at NTP; such an elevated level might be found in the vicinity of radioactive material. The aim of the gyro-BWO development is to produce $\sim$ 1 kW of THz power in a 100 microsecond pulse. When such radiation is focused to a spot of cross-sectional area $\sim \lambda^2$, the electric field would be sufficient to break down the air if the background ionization level were sufficiently elevated. With the time to breakdown dependent on background electron density n_o, an elevated value of n_o will manifest itself by causing a shortening of the transmitted or reflected THz pulse. The range and sensitivity of such a detection scheme will be discussed.

*This work was supported by the Office of Naval Research.

9:54

BO6 3 Self-excitation of a frequency-tunable THz-range gyro-backward-wave oscillator* GREGORY NUSINOVICH, *IREAP, University of Maryland* RUIFENG PU, JIAO YU, *University of Maryland* OLEKSANDR SINITSYN, VICTOR GRANATSTEIN, *IREAP, University of Maryland* GYROTRON TEAM TEAM, Gyro-backward-wave oscillators (gyro-BWOs) are known as high-power sources of millimeter-wave radiation which can be continuously tunable in a wide frequency range by varying either magnetic field or the beam voltage. Our group is planning to start experiments with frequency-tunable gyro-BWOs in the THz frequency range. The required magnetic field will be produced by a pulsed magnet delivering up to 40 T magnetic fields. To increase the tunability we plan to utilize slightly tapered waveguides. In the present paper, the self-excitation conditions in gyro-BWOs with such waveguides are analyzed. First, the analysis is performed assuming that the axial structure of the electromagnetic field in such waveguide, which consists of the region of electromagnetic propagation and the region where the wave frequency is below cutoff, can be approximated by the Airy function. The results of simulations performed with the use of the self-consistent code MAGY will be presented and compared with analytical data. These results will be used for estimating (a) parameters of the required electron gun and (b) tolerances on fabrication of the microwave circuit.

*This work is supported by the Office of Naval Research.

10:06

BO6 4 Single Mode Excitation in High Power Gyrotrons DMYTRO KASHYN, GREGORY NUSINOVICH, THOMAS ANTONSEN, *IREAP, University of Maryland* Megawatt-class, millimeter-wave gyrotrons are necessary for plasma heating and current drive in large-scale tokomaks and stellarators. These gyrotrons operate at very high-order modes with rather dense spectrum of eigenfrequencies. Therefore, when the voltage rises from zero to its nominal value, self-excitation conditions can be fulfilled for several modes. Analysis of gyrotrons start-up scenarios was performed by many authors. It was shown that in gyrotrons with diode-type electron guns the excitation of at least one parasitic mode is inevitable during the start up. We propose a method of eliminating this excitation. The method is based on usage of the diode-type electron guns where transition from the space-charge to temperature-limited emission takes place at higher voltages. As a result, in the regions where the self-excitation can be fulfilled for parasitic modes, the current density is lower than the required starting value. Results include analysis of beam current densities for different gun configurations as well as the dependence of starting currents on the beam voltage.

10:18

BO6 5 Properties and applications of mono-energetic gamma-rays from laser-Compton scattering FELICIE ALBERT, SCOTT ANDERSON, GERRY ANDERSON, SHAWN BETTS, DAVID GIBSON, CHRISTIAN HAGMANN, MICAH JOHNSON, MIKE MESSERLY, MIROSLAV SHVERDIN, FREDERIC HARTEMANN, CRAIG SIDERS, DENNIS McNABB, CHRISTOPHER BARTY, *Lawrence Livermore National Laboratory* Properties of a Mono-Energetic Gamma-Ray (MEGa-Ray) Compton scattering source are presented. It produces 0.1 MeV-0.9 MeV photons. Its experimental key parameters are: its size (0.01 mm^2), divergence (10x6 $mrad^2$), duration (ps), spectrum (15% bandwidth) and intensity (10^5 photons/shot), which yield an on-axis peak brightness of $\sim 10^{15}$ photons/mm^2/$mrad^2$/s/0.1% bandwidth at 0.478 MeV. We detected the 0.478 MeV nuclear resonance fluorescence (NRF) line of ^{7}Li. A LiH sample was in the beam path, and the NRF scattered photons were detected by a germanium detector oriented at 90° with respect to the incident beam axis. The resulting spectrum shows the 0.478 MeV line of ^{7}Li, with several characteristic lines from the interaction. With this experiment, we have shown that MEGa-Ray sources will provide a unique specific isotope detection capability. This work performed under the auspices of the U.S. Department of Energy by Lawrence Livermore National Laboratory under Contract DE-AC52-07NA27344.

10:30

BO6 6 MeV Mono-Energetic Gamma Ray Compton Scattering Source R&D* FRED HARTEMANN, *LLNL* FELICIE ALBERT, SCOTT ANDERSON, SAM CHU, RICK CROSS, CHRIS EBBERS, DAVID GIBSON, MIKE MESSERLY, VLAD SEMENOV, MIRO SHVERDIN, CRAIG SIDERS, DENNIS MCNABB, CHRIS BARTY, *LLNL* ARNOLD VLIEKS, SAMI TANTAWI, *SLAC* A precision, tunable gamma-ray source driven by a compact, high-gradient X-band linac is currently under development at LLNL. High-brightness, relativistic electron bunches produced by the linac interact with a Joule-class, 10 ps laser pulse to generate tunable γ-rays in the 0.5-2.5 MeV photon energy range via Compton scattering. The source will be used to excite nuclear resonance fluorescence lines in various isotopes; applications include homeland security, stockpile science and surveillance, nuclear fuel assay, and waste imaging and assay. The source design, key parameters, and current status are presented.

*This work performed under the auspices of the U.S. Department of Energy by Lawrence Livermore National Laboratory under Contract DE-AC52-07NA27344.

10:42

BO6 7 Compact Laser Technology for Compton Scattering Sources* M. SHVERDIN, F. ALBERT, S.G. ANDERSON, A. BAYRAMIAN, S.M. BETTS, C. EBBERS, D. GIBSON, M. MESSERLY, F.V. HARTEMANN, C.W. SIDERS, D.P. McNABB, C.P.J. BARTY, We describe compact laser technology for Mono-Energetic Gamma-Ray (MEGa-Ray) Compton scattering light source at LLNL. The high energy, 120W interaction laser utilizes chirped pulse amplification (CPA) in Nd:YAG to amplify a sub-nanometer bandwidth 20 μJ pulses from a fiber system to 1J. A novel pulse stretcher provides a dispersion of over 7000ps/nm to expand a several picosecond wide seed pulse to 6ns. After amplification, the pulse is recompressed to 10ps with a hyper-dispersive pulse compressor. We also describe a technique for over an order of magnitude increase in the generated gamma-ray flux by recirculation of the interaction laser pulse. This technique, termed Recirculation Injection by Nonlinear Gating (RING), consists of frequency doubling the incident laser pulse inside a dichroic mirror cavity. The resonator mirrors transmit at 1 ω and reflect at 2ω. The 2^{nd} harmonic of the incident pulse then becomes trapped inside the cavity. To date, we demonstrated 14 times cavity enhancement of 180mJ, 10ps, 532nm laser pulses.

*This work performed under the auspices of the U.S. Department of Energy by Lawrence Livermore National Laboratory under Contract DE-AC52-07NA27344.

10:54

BO6 8 Three-Dimensional Space-Charge Modeling of Intense Beams in a Circular Conducting Pipe* MARK HESS, CHONG SHIK PARK, *Indiana University Cyclotron Facility* We demonstrate a novel 3-D method for modeling the space-charge fields of intense beams in a circular conducting pipe. In this method, we can solve the electromagnetic space-charge fields using two time-dependent Green's functions. Since these Green's functions satisfy the Helmholtz wave equation, the method is completely free of numerical dispersion making this method an ideal alternative to the traditional FDTD methods which are typically used for fully electromagnetic simulations. In addition, we show how this method can be implemented numerically to compute the space-charge fields of intense beams undergoing non-trivial motion, such as breathing mode oscillations.

*This work is supported by the AFOSR under grant FA9550-08-1-0160.

11:06

BO6 9 Adiabatic thermal beam equilibrium in an alternating-gradient focusing channel* CHIPING CHEN, KSENIA SAMOKHVALOVA, *MIT* JING ZHOU, *Beam Power Technology* An adiabatic warm-fluid equilibrium theory for a thermal charged-particle beam in an alternating-gradient (AG) focusing field is presented. Warm-fluid equilibrium equations are solved in the paraxial approximation. The theory [K.R. Samokhvalova, J. Zhou and C. Chen, Phys. Plasmas **16**, 043115 (2009)] predicts that the

4D rms thermal emittance of the beam is conserved, but the 2D rms thermal emittances are not constant. The rms beam envelope equations and the self-consistent Poisson equation, governing the beam density and potential distributions, are derived. Although the presented rms beam envelope equations have the same form as the previously known rms beam envelope equations, the evolution of the rms emittances in the present theory is given by analytical expressions. The density does not have the simplest elliptical symmetry, but the constant-density contours are ellipses, and the aspect ratio of the elliptical constant-density contours decreases as the density decreases along the transverse displacement from the beam axis.

*Research supported by DOE Grant No. DE-FG02-95ER40919, and AFOSR Grant No. FA9550-06-1-0269.

11:18

BO6 10 Characterization of Plasmas in Negative Polarity Rod Pinch Diodes* MARK JOHNSTON, BRYAN OLIVER, JOSHUA LECKBEE, *Sandia National Laboratories* DALE WELCH, *Voss Scientific* DARRYL DROEMER, MARLON CRAIN, *National Security Technologies* Experiments at SNL are underway to investigate plasma formation in rod pinch diodes fielded in negative polarity on the RITS-6 accelerator (7.5MV and 180kA at 40 Ohms). The rod pinch diode consists of a small diameter metal rod which extends through a larger diameter metal cathode plate. Electrons formed at the cathode accelerate across the gap, become self-insulated, and are focused at the rod tip, generating x-rays used for flash radiography. Most of the previous rod pinch work has been performed in positive polarity; however, there is an interest in operating this diode in negative polarity at higher voltages, allowing more flexibility and incorporation into a wider variety of pulsed power devices. In an effort to better understand the basic physics, and the role ions play in the impedance behavior, a series of shots were taken looking at plasma formation in the diode. Diagnostics include optical imaging and spectroscopy using nanosecond gated ICCD cameras, streak cameras, and photodiode arrays. *Sandia is a multiprogram laboratory operated by Sandia Corporation, a Lockheed Martin Company, for the United States Department of Energy's National Nuclear Security Administration under contract DE-AC04-94AL85000.

11:30

BO6 11 Effects of external magnetic fields on the operation of rf accelerating structures* DIKTYS STRATAKIS, JUAN GALLARDO, ROBERT PALMER, *Brookhaven National Laboratory* Recent experiments on rf cavity breakdown have shown severe surface damage and a reduction of the maximum accelerating gradient when an external magnetic field is applied. This finding implies serious problems for cooling lattices in which rf cavities and external magnetic fields coexist, such as those of the proposed neutrino factory and muon collider. While existing data suggest that such operational problems were associated with the unwanted emission of electrons from locally enhanced field regions, the mechanism that drives the breakdown is poorly understood. We show that field-emitted electrons from one wall of a cavity are accelerated by the rf fields, and in the presence of a external magnetic field are focused into small spots at another location in the cavity where they heat the surface. We construct a simple model to analyze the dependence of wall temperature on emission current and external magnetic fields. We show that if the magnetic field strength is on the order of 1 T, the surface can suffer significant thermally-induced deformation that eventually limits the cavity's accelerating gradient. We compare the results from our model to existing experimental data from an 805-MHz cavity. Possible solutions and suggestions for future experiments to study those problems are offered.

*This work supported by the U.S. Department of Energy, contract no. DE-AC02-98CH10886.

11:42

BO6 12 Experimental Measurements of a High-Energy Pseudospark-Produced Electron Beam JING HU, JOSHUA L. ROVEY, *Missouri University of Science & Technology* SCOTT KOVALESKI, *University of Missouri-Columbia* AEROSPACE PLASMA LABORATORY TEAM, UNIVERSITY OF MISSOURI-COLUMBIA COLLABORATION, This paper presents the progress thus far in the investigation of pseudospark-produced electron beams for medical applications. A twenty-six-gap pseudospark device is fabricated with different insulators and tested as the electron beam source. The discharge capacitor between the anode and cathode to store electrical energy is incorporated into the stacked ring design to minimize inductance. The system is operated at 100kV. Two Rogowski coils are positioned in the hole of anode flange and external capacitors to measure the total beam and discharge currents. Further, a small Langmuir probe and a Faraday cup are used to determine the energy of the beam through the comparison of the time that the e-beam passes them. Results of the scaling study for the electron beam current with breakdown voltage, gas pressure, external capacitance, and the effect of insulator material on pseudospark operating characteristics are presented.

11:54

BO6 13 Numerical studies of multipactor in dielectric-loaded accelerator structures* OLEKSANDR SINITSYN, GREGORY NUSINOVICH, THOMAS ANTONSEN, *IREAP, University of Maryland* Multipactor (MP) is known as the avalanche growth of the number of secondary electrons emitted from a solid surface exposed to an rf electric field under vacuum conditions. MP may occur in various microwave and rf systems such as microwave tubes, rf windows and launchers, accelerating structures, and rf satellite payloads. In this work we present results of MP analysis in dielectric-loaded accelerator (DLA) structures. The starting point of our work was experimental and theoretical studies of DLA structures jointly done by Argonne National Laboratory and Naval Research Laboratory (J. G. Power et al., Phys. Rev. Lett. 92, 164801 (2004); J. G. Power et al., AIP Conf. Proc. 877, 362 (2006)). In the theoretical model developed during those studies the space-charge field due to the total number of particles is taken into account as a parameter. We perform our studies using a self-consistent approach with the help of time-dependent two-dimensional code developed at the University of Maryland (O. V. Sinitsyn et al., Phys. Plasmas 16, 073102 (2009)). Results include analysis of MP evolution at an early stage, detailed studies of individual electron trajectories, analysis of MP onset time under various conditions and comparison of some results with the experimental data.

*This work was supported by the Office of High Energy Physics of the U. S. Department of Energy.

12:06
BO6 14 Lithium alumino-silicate ion source development* PRABIR KUMAR ROY, PETER A. SEIDL, JOE W. KWAN, WAYNE G. GREENWAY, WILLIAM L. WALDRON, JAMES K. WU, KAVOUS MAZAHERI, *Lawrence Berkeley National laboratory* HIFS-VNL COLLABORATION, We report experimental progress on Li+ source development in preparation for warm dense matter heating experiments. To uniformly heat targets to electron-volt temperatures for the study of warm dense matter, we are pursuing the use of a low (E < 5 MeV) kinetic energy singly ionized lithium beam and a thin target. Two kinds of lithium (Li+) alumino-silicate ion sources, β-spodumene and β-eucryptite, each of area 0.31 cm2, have been fabricated for ion emission measurements. These surface ionization sources are heated to 1200 to 1300[r]C where they preferentially emit singly ionized alkali ions. Tight process controls were necessary in preparing and sintering the alumino-silicate to the porous tungsten substrate to produce an emitter that gives uniform ion emission, sufficient current density and low beam emittance. Current density limit of the two kinds have been measured, and ion species identification of possible contaminants has been verified with a Wien (E x B) filter.

*This work was supported by the Director, Office of Science, Office of Fusion Energy Sciences, of the U.S. Department of Energy under Contract No. DE-AC02-05CH11231.

SESSION BP8: POSTER SESSION I
Monday Morning, 2 November 2009
Grand Hall East at 9:30

BP8 1 PLASMA SOURCES AND BOUNDARIES

BP8 2 Modeling of tungsten surfaces bombardement with helium ions MARTIN NIETO, GONZALO RAMOS, *Instituto Politecnico Nacional* Tungsten is regarded as one of the top choices for the construction of plasma facing components (PFCs) in fusion reactors. As such, a good understanding of its behavior under plasma bombardment is needed. For the case of helium bombardment, the experimental evidence points to the formation of a very low density metal layer a few microns thick. In this work, Monte Carlo simulations of tungsten surfaces bombarded with helium ions is presented. The results of the simulations including ballistic effects only are contrasted against experimental observation, which may help determine, in a qualitative way, the importance of diffusive mechanisms in the formation of these structures.

BP8 3 Instability-Enhanced Collisional Friction Determines the Bohm Criterion in Multiple-Ion-Species Plasmas* S.D. BAALRUD, C.C. HEGNA, J.D. CALLEN, *Department of Engineering Physics, University of Wisconsin-Madison* Ion-ion streaming instabilities are excited in the presheath region of plasmas with multiple ion species if the ions are much colder than the electrons. Streaming instabilities onset when the relative fluid flow between ion species exceeds a critical speed, ΔV_c, of order the ion thermal speeds. Using a generalized Lenard-Balescu theory that accounts for instability-enhanced collective responses [1], one is able to show the instabilities rapidly enhance the collisional friction between ion species far beyond the contribution from Coulomb collisions alone. This strong frictional force determines the relative fluid speed between species. When this condition is combined with the Bohm criterion generalized for multiple ion species, the fluid speed of each ion species is determined at the sheath edge. For each species, this speed differs from the common "system" sound speed by a factor that depends on the species concentrations, masses and ΔV_c. [1] S.D. Baalrud, J.D. Callen, and C.C. Hegna, Phys. Plasmas **15**, 092111 (2008).

*This material is based upon work supported under a National Science Foundation Graduate Research Fellowship (S.D.B) and by U.S. Department of Energy Grant No. DE-FG02-86ER53218.

BP8 4 Dynamical Response of Continuum Regime Langmuir Probe H.L. RAPPAPORT, *Enig Associates, Inc.* Probe dynamic response is sometimes used as a way to increase the amount of information obtained from Langmuir probes [1]. In this poster, the effects of frequency dependent probe capacitance and coupling of probe fields to damped Langmuir waves and damped ion acoustic waves are considered. In the continuum regime, with small Debye length to spherical probe radius ratio, the probe DC current vs. voltage characteristic displays a hard saturation at sufficiently large probe potential [2]. In this regime, the sheath thickness varies little with the applied voltage although the plasma response can still be measured. A goal of the present investigation is to show that the probe dynamical response is richer as a result of modulation of sheath thickness or shielding particularly in the larger Debye length to probe radius ratio regime. Inertia inhibits ion response at sufficiently high frequency and deviation from the DC characteristic is shown. [1] D. N. Walker, R.F. Fernsler, D.D. Blackwell, and W.E. Amatucci, Phys. Plasmas 15, 123506 (2008). [2] E. Baum and R.L. Chapkis, AIAA J. 8, 1073 (1970).

BP8 5 Effect of ionization on a collisionless magnetized plasma near a wall* JÉRÔME GUTERL, NATALIA KRASHENINNIKOVA, VADIM ROYTERSHTEYN, XIANZHU TANG, *LANL* Plasma-wall interactions play a key role in controlled thermonuclear fusion experiments. Wall recycling produces a stream of neutrals which are ionized in the plasma. The ionization of slow neutrals near the wall can significantly affect the sheath and presheath of a magnetized plasma. This was considered previously using analytic models [1,2] for a plasma in which the system size is greater than the neutral ionization length but smaller than the Coulomb collision mean free path. The presence of this ionization source can alter electric field near the surface and affect sheath structure as well as background plasma and ionized particle flow to the wall. Here we present results of PIC simulation for such a simplified boundary plasma model with magnetic field normal to the wall. Employing the state-of-the-art VPIC[3] code, we consider 1D magnetized collisionless plasma. The ionization is modeled as a source which produces thermalized electrons and thermal ions. We examine the effects of source parameters, such as shape, intensity and spatial position on the sheath structure and plasma parameters near the wall. [1] S. Krasheninnikov et al. Contrib. Plasma Phys. 34, 210 (1994). [2] A. Bailey et al. Nucl. Fusion 24, 1439 (1984). [3] K. Bowers, et al., Phys. Plasmas 15, 055703 (2008).

*Work supported by OFES and LANL LDRD.

BP8 6 Plasma sheath dynamics for high-temperature low-density plasmas* XIANZHU TANG, NATALIA KRASHENINNIKOVA, VADIM ROYTERSHTEYN, *LANL* With an absorbing material wall, the plasma is thought to be able to access a state of high temperature but low density. This can lead to an interesting edge condition for magnetically confined plasmas and possibly new confinement regimes. The implication for tokamak plasmas has been recognized in recent years. The earlier concept of tandem mirrors depends on essentially the same physics for accessing high electron temperature. As a first step to understand such a plasma, we revisit the classical unmagnetized plasma sheath using a kinetic approach. Although kinetic simulation using VPIC [1] gives a full account of the physical processes, an emphasis of our approach is on how to interpret the unexpected plasma behavior from kinetic simulations (compared with conventional electrostatic sheath theory) using the fluid-moment formulation. [1] K. Bowers, et al., Phys. Plasmas 15, 055703 (2008).

*Work supported by OFES and LANL LDRD.

BP8 7 Are there internal sheaths in unmagnetized electronegative plasmas?* CHI-SHUNG YIP, NOAH HERSHKOWITZ, *University of Wisconsin - Madison* Bounded electronegative plasmas are predicted to have electropositive halos. A recent experiment [1] showed that for a negative ion to electron concentration ratio of $\alpha = 0.43$ for an Argon-Oxygen plasma, a positive halo was formed as a consequence of negative ions satisfying a Boltzmann relation. When $T_e/T_- > 5 + \sqrt{24}$ [2] and $\alpha > T_e/T_-$ [3], the negative ions are predicted to be confined by an internal sheath. Experiments are reported in $Ar - SF_6$ and $Ar - Cl_2$ plasmas aimed at finding the internal sheath by varying the gas concentrations. Experiments are carried out in a hot filament discharge in a multi-dipole chamber. Negative ions concentrations are determined from the phase velocity of C.W. Ion Acoustic Waves. Electron temperature and density are determined using Langmuir probes. Plasma potentials are determined by emissive probes. Argon drift velocities are determined by Laser Induced Flourescence. [1] Ghim, YC and Herskowitz, N, Applied Physics Letters. **94**, 15, 151503 (2009) [2] N. Braithwaite and J.E.Allen, J. Physics. D: Appl. Phys **21**, 1733 (1988) [3] R. N. Franklin, Plasma Sources Sci. Technol. **11**, A31, (2002)

*Work supported by the DoE grant no. DE-FG02-97ER54437.

BP8 8 Hot-filament discharge plasma in argon gas at 140 K* SHANNON DICKSON, SCOTT ROBERTSON, *University of Colorado* A hot-filament discharge plasma has been created in a double-walled vacuum chamber with the inner wall cooled by liquid nitrogen vapor. The inner brass chamber (16 cm dia. x 30 cm) is wound with copper tubing for cooling. This chamber has two tungsten filaments 10 cm in length oriented axially about 2.5 cm from the wall. Plasma measurements are made using a Pt wire probe. At 300 K, 0.6 mTorr argon in the outer chamber, and 2 mA emission, the electron density is 1 x10^8 cm^{-3} and the electron temperature is 0.054 eV. At 140 K, the density is 1.6 x10^8 cm^{-3} and their temperature is 0.11 eV confirming that the electrons are not cooled by elastic collisions with the gas. The floating potential of the probe is -2.4 V at 300 K and -0.6 V at 140 K as a consequence of the ion current to the probe being about doubled at the lower temperature. The higher ion current may be a consequence of charge-exchange collisions producing cold ions that are more easily captured by the probe. These collisions decrease the ion losses to the wall by slowing ions accelerated by the plasma potential. Electron losses are reduced because of the requirement of quasineutrality, thus reduced evaporative cooling of electrons may be the cause of the increased electron temperature in 140 K gas.

*Supported by DoE through the Plasma Science Intiative.

BP8 9 Waves, Currents, Drifts and Plasma Confinement Time in a Low Temperature, Pulsed, Toroidal, ECR Plasma MICHAEL LINDON, *West Virginia University* ARVIND THAKUR, P.K. SHARMA, K. SATYANARAYAN, P.R. PARMAR, CHETAN VIRANI, *Institute of Plasma Research* EARL SCIME, SAIED HOUSHMYANDAR, *West Virginia University* WEST VIRGINIA UNIVERSITY TEAM, INSTITUTE OF PLASMA RESEARCH TEAM, Typically the plasma in purely toroidal field experimental systems is created by a filament source or, in some cases, a helicon plasma source. Here we present measurements of plasma density, electron temperature, flow and confinement time for an electron cyclotron resonance (ECR) created plasma in a purely toroidal field at the Institute of Plasma Research (IPR) in India. A linear array of Langmuir probes was used to measure the density and temperature in a horizontal plane of the torus and a pair or probes is used to measure the vertical electric field arising from charge separation. Mach probes were used to measure bulk plasma flows in the same plane. Through measurements of the decay rate of the plasma density after the 2.45 GHz ECR microwave source turns off, the plasma confinement time as a function of initial toroidal magnetic field strength and fill pressure was investigated. This work was supported by the American Physical Society and the Indo-U.S. Science and Technology Forum (IUSSTF) through the India-U.S. Physics Visitation Program.

BP8 10 Laser Initiated, RF Sustained Air Plasmas* JOHN SCHARER, RYAN GIAR, JASON HUMMELT, JESSE WAY, *University of Wisconsin - Madison* Measurements and analysis of air breakdown processes by focusing 193 nm, 260 mJ, 10 MW high power UV laser radiation to 18 cm and 1.3 cm zones are examined. Quantum resonant multi-photon (REMPI) and collisional cascade ionization processes affect the breakdown and plasma formation. Our spectroscopic measurements show that REMPI (2+1) processes on nitrogen play a substantial role at lower pressures due to the high photon energy (6.4 eV). The REMPI process yields high density air plasmas (5 x 10^{16}/cc) for the 18 cm focus with the laser flux three orders of magnitude below the classical breakdown threshold intensity. Measurements of the f = 1.3 cm core laser plasma density (8x10^{17}/cc) and electron temperature decay via two color laser interferometry are made. The 18 cm focal length lens and its ionizing shock wave front are utilized to produce air seed plasma to initiate a large volume (500 cc) RF sustainment discharge coupled by means of a 6 cm diameter helical coil at up to 10 kW power levels.

*Research supported by AFOSR Grant No. FA9550-09-1-0357.

BP8 11 Low Pressure Discharge Initiation and LIF Diagnostic in a High Power Argon Helicon Plasma* MATT WIEBOLD, JOHN SCHARER, HE REN, *University of Wisconsin - Madison* A flowing argon helicon plasma is formed in a 10 cm diameter, 1.5 m long Pyrex chamber with a peaked axial magnetic field, variable up to 1 kG. Upgrades have allowed for operation at high, pulsed RF powers (up to 10 kW at 13.56 MHz) and low flow rates and pressures (as low as 1 sccm, 10^{-5} Torr). Neutral-collisional

plasma exists upstream of the half-turn, double helix antenna and neutral-collisionless plasma exists downstream, leading to bulk plasma acceleration due to reduced neutral drag. Microwave interferometry (105 GHz) and collisional radiative spectroscopic codes are used to measure electron density and temperature. An initial transient high-density peak ($> 10^{14}$/cc) is seen observed followed a neutrally depleted steady state plasma ($> 10^{12}$/cc). Neutral depletion is observed along with substantial plasma acceleration. Initial LIF results using a new MOPA system are reported. A static magnetic field threshold for discharge initiation is seen at low flow rates. Evidence is given that this is a consequence of the magnetic field quenching a multipactor discharge, which is the dominant mechanism for breakdown at low flow rates and pressures. A magnetic field ramping technique for starting discharges under these conditions is described.

*Research supported by AFOSR Grant No. FA9550-09-1-0357.

BP8 12 Hollow cathode plasma electron source for beam generation* C.D. COTHRAN, *Global Strategies Group (North America)* S.G. WALTON, R.F. FERNSLER, W.E. AMATUCCI, *Plasma Physics Division, U.S. Naval Research Laboratory* The characteristics of an electron beam produced by extracting electrons from a hollow cathode plasma is described. The anode to cathode surface area ratio is less than the root of the electron to ion (Argon) mass ratio such that an electron sheath forms at the anode; a bias on this anode then accelerates the electron flux into a beam. A magnetic field assists the beam collimation. Paschen breakdown in the few Torr range at 500V initiates the hollow cathode plasma, and typical continuous operation is at 130mTorr with about 300V required to sustain the plasma at 60mA. Variation of the hollow cathode current allows direct control of the beam current. Continuous beam at up to 5kV and 80mA has been produced with this device.

*Work supported by the Office of Naval Research.

BP8 13 Investigation of the Surface Wave Plasma on Cylindrical Dielectric Waveguide* RONGQING LIANG, QIONGRONG OU, XIJIANG CHANG, SHUYU ZHANG, LONG HE, ZEBING LI, *Fudan University* DEPARTMENT OF LIGHT SOURCES AND ILLUMINATING ENGINEERING TEAM, The surface wave plasma (SWP) generated by a cylindrical Teflon rod has been developed in our laboratory. A Teflon rod, diameter of 4cm, is adopted to be as waveguide in our experiment. The Microwave frequency is 2.45GHz, and the power is adjustable from about 100W to 800W. The pressure of working gas Argon is set around 20 Pascal. When microwave power is coupled into the cylindrical Teflon rod in a vacuum chamber, a surface wave will be conveyed along the surface of the Teflon rod in axial direction. Plasma could be excited by the electric field of surface wave. Plasma density is proportional with the input microwave power. With increasing density, plasma permittivity will decrease. The variable permittivity of plasma could result in the change of the transmitting mode of surface wave along the Teflon waveguide surrounded by the plasma. The correlative phenomena in our experiment were experimentally observed through the visible light pattern of SWP, and the involved mechanism is theoretically analyzed.

*Supported by NNSF of China, No. 10775034.

BP8 14 Plasmonic focusing and collimating of light beyond the conventional diffraction limit* KUAN-REN CHEN, *National Cheng Kung University* Diffraction sets the smallest achievable product of the line width and the divergence angle of a propagating light. While we still obey the fundamental wave concept, herein we demonstrate that by utilizing a new setup of a metallic subwavelength aperture as the plasmonic lens to preserve, generate and squeeze the sub-limit wave functions an incident light can be focused in the intermediate zone to a single-line width with its value smaller than the conventional diffraction limit of half the wavelength. The fields focused by the plasma effects on the structured lens with the focusing aperture beyond (FAB) the limit are verified to be radiative as of concern and in contrast to the evanescent near-field. With a different structure and plasmonic mechanism, our FDTD simulation has yielded super-collimated light beams with almost zero divergence angles in 2-D free space, as verified by our experimental NSOM measurement. Additionally, we have built an exposure machine; the widths of the exposed patterns at different distances remain almost same and thus verify the super-collimation. The light focusing and collimating processes of the FAB lens, besides being of academic interest, is expected to open up a wide range of application possibilities.

*This work was supported by NCKU Project of Promoting Academic Excellence & Developing World Class Research Centers.

BP8 15 Low Ion-Velocity Slowing Down in a Strongly Magnetized Plasma Target CLAUDE DEUTSCH, ROMAIN POPOFF, *LPGP UParis XI Orsay* LIVSD COLLABORATION, Ion projectile stopping at velocities smaller than target electron thermal velocity in a strong magnetic field is investigated within a novel diffusion formalism, based on Green- Kubo integrands evaluated in magnetized one-component-plasma models, respectively framed on target ions and electrons. Analytic expressions are reported for slowing down parallel and orthogonal to an an arbitrary large and steady magnetic field, which are free from usual uncertainties plaguing the standard binary collision/dielectric derivations. Magnetic and temperature dependences of the low velocity slowing down are thoroughly detailed for dense plasmas of fast ignition concern and ultracold plasmas envisioned for ion beam cooling, as well.

BP8 16 GYROKINETICS AND TURBULENCE

BP8 17 A Quarter-Century Later: Nonlinear Gyrokinetics Under Attack* J.A. KROMMES, *Princeton University* The nonlinear gyrokinetic equation (GKE) was first derived about a quarter-century ago. Subsequent technical developments have refined the GKE into a major tool for the description of both fusion and astrophysical plasmas. However, the GKE has suffered serious attacks on its veracity, two of which will be discussed: the possibilities that (i) the asymptotic expansion for the GK variables breaks down for torsional or stochastic magnetic fields[1]; (ii) conventional gyrokinetics is insufficiently accurate to determine the long-wavelength, axisymmetric part of the radial electric field.[2] The relevant physical pictures and detailed mathematics will be pdescribed for both sides of each issue. For (i), local and global coordinate systems must be distinguished; for (ii), the use of Lagrangian field theory is advocated.

*Work supported by U.S.D.o.E. Contract No. DE-AC02-09CH11466.

[1]L. E. Sugiyama, Guiding center plasma models in three dimensions, Phys. Plasmas **15**, 092112 (2008); J. A. Krommes, Comments on "Guiding center plasma models..." [Phys. Plasmas **15**, 092112 (2008)], Phys. Plasmas (2009, submitted); L. E. Sugiyama, Response to Comments of J. A. Krommes, Phys. Plasmas (2009, submitted).F. I. Parra and P. J. Catto, Limitations of gyrokinetics on transport time scales, Plasma Phys. Control. Fusion **50**, 065014 (2008).
[2]E. Sugiyama, Response to Comments of J. A. Krommes, Phys. Plasmas (2009, submitted).F. I. Parra and P. J. Catto, Limitations of gyrokinetics on transport time scales, Plasma Phys. Control. Fusion **50**, 065014 (2008).

BP8 18 Turbulence-Driven Magnetic Reconnection* WILLIAM NEVINS, ERIC WANG, ILON JOSEPH, *LLNL* JEFF CANDY, *GA* SCOTT PARKER, YANG CHEN, *U of CO* GREG REWOLDT, *PPPL* Data from finite-beta gyrokinetic simulations of ion temperature gradient turbulence show localized modifications to the magnetic shear in the neighborhood of low order rational surfaces. We analyze this data with the object of determining if these modifications result from magnetic reconnection. When magnetic reconnection occurs, we employ Poincaré surface-of-section plots to determine the degree to which the reconnection results in island formation or generalized magnetic stochasticity.

*This work performed under the auspices of the U.S. Department of Energy by Lawrence Livermore National Laboratory under Contract DE-AC52-07NA27344.

BP8 19 Properties of Multiscale Finite-Beta Gyrokinetic Plasmas W.W. LEE, E.A. STARTSEV, R.A. KOLESNIKOV, *Princeton Plasma Physics Laboratory* The numerical issues arise from the finite-β gyrokinetic Maxwell equation of the form, $[\nabla_\perp^2 - \beta m_i/m_e - \beta](\partial\psi/\partial t) = -\beta(\hat{\mathbf{b}}_0 \cdot \nabla)\int v_\parallel^3(\delta g_i - \delta g_e)dv_\parallel + (\hat{\mathbf{b}}_0 \cdot \nabla)\int v_\parallel(\delta g_i - \delta g_e)dv_\parallel + \beta\nabla\psi \times \hat{\mathbf{b}}_0 \cdot [(m_i/m_e)(\kappa_n + \kappa_{Te}) - (\kappa_n + \kappa_{Ti})/\tau)]$ will be discussed. The equation is the result of a new simulation scheme which separates out the fast particle response due to quasi-static bending of magnetic field lines by letting $\delta g = =F - (1 + \psi)F_0 - \int dx_\parallel \kappa \cdot \delta\mathbf{B}$, so that a new full density and/or temperature gradient, which is set up by the fast particles, is transverse to the direction of the full field, background plus perturbation, where $\hat{\mathbf{b}} = \hat{\mathbf{b}}_0 + \delta\mathbf{B}/B_0$, $\delta\mathbf{B} = \nabla A_\parallel \times \hat{\mathbf{b}}_0$, $\psi = \phi + \int(\partial A_\parallel/\partial t)dx_\parallel/c$, ϕ and $A_\parallel$ are the perturbed potentials, and κ represents the zeroth-order inhomogeneities. For $\beta m_i/m_e$ $(\equiv \rho_s^2/\delta_e^2) \gg 1$, it is found that, we need to use a computational grid based on the electron skin depth δ_e, which can be an order smaller than ρ_s, the length of interest, in agreement with the analytical perturbative methods in solving this type of singular equations. The adequacy of the above equation for the perturbations of the order of $k \sim \kappa$, [1] where k is the perturbed wavenumber, will also be presented along with their conservation properties. The issue of transition from δf to *total-F* in finite-β PIC simulations in general geometry, based on the particle weights, will also be discussed. [1]W. W. Lee and R. Kolesnikov, Phys. Plasmas **16**, 04506 (2009).

BP8 20 Linearized Model Collision Operators for Multiple Ion Species Plasmas HIDEO SUGAMA, TOMOHIKO WATANABE, MASANORI NUNAMI, *National Institute for Fusion Science* Linearized model collision operators for multiple ion species plasmas are presented, which conserve paricles, momentum, and enery, and satisfy adjointness relations and Boltzmann's H-theorem even for collisions between different particle species with unequal temperatures. The model collision operators are also written in the gyrophase-averaged form that can be applied to the gyrokinetic equation. Balance equations for the turbulent entropy density, the energy of electromagnetic fluctuations, the turbulent transport fluxes of particle and heat, and the collisional dissipation are derived from the gyrokinetic equation including the collision term and the Maxwell equations. It is shown that, in the steady turbulence, part of the heat generated by the turbulent transport fluxes produced in the unstable nonzonal-mode region is nonlinearly transferred into the stable zonal-mode region where the collisional dissipation occurs.

BP8 21 Proposal of a brand-new gyrokinetic algorithm for global MHD simulation* HIROSHI NAITOU, KENICHI KOBAYASHI, HIROKI HASHIMOTO, TAKEHISA ANDACHI, *Yamaguchi U.* WEI-LI LEE, *PPPL* SHINJI TOKUDA, *JAEA* MASATOSHI YAGI, *Kyushu U.* A new algorithm for the gyrokinetic PIC code is proposed. The basic equations are energy conserving and composed of (1) the gyrokinetic Vlasov (GKV) equation, (2) the Vortex equation, and (3) the generalized Ohm's law along the magnetic field. Equation (2) is used to advance electrostatic potential in time. Equation (3) is used to advance longitudinal component of vector potential in time as well as estimating longitudinal induced electric field to accelerate charged particles. The particle information is used to estimate pressure terms in equation (3). The idea was obtained in the process of reviewing the split-weight-scheme formalism. This algorithm was incorporated in the Gpic-MHD code. Preliminary results for the m=1/n=1 internal kink mode simulation in the cylindrical geometry indicate good energy conservation, quite low noise due to particle discreteness, and applicability to larger spatial scale and higher beta regimes. The advantage of new Gpic-MHD is that the lower order moments of the GKV equation are estimated by the moment equation while the particle information is used to evaluate the second order moment.

*Supported by the Grand-in-Aid for Scientific Research of MEXT.

BP8 22 Radial Propagation in the ITG CYCLONE Base Case* ERIC WANG, WILLIAM NEVINS, *Lawrence Livermore National Labs* Analysis of the ITG CYCLONE benchmark [A.M. Dimits et al, Phys. Plasmas 7, 969 (2000)] in the past focused on the characteristics of plasma microturbulence located at the outboard midplane ($\theta = 0$). The outboard midplane is chosen because this is the region of the tokamak that produces the most violent instabilities, while the third spatial is ignored because plasma microturbulence in tokamaks is anisotropic, with short spatial variations perpendicular to the magnetic field and long variations parallel. In the present work we revisit the CYCLONE base case using the nonlinear gyrokinetic microturbulence code GYRO[J. Candy and R.E. Waltz, J. of Comp. Phys., Volume 186, Issue 2, 10 April 2003], observing steady state turbulence in all three spatial dimensions plus time. Unexpectedly, the perturbed quantities (electrostatic potential, density, and temperature) all exhibit radial propagation inwards for spatial positions above the outboard midplane ($\theta < 0$) and outwards below the outboard midplane ($\theta > 0$). The characteristics of this propagation are presented in detail, along with a model for the cause of these structures.

*Prepared by LLNL under Contract DE-AC52-07NA27344.

BP8 23 Comparisons of Positivity Preserving Advection Algorithms for Edge Plasma Turbulence Simulations* G.W. HAMMETT, J.L. PETERSON, *Princeton Plasma Physics Laboratory* The steep density and temperature gradients associated with the edge and scrape off layer regions of a fusion plasma complicate the numerical simulation of plasma turbulence. Spectral methods and Arakawa finite differencing have the interesting property of exactly preserving certain conservation properties of Hamiltonian systems and work well for simulating well-resolved, small amplitude fluctuations. However, such algorithms can exhibit Gibbs phenomena, small overshoots in the vicinity of large gradients. While these overshoots are unimportant for small amplitude turbulence in the core region of tokamaks, these algorithms can lead to regions of negative density or temperature in the tokamak edge. Several finite volume methods of solving multi-dimensional hyperbolic equations can be constructed to prevent such negative solutions, and can be useful for both gyrokinetic and gyrofluid continuum simulations. We explore here different algorithms for positivity-preservation and their effects on efficiency. When combined with Strong Stability Preserving time-integration techniques, unphysical negative solutions can simply and quickly be eliminated.

*Supported at PPPL by USDOE contract DE-AC02-09CH11466.

BP8 24 Absolute equilibria of gyrokinetic fluctuations* JIANZHOU ZHU,† *University of Maryland* GREGORY HAMMETT, *Princeton Plasma Physics Laboratory* A paradigm based on the absolute equilibria of Fourier-truncated inviscid systems [R. H. Kraichnan and D. Montgomery, Rep. Prog. Phys. 43, 547 (1980)] to understand turbulence is applied to study gyrokinetic plasma turbulence. This approach has been successful in understanding fundamental issues of fluid turbulence, and provides useful benchmarks for analytical theories and numerical simulations. The existence of 2 conserved quantities (energy and enstrophy) in 2-D fluids gives rise to interesting features in the equilibrium spectrum, related to the existence of inverse cascade. We have derived the class of absolute equilibria for gyrokinetic fluctuations in 2 spatial dimensions and 1 (perpendicular) velocity dimension, including finite Larmor effects with the full Bessel functions in this framework. A range of spectra types are calculated with different parameters. Extensions to absolute equilibria in fully 5-D gyrokinetics are being explored. The implication of these results for ITG and ETG plasma turbulence will also be discussed.

*Supported by the Center for Multiscale Plasma Dynamics through DOE Grant DE-FC02-04ER54784
†also at Princeton Plasma Physics Laboratory

BP8 25 Characteristics of nonlinear interaction in entropy cascade* T. TATSUNO, G.G. PLUNK, W. DORLAND, *U Maryland* A.A. SCHEKOCHIHIN, *U Oxford* Two-dimensional electrostatic turbulence in weakly-collisional magnetized plasmas can be described as a turbulent cascade of entropy in phase space [1]. Nonlinear phase mixing [2] introduces small structures of distribution function in both position and velocity space. By invoking the Kolmogorov-type phenomenology applied in the phase space, it is argued that entropy cascades to smaller scales as energy or enstrophy does in the Navier-Stokes turbulence. In this presentation, we report the detailed characteristics of nonlinear interaction in the gyrokinetic turbulence. We diagnose the triad interaction in the wave-number as well as in the velocity dual space using the AstroGK code [3], and see how quantitatively the theoretical assumptions are satisfied, namely, (a) the scale locality of nonlinear intercation, and (b) constancy of entropy flux both in position and in velocity space. [1] T. Tatsuno *et al.*, Phys. Rev. Lett. **103**, 015003 (2009). [2] W. Dorland and G. Hammett, Phys. Fluids B **5**, 812 (1993). [3] http://www.physics.uiowa.edu/ghowes/astrogk/

*This work is supported by Maryland Fusion Theory Program.

BP8 26 Rotation dynamics with & without Internal Transport Barriers GUILHEM DIF-PRADALIER, PATRICK H. DIAMOND, *Center for Astrophysics and Space Sciences, UCSD, La Jolla, CA 92093, USA* C.S. CHANG, S. KU, *Courant Institute of Mathematical Sciences, New York University, NY 10012, USA* Y. SARAZIN, V. GRANDGIRARD, J. ABITEBOUL, X. GARBET, PH. GHENDRIH, A. STRUGAREK, *Association Euratom-CEA, CEA/IRFM, F-13108 St. Paul-lez-Durance cedex, France* We investigate the dynamics of both poloidal and toroidal flows in the presence (or absence) of a reversed safety factor profile through a scan in the incoming heat power applied to the plasma. Doing so, it incidentally also addresses the question of a power threshold for a self-consistent ITB formation in gyrokinetic modeling. As a prime candidate to drive the system away from its neoclassical prediction, we recently showed evidence of turbulence-generated poloidal rotation, consistently with earlier theories. Accurate calculation of the radial electric field is central. Accordingly, description of the mean profile dynamics, as done in *full–f* flux-driven models is shown to take on a very prominent role. The study is performed using both the scGysela and scXgc–1 gyrokinetic codes with Enhanced Reverse Shear (ERS)-like parameters.

BP8 27 Free Boundary Magnetohydrodynamic Equilibria with Flow* RONALD SCHMITT, GUNYOUNG PARK, CHOONGSEOCK CHANG, *New York University* LUCA GUAZZOTTO, *University of Rochester* HENRY STRAUSS, ELIEZER HAMEIRI, HAROLD WEITZNER, *New York University* Equilibria with flow are known to exhibit characteristics different from static equilibria. In particular, plasma rotation often reduces turbulent transport, as exhibited by H-mode confinement state observed in tokamaks. The equations that govern MHD equilibrium with flow are the generalized Grad-Shafranov equation and the magnetic Bernoulli equation. The finite element, free boundary equilibrium solver in the M3D code has been modified to included arbitrary toroidal and poloidal flows. The M3D+FLOW code differs from other codes in that, being a free boundary code, it includes the separatrix and the region outside the separatrix. Results for M3D+FLOW are presented for both subsonic and transonic flows. Application to data from the XGC gyrokinetic code is also presented.

*This research was supported in part by the Fusion Energy Sciences Postdoctoral Research Program of the U.S. Department of Energy administered by the Oak Ridge Institute for Science and Education (ORISE).

BP8 28 Integrated Edge-core multiscale simulation of Full-f ITG-turbulence in realistic tokamak geometry* SEUNG-HOE KU, *New York University, Courant Institute Mathematical Sciences* C.S. CHANG,† *KAIST* P.H. DIAMOND, *UCSD* CPES TEAM,‡ We report "the-tail-wagging-the-dog" phenomenon observed from the full-f XGC1 simulation of the whole-volume ITG turbulence in realistic tokamak geometry. In H-mode experiments, the core energy confinement is promptly enhanced with steepening

of the edge gradient under a strong core heating in diverted magnetic field geometry. The full-f XGC1 simulation studies the dynamical neoclassical and turbulence interaction without scale-separation. It is found that edge turbulence is nonlocally connected to the core through spatial energy propagation, modifying the core turbulence and driving a SOC. Strong core heating and self-organized ExB shear play important roles in this process. Detailed physics mechanisms and experimental implications will be discussed.

*Work supported by US DOE Office of Fusion Energy Science and Office of Advanced Scientific Computing Research.
†also New York University, Courant Institute
‡SciDAC FSP Prototype Center for Plasma Edge Simulation

BP8 29 Finite β Effects on TEM Turbulence* D.R. ERNST, *Mass. Inst. of Technology* J. LANG, *PPPL* W.M. NEVINS, *LLNL* P.N. GUZDAR, *Univ. Maryland* J. CANDY, R.E. WALTZ, *General Atomics* This work explores the β dependence of trapped electron mode turbulence and associated electron thermal energy and particle transport, using the GS2 (continuum), GEM (particle), and GYRO (continuum) codes. Leadership class computing facilities enable us to extend to shorter wavelengths that contribute significantly to electron thermal transport, which can increase with β in ITG dominated cases.[1] Analytic work on zonal flow modulational instabilities with finite β suggests interesting and non-monotonic β dependence, arising from competition between drift wave and drift-Alfvén wave pumps.[2] Finally, our previous TEM zonal flow studies[3] found that convergence was poor for $\eta_e > 3$, despite including wavenumbers $k_\alpha \rho_s \leqslant 4$. Additional physics, such as electromagnetic effects, could potentially resolve this.

*Supported by U.S. Dept. of Energy DE-FG02-91ER-54109, DE-FC02-99ER54966, and other DoE grants.

[1]J. Candy, Phys. Plasmas **12**, 072307 (2005). See posters by R. Waltz and W. Nevins, this conference.
[2]P. N. Guzdar *et al.*, Phys. Plasmas 8(9) 3907 (2001).
[3]D. R. Ernst, J. Lang, W. M. Nevins *et al.*, Phys. Plasmas 16, 055906 (2009).

BP8 30 Gyrokinetic study of the spatial entropy dynamics in turbulent plasmas with zonal flow KENJI IMADERA, YASUAKI KISHIMOTO, JIQUAN LI, *Kyoto University* TAKAYUKI UTSUMI, *Tokyo University of Science, Yamaguchi* We have developed a new computational algorithm based on the IDO-CF (Conservative Form of Interpolated Differential Operator) scheme [1], which is efficient in capturing sharp domain structure in long time scale, for solving full-f Gyrokineitc Vlasov-Poisson system. By using the developed code, we have performed the ITG simulation focusing on entropy dynamics and associated zonal flow formation. Here, we have introduced the modified local entropy defined as $\delta S_m(x) = \int \langle \delta f^2 / \{2 f_0 (- 1 + v_\parallel^2/T)\} \rangle_{yz} dv$, which retains the spatial information. It is found that the entropy balances with the acoustic coupling driven by ITG mode in the linear stage, and then the zonal flows expel the entropy to outside region via its convection. The spatial structure of the entropy is regulated by the zonal flows, and finally, the quasi-steady state where the entropy and zonal flows have similar structure is established. This indicates that the zonal flows couple with the entropy spatially [1] Y.Imai *et al.*, J. Comput. Phys. **227** (2008) 2263.

BP8 31 Catalytic Role of Zero-Frequency Zonal Modes in Saturation by Damped Eigenmodes P.W. TERRY, D.R. HATCH, *University of Wisconsin-Madison* W.M. NEVINS, *LLNL* F. JENKO, *IPP-Garching* Recent gyrokinetic simulations suggest that the effect of zonal flows on turbulence is catalytic, enabling energy to reach damped-eigenmode energy sinks in the wavenumber range of the instability. We investigate this issue, looking generically at three-wave coupling with a variety of analysis techniques. Using parametric instability analysis to study the excitation of general eigenmodes that are not linearly unstable, we find that energy transfer to damped-eigenmode energy sinks is sensitive to heavy reductions by phase mixing. Phase mixing is avoided if energy first goes to a set of catalytic modes and then to damped eigenmodes. The catalytic modes must have a zonal wavenumber (e.g., k_y=0), the linear wave frequency must be zero, but they do not have to be a flow or involve a flow, i.e., flow is not an essential aspect of the avoidance of phase mixing. Projections of ITG turbulence onto a linear-eigenmode basis indicate both the excitation of many virtually undamped, non flow-like k_y=o modes, and robustly damped $k_y \neq 0$ eigenmodes in the instability region.

BP8 32 Gyrokinetic particle characterization of transport in tokamaks* JEAN-NOEL LEBOEUF, *JNL Scientific* VIKTOR DECYK, *UCLA* DAVID NEWMAN, *UAF* RAUL SANCHEZ, *ORNL* We are characterizing transport using particles in gyrokinetic simulations of ion channel turbulence in tokamaks with the 3D global toroidal nonlinear parallel particle-in-cell UCAN code. Tracking of simulation particles through space and time and especially multiple processors, including restarts with different numbers of tagged particles, is now in production mode. The particle data thus tracked and stored comprise the positions and velocities for every tracked particle at each chosen instant of time. These particle data are analyzed with tools previously applied to passive marker particles in fluid turbulence simulations. The data from electrostatic UCAN simulations with adiabatic electrons and gyrokinetic ions show that radial transport is altered fundamentally by the presence of a sheared poloidal zonal flow, changing from diffusive to anti-correlated and subdiffusive. Convergence studies with both particle number and grid size confirm the standard resolution results. To facilitate these resource-intensive calculations two-dimensional domain decomposition is being implemented in UCAN.

*Work supported by USDOE/OFES.

BP8 33 The physics behind subdiffusive transport across an externally imposed sheared flow in drift-wave turbulence* D.E. NEWMAN, *Univ. of Alaska Fairbanks* R. SANCHEZ, *Oak Ridge National Lab* DEBASMITA SAMADDAR, J.N. LEBOEUF, *JNL Scientific* In recent gyrokinetic simulations of ITG turbulence it has been found that radial transport ceases to behave diffusively in the presence of a radially-sheared poloidal zonal flow [1]. We have observed a similar change in the character of transport across a shear flow in numerical simulations of 2D-turbulence in slab geometry using the BETA code, on which the sheared flow has been externally imposed [2]. The slab geometry and physics simplifies the search for the physics mechanism responsible for the onset of subdiffusion. The results suggest that subdiffusion is caused by the selection of a preferred sign for the vorticity carried out by the sheared flow throughout the 2D domain. This mechanism is likely to be important in a wide variety of turbulent systems. [1] R. Sanchez, D.E. Newman, J.N. Leboeuf,

V.K. Decyk and B.A. Carreras, Physical Review Letters **101**, 205002 (2008) [2] D.E. Newman, D. Samaddar, R. Sanchez and B.A. Carreras, in Proc. of the 35th EPS Conference on Plasma Physics, Hersonissos, 9-13 June 2008, ECA Vol. 32, p. 1.044 (2008)

*Supported in part by HPC resources from ARSC at the UAF, and DOE's NERSC and under DOE grants DE-AC05-00OR22725 and DE-FG02-04ER54741.

BP8 34 Transport suppression by shear reduction JULIO MARTINELL, *ICN, UNAM, Mexico* DIEGO DEL-CASTILLO-NEGRETE, *Oak Ridge National Laboratory* The relationship between transport and shear is a problem of considerable interest to magnetically confined plasmas. It is well known that there are cases in which an increase of flow shear can lead to a reduction of turbulent transport. However, this is not a generic result, and there are transport problems in which the opposite is the case. In particular, as originally discussed in Ref.[1], barriers to chaotic transport typically form in regions of vanishing shear. This property, which is generic to the so-called non-twist Hamiltonian systems[2], explains the observed resilience of transport barriers in non-monotonic zonal flows in plasmas and fluids and the robustness of shearless magnetic surfaces in reverse shear configurations. Here we study the role of finite Larmor radius (FLR) effects on the suppression of chaotic transport by shear reduction in a simplified model. Following Ref.[3] we consider a model consisting of a superposition of drift waves and a non-monotonic zonal flow. The FLR effects are incorporated by gyroaveraging the $\mathbf{E} \times \mathbf{B}$ velocity, and transport is studied by following the evolution of ensembles of test particles.

[1]del-Castillo-Negrete and Morrison, Phys. Fluids A **5**, 948 (1993)
[2]del-Castillo-Negrete, Greene, and Morrison, Physica D **91**, 1 (1996)
[3]del-Castillo-Negrete, Phys. Plasmas, **7**, 1702 (2000)

BP8 35 Coupled GEM-XGC Simulations of Edge Pedestal Plasmas* SCOTT PARKER, WEIGANG WAN, YANG CHEN, *University of Colorado* C.S. CHANG, S. KU, *New York University* N. PODHORSZKI, S. KLASKY, *ORNL* Global GEM gyrokinetic turbulence simulations of the edge pedestal are performed assuming closed flux surfaces and using numerical profiles obtained from the XGC0 neoclassical calculation[1]. The plasma profiles used in GEM are output from an XGC0 simulation of L- and H-mode DIII-D plasmas. For L-mode plasmas, it is found that electromagnetic effects are important and the heat diffusivities for both electrons and ions are much bigger than from equivalent simulations in the electrostatic limit. While electromagnetic ion and electron energy transport are comparable to experimental values, the particle transport is too high, and such particle diffusion coefficient would cause the pedestal crash in the XGC0 calculation. Adding carbon impurity may reduce the level of particle transport. Work is under way to incorporate the GEM/XGC coupling under the EFFIS – "End-to-end Framework for Fusion Integrated Simulation."

*Work supported by DOE SciDAC CPES project.

[1]Y. Chen and S. Parker, Phys. Plasmas **15**, 055905 (2008).

BP8 36 Global Turbulence Calculations with GEM for Experimental Cases and Experimental Comparisons* G. REWOLDT, D. MIKKELSEN, *PPPL* Y. CHEN, S. PARKER, *U. Colorado-Boulder* The GEM code is capable of global nonlinear turbulence calculations for experimentally-realistic cases, including trapped electrons, deuterium ions, carbon impurity ions, and hot beam ions, with electron collisions and electromagnetic effects, using a model MHD equilibrium with ellipticity and triangularity. For cases for the core region only of tokamaks such as NSTX and DIII-D, when the experimental level of the equilibrium ExB velocity is included, the cases are often completely stable, while if the ExB velocity is set to zero the cases can become unstable. However, even including the experimental ExB velocity, if the edge (pedestal) region also is included in the computation domain, the cases can be unstable, grow linearly, and saturate nonlinearly. In particular, the linearly stable core region could then have a significant level of anomalous transport, which would be evidence of turbulence spreading. For one particular NSTX case where the experimental ion energy transport is anomalous, the saturated GEM level of transport matches this in the edge region, but dies off more quickly radially going into the core region than the experimental transport. Results will be presented and discussed.

*Work Supported by U.S. DoE

BP8 37 Subdiffusive radial transport in a gyrokinetic Z-pinch plasma with zonal flows* KYLE GUSTAFSON, WILLIAM DORLAND, *University of Maryland* We report on numerical gyrokinetic studies of a confined, magnetized plasma in a Z-pinch configuration. Building upon previous results[1] for the entropy mode in a gyrokinetic Z-pinch, we examine the details of particle transport as diagnosed by the displacements of an ensemble of tracer particles in simulations[2]. The density-gradient driven entropy mode of instability leads to vertical zonal flow structures in the turbulence that impede particle transport in the radial direction. Tracer displacements in this study point to the existence of subdiffusive radial transport, such that the spreading of the tracers proceeds more slowly than predicted by a canonical turbulent diffusion equation. The relevance of this result to the usual predictions of confinement-time scaling for fusion machines is examined. We compare the effects of collisions and several values of the density gradient for significant periods of time, measured in $v_{thermal}/L$. We use continuous-time random walk and fractional diffusion equation models to understand the transport process more generally. The importance of long-range velocity correlations and scale-free transport is considered.

*Work supported by a Fannie and John Hertz Foundation Fellowship and the DOE Center for Multiscale Plasma Dynamics.

[1]Ricci et al PRL 97 245001 2006
[2]Broemstrup, Thesis University of Maryland

BP8 38 Formation of Coherent Vortex Structures and Transport Reduction in Electron Temperature Gradient Turbulence* MOTOKI NAKATA, *Graduate University for Advanced Studies* TOMO-HIKO WATANABE, HIDEO SUGAMA, *National Institute for Fusion Science* Formation of coherent vortex structures and related transport reduction in the slab ETG turbulence has been investigated by means of gyrokinetic Vlasov simulations with high phase-space resolution. A spontaneous transition of vortex structures from a turbulent state with finer-scale fluctuations to a coherent state dominated by large-scale vortices with zonal flows are found, where the electron heat flux is significantly reduced. The transport reduction in the coherent vortex state is mainly attributed to the phase matching of the potential and temperature fluctuations in association with the structural change of the velocity distribution function. A traveling wave solution of the Hasegawa-Mima type fluid equation including electron tempera-

ture gradient successfully describes the coherent vortex structures. It is also investigated how the parameters of η_e and $\Theta = k_{||}/k_\theta$ affect the formation of the coherent vortex structures and the resultant transport levels. Results of the toroidal ETG turbulence simulation will be also discussed.

*This work is supported by the Grant-in-Aid (No. 20-4017) for Japan Society for the Promotion of Science Fellows.

BP8 39 Eigenmode Analyses of Nonlinear Gyrokinetic Simulations D. HATCH, P. TERRY, *U. W. Madison* W. NEVINS, *LLNL* F. JENKO, F. MERZ, *IPP Garching* The excitation of damped eigenmodes is shown to be the dominant saturation mechanism for gyrokinetic ITG turbulence. Stable eigenmodes are excited to significant amplitude even at linearly unstable wavenumbers, revealing the collisionless gyrokinetic plasma to be a lossy medium, quite different from the conventional, nearly conservative medium requiring a cascade to short wavelengths for energy dissipation. This observation comes from eigenmode analyses of gyrokinetic simulations using the complete linear spectrum of the numerically discretized gyrokinetic operator. A projection procedure allows for explicit observation of the importance of each eigenmode with regard to transport, energy dissipation and energy content of the turbulence. This procedure has been applied to ITG driven turbulence where it is found that a series of stable eigenmodes are strongly excited, playing a vital role in energy balance and saturation. Comparisons with simulations for which zonal modes have been artificially suppressed indicate that zonal modes facilitate energy transfer to damped eigenmodes.

BP8 40 Source formulation for fluid turbulence simulations from atomic physics differential cross sections S.H. MULLER, C. HOLLAND, G.R. TYNAN, M. XU, J.H. YU, *UCSD* The derivation of the correct functional form of source terms in plasma fluid theory is revisited. The relation between the fluid source terms and atomic physics differential cross sections is established for particle-impact ionization. It is shown that the interface between atomic and plasma physics is completely described by three scalar functions of the incident particle energy, which are properties of the differential cross sections only. For electron-impact ionization, the BEB and BED models [Y.-K. Kim and M. E. Rudd, Phys. Rev. A, 50 (1994) 3954] are used to calculate these functions analytically, yielding expressions that both accurately capture the physics and can be efficiently evaluated within fluid simulation codes. The source terms explain the observed electron temperature regimes in a wide variety of basic plasma physics experiments, including the trends across different gases.

BP8 41 Physics behind the role of shear flow in turbulent transport of magnetic fields A. NEWTON, E. KIM, *University of Sheffield* Fundamental processes governing the dynamics of coherent structures and their interplay with turbulence in magnetized fluids present some of the most outstanding problems in classical physics. In particular, various observations indicate that typical magnetic activities in astrophysical plasmas must involve the fast transport of magnetic fields on time scales much shorter than the Ohmic diffusion time scale. In this contribution, we report on the first comprehensive direct numerical simulations of 2D sheared MHD turbulence to elucidate fundamental physical processes which accelerate or moderate turbulent transport of magnetic fields [1]. We show (i) that transport quenching by shear flows and resonant interactions are vitally important; (ii) that a shear flow plays a dual role of quenching transport by shearing and enhancing it by resonance and the overlap of resonant layers; (iii) that a strong suppression of transport by shear flow (magnetic fields) occurs when the shearing (Alfvénic) timescale is shortest among all the characteristic timescales. Specifically, without resonance, turbulent magnetic diffusivity η_T is quenched as $\eta_T \propto B_0^{-4}$ for weak shear (Ω) and strong magnetic field (B_0) while $\eta_T \propto \Omega^{-2.7}$ for strong shear and weak magnetic fields. In comparison, η_T is less severely quenched with resonance with the scaling $\eta_T \propto B_0^{-2} \propto \Omega^{-2}$ for strong shear and magnetic fields. [1] A. Newton and E. Kim, Phys. Rev. Lett., v102, 165002 (2009).

BP8 42 Universal Probability Distribution Function for Bursty Transport in Plasma Turbulence* INGMAR SANDBERG, *National Technical University of Athens, Association Euratom- Hellenic Republic, Greece* SADRUDDIN BENKADDA, *France-Japan Magnetic Fusion Laboratory, LIA 336/UMR 6633 CNRS-Universite de Provence, Marseille, France* XAVIER GARBET, *I.R.F.M., CEA Cadarache, France* GEORGE ROPOKIS, *National Observatory of Athens, Greece* KYRIAKOS HIZANIDIS, *National Technical University of Athens, Association Euratom - Hellenic Republic, Greece* Bursty transport phenomena associated with convective motion present universal statistical characteristics among different physical systems. A stochastic univariate model and the associated probability distribution function for the description of bursty transport in plasma turbulence is presented. The proposed stochastic process recovers the universal distribution of density fluctuations observed in plasma edge of several magnetic confinement devices and the remarkable scaling between their skewness S and kurtosis K. Similar statistical characteristics of variabilities have been also observed in other physical systems that are characterized by convection such as the X-ray fluctuations emitted by the Cygnus X-1 accretion disc plasmas and the sea surface temperature fluctuations.

*Supported under the Contract ERB5005CT990100 between the European Atomic Energy Community and the Hellenic Republic.

BP8 43 The effects of non-uniform magnetic field strength on test particle transport in drift wave turbulence RICHARD DENDY, *UKAEA Culham* JOSEPH DEWHURST, BOGDAN HNAT, *Warwick University* Our model of drift turbulence is a modified form of the Hasegawa-Wakatani equations, extended to include magnetic field inhomogeneity in the radial direction, thus incorporating interchange modes. Direct numerical simulation of this system yields local time series for: the turbulent E x B radial density flux Γ, whose probability density function (PDF) is analyzed in terms of skewness and kurtosis; and the relative phase and amplitude of fluctuations in density n, electrostatic potential ϕ and radial velocity v. We investigate how changes in the magnitude C of the magnetic field inhomogeneity affect the relative phases of n, ϕ and v and in consequence the skewness of the PDF of Γ. This is a consequence of the shift from drift to drift-interchange turbulence. The challenge is then to identify a Fickian expression linking Γ to the radial diffusivity that embodies C as a parameter, while noting the conservation of potential vorticity. This is achieved, assisted and confirmed by statistical analysis of the transport of ensembles of test particles in stationary turbulence and by measurements of the decay of correlation in potential vorticity.

BP8 44 Turbulence Spreading and Zonal Flow Evolution - A Non-Perturbative Theory A. ULVESTAD, M. MALKOV, P.H. DIAMOND, *CASS, U.C.S.D.* The interplay of turbulence spreading and zonal flows has been a subject of controversy in recent years. Previous work on this subject has utilized perturbative,

weak-coupling approaches (i.e. turbulence closures, envelope expansions, etc) to address this subject. Many of these calculations do not properly conserve momentum between fluctuations and flows. In this work, we study solutions of an asymptotic (i.e. eikonal) model without the use of a perturbative expansion. The model conserves momentum between fluctuations and zonal flows by treating the radial flux of turbulence potential enstrophy in the flow momentum balance. Results indicate intensity propagation depends strongly on fluctuation and flow dissipation profiles.

BP8 45 Particle in cell simulations of wave turbulence in solar wind in ion cyclotron frequency range VLADIMIR SVIDZINSKI, HUI LI, HARVEY ROSE, BRIAN ALBRIGHT, *LANL* KEVIN BOWERS, *D. E. Shaw Research* Fully electromagnetic particle in cell simulations of nonlinear waves propagation and interaction is performed in two-dimensional plane geometry in magnetized plasma in ion cyclotron frequency range. A spectrum of fast wave modes with different total energies with wave numbers parallel and perpendicular to uniform equilibrium magnetic field is launched into plasma and the nonlinear dynamics of these waves is analyzed. Results show that the wave magnetic energy spectrum cascades to smaller scales exhibiting strong anysotropy, it is wider in direction perpendicular to the equilibrium magnetic field. The shape of the cascade is established after a few ion cyclotron periods and most of the energy in the cascade stays in the fast wave oscillations. Collisionless damping on electrons is the main dissipation chanel in these results.

BP8 46 Role of linearly damped eigenmodes in several two field turbulence models K.D. MAKWANA, P.W. TERRY, *University of Wisconsin-Madison* Linearly damped eigenmodes have been shown to provide a significant finite-amplitude-induced energy sink for saturation in collision-less trapped electron turbulence(CTEM). Based on an analytic criterion, similar behaviour is predicted for seven other distinct fluid models in certain parameter regimes. These models (TEM, Rayleigh-Taylor, Local Resistive g-mode, Drift thermal, Micro-tearing with time dependent thermal force, Hasegawa-Wakatani and Ionization driven drift wave) are solved numerically and the solutions are projected onto the linear eigenmodes. The analytic criterion is explicitly evaluated for various parameter regimes and used to predict whether or not damped modes will significantly affect saturation. These regimes are investigated in the simulations and the predictions are verified by comparing stable mode amplitudes with unstable mode amplitudes in saturation. Fluxes are calculated and it is shown that quasilinear flux overestimates the true flux whenever damped modes contribute significantly to saturation. This invalidates the quasilinear approximation and shows that damped modes cannot be ignored in these models.

BP8 47 A Simple Dynamical Model of Flux-Driven Turbulence and Profile Evolution Z.H. WANG, P.H. DIAMOND, *UCSD, CA* C.S. CHANG, S. KU, *CIMS, NY University* X.G. WANG, *PKU, CHN* We study nonlocal, flux driven turbulence and profile evolution using a simple model of coupled nonlinear reaction-diffusion equation, heat transport equation and density source-diffusion equation. We study temperature profile evolution in the presence of turbulence produced by a strong edge source, which spreads inward and interacts with both heat pulses and locally driven core turbulence. Basic results are: 1)propagation of intensity and heat pulse differs in that the speed of the former grows and then decays as heat flux Q increases, while the latter grows and saturates at a value set by neoclassical transport. 2) speed of inward propagating turbulence is sensitive to Q. It first increase as $\sqrt{Q}$ and then decreases as 1/Q, following the formation of ITB. It suggests ITB location is determined by both heat flux and near edge conditions and ITB works as much by keeping turbulence out as by keeping heat in! 3) collisions of in to out and out to in pulses trigger local profile steeping, and (in some cases) ITB formation. Moreover, the interaction point varies with Q.

BP8 48 Zonal flow generation from trapped electron mode turbulence LU WANG, *School of Physics, Peking University* T.S. HAHM, *Princeton University, PPPL* Most existing zonal flow generation theory [1,2] has been developed with a usual assumption of $q_r\rho_{i\theta} << 1$ (q_r is the radial wave number of zonal flow, and $\rho_{i\theta}$ is the ion poloidal gyroradius). However, recent nonlinear gyrokinetic simulations of trapped electron mode (TEM) turbulence exhibit a relatively short radial scale of the zonal flows with $q_r\rho_{i\theta} \sim 1$ [3,4,5]. This work reports an extension of zonal flow growth calculation to this short wavelength regime via the wave kinetics approach. A generalized expression for the polarization shielding for arbitrary radial wavelength [6] which extends the Rosenbluth-Hinton formula in the long wavelength limit [7] is applied. The electron nonlinearity effects on zonal flow are investigated by using GTC simulation. This work was supported by the China Scholarship Council (LW), U.S. DoE Contract No. DE–AC02–09CH11466 (TSH, LW), the U. S. DOE SciDAC center for Gyrokinetic Particle Simulation of Turbulent Transport in Burning Plasmas, and the U. S. DOE SciDAC-FSP Center for Plasma Edge Simulation (TSH). [1] P. H. Diamond et al., IAEA-CN-69/TH3/1 (1998). [2] L. Chen, Z. Lin, and R. White, Phys. Plasmas **7**, 3129 (2000). [3] Z. Lin et al., IAEA-CN-138/TH/P2-8 (2006). [4] D. Ernst et al., Phys. Plasmas **16**, 055906 (2009). [5] Y. Xiao and Z. Lin, "Turbulent transport of trapped electron modes in collisionless plasmas," submitted to Phys. Rev. Lett. (2009). [6] Lu Wang and T.S. Hahm, Phys. Plasmas **16**, 062309 (2009). [7] M. N. Rosenbluth and F. L. Hinton, Phys. Rev. Lett. **80**, 724 (1998).

BP8 49 Transport studies of Toroidal Angular Momentum carried by Drift Resonance of Toroidal Ion Temperature Gradient Instability near Marginality* E.S. YOON, T.S. HAHM, *Princeton Plasma Physics Laboratory* We calculate transport of parallel momentum carried by drift resonance of toroidal ITG instability near marginality using quasilinear theory starting from a phase space conserving gyrokinetic equation [1] for ions. The principal results are: TEP pinch remains inward as the most robust term of pinch. In addition, ion temperature gradient driven pinch is inward for typical parameters. Interestingly, density gradient driven pinch is outward as in the previous kinetic results in slab geometry [2], but opposite to the results in the fluid regime [3]. Parameter dependency of momentum diffusivity and pinch velocity on the electron to ion temperature ratio ($\tau = T_e/T_i$) has been examined over a wide range of density profiles. [2] P.H. Diamond, C.J. McDevitt, and.D. Gürcan, *et. al.*, Nuclear Fusion, **15** 012303 (2008) [3] A.G. Peeters, C. Angioni and D. Strintzi, Phys. Rev. Lett., **98** 072302 (2007)

*We would like to acknowledge useful discussions with P.H. Diamond, S.D. Scott, and J. Rice. This work was supported by the U.S. Department of Energy Contract No. DE-AC02-09CH11466.

BP8 50 Construction of momentum theorem using cross moments T.S. HAHM, *Princeton University, Princeton Plasma Physics Laboratory, P.O. Box 451, Princeton, NJ 08543, USA* LU WANG, *School of Physics, Peking University, Beijing 100871, China* P.H. DIAMOND, *Center for Astrophysics and Space Science, U.C.S.D., La Jolla, CA 92093, USA* Charney-Drazin theorem has been extended to Hasegawa Wakatani system for zonal flow problem in magnetic fusion [P.H. Diamond, et al., Plasma Phys. Control. Fusion **50**, 124018 (2008)]. For this model, the guiding center density is the potential vorticity and zonal flow is influenced by the particle flux. In this work we construct momentum theorems in terms of a hierarchy of cross moments $\langle n_G^2 \rangle$, $\langle u_\phi n_G \rangle$, and $\langle p_i n_G \rangle$. Then we show that the particle flux, momentum flux, and heat flux influence the zonal flow for each system respectively. This work was supported by U. S. Department of Energy Contract No. DE–AC02–09CH11466 (TSH, LW), China Scholarship Council (LW), U. S. DOE SciDAC center for Gyrokinetic Particle Simulation of Turbulent Transport in Burning Plasmas, and the U. S. DOE SciDAC-FSP Center for Plasma Edge Simulation (TSH).

BP8 51 Role of stable eignmodes in ETG-driven turbulence* JUHYUNG KIM, PAUL T. TERRY, *Dept. of Physics, Univ. Wisconsin at Madison* The role of stable eigenmodes in the saturation of plasma turbulence is investigated in the framework of the ETG fluid model. Previously, Kelvin-Helmholtz instability has been involved as a saturation mechanism, applying to the transition from the linear to nonlinear regime where the structure of linearly unstable modes breaks down. This saturation mechanism is investigated from the "energetic" point of view with the damped eigenmodes. The nonlinear energy transfer between the unstable and damped eigenmodes is traced in the simulations. It is observed that the energy of the linearly unstable modes is transferred to the damped eigenmodes at the corresponding wavelength at the time of the linear structure break-down. Additional details of energy balances among eigenmodes in the nonlinear state are presented for a 2D sheared slab geometry. Extension to 3D has also been developed and results will be given. The analysis of energetics that complement dynamical approaches, such as the analysis of phase mixing, will be considered and described.

*This work is supported by the grant of DoE DE-FG02-89ER53291.

BP8 52 Angular Momentum Ejection and Recoil* O. OHIA, B. COPPI, *MIT* The spontaneous rotation phenomenon observed in axisymmetric magnetically confined plasmas has been explained by the "accretion theory" [1] that considers the plasma angular momentum as gained from its interaction with the magnetic field and the surrounding material wall. The ejection of angular momentum to the wall, and the consequent recoil are attributed to modes excited at the edge while the transport of the (recoil) angular momentum from the edge toward the center is attributed to a different kind of mode. The toroidal phase velocity of the edge mode, to which the sign of the ejected angular momentum is related, is considered to change its direction in the transition from the H-regime to the L-regime. For the latter case, edge modes with phase velocity in the direction of upv_{di} are driven by the temperature gradient of a cold ion population at the edge and damped on the "hot" ion population. The "balanced" double interaction [2] of the mode with the two populations, corresponding to a condition of marginal stability, leads to ejection of hot ions and loss of angular momentum in the direction of upv_{di} while the cold population acquires angular momentum in the opposite direction. In the H-regime resistive ballooning modes with phase velocities in the direction of upv_{de} are viewed as the best candidates for the excited edge modes. *Sponsored in part by the U.S. DOE. [1] B. Coppi, *Nucl. Fusion* **42**, 1 (2002) [2] B. Coppi and F. Pegoraro, *Nucl. Fusion* **17**, 969 (1977)

BP8 53 Wave Momentum, Radial Current and Intrinsic Rotation* P.H. DIAMOND, *University of California, San Diego* O.D. GURCAN, *Laboratoire de Physique et Technologie des Plasmas* In this paper, we extend ongoing work on the origins of intrinsic rotation in tokamaks to address general novel mechanisms for producing a non-diffusive Reynolds stress which drives intrinsic rotation. A unifying approach employs the calculation of momentum fluxes via consideration of transport of resonant particle and wave momentum. The latter is calculated via wave kinetics. Specific results include the calculations of radial current $\langle T_r \rangle$ and the associated toroidal acceleration due to wave turbulence and a more general calculation of parallel spin-up due to $k_\parallel$-symmetry breaking. The latter is shown to occur for any intensity gradient.

*This research was supported by U.S Department of Energy Grant Nos. DE-FG02-04ER54738, DE-FC02-08ER54959 and DE-FC02-08ER54983.

BP8 54 Momentum Theorems for Vlasov and Gyrokinetic Turbulence* L.T. NEKO, P.H. DIAMOND, C. McDEVITT, Y. KOSUGA, *University of California, San Diego* X. GARBET, *CEA Cadarache* O.D. GURCAN, *Laboratoire de Physique et Technologie des Plasmas* T.S. HAHM, *Princeton Plasma Physics Laboratory, Princeton University* In this work, we extend Charney-Drazin type momentum theorems to encompass Vlasov and gyrokinetic systems. The common key element of these and their fluid antecedents is the existence of a Kelvin's Theorem for a conserved circulation in the relevant phase space. A pseudomomentum, quadratic in the perturbed distribution function, is identified. In the non-resonant limit, we show that this pseudomomentum reduces to the familiar wave momentum density. Constraint relations for anomalous resistivity (1D) and GK zonal flow growth are derived. The relation to phase space density granulations is discussed.

*This research was supported by U.S Department of Energy Grant Nos. DE-FG02-04ER54738, DE-FC02-08ER54949 and DE-FC02-08ER54983.

BP8 55 Current-Driven Drift Wave Turbulence and Electron Thermal Transport in Tokamaks* C. LEE, P.H. DIAMOND, *University of California, San Diego* M. PORKOLAB, *PSFC, Massachusetts Institute of Technology* Recent analyses (Y. Lin, M. Porkolab; 2009) have indicated that the "usual suspects" for the mechanism of electron thermal transport, such as ITG, ETG, CTEM modes, etc, cannot explain results from modest density, $T_e > T_i$ plasmas, in either OH or ECH heating regimes. Interestingly, such plasmas exhibit very large toroidal current drift parameters v_d/c_s, thus naturally suggesting a re-visitation of current driven drift waves. In this paper, we discuss the linear, quasilinear and non-linear theory of current driven drift waves in tokamaks. Parallel electron velocity scattering, a critical effect beyond the capacity of most, gyrokinetic codes is a major focus of investigations. The coupled transport of current density and heat are considered. Work is ongoing and results will be presented.

*This research was supported by U.S Department of Energy Grant Nos. DE-FG02-04ER54738, DE-FC02-08ER54959 and DE-FC02-08ER54983.

BP8 56 Mesoscopic Lattice Boltzmann Representation for Quantum to Classical Turbulence* BO ZHANG, GEORGE VAHALA, *William & Mary* LINDA VAHALA, *Old Dominion University* Here we present a lattice Boltzmann (LB) mesoscopic representation of the Gross-Pitaevskii equation to examine the multiscale physics of turbulence spanning the quantum vortex core scales to the classical large scales were the quantization of vortices is unimportant. While the unitary mesoscopic algorithm faithfully represents the Hamiltonian structure of GP, the LB representation is at first glance dissipative. The macroscopic nonlinearities are recovered by phase shifts – just as in the mesoscopic qubit unitary algorithm. However, this dissipative effect can be rescaled in time. Soliton collisions as well as turbulence will be considered and compared to the unitary algorithm.

*Work supported by AFOSR.

BP8 57 Scalar Magnetic Field Distribution Function Approach to MHD Turbulence TAO WANG, GEORGE VAHALA, *William & Mary* LINDA VAHALA, *Old Dominion University* Lattice Boltzmann (LB) representations are mesoscopic algorithms that exploit a simple collide-stream scheme that is ideal for parallelization – even for non-periodic boundary conditions. Moreover, in LB one can enforce to machine accuracy. Typically one has introduced a vector distribution function for the magnetic field to account for the asymmetry tensor in the magnetic field evolution as opposed to the symmetric stress tensor in velocity evolution. Here we investigate 2D MHD turbulence by working with a scalar magnetic distribution function representation. A major advantage of the scalar representation is the much reduced computational memory requirements, simpler boundary condition enforcement, and simple entropic stabilization schemes. The Orszag-Tang vortex will be examined as well as some LES closure schemes using Elsasser variables.

BP8 58 Kolmogorov to Kelvin Wave Cascades in Turbulence: from large scales to quantum vortex core scales GEORGE VAHALA, *William & Mary* JEFFREY YEPEZ, *Air Force Research Lab., Hanscom* MIN SOE, *Rogers State University* LINDA VAHALA, *Old Dominion University* A novel unitary mesoscopic lattice algorithm with low memory requirements, permits simulations of the nonlinear Schrodinger equation (NLS) on spatial grids up to 5760^3. The algorithm is built from the collisional unitary entanglement of 2 qubits at each spatial node and then unitary streaming of this entangled state to neighboring sites. The algorithm scales perfectly – even to the full 163840 processors on Blue Gene P/Intrepid. Our simulations have determined 3 distinct power laws in the incompressible kinetic energy spectrum: a classical Kolmogorov $k^{-5/3}$ spectrum at large scales, and a quantum Kelvin wave cascade spectrum of at scales of the order of the quantum cores. In the adjoining semiclassical regime there is a non-universal steeper spectral decay adjoining the classical and quantum regimes. Our unitary (reversible) algorithm fully respects the Hamiltonian nature of the GP equation and approaches pseudo-spectral accuracy. Somewhat unexpectedly, we find a set of initial conditions that exhibit very short Poincare recurrence times.

BP8 59 Candidates for the Observed Electron Thermal Energy Transport and Micro-reconnecting Modes* C. CRABTREE, B. COPPI, *MIT* Two plausible candidates to explain the observed (anomalous) electron thermal energy transport in collisionless or weakly collisional plasmas are shown to be the trapped electron mode[1] (TEM) and the micro-reconnecting mode[2]. The first mode is driven by the combined effects of the plasma pressure and the magnetic field curvature. The second produces a string of magnetic islands and requires that the relative electron temperature gradient to be significantly larger than the relative temperature gradient. Both modes, when considering the largest transverse wavelengths for which they can be excited ($1/k_\perp \sim \rho_i$, for the first mode, $\rho_i =$ ion gyro-radius, and $1/k_\perp \sim c/\omega_{pe}$ for the second mode) require a phase space (non-fluid) description. For the second mode the transverse electron energy effective diffusion can be represented by $D^{th}_{e\perp} \sim (de/r_{te})cT_e/(eB)$ which does not involve a strong degradation of the energy confinement time as a function of the heating power. Here $r_{te} = -1/(duplnT_e/dr)$. A more complete form of the composite transport coefficient that is suitable for the numerical simulation of the transport properties of experimentally produced plasmas with different degrees of collisionality has been derived from the characteristics of the modes. *Supported in part by the U.S. D.O.E. [1] B. Coppi and G. Rewoldt, *Phys. Rev. Letts.* **33** 1329 (1974) [2] B. Coppi, in *Collective Phenomena in Macroscopic Systems*, p. 59 publ. *World Scientific* (2007).

BP8 60 A Green's function method for local and non-local parallel transport in general magnetic fields DIEGO DEL-CASTILLO-NEGRETE, LUIS CHACÓN, *Oak Ridge National Laboratory* The study of transport in magnetized plasmas is a problem of fundamental interest in controlled fusion and astrophysics research. Three issues make this problem particularly challenging: (i) The *extreme anisotropy* between the parallel (i.e., along the magnetic field), $\chi_\parallel$, and the perpendicular, $\chi_\perp$, conductivities ($\chi_\parallel/\chi_\perp$ may exceed 10^{10} in fusion plasmas); (ii) Magnetic *field lines chaos* which in general complicates (and may preclude) the construction of magnetic field line coordinates; and (iii) *Non-local parallel transport* in the limit of small collisionality. Motivated by these issues, we present a Lagrangian Green's function method to solve the local and non-local parallel transport equation applicable to integrable and chaotic magnetic fields. The numerical implementation employs a volume-preserving field-line integrator [Finn and Chacón, *Phys. Plasmas*, **12** (2005)] for an accurate representation of the magnetic field lines regardless of the level of stochasticity. The general formalism and its algorithmic properties are discussed along with illustrative analytical and nu-

merical examples. Problems of particular interest include: the departures from the Rochester–Rosenbluth diffusive scaling in the weak magnetic chaos regime, the interplay between non-locality and chaos, and the robustness of transport barriers in reverse shear configurations.

BP8 61 Self Consistently Calculated Zonal Flow Shears and Stability and Its Implications Y. KOSUGA, P.H. DIAMOND, *University of California, San Diego* In this work, we derive an *exact* expression for the zonal flow velocity profile using conservation of potential enstrophy for drift wave models, in a *stationary state*. This result extends the Charney-Drazin theorem, familiar from geophysical fluid dynamics, and should be contrasted to previous zonal flow models in that it: a.) is derived for the *stationary* turbulence-flow system, rather than for the transient growth phase. b.) links the zonal flow directly to the driving transport *flux*, which is *fixed*. c.) is formulated in *real* space, instead of Fourier space, which is critical to determine the strength of the shear and curvature of zonal flow (n.b. the former controls turbulent transport and the latter controls Kelvin-Helmholtz instability of zonal flows). We have obtained results for the flow shear profile and the flow curvature profile. Results indicate that: a.) zonal flow *shear* is determined primarily by the driving flux and the profile of the flow damping, which allows determination of the critical flux for reduction of turbulent transport. b.) zonal flow *curvature* is determined by the flow damping curvature, along with the profile of potential enstrophy dissipation, which determines a condition for KH stability. This research was supported by U.S Department of Energy Grant Nos. DE-FG02-04ER54738, DE-FC02-08ER54959 and DE-FC02-08ER54983.

BP8 62 On the mechanism responsible for subdiffusive transport across poloidal zonal flows in gyro-kinetic simulations of tokamak ITG turbulence* RAUL SANCHEZ, *Oak Ridge National Laboratory* DAVID NEWMAN, *University of Alaska* JEAN-NOEL LEBOEUF, *JNL Scientific, Inc.* VIKTOR DECYK, *UCLA* It has been recently found that radial transport ceases to behave diffusively in the presence of a radially-sheared poloidal zonal flow, becoming instead strongly subdiffusive [1]. The same behavior is observed in other simulations, suggesting that the mechanism responsible is rather general. In numerical simulations of 2D-turbulence, the change in character seems to be related to the selection by the sheared flow of a preferred sign of the axial vorticity (that of the sheared flow), further reinforced by the tilting of the turbulent eddies carried out by the shear [2]. In this contribution we look for evidence of the same mechanism in gyrokinetic simulations of tokamak ITG turbulence carried out by the UCAN code. The way in which these concepts must be modified to accommodate the toroidal geometry is discussed. [1] R. Sanchez et al, Physical Review Letters **101**, 205002 (2008) [2] D.E. Newman et al, in Proc. of the 35th EPS Conference on Plasma Physics, Hersonissos, 9-13 June 2008, ECA Vol. 32, p. 1.044 (2008)

*Work supported in part by US DOE under Contract No. DE-AC05-00OR22725. Simulations run at ARSC and NERSC.

BP8 63 COMPLEX, NON-NEUTRAL AND OTHER NOVEL PLASMAS

BP8 64 Low Velocity Ion Stopping in Dense and Multicomponent Plasmas BEKBOLAT TASHEV, *KazNu Almaty Kazakhstan* CLAUDE DEUTSCH, *LPGP UParis XI* PATRICE FROMY, *CRI UParis XI* KAZAKH COLLABORATION, We focus attention on low velocity ion slowing down (LIVSD) in dense and multicomponent plasmas of ICF and astrophysical interest. The target is treated in a dielectric formalism with classical electrons neutralizing binary ionic mixtures (BIM) of any relative proportion.We consider first charge symmetric BIM such as deuterium-tritium, proton-heliumlike iron ions in the solar interior or proton-helium ions considered in planetology as well as other mixtures of relevance to the heavy ion production of warm dense matter at Bragg peak conditions. We single out ion projectile velocities (so-called critical) at which target electron LIVSD matches the sum of target ion ones. Proton stopping in the white dwarf crust (carbon-helium BIM) is also considered.

BP8 65 Weibel instability in positron-electron plasma BARBARA SHRAUNER, *Washngton University* The Weibel or filamentation instability of counter-flowing beams described by a recent model is investigated. The model combined computer simulations and an analytic one-particle distribution function for the quasi-equilibrium of a positron-electron plasma. An electron-ion plasma is not considered. This instability is conjectured to give rise to turbulent magnetic fields in collisionless shocks. The linear growth rate and time dependence of the instability is determined from the Vlasov-Maxwell equations and confirms that the dominant mode for the magnetic field has the spatial dependence of the initial perturbed magnetic field as found by the simulations. The quasi-equilibrium distribution function is expanded in Hermite polynomials varying in two spatial variables, a generalization of earlier results for nonlinear transverse waves. The quasi-equilibrium in reference 1 is further constrained by the conservation of particle number and total energy. That quasi-equilibrium agrees only qualitatively with the simulation results. A nonlinear model is proposed with the sinh-Poisson equation. An analytic form for the vector potential is found for this nonlinear model in terms of Jacobian elliptic functions. A. Suzuki and T. Shigeyama, Astrophys. J. **695**, 1550-1558 (2009). B. Abraham-Shrauner, Phys. Fluids, **11**, 1162-1167 (1968).

BP8 66 Emittance Preservation of Positron Beams Traveling in Hollow Plasma Channels* XIAOYING LI, PATRIC MUGGLI, *University of Southern California* SAMUEL MARTINS, WARREN MORI, *University of California, Los Angeles* WAYNE D. MORI, *STI Optronics* Emittance preservation of the incoming beam is essential for all accelerators. In the blowout regime of plasma wakefield accelerator (PWFA), the electron bunch propagates in a uniform ion column and its emittance is preserved along the plasma. For a positron bunch propagating in a uniform plasma, the beam suffers emittance growth [P. Muggli et al., Phys. Rev. Lett. 2008]. However, it has been shown that when a positron bunch propagates in a hollow plasma, the axial accelerating field can be enhanced when compared to the uniform plasma case [S. Lee, PRE, 64, 045501(R), 2001]. We explore through numerical simulations the possibility of preserving emittance of positron beams by using a hollow plasma channel instead of a uniform plasma. We consider in particular the case of a drive/witness bunch train, necessary to accelerate the witness bunch with a high gradient and a narrow final energy spread. We explore a range of beam and channel parameters to maximize the acceleration and minimize the final energy spread and emittance of the witness bunch. Detailed simulation results will be presented.

*This work is supported by the US Department of Energy.

BP8 67 Metal Wire Explosions in Underwater Discharges DEOK-KYU KIM, SUNG-HYUN BAEK, INHO KIM, *Agency for Defense Development* Magnetohydrodynamics of metal wires exploding in underwater electrical discharges have been simulated and the results are compared with the experimental observations by streak camera. We use a one-dimensional time-dependent magnetohydrodynamic simulation code which employs an equation-of-state model and an electrical conductivity model for dense plasmas [1]. The rapidly expanding boundaries of metal plasmas and the resulting shock fronts propagating in the water are computed as function of time for comparison with the streak camera images, which shows fair agreements. In addition, the electrical conductivities of metal plasmas are reproduced from the measured current and voltage profiles and then discussed for verification of the conductivity model used in the simulation. [1] Deok-Kyu Kim and Inho Kim, Phys. Rev. E **68**, 056410 (2003); Contrib. Plasma Phys. **47**, 173 (2007).

BP8 68 SF_6 gas jet laser-produced plasma for strongly-coupled physics experiments J.M. TACCETTI, R.P. SHURTER, P.M. GOODWIN, *Los Alamos National Laboratory* A dense plasma for strongly-coupled physics experiments is formed by focusing a 10 ps laser pulse ($I \sim 5 \times 10^{16}$ W/cm^2) into a supersonic SF_6 gas jet. The desired plasma is a partially ionized non-equilibrium plasma of hot electrons ($\sim$ 125 eV) and cold ions (10-15 eV) with $n_e \sim 1 \times 10^{21}$ cm^{-3}. We will present detailed studies of the plasma formation dynamics for such a high-Z system. Such a strongly coupled ion plasma (initial ion-ion coupling parameter $\Gamma_{ii} \sim 3 - 5$) can be used to study temperature relaxation between the electrons and ions as a function of time. We plan to measure the electron and ion temperatures of the resulting plasma independently during and after heating, using collective Thomson scattering for electrons and a high-resolution x-ray spectrometer for the ions, measuring Doppler-broadened absorption lines.

BP8 69 X-ray absorption spectroscopy using short pulse laser isochoric heated targets* SOPHIA CHEN, R. SHEPHERD, *Lawrence Livermore National Laboratory* P. AUDEBERT, *Laboratoire d'Utilisation de Lasers Intenses (LULI), Palaiseau, France* P. RENAUDIN, B. LOUPIAS, *CEA/DIF, Bruyere Le Chatel, France* L. LECHERBOURG, *University of Toronto, Canada* B. WILSON, C. IGLESIAS, *Lawrence Livermore National Laboratory* R. MAJORIBANKS, *University of Toronto, Canada* H. CHEN, P. BEIERSDORFER, *Lawrence Livermore National Laboratory* We present a series of experiments to help quantify the effects of density on bounds states in plasmas. The experiments are performed by x-ray back-lighting aero-gel targets heated with an ultrashort pulse laser. The density and temperature is determined by assuming an isothermal expansion and using frequency domain interferometry measure the time-dependent position of the critical surface. Additional temperature verification is made using the target emissivity. The aero-gel target density is systematically increased and absorption spectra is used to monitor the effect of the increased density on the bound states. Preliminary experimental results will be presented.

*Work performed under the auspices of the U.S. Department of Energy by the Lawrence Livermore National Laboratory under Contract No. W-7405-ENG-48.

BP8 70 Strongly Coupled Plasma Dynamics Using the Particle-in-Cell Methodology* D.V. ROSE, T.C. GENONI, D.R. WELCH, R.E. CLARK, *Voss Scientific, LLC* T.A. MEHLHORN, R.B. CAMPBELL, D.G. FLICKER, W.A. STYGAR, *Sandia National Laboratories* Three-dimensional simulations of moderately to strongly coupled electron-ion and multi-component plasmas using the particle-in- cell method are presented. The simulations resolve sub-Debye- length inter-particle spacing to accurately model the dynamics of these systems. We consider realistic mass ratios and quasi- equilibrium conditions with different component temperatures which are relevant on short time scales. The simulation results are in very good agreement with classical hypernetted chain calculations for dense electron-ion and ion-ion plasmas [1]. Our results demonstrate the feasibility and utility of large- scale particle-in-cell simulations for the modeling and analysis of multi-component moderately and strongly coupled plasmas. Application of the simulation model to conductivity [2] and mass-stopping power of energetic ions in strongly coupled plasmas is discussed. [1] V. Schwarz, et al., Contrib. Plasma Phys. 47, 324 (2007). [2] W. A. Stygar, G. A. Gerdin, and D. L. Fehl, Phys. Rev. E 66, 046417 (2002).

*Work supported by Sandia National Laboratories through U.S. DOE.

BP8 71 Degenerate Mixing of Electrostatic Modes on a Finite-Length Nonneutral Plasma Column* M.W. ANDERSON, T.M. O'NEIL, *UCSD* Using cold fluid theory, we discuss the structure of standing electron plasma waves on a magnetized, nonneutral plasma column of finite length. Such eigenmodes can be surprisingly complex, involving a superposition of many component waves with different axial and transverse wavenumbers k_z and $k_\perp$. The dispersion relation[1] for the individual components [*i.e.*, $\omega = \omega_p k_z / \sqrt{k_z^2 + k_\perp^2}$] implies that waves with small k_z and $k_\perp$ can be degenerate with waves with large k_z and $k_\perp$. Reflection at the column ends mixes these degenerate components, yielding the complicated structure. We have in mind eigenmodes on a cryo-

genic plasma column, where cold fluid theory is valid even for waves with large k_z and $k_\perp$. In a warmer plasma, kinetic effects (*e.g.*, Landau damping of the large wavenumber components) spoils the degeneracy and kills the mixing.

*Supported by NSF PHY-0903877.

[1]A.W. Trivelpiece and R.W. Gould, J. Appl. Phys. **30**, 1784 (1959).

BP8 72 Electron Acoustic Waves in Pure Ion Plasmas* F. ANDEREGG, C.F. DRISCOLL, D.H.E. DUBIN, T.M. O'NEIL, *UCSD* Electron Acoustic Waves (EAW) are the low frequency branch of electrostatic plasma waves. These waves exist in neutralized plasmas, pure electron plasmas and in pure ion plasmas[1] (where the name is deceptive). Here, we observe standing $m_\theta = 0$ $m_z = 1$ EAWs in a pure ion plasma column. At small amplitude, the EAWs have a phase velocity $v_{ph} \simeq 1.4\bar{v}$, and the frequencies are in close agreement with theory. At moderate amplitudes, waves can be excited over a broad range of frequencies, with observed phase velocities in the range of $1.4\bar{v} \leqslant v_{ph} \leqslant 2.1\bar{v}$. This frequency variability comes from the plasma adjusting its velocity distribution so as to make the EAW resonant with the drive frequency. Our wave-coherent laser-induced fluorescence diagnostic shows that particles slower than v_{ph} oscillate in phase with the wave, while particles moving faster than v_{ph} oscillate 180 ° out of phase with the wave. From a fluid perspective, this gives an unusual negative dynamical compressibility. That is, the wave pressure oscillations are 180° out of phase from the density oscillations, almost fully canceling the electrostatic restoring force, giving the low and malleable frequency.

*Supported by NSF PHY-0903877.

[1]F. Anderegg *et al.*, PRL **102**, 095001 (2009) and PoP **16**, 055705 (2009).

BP8 73 Enhanced Neoclassical Transport and Mode Damping Caused by Chaos Near an Asymmetric Separatrix* D.H.E. DUBIN, *UCSD* YU.A. TSIDULKO, *Budker Inst.* Plasma loss due to apparatus asymmetries is a ubiquitous phenomenon in magnetic plasma confinement. Recent experiments have investigated the loss rate when a central squeeze potential is applied to a magnetized plasma column, creating two trapped particle populations separated by a separatrix.[1] These populations react differently to the asymmetries, leading to a collisional boundary layer at the separatrix. A loss rate scaling as $\sqrt{\nu/B}$ due to the boundary layer is expected theoretically,[1] provided that the separatrix itself is axisymmetric. However, when the separatrix is *asymmetric*, particles become trapped and detrapped as they follow collisionless orbits. This can lead to a chaotic region around the separatrix, giving enhanced transport scaling as $\nu^0 B^{-1}$. This effect also damps certain plasma modes. Predictions for damping of trapped particle diocotron modes will be compared to experiments.[2]

*Supported by NSF/DOE PHY-0613740 and NSF PHY-0903877.

[1]D.H.E. Dubin, Phys. Plasmas **15**, 072112 (2008); D.H.E. Dubin *et al.*, Neoclassical transport and plasma mode damping caused by collisionless scattering across an asymmetric separatrix, in preparation.
[2]A.A. Kabantsev, adjacent poster.

BP8 74 Damping of Diocotron Modes by Chaotic Dissipation on a θ-ruffled Separatrix* A.A. KABANTSEV, D.H.E. DUBIN, *UCSD* YU.A. TSIDULKO, *Budker Inst.* C.F. DRISCOLL, *UCSD* Diocotron mode damping measurements on pure electron plasma columns clearly distinguish the novel "chaotic" dissipation on a θ-ruffled separatrix from the usual collisional dissipation on a θ-symmetric separatrix. Here, an applied electrostatic "squeeze" barrier $\Phi_0(r)$ makes a separatrix between fast and slow electrons, and separatrix dissipation[1] causes the observed mode damping. We add controlled θ-ruffles $\Phi_m \cos(m\theta)$ to the separatrix by either static wall voltages or by other launched waves, and we quantify the enhanced damping in both cases. The chaotic dissipation results from electrons becoming trapped and untrapped as the plasma $E \times B$ drift rotates; and it is observed to scale as $\Phi_m^1 B^{-1}$. In contrast, the collisional dissipation scales as $B^{-1/2}$, and so tends to dominate at high magnetic fields. The transition from collisional to chaotic is unambiguously observed as the strength of the separatrix ruffle is increased. These experimental results are in quantitative agreement with nascent theory analyses[2] which treat the neoclassical transport and damping from θ-ruffled separatrices.

*Supported by NSF PHY-0903877.

[1]A.A. Kabantsev *et al.*, Phys. Rev. Lett. **101**, 065002 (2008).
[2]D.H.E. Dubin, adjacent abstract

BP8 75 Separatrix-Induced Transport, Damping, and Wave-Coupling* C.F. DRISCOLL, A.A. KABANTSEV, T.M. O'NEIL, D.H.E. DUBIN, *UCSD* YU.A. TSIDULKO, *Budker Inst.* Recent experiments have characterized a broad range of transport, damping, and wave-coupling effects caused by trapping separatrices in both the "collisional" and "chaotic" regimes. Here, the pure electron plasma columns have an electrostatic trapping separatrix created by an applied "squeeze" voltage; and this separatrix may have "θ-ruffles" from the applied voltages or from other $m_\theta \neq 0$ waves. For a θ-symmetric separatrix, traditional neoclassical theory predicts collisional dissipative effects scaling as $\nu_{ee}^{1/2} B^{-1/2}$. For a θ-ruffled separatrix, recent theory predicts chaotic dissipative effects scaling as $\nu_{ee}^0 B^{-1}$. The experiments have characterized the wave damping for both diocotron (drift) waves and Langmuir (plasma) waves, as well as the bulk plasma expansion that occurs when external confinement asymmetries (such as magnetic tilt) are present. For $B > 10$kG, the $E \times B$ drift rotation is slow and collisional effects tend to dominate; for $B < 1$kG, rapid plasma rotation around θ-ruffled separatrices causes chaotic effects to dominate. This novel chaotic transport may have applicability to low-collisionality stellarator and tokamak separatrices also, especially given the ubiquity of wave-induced separatrix ruffles.

*Supported by NSF PHY-0903877.

BP8 76 Progress Towards a Multicell Trap for Positron Storage* J.R. DANIELSON, T.R. WEBER, C.M. SURKO, *University of California, San Diego* There are many potential applications of high-capacity and/or portable antimatter traps. Here, we describe the latest progress toward the development of a novel multicell Penning-Malmberg trap that will be capable of accumulating orders of magnitude more positrons than is possible presently.[1] This design represents the next major step in antimatter storage technology. Described here is the design for a 21 cell trap capable of accumulating and storing more than 5×10^{11} positrons using 1 kV confinement potentials. Experiments with electron

plasmas establishing techniques critical to the implementation of a practical multicell trap are discussed. This trap could be used to multiplex the output of the new generation of positron sources, either operating now or currently under development, as well as to provide record-high bursts of positrons for a variety of applications.

*This work supported by NSF grant PHY 07-13958.

[1]J. R. Danielson, T. R. Weber and C. M. Surko, *Phys. Plasmas* **13**, 123502 (2006).

BP8 77 Magnetic multipole induced zero-rotation frequency bounce-resonant loss in a Penning-Malmberg trap used for antihydrogen trapping* JOEL FAJANS, *U.C. Berkeley* ALPHA TEAM, In many antihydrogen trapping schemes, antiprotons held in a short-well Penning-Malmberg trap are released into a longer well. This process necessarily causes the bounce-averaged rotation frequency Ω_r of the antiprotons around the trap axis to pass through zero. In the presence of a transverse magnetic multipole, experiments show that many antiprotons (over 30% in some cases) can be lost to a hitherto unidentified bounce-resonant process when Ω_r is close to zero. The results of these experiments will be presented, as well as an analytic model and numeric simulations

*This work was supported by CNPq, FINEP (Brazil), ISF (Israel), MEXT (Japan), FNU (Denmark), NSERC, NRC/TRIUMF (Canada), DOE (USA), and EPSRC and the Leverhulme Trust (UK).

BP8 78 Antihydrogen Induced Radial Redistribution of Antiprotons and Detection of Weakly Bound Antihydrogen NIELS MADSEN, *Swansea University* ALPHA COLLABORATION, Attempts to trap antihydrogen ($\bar{H}$) in a magnetic minimum trap are ongoing. The $\bar{H}$s is typically formed through direct mixing of plasmas of positrons (e^+) and antiprotons ($\bar{p}$), as this, thus far, has shown the highest yields of $\bar{H}$. The formation is believed to be dominated by a process in which two e^+s interact with a $\bar{p}$, such that one e^+ becomes bound and the second carries away excess momentum and energy. This process is expected to generate relatively weakly bound $\bar{H}$. We have found that, when using direct mixing, field-ionization of the weakly-bound $\bar{H}$ by the external electric fields, leads to radial redistribution of the $\bar{p}$s. We can use this effect to efficiently detect these weakly bound $\bar{H}$, by intentionally causing $\bar{p}$s at large radii in our trap to be lost on the introduction of a strong transverse octupole magnetic field and monitoring the losses. This technique, together with the direct detection of strongly-bound $\bar{H}$ (bound enough that it survives the various trap electric fields), allows us to measure the fraction of $\bar{H}$ formed in strongly-bound states. Since it is these states which survive the electric fields necessary for synthesis, they are those available for trapping if cold enough. Using this technique we can therefore optimize the synthesis for maximum generation of strongly-bound, potentially-trappable states, and hence increase the likelihood of trapping.

BP8 79 Energy Manipulation and Diagnostics of Charged Plasmas for Antihydrogen Production WILLIAM BERTSCHE, *University of Wales, Swansea* ALPHA COLLABORATION, In the focused efforts to trap antihydrogen for spectroscopic studies, currently proposed methods require the synthesis of antihydrogen atoms cold enough to be trapped in the relatively-shallow (1K) minimum-magnetic-field atom traps. Obviously the initial energy distribution and temperatures of the constituents of antihydrogen - positrons and antiprotons - are important to the final temperature of the anti-atoms formed. The techniques for cooling these particles, characterizing their distributions and maintaining desired distributions are important for the goal of anti-atom trapping. We present results from sensitive temperature measurement techniques based on particle dump profiles, and show progress towards cold particle distributions. Also, we have been able to directly tailor particle distributions by using an autoresonant-drive to tunably manipulate particle energies. Using these techniques, we have been able to tune our particle manipulation schemes to optimize production and maintenance of cold, non-neutral particles for use in production of antihydrogen.

BP8 80 Overview of recent results from non-neutral plasmas in the CNT stellarator* T. SUNN PEDERSEN, A.H. BOOZER, P.W. BRENNER, B. DURAND DE GEVIGNEY, M.S. HAHN, X. SARASOLA, A. SENTER, An overview of recent results from the Columbia Non-neutral Torus (CNT) will be given. CNT is a stellarator dedicated to studies of non-neutral and electron-positron plasmas [1]. CNT operates with a surplus of electrons – most of the time with only a trace amount of ions ($n_i/n_e < 1\%$), creating negative space potentials of several hundred volts despite having $T_e \approx 5$ eV [2]. This allows the study of neoclassical confinement with negative radial electric fields much larger than those that would arise from ambipolarity constraints, and also allows the study of pure electron plasmas in a minimum energy state. The overview will include results from studies of partially neutralized plasmas [3-5], recent improvements in confinement times, observations of transport jumps [6] and will give an update on our plans for the creation and study of pure electron plasmas. [1] T. Sunn Pedersen and A. H. Boozer, PRL **88** (2002) 205002 [2] J. P. Kremer *et al.*, PRL **97**, (2006) 095003 [3] P. W. Brenner *et al.*, this poster session [4] Q. R. Marksteiner *et al.*, PRL **100** (2008) 065002 [5] X. Sarasola Martin *et al.*, this poster session [6] M. S. Hahn et al., Phys. Plasmas **16** (2009) 022105

*Supported by NSF and DOE, grants NSF-PHY-04-49813 and NSF-PHY-06-13662.

BP8 81 Confinement of Pure Electron Plasmas in the Columbia Non-neutral Torus* P.W. BRENNER, T. SUNN PEDERSEN, M.S. HAHN, X. SARASOLA, *Columbia University* The plasmas studied in the Columbia Non-neutral Torus are uniquely different from non-neutral plasmas in other magnetic geometries. Confinement is primarily limited by transport resulting from insulating probes inserted into the plasma and electron neutral collisions. Recently the best measured confinement time has been increased by over an order of magnitude to 323 ms. The magnetic geometry allows for confinement of plasmas with arbitrary degree of neutralization but the geometry's complexity also introduces new challenges and sources of transport. An improved conducting boundary is being designed and installed to minimize potential variation along magnetic surfaces and externally diagnose the plasma. Three stellarator configurations can be studied in CNT by varying the angle between coils. Progress toward a comparison of each configuration will be presented. Methods to create plasmas unperturbed by internal rods and diagnose the plasma at or outside the edge are described and initial results are presented. A thorough understanding of these methods is a significant step towards the goal of studying electron-positron plasmas.

*Supported by the NSF CAREER Program, Grant no PHY-04-49813.

BP8 82 Numerical Studies of Transport in the Columbia Non-neutral Torus* BENOIT DURAND DE GEVIGNEY, THOMAS SUNN PEDERSEN, ALLEN H. BOOZER, *Columbia University* The Columbia Non-neutral Torus (CNT) is a stellarator dedicated to the study of non-neutral plasmas on magnetic surfaces. Due to space charge imbalance such plasmas exhibit a very large radial electric field. In the absence of parallel electric fields, the induced $\vec{E} \times \vec{B}$ rotation dominates over the radial magnetic drifts and closes the orbits. However the confinement of trajectories is sensitive to the electrostatic boundary conditions at the plasma edge. Variations of the electric potential on magnetic surfaces, inherent to the CNT equilibrium, can also lead to bad orbits. Insulated probes inserted into the plasma charge up negative and create large, localized potential variations leading to $\vec{E} \times \vec{B}$ plasma flow out of the confining region. A code was written to solve for the electric potential in CNT allowing for a large variety of boundary conditions and capable of resolving the perturbation of the probes. Using results from this code as input for a Monte-Carlo electron drift orbit code we study how these perturbations affect the loss rate of electrons at different magnetic field strengths, and we compare our results to experimental data.

*Supported by the NSF-DOE Partnership in basic plasma science, Grant no. NSF-06-13662.

BP8 83 First observations of partially neutralized and quasineutral plasmas in the Columbia Non-neutral Torus* XABIER SARASOLA, PAUL BRENNER, MICHAEL HAHN, THOMAS PEDERSEN, *Columbia University* The Columbia Non-neutral Torus (CNT) is the first stellarator devoted to the study of pure electron, partially neutralized and positron-electron plasmas. To date, CNT usually operates with electron rich plasmas (with negligible ion density) [1], but a stellarator can also confine plasmas of arbitrary degree of neutralization. In CNT the accumulation of ions alters the equilibrium of electron plasmas and a global instability has been observed when the ion fraction exceeds 10%. A characterization of this instability is presented in [2], analyzing its parameter dependence and spatial structure (non- resonant with rational surfaces). A new set of experiments is currently underway studying plasmas of arbitrary degree of neutralization, ranging from pure electron to quasineutral plasmas. Basic observations show that the plasma potential decouples from emitter bias when we increase the degree of the neutralization of our plasmas. Partially neutralized plasmas are also characterized by multiple mode behavior with dominant modes between 20 and 200 kHz. When the plasma becomes quasineutral, it reverts to single mode behavior. The first results on partially neutralized plasmas confined on magnetic surfaces will be presented. [1] J. Kremer, PRL 97, (2006) 095003 [2] Q. Marksteiner, PRL 100 (2008) 065002

*Supported by Fundación Caja Madrid and NSF-PHY-04-49813.

BP8 84 Electrostatic Charging of Insulating Rods and Resulting Particle Transport in the Columbia Non-neutral Torus* AARON SENTER, NIKOLAUS RATH, PAUL BRENNER, XABIER SARASOLA, THOMAS PEDERSEN, The Columbia Non-neutral Torus (CNT) is a stellarator created to study non-neutral plasmas confined on magnetic surfaces. To create and diagnose the electron plasma, filaments supported by ceramic rods are inserted into the plasma. These rods charge negatively allowing particles to $\vec{E} \times \vec{B}$ drift across the confining magnetic surfaces and out of the plasma. A simple model of this process has yielded good qualitative agreement with experimentally observed radial transport[1]. However, when the rod is retracted, it perturbs the plasma more than expected. To better understand the rod perturbations, externally biased conducting rods are now being used. We find the effect of the ceramic rods by measuring the increase in filament emission current with a rod installed. Comparing the radial transport rates of the ceramic and conducting rods, we aim to understand the charge distribution on the former, and to minimize the rod driven transport. Initial experiments show that a uniformly biased rod does not reproduce the transport observed. Experiments using a rod with a varying radial potential profile are being conducted and will be reported on. [1] J.W. Berkery *et al.*, Phys. Plasmas **14**, 062503 (2007).

*Supported by the NSF CAREER Program, Grant no PHY-04-49813.

BP8 85 Simulating the FTICR-MS signal of a decaying ^{7}Be Ion Plasma using a 2D PIC code M. TAKESHI NAKATA, GRANT W. HART, *Brigham Young University* BRYAN G. PETERSON, ROSS L. SPENCER, *Brigham Young University* Beryllium-7 (^{7}Be) decays only by electron capture into lithium-7 (^{7}Li) with a half life of 53 days. As a result, its decay rate varies with its environment. We desire to study the effect of ionization on its decay rate. We will do this by trapping a ^{7}Be ion plasma in a cylindrical Malmberg-Penning trap and measuring its and ^{7}Li's concentration as a function of time by using Fourier transform ion cyclotron resonance mass spectrometry (FTICR-MS). We use this ratio as a function of time to directly measure the decay rate of the confined ion plasma rather than using gamma detection. We have simulated these signals in a 2-dimensional electrostatic particle-in-cell (PIC) code. The two spectrum peaks merge at high densities and at low densities they can be resolved. The merged peak linearly shifts with the relative abundances of these species. We have also simulated singly-ionized beryllium-7 hydride (^{7}BeH$^+$) and ^{7}Li ion plasmas at high densities. These two separate peaks shift according to their relative abundances. We have developed an analytical model that explains how these peaks shift with their relative abundances.

BP8 86 Theory and simulation of m=0 Bernstein modes in a non-neutral plasma GRANT W. HART, ROSS L. SPENCER, M. TAKESHI NAKATA, *Brigham Young University* Axisymmetric upper-hybrid oscillations have been known to exist in non-neutral plasmas and FTICR/MS devices for a number of years. However, because they are electrostatic in nature and axisymmetric, they are self-shielding and therefore difficult to detect in long systems. When non-zero temperature is included the modes become analogous to Bernstein modes in slab geometry. Using a kinetic theory model We have analyzed the theory of these modes in a rigid-rotor thermal equilibrium. We find that in the central region (where the density is constant) the perturbed velocity is proportional to the Bessel function $J_1(\alpha r)$, with α having a distinct value for each mode. We have simulated these modes in our $r - \theta$ particle-in-cell code that includes a full Lorentz-force mover and find that in a mostly flat-top plasma the perturbed velocity closely matches this theoretical prediction. The dispersion relation derived from the theory also matches the values of ω and α seen in the simulation. There are still a few unresolved difficulties with the model. First, it is difficult to find the appropriate boundary condition to apply at the plasma edge. Second, the fundamental mode is undamped but all higher modes appear to be Landau damped. Progress in understanding these issues will be discussed.

BP8 87 Characterization of an ion trap to be used to determine the decay rate of ionized beryllium-7 BRYAN G. PETERSON, DANIEL ERICKSON, GRANT W. HART, *Brigham Young University* Beryllium-7 is an isotope with a 53-day half-life that decays exclusively by electron capture. The decay rate can be modified by changing the electron configuration, and the availability of electrons for capture. All previous measurements of the half-life were made with the Be-7 atoms embedded in a matrix of some kind that resulted in significant and not well characterized modifications to the electron configuration. We are building an ion trap to study the rate of decay of singly-ionized Be-7 to determine the rate when the electron configuration is well known. We are using a boron carbide plasma to characterize the behavior of the trap. The presence of boron-10, boron-11, and carbon-12 will also allow us to determine the resolution and sensitivity of the Fourier Transform Ion Cyclotron Resonance Mass Spectrometry technique that will be used to monitor the conversion of the Be-7 to Li-7 and to determine the half-life. The results of this characterization will be presented.

BP8 88 Autoresonant transition in the presence of noise and self-fields* IDO BARTH, *Hebrew University of Jerusalem* A sharp threshold on the driving amplitude for transition to adiabatic nonlinear phase-locking (autoresonance) is characteristic of a single, electrostatically trapped particle starting in equilibrium and driven by a chirped frequency perturbation. In the presence of a weak noise or a small temperature (T) initial distribution of trapped particles, the threshold develops a width, scaling as $T^{1/2}$. The inclusion of repulsive self-fields makes the width of the autoresonant transition narrower.

*Supported by the Israel Science Foundation, Grant No. 1080/06.

BP8 89 Measuring transport in a toroidal electron plasma* J. SMONIEWSKI, M.R. STONEKING, F. CHOUDHURY, E. FRATER, *Lawrence University* Global confinement times in excess of one second have been measured in the Lawrence Non-neutral Torus II using the frequency of the $m = 1$ diocotron mode as a diagnostic, coupled with modeling of the toroidal modifications of that mode. We now report measurements (and modeling) of the $m = 2$ mode frequency, which yields a measure of the average electron number density. The combined information provided using both modes permits the first measurements of transport rates in this experiment. Transport is initially faster than the previously reported global confinement times. We also report on initial experiments in which the plasma is allowed to expand from a 270° toroidal arc (in which all previous experiments were conducted in this device) into a fully toroidal (closed field line) trap.

*This work is supported by National Science Foundation Grant PHY-0812893.

BP8 90 Constraints on an empirical flux equation for asymmetry-induced transport* D.L. EGGLESTON, *Occidental College* Despite a large body of experimental work on asymmetry-induced transport, the correct theory remains elusive. We are currently developing an empirical model of the transport with an eye toward providing guidance for further theoretical development. In previous work[1] we have shown that the flux equation for the transport is empirically constrained to be of the form $\Gamma(\epsilon) = -(B_0/B)^{1.33} D(\epsilon)[\nabla n_0 + f(\epsilon)]$, where $\epsilon = \omega - l\omega_R$, ω is the asymmetry frequency, ω_R the plasma rotation frequency, l the azimuthal mode number, B the magnetic field, n_0 the density, B_0 an empirical constant, and $D(\epsilon)$ and $f(\epsilon)$ are unknown functions. To gain information about $D(\epsilon)$ and $f(\epsilon)$, we have examined data near the $\epsilon = 0$ point and compared it to a first order expansion of $\Gamma(\epsilon)$. This analysis shows that $dD/d\epsilon(0) \neq 0$, in contradiction to resonant particle theory[2]. We also find that $f(\epsilon)$ can only be a fraction of the size predicted by that theory, and that $dD/d\epsilon(0)$ is an increasing function of radius and scales with the inverse of the center wire bias. This last result suggests that ϵ may be scaled by ω_R rather than the axial bounce frequency.

*Supported by DOE grant DE-FG02-06ER54882

[1]D. L. Eggleston and J. M. Williams, Phys. Plasmas 15, 032305 (2008).
[2]D. L. Eggleston and T. M. O'Neil, Phys. Plasmas 6, 2699 (1999).

BP8 91 Experimental conditions to realize characteristic parameters of strongly coupled fine particle plasmas: An inverse problem* HIROO TOTSUJI, *Okayama Univ* Statistical properties of fine particle plasmas are characterized by dimensionless parameters such as strength of coupling. When the experimental conditions of density and temperatures are known, the dimensionless parameters are readily computed. However, it is straightforward to determine experimental conditions to realize a given combination of dimensionless parameters including charging condition of fine particles. In this presentation, we solve this inverse problem as much as possible analytically and give typical example by finally resorting to numerical methods[1]. The dependency of experimental conditions on various dimensionless characteristic parameters is obtained and it is shown that there exists a domain of dimensionless parameters where experimental conditions do not exist. We also analyze the dependency on species of neutral atoms. The results may be helpful to observe various phenomena related to the strong coupling between fine particles including possible existence of the critical point. [1] Earlier results have been given in, H. Totsuji, Plasma and Fusion Research, 3, 046(2008).

*Supported by the Grant-in-Aid for Scientific Research (C) of JSPS 21540512.

BP8 92 Theory of arbitrary amplitude dust ion-acoustic shock waves in a multi-ion dusty plasma* A.A. MAMUN, *Jahangirnagar University, Dhaka, Bangladesh* BENGT ELIASSON, PADMA K. SHUKLA, *Ruhr-University Bochum, Germany* We present a theory for arbitrary amplitude dust ion-acoustic shock waves in a multi-ion dusty Plasma, composed of electrons, light positive ions, heavy negative ions, and stationary massive dust grains. For this purpose, the coupled Poisson and dust-charging equations, which accounts for the fluctuation of charges on static dust, is solved numerically. We find that large amplitude shocks are associated with a sudden decrease of the electrostatic potential and of the dust grain charge. In the lower speed limit small amplitude shocks, which are smoother in space, are formed, but in the larger speed limit large amplitude shocks with sharper fronts are formed. It is anticipated that the profiles and amplitudes of the DIA shocks predicted here will be observed in forthcoming laboratory and space experiments.

*This work was partially supported by the DFG through the Research Unit 1048 and by the Swedish Research Council (VR).

BP8 93 Direct measurement of the out-of-plane (optical) phonon spectrum in a 2D complex plasma crystal L. COUEDEL, V. NOSENKO, S.K. ZHDANOV, A.V. IVLEV, H.M. THOMAS, G.E. MORFILL, *Max-Planck Institute for Extraterrestrial Physics* The out-of-plane phonon spectrum of a 2D complex plasma crystal in the sheath of a RF discharge was measured using a novel imaging technique that allowed us to resolve the particle motion in the 3 dimensions. The out-of-plane mode was proven to have negative optical dispersion, as predicted a long time ago. Comparison with theory showed a remarkably good agreement. The effect of the plasma wakes on the dispersion relation is discussed.

BP8 94 Effect of a floating circular aperture on a dc glow discharge dusty plasma* JONATHON R. HEINRICH, SUHYUN KIM, ROBERT L. MERLINO, *University of Iowa* We have investigated novel effects observed when a floating aperture, either 6 mm or 8 mm in diameter, is placed 1-2 cm in front of an anode disk (4 cm diameter) that is used to form a dc glow discharge dusty plasma. Dust is incorporated into the anode glow plasma from a tray located below the anode which contained kaolin powder. The glow discharge traps particles with an average size of 1 micron. When the aperture is placed in front of the disk, well-defined pear-shaped or spherical dust clouds are formed, depending on the diameter of the aperture and its distance from the anode. The dust interacts with the aperture through the potential structure associated with the floating (negative) plate in which the aperture is located. The dust cloud is imaged using a CCD camera and a thin sheet of 532 nm laser light. Some of the effects observed include: outwardly expanding spherical dust acoustic waves and shocks, dust rotation around a void formed at the aperture, and a dust/discharge instability in which the discharge is periodically quenched and reignited while the dust cloud expands and contracts, with the dust retaining a residual charge.

*Work supported by DOE

BP8 95 Thermal Characteristics of Dust Particles in Complex Plasmas with Dust Acoustic Waves* R. FISHER, E. THOMAS, *Auburn University* In a complex (dusty) plasma, charged micron-sized particles are suspended in a dc glow discharge plasma. The velocity space distribution of particles in the dust cloud was measured using stereoscopic particle image velocimetry (StereoPIV). As has been shown previously [J. Williams and E. Thomas, Jr, *Phys Plasmas*, **14**, 063702 (2007)] the velocity distribution of stable dust clouds can be modeled with a maxwellian distribution function, from which a characteristic kinetic temperature of the dust cloud can be obtained. In this study, the velocity distribution of dust particles was measured in dusty plasmas which contained driven dust acoustic waves (DAW). It was found that the measured velocity distributions of regions of the dust cloud containing DAW could not be adequately described by a maxwellian distribution function. This presentation describes the first attempts to find and interpret a suitable alternative velocity distribution model.

*This work is supported by the NSF-DOE Partnership in Basic Plasma Science and Engineering, NSF grant number: PHY-0810419

BP8 96 A Proposed Magnetized Dusty Plasma User Facility E. THOMAS, *Auburn University* R.L. MERLINO, *University of Iowa* M. ROSENBERG, *University of California - San Diego* As the experimental study of dusty (complex) plasmas has advanced over the last two decades, a great deal of new insight has been gained on the complex interaction between the background plasma and charged microparticles. Even through the charged dust grains in a typical experiment can acquire several thousand elementary charges, the large mass of the grains ensures that the charge-to-mass ratio is quite low. As a result, it has been considered experimentally challenging to design an experiment that can achieve full magnetization of ions, electrons, and the charged dust grains. However, with continuing improvements in magnet design and sub-micron particle imaging technologies, it is now possible to contemplate the development of a Magnetized Dusty Plasma Facility. This presentation discusses the design, experimental parameters, and scientific motivation for a flexible, superconducting, 4 Tesla magnetic field user facility for the study of magnetized dusty plasmas. This work is supported by NSF grant number PHY-0936470 (AU), DOE Grant No. DE-FG01-04ER54795 (UI) and DOE Grant No. DE-FG02-04ER54804 (UCSD)

BP8 97 Applying PIV analysis techniques to complex plasmas: reduced gravity and phase transition experiments* C. RÄTH, *MPE* E. THOMAS, *Auburn University* J. WILLIAMS, *Wittenberg University* M. THOMA, S. MITIC, L. COUEDEL, H. THOMAS, M. CHAUDHARI, *MPE* Particle image velocimetry (PIV) techniques have been applied to studies of complex (dusty) plasmas for over a decade. In these previous investigations, measurements were performed using specialized hardware configured specifically for PIV. However, with the increasing use of higher speed video imaging, i.e., in excess of 100 frames per second, it is possible to apply PIV analysis techniques directly to video data. This presentation will discuss techniques used to benchmark and validate the use of PIV in this manner. Then, it will describe recent applications of PIV to reduced gravity and phase transition measurements in complex plasmas. It is shown that PIV can reveal detailed information on particle flows and waves in these systems.

*This work is supported by the NSF-DOE Partnership in Basic Plasma Science and Engineering and by the DLR.

BP8 98 Preliminary measurements of thermal effects in the dust acoustic wave JEREMIAH WILLIAMS, *Wittenberg University* A complex (dusty) plasma (CDP) is a four-component system composed of ions, electrons, neutral particles and charged microparticles. The presence of the microparticles gives rise to new

plasma phenomena, including collective modes such as the dust acoustic wave. Recent measurements of the dispersion relationship of this wave mode [E. Thomas, Jr., *et. al.*, Phys. Plasmas 14, 123701 (2007), J.D. Williams, *et. al.*, Phys. Plasmas 15, 043704 (2008)] have shown that, over a range of neutral gas pressures, it is necessary to include thermal effects to accurately fit the measured dispersion relations. In this work, initial measurements of the dispersion relation in a new dusty plasma experiment, the Wittenberg University DUsty Plasma Experiment (WUDUPE), will be presented. In particular, the dependence of the kinetic dust temperature on the neutral gas pressure will be presented.

BP8 99 Non-ideal Effects on Drift Wave Instabilities in Magnetized Inhomogeneous Dusty Plasma ENRIQUE CASTRO, JULIO PUERTA, PABLO MARTIN, *Universidad Simon Bolivar, Depto. Fisica, Apdo. 89000, Caracas, Venezuela* Low-frequency drift wave instabilities, for perpendicular propagation, on magnetized inhomogeneous dusty plasmas are analyzed, considering a temperature gradient and using a kinetic treatment. The growth rate of the instabilities has been determined by using a four poles two-point quasi-rational approximation for the plasma dispersion function. For large grain radius or high particle densities, the non-ideal effects in the state equation can be considered and described by the Ree and Hoover Pade's type state equation. The contribution of non-ideal effects is analyzed for different plasma parameters such as temperature ratios, particle drift velocities, dust charge and mass values. Fluctuating charge effects are not considered in this work. Our results are compared with those where ideal contributions are considered.

BP8 100 Phase Transition Studies for Conducting Dust in a GEC Reference Cell JORGE CARMONA REYES, TRUELL HYDE, LORIN MATTHEWS, DAVID GEORGE, MIKE COOK, *CASPER - Baylor University* JIMMY SCHMOKE, *CASPER-Baylor University* Dust particles immersed in plasma typically acquire a negative charge. The resulting Yukawa interaction between grains in a two-dimensional horizontal layer leads to the formation of disordered or ordered structures depending on whether short or long range ordering dominates, as determined by the ratio of the particle's interparticle potential energy to its average kinetic energy. Various stable crystalline phases have been observed experimentally for dust particles residing within such two-dimensionally extended lattice planes with system dynamics driven in large part by particle charge. Although the charging process for insulating materials has been examined in some detail, conducting materials have not yet been fully investigated. This work experimentally examines the phases and phase transitions for both conductive (gold coated) and non-conductive (melamine formaldehyde) particles. Phase maps for each type of particle are obtained using data from pair correlation functions and voronoi diagrams for dust structures formed over a range of pressures and powers within a standard GEC reference cell.

BP8 101 Dust Particle Probes in a Complex Plasma ANGELA DOUGLASS, TRUELL HYDE, LORIN MATTHEWS, MICHAEL POPE, BERNARD SMITH, *CASPER - Baylor University* In dusty plasma experiments within a GEC rf reference cell, the confining potential is generally assumed to be parabolic. The validity of this assumption can be tested in a number of ways. One noninvasive method is to utilize the particles themselves as system probes. In this experiment a cw laser (0.1-5W, 532nm) was used to apply a radiation pressure force on a single MF particle. The particle's trajectory while the laser was on and off was recorded and the confining potential calculated. System power, pressure, DC bias, and cutout size of the plate placed on the powered electrode were varied in order to better understand their effects on the shape of the confining potential.

BP8 102 Measurements within a GEC rf Reference Cell JAMES CREEL, TRUELL HYDE, LORIN MATTHEWS, DAVID GEORGE, JORGE CARMONA REYES, *CASPER - Baylor University* BROOKS McMASTER, KE QIAO, MIKE COOK, JIMMY SCHMOKE, *CASPER-Baylor University* Since its introduction, the GEC rf Reference Cell has provided a baseline for comparison among various experiments performed within the complex (dusty) plasma community. The GEC cell, while providing for data comparison between systems due to its standardized design, does not exist without some variation between cells. In this work, two GEC rf Reference Cells located within the CASPER Hypervelocity Impacts & Dusty Plasmas Lab will be utilized to examine variations in operating parameters. Both standard analysis and Langmuir probe techniques will be employed in an attempt to gain insight into the experimental workings of a standard GEC rf Reference Cell.

BP8 103 Studying the interaction between two dust clouds of differently sized particles in complex plasma STEPHEN PICKETT, *CASPER, Baylor University, Waco, TX 76798, USA* VICTOR LAND, DIVYAPRAKASH SINGH, *Participant in Baylor University's High School Scholars Summer Research Program* DIANA BOLSER, *Participant in Baylor University's NSF Research Experience for Undergraduates Program* LORIN MATTHEWS, TRUELL HYDE, CASPER TEAM, Dust particles levitate in the sheath of an argon RF discharge in a modified GEC cell. Radial confinement is created by a circular cutout in a top-plate covering the lower electrode. By using differently sized MF particles, two 2D dust crystals are formed, levitated at different heights. By heating or cooling the lower electrode, the crystals are moved relative to each other by thermophoresis. When the crystals are far apart, two vertically aligned layers are visible. Upon approach, layer-splitting occurs and a *zig-zag* pattern appears. Upon further compression, longer aligned chains form. This behavior is studied using experimental data, as well as by using a combination of a fluid model and N-body code.

BP8 104 Effects of rotating dust grains on the instability of dust-acoustic waves in a complex Lorentzian plasma* MYOUNG-JAE LEE, KYU-SUN CHUNG, *Hanyang University* Charged non-spherical dust grains can rotate due to the interaction with surrounding plasmas or oscillating electric field. The rotational effect will modify the conventional plasma wave dispersion relations. In this work, the growing of dust-acoustic wave is investigated in the presence of the rotating dust grains in a complex Lorentzian plasma. Full spectrums of the growth rate of the dust-acoustic wave is obtained and the effect of dust grain rotation is discussed. The Lorentzian plasma effect on the growth rate is also analyzed. The growth rate was found to be enhanced by the rotation of dust grains, but suppressed by the Lorentzian plasmas.

*This research was supported by National R&D Program through the National Research Foundation of Korea (NRF) funded by the Ministry of Education, Science and Technology (Grant No. 20090082669 and No. R11-2008-072-02002-0).

BP8 105 The Dust Accelerator Facility at CCLDAS ANTHONY SHU, E. GRUN, M. HORANYI, S. LEBLANC, T. MUNSAT, S. ROBERTSON, R. SRAMA, Z. STERNOVSKY, E. THOMAS, M. WAGNER, T. WINGFIELD, *University of Colorado* AND THE CCLDAS TEAM, The lunar surface is continually bombarded with micrometeorites, primarily within the 0.1-1 μm and $\leqslant$ 100 km/s range. The impacts of such particles at the lunar surface introduce significant potential hazards to humans and instruments, but also create a scientifically rich complex system. Upon impact into the lunar regolith, cratering and micro-plasma creation can lead to liberation of many families of materials in to the charged lunar dusty plasma. To address the many scientific and technical questions surrounding the hypervelocity micrometeorites at the lunar surface, we describe an accelerator facility based on nuclear accelerator techniques, to be constructed at the Colorado Center for Lunar Dust and Atmospheric Studies at the University of Colorado. Key technical features of the 3 MV electrostatic accelerator include 1) high achievable charge and mass, up to realistic micrometeorite parameters, 2) precise selection of particle size and velocity for high experimental control, 3) high repetition and data acquisition rates. We present technical details of the accelerator and a description of the scientific questions to be addressed at such a facility within the Center.

BP8 106 Parametric Effects on the Charging of Dust in Plasma B.K. SAIKIA, S.S. KAUSIK,*M. CHAKRABORTY, B. KAKATI, *Centre of Plasma Physics, Nazirakhat, Sonapur-782402, Kamrup, Assam, India* M. BANDYOPADHYAY, *Institue for Plasma Research, Bhat, Gandhinagar-382428, Gujarat, India* This work reviews some recent experiments from the Centre of Plasma Physics on the charging of dust in plasma. Dust particles are produced *in-situ* by heating silver in a Tantalum boat at reduced pressure. They enter the plasma in the form of a dust beam due to differential pressure between the oven and the plasma chambers. A magnetic cage confines plasma produced by filament heating. The dust beam ultimately enters a deflection chamber where it is deflected and allowed to hit a collector plate. From this arrangement the charge accumulated on the dust is estimated. A Faraday cup with an electrometer measures the dust current ($\sim$ pA). We present the effects of discharge current and electron temperature. The charge distribution in the dust beam is also presented. Lastly, an experiment to coat tungsten dust particles with Cesium vapour is described. These Cesium coated tungsten dust produces negative hydrogen ions in hydrogen plasma, which could be useful in the Neutral Beam Injection in fusion plasma.

*membership pending

BP8 107 Time-resolved Schlieren imaging of electrohydrodynamic interaction induced by a dielectric barrier discharge* SIROUS NOURGOSTAR, NOAH HERSHKOWITZ, *University of Wisconsin-Madison* Commercially available transparent conducting electrodes provide an inexpensive way to investigate different configurations of dielectric barrier discharges (DBD), including so called plasma actuators. Although operation of atmospheric DBDs in a diffuse mode has been reported, they ares limited to very restricted range of operational parameters including the gas flow rate. In addition to diffuse and filamentary modes, there exists a patterned mode which like the diffuse one, is also severely limited by operational constraints. In the experiment, spatial and temporal evolution of both flow and plasma fields in parallel, tilted plate and asymmetric plasma actuator geometries are analyzed by the Schlieren method, and using gated intensified CCD.

*This work supported by NASA grant No.NNX07AB84A and Air Force Office of Scientific Research grant No.FA9550-07-1-0025.

BP8 108 Enhancement of electric force on ions by ion - neutral collisions* GENNADY MAKRINICH, AMNON FRUCHTMAN, *H.I.T. - Holon Institute of Technology* The force exerted by a radially-outward plasma and neutral flow from a Radial Plasma Source (RPS) [1], is measured. From the measured force, the electric force exerted on the ion flow by the applied electric field is deduced. This force is found to be larger than the electric force that can be exerted if the ions are collisionless. In addition, the increase of the gas pressure is found to result in an increase of the electric force despite a simultaneous decrease of the deposited electric power. Employing a simple model, we argue that these experimental findings result from the electric force being felt by the ions for a longer time; their residence time in the acceleration region is increased due to their slowing-down collisions with neutrals. In separate experiments, when no magnetic field is present, a plasma ball is formed, attached to the anode. We measure the force exerted by the plasma and neutrals flowing away from the ball. We relate the measured force to the estimated density and temperature of the plasma of the plasma ball. [1] G. Makrinich and A. Fruchtman, Phys. Plasmas **16**, 043507 (2009).

*This research has been supported by the Israel Science Foundation (Grant no. 864/07).

BP8 109 Controlling synthesis of carbon nanostructures by plasma means in arc discharge OLGA VOLOTSKOVA, ALEXEY SHASHURIN, JON TORREY, *GWU* YEVGENY RAITSES, *PPPL* MICHAEL KEIDAR, *GWU* Thermal stability of SWNTs at conditions of atmospheric arc is crucial for determination of region of their synthesis in arc and in general for clarification of the thermal regime of SWNT in arc plasmas. We investigated electrical resistance dependence on temperature of mats of SWNTs under variable pressures in helium atmosphere, in the air and in vacuum in high temperature ranges (300-1200K) which closely mimic conditions during the synthesis in arc discharge. Dependence of SWNT resistance on temperature exhibits similar "V-shape" behavior for all applied conditions which characterized by two temperatures: Tmin (temperature of the minimum of resistance) and Tcr (temperature of destruction of SWNT bundles). It is found that Tmin and Tcr increased with helium pressure, so that at 500 Torr Tcr was 1100K, while Tmin -900K. This is the temperature that corresponds to buffer region between the arc plasma and helium background in arc discharge. Based on that it can be suggested that region of formation of SWNTs in arc should be close to arc periphery. Our study also demonstrates a strong effect of electric and magnetic fields on properties and growth conditions of SWNTs and other carbon nanostructures such as graphene. These effects are quantified by variety of diagnostics tools: SEM, TEM, AFM - microcopies, TGA, RAMAN and UV-vis-NIR.

BP8 110 Particle-in-cell simulations of electron transport in complex shape dc discharges* ALEXANDER V. KHRABROV, IGOR D. KAGANOVICH, YEVGENY RAITSES, VLADIMIR I. DEMIDOV, DMYTRO SYDORENKO, *PPPL* A region of dc discharge near cathode, or negative glow, exists in very nonequlibrium state. Three distinct groups of electrons play different roles in discharge self-organization [1]: 1) fast electrons from cathode produce ionization; 2) very cold trapped electrons make up the plasma density; and 3) intermediate electrons conduct the current. These non-equilibrium conditions provide considerable freedom to choose optimal plasma parameters for many applications by controlling electron energy distribution function (EEDF). The EEDF modification is achieved by making use of additional biased electrodes or cathode voltage forms in afterglow [2]. We have performed particle-in-cell simulations in 1 and 2D geometry to demonstrate possible control of EEDF. This work was supported by AFOSR through STTR contract. [2] V.I. Demidov, C.A. DeJoseph, and V. Ya. Simonov, Appl. Phys. Lett. **91**, 201503 (2007).

*This work was supported by AFOSR through STTR contract.

BP8 111 Structure and stability of relativistic two-fluid electron-positron jets JESSE PINO, HUI LI, *Los Alamos National Laboratory* SWADESH MAHAJAN, *Institute for Fusion Studies, University of Texas at Austin* Magnetized, rotating compact objects can launch jets with large Lorentz factors. Using a temperature-transformed magnetofluid coupling formalism, we derive the relativistic two-fluid equations in vortex form. For the case of homentropic pair plasmas, we find analytic self-organized solutions in cylindrical geometry. Various temperature, density and Lorentz factor profiles are considered. We compare these solutions to previous jet models, focusing on magnetic tower type jets with an external return current. Finally, we investigate the stability of the equilibria to MHD and two-fluid perturbations.

SESSION BM9: MINI-CONFERENCE ON INNOVATIVE MAGNETIC MIRROR CONCEPTS AND APPLICATIONS I

Monday Morning, 2 November 2009
The Learning Center at 9:30
Xianzhu Tang, Los Alamos National Laboratory, presiding

9:30

BM9 1 Innovative Magnetic Mirror Concepts* THOMAS SIMONEN, MIRROR STUDY GROUP COLLABORATION, In the past two decades, while magnetic mirror research in the US was curtailed, several innovations have been proposed and many have been demonstrated in Japan and Russia in the Gamma 10 and GDT experiments. These advances have led to new scientific understanding, means of overcoming previous short comings, and reconsideration of magnetic mirror systems as a modest size material testing neutron source or as a fusion- fission hybrid system. Compared to toroidal systems, the linear geometry of mirror systems has the significant advantages of easing construction, operation and maintenance, but has a less developed data base. The recent innovations include reliance on axi-symmetric mirror coils, suppression of energetic-ion cyclotron-modes with potential confined warm plasma, and sheared ExB flow stabilization of drift waves. To enable increased electron temperature, the magnetic field expansion ratio from the mirror to the end wall is increased beyond the square root of the ion to electron mass ratio. This expansion inhibits electron thermal conduction, reduces the incident wall power flux to low levels, and isolates plasma-wall interactions far from the confined plasma.

*Supported in part by DOE - ORAU.

10:00

BM9 2 MHD-stable axisymmetric mirrors DMITRI RYUTOV, *Lawrence Livermore National Laboratory* The traditional way of making MHD-stable mirror configurations is to use quadrupolar magnets. This approach indeed provides stability, but only at the cost of creating complex three-dimensional plasma equilibria, with a number of undesirable features like enhanced cross-field transport, lower magnetic field, and engineering complexity. Over the years, numerous ideas have been suggested for achieving the MHD stability in axisymmetric mirrors. Some of them have been successfully tested experimentally. In this paper, a brief summary of various approaches to the axisymmetric mirror stability will be made that will include: stabilization by sloshing ions, non-paraxial stabilization, the use of magnetic divertors, sheared plasma rotation, and enhanced line-tying stabilization. Wherever possible, relation to existing experiments will be made. The general conclusion is that there are ways of providing MHD stability of the reactor-relevant plasma in axisymmetric mirrors. Prepared by LLNL under Contract DE-AC52-07NA27344.

10:30

BM9 3 Present status of the GAMMA 10 and future plan in University of Tsukuba TSUYOSHI IMAI, MAKOTO ICHIMURA, YOUSUKE NAKASHIMA, MASAYUKI YOSHIKAWA, ISAO KATANUMA, TSUYOSHI KARIYA, HITOSHI HOJO, RYUTARO MINAMI, YOSHIAKI MIYATA, YUUSUKE YAMAGUCHI, HIROYUKI SHIDARA, *Plasma Research Center, University of Tsukuba* GAMMA 10 TEAM, The studies of the formation of ion confining potential, the central electron heating, the suppression of drift type fluctuations by the ECH and various collaborative works have been carried out in the GAMMA 10 tandem mirror device. With high power plug ECH up to $\sim$ 500 kW, the ion confining potential of more than 2 kV was achieved. The drift type low frequency fluctuations were suppressed by the potential produced with plug ECH. The best central EC heating was observed with 100% X-mode excitation. The development of a gyrotron, the key tool of these ECH experiments, has been made in collaboration with NIFS (National Institute for Fusion Science), JAEA (Japan Atomic Energy Agency) and TETD (Toshiba). The plan of the new mirror program with modification of GAMMA 10 is in progress. The new program includes the physics studies of the divertor plasma and SOL plasma relevant to torus plasmas like ITER. The high heat flux experiments using the open end mirror throat and the edge physics with introduction of the divertor coil are in consideration.

11:00

BM9 4 Potential and density fluctuation suppressions by the potential formation and the newly installing Thomson scattering system in GAMMA 10 M. YOSHIKAWA, Y. MIYATA, M. MIZUGUCHI, N. IMAI, H. HOJO, M. ICHIMURA, T. KARIYA, I. KATANUMA, Y. NAKASHIMA, R. MINAMI, H. SHIDARA, Y. YAMAGUCHI, Y. SHIMA, Y. OHNO, F YAGUCHI, T. IMAI, *Univ. Tsukuba* K. KAWAHATA, I. YAMADA, H. FUNABA, *NIFS* Suppression phenomena of the potential and density fluctuation were clearly observed when the confinement potentials were produced by the application of electron cyclotron heating (ECH) in the tandem mirror GAMMA 10. We study the correlation between the suppression levels of both potential and density fluctuations and the effects of formed confinement potentials. Moreover, we show that the radial anomalous transport induces the radial particle transport which is estimated by the phase difference between the potential and density fluctuations obtained by using the gold neutral beam probe. We are now planning to measure the electron temperature by using a Thomson scattering system in GAMMA 10 by the collaboration with NIFS. In recent years, the direct electron heating experiments by central cell ECH have been carried out. The highest electron temperature, about over 500 eV, was estimated by a soft x-ray measurement. We will make a cross-check with the newly installing Thomson scattering system for more reliable data evaluation.

11:30

BM9 5 The Maryland Centrifugal Experiment* RICHARD ELLIS, ADIL HASSAM, *University of Maryland* The Maryland Centrifugal Experiment(MCX) produces supersonically rotating plasmas in a mirror geometry with a radial electric field produced by a coaxial core biased at high voltage. MCX has achieved high density (n> 10**20 m-3) fully ionized plasmas rotating with velocities of ~ 100 km/sec for times exceeding 8 ms under a wide range of conditions. Ion temperatures are 30 eV and confinement times ~ 100 microseconds. Sonic mach numbers are 1-3 and Alfven mach numbers somewhat less than 0.5; the maximum rotational velocity may be limited by the critical ionization velocity. MCX has achieved its major goals including the demonstration of supersonic rotation, radial velocity profiles with shear sufficient for MHD stability, overall MHD stability, and centrifugal confinement in the axial direction. Upgrade plans include a larger diameter vessel, higher field magnets, and higher discharge voltages. Possible applications to larger experiments will be discussed.

*Work supported by USDOE.

12:00

BM9 6 The GDT-based 14MeV neutron source for fission fuel systems ALEXANDER IVANOV, *Budker Institute of Nuclear Physics, Novosibirsk* BUDKER INSTITUTE OF NUCLEAR PHYSICS, NOVOSIBIRSK TEAM, The gas dynamic trap (GDT) is an axisymmetric mirror device with a high mirror ratio and with a mirror to mirror length exceeding a mean free path for the ion scattering into loss cone. A version of GDT with multi-component plasma was proposed for generation of high D-T neutron flux in localized zones to serve the needs of fusion material tests [1]. Conceptual studies demonstrated that the D-T neutron flux would reach ~ 2MW/m^2 in these zones if the device consumes 60MW. This approach can only be realized if the high beta plasma in the GDT with anisotropic fast ions is stable against MHD and kinetic instabilities. This has been already proven both theoretically and experimentally. Recently, application of the GDT neutron source as a driver for a fission –fusion hybrid and minor actinides burner was considered. This requires certain modifications to be introduced into the initial approach, since then overall efficiency of the driver becomes important. These physical and technical modifications are discussed in the paper. [1] I.A.Kotelnikov,V.V.Mirnov, V.P.Nagorny, D.D.Ryutov, In: Plasma Phys. Controll. Fusion Res., **2,** IAEA, Vienna, p.309, 1985

SESSION CI2: ACCELERATORS, BEAM DYNAMICS AND RADIATION

Monday Afternoon, 2 November 2009; Centennial I at 14:00; Joe Kwan, Lawrence Berkeley National Laboratory, presiding

14:00

CI2 1 Beam dynamics of NDCX-II, a novel pulse-compressing ion accelerator.*

ALEX FRIEDMAN, *LLNL & Heavy Ion Fusion Science VNL*

The near-term mission of the Heavy Ion Fusion Science Virtual National Laboratory (HIFS-VNL, a collaboration of LBNL, LLNL, and PPPL) is to study Warm Dense Matter (WDM) at ~ 1 eV in thin foils heated volumetrically by ion beams. An emerging mission is ion-direct-drive target physics for inertial fusion energy. These goals (especially the WDM mission) require rapid target heating. Beam bunch compression factors exceeding 50 are routinely achieved on the Neutralized Drift Compression Experiment (NDCX) at LBNL. The next facility for this research program, NDCX-II, will employ a unique approach to ion beam acceleration and pulse compression. Using modified induction cells from the decommissioned Advanced Test Accelerator at LLNL, NDCX-II will compress pulses of singly-charged Lithium ions from ~ 500 ns to ~ 1 ns as they are accelerated to 3-4 MeV. The required ~ sixfold speed-up and ~ hundredfold spatial compression are to be accomplished in ~ 15 m. The beam dynamics employs the strong longitudinal space charge field to halt, and then reverse, an initially imposed pulse compression. This initial compression enables efficient use of the Volt-seconds in the downstream induction cells. Those cells impose further acceleration and the head-to-tail velocity gradient that enables a final neutralized drift compression and focus onto the target. Discrete-particle simulations (1-D, 2-D, and 3-D) have been used to develop the "physics design" for NDCX-II. We present the elements of the design, and our progress toward building this machine at LBNL.

*This work was performed under the auspices of the USDOE by LLNL under Contract DE-AC52-07NA27344, by LBNL under Contract DE-AC02-05CH11231, and by PPPL under Contract DE-AC02-76CH03073.

14:30
CI2 2 Physics of neutralization of intense charged particle beam pulses by a background plasma.*
IGOR KAGANOVICH,† *PPPL*

Neutralization and focusing of intense charged particle beam pulses by a background plasma forms the basis for a wide range of applications to high energy accelerators and colliders, heavy ion fusion, and astrophysics. From the practical perspective of designing advanced plasma sources for beam neutralization, a robust theory should be able to predict the self-electric and self-magnetic fields during beam propagation through the background plasma. The major scaling relations for the self-electric and self-magnetic fields of intense ion charge bunches propagating through background plasma have been determined taking into account the effects of transients during beam entry into the plasma, the excitation of collective plasma waves, the effects of gas ionization, finite electron temperature, and applied solenoidal and dipole magnetic fields. Accounting for plasma production by gas ionization yields a larger self-magnetic field of the ion beam compared to the case without ionization, and a wake of current density and self-magnetic field perturbations is generated behind the beam pulse. A solenoidal magnetic field can be applied for controlling beam propagation. Making use of theoretical models and advanced numerical simulations, it is shown that even a small applied magnetic field of about 100G can strongly affect beam neutralization. It has also been demonstrated that in the presence of an applied magnetic field the ion beam pulse can excite large-amplitude whistler waves, thereby producing a complex wake structure of plasma density perturbations in the region of the ion beam pulse. The presence of an applied solenoidal magnetic field may also cause a strong enhancement of the radial self-electric field of the beam pulse propagating through the background plasma. If controlled, this physical effect can be used for optimized beam transport over long distances.

*Research supported by the US Department of Energy.
†in colloboration with E. A. Startsev, M. A. Dorf, A. B. Sefkow, and R.C. Davidson

15:00
CI2 3 Studies of Emittance Growth and Halo Particle Production in Intense Charged Particle Beams Using the Paul Trap Simulator Experiment.*
ERIK GILSON, *Princeton Plasma Physics Laboratory*

The Paul Trap Simulator Experiment (PTSX) is a compact laboratory experiment that places the physicist in the frame-of-reference of a long, charged-particle bunch coasting through a kilometers-long magnetic alternating-gradient (AG) transport system. The transverse dynamics of particles in both systems are described by the same set of equations, including nonlinear space-charge effects. The time-dependent voltages applied to the PTSX quadrupole electrodes are equivalent to the spatially-periodic magnetic fields applied in the AG system. The transverse emittance of the charge bunch, which is the area in the transverse phase space that the beam distribution occupies, is an important metric of beam quality. Maintaining low emittance is an important goal when defining AG system tolerances and when designing AG systems to perform beam manipulations such as transverse beam compression. Results will be presented from experiments in which white noise and colored noise of various amplitudes and durations has been applied to the PTSX electrodes. This noise is observed to drive continuous emittance growth over hundreds of lattice periods. Additional results will be presented from experiments that determine the conditions necessary to adiabatically reduce the charge bunch's transverse size. During adiabatic transitions, there is no change in the transverse emittance. The transverse compression can be achieved either by a gradual change in the PTSX voltage waveform amplitude or frequency.

*Research Supported by the U.S. Department of Energy.

15:30
CI2 4 Generalized Phase-Space Tomography for Intense Beams.*
DIKTYS STRATAKIS, *Brookhaven National Laboratory*

Many applications of accelerators, such as free electron lasers, pulsed neutron sources, and heavy ion drivers for warm dense matter experiments require good quality beams with high intensity, i.e., cold, high-current beams. At the low-energy end of such machines, collective interactions from space charge dominate the beam dynamics and the beam can be viewed as a nonneutral plasma capable of carrying waves. Consequently, the initial beam distribution significantly affects its downstream behavior and beam characterization at the source is an important requirement to understand its evolution. This work reports on a novel diagnostic for time-dependent beam phase space characterization by using tomographic techniques. Tomography here is the reconstruction of phase space from a number of projections onto configuration space. Application of tomography to beams with space charge is non-trivial since it involves assumptions about the beam distribution one is trying to measure.This talk will address this issue, as well as the implementation of this diagnostic to both solenoidal and quadrupole focusing lattices. Also discussed will be a series of proof-of-principle experiments conducted at the University of Maryland to test the diagnostic. The tomography is benchmarked both against self-consistent simulation using a particle-in-cell code and against a pinhole-scan direct experimental sampling of phase-space.

*This work is supported by the U.S. Department of Energy High Energy Physics and Fusion Energy Science, and by the Department of Defense Office of Naval Research and Joint Technology Office.

16:00
CI2 5 Advances in Modeling of Beam-Wave Interaction in Multi-Megawatt Gyrotrons.*
ALEXANDER VLASOV, *Naval Research Laboratory*

High-power gyrotrons, capable to produce several megawatts of CW radiation in millimeter wave range, are used in many magnetic fusion facilities, and planned to be used in ITER. The gyrotrons employ an interaction between a gyrating electron beam and very high order modes of open cylindrical or co-axial cavities to keep Ohmic losses on cavity walls on acceptable level. Since the gyrotron cavity supports a large number of eigenmodes with different azimuthal and radial indexes many of which are capable of interaction with electron beam at different frequencies. The code MAGY [1,2] has been developed to address the mode competition issue in gyro-devices. MAGY model is based on multi time-scale approach and uses electromagnetic fields expansion into series of eigenfunctions of local transverse cross-section. This approach leads to computationally efficient solution of the Maxwell's Equations. MAGY has been used for design and modeling of gyro-devices in CPI, MIT, UMD, NRL for last decade and demonstrated excellent agreement with experimental data. Modeling of Multi-Megawatt gyrotrons operating at high frequencies (170 GHz and above) presents a new challenge due to the unprecedented level of spectral mode density and higher level of beam current. A co-axial cavity gyrotron has been introduced to reduce this spectral density. To address these computational physics challenges a new MAGY model for mode interaction in gyrotrons with co-axial cavities has been implemented. MAGY has been used to model the FZK (Germany) 170 GHz co-axial gyrotron [3,4]. The results of this modeling will be presented. Further advances in the theoretical models for comparison with the existing experimental data will be discussed. [1] S.C. Cai, et al, *Int. J. Elect.*, 72, p. 759, 1992. [2] M. Botton, et al, *IEEE Trans on P S,* 26, p. 882, 1998. [3] B. Piosczyk, et al, *IEEE Trans. on P S.*, 32, 413, 2004. [4] A.N. Vlasov, et al, *IEEE Trans. on P S.*, 36, p. 606, 2008.

*This work was supported by the U.S. Office of Naval Research.

16:30
CI2 6 Wakefields in Photonic Crystal Accelerator Cavities.*
GREGORY WERNER, *University of Colorado*

The RF properties of photonic crystals (PhCs) can be exploited to avoid the parasitic higher order modes (HOMs) that degrade beam quality in accelerator cavities and reduce efficiency and power in RF generators. For example, an accelerator cavity can be designed using a PhC structure that traps only modes within a narrow frequency range, so that the cavity has only a single mode. Although the lack of HOMs is perhaps the most drastic difference between PhC cavities and traditional metal cavities, PhC cavities should allow a much wider range of materials and shapes, which could potentially lead to cavities that operate at higher electric fields and at higher frequencies (with lower losses). However, this greater flexibility introduces many challenges for building actual structures. A hybrid cavity that uses a dielectric 2D PhC along with metal plates to trap fields in the third dimension may offer the advantages of a PhC cavity while being relatively easy to construct. Although the 2D photonic structure may allow only a single mode, the 3D structure can in principle trap HOMs, such as guided modes in the dielectric rods that form the PhC; however, computer simulations show that long-range wake fields can be significantly reduced in such hybrid structures. For a 3D cavity based on a triangular lattice of dielectric rods, the rod positions can be optimized (breaking the lattice symmetry) to reduce radiation leakage using a fixed number of rods; moreover, the optimized structure can further reduce the wake fields.

*This work is supported by the U.S. Department of Energy grant DE-FG02-04ER41317.

SESSION CT3: TUTORIAL: FLOW DRIVEN MHD INSTABILITIES IN WEAKLY MAGNETIZED LABORATORY EXPERIMENTS: DYNAMOS AND MRI
Monday Afternoon, 2 November 2009; Centennial II at 14:00; Dylan Brennan, University of Tulsa, presiding

14:00
CT3 1 Flow Driven MHD instabilities in Weakly Magnetized Laboratory Experiments: Dynamos and MRI.
CARY FOREST, *University of Wisconsin, Madison*

Astrophysical plasmas are often characterized by high magnetic Reynolds number, turbulent, flowing plasma in which the flow energy is much larger than that of magnetic field. Examples include planetary interiors, accretion disks and the solar wind. Creating such conditions in laboratory plasma experiments is challenging since confinement is required to keep the plasma hot and conducting and requiring strong magnetic fields. For this reason, laboratory experiments using liquid metals have been addressing fundamental plasma processes in this unique parameter regime. This talk will begin by giving a elementary tutorial of two related processes: the dynamo in which magnetic energy is spontaneously generated from flow energy; and the magneto-rotational instability in which a weak magnetic field can act as a catalyst for transporting momentum. Then, I will then show how liquid metal experiments have been contributing the the under-

standing of such processes. Liquid metal experiments have (1) demonstrated self-excitation of magnetic fields, (2) two scale dynamos where a small scale flow drives a large scale magnetic field, (3) intermittent self-excitation and a variety of time dynamics including field reversals, (4) showed the existence of a turbulent electromotive force (mean-field current generation), and (5) MRI-like instabilities have been observed in Couette flow geometries. Liquid metals are, however, not plasmas: dynamos and MRI may differ in plasmas where the relative importance of viscosity, and resistivity can be interchanged, and new instability mechanisms, outside the scope of MHD may be critical in collisionless plasmas. This suggests that the next generation of experiments in this important astrophysics regime should be based upon plasmas.

SESSION DI3: GYROKINETIC THEORY AND SIMULATION
Monday Afternoon, 2 November 2009; Centennial II at 15:00; Ronald Waltz, General Atomics, presiding

15:00
DI3 1 Direct multi-scale coupling of a transport code to gyrokinetic turbulence codes, with comparisons to tokamak experiments.
MICHAEL BARNES, *University of Oxford*

To faithfully simulate ITER and other modern fusion devices, one must resolve electron and ion fluctuation scales in a five-dimensional phase space and time. Simultaneously, one must account for the interaction of this turbulence with the slow evolution of the large-scale plasma profiles. Because of the enormous range of scales involved and the high dimensionality of the problem, resolved first-principles simulations of the full core volume over the confinement time are very challenging using conventional (brute force) techniques. In order to address this problem, we have developed a new approach in which turbulence calculations from multiple gyrokinetic flux tube simulations are coupled together using gyrokinetic transport equations to obtain self-consistent equilibrium profiles and corresponding turbulent fluxes. This multi-scale approach is embodied in a new code, Trinity, which is capable of evolving equilibrium profiles for multiple species, including electromagnetic effects and realistic magnetic geometry, at a fraction of the cost of conventional direct numerical simulations. Key components in the cost reduction are the extreme parallelism enabled by the use of coupled flux tubes and the use of a nonlinear implicit algorithm to take large time steps when evolving the equilibrium. In this talk, we describe the multi-scale model employed in Trinity and present simulation results using nonlinear fluxes calculated with the gyrokinetic turbulence codes GS2 and GENE. We compare the numerical predictions from Trinity simulations with experimental results from a number of fusion devices, including JET and MAST.

15:30
DI3 2 Predictive Gyrokinetic Transport Simulations and Application of Synthetic Diagnostics.*
J. CANDY, *General Atomics*

In this work we make use of the gyrokinetic transport solver TGYRO [1] to predict kinetic plasma profiles consistent with energy and particle fluxes in the DIII-D tokamak. TGYRO uses direct nonlinear and neoclassical fluxes calculated by the GYRO and NEO codes, respectively, to solve for global, self-consistent temperature and density profiles via Newton iteration. Previous work has shown that gyrokinetic simulation results for DIII-D discharge 128913 match experimental data rather well in the plasma core, but with a discrepancy in both fluxes and fluctuation levels emerging closer to the edge ($r/a > 0.8$). The present work will expand on previous results by generating model predictions across the entire plasma core, rather than at isolated test radii. We show that TGYRO predicts temperature and density profiles in good agreement with experimental observations which simultaneously yield near-exact (to within experimental uncertainties) agreement with power balance calculations of the particle and energy fluxes for $r/a \leqslant 0.8$. Moreover, we use recently developed synthetic diagnostic algorithms [2] to show that TGYRO also predicts density and electron temperature fluctuation levels in close agreement with experimental measurements across the simulated plasma volume.

[1] J. Candy, C. Holland, R.E. Waltz, M.R. Fahey, and E. Belli, "Tokamak profile prediction using direct gyrokinetic and neoclassical simulation," Phys. Plasmas **16**, 060704 (2009).

[2] C. Holland, A.E. White, G.R. McKee, M.W. Shafer, J. Candy, R.E. Waltz, L. Schmitz, and G.R. Tynan, "Implementation and application of two synthetic diagnostics for validating simulations of core tokamak turbulence," Phys. Plasmas **16**, 052301 (2009).

*Supported by US DOE under DE-FG03-95ER54309.

16:00
DI3 3 Limitations of the gyrokinetic quasineutrality equation.*
FELIX I. PARRA, *Plasma Science & Fusion Center, MIT*

Traditional electrostatic gyrokinetic treatments consist of a gyrokinetic Fokker-Planck equation and a gyrokinetic quasineutrality equation. The equations implemented in full f codes are typically only consistent through first order in a gyroradius over macroscopic scale length expansion. In axisymmetric configurations such as the tokamak, we will show that these gyrokinetic descriptions are unable to correctly calculate the profile of toroidal rotation and hence the long wavelength radial electric field because even turbulence dominated tokamaks are intrinsically ambipolar. We study the vorticity equation or current conservation equation in the gyrokinetic regime, with wavelengths on the order of the ion gyroradius. We use the momentum conservation equation to determine the perpendicular current density, making explicit the dependence of the current on the transport of toroidal angular momentum. Employing the vorticity equation, it is possible to show that gyrokinetics needs to be calculated to fourth order in the gyroradius expansion if the radial electric field is to be retrieved from quasineutrality. However, existing full f simulations are based on first order gyrokinetic equations that are unreliable for wavelengths longer than the geometric average between the ion gyroradius and the macroscopic scale length. Finally, we replace quasineutrality by the conservation equation for toroidal angular momentum in a form that only requires an ion distribution function correct to second order in ion gyroradius over scale length, and by exploiting an expansion in $q >> 1$, we propose a scheme in which the first order gyrokinetic Fokker-Planck equation already implemented in codes is enough to find the axisymmetric radial electric field.

*Work supported by DoE and CMPD at the University of Maryland.

16:30
DI3 4 Gyrokinetic Models for Edge Plasmas.*
ANDRIS DIMITS, *Lawrence Livermore National Laboratory*

We address two key sets of issues in the development of gyrokinetic equations for magnetic fusion edge simulation codes. Starting with existing second-order gyrokinetic equations [1], we develop a "minimal" electromagnetic gyrokinetic model for edge simulations. Large-amplitude perturbations, believed to be present in the edge, result in time evolution of the gyrokinetic Poisson equation operator, and a need to retain second-order terms in the gyrocenter Hamiltonian to satisfy system energy conservation. These aspects have never been implemented in gyrokinetic simulations. We present methods for implementing the second-order terms in the equations of motion, as well as a practical direct finite-element discretization of the evolving gyrokinetic Poisson-equation operator. While tempting, the use of long-wavelength or Pade' approximations for this operator would result in violation of energy conservation. An appropriate model for Coulomb collisions comes from an extension of work on bilinear gyrokinetic collision operators [2,3] to include the first-order terms in the transformation from the gyrocenter- to physical-space distribution function prior to insertion in the Landau-Fokker-Planck operator. We also describe a gyrokinetic theory in an extended ordering in which the small parameter is the ratio of the ExB shearing rate to the gyrofrequency. This theory allows for long wavelength ExB flows of order the thermal velocity instead of the more restrictive standard orderings which require that either the electrostatic potential [1] or the ExB flow velocity [4] be small compared with the thermal levels.

[3] Z. Xiong et al., J. Comput. Phys. 227, 7192 (2008) [4] A.M. Dimits et al., Phys Fluids B **4**, 274 (1992).

*This work was performed for US DOE by LLNL under Contract DE-AC52-07NA27344 and is part of the ESL.

SESSION CO4: DIII-D TOKAMAK
Monday Afternoon, 2 November 2009
Regency VI at 14:00
Michael Mauel, Columbia University, presiding

14:00
CO4 1 Overview of Recent DIII-D Experimental Results*
M.E. FENSTERMACHER, *LLNL* DIII-D TEAM, DIII-D experiments in 2009 addressed critical ITER issues and physics understanding needed for extrapolation to future devices. Multiple schemes for rapid plasma shutdown were demonstrated including massive gas injection, large shattered D_2 pellets and impurity filled shell pellets. Detailed particle balance experiments show dramatically reduced wall uptake in ITER relevant H-mode compared with L-mode. Joint DIII-D/JET experiments showed no dependence of pedestal pressure width on ρ^*, indicating a favorable scaling to ITER. Torque from non-resonant magnetic perturbations improved access to QH-mode at low rotation. DIII-D demonstrated low voltage startup with ECH assist and low ℓ_i plasma rampdown, as well as solenoidless startup. Progress on qualifying Hybrid scenario plasmas for $Q = 10$ in ITER included $\beta_N = 2.5$ with ELM suppression by RMPs. Advances in physics understanding included: 1) systematic q_{min}, q_{95} scans showing the dependence of n_e and T_e profiles on $q(r)$, 2) plasma response to non-axisymmetric fields, 3) validation of core turbulence and thermal transport models and 4) intrinsic rotation studies.

*Work supported by the US DOE under DE-AC52-07NA27344 and DE-FC02-04ER54698.

14:12
CO4 2 Particle Control and Carbon Transport Experiments on DIII-D* S.L. ALLEN, *LLNL* E.A. UNTERBERG, *ORISE* N.H. BROOKS, M.A. MAHDAVI, *GA* D.G. WHITE, *MIT* J.W. DAVIS, A.A. HAASZ, B. FITZPATRICK, *U. Toronto* As part of the 2009 Joint Research Target, DIII-D, along with MIT and NSTX have completed a series of experiments on particle control

and transport. On DIII-D, both dynamic (calculated particle balance) and static (pumps closed or regenerated) particle balance experiments were carried out in both L- and H-mode with cryopumping. We find that the exhaust obtained from both techniques is comparable. We find that the uptake can be large in ohmic and L-mode, but in H-mode, the wall retention flux is very small, which is promising for long pulse burning plasma experiments. Also, in support of tritium control research for ITER, we have started a process to qualify the DIII-D internal components for an anticipated air bake (350°, 10 Torr) in 2010. We find issues with some copper components, but most components are compatible. Air baking removes the co-deposited carbon that can be rich in tritium in ITER with carbon walls.

*Work supported by the US DOE under DE-AC52-07NA27344, DE-AC05-06OR23100, and DE-FC02-04ER54698.

14:24

CO4 3 Observations of Thermal Transport Enhancement in Stochastic Boundary Experiments at DIII-D and TEXTOR* O. SCHMITZ, H. FRERICHS, *FZJ* M.E. AUSTIN, *U. Texas-Austin* B.D. BRAY, T.E. EVANS, T.H. OSBORNE, *GA* H. REIMERDES, *Columbia U.* M.E. FENSTERMACHER, C.J. LASNIER, *LLNL* M.W. JAKUBOWSKI, *MPI* S. MORDIJCK, R.A. MOYER, *UCSD* E.A. UNTERBERG, *ORISE* Comparison of stochastic boundary experiments in TEXTOR L-modes to DIII-D H-modes shows on both experiments a q_{95} resonance in the pedestal pressure p_e which is driven by a resonant decrease of the pedestal electron temperature T_e as q_{95} is varied. This decrease in T_e is correlated to an increase in the modeled stochastic layer width while the electron density does not show a strong q_{95} resonance. The T_e decrease is only seen for DIII-D in an ITER similar shape at high triangularity as opposed to an increase in T_e and a small effect only on the thermal transport for low triangularity plasmas. This indicates significant shape dependence for the q_{95} resonant thermal transport features in stochastic boundary experiments for suppression of type-I edge localized modes by RMP at DIII-D.

*Work supported in part by the US DOE under DE-FG03-97ER54415, DE-FC02-04ER54698, DE-FG02-89ER53297, DE-AC52-07NA27344, DE-FG02-07ER54917 and DE-AC05-06OR23100.

14:36

CO4 4 Correlation Between Density Pump-out and Free Streaming Particle Transport in Low Collisionality Resonant Magnetic Perturbation H-modes* S. MORDIJCK, R.A. MOYER, *UCSD* E.A. UNTERBERG, *ORISE* T.E. EVANS, *GA* Experimental pedestal density data shows a decrease in the gradient within the transport barrier during RMP H-mode, as compared to an ELMing H-mode. Recent modeling, with SOLPS5 and TRIP3D, indicates that this change is the result of an increase in particle transport. This increase in transport is the consequence of the creation of open field lines inside the traditional separatrix. The magnitude ($\sim 0.1\ m^2/s$) and radial extent of this free-streaming transport are well correlated with experimental changes. In this paper, we present a more systematic study, where we compare the increase in particle transport calculated with TRIP3D, directly with the changes in pedestal density. We notice that the experimental density pump-out during RMP H-mode is linearly correlated with the increase in free streaming transport for low collisionality plasmas.

*Work supported by the US DOE under DE-FG02-08ER54984, DE- DE-AC05-06OR23100, and DE-FC02-04ER54698.

14:48

CO4 5 Dependence of Bootstrap Current, Stability, and Transport on the Safety Factor Profile in DIII-D Steady-state Scenario Discharges* C.T. HOLCOMB, *LLNL* J.R. FERRON, T.C. LUCE, P.A. POLITZER, J.C. DEBOO, T.W. PETRIE, C.C. PETTY, R.J. LA HAYE, *GA* A.E. WHITE, F. TURCO, *ORISE* E.J. DOYLE, T.L. RHODES, L. ZENG, *UCLA* A high beta, high gain steady state tokamak scenario with large bootstrap current fraction will have strong coupling between the current density and the pressure gradient through turbulent transport and the bootstrap current. To address this coupling experimentally, a scan of the safety factor minimum (q_{min}, from 1.1 to over 2) and edge value (q_{95}, from 4.5 to 6.5) was performed. The bootstrap current fraction increases with q_{min} and q_{95} by virtue of increasing density gradients. Compared to lower q_{min}, $q_{min} > 2$ has lower $n = 1$ stability limits, enhanced drift wave growth rates, higher low-k density fluctuations, and lower confinement. At $q_{min} > 2$ and $q_{95} = 4.5$ the unsustainable condition $J_{BS} > J_{Total}$ occurs near the axis. These considerations suggest intermediate q is the optimal operating point.

*Work supported by the US DOE under DE-AC52-07NA27344, DE-FC02-04ER54698, DE-AC05-06OR23100, DE-FG03-08ER54984.

15:00

CO4 6 Global Structure of a Stable, Driven Kink Mode: DIII-D Measurements and Model Validation* M.J. LANCTOT, H. REIMERDES, J.M. HANSON, G.A. NAVRATIL, *Columbia U.* A.M. GAROFALO, M.S. CHU, G.L. JACKSON, R.J. LA HAYE, M.J. SCHAFFER, E.J. STRAIT, *GA* Y.Q. LIU, *UKAEA* M. OKABAYASHI, W.M. SOLOMON, *PPPL* Recent DIII-D measurements of the global structure of the non-axisymmetric plasma perturbation driven by applied $n = 1$ magnetic fields enable the quantitative test of ideal MHD theory. Extensive magnetic measurements show that the ideal MHD code MARS-F predicts the plasma response within 20% for values of beta up to 75% of the beta limit calculated without a conducting wall, but overestimates the perturbed field at higher pressures. Experiments varying the pitch angle of the applied field at different values of plasma current demonstrate the plasma response depends primarily on the match of the applied field to the kink mode structure. Toroidally distributed soft x-ray measurements indicate the kink-like internal perturbation structure depends on the plasma pressure. The measurements are used to test kinetic stabilization models in the MARS-K code.

*Work supported in part by the US DOE under DE-FG02-89ER53297, DE-FC02-04ER54698, and DE-AC02-09CH11466.

15:12

CO4 7 Synergy in Two-Frequency Fast Wave Cyclotron Harmonic Absorption in DIII-D* R.I. PINSKER, M. CHOI, *General Atomics* M. PORKOLAB, *MIT* W.W. HEIDBRINK, Y. ZHU, *UC-Irvine* F.W. BAITY, *ORNL* J.C. HOSEA, *PPPL* Fast waves (FWs) at 60 MHz and at 90 MHz are coupled to DIII-D discharges for central heating and current drive at net FW power levels up to 3.5 MW. In 2 T discharges with fast deuteron populations from neutral beam injection, 4th and 6th deuterium cyclotron harmonic absorption on the fast ions competes with direct electron damping and with edge losses. If the fast deuterons are accelerated by absorption of 60 MHz (4th harmonic) FWs, adding 90 MHz power (6th harmonic) increases the fusion neutron rate by a increment larger than the sum of the increments observed with separate 90 MHz and 60 MHz pulses (synergy). Synergy in the global confinement

is also observed. The regions of velocity space that are affected with the two-frequency FW heating are studied with fast-ion D_α spectroscopy and by detailed characterization of the dynamics of the neutron rate with modulated neutral beams.

*Work supported by the US DOE under DE-FC02-04ER54698, DE-FG02-90ER54084, SC-G903402, DE-AC05-00OR22725, and DE-AC02-09CH11466.

15:24

CO4 8 Measurements of the Spatial Structure of Geodesic Acoustic Modes in DIII-D* J.C. HILLESHEIM, W.A. PEEBLES, L. SCHMITZ, T.L. RHODES, T.A. CARTER, *UCLA* Geodesic acoustic modes (GAMs) are linearly stable, turbulence driven modes exhibiting oscillating axisymmetric ($m = 0$, $n = 0$) $E \times B$ flows. They potentially play an important role in establishing the saturated level of turbulence in fusion plasmas. Two Doppler backscattering (DBS) systems at locations separated toroidally by 180° are aligned to make simultaneous measurements at the same radial location ($\rho \approx 0.8$) and wavenumber ($k_\perp \sim 4\,\mathrm{cm}^{-1}$, $k_\perp \rho_s \sim 1$) in a beam-heated L-mode DIII-D plasma. Flow oscillations, which agree with the predicted GAM frequency scaling, correlate toroidally between the two DBS systems with an ensemble averaged cross-coherency of $\gamma \approx 0.6$ over 600 ms. The cross-phase between pairs of the DBS signals is consistent with the expected GAM structure. The radial variation in cross-phase agrees with descriptions of the GAM eigenmode as having an Airy function character with outward radial propagation; the measured radial wavelength is $\lambda_r \approx 2.8\,\mathrm{cm}$ and the calculated GAM characteristic length scale is $L_{GAM} = \rho_i^{2/3} L_T^{1/3} \approx 1.2\,\mathrm{cm}$.

*Supported by US DOE under DE-FG02-08ER54984. JCH's work performed through a DOE-ORISE FES Fellowship Program.

15:36

CO4 9 Heat Transport in Off-axis EC-Heated Discharges in DIII-D* M.E. AUSTIN, K.W. GENTLE, *U. Texas-Austin* C.C. PETTY, *GA* T.L. RHODES, L. SCHMITZ, G. WANG, *UCLA* In low-density H-mode discharges in DIII-D, ECH applied off-axis produces electron temperature profiles with strong peaking at the heating location and very slow penetration of heat into the core. This type of discharge is a counter example to the heat-pinch effect normally seen in tokamaks where off-axis heating propagates rapidly to the center. In a recent experiment on DIII-D, the conditions for producing these "bat-eared" T_e profiles were studied. It was observed that H-mode is a necessary condition; L-mode discharges exhibit the classic heat pinch. A region of low transport corresponds to the $q = 1$ surface as verified by the sawtooth inversion radius. Results of transport analysis are presented as well as measurements of n_e and T_e fluctuations.

*Work supported by the US DOE under DE-FG03-97ER54415, DE-FC02-04ER54698, and DE-FG02-08ER54984.

15:48

CO4 10 Studies of Runaway Electron Confinement in MHD Disruption Simulations* V.A. IZZO, E.M. HOLLMANN, A.N. JAMES, *UCSD* D.G. WHYTE, G. OLYNYK, *MIT* L.L. LAO, *GA* Formation of a runaway electron beam during an ITER disruption is a major concern for machine survival, particularly because the avalanche growth of a seed population will be many orders of magnitude larger than in present devices. Enhanced fast-electron losses due to stochastic fields produced during the disruption, or from applied non-symmetric fields, can combat avalanche growth. The confinement of fast electrons is studied in the context of MHD simulations using a newly developed capability in the NIMROD code to track single particle orbits as the magnetic fields evolve. Macroscopic drift-orbit displacements associated with highly relativistic electrons play an important role in confinement by averaging over perturbing fields during a poloidal transit, thus allowing good confinement in the presence of stochasticity. Verification of the model for a small number of electrons compares the orbits with and without drift terms directly. Confinement of fast electrons during a gas-jet-induced disruption on Alcator C-Mod, and during a controlled error field ramp on DIII-D are presented.

*Supported by US DOE under DE-FG03-95ER54309.

16:00

CO4 11 Solenoid-free Startup of DIII-D* J.A. LEUER, N. EIDIETIS, D.A. HUMPHREYS, A.W. HYATT, G.L. JACKSON, J. LOHR, P.A. POLITZER, R. PRATER, P.T. TAYLOR, M.L. WALKER, *GA* G. CUNNINGHAM, *Culham* D. GATES, D. MUELLER, *PPPL* Y.-K. OH, S.-W. YOON, S.-H. HAHN, *NFRI* J.H. YU, *UCSD* Inductive plasma current startup to 170 kA was achieved in the DIII-D tokamak without the use of inboard poloidal field coils (solenoidless startup). This was achieved with strong preionization/heating using electron cyclotron (EC) power. For outside breakdown and moderated field null quality, flux conversion efficiency to plasma current using only diverter and vertical field coils is similar to DIII-D's ohmic startup. At higher flux states null quality degrades and flux/current efficiency is reduced, possibly from a reduced in EC/breakdown region coupling. EC current drive was minimal for the plasma regime studied. Preliminary solenoidless handoff experiments to neutral beam current drive were also explored. This research is expected to reduce central solenoid requirements for next generation devices and provide a basis for solenoidless startup of toroidal devices with integration of appropriate current drive techniques.

*Supported in part by US DOE under DE-FC02-04ER54698, DE-AC02-09CH11366, and DE-FG02-07ER54917.

16:12

CO4 12 Identity Experiments in the Hybrid Regime on DIII-D and JET* C.D. CHALLIS, *EURATOM/UKAEA Fusion Assoc.* E. JOFFRIN, *Assoc. EURATOM-CEA* T.C. LUCE, P.A. POLITZER, *General Atomics* DIII-D TEAM, JET EFDA TEAM, Hybrid plasmas have the potential for high fusion yield and long pulse tokamak operation. However, performance extrapolation to future devices depends on an understanding of the transport scaling with machine size, which may not be adequately described by existing ELMy H-mode scalings. An identity match and ρ^* scan has been performed in the hybrid regime on DIII-D and JET to investigate the core confinement. A similar plasma shape and NBI heating were used and ν^*, ρ^*, β and Mach number profiles were all matched within about 20% at the plasma mid-radius. A ρ^* range of roughly 2.5 was covered across the two devices for plasmas with $q_0 \sim 1$ and normalized beta in the range $\sim$ 2.5-3.0. These experiments allow a comparison of transport in this domain on the two devices and an assessment of the ρ^* dependence of core confinement.

*Work supported by EURATOM and UK EPSRC and by the US Department of Energy under DE-FC02-04ER54698. For JET EFDA Team, see appendix of F. Romanelli et al., Fusion Energy Conf. 2008 (Proc. 22nd Int. FEC Geneva, 2008) IAEA (2008).

16:24

CO4 13 Scaling of H-mode Pedestal and ELM Characteristics With Gyroradius* T.H. OSBORNE, R.J. GROEBNER, A.W. LEONARD, P.B. SNYDER, *GA* M.N.A. BEURSKENS, L.D. HORTON, P. LOMAS, S. SAARELMA, *EURATOM/UKAEA* L. FRASSINETTI, *Assoc. EURATOM-VR* I. NUNES, *Centro de Fusao Nuclear* JET-EFDA TEAM, DIII-D TEAM, The dependence of the H-mode pedestal structure and ELMs on gyroradius ($\rho^* = \rho/a$) was examined in experiments combining data from the JET and DIII-D to produce a factor of 4 variation in ρ^*, while keeping the plasma shape, q, normalized pressure (β), collisionality, Mach number, and T_i/T_e at the pedestal top constant. In this scan, the width of the steep gradient region of T_e and n_e, Δ, was independent of ρ^* within uncertainties, $\Delta/a \sim (\rho^*)^{0.0\pm0.15}$. The pedestal pressures and widths were in quantitative agreement with the EPED1 model in which the pedestal structure is set by combining the peeling-ballooning and kinetic ballooning stability thresholds. The ELM energy loss normalized to the pedestal energy decreased from 40% to 10% as ρ^* decreased by a factor of 2 in DIII-D, but the trend did not continue in smaller ρ^* on JET.

*Supported by US DOE under DE-FC02-04ER54698.

16:36

CO4 14 Pedestal Density Fluctuations During Quiescent and ELMing H-mode Plasmas* Z. YAN, G.R. McKEE, M.W. SHAFER, *U. Wisc.-Madison* R.J. GROEBNER, P.B. SNYDER, K.H. BURRELL, T.H. OSBORNE, A.W. LEONARD, *General Atomics* T.L. RHODES, L. ZENG, *UCLA* Spatially resolved density fluctuation characteristics have been measured in the pedestal region of quasi-steady-state Type I ELMing plasmas and ELM-free quiescent H-mode (QH) plasmas using 2D beam emission spectroscopy measurements. During Type I ELMing plasmas, these fluctuations are modulated with the ELM cycles. Two distinct frequency bands (20-200 kHz and 250-450 kHz) are observed propagating in opposite directions. In QH-mode plasmas, discrete and coherent modes are observed in the pedestal region of particular discharges at relatively high-pedestal pressure. These modes appear from 50-250 kHz, peaking in amplitude around 150 kHz, with a uniform frequency separation of about 10 kHz. Observed characteristics of these modes will be compared with those from ELITE calculations of theoretically predicted pressure-gradient limiting instabilities, such as kinetic ballooning modes.

*Work supported by the US DOE under DE-FG02-08ER54999, DE-FG02-89ER53296, DE-FC02-04ER54698 and DE-FG03-08ER54984.

16:48

CO4 15 Quiescent H-Mode Plasmas with Rotation Driven by Static Non-axisymmetric Fields* A.M. GAROFALO, K.H. BURRELL, G.L. JACKSON, *General Atomics* A. COLE, *U. Wisc.* W.M. SOLOMON, *PPPL* M.J. LANCTOT, H. REIMERDES, *Columbia U.* A quiescent H-mode (QH-mode) edge allows ELM-free operation of a plasma with good confinement and good particle exhaust. Until recently, QH-mode operation required rather strong plasma toroidal rotation in order for the edge velocity shear to exceed a minimum value [1]. However, rapid rotation may not be feasible in a self-heated burning plasma with little or no momentum injection from neutral beams. New DIII-D experiments in ITER-similar plasmas show that the neoclassical torque from static, nonresonant magnetic fields (NRMFs) provides a useful knob to change the edge rotation profile shear. NRMF application resulted in QH-mode operation with less than half the rotation (evaluated on top of the pedestal) of previous QH-mode without the NRMFs. At this low rotation, the NRMF torque may be amplified by entering the theoretically predicted $1/\nu$ collisionality regime.[1] K.H. Burrell, *et al.*, Phys. Rev. Lett. **102**, 155003 (2009).

*Work supported in part by the US DOE under DE-FC02-04ER54698, DE-FG02-89ER53296, DE-FG02-09ER54999, DE-AC02-09CH11466, and DE-FG02-89ER53297.

SESSION CO5: EQUATION OF STATE, STRENGTH, AND HYDRODYNAMICS

Monday Afternoon, 2 November 2009
Hanover CDE at 14:00
Tom Boehly, University of Rochester, presiding

14:00

CO5 1 Laser-Shock Compression and Hugoniot Measurements of Liquid Hydrogen TAKAYOSHI SANO, *Osaka University* NORIMASA OZAKI, TATSUHIRO SAKAIYA, KEISUKE SHIGEMORI, MASAHIRO IKOMA, TOMOAKI KIMURA, KOHEI MIYANISHI, TAKASHI ENDO, AKIYUKI SHIROSHITA, HIDEKI TAKAHASHI, TATSUYA JITSUI, YASUNORI HORI, YOICHIRO HIRONAKA, AKIFUMI IWAMOTO, TOSHIHIKO KADONO, MITSUO NAKAI, TAKUO OKUCHI, KAZUTO OTANI, KATSUYA SHIMIZU, TADASHI KONDO, RYOSUKE KODAMA, KUNIOKI MIMA, Hugoniot data for liquid hydrogen were obtained up to 55 GPa under laser-driven shock loading using impedance matching to a quartz standard. The pressure range we achieved is about 5 times higher than the earlier experiments done by a two-stage gas gun. The experiment was performed on the Gekko/HIPER laser facility at the Institute of Laser Engineering, Osaka University. A significant improvement in the precision of velocity measurements because transparent standard allows direct measurement of the shock velocities for both the standard and hydrogen. The shocked temperature of hydrogen is determined concurrently from the brightness temperature. The temperature is $\sim$ 9000 K at 40 GPa, which is about twice as high as that of shocked deuterium at the same pressure. Compression and temperature along the primary Hugoniot are consistent with theoretical models of equation-of-state.

14:12

CO5 2 Inferring Electron Temperature of Shocked Liquid Deuterium Using Inelastic X-Ray Scattering S.P. REGAN, P.B. RADHA, T.R. BOEHLY, V.N. GONCHAROV, R.L. McCRORY, D.D. MEYERHOFER, T.C. SANGSTER, V.A. SMALYUK, *Laboratory for Laser Energetics, U. of Rochester* K. FALK, G. GREGORI, *U. of Oxford* T. DOEPPNER, S.H. GLENZER, O.L. LANDEN, *LLNL* A laser-ablation–driven shock wave (12 Mbar) was launched in a planar liquid-deuterium target on OMEGA, and the shocked conditions were diagnosed using inelastic x-ray scattering. The electron temperature (T_e) is inferred from the Doppler-broadened, Compton-downshifted peak of the noncollective x-ray scattering for $T_e > T_{Fermi}$. For this purpose, a saran backlighter foil was irradiated with a group of tightly focused beams having an overlapped intensity of $\sim 10^{16}$ W/cm^2. The spectrally resolved x-ray scattering of the Cl Ly$_\alpha$ emission ($h\nu$ = 2.96 keV) was recorded at 90[r]. The inferred $T_e = 20\pm 5$ eV is close to the

predicted T_e = 22 eV. The experimental design and initial results will be reported. This work was supported by the U.S. Department of Energy Office of Inertial Confinement Fusion under Cooperative Agreement No. DE-FC52-08NA28302. The work of G. Gregori and K. Falk was supported in part by EPSRC grant No. EP/G007187/1 and by the HiPER collaboration.

14:24

CO5 3 Measurements of electron density and temperature in shock-compressed Be from x-ray Thomson scattering H.J. LEE, *Department of Physics, University of California, Berkeley CA* S.H. GLENZER, T. DOEPPNER, O.L. LANDEN, R.W. LEE, *Lawrence Livermore National Laboratory, Livermore CA* R.W. FALCONE, *Department of Physics, University of California, Berkeley CA* X-ray Thomson scattering measurements have provided an insight into characterization of dense plasmas by determining electron temperature, density, and ionization state [1,2]. We have measured spectrally resolved 6 keV x-ray scattering spectra of shock-compressed matter created by counter-propagating shocks at the Omega laser facility. The spectra in non-collective scattering regime show Compton features that give evidence of Fermi-degenerate dense plasmas with a Fermi energy above 30 eV and temperatures of 10-15 eV. Detailed analysis in comparison with radiation-hydrodynamic modeling will be presented. [1] S. H. Glenzer *et al.*, Phys. Rev. Lett. 90, 175002 (2003); Phys. Rev. Lett. 98, 065002 (2007). [2] H. J. Lee *et al.*, Phys. Rev. Lett. 102, 115001 (2009). This work was performed under the auspices of the U.S. Department of Energy by University of California, Lawrence Livermore National Laboratory under Contract No. DE-AC52-07NA27344 and supported by the National Laboratory User Facility program.

14:36

CO5 4 Measurements of Strain-Induced Refractive Index Changes in Shocked and Ramp-Compressed Lithium Fluoride D.E. FRATANDUONO, M.A. BARRIOS, T.R. BOEHLY, D.D. MEYERHOFER, *Laboratory for Laser Energetics, U. of Rochester* R. SMITH, D.G. HICKS, P.M. CELLIERS, J.H. EGGERT, G.W. COLLINS, *LLNL* Lithium fluoride is frequently used as a window in equation-of-state experiments because it remains transparent for multishocks up to 5 Mbar. When compressed, its refractive index changes, affecting the sensitivity of velocity interferometry measurements. For shocked LiF, the refractive index has been measured for pressures up to 1.15 Mbar using gas gun flyer-plate experiments. It has become commonplace to extrapolate the linear dependence for higher-pressure experiments, i.e., those above 1.15 Mb. We report on experiments at the Omega/Omega EP Laser Facilities that use laser-driven shocks and ramp compression to compress diamond targets with LiF windows up to 5 Mbar. Diamond-free surface velocity and diamond/LiF interface velocities are measured. By comparing these velocities, the refractive index of compressed LiF is deduced. This work was supported by the U.S. Department of Energy Office of Inertial Confinement Fusion under Cooperative Agreement No. DE-FC52-08NA28302.

14:48

CO5 5 Theoretical Investigation of Strong Coupling and Degeneracy Effects in ICF Implosions S.X. HU, V.N. GONCHAROV, T.R. BOEHLY, P.B. RADHA, S. SKUPSKY, *Laboratory for Laser Energetics, U. of Rochester* B. MILITZE, *U. of California–Berkley* Accurate knowledge of the equation of state (EOS) and opacity is essential to inertial confinement fusion (ICF). Low-adiabat ICF implosion designs reach strongly coupled, degenerate plasma conditions. Using the first-principles, path-integral Monte Carlo method, we have established an EOS table of deuterium, spanning typical ICF shell conditions (densities of 0.001 to 100 g/cc and temperatures of 1 eV to 1 keV). Noticeable differences in energy/pressure at moderately coupled, degenerate regimes have been found in comparison to the *SESAME* and Thomas-Fermi EOS. Hydrodynamic simulations using these EOS's and opacities for OMEGA implosions will be presented. This work was supported by U.S. Department of Energy Office of Inertial Confinement Fusion under Cooperative Agreement No. DE-FC52-08NA28302.

15:00

CO5 6 Mixed equation of state: dynamical materials experiments on Z and multi-scale simulations* T.R. MATTSSON, S. ROOT, T.A. HAILL, *Sandia National Laboratories* N.L. BRUNER, *Voss Scientific* R.W. LEMKE, *Sandia National Laboratories* Significant progress in understanding properties of pure materials under extreme conditions has been made recently, with experiments and first-principles theoretical work providing detailed insights for many pure materials. Mixing poses additional fundamental questions regarding the fidelity of first-principles calculations, the reliability of mixing rules for equations of state, as well as the accuracy of experimental approaches. We will present experimental and theoretical results for mixed equation of state. By shock impact of magnetically launched flyer plates on doped poly(4-methyl-1-pentene) foams, we create multi-Mbar pressures in a dense plasma mixture of hydrogen, carbon, and dopant at temperatures of several eV. We analyze the system by multi-scale simulations, from density functional theory to continuum magneto-hydrodynamics simulations.

*Sandia is a multiprogram laboratory operated by Sandia Corporation, a Lockheed Martin Company, for the United States Department of Energy's National Nuclear Security Administration under contract DE-AC04-94AL85000.

15:12

CO5 7 Transport properties of Hydrogen and CH under ICF conditions JEAN CLEROUIN, VANINA RECOULES, CHARLES STARRETT, STEPHANE MAZEVET, FLAVIEN LAMBERT, BENOIT CANAUD, ALAIN DECOSTER, *CEA/DAM/DIF 91297 Arpajon Cedex France* We present ab initio evaluations of the thermal and of the electrical conductivity of hydrogen at a density of 80 g/cc [1] and 160 g/cc corresponding to the Inertial Confinement Fusion regime. Results are compared with different theories (Hubbard, Lee-More, Ichimaru) and with an average atom (AA) model coupled with a Kubo-Greenwood evaluation of transport coefficients. The Lorentz number, which is the ratio between the thermal to the electrical conductivity, given by the Wiedemann-Frantz law is checked in different regimes ranging from the highly degenerate to the kinetic one. We have also used ab initio calculations to compute the CH thermal conductivity and compared it to the AA approach using mixing rules. [1] V. Recoules, F. Lambert, A. Decoster, B. Canaud and J. Clerouin, "Ab initio determination of thermal conductivity of dense hydrogen plasmas," Phys. Rev. Letters 102, 075002 (2009).

15:24

CO5 8 Shock-Clump Interaction Studies in the Laboratory* B.E. BLUE, J.D. HUND, R.R. PAGUIO, J.F. HANSEN, *GA* J.M. FOSTER, P.A. ROSEN, R.J.R. WILLIAMS, *AWE* M. DOUGLAS, B.H. WILDE, *LANL* R. CARVER, J. PALMER, P. HARTIGAN, *Rice University* Large-scale directional outflows of supersonic plasma are driven by a wide variety of objects in the universe. Typical models of the outflows assume simplistic geometries; however, images of most outflows show a much more complex structure that consists of multiple clumps and shocks. To bridge the gap between the complex system in space and the simplified models, controlled scaled experiments were performed to elucidate the physics of a shock progressing through a clumpy medium. This talk will present experiments on the Omega Laser in which a shock impacts density discontinuities in order to understand the perturbed shock structure. Two types of discontinuities that had the same average density were tested: one with a uniformly distributed dopant and another with $\sim$ 47 randomly distributed high-density clumps. We have obtained high-resolution radiographs that detail the temporal evolution of the shock and density discontinuity.

*Work supported by the US DOE under DE-AC52-06NA27279.

15:36

CO5 9 Ramp loading by shock release of foam reservoirs for the NIF* SHON T. PRISBREY, BRUCE REMINGTON, HYE-SOOK PARK, ROBERT CAVALOO, STEPHEN POLLAINE, MARK MAY, *Lawrence Livermore National Laboratory* Previous work has shown that a ramped pressure wave created by the stagnation of an unloading, shocked reservoir can drive a quasi-isentropic compression experiment (ICE) [Edwards et al., **92** PRL 2004; Lorenz et al., **2** HEDP 2006]. The size of the shock at the back of the reservoir, the reservoir materials, the size of the gap between the reservoir and the sample, and the sample's sound speed places limits on (1) the thickness of the sample that can be studied before the ramp wave steepens into a shock that would impart significant shock heating into the sample, and (2) the size of the planar drive region. We present simulation and experimental data from a series of CRF foam laser shots done on the Omega Laser Facility to show that the presence of lower density materials in an ICE reservoir reduces the needed gap size between the reservoir and the sample, tailors the ramp drive, and can be simulated using the radiation-hydrodynamics code LASNEX. The combination of these factors have allowed for a compact design suitable for a laser-driven hohlraum that can reach 5 Mbar pressures and beyond on the National Ignition Facility.

*This work was performed under the auspices of the Lawrence Livermore National Security, LLC, (LLNS) under Contract No. DE-AC52-07NA27344

15:48

CO5 10 Rayleigh-Taylor stabilization by material strength at Mbar pressures* BRUCE REMINGTON, HYE-SOOK PARK, THOMAS LORENZ, ROBERT CAVALLO, STEPHEN POLLAINE, SHON PRISBREY, ROBERT RUDD, RICHARD BECKER, JOEL BERNIER, *LLNL* We present experiments on the Rayleigh-Taylor (RT) instability in the plastic flow regime of solid-state vanadium (V) foils at 1 Mbar pressures and strain rates of 1.e6-1.e8 1/s, using a laser based, ramped-pressure acceleration technique. High pressure material strength causes strong stabilization of the RT instability at short wavelengths. Comparisons with 2D simulations utilizing models of high pressure strength show that the V strength increases by factors of 3-4 at peak pressure, compared to its ambient strength. An effective lattice viscosity of 400 poise would have a similar effect. [1] Constitutive models, and theoretical implications of these experiments will be discussed. [1] H.S. Park, B.A. Remington et al., submitted for publication (July, 2009).

*This work was performed under the auspices of the Lawrence Livermore National Laboratory under Contract No. DE-AC52-07NA27344.

16:00

CO5 11 Designs for Solid-State Rayleigh-Taylor Experiments in Tantalum at Omega* STEPHEN POLLAINE, BRUCE REMINGTON, HYE-SOOK PARK, SHON PRISBREY, ROBERT CAVALLO, *Lawrence Livermore National Laboratory* We have designed an experiment for the Omega - EP laser facility to measure the Rayleigh-Taylor (RT) growth rate of solid-state Ta samples at $\sim$ 1 Mbar pressures and very high strain rates, 10^7-10^8 s^{-1}. A thin walled, hohlraum based, ramp-wave, quasi-isentropic drive has been developed for this experiment. Thick samples ($\sim$ 50 μm) of Ta, with a preimposed sinusoidal rippled on the driven side, will be accelerated. The ripple growth due to the RT instability is greatly reduced due to the dynamic material strength. We will show detailed designs, and a thorough error analysis used to optimize the experiment, minimize uncertainty, and predict strength model sensitivity.

*This work was performed under the auspices of the Lawrence Livermore National Security, LLC, (LLNS) under Contract No. DE-AC52-07NA27344.

16:12

CO5 12 Rayleigh–Taylor Measurements in Planar CH and SiO_2 Foils on OMEGA J.D. HAGER, V.A. SMALYUK, S.X. HU, D.D. MEYERHOFER, T.C. SANGSTER, *Laboratory for Laser Energetics, U. of Rochester* Understanding how areal-density modulations grow at unstable ablative Rayleigh–Taylor (RT) interfaces is crucial to achieving inertial confinement fusion ignition. Recent planar RT experiments demonstrated increased stabilization in CH targets driven at high intensities (1×10^{15} W/cm^2) compared to simulations. Planar experiments were preformed on the OMEGA laser using CH, SiO_2, and CH-SiO_2 targets with 2-D modulations (imprinted by drive beams or pre-imposed) using shaped drive pulses at high (1×10^{15} W/cm^2) and low (5×10^{14} W/cm^2) intensities. The temporal growth of these modulations was measured with face-on x-ray radiography using Pd and Dy x-ray backlighters. Experimental results will be compared with simulations. This work was supported by the U.S. Department of Energy Office of Inertial Confinement Fusion under Cooperative Agreement DE-FC52-08NA28302.

16:24

CO5 13 Potential of FAIR at Darmstadt and LHC at CERN for High Energy Density Physics Research: the HEDgeHOB Collaboration NAEEM A. TAHIR, *GSI Darmstadt* ALEXANDER SHUTOV, IGOR LOMONOSOV, *IPCP Chernogolovka* A.R. PIRIZ, *UCLM Ciudar Real* RUEDIGER SCHMIDT, *CERN* DIETER H.H. HOFFMANN, *TU Darmstadt* CLAUDE DEUTSCH, *LPGP University of Paris* Substantial progress in the development of technology of high quality, well focused, strongly bunched intense partile beams have led to development of a novel, very efficient technique of studying High Energy Density Matter (HEDM) in the laboratory. This method involves generation of

large samples of HEDM by isochoric and uniform heating of solid targets by these ion beams. Two huge accelerator projects are on the way in Europe. One is the Facility for Antiiprotons and Ion Research (FAIR), at Darmstadt and the other is the Large Hadron Collider (LHC) at CERN. Extensive theoretical work has been carried out over the past years to assess the potential of these accelerators to generate HEDM and several experimental schemes have been proposed [1-4]. A brief overview of this work is presented in this talk. [1] N.A. Tahir et al., PRL 95 (2005) 035001. [2] N.A. Tahir et al., PRL 94 (2005) 135004. [3] N.A. Tahir et al., Nucl. Instr. Meth. A 577 (2007) 238. [4] N.A. tahir et al., PRE 79 (2009) in print.

16:36

CO5 14 Analytical theory for the interaction of a planar shock wave with an isotropic 2D/3D isotropic density field* C. HUETE RUIZ DE LIRA, J.G. WOUCHUK, *ETSII-INEI Univ. Castilla-La Mancha, Ciudad Real, 13071, Spain* A.L. VELIKOVICH, *Plasma Physics Division, Naval Research Laboratory, Washington, DC 20375, USA* The response of a shock front to different kinds of perturbations in the fluid upstream is of paramount importance to several fields, in particular to ICF. We present here an analytical linear model that describes the interaction of a shock front with a random pre-shock density perturbation field. Exact expressions for the velocity, density, vorticity and pressure of the compressed fluid particles are obtained. For isotropic pre-shock conditions, the mode averaging can be easily implemented in 2D/3D. Fully closed analytical expressions for the kinetic energy, vorticity generation, density non-uniformity amplification and for the intensity of sound emitted downstream are shown in the whole range of gas compressibilities and shock intensities. A comparison to an existing model [J. G. Wouchuk *et al.*, Phys. Rev. E. **79**, 066315 (2009)] that describes the shock interaction with a turbulent vorticity field is also given.

*Work supported by: Ministry of Science, Junta de CLM, Spain (C. H. R. de L. and J. G. W.), US DOE (A. L. V.)

16:48

CO5 15 Modification of the Hugoniot adiabat due to turbulence generated in shocked deuterium-filled CH foams* A.L. VELIKOVICH, *Plasma Physics Division, Naval Research Laboratory* J.G. WOUCHUK, C. HUETE RUIZ DE LIRA, *UCLM, ETSII-INEI Campus s/n Ciudad Real, Spain* Direct-drive laser targets are often designed with DT-filled CH foam ablator. Accurate modeling of these targets requires understanding of shock propagation in such non-uniform media. The interaction of the shock front with the preshock random density non-uniformities generates a random motion (turbulence) in the postshock flow. The energy coupled into the postshock turbulent motion, in turn, modifies the shock adiabat. As first detected in simulations by G. Hazak *et al.*, Phys. Plasmas **5**, 4357 (1998), shock compression and shock velocity in a deuterium-filled foam would be, respectively, less and greater than those predicted for the uniform medium of the same average density. We report an exact analytical theory of this "shock undercompression" effect and present explicit formulas for the shock adiabat modification. We discuss the contributions of post-shock Reynolds stresses, acoustic energy flux emitted downstream and correlations between vortical and entropy perturbations and highlight the difference between the cases of 2D and 3D turbulence.

*Work supported by US DoE/NNSA (A. L. V.), Ministry of Science, MEC(FIS2006-05389) and Junta de CLM (PAI08-0182-3162), Spain (J. G. W and C. H. R. de L.)

SESSION CO6: MAGNETIC RECONNECTION AND TURBULENCE

Monday Afternoon, 2 November 2009
Room: Hanover FG at 14:00
William Daughton, Los Alamos National Laboratory, presiding

14:00

CO6 1 Instability of the Sweet Parker reconnection layer and onset of fast turbulent reconnection MARINA SKENDER, GIOVANNI LAPENTA, *KU Leuven* Within purely resistive MHD without any anomolous effects reconnection sets into a steady state knox to center around an elongated current sheet, the Sweet-Parker (SP) layer, where dissipations allow reconnection. However, such layer is known to be possibly unstable to tearing-like modes. A recent discovery [1,2] is that following the destabilisation of the SP layer reconnection can develop into a fast trubulent regime. This new regime requires no anomlous processes and it is purely resistive MHD, progressing as fast as the fastests kinetic or MHD processes. We investigate such transition. [1] Self-Feeding Turbulent Magnetic Reconnection on Macroscopic Scales Giovanni Lapenta, Phys. Rev. Lett. 100, 235001 (2008), DOI:10.1103/PhysRevLett.100.235001 [2] Turbulent Magnetic Reconnection in Two Dimensions: Loureiro, N. F.; Uzdensky, D. A.; Schekochihin, A. A.; Cowley, S. C.; Yousef, T. A.: eprint arXiv:0904.0823

14:12

CO6 2 Hall Resistive Tearing Mode: A Variational Formulation BHIMSEN SHIVAMOGGI, A unified linear tearing-mode formulation is given incorporating both resistivity and Hall effects. A variational method is used that appears to be best suited to deal with the difficulties peculiar to the triple-deck structure associated with the Hall resistive tearing mode but also to lead to a convenient analytical dispersion relation for the Hall resistive tearing mode. This analytical dispersion relation -
recovers the Furth-Killeen-Rosenbluth result for the resistive branch; gives a growth rate for the Hall branch which appears to be consistent with the growth rate of the electron-inertia driven tearing mode given previously by Coppi; recovers the scaling relation for the transition from the resistive regime to the Hall regime numerically established by Fitzpatrick in a driven Hall resistive reconnection situation.

14:24

CO6 3 Electron scale structure of thin current sheets in collisionless magnetic reconnection NEERAJ JAIN, SURJALAL SHARMA, *University of Maryland, College Park, MD-20742* Cluster observations have shown highly structured electron-scale current sheets (CS), viz. bifurcated, filamented and triple peak structures during magnetic reconnection. An electron-magnetohydrodynamic model shows that these structures develop at various stages of time dependent reconnection. The Lorentz force on electrons due to the interaction of electron outflow velocity and normal component of magnetic field bifurcates the CS in the outflow regions, with scale sizes of the individual peak $\sim 3d_e$ (d_e being electron skin depth), similar to those observed by Cluster spacecraft. The bifurcation limits the length of the reconnecting CS which is further reduced by the secondary instabilities growing on the bifurcated CS. The secondary instabilities causes filamentation of the CS in the outflow region. Such filamentary

structures have been observed by Cluster spacecraft in magnetopause. In the presence of many reconnection sites, triple peak structure of the CS forms at the secondary sites as a result of reconnection inside the bifurcated CS associated with the main reconnection site.

14:36

CO6 4 Fast magnetic reconnection in fluid models of collisionless pair plasma* EVAN JOHNSON, *UW-Madison* The original studies of the GEM magnetic reconnection challenge problem exhibited fast magnetic reconnection in models which included Hall term effects. Subsequent PIC simulations showed that fast reconnection occurs even in pair plasmas, where the Hall term is absent; these studies attributed fast reconnection to nongyrotropic pressure. So we ask, (1) *Can a model of pair plasma with isotropic pressure exhibit fast reconnection?*, and (2) *Can a fluid model replicate patterns of fast magnetic reconnection seen in PIC simulations*? We have simulated the GEM problem for a pair plasma using ten-moment gas-dynamics for each species coupled to Maxwell's equations. Surprisingly, we find that the adiabatic collisionless ten-moment model gives slow reconnection but that isotropization *increases* the rate of reconnection to typical fast rates. We hope to demonstrate fast reconnection in anisotropic pair plasma without direct isotropization by using a nonadiabatic closure for the generalized heat flux; in particular, we expect to report results for David Levermore's 10-moment closure.

*Supported by the Wisconsin Space Grant Consortium.

14:48

CO6 5 Phase-space signature of electron diffusion in collisionless magnetic reconnection: A standing electron phase-space hole* LI-JEN CHEN, *Space Science Center and Center for Integrated Computation and Analysis of Reconnection and Turbulence, University of New Hampshire* WILLIAM DAUGHTON, *Los Alamos National Laboratory* The structure and dynamics of the electron layer holds the ultimate mystery of how magnetic reconnection can occur in a collisionless plasma. Results from 2D fully kinetic simulations indicate that the electron crossing orbits within the electron layer is the main cause for the electron motion decoupling from the magnetic flux during collisionless magnetic reconnection with zero guide fields. The key evidence is revealed in a hole structure in the electron phase space that stands in the center of the electron layer. The hole structure starts to emerge at the beginning of the explosive growth phase of reconnection, becomes the most prominent when the reconnection rate peaks, and spatially extends, along the outflow direction, through the entire electron diffusion region. Corresponding to the electron hole are a layer of bipolar electric field embedded in the bipolar Hall electric field within the electron layer, and bifurcations of the electron density and the out-of-plane velocity. Flow diversion, energy conversion, as well as regulation of electric currents in the reconnection layer can be understood in terms of electron crossing orbit dynamics.

*Work supported by DOE and NSF.

15:00

CO6 6 Electron holes in PIC Simulations with Physical Mass Ratio GIOVANNI LAPENTA, *KU Leuven* MARTIN GOLDMAN, DAVID NEWMAN, *University of Colorado* ANDREY DIVIN, *KU Leuven* S. MARKIDIS, *UIUC* Numerical simulation of reconnection with the kinetic approach is presented. Calculations are performed using the implicit particle-in-cell code PARSEK. The initial configuration is taken to be a conventional Harris current sheet with a guide field and an initial X-point perturbation is superposed to drive the reconnection process. The simulations reproduce such typical features as the Hall structure, the plasma exhaust jets and particle acceleration near X-point. Our attention is focused on the study of kinetic processes near the separatrix. Fast electron flows formed by Hall current system are favourable for development of electrostatic instabilities (namely, electron-ion Buneman instability) [Pritchett, 2005], [Goldman, 2008] as electrons stream much faster than ions there. The distribution functions are investigated for the evidence of electron holes formed by the Buneman instability and the corresponding bipolar spots of electric field. The relation between those reconnection signatures and development of separatrix instability in simulations is discussed.

15:12

CO6 7 Dynamo action with flow shear and magnetic shear N. LEPROVOST, E. KIM, *University of Sheffield* Dynamo action is a fundamental mechanism that explains ubiquitous magnetic fields in a variety of systems, including astrophysical, geophysical and laboratory plasmas. In this contribution, we provide an analytical theory of dynamo (α and β effects) in 3D forced helical MHD turbulence [1]. By non-perturbatively incorporating the effect of shear, we show that the α and β effects are enhanced by a weak shear while strongly suppressed by strong shear. In particular, for strong shear, the β effect is shown to be much more strongly suppressed than the α effect with the scalings $\alpha \propto A^{-5/3}$ and $\beta \propto A^{-7/3}$, respectively (A is the strength of the shear). The quenching of the α and β effect by shear has recently been confirmed in a numerical experiment [2]. One of the interesting implications of these results is that the dynamo efficiency, conventionally measured by the dynamo number D, depends more strongly on the shear than conventionally assumed. Specifically, D scales as A^4 rather than A. Incorporating a shear in the magnetic field, we then discuss its effect on the stability. Magnetic shear is shown to destabilize when it is stronger than flow shear. On the other hand, a weak magnetic shear compared to flow shear weakens the stabilizing effect of flow shear, thereby leading to a stronger turbulence than in the case without magnetic shear. [1] N. Leprovost and E. Kim, Astrophys J Lett. v696, L125 (2009); Phys. Rev. Lett., v100, 144502 (2008) [2] D. Mitra et al, Astron & Astrophys, v495, 1 (2009)

15:24

CO6 8 The effect of two-dimensional turbulence on resistive-MHD reconnection NUNO LOUREIRO, *IPFN, IST Lisbon* DMITRI UZDENSKY,* *Princeton University/CMSO* ALEXANDER SCHEKOCHIHIN, *R. Peierls Centre for Theoretical Physics, University of Oxford* STEPHEN COWLEY, *EURATOM/UKAEA Culham Science Centre* TAREK YOUSEF, *Imperial College London* Two-dimensional numerical simulations of the effect of background turbulence on 2D resistive magnetic reconnection are presented. For sufficiently small values of the resistivity (η) and moderate values of the turbulent power (ϵ), the reconnection rate is found to have a much weaker dependence on η than the Sweet-Parker scaling of $\eta^{1/2}$ and is even consistent with an η − independent value. For a given value of η, the dependence of the reconnection rate on the turbulent power exhibits a critical threshold in ϵ above which the reconnection rate is significantly enhanced.

*supported by NSF

15:36

CO6 9 Fast 3D Reconnection of Weakly Stochastic Magnetic Field: Prospects of the Research ALEX LAZARIAN, *University of Wisconsin-Madison* ETHAN VISHNIAC, *McMaster University* GRZEGORZ KOWAL, HOANG THIEM, *University of Wisconsin-Madison* REINALDO LIMA, *University of Sao Paolo* If the necessary requirement for the fast reconnection is the fluid being collisionless, then most of MHD simulations, including those of interstellar medium, do not represent astrophysical reality, as high numerical diffusivity makes reconnection fast for present-day simulations. Fortunately, the model of fast reconnection proposed in Lazarian & Vishniac (1999) does not have these restrictive constraints as it allows for fast reconnection in MHD limit provided that magnetic field is weakly stochastic. As turbulence is ubiquitous in astrophysical environments, weak stochasticity of magnetic field lines is a default state for most of astrophysical magnetic fields. This still leaves a question of what is happening when the magnetic fields are rather laminar. Our research shows that the reconnection itself may increase the level of turbulence resulting in reconnection instability or bursts of reconnection. The most evident application of the model is related to explaining of Solar flares. The predictions of the model above include First Order Fermi acceleration of energetic particles within the extended reconnection layers predicted in the model as well as the removal of magnetic flux during star formation. More astrophysical applications of the process are to follow.

15:48

CO6 10 Spectrum of weak MHD turbulence* STANISLAV BOLDYREV, *U. Wisconsin-Madison* JEAN CARLOS PEREZ, *U. Wisconsin-Madison* Turbulence of magnetohydrodynamic waves in nature and in the laboratory is generally cross-helical or non-balanced, in that the energies of Afvén waves moving in opposite directions along the guide magnetic field are unequal. We propose that such turbulence spontaneously generates a condensate of the residual energy $E_v - E_b$ at small field-parallel wave numbers. As a result, the energy spectra of counter-propagating Alfvén waves are generally not scale-invariant. In the limit of infinite Reynolds number, the universality is asymptotically restored at large wave numbers, and both spectra attain the scaling $E(k) \propto k_\perp^{-2}$.

*Supported by the U.S. Department of Energy under Grant No. DE-FG02-07ER54932, and by the NSF Center for Magnetic Self-Organization in Laboratory and Astrophysical Plasmas at the UW-Madison.

16:00

CO6 11 Numerical studies of weak MHD turbulence* JEAN C. PEREZ, STANISLAV BOLDYREV, *University of Wisconsin-Madison* Results from numerical simulations of weak magnetohydrodynamic (MHD) turbulence in steady-state are presented, with resolutions as high as $1024^2 \times 256$ grid points. Weak turbulence refers to the limit of MHD turbulence in which the energy transfer toward smaller scales results from the weak interaction between Alfvén waves moving along of against a strong guide magnetic field. The energies of the Alfven waves moving in the opposite directions can be either equal, in which case the turbulence is called balanced, or unequal, in which case it is unbalanced. The numerical set up is optimized as to drive either balanced or unbalanced turbulent cascades. We obtain the spectra of Alfvén waves for various degrees of imbalance and Reynolds numbers. We discuss our results and compare with recent theories of weak MHD turbulence.

*This work was supported by the U.S. DOE under Grant No. DE-FG02-07ER54932, by the NSF Center for Magnetic Self-Organization in Laboratory and Astrophysical Plasmas at the UW-Madison, and in part by the NSF under Grant No. NSF PHY0821899.

16:12

CO6 12 Theory of incompressible MHD turbulence with scale dependent alignment and cross-helicity J.J. PODESTA, *LANL* A. BHATTACHARJEE, *UNH* Boldyrev's theory of incompressible MHD turbulence is different from that of Goldreich & Sridhar (1995) and others in that it contains a scale dependent alignment of velocity and magnetic field fluctuations in the inertial range. Evidence for this alignment comes from direct numerical simulations and from solar wind data. An extension of Boldyrev's theory to imbalanced turbulence has been proposed by Perez & Boldyrev. We propose a different theoretical approach which generalizes the results of Perez & Boldyrev and is based on two new solar wind observations. The first is the observation that the normalized cross-helicity is approximately constant in the inertial range. The second is the observation that the probabilities p and q are approximately constant in the inertial range, where p and q are the probabilities that the velocity and magnetic field fluctuations at a randomly chosen point (x,t) are either aligned or anti-aligned, respectively. Aligned means that the angle between the velocity and magnetic field fluctuations is between 0 and $\pi/2$; anti-aligned means that the angle is between $\pi/2$ and π. Using these two observational constraints, a generalization of Boldyrev's theory is constructed in which the cascades of the two Elsasser species are each in a state of critical balance and the eddy geometries are required to be scale-invariant. In the new theory, $E(k_\perp) \propto k_\perp^{-3/2}$, $k_\parallel \propto k_\perp^{1/2}$, and the normalized cross-helicity is scale-invariant (a constant).

16:24

CO6 13 Scaling criteria for high Reynolds number MHD turbulence* YE ZHOU, *Lawrence Livermore National Laboratory, Livermore, CA, 94551* Magnetohydrodynamic (MHD) turbulence has been employed as a physical model for a wide range of applications in astrophysical and space plasma physics. This paper addresses the following questions. At what MHD flow condition can investigators be sure that their numerical simulations have reproduced all of the most influential physics of the flows and fields of practical interest? Another question, perhaps more specific, is can one define a metric to indicate whether the necessary physics of the flows of interest have been captured and suitably resolved using the tools available to the researcher? This issue was previously addressed in the context of high energy density physics where the Reynolds number of the minimum state was determined to be 1.6×10^5 [Zhou, Phys. Plasma, 14, 082701 (2007)]. The current paper focuses on extending the threshold minimum state criteria to include the correspondingly high Magnetic Reynolds number influences in MHD applications.

*This work was performed under the auspices of the Lawrence Livermore National Security, LLC, (LLNS) under Contract No. DE-AC52-07NA27344.

16:36

CO6 14 Thermodynamics, Vertical Structure, and Coronal Power of Optically-Thick MRI-Turbulent Accretion Disks* DMITRI UZDENSKY, *Princeton Univ./CMSO* Determining the thermal structure of an accretion disk heated by the dissipation of MRI turbulence, and the fraction of accretion power released in the disk corona are two critical problems in plasma astrophysics. In this contribution, these two intertwined problems are considered in the case of a disk threaded by a weak vertical magnetic field. The vertical disk structure is calculated by balancing the local turbulent heating due to the disruption of MRI channel flows by parasitic instabilities, and the cooling by radiative diffusion. It is argued that, neglecting the effects of large-scale MHD disk dynamo, the MRI dissipation rate should be uniform across the disk, almost up to its photosphere. This enables one to obtain a self-consistent solution for the disk's thermal structure. Next, the efficiency of Parker instability, viewed as a secondary parasitic instability feeding off MRI channel flows, is assessed by comparing its growth rate with that of other parasitic instabilities. It is shown that Parker instability becomes important near the disk surface, leading to a certain minimal coronal power fraction.

*Work supported by NSF.

16:48

CO6 15 Magnetosphere-Ionosphere Coupling through Plasma Turbulence in Electrojet* Y.S. DIMANT, M.M. OPPENHEIM, *Boston University* Field-aligned currents enter the high latitude E-region ionosphere from the magnetosphere causing cross-field electric fields and currents. During periods of intense geomagnetic activity, these fields induce the formation of strong electrojets, plasma instabilities, and turbulence. This turbulence gives rise to intense anomalous electron heating and nonlinear transport which significantly affects the E-region conductivity. Electrojet conductivities play an important role in the Magnetosphere-Ionosphere system. These conductivities determine the polar-cap potential saturation level and the evolution of field-aligned currents. Quantitative understanding of turbulent conductivities and energy conversion issues is important to accurately model magnetic storms and substorms essential for Space Weather predictions. We will present results of recent theoretical efforts of global energy flow, along with results of 2D and 3D fully kinetic, particle-in-cell, simulations. These simulations reproduce many of the observational characteristics of radar signals and provide information useful in accurately modeling plasma turbulence. They demonstrate the significant progress we have made simulating physical processes in E-region electrojets.

*Work supported by NSF Grants ATM-0613624 and ATM-0819914.

SESSION CO7: LOW TEMPERATURE PLASMAS I
Monday Afternoon, 2 November 2009
Regency VII at 14:00
Michael Keidar, George Washington University, presiding

14:00

CO7 1 The Electrodeless Lorentz Force Thruster THOMAS WEBER, BRIAN NELSON, RICHARD MILROY, *Plasma Dynamics Laboratory, University of Washington* DAVID KIRTLEY, JOHN SLOUGH, *MSNW LLC* The Electrodeless Lorentz Force (ELF) thruster is a novel plasma thruster under development at MSNW and the University of Washington which utilizes Rotating Magnetic Field (RMF) current drive technology to ionize a neutral gas and drive an azimuthal current to form a Field Reversed Configuration (FRC) plasmoid in a diverging magnetic field. The magnetic gradient imparts a net force to the FRC which is ejected from the thruster at high velocity. ELF has been shown to operate from 10 - 100 kW, with an exhaust velocity of 15 - 40 km/s. The ELF thruster is expected to have an extremely large range of efficient power levels, high thrust density, high specific power, long lifetime, and the ability to utilize virtually any type of propellant. Thruster design and operation, novel diagnostics, and a discussion of experimental results detailing the key physical phenomena within the thruster and exhaust plume will be presented.

14:12

CO7 2 Self consistent kinetic simulations of SPT and HEMP thrusters including the near-field plume region RALF SCHNEIDER, KONSTANTIN MATYASH, ANDREAS MUTZKE, OLEKSANDR KALENTEV, *Max-Planck Institute for Plasmaphysics* FRANCESCO TACCOGNA, *IMIP-CNR Bari* NORBERT KOCH, MARTIN SCHIRRA, *THALES Electron Devices GmbH, Ulm, Germany* SPT (Stationary Plasma Thruster) and HEMP (High Efficiency Multistage Plasma) thrusters are both relying on the creation of propulsive ion beams by ionization of propellant atoms. The specific shape of the magnetic fields in both concepts is used to optimize efficiency and ion acceleration. 2d3v-PIC-MCC calculations are used to compare the two different thruster concepts. They result in quite different plasma-wall interaction characteristics. The SPT thruster relies on the strong secondary electron emission from the dielectric walls of the thruster channel, which causes a large ion flux over the whole channel surface and consequently high erosion rate. In contrast, in the HEMP thruster the plasma contact to the wall is limited only to very small areas of the magnetic field cusps, which results in much smaller ion flux to the thruster channel surface as compared to SPT. Consequently, experimental studies of HEMP gave no evidence of erosion. In order to study the wall erosion for both thrusters, the binary collision approximation (BCA) based Monte-Carlo code SDTrimSP is applied.

14:24

CO7 3 Initial Results of Time-Resolved VUV Spectroscopy of Pulsed Dielectric Surface Flashover in Atmosphere* GEORGE LAITY, KLAUS FRANK, GARRETT ROGERS, ANDREAS NEUBER, JAMES DICKENS, JAMES MOSS, *TTU Center for Pulsed Power and Power Electronics* This paper describes some initial results from an experimental setup designed for studying the optical emission during pulsed surface flashover for the wavelength range from 115 nm to 180 nm at atmospheric pressures. A VM 505 from Acton Research Corporation was used as the spectrograph, with an Andor DH740 series ICCD camera mounted at the exit flange. Spectra were measured in nitrogen and air at atmospheric pressure with a flashover spark length of 8 mm under pulsed 35 kV excitation. Emission intensities were measured during gated 50 ns intervals, and it was concluded that most VUV emission occurs during the first stage of the flashover event. This is important because it is believed only radiation below 180 nm is energetic enough to cause photoionization leading to streamer discharge, and very little is known about VUV emission during this initial stage. Utilizing the NIST Atomic Spectra Database, a library of temperature dependent emission spectra was generated with SpectraPlot, a spectral software suite developed at TTU. The measured spectra will be discussed in relation to the physics of surface flashover at atmospheric pressure.

*Work supported by the Air Force Office of Scientific Research.

14:36

CO7 4 Determination of OH radicals in the far downstream of an atmospheric pressure microwave helium plasma jet* NIMISHA SRIVASTAVA, CHUJI WANG, *Department of Physics & Astronomy, Mississippi State University, MS, US* A recent study has reported observation of OH radicals in the far downstream of an atmospheric argon microwave plasma jet. The far downstream is referred to as the location where the ratio of the distance from the jet orifice to the length of the jet column is $>$ 3. In this work we report that this phenomenon also exists in a similar plasma jet of 2.5 mm long, operating by helium gas. A detailed characterization of the helium microwave plasma jet was carried out by using UV pulsed cavity ringdown spectroscopy and optical emission spectroscopy. The nonthermal plasma temperatures were determined from stimulations of the emission spectra of several vibronic bands of the 2^{nd} positive system of N_2, the 1^{st} negative system of N_2^+, the (0,1,2,3-0) bands of NO (A-X), and the (0-0) band of OH (A-X). Absolute number densities of OH were measured along the plasma jet column. Dependence of OH concentration on plasma power and gas flow rate at different locations along the jet axis was characterized. The electron densities were also measured by recording Stark broadening of the hydrogen Balmer beta line (H_β) at 486.1 nm.

*This work was supported by National Science foundation, grant # CTS-0626302.

14:48

CO7 5 Studies of the vacuum breakdown behavior using refractory-metal thin film coated electrodes RANDOLPH FLAUTA, JOHN KIONKA, MARTIN JOHN NEUMANN, DAVID RUZIC, *Center for Plasma-Material Interactions, Department of Nuclear, Plasma, and Radiological Engineering, University of Illinois at Urbana-Champaign* JOHN CAUGHMAN, *Fusion Energy Division, Oak Ridge National Laboratory* UNIVERSITY OF ILLINOIS AT URBANA-CHAMPAIGN TEAM, OAK RIDGE NATIONAL LABORATORY COLLABORATION, A reliable operation of ICRF antennas in fusion devices is often limited by its breakdown threshold. Surface conditions of electrodes during high voltage operations have played a key role in affecting breakdowns. In this work, the effects of coating electrodes with refractory-metal thin films to improve on the reliability and power delivered by ICRF antennas have been investigated. Using the Surface Plasma Arcs by Radiofrequency - Control Study (SPARCS) facility at the Center for Plasma-Material Interactions which is designed as a DC system, the current and voltage breakdown patterns and the measured energy in the arc at an electric field of up to 150 MW/m were studied. Experiments with electrodes coated with W, Mo and Ta operated at high temperature of 600 ^oC and above were explored. Surface studies were also conducted on the electrodes to determine the electrode conditions and other surface reactions after the breakdown.

15:00

CO7 6 Design of experiments on a DC Steady State Atmospheric Pressure Plasma Sterilizer IGOR ALEXEFF, ARUN BALASUNDARAM, RAPINDER SAWHENY, *University of Tennessee* Our Resistive Barrier Discharge has been demonstrated to be successful on E. coli, Pseudomonas fluorescens (5RL), spores and bacteriophages. It has been tested successfully in sterilizing pagers at the St. Jude Research Hospital in Memphis, TN. In this recent work, we evaluate three primary factors in the atmospheric pressure resistive barrier discharge, hydrogen peroxide, charged ions and air (oxygen). The experiment used was Analysis of Variance (ANOVA) and regression analysis. The tests used 144 Petri Dishes and the bacteria used were E. coli. The hydrogen peroxide was used as a replacement for the water conductor on the resistive barrier discharge electrode. The charged ions were removed by a double charged wire mesh between the discharge and the Petri Dish. The air was displaced by a slow flow of nitrogen into the experimental area. The basic conclusions are that air, and charged ions are both extremely effective in killing bacteria. In addition, air and charged ions together strongly enhance each other. Hydrogen peroxide in our experiments did not enhance the kill rate.

SESSION CP8: POSTER SESSION II
Monday Afternoon, 2 November 2009
Grand Hall East at 14:00

CP8 1 DIAGNOSTICS, HEATING, CURRENT DRIVE

CP8 2 Enhancements to the Edge CXRS System on JET* T.M. BIEWER, D.L. HILLIS, *Oak Ridge Nat. Lab., USA* Y. ANDREW, N.C. HAWKES, K.-D. ZASTROW, *EURATOM/UKAEA Fusion Assoc., UK* K. CROMBE, *Assoc. EURATOM, Belgium* JET EFDA COLLABORATION, Enhancements have been made to 2 of the 4 instruments comprising the edge (r/a $\sim$ 0.5 to $\sim$ 1.0) charge-exchange recombination spectroscopy (CXRS) suite of diagnostics on the Joint European Torus (JET). Both enhanced instruments now consist of short focal length spectrometers coupled to fast-framing CCD cameras at "high dispersion." Between these two instruments the number of plasma viewing channels increases from 24 to 34. The time resolution is improved to 10 ms. The neutral-beam induced emission of C VI at 529.1 nm, of Ne X at 524.8 nm, and of Ar XVIII at 522.4 nm is observed simultaneously, complementing the existing edge CXRS instruments, which can be tuned to observe any visible wavelength of interest. These enhancements enable the simultaneous observation of the temperature, rotation, and concentration of multiple plasma impurity ions at improved temporal and spatial resolution. Preliminary data will be shown from the recent JET campaign.

*This work was supported by the US D.O.E. contract DE-AC05-00OR22725, and has been performed under the European Fusion Development Agreement.

CP8 3 Measurement of Type-I ELM Pulse Propagation in Scrape-Off Layer Using Optical System of Motional Stark Effect Diagnostics in JT-60U TAKAHIRO SUZUKI, NAOYUKI OYAMA, NOBUYUKI ASAKURA, *Japan Atomic Energy Agency* Propagation of plasma ejected by type-I ELM has been measured in scrape-off layer (SOL), using optical system of motional Stark effect (MSE) diagnostics in JT-60U as beam emission spectroscopy (BES) diagnostics. This MSE/BES system measures Dalpha emission from heating neutral beam excited by collisions with the ejected plasma, as well as background light (e.g. bremsstrahlung). In order to separate the beam emission and the back-

ground light, a two-wavelength detector is introduced into the MSE/BES system The detector observes simultaneously at the same spatial point in two distinct wavelengths using two photomultiplier tubes through two interference filters. One of the filters is adjusted to the central wavelength of the beam emission and the other is outside the beam emission spectrum Subtracting the background light, temporal change in the net beam emission in SOL has been evaluated Comparing conditionally-averaged beam emission with respect to 594 ELMs at 5 spatial channels (0.02-0.3 m outside the main plasma near equatorial plane), radial velocity of the ELM pulse propagation in SOL is about 0.8-1.8 km/s. Work supported by Grand-in-Aid for Young Scientists (B) No. 20760586

CP8 4 Progress on a 200kW Diagnostic Neutral Beam ETHAN SCHARTMAN, E.L. FOLEY, F. LEVINTON, *Nova Photonics, Inc* J.W. KWAN, K.N. LEUNG, Y. WU, H. VAINIONPAA, *Lawrence Berkeley Laboratory* The interaction of neutral beam atoms with a magnetized plasma provides diagnostic access to the interiors of fusion experiments. Parameters which can be measured using neutral beams include ion temperature and velocity, density fluctuations and also local magnetic field direction. Nova Photonics, Inc and Lawrence Berkeley National Laboratory are developing a diagnostic neutral beam for use in fusion experiments which lack neutral heating beams, or on which the heating beam is not suitable for diagnostics. Our apparatus is designed to produce a 1 s duration, 5 x 8 cm elliptical cross section hydrogen beam at energies up to 40 kV and up to 5 A current. Hydrogen ions are produced in a multicusp 13 kW, 13 MHz RF source. The extracted ions have current densities of 100 - 150 mA/cm^2. The proton fraction of the hydrogen ions is 85%. Beams are extracted from the source with a rectangular, multi-aperature grids. Details of the source performance will be presented as well as initial operation of the extraction optics and neutralizer region. This work is supported by the U.S. DOE under grant DE-FG02-05ER86256.

CP8 5 Relativistic Depolarization Effects in Thomson Scattering E. PARKE, V.V. MIRNOV, D.J. DEN HARTOG, Y.M. YANG, *University of Wisconsin-Madison* Relativistic depolarization effects have been well studied for several cases of Thomson scattering - particularly the simplifying case of 180 ° backscattering utilized in LIDAR Thomson scattering systems [K. V. Beausang and S. L. Prunty, Plasma Phys. Control. Fusion 50, 095001 (2008)], as well as the more general case where the detector is assumed to collect only scattered radiation with the component of the scattered electric field parallel to the incident wave electric field [O. Naito, H. Yoshida, and T. Matoba, Phys. Fluids B 5, 4256 (1993)]. These results are not valid for the Thomson scattering diagnostic on the MST reversed-field pinch, which collects all polarizations of the scattered radiation and measures radiation scattered at many different angles. We derive a compact form for the scattering spectrum for this case and present an analytic approximation. The accuracy of this approximation is determined for temperatures up to 40 keV. This derivation improves the accuracy of Thomson scattering measurements made on the MST without sacrificing calculation speed; even at temperatures of a few keV, the onset of relativistic depolarization can significantly alter the scattering spectrum. Furthermore, this approximation provides an accurate spectrum of interest in the study of higher-temperature fusion plasmas. *This work was supported by the U.S. Department of Energy.

CP8 6 Dual-Array Electron Cyclotron Emission Imaging (ECEI): a New Millimeter Wave Imaging System for Electron Temperature Fluctuation on the DIII-D Tokamak* N.C. LUHMANN, JR., B.J. TOBIAS, C.W. DOMIER, X. KONG, T. LIANG, *University of California* R. JASPERS, A.J.H. DONNE, *FOM-Institute for Plasma Physics Rijnhuizen* M. SMITH, R. NAZIKIAN, *Princeton Plasma Physics Laboratory* H.K. PARK, *Pohang University of Science and Technology* A new diagnostic tool has been developed for simultaneous real-time imaging of electron temperature fluctuations at both the high and low field sides. Separate imaging arrays spanning 75 to 110 and 90 to 140 GHz, respectively consist of 160 channels (20 vertical by 8 radial) with $\sim$ 1 cm^2 resolution, providing up to 55 cm of vertical plasma coverage. Fluctuations of 1% are measurable on μs time-scales. The technical capabilities of this diagnostic, as well as potential physics issues to be investigated, are discussed. The details of the constituent technologies, including advanced antennas and substrate lenses, quasi-optical planar filter components, and double down-conversion heterodyne signal detection will be addressed.

*Work supported by U.S. DOE Grants DE-FG02-99ER54531 and DE-AC02-76CHO307, POSTECH, and by NWO and the Association EURATOM-FOM.

CP8 7 Advances in Velocimetry Techniques for Plasma Turbulence BENJAMIN BROWN, T. MUNSAT, Y. SECHREST, N. SEN, *University of Colorado* The HOP-V (Hybrid OPtical-flow Velocimetry) code has been developed for extracting time-resolved 2-D velocity maps from turbulence imaging diagnostics. The HOP-V code combines optical-flow and local pattern-matching techniques to derive "dense" velocity fields at the full temporal resolution and a fraction of the spatial resolution of the underlying image frames, often tens of pixels per side and thousands of timepoints in duration, with temporal and spatial resolution sufficient to resolve the relevant coherence decay quantities. Recent work has resulted in a new module to the HOP-V code, using a "next generation" optical flow approach capable of obtaining accurate flow-fields from highly nonrigid motion, as is commonly the case in turbulent scalar measurements. This approach not only derives flow fields containing local curl, but also simultaneously provides a decomposition of the flow field into a coherent pattern with separable small-scale patterns. This can be particularly important in separating the local "swirling" motion from flows having a more global impact on transport.

CP8 8 Validation of Velocimetry Techniques using Synthetic Diagnostics in Edge Turbulence Simulations Y. SECHREST, B. BROWN, T. MUNSAT, N. SEN, *University of Colorado* X. XU, *LLNL* S. ZWEBEN, *PPPL* The HOP-V (Hybrid OPtical-flow Velocimetry) code, developed for extracting time-resolved 2-D velocity maps from turbulence imaging diagnostics, combines optical-flow and local pattern-matching techniques to derive "dense" velocity fields at the full temporal resolution and a fraction of the spatial resolution of the underlying image frames, often tens of pixels per side and thousands of timepoints in duration, with temporal and spatial resolution sufficient to resolve the relevant turbulent structures. The code has been validated for a variety of artificial test patterns of convective flow, including highly sheared cases. Beyond verifying the validity of the velocimetry algorithms for extracting the true motion of the visible structures lies the physical interpretation of the derived velocity fields. To approach this question, we have implemented a synthetic diagnostic (similar to the Gas Puff Imaging instrument) to analyze the

output of the BOUT edge turbulence simulation. Here we present the results of a study directly comparing the derived velocity fields to the known plasma quantities from the simulation, in an attempt to define the connection between the observed velocities and underlying plasma behavior.

CP8 9 Fullwave Simulation of Doppler Reflectometry in Turbulent Plasmas CARSTEN LECHTE, ULRICH STROTH, *Institut fuer Plasmaforschung, Universitaet Stuttgart, Germany* GARRARD CONWAY, *Max-Planck-Institut fuer Plasmaphysik, EURATOM Assoziation* Doppler reflectometry is a microwave diagnostic for plasma density fluctuations and flow velocities. A meaningful interpretation of Doppler reflectometry measurements necessitates the analysis of the wave propagation in the plasma using simulations methods. While the beam path can usually be reconstructed with beam tracing methods, the modeling of the scattering process demands the use of wave simulation codes. Furthermore, in the presence of strong density fluctuations, the response from the plasma is dominated by dispersion and multiple scattering, and hence becomes non-linear. IPF-FD3D [1] is the finite difference time domain code used to investigate the dependence of the scattering efficiency on the various plasma conditions. It uses the full set of Maxwell equations and the electron equation of motion. First results in slab geometry indicate a strong dependence of the scattering efficiency on the density gradient, the turbulent fluctuation strength, and the wave polarisation. In addition, the actual plasma conditions in ASDEX-Upgrade are recreated in the simulation in order to interpret experimental measurements. [1] C. Lechte, IEEE Trans. Plasma Sci. 37 (6), 2009

CP8 10 Transmitter Upgrade for JET Alfvén Eigenmode Fast Particle Interaction Studies* P. WOSKOV, M. PORKOLAB, *MIT PSFC* A. FASOLI, P. BLANCHARD, *CRPP-EPFL* One of the main missions of the worldwide fusion R&D effort is to develop predictive and control capability of burning plasmas in support of ITER. A unique 8-coil antenna system has been implemented on JET to study fast-ion interactions with Alfvén eigenmodes in the 50 – 500 kHz range that could potentially increase losses of α particles and reduce fusion gain. The single 4 kW transmitter will be replaced with eight 1 kW transmitters that will independently power each antenna to more uniformly distribute the power among the antennas. This will improve the coupling to higher order modes (n = 5 - 30) for damping studies. Independent drivers will also be used to make possible multi frequency and arbitrary phase studies of multiple modes and traveling modes. Various analog and digital driver approaches are being considered to provide the needed flexibility. A systems design will be presented.

*Supported by U. S. DOE.

CP8 11 X-ray GEM Detectors for Burning Plasma Experiments S. PUDDU, *Universita di Cagliari* F. BOMBARDA, G. PIZZICAROLI, *ENEA* F. MURTAS, *INFN-LNF, Italy* The harsh environment and higher values of plasma parameters to be expected in future burning plasma experiments (and even more so in future power producing fusion reactors) is prompting the development of new, advanced diagnostic systems. The detection of radiation emitted by the plasma in the X-ray spectral region is likely to play the role that visible or UV radiation have in present day experiments. GEM gas detectors, developed at CERN, are the natural evolution of Multiwire Proportional Chambers, with a number of advantages: higher counting rates, lower noise, good energy resolution, low sensitivity to background radiation. GEM's can be used in several different ways, but two specific applications are being explored in the framework of the Ignitor program, one for plasma position control and the other for high resolution spectroscopy. The diagnostic layout on the Ignitor machine is such that the detectors will not be in direct view of the plasma, at locations where they can be efficiently screened by the background radiation. Prototype detectors 10 $\times$ 10 cm^2 in area have been assembled and will be tested to assess the optimal geometrical parameters and operating conditions, regarding in particular the choice between Single and Triple GEM configurations, the gas mixture, and the problem of fan-out associated with the high number of output channels required for high resolution crystal spectrometers.

CP8 12 SSPX discharges with tungsten hexacarbonyl prefill J. CLEMENTSON, P. BEIERSDORFER, H.S. McLEAN, R.D. WOOD, E.W. MAGEE, *Lawrence Livermore National Laboratory* The ITER tokamak will have a tungsten divertor and, consequently, the plasmas are expected to contain tungsten ions. The spectral emission from these ions can serve to diagnose the divertor for plasma parameters such as tungsten concentrations, densities, ion and electron temperatures, and flow velocities. The ITER divertor plasmas will have densities around 10^{14-15} cm^{-3} and temperatures below 100 eV. These conditions are similar to the plasmas at the Sustained Spheromak Physics Experiment (SSPX) in Livermore. To simulate ITER divertor plasmas, a tungsten impurity was introduced into the SSPX spheromak by prefilling it with tungsten hexacarbonyl at injection pressures up to 1 Torr prior to the usual hydrogen gas injection and initiation of the plasma discharge. These discharges lasted a few milliseconds and achieved plasma currents up to 1 MA. The possibility of using the emission from low charge state tungsten ions to diagnose tokamak plasmas was investigated using a high-resolution EUV spectrometer in the 50 to 450 Å range. Work performed under the auspices of the US DOE by LLNL under contract DE-AC52-07NA-27344.

CP8 13 Determination of Experimental Mutual Inductances in Magnetic Diagnostics Through Linear Modeling JONATHAN HEBERT, *Auburn University* JAMES HANSON, BENJAMIN STEVENSON, When using magnetic diagnostics for equilibrium reconstruction of a plasma, it is necessary to know the mutual inductances between the diagnostics and known sources of current, such as field generating coils. The mutual inductance is a purely geometric factor and, as such, can be found computationally given the locations of the target coils. Even so, direct calculation may not be the most accurate method of determination. This method does not, for example, take into account the error inherent in the placing of the coils (which can have a large effect when a perfectly placed coil should have an extremely low inductance). A method for experimentally determining the mutual inductances, explored here, is possible through a linear model. The flux in each diagnostic is measured during a plasma-free (vacuum) shot. Under the assumption that any flux in the magnetic diagnostics during such a shot is the product of measured coil currents and their mutual inductances with the diagnostic, a chi-squared minimization is done on the difference between the measured flux data and the product of the model. This method also has the advantage of offering some insight into the modeling of induced currents in the vacuum vessel.

CP8 14 Miniature magnetic field probes for use in high temperature plasmas K.E. MILLER, K.M. VELAS, D.E. LOTZ, *University of Washington, Redmond Plasma Physics Laboratory* An ideal internal magnetic probe would provide high temporal and spatial resolution, without perturbing the plasma. Optimizing the following moves towards this ideal: Size - as small as possible; Plasma facing material - insulating, difficult to ablate, low Z; Shielding - electrostatic, short field penetration time; Electronics - high gain integration, long term stability. Over the years, significant improvements in these areas have been made. The latest probe, built for TCSU, is 3 axis with 96 windings. It is BN clad with a 6 mm outside diameter, is UHV compatible, and can be baked to 200 C. The integrators used are gated, with a 10 usec RC time, and have less then a 10 mV drift per second. Plasmas with widely varying parameters have been probed. A few hundred eV, 1e20 m-3 density plasma with a 1 msec duration represents a reasonable upper limit for probe usability. Plasma duration, density, and temperature can be traded for each other. Design criterion and construction details will be presented, with a focus on the "how to" of actually building one.

CP8 15 A Baffled-Probe Technique for Real-Time Edge Diagnostics VLADIMIR DEMIDOV, MARK KOEPKE, *WVU* YEVGENY RAITSES, *PPPL* A baffled probe offers the advantages of direct measurements of the plasma fluid observables, while being non-emitting and electrically floating [1]. The principle of operation of the probe is based on the dependence of the voltage drop in the plasma-probe sheath on the direction of the local magnetic field. When the magnetic field is parallel to the probe surface, the electron-repelling sheath can be significantly reduced as the magnetic field also impedes the cross-field electron flow and therefore, a smaller sheath voltage is needed to maintain the zero current balance to the floating probe. As a result, the accuracy of direct measurement of the plasma potential is greatly increased by eliminating the contribution of electron temperature to the floating-potential measurement. The baffled-probe designs proposed for edge diagnostics will increase the capability to characterize separately plasma properties in real-time for understanding of underlying physics in the edge plasma of tokamaks. [1] V. I. Demidov et al., Rev. Sci. Instrum. 73, 3409 (2002).

CP8 16 Self-consistent simulations of rf heating in the ion cyclotron range of frequencies D.L. GREEN, E.F. JAEGER, L.A. BERRY, *Oak Ridge National Laboratory* M. CHOI, *General Atomics* RF-SCIDAC TEAM,* The rf-SciDAC collaboration is developing computer simulations to predict the damping of radio frequency (rf) waves in fusion plasmas. The recent iterative coupling of the all-orders spectral wave solver AORSA to the Monte-Carlo particle codes ORBIT-rf and sMC+rf allows finite width ion orbits and rf induced spatial transport to be studied in the ion cyclotron range of frequencies [Green et al., *Proc. of 18th Topical Conference on Radio Frequency Power in Plasmas, Gent, Belgium*]. Here we investigate the effects of including finite ion orbits and the importance of using the full $\vec{k}$ spectrum when constructing the quasi-linear (QL) rf heating operator. Power absorption and deposition results for simulations with and without finite ion orbits and for various QL heating operators are compared for heating scenarios including minority H on Alcator C-Mod, beam heating on DIII-D and high harmonic fast wave heating on NSTX. Additionally we present the preliminary results of extending AORSA to calculate the linear wave solution in the open field line region outside the last close flux surface on NSTX.

*See author list of Jaeger et al., Phys. of Plasmas, 15, 072512 (2008), DOI: 10.1063/1.2959128

CP8 17 ICRF Heating Scenarios for the Reduced Magnetic Field, Non-nuclear Phase of ITER* E.F. JAEGER, L.A. BERRY, *Oak Ridge National Laboratory* P.U. LAMALLE, A. LOARTE, A. POLEVOI, *ITER Organization* A. IVANOV, *Keldysh Inst. of Appl. Math* RF SCIDAC TEAM, Radio frequency power in the ion cyclotron range of frequencies (ICRF) is one of three external heating sources planned for ITER. Previous full-wave simulations of high-power electromagnetic wave heating in ITER using the AORSA code [1] have concentrated on the burning plasma regime at full magnetic field and plasma current. Here, we consider instead the startup, non-nuclear phase of ITER. ASTRA modeled plasma profiles are assumed for hydrogen plasmas at 7.5 MA and 2.65 T with 3% minority He^3 ions. The 2^{nd} harmonic He ^{3} resonance occurs near the magnetic axis, while the fundamental H resonance occurs on the inboard edge. Three cases represent a good range of conditions to study the application of ICRF: 1) L-mode conditions before ICRF is applied and well away from the H-mode threshold, 2) L-mode conditions with ICRF approaching the H-mode threshold, and 3) fully developed H-mode with all power available.

*This research used resources of the National Center for Computational Sciences at Oak Ridge National Laboratory, which is supported by the Office of Science of the U.S. Department of Energy under Contract No. DE-AC05-00OR22725.

CP8 18 Modeling of an ITER Antenna Module, in Vacuum, and with Facing Plasma DAVID SMITHE, JOHAN CARLSSON, TRAVIS AUSTIN, PETER STOLTZ, DAN KARIPIDES, *Tech-X Corporation* RF SCIDAC TEAM, We report on the process of modeling the electromagnetic properties of a single ITER module, including Faraday screen, with the finite-difference time-domain software, VORPAL. CAD drawings and other descriptive materials are used to create an input file and geometry description suitable for EM modeling. Though finite-difference based, this software provides finite-element-like accuracy in the geometry representation, due to its cut-cell boundary capability. Parametric descriptions and enhancements are also used to resolve issues, add drive terms, and diagnostic features, and to insure reusability, e.g., for simulation of an entire antenna assembly in the future, and for installation into a larger toroidal-geometry simulation. Vacuum electromagnetic properties, such as peak fields and radiation impedance are measured, and compared with existing data, where possible. In addition, this software contains a time-domain plasma model that allows seamless integration with edge and possibly even internal plasma. An investigation of the electrical properties is then repeated for sensible edge plasma parameters.

CP8 19 RF propagation in the turbulent edge plasma* J.R. MYRA, D.A. D'IPPOLITO, *Lodestar Research Corp.* Most present day codes treat the propagation of rf through the edge plasma in relatively simple models in which the background plasma is steady state, laminar, and one dimensional (varying only in the flux coordinate). In reality, the edge plasma is strongly turbulent and intermittent in both space and time. As a first approximation, we consider the SOL to consist of a tenuous background plasma upon which denser filamentary field-aligned blobs of plasma are superimposed. Thus the (time and poloidally averaged) mean and local densities are very different. The blobs are regarded as stationary on the rf time-scale. Questions include phenomenology near resonances and cutoffs in intermittent plasmas, wave propagation and evanescence (e.g. when the blob and background are on opposite sides of a cutoff), and scattered power. We begin to address these questions by reporting on the scattering of a fast or slow plane-wave from a field-aligned cylinder of higher density plasma, in the cold plasma model.

*Supported by the USDOE under grants DE-FG02-97ER54392 and DE-FC02-05ER54823.

CP8 20 A numerical analysis of the RF wave propagation under the sheath boundary condition in the ion cyclotron range of frequencies* HARUHIKO KOHNO, *Massachusetts Institute of Technology, Plasma Science and Fusion Center* J.R. MYRA, D.A. D'IPPOLITO, *Lodestar Research Corporation* Applying radio-frequency (RF) waves to heat plasmas and drive current is an important technique for magnetic fusion, and much research effort has been spent on improving the methods, particularly in the ion cyclotron range of frequencies. In this study, a numerical analysis is carried out in order to observe the RF wave propagation and its interaction with the sheath in the scrape-off layer. A two-dimensional finite element code is developed to test the effect of sheaths on waves in cold plasma with the equilibrium magnetic field having a small component into the wall. Here the C-Mod like parameters are used to construct the calculation domain, on which the sheath boundary condition proposed by D'Ippolito and Myra, and the absorbing boundary condition are imposed. Various mechanisms for antenna coupling to the slow wave (SW) and fast-wave coupling to the SW by the sheath boundary condition are qualitatively investigated.

*This work was supported in part by DoE contracts DE-FC02-ER54648 and DE-FC02-05ER54823.

CP8 21 Reconstructing lower hybrid wave fields from ray tracing data* A.S. RICHARDSON, P. BONOLI, J. WRIGHT, *MIT Plasma Science and Fusion Center* Full wave simulations of lower-hybrid waves in plasmas can now be performed, and some of the results display features that look like rays or beams [1]. While some features of the full wave results can be reproduced using ray tracing methods, other features cannot be. In this work, we use the higher order terms in the ray tracing approximation to construct an approximate wave field from ray tracing data. In order to correctly deal with caustics - such as the reflection of the lower hybrid wave from the cutoff at the plasma boundary - we implemented a field reconstruction algorithm based on wave packet dynamics [2]. We then applied this algorithm to the case of a lower hybrid wave reflecting from the cutoff in a cold plasma slab model, and the preliminary results show good agreement with the analytical solution. [1] J. Wright, et al. Full wave simulations of lower hybrid wave propagation in tokamaks. Proceedings of the 18th Topical Conference on Radio Frequency Power in Plasmas, 2009. [2] R. Littlejohn. The semiclassical evolution of wave packets. Physics Reports, 138(4-5):193-291, May 1986.

*Work supported by the DOE OFES.

CP8 22 Towards the modeling of ICRH using the delta-f particle-in-cell method in RZ geometry* TRAVIS AUSTIN, DAVID SMITHE, VAHID RANJBAR, MATT WROBEL, *Tech-X Corporation* The delta-f particle-in-cell (DFPIC) method is a PIC method with a high signal-to-noise ratio which has been used for modeling electron Bernstein waves and ion cyclotron fast waves. It offers the capacity to model particle behavior such as multiple pass resonance, banana orbits, and superadiabaticity. It presents an alternative to linear wave codes like AORSA and TORIC which include only first-order parallel and perpendicular gradient variations of cyclotron frequency. Here we explore the use of the DFPIC method in the VORPAL computational framework for ion cyclotron resonance heating in RZ geometries based on eqdisk fusion data. We also consider the coupling to the bounce-averaged nonlinear Fokker-Planck code, CQL3D, through the generation of quasi-linear diffusion coefficients using a novel approach based on the DFPIC method. A benchmarking of the quasi-linear diffusion coefficients generated with the DFPIC method will be presented in 1D.

*Work funded by Department of Energy SBIR Grant #DE-FG02-07ER84722.

CP8 23 AORSA-1D simulation of parametric decay instability (PDI) in tokamak plasmas* GUANGYE CHEN, F.E. JAEGER, L.A. BERRY, *ORNL* J.R. MYRA, *Lodestar* Theory and experiment have suggested that PDI is a possible nonlinear edge loss mechanism. This study simulates the PDI in ICRF heating for the C-MOD and NSTX tokamaks, using an extended 1D full wave spectral code, AORSA [1], where a non-uniform plasma is taken into account. PDI is described by a set of coupled equations for a long-wavelength "dipole" pump and short-wavelength daughter waves. Fixing the pump wave, so that a direct method can be used to find the solution, eliminates possible numerical instability associated with iterative methods. We successfully excite the decay instability into an ion Bernstein wave and an ion cyclotron quasi-mode. Simulation shows the PDI threshold of C-MOD is consistent with the estimate from experiment, and the linear damping is so weak that non-linearly excited waves can propagate into the bulk plasma. NSTX has a much lower PDI threshold, and the narrow distance between harmonics prevents the daughter wave energy from getting into the bulk plasma. Comparison with local dispersion relation calculations shows strong effects of damping and poloidal wave number k_y on the PDI. [1] E.F. Jaeger, et al., Phys. Plasmas 7, 3319, 2000.

*Research sponsored by the U.S. DOE under Contract DE-AC05-00OR22725 with UT-Battelle, LLC.

CP8 24 JET ITER-Like Antenna Simulation Using the TOPICA Code DANIELE MILANESIO, RICCARDO MAGGIORA, *Politecnico di Torino, Italy* In this work, we carried out the analysis of the recently installed JET ITER-Like antenna with TOPICA code. Comparisons between TOPICA simulations and measurements taken during the actual experiment are presented. As routinely done for all simulated antennas, TOPICA inputs are

the technical drawings of the launcher and the accurate density and temperature profiles, which, in this case, have been provided by the JET team. The standard outputs are the input parameters of the antenna, namely the impedance matrix, the electric current distribution and the electric field pattern at the interface between the antenna region and the plasma column. This work provides an additional proof that the code can be adopted to predict the behavior of the ITER antenna, and to confidently use TOPICA for the challenging task of optimizing the complex design of the actual ITER antenna. More generally viewed, the possibility to reliably simulate the detailed geometry of an ICRF antenna, given a realistic plasma description, and to obtain the actual antenna input parameters, is of paramount importance to evaluate and predict the system performances, and to assist in system operation.

CP8 25 Simulations of lower-hybrid coupling in the Madison Symmetric Torus* JOHAN CARLSSON, DAVID SMITHE, *Tech-X Corporation* MARK CARTER, *Oak Ridge National Laboratory* MICHAEL KAUFMAN, *University of Wisconsin-Madison* An analysis will be presented of radio-frequency (RF) coupling with the inter-digital line slow-wave antenna used for lower-hybrid (LH) heating and current drive at 800 MHz in the Madison Symmetric Torus (MST) reversed-field pinch (RFP). The primary simulation tool was the VORPAL code, but MicroWave Studio and RANT3D/AORSA1D-H were also used. Due to the special requirements of the RFP configuration (tight-fitting conducting shell in which only minimal portholes are acceptable to maintain MHD stability), the unusual inter-digital line antenna was chosen. Accessibility in MST requires a very large parallel wave number $k_\parallel$, with $N_\parallel = ck_\parallel/\omega > 7.5$. A blind V&V exercise done in vacuum showed excellent agreement for the phase difference between the antenna rods, with VORPAL and measurement differing by only 1.0°, but with MWS deviating more. Unfortunately the phasing excites a wave with $N_\parallel$ approximately 10% too small. With plasma, VORPAL gives $N_\parallel$ around 15% below the accessibility limit. VORPAL simulations performed on ANL Intrepid to investigate antenna modifications to increase $N_\parallel$ will also be presented.

*Work supported by Oak Ridge National Laboratory

CP8 26 Examination of Up-Down Asymmetry Effects on CQL3D Calculation of ECCD and Multi-Species FW Heating in the DIII-D Tokamak* R.W. HARVEY, *CompX* R. PRATER, *General Atomics* E.F. JAEGER, *ORNL* The CQL3D Fokker-Planck code [1] which calculates the 3D (r, $v_\perp$, $v_{//}$), time-dependent electron and ion distributions has been recently upgraded to include effects of non-up-down symmetry, and also to simulate simultaneous quasilinear diffusion of multiple ion species. We make applications to two types of previous modeling of the DIII-D experiment: (1) ECCD, now particularly as regards effects on up-down asymmetric equilibria; and (2) D/minority-H modeling of a canonical DIII-D fast wave shot. Code modification issues, and results for ECCD and the effects of minority-H on the higher harmonic ion absorption of the FW, are presented. [1] R.W. Harvey and M. McCoy, The CQL3D Fokker Planck Code, Proceedings of the IAEA Technical Committee Meeting on Simulation and Modeling of Thermonuclear Plasmas, Montreal, Canada, 1992; also, http://www.compxco.com/cql3d.html.

*Supported under USDOE DE-FC02-04ER54698 and DE-AC02-05CH11231.

CP8 27 Kinetic evolution of electron distribution function in presence of RF waves* Y. KOMINIS, *NTUA, Athens, Greece* A.K. RAM, *PSFC, MIT* K. HIZANIDIS, *NTUA, Athens, Greece* Radio frequency (RF) waves are routinely used to modify the current profile in tokamaks. In ITER, electron cyclotron waves will be used for such a purpose. We have formulated a kinetic description for the evolution of the electron distribution function f_e in the presence of RF waves in a tokamak magnetic geometry [1]. The evolution of f_e and the electron orbits is treated simultaneously, so that the evolution equation for f_e is a functional mapping. This is useful as the electron phase space is inhomogeneous and bounded. All possible electron orbits, correlated and uncorrelated, are properly included. We use action-angle variables of an axisymmetric toroidal plasma. If we assume that f_e is randomly distributed in one or all of the angles, a diffusion-like equation for the evolution of f_e is obtained. The diffusion coefficient is time dependent and non-singular. In the limit of infinite time, we obtain the usual, singular, quasilinear diffusion coefficient. However, this description is incorrect as the time scale for the evolution of f_e is inconsistent with the infinite time scale for determining the diffusion coefficient. The consequences of our description on the evolution of f_e will be discussed. [1] Y. Kominis et al., Phys. Plasmas **15**, 122501 (2008).

*Supported by DoE, EFDA, and Assoc. EURATOM-Helenic Republic.

CP8 28 Nonlinear heating of ions by electron cyclotron frequency waves in tokamaks* K. HIZANIDIS, Y. KOMINIS, *NTUA, Athens, Greece* A.K. RAM, *PSFC, MIT* Previously it has been shown that small amplitude waves in the lower hybrid frequency range can nonlinearly heat ions in plasmas [1]. We study the possibility of heating ions by two electron cyclotron (EC) waves with slightly different frequencies in tokamak plasmas. The EC beams can be either the X or O waves and propagate at two different angles with respect to the local magnetic field. The ion motion in the interaction region, where the beams overlap spatially, is determined by canonical perturbation theory applied to the Hamiltonian of the ion motion. An analysis of the EC beam parameters for the two waves that are required to energize ions is presented. We consider the possibility of using such a scheme to heat ions in ITER-type plasmas. [1] D. Bénisti, A. K. Ram, and A. Bers, Phys. Plasmas **5**, 3224 (1998); A. K. Ram, A. Bers, and D. Bénisti, J. Geophys. Res. **103**, 9431 (1998).

*Work supported by DoE grants DE-FG02-99ER-54521 and DE-FG02-91ER-54109, EFDA, and Association EURATOM-Helenic Republic.

CP8 29 Scattering of radio frequency waves by edge density fluctuations* A.K. RAM, *PSFC, MIT* K. HIZANIDIS, Y. KOMINIS, *NTUA, Athens, Greece* The coupling of externally launched radio frequency (RF) waves to a plasma is through an edge region with fluctuating density. The fluctuations can lead to scattering of the waves and hinder their coupling into the core plasma. Consequently, the efficiency for heating and/or current drive by RF waves is lowered. We study the effect of density fluctuations on RF waves in the ion cyclotron, lower hybrid, and electron cyclotron range of frequencies. We compare the full wave effects with a model where the waves are represented by rays. Then the Hamilton-Jacobi equations are applicable. A statistical model for

the refraction of rays due to the fluctuating part of the plasma permittivity is developed. We will present results from this model showing the effect of fluctuations on the coupling of various RF waves.

*Work supported by DoE grants DE-FG02-99ER-54521 and DE-FG02-91ER-54109, EFDA, and Association EURATOM-Helenic Republic.

CP8 30 Drift of circulating orbits due to toroidal electrical field XIAOYIN GUAN, HONG QIN, NATHANIEL J. FISCH, *Princeton University* The drift orbit of circulating particles in a tokamak geometry with a toroidal electric field is studied. Unlike trapped particles, which move significantly due to the Ware-pinch effect, circulating particles deviate far less across flux surfaces. The orbits of circulating particles drift away from the center of tokamak with a velocity smaller than the ware pinch velocity, but larger than the $\mathbf{E} \times \mathbf{B}$ drift velocity. For trapped particles, the Ware pinch effect is accompanied by acceleration in the parallel direction. Thus, trapped particles first are pinched inward, then untrapped and then the resulting untrapped particles drift outwards. Thus, trapped particles first are pinched inward, are then untrapped, and then the resulting untrapped particles drift outwards. This effect may be relevant to toroidal rotation observed in the presence of lower hybrid (LH) waves, where resonant trapped particles may be pinched inward, whereas resonant circulating particles may drift away from the center of tokamak. Both transport mechanisms could affect the radial electric field, which generates the rotation in the toroidal direction.

CP8 31 Novel visualization and computational methods for iterated conversions in tokamak RF heating* E.R. TRACY, *William & Mary* A.S. RICHARDSON, *MIT PSFC* A.N. KAUFMAN, *LBNL and UCBerkeley* N. ZOBIN, *William & Mary Mathematics* A.J. BRIZARD, *St. Michaels* Mode conversion is of great interest as a tool for RF heating and control of flow and current in fusion devices. In a closed system, waves convert many times, leading to a complex interference pattern. To aid in visualization, we introduce the concept of a 'room' associated with each of two uncoupled modes, and illustrate the idea with a tokamak model for its two- dimensional poloidal cross-section (hence the ray phase space is four-dimensional). Each of the two dispersion surfaces, $D_j(x,y,k_x,k_y) = 0$ for $j = 1,2$, is three-dimensional, hence they can be visualized as two separate 3-spaces. The set of points where conversion can occur is a two-dimensional surface in each room. When a ray of type 1 in room 1 punctures the conversion surface, it continues in room 1 as a transmitted ray, but it also spawns a daughter ray of type 2 in room 2. Starting from a point on the conversion surface, we can follow a ray of either type in the relevant room to construct two maps, which take the conversion surface to itself. All possible sequences of conversions can be summarized by all possible combinations of the maps.

*Supported by the DOE OFES and NSF-DOE.

CP8 32 Mitigation of the Thermonuclear Instability by Low-Power ICRH Minority Heating in Ignitor* A. CARDINALI, *ENEA; Italy* B. COPPI, *MIT* The expected ability of Ignitor to achieve ignition with high peak densities ($n_0 \cong 10^{21}\mathrm{m}^{-3}$) and relatively low temperatures makes it possible to investigate the thermonuclear instability that can develop in these regimes. As a consequence of the instability, self-heating of the plasma by the fusion produced α-particles can lead to a significant rise of the plasma temperature and, with this, to an increase of its pressure. Then, internal plasma modes may be excited and saturate the thermonuclear instability at acceptable levels without external intervention. In the case where an internal process may not be effective, a scenario is considered whereby Ignitor is led to operate in a slightly subcritical regime, i.e. the plasma parameters are so chosen that the thermonuclear heating power is slightly less than the power lost, and a small fraction of ^{3}He is added to the optimal Deuterium-Tritium mixture. The difference between power lost and α-heating is compensated by additional ICRH heating, which should be able to energize the minority species (minority heating) directly, which can transfer the power to the main plasma species by collisions. Other options to control the thermonuclear instability are discussed.

*Sponsored in part by ENEA of Italy and by the U.S. D.O.E.

CP8 33 RF Power to Plasma Increase Using EBG Surfaces in IC and LH Antennas SAUL GUADAMUZ, RICCARDO MAGGIORA, *Politecnico di Torino, Italy* High impedance surfaces or electromagnetic band gap (EBG) surfaces have proved themselves to be useful in wireless communications applications due to their unique characteristics such as no propagating surface wave support, no conduction of RF current for a given bandwidth, in-phase electromagnetic reflection and non-inverted image of the electric charge in front of them [1]. These characteristics make possible to design compact antennas achieving better performance in terms of radiation and input impedance. ICRF and LH antennas in plasma experiments can take advantage of using EBG surfaces. One of the main issues in ICRF plasma heating is the high mismatch between the feeding lines and the antenna inputs. The adoption of EBG surfaces in the ICRF antenna structure and the advantages offered by a predictive designing tool as TOPICA [2] offer the possibility to improve significantly the coupled power to plasma. The adoption of EBG surfaces in the LH waveguides permits to reduce the major dimension of waveguides not affecting the propagation. It is then possible to manufacture compact LH arrays of waveguides. [1] IEEE Trans. Microwave Theory Tech., vol. **47**, pp. 2059–2074, Nov. 1999. [2] Nucl. Fusion, **46** (2006) S476.

CP8 34 Toroidal plasma start-up, refluxing and sustainment by repetitive plasma injection* SIMON WOODRUFF, ANGUS MACNAB, JENNIFER BAERNY, COSMO SMITH, TIM ZIEMBA, *Woodruff Scientific Inc* A critical problem for most toroidal plasma configurations is to demonstrate solenoid-free start-up and sustainment: one solution might be to repetitively inject helicity-bearing plasmoids. We are exploring this concept in the Pulsed Build-up Experiment (PBX) [1] and with 3D MHD simulations [2]. PBX is designed to produce three spheromaks by energizing magnetized planar coaxial electrodes, and inject each subsequent spheromak into a copper flux-conserver. Three 32uF, 8kV banks produce 100kA currents in 10us pulses to form the plasmas, and six 16uF banks are used to energize compression coils. Magnetic energy in the flux conserver is monitored by use of magnetic field coils. We report first results from the experiment and summarize theoretical and computational understanding that points to favorable start-up, refluxing and sustainment scenarios that are not deleterious to confinement. Applications to other closely related toroidal plasma configurations is discussed. [1] S. Woodruff et al J. Fusion Energy v28, p229-234 (2009) [2] A. I. D. Macnab et al J. Fusion Energy v28, p183-186 (2009).

*This work is supported by the DOE under contract DE-FG02-06ER84449.

CP8 35 Extended MHD simulations of repetitive spheromak injection for non-inductive start-up and sustainment* ANGUS MACNAB, SIMON WOODRUFF, *Woodruff Scientific, Inc.* NIMROD TEAM, We present 3D extended MHD simulations using the NIMROD code [1] to demonstrate repetitive spheromak injection to address current drive in toroidal plasmas [2]. Simulations initialize three finite beta spheromak equilibria, $n = 5 \times 10^{20} m^{-3}$, $T = 7.5eV$, $B_{tor} = 1T$, in a segmented flux-conserving canister. Two theta-pinch coils are successively pulsed to accelerate two of the spheromaks into the sustainment region to drive co-helicity spheromak merging. The resulting spheromak gains helicity and current in a step-wise manner with each injection [3]. Ohmic and viscous heating models are applied in addition to most aspects of the Braginskii transport model. Magnetic reconnection during the merging process and its dependence on the Hall parameter is discussed. Non-linear stability to current and pressure driven modes during the acceleration, merging and heating periods are also addressed. While the breaking of field lines during spheromak merging tends to cool the plasma, the resulting current increase leads to strong Ohmic heating once the configuration heals. [1] C.R. Sovinec et al. J. Comp. Phys., **195**, 355 (2004) [2] S. Woodruff et al J. Fusion Energy **28**, 229 (2009) [3] A. I. D. Macnab et al J. Fusion Energy **28**, 183 (2009).

*Supported by grants DE-FG02-07ER84924 and DE-FG02-06ER84449.

CP8 36 DIAGNOSTICS, LASER PLASMA INTERACTIONS, AND FAST IGNITION

CP8 37 Absolute X-Ray Yields from Laser-Irradiated Metal-Doped Low-Density Aerogels* K.B. FOURNIER, J.D. COLVIN, M.J. MAY, C.M. SORCE, *Lawrence Livermore National Laboratory* F. GIRARD, B. VILLETTE, *Commissariat à l Energie Atomique* C.A. COVERDALE, *Sandia National Laboratory* M. TANABE, H. NISHIMURA, *Institute of Laser Engineering, Osaka University* J.F. DAVIS, *DTRA* The X-ray yields from laser-irradiated, high-Z-doped, ultra-low-density aerogel plasmas have been measured in the energy range from sub-keV to 13 keV at the 20 kJ OMEGA laser. The targets' X-ray yields have been studied for variation in target size, aerogel density, laser pulse length and intensity. For Ti-doped targets that result in plasmas with electron densities in the range of $\sim$ 10% of the laser's critical density, one can expect $\sim$ 2% laser-to-X-ray conversion efficiency (CE) in the 4 - 6 keV energy band; for Zn-doped aerogels, $\sim$ 1% CE has been measured for 9 keV X rays. For Ge-doped aerogels, one can expect $\sim$ 0.7% laser-to-X-ray CE for X-rays above 9 keV, and $\sim$ 40% CE for energies below 3.5 keV. These results for doped-aerogel targets are consistent with other CE measurements made recently at the GEKKO laser for metallic Ti nano-fiber materials, and are also consistent with recent measurements of CEs for Ge-lined cavities, but are below the CEs measured for Ti-lined cavities and below the CEs measured for pre-exploded Ti foils.

*This work was performed under the auspices of the U.S. Department of Energy by LLNL under Contract No. DE-AC52-07NA27344.

CP8 38 X-ray conversion efficiency measurements for CsI and Sn* JOHN BENAGE, PAUL KEITER, NICK LANIER, *Los Alamos National Lab* We measured the absolute conversion efficiency of Sn and CsI in the energy range of 3900 to 5600 eV using the Omega laser at the Laboratory for Laser Energetics. The laser intensity was varied from $2x10^{15}$ W/cm^2 to $2x10^{16}$ W/cm^2. The efficiency measurements were for 1 ns laser pulse widths and were determined based on previous calibration measurements for several x-ray films. To obtain the efficiencies, we measured absolute film exposures in several energy bands by employing different x-ray filters. The overall efficiency was then determined by calibrating these individual band measurements to the overall spectrum. One band was used as a high energy background measurement. Our results indicate the overall conversion efficiency was relatively insensitive to intensity in this regime and in general was of order 0.1-1%. We conclude with a discussion of the usefulness of such broadband backlighters for HED experiments.

*Work supported by US DOE/NNSA under Contract DE-AC52-06NA25396.

CP8 39 Development of Laser-Produced High-Energy X-ray Sources for Phase Contrast Imaging* JONATHAN WORKMAN, J. COBBLE, K. FLIPPO, D.C. GAUTIER, S. LETZRING, D.S. MONTGOMERY, *Los Alamos National Laboratory* S. GAILLARD, *University of Nevada Reno* Experiments performed on the TRIDENT-200TW facility show phase contrast effects from K-alpha x-ray sources produced from 2-ps laser pulses using 17-keV Mo backlighters. These low magnification images show high-spatial resolution and enhanced contrast on these 3-mm undriven CH disks. We will compare these results to some predictions and discuss plans to measure dynamic properties of shocked material on the OMEGA-EP facility. Results from pulse duration scaling on OMEGA-EP will also be presented.

*Work performed under the auspices of the Dept. of Energy under contract DE-AC52-06NA25396.

CP8 40 X-ray generation from laser irradiated low Z gas embedded with high Z atoms* ASHOK KUMAR SHARMA, UPDESH VERMA, *IIT Delhi, India* Plasma of mixture of gases (Hydrogen 95% and Xenon 5%) is impinged by a pre pulse of intensity $I \sim 10^{14}\, W/cm^2$ ionizes hydrogen atoms fully whereas Xenon atoms are only singly ionizes and create hydrogen plasma with partially ionized Xenon. After first pulse is gone plasma expands in about 1ns to produce a hydrogen plasma channel with minimum density on the axis. A second intense short pulse laser of intensity $I \sim 10^{17}\, W/cm^2$ self focuses and travel guided in the channel. Due to self focusing intensity of the second pulse enhanced and it tunnel ionizes the remaining Xenon. The Xenon acquires Xe^{8+} charge state after loosing 8 ions and acquires Neon like configuration and emits X-rays.

*The author is thankful to DRDO, Delhi, India.

CP8 41 Reflectometer Measurement for LDX* B. KARDON, *MIT PSFC* D. GARNIER, *Columbia Univ* J. KESNER, P. WOSKOV, *MIT PSFC* M. MANUEL, *Columbia Univ* A flexible and general purpose microwave reflectometer system is being developed for density measurement in the Levitated Dipole Experiment. LDX is uniquely suited for reflectometry due to its observed high density gradients and shear-free magnetic field. Various diagnostics exist in LDX to make chordal measurements of the

plasma, including an interferometer and visible light diagnostics; the reflectometer will be able to make non-perturbative local measurements in the core of the plasma. In its initial configuration, the reflectometer will be used to determine the peak plasma density. It will sweep the frequency of launched waves through the peak density O-mode cutoff frequency. Once it passes above that frequency, a sharp jump in time of flight will be observed due to waves passing through the entire radius of the plasma and reflecting off the floating coil at the center of the vessel. The reflectometer will be reconfigured to measure density fluctuations by using a fixed frequency and observing the time of flight as the location of the density-dependent cutoff layer fluctuates. First results will be presented.

*Supported by US DOE Grants: DE-FG02-98ER54458/9

CP8 42 Rotational temperature measurements of the Princeton FRC using non-optical electron-impact excitation selection rules* D.R. FARLEY, *Innovative Energy Concepts* S.A. COHEN, *Princeton Plasma Physics Laboratory* Spectroscopic rotational temperature measurement techniques are often used in molecular gas dynamics and generally can be related to the gas translational temperature. Many authors assume a low-mass electron cannot significantly disturb the molecular rotational level distribution, enforcing a rotational selection rule $\Delta K = 0$. Others believe optical selection rules apply ($\Delta K = 0, \pm 1$). In either case, these selection rules allow for the use of simple Boltzmann plots to estimate the rotational temperature. However, rotational transitions for $\Delta K > 1$ are in fact allowed by molecular symmetries and dipole selection rules. It has been found through this study that these larger transitions ($\Delta K = \pm 2$) for the hydrogen Fulcher-α emission ($H_2 d^3\Pi_u \rightarrow a^3\Sigma_g^+$) can affect the rotational distributions by up to 40% for $K = 5$ upper rotational states and also results in inferred rotational temperatures about 30% lower than would be obtained with Boltzmann plots and optical selection rules. This broader use of non-optical selection rules is applied to measuring rotational temperatures radially across the plasma column of the Princeton Field-Reversed Configuration device at a variety of pressures.

*Supported in part by US DOE Contract No. DE-AC02-76-CHO-3073

CP8 43 Development of diffractive XUV-VUV light extractors for fusion plasma diagnostic D. STUTMAN, G. CARAVELLI, L. DELGADO-APARICIO, M. FINKENTHAL, K. TRITZ, *Johns Hopkins University* R. KAITA, L. ROQUEMORE, *Princeton University* The diagnostic and control of next generation MFE and ICF fusion experiments will require optical light extractors capable of withstanding intense plasma and radiation exposure. A solution applicable from the XUV to the infrared is to use free-standing diffractive optics such as transmission gratings or zone plates. Here we present results on XUV-VUV diffractive extractors for the diagnostic of boundary MFE plasmas. For the VUV range we developed Si transmission gratings having 1 μm period, 5 μm thickness, 40% open fraction, 1x2 mm active area, and coated with Ni, while for the XUV range we use SiN gratings having 0.2 μm period, 0.3 μm thickness, 1x1 mm area, and coated with Ta. The grating extractors are spectrally and spatially calibrated in the laboratory using a newly developed extended XUV-VUV source and will be employed for imaging spectrometry on the NSTX experiment. The operational characteristics of the extended source and first space resolved XUV-VUV spectra will be presented. Work supported by DoE Grant DE-FG02-99ER54523 at JHU and Contract DE-AC02-09CH11466 at PU.

CP8 44 Coherent population trapping to measure magnetic fields in hydrogen plasma* J.M. MITRANI, *Physics Dept., Princeton University* D.R. FARLEY, *Innovative Energy Concepts LLC, Plainsboro, NJ* S.A. COHEN, *Princeton Plasma Physics Laboratory* A laser-based diagnostic to measure weak magnetic fields in hydrogen plasmas using the quantum optics phenomenon of coherent population trapping (CPT) is described. In CPT, a bichromatic laser beam causes non-linear optical-pumping of a 3-state (Λ) atomic system whose lower states' separation is set by the externally applied magnetic field (Zeeman effect). At CPT resonance, fluorescence from the upper state decreases significantly. The frequency difference of the bichromatic laser beam can be adjusted in search of the Zeeman splitting corresponding to magnetic field strengths present. Magnetic field direction can be obtained from polarization information. Critical physics issues, studied with Bloch equations, include the effects of all possible n=3→ 2 transitions, Doppler broadening, hyperfine structure, and Stark shift. For sub-keV H^0 temperatures, CPT resonance does not depend on Doppler shift, but Doppler broadening of multiple transitions of the n=3→ 2 manifold will decrease CPT contrast.

*Supported by USDOE Contract No. DE-AC02-76-CHO-3073.

CP8 45 Plasma signatures on radially resolved line emission S.B. HANSEN, B. JONES, G.A. ROCHAU, J.E. BAILEY, D.J. AMPLEFORD, C.A. JENNINGS, C.A. COVERDALE, M.E. CUNEO, *Sandia National Labs* Y. MARON, V. FISHER, V. BERNSHTAM, A. STAROBINETS, L. WEINGARTEN, *Weizmann Institute* In the last few years, various intriguing emission profiles have been observed in time-gated, radially resolved measurements of K-shell line emission from imploding and stagnating Z-pinch plasmas. The radially resolved lines have appeared as hollow or closed ovals whose extents in the spatial and (Doppler-shifted) wavelength dimensions record the plasma radius and velocity, respectively. Optically thick lines can lead to asymmetries in both spatial and wavelength dimensions, such as limb darkening and preferential absorption of velocity-matched wavelengths. We present the results of a comprehensive investigation of density, temperature, and velocity gradients and their effects on radially resolved emission lines, listing the combinations of plasma conditions that can give rise to signature emission features. Sandia is a multi-program laboratory operated by Sandia Corporation, a Lockheed Martin Company, for the United States Department of Energy's National Nuclear Security Administration under contract DE-AC04-94AL85000.

CP8 46 Magnetooptical Faraday and Light-Scattering Diagnostics of Laser Plasma in Leopard Laser Facility at UNR/NTF G.S. SARKISOV, *Ktech Corp.* K. YATES, V.V. IVANOV, V.I. SOTNIKOV, E. YASIN, P. WIEWIOR, A. ASTANOVITSKY, O. CHALY, J. KINDEL, *UNR* Laser plasma of the solid target on Leopard Laser Facility at University of Nevada Reno was investigated using polarimetry, interferometry and laser-scattering diagnostics. 50 TW Nd:glass Leopard laser operates on 1056 nm wavelength, 10 J energy and 1ns/400 fs pulse width. Power flux on a target surface varied from 10^{14} to 10^{19}W/cm^2 with 20 μm focus spot from off-axis parabola. The diagnostic of spon-

taneous magnetic fields in laser plasma was carried out using three-channel polarinterferometer with Faraday, shadow and interferogram channels. Ultrafast two-frame shadowgrams/ interferograms with two probing beams with orthogonal polarizations were used for investigation of fast moving plasma phenomena (jets, ionization front propagation). Continuous 1W green DPSS-laser with external modulation was used for light scattering experiments for investigation of the late-time microparticles generation in laser plasma with expected large charge number of the grain Z ~ 100-1000.

CP8 47 Thomson-Scattering from electron plasma waves in a magnetized laser-produced plasma BRADLEY POLLOCK, *University of California, San DIego* LAURENT DIVOL, SIEGFRIED GLENZER, JOHN PALASTRO, *Lawrence Livermore National Laboratory* JAMES ROSS, GEORGE TYNAN, *University of California, San DIego* DUSTIN FROULA, *Lawrence Livermore National Laboratory* We present temporally resolved Thomson-scattering measurements of the electron temperature and density of a magnetized laser-produced plasma. Our experiment demonstrates that by applying a 25T external magnetic field parallel to a laser beam in the plasma the electron temperature increases by nearly a factor of 2. Comparison with hydrodynamic modeling indicates the formation of a plasma channel suitable for guiding ultra-short pulse laser beams at conditions for GeV laser wakefield acceleration. This experiment was performed at the Jupiter Laser Facility, Lawrence Livermore National Laboratory, using a 527 nm, 5-ns long, 420 J laser beam focused with a random phase plate to an intensity of 1x 10^{15} W/cm^2. He gas from a 1.5 mm gas jet is ionized to produce a plasma with an initial electron density of 3x10^{18} cm^{-3}. This work was performed under the auspices of the U.S. Department of Energy by Lawrence Livermore National Laboratory under Contract DE-AC52-07NA27344 and was partially funded by the Laboratory Directed Research and Development Program under project tracking code 06-ERD-056.

CP8 48 Imaging X-ray Thomson Scattering Development at Trident D.S. MONTGOMERY, J.L. KLINE, D.T. OFFERMAN, M.S. MURILLO, *LANL* T.E. LOCKARD, I.M. HALL, S.A. GAILLARD, *Univ. Nevada, Reno* X-ray Thomson scattering is a powerful technique to accurately measure conditions such as density, temperature, and ionization state in near-solid density plasmas. Such measurements are required to assess equation of state variables, for example, in the warm dense matter regime. Experiments using x-ray Thomson scattering reported by other research groups utilized high-collection-efficiency x-ray spectrometers with high spectral resolution, but very poor spatial resolution. Thus, those experiments required fairly uniform conditions within the volume of dense plasma being probed. In this present research, we report the development of a high-collection-efficiency toroidally curved imaging spectrometer, with high spectral and spatial resolution (2 eV, 20 μm) for x-ray photon energies in the 4 to 5 keV region. In principle, it can be used as part of an imaging x-ray Thomson scattering experiment whereby spatial gradients in dense plasma conditions can be measured. The spectrometer was fielded on Trident to demonstrate its resolution characteristics, and to demonstrate a proof-of-principle use of imaging x-ray Thomson scattering by nonuniformly heating a solid-density target. We report preliminary results from these experiments, and future prospects for this diagnostic capability.

CP8 49 Localized Density Measurement by Scattered X-Ray Imaging* C.M. HUNTINGTON, C.M. KRAULAND, C.C. KURANZ, *AOSS, University of Michigan* S.H. GLENZER, *Lawrence Livermore National Lab* J.P. KNAUER, *Lab for Laser Energetics, University of Rochester NY* R.P. DRAKE, *AOSS, University of Michigan* Transmission x-ray radiography has been used successfully as a diagnostic for high energy density experiments for many years. This method is limited, though, as radiographs provide only integrated density measurements along the x-ray path and require a collinear source-detector configuration. These constraints do not exist for the imaging of x-rays, which may provide localized, point-wise interrogation of density structure inside an experimental package and allows much greater flexibility in source-detector experimental geometry. Here we describe the method of scattered x-ray imaging by defining the forward problem, applying it to model systems, and exploring methods of solving the related inverse problem. Also presented are initial experimental results from scattered x-ray imaging experiments on the Omega Laser at the Lab for Laser Energetics.

*Supported by the US DOE NNSA under the Predictive Sci. Academic Alliance Program by grant DE-FC52-08NA28616, the Stewardship Sci. Academic Alliances program by grant DE-FG52-04NA00064, and the Nat. Laser User Facility by grant DE-FG03-00SF22021.

CP8 50 Core spatial structure and areal-density modulation in OMEGA direct-drive implosions cores* T. NAGAYAMA, H.M. JOHNS, R. MANCINI, R. FLORIDO, *University of Nevada, Reno, Physics Department, Reno, NV 89557, USA* R. TOMMASINI, J. KOCH, *Lawrence Livermore National Laboratory, Livermore, CA 94550, USA* J. DELETTREZ, S. REGAN, V. SMALYUK, *Laboratory for Laser Energetics, University of Rochester, NY 14623, USA* We discuss the observation of spectrally resolved image data from argon-doped, deuterium-filled OMEGA direct-drive implosions. A titanium-doped tracer layer is also embedded in the plastic shell. The image data were recorded simultaneously along three quasi-orthogonal lines of sight (LOS) using three identical, gated Direct-Drive Multi-Monochromatic x-ray Imagers (DDMMI). For each LOS, a set of space-resolved argon emission and titanium absorption line spectra can be extracted from the spectrally resolved core image data recorded with the DDMMI instruments. The argon x-ray emission emitted at the collapse of the implosion provides a spectroscopic signature for the spatial structure of the imploded core, while the titanium line absorption of continuum radiation has information about the areal-density modulations in the compressed shell. We discuss the connection between the areal-density modulations observed along the three LOS and the spatial-structure of the core.

*Work supported by DOE/NLUF Grant DE-FG52-09NA29042, and LLNL.

CP8 51 X-Ray Spectroscopy of Shock-Ignition Implosions* R.C. MANCINI, R. FLORIDO,†T. NAGAYAMA, *Physics Department, University of Nevada, Reno, NV 89557, USA* R. TOMMASINI, *Lawrence Livermore National Laboratory, Livermore, CA 94550, USA* J. DELETTREZ, S.P. REGAN, V. SMALYUK, *Laboratory for Laser Energetics, University of Rochester, NY 14623, USA* We discuss the observation and spectroscopic analysis of argon K-shell x-ray line spectra from argon-doped deuterium-filled OMEGA direct-drive shock-ignition implosions based on data recorded with streaked crystal spectrometers. The argon line

spectrum is primarily emitted at the collapse of the implosion thus providing a spectroscopic signature of the state of the imploded core. The observed spectra includes parent and satellite line transitions in H-, He- and Li-like Ar ions thus covering a broad photon energy range from 3200 eV to 4200 eV with a spectral resolution power of approximately 500. Both optically thick and thin lines are simultaneously modeled, including line overlapping and Stark-broadening effects. The spectroscopic analysis results show core temperature and density time-histories associated with the collapse implosions. A comparison is also made with LILAC hydrodynamic simulations.

*Work supported by DOE/NLUF Grant DE-FG52-09NA29042, and LLNL.

†Permanent address: Departamento de Física, ULPGC, Spain

CP8 52 Absolute Calibration of X-ray Filters Employed By Laser-Produced Plasma Diagnostics GREGORY BROWN, PETER BEIERSDORFER, JOEL CLEMENTSON, JIM EMIG, *Lawrence Livermore National Laboratory* MIRIAM FRANKEL, *Imperial College* MING GU, *UC Berkeley Space Science Lab* ROBERT HEETER, ED MAGEE, *Lawrence Livermore National Laboratory* DANIEL THORN, *GSI* KLAUS WIDMANN, *Lawrence Livermore National Laboratory* The electron beam ion trap (EBIT) facility at the Lawrence Livermore National Laboratory is being used to absolutely calibrate the transmission efficiency of X-ray filters employed by diodes and spectrometers used to diagnose laser-produced plasmas. EBIT emits strong, discrete mono-energetic lines at appropriately chosen X-ray energies. X rays are detected using the high-resolution EBIT calorimeter spectrometer (ECS), developed for LLNL at the NASA/Goddard Space Flight Center. X-ray filter transmission efficiency is determined by dividing the X-ray counts detected when the filter is in the line of sight by those detected when out of the line of sight. Verification of filter thickness can be completed in only a few hours, and absolute efficiencies can be calibrated in a single day over a broad range from about 0.1 to 15 keV. An overview of these activities will be discussed. Prepared by LLNL under Contract DE-AC52-07NA27344.

CP8 53 Kirkpatrick-Baez Microscope for Hot-electron Transport Imaging in Fast Ignition Experiments H. FRIESEN, Y.Y. TSUI, R. FEDOSEJEVS, *Univ Alberta* K.U. AKLI, R.B. STEPHENS, *GA* M.S. WEI, H. SAWADA, S. CHAWLA, N. NAKANII, D.P. HIGGINSON, F.N. BEG, *UCSD* D. HEY, S. LE PAPE, A. MACPHEE, C.D. CHEN, Y. PING, M.K. KEY, H. MCLEAN, P. PATEL, A. MACKINNON, *LLNL* E. KEMP, A. LINK, D.W. SCHUMACHER, R.R. FREEMAN, L.D. VAN WOERKOM, *OSU* H. TIEDJE, A. ALI, N. VAFAEI-NAJAFABADI, Univ Alberta, T. MA, L. JARROT, D. MARISCAL, C.W. MURPHY, B. WESTOVER, B.S. PARADKAR, T. YABUUCHI, UCSD - K-alpha emission from tracer layers is a powerful diagnostic for quantitatively measuring the generation and transport of MeV electrons in studies of Fast Ignition Fusion. We are developing a Kirkpatrick-Baez microscope for such experiments at the Titan Laser Facility using grazing incidence platinum coated mirrors together with metal filters to detect copper K-alpha emission from tracer layers in planar and cone-wire targets. The instrument performance has been modeled using ray tracing and characterized by a cw x-ray source. Broadband multilayer grazing incidence mirrors are also being designed for both copper K-alpha and silver K-alpha imaging. The characteristics of the KB microscope and initial experimental results on electron transport will be presented.

CP8 54 The NIF wedge-range-filter proton spectrometer M.J. ROSENBERG, F.H. SEGUIN, N. SINENIAN, J.A. FRENJE, C.K. LI, R.D. PETRASSO, *MIT* A new wedge-range-filter (WRF) proton spectrometer has been designed for implementation at the National Ignition Facility. Based on the existing WRF spectrometers currently in use at the OMEGA laser facility, this model will be modified to optimize performance in the NIF environment. The WRFs will measure proton spectra from 4 to 25 MeV, and a primary application will be diagnosis of ablator ρR and ρR asymmetry in DT implosions (through measurements of knock-on ablator protons). Calibration of these WRFs will be performed using 15-MeV D^3He protons produced in the MIT Nuclear Products Generator. The WRFs will be ready for installation at the NIF for the Ignition Campaign. This work was supported in part by US DoE, LLNL, and LLE.

CP8 55 Reconstruction of proton paths in CR-39 for radiography experiments H.G. RINDERKNECHT, D.T. CASEY, N. SINENIAN, F.H. SEGUIN, C.K. LI, J.A. FRENJE, R.D. PETRASSO, *MIT* Recent mono-energetic proton backlighter experiments on the dynamics of laser-plasma interaction and inertial fusion implosions have revealed high-intensity magnetic and electric fields in high-energy-density regime plasmas. Current radiographic methods measure particle fluence and energy at the detector surface. By reconstructing incident proton trajectory on the detector, radiography techniques may strongly constrain the strength and location of fields in ICF capsule implosions, hohlraum implosions, and other complex high-energy-density plasmas of interest. A new diagnostic method developed on the MIT Nuclear Products Generator, utilizing CR-39 as a multiple-stage particle detector, is presented and the applications of this method to experiments at LLE and NIF are discussed. This work was supported in part by US DoE, LLNL, and LLE.

CP8 56 Using proton radiography to measure Rayleigh-Taylor-induced magnetic fields M. MANUEL, C.K. LI, F.H. SEGUIN, J.A. FRENJE, D.T. CASEY, N. SINENIAN, R.D. PETRASSO, *MIT* R. BETTI, V.A. SMALYUK, J. HAGER, *LLE* J.P. TOWN, *LLNL* The Rayleigh-Taylor (RT) hydrodynamic instability has been a concern for shell integrity during the acceleration phase of Inertial Confinement Fusion (ICF) implosions. RT-induced magnetic fields on the order of a mega-Gauss have been theoretically predicted and simulated, but never measured. If present, these self-generated fields will reduce heat flux and affect implosion dynamics. An experimental method for measuring these elusive fields using a combination of mono-energetic proton radiography, X-ray radiography, and Monte-Carlo simulations is described, and experimental measurements of RT-induced magnetic fields are presented. This work was performed at the LLE NLUF, and was supported in part by the FSC at U. of R., US DoE, LLNL, and LLE.

CP8 57 Diagnostics for heavy ion beam driven Warm dense matter experiments PAVEL NI, FRANK BIENIOSEK, STEVE LIDIA, PETER SEIDL, WILL WALDRON, *LBNL* A set of diagnostic has been developed for the WDM experiments at Berkeley. The diagnostics are aimed at the in-situ measurement of temperature, expansion velocity and pressure of a WDM sample.A specially developed two-channel pyrometer probes color temperatures at 750 nm,1000 nm and 1400 nm, with 75 ps temporal resolution. The system has a broad dynamic range with a lower limit ~ 2000

K and upper limit ~ 100000 K. The pyrometer design is based on custom spectrally selective beam splitters and can be upgraded up to seven channels. Continuous target emission from 450 nm to 850 nm is recorder by a custom spectrometer, consisting of a high dynamic range Hamamatsu streak camera and a holographic grating. The system is calibrated absolutely with a tungsten ribbon lamp (NIST traceable). The various sweeping times of the streak unit allows for temporal resolution varying from 1 ps to 1 us. The spectrometer has a lower sensitivity than the pyrometer and applied in experiments with higher temperatures. Hydrodynamic expansion velocity of a target's free surface is measured by a commercially available all- fiber Doppler shift laser interferometer (VISAR). The installed delay etalon allows for velocity detection with 2 m/s precision and 0.5 ns resolution.

CP8 58 Thomson Parabola Ion Energy Analyzer JAMES COBBLE, SAM LETZRING, FRAND LOPEZ, *Los Alamos National Laboratory* A new, versatile Thomson parabola ion energy (TPIE) analyzer has been designed and constructed for use at the OMEGA-EP facility. Multi-MeV ions from EP targets are transmitted through a W pinhole into a (5- or 8-kG) magnetic field and subsequently through a parallel electric field of up to 24 kV/cm. The ion drift region may have a user-selected length of 10, 50, or 80 cm. With the highest fields, 500-MeV C^{6+} and C^{5+} may be resolved. TPIE is TIM-mounted at OMEGA-EP and can be used opposite either of the EP ps beams. The instrument runs on pressure-interlocked 15-VDC power available in EP TIM carts. It may be inserted to within several inches of the target to attain sufficient flux for a measurement. For additional flux control, the user may select a square-aperture W pinhole of 100 μm or 250 μm. The detector consists of CR-39 backed by an image plate. The fully relativistic design code and design features will be discussed. Ion spectral results from first use at OMEGA-EP are expected.

CP8 59 Measurements of down-scattered and TT neutrons at OMEGA using the Magnetic Recoil Spectrometer D.T. CASEY, J.A. FRENJE, F.H. SEGUIN, C.K. LI, M. MANUEL, H.G. RINDERKNECHT, *MIT* N. SINENIAN, R.D. PETRASSO, *MIT* V. YU. GLEBOV, D.D. MEYERHOFER, T.C. SANGSTER, P.B. RADHA, S. ROBERTS, M. BURKE, J. ULREICH, *LLE* K. FLETCHER, *SUNY Geneseo* A Magnetic Recoil Spectrometer (MRS) was built and is currently being used on the OMEGA laser for absolute measurements of down-scattered and primary neutrons. The areal densities of CH and cryogenic DT implosions have been inferred from the down-scattered neutron spectrum. TT neutrons have also been observed in the down-scattered continuum. To correctly interpret these measurements, the MRS response function was characterized using the Monte Carlo code GEANT4 and diagnostic activation experiments. Measurements of the absolute neutron spectrum at OMEGA, inferred using the MRS response function, will be presented. This work was supported in part by the U.S. DoE, LLE, and LLNL.

CP8 60 Processing of the HXR and neutron signals registered with the time resolved scintillation detectors* EKATERINA LITSEVA, PAVEL KUBES, KAREL REZAC, *FEE CTU in Prague* The DD fusion reaction was studied experimentally on the PF-1000 plasma focus (IPPLM, Warsaw, 1-2 MA current and 1011 neutrons per shot). The neutron measurements were carried out with the set of detectors in the downstream, upstream and radial directions, which make possible to estimate the time dependence of neutron energy distribution. The signals from the detectors consist of a few of the hard X-ray and neutron pulses. The signals are distorted by the dimensions and characteristics of the detectors and photomultipliers. Hard X-rays are influenced by the transit time of the electrons before collisions with the walls of the chamber. Neutron signals are influenced by the moderated and scattered neutrons. In order to remove these distortions from the signals, the supposition of the linear dependence of delayed particles on the time and intensity is used. The processing includes the filtration of the signals and further the adjustment of the neutron signals with the supposition of the 10%, 30% and 50% delayed particles.

*This research has been supported by the research program No. LA08024, No. ME09087, No. LC528, the GACR grants No. 202-08-H057, No. 202-08-P084 and grant CRA IAEA No. 14817.

CP8 61 Determination of average kinetic energy of reacting deuterons on the basis of neutron time-of-flight diagnostics* KAREL REZAC, DANIEL KLIR, PAVEL KUBES, JOZEF KRAVARIK, *FEE CTU in Prague* S 300 TEAM, The kinetic energy of reacting deuterons is one of the important parameter of the fusion plasma where deuterium is presented in a load. The energy of deuterons is determined from the reconstructed neutron energy spectra which are obtained by extended time-of-flight (TOF) method where time-resolved neutron detectors are placed at several distances on two opposite directions from the neutron source. Provided that the deuteron energy is much smaller than the fusion Q-value, it is possible to show that the neutron energy is only a function of the component of the deuteron kinetic energy (and vice versa) in the direction of neutron detection. Consequently, the side- on and end-on energy components of deuterons can be found on the basis of TOF measurement of neutrons in the radial and axial directions. Finally, the average kinetic energy of reacting deuterons can be evaluated on an assumption of radial symmetry of neutron production from Z-pinch plasma.

*Work supported by MEYS No. LA08024, No. ME09087, No. LC528, by GACR grants No. 202-08-H057, No. 202-08-P084, and grant CRA IAEA No. 14817.

CP8 62 Nuclear diagnostics utilizing robust CR-39 for OMEGA, OMEGA-EP, and the NIF N. SINENIAN, D.T. CASEY, M. MANUEL, H.G. RINDERKNECHT, M.J. ROSENBERG, F.H. SEGUIN, J.A. FRENJE, C.K. LI, R.D. PETRASSO, *MIT* Harsh EMP/x-ray/gamma-ray environments such as those found at OMEGA and OMEGA-EP (and soon the NIF) hinder electronic detection schemes for sensitive measurements of charged particles and neutrons. This has made passive particle detectors such as CR-39 attractive, especially since they measure the position, energy, and species of individual charged particles. To enhance the accuracy of CR-39-based measurements, and to lay the groundwork for new applications, new measurements of CR-39 response to accelerator-generated protons (from 0.35 MeV to 11.7 MeV) and 2.5-MeV neutrons have been made using a variety of CR-39 types and CR-39 processing techniques. Results include determination of energy-measurement accuracy and the sensitivity of energy measurements to CR-39 thickness, vacuum exposure, heat exposure, and various processing parameters. Application to a new and sensitive neutron detector for OMEGA, OMEGA-EP, and the NIF will be presented. This work was supported in part by US DoE, LLNL, and LLE.

CP8 63 Interaction of ultra-intense ultra-short laser light with a magnetized target* PHILIPPE LEBLANC, YASUHIKO SENTOKU, RADU PRESURA, *University of Nevada, Reno* An ultra-intense short-pulse laser is an important tool capable of isochorically heating a thin solid target to beyond 100eV in a picosecond before hydrodynamic effects force it to expand. The temperature we could achieve depends on the dynamics of hot electron transport inside the target. We have simulated in 2D the hot electron transport in solid density plasmas using a collisional particle-in-cell code, PICLS. Because of rapid lateral motion of hot electrons the target heating is less efficient especially in low Z targets, such as a CH target. We have proposed uniformly magnetized isochoric heating by using a 1MA Z-pinch machine as a MG field generator and have studied the hot electron diffusion across the imposed magnetic field. We found that the external magnetic field was partially expelled from the heated region due to the circular motion of the hot electrons, and was compressed at the edge of the region. That is why the presence of an external MG field is able to slow down the hot electrons' lateral diffusion, and improve the bulk heating efficiency significantly. We will also show the effects of scaling the external magnetic field on the confinement of hot electrons.

*This work was supported by DOE/NNSA Grant No. DE-FC52-06NA27616.

CP8 64 Algorithm Development for Simulation of the Interaction of Intense Laser Light with a Multiscale Plasma* BRUCE COHEN, ANDREAS KEMP, LAURENT DIVOL, *Lawrence Livermore National Laboratory* The kinetic simulation of the interaction of intense laser light with plasma in a multiscale limit presents severe challenges. Conventional, explicit-integration, particle-in-cell (PIC) methods require resolving the light waves and electron plasma waves with appropriately small time steps and mesh sizes in order that the simulation be both numerically stable and accurate. In the simulation of laser light interacting with a fast-ignition target plasma, the domain spans a range of electron densities going from vacuum to thousands of times the critical density. For the electron temperatures in the target plasmas, the underdense plasma is collisionless and the overdense plasma becomes highly collisional. We have introduced a new two-region algorithm that is well suited to the simulation of fast ignition, employing explicit PIC with complete Maxwell's equations at low densities through densities above critical and a reduced set based on Ohm's law for higher densities. Collisions in the high-density region set limits on time steps, and we examine subcycling the collisions to improve efficiency. Analysis and demonstrations of the algorithm are presented.

*Work performed under the auspices of the U.S. Department of Energy under contract DE-AC52-07NA27344 at LLNL.

CP8 65 ePLAS code improvements for short pulse laser-matter interaction studies* R.J. MASON, J. AMBROSIANO, W. ATCHISON, R. FAEHL, D. HENDERSON, R. KIRKPATRICK, *Research Applications Corp* D. BARNES, *Coronado Consulting* We detail new features for ePLAS, a 2D implicit/hybrid simulation model in use for Fast Ignition. The hybrid/PIC code tracks laser light with ponderomotive force, depositing at critical into relativistic hot particle electrons, while pulling cold collisional, return-current Van Leer fluid electrons through fluid ions by means of self-consistent Implicit Moment[1] $E -$ and $B -$ fields. The new features include: a 1D formulation for light absorption studies with generalized *E- and B-* fields, multiple laser beams, real EOS data from analytic models or the Sesame tables, K_α imaging, generalized cold electron elevation to hots, particle ions for fast ion fusion, improved graphical options, and new Linux and Mac OS X implementations. The focus of the talk is code enhancements.

*Work supported in part by DOE SBIR Grant DE-FG02-07ER84723.

[1]R. J. Mason, J. Comp. Phys. **71,** 429 (1987).

CP8 66 ePLAS examination of short-pulse laser- wire and foil interactions* R. FAEHL, R.J. MASON, *Research Applications Corp* M. WEI, T. MA, F.N. BEG, *UCSD* R. STEPHENS, *General Atomics* An enhanced 2D implicit hybrid simulation code ePLAS has been used to examine short-pulse laser interactions with cone-wire and foil targets. The code deposits picosecond pulses of 1 μm, $\sim 3\text{x}10^{20}$ W/cm^2 laser light near critical, and tracks resultant megavolt "hot" particle-in-cell (PIC) electrons through an ionized copper or carbon background plasma. The background is modeled as collisional Van Leer "cold electron" and ion fluids. The code now elevates the returning fluid colds to hot particles, when their energy exceeds a specified threshold (e.g. 20 keV). It also uses real equations of state from analytic models or the Sesame Tables. Cylindrical and Cartesian results are compared. The emphasis will be on recent cone/nail-wire experiments[1] with target heads of varying mass, and revisited foil studies.[2]

*Research partly supported by the USDOE under DE-FG02-07ER84723.

[1]T. Ma et al., "Transport of energy by ultra-intense laser-generated electrons in nail-wire targets," submitted to Physics of Plasmas
[2]R. J. Mason, et al. Phys. Rev. E **72,** 01540 (R) (2005).

CP8 67 Ultrashort laser pulse absorption in dense targets S.G. BOCHKAREV, W. ROZMUS, *University of Alberta, Canada* M. SHERLOCK, *Imperial College, UK* A.V. BRANTOV, V. YU. BYCHENKOV, *Lebedev Physics Institute, Russia* A theory of ultrashort laser pulse absorption in dense targets is important for modeling of basic physics and applications of short laser pulse plasma interactions. Recent absorption measurements and large number of indirect observations point to complex scenarios of short laser pulse absorption where the laser prepulse, ionization physics, density profile modifications, collisional processes and collisionless mechanisms occur all within short pulse duration and contribute to the absorbed fraction of the incident laser energy. A model of ultrashort laser pulse absorption, which includes linear absorption and thermal transport into dense plasma will be described. Plasma dielectric function in our model describes collisional and collisionless absorption mechanisms including the effect of electron-electron collisions. Thermal transport is modeled using nonlocal expressions that are valid in the weakly collisional regime. The inhibited and nonlocal thermal transport can contribute to the increase of the electron temperature in the skin layer. Theoretical predictions will be compared with the results of Vlasov-Fokker-Planck simulations for moderate laser intensities. Also numerical simulations will illustrate transition into relativistic regime of laser intensities.

CP8 68 Laser acceleration of monoenergetic protons via a double layer emerging from an ultra-thin foil* BENGT ELIASSON, *Ruhr-University Bochum, Germany* CHUAN S. LIU, XI SHAO, ROALD SAGDEEV, *University of Maryland, College park, MD* PADMA K. SHUKLA, *Ruhr-University Bochum, Germany* GALINA DUDNIKOVA, T.C. LIU, *University of Maryland, College park, MD* Theoretical and numerical studies are presented of the acceleration of monoenergetic protons in a double layer formed by the laser irradiation of an ultra-thin film. The ponderomotive force of the laser light pushes the electrons forward, and the induced space charge electric field pulls the ions and makes the thin foil accelerate as a whole. A stable double layer is formed, in which the ions are trapped by the combined electric field and inertial force in the accelerated frame, together with the electrons that are trapped in the well of the ponderomotive and ion electric field. The trapped ions reach monoenergetic energies up to 100 MeV and beyond, making them suitable for cancer treatment. We present an analytic theory for the laser-accelerated ion energy as a function of the laser intensity, foil thickness and the plasma number density. The underlying physics of the trapped and untrapped ions and of the stabilization of the Rayleigh-Taylor instability are discussed.

*This work was partially supported by the DFG through the Research Unit 1048 and by the Swedish Research Council (VR).

CP8 69 Abundant generation of quasimonoenergetic ions by Coulomb explosions of optimized nanostructure MASAKATSU MURAKAMI, KUNIOKI MIMA, *ILE, Osaka Univ.* In Coulomb explosions of spherical clusters composed of two ion species (light and heavy), the initial density profile of light ions is optimized to have iso-Coulomb potentials. This results in the generation of many quasimonoenergetic ions with the highest possible energy coupling. The overall coupling efficiency (equal to the summed kinetic energy of the light ions in the highest 1-percent energy band divided by total kinetic energy of both ions) is estimated to be as high as 30-40 percent in a one-dimensional simulation. The monoenergeticity and efficiency can be further improved by using even more ion species or by exploiting different ionization levels of the heavy ions. The present scheme has high potential to provide a reasonably efficient method for generating quasimonoenergetic ions for practical applications.

CP8 70 Ionization dynamics of high-intensity laser-target interactions* GEORGE PETROV, *Naval Research Laboratory* TZVETELINA PETROVA, *Berkeley Scholars, Inc.* KARL KRUSHELNICK, ANATOLY MAKSIMCHUK, LOUISE WILLINGALE, *University of Michigan* KENNETH WHITNEY, *Berkeley Scholars, Inc.* JACK DAVIS, *Naval Research Laboratory* The ionization dynamics of thin foils irradiated by an ultrashort pulse laser is investigated with a fully relativistic 2D particle-in-cell model. The PIC model is integrated with a ionization dynamics model, which includes optical field and collisional ionizations. The spatio-temporal evolution of the ion charge and electron density of a 5 micron aluminum foil are studied for peak laser intensities 10^{18}-10^{20} W/cm^2 and laser pulse duration of 80 fs. The optical field ionization dominates in the pre-plasma region, creating a dense plasma of highly charged ions, while the collisional ionization is most effective in the bulk of the target. A series of ionization waves launched at the front surface of the foil propagate with high velocity ($\sim 0.2c$) through the target.

*This work was supported by the DTRA and NRL under the 6.1 program.

CP8 71 Comparison of radiaton cooling models for particle-in-cell simulations* MARIJA VRANIC, JOANA L. MARTINS, LUIS O. SILVA, *GoLP/IPFN, Instituto Superior Técnico, Lisboa, Portugal* Under extreme acceleration, charged particles can radiate strongly and the corresponding radiation damping/cooling can become important in the plasma energetics and dynamics. This occurs when radiated energy in the interaction time is comparable to mc^2. In particular, under the presence of ultra high intensity lasers or other intense electro/magnetic fields the motion of particles in the ultrarelativistic regime can be severely limited by radiation damping. The standard Particle-in-Cell (PIC) algorithms do not include radiation damping/cooling effects. Even though this is a well known mechanism, there is not yet a definite algorithm nor a standard technique to include radiation cooling in PIC codes. We have compared several models for the calculation of radiation damping force, with the goal of developing an algorithm for radiation damping in Osiris [1]. The results of the different models are compared with analytical models and standard results, and the relevance/advantages of each model are discussed.

*Work partially supported by FCT (Portugal).

CP8 72 Non-Equilibrium Plasma Dynamics Modeling of Xenon Clusters Irradiated by an Intense Laser Pulse* TZVETELINA PETROVA, KENNETH WHITNEY, *Berkeley Research, Inc.* GEORGE PETROV, JACK DAVIS, *Naval Research Laboratory* Population inversions have been experimentally observed when small xenon clusters of 5-20 atoms are irradiated by $\sim$ 230 fs high intensity laser of 10^{19} W/cm^2 and wavelength of 248 nm [1]. Consequently, a plasma channel $\sim$ 1.5-2 cm in length and $\sim$ 1.5–2 μm in diameter is formed which produces amplified x-ray emissions with gains $\sim$ 20-60 for wavelengths in the range 2.71-3 Å. It has been conjectured [2], that population inversions in laser generated xenon plasmas may be efficiently created within M-shell ionization stages by photo- or collisional-ionization of 2s and 2p inner shell electrons. In this study we focus our attention on the influence of non-Maxwellian electron energy distributions on the collisional dynamics by which hollow atoms are generated in different ionization stages of xenon. These distributions are calculated from a relativistic molecular dynamics model. [1] A. B. Borisov, *et al.*, J. Phys. B **40**, F307 (2007). [2] W. A. Schroeder, *et al.*, J. Phys. B **34**, 297 (2001).

*Work supported by NRL under the 6.1 program.

CP8 73 Cluster mass fraction and size distribution determined by fs-time-resolved measurements XIAOHUI GAO, XIAOMING WANG, BONGGU SHIM, ALEXEY AREFIEV, MIKHAIL TUSHENTSOV, BORIS BREIZMAN, MIKE DOWNER, *University of Texas at Austin* Characterization of supersonic gas jets is important for accurate interpretation and control of laser-cluster experiments. While average size and total atomic density can be found by standard Rayleigh scatter and interferometry, cluster mass fraction and size distribution are usually difficult to measure. Here we determine the cluster fraction and the size distribution with fs-time-resolved refractive index and absorption measurements in cluster gas jets after ionization and heating by an intense pump pulse. The fs-time-resolved refractive index measured with frequency domain interferometer (FDI) shows different contributions from monomer plasma and cluster plasma in the time domain, enabling us to determine the cluster fraction. The fs-time-resolved absorption measured by a delayed probe shows the contribution from clusters of various sizes, allowing us to find the size distribution.

CP8 74 Size distribution of microclusters in laser-irradiated plasmas MIKHAIL TUSHENTSOV, BORIS BREIZMAN, XIAOHUI GAO, ALEXEY AREFIEV, *Institute for Fusion Studies, The University of Texas at Austin* Laser interactions with a mixture of a gaseous plasma and microclusters depend strongly on the cluster-size distribution, which is usually difficult to measure directly. We present a new approach for recovering the cluster-size distribution from time-resolved measurements of the absorbed energy in a pump-probe experiment. The pump pulse ionizes microclusters to a peak density that exceeds the critical plasma density for the probe pulse. The existence of plasma resonances enhances the energy absorption for individual clusters. As a cluster expands, its peak density decreases and the resonance eventually disappears. The expansion time is shorter for smaller clusters than for larger ones, which makes the absorbed energy dependent on the cluster-size distribution. We can then find the cluster-size distribution by matching a convolution of the distribution with a single cluster absorption curve to the measured absorption. We demonstrate feasibility of this technique by analyzing the data from recent pump-probe experiments at the University of Texas.

CP8 75 High temperature deuterium plasmas produced by laser irradiation of clusters in a confining magnetic field M. WISHER, H.J. QUEVEDO, M. McCORMICK, ROGER D. BENGTSON, T. DITMIRE, *University of Texas at Austin* K.W. STRUVE, D.C. ROVANG, M. SAVAGE, J.L. PORTER, *Sandia National Laboratories* Experiments have shown that interactions of intense ultrafast lasers with targets of small atomic clusters with thousands of atoms can create plasmas with high density and high average ion energies ($>>$ 1keV). DD fusion neutrons can be produced with laser pulses of a few joules to kilojoules. The fusion yield is limited by the fast expansion time ($<$ 100 ps)of the plasma. The expansion could be affected by a large magnetic field ($>$ 100 T) to limit transport in the radial direction that would lead to an increase of fusion neutron yield. We present preliminary design of the magnetic field generator for fields as large as 200 T. This includes a 100 kV capacitor bank that can deliver 2.2 MA through coaxial cables that feed into a conical transmission line. This line is connected to two destructible concentric millimeter coils in a mirror configuration to generate the high magnetic field for a microsecond. We will use a cryogenically cooled gas jet to produce 10 nm deuterium clusters as the laser target. The jet will be irradiated by a femtosecond laser beam propagating on the axis of a 100 T magnetic field.

CP8 76 Effect of micro-structure growth on x-ray production* J.T. MORRISON, E.A. CHOWDHURY, R.L. DASKALOVA, A.G. KRYGIER, A. LINK, V.M. OVCHINNIKOV, C.R. WILLIS, D. CLARK, D.W. SCHUMACHER, L.D. VAN WOERKOM, R.R. FREEMAN, *The Ohio State University* High intensity short pulse laser interactions with solid targets have been shown to produce an x-ray burst. The effect of micro-structures on laser coupling efficiency to x-rays was investigated. Metallic targets with and without micro-structure growth were shot at the Scarlet Laser Facility with an intensity near than 3 x 10^{19} W/cm^2 and energy near 1J. Results will be presented on the enhancement of x-rays.

*This work was supported by the U.S. Defense Threat Reduction Agency under contract HDTRA1-08-1-0018.

CP8 77 An interaction between strong laser field and carbon nantubes* TOSHIHIRO TAGUCHI, *Setsunan University* THOMAS ANTONSEN, HOWARD MILCHBERG, *University of Maryland* MASAHIKO INOUE, *Setsunan University* An interaction between strong laser field and carbon nanotubes has been investigated using a particle-in-cell code, which includes a collisional and ionization effect. Carbon nanotubes are considered as a nano-scale solid cylinder. According to a series of our works about laser-cluster interaction using the PIC code[1–2], electrons in a nano-cylinder absorb large amount of laser energy through a resonant absorption. Such a strong excitation of electron oscillation can cause a nonlinear excitation of a low frequency radiation such as terahertz waves. We will present about the simulation results of the interaction between carbon nanotubes and a strong laser field. We will also show a possibility of a coherent radiation from a periodically arrayed carbon nanotubes. [1] T. Taguchi, et al., Phys. Rev. Lett., 92, 20, 2004, 205003. [2] T. M. Antonsen, Jr., et al., Phys. Plasmas 12, 5, (2005), 056703.

*Grant-in-aid for scientific research from JSPS.

CP8 78 Calculations of fast electron transport through different materials at solid density using a robust hybrid code STEVE HUGHES, DAVID CHAPMAN, *AWE* Development of a robust hybrid code is useful for efficient calculation of fast electron transport, in conjunction with a radiation hydrodynamics code. The code THOR has been developed for coupling to a fluid code in this fashion for modelling this fast electron population generated during short-pulse laser experiments. It is built on the hybrid philosophy of work by J.R. Davies, which provides an intuitive and relatively straightforward computational framework, and makes it easier to take advantage of parallelism for reducing noise in the solution. The basic algorithms of the code are described along with the approximations and limitations of the current implementation. Recent experiments by D. Hoarty at AWE have demonstrated a method of heating solid density Aluminium layers to hundreds of eV, buried at various depths in a plastic target. Application of the THOR code in reproducing these measurements is shown with encouraging results. The quality of the match to the data is discussed with layers placed at various depths as in the experiments, and with different laser sources. The problems of comparing the code outputs with the measurement technique used in the experiment are also described.

CP8 79 Relativistic Electrons from Slab Targets Interacting Strongly with Intense Light in Vacuum from High-Contrast Laser Pulses T.W. JOHNSTON, *INRS-EMT* L. NIKOLIC, *Now Univ. Alberta, Edmonton, AB, Canada* Y. TYSHETSKIY, *Now Univ. Sydney, Sydney, NSW, Australia* F. VIDAL, *INRS-EMT, Varennes, QC, Canada* When light of electron-relativistic intensity in several-cycle laser pulses are obliquely incident on slab targets with extremely low pre-pulse energy, copious amounts of high laser harmonic light emerge [1] (See also ongoing work at the ALLS 200 TW Ti-Saph laser at INRS EMT. (Pulses are 24 fs at 10 Hz with 10^{-10} contrast, even without plasma mirrors).) 2-D PIC (OSIRIS code at INRS) simulations [2] (and earlier work by Naumova et al. [3] have shown that intense beams of electrons are not only injected into the target [2] but that significant relativistic electrons are also emitted more or less along with the emitted light. These frontally-emitted relativistic electrons emerge from the narrow regions of intense current responsible for the harmonics [2] and interact strongly with the incident and emitted light. [1] B. Dromey et al Nature Phys. Lett., 2, 456-459 (2006). [2] T.

Johnston et al. Poster YP8 48, Bull. Amer. Phys. Soc 52, 16 November (2007). [3] N. Naumova, et al., Phys. Rev. Lett. 93, 195003 (2004). Note: This is work meant to be reported in 2008, but was not for medical reasons. This is likely to be the last Bulletin Abstract submitted by the lead author.

CP8 80 Magnetic Field Measurement in Laser-Plasma Interaction via Relativistic Electron Deflectometry NOBUHIKO NAKANII, HIDEAKI HABARA, KAZUO A. TANAKA, *Osaka University* TOSHINORI YABUUCHI, HIROSHI SAWADA, BHOOSHAN S. PARADKAR, MINGSHENG WEI, FARHAT N. BEG, *UC San Diego* RICHARD B. STEPHENS, *General Atomics* In laser matter interactions, whether it is with a short pulse laser or a long pulse laser, magnetic fields are produced which can affect the energy transport in the target. So characterization of these fields is important. Recently, protons are used for magnetic field measurements. We report a theoretical study to assess use of relativistic electrons for the detection of magnetic field. Electrons are produced in short pulse laser matter interactions. In this modeling rad-hydro code h2d was used to produce magnetic field by a long laser pulse ($\sim 10^{14}$W/cm^2) due to the thermoelectric effect. The probe electron beam was produced using a hybrid particle-in-cell code LSP. Results show that the field and their shape can be characterized by the deflection of the electron beam. Results will be discussed at the meeting. Work supported by Research Fellowship of the JSPS, and by the Dept. of Energy under contract DE-FG-02-05ER54834.

CP8 81 Suppression of parasitic noise by strong Langmuir wave damping in quasitransient regimes of backward Raman amplification of intense laser pulses in plasmas.* VLADIMIR MALKIN, NATHANIEL FISCH, *Princeton University* Currently built powerful soft x-ray sources may be able to access intensities needed for backward Raman amplification (BRA) of x-ray pulses in plasmas. However, high plasma densities, needed to provide enough coupling between the pump and seed x-ray pulsed, cause strong damping of the Langmuir wave that mediates energy transfer from the pump to the seed pulse. Such damping could reduce the coupling, thus making efficient BRA impossible. This work shows that efficient BRA can survive despite the Langmuir wave damping significantly exceeding the linear BRA growth rate. Moreover, the strong Langmuir wave damping can suppress deleterious instabilities of BRA seeded by the thermal noise. This shows that it may be feasible to observe x-ray BRA for the first time soon.

*This work was supported in part by the NNSA under the SSAA Program through DOE Research Grant No. DE-FG52-04NA00139.

CP8 82 A Simple Model for the Performance of the First Empty Hohlraum Experiments on NIF* MORDECAI ROSEN, *LLNL* We present a simple energy balance model for predicting the performance of the first hohlraums to be irradiated on the National Ignition Facility (NIF) as the input energy and power is varied. Key ingredients include the scaling of x-ray conversion efficiency with irradiance (as well as with pulse length), as well as some assumptions about the absorption fraction. Wall loss formulae follow the results of Hammer & Rosen (PoP 10, 1829 (2003)). Other fine points are also considered. Specifically they involve the difference between the Au wall material temperature and a "virtual" drive temperature; the latter differs from the former due to Milne conditions. Also analyzed is the predicted "observed via Dante" temperature which differs yet again from the two former quantities due to albedo / Marshak limb brightening angle-of-view effects.

*This work performed under the auspices of the U.S. Department of Energy by Lawrence Livermore National Laboratory under Contract DE-AC52-07NA27344.

CP8 83 Simulation of Asymmetrically Driven Hohlraum Experiments on OMEGA STUART McALPIN, RICHARD STEVENSON, KELLY VAUGHAN, JOHN FOSTER, *AWE* A campaign of experiments is being undertaken on the OMEGA laser to asymmetrically drive an imploding capsule within a hohlraum. This acts as a stringent test of the modeling of both the conditions inside the hohlraum and the evolution of complex hydrodynamic systems. These experiments are being modeled using two methodologies. Simulating the laser deposition and early-time evolution in a Lagrangian code, before linking to an Eulerian code for the late-time evolution, is a well established route. Simulation of the entire evolution using an ALE (Arbitrary Lagrangian Eulerian) code is also being attempted. A number of techniques have been identified which potentially offer significant control of both the spatial and temporal asymmetry of the drive on the capsule. These are being tested systematically in two ways. Uniform density aerogel spheres are used to resolve the temporal variation in drive and thin glass shells with a GDP ablator are used to resolve the spatial variation in drive. In both cases the evolution of the configuration is being determined using titanium area backlighting at 4.7 keV combined with a gated x-ray imaging system.

CP8 84 Multi-Variable Sensitivity Studies of the Beryllium NIF Ignition Target* JAY SALMONSON, STEVEN HAAN, DANIEL CLARK, DEBRA CALLAHAN, *Lawrence Livermore National Laboratory* We report the results of our continuing effort to optimize and control sensitivities for the Beryllium (Be) NIF ignition capsule. We will compare the two candidate scales for the latest (Revision 4) Be capsule: maximum hohlraum radiation temperature of 285 eV (capsule radius 1.18 mm) and 270 eV (1.3 mm). The performance of these capsules is assessed by performing a sensitivity analysis which integrates 35 1D capsule design parameters with 2D surface roughness specifications for each of the seven distinct capsule layer interfaces as well as laser drive asymmetry specifications. We will highlight efforts to understand and control the sensitivities deriving from inhomogeneities within the sputtered Be ablator material including the diffusion of Copper across the internal graded doped layers as well a clumping of impurities such as Argon associated with the Be crystal microstructure.

*This work was performed under the auspices of the U.S. Department of Energy by Lawrence Livermore National Laboratory under Contract DE-AC52-07NA27344.

CP8 85 Sensitivity of Thermonuclear Burn to Charged Particle Stopping Power Models in NIF-like Targets* MATTHEW TERRY, GREGORY MOSES, *University of Wisconsin-Madison* Accurate treatment of fusion product charged particle transport (in particular the 3.5 MeV alpha particles) is very important for the accurate simulation of ICF ignition, bootstrap heating and burn. Models have been proposed by many authors to account for collisional scattering, dielectric scattering, degeneracy effect, and

combined collisional-dielectric behavior. We present 1D calculations comparing the behavior of NIF ignition-like targets for a series of different stopping power models. As each of these models has complicated validity constraints, we keep track of validity violations in terms of the amount of energy deposited while using a theoretically invalid stopping power. For our calculations we use the radiation-hydrodynamics code BUCKY and have developed a stopping power library: Deeks. Deeks implements the stopping power models of Landau; Spitzer; Li and Petrasso; Brown, Preston and Singleton; Kihara and Aono; May and Cramer; Brysk; Skupsky; and a degenerate extension of Li and Petrasso's model in the library Deeks. Additionally, Deeks can mix electron and ion components of different models while retaining validity checks for the hybrid model.

*Work supported by Sandia National Laboratories through NPSC Fellowship.

CP8 86 Automated parameter space searches for calibrating mix models in NIF ignition implosions* NELSON HOFFMAN, *LANL* BRUCE HAMMEL, OLEG SCHILLING, *LLNL* Turbulent transport ("mix") models typically have many adjustable coefficents, which must be calibrated against experimental or numerical simulation data. We calibrate mix models against high-resolution 2D simulations of NIF ignition capsules [Hammel *et al.*, *J. Phys.: Conf. Ser.* **112**, 022007 (2008)]. The time-varying radial profiles of species composition in the imploding capsule serve as the calibration reference. We perform one-dimensional implosion simulations using two mix models: one from Zhou, Zimmerman, and Burke [*Phys. Rev. E* **65,** 056303 (2002)] and a $k - \varepsilon$ model by one of us (OS). We can calibrate so that one-dimensional composition profiles roughly match the simulation profiles for a Rev3 CH(Ge) ignition capsule at several times, although non-monotonic features of the profiles cannot be represented by the mix models. For fitting, we use automated scripts and fitting metrics, which allow parameter spaces of up to five dimensions to be searched rapidly. Besides identifying optimal coefficient sets, such searches reveal the sensitivity of model results to variations in inputs.

*Work supported by US DOE/NNSA under Contract DE-AC52-06NA25396.

CP8 87 Shock interaction with an isotropic field of sound waves* J.G. WOUCHUK, C. HUETE RUIZ DE LIRA, *ETSII-INEI UCLM Ciudad Real 13071 Spain* A.L. VELIKOVICH, *Plasma Physics Division, NRL, USA* Interaction of shock waves with vortical, entropic and acoustic preshock fluid perturbations must be well understood to study and model shock interaction with more general turbulent flows, which is important for ICF and many other areas. We focus here on the interaction of a shock front with a random isotropic field of acoustic waves. The dynamics of the shock interaction with a single-mode pre-shock acoustic perturbation field is analyzed in detail and mode averaging is performed to study the turbulence generated downstream. Analytical results are shown for the postshock turbulent kinetic energy, vorticity, acoustic energy flux, internal energy, and noise level as a function of the fluid compressibility and shock strength. Good agreement with previous theoretical results is demonstrated. Comparison to the shock interaction with vortical [J. G. Wouchuk *et al.*, Phys. Rev. E 79, 066315 (2009)] and entropic perturbations is also presented.

*Work supported by US DoE/NNSA (A. L. V.), Ministry of Science, MEC(FIS2006-05389) and Junta de CLM (PAI08-0182-3162), Spain (J. G. W and C. H. R. de L.)

CP8 88 Influence of binary particle collisions on trapped particle nonlinearities and the onset of stimulated Raman backscatter in the kinetic regime* S.M. FINNEGAN, L. YIN, B.J. ALBRIGHT, K.J. BOWERS,†J.L. KLINE, *Los Alamos National Laboratory* The onset of stimulated Raman backscatter (SRBS) in a single laser speckle is examined in the kinetic regime using 1D and 2D VPIC [K. J. Bowers et *al.*, Phys. Plasmas **15**, 055702] simulations. A binary particle collision model [T. Takizuka and H. Abe, J. Comput. Phys. **25**, 205] is used to isolate and independently study the effects of like-particle (e-e) and pair-particle (e-i) collisions on trapped particle nonlinearities (e.g., frequency shift) in relation to SRBS onset, under conditions relevant to short-pulse ($\sim$ 3 ps at FWHM), single-speckle experiments at Trident [J. L. Kline et *al.*, J. Phys.: Conf. Series **112**, 022042]. Regimes of weak and strong collisionality are identified and collisional results are compared with those obtained in the collisionless limit [L. Yin et *al.*, J. Phys.: Conf. Ser. **112**, 022033].

*This work was performed under the auspices of the US DOE.
†Guest Scientist. Currently with D. E. Shaw Research, LLC, New York, NY 10036

CP8 89 Initiation and Saturation of Backward Stimulated Raman and Brillouin Scatter in Single Speckles: Influence of Scattered-Light Seeds and Collisional Heating L. YIN, B.J. ALBRIGHT, H.A. ROSE, K.J. BOWERS, B. BERGEN, S.M. FINNEGAN, *LANL* A suite of 2D and 3D PIC simulations of backward stimulated Raman and Brillouin scattering (SRS and SBS) in ICF hohlraum and Trident plasma have been performed on the heterogeneous multi-core supercomputer, Roadrunner. These calculations reveal that the physics governing the nonlinear saturation of SRS in 3D is consistent with that of prior 2D studies [L. Yin, et al. Phys. Rev. Lett., 99, 265004, 2007], but with important differences arising from enhanced diffraction and side loss in 3D compared with 2D. In addition to wavefront bowing of electron plasma waves (EPW), we find that EPW self-focusing also exhibits loss of angular coherence by formation of a filament necklace, a process not available in 2D. These processes in higher dimensions increase the side-loss rate of trapped electrons, increase wave damping, decrease source coherence for backscattered light, and fundamentally limit how much backscatter can occur from a laser speckle. The SRS onset threshold is lower if initiated by SRS seeds compared with the onset threshold if SRS is initiated by thermal electron density fluctuations alone. Furthermore, we show that the presence or absence of SBS may be sensitively determined by collisional heating and transverse electron temperature variations.

CP8 90 Role of kinetic nonlinearities in Raman scatter in NIF ignition targets* BRUCE LANGDON, DENISE HINKEL, BERT STILL, DAVID STROZZI, EDWARD WILLIAMS, *Lawrence Livermore National Laboratory* Raman scattered light generated over the capsule in an ignition target propagates back towards the laser entrance hole (LEH). Along this path, several millimeters in length, the light may undergo a further Raman decay; the resulting rescattered light will not likely be observable outside the hohlraum. In the LEH region, where many incoming beams overlap, the Raman scattered light may also undergo further amplification, driven by the intensity of the overlapped beams. We analyze kinetic simulations along the lengthy beam path, between LEH and capsule, for the role of nonlinearities, including "inflation" and hot electron production.

*This work performed under the auspices of the U.S. Department of Energy by Lawrence Livermore National Laboratory under Contract DE-AC52-07NA27344.

CP8 91 Considerations of stimulated sideward scattering in NIF ignition-scale hohlraums* WILLIAM KRUER, *University of California, Davis* It's prudent to consider the possibility of stimulated Raman and Brillouin sideward scattering in NIF ignition-scale hohlraums. NIF beam spots are quite large (with diameter $>$ 1mm), and the gradient threshold intensities for these instabilities are rather low. Some simple calculations are given for the convective gain of sideward scattering assuming heavily-damped electrostatic waves. A possible enhancement of sideward scattering in the azimuthal direction is examined. Various ways to detect sideward scattering and its effects are discussed. For seeded angular scattering in the region where the laser beams overlap, see recent calculations by P. Michel *et. al.*[1]

*This work performed under the auspices of the U.S. Department of Energy by Lawrence Livermore National Laboratory under Contract DE-AC52-07NA27344.

[1]P. Michel *et. al.*, 39th Anomalous Absorption Conference, Bodega Bay, CA (June 14-19, 2009)

CP8 92 Suppression of stimulated Raman scattering due to localization of electron plasma wave in laser beam filaments PRERANA SHARMA, RAMPAL SHARMA, *Indian Institute of Technology, Delhi, India* The filamentation of the high power laser beam by taking off-axial contribution is investigated when ponderomotive nonlinearity is taken into account. The splitted profile of the laser beam is obtained due to uneven focusing of the off-axial rays. It is observed that the weak electron plasma wave (EPW) propagating in the z direction is nonlinearly coupled in the modified filamentary regions of the laser beam. The semi-analytical solution of the nonlinear coupled EPW equation in the presence of laser beam filaments has been found and it is observed that the nonlinear coupling between these two waves leads to localization of the EPW. Stimulated Raman scattering (SRS) of this EPW is studied and back reflectivity has been calculated. Further, the localization of EPW affects the eigen frequency and damping of plasma wave. As a result of this, mismatch and modified enhanced Landau damping lead to the disruption of SRS process and a substantial reduction in the back reflectivity. For the typical laser beam and plasma parameters with wavelength (λ=1064nm), power flux ($\approx 10^{16}$W cm^{-2}), and plasma density (n/n_{cr}) = 0.2; the back reflectivity was found to be suppressed by a factor of around 20%.

CP8 93 The growth and saturation of the two-plasmon decay instability in inertial confinement fusion* R. YAN, A. MAXIMOV, C. REN, *University of Rochester* F. TSUNG, *UCLA* We present particle-in-cell (PIC) and fluid simulations on the two-plasmon-decay (TPD) instability under conditions relevant to direct-drive inertial confinement fusion experiments. The PIC simulations show a wide TPD spectrum, with modes whose perpendicular mode number $k_\perp$ larger than the cutoff predicted by the linear theory for absolute modes. The fluid simulations, solving the full set of the linear equations of TPD, show that large-$k_\perp$ modes are convective and have linear growth rates comparable to the absolute modes. The convective modes grow at the lower density region and can cause pump depletion, reducing the growth of the absolute modes. The convective modes, saturating before reaching the convective limit, are energetically dominant in the nonlinear stage. The PIC simulations show that both the absolute and convective modes saturate due to ion density fluctuations. The results show that the convective modes of TPD are important to the performance of current and future direct-drive experiments.

*Supported by DoE under Grants Nos. DE-FG02-06ER54879 and DE-FC02-04ER54789. The research used resources of NERSC.

CP8 94 The Effects of Plasma Packets and Local Pump Depletion in Stimulated Raman Scattering* B.J. WINJUM, J.E. FAHLEN, F.S. TSUNG, W.B. MORI, *UCLA* Stimulated Raman scattering (SRS) for NIF-relevant parameters involves nonlinear, kinetic physics. Previous simulations have focused on the nonlinear physics involved in SRS saturation (such as nonlinear frequency shifts and trapped-particle sideband instabilities) in isolation from and without regard to finite spatial effects. However, SRS is bursty in both space and time, generating plasma wave packets that locally generate bursts of reflected light, deplete incident laser light, and interact with each other through scattered light. The recurrence rate of SRS reflectivity is shown to depend on the nonlinear packet speed and the nonlinear frequency shift of plasma waves in packets. Packets are shown to locally deplete the incident laser energy, but as the packets are etched away and new laser energy propagates past the packet edge without being depleted, packets undergo renewed growth, resulting in new bursts of reflectivity. For interaction lengths that allow several packets to grow and convect simultaneousl, backscattered light from one packet provides an enhanced seed for a nearby packet. This causes the reflectivity to increase as a function of time. We present results for both 1D and 2D simulations.

*Supported by DOE and NSF.

CP8 95 Nonlinear, Local Kinetic Damping of Finite-Size Plasma Waves Relevant to Stimulated Raman Scattering WARREN MORI, JAY FAHLEN, BENJAMIN WINJUM, THOMAS GRISMAYER, VIKTOR DECYK, Computer simulations of stimulated Raman scattering (SRS) indicate that the instability is bursty in time and space, leading to finite-size plasma waves in both the longitudinal and transverse directions. Using particle-in-cell (PIC) simulations with an external, ponderomotive impulse driver, we present the results of detailed study of the nonlinear behavior of finite-sized plasma waves in order to better understand the long-time behavior of SRS reflectivities. In one dimension, we present recently published results (Fahlen *et al.*, PRL **102**, 245002 (2009)) showing that finite-length plasma waves erode from the rear edge as new resonant particles enter and locally damp the packet. In multiple dimensions, recent results show that finite-width plasma waves localize about their axis due primarily to

local, kinetic damping at the edges. The simulations are performed using a 1D and 2D electrostatic PIC code, and also using a 2D Darwin PIC code. This work was supported by DOE under Grant Nos. DE-FG52-03-NA00065, DE-FG52-06NA26195, and DE-FG02-03ER54721.

CP8 96 A PIC simulation study on the evolution of the real and imaginary frequencies of 1D plasma waves* THOMAS GRISMAYER, JAY FAHLEN, BENJAMIN WINJUM, FRANK TSUNG, GEORGE MORALES, WARREN MORI, UCLA TEAM, We use electrostatic PIC simulations to study the evolution of both the real and complex frequency of 1D plasma waves. We are considering especially the linear regime where the asymptotic damping rate is much bigger than the bounce frequency. In this regime the waves are typically very small and below the thermal noise. These waves can be studied using a subtraction technique where two simulations where identical random number generation seeds are carried out. In the first, a small amplitude wave is excited. In the second simulation no wave is excited. The results from each simulation are subtracted providing a clean linear wave that can be studied. As previously predicted, the damping is divided in two stages, an initial transient and an asymptotic decay (Landau's formula). The time-dependent resonant width measured in the simulations is compared with the theoretical prediction. In typical ICF plasmas $nl_d^3 < \sim 10^3$. Therefore, the number of resonant electrons can be small for linear waves. We will consider the effects of small numbers of resonant particles and their consequences of the observed damping.

*This work was supported by DOE under grant Nos. DE-FG52-03-NA00065, DE-FG52-06NA26195, DE-FG02-03ER54721.

CP8 97 Simulations for plasma heating of the core plasma in fast ignition ATSUNORI OKABAYASHI, HIDEAKI HABARA, KAZUO A. TANAKA, *Osaka University* AMITA DAS, *Institute of Plasma Physics, India* G. RAVINDRA KUMAR, *Tata Institute of Foundermental Research, India* PREDHIMAN KAW, *Institute of Plasma Physics* TOSHINORI YABUUCHI, *UC, San Diego* SUDIP S. GUPTA, *Institute of Plasma Physics, India* Heating of core plasma by fast electrons is a backmost and utmost issue in fast ignition. Although several efforts in simulation to understand the heating mechanism and consequently the deposit energy in the core, it has been unknown due to complicated physical processes and insufficient computer resource for a full-scale simulation. For this situation, we separate collisional and collective processes by using different type of simulations. In order to simulate collisional energy deposition, we performed a Monte-Carlo code, EGS5, to estimate the core temperature by using the previous integrated experiment as the calculation condition [1]. In the results, the temperature increases from the low dense to the core where the maximum temperature is obtained up to several tens eV, which is near the half of the temperature in the experiment In addition, we found the electrons around 1 MeV mostly contribute to the heating. On the other hand, we observe the significant reduction of electrons up to 10 MeV possibly by depositing their energies on the core in the above experiment and indicate a new collective energy deposition mechanism in EMHD framework [2]. We're developing a new code to verify the EMHD approach. [1] R. Kodama et al., Nature 412, 23 (2001). [2] T. Yabuuchi et al., submitted to New J. Phys. (2009).

CP8 98 Hybrid simulations of strong filamentation of relativistic electron beam propagating through collisionless plasma.* VLADIMIR KHUDIK, GENNADY SHVETS, *Institute for Fusion Studies, The University of Texas at Austin* IGOR KAGANOVICH, *Princeton Plasma Physics Laboratory* Development of the Weibel instability during propagation of relativistic beam through ambient plasma leads to formation of low-current filaments, which continue to merge with each other and eventually form filaments with large currents. Analytical theory and computationally efficient simulations of this nonlinear stage of Weibel instability are presented. In our hybrid approach [1] beam electrons are modeled using numerical macroparticles while plasma electrons are modeled as a passive fluid responding to the beam evolution. But in contrast to [1], present analysis captures effects of violation of the charge quasi-neutrality near the boundaries of high-current filaments and reproduces in details the structure of the electron plasma-void regions. This approach is especially effective in the cases when beam electrons have a large relativistic factor. Results of hybrid simulations are compared with those obtained from direct fully electromagnetic PIC simulations and applicability limits of the developed model are established. [1] Oleg Polomarov et al., Phys. Plasmas 14,043103 (2007).

*Supported by the US DOE grant DE-FG02-05ER54840.

CP8 99 Modeling of Plasma Heating and Neutron Production in Collisions of CD Planar Foils at Velocities of ~ 1000 km/s* STEVEN ZALESAK, *Berkeley Research Associates* M. KARASIK, J.W. BATES, A.J. SCHMITT, A.L. VELIKOVICH, *Plasma Physics Division, NRL* Y. AGLITSKIY, *Science Applications International Corporation* N. METZLER, *ARTEP, Inc.* M. MURAKAMI, *Institute of Laser Engineering, Osaka University* Recent experiments on NRL's Nike laser have for the first time accelerated CD planar foils to velocities of 700-1000 km/s [1]. When the CD foils collide with stationary graphite foils, on the order of 10^6 thermonuclear neutrons are produced, with ion temperatures in the range of 2-3 keV. The success of this set of experiments suggests optimism for ICF concepts such as shock ignition and Impact Ignition [2,3]. We present numerical simulations of these experiments using NRL's FAST3D radiation hydrodynamics code, which we use both to better understand the details of the experiment and to validate the code for fusion reactor pellet design. [1] M. Karasik, invited talk, this conference [2] M. Murakami *et al.*, Nucl. Fusion **46**, 99 (2006) [3] H. Azechi *et al.*, PRL **102**, 235002 (2009).

*This work was supported by the U.S. Department of Energy.

CP8 100 Progress in indirect drive fast ignition capsule design for the National Ignition Facility DANIEL CLARK, PETER AMENDT, BARBARA LASINSKI, DONALD MEEKER, HENRY SHAY, MAX TABAK, RICHARD TOWN, *Lawrence Livermore National Laboratory* We describe our ongoing work in developing indirect drive Fast Ignition (FI) target designs to be fielded on the National Ignition Facility. Previous efforts [Bull. Am. Phys. Soc. 53, 52 (2008)] focused on capsule designs using deuterium-tritium fuel and doped beryllium ablators. In keeping with the need to diagnose electron beam heating of the assembled fuel at low beam energies, these target designs have evolved into non-cryogenic surrogate targets using silver-doped, deuterated plastic "fuel" layers and plastic ablators. Two designs are described in detail, one using a single shock pulse shape followed by a quasi-isentropic compression and a second using a more con-

ventional four-shock pulse shape. The control of pre-heating of the reentrant gold cone in FI targets is particularly problematic in the hard x-ray environment of indirect drive, and a variety of shell dopant materials are investigated in these designs to mitigate the pre-heat. Finally, the reliability of these target designs in assembling the required fuel areal density is assessed in the face of expected target and radiation drive uncertainties using a series of statistical scans including all expected 1-D sources of error.

CP8 101 On the role of relativistic shocks in fast ignition FREDERICO FIUZA, RICARDO FONSECA, LUIS SILVA, *GoLP/IPFN - Instituto Superior Tecnico* JOHN TONGE, JOSHUA MAY, *Department of Physics & Astronomy, University of California, Los Angeles* WARREN MORI, *Department of Electrical Engineering and Department of Physics & Astronomy, University of California, Los Angeles* CHUANG REN, *University of Rochester* One of the critical issues for fast ignition of fusion targets is to understand/optimize the coupling of the ignition laser to the fast particles, and their transport in the mildly to high dense region of the target. We have performed a series of 2D PIC simulations in order to examine laser absorption and electron transport using ignition lasers with ultra-high intensities, up to $5x10^{21}$W/cm^2, and density gradients up to 1000 nc. Our results indicate that the dynamics of the Weibel/streaming instabilities leads to an isotropization of inward heat flux. This causes energy to be bottled up near the laser interaction point causing a shock to be launched. In uniform plasmas, this process and the emission of plasmons by the inward flowing electrons leads to a softening of the electron energy spectrum to the 1-3 MeV range for ultra-high laser intensities. In fast ignition (both channel and cone guided) this shock and the associated heat flux need to propagate up a density gradient to the core. The inclusion of the density gradient is observed to be crucial, leading to a stronger energy release by the shock structure and therefore to potentially higher efficiencies.

CP8 102 Dependence of core heating properties on heating pulse duration and intensity TOMOYUKI JOHZAKI, HIDEO NAGATOMO, ATSUSHI SUNAHARA, *ILE, Osaka University* HONGBO CAI, *ILE, Osaka Univ.* HITOSHI SAKAGAMI, *NIFS* KUNIOKI MIMA, *ILE, Osaka University* In the cone-guiding fast ignition, an imploded core is heated by the energy transport of fast electrons generated by the ultra-intense short-pulse laser at the cone inner surface. The fast core heating ($\sim$ 800eV) has been demonstrated at integrated experiments with GEKKO-XII+ PW laser systems. As the next step, experiments using more powerful heating laser, FIREX, have been started at ILE, Osaka university. In FIREX-I (phase-I of FIREX), our goal is the demonstration of efficient core heating ($T_i \sim$ 5keV) using a newly developed 10kJ LFEX laser. In the first integrated experiments, the LFEX laser is operated with low energy mode ($\sim$ 0.5kJ/4ps) to validate the previous GEKKO+PW experiments. Between the two experiments, though the laser energy is similar ($\sim$ 0.5kJ), the duration is different; $\sim$ 0.5ps in the PW laser and $\sim$ 4ps in the LFEX laser. In this paper, we evaluate the dependence of core heating properties on the heating pulse duration on the basis of integrated simulations with FI^3 (Fast Ignition Integrated Interconnecting) code system.

CP8 103 Study of fast electron transport in warm dense plasma targets* M.S. WEI, H. SAWADA, S. CHAWLA, N. NAKANII, D.P. HIGGINSON, B.S. PARADKAR, T. YABUUCHI, F.N. BEG, *UC San Diego* K.U. AKLI, R.B. STEPHENS, *General Atomics* A. MACPHEE, D. HEY, S. LE PAPE, H.S. MCLEAN, M. FOORD, M.K. KEY, P.K. PATEL, A.J. MACKINNON, *LLNL* H. FRIESEN, H. TIEDJE, Y.Y. TSUI, R. FEDOSEJEVS, *Univ. of Alberta, Canada* J. PASLEY, *Univ. of York, UK* A. MORACE, D. BATANI, *Univ. of Milano, Italy* Recent experiments [Le Pape et al., RSI 79, 106104, 2008] successfully demonstrated creation of a warm dense plasma using ns laser driven shock compression in a low-density foam target. Fast electron transport in such shock heated targets relevant to fast ignition is investigated using the Titan laser at LLNL. K-shell x-ray emission from the Cu fluorescent layer in the foam package targets is measured using Bragg crystal imagers and HOPG spectrometers. Electron transport through cold, conductor and shocked compressed foam targets is compared. The experiment is modeled using a 2D radiation hydro code and the hybrid PIC code LSP.

*Work supported by US DOE under contracts DE-FC02-04ER54789 (Fusion Science Center) and DE-FG02-05ER54834 (ACE).

CP8 104 Creation of warm dense matter with a proton beam generated by the OMEGA EP laser beam SUGREEV CHAWLA, *UCSD,LLNL* F.N. BEG, *UCSD* A.G. MACPHEE, M. FOORD, M.B. SCHNEIDER, T. DOEPPNER, D.L. JAMES, A. ELSHOLZ, J. EMIG, A.J. MACKINNON, H.S. MCLEAN, R.B. STEPHENS, K.U. AKLI, C. FREDERICK, The creation of warm dense states of matter has important implications in astrophysics and the fast ignition scheme for inertial confinement fusion. We report on an experiment performed using OMEGA EP laser (1 kJ, 10 ps), which was focused on a hollow Cu hemisphere to produce an intense, focused proton beam. This proton beam was used to heat a 25 um thick, 2 mm diameter Be disk placed 375 um from the apex of the hemisphere. Variable spaced grating spectrometers were used to diagnose the continuum spectrum emitted from the rear side of the disk. The results were then compared to LASNEX simulations to infer a bulk temperature. A detailed analysis will be presented. Work performed under the auspices of the U.S. DOE by LLNL under contracts DE-AC52-07NA27344 and DE-FG-02-05ER54834. The authors acknowledge the support of OMEGA EP and LLNL technical staff.

CP8 105 Fast electron transport in shock-wave heated planar Au targets H. SAWADA, M.S. WEI, S. CHAWLA, N. NAKANII, B.S. PARADKAR, T. YABUUCHI, F.N. BEG, *UCSD* K. AKLI, R.B. STEPHENS, *GA* A.G. MACPHEE, D. HEY, S. LE PAPE, Y. PING, M. FOORD, H. MCLEAN, M. KEY, A.J. MACKINNON, P. PATEL, *LLNL* H. FRIESEN, H. TIEDJE, Y. TSUI, R. FEDOSEJEVS, *U of Alberta* J. PASLEY, *U of York* A. MORACE, D. BATANI, *U of Milano* Hydro modeling shows that in a re-entrant cone-guided Fast Ignition, shell compression launches a shock into the tip of the cone through which the ignition electrons must propagate. The transport of fast electrons through shocked and unshocked Au targets is investigated using the Titan laser at LLNL. A shock wave is launched by the long pulse (300 J, 3ns, 532 nm) interacting with the CH of a CH/Cu/Au target. Fast electrons generated by the short pulse (150J, 0.7 ps, 10^{20} W/cm^2) interacting with the Au are transported through the gold. Cu K-alpha induced by the electrons is recorded with HOPG

spectrometers and spherical Bragg crystal imagers as a function of the delay of two pulses. Detailed analysis of results will be presented. This work was supported by the US DOE under contracts DE-FC02-04ER54789 (Fusion Science Center) and DE-FG-02-05ER54834 (ACE).

CP8 106 Fast electron generation and transport in cone-attached wire targets irradiated by 800 J, 10 ps OMEGA EP laser pulses* T. YABUUCHI, H. SAWADA, T. MA, T. BARTAL, M.S. WEI, F.N. BEG, *UCSD* K.U. AKLI, R.B. STEPHENS, *GA* H. CHEN, A.J. ELSHOLZ, J.A. EMIG, M.H. KEY, A.J. MACKINNON, R.D. VAN MAREN, H.S. McLEAN, P.K. PATEL, Y. PING, *LLNL* D. BATANI, R. JAFER, *Univ. of Milano, Bicocca* S.D. BATON, *LULI* L.A. GIZZI, *IPCF-CNR* P.A. NORREYS, C. SPINDLOE, *STFC RAL* R. BETTI, W. THEOBALD, *LLE* Study of fast electron generation and transport is of a fundamental importance for the success of fast ignition of ICF. OMEGA EP provides an important platform to carry out such a study. We report experiments using copper wires attached to gold cones with 800 J, 10 ps pulses at the OMEGA EP laser facility. The fast electron generation and transport were investigated with the Cu K α x-rays, to show energy coupling into the wire, from the emitted electrons, to show their energy spectrum, and by backlighting with an MeV proton beam to show electrostatic fields around the target. Experimental results are compared with 150 J, 1 ps pulses using the Titan laser at LLNL.

*This work was performed in part at the LLE NLUF, and supported by US DOE under contracts DE-FG02-05ER54834 and DE-FC02-04ER54789.

CP8 107 A Hybrid Ion/Electron Beam Fast Ignition Concept B.J. ALBRIGHT, *Los Alamos National Laboratory* Fast ignition (FI) inertial confinement fusion is an approach to high-gain inertial fusion, whereby a dense core of deuterium/tritium fuel is assembled via direct or indirect drive and then a hot spot within the core is heated rapidly (over a time scale of order 10 ps) to ignition conditions by beams of fast charged particles. These particle beams are generated outside the capsule by the interaction of ultra-intense laser pulses with solid density targets. Most study of FI to date has focused on the use of electron [Tabak et al., Phys. Plasmas 1, 1696 (1994)] or ion [Fernández et al., Nuclear Fusion 49, 065004 (2009)] beams, however a hybrid approach involving both may have advantages. This paper will describe recent work in this arena. Work performed under the auspices of the U. S. Dept. of Energy by the Los Alamos National Security, Los Alamos National Laboratory. This work was supported by LANL Laboratory Directed Research and Development (LDRD).

CP8 108 Laser Energy Absorption Scaling and Ion Production in Thick and Thin Targets* MALCOLM HAINES, *Imperial College, London* MINGSHENG WEI, FARHAT BEG, *University of California San Diego* RICHARD STEPHENS, *General Atomics San Diego* A fully relativistic model has been developed for the interaction of an intense laser with an overdense plasma. The model is based on conservation laws in one dimension for momentum flux and energy flux across the vacuum-plasma boundary. The main results are (a) that the maximum hot electron temperature scales as $(1 + 2^{1/2}a_0)^{1/2} - 1$, in units of the electron rest mass energy and (b) the light absorption can be 80%-90% for intensity $> 10^{19}$ W cm^{-2} This theory has been extended to the case of a thin target, at the rear boundary of which fast electrons can reflux. Momentum and energy flux conservation leads to surface ion acceleration (typically protons in experiments), while refluxing electrons re-entering the front boundary region lead to greatly reduced laser-light absorption. This is relevant to proton driven fast ignition.

*Work supported by US DOE under contracts DE-FC02-04ER54789 (Fusion Science Center) and DE-FG02-05ER54834 (ACE).

CP8 109 On the Advantages of Fast Ignition with Ultra-High Intensity Lasers* J. TONGE, J. MAY, W.B. MORI, *UCLA* F. FIUZA, R.A. FONSECA, L.O. SILVA, *Instituto Superior Técnico* C. REN, *University of Rochester* One of the critical design constraints for fast ignition targets is the need to have a small cross section for the hot spot at the target core while delivering enough power to the hot spot with hot electrons of the proper energy range, $\sim$ 1-3 MeV, to couple to the core. We use two-dimensional Particle-In-Cell simulations of isolated targets to investigate the feasibility of using 1μm ignition lasers with ultra-high intensities, up to 8x10^{20}W/cm^2, for fast ignition. The self-consistent absorption of energy from an ultra-high intensity laser by overdense plasma and the subsequent energy transport through the collisionless overdense plasma, $\nu_{ei} < \omega_p$, of a 50μm radius isolated target, is explored in detail. At these ultra-high intensities, we find that most of the energy transport is in a hot bulk and not in the super-hot tail of the electron distribution. Electrons in a relatively low energy range, below 3MeV, transport 90% of the heat flux through 50μm of 100n$_c$ plasma to the target core.

*The authors acknowledge support by NSF under PHY-0078508, and DOE under DE-FG03-NA0065 and DE-FG02-03ER54721 and DE-FG02-06ER54879, and of the HiPER project (EC FP7 #211737).

CP8 110 Hosing in Laser Channeling in Fast Ignition G. LI, R. YAN, C. REN, V.N. GONCHAROV, *Laboratory for Laser Energetics, U. of Rochester* J. TONGE, W.B. MORI, *UCLA* Laser channeling aims to reduce the energy loss of an ignition pulse in the mm-scale underdense plasma of fast ignition targets. Previous full-scale particle-in-cell (PIC) simulations in 2D identified laser and channel hosing as an important instability that causes channel-bifurcation and limits channeling speed [1]. Hosing in 3D has also been observed in recent PIC simulations, which show that hosing grows slower in 3D than in 2D. Laser hosing in this long wavelength regime is through coupling with the ion acoustic waves. A variational analysis of hosing in 2D and 3D will also be presented. This work was supported by the U.S. Department of Energy under Cooperative Agreement Nos. DE-FC52-92SF19460, DE-FC02-04ER54789, and DE-FG02-06ER54879. [1] G. Li et al., Phys. Rev. Lett. 100, 125002(2008).

CP8 111 Electron Acceleration by High Intensity Lasers at Sharp Matter Interfaces* J. MAY, J. TONGE, W.B. MORI, *UCLA* F. FIUZA, R. FONSECA, L. SILVA, *GoLP/IPFN, IST* C. REN, *University of Rochester* A key question in the fast ignition approach to nuclear fusion is how electrons are accelerated at a light-plasma interface by very intense lasers. To investigate this, we use the PIC code OSIRIS to model the interaction of high intensity lasers (I> =5x10^{19} W/cm^2) with a sharp boundary of an over-critical plasma (n> >n$_c$). We find that, for these experimental parameters, none of the commonly proposed absorption mecha-

nisms – i.e., inverse Bremsstrahlung, JxB, Brunel heating – can account for the spectrum of forward accelerated electrons. Instead, we propose a mechanism in which these electrons thermally exit the plasma, resonantly interact with the incoming and reflected laser light within a quarter wavelength of the surface, and then turn back into the plasma - gaining in the process up to twice the quiver velocity. Electrons must leave the plasma at high energies, specific angles, and in phase with the laser wave in order to be accelerated. This mechanism is confirmed by 2D OSIRIS simulations with particle tracking, as well as from the results of a 1D numerical imposed field model.

*The authors acknowledge support by NSF and DOE.

CP8 112 Numerical Simulation of Pre-formed Plasma Generated by Low Intensity Pre-Pulse Before Main Heating Laser in Fast-Ignition ATSUSHI SUNAHARA, CAI HONGBO, TOMOYUKI JOHZAKI, HIDEO NAGATOMO, KUNIOKI MIMA, *Intitute of Laser Enginnering Osaka Univ.* We investigated the plasma expansion of the inner surface of the cone used for the fast-ignition scheme of the inertial confinement fusion (ICF). LFEX laser [1] in Osaka University is high intense and short pulse laser system, which has 10^{19}W/cm^2 to 10^{20}W/cm^2, and ps pulse duration. However, it has also low intense pre-pulse with the contrast ranging from 10^5 to 10^8. It is high enough to ablate the inner surface of the cone wall used for fast ignition target. We developed the two-dimensional simulation code (Star-2D) [2], and simulate plasma expansion of the inner surface of the cone. We will discuss our simulation results, and also effects of the pre-plasma expansion on fast electron production. On the other hand, our code has been applied to simulate the laser-produced plasmas for Extreme-Ultraviolet research, and its accuracy has been tested with various experiments. We will also discuss the accuracy of our simulations. [1] H. Azechi et at., in EPS. [2] A. Sunahara et al., *Journal of Physics: Conference Series* 112(2008) 042048-1-4.

CP8 113 Application of a New Turbulent Transport Model to Double-Shell Inertial Confinement Fusion Capsule Implosions* OLEG SCHILLING, HARRY ROBEY, PETER AMENDT, *Lawrence Livermore National Laboratory* Recent progress in the modeling of the performance of non- cryogenic double-shell inertial confinement fusion capsules is discussed. A new two-equation eddy viscosity-based K- ϵ turbulent transport and mixing model is briefly described and then applied to a set of double-shell capsules with glass and plastic inner shells. One- and two-dimensional simulations are presented and compared to measurements previously obtained from experiments on the OMEGA laser. It is shown that the model predictions, using coefficients consistent with both high resolution numerical simulation data of Rayleigh- Taylor instability-induced turbulence and with analytical solutions of the model in particular limiting cases, are well within the uncertainties of the experimentally measured capsule yields. Various quantities from the capsule simulations are discussed and interpreted physically within the context of both ICF physics and turbulence.

*This work was performed under the auspices of the U.S. Department of Energy by Lawrence Livermore National Laboratory under Contract DE-AC52-07NA27344.

CP8 114 Laser-Plasma Interaction Experiments in Gas-Filled Hohlraums at the LIL Facility* PAUL-EDOUARD MASSON-LABORDE, *CEA, DAM, DIF, F-91297 Arpajon, France* PASCAL LOISEAU, *CEA, DAM, DIF* MICHEL CASANOVA, CHRISTOPHE ROUSSEAUX, DENIS TEYCHENNE, STEPHANE LAFFITE, GAEL HUSER, *CEA, DAM, DIF, F-91297 Arpajon, France* The first laser-plasma interaction campaign conducted at the LIL facility, using gas-filled hohlraums, ended in spring 09. Two different gas-filled hohlraums have been designed in order to mimic plasma conditions expected along two particular beam paths in ignition hohlraums. The targets consist of 3- or 4-millimeters long, 1 atm neo-pentane gas-filled gold hohlraums. The LIL quadruplet is aligned with the hohlraum's axis and delivers a 6-ns long pulse with 15 kJ at 3ω. Optical smoothing is achieved by longitudinal dispersion and a phase plate giving a near 10^{15} W/cm^2 mean intensity on the focal spot at maximum power. Plasma conditions from hydrodynamic calculations allow to calcule SBS and SRS linear gain with the PIRANAH code. The calculated spectra are compared to experimental results. We use the paraxial code HERA to investigate the propagation of the LIL quad. Finally, 1D and 2D PIC simulations based on the plasma conditions of the cavity will be discussed in order to understand experimental SRS spectrum.

*paul-edouard.masson-laborde@cea.fr

SESSION CM9: MINI-CONFERENCE ON INNOVATIVE MAGNETIC MIRROR CONCEPTS AND APPLICATIONS II

Monday Afternoon, 2 November 2009
The Learning Center at 14:00
E. Bick Hooper, Lawrence Livermore National Laboratory, presiding

14:00

CM9 1 Vortex Confinement of Plasmas in Axially Symmetric Mirrors ALEXEI BEKLEMISHEV, PETER BAGRYANSKY, MAXIM CHASCHIN, ELENA SOLDATKINA, *Budker Institute of Nuclear Physics* Efforts to optimize operation of the Gas Dynamic Trap with variation of plasma rotation led to discovery of a new way of efficient plasma confinement. Its nature is similar to confinement of material in the dead zone of a vortex flow. It is achieved by applying voltage to the limiters and the endplates of the device, thus creating shear-flow layer, which surrounds the core of the discharge. In this regime the gas-dynamic stabilization is shown to be unnecessary, as the confinement is excellent even with straight field lines in the expanders. While the axisymmetric equilibrium remains unstable, there appears a new dynamic state of confinement with approximate axial symmetry and low convective losses. The needed power consumption is a fraction of parallel ion losses (30kW), while the theoretical scaling predicts the scheme to work even at fusion temperatures. The talk will contain simplified analytic theory of the nonlinear dissipative saturation of the m=1 mode in the presence of the externally-driven vortex flow, and the two-dimensional drift-ordered MHD simulation of the vortex confinement in the GDT.

14:30

CM9 2 The Design of anchor divertor of GAMMA10 ISAO KATANUMA, KOTARO YAGI, YOSUKE NAKASHIMA, MASAYUKI YOSHIKAWA, MAKOTO ICHIMURA, TSUYOSHI IMAI, *University of Tsukuba* The plan that one of the anchor mirror cells, which was installed for the flute interchange mode stability, is replaced by an axisymmetric divertor mirror cell is in progress. The main object of the divertor mirror is to simulate the ITER divertor physics. Then the scenario on the effective evacuation of core plasma in the divertor mirror cell to the magnetic null region is required in order to obtain a high power plasma flow outside the divertor mirror cell region. We are designing the divertor mirror coil system in GAMMA10 and estimating the plasma parameter in the divertor system and radial energy loss flux outside the magnetic null. The MHD stability is determined with help of the kinetic analysis of flute mode by taking into account the ion FLR, magnetic field line curvature and plasma compressibility. The stored energy is calculated by the bounce-averaged Fokker-Planck code. The radial evacuation of hot ions is estimated by the reduced MHD simulation taking into account the flute-like electrostatic potential fluctuations.

15:00

CM9 3 Trapped Particle Instability in Kinetic Stabilized Tandem Mirror HERBERT BERK, JANE PRATT, *IFS, UT Austin* The kinetic stabilizer tandem mirror (KSTM) devised by R. F. Post (J. Fus. Energy 2007) is an innovative concept devised to stabilize a symmetric tandem mirror machines using a concept devised by D. Ryutov (Proc. of Course and Workshop, Varenna, Italy, 1987) and empirically verified in the Gas Dynamic Trap (Ivanov, et. al. Trans. Fusion Technology 39, 127, 2001). The KSTM uses the momentum flux of unconfined particles that only sample the outer end regions of the mirror where there is very favorable field line curvature. Charged ion beams at relatively low energy are externally injected into the ends and reflected out from the ends. MHD stability with a power drain less than the fusion power production can be achieved. We examine the effect of fast growing trapped particle instability (Berk et. al. Sov J. Plasma Phys. 1983) on the overall stability. In this case stability is very sensitive to the electron connection between the stabilizer and end plug.

15:15

CM9 4 The TASKA, TDF, and TASKA-M Fusion Neutron Materials Test Facilities* JOHN SANTARIUS, GERALD KULCINSKI, *University of Wisconsin* This talk will summarize key features of three conceptual fusion neutron test facilities designed in the early 1980s: TASKA,[1] TDF,[2] and TASKA-M.[3] Motivated by the accessibility and maintainability of cylindrical geometry, these magnetic-mirror designs possess a simple central cell, as in a fusion neutron test facility based on the gas dynamic trap (GDT).[4] The TASKA-M design, like today's GDT designs, included the injection of neutral beams into the central cell to create a sloshing-ion distribution that gives density peaks near the materials test modules. In TASKA and TDF, the minimum-B end-cell designs contained thermal barriers, regions of low electrostatic potential to reduce electron flow between central cell and end cells. Thermal barriers improve performance but require more complicated input power systems, and their physics basis is less well established than that of simple mirrors. For TASKA-M, a more conservative design, minimum-B end cells provided MHD stability, but thermal barriers and an end-plug potential peak were absent. [1] B. Badger, et al., UW FTI Report UWFDM-500 (1982). [2] T.H. Batzer, et al., LLNL Report UCID-19328 (1983). [3] B. Badger, al., UW FTI Report UWFDM-600 (1984). [4] P.A. Bagryanski, et al., *Fus. Eng. Design* **70**, 13 (2004).

*Research sponsored by UW-Madison and ORISE.

15:30

CM9 5 Minimum B mirror with expander aimed for transmutation and energy production OLOV ÅGREN, *Uppsala University* V.E. MOISEENKO, *IPP NSC KhIPT, Kharkov* KLAUS NOACK, ANDERS HAGNESTÅL, A comparatively simple fusion driven fission device may be developed for industrial transmutation and energy production from spent nuclear waste [1-2]. This opportunity stems from the large fission to fusion power production ratio, $P_{fis}/P_{fus} \approx 150$, in a subcritical fusion device surrounded by a fission mantle with the neutron multiplicity k_{eff}=0.96. Power production is predicted if the electron temperature exceeds 700 eV. The expanders may improve the electron temperature by a formation of an ambipolar potential. Theoretical studies include RF heating, magnetic coil designs, fission mantle kinetics and some basic plasma investigations. A 20 m long mirror with a 40 cm plasma radius could be sufficient for a electric power production of 500 MW. [1] S. Taczanowski, "Premises for development of fusion-fission hybrid systems" in IAEA-RC-870.3, TWG-FR/132, Chennai, India 15 – 19 January 2007. [2] O. Ågren, V.E. Moiseenko, A. Hagnestål, "The straight field line mirror concept and applications," Problems of atomic science and technology **6**. *Series:* Plasma Physics, 8 (2008).

15:45

CM9 6 Gas Dynamic Trap Neutron Source (DTNS) – applications and development path* A.W. MOLVIK, T.C. SIMONEN, *ORAU* D.D. RYUTOV, *LLNL* The successes in the Gas Dynamic Trap at the Budker Institute of Nuclear Physics – stable operation to $\beta \sim 60\%$, T_e increasing with neutral beam power to > 200 eV, and classical behavior of hot ions (Ivanov and Beklemishev, this conf.) – motivate building a DTNS. The DTNS provides ~ 2 MW/m^{2}neutron flux, and 20 l irradiated volume (in a 2.5 cm thick annulus) to enable aggressive programs in fusion materials development, tritium-breeding blankets (which do not have to breed initially because the DTNS burns less than 200 g/yr of T), and hybrid fission blankets. The major issue is steady-state operation of a configuration that has been demonstrated during 5 ms pulses. The known issues are all engineering: cooling components impinged by beams, pumping the gas and regenerating the pumps. Possible plasma physics issues, such as drift waves, are expected to have slow growth times enabling suppression or saturation at low levels.

*This work performed under the auspices of the U.S. Department of Energy by ORAU and by Lawrence Livermore National Laboratory under Contract DE-AC52-07NA27344.

16:00

CM9 7 Investigations of axisymmetric mirror boundary conditions using Reconnection Scaling Experiment* T.P. INTRATOR, *Los Alamos Natl Lab, P-24 Plasma Physics* R.J. OBERTO, T.D. OLSON, Axisymmetric magnetic mirrors such the Gas Dynamic Trap (GDT) concept do not need complex and expensive minimum B magnetic coil structures to enhance MHD stability. GDTs and related mirror designs typically contain a large end loss region region of flared and expanding magnetic field lines between a mirror coil and an end cell with radial and axial end walls. This

end loss region can furnish pressure weighted good curvature field line forces that stabilize MHD behavior, and also provide electrostatic sheaths that confine electron heat loss. Investigations of axial boundary conditions will be useful to determine how and why MHD stability can be enhanced, and how to improve confinement of electron heat flux. The Reconnection Scaling Experiment (RSX) has been used to for a wide range of conditions in an MHD relevant experiment. We have demonstrated a continuous range of adjustability between line tied (fixed) and non line tied (free) axial boundary conditions.

*Supported by LANS Contract No. DE-AC52-06NA25396, and Center for Magnetic Self Organization funded by the National Science Foundation and the Department of Energy.

16:15

CM9 8 MHD-Stabilization of Axisymmetric Mirror Systems Using Pulsed ECRH R.F. POST, *Lawrence Livermore National Laboratory* A method of MHD-stabilizing axisymmetric mirror systems, demonstrated in the Gas Dynamic Trap [1] and analyzed by Ryutov [2] employs low pressure plasma on expanding field lines outside the mirrors. Methods of creating such plasmas have been analyzed [3]. This paper studies another technique: Pulsed ECRH in regions of positive curvature. The ansatz: If the repetition time is shorter than the MHD growth time, and if their time-averaged amplitude is exceeds that required by the theory the system will be stable. The calculations confirm the ansatz. Applications include axisymmetric tandem mirror and multiple-mirror systems. In the latter it might perform the functions of MHD-stabilization and of biasing cell-loss probabilities inwardly. Post and Li [4] showed that such biasing leads to confinement times that increase exponentially with the number of cells, rather than linearly, as occurs with symmetric losses. Prepared by LLNL under Contract DE-AC52-07NA27344. [1] P. A. Bagryansky, et. al., Trans. Fusion Tech. **35**, 79 (1999) [2] D. D. Ryutov, Proc. of Course and Workshop, Varenna, Italy, Vol II, 791 (1987) [3] R. F. Post, Trans. Fusion Tech., **39**, 25 (2001) [4] R. F. Post and X. Z. Li, Nuc. Fusion, **21**, 135 (1981).

16:30

CM9 9 Alpha-Channeling in Mirror Machines ANDREY ZHMOGINOV, NATHANIEL FISCH, *Princeton University* Linear magnetic trap is an attractive concept for fusion research and plasma applications due to its relative engineering simplicity and high-beta operation. Application of the alpha-channeling technique to mirror machines can benefit this concept by efficiently redirecting alpha particle energy to fuel ion heating or sustaining plasma confinement, thus increasing the effective fusion reactivity. To identify waves suitable for alpha-channeling a rough optimization of the energy extraction rate with respect to the wave parameters is performed. After the optimal regime is identified, the systematic search for modes with similar parameters in mirror plasmas is performed by assuming quasi-longitudinal, or quasi-transverse wave propagation. As a result, modes suitable for alpha particle energy extraction are identified in several device designs including the LAPD experiment. Under a proper choice of the tandem mirror device parameters, the predicted modes are expected to feed ICRH waves in the device plugs, thus redirecting the extracted energy to sustaining the plasma confinement.

16:45

CM9 10 Alpha channeling using stationary waves in a centrifugal mirro* ABRAHAM FETTERMAN, NATHANIEL FISCH, *Princeton University* In a mirror with supersonic rotation, charged fusion products might interact with radio-frequency waves to maintain the rotation against drag forces. Magnetic ripples that are stationary in the lab frame can match the cyclotron frequency in the particle frame, allowing resonant interaction without requiring power input. We examine the feasibility of using these waves in a fusion device with a deuterium-tritium plasma.

*This work was supported by DOE Contracts DE-FG02-06ER54851 and DE-AC0276-CH03073.

17:00

CM9 11 Proposed Thomson scattering measurements on the Gas Dynamic Trap HARRY McLEAN, *Lawrence Livermore National Laboratory* DANIEL DEN HARTOG, *University of Wisconsin-Madison* We describe a proposed short-term collaborative experimental investigation of electron temperature on the Gas Dynamic Trap (GDT) experiment at the Budker Institute in Novosibirsk, Russia using the double-pulse multipoint Thomson scattering diagnostic from the decommissioned SSPX spheromak at Lawrence Livermore National Laboratory. Electron temperature is a critical parameter in the gas dynamic trap (GDT) since fast-ion energy losses are governed by electron drag, which decreases with increased electron temperature. Higher fast-ion densities lead to higher neutron production in fusion neutron sources based on the GDT concept. Expected plasma conditions and measurement capabilities will be compared. Suitable experimental campaigns will be presented. This work performed under the auspices of the U.S. DoE by LLNL under Contract DE-AC52-07NA27344.

17:15

CM9 12 Extension of XGC kinetic simulation codes to magnetic mirror configurations G. BATEMAN, A.Y. PANKIN, A.H. KRITZ, T. RAFIQ, *Lehigh U.* G.Y. PARK, S. KU, C.S. CHANG, *NYU Courant Institute* W. HORTON, J. PRATT, *UT Austin, IFS* The XGC codes, developed to simulate the edge regions of tokamak plasmas, are modified to carry out kinetic simulations of axisymmetric magnetic mirror configurations. The XGC codes are particle in cell kinetic codes that include a virtual sheath condition where magnetic field lines run into end plates. The XGC1 code is a fully five dimensional kinetic code that is used to investigate turbulence, while the faster XGC0 code uses the axisymmetric average electrostatic potential in order to simulate charged particle drifts, losses and collisional effects. Kinetic electron computations, neutral beam injection, atomic physics and the effects of thermal neutrals are included in the XGC codes. Changes are being made to allow the XGC codes to accept mirror equilibria and to run without a toroidal magnetic field component. The XGC0 code will be used to compute particle dynamics, electrostatic potentials, and moments of the distribution functions including plasma flows in mirror configurations. [1] C.S. Chang, S. Ku, H. Weitzner, Phys. Plasmas **11** (2004) 2649

SESSION EE1: PANEL DISCUSSION: TOOLS NEEDED TO SURVIVE IN SCIENCE
Monday Evening, 2 November 2009; Regency VI at 17:30

17:30
EE1 1 Panel Discussion
PETER J. FEIBELMAN, *Sandia National Laboratories*
TUDOR JOHNSTON, *University of Quebec, Canada*

SESSION EE2: UNIVERSITY FUSION ASSOCIATION GENERAL MEETING, INCLUDING TOWN MEETING ON DOE RESEARCH NEEDS WORKSHOPS
Monday Evening, 2 November 2009; Hanover CDE at 19:00

SESSION EE3: TOWN HALL MEETING ON THE HIGH ENERGY DENSITY LABORATORY PLASMA RESEARCH NEEDS WORKSHOP
Monday Evening, 2 November 2009; Hanover FG at 21:00

SESSION FR1: REVIEW: ION ACCELERATION USING ULTRA-HIGH INTENSITY LASERS
Tuesday Morning, 3 November 2009; Centennial I-II at 8:00; Chan Joshi, University of California, Los Angeles, presiding

8:00
FR1 1 Ion acceleration using ultra-high intensity lasers.
KARL KRUSHELNICK, *University of Michigan*

For the past several years there has been significant experimental and theoretical developments into the generation of highly directional energetic proton and ion beams from the interaction of intense ultra-short laser pulses with thin solid targets. Recent results have shown that these beams can be produced with mono-energetic features and that they can also be generated from underdense interactions. With the recent construction of many Petawatt-class high intensity laser systems around the world – both high energy picosecond laser systems as well as Titanium:Sapphire high repetition rate lasers (including the HERCULES laser system at Michigan) – ion/proton beams having energies of several hundred MeV may soon be produced. New mechanisms for the generation of very energetic beams have also been proposed which use ultra-thin (less than 100 nm) targets. Such experiments consequently require very careful control of the properties of the laser pulses used. The proton beams produced from present experiments are already important as a diagnostic of electric/magnetic fields within laser-produced plasmas and using the new facilities under construction these beams may soon become relevant for fusion, medicine and homeland security applications.

SESSION GI2: MICRO AND LOW-TEMPERATURE PLASMAS
Tuesday Morning, 3 November 2009; Centennial I at 9:30; Martin Lampe, Naval Research Laboratory, presiding

9:30
GI2 1 Microplasma assembly for novel electromagnetic media.
OSAMU SAKAI, *Kyoto University*

Microplasmas whose sizes are smaller than a few millimeters can perform functionality for chemical micro-reactors, conversion fields for biomaterials, and interactive media for photons. In particular, as far as interaction with photons or electromagnetic waves is concerned, in addition to microplasma generation and photon emission in an intensified electric field of waves, microplasmas can also play a number of potential roles of controllers for propagating waves. This report focuses on novel physics of microplasma assembly for electromagnetic media [1]. When we make an assembly composed of microplasmas, novel functions are expected due to its complex dielectric function arising from dielectric and lossy properties. The dielectric property creates photonic band gaps (PBGs), and the lossy property drastically changes transmittance around the PBGs. As a result, a "complex" dispersion relation or band diagram in the three-dimensional space of real and imaginary wavenumbers and wave frequency will open new possibilities to control electromagnetic waves by complex-value filters composed of microplasma assembly. [1] O. Sakai et al., Plasma Physics and Controlled Fusion, vol. 49 (2007), pp. B453-B463.

10:00
GI2 2 Kinetic effects in low-pressure discharges with secondary electron emission.*
DMYTRO SYDORENKO, *University of Alberta, Edmonton, Alberta, Canada*

Secondary electron emission (SEE) from material surfaces can result in efficient plasma cooling and large energy losses from the plasma. This is relevant to Hall thrusters and divertors, where the electron temperature is high enough to provide strong SEE. The SEE reduces negative charge of a wall immersed into a plasma and increases the flux of plasma electrons to the wall. If the plasma is hot enough to produce intense SEE, the plasma potential relative to the wall can be several times lower than that without the SEE. Then the electron heat flux to the wall will be extremely high provided the plasma electron velocity distribution function (EVDF) is Maxwellian, with a large number of electrons flying toward the walls and capable to penetrate the sheath potential barrier. This is the case if the electron mean free path is small compared to the plasma dimensions. Further increase of the electron temperature saturates the wall losses once the space charge limited (SCL) regime of the sheath establishes. In low-pressure plasmas, however, amplification of the electron heat flux to the wall due to the SEE is much weaker because the electron mean free path is large compared to the plasma dimensions. In such plasmas, the EVDF is depleted of the energetic electrons flying toward the walls. This considerably reduces the flux of hot electrons to the walls. The secondary electrons propagate freely between the walls forming electron beams that do not mix with the plasma electrons. The presence of these secondary electron beams with intense current and relatively low energy prevents the occurrence of a steady SCL sheath. Instead, relaxation oscillations of the sheath between the SCL and non-SCL states may occur under conditions with intense anisotropic heating.

*In collaboration with I. Kaganovich, Y. Raitses, PPPL, and A. Smolyakov, University of Saskatchewan.

10:30
GI2 3 Kinetic Theory of Instability-Enhanced Collisional Effects.*
SCOTT D. BAALRUD, *Department of Engineering Physics, University of Wisconsin-Madison*

A generalization of the Lenard-Balescu collision operator is derived which accounts for the scattering of particles by instability amplified fluctuations that originate from the thermal motion of discrete particles (in contrast to evoking a fluctuation level externally, as is done in quasilinear kinetic theory) [1]. Emphasis is placed on plasmas with convective instabilities. It is shown that an instability-enhanced collective response results which can be the primary mechanism for scattering particles, being orders of magnitude more frequent than conventional Coulomb collisions, even though the fluctuations are in a linear growth phase. The resulting collision operator is shown to obey conservation laws (energy, momentum, and density), Galilean invariance, and the Boltzmann $\mathcal{H}$-theorem. It has the property that Maxwellian is the unique equilibrium distribution function; again in contrast to weak turbulence or quasilinear theories. Instability-enhanced collisional effects can dominate particle scattering and cause strong frictional forces. For example, this theory has been applied to two outstanding problems: Langmuir's paradox [2] and determining Bohm's criterion for plasmas with multiple ion species [3]. Langmuir's paradox is a measurement of anomalous electron scattering rapidly establishing a Maxwellian distribution in gas discharges with low temperature and pressure. This may be explained by instability-enhanced scattering in the plasma-boundary transition region (presheath) where convective ion-acoustic instabilities are excited. Bohm's criterion for multiple ion species is a single condition that the ion fluid speeds must obey at the sheath edge; but it is insufficient to determine the speed of individual species. It is shown that an instability-enhanced collisional friction, due to streaming instabilities in the presheath, determines this criterion.

[1] S.D. Baalrud, J.D. Callen, and C.C. Hegna, Phys. Plasmas **15**, 092111 (2008).
[2] S.D. Baalrud, J.D. Callen, and C.C. Hegna, Phys. Rev. Lett. **102**, 245005 (2009).
[3] S.D. Baalrud, C.C. Hegna, and J.D. Callen (submitted July 2009); preprint UW-CPTC 09-5 at www.cptc.wisc.edu.

*This material is based upon work supported under a NSF Graduate Research Fellowship and by U.S. DoE Grant No. DE-FG02-86ER53218. This work was done in collaboration with C.C. Hegna and J.D. Callen.

11:00
GI2 4 Cold microplasmas at one atmosphere: Simulation and characterization.*
JEFFREY HOPWOOD, *Tufts University*

Cold atmospheric pressure plasma offers many of the same technical advantages as conventional low pressure glow discharges, but without the need for a vacuum system. The cold atmospheric plasma is distinct from most high-pressure plasmas, such as arcs and sparks, because the low gas temperature allows for the treatment of temperature sensitive materials. This talk focuses on the generation of microwave-frequency microplasmas of air and inert gases. These plasmas exhibit gas temperatures of 300-600 K, but electron temperatures of 1-2x10^4 K. The electron density is greater than 10 ^{14} cm^{-3}. Microplasma is generated in a 200 micron-wide gap in a ring-shaped microstrip transmission line. When operated at electrical resonance, a microwave potential forms across the discharge gap and generates a microplasma. Microplasma generation becomes more efficient at higher frequencies. Inert gas microplasmas are characterized using excitation frequencies of 450 MHz, 900 MHz, and 1.8 GHz at both 1 atm and 0.5 mbar. The microplasma resistance decreases with increasing frequency. Simultaneously, the reactive sheath impedance and the microwave electrode voltage also decrease. At higher microwave frequency, the decreased electrode voltage reduces both the plasma potential and the ion kinetic energy losses, thus increasing the electron density. A three-dimensional fluid model confirms these experimental measurements.

*This research is supported by the National Science Foundation under Grant No. CBET-0755761 and the Agilent Foundation.

11:30
GI2 5 Tailored Positron Beams from Trapped Single-component Plasmas.*
T.R. WEBER, *University of California, San Diego*

There are a number of important uses of antiparticles (e.g., positrons and antiprotons) including the creation of antihydrogen, modeling astrophysical processes, and the characterization of materials and material surfaces. Much of this progress has been driven by the development of new plasma techniques to accumulate, manipulate and store antiparticles. This talk focuses on recent work[2,3] to create specially tailored positron beams with small transverse spatial extent ρ_b, narrow energy spreads ΔE, and high brightness by pulsed extraction from plasmas in a Penning-Malmberg trap. Experiments are presented using electron plasmas for increased data rate. By briefly lowering the exit-gate potential, beam pulses ($\Delta t < 10$ μsec) from near the plasma center are created with $\rho_b = 2\lambda_D$ (HW $1/e$) and $\Delta E \approx T$, where λ_D is the plasma Debye length, and T is the plasma temperature. Specifically, by tailoring the plasma temperature to $T \approx 25$ meV and density to $n_0 \approx 10^{10}$ cm^{-3}, beams are created with $\Delta E < 35$ meV and $\rho_b < 50$ μm. A nonlinear model for beam extraction is used to derive expressions for the beam amplitude N_b, transverse spatial profile $\sigma_b(r)$,

and single particle energy distribution as a function of the exit-gate potential V_E, trap wall radius R_W, and plasma parameters.[2] All predictions are verified for a wide range of plasmas. Protocols to optimize ρ_b and ΔE for various applications will be discussed. Prospects for cryogenic beams and pulsed extraction from the confining B field (to $B = 0$, for brightness enhancement and electrostatic focusing) will be discussed along with selected applications.

*This work is done in collaboration with J. R. Danielson and C. M. Surko and is supported by NSF grant PHY 07-13958.

[1]T. R. Weber, J. R. Danielson and C. M. Surko, Phys. Plasmas **15**, 012106 (2008).
[2]T. R. Weber, J. R. Danielson and C. M. Surko, Phys. Plasmas **16**, 057105 (2009).

12:00
GI2 6 Exploring Plasma Mechanisms of Carbon Nanostructures Synthesis in Arc Discharge.
MICHAEL KEIDAR, *George Washington University*

Plasma enhanced approached are widely used for synthesis of carbon nanostructures. Among several methods for synthesis carbon nanostructures (single wall carbon nanotubes (SWNT), multi-wall carbon nanotubes (MWNT), graphene) arc discharge is the most practical one for scientific and technological purposes due to the number of advantages in comparison with other techniques. Firstly, arc discharge method yields highly graphitized nanostructures with very small defects, because the synthesis occurs at a very high temperature. As results, arc-grown SWNTs demonstrate the highest time of emission capability degradation than those produced by other techniques. Secondly, nanotubes produced in arc usually demonstrate a high flexibility, thus eventually demonstrating higher strength characteristics. The primary focus of this presentation is to review state of the art understanding of SWNT synthesis mechanism in arc discharge, methods and approaches to control parameters of arc discharge. Fundamental issues related to synthesis of SWNTs, which is relationship between plasma parameters and SWNT characteristics will be considered. It is believed that characteristics of synthesized SWNTs can be controlled by means of plasma parameters and arc discharge conditions. Effects of electrical and magnetic fields applied during SWNT synthesis in arc plasma will be explored. For instance, our recent experiments suggest that magnetic field has very strong effect on the arc discharge and the carbon nanostructures synthesis. It is also demonstrated that the magnetic field has a profound effect on the length of a SWNT synthesized in the arc discharge. An average length of SWNT increases by a factor of 2 in discharge with magnetic field as compared with the discharge without magnetic field, and an amount of long nanotubes with the length above 5 micron also increases. Electric and magnetic fields allow effective SWNT transport to the collection area, in-situ SWNT filtration from the soot and SWNT separation by their characteristics (e.g. by chirality, length, structural properties).

SESSION GI3: ISLANDS, KINKS AND SAWTEETH
Tuesday Morning, 3 November 2009; Centennial II at 9:30; Jill Foley, Nova Photonics, Inc, presiding

9:30
GI3 1 A New View of Internal Kink Modes and Their Relation to the Sawtooth Instability.*
A.D. TURNBULL, *General Atomics*

Understanding the physics of sawteeth is crucial for avoiding large sawtooth crashes in tokamaks. Analyses of equilibria reconstructed through consecutive cycles of the ramp and crash phases of DIII-D sawtooth experiments have shed new light on the interplay of the underlying ideal MHD instabilities, the cross section, and the profiles, and a consistent picture is emerging. The discharges comprised two low beta oval and bean shaped discharges and a single null ICRF heated discharge, chosen since they have very different sawtooth characteristics. The crash in the bean is fast and violent but the oval is slow with negligible energy loss. The ICRF discharge exhibited giant sawteeth. The aim is to understand the different characteristics through analysis of both the crash and ramp phases since they are inextricably linked through the triggering mode — the onset from the linear threshold and the crash by the nonlinear consequences. The results are surprising in view of the conventional sawtooth picture. The underlying ideal mode can have characteristics more like the quasi-interchange mode and this leads to the qualitatively different crash features observed experimentally. Also, the ideal stability does not necessarily degrade during the ramp as q_0 decreases; the sawtooth is generally triggered by weakening of the kinetic stabilization. MHD relaxation events observed during the ramp are found to be associated with a non-monotonic q profile near unity and an underlying quasi-interchange mode, with apparent reconnection at the inner $q = 1$ surface. The crash onset itself is described qualitatively by a Porcelli-like model and the return to $q \sim 1$ by full reconnection. However, if the model is to be a quantitative predictor of the crash onset, it will require plausible but specific adjustments to some key terms and coefficients.

*Supported by US DOE under DE-FG03-95ER54309.

10:00
GI3 2 Theoretical and JET experimental evidence of a new sawtooth control mechanism by off-axis toroidally propagating ICRF waves.*
JONATHAN GRAVES, *Ecole Polytechnique Federale de Lausanne (EPFL), Centre de Recherches en Physique des Plasmas, Association EURATOM-Confederation Suisse, 1015 Lausanne*

A new explanation has been given [J. P. Graves, et al, Phys. Rev. Lett. 102, 065005 (2009)] for the highly effective nature of sawtooth control using off-axis toroidally propagating ion cyclotron resonance waves in tokamaks. Energetic passing ions influence the internal kink mode when the distribution of ions is asymmetric in the parallel velocity, a natural feature of co or counter propagating ICRH waves. Dedicated JET experiments have been devised in order to eliminate an alternative explanation of modified sawteeth involving magnetic shear modification. Low concentration He-3 minority was employed because the large drag current of the background plasma yields very poor current drive efficiency. Nevertheless, these ITER relevant ICRH scenarios in JET demonstrate that sawteeth can be controlled effectively. Modelling of these experiments quantifies the role played by the fast ions. Importantly, the extreme sensitivity of the fast ion mechanism to RF deposition location is consistent with the variation of the observed sawtooth period over a change in the magnetic field strength of only a few percent. The success of these JET experiments in controlling sawteeth, and validating the theory, greatly improves the prospect of using the planned ICRH system in ITER to shorten or lengthen sawteeth.

*Collaborators include I. Chapman, S. Coda, T. Johnson, M. Lennholm and JET-EFDA contributors. This work was partly supported by the Swiss National Science Foundation and by the European Communities under a contract of association.

10:30
GI3 3 Islands in the Stream: The Effect of Plasma Flow on Tearing Stability.*
R.J. LA HAYE, *General Atomics*

Reducing plasma flow clearly decreases the stability of tearing modes in multiple regimes (sawtooth, hybrid) in both high- and low-aspect-ratio tokamaks (DIII-D, JET, NSTX, each with distinct means of lessening rotation). Further, reducing flow makes preexisting "saturated" islands larger at the same beta. Thus lower plasma flow impairs high-beta operation owing both to the destabilization and to the impact of tearing-mode islands. The physics is that *flow shear* (not flow) at the tearing rational surface is classically stabilizing, making the tearing stability index Δ' more negative (more stable). In this picture, with profiles and all else the same, the critical beta at which neoclassical tearing modes (NTMs) destabilize is proportional to $-\Delta'$ and hence lower flow and flow shear lead to destabilization at lower beta. Similarly, if destabilized, the saturated NTM island width is proportional to $-\beta/\Delta'$ and thus increases as flow and flow shear are reduced. A working model for a significant level of stabilizing shear in the plasma toroidal angular flow $-d\Omega_\phi/dr$ at a given rational surface is of order of the inverse of the product of the local values of the parallel magnetic shear length L_s and the Alfvèn time τ_A. Experimental data are fitted for the effect of this normalization of flow shear in a simple empirical model for both onset and saturation of tearing modes. Most theoretical literature is on the consequence of flow shear on classical tearing stability at zero beta; tokamaks at high beta have large magnetic Prandtl number (an issue for the sign of the flow effect) and very large Lundquist number. It is in this regime that theory will be compared to experimentally based empirical models. The consequence for future tokamaks with low rotation may be lower tearing stability than now expected.

*Supported by US DOE under DE-FC02-04ER54698.

11:00
GI3 4 Electron thermal transport within magnetic islands in the RFP.*
HILLARY STEPHENS, *University of Wisconsin - Madison*

Magnetic islands formed by tearing reconnection have a significant impact on the thermal characteristics of magnetically confined plasmas such as the reversed-field pinch (RFP). New Thomson scattering diagnostic capability on the MST RFP has enabled measurement of the thermal transport characteristics of islands. Electron temperature (Te) profiles can now be acquired at 25 kHz, sufficient to measure the effect of an island on the profile as it rapidly rotates by the measurement point. In standard plasmas with a spectrum of tearing modes, islands tend to flatten the Te profile across resonant surfaces, as observed in tokamaks. This flattening is characteristic of parallel heat conduction inside the island and is not the result of a stochastic field as it was previously thought. In striking contrast, a temperature gradient within an island is observed in improved confinement plasmas, brought about by a reduction in tearing instability. This suggests local heating and relatively good confinement within the island; local power balance calculations are underway to quantify the island thermal transport. Measurement of transport in 3D magnetic structures is key to understanding the self-organized helical equilibrium in the RFP in which one large island reorganizes the central magnetic field topology. The high rep-rate Thomson scattering diagnostic has also been used to resolve electron thermal transport during the periodic growth and

decay of the tearing modes in MST. The measured electron heat conductivity is less than that predicted for transport in a fully stochastic magnetic field (Rechester-Rosenbluth). This suggests that remnant island structures are present, consistent with the direct observations described above. The stochastic field was modeled with 3D nonlinear resistive MHD simulations (DEBS code) with Lundquist numbers matching those in MST during standard discharges.

*This work supported by US DOE.

11:30
GI3 5 The Role of Kinetic Effects, Including Plasma Rotation and Energetic Particles, in Resistive Wall Mode Stability.*
JOHN W. BERKERY,† *Columbia University*

Continuous, disruption-free operation of tokamaks requires stabilization of the resistive wall mode (RWM). Theoretically, the RWM is thought to be stabilized by energy dissipation mechanisms that depend on plasma rotation and other parameters, with kinetic effects being emphasized.[1] Experiments in NSTX show that the RWM can be destabilized in high rotation plasmas while low rotation plasmas can be stable, which calls into question the concept of a simple critical plasma rotation threshold for stability. The present work tests theoretical stabilization mechanisms against experimental discharges with various plasma rotation profiles created by applying non-resonant n=3 braking, and with various fast particle fractions. Kinetic modification of ideal stability is calculated with the MISK code, using experimental equilibrium reconstructions. Analysis of NSTX discharges with unstable RWMs predicts near-marginal mode growth rates. Trapped ions provide the dominant kinetic resonances, while fast particles contribute an important stabilizing effect. Increasing or decreasing rotation in the calculation drives the prediction farther from the marginal point, showing that unlike simpler critical rotation theories, kinetic theory allows a more complex relationship between plasma rotation and RWM stability. Results from JT-60U show that energetic particle modes can trigger RWMs[2]. Kinetic theory may explain how fast particle loss can trigger RWMs through the loss of an important stabilization mechanism. These results are applied to ITER advanced scenario equilibria to determine the impact on RWM stability.

*Supported by U.S. DOE Contracts DE-FG02-99ER54524 and DE-AC02-09CH11466.
†With S.A. Sabbagh, H. Reimerdes, R. Betti, and B. Hu.

[1]B. Hu et al., *Phys. Plasmas* **12** (2005) 057301.
[2]G. Matsunaga et al., IAEA FEC 2008 Paper EX/5-2.

12:00
GI3 6 Kinetic Analysis of Resistive Wall Modes in ITER Advanced Tokamak Scenario.*
L.J. ZHENG, *University of Texas at Austin, Institute for Fusion Studies*

A fully kinetic analysis of the stability of resistive wall modes in tokamaks is important. However, it is also challenging: first, because the conventional gyrokinetic equation cannot recover MHD; and, second, because the coupling to Alfvén continuum damping requires high-resolution computation of a mode near its singular surfaces, which is difficult to achieve with usual non-adaptive codes. Our current effort is aimed at resolving these two difficulties. First, we will describe our new derivation of an extended gyrokinetic theory that can fully recover MHD. Second, we will describe our numerical work to implement this extended gyrokinetic theory in the non-perturbative and non-hybrid kinetic code AEGIS-K as an adaptation of our existing, well-benchmarked AEGIS code. Our numerical results show that n=1 resistive wall modes in the ITER advanced tokamak scenario can be fully stabilized by modestly low rotation with a rotation frequency (normalized to the Alfvén frequency at the magnetic axis) of about 0.75%. Wave-particle resonances, shear Alfvén continuum damping, trapped particle effects, and the parallel electric field effects are all taken into account. The rotation frequency for full stabilization is much larger than the diamagnetic drift frequency; therefore, finite Larmor radius effects are negligible. We also find that the window for rotation stabilization window opens first near the ideal wall limit.

*Work in collaboration with M. T. Kotschenreuther and J. W. Van Dam and supported by USDOE grant DE-FG02-04ER54742.

SESSION GO4: C MOD TOKAMAK
Tuesday Morning, 3 November 2009
Regency VI at 9:30
Steve Allen, LLNL/General Atomics, presiding

9:30

GO4 1 Overview of Recent Research on the Alcator C-Mod Tokamak AMANDA HUBBARD, *MIT Plasma Science and Fusion Center* AND THE ALCATOR C-MOD TEAM,* Recent experiments on Alcator C-Mod exploit high power density RF heating and current drive and metal walls, focusing on key issues for ITER. These include hydrogenic retention in metal walls, and impurity generation by RF sheaths. New edge diagnostics and coated tiles have been added to study sheath effects, as well as divertor and SOL heat flux widths. SOL turbulence has been compared to gyrofluid simulations. Improved lower hybrid and ion cyclotron models, both ray tracing and full wave, are benchmarked against experiments. Assessment of LHCD at high densities, and rotation generated by both mode converted ICRF and LHCD, are of particular interest. Transport studies include assessment of rotation in internal transport barriers, particle transport and peaking in low collisionality discharges, and comparison of core turbulence with GYRO. The "improved L-Mode" regime, featuring a T_e pedestal without a particle barrier, has been extended to longer durations and reached $H_{ITER-98-Y2} \sim 1.0$. Disruption and gas jet mitigation experiments show runaways, seeded by LHCD, are suppressed by stochastic transport.

*Supported by the USDOE Office of Fusion Energy Sciences.

9:42

GO4 2 Studies of enhanced energy confinement discharges with L-mode-like edge particle transport in Alcator C-Mod* E. MARMAR, B. LIPSCHULTZ, A. DOMINGUEZ, M. GREENWALD, N. HOWARD, A. HUBBARD, J. HUGHES, B. LABOMBARD, R. McDERMOTT, M. REINKE, D. WHYTE, *MIT* C. KESSEL, *PPPL* A regime of enhanced energy confinement on Alcator C-Mod exhibits an H-mode-like temperature pedestal, but with edge particle transport and density profiles like those in L-mode. Access to this "improved L-mode" is achieved by operating just below the H-mode power threshold, with ion drift in the unfavorable direction, away from the x-point. Increases of power, up to a factor of three above that required for entry to H-mode with favorable drift, yield global confinement comparable to H-mode (H_ITER-98~ 1.0), but with no density or impurity accumulation, and no need for ELMs to regulate the edge. Edge fluctuations seen with magnetics typically cover the range from 80 kHz to 150 kHz, somewhat broader than the quasi-coherent mode responsible for edge particle transport in EDA H-mode. The resulting high temperature, low density edge pedestal has low collisionality, and modeling indicates this could be an attractive target for Lower Hybrid Current Drive in advanced scenarios.

*Work supported by DoE awards DE-FC02-99ER54512 and DE-AC02-76CH03073.

9:54

GO4 3 Analysis of Rotation and Transport Data in C-Mod ITB Plasmas* C.L. FIORE, J.E. RICE, M.L. REINKE, Y. PODPALY, *MIT-PSFC* I.O. BESPAMYATNOV, W.L. ROWAN, *FRC-UT Austin* Internal transport barriers (ITBs) spontaneously form near the half radius of Alcator C-Mod plasmas when the EDA H-mode is sustained for several energy confinement times in either off-axis ICRF heated discharges or in purely ohmic heated plasmas. These plasmas exhibit strongly peaked density and pressure profiles, static or peaking temperature profiles, peaking impurity density profiles, and thermal transport coefficients that approach neoclassical values in the core. It has long been observed that the intrinsic central plasma rotation that is strongly co-current following the H-mode transition slows and often reverses as the density peaks as the ITB forms. Recent spatial measurements demonstrate that the rotation profile develops a well in the core region that decreases continuously as central density rises while the value outside of the core remains strongly co-current. This results in the formation of a steep potential gradient/strong electric field at the location of the foot of the ITB density profile. The resulting E X B shearing rate is also quite significant at the foot. These analyses and the implications for plasma transport and stability will be presented.

*Work supported by US-DoE DE-FC02-99ER54512 and DE-FG03-96ER54373.

10:06

GO4 4 Studies of Filament Formation during Lithium Pellet Injection in Alcator C-Mod* B. BOSE, E. MARMAR, *PSFC* D.R. MIKKELSEN, *PPPL* Using a high speed CCD camera, (frame rate up to 500 kHz) and a stereoscopic imaging system, the detailed three dimensional evolution of filaments formed in the ablation clouds of injected lithium pellets has been studied on the Alcator C-Mod tokamak. After formation, the filaments move primarily in the poloidal direction during the first $10\mu s$ after their formation. During the '07 and '08 campaigns the stereo-imaging system was employed to make a survey of the characteristics of filament trajectories in a variety of background plasmas and was then used to determine the filaments' statistical properties. The distributions of poloidal velocities of the filaments show no statistical variation with local density, temperature or magnetic shear, but do show significant variation with the local safety factor and plasma collisionality. The filament velocity distributions and the spatial scales of the filament trajectories are compared with simulated turbulent ExB flows from the nonlinear gyrokinetic solver GYRO. Simulations using plasma profiles just prior to the injection do not generate large enough fluctuations in ExB drift to be consistent with experimental data from the imaging diagnostic. Additional simulations using estimates of the strongly perturbed temperature and density profiles will also be discussed.

*Supported by USDoE award DE-FC02-99ER54512.

10:18

GO4 5 Measurement of the adiabatic index through the temperature scaling of reversed shear Alfvén eigenmodes E.M. EDLUND, M. PORKOLAB, Y. LIN, N. TSUJII, S.J. WUKITCH, *MIT PSFC* L. LIN, *UCLA* G.J. KRAMER, *PPPL* Reversed shear Alfvén eigenmodes (RSAEs) have been excited in Alcator C-Mod during the current ramp phase at ITER relevant densities of $rmn_{e0} \leq 1.5 \times 10^{20} rmm^{-3}$ with (2-5) MW of ICRH power absorbed by H minority heating [1]. We have studied the scaling of the minimum frequency of the RSAEs by varying the temperature of the electrons and majority ions and compare the results to

theoretical scalings from the code scNOVA [2] and an analytic dispersion relation [3]. Taking the adiabatic index (γ) as a free parameter, a best fit to the data indicates $\gamma = 1.40 \pm 0.15$, excluding the ideal gas limit of $\gamma = 5/3$. A limiting value of $\gamma = 3/2$ is predicted from consideration of the energy and pressure of shear Alfven waves [4]. Kinetic electron response is considered as a possible correction to the theoretical treatment. Work supported by DOE under DE-FG02-94-ER54235 and DE-FC02-99-ER54512. [1] M. Porkolab *et al.*, IEEE Trans. Plasma Sci. **34**, 229 (2006). [2] C.Z. Cheng and M.S. Chance, J. Comput. Phys. **71**, 124 (1987). [3] B.N. Breizman *et al.*, Phys. Plasmas **12**, 112506 (2005). [4] C.F. McKee and E.G. Zweibel, Astro. J. **440**, 686 (1995).

10:30

GO4 6 ICRF Mode Conversion Flow Drive on Alcator C-Mod* Y. LIN, J.E. RICE, S.J. WUKITCH, M.J. GREENWALD, A.E. HUBBARD, A. INCE-CUSHMAN, L. LIN, E.S. MARMAR, M. PORKOLAB, M.L. REINKE, N. TSUJII, J.C. WRIGHT, *MIT, PSFC* Plasma flow driven by externally launched waves could be important for tokamaks. We have observed both toroidal (V_ϕ) and poloidal (V_θ) flows driven via an ICRF mode conversion (MC) process in D(^{3}He) plasmas on Alcator C-Mod [1, 2]. Strong V_ϕ in the co-current direction is observed by x-ray spectroscopy in L-mode plasmas heated with 50 MHz RF power at $B_{t0} \sim 5.1$ T and $n_{3He}/n_e \sim 8\%$. The central V_ϕ scales with the applied RF power and is at least a factor of 2 more than the intrinsic plasma rotation. The MC ion cyclotron wave (MC ICW) is detected by a phase contrast imaging system. The MC physics have been studied by 2-D full wave TORIC simulation. We hypothesize that an MC scenario where MC slow waves are strongly damped on ions may be necessary for MC flow drive. Momentum transport modeling has been applied to infer the total flow drive force. Results from flow drive optimization experiments will be reported. The feasibility of creating such an MC scenario, thus potentially driving plasma flow, in larger tokamaks like JET and ITER will also be discussed. [1] Y. Lin et al, Phys. Rev. Lett. 101, 235002 (2008). [2] Y. Lin et al, Phys. Phys. 16, 056102 (2009).

*Work supported by US DoE award DE-FC02-99ER54512.

10:42

GO4 7 Evaluation of ICRF heated discharges with boron coated molybdenum tiles* S.J. WUKITCH, *MIT PSFC* B. LABOMBARD, Y. LIN, B. LIPSCHULTZ, E. MARMAR, R. OCHOUKOV, M.L. REINKE, D.G. WHYTE, AND ALCATOR C-MOD TEAM, One of the primary utilization challenges is to minimize impurity production associated with ICRF operation. In present experiments, boronization is frequently applied to control impurities and its lifetime has been observed to be proportional to number of RF Joules injected. We have also observed that RF sheaths localized to field lines connected to the active antenna were responsible for the boron erosion and subsequent impurity generation. In an effort to identify important erosion and impurity source locations, we have vacuum plasma sprayed ~ 100 μm of boron on molybdenum tiles from the outer divertor shelf, main plasma limiters, and the RF antennas. We have also modified the shape of the main plasma limiter and increased our spectroscopic monitoring diagnostics of the main plasma limiter. We have installed a set of probes to monitor the plasma potential and RF fields on field lines connected an antenna. Results from experiments investigating plasma performance and ICRF generated impurities will be presented.

*Work supported by USDoE award DE-FC02-99ER54512.

10:54

GO4 8 Observations of Lower Hybrid Wave Interactions in the Scrape-Off-Layer of a Diverted Tokamak* G.M. WALLACE, R.R. PARKER, P.T. BONOLI, O. MENEGHINI, A.E. SCHMIDT, S. SHIRAIWA, D.G. WHYTE, J.C. WRIGHT, S.J. WUKITCH, *MIT Plasma Science and Fusion Center* R.W. HARVEY, A.P. SMIRNOV, *CompX* J.R. WILSON, *Princeton Plasma Physics Laboratory* AND THE ALCATOR C-MOD TEAM, Experiments with LHCD on Alcator C-Mod indicate that, at high density, significant power is deposited directly in the SOL, thereby reducing the effective current drive efficiency. This phenomenon is observed in plasmas which are accessible to LH waves and below the density limit attributed to parametric decay as $\omega \rightarrow 2\omega_{LH}$. Current densities of ~ 500 kA/m^2 are measured just outside the separatrix during high power LH operation above $\bar{n}_e \sim 1 \times 10^{20}$ m^{-3}. Line integrated hard X-ray emission also drops sharply above $\bar{n}_e \sim 1 \times 10^{20}$ m^{-3}. Ray tracing/Fokker-Planck simulations over-estimate the line integrated X-ray emissivity by a factor of ~ 500 at $\bar{n}_e = 1.4 \times 10^{20}$ m^{-3} as compared to a factor of 3-4 at $\bar{n}_e = 0.6 \times 10^{20}$ m^{-3}. Simulations including a realistic SOL with collisional damping show substantial improvement in agreement with experiment.

*Work supported by USDOE awards DE-FC02-99ER54512 and DE-AC02-76CH03073.

11:06

GO4 9 Closing the Poloidal Flow Loop in the High-Field Side Scrape-off Layer of Alcator C-Mod* NOAH SMICK, BRIAN LABOMBARD, *MIT PSFC* Observations of near-sonic parallel flows towards the high-field side (HFS) divertor have suggested a ballooning-like transport drive on the low-field side. However, the mechanisms that close the implied particle flow loop have not been identified experimentally. To investigate this phenomenon, a magnetically-actuated scanning probe was operated on the HFS midplane during C-Mod's '07-'09 campaigns. This probe is capable of measuring the total flow vector in the SOL, including radial fluctuation-induced fluxes. ExB drift measurements confirm that the net poloidal flow is indeed directed towards the HFS divertor. Two mechanisms for closing the particle loop have been identified as important contributors. Measurements of the fluctuation-induced particle fluxes on the HFS show an inward pinch velocity of ~ 10 m/s at or just inside the separatrix, sufficient to balance the midplane poloidal particle flux. Neutral penetration from inner divertor recycling has been quantified using a 1-D kinetic code, indicating that it can also account for a significant fraction of the total poloidal flux.

*Supported by USDoE award **DE- FC02-99ER54512.

11:18

GO4 10 Poloidal and Radial Characteristics of Edge Turbulence at the High-field-side Midplane of Alcator C-Mod* J.L. TERRY, I. CZIEGLER, B. LABOMBARD, *MIT-PSFC* S.J. ZWEBEN, *PPPL* Previous measurements have shown that edge turbulence on the high-field, "good" curvature side is much reduced (x 0.1-0.3) compared to that on the low-field, 'bad' curvature side. This has been shown by both Gas-Puff-Imaging (GPI) and scanning probe measurements. A recent upgrade to the high-field-side GPI view on C-Mod allows 2D (radial and poloidal) resolution of emission from the midplane region there. The 2D array of view spans a radial region ~ 2.3 cm around the separatrix and a poloidal region from Z=-0.5 to 1.7 cm with ~ 0.38 cm resolution. This

allows investigation of the 2D characteristics of edge phenomena like blobs/filaments, the Quasi-Coherent Mode, ELMs, and broadband turbulence. Of particular interest are the existence and structure of both filaments and the QCM on the inboard midplane, and the dynamics and structure of both the ELM perturbation and the broadband turbulence there. Results of these investigations will be presented and compared to observations made on the low-field-side.

*Supported by USDoE awards DE-FC02-99ER54512 and DE-AC02-09CH11466.

11:30

GO4 11 Relationship of SOL turbulence to SOL width in Alcator C-Mod* STEWART ZWEBEN, *PPPL* JAMES TERRY, BRIAN LABOMBARD, *MIT* DAREN STOTLER, D.P. LUNDBERG, *PPPL* R.H. COHEN, M. UMANSKY, *LLNL* D.A. BAVER, D.A. D'IPPOLITO, J.R. MYRA, D.A. RUSSELL, *Lodestar* Measurements of SOL turbulence in Alcator C-Mod show a strong variation with poloidal angle [1], therefore it is likely this variation will affect the SOL width. The poloidal variation of the SOL turbulence will be measured as a function of the SOL collisionality, plasma shape, and normalized gyroradius, and the results will be compared with theoretical models for these variations. The radial transport due to the SOL turbulence will be estimated from the radial propagation and correlation length at each poloidal angle, and the results will be compared with the local temperature/density SOL widths measured by Langmuir probes and D_α emission. The expected relationship between these local SOL widths and the total heat flux SOL width at the divertor plate will be discussed. [1] J.L. Terry, S.J. Zweben et al, J. Nucl. Mat. 390-391, 339 (2009)

*This work was supported by Work supported by US DOE Contracts #DE-AC02-09CH11466 and DE-FC02-99ER54512.

11:42

GO4 12 Initial results from the swept frequency O-mode correlation reflectometer system in Alcator C-Mod* A. DOMINGUEZ, E. MARMAR, *MIT PSFC* G.J. KRAMER, E. VALEO, *PPPL* AND ALCATOR C-MOD TEAM, Turbulent eddies are believed to be largely responsible for increased cross-field particle and energy transport in confined plasma devices. One of the tools that has been used to characterize this turbulence is correlation reflectometry whereby the spatial extent of the eddies in the direction of propagation of the reflectometry waves can be determined. A swept frequency O-mode reflectometer has been installed on the Alcator C-Mod tokamak. The system has a midplane view of the plasma from the low field side and covers the frequency range of 110GHz-140GHz, corresponding to electron density cutoffs of 1.50-2.43 $x10^{20}m^{-3}$. In conjunction with two fixed frequency O-mode reflectometry channels at 110GHz and 140GHz, it is possible to determine radial correlation lengths, which can be mapped to the turbulent radial correlation lengths with the use of a 2-D synthetic diagnostic code[1]. Initial results from the analysis of results from various plasma conditions using this system will be presented. [1] E.J. Valeo, G.J. Kramer, R. Nazikian, Plasma Phys. Control. Fus. 44 (2002) L1

*Supported by USDoE award DE-FC02-99ER54512.

11:54

GO4 13 Intrinsic Toroidal Rotation Reversal Comparison between TCV and CMOD B.P. DUVAL, A. BORTOLON, *CRPP-EPFL, CH-1015 Lausanne, Association Euratom-Confédération, Switzerland* J. RICE, M. REINKE, *PSFC-MIT, Boston, USA* R. McDERMOTT, *IPP-Garching, Germany* Toroidal reversal was observed on the TCV tokamak using a CXRS system with a diagnostic beam that did not perturb the plasma motion. Support experiments were performed on CMOD where the core rotation is measured with an X-ray imaging spectrometer and edge CHEERS so the measured rotation may again be considered "intrinsic." Rotation reversal was observed on both machines when q~ 3 across a density ramp. The plasma shape used on CMOD was repeated on TCV and the toroidal rotation for this marginally diverted discharge shows behavior similar to limited discharges on TCV. This paper will report the diagnostic measurements including preliminary PCI turbulence data that does not indicate a strong role of turbulence for rotation reversal as suggested by several theoretical approaches. In both machines there is evidence that the change in torque can not be entirely attributed to changes in the plasma edge necessitating a model that applied torque directly to the plasma bulk.

SESSION GO5: Z-PINCHES, X-PINCHES, AND DENSE PLASMA FOCUS
Tuesday Morning, 3 November 2009
Hanover CDE at 9:30
Mike Cuneo, Sandia National Laboratories, presiding

9:30

GO5 1 Structure of Imploding Plasma in Coiled Wire Arrays GARETH HALL, *Imperial College* SERGEY LEBEDEV, SIMON BLAND, JEREMY CHITTENDEN, JAMES PALMER, FRANCISCO SUZUKI-VIDAL, ADAM HARVEY-THOMPSON, GEORGE SWADLING, GUY BURDIAK, LOUISA PICKWORTH, NICOLAS NIASSE, Coiled arrays, a cylindrical array in which each wire is formed into a single helix, suppress the modulation of ablation at the fundamental wavelength. Instead, ablation flow is modulated at the wavelength of the coil. Large wavelength coils produce wire beaks with sufficient axial separation that perturbations in the implosion sheath do not merge, producing an organised mode of implosion in which the global instability can be controlled and the perturbations correlated between all the wires in the array. The inductance of the current paths that may be established by an organised implosion are considered. This suggests that, for a given inductive voltage drop across the load, coiled arrays are capable of achieving significantly higher current convergence to the axis than straight arrays. These experiments were carried out on the MAGPIE generator at Imperial College. This research was sponsored by Sandia National Laboratories Albuquerque, the SSAA program of NNSA under DOE Cooperative Agreement DE-FC03-02NA00057.

9:42

GO5 2 Measurement of Linear Magneto-Rayleigh-Taylor Instability Growth in Solid Liners* DANIEL SINARS, STEVE SLUTZ, MARK HERRMANN, KYLE PETERSON, ROGER VESEY, *Sandia National Laboratories* BRENT BLUE, *General Atomics* The magneto-Rayleigh-Taylor (MRT) instability is ubiquitous to pinch plasmas compressed by magnetic pressure, and is an important factor in determining whether a cylindrical liner can reach the axis in a relatively intact form. While there are many RT characterization experiments, there are few well-characterized MRT experiments and none for fast ($\sim$ 100 ns) z-pinch implosions in which the magnetic pressure quickly dominates over material strength. We present data from an initial series of MRT growth experiments on the 20 MA Z-machine that used solid Al liners with outer radii of 3.16 mm and aspect ratios (radius/thickness) of 10. The MRT instability was seeded with sinusoidal perturbations of 200 and 400 μm and peak-to-valley amplitudes of 5 and 10 μm, respectively. Radiographs showing the evolution of the MRT instability are compared with codes being used to design magnetized liner inertial fusion loads [see S.A. Slutz, "Magnetized liner inertial fusion," this conference.]

*Sandia is a multiprogram laboratory operated by Sandia Corporation, a Lockheed Martin Company, for the U.S. DOE's NNSA under contract DE-AC04-94AL85000.

9:54

GO5 3 Three dimensional simulations of DT fuel compression by an imploding Z-pinch liner J.P. CHITTENDEN, *Imperial College* B. APPELBE, S.A. SLUTZ, *Sandia National Laboratory* R.A. VESEY, K. PETERSON, D.B. SINARS, M.E. CUNEO, M.C. HERRMANN, Z-pinch implosions provide a method of directly compressing fusion fuel to high densities and temperatures, with excellent energy coupling efficiency. The presence of large magnetic fields also provides a method of suppressing thermal conduction losses and increasing alpha particle confinement, significantly reducing the rho-R criterion required for ignition. We present three dimensional resistive magneto-hydrodynamic simulation results of one such scheme (S.A. Slutz et. al., this conference), in which a preheated, magnetised fuel is compressed by an imploding metal liner Z-pinch. Large scale parallel computing methods allowed the full liner volume to be modelled at relatively fine scale resolution. The results are used to examine how important the three dimensional structure of the magneto-Rayleigh-Taylor instability is in determining the neutron yield. Sensitivities of the fusion performance to fuel pre-heat, magnetic field configuration and current pulse shaping are also examined. This work was supported by Sandia National Laboratories.

10:06

GO5 4 Nonlinear Rayleigh-Taylor instabilities in fast z-pinches* AARON MILES, *Lawrence Livermore National Laboratory* Simplified analytic models are used to describe the implosion of a cylindrical plasma by an azimuthal magnetic field of sufficient magnitude to drive a strong shock wave into the plasma. These models are employed together with buoyancy-drag-based models of nonlinear single-mode and turbulent multimode Rayleigh-Taylor (RT) growth to investigate the mixing process in such fast z-pinches. Together, the implosion and instability models give predictions that characterize limitations that instabilities can impose on the implosion in terms of maximum convergence ratios (CR) attainable for an axially coherent pinch. Results from high-resolution numerical simulations are used to validate both implosion and instability models.

*This work performed under the auspices of the U.S. Department of Energy by Lawrence Livermore National Laboratory under Contract DE-AC52-07NA27344.

10:18

GO5 5 Modifying implosion dynamics of a wire array by using an inverse wire array z-pinch as a current switch* SERGEY LEBEDEV, A. HARVEY-THOMSON, G.N. HALL, S.N. BLAND, G. BURDIAK, F.A. SUZUKI-VIDAL, G. SWADLING, E. KHOORY, J.P. CHITTENDEN, L. PICKWORTH, *Imperial College* We will describe experiments on the MAGPIE facility (1.5MA, 250ns) in which an inverse wire array (with the wires acting as a return current cage placed around a central current conductor) operated as a fast current switch. This allowed to significantly reduce the rise-time of the current pulse ($<$ 100ns) delivered to a separate, standard imploding wire array z-pinch load. It was found that this arrangement generates a short current pre-pulse ($\sim$ 5kA, $<$ 15ns) through the imploding array, followed by a $\sim$ 140ns interval with zero current, before the main fast rising current pulse is switched into the array. This led to a significant change in the implosion dynamics, suppressing the ablation phase, introducing a 0-D-like implosion and reducing the level of trailing mass.

*This research was sponsored by the NNSA under DOE Cooperative Agreement DE-FC03-02NA00057.

10:30

GO5 6 Influence of ion temperature gradient effects on magnetic-curvature-driven flute instability* V.I. SOTNIKOV, J.M. KINDEL, O.G. ONISHCHENKO, E. YASIN, *University of Nevada at Reno, NV 89557, USA* J.N. LEBOEUF, *JNL Scientific, Casa Grande, AZ 85294, USA* B.V. OLIVER, T.A. MEHLHORN, *Sandia National Laboratories, Albuquerque, NM 87123, USA* C. DEENEY, *Department of Energy, Washington, DC 20585, USA* In order to study flute mode instability in the presence of ion temperature gradient effects, a nonlinear system of equations in two fluid approximation applicable for spatial scales comparable with the ion Larmor radius was derived. Linear analysis of this system shows that the range of unstable wavelengths in a plasma with large ion charge numbers extends into the region of spatial scales of the order of the ion Larmor radius. Nonlinear stage of the instability was analyzed with the modified version of the numerical code FLUTE. Mixing length estimates of nonlinear saturation levels are in good agreement with simulation results.

*Work supported by the US Department of Energy under Grant No. DE-FC52-06NA27616 at UNR, ISTC through the grant N3520 and Grant No. DE-AC04-94AL85000 at Sandia National Laboratories.

10:42

GO5 7 Polarity Contact and Risetime Effects on Wire Array Z-Pinches* DAVID CHALENSKI, BRUCE KUSSE, *Cornell University Lab of Plasma Studies* The Cornell COBRA pulser is a 1MA, negative polarity machine. COBRA can operate with 100 to 200 ns current risetimes. Wires are typically strung with a "press" contact to the electrode hardware, where the wire is loosely pulled against the hardware and held there to establish electrical contact. The machine is normally negative, but a bolt-on convolute can be used to modify the current path and change the electric field at the wires, thereby producing positive polarity with respect to ground at the load. Data presented are the culmination of experiments studying the combined effects of contact, polarity and risetime on wire array z-pinches. Data were collected on 16-wire Aluminum z-pinch arrays in both negative and positive polarity, with solder and non-solder contacts, and with slow and fast risetimes (100ns and 200ns). Five shots were collected for each case. The initiation, ablation, implosion and stagnation phases were compared for the various cases.

*This research was supported by the NNSA SSAA program under DOE Cooperative Agreement DE-FC03-02NA00057.

10:54

GO5 8 Precursor focusing by conical electrodes inside wire array Z-pinches* J.B. GREENLY, D.A. CHALENSKI, P.F. KNAPP, T.A. SHELKOVENKO, S.A. PIKUZ, *Cornell University* The addition of conical extensions of the anode and cathode electrodes into the interior of wire array Z-pinches is being studied. So far, 30 and 45 degree simple solid cones have been added to both electrodes, for instance, 16 mm base diameter, 8 mm tall cones, centered on axis, projecting from both electrodes into a 20 mm diameter (16 x 12 micron dia. Aluminum) wire array (thus leaving a 4 mm gap between the points of the cones on axis).The inward flow of ablation streams from the wires is strongly modified by the cones, especially on the anode side: the effects are not symmetrical at anode and cathode. At the anode, the streams are redirected to form a well-defined layer of flow along the cone and come to a focus $\sim$ 1.5 mm off the tip of the cone, forming a hot, high-density spot $\sim$ 1.5 mm diameter which persists in a nearly steady state for 10's of ns during the ablation phase. Images and x-ray spectra will be presented to quantify the characteristics of this focal spot and other phenomena of the ablation flows with cones.

*This work was sponsored by NNSA under DOE Cooperative Agreement DE-FC-03-02NA00057

11:06

GO5 9 High energy density plasma experiments using radial foils P.-A. GOURDAIN, I.C. BLESENER, J.B. GREENLY, D.A. HAMMER, P.F. KNAPP, B.R. KUSSE, P.C. SCHRAFEL, *Cornell University* A novel technique involving radial foil explosions can produce high energy density plasmas (HEDP). A current flows radially inward in a 5-micron thick aluminum foil from a circular anode, which contacts the foil on its outer rim, to the cathode, which connects to the foil at its geometrical center. JxB forces lift the foil upward, forming a plasma shell, with electron density above $5x10^{19}$ cm^{-3}, around a central plasma column, carrying most of the current. When using very small "pin" cathodes ($\sim$ 1 mm in diameter) on a medium size pulsed-current generator such as the COrnell Beam Research Accelerator (COBRA), central magnetic fields approach 2 Mgauss and local JxB force densities are on the order of a mega-newton per cubic millimeter. Combining well-established diagnostics, such as laser backlighting, interferometry and fast camera imaging, with new measurements techniques, such as micro B-dot probes, we will present the magneto-hydrodynamics properties of such plasmas. Particular attention will be given to flow and magnetic field measurements.

11:18

GO5 10 Recent Developments and Future Research at the Nevada Terawatt Facility* JOSEPH KINDEL, *Nevada Terawatt Facility, University of Nevada, Reno, NV 89557 USA* High Energy Density Physics is the focus of research at the Nevada Terawatt Facility (NTF). The NTF consists of a 1 MA, 2 TW Z-pinch, achieving 400 shots a year, and a 50 TW, 400ps, one micron glass laser. Experiments are undertaken in three ways: Z-pinch only, Z-pinch coupled with laser and laser only. Our facility generates Terawatt x-ray bursts, Megagauss magnetic fields, and investigates magnetized laser plasmas, including astrophysical like plasmas. Plasma diagnostics include a multiframe laser probing, optical and x-ray imaging, particle diagnostics, and x-ray spectroscopy. Wire array pinch experiments show significant structure due to the magnetic Rayleigh-Taylor instability. The magnetic Rayleigh-Taylor instabilities are modeled with nonlinear hydrodynamic modeling. This fluid modeling is capable of describing a wide range of instabilities in high beta plasmas on scales of an ion Larmor radius.

**Work supported by the US Department of Energy under Grant No. DE-FC52-06NA27616 at UNR.

11:30

GO5 11 Multi-Planar Wire Array Precursor Formation on the 1MA Zebra Generator* KENNETH WILLIAMSON, VICTOR KANTSYREV, ANDRE ESAULOV, ALLA SAFRONOVA, ISHOR SHRESTHA, GLENN OSBORNE, MICHAEL WELLER, VERONICA SHLYAPTSEVA, *University of Nevada, Reno* PLASMA PHYSICS AND DIAGNOSTICS LABORATORY TEAM, The double-planar wire array (DPWA) is the most promising z-pinch load studied on the 1MA Zebra generator for application to radiation physics and ICF studies. Initial investigation of this load revealed unique implosion dynamics: each plane implodes independently into two off-axis columns before coalescing into the final pinch.[1] New results are presented exploring the formation of these off-axis plasma columns with laser shadowgraphy and time-gated x-ray imaging, each fielded parallel to wire planes 6mm apart. Simulated radial current distribution and ablation effects[2] along with simple 3-D calculations were used to establish the processes that created the observed structures. These dynamics are then compared with triple-planar wire array (TPWA) loads.

*Work was supported by DOE/NNSA cooperative agreements DE-FC52-06NA27586, DE-FC52-06NA27588, and in part by DE-FC52-06NA27616.

[1]V. L. Kantsyrev, et. al., PoP, **15**, 030704 (2008)
[2]A. A. Esaulov, et. al., HEDP, **5** (2009), in press

11:42

GO5 12 Z-pinch stability in the presence of an axial flow* R. PRESURA, D. MARTINEZ, S. STEIN, C. PLECHATY, S. NEFF, *Nevada Terawatt Facility, University of Nevada, Reno, NV 89506* In axially symmetric wire array z-pinches, axial flow can be produced by tilting the wires radially. Adding a wire on the axis of the resulting conical wire array introduces a radial profile in the axial velocity of the flow. For certain conditions, such a shear flow has been predicted theoretically to have a mitigating effect on z-pinch instabilities, but experimental support for this stabilization

mechanism is scarce. At the Nevada Terawatt Facility, experiments with conical wire arrays driven by the 1 MA Zebra z-pinch showed improved stability both in the precursor and the stagnation phases of the z-pinch. To focus on the kink (m=1) instability, the study included central wires with helical perturbations. Strong experimental evidence supports the formation of shear flow in the presence of a central wire. The stabilizing effect of the shear flow was assessed by comparing the evolution of the pre-imposed perturbation in equivalent conical and cylindrical arrays.

*This work was supported by the DOE/NNSA grant DE-FC52-06NA27616.

11:54

GO5 13 Impact of load geometry on plasma formation and radiative properties of Z-pinches at stagnation* V.L. KANTSYREV, A.S. SAFRONOVA, A.A. ESAULOV, *UNR* A.L. VELIKOVICH, *NRL* L.I. RUDAKOV, *Icarus Inc.* A.S. CHUVATIN, *Ecole Politechnique* K.M. WILLIAMSON, M.F. YILMAZ, G.C. OSBORNE, M.E. WELLER, I. SHRESTHA, V.V. SHLYAPTSEVA, *UNR* The double planar wire array (DPWA) is the best x-ray radiator at 1 MA [V. Kantsyrev *et al.*, HEDP 5 (2009), in press]. To improve its radiative performance by reducing the MRT instability growth rate, Al, brass and W DPWAs were skewed to produce initial axial magnetic field Bz. The diagnostics included x-ray devices and laser shadowgraphy. Experiments on 1.6 MA Zebra generator at UNR and MHD modeling have shown that Bz mitigated the MRT instability in the precursor. The stagnation starts in the middle of the A-K gap, and more uniform plasma column with a higher temperature Te is formed compared to a standard DPWA. The yield and power were comparable with standard DPWA. Highest yield and power were for W and brass, respectively. Feasibility of the x-ray pulse shaping was demonstrated in experiments. Research plans are discussed.

*Work supported by NNSA/DOE Cooperative Agreements DE-FC52-06NA27586, DE-FC52-06NA27588, and in part by DE-FC52-06NA27616.

12:06

GO5 14 A Low Voltage, High Current Dense Plasma Focus using an Impedance Transformer* BRIAN BURES, MAHADEVAN KRISHNAN, KRISTI WILSON-ELLIOT, ROBERT MADDEN, FLORIAN BLOBNER, *Alameda Applied Sciences Corp* The dense plasma focus is a high voltage, high current device. In principle, high voltage is unnecessary as the dense plasma focus (DPF) is a low impedance load. The impedance of the driver usually dominates the impedance of the circuit. An alternative approach is to use a step down transformer to increase the current and reduce the voltage at the load. Additional benefits of this approach are: reducing driver inductance to less than 5nH from a $>$ 30nH driver; reducing stored energy to achieve a large current; minimizing consumable switches; and reducing anode heating. A module capable of producing 33 kA with a quarter period of 350 ns was demonstrated using a 3:1 current step-up transformer. The source stored only 40 J and produced $\sim$ 1E4 n/pulse using deuterium gas, while using a single Thyratron switch. The new module is a 6:1 current step up transformer which is projected to produce 60-66kA with 50J stored. Key performance metrics for the DPF including peak current, energy stored, and neutron yield will be described.

*Work supported by the Domestic Nuclear Dection Office

12:18

GO5 15 Deuterium Gas-Puff Experiments on the S-300 Z-pinch* DANIEL KLIR, JOZEF KRAVARIK, PAVEL KUBES, KAREL REZAC, *FEE CTU in Prague* S 300 TEAM, The neutron production from a deuterium gas-puff Z-pinch has been studied on the S-300 Z-pinch (Kurchatov Institute, Moscow). Neutron time-of-flight diagnostics was used to give an insight into the acceleration of fast deuterons. The emphasis was put on the finding of (i) the energy distribution of deuterons which produced fusion neutrons, (ii) the anisotropy of neutron emission, and (iii) the time and duration of neutron production with respect to the general Z-pinch dynamics. The peak neutron yield above 10^{10} was achieved on the current level of 2 MA. The fusion neutrons were generated for 30 ns during the stagnation and at the beginning of the expansion of a plasma column. The side-on neutron energy spectra peaked at 2.42$\pm$ 0.04 MeV with about 400 keV FWHM. In the downstream direction (i.e. the direction of the current flow from the anode towards the cathode), the peak neutron energy was 2.6 $\pm$ 0.1 MeV. The average kinetic energy of reacting deuterons was about 100 keV. The broad width of radial neutron spectra implied a high radial component of deuteron velocity. On the basis of these experimental data, it is possible to discuss acceleration of deuterons and fusion neutron production.

*Work supported by MSMT and GACR projects No. LA08024, ME09087, LC528, 202-08-H057, 202-08-P084, and IAEA grant 14817.

SESSION GO6: LASER ACCELERATION AND TRANSPORT; RADIATION AND FELS

Tuesday Morning, 3 November 2009
Hanover FG at 9:30
Carl Schroeder, Lawrence Berkeley National Laboratory, presiding

9:30

GO6 1 Laser Proton acceleration from mass limited silicon foils K. ZEIL, S. KRAFT, T. RICHTER, J. METZKES, M. BUSSMANN, U. SCHRAMM, R. SAUERBREY, T.E. COWAN, *Forschungszentrum Dresden-Rossendorf* J. FUCHS, S. BUFFECHOUX, *LULI* We present recent studies on laser proton acceleration experiments using mass limited silicon targets. Small micro machined silicon foils with 2 μm thickness and 20x20 μm2 to 100x100μm2 size mounted on very tiny stalks were shot with the 100 TW LULI Laser (long pulse 150 fs) and with the new 150 TW DRACO Laser facility (short pulse 30 fs) of the Research Centre Dresden-Rossendorf. The experiments were carried out using high contrast levels. Proton spectra have been measured with magnetic spectrometers and radio chromic film stacks.

9:42

GO6 2 First Laser-Accelerated Ion Observations From the Omega EP Laser at 1000 J in 10 ps* K.A. FLIPPO, M.J. SCHMITT, J.C. COBBLE, D.C. GAUTIER, D. OFFERMANN, *LANL* T. BARTAL, S. CHAWLA, F.N. BEG, *UCSD* P.M. NILSON, *LLE, Univ. of Rochester* A. MacPHEE, S. LE PAPE, D. HEY, A. MacKINNON, *LLNL* The efficient generation of ion beams using short intense laser pulses has many applications including active interrogation, providing a temporally-precise perturbation source for ICF capsule implosions, and providing a hot spot for ion fast ignition schemes. All applications benefit by im-

provements in the laser-to-ion conversion efficiency. For example, ion fast ignition fusion which promises order-of-magnitude reduction in laser driver energies, requires a conversion efficiency of order 10% to avoid the short-pulse lasers from becoming impractically large and expensive. Presently, ion acceleration at the shortest pulse lengths ($\tau_{pulse} < 1$ ps) has been limited. For integrated fast ignition experiments short-pulse laser energies in excess of 10's of kJ will be required necessitating longer pulse lengths on the order of $\tau_{pulse} \geqslant 10$ ps. There is a lack of experimental data in this pulse length regime. For the first time the OMEGA EP laser has been focused onto small foils with 1000 J in 10 ps to produce proton beams up to nearly 50 MeV with high efficiencies. Results of ion energy and conversion efficiency as a function of target size, target thickness, and intensity will be presented.

*This work supported by US DOE/NNSA, performed at LANL, operated by LANS LLC under Contract DE-AC52-06NA25396.

9:54

GO6 3 65+ MeV Protons from Short-Pulse-Laser Micro-Cone-Target Interactions* S.A. GAILLARD, *FZD/UNR* K.A. FLIPPO, D.C. GAUTIER, D.T. OFFERMANN, J.B. WORKMAN, F. ARCHULETA, R. GONZALES, T. HURRY, R.P. JOHNSON, S. LETZRING, D.S. MONTGOMERY, S.-M. REID, T. SHIMADA, *LANL* T. LOCKARD, Y. SENTOKU, *UNR* M.E. LOWENSTERN, J.E. MUCINO, *AOSS, U of M, Ann Arbor* B.B. GALL, *U of Mo, Columbia* E. D'HUMIERES, *U. Bordeaux 1* M. GEISSEL, M. SCHOLLMEIER, *SNL* M. BUSSMAN, T.E. COWAN, T. KLUGE, J.M. RASSUCHINE, *FZD* Two sets of laser-ion acceleration experiments at the LANL 200 TW Trident laser at $\sim 10^{20}$ W/cm^2 (1 μm, 80 J, $\sim$ 600 fs) with high ($> 10^{10}$) and low ($> 10^8$) contrast are compared for regular size flat foils ($\sim$ 2x2 mm), reduced mass targets (RMT, 200-500 μm diameter) and new micro-cone targets in various geometries to elucidate the production of hot electrons and ions in these targets. Results from the latest experiment at high contrast show proton energies in excess of 65 MeV for flat-top cones, compared to $\sim$ 55 MeV for RMTs and $\sim$ 45 MeV for flat foils. Data from a Cu Kα 2D imaging crystal, an electron spectrometer and an RCF stack are presented and compared, showing the importance of not just generating hot electrons, but efficiently propagating these hot electrons to the accelerating "tip," where they can then be converted to ion energy, as well as the importance of the micro-cones' supporting foil size.

*The TRIDENT laser and the experiment were funded by the LANL LDRD program

10:06

GO6 4 Experimental study of channel formation by 30 ps intense laser pulses in near-critical, mm-scale plasmas GIANLUCA SARRI, *Queen's University Belfast* PETER NORREYS, *STFC Rutherford Appleton Laboratory and Blackett Laboratory, Imperial College, UK* KATE LANCASTER, *STFC Rutherford Appleton Laboratory, UK* MARCO BORGHESI, *School of Mathematics and Physics, Queens University Belfast, UK* T. TANIMOTO, *Osaka University, Japan* E. CLARK, *Technological Educational Institute of Crete, Greece* S. HASSAN, *Blackett Laboratory, Imperial College London, UK* N. KAGEIWA, *Osaka University, Japan* Z. NAJMUDIN, *Blackett Laboratory, Imperial College London, UK* R. SCOTT, *STFC Rutherford Appleton Laboratory and Blackett Laboratory, Imperial College, UK* A. REHMAN, *Blackett Laboratory, Imperial College London, UK* K. TANAKA, *Osaka University, Japan* RAOUL TRINES, *STFC Rutherford Appleton Laboratory, Didcot, UK* We will present results, obtained at the VULCAN laser (RAL, UK), of an experiment investigating channel creation in deuterium gasjets at different plasma densities (from 10^{18}cm^{-3} up to 10^{20}cm^{-3}) using laser pulses with parameters of Fast Ignitor relevance (T$\approx$ 30ps, I$\approx 10^{18}$ W/cm^2) and a range of diagnostics including optical and proton probing. For densities up to few times 10^{18}cm^{-3}, smooth and several mm long, strongly evacuated channels with sharp walls are created. For higher densities, the interaction appears to be more chaotic, with possible indication of unstable explosion of the channel walls. Soliton-like features are also observed in the channel vicinities.

10:18

GO6 5 Tight focusing of ultra-intense laser pulses by innovative plasma optics toward extreme intensity M. NAKATSUTSUMI, *LULI, France* A. KON, *Osaka U. JPN* J. FUCHS, S. BUFFECHOUX, P. AUDEBERT, *LULI* R. KODAMA, *Osaka U.* With rapid advances in laser technology, laser beams are now available that can be routinely focused to intensities approaching $> 10^{21}$ Wcm^{-2}. Enhancement of laser intensity is achieved by truncating the pulse width, increasing the laser-energy, or reducing the focal spot size. Although the reduction of the spot size is the simplest among those, by using low f-number optics, this method is not frequently employed because of the difficulty in avoiding damage from target debris or complexity of alignment procedure. We developed for the first time very compact (< 1 cm^3) extremely low f-number (0.4) plasma-based, confocal ellipsoid focusing systems. Direct measurement of the laser focal spot using low-energy laser indicates 1/5 reduction of spot size compared to standard focusing (using a f/3 optics). Around tenfold enhancement of laser intensity by reduction of the spot size for high power shots is clearly evidenced by remarkable enhancement of proton energy. The experiment was performed at LULI 100TW laser facility.

10:30

GO6 6 Charged particle dynamics and nano-target evolution in relativistic tightly focused electromagnetic fields KONSTANTIN POPOV, *University of Alberta, Canada* VALERY BYCHENKOV, *Lebedev Physics Institute, Russia* WOJCIECH ROZMUS, RICHARD SYDORA, *University of Alberta, Canada* The electromagnetic field structure of a tightly focused laser pulse is calculated using Stratton-Chu integrals over the surface of a focusing mirror. The details of acceleration mechanisms and characteristic scalings of maximum attainable particle energy vs. maximum laser power and focusing optics were studied. The applicability of paraxial Gaussian beams is discussed. The 3D particle-in-cell (PIC) simulations of interaction between a tightly focused laser and nano-targets such as clusters and ultra-thin foils were performed with electromagnetic code SCPIC. In addition to the dynamical properties found in the test particle simulations, a new mechanism of Coulomb field assisted attosecond electron bunch formation has been identified. This basic mechanism includes the interplay between the laser and electrostatic fields of the partially evacuated target. Each bunch contains mono-energetic electrons. The length, density and average energy of the bunch are given in terms of simple analytical expressions. Electron acceleration and bunch formation have been also studied under more realistic conditions of the targets having a pre-plasma.

10:42

GO6 7 THz Generation by Two Superposed Short Laser Pulses* ANIL KUMAR MALIK, HITENDER KUMAR MALIK, *Indian Institute of Technology Delhi 110016* THz radiation generation is a subject of current interest due to its potential applications in various fields. The use of collective properties of laser-

produced plasma underlies a number of methods of THz generation, particularly based on the phenomenon of nonlinear ponderomotive force induced excitation of plasma wake oscillations. A theoretical and simulation study has been done for THz generation based on tunnel - ionization of gas jet when two superposed short pulse lasers (circularly polarized and linearly polarized with same frequency while different amplitudes and phases) are focused on to it. In the proposed scheme a transverse transient current is caused by the presence of residual momentum after passing of the laser pulse. The effect of radial variation of electron density in the plasma channel on the frequency of plasma cylinder oscillation and hence on frequency of emitted THz radiations is examined. With optimum initial phase of the laser envelope and width of the channel, the mechanism seems to be much more efficient than some of other nonlinear phenomenon base mechanisms.

*UGC, Govt. of India

10:54

GO6 8 Relativistic Spherical Wake Wave in Plasma. Relativistic focusing spherical mirror and Schwinger pair production STEPAN BULANOV, ANATOLY MAKSIMCHUK, *CUOS, University of Michigan* ALEXEI ZHIDKOV, *Central Research Institute of Electric Power Industry, Japan* We report on the analytic and computer simulation study of a relativistic spherical wake wave. Such a wave in the breaking regime, traveling towards the center is able to reflect and focus the incoming radiation and up-shifting its frequency. The reflected and focused electromagnetic pulse can have such high intensity, that it is able to create e^+e^- pairs via Schwinger process.

11:06

GO6 9 Light scattering by a dense ionization plasma wave with a tunable velocity ALEXEI ZHIDKOV, TAKASHI FUJII, *CRIEPI, Japan* TIMUR ESIRKEPOV, JAMES KOGA, *JAEA, Japan* KOSHICHI NEMOTO, *CRIEPI, Japan* SERGEI BULANOV, *JAEA, Japan* An optically-dense ionization wave (*IW*) produced by two femtosecond laser pulses focused cylindrically and crossing each other is shown to be an efficient coherent x-ray converter. The resulting velocity of a quasi-plane *IW* in the vicinity of pulse intersection increases with the angle between the pulses from the group velocity of ionizing pulses to infinity allowing an easy tuning the wavelength of x-rays. We study the conversion of a coherent light to x-rays by means of particle-in-cell simulation and by solution of continuous equation with the correct current. The x-ray spectra of a converted, lower frequency coherent light change from the monochromatic to a high order harmonic-like with the duration of ionizing pulses and the intensity of scattered pulses; the spectrum are not symmetrical at $V < c$ and $V > c$.

11:18

GO6 10 Coherent radiation from the interaction of high-power femtosecond laser with a thin film target and the generation of attosecond pulses SANG-YOUNG CHUNG, *Pusan National University* KITAE LEE, *Korea Atomic Energy Research Institute* DONG EON KIM, *POSTECH* SEOK WON HWANG, HAE JUNE LEE, *Pusan National University* The simulation studies about the generation of attosecond X-ray pulses have been reported from the relativistic nonlinear Thomson scattering (RNTS) of a single electron [Phys. Plasmas 12, 043107 (2005)]. However, even if one electron generates an ultrashort pulse, the radiation is summation from many electrons in a real experiment. The coherency among the RNTS radiation from each electron needs to be considered to confirm the generation of ultrashort pulse radiations. In this presentation, the coherent RNTS radiation from a thin film target is proposed and verified using a particle-in-cell simulation. The radiation from RNTS is squeezed in a narrow angular region and the specific angle is varied by the laser intensity. The coherence is controlled from the angular property of the radiation and attosecond pulses are generated.

11:30

GO6 11 Underwater Laser Plasma Acoustic Source Directivity and Frequency Control Demonstration* T.G. JONES, M. HORNSTEIN, A. TING, *Naval Research Laboratory, Plasma Phys Div* M. NICHOLAS, *NRL, Acoustics Div* A remote underwater laser acoustic source is under development at NRL. Sound is generated by intense laser pulses propagating through air and water, followed by underwater optical compression and laser-induced breakdown (LIB). Such an acoustic source would be useful for communications, navigation, and sonar imaging. Recent experiments demonstrated control of the shape of the LIB plasma volume, and thereby control of the acoustic frequency spectrum and sound pressure level as a function of acoustic propagation direction. Femtosecond and nanosecond lasers were used for lens-focused acoustic generation near the water surface. The LIB volume shape was controlled by varying laser pulse length, energy, optical bandwidth, and focusing angle. Aspherical LIB volumes produced strongly anisotropic acoustic sources. Initial results of acoustic propagation studies in a 30,000 gallon bubbly salt water tank suggest both ultrasonic and bubble-induced attenuation. Recent results will be discussed.

*This work is supported by ONR.

11:42

GO6 12 Observation of Very High-order Electron-radiation Coupling in a 7^{th} Harmonic IFEL Experiment SERGEI TOCHITSKY, *Department of Electrical Engineering, UCLA* OLIVER WILLIAMS, PIETRO MUSUMECI, *Department of Physics, UCLA* CHIEH SUNG, DANIEL HABERBERGER, *Department of Electrical Engineering, UCLA* ALAN COOK, JAMES ROSENZWEIG, *Department of Physics, UCLA* CHAN JOSHI, *Department of Electrical Engineering, UCLA* FEL/IFELs based on the resonant interaction between laser and electron beams in an undulator would benefit from using efficient high-order resonances. The high-order harmonic FEL/IFEL interactions were considered theoretically as a technique for reduction of the beam energy without corresponding decrease in the undulator period and the magnetic field strength in a single-pass X-ray FEL. We demonstrate microbunching of the 12.3 MeV electrons in a 7 th order IFEL interaction, where the seed radiation frequency is seven times higher then the undulator's fundamental frequency. Strong longitudinal modulation of the beam is inferred from the observation of the first, second and third harmonics of the seed radiation in a Coherent Transition Radiation spectrum. The highest CTR frequency is the 21^{st} harmonic of the fundamental interaction. The level of seed power is comparable to that required for microbunching at the fundamental frequency in this undulator. This work was supported by DOE grant DE-FG03-92ER40727.

11:54
GO6 13 High Transformer ratio PWFA for Applications on XFELs WEI LU, WEIMING AN, CHENGKUN HUANG, CHAN JOSHI, WARREN B. MORI, *UCLA* MARK HOGAN, T.O. RAUBENHEIMER, A. SERYI, *SLAC* PATRIC MUGGLI, *USC* TOM KATSOULEAS, *Duke* UCLA COLLABORATION, SLAC COLLABORATION, USC COLLABORATION, DUKE COLLABORATION, Fourth generation of light sources (e.g.,LCLS and the XFEL) require high energy electron drivers (16-20GeV) of very high quality. We are exploring the possibility of using a high transformer ratio PWFA to meet these challenging requirements. This may have the potential to reduce the size of the electron drivers by a factor of 5 or more, therefore making these light source much smaller and more affordable. In our design, a high charge (5-10nC) low energy driver (1-3GeV) with an elongated current profile is used to drive a plasma wake in the blowout regime with a high transformer ratio (5 or more). A second ultrashort beam that has high quality and low charge beam (1nC) can be loaded into the wake at a proper phase and be accelerated to high energy (5-15GeV) in very short distances (10s of cms). The parameters can be optimized, such that high quality (0.1% energy spread and 1mm mrad normalized emittance) and high efficiency (60-80%) can be simultaneously achieved. The major obstacle for achieving the above goals is the electron hosing instabilities in the blowout regime. In this poster, we will use both theoretical analysis and PIC simulations to study this concept.

12:06
GO6 14 The Generation of Transient Transparent Aluminum with Intense Femtosecond XUV Light JUSTIN WARK, *University of Oxford* PEAK BRIGHTNESS COLLABORATION, Fourth generation light sources have spectral brightnesses ten orders of magnitude brighter than any synchrotron, and when their output is focussed down to small spots, they can create solid density, "crystalline" plasmas on femtosecond timescales, long before the atoms have had time to move. We report specifically on the first experiments performed using the FLASH XUV laser in Hamburg. This laser can produce 15 fsec pulses of XUV radiation containing tens of μJ per pulse. Using a multi-layer-coated off-axis parabola, we have focused 13.5nm radiation to spots of order a few microns in diameter, corresponding to peak intensities in excess of 10^{16}Wcm $^{-2}$ - a region of intensity that had, until recently, been the domain of optical high power lasers. We discuss here some of the interesting absorption physics that takes place at this new frontier, where the intensity is so great that we can eject L-shell electrons from every atom in an aluminum target placed in the focal region of the laser,[1] and how the observed saturable absorption may impact on the creation and diagnosis of warm dense matter. [1] Bob Nagler et al, Nature Physics, to be published

12:18
GO6 15 Electronic Structure of a Photo-Generated Solid-Density Aluminum Plasma SAM VINKO, *University of Oxford* PEAK BRIGHTNESS COLLABORATION, Using high intensity radiation from the FLASH free electron XUV laser, we have created highly excited exotic states of matter in solid-density aluminum samples on time scales short compared with ion motion. The XUV intensity is sufficiently high to eject an inner-shell electron from every atom in the focal region. As the photo-excited electrons in this plasma recombine, the associated fluorescence signal provides information on the shape of the electronic density of states in the valence band, as well as the electron temperature. We demonstrate that the combination of normal and photo-ionized Al ion-cores alter the density of states in a very similar manner to that which would be expected in a binary alloy. Detailed calculations of the electronic structure, based on density functional theory, are in good agreement with the observed emission spectra.

SESSION GP8: POSTER SESSION III
Tuesday Morning, 3 November 2009
Grand Hall East at 9:30

GP8 1 ITER, GENERAL TOKAMAK, SIMULATION AND MODELING

GP8 2 Revisiting the Design of a Fusion Development Facility* V.S. CHAN, R.D. STAMBAUGH, A.M. GAROFALO, J.P. SMITH, C.P.C. WONG, *General Atomics* A Fusion Development Facility (FDF) is proposed to make possible a DEMO of the ARIES-AT type as the next step after ITER. The mission of the FDF should be to carry forward advanced tokamak physics and enable development of fusion nuclear science and technology. We have added more realism to the initial FDF concept [1] including inner and outer gaps from the plasma to the first wall; an improved estimate of the inboard/outboard blanket/shield thickness to protect the magnets/insulators; control coil positions; and realistic divertor geometry. Optimizing the mix of heating and current drive power has high leverage on the operating power. We have also revisited the assumed impurity fraction and the density profile peakedness.[1] R.D. Stambaugh, *et al.*, Bull. Am. Phys. Soc. **53**, 259 (2008).

*Supported by GA IR&D funding.

GP8 3 Fusion Nuclear Science Facility Design Points* R.D. STAMBAUGH, V.S. CHAN, A.M. GAROFALO, J.P. SMITH, C.P.C. WONG, *General Atomics* A Fusion Nuclear Science Facility (FNSF) is needed to fill the gaps between ITER and current experiments and a fusion demonstration power plant (DEMO). Characteristics should be neutron flux at the outboard midplane of 1-2 MW/m^2, continuous operation for periods up to two weeks, a goal of a duty factor of 0.3 on a year and fluences of 3-6 MW-yr/m ^{2} in ten years of operation to enable development of blankets suitable for tritium, electricity, and hydrogen production. Systems code analysis that implements constant physics and technology assumptions over a wide range of aspect ratio has been updated for more detailed design considerations and neutronics calculations. Conventional copper-coil tokamaks with inboard breeding/shielding and an OH solenoid optimize at high aspect ratio with devices between DIII-D and JET in size. Removal of the inboard breeding/shielding and OH coil results in the distinct ST branch with devices about half the size and $A < 1.8$. All these devices are generally $Q < 5$ but possible avenues to higher Q will be discussed.

*Supported by GA IR&D funding.

GP8 4 Low Aspect Ratio Fusion Nuclear Science Facility Mission and Parameter Space* Y.-K.M. PENG, A. SONTAG, S. DIEM, J. CANIK, M. COLE, *ORNL* P.J. FOGARTY, *DevTech* M. KOTSCHENREUTHER, P. VALANJU, *UT-Austin* A Fusion Nuclear Science Facility (FNSF) is needed to bridge critical knowledge gaps between ITER and current R&D toward a fusion DEMO. The FNSF aims to subject, *for the first time*, components that tame the plasma-material interface and harness fusion power to the rigors of a full fusion nuclear environment, continuously for up to 10^6 s. This would test and reveal new physical properties and issues of interest, encourage R&D to innovate and improve, and iterate to arrive at the component design knowledge needed to begin power engineering and technology testing. Physical properties include, for example, tritium permeation through material layers of plasma facing components; tritium extraction from solid breeders; thresholds of measurement of tritium concentration in fusion chamber. These encompass wide ranges of time constants (10^3 – 10^6 s) and fusion neutron fluxes (0.01 – 1 MW/m^2). A set of aspect-ratio-dependent plasma physics and engineering assumptions are used to estimate the parameter space of the FNSF, covering the entire range of neutron flux. It is found that for plasmas with R = 1.2 m, B = 2.2 T, A = 1.5, and kappa = 3, the required plasma current ranges from 3.5 MA to 8.5 MA, q_{cyl} = 8.5 to 3.5, and Q = 0.05 to 2.5. The relationship with design parameters of higher aspect ratios will also be discussed.

*Oak Ridge National Laboratory is managed by UT-Battelle, LLC, for the U.S. Dept. of Energy under contract DE-AC05-00OR22725.

GP8 5 To Demonstrate an Integrated Solution for Plasma-Material Interfaces Compatible with an Optimized Core Plasma* ROBERT GOLDSTON, *PPPL* JEFFREY BROOKS, *Purdue* AMANDA HUBBARD, *MIT* ANTHONY LEONARD, *GA* BRUCE LIPSCHULTZ, *MIT* RAJESH MAINGI, *ORNL* MICHAEL ULRICKSON, *SNL* DENNIS WHYTE, *MIT* The plasma facing components in a Demo reactor will face much more extreme boundary plasma conditions and operating requirements than any present or planned experiment. These include 1) Power density a factor of four or more greater than in ITER, 2) Continuous operation resulting in annual energy and particle throughput 100-200 times larger than ITER, 3) Elevated surface operating temperature for efficient electricity production, 4) Tritium fuel cycle control for safety and breeding requirements, and 5) Steady state plasma confinement and control. Consistent with ReNeW Thrust 12, design options are being explored for a new moderate-scale facility to assess core-edge interaction issues and solutions. Key desired features include high power density, sufficient pulse length and duty cycle, elevated wall temperature, steady-state control of an optimized core plasma, and flexibility in changing boundary components as well as access for comprehensive measurements.

*This work supported in part by U.S. DOE Contract # DE-AC02-09CH11466.

GP8 6 Design studies of Vulcan, a compact steady-state tokamak for boundary studies using HTS magnets* L. BROMBERG, P.T. BONOLI, A.E. HUBBARD, J. SCHULZ, D. WHYTE, *MIT PSFC, Cambridge MA 02139* Recent advances in high temperature superconductors (HTS) have been dramatic. We present investigation of a near-term tokamak design using present day HTS materials, conventional structures and manufacturing. The device is intermediate-scale (~ 1 m major radius, 7 T on axis), operating in H and limited D, for studies involving long-term operation with surface averaged power density ~ 1 MW/m^2 and hot walls to study plasma-facing component issues and plasma sustainment under conditions relevant to fusion reactors. We will discuss operation time required under different plasma conditions to achieve steady state conditions. The design uses demountable joints at 40-50 K for easy access to the first wall and divertor, with capability for single-piece maintenance. Compact designs for He cooled first walls are described. Plasma heating and current drive options for this compact, high density plasma will be presented. Engineering/plasma tradeoffs will be described, including performance as a function of machine size and cost.

*Supported by the US DoE OFES under Grant Number DE-FC02-93ER54186.

GP8 7 Simulation experiment of interaction of plasma facing materials and transient heat loads in ITER divertor by use of magnetized coaxial plasma gun M. NAKATSUKA, K. ANDO, T. HIGASHI, Y. KIKUCHI, N. FUKUMOTO, M. NAGATA, *University of Hyogo* Interaction of plasma facing materials and transient head loads such as type I ELMs is one of the critical issues in ITER divertor. The heat load to the ITER divertor during type I ELMs is estimated to be 0.5-3 MJ/m^2 with a pulse length of 0.1-0.5 ms. We have developed a magnetized coaxial plasma gun (MCPG) for the simulation experiment of transient heat load during type I ELMs in ITER divertor. The MCPG has inner and outer electrodes made of stainless steel 304. In addition, the inner electrode is covered with molybdenum so as to suppress the release of impurities from the electrode during the discharge. The diameters of inner and outer electrodes are 0.06 m and 0.14 m, respectively. The power supply for the MCPG is a capacitor bank (7 kV, 1 mF, 25 kJ). The plasma velocity estimated by the time of flight measurement of the magnetic fields was about 50 km/s, corresponding to the ion energy of 15 eV (H) or 30 eV (D). The absorbed energy density of the plasma stream was measured a calorimeter made of graphite. It was found that the absorbed energy density was 0.9 MJ/m^2 with a pulse width of 0.5 ms at the distance of 100 mm from the inner electrode. In the conference, experimental results of plasma exposure on the plasma facing materials in ITER divertor will be shown.

GP8 8 Models and Simulations of C60-Fullerene Plasma Jets for Disruption Mitigation and Magneto-Inertial Fusion* IOAN-NICULAE BOGATU, SERGEI A. GALKIN, JIN-SOO KIM, *FAR-TECH, Inc.* We present the models and simulation results of C60-fullerene plasma jets proposed to be used for the disruption mitigation on ITER and for magneto-inertial fusion (MIF). The model describing the fast production of a large mass of C60 molecular gas in the pulsed power source by explosive sublimation of C60 micro-grains is detailed. Several aspects of the magnetic "piston" model and the 2D interchange (magnetic Rayleigh-Taylor) instability in the rail gun arc dynamics are described. A plasma jet adiabatic expansion model is used to investigate the in-flight three-body recombination during jet transport to the plasma boundary. Our LSP PIC code 3D simulations show that heavy C60 plasmoid penetrates deeply through a transverse magnetic barrier demonstrating self-polarization and magnetic field expulsion effects. The LSP code 3D simulation of two plasma jets head-on injection along a magnetic field lines for MIF are also discussed.

*Work supported by the US DOE DE-FG02-08ER85196 and DE-FG02-05ER84185 SBIR grants.

GP8 9 The Motional Stark Effect Diagnostic for ITER* FRED LEVINTON, ELIZABETH FOLEY, HOWARD YUH, *Nova Photonics* The United States has been tasked with the development and implementation of a Motional Stark Effect (MSE) system on ITER. In the harsh ITER environment, in order to transmit light to a detector, a shielded labyrinth is required to mitigate the effect of neutrons and radiation. This necessitates the use of several mirrors to relay the light to the vacuum interface outside the shielded region. However, the plasma facing mirror is susceptible to coating and erosion. This is problematic for any optical diagnostic and particularly polarimetry measurements such as MSE. Even thin coatings can change the phase and reflectivity of s and p polarized light when reflected from a mirror. This makes maintaining and tracking the MSE calibration very challenging. Our proposed approach to the MSE diagnostic is to implement a combination of conventional MSE polarimetry and a new approach to measure the magnitude of the magnetic field from the line shift of the Stark spectrum. The advantage of the latter approach is that the line shifts are independent of polarization. Results of this and conceptual designs of the proposed MSE system for ITER will be discussed.

*Work supported by DOE Grant No. DE-FG02-08ER85205.

GP8 10 Design of a Prototype for the In Situ Calibration Source for the ECE Diagnostic on ITER* P.E. PHILLIPS, M. E. AUSTIN, W.L. ROWAN, *Fusion Research Center, Univ. of Texas* J. BENO, A. OUROUA, *CEM-UTA* R.F. ELLIS, *Univ. of MD* A large area (200mm diameter) calibration source will be prototyped for ITER. The source will generate blackbody emission (emissivity $>$ 0.7) for frequencies greater than 120 GHz in the ITER vacuum environment. The device is a primary vacuum component (VQC 1B) and is subject to stringent vacuum requirements that will be tested in the case of this prototype. The source will operate at temperatures up to 800 °C though it will not be actively heated during plasma operation. A major challenge is to assure high reliability both in maintenance of calibration and mechanical integrity. SiC has been selected as the active emissive surface. Prior to construction of the prototype, candidate-heating methods will be critically examined for reliability, efficiency, and ITER compatibility. Results of test of a resistively heated source will be presented. A progress report on the development of the prototype will also be presented.

*Supported by US-IPO under PPPL-S0007684-R.

GP8 11 Performance of ITER H-mode discharges with various mixes of external heating computed using the MMM08 transport model in PTRANSP simulations A.H. KRITZ, G. BATEMAN, F.D. HALPERN,*A.Y. PANKIN, T. RAFIQ, *Lehigh U.* R.V. BUDNY, D.C. McCUNE, *PPPL* The new MMM08 Multi-Mode transport model [1] is used in PTRANSP simulations to predict the time evolution of temperature and toroidal angular frequency profiles in ITER H-mode discharges. External heating and current drive sources include NBI, ECRH and ICRH, computed using NUBEAM, TORAY and TORIC respectively. Five mixes of heating (with associated current and torque drives, and fueling) are considered in order to examine various possibilities and contingencies for ITER. The evolution of the magnetic q profile is computed using the NCLASS module for neoclassical resistivity and bootstrap current together with the KDSAW module for the effect of sawtooth crashes. The fusion power production and fusion Q, computed as a function of heating power mix and pedestal height, are compared with those obtained using the GLF23 model [2]. [1] F.D. Halpern *et al.,* Phys. Plasmas 15 (2008) 065033; J.Weiland *et al.,* Nucl. Fusion 49 (2009) 965933; A.Kritz et al., EPS (2009) [2] R.V. Budny, Nucl. Fusion 49 (2009) 085008

*Current address, Ecole Polytechnique, Palaiseau, France

GP8 12 Quasilinear Relaxation of Alpha Particle Profiles in Burning Plasmas* KATY GHANTOUS, N.N. GORELENKOV, M. ZARNSTORFF, *Princeton Plasma Physics Lab* Using local quasilinear theory and analytic methods, we reconstruct the relaxed fast ion profile in burning plasmas and get information on the losses. With a local alpha drive and background dampings of TAE modes, we compute the critical alpha particle beta profile beyond which the modes destabilize. Previous local theory is improved by including more sophisticated damping and drive mechanisms such as the effect of alpha particle finite orbit width. Solving the equation for this threshold condition in the unstable regions, and taking into account conservation laws, we integrate a relaxed profile for the alpha particles and deduce losses if any. The theory allows to predict ITER scenarios with good alpha confinement where it is hazardous to operate in regimes with more than 5% losses of energetic particles.

*This work supported, in part, by US DOE Contract No. DE-AC02-CH0911466.

GP8 13 Status of ITER ICH Matching System Design* D. SWAIN, R. GOULDING, D. RASMUSSEN, *ORNL* Work on the design of the ITER ICH matching system is progressing. The system will deliver a total power of 20 MW for long-pulse ($>$ 3000 s) operation. The present matching system design has: hybrid combiner-splitter circuits for ELM resilience, active matching during a shot using a double-stub tuner circuit, decouplers between the eight inputs to each antenna, water-cooled matching components, and air-cooled matched transmission lines using turbulent cooling. The matching/decoupling system is evolving. While the main components are fairly well determined, the configuration of the decoupler connections and tuning of the decouplers is still under discussion. More detailed specifications and predicted performance of the rf system under different plasma conditions will be presented.

*The submitted manuscript has been authored by a contractor of the U.S. Government under contract DE-AC05-00OR22725. Accordingly, the U.S. Govt retains a nonexclusive, royalty-free license to publish or reproduce the published form of this contribution.

GP8 14 ITER ECH Transmission System Test Stand and Prototype Development T.S. BIGELOW, J.B. CAUGHMAN, D.A. RASMUSSEN, T.E. WHITTLE, *Oak Ridge National Laboratory* M.A. SHAPIRO, J.R. SIRIGIRI, R.J. TEMKIN, *Massachusetts Institute of Technology* Progress in acquisition and testing of prototype components and developing a high power test stand will be described. The US ITER Project Office is responsible for providing the ECH transmission lines that are based on evacuated 63.5 mm diameter corrugated waveguide. Each line is designed to handle 170 GHz power at 1 MW and possibly up to 2 MW in the HE_{11} mode. A total of 24 lines are planned. The ITER Organization has completed a conceptual design of the system. A number of prototype components have been procured primarily from industrial suppliers and testing of vacuum performance and mechanical

alignment have been performed. A 140[r] miter bend was developed and tested at low power as an alternative to two adjacent 90 degree miter bends. A waveguide pumpout prototype and a compact waveguide switch have been built. Testing at high power is planned on a test stand being setup at ORNL. Work on installing a power supply and interim 400 kW 140 GHz gyrotron has progressed and procurement of a 170 GHz 0.5-1 MW gyrotron has begun. Low power testing is underway of a grating coupler to be used in a resonant ring for very high power testing of components at the 2 MW level or higher.

GP8 15 Loss Estimate for ITER ECH Transmission Line* M.A. SHAPIRO, E.J. KOWALSKI, J.R. SIRIGIRI, D.S. TAX, R.J. TEMKIN, *MIT PSFC* T.S. BIGELOW, D.A. RASMUSSEN, *US ITER Project, ORNL* The ITER ECH Transmission Lines (TL) are 63.5 mm diameter corrugated waveguides that will each carry 1 MW of power at 170 GHz. The current specifications require that the transmission efficiency of the HE_{11} mode from the gyrotron to the plasma should exceed 83%. The transmission losses on the ITER TL have been calculated for four possible cases corresponding to having HE_{11} mode purity at the input of the TL of 100%, 97%, 90% and 80%. The losses due to coupling, Ohmic and mode conversion loss are evaluated. Estimates of the calorimetric loss on the line show that the output power is reduced by about 5 $\pm$ 1 % due to Ohmic loss in each of the four cases. Estimates of the mode conversion loss show that the fraction of output power in the HE_{11} mode is about 3% smaller than the fraction of input power in the HE_{11} mode. High output mode purity therefore can only be achieved with significantly higher input mode purity. We also present a new conservation theorem relating the field distribution offset and propagation angle due to any two linearly polarized LP_{mn} modes propagating in the corrugated waveguide.

*Supported by US DOE and US ITER Project.

GP8 16 The Ignitor-Columbus Path in Fusion Research* MATTEO SALVETTI, BRUNO COPPI, *M.I.T.* The Ignitor and Columbus [1] machines are based on the use of normal conducting magnets to produce high magnetic fields and are designed to reach ignition by exploiting the favorable confinement characteristics of high plasma density regimes ($n_0 \cong 10^{21}$ m^{-3}) [2]. The Columbus experiment is proposed as a parallel US project to the Ignitor program carried out in Italy. The possible discovery of new phenomena and the understanding of known ones, i.e. sawtooth oscillations, under fusion burning conditions will drive the design of future fusion reactors. Columbus is designed to reach ignition conditions in D-T plasmas where the α-particles heating compensates for all energy losses and it takes advantage of the Ignitor R&D effort and the technology acquired during the construction of its full size component prototypes. Columbus is geometrically self similar to Ignitor, the dimensions being increased by 25/22 ($R_0 \cong$ 1.5 m) and the volume by about 50%. The toroidal magnetic field is decreased by the factor 12.6/13 and the average poloidal field produced by the plasma current is about equal to that of Ignitor for comparable values of the magnetic safety factor (q_a). The reference plasma current is $I_p \cong$ 12.2 MA, the value that ITER would produce for the same q_a but without reaching ignition. [1] B. Coppi and M. Salvetti, MIT-RLE report PTP (2003). [2] B. Coppi, MIT-RLE report PTP02/04 (2002), Presentation to the NRC.

*Sponsored in part by the US DOE.

GP8 17 Improved Confinement Regimes for the Ignitor Experiment[1] A. AIROLDI, G. CENACCHI, *CREATE* P. DETRAGIACHE, G. CLAI, *ENEA, Italy* B. COPPI, *MIT* The Ignitor experiment[2] is designed to achieve ignition in well confined deuterium-tritium plasmas, with Ohmic heating only or small amounts of additional RF heating. Thanks to its unique features ($B_T \leq$ 13 T, $I_p \leq$ 11 MA, $\langle n \rangle \leq 5 \times 10^{20}$m^{-3}), Ignitor is the only device capable of accessing plasma parameters that are relevant to a net power producing D-T reactor. In fact, plasma regimes suitable to operate a reactor have yet to be produced. The Poloidal Field System in Ignitor makes it possible to operate with different configurations, from the reference "extended limiter" configuration to the configuration with double X-points just inside or just outside the first wall. X-point configurations are interesting as they may lead to a high confinement regime (H- mode) when the heating power is larger than a threshold value. H-mode operation in Ignitor has been assessed both with 0D calculations as well as 1 1/2D transport simulations. Quasi-stationary conditions can be attained when a process producing re-distribution of pressure and current profiles is active. The accessibility to improved confinement regimes with or without edge pedestal that have been observed on existing experiments is assessed. [1]Sponsored in part by ENEA of Italy and by the U.S. D.O.E. [2]B.Coppi, A.Airoldi, F.Bombarda, et al.,*Nucl. Fusion* **41**, 1253 (2001)

GP8 18 Design of MgB_2 Superconducting coils for the Ignitor Experiment* G. GRASSO, R. PENCO, S. BERTA, *Columbus (Genova, Italy)* B. COPPI, *MIT* G. GIUNCHI, *(Milano, Italy)* A feasibility study for the adoption of MgB_2 superconducting cables for the largest (about 5 m in diameter) of the poloidal field coils of the Ignitor machine is being carried out. This initiative was prompted by the progress made in the fabrication of MgB_2 long cables, and related superconducting magnets of relatively large dimensions. These magnets will be cryocooled at the operating temperature of 10-15 K that is compatible with the He-gas cryogenic cooling system of Ignitor as well as with the projected superconducting current density of the MgB_2 material, at the magnetic field values ($\simeq 4 - 5$ T) in which these coils are designed to operate. The optimal cable configuration has been identified that can provide an efficient cooling of the MgB_2 conductors over times compatible with the machine duty cycles. MgB_2 superconductors hold the promise of becoming suitable for high field magnets by appropriate doping of the material and of replacing gradually the normal conducting coils adopted, by necessity, in high field experiments. Therefore, an appropriate R&D program on the development of improved MgB_2 material and related superconducting cabling options has been undertaken, involving different institutions.

GP8 19 Experiments with the Ignitor Pellet Injector (IPI)* A. FRATTOLILLO, S. MIGLIORI, S. PODDA, F. BOMBARDA, *ENEA, Italy* L.R. BAYLOR, J.B.O. CAUGHMAN, S.K. COMBS, C. FOUST, D. FEHLING, J.M. McJILL, S. MEITNER, *ORNL* G. ROVETA, *CRIOTEC Impianti, Italy* The four barrel, two-stage pneumatic injector for the Ignitor experiment (IPI), built by ENEA and ORNL, has been tested in the course of three esperimental campaigns. The optimal shaping of the propellant pressure pulse to improve pellet acceleration is provided by specially designed Pulse Shaping Valves. These have been modified and tested on a new facility that allows operating pellet injector components in conditions close to those at which they will have to operate on the IPI. Fast closing ($<$ 10 ms) valves drastically reduce the expan-

sion volumes needed to remove the propellant gas at the end of the guiding tube. The four barrel (2.1, 2.2, 3.0 and 4.6 mm bores) pipe-gun cryostat is cooled down by a closed cycle refrigerator, and pellet diagnostics for measuring speed and mass of the pellets, as well as for capturing in-flight pictures of all four pellets were developed for this application. The final impact target is equipped with a shock accelerometer. The injector is designed to deliver pellets with velocities up to 4 km/s (2 km/s already achieved): the results of the latest experimental campaign will be reported.

*Sponsored in part by ENEA of Italy and by the U.S. D.O.E.

GP8 20 Ignitor Structural Analysis for Double X-points Configurations and Machine Cooling System* A. BIANCHI, *ANSALDO Energia* P. FROSI, *ENEA, Italy* B. COPPI, *MIT* Recent activities carried out by ANSALDO for the Ignitor program include the structural analysis of the machine Load Assembly for two new scenarios that extend the operation of the machine to H-regimes, where the plasma equilibrium configuration is of the double X- point type and the out-of-plane forces increase. A complete structural analysis was carried out for three scenarios with $B_T = 13$ T and $I_p = 9$ and 10 MA and double X points just outside the plasma chamber, and $I_p = 9$ MA and double X points just inside the plasma chamber. The lowered values of the plasma current can offset the increase of stress due to the less favorable X-point configuration relative to the "extended limiter" configuration. With the cryogenic plant involving gaseous helium and studied by LINDE KRYOTECHNIK AG, the toroidal field coils reach temperatures up to 230 K and the central solenoid coils approach 220 K after a pulse at the most extreme machine parameters, while the vertical field coils remain under 100 K. Several hours are needed to re-cool the machine down to 30 K before each pulse. New calculations are underway to verify the plant cooling performance at reduced parameters but with more stringent cooling times between shots.

*Sponsored in part by ENEA of Italy and by the U.S. D.O.E.

GP8 21 ICRH Component Prototypes for the Ignitor Expe-riment* M. SASSI, S. MANTOVANI, P. FROSI, A. CARDINALI, *ENEA* A. BIANCHI, *ANSALDO Energia, Italy* The ICRH system for the Ignitor experiment is designed with a modular configuration to launch the power into the plasma through 4-strap antennas located in four of the 12 horizontal ports. Each module consists of 4 high power generators, operating in the frequency range 80-120 MHz, whose power is split over two ports (8 straps). A 30 Ω vacuum transmission line (VTL) transfers 0.4 MW of power per strap for a total power of 1.6 MW (at 115 MHz) per port in order to keep the maximum electric field below 5 kV/cm in the vacuum region of the straps and trasmission line. The RF configuration of the modules allows a full phase controls (toroidal and poloidal) of the straps though a PLL phase control. A detailed design of the ICRH antenna has been carried out, including the Faraday shield, the current straps, the vacuum transmission lines and the vacuum feed-through, and the antenna design has been integrated with the plasma chamber. An innovative plug-in system has been designed that should allow a simple installation of the antenna by remote handling. An improved port will be welded to the existing prototype of the D- shaped sector of the plasma chamber. A set of four strap will then be installed to test their coupling with the VTL coaxial cable. This facility will be used for the testing of welding procedures, vacuum tightness, plug-in system, and high voltage components.

*Sponsored in part by ENEA of Italy and by the U.S. D.O.E.

GP8 22 HBT-EP External Kink Mode Control Research Program: Recent Progress and Future Plans* G.A. NAVRATIL, B. DEBONO, J.P. LEVESQUE, M.E. MAUEL, D.A. MAURER, T.S. PEDERSEN, N. RATH, D. SHIRAKI, *Columbia University* HBT-EP TEAM, HBT-EP MHD mode control research is studying ITER relevant internal modular feedback control coil configurations and their impact on kink mode rigidity, advanced digital control algorithms, and the effects of plasma rotation on MHD mode stability. HBT-EP is installing a new segmented adjustable conducting wall with internal modular feedback control coils of varying toroidal angular coverage similar to that of the ITER 'VAC02' internal coil design to test RWM interaction and multi-mode response to such highly localized control fields. In parallel with this hardware development, we have also extended our 3-D VALEN feedback modeling code to include the effects of multi-mode plasma response. This enhanced VALEN physics capability will allow detailed comparison and benchmarking of its new plasma model with our new wall, control and sensor coil geometry measurements. Multi-mode VALEN is now being tested and initial calculations of plasma stability for HBT-EP and NSTX will be presented along with details of the design and construction of our new wall-feedback coil system and future experimental plans.

*Supported by U.S. DOE Grant DE-FG02-86ER53222.

GP8 23 Design and Construction of New HBT-EP Passive Wall, Control and Sensor Coil System for Kink Rigidity Studies D.A. MAURER, B. DEBONO, J.P. LEVESQUE, M.E. MAUEL, G.A. NAVRATIL, T.S. PEDERSEN, N. RATH, D. SHIRAKI, *Columbia University* An important plasma response issue is to quantify the extent to which one can perform feedback on one unstable mode without destabilizing other stable MHD modes when they approach marginal stability as the plasma pressure is increased near the ideal wall limit. The HBT-EP experiment is investigating this effect of non-rigid, multimode plasma response during feedback control of the external kink using a new passive stabilizing wall geometry and new set of 120 modular feedback coils of varying toroidal angular coverage. Plasma multimode magnetic response will be measured and quantified using new pickup coil arrays containing 216 poloidal and radial magnetic sensors. This new passive wall-feedback coil system will allow the first detailed measurement of multi-mode, non-rigid kink mode response, first investigation of multi-mode feedback control of the kink mode, and allow the development of feedback strategies to mitigate sideband coupling to stable plasma modes thus limiting plasma non-rigid response and increasing feedback effectiveness. Design, construction, and installation details of the new wall and coil sets will be presented and discussed. Supported by U.S. DOE Grant DE-FG02-86ER53222.

GP8 24 Evaluation of Non-axisymmetric Position Measurements of the HBT-EP Vacuum Chamber and Equilibrium Coils J.P. LEVESQUE, B.A. DEBONO, M.E. MAUEL, D.A. MAURER, G.A. NAVRATIL, T.S. PEDERSEN, N. RATH, D. SHIRAKI, *Columbia University* The ability to do future multi-mode and non-rigid external kink studies on the HBT-EP tokamak will largely depend on alignment of the newly installed wall, sensors, and control coils. Also, small non-axisymmetric equilibrium field errors in tokamaks can have a dramatic impact on plasma performance [1], and reducing these field errors can improve plasma behavior. A measurement arm was built on a rotating axis in the center of HBT-EP in order to accurately locate and quantify misalignments of the equilibrium field coils, vacuum chamber,

new wall segments, sensors, and control coils. The measurement arm is capable of determining locations of equilibrium coils and vacuum chamber ports to within 0.5 mm. Measurements are being used to correct small misalignments of magnetic coils and chamber components during installation of the new wall and magnetic feedback coils in HBT-EP. A ROMER coordinate measuring machine is used in conjunction with the measurement arm to verify coil alignment and to position the new wall segments in the vacuum vessel. Details of the measurement system and analysis of field errors produced by small misalignments of the equilibrium field coils will be presented. Supported by U.S. DOE Grant DE-FG02-86ER53222. [1] J.K. Park *et al*, Phys. Rev. Let. 99, 195003 (2007)

GP8 25 Magnetics Design and Calibration for Multimode Plasma Response Measurements on HBT-EP D. SHIRAKI, B. DEBONO, J.P. LEVESQUE, M.E. MAUEL, D.A. MAURER, G.A. NAVRATIL, T.S. PEDERSEN, N. RATH, Accurate measurements of multimode plasma magnetic response are important for quantifying the effects of a variety of MHD phenomena. A new array of 216 poloidal and radial magnetic sensors has been designed, installed, and calibrated on the HBT- EP tokamak to measure multimode kink dynamics under feedback control. The new system provides double the toroidal resolution for real-time feedback over the previous system, as well as two complete poloidal and one complete toroidal array for high mode-number detection. A Monte Carlo simulation was used to determine the required accuracies, and a combination of bench and a new novel in-situ calibration were used to achieve this required performance. The in-situ calibration was carried out with four current ring sources which were built and installed in the vacuum chamber during an up to air period near the location of the plasma core, as well as the external vertical field, ohmic heating, and toroidal field coils. This calibration procedure is based on a linearized least squares algorithm to verify the location and orientation of each individual sensor. The new system will allow extensive multimode RWM studies, high mode-number feedback, and more accurate MHD spectroscopy detection of possible non-rigid, multimode kink dynamics. Supported by U.S. DOE Grant DE-FG02-86ER53222.

GP8 26 Equilibrium Reconstruction and Ideal Stability Analysis of HBT-EP plasmas N. RATH, B. DEBONO, J.P. LEVESQUE, M.E. MAUEL, D.A. MAURER, G.A. NAVRATIL, T.S. PEDERSEN, D. SHIRAKI, *Columbia University* Accurate knowledge of the safety factor profile is needed to evaluate MHD stability for resistive wall kink modes. In HBT-EP, we reconstruct the time evolution of the safety factor profile with the Tokamac code from equilibrium measurements of external magnetic fields and fluxes along with equilibrium coil currents. Additionally, internal magnetic field information is measured using movable edge magnetic probes to constrain the profile reconstruction. Recent installation of a new passive stabilizing wall for multimode kink studies has substantially increased the magnetic diagnostic measurement set available. Incorporation of this enhanced magnetic capability into the Tokamac code will be described. Eddy currents can have a large effect on the equilibrium of HBT-EP plasmas due to the new close fitting conducting wall used to stabilize the ideal kink. Eddy-currents in these wall segments will be modeled as a superposition of pre-calculated current eigenmodes whose weights are included in the equilibrium fitting procedure. Direct measurement of the eddy-currents from a known toroidal source current will be used to verify the eddy-current model. Ideal stability analysis of these equilibria using the DCON code will also be presented for a series of reconstructed equilibria. Supported by U.S. DOE Grant DE-FG02-86ER53222.

GP8 27 MHD Mode Rotation and Amplitude Changes Induced by a Biased Electrode and Applied Resonant Magnetic Perturbations B. DEBONO, J.P. LEVESQUE, M.E. MAUEL, D.A. MAURER, G.A. NAVRATIL, T.S. PEDERSEN, N. RATH, D. SHIRAKI, *Columbia University* The effect of plasma rotation on the behavior of MHD modes is a topic of importance for both resistive wall and tearing mode stability. On HBT-EP, a biased molybdenum electrode inserted into the edge plasma is used to change the intrinsic ExB rotation of MHD activity of both kink and tearing mode fluctuations and magnetic torque is applied by currents in control coils to effect mode rotation and amplitude. Applied resonant magnetic fields have been observed to lead to characteristic mode amplitude modulations due to the applied slowing torque. For large applied bias voltage, kink fluctuations are observed to accelerate in the direction opposite to the naturally occurring mode rotation with frequencies up to two or three times the natural rotation rate. With the use of strong edge biasing, large (n,m)=(3,1) external kink modes are observed to change their rotation rate from +4 kHz to -30 kHz. At these velocities, the conducting wall segments behave like an ideal wall with a small amplitude rotating ideal kink mode still observable. Magnetic analysis of the behavior of the external kink under these fast rotating conditions will be discussed. Supported by U.S. DOE Grant DE-FG02-86ER53222.

GP8 28 Plasma Rotation in Tokamaks for Steady State Conditions* PABLO MARTIN, ENRIQUE CASTRO, *Universidad Simon Bolivar, Depto. Fisica, Apdo. 89000, Caracas, Venezuela* New equations for tokamaks plasmas in steady state conditions have been found, which allow to find the plasma rotation velocities from the plasma geometry and some parameters such as ellipticity, triangularity, safety factor, shear and inductive electric field. The starting point of our treatment is the resistive MHD equilibrium equation. By additional operation with the del operator, a set of new differential equations has been found. These equations, together with the magnetic surface equations, allow determining the plasma velocities as a function of some experimental parameters, usually determined in most of the tokamaks. Particular cases, as circular geometry, can be treated in a simplified way. These results illustrate more realistic geometries with ellipticity and triangularity, which can only be solved numerically. The coordinates used in this word are those previously presented in several papers [1] P. Martin, E. Castro and M. G. Haines, Phys Plasmas **12**, 102505 (2005)

*This research has been suppored by funds of the group G-22 DID USB.

GP8 29 Parameter dependences of toroidal rotation and momentum transport in JT-60U MAIKO YOSHIDA, YUTAKA KAMADA, HIDENOBU TAKENAGA, YOSHITERU SAKAMOTO, NAOYUKI OYAMA, HAJIME URANO, *Japan Atomic Energy Agency* Prediction and controllability of the toroidal rotation profile are open issues in ITER because parameter dependences of the ratio of the toroidal momentum diffusivity to the thermal diffusivity and the ratio of the convection velocity to the

toroidal momentum diffusivity are not understood well. Parameter dependences of these ratios are essential to understand the mechanisms determining the rotation profile and the level of momentum transport. In this paper, dimensional and non-dimensional parameter dependences of the momentum transport coefficients and these ratios are investigated. It is found that the ratio of the toroidal momentum diffusivity to the thermal diffusivity increases with increasing the normalized poloidal Larmor radius. The ratio of the inward convection velocity to the toroidal momentum diffusivity decreases with increasing the normalized collisionality and decreasing the normalized poloidal Larmor radius. Relations between core and edge rotations are found and the physics mechanisms are discussed form the viewpoints of pinch effect and intrinsic rotation.

GP8 30 Tokamak edge flows and their effect on the L-H transition power threshold A.Y. AYDEMIR, *The University of Texas at Austin, Institute for Fusion Studies* At the edge collisional effects lead to a residual vertical electric field associated with the Pfirsch-Schlüter currents. Non-neutralized portion of this field, whose origin can be traced back to charge-dependent classical grad-B and curvature drifts, drives an ExB flow at the edge. Its poloidal component is in the direction of increasing major radius, regardless of the orientation of the fields and currents. The toroidal component is anti-symmetric about the mid-plane for an up-down symmetric system and reverses with the toroidal field. These flows have many features in common with the observed edge flows in tokamaks. A more careful analysis leads to a radial electric field that depends on the edge temperature gradient and shear. Without up-down symmetry, total contribution to the toroidal momentum and the edge E_ψ clearly depends on the toroidal field direction. When the grad-B drift direction points towards the X- point, the net effect is positive; with toroidal field reversal, E_ψ and the toroidal flow oppose the ambient flows and electric field due to, for example, the ion-orbit loss mechanism. The magnitude of this positive/negative contribution is also plasma-shape dependent. These features provide a compelling explanation for the grad-B drift-dependence of the L-H transition power threshold. We are continuing to study these effects using both initial value and free-boundary equilibrium codes.

GP8 31 Modeling Flow Suppression of Error-field-induced Magnetic Islands in Tokamaks J.A. BRESLAU, W. PARK, *Princeton Plasma Physics Laboratory* Small deviations from axisymmetry in applied tokamak magnetic fields can induce island formation at magnetic surfaces whose rotational transform resonates with the perturbation. These islands have a braking effect on plasma rotation that can destabilize resistive wall modes. The IPEC code[1] is useful for computing plasma response to harmonic perturbations in the infinite-conducting limit, assuming perfect shielding at the resonant surface, but cannot predict the nonlinear effects of finite-sized islands. Using the nonlinear extended MHD code M3D,[2] we explore the effects of a 2,1 perturbation on the nonlinear evolution of a family of equilibria with finite resistivity. Particular attention is paid to the effects of toroidal flow on suppressing island formation, making contact with the analytic theory of Fitzpatrick.[3] Island suppression is shown to depend strongly on the tearing mode stability properties of the equilibrium.

[1]J.K. Park, et al., *Phys. Plasmas* **14**, 052110 (2007).
[2]W. Park, *et al.*, *Phys. Plasmas* **6**, 1796 (1999).
[3]R. Fitzpatrick, *Phys. Plasmas* **5**, 3325 (1998).

GP8 32 Neoclassical toroidal plasma viscosity in the vicinity of the magnetic axis in tokamaks K.C. SHAING, *Plasma and Space Science Center, National Cheng Kung University and University of Wisconsin* Y. SUN, *Forschungszentrum Julich, Association EURATOM-FZJ* S.A. SABBAGH, *Columbia University* M.S. CHU, *General Atomics* Error fields in tokamaks do not vanish on the magnetic axis. Thus, neoclassical toroidal plasma viscosity does not vanish on the axis either. Here, the theory for neoclassical toroidal plasma viscosity is extended to the region near the magnetic axis. Two isomorphic models are presented to investigate the neoclassical toroidal plasma viscosity in that region. The analytic expressions for the viscosity in the low collisionality regimes are calculated. The results can be compared to the experimentally measured toroidal flow damping rate in the near magnetic axis region. The isomorphic transformation developed here can also be used to transform all the analytic expressions of the neoclassical toroidal plasma viscosity calculated for tokamaks to any toroidal system with arbitrary equilibrium symmetry property.

GP8 33 Bootstrap current and transport fluxes associated with bounce-transit and drift resonance in tokamaks B.C. TRANS, *Plasma and Space Science Center, National Cheng Kung Univerrsity* K.C. SHAING, *Plasma and Space Science Center, National Cheng Kung University* M.S. CHU, *General Atomics* S.A. SABBAGH, *Columbia University* Bootstrap current and transport fluxes caused by the bounce-transit and drift resonance are calculated by solving parallel and toroidal momentum balance equations in tokamaks that have error fields and magnetohydrodynamic (MHD) activities. Because error fields are not localized around a surface where the safety factor is a rational number, the bootstrap current densities on either side of the rational surface do not cancel. Thus, there is a net contribution to the equilibrium bootstrap current. This may offer a possibility to control bootstrap current by error fields. Other transport quantities of interest such as parallel flow speed, radial electric field, and particle and heat flux are also calculated.

GP8 34 Real-time MHD Mode Localization in ECE Measurements on ASDEX Upgrade N.K. HICKS, M. GARCIA-MUNOZ, V. IGOCHINE, M. MARASCHEK, M. REICH, J. STOBER, W. SUTTROP, W. TREUTTERER, *Max Planck Insitut fuer Plasma Physik, Boltzmannstrasse 2, 85748 Garching, Germany* ASDEX UPGRADE TEAM, Electron cyclotron emission (ECE) measurements of the electron temperature (T_e) radial profile obtained with the 60-channel radiometer on the ASDEX Upgrade (AUG) tokamak are used to determine the locations of MHD modes that arise in the plasma. A neoclassical tearing mode (NTM) exhibits a phase reversal in T_e fluctuations, and localizing this signature in the ECE T_e profile identifies the radial position of the mode. This technique is part of the development at AUG of a real-time system for NTM suppression, as will be needed for successful operation of ITER. To improve the detection, ECE signals are correlated with magnetic signals. Results are presented on the performance of tracking NTMs in real-time during AUG discharges, and the prospects for the feasibility of this approach in closed-loop real-time NTM suppression are assessed. Building on the correlation approach for NTM tracking, a framework for correlation of ECE signals with other diagnostics is being developed, e.g. to localize Alfvén eigenmodes.

GP8 35 Extremum-Seeking Stabilization of Neoclassical Tearing Modes in Tokamak Plasmas* WILLIAM WEHNER, EUGENIO SCHUSTER, *Lehigh University* Current injection by Electron Cyclotron Current Drive (ECCD) has been proved experimentally as an effective method to stabilize neoclassical tearing modes (NTM). The effectiveness of this method is limited in practice by the uncertainties in the width of the island, the alignment between the island and the EC beam, and the EC power threshold for NTM stabilization. Heuristic search and suppress algorithms have been proposed and shown effective to improve the alignment of the EC beam with the island by just using an estimate of the island width. Making use of this estimate, a real-time, non-model-based, extremum-seeking, optimization algorithm is proposed in this work for EC beam steering and modulation in order to minimize the time (control energy) required for NTM stabilization. A model is proposed for the dynamic response of the island width to different parameters of the EC beam such as alignment, width, power, modulation duty-cycle and modulation phase. The efficiency of the proposed method is compared with traditional search and suppress algorithms.

*Supported by the NSF CAREER award program (ECCS-0645086).

GP8 36 Simultaneous Control of Electron Density and Effective Atomic Number in Non-burning Tokamak Plasmas* DANIEL BOYER, PATRICK BOYLE, EUGENIO SCHUSTER, GLENN BATEMAN, ARNOLD KRITZ, *Lehigh University* The control of plasma kinetic profiles is one of the most fundamental problems in tokamaks. Precise regulation of electron density and effective atomic number, or alternatively hydrogen and impurity densities, is required during routine operation. A common means of actuation toward this end is the use of fast-acting gas valves for the injection of different species. However, non-linear coupling may lead to a closed-loop oscillatory behavior when there is a failure to properly account for the multi-input-multi-output nature of the problem. In this work, controllers are sought to regulate both the average value and spatial profiles of the electron density and effective atomic number. One-dimensional transport equations for these variables are represented in cylindrical coordinates by a set of partial differential equations (PDEs) and used for control synthesis based on nonlinear and backstepping techniques. Numerical simulations illustrating the effectiveness of the resulting control laws are presented.

*Supported by the NSF CAREER award program (ECCS-0645086).

GP8 37 Estimation of Angular Momentum Transport Coefficients via Extended Kalman Filtering Theory* CHAO XU, EUGENIO SCHUSTER, *Lehigh University* The accuracy of first-principles predictive models for the evolution of plasma profiles is sometimes limited by the lack of understanding of the plasma transport phenomena. In this work we use the extended Kalman filtering theory to provide real-time estimates of poorly known or totally unknown angular momentum transport coefficients. These estimates are based solely on input-output diagnostic data and limited understanding of the transport physics. We first assume that the plasma dynamics can be governed by a tractable model obtained by first principles but the transport coefficients are considered unknown and to-be-estimated. The partial-differential-equation model is discretized both in space and time to obtain a finite-dimensional discrete-time state-space representation. The system states and to-be-estimated coefficients are then combined into an augmented state vector. The resulting nonlinear state-space model is used for the design of an extended Kalman filter that provides real-time estimations not only of the system states but also of the unknown transport coefficients.

*Supported by the NSF CAREER award program (ECCS-0645086).

GP8 38 Remediating the Effects of Time Delays in Axisymmetric Plasma Controllers via Optimal Tuning and Predictor Augmentation* REZA ARASTOO, EUGENIO SCHUSTER, *Lehigh University* MICHAEL WALKER, *General Atomics* Introducing extra time delays into the axisymmetric control loops of certain superconducting tokamaks can have significant detrimental consequences. This study exposes and quantifies these effects by focusing on plasma current and radial position control in a vertically-stable circular plasma in KSTAR. Delays in the power supplies, data acquisition, and vessel structure are taken into account. Extremum-seeking-based optimal tuning of PID controllers is proposed as a possible method for remediating the negative effects of time delays. In addition, an augmentation of the control loop by the introduction of a predictor is proposed to improve the performance of the time-delayed closed-loop system. It is shown that the proposed predictor is robust against uncertainties in the values of the delays. The dual-locus technique is employed to assess stability of the closed-loop systems in the presence of time delays.

*Supported by the NSF CAREER award program (ECCS-0645086).

GP8 39 Numerical Simulation on Applicability of Resonant Magnetic Perturbation to KSTAR Tokamak DOOHYUN KIM, HYUNSUN HAN, KI MIN KIM, SANG HEE HONG, *Department of Nuclear Engineering, Seoul National University* FUSION AND PLASMA APPLICATION LABORATORY TEAM, A numerical simulation is carried out to investigate the perturbed magnetic field configurations for a feasibility study on the resonant magnetic perturbation(RMP) to mitigate ELM damages to the divertor in KSTAR tokamak. The perturbed magnetic fields are described by vacuum superposition of equilibrium fields and fluctuating fields induced from the in- vessel control coils (IVCCs) will be installed in KSTAR. The equilibrium and induced fields are calculated using Grad- Shafranov equation and Biot-Savart law, respectively. For visualizing the magnetic field configurations, a field line tracing code has been developed using the 4th-order Runge-Kutta method. Magnetic field perturbations and island configurations can be found with this tracing code by describing poloidal positions of field lines as the increment of toroidal angle. And the Chirikov parameter is calculated to verify the generation of stochastic layer by overlap of magnetic islands. From this numerical work, it is confirmed that stochastic magnetic field lines are formed when the IVCC magnetic fields are generated, and the effect of RMP on KSTAR operation is discussed.

GP8 40 Electron Cyclotron Emission Imaging on KSTAR* T. LIANG, C.W. DOMIER, N.C. LUHMANN, JR., B.J. TOBIAS, *University of California* H.K. PARK, G.S. YUN, W. LEE, *Pohang University of Science and Technology* An innovative, four array electron cyclotron emission imaging (ECEI) system is under development to generate 2-D localized, time-resolved electron tem-

perature T_e images of the KSTAR plasma. The KSTAR system consists of two ECEI instruments on widely separated toroidal locations. Each instrument comprises a pair of imaging arrays which view the plasma through a single midplane port, with a quasi-optical beamsplitter to separate the high field and low field side signals.Translatable optics allow each array to independently focus on different portions of the KSTAR plasma, with each array forming 24 (v) × 8 (h) = 192 channel images of T_e profiles and fluctuations. The ECEI instrument is scheduled for installation on the KSTAR tokamak in early 2010. ECEI will be employed in a wide range of physics studies, but will focus on unraveling the magnetic reconnection physics associated with the sawtooth oscillation. Technical capabilities of this diagnostic will be presented. Work supported by U.S. DOE Grant DE-FG02-99ER54531 and by POSTECH and KNRF.

*Technical capabilities of this diagnostic will be presented. Work supported by U.S. DOE Grant DE-FG02-99ER54531 and by POSTECH and KNRF.

GP8 41 MHD Stability Study of Oblate FRCs G.A. CONE, R.D. MILROY, C.C. KIM, *PSI-Center, University of Washington* The $n = 1$ tilt, interchange, and shift modes of oblate FRC plasmas are simulated using the ttNIMROD code. The grid geometry approximates the shaped, close-fitting flux conserver used in the Swarthmore Spheromak eXperiment (SSX) oblate FRC study[1]. The results validate the work by Belova et al[2] which characterized important thresholds for these instabilities. The tilt mode changes from an internal mode to an external mode with decreasing FRC elongation, and in the oblate case it can be stabilized with a close-fitting conducting wall. By increasing the edge separatrix pressure for wall-supported FRCs, the growth rate of interchange mode decreases, and complete stabilization is achieved when the separatrix beta exceeds 30%. Simulations of the dynamics of FRC formation from two counter-helicity spheromaks are beginning, and preliminary results will be presented.

[1]M. J. Schaffer, M. Brown, C. Cothran, N. Murphy, An oblate FRC concept for SSX, ICC Workshop, College Park, MD, Feb 2007
[2]E. V. Belova, S. C. Jardin, H. Ji, M. Yamada, R. Kulsrud, Numerical study of global stability of oblate field-reversed configurations, Phys. Plasmas, **8**(4), 1267 (2001)

GP8 42 Physics-Based Preconditioning for a Radially Compressed FRC Model A.H. GLASSER, *University of Washington* V.S. LUKIN, *Naval Research Laboratory* SEL is a parallel code for solving initial-boundary value problems for coupled nonlinear fluid equations, using high-order spectral elements for discretization in 2 spatial dimensions, and a fully-implicit time step. Efficient parallel operation requires a scalable method for solving large, sparse matrices. In previous work, a framework for such a solver has been developed, separated into general-purpose modules for all applications and problem-specific code for each application. The heart of the method is physics-based preconditioning, which reduces the order and enhances the diagonal dominance of the linear systems to be solved. Approximations introduced at this stage are eliminated by matrix-free Newton-Krylov iteration on the full nonlinear system. The details of the approach depend on the coupling of the various physical variables. It has been successfully tested for ideal MHD waves in a doubly periodic plane. The purpose of this presentation is to describe the development and testing of physics-based preconditioning for a more interesting test case, modeling a radially compressed FRC with extend MHD.

GP8 43 Perfecting Braginskii's eletron transport coefficients for high collisionality plasmas* JEONG-YOUNG JI, E.D. HELD, *Utah State University* It is known that Braginskii's transport coefficients for the heat flow and frictional force are in error up to 65% for some finite values of $x = \Omega\tau$ and have significant error in the large-x limit.[1] Here Ω is the electron-cyclotron frequency, and τ is the electron-ion collision time. In this work, we find fitting formulas which are practically exact (less than 1% error) for the whole range of x and Z, the ion charge, checked up to $Z=100$. The new fitting formulas are based on calculations with 160 moments (Laguerre polynomials)[2] for $x < 100$ and on the asymptotic form for large x-values.

*Research supported by the U.S. DOE under grant nos. DE-FG02-04ER54746, DE-FC02-04ER54798 and DE-FC02-05ER54812. Work performed in conjunction with the Plasma Science and Innovation (PSI) Center and the Center for Extended MHD Modeling (CEMM).

[1]E. M. Epperlein and M. G. Haines, Phys. Fluids **29**, 1029 (1986).
[2]J.-Y. Ji and E. D. Held, Phys. Plasmas **13**, 102103 (2006); **15**, 102101 (2008).

GP8 44 Hybrid Kinetic-MHD Studies of ICC Devices using Lorentz PIC in Finite Elements CHARLSON C. KIM, *PSI Center - U. Washington* NIMROD TEAM, Progress on the implementation of a Lorentz force particle in cell (PIC) module for the NIMROD code wil be presented. This is an extension of the drift kinetic δf PIC module already in place in NIMROD[1]. Particular challenges of the implementation are PIC in high order finite element grids, resolving the finite Larmour radius (FLR) effect resulting from the Lorentz force (both spatially and temporally), and coupling to the resistive time scales of the MHD fluid variables. The Lorentz force PIC module will be used to study the effects of energetic ions on stability and confinement of innovative confinement concept (ICC) devices. FLR effects may also be important in the high energy tails of energetic particle distributions found in tokamaks. As an initial application, we use the the Lorentz PIC module as tracer particles to study trajectories in ICC devices and the resultant phase space distribution function. We also present simulations of FLR effects on tearing modes of reversed field pinch configurations. Comparisons with the drift kinetic model will also be presented where possible.

[1]C. C. Kim "Impact of velocity space distribution on hybrid kinetic-magnetohydrodynamic simulation of the (1,1) mode," Phys. Plasmas 15, 072507 (2008)

GP8 45 A Tetrahedral Mesh 3-D Ideal MHD Equilibrium Code GEORGE J. MARKLIN, CHRIS HANSEN, *PSI Center, University of Washington, Seattle WA 98195* A new code has been developed to solve the zero beta equilibrium equation mu0*J = curl(B) = Lambda*B on a tetrahedral mesh in an arbitrary 3-D geometry. The function Lambda(x) must be constant along field lines and on flux surfaces, but may be specified arbitrarily across surfaces, where surfaces exist. It must be spatially constant in ergodic regions where there are no surfaces. The solution is computed by alternately solving curl(B) = Lambda*B with Lambda specified, and then updating Lambda = Lambda(B) and iterating until converged. The first equation is easily solved using standard methods for computing Taylor states. The Lambda update is most easily accomplished by tracing field lines and attempting to find the q value, which is constant on a magnetic surface but generally

does not exist for lines that do not lie on surfaces. Lambda may then be specified as a function of q where the q value exists, and constant where the q value does not exist. Examples will be presented of 3-D equilibria in HIT-SI for different ratios of spheromak current to injector current and injector current to injector flux.

GP8 46 Plasma Solution Quality in Distorted, Body-Fitted Meshes in HiFi/SEL WESTON LOWRIE, *University of Washington* VYACHESLAV LUKIN, *Naval Research Laboratory* URI SHUMLAK, *University of Washington* PLASMA SCIENCE AND INNOVATION CENTER COLLABORATION, Highly distorted meshes can yield significant errors in field solutions. Mesh metrics have been widely used to quantify distortion on computational meshes, although they rarely make strong correlations to solution accuracy. In this study several mesh quality metrics are compared to solution error norms for varying types and degrees of mesh deformation. The goal is to be able to better predict the solution error magnitudes based solely on mesh metrics. This work is done using the HiFi/SEL high-order finite (spectral) element code, which is a code that can incorporate many physics models, including the extended MHD plasma model. The code also makes use of a multiblock framework, where several structured logical blocks are coupled together into one computational domain. Each block uses a logical to physical grid transformation to deform the mesh into some physical shape of interest. This can sometimes yield highly distorted meshes, and it is important to know if a particular region of the domain is of acceptable quality.

GP8 47 Non-reflecting boundary conditions for dissipative MHD* E.T. MEIER, A.H. GLASSER, *University of Washington* V.S. LUKIN, *Naval Research Laboratory* U. SHUMLAK, *University of Washington* PSI-CENTER COLLABORATION, Non-reflecting boundary conditions (NRBCs) are frequently used to truncate computational domains without disruptive boundary effects. NRBC techniques are well established for hyperbolic problems, but not for mixed hyperbolic/parabolic equation systems like dissipative MHD. Practical MHD computation with C0-continuous spectral or finite element codes (the focus of this research) requires dissipation to ensure finite gradient length scales. For the Euler and ideal MHD equations, a hyperbolic-based NRBC has been implemented in SEL/HiFi. Simulation results and details of the implementation are presented. Progress toward an effective and stable NRBC for more complicated mixed hyperbolic/parabolic systems like disspative MHD and extended MHD is discussed. Derivations of well-posed NRBC for the Navier-Stokes equations (e.g. [1]) provide a basis for further development. [1] J. Nordstrom and M. Svard, Well-posed boundary conditions for the Navier-Stokes equations, SIAM J. Numer. Anal., 43 (2005) 1231

*Supported by DOE/OFES grant.

GP8 48 Nimrod Simulations of FRC Formation with Rotating Magnetic Field Current Drive R.D. MILROY, C.C. KIM, *PSI-Center, University of Washington* C.R. SOVINEC, *PSI-Center, University of Wisconsin, Madison* Three dimensional simulations of Field Reversed Configuration (FRC) formation and sustainment with Rotating Magnetic Field (RMF) current drive have been performed with the NIMROD code. The Hall term is a zeroth order effect with strong coupling between Fourier components, and recent enhancements to the NIMROD preconditioner allow much larger timesteps than was previously possible. A two-fluid option with a finite electron mass set equal to 1/100 of the ion mass is used. Boundary conditions to capture the effects of a finite length RMF antenna have been added, and simulations of FRC formation from a uniform background gas have been performed with parameters relevant to the TCSU experiment at the University of Washington. Results will be compared with experimental observations. The calculations indicate that the current drive extends considerably beyond the ends of the antenna, that the RMF appears to have a strong stabilizing effect on the configuration, and that an electron poloidal flow (poloidal current) provides the current drive on the inner field lines.

GP8 49 Simulation and Visualization Progress of the PSI-Center Interfacing Group B.A. NELSON, C.C. KIM, R.D. MILROY, T.R. JARBOE, *University of Washington* THE PSI-CENTER GROUP TEAM, The Interfacing Group of the Plasma Science and Innovation Center (PSI-Center - http://www.psicenter.org) performs simulations of collaborating Innovative Confinement Concept (ICC) experiments. Collaborators include the Bellan Plasma Group (Caltech), FRX-L (Los Alamos National Laboratory), HIT-SI (Univ of Wash - UW), LDX (M.I.T.), MST, Pegasus (Univ of Wisc-Madison), PHD (UW), SSPX (Lawrence Livermore National Laboratory), SSX (Swarthmore College), TCS (UW), and ZaP (UW). Extensive simulations of the Caltech experiment study the formation of a kink mode and its dependence on vessel size and current waveform. Simulations of translation and formation of field-reversed configurations (FRCs) continue. Initial Z-pinch sheared-flow stabilization studies are being performed. Output files from NIMROD and its nimplot postprocessor suite are interfaced to the powerful 3-D visualization program, VisIt (http://www.llnl.gov/visit). Results from these simulations, as well as an overview of the Interfacing Group status will be presented.

GP8 50 Numerical Simulation of Non-inductive Startup and Flux Compression in the Pegasus Toroidal Experiment* J.B. O'BRYAN, C.R. SOVINEC, D.J. BATTAGLIA, T.M. BIRD, *Univ. of Wisconsin* Nonlinear numerical computation is used to investigate DC helicity injection from washer-gun plasma sources in a spherical torus. The simulations model non-inductive startup in the Pegasus Toroidal Experiment (Univ. of Wisconsin), including relaxation of the current channels into a "tokamak-like" plasma and current amplification through flux compression. Our resistive MHD simulations with the NIMROD code (nimrodteam.org) use three-dimensional, anisotropic, temperature-dependent thermal conduction—corrected for regions of low-magnetization [Braginskii, Reviews of Plasma Physics, 1965]—and temperature-dependent resistivity. We investigate the effectiveness of the relaxation and flux compression, in terms of current drive, heating, and confinement. Preliminary results on current amplification are in rough agreement with the experiment and indicate significant plasma heating.

*Work supported by the U.S. Dept. of Energy.

GP8 51 Status of TRANSP and PTRANSP* DOUGLAS McCUNE, ROBERT ANDRE, ELIOT FEIBUSH, MARINA GORELENKOVA, K. INDIRESHKUMAR, CHRISTIANE LUDESCHER-FURTH, LEW RANDERSON, *PPPL* GLENN BATEMAN, ARNOLD KRITZ, *Lehigh University* This poster describes the status of TRANSP and PTRANSP code development and run production operations. Production rates continue to climb

as new users and tokamaks are added; statistics will be shown, including utilization of the recently added TRANSP MPI capability. New code features include greatly expanded flexibility in specification of transport models for density, temperature, and angular momentum profile prediction in PTRANSP runs. A new replay option enables retrieval of sources from TRANSP analysis runs for PTRANSP validation. TRANSP / PTRANSP free boundary MHD modeling options have been enhanced. New RF modeling capabilities, such as the ability to model ICRF with full toroidal mode spectrum, have been added. NUBEAM upgrades include improvements to deposition atomic physics and loss orbit distribution capture. Fusion Grid post-processing of TRANSP results has been improved using extraction of SWIM-SciDAC Plasma State files from TRANSP archives. Opportunities for PTRANSP support of SciDAC and FSP efforts will be presented.

*Work Supported by U.S. DOE Contract DE-AC02-09-CH11466.

GP8 52 New RF heating and current drive codes in TRANSP K. INDIRESHKUMAR, D. McCUNE, *Princeton Plasma Physics Lab* J. WRIGHT, *MIT-PSFC* R.W. HARVEY, A.P. SMIRNOV, *CompX* Radio Frequency (RF) heating/current drive comprise an important aspect of present and future tokamaks. The PPPL tokamak transport code (TRANSP) has many RF modules currently available. This poster describes improvements to the RF modeling capabilities of TRANSP by incorporating the general ray tracing code (GENRAY) and upgrading the capabilities of the currently available TORIC code by including its parallel solver capabilities. Currently efforts are underway to incorporate the electron cyclotron (EC) heating/current drive aspects of GENRAY into transp. GENRAY has been built as a TRANSP library and a transp-based executable has been written. Routines from GENRAY have been adapted to produce the input files to GENRAY from the PPPL plasma state software and load the results into the plasma state. In regard to parallel TORIC, a transp executable has been developed and tested. Routines have been developed to broadcast the input data for parallel toric operation. Scaling studies of TORIC are underway on the PPPL Kruskal cluster. This poster will describe the status of GENRAY and Parallel TORIC in TRANSP along with results of scaling studies.

GP8 53 Effect of anomalous transport on kinetic simulations of the H-mode pedestal G. BATEMAN, A.Y. PANKIN, A.H. KRITZ, T. RAFIQ, *Lehigh U.* G.Y. PARK, S. KU, C.S. CHANG, *NYU Courant Institute* The MMM08 and MMM95 Multi-Mode transport models [1,2], are used to investigate the effect of anomalous transport in XGC0 gyrokinetic simulations [3] of tokamak H-mode pedestal growth. Transport models are implemented in XGC0 using the Framework for Modernization and Componentization of Fusion Modules (FMCFM). Anomalous transport is driven by steep temperature and density gradients and is suppressed by high values of flow shear in the pedestal. The radial electric field, used to calculate the flow shear rate, is computed self-consistently in the XGC0 code with the anomalous transport, Lagrangian charged particle dynamics and neutral particle effects. XGC0 simulations are used to provide insight into how thermal and particle transport, together with the sources of heat and charged particles, determine the shape and growth rate of the temperature and density profiles. [1] F.D. Halpern *et al.*, Phys. Plasmas 15 (2008) 065033; J.Weiland *et al.*, Nucl. Fusion 49 (2009) 965933; A.Kritz*et al.*, EPS (2009) [2] G. Bateman, *et al,* Phys. Plasmas **5** (1998) 1793 [3] C.S. Chang, S. Ku, H. Weitzner, Phys. Plasmas **11** (2004) 2649

GP8 54 Study of neoclassical effects on the pedestal structure in ELMy H-mode plasmas A.Y. PANKIN, G. BATEMAN, A.H. KRITZ, T. RAFIQ, *Lehigh U.* G.Y. PARK, S. KU, C.S. CHANG, *NYU Courant Institute* P.B. SNYDER, *General Atomics* The neoclassical effects on the H-mode pedestal structure are investigated in this study. First principles' kinetic simulations of the neoclassical pedestal dynamics are combined with the MHD stability conditions for triggering ELM crashes that limit the pedestal width and height in H-mode plasmas. The neoclassical kinetic XGC0 code [1] is used to produce systematic scans over plasma parameters including plasma current, elongation, and triangularity. As plasma profiles evolve, the MHD stability limits of these profiles are analyzed with the ideal MHD stability ELITE code [2]. The scalings of the pedestal width and height are presented as a function of the scanned plasma parameters. Simulations with the XGC0 code, which include coupled ion-electron dynamics, yield predictions for both ion and electron pedestal profiles. Differences in the electron and ion pedestal scalings are investigated. [1] C.S. Chang et al, Phys. Plasmas 11 (2004) 2649. [2] P.B. Snyder et al, Phys. Plasmas, 9 (2002) 2037.

GP8 55 Plans for kinetic particle-based predictive transport modeling of whole-volume tokamak plasma C.S. CHANG, G. PARK, S. KU, H. STRAUSS, *NYU* L. SUGIYAMA, *MIT* G. BATEMAN, A. KRITZ, *Lehigh U.* D. STOTLER, *PPPL* J. CUMMINGS, *Caltech* S. PARKER, *U. Colorado* S. KLASKY, *ORNL* CPES TEAM, Predictive transport modeling codes, such as PTRANSP, are based upon reduced transport equations, and require ad-hoc closures for most of the critical equilibrium physics phenomena (finite banana width effect, ExB shearing rate profile, orbit loss, MHD- effect, rf-driven transport, impurity transport, alpha particle transport, etc). SciDAC proto-FSP CPES is developing a kinetic particle-based transport modeling code XGC0, which utilizes the modern parallel computing environment (~ 1,000 processors) and which can evaluate these equilibrium kinetic physics phenomena at first principles level. The basic dynamics of ion, electron and impurity particles obey the Lagrangian guiding-center equation of motion in the self-consistent equilibrium electric field. The modeling region is the whole volume, from the magnetic axis to the material wall. The physics capability includes or will include radial anomalous transport coefficients, Ohmic heating, various auxiliary heatings, neutral kinetic transport with wall-recycling, impurity transport, MHD instabilities (in code integration), fusion reaction, and alpha particles.

GP8 56 Transport analysis in toroidal helical plasmas using the integrated code: TASK3D* A. WAKASA, A. FUKUYAMA, S. MURAKAMI, *Kyoto University* C.D. BEIDLER, H. MAASSBERG, *Max-Planck-Institute fur Plasmaphysik* M. YOKOYAMA, M. SATO, *National Institute for Fusion Science* The integrated simulation code in helical plasmas, TASK3D, is being developed on the basis of an integrated modeling code for tokamak plasma, TASK. In helical systems, the neoclassical transport is one of the important issues in addition to the anomalous transport, because of strong temperature dependence of heat conductivity and an important role in determining the radial electric field. We have already constructed the neoclassical transport database in LHD, DGN/LHD. The mono-energetic diffusion coefficients are evaluated based on the Monte Carlo method by DCOM code and the mono-energetic diffusion coefficients database is constructed using a neural network technique. Also we apply GSRAKE code, which

solves the ripple-averaged drift kinetic equation, to obtain transport coefficients in highly collisionless regime. We have newly incorporated the DGN/LHD module into TASK3D. We will present several results of transport simulation in typical LHD plasmas.

*This work is supported by Grant-in-Aid for Scientific Research (S) (20226017) from JSPS.

GP8 57 Recent Advances in Simulation of Wave Interactions with Extended MHD Phenomena* DONALD BATCHELOR, *ORNL* SWIM TEAM The Integrated Plasma Simulator (IPS), developed by the Simulation of Wave interactions with MHD (SWIM), project provides a framework within which some of the most advanced, massively-parallel fusion modeling codes can be interoperated to provide a detailed picture of the multi-physics processes involved in fusion experiments. The presentation will cover four topics: 1) recent improvements to the IPS, 2) application of the IPS for very high resolution simulations of ITER scenarios, 3) studies of resistive and ideal MHD stability in tokamak discharges using IPS facilities, and 4) the application of RF power in the electron cyclotron range of frequencies to control slowly growing MHD modes in tokamaks and initial evaluations of optimized location for RF power deposition.

*The SciDAC project Simulation of Wave Interactions with MHD is supported jointly by U.S. Dept. of Energy offices of Fusion Energy Science and Advanced Scientific Computing Research.

GP8 58 Modeling ECCD/MHD coupling using NIMROD, GENRAY, and the Integrated Plasma Simulator THOMAS G. JENKINS, D.D. SCHNACK, C.R. SOVINEC, C.C. HEGNA, J.D. CALLEN, F. EBRAHIMI, *UW-Madison* S.E. KRUGER, J. CARLSSON, *Tech-X* E.D. HELD, J.-Y. JI, *Utah State U.* R.W. HARVEY, A.P. SMIRNOV, *CompX* W.R. ELWASIF, *ORNL* SWIM PROJECT TEAM, We summarize ongoing theoretical/numerical work relevant to the development of a self–consistent framework for the inclusion of RF effects in fluid simulations; specifically, we consider the stabilization of resistive tearing modes in tokamak geometry by electron cyclotron current drive. In the fluid equations, ad hoc models for the RF–induced currents have previously been shown to shrink or altogether suppress the nonlinearly saturated magnetic islands generated by tearing modes; progress toward a self–consistent model is reported. The interfacing of the NIMROD [1] code with the GENRAY/CQL3D [2] codes (which calculate RF propagation and energy/momentum deposition) via the Integrated Plasma Simulator (IPS) framework [3] is explained, RF-induced rational surface motion and the equilibration of RF–induced currents over plasma flux surfaces are investigated, and the efficient reduction of saturated island widths through time modulation and spatial localization of the ECCD is explored. [1] Sovinec *et al.*, JCP **195**, 355 (2004) [2]www.compxco.com [3] Both the IPS development and the research presented here are part of the SWIM project. Funded by U.S. DoE.

GP8 59 Correlation Effects in ICRF Diffusion Coefficients* YU. PETROV, R.W. HARVEY, *CompX* E.F. JAEGER, L.A. BERRY, D.B. BATCHELOR, *ORNL* P.T. BONOLI, J.C. WRIGHT, *MIT/PSFC* RF quasi-linear (QL) theory of wave-plasma interaction assumes at each resonant surface that a group of ions has no gyrophase-memory from the previous crossings. In contrast, the DC (Diffusion Coefficient) code obtains coefficients by direct numerical integration of the Lorentz force equation for ion motion in combined equilibrium and RF fields from the AORSA full-wave code, thus keeping gyrophase information. For a single toroidal mode, strong correlation effects are observed in form of peaks and dips in momentum space. Nevertheless, for a C-Mod minority ion ICRF heating test case, the radial profiles of power absorption calculated by the CQL3D Fokker-Planck code using DC results, agree well with those calculated by AORSA based on QL theory, at least at early times where the ion distribution is isotropic about the B-field. However, as the ion distribution develops anisotropy, differences in power absorption appear. We also examine effects of multiple ICRF toroidal modes in ITER.

*Supported under US DOE grants ER54649 and ER54856.

GP8 60 Equilibrium relations in a two-fluid and drift-kinetic theory of weakly collisional, magnetically confined plasmas* J.J. RAMOS, *M.I.T. Plasma Science and Fusion Center* A two-fluid system with finite-Larmor-radius drift-kinetic closures, applicable to weakly collisional, magnetically confined plasmas is presented. The ordering of the collisionality differs from more traditional approaches in that the ratio of mean free paths to equilibrium confinement lengths is assumed to be of the same order as the ratio of such macroscopic plasma lengths to the ion gyroradius, the inverse of which is adopted as the basic expansion parameter $\delta \ll 1$. The drift-kinetic equations are expressed in the moving reference frames of the macroscopic flows, which facilitates their coupling to and precise compatibility with the complementary two-fluid, extended-MHD equations, and the macroscopic flows are assumed of the order of the diamagnetic drift velocities. Different electron and ion equations are derived, based on the ordering of the small mass ratio as δ^2. Considering axisymmetric equilibria with diamagnetic flows, several new results are obtained. These include specific relations for the particle and heat flows, the electric potential, the density and the pressure anisotropies, a precise evaluation of the ion gyroviscosity and a novel expression for the parallel collisional friction force.

*Work supported by the U.S. Department of Energy.

GP8 61 Neoclassical parallel closures for toroidal plasmas MUKTA SHARMA, E.D. HELD, J.Y. JI, *Utah State University* Closures for the parallel conductive heat fluxes and stresses are derived. A Chapman-Enskog-like approach is adopted and time-dependent effects are ordered small compared to parallel free streaming, collisional effects and particle trapping in magnetic wells. The distribution function is written as the sum of a dynamic Maxwellian and a kinetic distortion, F, expanded in Legendre polynomials. To lowest order, the magnetic moment and total energy of the particles are conserved. For an accurate treatment of collisional effects, a moment approach is applied to the full, albeit linearized, Coulomb collision operator. In contrast to previous derivations[1], this work does not bounce-average when solving the lowest-order drift kinetic equation. In contrast, a Fast Fourier Transform algorithm is used to treat the one-dimensional spatial domain along the magnetic field and the drift kinetic equation is solved on a grid in the speed variable, $s = v/v_T$. This approach allows for parallel acceleration as well as examination of the closures in all collisionality regimes, i.e., Pfirsch-Schlueter, plateau and banana. The application of these closures in the NIMROD code is also discussed.

[1]E.D. Held, *et al.*, Phys. Plasmas **10**, 3933 (2003).

GP8 62 Warping Simulation Time: Multi-Dimensional Asynchronous Hybrid Simulations* YURI OMELCHENKO, HOMA KARIMABADI, *SciberQuest, Inc* Fusion and space plasmas are often characterized by the strong presence of ion kinetic effects and multiple temporal scales associated with plasma and magnetic field inhomogeneities. Traditional hybrid (electron fluid/particle ion) simulations of such systems face severe restrictions on the global timestep and sometimes even fail to resolve fine spatial structures. Recently we introduced a new approach to multi-scale modeling [1]: Discrete-Event Simulation (DES). Our new multi-dimensional code, HYPERS (HYbrid-Particle Event-Resolved Simulation) proceeds by adaptively selecting physically appropriate time increments for individual particles and local electromagnetic fields. As a result, numerical updates are always carried out when needed only. This enables fast, reliable and accurate simulations of energetic plasmas immersed in highly inhomogeneous magnetic fields. We report preliminary results from simulations of the interaction of streaming plasmas with dipole magnetic obstacles and discuss the applicability of this technique to other plasma configurations (magnetic confinement schemes) and theoretical approximations (MHD, two-fluid,Vlasov). [1] Y.A. Omelchenko, and H. Karimabadi, J. Comp. Phys. 216, 153 (2006).

*Supported by DOE/NSF Grant PHY-0613410.

GP8 63 Modeling of Anomalous Plasma Current Evolution in Tokamak Hybrid Operation Scenarios HYUNSEOK KIM, WONJAE LEE, YONG-SU NA, *Seoul National University* FUSION AND PLASMA APPLICATION LABORATORY TEAM, Tokamak experiments worldwide have discovered hybrid scenarios, which exhibit high confinement and stability simultaneously, where the q-profile is relatively flat at the centre with qmin q0 1 in stationary conditions. However, the reasons for high fusion performance and for sustainment of flat q-profiles in hybrid scenarios are not clarified yet. In this work, a numerical modeling is carried out using ASTRA to simulate an anomalous current evolution, observed in some experiments and to figure out factors which affect the flat and stationary q- profile in hybrid scenarios. Firstly, the neoclassical resistivity is used for the simulation and compared with experiments. Then, the additional terms based on the ohm's law, like an anomalous parallel plasma resistivity, a hyper resistive term and etc., are introduced and their effects are investigated by comparing with experiments. Here, the parallel ohm's law for mean magnetic fields is adopted for current diffusion. The modeling results are expected to contribute to understand physical background of improvement of confinement and stability in hybrid operation scenarios.

GP8 64 TGLF Transport Modeling With PTRANSP/GCNMP* H.E. ST. JOHN, L.L. LAO, G.M. STAEBLER, J.E. KINSEY, P.B. SNYDER, *GA* R.V. BUDNY, D. McCUNE, *PPPL* We describe our effort in getting the turbulent TGLF confinement model operational with the PTRANSP transport code. Numerically intensive, TGLF requires parallel operation for determination of turbulent fluxes. This has driven our interface design to PTRANSP and motivated the purchase of a small parallel computing cluster for development. We note that larger clusters would be appropriate to exploit further parallel structure present in TGLF. A direct flux solver was developed to solve both the time-dependent and time-independent transport equations over a variable radial transport grid. A universal communication scheme based on netcdf data representation is under continuing development that will allow translation of PTRANSP, ONETWO, GCNMP, XPTOR, and GYRO code run time information from any of the codes to any other. Cross validation of results thus becomes much more feasible. Our initial efforts comparing XPTOR and PTRANSP/GCNMP calculations are discussed. Our initial foray into EPED1 type edge stability analysis is described.

*Work supported by the US DOE under DE-FG02-07ER54935 and DE-AC02-09CH11466.

GP8 65 On the Development of a Scalable Implicit Stabilized Finite-Element Resistive MHD Solver L. CHACÓN, *ORNL* J.N. SHADID, R.P. PAWLOWSKI, *SNL* We explore the development of a massively parallel, scalable fully-implicit stabilized unstructured finite element (FE) capability for low-Mach-number resistive MHD. We focus on the development of the stabilized FE formulation and the underlying fully-coupled preconditioned Newton-Krylov nonlinear iterative solver. To enable robust, scalable and efficient solution of the large-scale sparse linear systems generated by the Newton linearization, fully-coupled algebraic multilevel preconditioners are employed. These preconditioning methods are based on a variable-overlap additive one- level Schwarz preconditioner and a relatively new algebraic multilevel technique that employs a graph-based aggressive-coarsening aggregation method applied to the nonzero block structure of the Jacobian matrix. We will present verification results that demonstrate the expected order-of-accuracy, including prototype problems such as an MHD Faraday conduction pump, the hydromagnetic Rayleigh-Bernard instability, the magnetic island coalescence problem, and 3D tokamak calculations using Solove'ev equilibria. We will discuss initial encouraging results that explore the scaling of the solution methods on up to 4096 processors for problems with up to 64M unknowns on a CrayXT3/4, and will demonstrate a successful large-scale proof-of-capability calculation for 1 billion unknowns for the MHD Faraday pump problem on 24,000 cores.

GP8 66 Nonlinear Simulations of Energetic Particle-induced Geodesic Acoustic Mode G.Y. FU, R. NAZIKIAN, R. BUDNY, M. GORELENKOVA, *Princeton University* An Energetic Particle-induced Geodesic Acoustic Modes (EGAM) was previously shown to exist based on analytic theory and numerical simulation [1], in agreement with the recent experimental results of the beam-driven GAM-like n=0 mode in DIII-D [2]. In this work, nonlinear simulations of EGAM are carried out using a hybrid model in which the thermal plasma is modeled as a fluid whereas the energetic particle component is described by the drift-kinetic equation. For an analytic energetic particle distribution function, simulation results show initial saturation due to the flattening of particle distribution function in velocity space, followed by a bursting feature with frequency chirping. In order to model the DIII-D experiments more closely, realistic simulations have been carried out using the experimental neutral beam deposition profile from the TRANSP/NUBEAM code. Numerical results show mode bursting with clear radial propagation. The calculated mode frequency, mode radial extent, and density fluctuation level are consistent with the experimental observation in DIII-D [1] G. Y. Fu, Phys. Rev. Letts. 101, 185001 (2008) [2] R. Nazikian et al., Phys. Rev. Letts. 101, 185001 (2008).

GP8 67 An Efficient Method for Verifying Gyrokinetic Microstability Codes* R. BRAVENEC, *Fourth State Research* J. CANDY, *General Atomics* W. DORLAND, *U. Maryland* C. HOLLAND, *UCSD* Benchmarks for gyrokinetic microstability codes can be developed through successful "apples-to-apples" comparisons among them. Unlike previous efforts, we perform the com-

parisons for actual discharges, rendering the verification efforts relevant to existing experiments and future devices (ITER). The process requires i) assembling the experimental analyses at multiple times, radii, discharges, and devices, ii) creating the input files ensuring that the input parameters are faithfully translated code-to-code, iii) running the codes, and iv) comparing the results, all in an organized fashion. The purpose of this work is to automate this process as much as possible: At present, a python routine is used to generate and organize GYRO input files from TRANSP or ONETWO analyses. Another routine translates the GYRO input files into GS2 input files. (Translation software for other codes has not yet been written.) Other python codes submit the multiple GYRO and GS2 jobs, organize the results, and collect them into a table suitable for plotting. (These separate python routines could easily be consolidated.) An example of the process – a linear comparison between GYRO and GS2 for a DIII-D discharge at multiple radii – will be presented.

*Supported by USDoE through grant DE-FG02-08ER54978.

GP8 68 The para-real algorithm applied to a simple drift-wave turbulence model for transport timescale studies DEBASMITA SAMADDAR, DAVID E. NEWMAN, *University of Alaska Fairbanks* RAUL SANCHEZ, *Oak Ridge National Laboratory* We will present the results of applying the para-real algorithm[1] to a fluid turbulence code. This new technique efficiently parallelizes the time domain and has been found to significantly reduce the computational wall time. If successfully applied, this will allow study of the turbulent transport dynamics on transport time scales - something that has heretofore been very difficult. We apply this algorithm to simulations of drift-wave turbulence[2] in slab geometry as a function of the model and sheared flow. Preliminary science results as well as computational results will be presented. These include cases in which the relative dominance ExB nonlinearities will be tuned artificially and the transport exponents will be explored as the sheared flow changes.

[1]Martin J. Gander et al, Siam J. Sci. Comput. Vol.29, No.2, pp.556-578
[2]D.E. Newman et al, Phys. Fluids B 5, 1140 (1993)

GP8 69 Benchmarking of the 2DX eigenvalue code D.A. BAVER, J.R. MYRA, *Lodestar Research Corporation* M. UMANSKY, *Lawrence Livermore National Laboratory* The 2DX code is a linear eigenmode solver designed for toroidal plasma configurations with an x-point topology. Together with recent upgrades to BOUT, it is part of a project to provide validation and verification capability for large-scale turbulence codes. Comparing linear growth rates to a single simple linear code provides a reproducible result that can be used as a common standard. In addition to its topological capabilities, the 2DX code is distinct in its use of an equation language to input equations to be solved. This gives it the flexibility to handle nearly arbitrary systems of equations, giving it potential applications far beyond the scope of the current project. For purposes of the present project, however, editing the equation language is a potential source of error, so we will be presenting results from a standardized 6-field model instead. We will present 2DX results from both analytic and full geometry test cases. We will also present comparisons with BOUT. These tests will serve to build confidence in the 2DX code as a valuable tool for V&V. Work supported by the U.S. DOE under grant DE-FG02-07ER84718.

GP8 70 Progress on the Collisional-Radiative Modeling and the Analysis of Local Line Emission Profiles of Carbon Impurities from TJ-II Plasmas* R. FLORIDO, D. SUAREZ, R. RODRIGUEZ, J.M. GIL, J.G. RUBIANO, P. MARTEL, *Departamento de Fisica, Universidad de Las Palmas de Gran Canaria, Spain* E. MINGUEZ, *Instituto de Fusion Nuclear, Universidad Politecnica de Madrid, Spain* B. ZURRO, A. BACIERO, *Laboratorio Nacional de Fusion, Asociacion Euratom-CIEMAT, Madrid, Spain* In a simple previous analysis the ratio of local emission profiles of carbon impurities (C^{4+} at 227.1 nm and C^{5+} at 529.0 nm) measured from TJ-II plasmas was found to have a significant dependence of neutral density profile. Hence, the aim of this work is to have a better theoretical understanding of this system and finally validate or discard the carbon spectral line ratio as a useful tool to estimate the neutral density profile in ECRH TJ-II plasmas. To assist in the theoretical modeling of this carbon system we use the collisional-radiative code ABAKO, which has been successfully applied to different ICF problems. Progress on the collisional-radiative modeling and simulation of MCF TJ-II plasmas are reported, paying particular attention to the influence of the charge-exchange recombination processes on the charge state distribution and carbon line ratio radial profiles.

*Work supported by Research Project ENE2008-06668-C02/FTN of the Spanish Ministry of Science and Innovation.

GP8 71 3D-MAPTOR Code for computation of magnetic fields in tokamaks* ESTEBAN CHÁVEZ-ALARCÓN, *Instituto Nacional de Investigaciones Nucleares* JULIO HERRERA-VELÁZQUEZ,† *Universidad Nacional Autónoma de México* A 3dimensional code has been developed in order to determine the magnetic field in tokamaks, starting from the assumption that the toroidal and vertical field coils are all circular, as well as the cross section of the plasma current distribution. It was earlier used to study the stochastization of the outer magnetic surfaces [1] and to reconstruct the evolution of the plasma column, using the experimental signals of tokamak discharges. These results were compared with tomographic reconsructions of the ISTTOK tokamak [2]. We present an upgrade of the code, in which rectangular toroidal field coils and D shaped plasma current cross sections can be included. The code is particularly useful to study the effect of the ripple along the toroidal coordinate. [1] E. Chávez, et al., "Stochastization of Magnetic Field Surfaces in Tokamaks by an Inner Coil" in Plasma and Fusion Science, AIP Conference Proceedings Series 875 (2006) pp.347-349. [2] B.B. Carvalho, et al., "Real-time plasma control based on the ISTTOK tomography diagnostic," Rev. Sci. Instrum. 79 (2008)10F329.

*This work is partially supported by CONACyT projects 44324-F and U47899-E.
†Instituto de Ciencias Nucleares

GP8 72 Nonlinear simulation of Toroidicity-induced Alfvén Eigenmode with source and sink JIANYING LANG, GUOYONG FU, *Princeton Plasma Physics Laboratory* YANG CHEN, *Univ. of Colorado at Boulder* It has been known that in collisionless plasmas the nonlinear saturation of energetic particle-driven modes is caused by wave-particle trapping effect, which flattens the spatial distribution function of resonant particles and reduces the drive. However, when energetic particles are sufficiently collisional, much more complicated physics is involved during the nonlinear process. The nonlinear behavior of a single TAE is studied using the kinetic/MHD hybrid code m3d-K [Fu, Phys. Plas-

mas, 2006] in the presence of pitch-angle scattering, source, sink, and the slowing-down process. In the presence of only pitch-angle scattering, both steady state and pulsation behaviors are observed depending on the regime of collision rate. For steady state cases, the scaling of nonlinear saturation level with collision rate agrees with the analytical prediction [Berk, Phys. Plasmas, 1990]. Our preliminary simulations with source, sink, and slowing-down process have obtained nonlinear steady state, where the saturation level increases with slowing-down rate. Flattening in the spatial distribution function is observed during nonlinear saturation. Detailed variation of distribution function and parameter scaling will be further explored and compared to analytic theories. This work is supported by DOE Energetic Particle Simulation Center PEPSC.

GP8 73 Edge Biasing of SINP-Tokamak Plasma in High-Q Regime* RABINDRANATH PAL, DEBJYOTI BASU, *Saha Institute of Nuclear Physics, 1/AF Bidhannagar Kolkata - 700064 India* In high q regime ($q_{edge} = 5 - 7$) of SINP-TOKAMAK [an iron-core device having major and minor radii of 30 and 7.5 cm, respectively and $B_{toroidal} = 1.2$ Tesla] fast edge biasing experiment is carried out introducing a Molybdenum electrode of 5mm in diameter, radially positioned at 7.0 cm. Biasing seems to cause a change in plasma current density profile forming a negative shear in the region 6.4-6.9 cm and it leads to better confinement and longer duration of plasma current as was observed[1] also in very low q (VLQ) regimes of the same machine. The electrode current drawn in this regime is about 5-10 amp. Lowering of H_α signal and loop voltage is also observed indicating better confinement, independently confirmed by diamagnetic loop too. On applying bias, electron density and temperature profile develop sharper gradient near the edge. Interestingly, electrostatic and magnetic fluctuations, observed by inserting electric and magnetic probes in the edge plasma, are suppressed in the inner region (6.4-6.8 cm) in the frequency range of 30-70 kHz by the effect of electrode biasing.

*Supported by D.A.E. of Govt. of India.

[1]Ghosh J., Pal R., Chattopadhyay P. K. and Basu D. 2007 Nucl. Fusion **47** 331

GP8 74 MHD, LINEAR AND NONLINEAR PHENOMENA

GP8 75 Measurements of reduced parallel electron distributions using whistler wave absorption* DEREK THUECKS, *Univ of Wisconsin-Madison* FRED SKIFF, CRAIG KLETZING, *Univ of Iowa* STEPHEN VINCENA, *UCLA* We present the first results of a diagnostic designed to measure the reduced parallel electron distribution using resonant absorption of whistler waves at the electron cyclotron frequency. According to warm-plasma theory, a whistler wave that is swept in frequency is Doppler-shifted into resonance with those parts of the electron phase space density with a velocity component parallel to B_0. In our experiments, whistler waves were launched and received by a pair of dipole antennas immersed in a cylindrical discharge plasma at two positions along the axial background magnetic field. The whistler wave frequency was swept from somewhat below and up to $|\omega_{ce}|$ The measured wave absorption through the plasma was proportional to the reduced parallel electron distribution function. The background theory and initial results from this diagnostic are presented here. These first results show that this diagnostic succeeds in measuring changes to the distribution function due to cooling of the plasma during the transition from the discharge to the afterglow.

*Supported by DOE and NSF.

GP8 76 Measurements of Turbulent Transport of Fast Ions* SHU ZHOU, HEINRICH BOEHMER, WILLIAM HEIDBRINK, ROGER McWILLIAMS, TROY CATER, PAVEL POPOVICH, SHREEKRISHNA TRIPATHI, STEVE VINCENA, *University of California, Irvine* Due to gyroradius averaging and drift-orbit averaging, the transport of fast ions by microturbulence is often smaller than for thermal ions. In this experiment, spatial transport of lithium fast ions [1] with gyroradii of 5.9 cm is studied in the LArge Plasma Device (LAPD). The baseline condition is a uniform quiet plasma; in the comparison condition, the cylindrical plasma column is compressed so the helical fast-ion orbits pass through the turbulent edge region (broadband drift-wave fluctuations with density fluctuations of $\sim$ 20%) The fast-ion energy and pitch are varied to study drift averaging. Initial observations indicate that changes in parallel energy are more evident than radial transport. Measurements of the fluctuations by triple, swept Langmuir, and B-dot probes are compared with two-fluid simulations by the BOUT code. Calculations of the expected fast-ion transport in the simulated turbulence will be compared with the experimental profiles. [1] Y. Zhang et al., Rev. Sci. Instrum. 78, 013302 (2007).

*Supported by U.S. DoE.

GP8 77 Confinement regimes in simple magnetized toroidal plasmas* IVO FURNO, AMBROGIO FASOLI, BENOIT LABIT, PAOLO RICCI, CHRISTIAN THEILER, *Centre de Recherches en Physique des Plasmas-Ecole Polytechnique Federale de Lausanne, Association EURATOM-Confederation Suisse, CH-1015 Lausanne* BARRETT ROGERS, *Dartmouth College, Hanover, New Hampshire, 03755, USA* In the simple magnetized torus TORPEX (R = 1 m, a = 0.2 m), we explore experimentally the accessibility of a high confinement mode, which is predicted by theory for this configuration [P. Ricci, et al., Phys. Rev. Lett. **100**, 225002 (2008)]. We consider different gases (H_2, D, He, Ne, N_2) and we measure the dependence of the temperature and density gradients upon the ratio γ/v'_{ExB} (γ is the interchange linear growth rate and v'_{ExB} is the velocity shear). We observe that γ/v'_{ExB} decreases from $\gamma/v'_{ExB} \sim$ 6-7 for hydrogen to $\gamma/v'_{ExB} \sim$ 0.3-0.4 for neon. Consistently with theory, temperature and density profiles steepen when γ/v'_{ExB} drops below unity. The perpendicular particle flux is estimated by particle balance and measured using a multi-pin flux probe. First simulation results are presented with a global fluid code that solves the drift-reduced Braginskii equations in the whole TORPEX domain.

*This work is partly funded by the Fonds National Suisse de la Recherche Scientifique.

GP8 78 Interchange instabilities, turbulence and fast ion interactions in the TORPEX device* A. FASOLI, A. DIALLO, L. FEDERSPIEL, I. FURNO, D. IRAJI, E. KUNG, B. LABIT, S. MULLER, G. PLYUSHCHEV, M. PODESTA, F. POLI, P. RICCI, C. THEILER, *CRPP-EPFL, Switzerland* Electrostatic turbulence, related structures and their effect on transport are investigated on TORPEX simple magnetized plasmas using high resolution diagnostics and several control parameters, fluid models and numerical simulations. A critical pressure gradient to drive the interchange instability is experimentally identified, consistently with linear theory. Interchange modes nonlinearly develop blobs, radially propagating filaments of enhanced plasma pressure. Blob velocities and sizes are obtained from probe measurements using pattern recognition and are described by an analytical expression that includes ion polarization currents, parallel sheath currents and ion-neutral collisions. Limiter configurations with varying angles between field lines and the metal surface are explored. To complement probe data, a fast framing camera and a movable gas puff system are installed. Density and light fluctuations show similar signatures of drift-interchange activity. Further developments of optical diagnostics, including an image intensifier and LIF, will be discussed. The effect of interchange turbulence on fast ion phase space dynamics is studied using movable fast ion source and detector in scenarios for which the development from linear waves into blobs is fully characterized.

*Partly funded by the Fonds National Suisse de la Recherche Scientifique.

GP8 79 Langmuir wave linear evolution in inhomogeneous nonstationary anisotropic plasma* I.Y. DODIN, V.I. GEYKO, N.J. FISCH, *Princeton University* Equations describing the linear evolution of a nondissipative Langmuir wave in inhomogeneous nonstationary anisotropic plasma without magnetic field are derived in the geometrical optics approximation. A continuity equation is obtained for the wave action density, and the conditions for the action conservation are formulated. In homogeneous plasma, the wave field $\tilde{E}$ universally scales with the electron density N as $\tilde{E} \propto N^{3/4}$, thereby resulting in a modified adiabatic index of the plasma $\gamma = 3/2$, whereas the wavevector evolution varies depending on the wave geometry.

*This work was supported by the NNSA under the SSAA Program through DOE Research Grant No. DE-FG52-04NA00139.

GP8 80 Numerical studies of electrostatic eigenmodes in a pair-ion plasma SUWON CHO, *Kyonggi University* It has been known that there exist various waves in a pair-ion plasma having ions of equal mass and opposite charge without electrons and that a branch in the intermediate frequency range is a backward wave. The dispersion relation of electrostatic eigenmodes is studied to analysis these experimental results. Including the non-uniform density profile in a bounded plasma, the wave equation is converted to a matrix eigenvalue equation via the finite difference method, which is then solved numerically. The shooting method is also used to confirm the results. Numerical results shows that there can be a backward wave in a bounded plasma, while it is absent in the corresponding infinite plasma. In addition, the eigenmodes in an ordinary electron-ion plasma are examined for comparison.

GP8 81 Nonlinear Wave Driven Processes in Plasmas ROBERT BINGHAM, R.M.G.M. TRINES, *STFC Rutherford Appleton Laboratory* L.O. SILVA, *GoLP* J.J. SANTOS, *CELIA, Universite, Bordeaux 1-CNRS-CEA, Talence, France* B. BRANDAO, J.T. MENDONCA, *GoLP, IST Portugal* P.K. SHUKLA, *Institut fur Theoretische Physik IV* Nonlinear wave driven processes in plasmas are normally described by either a monochromatic pump wave that couples to other monochromatic waves, or as a random phase wave coupling to other random phase waves. An alternative approach involves a random or broadband pump coupling to monochromatic and/or coherent structures in plasmas. This approach can be implemented through the wave kinetic model. In this model, the incoming pump wave is described by wither a bunch (for coherent waves) or a rea (for random phase waves) of quasi-particles. We will present a generalized statistical theory describing a range of phenomena that include generation of zonal flows from drift mode turbulence, photon acceleration of intense lasers and intense radio waves and photon shocks. Possible applications include a diagnostic of large amplitude plasma waves and studies of zonal flows in planetary atmospheres will also be discussed.

GP8 82 Equal energy phase space trajectories in resonant wave interactions* ODED YAAKOBI, LAZAR FRIEDLAND, *Hebrew University of Jerusalem* Adiabatic evolution of a nonlinear resonantly driven wave system and two/three coupled waves system generic to a variety of plasma physics problems is studied. The corresponding Hamiltonian, depending on the coupling, detuning and nonlinear frequency shift parameters has a variable number of fixed points. The system can be bistable due to repeated separatrix crossing in the phase space. It is analytically shown that the oscillation periods along trajectories corresponding to the same value of the Hamiltonian are equal, and the difference of the corresponding areas under them is obtained as a function of the system parameters. A scheme of simultaneous adiabatic change of system parameters is constructed, in such a way that any pair of trajectories that have equal energy at some time will continue to have the same energy anytime. These results are generalizations of a previous work [O. Polomarov and G. Shvets, Phys. Plasmas, 13, 054502 (2006)] for a single resonantly driven wave.

*Supported by the US-Israel Binational Science Foundation, Grant No. 2004033.

GP8 83 Multidimensional autoresonant three-wave interactions* LAZAR FRIEDLAND, ODED YAAKOBI, *Hebrew University of Jerusalem* The theory of autoresonant three-wave interactions is generalized to more than one space and/or time variation of the background medium. In the most general case, the three waves propagate in a four-dimensional (4D) slowly space-time varying background, with an embedded 3D linear resonance hypersurface, where the linear frequency and wave-vector matching conditions of the three waves are satisfied exactly. The autoresonance in the system is the result of weak nonlinear frequency shifts and nonuniformity in the problem and is manifested by satisfaction of the nonlinear resonance conditions in an extended region of space-time adjacent to the resonance surface despite the variation of the background. The threshold condition for autoresonance is found. Asymptotic description of the autoresonant waves far away from the resonance surface is obtained. The theory is illustrated and tested in 2D numerical simulations. An application to stimulated Raman scattering in a nonuniform, time-dependent plasma case is discussed.

*Supported by the US-Israel Binational Science Foundation, Grant No. 2004033.

GP8 84 A Simple Analytic Double Layer FRANCIS PERKINS, *University of Colorado* A simple model comprised of Debye-shielding electrons and inter-penetrating ion beams leads to formation of double layers. The key non dimensional parameter is the ion-beam energy to electron temperature ratio. The simple model permits an analytic solution which will be presented.

GP8 85 Nonlinear traveling waves in energetic particle phase space* BORIS BREIZMAN, *Institute for Fusion Studies, The University of Texas at Austin* The near-threshold regimes of wave excitation by energetic particles reveal a rich family of nonlinear scenarios, including formation of nonlinear structures with time-dependent frequencies. Previous descriptions of such structures were limited to the case of small deviations of their frequencies from bulk plasma eigenfrequencies. However, in many frequency-sweeping events, the range of sweeping is comparable to the frequency itself. The need to interpret such dramatic phenomena requires a non-perturbative formalism, which this work presents. The underlying idea is that the time-dependent frequencies represent nonlinear traveling waves in fast-particle phase space. Such waves form due to initial instability and resonant particle trapping, and they then evolve slowly due to dissipation. The coherent bunches of trapped particles slow down considerably during this process, which results in significant frequency sweeping. An analytic solution of this type has been constructed for a simple one-dimensional model. This solution suggests an efficient numerical approach to modeling frequency-sweeping events in tokamaks.

*Supported by U.S. DOE Contract DE-FG03-96ER-54326.

GP8 86 Interaction of Electron Holes with Ion Density Perturbations* DAVID L. NEWMAN, MARTIN V. GOLDMAN, NARESH SEN, HAIHONG CHE, *University of Colorado* Kinetic simulations show that electron phase space holes in a homogeneous ion background can persist for long times with little change in speed, shape, or size. Spatial perturbations in the ion density change this situation: Short-scale ion perturbations comparable in length to the size of the holes themselves can degrade the coherence of individual holes. Ion perturbations with much longer scale lengths, however, have a quite different effect, causing holes to accelerate toward density maxima with little degradation. This latter behavior may account for the correlation between the hole spatial location and the location of density maxima observed in two recent 2-D Vlasov simulation studies: In the first case, the perturbations are due to ion-Bernstein waves near double layers in Earth's auroral zone [N. Sen, Ph.D. Thesis, Univ. of Colorado, 2009]. In the second case the density maxima are due to lower-hybrid waves in Buneman-unstable current channels [D. L. Newman and M. V. Goldman, 2008 Fall AGU Meeting, SM31B-1735] inferred from the separatrix region in published PIC simulations of magnetic reconnection. The detailed nature of the interaction of holes and various scale density perturbations will be addressed using 1-D and 2-D Vlasov simulations.

*Research supported by NSF, NASA, and DOE.

GP8 87 Parallel Electric Field in Nonlinear Magnetosonic Waves in Tow- and Three-Component Plasmas SEIICHI TAKAHASHI, YUKIHARU OHSAWA, *Department of Physics, Nagoya University, Nagoya 464-8602, Japan* With theory and electromagnetic particle simulations, we have studied the electric field parallel to the magnetic field, $E_\parallel$, in nonlinear magnetosonic waves in an electron-ion (e-i) plasma and in an electron-positron-ion (e-p-i) plasma. Our theory for the e-i plasma shows that the integral of $E_\parallel$ along the magnetic field, $F = -\int E_\parallel ds$, is given as $eF \sim \epsilon \Gamma_e T_e$ in small-amplitude ($\epsilon \ll 1$) pulses in a warm plasma with electron temperature T_e, where Γ_e is the specific heat ratio. In a cold plasma, it is given as $eF \sim \epsilon^2 m_i v_A^2$, where v_A is the Alfven speed. For the e-p-i plasma, F is large if the positron-to-ion density ratio n_{p0}/n_{i0} is small. These theoretical predictions were verified with simulations. Furthermore, the relation $n_{e0}eF \sim \epsilon(\rho v_A^2 + \Gamma_e p_{e0})(n_{i0}/n_{e0})$ is found to fit fairly well to the simulation results for shock waves with $\epsilon \sim O(1)$ in e-i and e-p-i plasmas, where ρ is the mass density and p_{e0} is the electron pressure. These results indicate that $E_\parallel$ can be strong in nonlinear magnetosonic waves.

GP8 88 Second Harmonics of Reversed Shear TAE in Alcator C-Mod Geometry EUGENE CHEN, HERBERT BERK, BORIS BREIZMAN, LINJIN ZHENG, *IFS, UT Austin* Experiments on Alcator C-Mod, operating with reversed magnetic shear, reveal Toroidal Alfven Eigenmodes (TAE) together with signals at twice the mode frequency. The double frequency signals can be viewed as second harmonic sidebands driven by quadratic non-linear terms in the MHD equations, in analogy with a corresponding theory for Alfven Cascades [1]. However, these nonlinear sidebands have not yet been quantified by any of the existing codes. In this work, we extend AEGIS code [2] to capture nonlinear effects iteratively by treating the nonlinear terms as a driving source in the linear MHD solver. We first compute the TAE mode structure for realistic geometry and q-profile and then use it to find the spatial structure of the second harmonic density perturbation, which can be directly compared with PCI measurements at Alcator C-Mod. [1] H. Smith, B. N. Breizman, M. Lisak and D. Anderson, Physics of Plasmas 13 042504 (2006) [2] L. J. Zheng and M. Kotschenreuther, Journal of Computational Physics 211 (2006) 748-766

GP8 89 Studies of HF-induced Strong Langmuir Turbulence at the HAARP Ionospheric Observatory J.P. SHEERIN, J.M. GERRES, M.R. KEITH, N. ADHAM, A. WITTBRODT, *Eastern Michigan U.* B.J. WATKINS, W.A. BRISTOW, *U. Alaska-Fairbanks* P.A. BERNHARDT, C.A. SELCHER, *NRL* High power HF transmitters may induce a number of plasma instabilities in the interaction region of overdense ionospheric plasma. We report re-

sults from our recent experiments using over one gigawatt of HF power (ERP) to generate and study strong Langmuir turbulence (SLT) and particle acceleration at the HAARP Observatory, Gakona, Alaska. Among the effects observed and studied are: SLT spectra including the outshifted plasma line or free-mode, appearance of a short timescale ponderomotive overshoot effect, collapse, cascade and co-existing spectra, control of artificial field-aligned irregularities (AFAI), the aspect angle dependence of the plasma line spectra, and suprathermal electrons. Mapping the intensity of SLT versus pointing angle, we have discovered a number of regions of strong interaction displaced from the primary HF interaction region. Experimental results are compared to previous high latitude experiments and predictions from recent modeling efforts.

GP8 90 Nonlinear vacuum polarization in intense blackbody radiation and its effects on the radiation spectrum SHELDON WU, FREDERIC HARTEMANN, CRAIG SIDERS, CHRISTOPHER BARTY, *Lawrence Livermore National Laboratory* A study of thermally induced vacuum polarization stemming from the Euler-Heisenberg radiation correction to Maxwell equations is conducted. While nonlinear effects associated with interactions of electromagnetic pulse with a background photon gas had been previously calculated, we examine the possibility of nonlinear corrective terms to the blackbody radiation spectrum. Suitable conditions can be found in both astrophysical and laboratory environments. Inertial confined, ignited thermonuclear plasmas will produce intense blackbody radiation at temperatures in excess of 20 keV. In this theoretical investigation, our analysis shows that in an ideal incoherent blackbody the radiation spectrum is unaffected in the regime studied. This work performed under the auspices of the U.S. Department of Energy by Lawrence Livermore National Laboratory under Contract DE-AC52-07NA27344.

GP8 91 The refraction phenomena in the shock wave dispersion on plasma inhomogenities ANNA MARKHOTOK, *MMA* SVETOZAR POPOVIC, *ODU* Recently we introduced a new mechanism of the shock wave (SW) dispersion on a boundary [1] and then employed it to control the structure of a SW front as it interacts with plasma. Now we consider same effect but under specific conditions on the interface with weak gradients at the interface, but stronger in the bulk. These conditions appear more realistic for most applications, and what is also important, the SW dispersion in this case becomes stronger. We derive all relations using the approach similar to [1]. Then the model applied to calculate the structure of the SW front dispersed on a plasma sphere numerically and compared with the existing experiments. The strength of the effect is demonstrated by comparing results of calculation for different conditions on the interface. Comparative calculations show significant difference in the shock front shapes and they are in complete agreement with the experiments. More results are underway which can contribute to understanding of basic phenomena in weakly ionized gases, combustion, and shock dynamics on the interfaces. [1] A. Markhotok, S. Popovic, L. Vuskovic, Phys. of Plasmas J. **15**, 3 (2008).

GP8 92 Stability Control for High-beta Plasmas on JT-60SA G. MATSUNAGA, M. TAKECHI, S. SAKURAI, S. IDE, M. MATSUKAWA, N. OYAMA, N. AIBA, G. KURITA, *Japan Atomic Energy Agency* A. FERRO, E. GAIO, L. NOVELLO, *Consorzio RFX, Associazione Euratom-Enea sulla fusione* S. SAKASAI, Y. KAMADA, *Japan Atomic Energy Agency* JT-60SA TEAM, JT-60SA is designed and under construction as fully superconducting tokamak under a combined project of the ITER satellite tokamak program of EU-JA (Broader Approach Activities) and the Japanese national program. One of the main purposes of JT-60SA is the steady-state high-beta operation above the ideal no-wall beta-limit with suppressing resistive wall modes (RWMs). In order to control the RWMs, the RWM control coils and error field correction coils (EFCCs) are to be installed. The current design of these coils composes of 18 sector coils (6 coils in toroidally and 3 coils in poloidally) so as to suppress n=1-3 RWMs and to compensate various error fields. The EFCCs can also be utilized to apply the resonant magnetic perturbation to ergodize the peripheral magnetic filed structure to mitigate and avoid the large edge localized modes. The design and analysis of these in-vessel tools for high-beta plasmas on JT-60SA will be presented.

GP8 93 Investigation of equilibrium plasma beta limits in 3D magnetic topologies* MARK SCHLUTT, C.C. HEGNA, *Univ. of Wisconsin* E. HELD, *Utah State Univ.* S.E. KRUGER, *Tech-X Corporation* A fluid model is used to investigate pressure-induced magnetic islands in 3D equilibria. We revisit previous analytic island calculations, allowing for finite parallel heat transport, to find an equation for equilibrium island widths. Finite parallel heat transport can alter the resistive interchange and bootstrap current contributions to magnetic island formation. However, the effect of Pfirsch-Schlüter currents driven by resonant components in $1/B^2$ on magnetic island formation is largely unaffected by transport processes. 3D MHD equilibria are modeled using NIMROD. A vacuum equilibrium helical magnetic field is loaded into the geometry of a straight stellarator. The symmetry of the vacuum field with a dominant magnetic harmonic can be spoiled by adding small magnetic perturbations. These perturbations alter the magnetic spectrum, producing magnetic islands and stochastic regions. Numerical simulations are performed that include a heating source and self-consistent anisotropic transport in different magnetic configurations. The support of pressure gradients in stochastic regions is investigated. The connection between flux surface destruction and the breaching of MHD stability boundaries is also considered.

*Supported by U.S. DOE Grant No. DE-FG02-99ER54546.

GP8 94 Three dimensional Simulations of Self-Organization in a Driven Dissipative Plasma System DASTGEER SHAIKH, B. DASGUPTA, Q. HU, G.P. ZANK, *The University of Alabama in Huntsville,* We perform a fully self-consistent 3-D numerical simulation for a compressible, driven dissipative magneto-plasma driven by large-scale perturbations, that contain a fairly broader spectrum of characteristic modes, ranging from largest scales to intermediate scales and down to the smallest scales, where the energy of the system are dissipated by collisional (Ohmic) and viscous dissipations. Additionally, our simulation includes nonlinear interactions amongst a wide range of ?uctuations that are initialized with random spectral amplitudes, leading to the cascade of spectral energy in the inertial range spectrum, and takes into account large scale as well as small scale perturbation that may have been induced by the background plasma ?uctuations, also the non adiabatic exchange of energy leading to the migration of energy from the energy containing modes or randomly injected energy driven by perturbations and further dissipated by the smaller scales. Besides demonstrating the comparative decays of total energy and dissipation rate of energy, our results show the existence of a perpendicular component of current, thus clearly con?rming that the self-organized state is non-force free.

GP8 95 Kinetic Effects of Energetic Particles on Nonlinear Resistive MHD Stability* R. TAKAHASHI, D.P. BRENNAN, *University of Tulsa* C.C. KIM, *University of Washington* Kinetic effects of energetic particles can play a crucial role in the stability of the 2/1 tearing mode in tokamaks (JET, JT-60U, and DIII-D), where the fraction of energetic particle $\beta_{frac} = \beta_h/\beta$is high. Using model equilibria based on experimental reconstructions, it has been shown that energetic particles have significant damping and stabilizing effects at experimentally relevant $\beta_N$sgβ_{frac}, and S, and weaker damping and stabilizing effects in the ideal unstable regime, and excite a real frequency of the 2/1 mode [1,2]. Initial nonlinear and two-fluid effects are now investigated. A qualitative extrapolation of these results is discussed for what to expect from energetic particle effects on resistive MHD modes in ITER. [1] R. Takahashi, *et al.*, Phys. Rev. Lett. 102, 135001 (2009). [2] R. Takahashi, *et al.*, Nucl. Fusion 49, 065032 (2009).

*Supported by US DOE Grant DE-FG02-07ER54931.

GP8 96 2D Langmuir Maps of Kinked UW-RWM Plasma DAVID HANNUM, MATT BROOKHART, CARY FOREST, ROCH KENDRICK, GABRIEL MENGIN, CARLOS PAZ-SOLDAN, *UW-Madison* The rotating wall machine is a linear screw-pinch built to study the role of different wall boundary conditions on the Resistive Wall Mode (RWM). Its plasma is created by a hexagonal array of seven electrostatic guns. The guns can be biased to discharge up to 1 kA of current each, firing independently or in tandem. The 20 cm diameter, 1.2 m long plasma column is held in place by a 500 G (max) axial guide field. A singletip Langmuir probe inserted from the opposite end of the chamber yields measurements of T_e,n_e and V_p in r and z. Though it is tied to the guns at the cathode end, the plasma column is free to slip over the anode end. At higher plasma currents, the kinking column oscillates past the probe tip. Ensemble averaging of the I-V curves is required to derive reliable Langmuir measurements for these plasmas. I will present 2D Langmuir profiles in configurations scanning the plasma current I_p, guide field B_z, and number of plasma sources (one gun / seven guns).

GP8 97 Resistive Wall Mode Study in a Line-tied Screw Pinch* CARLOS PAZ-SOLDAN, MATTHEW BROOKHART, GABRIEL MENGIN, DAVID HANNUM, ROCH KENDRICK, CARY FOREST, *University of Wisconsin-Madison* Recent studies on the University of Wisconsin - Rotating Wall Machine (UW-RWM) are presented. The device has been constructed to test the hypothesis that the resistive wall mode (RWM) can be stabilized by two differentially rotating solid conducting walls. The RWM can rotate with (or lock to) either the stationary or the moving wall, but not both simultaneously. This allows stabilizing image currents to persist despite finite wall resistivity. This method has application to future breeder blanket designs, with the rotating wall replaced by flowing liquid metal. A rotating wall of 21cm diameter is under construction that will be capable of reaching 6000 rpm. Engineering design and performance of this wall will be presented. The timing and role of the MHD safety factor (q) on the RWM in the static wall case will also be presented. Recent spectroscopic studies of neutral and impurity interactions will be described. The UW-RWM studies the RWM through 120 radial, axial, and azimuthal flux loops in screw pinch geometry 1m long and 20cm across. Discharges up to 7kA can be maintained at flat top for 20ms or ramped by a pulse width modulation scheme.

*Supported by DOE and NSERC (Canada).

GP8 98 Studies of Line-tied Reconnection on the RWM Experiment* M. BROOKHART, C.B. FOREST, D.A. HANNUM, R. KENDRICK, G. MENGIN, C. PAZ-SOLDAN, *University of Wisconsin - Madison* An internal kink instability has been observed to grow and saturate in the Rotating Wall Machine Experiment. Detailed measurements show that an ideal, line-tied kink mode begins growing when the safety factor drops sufficiently below 1 inside the plasma; the saturated state corresponds to a rotating helical equilibrium. In addition to the ideal mode, reconnection events have been observed to periodically flatten the current profile and change the magnetic topology. The reconnection events strongly resemble the reconnection phenomena described in numerical simulations of a nearly identical geometry. Recently, the 2D equilibrium current profile has been measured using an axially and radially scanning magnetic probe so that better comparisons between experiment and theory can be carried out. The measurements show the current channel diffuses radially, inconsistent with Spitzer resistivity. To determine the effect of neutrals on conductivity, neutral fraction is being independently quantified via Hα emission. Future work will involve the construction and installation of a 2D coil array to measure fluctuations in the current at the axial midpoint of the experiment in an effort to characterize the reconnection rate in this inherently 3D geometry.

*Supported by NSF.

GP8 99 Toroidal Mode Coupling in Tokamaks with Anisotropic Viscosity S.E. KRUGER, *Tech-X Corporation* D.P. BRENNAN, *University of Tulsa* E.D. HELD, *Utah State University* C.R. SOVINEC, C.C. HEGNA, *University of Wisconsin-Madison* Most linear and nonlinear theories of toroidal mode coupling of tearing modes in tokamaks [1,2] have used isotropic viscosity. NIMROD's implementation of Braginskii's anisotropic parallel viscosity, however, enables an evaluation of the effect of stress anisotropy on mode coupling for a wide range of collisionality. Numerical simulations with the NIMROD code are used to compare the effect of anisotropy on mode coupling in conditions representing low collisionality. To simplify the analysis, we choose a high aspect ratio, circular cross-section equilibrium. We also present preliminary comparisons with a more complicated coupling of tearing modes with a 1/1 mode using a realistic free-boundary, high beta DIII-D equilibrium [2] R. Fitzpatrick, Nucl. Fusion **33**, 1533 (1993). [3] D.P. Brennan, S.E. Kruger, and R.J. LaHaye, *to be submitted to Physics of Plasmas*

GP8 100 Effects of Electron inertia on the Waves in Hall Magnetohydrodynamics B. DASGUPTA, DASTGEER SHAIKH, G.P. ZANK, *The University of Alabama in Huntsville* Electromagnetic waves in Hall Magnetohydrodynamics (HMHD) exhibit a variety of complex and interesting features. Earlier works have shown the mode conversion of incompressible MHD shear Alfvén wave into a compressible, the fast wave becoming mostly electromagnetic and the slow wave becomes almost a fluid-dynamical wave. These features have been supported partially by numerical simulations of Shaikh & Zank (ApJ,640,L195,2006). Also, recent numerical simulations on solar wind turbulence show some interesting features for the power spectra, like the predominance of Whistler cascades in the range kde $<$ 1, where k is the wave number and de is the electron inertial length. In this work, we first consider the linear dispersion relation for a complete two-fluid plasma with a finite electron mass. We analyze the different branches of the dispersion relation for different ranges of kde, i.e., kde $>$ 1 and kde $<$ 1, in addition to the ranges kdi $>$ 1 and kdi $<$ 1. The wave characteristics,revealing many significant features, are discussed.

GP8 101 Does a contact discontinuity exist within the Hall-MHD model?* ELIEZER HAMEIRI, *New York University, Courant Institute of Mathematical Sciences* The stability analysis of a z-pinch equilibrium state with a surface discontinuity, carried out within the Hall-MHD model (1), indicates that one jump condition across the discontinuity is missing. Indeed, Ref. (1) resorts to an extraneous condition based on mathematical convenience which seems not justifiable physically, with the result of the analysis being very different from equilibrium with continuous profiles albeit with sharp gradients. We attempt to generate the missing jump condition using a variational analysis for the equilibrium state. Surprisingly, the allowed equilibria appears so restricted, that they are practically irrelevant for fusion-related configurations. For example, the total plasma current must vanish. We give further indications for the correctness of this conclusion. (1) U. Schaper, J. Plasma Phys. 30, 169 (1983).

*This work is supported by U.S. Dept. of Energy Grant No. DE-FG02-86ER53223.

GP8 102 Implicit Time Integration Schemes for a Finite Element Two-Fluid Plasma Code BHUVANA SRINIVASAN, URI SHUMLAK, *Aerospace & Energetics Research Program, University of Washington* The two-fluid model consists of the complete Euler equations for the ion and electron fluids and Maxwell's equations for the electric and magnetic fields. Two-fluid effects become significant when the characteristic spatial scales are on the order of the ion skin depth and the characteristic time scales are on the order of the inverse ion cyclotron frequency. In regimes where two-fluid physics is significant, it is necessary to account for the Hall term and the diamagnetic drift term that are missed in single-fluid MHD. WARPX is a finite element code based on the two-fluid plasma model which uses the Runge-Kutta discontinuous Galerkin method. The two-fluid plasma model has characteristic speeds ranging from the fluid sound speeds to the speed of light. As a result, the explicit time stepping schemes have a very restrictive time step governed by either the speed of light or the electron plasma frequency. This provides the motivation to study implicit time stepping schemes for the two-fluid plasma model where accuracy considerations alone determine the time-step.

GP8 103 WAVES AND INSTABILITIES IN BASIC PLASMAS

GP8 104 Linear and nonlinear waves with orbital angular momentum in magnetized plasma SHAHID ALI, *Instituto Superior Tecnico, Lisboa, Portugal* PADMA KANT SHUKLA, *Ruhr Universitat, Bochum, Germany* JOSÉ TITO MENDONCA, *Instituto Superior Tecnico, Lisboa, Portugal* Here we discuss the concept of orbital angular momentum (OAM) for electromagnetic waves in a magnetized plasma. Nonlinear effects of photons with spin and OAM will be considered. In particular, we examine the case of parametric interactions between circularly polarized electromagnetic waves and Langmuir and ion acoustic waves, including the ponderomotive force of light with OAM in magnetized plasma (Shukla & Stenflo, PRA). This will be a generalization of recent results published in PRL by J.T. Mendonca and B. Thide. We also examine the influence of OAM on the magnetic field generation by the inverse Faraday effect.

GP8 105 Wave propagatiom and magnetic field generation in Rydberg plasmas HUGO TERCAS, NITIN SHUKLA, *Instituto Superior Tecnico, Lisboa, Portugal* P.K. SHUKLA, *Ruhr Universitat, Bochum, Germany* J. LOUREIRO, J.T. MENDONCA, *Instituto Superior Tecnico, Lisboa, Portugal* We call Rydberg plasma the weakly ionized gas produced in magneto-optical traps. In such a plasma, the neutral atoms can be excited in Rydberg states. Wave propagation in Rydberg plasmas, and the mutual influence of plasma dispersion and atomic dispersion is considered. New dispersion relations are established, showing new instability regimes and new cut-off frequencies. It is also shown that the ponderomotive force of a large-amplitude electromagnetic wave in Rydberg plasmas can generate quasi-stationary magnetic fields. The present result can account for the origin of seed magnetic fields in ultracold Rydberg plasmas when they are irradiated by the high-frequency electromagnetic wave.

GP8 106 Stability Analysis of Low Frequency Electrostatic Modes in a Large Scale Helicon Plasma in the Presence of Sheared Flows* M. GILMORE, S. XIE, L. YAN, C. WATTS, A.G. LYNN, *University of New Mexico* D.E. NEWMAN, D. SAMMADAR, *University of Alaska - Fairbanks* Experiments in the linear HelCat device, which investigate the nonlinear dynamics of edge fluctuations in the presence of varying flows affected by plasma biasing, show increasingly chaotic behavior as the bias is increased. These experiments have been conducted in a weakly turbulent regime near marginal stability. It is found that as bias is increased, flow shear penetrates into the plasma core from the edge, drift waves (DW's) suppress, and Kelvin-Helmholtz (KH) modes are excited. It is postulated that a 3-dynamical variables-type interaction between the DW, KH and the *local* flow leads to chaotic behavior. Building on a linear theory by Light, *et al* [Phys Plasmas **8**(10), 4675, 2001], a resonant interaction between the mode and the local flow, where mode conversion can occur, is investigated. We report on the linear stability, as well as progress on modelling the plasma with a 2D nonlinear fluid code.

*Work supported by the U.S. D.o.E. Grant no. DE-FG02-04ER54791.

GP8 107 Nonlinear Dynamics under Applied Electrical Field at Magnetized Laboratory Plasma Edge* SHUANGWEI XIE, MARK GILMORE, CHRISTOPHER WATTS, LINCAN YAN, *University of New Mexico* Experiments conducted on a linear helicon plasma (HelCat) device shows evidence of drift wave instability fluctuations, which are suppressed when an increased positive DC electric potential is applied perpendicular to the magnetic field. Simultaneously, a new K-H instability appears, and deterministic chaos also can be observed during this transaction. Measurements show both axial and azimuthal flow speed, as well as Reynolds stress change under the effect of E× B flow shear caused by this external disturbance. When neutral gas pressure is increased during the process, the suppression, requires a higher DC bias, and the K-H transition is not observed. From axial flow measurements, a possible mechanism is suggested from the reduced flow speed which may caused by increased collisions between charged particles and neutrals. Two simple models are presented to predict neutral change with increased gas pressure.

*Work supported by the U.S. D.o.E. under Grant no. DE-FG02-04ER54791.

GP8 108 Parallel shear and turbulence TIFFANY HAYES, MARK GILMORE, CHRISTOPHER WATTS, SHUANGWEI XIE, LINCAN YAN, *UNM* Instabilities may be caused in plasma due to (shear) flow. These flows can be transverse or parallel to the magnetic field. Past work has generally focussed on controlling and understanding the processes that occur from (shear) flow transverse to the magnetic field. At UNM experimental work is being performed in the the HelCat device (Helicon Cathode) to control the parallel flow in order to study and understand the processes that arise from this situation. It is also our aim to be able to control the transverse flow simulatneously, but independently of the parallel flow. By inserting a system of biased rings and grids into the plasma we are able to modify the flows, and hence the turbulence. Flows are measured using a seven-tip Mach probe. Results of our ability to control the flows independently are presented.

GP8 109 The HelCat Helicon-Cathode Device at UNM BRICETTE CYRIN, CHRISTOPHER WATTS, MARK GILMORE, TIFFANY HAYES, RALPH KELLY, CHRISTOPHER LEACH, ALAN LYNN, ANDREW SANCHEZ, SHUANGWEI XIE, LINCAN YAN, YUE ZHANG, *University of New Mexico* The HelCat helicon-cathode device is a dual-source linear plasma device for investigating a wide variety of basic plasma phenomena. HelCat is 4 m long, 50 cm diameter, with axial magnetic field $<$ 2.2 kG. An RF helicon source is at one end of the device, and a thermionic BaO-Ni cathode is at the other end. Current research topics include the relationship of turbulence to sheared plasma flows, deterministic chaos, Alfvén wave propagation and damping, and merging plasma interaction. We present an overview of the ongoing research, and focus on recent results of merging helicon and cathode plasma. We will present some really cool movies.

GP8 110 Spectral diagnostics for the HelCat helicon/cathode linear plasma device CHRISTOPHER LEACH, JAKSA OSINSKI, EDL SCHAMILOGLU, CHRISTOPHER WATTS, *Dept. of Electrical and Computer Engineering, University of New Mexico, Albuquerque, NM 87131-0001* Several new optical spectroscopy diagnostics installed on the HelCat (Helicon-Cathode) device expand the measurement capabilities of the plasma characteristics to include ion temperature, neutral characteristics, as well as alternative and convenient ways to determine drift velocities, temperatures, densities, and species recognition. These are in addition to the numerous probe diagnostics that provide density, potential, temperature, saturation current, and other data for HelCat. A highly directive lens system allow analysis of specific regions of the plasma by a survey spectrometer and a 4m McPherson spectrometer inputted by a compact and finely tunable optical slit input apparatus that allows adjustment along three separate axes. We present an overview of the system design and initial data.

GP8 111 Effects of Biasing and Boundary Conditions on Convective Blobs in Magnetized Laboratory Plasmas* L. YAN, M. GILMORE, C. WATTS, *University of New Mexico* T.A. CARTER, *UCLA* Intermittent convective plasma transport across magnetic field lines ("blobs") has been one of the most important issues in fusion-related edge plasma physics, and is thought to play a key role in cross-field transport in the tokamak scrape-off layer. Fundamental experiments on blobs are being conducted in both the linear LAPD and HelCat devices. HelCat is a 4 m long, 50 cm diameter device with B $<$ 0.22 T and both RF helicon and cathode sources. Blobs are always observed in LAPD and HelCat cathode plasmas. However, blobs are seen in HelCat helicon plasmas only under certain conditions. Biased electrodes (HelCat), and biasing of the cathode with respect to the wall (LAPD), are utilized to affect the sheared ExB flow profiles. Fluctuations, flux, and flows are monitored with probes. Measurements with biasing in both devices show that flow shear is modified at the edge and blob characteristics change. In HelCat, flows and blobs also change with axial and radial boundary conditions.

*Work supported by the U.S. D.o.E. under grant no. DE-FG02-04ER54791.

GP8 112 Observation of Lower-Hybrid Cavitons in Laboratory Plasma* TAKAO TANIKAWA, *Tokai Univ.* TAISEI MOTOMURA, SHUNJIRO SHINOHARA, *Kyushu Univ.* Lower-hybrid (LH) cavitons are localized wave activities trapped inside density depletions whose frequencies are in the range of the lower-hybrid frequency. In order to investigate the relationship between LH cavitons and lower-hybrid solitary structures (LHSS's) observed in space plasmas, we have constructed Tokai Helicon Device (THD) which is a specially designed rf plasma device and utilizes helicon-type discharge with a flat segmented multi-loop antenna [1]. Plasma is produced repetitively ($\sim$ 10 Hz) with a typical discharge pulse duration of $\sim$ 10 ms. A second rf pulse of short duration (a few μs) is injected into an afterglow plasma using the same antenna as used for plasma production. A large amplitude LH wave can be excited at the resonance layer; then density depletion can appear if the condition is right. It can evolve to become an LH caviton. The process has been under investigation. The possibility of particle acceleration due to LH cavitons will be discussed. The characteristics of plasma produced in THD will also be presented. [1] T. Tanikawa *et al.*, Bull. Ameri. Phys. Soc. **51** (7), 164 (2006); T. Tanikawa and S. Shinohara, *ibid.* **53** (14), 174 (2008).

*Work supported by Grant-in-Aid for Scientific Research, Japan.

GP8 113 Wave Characteristics of Large-Diameter, High-Density Helicon Plasma with Short Axial Length II* TAISEI MOTOMURA, SHUNJIRO SHINOHARA, *Kyushu Univ., Japan* TAKAO TANIKAWA, *Tokai Univ., Japan* KONSTANTIN P. SHAMRAI, *INR, Ukraine* We have demonstrated that a large-diameter, high-density ($\geqslant$ 10^{12} cm^{-3}) helicon plasma can be produced in a low aspect ratio (the ratio of the axial length L to the diameter R; in our case, R =73.8 cm and 5.5 cm $\leqslant L \leqslant$ 35 cm) device using a flat spiral antenna (4-turn, 43 cm in diameter) installed just outside the quartz-glass window at one end of the device [1]. As a first step to understand the role of helicon waves in the discharge process, helicon wave characteristics in plasma has been investigated in detail [2]. It has been found that discrete axial eigenmodes, whose characteristics depend on the plasma density profile and the axial boundary conditions, exist in the excited helicon wave. The effects of the background magnetic field profile and the rf input power on the excited wave have also been examined in detail. [1] T. Motomura *et al.*, J. Plasma Fusion Res. Ser., in press. [2] T. Motomura *et al.*, Bull. Ameri. Phys. Soc. **53** (14), 175 (2008).

*Our experiments were carried out at ISAS/JAXA. Work supported by Grant-in-Aid for Scientific Research, Japan as well as ISAS/JAXA.

GP8 114 Adiabatic invariance for eigenmodes and continuum modes in nonuniform plasmas MAKOTO HIROTA, SHINJI TOKUDA, *Japan Atomic Energy Agency* Adiabatic invariance of wave action is investigated for general eigenmodes and continuum modes by exploiting the variational principle for linearized dynamical systems. This theory applies to various dissipationless plasma models and serves to explain quasi-linear evolution of modal behavior, for which the standard eikonal limit is not always suitable. Given a sufficiently slow evolution of the background fields, the wave action (or the action variable) attributed to each mode is conserved as long as the corresponding discrete or continuous spectrum is isolated from other spectra and zero frequency. The resonant coupling allows exchange of wave action among these modes. The invariance of wave action is demonstrated for the case of Alfvén and sound resonances in the MHD model, which leads to a new wave-quantum interpretation of the continuum damping and the resonant growth. The sign of the wave action generally determines whether the resonant instability occurs or not.

GP8 115 EMIC Wave Characteristics and Their Effects on the Lifetime of Energetic Electrons in Earth's Inner Radiation Belt X. SHAO, K. PAPADOPOULOS, A.S. SHARMA, A. KARAVAEV, *Univ. of Maryland* The stably trapped electrons with energies ($>$ 100 keV) in inner radiation belt have lifetimes of years and can have serious effects on spacecrafts and satellites. One possible way of mitigating these hazards is to reduce electron life times through pitch angle scattering by waves. At frequencies close to the ion gyro-frequencies, the Electromagnetic Ion-Cyclotron (EMIC) waves can have wavelengths short enough to gyro-resonate with energetic electrons, which can lead to significant changes in lifetimes of electrons in inner belt. We investigated the lifetime of inner belt energetic electrons subject to pitch angle scattering with EMIC waves by calculating the diffusion coefficient. For several hundred Watts of broadband EMIC waves in the shell volume enclosed by magnetic field lines at L = 2.0 with width dL = 0.1, the lifetime of 1 MeV electrons can be reduced to a few months. This is a considerable reduction and has important consequences, including remediation of artificially enhanced energetic electron fluxes. The key issues to be investigated further are: the validity of the model of excitation and propagation of EMIC wave in a multi-ion plasma with non-uniform ambient magnetic field, the energy conversion between EMIC waves and multi-ion plasma. These are addressed by the comparing models and laboratory experiments. The work was sponsored by ONR MURI grant.

GP8 116 Pitch Angle Scattering of Energetic Particles by Waves Generated from a Rotating Magnetic Field Source A. KARAVAEV, X. SHAO, A.S. SHARMA, K. PAPADOPOULOS, N.A. GUMEROV, *Univ. of Maryland* A. GIGLIOTTI, W. GEKELMAN, *UCLA Dept. Physics* Injection of whistler waves into Earth's inner radiation belt to enhance precipitation of energetic electrons has been an active research area. Most mechanisms of pitch angle scattering of energetic particles are based on gyro-resonant wave-particle interaction. Recent experiments and simulations show that Rotating Magnetic Field (RMF) antennas in plasmas can be efficient radiation sources of MHD and whistler waves. In experiments conducted in the Large Plasma Device at UCLA, poly-phased current loops drove the RMF antenna. These experiments and simulations show that 75-85% of the radiation generated is in guided propagation. The waves have non-local magnetic field gradients in the transverse direction and these provide ways to break the adiabatic invariants of electrons and precipitate them via a non-resonant scattering. Here we present simulations of non-resonant pitch angle scattering of particles by waves generated by RMF sources. EMHD simulations are used to model whistlers and the resultant EM fields are used in particle tracing codes to study pitch angle scattering. The simulations are conducted for a wide range of wave magnetic fields, including fields much larger than the ambient magnetic field in space plasma environments. The work was sponsored by ONR MURI grant.

GP8 117 Experiments on the scattering of fast electrons by Alfvén waves* ALEX GIGLIOTTI, WALTER GEKELMAN, PATRICK PRIBYL, YUHOU WANG, *UCLA Dept of Physics* ALEXEY KARAVAEV, XI SHAO, DENNIS PAPADOPOULOS, *Univversity of Maryland* High energy ions and electrons with anisotropic distribution functions can be trapped in the earth's radiation belts for months, which pose a danger for satellites. A electron population with large $v_\perp$ and was introduced in the afterglow of the background LAPD plasma ($n_e = 2.0e^{11}cm^{-3}$, $T_e = .25eV$).Microwaves at 2.45 GHz were launched into the plasma at an axial and radial location where $f_{micro} = f_{UH}$. A small (2 cm dia) electron hot spot was generated. Shear Alfvén waves (f = 192 kHz) launched by an orthogonal loop antenna, with magnitude $B_{wave} \sim 2G$ destroyed the hot spot within 10 cycles. The hot spot returns when the Alfven wave is shut off. Space-time evolution of the plasma density, flow and electron are presented. The mechanism of the electron de-trapping is under investigation. Planned experiments involve the interaction of fast ion rings with shear Alfvén waves, and whistler waves with the anisotropic electrons.

*This work supported by The Office of Naval Research under a MURI award

GP8 118 Direct Measurement of the Impedance of a Dipole Antenna* PATRICK PRIBYL, WALTER GEKELMAN, *UCLA Dept of Physics* ALEX GIGLIOTTI, *UCLA, Dept Physics* The impedance of a dipole antenna radiating whistler waves has been determined by measuring the current and voltage directly at the antenna tips. The experiment was done at the Large Plasma Device at UCLA. The antenna was immersed in a magneto-plasma at the background magnetic field and plasma density, were both varied. The impedance was measured as a function of f_{pe}/f_{ce}. The standard technique is to measure forward and reflected power at the driven end of the probe shaft, and backing out transmission line properties and system reflections and resonances. Doing this accurately involves detailed knowledge of the circuit and transmission line properties associated with the antenna. The alternate technique we present is advantageous in that we can determine the impedance directly, accurate to zeroth order with transmission line effects only entering as corrections. Data of the radiation impedance from the lower hybrid frequency to higher than fce/2 will be presented.

*This work supported by The Office of Naval Research under a MURI award.

GP8 119 Non-localized waves in a magnetized argon plasma column* A. DUBOIS, A. EADON, E. THOMAS, *Auburn University* The Auburn Linear EXperiment for Instability Studies (ALEXIS), a 170 cm long, 10 cm diameter plasma column, has been used for studies of sheared flows in plasmas. These flows

play an important role in plasma stability and have led to observations of spatially localized ion cyclotron waves. In new experiments reported in this presentation, observations have been made of non-localized, low frequency waves in Argon plasmas. These waves are observed to extend over the entire radius of the column and vary with neutral gas pressure and magnetic field strength. Probe measurements of plasma parameters, such as plasma potential, density, and electron temperature, in various magnetic field strengths, will be presented. Initial data suggests these low frequency waves are driven by gradients in the density profile.

*This work is supported by US Dept. of Energy Grant Number: DE-FG02-00ER54476

GP8 120 Effect of sheared flows on different gas species in a magnetized plasma column* ASHLEY EADON, AMI DUBOIS, EDWARD THOMAS, *Auburn University* Transverse and parallel sheared flows are important topics in both space and fusion plasmas, and have been the subjects of extensive study. In an effort to understand the plasma response to these flows across a large parameter space, a series of coordinated multi-scale experiments is being performed on three different devices that span the space (Space Plasma Simulation Chamber, SPSC) to fusion (Compact Toroidal Hybrid, CTH stellarator) regimes. The Auburn Linear EXperiment for Instability Studies (ALEXIS) is a 170 cm long, 10 cm diameter linear magnetized, rf generated plasma column, and acts as the "bridge" between the space and fusion devices. Multiple gas species (He, N, Ar) are being evaluated to determine the ideal combination of gas, magnetic field strength, and imposed electric potential structure to best study the plasma response to sheared flows of many different scale sizes. Measurements will be presented on the correlation between different low frequency wave features and the electric field structure in the plasma.

*This work supported by the US Dept. of Energy, grant number: DE-FG02-00ER54476.

GP8 121 Measurements of electric field induced fluctuations in the Compact Toroidal Hybrid stellarator* M. CIANCIOSA, E. THOMAS, B.A. STEVENSON, G. HARTWELL, S. KNOWLTON, *Physics Department, Auburn University* Sheared flows arising from spatially inhomogeneous, transverse electric fields are of interest in space, laboratory and fusion plasmas. In fusion plasmas strongly sheared flows at the plasma edge can lead to a reduction of core fluctuations and enhanced core plasma parameters. The effects of sheared flows on plasmas in the Compact Toroidal Hybrid (CTH) stellarator (R_0 = 0.75 m, a $\sim$ 0.2 m, $B_0 \leq$ 0.7 T, $\bar{n}_e$ = 0.2 – 1.5 x 10^{19} m^{-3}), are studied using a biased electrode inserted into the edge plasma to alter the radial profile of the electric potential. The enhancement or suppression of fluctuations associated with the application of different applied potentials and electric fields is measured with a triple probe. Results will be presented for different biased limiters – one with a single-tip and another with two axially-separated, individually biased electrodes.

*Supported by US DOE Grant DE-FG02-00ER54476.

GP8 122 Laboratory Studies of Electromagnetic Velocity Shear-Driven Instabilities ERIK TEJERO, *Global Strategies Group (NA), Inc. and Auburn University* WILLIAM AMATUCCI, GURUDAS GANGULI, *Naval Research Laboratory* EDWARD THOMAS, *Auburn University* Observations of low frequency, electromagnetic ion cyclotron waves have been made in many regions of the space environment. Many theoretical mechanisms have been presented to account for these waves and the resulting transversely accelerated ions. Sheared flows produced by localized electric fields coupled with a perpendicular magnetic field are a potentially important energy source that can create waves of this type. *In situ* observations of sheared plasma flows collocated with electromagnetic wave activity have led to a laboratory effort to investigate the impact of electromagnetic, velocity shear-driven instabilities on the near-Earth space plasma dynamics. Under scaled ionospheric conditions in the NRL Space Physics Simulation Chamber, the transition from electrostatic to electromagnetic ion cyclotron wave propagation is being investigated. Results from experiments to characterize instability threshold and wave dispersion characteristics will be presented. Work supported by the Office of Naval Research.

GP8 123 Experimental Investigation of Whistler Wave Propagation in the NRL SPSC* DAVID BLACKWELL, WILLIAM AMATUCCI, GURUDAS GANGULI, GEORGE GATLING, *US Naval Research Lab* CHRISTOPHER COMPTON, CHRISTOPHER COTHRAN, ERIK TEJERO, DAVID WALKER, *Global Strategies Group North America, Inc.* Recent results of whistler wave propagation experiments in the Space Physics Simulation Chamber facility at the Naval Research Lab are presented. The full spectrum of whistler waves up to the electron cyclotron frequency cutoff is explored. Changing antenna near and far field radiation patterns are compared to varying transmitter power and plasma parameters. Transitions between helicon-like perpendicular long wavelength modes and short wavelength parallel whistler modes are clearly evident. These results are compared with transmitted antenna power measurements vs. frequency for recommendations of optimum operating conditions and antenna design. The background spectrum of whistlers excited by a filament plasma source and the interaction of driven whistlers with this spectrum is also explored. The waves are driven and detected using balanced dipole and loop antennas which measure the amplitude and phase of the wave in two dimensions (r and z). The magnetic field is varied from a few Gauss to 200 Gauss, with the density variable over three decades from 10^7-$10^{10}$$cm^{-3}$.

*Work supported by ONR.

GP8 124 Laboratory Investigation of Whistler and Lower Hybrid Wave Propagation* B. AMATUCCI, D. BLACKWELL, G. GANGULI, G. GATLING, *Naval Research Lab* C.D. COTHRAN, D. WALKER, *Global Strategies Inc.* An experimental investigation of the generation and propagation of waves on the whistler/lower hybrid branch is underway in the NRL Space Physics Simulation Chamber. The plasma conditions have been scaled to the inner magnetosphere. These studies are carried out in both homogeneous plasma and plasma containing density structuring. In homogeneous plasma, resonance cone propagation of the waves is observed, consistent with theoretical predictions. In plasma containing a density depletion layer, wave ducting within the layer has been observed. Experimental results on the observed whistler/lower hybrid wave propagation characteristics will be presented.

*Work sponsored by the Office of Naval Research.

GP8 125 Determining plasma potential from rf measurements using an impedance probe* DAVID WALKER, *Global Strategies Group,Inc* RICHARD FERNSLER, DAVID BLACKWELL, WILLIAM AMATUCCI, *Naval Research Laboratory* By using rf techniques with plasma probes in laboratory experiments we have demonstrated the existence of collisionless resistance in the sheath

of a spherical probe, shown that this leads to a method of finding the electron sheath density profile, and proposed a method of measuring electron temperature using the rf results.[1] Most recently we are able to determine plasma potential and the electron distribution function from the rf measurements, the latter requiring only a first derivative of the inverse ac resistance with respect to bias. The technique has general application to diverse areas of plasma investigations in the laboratory, or in space plasma measurement application. It can be used with *in situ* instrumentation itself and can be extended to provide an estimate of the sheath structure for arbitrarily shaped surfaces. Because the magnitude of the applied signal used is much smaller in magnitude than typical applied dc potentials, it is transparent to the existing plasma/probe interface.

*This work supported by the Office of Naval Research.

[1]Walker, D.N., R.F. Fernsler, D.D. Blackwell, W.E. Amatucci, *Phys of Plasmas*, **15**, 123506 (2008)

GP8 126 Particle-in-Cell simulation of energetic particles driven instabilities* YANG CHEN, SCOTT E. PARKER, *University of Colorado at Boulder* JIANYING LANG, GUOYONG FU, *PPPL* We present simulations of the evolution of energetic particles driven modes with the gyrokinetic turbulence code GEM[1], except that kinetic electrons are replaced by a mass-less fluid model. PIC simulations of energetic particles use either the conventional full-f method or the δf method. The latter is adequate for low-amplitude fluctuation amplitudes. The collisional δf-method[2] is used to systematically account for collisions and particle source and sink. Steady state saturation amplitudes are benchmarked with predictions of analytic theory. We also employ full-f simulations[3] to study bursty events in which the instabilities reach large amplitudes and cause macroscopic redistribution or loss of the particles. With full-f it is easy to retain all the nonlinear effects and treat accurately discontinuities in the distribution function at phase-space boundaries. Whereas the energetic particle current is neglegible in the Ampere's law in δf simulations, it is important in full-f simulations. Thermal ion kinetic effects are observed to be important.

*Work supported by DOE Plasma Energetic Particles Simulation Center.

[1]Y. Chen and S. E. Parker, J. Comp. Phys. **220**, 839 (2007)
[2]Y. Chen and R. White, Phys. Plasmas **4**, 3591 (1997)
[3]Y. Todo *et. al*, Phys. Plasmas 10, 2888 (2003)

GP8 127 Geodesic Acoustic Modes Induced by Energetic Particles TIANCHUN ZHOU, HERBERT BERK, *IFS, The University of Texas at Austin* A global geodesic acoustic mode driven by energetic particles (EGAM) has been observed in JET[1, 2] and DIII D[3, 4]. The mode is to be treated fully kinetically. The descriptions of the background electrons and ions are based on standard high and low bounce frequency expansion respectively with respect to the mode frequency. However, the energetic ions must be treated without any expansion of ratio between their bounce frequency and the mode frequency since they are comparable. Under electrostatic perturbation, we construct a quadratic form for the wave amplitude, from which an integro-differential equation is derived. In the limit where the drift orbit width is small comparison with the mode width, a differential equation for perturbed electrostatic field is obtained. Solution is obtained both analytically and numerically. We find that beam counterinjection enhances the instability of the mode. Landau damping due to thermal species is investigated.

GP8 128 Anomalous Resistivity Generated By Ion Acoustic Instabilities in Weakly Collisional Plasmas C. BLACK, A. BHATTACHARJEE, K. GERMASCHEWSKI, *University of New Hampshire* C.-S. NG, *University of Alaska Fairbanks* The anomalous resistivity associated with the current-driven ion-acoustic instability has been proposed as a mechanism for magnetic reconnection, and other forms of transport and dissipation. Recently, it has been shown that the underlying eigenmode spectrum of weakly collisional plasmas in the limit of small collisions is fundamentally different from that of collisionless plasmas [C. S. Ng, A. Bhattacharjee, and F. Skiff, Phys. Rev. Lett. 83, 1974 (1999)]. This raises the question of how quasilinear predictions of anomalous resistivity derived from the Vlasov equation differ from those obtained from a weakly collisional theory, even in the limit of zero collisions. We have reformulated traditional quasilinear theory for the Vlasov equation by including the Lenard-Bernstein collision operator. We compare the predictions of quasilinear theory with simulation results obtained from a code which integrates the kinetic Lenard- Bernstein equation coupled to the Poisson equation. We compare our results with classical estimates given by Sagdeev in the absence of collisions, and extend these estimates to the collisional regime. Comparisons will be made also with other numerical studies in the collisionless regime.

GP8 129 Study of Toroidicity-Induced Alfvén Eigenmodes on the Madison Symmetric Torus J.J. KOLINER, C.B. FOREST, S. OLIVA, J.K. ANDERSON, J.S. SARFF, A.R. ALMAGRI, *University of Wisconsin - Madison* D. SPONG, *Oak Ridge National Laboratory* Alfvén waves are likely of fundamental importance in the reversed-field pinch (RFP). The large magnetic fluctuations are expected to inject energy into Alfvén modes, and their subsequent cascade to shorter wavelengths may drive ion heating. A new effort is in progress to understand toroidicity-induced Alfvén eigenmodes (TAE's) through their structure, driving terms and damping mechanisms on the MST. Coupling of multiple eigenmodes can introduce undamped TAE's with frequencies from hundreds of kHz up to the cyclotron frequency at over 2 MHz. These modes can also become unstable by inverse Landau damping due to fast ions, a condition pertinent to neutral beam injection heating on MST and fusion alpha particles in future RFP devices. Frequencies of weakly damped modes have been calculated by solving a 3D partial differential equation that describes shear Alfvén dynamics numerically based on MST equilibrium conditions. To excite the calculated modes, a single strap poloidal antenna connected to a 1 kW broadband amplifier will be employed. An array of 64 toroidally distributed magnetic pickup coils will be utilized synchronously to resolve power spectra and mode numbers in the relevant range of frequencies.

GP8 130 Waves for Alpha-Channeling in Mirror Machines ANDREY ZHMOGINOV, NATHANIEL FISCH, *Princeton University* Alpha-channeling is a technique for extracting energy from alpha particles and using it to sustain fusion reaction by means of using waves to control the particle dynamics. The rough optimization of the energy transfer efficiency with respect to rf region parameters performed earlier for a mirror machine suggested that up to 60% of alpha particle energy can be redirected to fuel ions. However, the limitations on the wave parameters imposed by plasmas were not previously considered. Using kinetic plasma dispersion relation and assuming quasi-longitudinal, or quasi-transverse wave propagation, we systematically search for modes which can be used to extract alpha particle energy in mirror plasmas. This

method is further used to identify such modes in several device designs including the LAPD experiment. Since the damping rate of the suitable modes on fuel ions is small compared to the damping rate on electrons, coupling the identified modes to the waves in the plug is shown to be a mechanism which can potentially increase the effective reactivity of tandem mirrors.

GP8 131 Stimulated Raman scattering of a laser pulse in magnetized plasma SUKHDEEP KAUR, A.K. SHARMA, *Indian Institute of Technology, Delhi, India* A Gaussian laser beam propagating through a magnetized plasma pushes the plasma radially outward, creating a plasma channel. The channel guides and self focuses the laser. However, the channel is susceptible to Stimulated Raman back Scattering. In this process laser couples to a space charge mode to produce the frequency downshifted electromagnetic side band and the laser exert a ponderomotive force on the electrons, driving the space charge mode. The nonlocal effects reduce the growth rate or the Raman process.

GP8 132 Electric Field Measurements in a Helicon Source Based on Stark Splitting of Neutral Helium Lines STEPHANIE SEARS, SAIED HOUSHMANDYAR, JERRY CARR, MATTHEW GALANTE, KATHERINE TALLAKSEN, SAIKAT CHAKRABORTY THAKUR, EARL SCIME, *West Virginia University* For laser injection along the axial magnetic field, splitting of the 587.56 nm line of neutral helium has been observed during laser-induced-fluorescence experiments in a helicon plasma source. In a radially uniform region of magnetic field, the line splitting is localized to within $\pm$ 1 cm of the axis of the device. The spatial localization and independence of magnitude of the splitting on the source magnetic field strength rule out Zeeman splitting as an explanation for the observations. When compared to previous measurements of Stark splitting of the 587.56 nm He I line [*Ritschl,* 1934], the observed line splitting suggests electric field strengths on the order of kV/cm. Here we report measurements of the observed line splitting (and absolute shifts) as a function of neutral pressure, plasma density, plasma density profile, and magnetic field strength. Similar measurements are presented for the nearby, but weaker, He I line at 587.60. This work was supported by NSF award PHY-0611571.

GP8 133 Cavity Ring Down Spectroscopy measurements of Ar-II velocity distribution functions SAIKAT CHAKRABORTY THAKUR, JERRY CARR JR., EARL SCIME, *West Virginia University* The WVU helicon source group routinely uses laser induced florescence (LIF) to measure the ion velocity distribution function (ivdf) of argon plasmas. We are constructing a continuous wave Cavity Ring Down Spectroscopy (cw-CRDS) system that will provide an alternate approach to measuring the ivdf. CRDS is a proven, ultra-sensitive, laser absorption technique that will provide sufficient resolution to measure the Doppler broadened absorption line of Argon and other plasma species. We will use a CW tunable diode laser at 668.43 nm, pumping the Ar-II metastable $3d^4F_{7/2}$ level to the $4p^4D_{5/2}$ level, to gather data from our steady state, high density, helicon plasma source CHEWIE (the Compact HElicon Waves and Instabilities Experiment). The cw-CRDS data will then be compared to LIF measurements. Once optimized for the Ar-II transition, we will use a similar experimental configuration to complete the difficult measurement of the ivdf for He-II transition at 1012.36 nm. This report will present completed design schematics for the CRDS system as well as initial data gathered through the early stages of operation.

GP8 134 Comparison of Particle in Cell Simulations of Double Layers in a Xe-Ar Helicon Plasma with Experimental Results ALEXANDER HANSEN, I.A. BILOIU, E.E. SCIME, *West Virginia Univ. Physics Dept.* A. MEIGE, *Ecole Polytechnique* Recent experiments in plasma sheaths at grounded boundaries confirmed theoretical predictions that in a multi-ion species plasma presheath, ions do not accelerate up to their own Bohm, i.e., sound, speed in the presheath but instead accelerate up to a common bulk sound speed at the sheath-presheath boundary. Those ion speed measurements were obtained in argon plasmas doped with lighter helium and in xenon plasmas doped with lighter argon. Since the double layer (DL) that forms in expanding helicon source plasmas is essentially a plasma sheath in the plasma volume instead of at the plasma boundary, it was expected that similar effects would be observed in the DL presheath. However, in preliminary experiments on the HELIX device at West Virginia University [Biliou, Ph.D. thesis, WVU], we have found that addition of a small amount of argon in xenon plasma DL experiments suppresses formation of the DL in xenon plasmas. In order to understand this observation, we have performed simulations using a particle-in-cell code with Monte Carlo collisions, [Meige *et al.*, *PoP* (2005)] which we have modified to handle the presence of two ion species in the plasma. We present results from the simulation for unmixed argon and xenon plasmas, for mixed argon and xenon ions, and compare the results with those from the experiment.

GP8 135 Time Resolved Studies of Ion Beam Formation in Pulsed Helicon Argon Plasma* JERRY CARR JR., SAIKAT CHAKRABORTY THAKUR, ALEX HANSEN, SAEID HOUSHMANDYAR, STEPHANIE SEARS, EARL SCIME, *West Virginia University* WEST VIRGINIA UNIVERSITY PLASMA TEAM, Previous laser induced fluorescence (LIF) measurements of the parallel ion velocity distribution function (ivdf) in expanding, steady-state, argon helicon plasma demonstrated the existence of an accelerated population of ions co-existing with a stationary ion background. Downstream of the expansion region, a clear ion beam (evidence of a double layer) is seen only for source frequencies greater than a critical frequency. To investigate the ion beam formation, the plasma is pulsed at 5 Hz with a 50% duty cycle. The parallel ivdf, obtained with high time resolution LIF, and electrostatic fluctuations are measured both upstream and downstream at several plasma frequencies. At lower frequencies, large electrostatic instabilities appear and the ion beam vanishes. Below the critical frequency, large electrostatic instabilities are observed after the ion beam begins to appear in the LIF measurements. The beam vanishes and the electrostatic fluctuations decay later in the discharge. Above the critical frequency, we observe a less energetic beam and no electrostatic fluctuations.

*Jerry Carr Jr. would like to acknowledge the NASA WV Space Grant for their support of this work.

GP8 136 Propagation of Alfvén Waves from Kinetic to Inertial Regimes in a Helicon Plasma Source SAEID HOUSHMANDYAR, EARL SCIME, *West Virginia University* Ion heating by Alfvén waves is an active area of research in both laboratory and space plasma physics. As new instruments have enabled more detailed exploration of the solar corona (e.g. *Hinode* spacecraft, *Science*, Dec. 2007), the evidence in support of significant role of Alfvén waves in coronal ion heating continues to accumulate. Due to their high density, helicon sources can be employed for coronal plasma studies (e.g., $\beta_{HELIX}/\beta_{Corona} \cong 0.1 - 1$). However, the

non-uniform electron density and temperature profiles of helicon sources ($\bar{\beta} = \beta_{HELIX} m_i/v_A)^2 m_e = (v_{th-e}/v_A)^2 = 0.1 - 20$) lead to kinetic and inertial regimes in Alfvén wave propagation. As showed by Vincena *et al.* (PRL, **93**, 105003, 2004), the accumulation of magnetic field energy at the kinetic-inertial boundary results from a turning point in the perpendicular group velocity. Here we present observation of Alfvén waves in HELIX (Hot hELIcon eXperiment) launched by a dipole antenna whose axis is aligned along the background magnetic field. The waves are excited at sub-cyclotronic frequencies within the high density region of a helium plasma. Profile measurements of the wave amplitude show evidence of ducting of the waves along the high density core of the plasma as well as wave energy accumulation at the kinetic-inertial boundary. Furthermore, phase and group velocities measurements are also compared to Alfvén wave dispersion models.

GP8 137 Kinetic correlations in driftwave fluctuations* FRED SKIFF, VIKRAM PATEL, *University of Iowa* SHUNJIRO SHINOHARA, *Interdisciplinary Graduate School of Engineering Sciences, Kyushu University* We report measurements of kinetic fluctuations in dissipative driftwave fluctuations in a uniformly magnetized plasma cylinder. A singly ionized CW Argon plasma produced by an inductive plasma source is probed using two independent diode-laser based laser-induced fluorescence systems operating on transitions from separate metastable states (transitions at 668nm and 1047nm). The ions are weakly collisional in the $n = 10^9$ cm^{-3}, Te=2 eV,Ti=0.1 eV plasma with a neutral pressure of 2x10^{-4} Torr. Earlier measurements have been made using a single laser beam and were therefore limited to correlations at the same ion velocity. Here we look at the use of two laser beams, as well as the fast wavelength scanning of a single laser, to detect correlations between ions at different velocities parallel to the confining magnetic field. Tests are performed to explore correlations due to optical pumping (which are clearly observed at high laser power between the metastable magnetic sublevels). Of particular interest is the correlation width in velocity space, which pertains to the effective degrees of freedom of the plasma.

*Work supported by US Department of Energy Grant DE-FG02-99ER54543.

GP8 138 Frequency Domain Nonlinear Energy Transfer Study in a Laboratory Plasma M. XU, G.R. TYNAN, C. HOLLAND, Z. YAN, S.H. MULLER, J.H. YU, *University of CA, San Diego* We report here the experimentally measured internal and kinetic nonlinear energy transfer rates in a linear plasma device CSDX (Controlled Shear Decorrelation Experiment) using a recently developed technique [1]. The results clearly show net kinetic energy transfer from turbulence to zonal flows, thus directly show the turbulence-driven mechanism of shear flows. In addition, it was found that the radial flux of vorticity is dominantly responsible for the redistribution of kinetic turbulent energy among different frequencies (or different scales). Combined with published results [2], we know that it plays dual roles: the spreading of momentum in configuration space and the spreading of energy among different scales. The bicoherence was also computed, which shows that the phase coherence between zonal flows and turbulence plays an important role in the nonlinear energy transfer from turbulence to zonal flows. We also report the results from linear eigenmode stability analysis based on the Hasegawa-Wakatani model. Despite the use of flat profiles of electron temperature, ion viscosity, etc., it shows that the first two radial eigenmodes n=1 and n=2 are linearly unstable at the typical CSDX condition, suggesting that these two radial eigenmodes are the driving source for zonal flows. [1] M. Xu et al, Phys. Plasmas 16 042312 (2009). [2] Holland C et al, Phys. Rev. Lett. 96 195002 (2006)

GP8 139 Search for chaos in the transition to drift wave turbulence M.J. BURIN, J.A. NOGUEZ, *CSU San Marcos* G.R. TYNAN, S.H. MULLER, M. XU, *UCSD* In the transition to fully developed turbulence one may encounter chaotic regimes, as has been demonstrated both theoretically and experimentally in a variety of flows, including within magnetized plasmas. Such regimes appear as windows of low-dimensional order, allowing for a better understanding of the underlying nonlinear dynamics, which may in turn allow for new avenues of control. We have recently begun a study of the turbulent transition in the Controlled Shear Decorrelation Experiment (CSDX), a helicon-powered magnetized plasma column at UCSD, in light of chaotic signatures such as the maximum Lyapunov exponent as derived from Langmuir probe time-series. We report our preliminary results on the role of chaos in the transition in general and with respect to the emergence of a self-organized shear layer (zonal flow) in particular.

GP8 140 Temperature and Density Measurements in Low Density, Magnetized Plasmas Using a Multipass Thomson Scattering Cavity DEREK SCHAEFFER, CARMEN CONSTANTIN, NATHAN KUGLAND, ERIK EVERSON, CHRISTOPH NIEMANN, *University of California, Los Angeles* CHRIS EBBERS, SIEGFRIED GLENZER, *Lawrence Livermore National Laboratory* We present experiments to study the temperature and density in low density, magnetized plasmas in UCLA's Large Plasma Device (density $\sim 10^{12}$ cm^{-3}, temperature $\sim$ 5 eV) using a single-shot multipass Thomson scattering cavity with small scattering parameter alpha (non-collective regime). We frequency double the Phoenix laser (1064 nm, 10 J, 5 ns) to a 532 nm probe beam and send the beam $\sim$ 20 times through the target point in an image-relayed cavity, with the resulting mulitpassed beam yielding an effective probing energy of $\sim$ 100 J over $\sim$ 100 ns. The data will be compared to Langmuir probe measurements to characterize the ambient plasma and the setup will be used in future experiments to characterize exploding plasmas.

GP8 141 Experimental and Numerical Study of Drift Alfvén Waves in LAPD BRETT FRIEDMAN, P. POPOVICH, T.A. CARTER, D. AUERBACH, D. SCHAFFNER, *UCLA* We present a study of drift Alfvén waves in linear geometry using experiments in the Large Plasma Device (LAPD) at UCLA and simulations from the Boundary Turbulence code (BOUT). BOUT solves the 3D time evolution of plasma parameters and turbulence using Braginskii fluid equations. First, we present a verification study of linear drift Alfven wave physics in BOUT, which has been modified to simulate the cylindrical geometry of LAPD. Second, we present measurements of density and magnetic field fluctuations in the LAPD plasma and the correlation of these fluctuations as a function of plasma parameters, including strength of the background field and discharge current. We also compare the measurements to nonlinear BOUT calculations using experimental LAPD profiles.

GP8 142 Drift wave turbulence simulations in LAPD P. POPOVICH, *UCLA* M. UMANSKY, *LLNL* T.A. CARTER, D.W. AUERBACH, B. FRIEDMAN, D. SCHAFFNER, S. VINCENA, We present numerical simulations of turbulence in LAPD plasmas using the 3D electromagnetic code BOUT (BOUndary Turbulence). BOUT solves a system of fluid moment equations in a

general toroidal equlibrium geometry near the plasma boundary. The underlying assumptions for the validity of the fluid model are well satisfied for drift waves in LAPD plasmas (typical plasma parameters $n_e \sim 1 \times 10^{12}\text{cm}^{-3}$, $T_e \sim 10\text{eV}$, and $B \sim 1\text{kG}$), which makes BOUT a perfect tool for simulating LAPD. We have adapted BOUT for the cylindrical geometry of LAPD and have extended the model to include the background flows required for simulations of recent bias-driven rotation experiments. We have successfully verified the code for several linear instabilities, including resistive drift waves, Kelvin-Helmholtz and rotation-driven interchange. We will discuss first non-linear simulations and quasi-stationary solutions with self-consistent plasma flows and saturated density profiles.

GP8 143 Resonant Drive and Suppression of Unstable Drift-Alfvén Waves Using Alfvénic Quasimodes D.W. AUERBACH, S. VINCENA, T.A. CARTER, P. POPOVICH, B. FRIEDMAN, D. SCHAFFNER, *UCLA* We report here on the interaction between antenna-driven quasimodes and pressure-gradient driven drift-Alfven waves in the LAPD experiment at UCLA. A cylindrical low-density ($1 \times 10^{12} cm^{-3}$) depletion in the center of the higher density ($3 \times 10^{12} cm^{-3}$) bulk plasma is generated by selectively blocking primary electrons and therefore plasma producton. A broad frequency range (on the order of 10 kHz) of drift-Alfvén waves (DAW) form in the gradient region. Using a dual-strap Alfvén wave antenna, a low-frequency (1 kHz to 30 kHz) beat-wave quasimode between two co-propagating higher frequency Alfvén waves is driven into the cylindrical density gradient region. When the beat-frequency quasi-mode is at the spontaneous DAW frequency, we see resonant driving of the mode. More interestingly, when the quasi-mode is driven off-resonance, we observe strong suppression of the drift-Alfvén instability. By varying the beat-frequency, a range of suppression behavior is achieved. Both single coherent-mode fluctuations and broad-band turbulent fluctuations are suppressed. We provide experimental details of the observed quasimode-DAW interaction and discuss future plans for theory and simulation efforts to uncover the mechanism for the suppression.

GP8 144 Investigation of flows in LAPD and their relation to edge turbulence and intermittency D. SCHAFFNER, T.A. CARTER, B. FRIEDMAN, S. VINCENA, D.W. AUERBACH, P. POPOVICH, *UCLA* We report on measurements of spontaneous flows and turbulence in the Large Plasma Device (LAPD) at UCLA. Measurements of perpendicular and parallel flow using a six-sided Mach probe reveal edge-localized perpendicular flows. The source of this flow is under investigation and may be generated by boundary effects or turbulent processes. Particular cases where a plasma depletion zone is created, including inserting a blocking disk within the cathode region and forming a compressed column, are used to analyze the effects on plasma flows. Ultimately, the relationship between the flows, turbulence and intermittency—the formation of blobs—is sought.

GP8 145 Studies of a plasma with a hot dense core in LAPD BART VAN COMPERNOLLE, WALTER GEKELMAN, PATRICK PRIBYL, CHRIS COOPER, *UCLA* Recently, considerable effort in the LArge Plasma Device at UCLA (LAPD) has gone into the study of large cathodes which would enable higher discharge currents and higher densities. The new cathode is made out of Lanthanum HexaBoride (LaB6). LaB6 has a low work function and has higher emissivity than Barium oxide coated cathodes. The operating temperature of LaB6 cathodes lies above 1600 degrees Celsius. Tests of this cathode in the Enormous Toroidal Plasma Device (ETPD) showed that densities in excess of $2 10^{13}\text{cm}^{-3}$ and electron temperatures of 12 eV are feasible. Small LaB6 cathodes (3mm - 2cm) have been used before in LAPD in several experiments on heat transport and on magnetized flux ropes. The cathode presented in this paper has a 8 cm diameter, and can be positioned at different radial locations. The cathode will be pulsed into the standard background plasma ($n_e = 2 10^{12}\,\text{cm}^{-3}, .25 \leqslant T_e \leqslant 6\text{eV}$, dia $= 60\,\text{cm}$,L $= 18\,\text{m}$) creating a plasma with a hot dense core. We present the characterization of the core plasma at different conditions. Studies of the heat transport and density spreading at the interface between the core plasma and background plasma will be done by use of a variety of probes (Langmuir, magnetic, Mach, emissive) as well as fast photography.

GP8 146 Temporal sequences in the evolution of fluctuations on LMD-U* H. ARAKAWA, S. INAGAKI, K. KAMATAKI, M. YAGI, S. SUGITA, S.-I. ITOH, *Kyushu Univ., Japan* Y. NAGASHIMA, T. YAMADA, *Univ. Tokyo, Japan* N. KASUYA, A. FUJISAWA, K. ITOH, *NIFS, Japan* We investigate the dynamics of turbulence in linear magnetized plasma confined in LMD-U device. By use of poloidal array of probes and 2D-movable probe, spatio-temporal structure of drift wave fluctuations are studied. Abrupt changes of the density fluctuations are observed, and temporal evolution of Fourier-decomposed elements (both in poloidal direction and in frequency space) at the onset of transition is studied in detail. Primary components that lead the transition are identified. Then, delay times of higher harmonics after the sudden jump of primary components are measured using the conditional averaging and the cross correlation technique. This reveals the coupling between many Fourier components and yields the time for dynamical evolution in cascades. This experiment provides quantitative information of nonlinear interactions.

*Work supported by the grant-in-aid for Scientific Research of JSPS (21224014, 20560767), and by the collaboration programs of RIAM of Kyushu Univ. and of NIFS (NIFS07KOAP017).

GP8 147 Experimental Investigation of the ETG Nonlinear Saturation Mechanism* XIAO WEI, VLADIMIR SOKOLOV, AMIYA K. SEN, *Columbia University* We have produced and identified the slab electron temperature gradient (ETG) mode in the Columbia Linear Machine (CLM) [1]. Now we investigate the nonlinear saturation mechanism of the ETG modes. We study 3-wave coupling physics via the bi- coherence investigation and find signatures of the interaction between ETG modes and some low frequency modes. The saturation mechanism of the ETG modes is suspected to be related to the damping of low frequency modes. More detailed identification of the low frequency modes including their dispersion will be reported. [1] X. Wei, V. Sokolov, A.K. Sen, APS DPP08 TP6.00131

*This research was supported by U.S. Department of Energy Grant No. DE-FG02-98ER-54464.

GP8 148 Experimental Study of Local Anomalous Ion Thermal Transport with A Novel Time Dependent Energy Analyzer* VLADIMIR SOKOLOV, AMIYA K. SEN, *Columbia University* In the past we have reported measurements of global ion thermal transport due to ion temperature gradient (ITG) modes [1]. It is clearly more desirable to obtain local measurements of the same, which we now report for basic experiments in the Columbia Linear Machine. For local measurement of radial ion thermal transport we used a novel time dependent ion energy analyzer. For compensation of plasma potential fluctuations in energy analyzer measurements, we use floating potential fluctuation of Langmuir probe as a feedback signal with gain +1 and apply this voltage on energy selector grid. The simultaneous measurement of the ion current fluctuations of analyzer $\tilde{I}_{IEA}(t)$ and the fluctuation of ion saturation current of Langmuir probe $\tilde{I}_{SAT}(t)$ allow us to determine local fluctuations of ion temperature $\tilde{T}_i(t)$. The local thermal flux is obtained from cross-correlation of ion temperature fluctuations and potential fluctuations. The radial profiles of the plasma density, ion temperature, and total thermal flux were obtained at different levels of ITG mode. The results indicate that the ion thermal transport is $\Gamma \propto (\partial T_I/\partial r)^{\alpha}, \alpha > 1$. [1] B. Song, J. Chen, and A.K. Sen, Phys. Rev. Lett. 70, 2407 (1993).

*This research was supported by U.S. Department of Energy Grant No. DE-FG02-98ER-54464.

GP8 149 Measurement of neutral flow velocity field associated with an anti-E× B vortex KOHEI OGIWARA, *Kyushu University* MITSUTOSHI ARAMAKI, *Nagoya University* SHINJI YOSHIMURA, *National Institute for Fusion Science* MASAYOSHI Y. TANAKA, *Kyushu University* Recently, a class of vortices, which rotate opposite to the direction of E× B drift, have been observed in a magnetized plasma. It is considered that this vortex is driven by the force generated through the momentum transfer due to charge exchange collisions between ions and neutrals. To confirm the mechanism of the vortex formation, we have developed a high resolution LIF system and measured the neutral flow velocity field, in which the LIF system with an extended cavity diode laser is combined with saturated absorption spectroscopy to achieve high wavelength resolution (± 5fm). The LIF spectra of argon metastable atoms have been measured by tuning the laser wavelength to 696.735 nm and detecting the fluorescence photons of 826.679 nm. The neutral flow velocity field has been visualized for the first time. It is found that the radial flow is directed to the center of vortex with its maximum velocity of about 40 m/s. The direction of the azimuthal rotation is the same as that of the ion flow.

GP8 150 Coupling of axial plasma jets to compressional Alfven waves* STEPHEN VINCENA, WALTER GEKELMAN, *UCLA Department of Physics and Astronomy* The coupling of mass, energy, and momentum from a localized, dense, and rapidly expanding plasma into a large-scale magnetized background plasma is central to understanding many physical processes; these include galactic jets, coronal mass ejections, tokamak pellet fueling, high-altitude nuclear detonations, chemical releases in the ionosphere, and supernovae. The large-scale magnetized plasmas are capable of supporting Alfvén waves, which mediate the flow of currents and associated changes of magnetic topology on the largest size scales of the external system. We present initial results from a laboratory experiment wherein a fast-moving, laser-produced plasma (LPP) is allowed to propagate along the magnetic field lines of a pre-existing plasma column (17m long by 60 cm diameter). The LPP is generated using a 1J, 8ns Nd:YAG laser fired at a graphite target. The laser is pulsed along with the background plasma at 1Hz. This work focuses on the coupling of the LPP to compressional Alfvén waves in the background plasma. The experiments are conducted at UCLA's Basic Plasma Science Facility in the Large Plasma Device.

*This work is funded through a cooperative agreement between the DOE and NSF

GP8 151 Effect of two ion-species on the propagation of shear Alfven waves* G.J. MORALES, S.T. VINCENA, *UCLA* J.E. MAGGS, An experimental and theoretical modeling study of the propagation properties of shear Alfven waves of small transverse scale in the presence of two ion-species is presented. In a two-ion plasma, depending on the mass of the heavier species, ion kinetic effects can become prominent, and significant parallel electric fields result in electron acceleration. Theory predicts the appearance of frequency propagation gaps, and spatial structures that mix the cone-propagation characteristics of Alfven waves with radially expanding ion Bernstein modes. The experiments are performed at the Basic Plasma Science Facility (BaPSF) at UCLA and consist of the spatial mapping of shear waves launched by a small disk exciter and by a large loop antenna. A variety of two ion-species combinations are explored by mixing the basic gases Helium, Neon, Argon and Hydrogen to generate highly reproducible plasmas. It is found that propagation bands below the ion cyclotron frequency of each of the two species can be identified, but there appears to be a large damping mechanism whose strength increases with the mass of the heavier species. For a 50-50 mix of Argon-Neon the damping is so severe that no signals can be observed in the Neon propagation band.

*Supported by DOE/NSF, and by ONR under a MURI grant.

GP8 152 On generation of Alfvénic-like fluctuations by drift wave-zonal flow system in Large Plasma Device experiments* C.E. CORREA, W. HORTON, *Institute of Fusion Studies, University of Texas at Austin* G.D. CHAGELISHVILI, V.S. AVSARKISOV, J.G. LOMINADZE, *Georgian National Astrophysical Observatory, The Chavchavadze State University* J.-H. KIM, J.C. PEREZ, *Department of Physics, University of Wisconsin-Madison* TROY CARTER, *Department of Physics, University of California, Los Angeles* According to recent experiments, magnetically confined fusion plasmas with "drift wave-zonal flow turbulence" (DW-ZF) give rise to broadband electromagnetic waves. Sharapov et al (2008) report an abrupt change in the magnetic turbulence during L-H transitions in Joint European Torus [P. H. Rebut and B. E. Keen, Fusion Technol. **11**, 13 (1987)] plasmas. A broad spectrum of Alfvénic-like fluctuations appear from $\mathbf{E} \times \mathbf{B}$ flow driven turbulence in the Large Plasma Device (LAPD) [W. Gekelman et al., Rev. Sci. Instrum. **62**, 2875 (1991)]. We present one possible theoretical explanation of electromagnetic fluctuations in DW-ZF systems in LAPD experiments. Fluctuation modes of spectrally stable sheared flows are non-normal. The linear operators of the fluctuations modal analysis are non-normal and the corresponding eigenmodes are not orthogonal. The non-normality results in linear transient growth with bursts of the perturbations and the mode coupling, which causes electromagnetic waves. The transient growth substantially exceeds the growth of the classical dissipative trapped-particle instability.

*This work was supported by ISTC grant G-1217 and by NSF ATM-0638480.

GP8 153 A Krein-Like Theorem for the Linearized Vlasov-Poisson Equation GEORGE HAGSTROM, PHILIP MORRISON, *University of Texas at Austin* We consider the linearized Vlasov-Poisson equation in the Banach space with the norm $\|\{f_k\}\| = \Sigma_k k^2 \|f_k\|_{W_{1,1}}$. We perturb the equations by changing the equillibrium solution f_0. We prove that that always exists an infinitesimal perturbation of f_0' in the $W_{1,1}$ norm can create an instability at any solution of the equation $f_0'(v) = 0$. If we restrict to dynamically accessible perturbations we instead recover a result similar to Krein's theorem for linear finite dimensional Hamiltonian systems.

SESSION GM9: MINI-CONFERENCE ON UNSTEADY RECONNECTION IN LABORATORY AND NATURE I: RECONNECTION RATE AND DYNAMICS
Tuesday Morning, 3 November 2009
Regency V at 9:30
Giovanni Lapenta, Centre for Space Weather, Leuven, Belgium, presiding

9:30
GM9 1 Reconnection in the Solar Wind: An Update JOHN GOSLING, *University of Colorado* Magnetic reconnection plays a central role in a wide variety of observed solar and space phenomena. In the solar wind magnetic reconnection commonly occurs in a quasi-stationary mode at extended X-lines. It produces Petscheklike exhausts of roughly Alfvénic jetting plasma typically bounded by back-to-back rotational discontinuities that bifurcate a reconnecting current sheet. It occurs at thin current sheets most frequently associated with relatively small (less than 90 deg) magnetic field rotations in low beta plasma. Reconnection exhausts are observed most frequently (typically 1-3 events/day at 1 AU) in the low-speed wind and within interplanetary coronal mass ejections, and less frequently (0.6 events/day) in the Alfvénic turbulence characteristic of the high-speed wind from coronal holes. Reconnection occurs relatively infrequently at the heliospheric current sheet, HCS, but observations of exhausts at the HCS are particularly revealing of the magnetic field topology changes associated with the reconnection process. Reconnection in the solar wind is usually fast, but not explosive – the magnetic energy release occurs over a long time interval following reconnection as the Alfvénic disturbances initiated by the process propagate into the surrounding solar wind plasma. There is as yet no hard evidence that indicates that reconnection in the solar wind ever produces substantial particle acceleration.

9:55
GM9 2 The Tectonics Model of Coronal Heating: Unsteady Dynamics and Scaling in Statistical Steady State* C.S. NG, *Geophysical Institute, University of Alaska Fairbanks* L. LIN, A. BHATTACHARJEE, *Center for Integrated Computation and Analysis of Reconnection and Turbulence, University of New Hampshire* The tectonics model of coronal heating, proposed by Priest et al. [Astrophys. J., **576**, 533 (2002)] envisions coronal heating caused by a hierarchy of current sheets produced by the movement of a myriad of flux elements in the magnetic carpet covering the Sun. We have recently obtained new scaling results in two dimensions (2D) suggesting that the heating rate becomes independent of resistivity in a *statistical* steady state [C. S. Ng and A. Bhattacharjee, Astrophys. J., **675**, 899 (2008)]. Our numerical work has now been extended to 3D. Random photospheric footpoint motion is applied to obtain converged average coronal heating rates. In the large Lundquist number limit, we find that the heating rate is independent of the Lundquist number, with average magnetic energy saturating at a constant level due to the formation of strong current layers and subsequent disruptions. In this talk, we will present our latest numerical results from large-scale 3D simulations, and discuss differences with previous scaling laws.

*This work is supported by NSF grant AST-0434322, NASA grants NNX08BA71G, NNX06AC19G and DOE grant DE-FG02-07ER54832.

10:15
GM9 3 Energy conversion by magnetic reconnection JOACHIM BIRN, *Los Alamos National Laboratory* MICHAEL HESSE, *NASA/Goddard Space Flight Center* The energy release and conversion by magnetic reconnection is discussed on the basis of magnetohydrodynamic (MHD) and particle-in-cell (PIC) simulations. Contrary to common assumptions, the energy conversion to enthalpy flux (convected heat) plays a major role, which typically exceeds the conversion to bulk kinetic energy flux. Direct Joule dissipation plays only a minor role in the energy release and transfer. These results are found consistently between PIC and MHD simulations, provided that the imposed resistivity is strongly localized or sufficiently small in magnitude. Approximate conservation of entropy on magnetic flux tubes is responsible for governing the structure of final equilibrium in closed systems.

10:40
GM9 4 Dipolarization fronts as a distinctive feature of transient reconnection in the magnetotail: Particle simulations with open boundaries and THEMIS observations M. SITNOV, *JHU/APL* A. RUNOV, V. ANGELOPOULOS, *UCLA/IGPP* M. SWISDAK, P. GUZDAR, *UMD/IREAP* A. DIVIN, *KUL, Belgium* V. SERGEEV, *SPbU* S. OHTANI, B. MAUK, *JHU/APL* J. BONNELL, J. McFADDEN, D. LARSON, *UCB/SSL* K.-H. GLASSMEIER, U. AUSTER, *TUBS/IGEP* Particle simulations with open boundary conditions revealed an interesting new phenomenon in the outflow regions of the collisionless reconnection pattern. It was found that transient reconnection may result in the formation of dipolarization fronts (DFs), regions of the strong magnetic flux pileup propagating with the speed of the order of the Alfven speed in the reconnection exhausts. The flux pileup is accompanied by a drop of the plasma density making the front similar to a plasma bubble. Similar phenomena have been observed in the tail of the Earth's magnetosphere by Geotail, Cluster and other missions. Here we present the results of simulations of DFs using the explicit massively parallelized full-particle code P3D [Zeiler et al., JGR, 107, 1230, 2002] with open boundaries [Divin et al., GRL, 34, L09109, 2007] and compare them with observations of DFs in the magnetosphere using five-satellite THEMIS mission. DFs are found to be microscopic shock-like boundaries with the thickness of the order of the ion inertial length that propagate over a macroscopic distance up to ten Earth radii.

11:00

GM9 5 A Hall-MHD model for dipolarization fronts P.N. GUZDAR, *IREAP, University of Maryland, MD, USA* M.I. SITNOV, *APL, Johns Hopkins University, Laurel, MD, USA* A.B. HASSAM, M. SWISDAK, *IREAP, University of Maryland, MD, USA* In recent studies of transient reconnection, dipolarization fronts which are characterized by a steep increase or jump in the z component of the earth's tail magnetic field, have been reported in kinetic simulations with open boundaries as well as in many satellite observation, including the most recent five-probe THEMIS mission. One possible interpretation of these jumps is the formation of supersonic shocks using the standard MHD Rankine-Hugoniot relations. The observed jumps in the measured quantities like the density, magnetic field and velocity components are compared with the different kinds of oblique shocks that can occur in MHD. Using these jump conditions obtained from MHD, an initial value code for the 1D Hall-MHD system of equations is then solved to investigate the role of Hall physics on these shocks. Because of the strong coupling between the z component and an out-of-plane y component of the magnetic field in Hall-MHD, a discontinuous y component develops when the initial condition does not have a B_y component. The sharp shock discontinuity leads to the generation of whistler waves which have different propagation characteristics on either side of the shock boundary.

11:20

GM9 6 What Causes Electron Holes During Magnetic Reconnection and What Can We Learn From Them* MARTIN V. GOLDMAN, DAVID L. NEWMAN, *University of Colorado at Boulder* GIOVANNI LAPENTA, ANDRE DIVIN, *Katholieke Universiteit Leuven, Belgium* FRANCESCO CALIFANO, *University of Pisa, Italy* HAIHONG CHE, *University of Colorado* Weak bipolar electrostatic fields are commonly observed in association with magnetic reconnection. Recent attention has focused on their origin due to nonlinear evolution of electrostatic instabilities.[1,2,3] We present evidence from both older and new reconnection simulations for the SPATIAL dependence of electrostatically unstable electron distributions along the separatrix during guide-field magnetic reconection. Particle distributions further from the reconnection region tend to be Buneman (electron-ion) unstable, while distributions closer to the reconnection region tend to be two-stream (electron-electron) unstable. It may be possible to infer properties of the particle distributions from measurements of the speed, half-width, amplitude and aspect ratio of weak electron holes.

*Research Supported by NASA Grant # NNX08AO84G.

[1]Goldman, M. V., D. L. Newman, and P. Pritchett, *GRL*, **35**, doi:10.1029/2008GL035608 (2008).

[2]Newman, D. L. and M. V. Goldman, SM31B-1735, AGU Fall Meeting (2008).

[3]Che, H., J. F. Drake, M. Swisdak, and P. H. Yoon, *PRL*, **102**, 145004 (2009).

11:40

GM9 7 Dissipation of Thin Current Sheets Interacting with Nonlinear Alfven Waves in Relativistic Plasmas EDISON LIANG, GUY HILBURN, *Rice University* HUI LI, WEI LIU, *Los Alamos National Laboratory* We present results from 2.5D and 3D particle-in-cell simulations of the interaction of thin current sheets with nonlinear Alfven waves in relativistic plasmas. We find that the Alfven waves cause the current sheet to bend and kink and enhance its dissipation rate. The electrons are heated by several competing mechanisms, eventually forming a double Maxwellian population. The cooler Maxwellian is heated mainly by Alfven turbulence cascade while the hotter Maxwellian is heated by the drift kink instability. The implications of these results for the kinetic dissipation of turbulence driven by the magnetorotational instability (MRI) will be discussed. Potential applications to the emissions of low-luminosity black hole accretion flows will be studied.

12:00

GM9 8 Evolving Magnetic Reconnection in Well Confined Plasmas with Low Collisionalities* B. COPPI, *MIT* There are two kinds of modes, producing large scale magnetic islands in well confined plasmas with low degrees of collisionality. These have phase velocities of opposite signs and are expected to emerge following the excitation of other modes as they cannot be found to be linearly unstable. One type is the "drift-tearing" [1] mode with a phase velocity in the direction of the electron diamagnetic velocity (upv_{de}) and the other is classified as an "inductive" mode [2] with a phase velocity in the direction of upv_{di}. The "drift-tearing" can be excited after a mode that has the effect of decreasing the ratio of the longitudinal to the transverse electron thermal conductivity, like the "micro-reconnecting" mode discussed in Ref. [3]. The second type requires the previous excitation of a pressure gradient driven mode [4] that has a flow velocity in the upv_{di} direction. Moreover, a mode-particle resonance with a high energy particle population [1] is involved in the growth of both the primary and the secondary (reconnecting) mode. Recent experimental observations [4] are consistent with these conclusions. Sawtooth oscillations that involve periodic reconnection events and modes that are related to those described earlier are discussed. *Sponsored in part by the U.S. DoE. [1] B. Coppi, *Phys. Fluids* **8**, 2273 (1965) [2] B. Coppi, Bull. *Am. Phys. Soc* **45**, 366 (2000) [3] B. Coppi, in "Collective Phenomena etc." pg. 59, Eds. G. Bertin *et. al., Publ. World Scientific* (2007) [4] P. Buratti *et al.* Paper 02.007, 2009 E.P.S. Conference

SESSION JI2: ICF COMPRESSION, EQUATIONS OF STATE AND Z-PINCHES

Tuesday Afternoon, 3 November 2009; Centennial I at 14:00; Tom Mehlhorn, Sandia National Laboratories, presiding

14:00

JI2 1 Hugoniot Measurements of Diamond and α-Quartz in the TPa Regime: Implications for Astrophysics, ICF, and HED Physics.*

MARCUS KNUDSON,† *Sandia National Laboratories*

The development of an ultra-high velocity ($>$ 40 km/s) flyer plate capability at the Sandia Z Machine has enabled TPa shock wave experiments with unprecedented accuracy. Here we present the results of Hugoniot measurements on

diamond and z-cut, α-quartz in the 0.5-1.5 and 0.1-1.6 TPa regime, respectively. The diamond measurements are inclusive of a large solid-liquid coexistence region, and together with quantum molecular dynamics (QMD) calculations, provide compelling evidence for the existence of a diamond-bc8-liquid triple point along the Hugoniot. The new quartz Hugoniot data reveal significant errors in the current, widely-used quartz standard and have immediate ramification for the equations of state of deuterium, helium, and diamond at pressures relevant to giant planets and other high energy density conditions. This work provides a foundation for the use of quartz as an extremely accurate standard for use in multi-Mbar shock wave experiments, as well as a benchmark for first-principles calculations of high-pressure material response where processes such as disorder, dissociation, and ionization are significant.

*Sandia is a multiprogram laboratory operated by Sandia Corporation, a Lockheed Martin Company, for the United States Department of Energy's National Nuclear Security Administration under contract DE-AC04-94AL85000.
†In collaboration with M.P. Desjarlais and D.H. Dolan

14:30
JI2 2 High-Precision Measurements of the Equation of State of Polymers at 100 to 1000 GPa Using Laser-Driven Shock Waves.
M.A. BARRIOS, *Laboratory for Laser Energetics, U. of Rochester*

The equation of state (EOS) of materials at extreme temperatures and pressures is of interest to astrophysics, high-energy-density physics, and inertial confinement fusion (ICF). The high-pressure ($>$ 100 GPa) behavior of polymer materials is essential to the understanding of ablator materials for ignition targets. EOS measurements on CH_x provide benchmarks on the behavior of polymers under extreme conditions and the effect of stoichiometry (i.e., the C:H ratio) on that behavior. High-power lasers produce shock pressures greater than 100 GPa, and recent advances in diagnostics and analysis have made it possible to perform highly accurate measurements of shock velocity. This improves upon the impedance-matching technique for laser-driven shock experiments, producing $\sim$ 1% precision at extreme pressures. The OMEGA laser is used to produce principal (single-shock) Hugoniot EOS measurements on polystyrene (CH), polypropylene (CH_2), GDP ($C_{43}H_{56}O$), and Ge-doped GDP at shock pressures of $\sim$ 100 to 1000 GPa. We also present a novel target design that provides double-shock (re-shock) data together with the above data. These data are pertinent to ICF target designs that use multiple shocks to approximate an isentropic compression. Results of the single- and double-shock experiments on these polymers are presented and compared to various EOS models. This work was supported by the U.S. Department of Energy Office of Inertial Confinement Fusion under Cooperative Agreement No. DE-FC52-08NA28302. In collaboration with T.R. Boehly, D.E. Fratanduono, D.D. Meyerhofer (LLE), D.G. Hicks, P.M. Celliers, and G.W. Collins (LLNL).

15:00
JI2 3 X-ray Radiography and Scattering Diagnosis of Dense Shock-Compressed Matter.
SEBASTIEN LEPAPE, *Lawrence Livermore National Laboratory*

Spectrally resolved x-ray Thomson scattering is an established technique that allows characterizing Fermi degenerate dense plasmas accessible in laser shocked-compressed foil experiments. It has been used in a variety of experiments that, besides measuring plasma density and temperature, served as critical test for models that calculate important plasma parameters like structure factors, bound-free contributions, and ionization energy lowering in warm dense matter. Experiments realized at the TITAN facility at Lawrence Livermore National Laboratory apply ultra-short pulse laser produced K- x rays to characterize plasmas at pressures above 1.5 Mbar that are produced with an energetic nanosecond laser. High energy x-rays produced by the short pulse laser allow probing compressed matter with a high temporal resolution (about 10 ps). From collective and non-collective scattering spectra mass density of the compressed Boron is inferred. X-ray radiography has been used as an independent way to characterize the mass density of matter for identical drive conditions. Here, we use K- X rays in a point projection scheme to probe the shock wave. Densities ranging from 3 to 4 g/cc have been measured, in excellent agreement with the x-ray Thomson scattering data. These radiography data combined with accurate measurement of the Plasmon dispersion in shocked Boron help improving the accuracy of the collision model as well as structure factor calculation.

15:30
JI2 4 Validated, 3-dimensional, magneto-hydrodynamic simulations of optimized single and nested wire array z-pinches with detailed circuit coupling.*
CHRISTOPHER JENNINGS, *Sandia National Laboratories*

Wire array Z-pinches have been used successfully for many years as a powerful x-ray source, as a dynamic hohlraum, and as an intense K-shell source. Significant progress has been made in modeling these 3D resistive plasmas however predictive modeling also requires an accurate representation of the power delivered to the load, which is an uncertainty potentially as large as the MHD implosion dynamics. We present 3D resistive MHD simulations of wire arrays that are coupled to a transmission line equivalent of the Z generator separately representing the 4 vacuum insulated transmission lines that join through a double post-hole convolute into a final feed to the array. Significant (multi-MA) current losses are shown to occur in the convolute and the final feed. This limits the array performance and must be correctly accounted

for to accurately represent the generator response. Our simulations are validated against data for compact, 20mm diameter, 10mm long wire arrays. This is the most comprehensive experimental data set for single and nested wire arrays and includes voltage, current, x-ray power and energy, and multiple mass distribution measurements. These data tightly constrain our simulation results and allow us to describe, for the first time, the detailed mechanism by which nested arrays can be used to narrow the radial mass distribution and increase the peak x-ray power. We use these results to define criteria for optimizing the x-ray power output from these and other nested wire array sources. In collaboration with: M. E. Cuneo, J.P.Chittenden, W.A. Stygar, B. Jones, D. J. Ampleford, E.M. Waisman, M.E. Savage, K. LeChien, D.B. Sinars

*Sandia is a multi-program laboratory operated by Sandia Corporation, a Lockheed Martin Company, for the United States Department of Energy's NNSA under contract DE-AC04-94AL85000.

16:00
JI2 5 Acceleration to High Velocities and Heating by Impact Using Nike KrF laser.
MAX KARASIK,* *Plasma Physics Division, Naval Research Laboratory, Washington DC*

Shock ignition, impact ignition, as well as higher intensity conventional hot spot ignition designs reduce driver energy requirement by pushing the envelope in laser intensity and target implosion velocities. This talk will describe experiments that for the first time reach target velocities in the range of 700 – 1000 km/s. The highly accelerated planar foils of deuterated polystyrene, some with bromine doping, are made to collide with a witness foil to produce extreme shock pressures and result in heating of matter to thermonuclear temperatures. Target acceleration and collision are diagnosed using large field of view monochromatic x-ray imaging with backlighting as well as bremsstrahlung self-emission. The impact conditions are diagnosed using DD fusion neutron yield, with over 10^6 neutrons produced during the collision. Time-of-flight neutron detectors are used to measure the ion temperature upon impact, which reaches 2 – 3 keV. The experiments are performed on the Nike facility, reconfigured specifically for high intensity operation. The short wavelength and high illumination uniformity of Nike KrF laser uniquely enable access to this new parameter regime. Intensities of $(0.4 - -1.2) \times 10^{15}$ W/cm^2 and pulse durations of $0.4 - -2$ ns were utilized. Modeling of the target acceleration, collision, and neutron production is performed using the FAST3D radiation hydrodynamics code with a non-LTE radiation model. Work is supported by US Department of Energy.

*In collaboration with J. L. Weaver, Y. Aglitskiy (SAIC), A. L. Velikovich, S. T. Zalesak, J. W. Bates, J. Oh (RSI), S. P. Obenschain, Naval Research Lab and Y. Arikawa, T. Watari, T. Sakaiya, M. Murakami, H.Azechi, Institute of Laser Engineering, Japan

16:30
JI2 6 Magnetized Liner Inertial Fusion.*
STEPHEN SLUTZ, *Sandia National Laboratories, Albuquerque, NM, USA 87185*

The natural geometry for magnetically driven implosions is cylindrical, but cylindrical implosions require more radial convergence than spherical implosions due to reduced volume convergence. Fuel magnetization and preheat can ameliorate this problem by reducing conduction losses and the required compressive heating. Assuming a deuterium-tritium fuel preheated to 200-500 eV and magnetized with a 10T field, numerical simulations indicate that fusion conditions could be obtained by cylindrical liner implosions driven by the Z accelerator. According to the simulations the initial axial magnetic field is compressed to more than 100 MG, which inhibits thermal conduction and the escape of alpha particles. The inhibited thermal transport allows the fuel to reach temperatures exceeding 5 keV despite an implosion velocity of only 10 cm/μs. The final fuel density is about 1 g/cc, which is high enough to axially trap alpha particles for cylinders less than 1 cm long with a purely axial magnetic field. Analytic and numeric calculations indicate that the fuel can be heated to 200-500 eV with 3-10 kJ of green laser light, which could be provided by the Z-Beamlet laser. The Magneto-Rayleigh-Taylor instability poses the greatest threat to this approach to fusion. 2D numerical simulations indicate that the liner walls must have a substantial initial thickness (15-30% of the radius) to maintain integrity throughout the implosion. Z and Z Beamlet experiments are underway to test the various components of this concept.

*Sandia is a multiprogram laboratory operated by Sandia Corporation, a Lockheed Martin Company, for the United States Department of Energy's National Nuclear Security Administration under contract DE-AC04-94AL85000.

SESSION JT3: TUTORIAL: VERIFICATION AND VALIDATION FOR MAGNETIC FUSION: MOVING TOWARD PREDICTIVE CAPABILITY

Tuesday Afternoon, 3 November 2009; Centennial II at 14:00; Bill Heidbrink, University of California, Irvine, presiding

14:00

JT3 1 Verification and Validation for Magnetic Fusion: Moving Toward Predictive Capability.

MARTIN GREENWALD, *MIT-Plasma Science & Fusion Center*

Dramatic progress in the scope and power of plasma simulations over the past decade has extended our understanding of these complex phenomena. However, as codes embody imperfect models for physical reality, a necessary step towards developing a predictive capability is demonstrating agreement, without bias, between simulations and experimental results. While comparisons between computer calculations and experimental data are common, there is a compelling need to make these comparisons more systematic and more quantitative. Tests of models are divided into two phases, usually called verification and validation. Verification is an essentially mathematical demonstration that a chosen physical model, rendered as a set of equations, has been accurately solved by a computer code. Validation is a physical process which attempts to ascertain the extent to which the model used by a code correctly represents reality within some domain of applicability, to some specified level of accuracy. Verification assesses errors from spatial or temporal gridding, algorithms, numerics and convergence, as well as coding errors and bugs in compilers. In the arsenal of verification methodology are formal convergence tests, theory to code comparisons, code to code comparisons, and specialized tools like the method of manufactured solutions. The process of code validation requires an assessment of the critical elements in a physical model and a quantitative approach for testing these elements individually and in combination. Dedicated experiments are typically required along with careful analysis of errors and sensitivity. A recent development has been "synthetic" diagnostics, which allow more direct comparisons between simulations and measurements. This talk will cover principles and practices for verification and validation including lessons learned from related fields.

SESSION KI3: TURBULENT TRANSPORT MEASUREMENT AND MODELING

Tuesday Afternoon, 3 November 2009; Centennial II at 15:00; Chris Holland, University of California, San Diego, presiding

15:00

KI3 1 Marshall N. Rosenbluth Outstanding Doctoral Thesis Award Talk: Simultaneous Measurement of Electron Temperature and Density Fluctuations in the Core of DIII-D Plasmas.*

A.E. WHITE, *UCLA (presently at ORISE)*

Multi-field fluctuation measurements provide opportunities for rigorous comparison between experiment and nonlinear gyrokinetic turbulence simulations. A unique set of diagnostics on DIII-D allows for simultaneous study of local, long-wavelength ($0 < k_\theta \rho_s < 0.5$) electron temperature and density fluctuations in the core plasma ($0.4 < \rho < 0.8$). Previous experiments in L-mode indicate that normalized electron temperature fluctuation levels ($40 < f < 400$ kHz) increase with radius from $\sim$ 0.4% at $\rho = 0.5$ to $\sim$ 2% at $\rho = 0.8$, similar to simultaneously measured density fluctuations. Electron cyclotron heating (ECH) is used to increase T_e, which increases electron temperature fluctuation levels and electron heat transport in the experiments. In contrast, long wavelength density fluctuation levels change very little. The different responses are consistent with increased TEM drive relative to ITG-mode drive. A new capability at DIII-D is the measurement of phase angle between electron temperature and density fluctuations using coupled correlation electron cyclotron emission radiometer and reflectometer diagnostics. Linear and nonlinear GYRO runs have been used to design validation experiments that focus on measurements of the phase angle. GYRO shows that if T_e and ∇T_e increase 50% in a beam-heated L-mode plasma ($\rho = 0.5$), then the phase angle between electron temperature and density fluctuations decreases 30%-50% and electron temperature fluctuation levels increase a factor of two more than density fluctuations. Comparisons between these predictions and experimental results will be presented.

*Supported by US DOE under DE-AC05-06OR23100 and DE-FC02-04ER54698.

15:30
KI3 2 Comparison of experimental measurements and gyrokinetic turbulent electron transport models in Alcator C-Mod plasmas.*
LIANG LIN, *MIT/UCLA*

We present results of core turbulence measurements and associated transport in Alcator C-Mod using phase contrast imaging (PCI) diagnostic. In order to interpret and better understand the measurements we quantitatively compared the results with extensive simulations with the gyrokinetic code GYRO through a synthetic PCI diagnostic. Both L-Mode and H-Mode plasmas were examined. The L-Mode experiments were carried out over the range of densities covering the "neo-Alcator" (linear confinement time scaling with density) to the "saturated ohmic" regime. The key role played by the ion temperature gradient (ITG) turbulence has been verified by measurements of turbulent wave propagation which was dominantly in the ion diamagnetic direction in the laboratory frame. The absolute fluctuation intensity also agreed with simulation within experimental error. In the saturated ohmic and H-Mode regime where ion transport dominates, the simulated ion and electron thermal diffusivities also agree with experiments after varying the ion temperature gradient or adding E× B shear suppression within experimental uncertainty. However, in the linear ohmic regime where electron transport dominates, GYRO does not agree with experiments, showing significantly larger ion thermal transport and smaller electron thermal transport. Our study shows that although the electron temperature gradient (ETG) mode is unstable, the nonlinear simulation with $k_\theta \rho_s$ up to 4 does not raise the electron thermal diffusivity to the experimental level. Further work to explore even higher-k ETG regimes with GYRO is underway and the results will be presented. Work supported by U. S. DOE under DE-FG02-94-ER54235 and DE-FC02-99-ER54512.

*In collaboration with M. Porkolab, E.M. Edlund, J.C. Rost, C.L. Fiore, M. Greenwald, Y. Ma, N. Tsujii (MIT), J. Candy, R.E. Waltz (GA), D.R. Mikkelsen (PPPL), W.M. Nevins (LLNL).

16:00
KI3 3 Probing Plasma Turbulence by Modulating the Electron Temperature Gradient.*
J.C. DEBOO, *General Atomics*

Validating transport models is an essential step toward accurate predictive capability of plasma transport in tokamak plasmas. Experiments with a single key parameter varied and the turbulence response measured provide excellent data sets for model validation studies. One such experiment on DIII-D will be discussed where the electron temperature gradient was systematically varied and the turbulence response documented and compared with predictions from the gyrokinetic turbulence code GYRO. The temperature gradient scale length a/L_{Te} was varied at the plasma mid-radius by repetitively switching from ECH deposition just inside to just outside the mid-radius which modulated a/L_{Te} at essentially fixed T_e. Electron density fluctuations at wavenumbers $k_\theta = 5\text{–}6\ \mathrm{cm}^{-1}$, typically associated with TEM turbulence, were measured with a Doppler backscattering system (DBS) and were well correlated spatially and temporally with the variation produced in a/L_{Te}. The turbulence amplitude modulation was spatially localized, peaked between the two ECH deposition regions, and was consistent with expectations based on a/L_{Te} being a drive term for TEM turbulence. The DBS lab frame frequency was observed to increase when a/L_{Te} decreased. However, this is likely a result of variations in poloidal $E \times B$ motion rather than changes in the turbulence frequency. A direct comparison of GYRO predictions using a synthetic diagnostic module developed for DBS shows agreement within experimental uncertainties with measured turbulence amplitude variation but disagreement in spectral shape and considerable disagreement between predicted heat fluxes and power balance analysis. This is an area of ongoing investigation. Additional experiments at larger plasma radii were carried out where modulation of temperature fluctuations were also seen and will be discussed.

*Supported by US DOE under DE-FC02-04ER54698.

16:30
KI3 4 Fluctuation-Induced Particle Transport and Density Relaxation in a Stochastic Magnetic Field.*
DAVID L. BROWER, *University of California, Los Angeles*

Particle transport and density relaxation associated with electromagnetic fluctuations is an unresolved problem of long standing in plasma physics and magnetic fusion research. In toroidal fusion plasmas, magnetic field fluctuations can arise spontaneously from global MHD instabilities, e.g., tearing fluctuations associated with sawtooth oscillations. Resonant magnetic perturbations (RMP) have also been externally imposed to mitigate the effect of edge localized modes (ELMs) by locally enhancing edge transport in Tokamaks. Understanding stochastic-field-driven transport processes is thus not only of basic science interest but possibly critical to ELM control in ITER. We report on the first direct measurement of magnetic fluctuation-induced particle transport in the core of a high-temperature plasma, the MST reversed field pinch. Measurements focus on the sawtooth crash, when the stochastic field resulting from tearing reconnection is strongest, and are accomplished using newly developed, laser-based, differential interferometry and Faraday rotation techniques. The measured electron particle flux, resulting from the correlated product of electron density (δn) and radial magnetic fluctuations (δb_r), accounts for density profile relaxation during these magnetic reconnection events. Surprisingly, the electron diffusion is 30 times larger than estimates of ambipolarity-constrained transport in a stochastic magnetic field.

A significant ion flux associated with parallel ion flow velocity fluctuations ($\delta v_{i,//}$) correlated with δb_r appears responsible for transport larger than predictions from the quasi-linear test particle model. These results indicate the need for improved understanding of particle transport in a stochastic magnetic field. Work performed in collaboration with W.X. Ding, W.F. Bergerson, T.F. Yates, UCLA; D.J. Den Hartog, G. Fiksel, S.C. Prager, J.S. Sarff and the MST Group, University of Wisconsin-Madison.

*Work supported by US Department of Energy.

SESSION JO4: NSTX SPHERICAL TORUS
Tuesday Afternoon, 3 November 2009
Regency VI at 14:00
Houyang Guo, Tri Alpha Energy, presiding

14:00
JO4 1 Overview of Results from the NSTX FY09 Run ROGER RAMAN, *University of Washington, for the NSTX Research Team* NSTX research in toroidal magnetic confinement at low aspect ratio has made extensive use this year of both lithium coatings for wall conditioning and external non-axisymmetric field correction to reliably produce high-performance discharges extending to 1.7s in duration. Toroidal beta above 25% has been sustained for up to 0.4s. The error-field correction coils have been used to trigger ELMs for controlled ELM pace-making and have also contributed to an improved understanding of both neoclassical tearing mode and resistive wall mode physics. The supersonic gas injector has been used to fuel long-pulse high-performance discharges without reliance on the high field side fueling previously employed. The edge pedestal of ELM-free H-mode plasmas has been studied using transient edge probes, fast infrared cameras and divertor bolometers. A reduction in the required central solenoid flux has been realized in NSTX when discharges initiated by coaxial helicity injection were ramped in current using induction. Other experiments have been conducted to address research of high priority to the ITPA and ITER. This work supported by U.S. DOE Contracts DE-AC02-09CH11466 and DE-FG02-99ER54519 AM08.

14:12
JO4 2 Plasma Response to Lithium-Coated Plasma-Facing Components in NSTX* M.G. BELL, H. KUGEL, D. MANSFIELD, R. KAITA, S. GERHARDT, S. PAUL, R.E. BELL, *PPPL* R. MAINGI, J. CANIK, *ORNL* NSTX TEAM, Lithium coatings have been routinely applied by evaporation onto the carbon surfaces of the lower divertor and other plasma-facing components in NSTX. In NBI-heated, deuterium H-mode plasmas, the lithium decreased the density in the plasma edge, reduced the inductive flux consumption, and increased the electron temperature, ion temperature and energy confinement time. Reductions in ELM frequency occurred, including complete ELM suppression for periods up to about 1s, apparently as a result of altering the stability of the edge. With ELM suppression, the effective ion charge and radiated power increased as a result of a buildup in carbon and metallic impurities, although lithium itself remained at a low level in the core, $< 0.1\%$. The impurity buildup could be inhibited by repetitively triggering ELMs with brief pulses of an n = 3 field perturbation. Lithium powder has also been injected directly into the scrape-off layer where it became ionized and flowed along the magnetic field to the divertor plates. This method of coating produced similar effects to evaporated lithium but at much lower amounts.

*Supported by US DOE contract DE-AC02-09CH11466

14:24
JO4 3 Reversed magnetic shear suppression of electron-scale turbulence on NSTX* HOWARD Y. YUH, F.M. LEVINTON, *Nova Photonics* R.E. BELL, J.C. HOSEA, S.M. KAYE, B.P. LEBLANC, E. MAZZUCATO, *PPPL* D.R. SMITH, *UW-Madison* C.W. DOMIER, N.C. LUHMANN, *UC Davis* H.K. PARK, *POSTECH* Electron thermal internal transport barriers (e-ITBs) are observed in reversed (negative) magnetic shear NSTX discharges[1]. These e-ITBs can be created with either neutral beam heating or High Harmonic Fast Wave (HHFW) RF heating. The e-ITB location occurs at the location of minimum magnetic shear determined by Motional Stark Effect (MSE) constrained equilibria. Statistical studies show a threshold condition in magnetic shear for e-ITB formation. High-k fluctuation measurements at electron turbulence wavenumbers[3] have been made under several different transport regimes, including a bursty regime that limits temperature gradients at intermediate magnetic shear. The growth rate of fluctuations has been calculated immediately following a change in the local magnetic shear, resulting in electron temperature gradient relaxation. Linear gyrokinetic simulation results for NSTX show that while measured electron temperature gradients exceed critical linear thresholds for ETG instability, growth rates can remain low under reversed shear conditions up to high electron temperatures gradients. [1]H. Yuh, et. al., PoP **16**, 056120 [2]D.R. Smith, E. Mazzucato et al., RSI **75**, 3840 [3]E. Mazzucato, D.R. Smith et al., PRL **101**, 075001

*Supported by DE-FG02-99ER54520 and DE-AC02-09CH11466.

14:36
JO4 4 Advanced Scenario and Plasma Control Development on NSTX* DAVID GATES, S.P. GERHARDT, E. KOLEMEN, *Princeton Plasma Physics Laboratory* AND THE NSTX TEAM, The NSTX extreme shaping regime ($\kappa \sim 3$, $\delta \sim 0.8$) and $\beta_N \sim 6$, has been extended to include lower q95 plasmas at high $< \beta_t > \sim 25\%$. These plasmas aim at the operating regime required for future ST reactors such as ARIES-ST. Additionally, record low sustained surface voltages have been sustained at higher q95 $\sim$ 13. The non-inductive current drive fraction is calculated to be $f_{BS} \sim 65\%$, however actual values may be higher as the sum of the calculated inductive and non-inductive currents is less than the measured plasma currents. Possible causes of this discrepancy will be discussed. These plasmas aim at the regime envisioned for proposed future spherical torus devices, such as NHTX and ST-CTF which plan to operate in this strongly shaped regime but at lower β_t. These plasmas utilized n=1 RFA/RWM suppression and n=3 error field correction. Lithium evaporation was used to improve plasma confinement. Divertor strike point control experiments in support of the planned liquid lithium divertor upgrade will also be described.

*This work was supported by DoE contract No. DE-AC02-09CH11466

14:48
JO4 5 Discharge Evolution Control via 3D Field ELM Pacing in NSTX* A.C. SONTAG, J.M. CANIK, R. MAINGI, *ORNL* D.A. GATES, S.P. GERHARDT, *PPPL* V.A. SOUKHANOVSKII, *LLNL* ELMs triggered by externally applied 3D magnetic perturbations in conjunction with fueling optimization have been used to prevent the uncontrolled rise in density, radiated power and impurity accumulation observed in otherwise ELM-free NSTX discharges. The frequency of n=3 perturbations was scanned from 10 to 80 Hz with 100% ELM triggering achieved up to 60 Hz. Triggered ELMs arrested the rise in radiated power with only a 10% decrease in the total stored energy. Gas fueling optimization by replacing the typical single-pulse high field side fueling with pulsed supersonic gas injection resulted in elimination of the secular density rise during the discharge. Density remained below $5 \times 10^{19} m^{-3}$ for the first time throughout the length of a high-performance discharge. Negative amplitude current pulses in the n=3 coils subsequent to the triggering pulses were successful in minimizing the duration of the n=3 perturbations at the surface of the plasma. This resulted in less rotation braking and delayed the appearance of deleterious MHD.

*Work supported by U.S. DOE Contracts DE-AC05-00OR22725, DE-AC52-07NA27344 and DE-AC02-09CH11466.

15:00
JO4 6 Fine structure of heat flux deposition for different ELM types in NSTX JOON-WOOK AHN, RAJESH MAINGI, *Oak Ridge National Laboratory* LANE ROQUEMORE, HENRY KUGEL, *Princeton Plasma Physics Laboratory* VLAD SOUKHANOVSKII, *Lawrence Livermore National Laboratory* Investigation of heat flux deposition onto the divertor plates for different ELM types has been carried out in NSTX using a high temporal resolution IR camera, and revealed distinctive features for each ELM type. A single Type-III ELM is found to carry up to ~ 5% of total plasma energy to the divertor, during which typical peak heat flux (q_{peak}) values are 30-60 MW/m^2 with near SOL e-folding length (λ_q) of 3-4cm. Peak heat flux during the inter-ELM period is typically 3-5MW/m^2 with λ_q=1-1.5cm. On the other hand, the small, Type-V ELMs exhibit very different heat deposition characteristics. Due to the presence of multiple ELM filaments for a single time slice, q_{peak} becomes significantly lower and λ_q larger, q_{peak}=1-2MW/m^2 and λ_q=2-3cm. Filaments also make the far SOL λ_q very long, $\lambda_q \geq$ 10cm. As a result, Type-V ELMs are found to effectively disperse heat flux onto a large area of divertor plates with significantly lower q_{peak}. A detailed data analysis for heat flux deposition for different ELM types will be presented and implications for the future machine will be discussed. This work was supported by the US Department of Energy, contract numbers DE-AC05-00OR22725, DE-AC02-09CH11466, and DE-AC52-07NA27344.

15:12
JO4 7 Edge current profile measurements of peeling-like modes at high $\langle j_{edge}/B \rangle$ in PEGASUS* M.W. BONGARD, R.J. FONCK, E.T. HINSON, B.T. LEWICKI, A.J. REDD, *University of Wisconsin-Madison* Large-scale, coherent, high-n filamentary edge instabilities are routinely observed under conditions of high $\langle j_{edge}/B \rangle$ in PEGASUS. These ELM-like filaments are characterized with high-speed imaging, as well as scanning magnetic and Langmuir probes. Their properties include: low- to intermediate-n; a coherent electromagnetic signature; large poloidal coherence lengths; rotation with the bulk plasma; and explosive detachment from the edge with outboard radial propagation. Stability is sensitive to j_{edge}, with mode drive or suppression dependent on the sign of $\dot{I}_p$. The extremely low **B** ($B_{t,0} \leq$ 0.1 T) and high $j_{edge} \approx$ 0.1 MA/m^2 in PEGASUS lead to high peeling instability drive, proportional to $\langle j_{edge}/B \rangle$, comparable to that achieved in H-mode on larger experiments. However, in PEGASUS j_{edge} is driven by large $\dot{I}_p$ ($\leq$ 50 MA/s) and associated skin currents as opposed to a localized region of high bootstrap current in an H-mode pedestal. A new radial array of Hall-effect sensors measures internal $B_{\theta,edge}(R)$ directly with high spatial and temporal resolution to provide strong experimental constraint on $j_{edge}(\psi)$ in equilibrium reconstructions. Such equilibria may be used to uniquely test predictions of peeling-ballooning stability theory.

*Supported by U.S. D.O.E. Grant DE-FG02-96ER54375.

15:24
JO4 8 Deuterium retention in NSTX with lithium conditioning* C.H. SKINNER, H.W. KUGEL, L. ROQUEMORE, *P.P.P.L.* J.P. ALLAIN, C.N. TAYLOR, *Purdue U.* V. SOUKHANOVSKII, *L.L.N.L.* Fuel retention is an important constraint in the selection of plasma facing materials for next-step tokamaks. Gas balance measurements of retention in NSTX have been performed before- and with lithiumization of the vessel. The gas retained in ohmic discharges was measured by comparing the vessel pressure rise after a discharge to that of a gas-only pulse with the pumping valves closed. For neutral beam heated discharges the gas input and gas pumped by the NB cryopanels was tracked. Preliminary results show high (~ 90%) prompt retention both with- and without lithiumization. Outgassing of deuterium follows, initially at a high rate that then slowed over the following 24 hours to become comparable to the baseline vessel presure rate of rise and reduced the retention to the ~ 50% level. Four material samples were exposed to the plasma and analysed in-vacuo the same evening in order to investigate the fundamental processes governing particle balance with lithium coatings.

*Support is provided by the U.S. DOE Contract Nos. DE AC02-09CH11466 and DE-AC52-07NA27344.

15:36
JO4 9 Error Field Physics and Correction at High Beta in NSTX STEFAN GERHARDT, JON MENARD, JONG-KYU PARK, RON BELL, DAVE GATES, BENOIT LEBLANC, *PPPL* STEVE SABBAGH, *Columbia Univ.* HOWARD YUH, *Nova Photonics* NSTX experiments over the past two years have made progress in understanding the physics and correction of both resonant and non-resonant error fields (EFs). By varying the amplitude and phase of an applied n=3 field, it has been demonstrated that there is an intrinsic n=3 EF. The EF source has been isolated to the main vertical field coil by experimentally determining the optimal correction for various values of plasma current, toroidal field, and elongation. This coil is measured to be slightly out of round, producing a dominantly n=3 EF; both vacuum field and neoclassical toroidal viscosity torque calculations indicate a correcting field similar in magnitude and phase to the experimental correction. Measurements of n=1 EF penetration at high-beta show that the critical error field for driving an island is substantially smaller than the standard density scaling would predict. The critical role of the high-beta plasma response in determining the penetration threshold will be discussed, using results from the IPEC code. This research is funded by the US Department of Energy contract # DE-AC02-09CH11466.

15:48

JO4 10 Search for Multiple Resistive Wall Modes at High Normalized Beta in NSTX* S.A. SABBAGH, J.W. BERKERY, J.M. BIALEK, *Columbia U.* L. DELGADO-APARICIO, K. TRITZ, *JHU* R.E. BELL, S.P. GERHARDT, B. LEBLANC, *PPPL* Resistive wall mode (RWM) research has focused on the behavior and control of the least stable mode. However, at sufficiently high normalized beta, multi-mode theory suggests that stable modes may significantly influence the plasma dynamics. [1] This may affect active RWM control reliability in high beta plasmas. [2] Experiments at very high normalized beta have been conducted in NSTX to search for direct evidence of multi-mode RWM dynamics. Discharges were created with normalized beta reaching 7.4 in conditions with the ideal MHD no-wall limit near 4. Evidence of stable RWMs is examined by both kinetic and magnetic means. Characteristics are consistent with RWM behavior. At sufficiently high normalized beta, stable RWM-level low frequency activity is observed. X-ray data amplitude depends on beta, shows the activity to be global, and propagates in the co-NBI direction at frequencies near the expected peak in resonant magnetic field amplification. Observed growing RWMs appear to be separate from the stable mode activity, with different radial extent, supporting the hypothesis of multiple modes. [1] A.H. Boozer, Phys. Plasmas **10** (2003) 1458. [2] S.A. Sabbagh, et al., Phys. Rev. Lett. **97** (2006) 045004.

*Work supported by U.S. DOE Contracts DE-FG02-99ER54524 and DE-AC02-09CH11466.

16:00

JO4 11 On the Analysis of HHFW Heated Plasmas in NSTX* B.P. LEBLANC, R.E. BELL, *PPPL* L.A. BERRY, *ORNL* P. BONOLI, *PSFC-MIT* D.L. GREEN, *ORNL* R.W. HARVEY, *CompX* J.C. HOSEA, E. MAZZUCATO, C.K. PHILLIPS, A.L. ROQUEMORE, *PPPL* P.M. RYAN, *ORNL* G. TAYLOR, J.R. WILSON, *PPPL* J. WRIGHT, *PSFC-MIT* H. YUH, *Nova Photonics* Recent developments in the HHFW research program include a better understanding of edge effects that has enabled improved heating, leading to Te $\sim$ 5 KeV, and installation of an upgraded antenna that should nearly double power delivery. While the time-dependent analysis of a HHFW-only discharge can be simulated using the TORIC module in TRANSP, a self consistent treatment of the fast ion evolution during combined HHFW and NBI heating is not yet possible because the computed power deposited into the fast ions is not transferred into the fast particles via Fokker-Planck calculations. To remedy this problem we intend to use CQL3D with wave fields from the GENRAY, AORSA or TORIC codes to evolve the fast-ion distribution at a given time-slice. Combining these results with TRANSP should improve understanding of the behavior of the fast ions during HHFW heating.

*Work supported by DE-AC02-09CH11466.

16:12

JO4 12 Point-source helicity injection for ST plasma startup in PEGASUS* A.J. REDD, D.J. BATTAGLIA, M.W. BONGARD, R.J. FONCK, D.J. SCHLOSSBERG, *University of Wisconsin, Madison* Plasma current guns are used as point-source DC helicity injectors for forming non-solenoidal tokamak plasmas in the PEGASUS Toroidal Experiment. Discharges driven by this injection scheme have achieved $I_p \geq 100$ kA using $I_{inj} \leq 4$ kA. They form at the outboard midplane, transition to a tokamak-like equilibrium, and continue to grow inward as I_p increases due to helicity injection and outer- PF induction. The maximum I_p is determined by helicity balance (injection rate *vs* resistive dissipation) and a Taylor relaxation limit, in which $I_p \propto \sqrt{I_{TF} I_{inj}/w}$, where w is the radial thickness of the gun-driven edge. Preliminary experiments tentatively confirm these scalings with I_{TF}, I_{inj}, and w, increasing confidence in this simple relaxation model. Adding solenoidal inductive drive during helicity injection can push I_p up to, but not beyond, the predicted relaxation limit, demonstrating that this is a hard performance limit. Present experiments are focused on increasing the injection voltage (*i.e.*, helicity injection rate) and reducing w. Near-term goals are to further test scalings predicted by the simple relaxation model and to study in detail the observed bursty $n=1$ activity correlated with rapid increases in I_p.

*Work supported by US DOE OFES, grant DE-FG02-96ER54375

16:24

JO4 13 Absorber arc mitigation during CHI on NSTX* D. MUELLER, M.G. BELL, A.L. ROQUEMORE, *Princeton University* R. RAMAN, B.A. NELSON, T.R. JARBOE, *University of Washington* A method of non-inductive startup, referred to as transient coaxial helicity injection (CHI), was successfully developed on the Helicity Injected Torus (HIT-II) experiment and employed on the National Spherical Torus Experiment (NSTX). This technique has produced 160 kA of plasma current on closed flux surfaces. Over 100 kA of the CHI current has been coupled to inductively driven current ramp-up. In transient CHI, a voltage is applied across the insulating gap separating the inner and outer vacuum vessel and gas is introduced at the lower gap (the injector). The resulting current in the injector follows the helical magnetic field connecting the electrodes, forms a toroidal current and expands into the vacuum vessel. At higher CHI current, the poloidal field due to the plasma can connect the inner and outer vessels at the insulating gap at the top (called the absorber) of NSTX and lower the impedance there. This results in arcs in the absorber which are a source of impurities and which reduce the desired current in the injector. Two coils installed in the absorber will be used to reduce the magnetic field across the absorber gap and mitigate the absorber arcs.

*Work supported by U.S. DOE Contract Nos. DE-AC02-09-CH11466 and DE-FG03-96ER54361.

16:36

JO4 14 Overview of recent results from MAST SIMON PINCHES, *Euratom/UKAEA Fusion Association* MAST TEAM, The MAST programme continues to address key issues for ITER and beyond, whilst undertaking research and development to establish the physics basis for a CTF based upon a spherical tokamak. The programme is benefiting from a range of technical enhancements which include: two long-pulse neutral beam PINIs; a twelve coil array of internal coils for ELM control; a multi-chord MSE diagnostic with 35 channels, 2.5 cm spatial resolution and down to 0.5ms time resolution, a new long pulse 28 GHz gyrotron (on loan from ORNL) allowing EBW start-up studies at higher power; an upgraded Thompson scattering system (240Hz, 120 core channels) together with a "smart" triggering system; a divertor science facility; and a disruption mitigation valve (on loan from FZJ). Recent studies include: ELM control using RMPs; transport and confinement including the effects of collisionality; off-axis current drive including the impact of fast particle instabilities; a campaign of counter injected neutral beam; and NTV studies in collaboration with the NSTX team. This presentation will provide an overview of recent results and future plans. Funded by EPSRC and EURATOM.

16:48

JO4 15 Exploitation of high resolution beam spectroscopy diagnostics on MAST CLIVE MICHAEL, MAARTEN DEBOCK, NEIL CONWAY, ROB AKERS, LYNTON APPEL, ANTHONY FIELD, MIKE WALSH, MARCO WISSE, *Euratom/UKAEA Fusion Association, Culham Science Centre, Abingdon, OX14 3DB, UK* MAST TEAM, Recent developments in beam spectroscopy on MAST, including CXRS, MSE and a pilot FIDA system have revealed new information about phenomena such as ITBs, MHD instabilities, transport and fast particle physics. For example, ITBs in the ion temperature and toroidal rotation have been observed with the 64ch CXRS system, while reverse-shear q profiles have been observed with the recently commissioned 35ch MSE system. Thus, the synergy of these diagnostics helps us to understand, among other things, the role of magnetic and rotational shear on ITBs. MSE measurements have also helped to understand MHD phenomena such as locked modes (characterized by changes in toroidal momentum, revealed by CXRS), sawteeth, and internal reconnection events. Finally, the temporal/spatial resolution and SNR of the MSE system have been exploited. Interesting results include the detection of low frequency ($\sim$ 2kHz) magnetic field fluctuations, characterization of the radial structure of higher frequency ($<$ 100kHz) broadband and coherent density (BES) fluctuations, and the identification of short scale length features ($\sim$ 1.8cm) in the current profile near the edge pedestal.

17:00

JO4 16 Modeling of Optimization and Control of EBW Heating and Current Drive* JAKUB URBAN, *EURATOM/IPP.CR Association, IPP AS CR, Prague* JOAN DECKER, YVES PEYSSON, *EURATOM-CEA, Cadarache, France* JOSEF PREINHAELTER, *EURATOM/IPP.CR Association, IPP AS CR, Prague* GARY TAYLOR, *Princeton Plasma Physics Laboratory, Princeton, NJ, USA* LINDA VAHALA, *Old Dominion University, Norfolk, VA, USA* GEORGE VAHALA, *College of William & Mary, Williamsburg, VA, USA* We present a modeling of Electron Bernstein waves (EBWs) by recently coupled AMR (Antenna—Mode-conversion—Ray-tracing) and LUKE (3D Fokker-Planck) codes. The electrostatic EBW is a promising candidate for localized heating and current drive in high-β plasmas, where the standard electron cyclotron O- and X-waves are cutoff. EBW heating and current drive is simulated here in spherical tokamak conditions, particularly in typical NSTX and MAST equilibria and also in equilibria predicted by transport modeling. The EBW injection parameters are varied in order to find optimized scenarios and a possible way to control the deposition location and the driven current. This task is rather challenging because EBW ray trajectories and $N_{\|}$ spectra are strongly dependent on the plasma parameters.

*Work Supported by EFDA, by DoE, by AS CR project AV0Z-20430508, and by EURATOM.

SESSION JO5: LASER-PLASMA COUPLING AT LONG SCALE LENGTHS

Tuesday Afternoon, 3 November 2009
Hanover CDE at 14:00
Larry Suter, Lawrence Livermore National Laboratory, presiding

14:00

JO5 1 Optical backscatter measurements to study laser plasma interactions on NIF J. MOODY, P. DATTE, K. KRAUTER, E. BOND, R. HIBBARD, P. MICHEL, B.J. MACGOWAN, S.H. GLENZER, L. SUTTER, N. MEEZAN, R. LONDON, J.L. KLINE, K. WIDMANN, L. DIVOL, J. JACKSON, *LLNL* C. NIEMANN, *UCLA* S. VERNON, *NSTech* We describe measurements of backscattered light from NIF targets under a variety of laser conditions. These measurements will initially be used to validate the point design hohlraum and select phase plates for the ignition experiments. Backscatter measurements are made on two separate groups of 4 beams (a quad). One quad is 30 ° from the hohlraum axis and the other at 50 °. The backscatter measurement utilizes a full aperture backscatter system (FABS) to measure light backscattered into the final focus lens of each beam in the quad and a near backscatter imager (NBI) to measure light backscattered outside of the beam quad. Both instruments must work in conjunction to provide spectrally and temporally resolved backscattered power. We describe the measurements, analysis, and comparison with simulations. This work was performed under the auspices of the U.S. Department of Energy by University of California, Lawrence Livermore National Laboratory under Contract W-7405-Eng-48.

14:12

JO5 2 Scaling Stimulated Brillouin Scattering from OMEGA gas-filled hohlraums to NIF hohlraums with gold-boron layers RICHARD BERGER, LAURENT DIVOL, DUSTIN FROULA, SIEGFRIED GLENZER, RICHARD LONDON, NATHAN MEEZAN, LAURENCE SUTER, *Lawrence Livermore National Laboratory* The long laser pulse length required to achieve ignition on the National Ignition Facility (NIF) creates long scale-length, hot, high-Z plasma inside the hohlraum from which stimulated Brillouin scatter (SBS) is predicted to be 20-40%. Adding $\sim$ 40% Boron to a thin layer of the high-Z wall reduces the predicted SBS to less than a percent. A number of experiments at the OMEGA laser facility have tested elements of the physics of SBS in gold-boron and the modeling tools. The damping rates for pure gold plasma and plasmas with various gold-boron mixtures can be duplicated with mixtures of CO_2 and hydrocarbon gasses. By combining the rad-hydro code HYDRA to compute bulk plasma parameters and the paraxial-wave-solver pF3d to compute backscatter, levels of stimulated Brillouin backscatter that agree with the measurements have been predicted in advance of the experiments. Although the SBS increases with the calculated average gain as expected, closer examination shows that, for the same gain, plasmas with very weakly damped ion acoustic waves Brillouin scatter light more strongly than plasmas with more strongly damped ion acoustic waves. We present theory and simulations to explain this behavior in the OMEGA and NIF experiments.

14:24

JO5 3 Gas-Filled Targets to Study Laser Backscatter on the National Ignition Facility* R.A. LONDON, E.A. WILLIAMS, D.E. HINKEL, J.D. MOODY, L.J. SUTER, *Lawrence Livermore National Laboratory* To achieve indirect drive fusion at the National Ignition Facility (NIF), laser beams must propagate through several millimeters of high-density plasma to reach the hohlraum walls. Stimulated Brillouin and Raman backscatter could create problems with energetics and/or symmetry. Laser backscatter at NIF will be diagnosed with full aperture backscatter systems (FABS) and near backscatter imagers (NBI). Several gas-filled targets ("gas pipes") have been designed to provide backscatter sources to commission the diagnostics. The 7-mm long gas pipes are filled with various gases, including C_5H_{12} and CO_2, and are irradiated by a NIF quad with 16 kJ of energy in 2-4 ns pulses. We describe the design of the gas pipes using hydrodynamics and laser-plasma-interaction computer codes. The relationship between the design parameters (gas composition and density and laser pulse shape) and the character of the backscatter (Brillouin versus Raman and narrow versus broad angle) are discussed. Comparisons of predicted and measured backscatter distributions and levels are discussed.

*Prepared by LLNL under Contract DE-AC52-07NA27344.

14:36

JO5 4 Laser-plasma interaction analyses of National Ignition Campaign energetics experiments* D.E. HINKEL, C.H. STILL, A.B. LANGDON, E.A. WILLIAMS, *Lawrence Livermore National Laboratory* The National Ignition Campaign is beginning a series of energetic experiments[1,2] at the National Ignition Facility (NIF), to be performed in the summer and fall of 2009. These experiments will test our understanding of, and our ability to, simulate laser-plasma interactions under NIF-like conditions. To this end, we will perform pF3D[3] simulations of beam propagation of energetics campaign targets. Reflectivity levels and spectra, images of the scattered light angular distribution, and hot electron estimates will be presented and compared to experimental results. Modification of the energy deposition by laser-plasma interactions, and the impact on symmetry, will also be presented. 1. S. H. Glenzer et al., this meeting. 2. N. B. Meezan et al., this meeting. 3. R. L. Berger, C. H. Still, E. A. Williams, and A. B Langdon, Phys. Plasmas 5, 4337 (1998); C. H. Still, R. L. Berger, A. B. Langdon, D. E. Hinkel, L. J. Suter, and E. A. Williams, Phys. Plasmas 7, 2023 (2000).

*Performed by LLNL under Contract DE-AC52-07NA27344.

14:48

JO5 5 Modeling laser-plasma interactions in NIF vacuum hohlraums* E.A. WILLIAMS, D.E. HINKEL, *Lawrence Livermore National Laboratory* C.H. STILL, A.B. LANGDON, *Lawrence Livermore National Laboratory* R.E. OLSON, *Sandia National Laboratory* J. KLINE, *Los Alamos National Laboratory* In preparation for the NIF ignition campaign, a series of experiments are underway firing 96 and 192 beams of the NIF laser into empty gold hohlraums. The primary purpose of these experiments is to qualify the DANTE filtered x-ray diode radiation temerature diagnostic. We plan to have backscatter diagnostics available, giving us an opportunity to test our LPI modeling on the NIF scale. In addition to scaling with energy, we test the use of a gold-boron coating on the hohlraum wall to reduce SBS via increased ion Landau damping of the ion-acoustic waves. We use Lasnex to simulate the hydrodynamic evolution of the hohlraum plasma. Steady state gains were computed using our diagnostic NEWLIP. These were used to suggest appropriate backscatter simulations to be performed with pF3D, a massivel parallel code that couples paraxial light propagation with fluid models of the stimulated plasma ansd ion waves evolving on a background plasma. We describe the results of these simulations, pre- and post-shot, and compare them with experimental results.

*Performed by LLNL under Contract DE-AC52-07NA27344.

15:00

JO5 6 Light Amplification by Seeded Stimulated Raman Scattering of a Crossing Beam and Its Saturation as is Relevant to Ignition Experiments R.K. KIRKWOOD, Y. PING, S.C. WILKS, N. MEEZAN, P. MICHEL, E.A. WILLIAMS, D. CLARK, L.J. SUTER, O.L. LANDEN, *LLNL* N.J. FISCH, E.O. VALEO, V. MALKIN, *Princeton* J. WURTELE, *UCB/LBL* T.L. WANG, S.F. MARTINS, C. JOSHI, *UCLA* Experiments with Janus laser seed the SRS of a 1ns 1054 nm beam with a frequency shifted 3.5 ps pulse, in a plasma in which the resonant density and temperature exist over a $< \sim$ 2mm interaction length. The hot ($< \sim$ 240 eV), low density (n/nc = 0.01), plasma created in the experiments produces a low gain spatial rate, similar to what is experienced by the outgoing SRS scatter which is generated in the interior of indirect drive ignition targets when it subsequently interacts with multiple incoming beams. The experiments show that even with a 1 x 10^{14} W/cm^2 pump intensity, gains of greater than 20x can occur under these conditions. The observed amplification is seen to reduce as seed energy increases, consistent with the scattering waves being saturated by electron kinetic effects that operate on the 3.5 ps time scale, (ie; electron trapping), and scaling like 1D PIC simulations. These results benchmark models used to design USP plasma amplifiers, and indirect drive ignition targets. This Work was performed under the auspices of the U.S. DOE by Lawrence Livermore Lab under contract No. DE-AC52- A27344, LLNL-ABS-405480.

15:12

JO5 7 Laser Plasma Instability (LPI) Driven Light Scattering Measurements with 44 beam-lines of Nike KrF Laser* J. OH, *Research Support Instruments* J.L. WEAVER, D.M. KEHNE, L.S. PHILLIPS, S.P. OBENSCHAIN, V. SERLIN, *Naval Research Laboratory* E.A. McLEAN, R.H. LEHMBERG, C.K. MANKA, *Research Support Instruments* With short wavelength (248 nm), large bandwidth ($\sim 1\ THz$), and ISI beam smoothing, Nike KrF laser provides unique opportunities of LPI research for direct-drive inertial confinement fusion. Previous experiments at intensities ($10^{15} \sim 10^{16} W/cm^2$) exceeded two-plasmon decay (TPD) instability threshold using 12 beam-lines of Nike laser.[a,b] For further experiments to study LPI excitation in bigger plasma volumes, 44 Nike main beams have been used to produce plasmas with total laser energies up to 1 kJ of $\sim$ 350 psec FWHM pulses. This talk will present results of the recent LPI experiment focusing on light emission data in spectral ranges relevant to the Raman (SRS) and TPD instabilities. The primary diagnostics were time-resolved spectrometers with an absolute-intensity-calibrated photodiode array in $(0.4 \sim 0.8)\omega_0$ and a streak camera near $0.5\omega_0$. Blackbody temperature and expansion speed measurements of the plasmas were also made. The experiment was conducted at laser intensities of $(1 \sim 4) \times 10^{15}\ W/cm^2$ on solid planar CH targets. [a] J. L. Weaver, et al, NO4.14, APS DPP (2008) [b] J. Oh, et al, NO4.15, APS DPP (2008) * Work supported by DoE/NNSA and performed at Naval Research Laboratory.

15:24

JO5 8 Updated LPI Thresholds for the Nike Laser* J.L. WEAVER, *Laser Plasma Branch, Plasma Physics Division, NRL* J. OH, *Research Support Instruments (RSI)* B. AFEYAN, *Polymath Research Inc.* L. PHILLIPS, J. SEELY, D. KEHNE, C. BROWN, S.P. OBENSCHAIN, V. SERLIN, A.J. SCHMITT, *NRL* U. FELDMAN, *ARTEP* G. HOLLAND, *NIST* C. MANKA, R.H. LEHMBERG, E. McLEAN, *RSI* Advanced implosion designs for direct drive inertial confinement fusion use high laser intensities (10^{15}-10^{16} W/cm^2) to achieve gain (g> 100) with a reduction in total laser energy (E< 1 MJ). Krypton-fluoride lasers such as the Nike laser at NRL are an attractive choice due to their combination of short wavelength (248 nm), large bandwidth (1-2 THz), and beam smoothing by induced spatial incoherence but the potential threat from laser-plasma instabilities (LPI) needs to be assessed. The 2008 LPI campaign at Nike yielded threshold intensities above 10^{15} W/cm^{2}for the two-plasmon instability, a value higher than reported for 351 nm glass lasers. The experiments used a planar geometry, solid polystyrene targets, and a subset of beams (E< 200 J) with a reduced focal spot (d< 125 μm). The 2009 campaign extended the shot parameters to higher laser energies (E < 1 kJ) and larger spot sizes (d< 300 μm). Spectrally-resolved and time-resolved measurements of x-rays and emission near $^1/_2\omega_o$ and $^3/_2\omega_o$ harmonics of the laser wavelength show threshold intensities consistent with the 2008 results. *Work supported by DoE/NNSA

15:36

JO5 9 Two-Plasmon Decay: Simulations and Experiments on the NIKE Laser System* LEE PHILLIPS, J.L. WEAVER, J. OH, A.J. SCHMITT, S. OBENSCHAIN, D. COLOMBANT, *Naval Research Laboratory* NIKE is a Krf laser system at the Naval Research Laboratory used to explore hydrodynamic stability, equation of state, and other issues arising in the research toward inertial fusion energy. The relatively small KrF wavelength, according to widely used theories, raises the threshold of most parametric instabilities. We report on simulations performed using the FAST3d radiation hydrocode to design TPD experiments. By post-processing the results of the simulations we have designed experiments that have explored the use of simple threshold formulas (from developing theories) and help establish the soundness of our simulational approach. Turning to the targets proposed for ICF energy research, we have found that among the designs for the proposed Fusion Test Facility (Obenschain et al., Phys. Plasmas 13 056320 (2006)), are some that are below LPI thresholds. We have also studied high-gain KrF shock ignition designs and found that they are below LPI thresholds for most of the implosion, becoming susceptible to TPD only late in the pulse.

*This research is funded by the US DOE.

15:48

JO5 10 Mitigation of Fast-Electron Production by the Two-Plasmon-Decay Instability in Directly Driven Targets. W. SEKA, D.H. EDGELL, J.F. MYATT, A.V. MAXIMOV, R.W. SHORT, R.S. CRAXTON, *Laboratory for Laser Energetics, U. of Rochester* D. RUSSELL, *Lodestar* D.F. DUBOIS, *LANL* H.X. VU, *U. of California, San Diego* Under certain conditions the fast-electron production caused by the two-plasmon-decay (TPD) instability can be mitigated through modulation of the laser pulse shape. This mitigation can be enhanced when combined with a target that contains a high-Z material. Planar- and spherical-target experiments on OMEGA that show this mitigation are diagnosed using hard x-ray diagnostics and Thomson scattering for the TPD plasma waves. The results of these experiments will be presented. This work was supported by the U.S. Department of Energy Office of Inertial Confinement Fusion under Cooperative Agreement No. DE-FC52-08NA28302.

16:00

JO5 11 Growth and Saturation of Two-Plasmon-Decay Instability Driven by Crossing Laser Beams in OMEGA Plasmas A.V. MAXIMOV, J.F. MYATT, R.W. SHORT, W. SEKA, C. STOECKL, J.A. DELETTREZ, *Laboratory for Laser Energetics, U. of Rochester* Under the conditions of direct-drive inertial confinement fusion experiments on the OMEGA Laser System, the threshold of two-plasmon-decay (TPD) instability is typically exceeded, and the TPD instability can generate fast electrons that are important for target implosions.[1,2] The characteristic feature of OMEGA experiments and of experiments at the National Ignition Facility is that the laser–plasma interaction is driven by multiple crossing laser beams that are randomized in space because of distributed phase plates, and randomized in time because of smoothing by spectral dispersion. The thresholds and growth rates of TPD instability are calculated and compared with the results of the three-wave TPD model.[3] The saturation of TPD instability is found to be caused by low-frequency ion-acoustic perturbations driven by the laser beams and also by the ponderomotive force of plasma waves, including the Langmuir decay instability. This work was supported by the U.S. Department of Energy Office of Inertial Confinement Fusion under Cooperative Agreement No. DE-FC52-08NA28302.

[1]C. Stoeckl *et al.*, Phys. Rev. Lett. **90**, 235002 (2003).
[2]W. Seka *et al.*, Phys. Plasmas **16**, 052701 (2009).
[3]A. Simon *et al.*, Phys. Fluids **26**, 3107 (1983).

16:12

JO5 12 Anisotropy and Angular Dependence of Two-Plasmon Decay Driven by Multiple Overlapping Laser Beams in Direct-Drive Geometry R.W. SHORT, *Laboratory for Laser Energetics, U. of Rochester* Experimental observations of half-harmonic and hard x-ray emission on OMEGA have shown that two-plasmon-decay (TPD) signals depend on the collective rather than the single-beam intensity.[1] Previous theoretical work has shown that if one of the plasmon wave vectors is aligned along the density gradient and the axis of symmetry of several laser beams, the beams act in concert and result in the same growth as would be obtained for a single beam at the combined intensity.[2] In this talk this analysis will be extended to plasmon wave vectors that deviate from the beam axis of symmetry or from the density gradient. The dependence of the integrated spatial growth of the instability on the angle of deviation will be determined. In a direct-drive spherical configuration this dependence determines the anisotropy of the resulting hot-electron distribution, so it is important in modeling the preheat of the core by TPD-generated hot electrons.[3] This work was supported by the U.S. Department of Energy Office of Inertial Confinement Fusion under Cooperative Agreement No. DE-FC52-08NA28302.

[1]C. Stoeckl *et al.*, Phys. Rev. Lett. **90**, 235002 (2003).
[2]R. W. Short, Bull. Am. Phys. Soc. **53**, 245 (2008).
[3]J. A. Delettrez *et al.*, Bull. Am. Phys. Soc. **53**, 248 (2008).

16:24
JO5 13 Extended Zakharov Modeling of Preheat Caused by the Two-Plasmon Decay Instability in Direct-Drive ICF Plasmas. J.F. MYATT, J.A. DELETTREZ, W. SEKA, D.H. EDGELL, A.V. MAXIMOV, R.W. SHORT, *Laboratory for Laser Energetics, U. of Rochester* D.F. DUBOIS, *LANL and Lodestar Research Corp.* D.A. RUSSELL, *Lodestar Research Corp.* H.X. VU, *U. of California–San Diego* The results of two-dimensional extended Zakharov calculations[1] of saturated two-plasmon-decay spectra and absorption will be presented in inhomogeneous long-scale-length plasma—the plasma parameters motivated by OMEGA-scale designs. Estimates of hot-electron production and preheat are obtained from the Zakharov calculations using a "test particle" approach and a *LILAC* model for target hydrodynamic evolution.[2] This work was supported by the U.S. Department of Energy Office of Inertial Confinement Fusion under Cooperative Agreement No. DE-FC52-08NA28302.

[1]D. F. DuBois, D. A. Russell, and H. A. Rose, Phys. Rev. Lett. **74**, 3983 (1995).
[2]J. Delettrez *et al.*, Phys. Rev. A **36**, 3926 (1987).

16:36
JO5 14 Cross-Beam Energy Transport in Direct-Drive-Implosion Experiments D.H. EDGELL, W. SEKA, J.A. DELETTREZ, R.S. CRAXTON, V.N. GONCHAROV, I.V. IGUMENSHCHEV, J.F. MYATT, A.V. MAXIMOV, R.W. SHORT, T.C. SANGSTER, R.E. BAHR, *Laboratory for Laser Energetics, U. of Rochester* Time-resolved scattered-light spectroscopy from spherical-target implosions on OMEGA provides information about the time-dependent absorbed power and the spectral shift of the scattered light. Modeled spectra reproduce the major features in the observed spectral shifts but not the absolute magnitudes of the predicted spectral shifts and the total scattered light, suggesting that modeling overpredicts absorption (typically a difference of 10% to 15% of the total time-integrated laser-pulse power). Cross-beam energy transfer appears to explain the discrepancy and its effect on the absorbed power, scattered-light spectra, and bang-time and is examined for a series of implosions with varying intensity. This work was supported by the U.S. Department of Energy Office of Inertial Confinement Fusion under Cooperative Agreement No. DE-FC52-08NA28302.

16:48
JO5 15 Modeling Crossed-Beam Energy Transfer in Implosion Experiments on OMEGA I.V. IGUMENSHCHEV, D.H. EDGELL, V.N. GONCHAROV, J.A. DELETTREZ, A.V. MAXIMOV, J.F. MYATT, W. SEKA, A. SHVYDKY, *Laboratory for Laser Energetics, U. of Rochester* Scattered-light measurements in direct-drive-implosion experiments on the OMEGA Laser System indicate enhanced light scattering in comparison with radiative-hydrodynamic simulations that include inverse bremsstrahlung as the primary absorption mechanism of the laser light. Beam-to-beam energy transfer caused by stimulated Brillouin scattering (SBS) is likely responsible for the reduction in absorbed energy at the end of drive pulses in OMEGA implosions. We have developed a simplified model for crossed-beam energy transfer that accounts for the propagation and coupling of multiple laser beams and associated plasma waves in spherically symmetric plasmas. This model has been implemented in the radiative-hydrodynamic code *LILAC*, demonstrating effects of SBS in implosion experiments on OMEGA. This work was supported by the U.S. Department of Energy Office of Inertial Confinement Fusion under Cooperative Agreement No. DE-FC52-08NA28302.

SESSION JO6: WAVES, TURBULENCE, AND BOUNDARY EFFECTS IN LABORATORY AND SPACE PLASMAS I
Tuesday Afternoon, 3 November 2009
Hanover FG at 14:00
Mark Gilmore, University of New Mexico, presiding

14:00
JO6 1 Observations of intense whistler-mode waves and simulations of associated acceleration of electrons CYNTHIA CATTELL, *School of Physics and Astronomy, University of Minnesota, Minneapolis MN* AARON BRENEMAN, KEITH GOETZ, PAUL KELLOGG, KRIS KERSTEN, LYNN WILSON III, JOHN WYGANT, *SPA, UMn* STUART BALE, ILAN ROTH, *SSL, UC, Berkeley CA* MILAN MAKSIMOVIC, *LESIA, Meudon, France* Observations from waveform capture instruments on STEREO and Wind have shown that large amplitude whistler-mode wave packets occur in the Earth's radiation belts, in stream interaction regions and at shocks. Amplitudes are 1 to 2 orders of magnitude larger than previously reported from observations and than those assumed in most theoretical models of wave/particle interactions in these regions. The waves are often monochromatic, obliquely propagating, and have both large longitudinal components and components parallel to the background magnetic field. Particle tracing code results show that, in the radiation belts, the waves can result in energization by many MeV during a single wave packet encounter due to coherent, nonlinear processes including trapping. Simulation results also indicate that the waves can scatter electrons by 10s of degrees in both solar wind and magnetospheric conditions. The results suggest that coherent processes with time scales of seconds, rather than quasi-linear processes with timescales of hours to days, may sometimes dominate scattering and energization by waves.

14:12
JO6 2 Warm electromagnetic lower hybrid wave dispersion ALIX VERDON, IVER CAIRNS, DON MELROSE, PETER ROBINSON, *School of Physics, The University of Sydney, NSW 2006, Australia* Lower hybrid (LH) waves can interact resonantly with both electrons and ions, and so can transfer energy between electrons and ions. This property of LH waves is unusual and suggests that they may play a role in particle acceleration and heating in the wide variety of physical contexts in which they occur. Specifically, LH waves are believed to be relevant to the generation of radio emissions in the outer heliosphere, and possibly also to electron and ion acceleration in magnetic reconnection regions in Earth's magnetosphere and the solar atmosphere. In this paper a new analytic dispersion relation for LH waves is presented and compared with numerical results calculated using a fully electromagnetic code. It is shown that the new analytic dispersion relation agrees closely with the numerical results for the real part of the frequency. Surprisingly, ion magnetization effects are important for the imaginary part of the frequency (or equivalently, the damping rate), and can cause the continuous LH mode to break up into a series of segments of ion Bernstein modes. In addition, in situations where the electrons and ions have a net relative drift parallel to the magnetic field of many times the electron thermal speed, numerical results show that wave growth may occur in a mode near the LH frequency. Again, ion magnetization effects play an important role.

14:24

JO6 3 Investigation of drift flute turbulence in high beta plasmas in the presence of shear flows* I. PARASCHIV, V.I. SOTNIKOV, *University of Nevada, Reno, Reno, NV 89557* J.N. LEBOEUF, *JNL Scientific, Casa Grande, AZ 85294* O.G. ONISHCHENKO, E. YASIN, R. PRESURA, J. KINDEL, *University of Nevada, Reno, Reno, NV 89557* Laboratory experiments performed at the Nevada Terawatt Facility have studied the propagation of a plasma plume across a magnetic field. These experiments have shown that there are instabilities growing at the plasma-field interface, which could be explained by the excitation of flute drift modes. Experimental results also suggest that transverse ExB flows may have an important effect on these instabilities. Using the two-fluid equations in the low-frequency approximation, a nonlinear set of equations for the electrostatic potential, magnetic field and density perturbations was derived, taking into account finite ion Larmor radius effects. The resulting nonlinear equations describe the evolution of small-scale flute turbulence, and the generation of large scale zonal structures in the presence of shear flows.

*Work supported by the NNSA/DOE grant no. DE-FC52-06NA27616

14:36

JO6 4 Intermittency in self-organized shear flows EUN-JIN KIM, *University of Sheffield* H.-L. LIU, *HAO/NCAR* J. ANDERSON, *University of Sheffield* Understanding multi-scale interactions is an outstanding problem in astrophysical plasmas. Despite complex nonlinear dynamics, coherent structures such as shear flows often form from small-scale turbulence, which then feed back on small-scales. A remarkable consequence of this mutual interaction is self-organization, which provides a powerful paradigm for understanding complexity in many systems. In this contribution, we present a novel statistical theory of self-organisation of forced shear flows, modeled by a nonlinear diffusion equation [1]. A non-perturbative method based on a coherent structure is utilized for the prediction of the PDFs, showing strong intermittency with exponential tails. We confirm these results by numerical simulations. The predicted power spectra are also in a good agreement with simulation results. Furthermore, the results reveal a significant probability of supercritical states due to stochastic perturbation. To elucidate a crucial role of relative time scales of relaxation and disturbance in the determination of the PDFs, we present results obtained in a threshold model where the diffusion is given by discontinuous values. Our results highlight the importance of the statistical description of gradients, rather than their average value as has conventionally been done. [2] E Kim and J Anderson, Phys. Plasmas, v15, 114506 (2008).

14:48

JO6 5 Experimental test of Baalrud's model for ion velocity at the sheath edge for a two ion species plasma* NOAH HERSHKOWITZ, CHI-SHUNG YIP, *University of Wisconsin-Madison* GREG SEVERN, *University of San Diego* Recent experiments have shown that ions in plasmas containing two ion species reach a common velocity at the sheath-presheath boundary [1]. A new theory [2] suggests that collisional friction between the two ion species enhanced by two stream instability affects the drift velocity of each ion species near the sheath edge and finds that the difference in ion velocities at the sheath-presheath boundary is given by $\sqrt{1/2\alpha(v_{th1}^2+\alpha v_{th2}^2)}$, where $\alpha = n_1M_1/(n_2M_2)$. We report the first experimental test of this model. We measure ion velocity distribution functions (ivdfs) near sheath edge in Argon/Xenon and Argon/Helium plasmas as a function of the concentration ratios. We show that for sufficiently great relative Xenon concentration, ions do not reach a common speed at the sheath edge. The relative concentration of the two ion species, which determines α, is inferred from Ion Acoustic Wave phase velocity measurements, the ivdfs are determined by Laser Induced Florescence. [1] Lee, D; Hershkowitz, N; Severn, GD. Appl. Phys. Lett. 91, 041505 (2007) [2] S.D. Baalrud, J.D. Callen, and C.C. Hegna, GEC 2009

*Work supported by the DoE grants nos. DE-FG02-97ER54437, and DE-FG02-97ER54728

15:00

JO6 6 Detailed reconstruction of the magnetic-field profile penetrating into a nearly-collisionless plasma RAMY DORON, BOAZ RUBINSTEIN, JONATAN CITRIN, RON ARAD, YITZHAK MARON, *Weizmann Institute of Science* AMNON FRUCHTMAN, *Holon Academic Institute of Technology* Observations of nearly-collisionless plasmas interacting with pulsed magnetic fields reveal rich physics and intriguing, unexplained phenomena. Among these are the mechanism of rapid (non-diffusive) magnetic-field penetration, the structure of the propagating magnetic front, the fate of the dissipated magnetic energy, and the particle dynamics. We utilize highly-resolved spectroscopy to study the penetration of a $\sim$ 1 T magnetic field into a low resistivity plasma ($n_e \sim 10^{14}$ cm^{-3}, $T_e \sim$ 6 eV). The magnetic-field profile is determined from Doppler-shifted line-emission of ions at the *edge* of a trace-element column that are pushed by the magnetic field. This technique allows for achieving submilimeter spatial resolution, approaching the electron skin-depth scale. Reliable Doppler-shift measurements allow for determining field magnitudes as low as 0.2 T, which are extremely difficult to measure via Zeeman spectroscopy under the present conditions. Moreover, the measured ion velocities enable to calculate self-consistently the plasma compression. These calculations predict the build up of a density shock that may induce instabilities behind the penetrating magnetic front.

15:12

JO6 7 Neutral depletion in magnetized plasmas* AMNON FRUCHTMAN, GENNADY MAKRINICH, *H.I.T. - Holon Institute of Technology* The effect of neutral depletion on the steady-state of a low temperature magnetized plasma is studied. The nonlinear cross- field diffusion is assumed ambipolar. The nonlinearity results from the dependence of the transport coefficients on the plasma and neutral densities. Recent results are described. It is shown that when the dominant electron collisions are with neutrals, neutral depletion results in a peaking of the density on-axis. If, however, electrons collide mostly with ions, neutral depletion results in flattening of the radial density profile. The nonlinear dependence of the density on the plasma flux is shown to differ for the two cases. There is a fast exponential increase of the plasma density with an increase of the plasma flux, when electrons collide mostly with neutrals, while the plasma density increases only logarithmically with the plasma flux when electron collisions with ions are dominant [1]. We then show how the 2D transport along and across magnetic field in the presence of neutral depletion result in a hollow cylindrical profile of the plasma density, in which the plasma density has a minimum on the cylinder axis. [1] A. Fruchtman, Plasma Sources Sci. Technol. **18**, 025033 (2009).

*This research was supported by the Israel Science Foundation (Grant no. 864/07).

15:24
JO6 8 Kappa: A New Universal Constant in Turbulent Behaviors C.T. RAYNOR, A.B. ALEXANDER, M. ROBINSON, J.A. JOHNSON III, *Florida A&M University* When turbulence physics is characterized as a Ginzburg-Landau phase transformation with the tools from BCS Theory, a new universal constant is derived, defined as κ, which can be determined from measured quantities in a turbulent glow discharge plasma. Such a constant would provide a new constraint in the MHD equations for turbulent plasma simulations. Values of κ are calculated for a wide range of noble gases subjected to an axial magnetic field in the range 0-500 gauss. We report first efforts at a determination of the sensitivity of κ to changes in the local molecular constituent and the strength of the local magnetic field. We will also evaluate the implications from these results for new turbulence physics.

15:36
JO6 9 Characteristic Frequencies and Critical Energies in Magnetized Turbulent Glow Discharge Plasmas* M. ROBINSON, A.B. ALEXANDER, C.T. RAYNOR, J.A. JOHNSON III, *Florida A&M University* Previous studies have revealed that dynamic axial magnetic fields can significantly influence the critical turbulent energy and the characteristic turbulent frequencies in glow discharge plasmas. To this end, we analyze the light signatures of several noble gases at constant pressure of 500mtorr and under the influence of static axial magnetic fields ranging from 0 to 500 Gauss. We find that there may be a relationship between the mass of the gas and the slope of its critical turbulent energy when plotted versus magnetic field. We find that this behavior is echoed in the characteristic turbulent frequencies. Further, for all masses and all magnetic fields, we find a high degree of correlation between the two parameters, with important implications for new turbulence physics.

*Research funded in part by the National Science Foundation and by the Department of Energy.

15:48
JO6 10 Evidence of New Turbulence Physics in Madison Symmetric Torus Plasmas using a Second Order Phase Transformation Interpretation* E.D. MEZONLIN, J.B. TITUS, J.A. JOHNSON III, K.M. WILLIAMS, C.T. RAYNOR, C.A. WEATHERFORD, *Florida A&M University* When turbulence physics is characterized as a Ginzburg-Landau phase transformation with the tools from BCS Theory, a new universal constant is derived, defined as κ, which can be determined from measured quantities in the turbulent MST plasmas. Such a constant would provide a new constraint in the MHD equations for fusion plasma simulations. Values of κ are calculated from light and magnetic field fluctuations for a wide range of MST operating conditions. The implications from these results are evaluated for new turbulence physics and new fusion simulation methodologies. We would like to thank the MST group for providing data used in these analyses.

*Research funded in part by the National Science Foundation and by the Department of Energy.

16:00
JO6 11 Turbulent Parameters during Magnetic Field and Particle Diffusion Fluctuations in the Madison Symmetric Torus* J.B. TITUS, E.D. MEZONLIN, J.A. JOHNSON III, K.M. WILLIAMS, C.T. RAYNOR, *Florida A&M University* Turbulence physics may be characterized as a Ginzburg-Landau phase transformation with the tools from BCS Theory. Such a characterization predicts anomalous enhancements of transport at critical turbulent energies. The standard turbulent parameters have been studied during the magnetic field fluctuations and the particle and thermal diffusion coefficient fluctuations. We will determine correlations between the associated transport coefficients and the turbulent parameters in search of evidence of turbulence driven heating and diffusion enhancements at MST. We would like to thank the MST group for providing data used in these analyses.

*Research funded in part by the National Science Foundation and by the Department of Energy

16:12
JO6 12 First Evidence of Inverse Bremsstrahlung in Laser Enhanced Laser Induced Plasmas* D.L. WIGGINS, C.T. RAYNOR, E.D. MEZONLIN, J.A. JOHNSON III, *Florida A&M University* Plasmas are created using a Nd-YAG 1020mJ laser at 532nm in air at atmospheric pressures. We bathed the plasma with a1080nm laser beam from a continuous wave fiber laser with powers of 50 W to 1 kW. We have observed the apparent effects of inverse bremsstrahlung in the plasma as the cw laser power increases. Specifically, with increasing cw fiber laser power the electron temperature increases and then begins to saturate after a threshold as predicted due to inverse bremsstrahlung. Furthermore, after a threshold, the signal to noise in the ion lines increases and the signal to noise in the neutral lines decreases as predicted. Implications from these results for astrophysical plasmas as well as plasmas produced for remote sensing in laser induced breakdown spectroscopy are discussed.

*Research funded in part by the National Science Foundation, the Department of Energy and the Department of Defense.

16:24
JO6 13 Pre- and Post-Shock Wave Self-Induced Magnetic Field Geometry in a Hypersonic Arc Driven Shock Tube* K.M. WILLAMS, J.B. TITUS, A.B. ALEXANDER, C.T. RAYNOR, M. SCOTT, J.A. JOHNSON, *Florida A&M University* Using a version of the motional Stark Effect method based on relative line intensities to determine the internal magnetic field of the arc driven shock tube, a study comparing the magnetic field geometry before and after the primary and reflected shock wave plasma is conducted for different Noble gases. Using spectral line emissions from He, Ar, Kr, and other Noble gases measurements of the internal magnetic field of the shock tube are obtained. When the data for pre-primary shock region, post-primary shock region, pre-reflected and post-reflected shock regions are compared evidence of reconnection events is confirmed. When the magnetic field intensity and the direction evolve with turbulent energy, the B-field direction displays a discontinuity similar to a 2^{nd}-order phase transition.

*Research funded in part by the National Science Foundation and by the Department of Energy.

SESSION JP8: POSTER SESSION IV
Tuesday Afternoon, 3 November 2009
Grand Hall East at 14:00

JP8 1 EDUCATION AND OUTREACH

JP8 2 Plasma Science and Applications at the Intel Science Fair: A Retrospective* LEE BERRY,† *Oak Ridge National Laboratory* For the past five years, the Coalition for Plasma Science (CPS) has presented an award for a plasma project at the Intel International Science and Engineering Fair (ISEF). Eligible projects have ranged from grape-based plasma production in a microwave oven to observation of the effects of viscosity in a fluid model of quark-gluon plasma. Most projects have been aimed at applications, including fusion, thrusters, lighting, materials processing, and GPS improvements. However diagnostics (spectroscopy), technology (magnets), and theory (quark-gluon plasmas) have also been represented. All of the CPS award-winning projects so far have been based on experiments, with two awards going to women students and three to men. Since the award was initiated, both the number and quality of plasma projects has increased. The CPS expects this trend to continue, and looks forward to continuing its work with students who are excited about the possibilities of plasma. You too can share this excitement by judging at the 2010 fair in San Jose on May 11-12.

*Research supported by the U. S. Department of Energy; member universities, industries, laboratories, and individuals; and sponsoring organizations.
†on behalf of the Coalition for Plasma Science

JP8 3 Science Education Research Using Web-based Video* LISA TARMAN, *William Penn Senior High* PAMELLA FERRIS, *Riverside Middle School* DAN BRUDER, *Rensselaer Polytechnic Institute* NICK GILLIGAN, *The Pingry School* JAMES MORGAN, JOHN DELOOPER, *Princeton Plasma Physics Lab* The Princeton Plasma Physics Laboratory in collaboration with teachers and students has developed a variety of educational outreach activities to demonstrate basic physical science principles using a variety of instructive and entertaining science demonstrations at elementary, middle and high school levels. A new effort has been initiated to demonstrate this material using web based videos. This can be a resource for the teacher, parent or student. In addition, the video is coupled to web-based lesson plans for the educator. The goal of these videos and lesson plans is to create enthusiasm and stimulate curiosity among students and teachers, showing them that science is interesting, fun, and within their grasp. The first video demonstrates a number of activities one can accomplish using a half-coated fluorescent tube. Additional demonstrations will be added over time.

*This work performed under the auspices of the U.S. Department of Energy by the Princeton Plasma Physics Laboratory under Contract No. DE-AC02-09CH11466.

JP8 4 Plasma Display at the Liberty Science Center* DAN BRUDER, *Rensselaer Polytechnic Institute* NICK GILLIGAN, *The Pingry School* LISA TARMAN, *William Penn Senior High* PAMELLA FERRIS, *Riverside Middle School* JAMES MORGAN, JOHN DELOOPER, ANDREW ZWICKER, *Princeton Plasma Physics Lab* The Liberty Science Center (LSC) is the largest (300,000 sq. ft.) education resource in the New Jersey – New York City region. PPPL in collaboration with the LSC has had a display at the center since 2007 More than 1.5 million visitors have come to the museum since the plasma display has been introduced. The plasma display has had significant use during that time frame. During the summer of 2009 a redesigned plasma exhibit was created by a student teacher-team using the lessons learned from the existing exhibit. The display includes a DC glow discharge tube with a permanent external magnet allowing visitors to manipulate the plasma and see how plasma can be used for fusion research. The goal of the display is to allow an individual to see a plasma and understand the potential benefits of fusion energy.

*This work performed under the auspices of the U.S. Department of Energy by the Princeton Plasma Physics Laboratory under Contract No. DE-AC02-09CH11466.

JP8 5 Calibrating and characterizing X-ray diagnostics using the Lawrence Livermore National Laboratory's Electron Beam Ion Trap: A Physics teacher's perspective CHAD GILLIS, PETER BEIERSDORFER, GREG BROWN, JOEL CLEMENTSON, ALEX DIXON, RONNY ELOR, EDWARD MAGEE, ELMAR TRABERT, Using Lawrence Livermore National Laboratory's Electron Beam Ion Trap (EBIT) as an X-ray source, we characterized a flat-field grating spectrometer and calibrated the X-ray transmission of optical-blocking filters. The flat-field grating spectrometer is being used to diagnose magnetically confined plasma and the optical-blocking filters are part of a variety of X-ray diagnostics used to study a plethora of sources including inertial confinement fusion plasma, high energy density plasma, and astrophysical plasma. I will give an overview of the calibration process and also discuss how I expect to relate this experience to teaching high school physics students. This work was performed under the auspices of the U.S. Department of Energy by the Lawrence Livermore National Laboratory under Contract DE-AC52-07NA27344 and is also supported by California State University.

JP8 6 On the Role of an Authentic Research Experience for K-12 Science Teachers ANDREW ZWICKER, JAMES MORGAN, JOHN DELOOPER, *PPPL* A variety of programs exist that offer K-12 teachers an opportunity to perform scientific research during the summer. Since 2001, the NSF has offered a Research Experience for Teachers, based upon the more common Research Experience for Undergraduates (REU). The DOE has had the Teacher Research Associate (TRAC) program since 1989 and currently sponsors the Academies Creating Teacher-Scientists (ACTS). In each of these, teachers spend 2-8 weeks performing research and developing classroom activities based upon this experience. Many programs assess changes in knowledge or attitude towards science, a few look at teacher retention, and one looked at student achievement after a teacher completed a program. Currently, PPPL runs two research programs for teachers, one running for two weeks, one for six weeks. One program recruits teachers nationally, while the other concentrates its efforts on a single

school district. Each program will initially run for three years and we will report on our initial data that looks at attitudes, teaching philosophy, and content knowledge before beginning the research project. We will also report on expected outcomes after completion of the program.

JP8 7 UNDERGRADUATE AND HIGH SCHOOL RESEARCH

JP8 8 Calculation of stochastic broadening due to low mn magnetic perturbation in the simple map in action-angle coordinates COURTNEY HINTON, ALKESH PUNJABI, HALIMA ALI, *Hampton University* The simple map is the simplest map that has topology of divertor tokamaks [A. Punjabi, H. Ali, T. Evans, and A. Boozer, Phys. Let. A **364**, 140–145 (2007)]. Recently, the action-angle coordinates for simple map are analytically calculated, and simple map is constructed in action-angle coordinates [O. Kerwin, A. Punjabi, and H. Ali, Phys. Plasmas **15**, 072504 (2008)]. Action-angle coordinates for simple map cannot be inverted to real space coordinates (R,Z). Because there is logarithmic singularity on the ideal separatrix, trajectories cannot cross separatrix [*op cit*]. Simple map in action-angle coordinates is applied to calculate stochastic broadening due to the low mn magnetic perturbation with mode numbers m=1, and n=± 1. The width of stochastic layer near the X-point scales as 0.63 power of the amplitude δ of low mn perturbation, toroidal flux loss scales as 1.16 power of δ, and poloidal flux loss scales as 1.26 power of δ. Scaling of width deviates from Boozer-Rechester scaling by 26% [A. Boozer, and A. Rechester, *Phys. Fluids* **21**, 682 (1978)]. This work is supported by US Department of Energy grants DE-FG02-07ER54937, DE-FG02-01ER54624 and DE-FG02-04ER54793.

JP8 9 Creation of a magnetic barrier at a noble q close to physical midpoint between two resonant surfaces in the ASDEX UG tokamak JUSTIN VAZQUEZ, *College of William and Mary* HALIMA ALI, ALKESH PUNJABI, *Hampton University* Ciraolo, Vittot and Chandre method of building invariant manifolds inside chaos in Hamiltonian systems [Ali H. and Punjabi A, Plasma Phys. Control. Fusion, **49**, 1565–1582 (2007)] is used in the ASDEX UG tokamak. In this method, a second order perturbation is added to the perturbed Hamiltonian [*op cit*]. It creates an invariant torus inside the chaos, and reduces the plasma transport. The perturbation that is added to the equilibrium Hamiltonian is at least an order of magnitude smaller than the perturbation that causes chaos. This additional term has a finite, limited number of Fourier modes. Resonant magnetic perturbations (m,n) = (3,2) +(4,3) are added to the field line Hamiltonian for the ASDEX UG. An area-preserving map for the field line trajectories in the ASDEX UG is used. The common amplitude δ of these modes that gives complete chaos between the resonant surfaces $\Psi 43$ and $\Psi 32$ is determined. A magnetic barrier is built at a surface with noble q that is very nearly equals to the q at the physical midpoint between the two resonant surfaces. The maximum amplitude of magnetic perturbation for which this barrier can be sustained is determined. This work is supported by US Department of Energy grants DE-FG02-07ER54937, DE-FG02-01ER54624 and DE-FG02-04ER54793.

JP8 10 A symplectic map for trajectories of magnetic field lines in double-null divertor tokamaks WILLIE CRANK, HALIMA ALI, ALKESH PUNJABI, *Hampton University* The coordinates of the area-preserving map equations for integration of magnetic field line trajectories in tokamaks can be any coordinates for which a transformation to (ψ, θ, ϕ) coordinates exists [A. Punjabi, H. Ali, T. Evans, and A. Boozer, Phys. Lett. A **364**, 140 (2007)]. ψ is toroidal magnetic flux, θ is poloidal angle, and ϕ is toroidal angle. This freedom is exploited to construct a map that represents the magnetic topology of double-null divertor tokamaks. For this purpose, the generating function of the simple map [A. Punjabi, A. Verma, and A. Boozer, Phys. Rev. Lett. **69**, 3322 (1992)] is slightly modified. The resulting map equations for the double-null divertor tokamaks are: $x_1 = x_0 - k y_0 (1 - y_0^2)$, $y_1 = y_0 + k x_1$. k is the map parameter. It represents the generic topological effects of toroidal asymmetries. The O-point is at (0.0). The X-points are at (0,± 1). The equilibrium magnetic surfaces are calculated. These surfaces are symmetric about the x- and y- axes. The widths of stochastic layer near the X-points in the principal plane, and the fractal dimensions of the magnetic footprints on the inboard and outboard side of upper and lower X-points are calculated from the map. This work is supported by US Department of Energy grants DE-FG02-07ER54937, DE-FG02-01ER54624 and DE-FG02-04ER54793.

JP8 11 Scaling of the stochastic broadening from low mn, high mn, and peeling-ballooning magnetic perturbations in the DIII-D tokamak MICHAEL ZHAO, ALKESH PUNJABI, HALIMA ALI, *Hampton University* The equilibrium EFIT data for the DIII-D shot 115467 is used to construct the equilibrium generating function for magnetic field line trajectories in the DIII-D tokamak in natural canonical coordinates [A. Punjabi, and H. Ali, Phys. Plasmas **15**, 122502 (2008)]. A canonical transformation is used to construct an area-preserving map for field line trajectories in the natural canonical coordinates in the DIII-D. Maps in natural canonical coordinates have the advantage that natural canonical coordinates can be inverted to calculate real space coordinates (R,Z,ϕ), and there is no problem in crossing the separatrix. This is not possible for magnetic coordinates [O. Kerwin, A. Punjabi, and H. Ali, Phys. Plasmas **15**, 072504 (2008)]. This map is applied to calculate stochastic broadening from the low mn (m,n)=(1,1)+(1,-1); high mn (m,n)=(4,1)+(3,1); and the peeling-ballooning (m,n)=(40,10)+(30,10) magnetic perturbations. In all three cases, the scaling of the widths of stochastic layer near the X-point in the principal plane of the DIII-D deviates at most by 6% from the $^{.5}$ker$n$ − $.1em$/ker$n$ − $.15em_{.25}$ power Boozer-Rechester scaling [A. Boozer, and A. Rechester, *Phys. Fluids* **21**, 682 (1978)]. This work is supported by US Department of Energy grants DE-FG02-07ER54937, DE-FG02-01ER54624 and DE-FG02-04ER54793.

JP8 12 Beryllium Drive Disc Characterization for Laboratory Astrophysics Experiments* J.R. DITMAR, R.P. DRAKE, C.C. KURANZ, M.J. GROSSKOPF, *University of Michigan* Laboratory Astrophysics scales large-scale phenomena, such as core-collapse supernovae shocks, down to the sub-millimeter scale for investigation in a laboratory setting. In some experiments, targets are constructed with a 20μm thick beryllium disc attached to a polyimide tube. A shockwave is created by irradiating the Be disc with ~ 4kJ of energy from the Omega Laser. The Be material is rolled into a 20μm sheet and then machined to a 2.5mm diameter. Characterizing the roughness and knowing if there are any major features on the initial surface could affect interpretations of data

taken during experiments. Structure in the Beryllium discs could become an important parameter in future high-fidelity computer simulations. Surfaces were characterized with a Scanning Electron Microscope and an Atomic Force Microscope.

*Supported by the US DOE NNSA under the Predictive Sci. Academic Alliance Program by grant DE-FC52-08NA28616, the Stewardship Sci. Academic Alliances program by grant DE-FG52-04NA00064, and the Nat. Laser User Facility by grant DE-FG03-00SF22021.

JP8 13 1D Hyades Study of Varying Input Parameters of a Gaussian Distribution* N. GJECI, R.P. DRAKE, E.M. RUTTER, M.J. GROSSKOPF, C.C. KURANZ, B. FRYXELL, *University of Michigan* The Center for Radiative Shock Hydrodynamics (CRASH) at the University of Michigan is a collaborative effort in predictive sciences associated with radiative hydrodynamics. Computer simulations aid in high-energy-density physics experiments performed at the OMEGA laser in Rochester, NY. The high intensity laser driven shocks are modeled using 1D Hyades, a Lagrangian radiation-hydrodynamic code. A data set varying input parameters over a Gaussian distribution is created and, using a Latin Hypercube sampling process, used to build sets of simulations to cover the input parameter space. This will advance the uncertainty quantification process, determining the impact of the variance of the experimental parameters. A Latin Hypercube Sampling distribution provides a multi-dimensional sensitivity analysis of the physical parameters of the experiment, enhancing the predictive capabilities of CRASH code.

*Supported by the US DOE NNSA under the Predictive Sci. Academic Alliance Program by grant DE-FC52-08NA28616, the Stewardship Sci. Academic Alliances program by grant DE-FG52-04NA00064, and the Nat. Laser User Facility by grant DE-FG03-00SF22021.

JP8 14 Absorption Spectra of BaF_2 Sm_2O_3, Sm, Gd, and Ho Plasmas MICHAEL MARTIN, *UCLA* SERENA BASTIANI-CECCOTTI, *Ecole Polytechnique* Knowledge of the opacities of high Z element plasmas is important in indirect drive ICF and the study of stellar evolution. There are few experimental measurements of this quantity, and its theoretical determination is difficult due to the number of possible bound electron configurations. This study aims to better the theoretical understanding of this parameter by looking at the 3d-4f transitions of BaF_2, Sm_2O_3, Sm, Gd, and Ho plasmas at the LULI2000 facility. The plasmas are produced by radiative heating and are cold, 15 – 40 eV, and relatively dense, $\sim$ .01gm/cm^3 A plasma is produced by a.5 ns laser pulse irradiating a gold hohlraum and then probed by an x-ray source created by a gold foil irradiated by a 10 ps laser pulse. The transmission is found with simultaneous source and absorption measurements by an x-ray spectrometer in the 8 - 20 Å range We will compare the results with statistical atomic structure codes. From this experiment we will gain further insight into the spectral broadening of neighboring Z elements due to changing plasma temperature and into mixture thermodynamics. This is a first step towards an experimental study of astrophysical domains.

JP8 15 BECOOL: a magnetohydrodynamic ballooning mode eigenvalue solver based on variable order Legendre polynomial basis functions GUY A. COOPER, RANDOLPH S. PETERSON, *University of the South, Sewanee, TN 37383* RALF GRUBER, W. ANTHONY COOPER, JONATHAN P. GRAVES, *Ecole Polytechnique Federale de Lausanne CRPP, Association Euratom-Suisse, Lausanne, Switzerland* An incompressible variational ideal ballooning mode equation is discretized with the COOL finite element discretization scheme using basis functions composed of variable order Legendre polynomials.[1] This reduces the second order ordinary differential equation to a special block pentadiagonal matrix equation that is solved using an inverse vector iteration method. A benchmark test of BECOOL (Ballooning Eigensolver using COOL finite elements) with second order Legendre polynomials recovers precisely the eigenvalues computed by the VVBAL shooting code.[2] Timing runs reveal the need to determine an optimal lower order case. Eigenvalue convergence runs show that cubic Legendre polynomials construct the optimal ballooning mode equation for intensive computations.

[1]G. A. Cooper, J. P. Graves, W. A. Cooper, R. Gruber and R. S. Peterson, J. Comput. Phys. **228** (2009) 4911-4916.
[2]A. Cooper, Plasma Phys. Control. Fusion **34** (1992) 1011-1036.

JP8 16 Comparison of Magnetospheric Ion Temperature Maps from In-Situ Measurements with Remote ENA-based Measurements KATHARINE TALLAKSEN, AMY KEESEE, EARL SCIME, *West Virginia University* Ion temperatures in the magnetosphere exhibit significant variations that are strongly correlated with solar wind conditions not only during geomagnetic storms, but also during quiet times. Using data that did not distinguish between storm and quiet times, *Borovsky et al.* showed a strong, linear correlation with the solar wind velocity of ion temperatures at 12 Earth radii downtail and at geosynchronous orbit on the nightside of the Earth [*Borovsky et al.,* 1998]. However, *Borovsky's* empirical relations between solar wind speed and magnetosphere ion temperature are only valid for these two spatial locations. Remote measurements of the energetic neutral atom (ENA) flux emitted by the magnetosphere can provide global magnetospheric ion temperature maps that can be used to understand how the solar wind conditions affect different regions of the magnetosphere. These remote measurements can be compared to in-situ measurements to confirm the accuracy of the ENA-based analysis. We will present ion temperature maps of the Earth's magnetosphere constructed from data from the TWINS, Geotail, Cluster, and THEMIS spacecraft and sorted by solar wind velocity (high speed (greater than 400 km/s) wind and low speed wind). The data used cover the interval from January 2008 through April 2009. This work supported by NASA.

JP8 17 GPU-Accelerated FDTD Full-Wave Codes for Reflectometry Simulations* B.C. ROSE, *Purdue U.* S. KUBOTA, W.A. PEEBLES, *UCLA* Recently, GPGPU (General-Purpose computing on Graphics Processing Units) has been gaining popularity in many engineering and science fields as an inexpensive platform for accelerating compute-intensive codes. Here, we report on the application of GPU-computing to microwave reflectometry simulations for NSTX (National Spherical Torus eXperiment) plasmas. Reflectometry is a widespread diagnostic for studying both coherent and turbulent electron density fluctuations in fusion plasmas. A suite of FDTD (Finite-Difference Time-Domain) full-wave microwave propagation codes has been ported to utilize the massively parallel processing capabilities of the NVIDIA C870 GPU. The C

for CUDA (Compute Unified Device Architecture) extension of the C programming language was used. For the 1-D FDTD code, it was found that the parallel version ran roughly 6 times faster than the linear equivalent. A more detailed benchmarking of both 1-D and 2-D codes for the GPU and traditional multicore processors will be presented.

*Supported by U.S. DoE Grant DE-FG03-99-ER54527 and the DoE National Undergraduate Fusion Fellowship.

JP8 18 Fluctuations and Turbulence in the Enormous Toroidal Plasma Device at UCLA* ROBERT NIEDERRITER, *Lawrence University* CHRIS COOPER, TROY CARTER, PAVEL POPOVICH, *UCLA* Turbulence and transport across magnetic field lines disrupt plasma confinement, which is particularly troublesome in toroidal geometries potentially useful for fusion energy. We investigate fluctuations of a helium plasma in the Enormous Toroidal Plasma Device (ETPD) at UCLA using 4-tip Langmuir probes to measure potential and ion saturation current. ETPD is a simple magnetized torus with major radius 5 m. The toroidal vacuum chamber has a rectangular cross section that is 3 m tall and 2 m wide. Plasma is generated by a lanthanum hexaboride (LaB6) cathode discharge into a helical magnetic field produced by a $\sim$ 200 G toroidal field and a $\sim$ 6 G vertical field. Typical plasma density is $n_e \sim 10^{13}$ cm^{-3} and typical electron temperature is $T_e \sim 10 - 20$ eV. Observed fluctuations are characterized and compared with theories of drift waves and interchange modes.

*This work was supported by the National Science Foundation through the Research Experience for Undergraduates (REU) program at UCLA.

JP8 19 Attempts to produce nearly steady-state conditions in a fully toroidal electron plasma ERIC FRATER, FARAZ CHOUDHURY, MATTHEW STONEKING, *Lawrence University* The Lawrence Non-neutral Torus II (major radius = 17.4 cm, minor radius = 1.27 cm, B $\sim$ 550 G) confines non-neutral (electron) plasmas in a purely toroidal magnetic field. By employing techniques used in cylindrical Penning-Malmberg traps, electron plasmas are confined in a 270° toroidal arc for times exceeding one second. The observed long confinement times indicate the production of nearly steady-state conditions and permit study of intrinsic toroidal effects on dynamics and transport. We report on attempts to trap electrons in a *full* torus. This is done by filling the trap and confining electrons in a partial torus, retracting the electron source, and then removing the electric potential barriers to allow the plasma to occupy the full torus. The long confinement times achieved in the partial torus make this experiment possible. The plasma is diagnosed by measuring the flow of image charge to and from isolated sectors of the fully segmented conducting shell. Electron plasmas (n $\sim$ 5x10^6 cm^{-3}) are confined and exhibit toroidal versions of diocotron modes. Frequency measurements of the m=1 diocotron mode along with numerical models yield the total charge in the plasma. This work is supported by National Science Foundation Grant PHY-0812893.

JP8 20 Redesign of Gas Delivery System and Calibration Setup for Magnetic Probes in the Maryland Centrifugal Experiment* GRAHAM TAYLOR, CARLOS A. ROMERO-TALAMAS, RICHARD ELLIS, ADIL HASSAM, CATALIN TEODORESCU, WILLIAM YOUNG, *University of Maryland* This work consists of two parts. The first part is the design of a new gas feed system for the Maryland Centrifugal Experiment. The system is designed to maintain high vacuum conditions, prevent back flow, and allow for gas mixtures to be used in the experiment. The second part of this work describes a setup to calibrate magnetic probes at different frequencies. The setup will produce different resonance frequencies by adjusting the capacitance in a LRC circuit. The total capacitance is adjusted by connecting capacitors in series or in parallel with jumper cables.

*Supported by the US Department of Energy.

JP8 21 Optimization of Hot Electron ECE Diagnostics on LDX* S.H. NOGAMI, *University of San Diego* P.P. WOSKOV, J. KESNER, *PSFC MIT* D.T. GARNIER, M.E. MAUEL, *Columbia University* The Levitated Dipole Experiment (LDX) is evaluating the dipole magnetic field configuration for fusion confinement with a levitated 1.1 MA, 68 cm mean diameter, 560 kg superconducting coil (F-coil) inside a 5 m diameter vacuum vessel. Highly peaked plasmas ($\sim 1/r^4$) are generated by up to 17 kW electron cyclotron resonance heating at 2.45, 6.4, and 10.5 GHz. The high magnetic field gradient around the outside of the dipole coil where the plasma is confined represents a new regime for modeling ECE diagnostics. Millimeter wave radiometers at 110, 137, and 165 GHZ in use on LDX can view ECE harmonics from the 2nd through the 55th depending on the location of the radiometers with respect to the plasma. A study of the viewable harmonics from each of the available radiometers at various positions and proximities to the plasma is necessary to determine the interpretation of the ECE in terms of the hot electron temperatures and densities and the optimum receiver placement for the best measurements.

*Supported by the US DOE and National Undergraduate Fellowship Program.

JP8 22 Python Graphical User Interface (GUI) for Control of the Levitated Dipole Experiment* DAVID JACOME, *Saint Peters College* DARREN GARNIER, *Columbia University* PAUL WOSKOV, JAY KESNER, *MIT* The Levitated Dipole Experiment (LDX) is used to study the confinement properties of plasmas in a magnetic dipole field. In LDX a superconducting coil is levitated for up to 3 hours within a large vacuum chamber to produce the confining dipole field. The plasma experiments take place during this time, with $\sim$ 10 second plasma shots, one shot every $\sim$ 5 min. MDSplus software is used to run the experiment and store the data. The software is currently controlled by command line operations. Since levitation time is limited, it's important to maximize efficiency and accuracy of experimental operations. Here, we present a Graphical User Interface (GUI) to efficiently control the operation of the experiment. The need for a GUI that integrates the MDSplus data cycle, cell access control, and routine experimental parameter controls is necessary. The GUI program provides a simple method for monitoring and setting experiment parameters. Python is used as the primary language to run the commands. A program called XRCed distributed by wxPython works as a visual tool.

*Supported by the National Undergraduate Fellowship in Plasma Physics and Fusion Energy Sciences.

JP8 23 Intra-shell diffusion in Yukawa balls PAUL LA PLANTE, *Loyola University Maryland* TORBEN OTT, MICHAEL BONITZ, Diffusion of micrometer sized particles has recently been studied in dusty plasmas. When examined experimentally and theoretically in the 2D and quasi-2D case [1], super-

diffusion was observed, i.e. the mean-squared displacement of the particles in the long time case was larger than that predicted by the Einstein relation $\langle |r(t)|^2 \rangle \sim t$. In the case of superdiffusion, the mean-squared displacement grows as t^α, where $\alpha > 1$. In this contribution, we study spherically confined small dust clusters where the particles arrange in a series of concentric spherical shells. We present the results of molecular dynamics simulation, both in the case where the coupling parameter $\Gamma = (Q^2/4\pi\epsilon_0) \times (1/a_{ws}k_BT)$ is held constant and the inverse screening parameter varies and vice versa. We also examine different particle numbers that lead to between one and three shells of the Yukawa ball. In most cases studied, normal diffusion or subdiffusion ($\alpha < 1$) was exhibited by the dust particles on the shells. [1] T. Ott, M. Bonitz, Z. Donkó, and P. Hartmann, PRE 78, 026409 (2008)

JP8 24 Stark Broadening Density Profile Measurements in the ZaP Experiment G.V. VOGMAN, U. SHUMLAK, *Aerospace and Energetics Research Program, University of Washington* The ZaP Flow Z-Pinch experiment uses sheared flow to mitigate MHD instabilities. The high-pressure plasma pinches exhibit Stark broadened emission spectra, which are analyzed to determine plasma density. A 20-chord spectroscopic system has been calibrated to quantify chord-to-chord variation in throughput, optical curvature effects, instrument wavelength displacement, and instrument broadening. By correcting for these effects and accounting for Doppler broadening, a Stark broadening profile can be resolved and used as a measure of plasma density. The local electric field from the plasma Stark broadens the spectral shape of line emission producing a Voigt profile. A Fourier expansion technique is used to approximate the Voigt profile for a C III spectral line, which is emitted from the center of the plasma column, and the H_β line, which is used to resolve density in the peripheral regions of the plasma. By measuring density at different locations, a radial density profile is generated. This profile is then compared to interferometry measurements and is used to gain a better understanding of Z-pinch equilibrium.

JP8 25 Calibration of the Thomson Scattering System on the ZaP Experiment R.J. OBERTO, U. SHUMLAK, B.A. NELSON, R.P. GOLINGO, *Aerospace and Energetics Research Program, University of Washington* D.J. DEN HARTOG, *University of Wisconsin-Madison* The ZaP Experiment studies the sheared flow stabilization of a Z-pinch plasma. A Thomson scattering system measures the local electron temperature and density in the pinch using a 10 J ruby laser. The scattered light is collected by a fiber optic bundle, separated by a single-grating spectrometer with ruby and H_α filters, and binned by an array of photomultiplier tubes (PMTs). The PMT response is digitized, providing a time-resolved signal. Preliminary measurements using a preliminary calibration indicate temperatures from 50 to 150 eV. To calibrate the system completely, a tungsten lamp has been used to measure the system's spectral response, determine PMT gain, and characterize the filters in the spectrometer. The instrument function of the spectrometer has been characterized using a helium-neon laser. The total system throughput will be determined by comparing predicted and measured Raman scattering signals. The calibration will enable absolute density measurements, improved analysis codes, and system optimization.

JP8 26 Implementation of a Hall Probe Array to Characterize Magnetic Fields in the Madison Dynamo Experiment A.M. RASMUS, C.B. FOREST, E.J. KAPLAN, R.D. KENDRICK, N.Z. TAYLOR, *UW Madison* This poster will provide an overview of improvements to the Hall probe array diagnostic on the Madison Dynamo Experiment. Two counter-rotating impellers driven by two 75kW motors are used to create a turbulent flow of liquid sodium in a one meter-diameter sphere. One of the goals of the experiment is to observe a dynamo; the spontaneous generation of magnetic fields by converting kinetic energy into magnetic energy. Previously, an intermittently self-excited magnetic field and a turbulent electromotive force were observed, but no sustained self-excited field was seen. A number of improvements to the experiment are being implemented and are predicted to allow sustained self-excited magnetic fields. In order to characterize the induced magnetic field, a new Hall probe array is being installed. The array consists of 6 radial probes as well as an equatorial array, which will allow for measurements of the magnetic field near the center of the vessel. These internal hall elements will be spaced 2 cm apart and measure the magnetic field in all three directions. Combined with 74 external probes, these diagnostics will allow us to decompose our magnetic field into spherical harmonics for further data analysis.

JP8 27 Flow Measurements of a Hot, Rotating, Unmagnetized Plasma J. JARA-ALMONTE, C.B. FOREST, R. KENDRICK, C. COLLINS, *University of Wisconsin Madison* The initial construction of the Plasma Couette Experiment (PCX) has been completed at the University of Wisconsin Madison. PCX aims to demonstrate magnetorotational instability (MRI), a proposed mechanism for angular transport in accretion disks, in a laboratory plasma. A hot and unmagnetized plasma is created using a lanthanum hexaboride cathode inside a high-order axisymmetric multicusp confinement scheme consisting or rings of permanent magnets. Electrodes located between cusp lines drive ExB drift of the plasma at the boundary, and viscous coupling provides bulk plasma rotation. Flow measurements are made using a Mach probe, and plasma parameters are established using a swept Langmuir probe. This poster will present an overview of the PCX, as well as initial data from the probes.

JP8 28 Spectral Analysis Software for the Compact Toroid Injection Experiment* DONALD BELKNAP, *Rice University* The Compact Toroid Injection Experiment (CTIX) operated by UC Davis functions by producing a spheromak-like plasma which is accelerated via a coaxial railgun. In order to examine features of the plasma such as impurities and temperature, the spectrum of the plasma is measured during a shot. Because of the number of shots that may be taken in a single day, a computer analysis program is an expedient method of analyzing the spectra. A graphic user interface (GUI) was designed to allow the user to easily read the spectral images from an archived data file and interactively perform functions such as CCD camera tilt correction, background subtraction, and wavelength calibration. The code for the GUI, background subtraction, wavelength calibration, and tilt correction algorithms are written in a high-level programming language, Igor,

to allow for easy extension by CTIX scientists. The code can be extended to add features that can perform analysis on large numbers of spectra. Results of CTIX shots and calibration spectra will be presented.

*Supported by U.S. DOE Grant DE-FG02-03ER54732; Completed as part of the National Undergraduate Fellowship in Plasma Physics (NUF).

JP8 29 Efficient Spherical Numeric Integration in Multiple Dimensions* MICHELLE JAMER, *Seton Hall University* Numeric integration in three dimensions through approximation can be computationally intensive. Computers using numeric integration find an approximation of the integral by a finite representation. In order to make an accurate approximation, the computer uses many quadrature points in order to evaluate which causes the three-dimensional analysis to be time intensive. The goal of this research is developing a quadrature rule which would use fewer points and thus reduce the computational expense in both two and three dimensional contexts. The research for the most efficient rule is done by testing various numerical integration rules, such as the midpoint rule and Simpson's rule, in the Python programming language. For this project the focus is on symmetrical domains such as spheres and circles. To test the accuracy of the integration rule on a given function, the convergence between both the exact and computed integrals is measured. The best quadrature rule converges and has minimal error when a modest amount of points are used. After analyzing the errors, one can see which quadrature rule fits the integral the best for radially symmetric two and three-dimensional shapes.

*Completed as part of the National Undergraduate Fellowship for Plasma Physics, Supported by U.S. DOE Grant DE-FG02-03ER54732.

JP8 30 First Plasmas in the Wheaton Impulsive Reconnection eXperiment (WIRX) D. STAPLETON, D. BLASING, D. COSTER, D. CRAIG, J. DAHLIN, *Wheaton College, Wheaton IL USA* WIRX is a new experiment that will be studying the three dimensional and impulsive aspects of reconnection. The experiment is composed of two parallel electrodes, linked by a magnetic arcade that is generated by a coil surrounding the electrodes. First plasmas were obtained in April of 2009. A preliminary exploration of WIRX parameter space is presented. An adjustable high power resistor is installed in series with the plasma, allowing plasma currents from 0.5 to 11 kA. A full range of magnetic field strengths are tested from 80 to 400 Gauss. Fueling from one end of the cathode and along the cathode has been investigated. Both allow breakdown with at least 800V across the electrodes but the second allows a longer arcade along the electrodes. The resistance of the plasma exhibits an upper boundary that falls with increased plasma current. Plasma instability is expected to increase with the ratio of plasma current over coil current. Experimental results show a sharp transition between stability in the plasma and instability. Fast camera images of plasmas will be compared with these experimental results. Work supported by U.S.D.O.E. grant DE-FG02-08ER55002.

JP8 31 Design of a pinhole photodiode camera for the Wheaton Impulsive Reconnection Experiment D. BLASING, D. COSTER, D. CRAIG, J. DAHLIN, D. STAPLETON, *Wheaton College, Wheaton IL USA* Absolute extreme ultraviolet (AXUV) photodiode arrays are utilized in the design of two pinhole photodiode cameras to examine the dynamics of the plasma evolution during a single shot. The cameras will resolve the discharge horizontally and vertically into 20 viewing slices each of width $\sim$ 1 cm. Each camera will monitor the entire plasma shot with 0.2μs resolution. This compliments the existing fast ICCD cameras which only take two pictures per shot but have spatial resolution $\sim$ 1mm. Fast ICCD time scan pictures taken from multiple shots are displayed. The spectrum and the total power of the light emitted by the plasma has been measured and incorporated into the camera design. The expected photodiode current has been estimated. Work supported by U.S.D.O.E. grant DE-FG02-08ER55002.

JP8 32 Three dimensional magnetic field structure of magnetic reconnection using plasma flux ropes THIAGO OLSON, *Vanderbilt University* TOM INTRATOR, *LANL* RACHEL OBERTO, *Washington University* XUAN SUN, *LANL* In nature, magnetic reconnection releases energy stored in stressed magnetic fields, and thus accelerates particles. This type of magnetic relaxation topologically rearranges magnetic field structure. In nature these processes are intrinsically 3D, whereas most models, theories and experiments are 2D, staying within the classic Sweet-Parker picture. The Reconnection Scaling eXperiment (RSX) at Los Alamos National Laboratory includes magnetic fields and current systems in the plasma that support these natural 3D fields. 2D studies have shed much light on the physics, but 3D aspects are largely unconsidered and unknown. Explanation of this behavior demands the need of a 3D picture or map. We present the B-dot probe design needed to map out the B-field structure in the plasma, and the results of the 3D merging of plasma flux ropes. RSX has already yielded data showing the onset, flux pileup, and stagnation of magnetic reconnection between two interacting plasma flux ropes. B-dot probe, and 3D positioner design and construction will be discussed in depth. This work was supported by the Los Alamos Laboratory Directed R&D program, and the Physics Frontier Center for Magnetic Self Organization in Laboratory and Astrophysical? Plasmas, jointly funded by NSF and DOE.

JP8 33 Neutron Activation Diagnostics for FRCHX at AFRL D.A. SUTHERLAND, *Massachusetts Institute of Technology* G.A. WURDEN, T.P. INTRATOR, *Los Alamos National Laboratory* KIRTLAND AIR FORCE RESEARCH LABORATORY COLLABORATION, Neutron diagnostics have been developed for MTF on the field reversed configuration heating experiment (FRCHX) to detect both DD and DT neutrons. We are working with time-integrated activation counting systems for absolute measurements of neutron yields, in the range of 10^6-10^{13} neutrons/shot. We are using multiple diagnostics due to different activation thresholds and need for diagnostic redundancy. The first system is indium-activation, with an Ortec germanium detector (GEM-10185) coupled to a multichannel analyzer. Indium is sensitive to and provides a count of DD neutrons. The second diagnostic system is Arsenic-activation that will also detect DD neutrons. The third system is Copper-activation, using a sodium iodide (NaI) coincidence system. Only DT neutrons are detected by this system. A fourth system consists of BTI Bubble detectors that are sensitive to both DD and DT neutrons. Thus, four systems will provide an absolute count of DD or DT neutrons from the FRC plasma implosion in FRCHX at the AFRL in Albuquerque later this year.

JP8 34 Applications of a Nd:YAG Laser for In-Situ Removal of Tritium from Plasma Facing Components in a Fusion Reactor Environment* PAUL SEDITA, *Canandaigua Academy* CHARLES GENTILE, *Princeton Plasma Physics Laboratory* CHRISTINA McGAHAN, *Gettysburg College* Studies from TFTR and JET have indicated that long term retention of tritium in plasma facing components account for a significant fraction of the tritium inventory; thus requiring periodic removal of T interned within these first wall components. This investigation will determine the efficacy of removing tritium in an in-situ fashion from co-deposits layers in PFC's employing a continuous wave 325 w Nd:YAG laser. The laser is configured to rapidly heat first wall surfaces using a rastering motion to effectively scan the exposed surfaces within the target area. The top 100 μm of the target surface is expected to transiently heat up to $\sim$ 1000 C within several seconds, subsequently releasing the trapped (un-expended) tritium for re-use within the fusion fuel cycle. The presentation will discuss the efficacy of this method using empirical data (destructive and non-destructive measurements) from pre and post surface laser heating.

*Supported by DOE Contract: DE-AC02-09CH1146.

JP8 35 Evaluation of a Non-Destructive Method for the Removal of Dust, Debris, and Co-deposited Tritium from First Wall Surfaces and Plasma Surface Interfaces (PSI) in a Fusion Reactor* CHRISTINA McGAHAN, *Gettysburg College* CHARLES GENTILE, *Princeton University* Diagnostic mirrors and windows located within the vacuum vessel boundary of fusion reactors will be subjected to dust and debris collection, causing reflectivity and clarity respectively to degrade and thus undermining data accuracy and machine performance. Additionally, co-deposited tritium must be removed in an efficient manner so unexpended tritium can be re-introduced into the fusion fuel cycle. A technique for removing carbon, beryllium, and co-deposited tritium from first wall components using a rastering 325 watt continuous wave neodymium-doped yttrium aluminum garnet (Nd:YAG) laser is under investigation. This technique has shown promise in ablating dust and debris without damaging reflective surfaces in addition to removing co-deposited layers of tritium from various diagnostic and PSI components in a non-destructive fashion. We will discuss the physical effects on surfaces and components pre and post laser interaction(s).

*Supported by DOE Contract # DE-AC02-09CH11466.

JP8 36 In-Situ Removal of Beryllium and Carbon Deposits from ITER Diagnostic Mirrors and Windows Utilizing Nd:YAG Laser* JENNIFER ZELENTY, *University of Chicago* CHARLES GENTILE, *PPPL* Studies from the Joint European Torus (JET) indicate that plasma deposits such as beryllium and carbon will collect on ITER diagnostic mirrors and windows. The presence of such deposits will cause a decrease in reflectivity and light transmission on these diagnostic related surfaces. This investigation will determine the effectiveness of removing plasma deposits from diagnostic mirrors and windows using a 325W continuous wave (cw) Neodymium-doped Yttrium Aluminum Garnet (Nd:YAG) Laser. In this study, laser cleaning will be tested on single crystal molybdenum mirror substrates, the material proposed for ITER first mirrors. The mirrors will be coated with either beryllium or carbon deposits. The Nd:YAG laser, directed by a computer controlled laser scanner, will raster the mirror substrates, ablating the deposits on the surfaces. The reflectivity and polarization properties will be tested before and after to determine the efficacy of this laser cleaning technique. The results will be presented and discussed.

*Supported by DOE Contract: DE-AC02-09CH11466.

JP8 37 Concept for a Low Pressure Gas Fill in a Direct Drive IFE Target Chamber* SASWATHI NATTA, MARIA ARISTOVA, CHARLES GENTILE, *Princeton Plasma Physics Laboratory* A concept using a low pressure nobel gas has been advanced for attenuating the interaction of (post detonation) He ions on first wall components. In this configuration approximately 1 torr of Ar gas is introduced into the target chamber for the purpose of interacting with energetic He ions before they impinge on first wall surfaces. As a result, effluent processing systems must be designed to take into account a high Ar gas load. Therefore, a two-stage cryopumping system will be configured in line with an array of turbomolecular drag pumps to remove Ar from the effluent gas stream. After exiting the reaction chamber, effluent will pass through the first cryopump stage, at liquid nitrogen temperature (77 K), which will remove argon as well as any trace contaminants from the gas stream. The remaining effluent, consisting of H and He, will pass through the second cryopumping stage, at liquid He temperature (4.2 K), to remove H isotopes from the gas stream. This poster will discuss specific concepts for efficient plasma exhaust processing.

*Supported by DOE Contract No. DE-AC0276CH03073

JP8 38 Development of one- and two-dimensional simulations of a thermal dusty plasma* R.A. JEFFERSON, M. CIANCIOSA, E. THOMAS, *Auburn University* In a "dusty" plasma, charged microparticles ("dust") is added to a background of ions, electrons, and neutral particles. These dust particles fully interact with the surrounding plasma and self-consistently alters the plasma environment leading to the emergence of new plasma behavior. Numerical tools that complement experimental investigations can provide important new insights into the properties of dusty plasmas. This presentation will focus on the initial results from a newly developed code that models transport and thermal properties of dusty plasmas. The code uses a fourth-order Runge-Kutta algorithm with adaptive time steps to solve the equations of motion for a group of microparticles confined in a trapping potential and subject to a neutral drag force and interaction through a screened Coulomb force. This presentation will discuss the physics basis for the 1-D code and extensions to a 2-D version of the code.

*This work is supported by the NSF-DOE Partnership in Basic Plasma Science and Engineering, NSF grant number: PHY-0810419.

JP8 39 Dust Particle Dynamics in a Varying Gravitational Field ALIYA MERALI, *TCNJ* ANDREW ZWICKER, *PPPL* DPX TEAM, The properties of silica dust suspended in an argon DC glow discharge plasma are analyzed in varying gravitational field. The plasma was created in a 6" x 1.5" glass chamber. 340 V was applied to the top of two stainless steel electrodes, placed 4" apart. In order to trap the dust during microgravity, a floating stainless steel mesh was suspended from the top electrode. The experiment used a current of 1-2 mA and a pressure of 80 to 155

mTorr while gravity ranged from 0 to 1.8g by flying through a series of 30 parabolas. Two CCD cameras recorded the dust cloud illuminated by a 5 mW laser sheet. One camera allowed observation of the interparticle spacing of the dust cloud and individual particle motion. The second camera recorded a wide field view of the overall cloud motion. In hyper-gravity, the dust cloud was 0.26 cm by 1.4 cm. As the gravitational field approached zero, the cloud moved from the center of the chamber, disassembled and reformed on the chamber wall. As gravity increased, the dust particles returned to the center of the chamber and reorganized in their initial formation. During the decrease in the gravitational field, a dust acoustic wave was spontaneously formed as the density of the cloud increased. To better understand the motion of the particles, the electrostatic field was modeled using a particle in cell code.

JP8 40 Measurement of Plasma Parameters in an Argon DC Glow Discharge Dusty Plasma ARTHUR SAFIRA, ANDREW ZWICKER, *PPPL, Princeton University* TAYLOR CALIGARIS, *PPPL* DPX TEAM, Dust particles in plasmas can gain a charge due to the free ions and electrons. The particles can then be suspended in space by opposing gravitational and electrical forces. These dusty plasmas appear as impurities in plasma processes and fusion reactors, but are also observed in astrophysics in planetary rings and nebulae. In an argon DC glow discharge plasma, dust cloud formation was studied by varying the dust tray location, the dust tray bias, the electrode bias, and the neutral gas pressure. In this set up, two 4 inch ring electrodes were set concentrically, and two 30 fps CCD cameras were used for data collection. Silica, a fluorescent dust mixture, glass beads, and quantum dots were tested as dust cloud substances. Plasma parameters near these dust clouds were measured using a Languimir probe. Dust clouds were readily produced with a pressure of 85± 5mTorr, cathode voltage of 253± 30V, anode voltage of 110± 20V, and the dust tray 4 inches from the anode. Dust tray biases proved useful in cloud positioning with -30CV< V_{dt} < +80V, but at other voltages clouds would not form due to plasma spots or dust tray proximity. Probe measurements indicated an electron density and temperature of $10^{14}m^3$ and 2eV, respectively. In addition, at P< 60mTorr spontaneous dust acoustical waves were observed and studied with a 500,000 fps 28 frame PSI-4 CCD camera.

JP8 41 Nonlocal transport in the hydrodynamics of laser plasma interactions BRENDAN C. LYONS, *Princeton University, USA* STEFAN HÜLLER, *CPHT, CNRS, Ecole Polytechnique, France* For the modeling of laser plasma interactions in hot plasmas, the assumption of an isothermal plasma can be justified as long as the thermal transport rapidly diffuses the absorbed laser energy. For electron temperatures below around 500eV, local heating may be non-negligible, requiring the solving of the energy equation together with the hydrodynamic equations for continuity and momentum. Furthermore, nonlocal transport effects have to be considered when the electron mean free path is comparable to the size of the laser hot spots which give rise to local heating. In this study, electron heat conduction and laser absorption are included in a Eulerian hydrodynamic scheme. The corrections to the transport and coupling coefficients are also taken into account following models which consider laser-induced anisotropy and nonlocal transport. Refs.: A. Brantov, V. Bychenkov et al. Phys. Plasmas 5, 2742 (1998); Phys. Plasmas 6, 3002 (1999); Phys. Plasmas 7, 1511 (2000), A. Bendib et al., Phys. Plasmas 12(3), 032308 (2005).

JP8 42 Picosecond Neutron Yields from Ultra-Intense Laser-Target Interactions C. LELAND ELLISON, *University of Colorado, Boulder* JULIEN FUCHS, *Laboratoire pour l'Utilisation des Lasers Intenses (LULI), Ecole Polytechnique* High-flux neutron sources for neutron imaging and materials analysis applications have typically been provided by accelerator-based (Spallation Neutron Source) and reactor-based (High Flux Isotope Reactor) neutron sources. A novel approach is to use ultra-intense (> 10^{18} W/cm^2) laser-target interactions to generate picosecond, collimated neutrons. Here we examine the feasibility of a source based on current (LULI) and upcoming laser facility capabilities. A Monte-Carlo code calculates angular and energy distributions of neutrons generated by D-D fusion events occurring within a deuterated target for a given incident beam of D+ ions. The parameters of the deuteron beam are well understood from laser-plasma and laser-target studies relevant to fast-ignition fusion. Expected neutron yields are presented in comparison to conventional neutron sources, previous experimental neutron yields, and within the context of neutron shielding safety requirements.

JP8 43 Use of Mirnov Coil Array in Detection of Magneto-Coriolis Waves KRISTINE GAROT, *University of Wisconsin, Madison* ERIK SPENCE, MARK NORNBERG, ETHAN SCHARTMAN, AUSTIN ROACH, DYLAN COSTER, CYPRIAN CZARNOCKI, HANTAO JI, It is the goal of the Princeton Magnetorotational Instability (MRI) experiment to better understand the process by which angular momentum is transported in accretion disks. The MRI experiment is a liquid gallium Taylor-Couette experiment with independently spinning disks at the ends and an applied axial magnetic field. Under turbulent conditions and a strong enough magnetic field, magneto-Coriolis waves are observed using a 2-D Mirnov coil array and global mode analysis. A new array has been constructed and added to the previous array, and the positions of the new coils have been chosen to increase the mode resolution. Discussion of the observed waves using both the new and old Mirnov coil arrays, along with spectra of the fit modes will be presented.

JP8 44 Wavenumber and Frequency Spectral Analysis from Free-Surface MHD Experiments B. BARTELL, *Union College* M.D. NORNBERG, J.R. RHOADS, H. JI, *PPPL* Characterizing turbulent free-surface magnetohydrodynamic flow in a region with a strong magnetic field is critical to understanding some astrophysical phenomena as well as designing a liquid-metal first wall diverter in a fusion reactor. To isolate the effect of a magnetic field on free-surface MHD, an experiment is performed in which liquid gallium flows down a wide aspect ratio channel perpendicular to a uniform, static, magnetic field of up to 2 kG. We measure disturbances in the flow at two locations by tracking the position of laser beam reflections from the liquid's surface with position sensitive photodiodes as a function of time. The distance between the incident lasers on the surface of the stationary liquid metal is 1.2 cm downstream. Given the two time-series and the distance between the measured locations on the surface, we estimate the local wavenumber and frequency spectra using two-point correlation analysis. Evidence from these spectra indicates that turbulence and wave features parallel to the magnetic field are largely damped as the magnetic field increases, thereby reducing the turbulence from three dimensions to two.

JP8 45 MRI Dispersion for a Helicon Plasma COURTNEY KAITA, *University of Michigan-Ann Arbor* HANTAO JI, *Princeton Plasma Physics Laboratory* CAMI COLLINS, *University of Wisconsin-Madison* The magnetorotational instability (MRI) is a basic MHD instability that occurs when a weak magnetic field is present in a differentially rotating disk. MRI is a likely reason for fast angular momentum transport in astrophysical accretion disks. A cohesive understanding of MRI with a range of plasma parameters pertaining to the wide variety of accretion disk systems has become an increasingly pressing concern. In the helicon plasma MRI experiment, plasma is created by a spiral antenna in an axial magnetic field produced by a solenoid. A radial potential difference is applied between a three-ring electrode system which creates plasma rotation through ExB drift. In this experiment, the ion gyro-orbit is much larger than for electrons. The Hall term due to different ion and electron velocities is added to the MHD model, resulting in additional two-fluid effects in the MRI dispersion relation. The characteristic MRI growth rates for the given experimental parameters are examined.

JP8 46 Experimental Characterization of Azimuthal Velocity with Varying Reynolds Numbers in short Taylor-Couette Flow CYPRIAN CZARNOCKI, *California State University San Marcos* PETER HUMANIK, *Bergen County Academies* AUSTIN ROACH, MARK NORNBERG, ERIK SPENCE, *Princeton Plasma Physics Laboratory* MICHAEL BURIN, *California State University San Marcos* HANTAO JI, *Princeton Plasma Physics Laboratory* Simulations of Taylor-Couette flow are difficult to reconcile with experimental measurements since the available Reynolds number of the simulations is normally much smaller than in most experiments. The ability to increase fluid viscosity by adding glycerol to water will allow for experiments to be run with a lower Reynolds number, allowing for the experimental results to be compared with simulations. In this experiment a Laser Doppler Velocimeter (LDV) is used to measure internal flow velocity within a short Taylor-Couette apparatus. The azimuthal velocity profiles are measured over a range of radial and axial positions with varying fluid viscosities. A comparison of both simulation and experimental results of azimuthal velocity profiles is presented. The goal for this experiment is to achieve good agreement between the experimental and simulation results and to help better understand the Ekman circulation and its suppression in the Princeton Magnetorotational Instability (MRI) Experiment.

JP8 47 Experimental Investigation of Flow Inside a Short Taylor-Couette Apparatus With an Air Vortex PETER HUMANIK, *Bergen County Academies* CYPRIAN CZARNOCKI, *California State University San Marcos* AUSTIN ROACH, ERIK SPENCE, MARK NORNBERG, HANTAO JI, *Princeton Plasma Physics Lab* The study of magnetohydrodynamics (MHD) and the instabilities involved with systems is one of great interest in astrophysics. Due to the limitations in tracking the flow of fluid conductors, such as the opacity of galintan, systems involving the movement of water and other easily traceable fluids are of great relevance towards predicting flows. In this experiment, the characteristics of a vortex of air that is formed around a cylinder rotating inside a larger coaxial cylinder which is rotating at a different rate are recorded. Laser Doppler Velocimetry (LDV) provides a profile of the speed of particles in the water near the vortex. Using the data about the water speed near the vortex and the characteristics of the vortex, the flow along the air-water boundary can be predicted. The experiment will be conducted over a range of viscosities which can be achieved from mixing glycerol with the water. The results can be used as a reference for further experiments in MHD involving similar vortices.

JP8 48 Evaporative ion cooling in SSX* M. KOREIN, D. WEINHOLD, J. SANTNER, T. GRAY, M.R. BROWN, *Swarthmore College* V.S. LUKIN, *NRL* Reconnection of merged plasmas in SSX results in rapid heating of ions and electrons. The SSX ion Doppler spectrometer shows heating of carbon and helium ions up to $100eV$ in a new slightly prolate flux conserver ($R = 0.2m, L = 0.4m$). A particle orbit simulation in realistic SSX magnetic fields shows that energetic ions are rapidly lost to the walls leaving behind a cooler ion population. We refer to this phenomenon as evaporative ion cooling. A retarding grid energy analyzer and a Mach probe are being used to study energetic ion flux and high velocity flows. Both probes are $\sim 1.5cm$ in diameter and can be scanned across the radius of the device at the mid-plane. Following reconnection, local flow speeds of greater than $60km/s$ (Mach number > 2) have been measured by the Mach probe in the present geometry. Preliminary data indicates bi-directional outflows during merging shots. Energetic ion data will be presented if available. The particle orbit code is being used to simulate $\sim 10^6$ particles with random initial conditions in SSX. The simulation traces particle orbits and models the probe structure in order to generate predictions of actual probe signals.

*Work supported by DOE and NSF CMSO.

JP8 49 Effect of Current Loop Perturbations on Fast Reconnection in MRX K.R. LABE, *Swarthmore College, SULI, PPPL* S. DORFMAN, M. YAMADA, H. JI, E. OZ, J. YOO, J. XIE, *CMSO, PPPL* The Magnetic Reconnection Experiment (MRX) investigates the mechanism responsible for fast reconnection. Two toroidal flux cores produce the plasma and drive the reconnection; the current flows toroidally [1]. A 20 cm diameter circular current loop was installed at one toroidal position at the center of the current sheet; it could be oriented to produce magnetic field either out-of-plane or along the reconnecting field. A voltage of up to 10 kV was applied to the loop for 100 us; the effect of its large-scale perturbations on the reconnection process was measured at several toroidal locations. Preliminary results show that the reconnection rate, as manifested by the flux evolution, is resilient to current loop perturbations. By contrast, detailed characteristics of the reconnection process (e.g. electromagnetic fluctuations, magnetic field profile) are globally affected by even small current loop perturbations. Effects of varying the plasma density as well as the loop voltage and timing will be reported. [1] M. Yamada, et al., Phys. Plasmas **4**(5), 1936 (1997).

JP8 50 Reconnection Line Breaking Interpreted in Terms of Electron Trajectories DANIEL LECOANET, *UW - Madison, Madison, WI 53706, PPPL, Princeton, NJ 08540* RUSSELL KULSRUD, MASAAKI YAMADA, *PPPL, Princeton, NJ 08540* In many physical situations, the width of the reconnection layer as predicted by the classical Sweet-Parker theory is smaller than the ion skin depth. In this case, the electrons and ions decouple, and the plasma must be treated as two fluids resulting in a fast reconnection rate with the layer width set by the ion skin depth. The line breaking mechanism in the two-fluid regime is no longer resistive but is driven by the anisotropic electron pressure tensor. By calculating electron trajectories near the origin, we show numerically

that this can be interpreted in terms of an unmagnetized region [1]. We find the electrons in the unmagnetized region are freely accelerated by the induced electric field, producing the reconnection current. We measure the average time electrons are accelerated in the unmagnetized region. For plasma parameters similar to those in the Magnetic Reconnection Experiment [2], we find this acceleration time is shorter than the collision time, implying an effective resistivity larger than the classical Spitzer resistivity. Understanding electron trajectories elucidates the reconnection mechanism and places additional constraints on analytic theories of two-fluid reconnection. [1] R. Kulsrud et al, Phys. Plasmas 12, 082301 (2005). [2] M. Yamada et al, Phys. Plasmas 4, 1936 (1997).

JP8 51 Numerical Study of Random Noise-Induced Beam Degradation in High Energy Accelerators* ARJUN LANDES, RONALD DAVIDSON, HONG QIN, *Plasma Physics Laboratory, Princeton University* Random noise caused by small machine errors is an inevitable and potentially significant source of beam degradation in high-energy accelerators. Understanding the detailed effects of such noise on beam quality is critical to evaluating the viability of accelerator design and operation. To this end, we study the dynamics of a single particle under the combined influence of random noise and a quadrupole focusing field. The equation of motion for a beam particle propagating through a sinusoidal quadrupole lattice takes the form of the Mathieu equation. We introduce a small random error into the amplitude of the oscillating term in the Mathieu equation, and solve the resulting dynamical equation numerically using Mathematica, employing stochastic integration techniques, to obtain matched solutions to the perturbed equation of motion. These solutions are then compared with the matched solutions to the standard Mathieu equation to determine the effects of the random noise, e.g., as measured by the increase in mean-square displacement of the particle from the beam axis. Statistical properties of the resulting particle dynamics are measured to assess quantitatively the degree of noise-induced degradation in beam quality.

*Research supported by the U.S. Department of Energy.

JP8 52 Investigation of Carbon Wire X-pinch backlighting for Pulsed Power Driven Exploding Wire Experiments SEAN McGRAW, *Ashland University* SIMON BOTT, FARHAT BEG, *University of California San Diego* Exploding wire experiments have many important applications, including inertial confinement fusion research and laboratory astrophysical plasmas. Understanding of the dynamics of wire arrays is crucial to these applications. Details of wire ablation remain somewhat unclear, which lead to uncertainties in scaling to higher drive currents. The ablated coronal plasma is typically investigated using x-rays in the 3-5 keV range, however much of this plasma is highly transparent to this radiation, and information about the dynamics of coronal plasma above 10^{19}/cc is therefore lacking. A possible candidate for lower energy radiography is the carbon x-pinch, which produces x-rays below 1 keV. Experiments are conducted on GenASIS, a linear transformer driver, to study carbon x-pinches for wire array x-ray backlighting. This pulsed power system drives 250 kA into a short circuit and 200 kA into an x-pinch load. X-pinches formed from 20 μm titanium and 10 μm stainless steel wires are compared to the carbon system to provide more insight into the evolution and structure of exploding wires. Information from these comparisons will feed directly into the ongoing discussion of wire ablation at high currents.

JP8 53 An experimental study of ion acoustic waves (IAW) in electronegative plasmas: can IAW measurements calibrate diagnostics for the measure of the negative ion fraction?* CAMRON PROCTOR, GREG SEVERN, *University of San Diego* Electronegative plasmas are found in nature, in the lower ionosphere for example, and in plasma processing applications, such as vapor deposition, plasma etching, and particle beam sources. To understand the full potential of electronegative plasmas, a better diagnostic of their properties needs to exist. The negative ion fraction $\alpha = n_-/n_e$ determines, in part, the degree of electronegativity of plasmas. The fast mode of Ion acoustic waves (IAWs) are often used as a diagnostic for α, and are here studied with the intent to use IAWs to calibrate other diagnostics, such as the laser photodetachment technique, which does not furnish absolute measurements. The various diagnostics of α are reviewed. The electronegative plasmas studied were Oxygen and Argon/Oxygen DC discharges confined with a multidipole arrangement of permanent magnets, producing low temperature, low pressure, ($T_e < 1eV, T_i \ll T_e, p_0 < 1mTorr$) weakly collisional plasmas.

*Work funded by DOE grant No. DE-FG02-03ER54728.

JP8 54 Particle and thermal transport due to drift resistive ballooning modes T. GOLDSTEIN,*T. RAFIQ, A.H. KRITZ, G. BATEMAN, A.Y. PANKIN, *Lehigh U.* The ion-temperature-gradient and trapped electron modes are primary candidates for producing the turbulence that drives anomalous transport in the core of magnetically confined plasmas. The situation at the edge is different. Since the edge plasma is influenced strongly by collisions, it is expected that resistive ballooning modes (RBMs) are an important driver of turbulence in the edge region. In this work, a new advanced RBM model [1] is tested as a function of plasma parameters. In this model, the eigenvalues and eigenvectors are used together with a quasi-linear mixing length estimate to determine fluxes and diffusivities. Particle and thermal transport coefficients are investigated in systematic scans over plasma density, density gradient, electron and ion temperature gradients, magnetic q, collisions, magnetic shear, finite Larmor radius effects, and pressure gradient. In the low temperature plasma region, it is found that RBM diffusivities increase with increasing density gradient, magnetic q, and collisionality. [1] T. Rafiq, et al, poster at this APS meeting

*Syracuse U. undergraduate supported by NSF REU grant PHY 0849416

JP8 55 Normal Modes of Magnetized Finite Two-Dimensional Yukawa Crystals GABRIEL-DOMINIQUE MARLEAU, *McGill University* HANNO KAEHLERT, MICHAEL BONITZ, *ITAP, University of Kiel* The normal modes of a finite two-dimensional dusty plasma in an isotropic parabolic confinement, including the simultaneous effects of friction and an external magnetic field, are studied. The ground states are found from molecular dynamics simulations with simulated annealing, and the influence of screening, friction, and magnetic field on the mode frequencies is investigated in detail. The two-particle problem is solved analytically and the limiting cases of weak and strong magnetic fields are discussed. [1] C. Henning, H. Kählert, P. Ludwig, A. Melzer, and M.Bonitz. J. Phys. A **42**, 214023 (2009) [2] B. Farokhi, M. Shahmansouri, and P. K. Shukla. Phys.Plasmas **16**, 063703 (2009) [3] L. Cândido, J.-P. Rino, N. Studart, and F. M. Peeters. J. Phys.: Condens. Matter **10**, 11627–11644 (1998)

JP8 56 Simulation of Power Supply for Vertical Stabilization of Plasmas at ITER MAXIMILIAN SWIATLOWSKI, *Harvard University* CHARLES NEUMEYER, *Princeton Plasma Physics Lab* We present the results of simulations of the power supply of an ITER vertical stabilization magnet system. ITER's elongated tokamak geometry enables increased plasma pressures at the cost of the loss of vertical stability, as the vertical-horizontal asymmetry allows small vertical perturbations to grow to dangerous levels. The ITER design calls for three independent magnetic systems to control this unstable growth; we describe the VS3 system which uses a set of in-vessel coils to actively generate a magnetic response when drift is detected. The primary requirements of the power- supply are to provide 80 kA for 0.3 s pulses every 10 s, while maintaining 20 kA during 1 s events every 2 s and 10 kA otherwise. An IGCT chopper design with variable pulse-width-modulation frequency is chosen to minimize cost and thermal losses. A full model of the circuit is developed in the time-domain simulation program PSCAD, and the design is demonstrated to be capable of delivering the specified signals. A thermal model is created to determine the optimal number of chopper bridges; a 4-wire plasma model is written to ensure the magnet's stabilization properties. We conclude that an IGCT chopper power supply is an effective system to drive the current of the VS3 in-vessel stabilization magnets at ITER.

JP8 57 Use of machine learning techniques for analysis of plasma data LOGAN MAINGI, *University of Oklahoma* HARRY MYNICK, NEIL POMPHREY, *Princeton Plasma Physics Laboratory* We consider the application of machine learning techniques to results from gyrokinetic (GK) codes such as Gene [1]. GK codes allow accurate computation of physical quantities such as radial fluxes, potential fluctuations, etc. However, such codes are computationally expensive, so use of techniques (eg, neural networks) to reduce the number of simulations necessary is desirable. Strategies are considered to minimize the requisite number of training examples for such a network without risk of error due to underfitting or overfitting. [1] F. Jenko, W. Dorland, M. Kotschenreuther, B.N. Rogers, Phys. Plasmas < 7> , 1904 (2000).

JP8 58 Parallelization of the GKEM Electromagnetic PIC code using MPI and OpenMP MARK BENJAMIN, STEPHANE ETHIER, WEI-LI LEE, *PPPL* GKEM is a legacy gyrokinetic PIC code in slab geometry that calculates anomalous transport in fusion plasmas due to drift wave microturbulence. It is currently being used to develop new algorithms for high-beta electromagnetic PIC simulations. This work focuses on the modernization and performance improvement of GKEM through the use of FORTRAN 90 language features and parallelization. MPI-based particle parallelization was implemented as well as loop-level multithreading using OpenMP directives. Performance improvements and speedup curves for the different stages of the code are discussed. Project supported by the DOE-PPPL High School Internship Program and DOE contract DE-AC02-09CH11466.

JP8 59 Parallelization of LSODE in PIES Using NVIDIA's CUDA Architecture for GPGPU PAUL THOMPSON, *Western Michigan University* STEPHANE ETHIER, *Princeton Plasma Physics Lab* The Princeton Iterative Equilibrium Solver (PIES) is a powerful tool for computing three dimensional MHD equilibria, without making assumptions about the form of the magnetic field. Part of its strength comes from its ability to handle equilibria with islands and stochastic regions. However, a high-resolution PIES calculation often takes several hours to complete, spending most of its time in the Livermore Solver for Ordinary Differential Equations (LSODE) to follow field-line trajectories. This work examines the feasibility of speeding up these calculations by taking advantage of the parallel computing resources of programmable Graphic Processor Units (GPUs). To this end, the LSODA variant version of LSODE is converted to NVIDIA's C for CUDA application programming interface and tested against its original Fortran version on an NVIDIA Tesla Cluster. Run times are compared between the serial and parallel versions, with special attention given to different scaling options. The new code is also analyzed for bottlenecks and opportunities for additional speedups, with the ultimate goal of developing a PIES-based MHD solver capable of running between experimental shots.

JP8 60 Providing Complete Distribution Function Analysis with NUBEAM FGen CASEY STARK, *University of Southern California* DOUGLAS McCUNE, ELIOT FEIBUSH, *PPPL* The TRANSP libraries provide many robust tools for analyzing tokamak plasmas. The development of this long-standing code has focused on physics modeling and producing efficient plasma calculations. In order to make these powerful libraries accessible to more scientists, parts of the code have been incorporated into web services, which can be run using the ElVis scientific graphics display. We present NUBEAM FGen, a new graphical web service interface focusing on distribution function (DF) simulation and analysis now integrated into ElVis. This interface can acquire TRANSP run data and given simulation parameters (a time of interest, duration, number of particles, etc.), will run a NUBEAM simulation on extracted Plasma State files. This simulation outputs the full distribution function in energy, pitch, x, and theta space. The user can analyze the DF data with an interactive get_fbm session, allowing them to visualize the DF with various plots (contour, slice, 3D, etc.). Users can also download the output for their own processing. The ease of this new approach to DF analysis will allow a much wider audience to utilize the DF tools provided by TRANSP in their own research.

JP8 61 Application of Piecewise Continuous Waveforms in the Paul Trap Simulator Experiment* M.S. GUTIERREZ, *University of California, Los Angeles* E.P. GILSON, R.C. DAVIDSON, *Princeton Plasma Physics Laboratory* A.N. KABCENELL, *Weston High School* The Paul Trap Simulator Experiment (PTSX) is a compact linear Paul trap that simulates a long, thin charged-particle bunch coasting through a kilometers-long magnetic alternating-gradient (AG) transport system by putting the physicist in the frame-of- reference of the beam. Both systems share the same equations of motion which allows for many AG focusing configurations to be studied in a compact laboratory environment instead of a kilometers-long machine. AG systems contain discrete quadrupole magnets but have been modeled with a continuously varying sinusoidal field of equivalent average transverse focusing strength in PTSX. The average transverse focusing frequency characterizes the strength of the transverse confinement in the smooth focusing model, where fast oscillations are averaged over. Initial experimental results demonstrate the validity of the smooth focusing model by applying periodic-step waveforms and sinusoidal waveforms, of equal average transverse focusing strength, to the electrodes of the Paul trap and comparing the resulting radial density profiles.

*This research is supported by the U.S. Department of Energy.

JP8 62 Diamond Synthesis in a Hybrid PVD/CVD ECR Thin Film Deposition System WILLIAM SOMERS, ANDREW ZWICKER, *Princeton Plasma Physics Laboratory* Diamond thin films are extremely hard, thermally conductive, resistant to chemical corrosion, and excellent insulators making them an ideal coating for semiconductors. In our electron cyclotron resonance (ECR) system, physical vapor deposition (PVD) and chemical vapor deposition (CVD) are used to create diamond thin films in a hybrid physical-chemical vapor deposition (HPCVD) system. In this process, a gas mixture that consists of 1% methane and 99% hydrogen is heated with a 2.45 GHz / 2.5 kW microwave source. Diamond deposition occurs from the physical sputtering of carbon from a negatively biased graphite target (PVD) and chemically from the stripped methane, CH_4, molecules (CVD). A major advantage of our hybrid plasma processing system is that it can sputter diamond at a much lower temperature than typical CVD. A silicon wafer substrate handling system allows us to control rotational speed, bias, and temperature and allows for increased control of diamond deposition. The quality of the diamond films is measured by Raman spectra and SEM images. Initial results of growth rate, uniformity, and quality will be presented.

JP8 63 Optical Analysis of Plasma Ball Filaments SCOTT VASQUEZ, MICHAEL CAMPANELL, STEWART J. ZWEBEN, *PPPL* Optical methods were used to study the properties of a commercial plasma ball. Using spectrometry, the gas composition of the plasma ball was analyzed. Spectra of known gases were compared with the plasma ball spectrum, confirming the presence of Neon and Xenon. The spectra indicate that faint amounts of Nitrogen may also be present. Photomultiplier tubes were used to measure the radial velocity of filaments in the plasma ball. Digital oscilloscope traces produced with the photomultiplier tubes show that the filaments propagate radially at an average velocity on the order of 10,000 m/s. Furthermore, these traces suggest that that the radial velocity decreases with increasing distance from the electrode. A hotwired commercial plasma ball, with connections for a pulse generator and Variac has been built, allowing for the study of filament velocity at different operating voltages and frequencies. A custom plasma ball whose parameters, such as gas mixture, pressure, electrode configuration, and applied voltage waveform can be varied, has also been constructed. Analysis of the custom plasma ball will give further insight to how such parameters affect the plasma ball's filament formation and behavior. Initial results will be presented. Ultimately, this custom plasma ball, along with the methods used to measure its properties, will be incorporated into an undergraduate physics lab.

JP8 64 High-Speed Imaging Analysis of Discharge Oscillations in the Cylindrical Hall Thruster* EVAN DAVIS, *University of California, Riverside* JEFFREY B. PARKER, YEVGENY RAITSES, *Princeton Plasma Physics Laboratory* The cylindrical Hall Thruster is a cross-field plasma discharge device, which employs mirror and cusp shaped magnetic field configurations [1]. Several modes of discharge oscillations in the plasma have been observed by a high-speed camera, including a circumferentially propagating spoke and a longitudinal breathing mode. The occurrence and characteristics of these oscillations are strongly influenced by the operating conditions of the thruster discharge. A data analysis package employing various signal processing techniques was developed to parametrically characterize both the spoke and the breathing mode oscillations under variations of the background gas pressure, the discharge voltage, and the magnetic field. [1] Y. Raitses and N. J. Fisch, Physics of Plasmas **8**, 2579 (2001).

*Work supported by USDOE DE-AC02-09CH11466.

JP8 65 Recent Bolometry Upgrades and Results from the HIT-SI and NSTX Experiments M.A. CHILENSKI, T.R. JARBOE, B.A. NELSON, R. RAMAN, *University of Washington* L. ROQUEMORE, *Princeton Plasma Physics Laboratory* B.M. JONES, *Sandia National Laboratory* The bolometry suite on the Helicity-Injected Torus (HIT-SI) has recently been upgraded with two new channels in order to measure the radiated power in the mouth of one of the helicity injectors, as well as an upgraded wide-view bolometer to maximize the solid angle imaged at the midplane. This upgrade will allow a better understanding of the magnitude of the power radiated in the injectors versus the confinement region. In addition to a multi-chord bolometer array, the National Spherical Torus Experiment (NSTX) is also equipped with three wide-view bolometers looking at various regions of the plasma. One bolometer looks into the main confinement region at midplane along a chord parallel to the midplane, one looks down to the lower divertor/injector region and one looks from the bottom up. Work is proceeding to cross-calibrate these bolometers to the multi-chord array. Once this calibration is complete, it will be possible to obtain rapid estimates of the total radiated power, which will be compared to the total input power.

JP8 66 Development and Evaluation of a Motional Stark Effect with Laser Induced Fluorescence Diagnostic for Determining the Magnetic Field Magnitude and Angle in NSTX ADAM STEINER, *NCSU* E.L. FOLEY, F.M. LEVINTON, *Nova Photonics* A. BARLIS, *Williams College* The motional Stark effect (MSE) diagnostic has been widely used for determining the magnetic field pitch angle profile in the high magnetic fields of large tokamaks. Incorporating laser induced fluorescence (LIF) and a dedicated diagnostic neutral beam into MSE systems has been shown to extend the range of applicability to lower field systems and to provide simultaneous measurements of magnetic field magnitude. An MSE-LIF system built by Nova Photonics has been characterized and redesigned for installation on NSTX. The design has taken into account spatial considerations of interfacing between the system and NSTX and allowed for the inclusion of neutral beam measurement devices including a Faraday probe and a calorimeter. An electrically insulated magnetic shielding system was developed to prevent interference from the external magnetic field of NSTX. Characterization of the neutral beam has shown good performance and agreement with theoretical values with respect to the neutral-ion ratio and species fraction.

JP8 67 RF power deposition during HHFW heating in NSTX* TERESA BRECHT, *UMN* R. BELL, J. HOSEA, B. LEBLANC, C.K. PHILLIPS, G. TAYLOR, E. VALEO, J.R. WILSON, *PPPL* P.M. RYAN, *ORNL* P.J. BONOLI, J. WRIGHT, *PSTC-MIT* THE NSTX TEAM, High harmonic fast wave (HHFW) heating and current drive (CD) research on the National Spherical Torus Experiment (NSTX) employs a 12 strap antenna which launches radio frequency (RF) waves into the plasma. Improved core heating efficiency is achieved by moving the onset of wave propagation away from the antenna. Current research focuses on understanding RF power losses at the edge region and power partitioning among the plasma species under various discharge conditions. The full-

wave code TORIC was used to simulate discharges of interest using equilibrium fits and temperature and density profiles from NSTX discharges. Ion species concentrations, as well as the launched wavelength strongly effect power deposition. Simulation of the power partitioning in L-mode and H-mode, with and without neutral beam injection (NBI) will be discussed.

*Work supported by DE-AC02-09CH11466.

JP8 68 Heat Flux Characterization in the NSTX* JONATHAN SURANY, *Princeton University* RAJESH MAINGI, *ORNL* NSTX TEAM, Management of the heat flux profile is critically important in spherical tokamaks because they are high power density systems. More specifically, peak heat fluxes as high as 10 MW/m^2 have been measured in the National Spherical Torus Experiment (NSTX). Infrared cameras placed to view the upper and lower divertors on the NSTX are used to measure the tile temperature and to calculate the heat flux profiles. In this study, we present the dependence of the heat flux profile on neutral beam injected power, plasma current, magnetic balance and magnetic flux expansion, and triangularity. For example, peak heat flux increases linearly with increases in neutral beam injected power, and varies inversely with magnetic flux expansion. These trends follow their basic theoretical expectations.

*Supported by Princeton Plasma Physics Laboratory.

JP8 69 3-D reconstruction of incandescent lithium dust particle trajectories in NSTX* JACOB NICHOLS, *Cornell University* LANE ROQUEMORE, *Princeton Plasma Physics Laboratory* WERNER BOEGLIN, *Florida International University* WILLIAM DAVIS, DENNIS MANSFIELD, CHARLES SKINNER, HANS SCHNEIDER, *Princeton Plasma Physics Laboratory* RAHUL PATEL, *Florida International University* Dust control is a key safety and stability concern for "next-step" fusion devices, so understanding the dynamics of dust in a fusion grade reactor is an important issue. Here, a large ensemble of trajectories from pre-characterized lithium dust is collected with the goal of verifying the various dust transport codes. Precise amounts of 40 μ lithium dust (varying from 1-150 mg) are injected into the National Spherical Torus Experiment (NSTX) plasma using a powder dropper based on a vibrating piezo crystal. The particles are heated to incandescence by electron bombardment, allowing them to be viewed by two separated visible-range fast cameras operating at $\sim$ 10,000 frames per second. The tracks from both cameras can be combined to form a single, 3-D trajectory. Particles are observed to undergo a variety of accelerations both parallel and perpendicular to the magnetic field, depending on their proximity to the scrape-off layer. The velocity, lifetime, and ionization state of the particles will be discussed.

*Work supported by US DOE Contract #DE-AC02-09CH11466.

JP8 70 Magnetic Transport Barriers in the DIII-D Tokamak* J. KESSLER, *SE Missouri State U.* F. VOLPE, *U. Wisc.-Madison* T.E. EVANS, *GA* H. ALI, A. PUNJABI, *Hampton U.* Large overlapping magnetic islands generate chaotic fields. However, a previous work [1] showed that second or third order perturbations of special topology and strength can also generate magnetic diffusion "barriers" in the middle of stochastic regions. In the present study, we numerically assess their experimental feasibility at DIII-D. For this, realistic I- and C-coils perturbations are superimposed on the equilibrium field and puncture plots are generated with a field-line tracer. A criterion is defined for the automatic recognition of barriers and successfully tested on earlier symplectic maps in magnetic coordinates. The criterion is systematically applied to the new puncture plots in search for dependencies, e.g. upon the edge safety factor q_{95}, which might be relevant to edge localized mode (ELM) stability, as well as to assess the robustness of barriers against fluctuations of the plasma parameters and coil currents.[1] H. Ali and A. Punjabi, Plasma Phys. Control. Fusion **49**, 1565 (2007).

*Work supported in part by the US DOE under a National Undergraduate Fusion Fellowship and DE-FC02-04ER54698.

JP8 71 Evaluation and Implementation of Helium Line Ratio Technique for Measurement of Edge Density and Temperature on DIII-D* L. HURD, *Clemson U.* N.H. BROOKS, *GA* E.A. UNTERBERG, *ORISE* O. SCHMITZ, *FZ-Juelich* The electron density and temperature in the scrape-off layer of DIII-D have been determined in pure helium plasmas by the helium line ratio technique [1] employing spectral line monitors and an intensified fast-framing CCD camera. Both diagnostics viewed the plasma tangentially on the midplane of the vessel. Three visible He I transitions, one triplet ($3^3S\rightarrow 2^3P$) and two singlets ($3^1D\rightarrow 2^1P$ and $3^1S\rightarrow 2^1P$), were measured simultaneously — along a single spatial chord with the line monitors and over a 2D region of the outer midplane with the intensified camera. Column brightnesses through the emission shell recorded with the camera were Abel-inverted to yield local intensities with a spatial resolution of a few millimeters. The electron densities and temperatures deduced by the helium line ratio method are compared with results from the Thomson scattering diagnostic on DIII-D.[1] O. Schmitz *et al.*, Plasma Phys. Control. Fusion **50** (2008) 115004.

*Work supported in part by the US DOE National Undergraduate Fellowship, DE-FC02-04ER54698, and DE-AC05-06OR23100.

JP8 72 Comparison of Moderate to High Ion Cyclotron Absorption on Energetic Ions in NSTX and DIII-D* J. BURBY, *Cornell University* R.I. PINSKER, M. CHOI, *General Atomics* Strong absorption of fast waves (FWs) on injected deuterons at ion cyclotron harmonic numbers in the 4-10 range is observed on both DIII-D and NSTX. The results from fast ion D_α spectroscopic measurements from the two devices differ significantly: deposition on fast ions peaks near the cyclotron harmonic layer closest to the magnetic axis in the conventional-aspect-ratio DIII-D, while results from the low-aspect-ratio NSTX show a broader deposition profile [1]. One root of the difference stems from the absorbing fast ions sampling more harmonic layers in NSTX than in DIII-D. We investigate cyclotron absorption in cases with multiple harmonic layers within a single ion gyroradius and related phenomena numerically and analytically by examining the response of individual charged particles to rf fields in various field configurations.[1] M. Podesta *et al.*, *RF Power in Plasmas* (Proc.18th Top. Conf., Gent, Belgium, 2009), to be published.

*Supported by the US DOE under a National Undergraduate Fusion Fellowship, DE-FC02-04ER554698, and DE-FG03-95ER54309.

JP8 73 Investigation of Ion Cyclotron Emissions on DIII-D During Neutral Beam Injection and Fast Wave Heating* A. AXLEY, *UCLA* R.I. PINSKER, *General Atomics* Ion cyclotron emission (ICE) spectra are measured with small rf loop antennas at 4 locations in the DIII-D vessel. Two of the loops are located on

the centerpost while the other two are on the outboard wall of DIII-D. Both sets of loops are near the midplane. The signal processing is done in software using data from a 1 Gigasample/s 4-channel digitizer to measure the output of these antennas rather than the traditional technique of using an analog spectrum analyzer. Specifically, an FFT is used to determine the spectra up to 500 MHz of each signal. The analysis is performed on data recorded during neutral beam injection, and during high power fast wave (FW) heating. This technique should be capable of resolving the bursting character of ICE in time, as has been often observed in the neutral beam injection case, as well as extending the observations of parametric decay instabilities during FW injection to include the pump (60 or 90 MHz) and its first several harmonics.

*Supported by US DOE National Undergraduate Fusion Fellowship, and DE-FC02-04ER54698.

JP8 74 Visualization of Turbulence with OpenGL* A. AVRIL, *Princeton U.* M.A. MAKOWSKI, M. UMANSKY, *Lawrence Livermore National Laboratory* R. KALLING, D.P. SCHISSEL, *General Atomics* Turbulence is an all-pervasive phenomenon in plasmas. The edge turbulence is of particular interest for the containment of plasmas during fusion processes. It is simulated with BOUT, a 4D (3 spatial + time coordinates) edge turbulence simulation code that is typical of modern codes in many ways. While predictive, the 4D outputs of these codes are difficult to visualize. In an effort to better understand the macroscopic trends of edge turbulence in toroidal plasmas, we are developing routines to render the BOUT output, using the OpenGL framework in C^{++}. These routines will allow us to follow the evolution of isosurfaces through time, and we anticipate gaining insight into the nonlinear dynamics of turbulence as a result. Additionally, these routines could potentially be used to visualize the output of other modeling codes.

*Work supported by a US DOE National Undergraduate Fellowship, DE-AC52-07NA27344, and DE-FC02-04ER54698.

JP8 75 Multi-Parameter Scaling of Divertor Heat Flux Profile Width* C.J. MILES, *Massachusetts Institute of Technology* D.N. HILL, C.J. LASNIER, M.A. MAKOWSKI, *Lawrence Livermore National Laboratory* A.M. GAROFALO, *General Atomics* We will explore the dependence of the divertor heat flux profile on plasma current, heating power, midplane edge heat flux, magnetic field strength, and other variables. In divertor tokamaks, a major part of the heating power is lost by thermal transport across the plasma boundary into the scrape-off layer (SOL) where the power is primarily transported along field lines to the divertor. It is important that this high heat flux to the divertor surfaces stays below the technologically feasible perpendicular heat flux of approximately 10 MW/m^2. Thus, it is valuable to determine a multi-parameter scaling of heat flux profile width for projections to a fusion reactor. We will attempt to do so by analyzing divertor heat flux data inferred from high-speed infrared camera measurements of the surface temperature over time

*Work supported by the US DOE under a National Undergraduate Fellowship in Plasma Physics and Fusion Energy Sciences, DE-ACD52-07NA27344, and DE-FC02-04ER54698.

JP8 76 Confinement Trends in DIII-D High Performance Plasmas* A. NEFF, *Mesa State College* A.M. GAROFALO, T.C. LUCE, *General Atomics* A research goal on the DIII-D tokamak is to develop the physics basis for steady-state, high performance plasma operation for ITER and future burning plasma devices. To achieve high fusion power density and steady-state with minimal external power requirements, a fusion reactor requires good energy confinement and high bootstrap (self-generated) fraction of the total plasma current. However, a coarse view of DIII-D and JET databases of high performance discharges suggests a decrease in quality of confinement with increasing noninductive current fraction. To assess this trend, and investigate possible causes, a code is being developed to retrieve and analyze the DIII-D experimental data, and generate a database of high confinement plasma discharges. The code uses specified criteria to evaluate the plasma duration at high confinement, and stores various plasma parameters calculated in this time range. Comparisons of the experimental energy confinement time to various inter-device scaling laws, and the dependence on key plasma parameters will be discussed.

*Work supported by a US DOE National Undergraduate Fusion Fellowship and DE-FC02-04ER54698.

JP8 77 Optimization of Optical Filters for the LIBEAM Diagnostic* SEAN McGUIRE, *Whitworth University* C.C. PETTY, D.M. THOMAS, *General Atomics* B. HUDSON, *ORISE* In tokamak plasmas with an edge transport barrier, a measurement of the edge current density is necessary to understand plasma stability. A LIBEAM diagnostic system has been deployed on DIII-D that measures Zeeman polarimetry of the 2S-2P lithium resonance line in order to determine the magnetic field and corresponding current density within the edge pedestal region. Emission of the lithium resonance line is split by the local magnetic field producing three closely spaced spectral components; isolation of the σ^- spectral component is required for measurement of the local magnetic field. A double Fabry-Perot etalon system is currently used for this purpose but a narrower bandpass is desired. This research will determine whether the installation of an exit pinhole will improve the etalon's finesse. However, transmitted light intensity is near a minimum threshold and the efficiency of the entire optical system must be examined and maximized. Optimization may include the installation of new detectors, lenses and fibers.

*Work supported by US DOE National Undergraduate Fusion Fellowship, DE-FC02-04ER54698, and DE-AC05-06OR23100.

JP8 78 Electron Cyclotron Emission Radiometer CRISTINA MORALES, *University of Maryland TREND, Florida International University McNair Program* There is much interest in studying plasmas that generate hot electrons. The goal of this project is to develop a wide band electron cyclotron radiometer to measure the non-Maxwellian rapid rises in electron temperature. These rapid increases in temperature will then be correlated to instabilities in the plasma. This project explores a type of noncontact temperature measurement. We will attempt to show the feasibility of electron cyclotron emissions to measure the Maryland Centrifugal Experiment's electron plasma temperature. The radiometer has been designed to have 100dB of gain and a sensitivity of 24mV/dB given by its logarithmic amplifier. If successful, this radiometer will be used as a diagnostic tool in later projects such as the proposed experiment studying magnetic reconnection using solar flux loops.

JP8 79 DIII-D TOKAMAK II

JP8 80 Non-axisymmetric Plasma Response to External Magnetic Perturbations* M.S. CHU, L.L. LAO, T.E. EVANS, M.J. SCHAFFER, E.J. STRAIT, *General Atomics* Y.Q. LIU, *Culham* M.J. LANCTOT, H. REIMERDES, *Columbia U.* Very low frequency non-axisymmetric magnetic response in tokamaks excited by external magnetic perturbations is studied with the MARS-F code [1] using different assumptions on the plasma dynamics. In the limit of vacuum plasma response, the fields are benchmarked against the SURFMN [2] code and an analytic model. In other plasma models, the response is affected by plasma pressure, resistivity, toroidal flow, and the kinetic effects associated with the particle drifts. Depending on the coil arrangement, the plasma response could be dominated by the resonant or non-resonant components of the external field. The responses can be tested by employing different combinations of currents in appropriately designed external coils as those in DIII-D. The combined magnetic field of the axisymmetric plasma equilibrium and its non-axisymmetic responses corresponds to a perturbed 3D plasma equilibrium.[1] Y.Q. Liu, *et al.*, Phys. Plasmas **7** (2000) 3681.[2] M.J. Schaffer, *et al.*, Nucl. Fusion **48** (2008) 024004.

*Work supported in part by the US DOE under DE-FG02-95ER54309 and DE-FG02-89ER53297.

JP8 81 Measurement and Modeling of the Plasma Response to Externally Applied Non-axisymmetric Magnetic Fields* H. REIMERDES, M.J. LANCTOT, J.M. HANSON, *Columbia U.* A.M. GAROFALO, M.S. CHU, G.L. JACKSON, R.J. LA HAYE, M.J. SCHAFFER, E.J. STRAIT, *General Atomics* O. SCHMITZ, *FZ Juelich* Y.Q. LIU, *UKAEA* M. OKABAYASHI, W.M. SOLOMON, *PPPL* Magnetic measurements in DIII-D H-mode plasmas reveal a beta dependent plasma response to externally applied low n magnetic fields. The plasma response must be significant since it correlates with effects on the plasma such as magnetic braking of rotation. This is confirmed by modeling using the ideal MHD plasma response model in the MARS-F code, which predicts the measured plasma response to external $n = 1$ fields for values of beta up to $\sim 75\%$ of the ideal MHD beta limit calculated without a conducting wall. At higher beta non-ideal effects have to be taken into account. The increasing plasma response is responsible for the decrease of the error field tolerance with beta. The knowledge of the perturbed field inside the plasma is an important step towards a quantitative understanding of the error field tolerance and the underlying braking models.

*Work supported in part by the US DOE under DE-FG02-04ER54761, DE-FC02-04ER54698, and DE-AC02-09CH11466.

JP8 82 Measuring Resistive Wall Mode Stability in Real-time* J.M. HANSON, M.J. LANCTOT, G.A. NAVRATIL, H. REIMERDES, *Columbia U.* E.J. STRAIT, *General Atomics* Measurements of the plasma response to externally applied, low-n magnetic fields can be used to determine the resistive wall mode (RWM) stability of the plasma equilibrium. Such a method, if implemented as a real-time algorithm, can be used to gate error field correction, profile control, and RWM feedback control algorithms, enabling operation close to the no-wall stability limit. In addition, the stability estimate can be used to directly update parameters in an advanced RWM controller as the plasma evolves. We have developed an efficient scheme that uses an external field rotating at a single fixed frequency. Because only one frequency is applied, the plasma response can be calculated from measurements by Fourier-analyzing the measurements at only the applied frequency and subtracting the known vacuum pickup due to the control coils. This single-frequency, Fourier-domain analysis uses a small number of arithmetical operations, which is a requisite for real-time implementation.

*Work supported by the US DOE under DE-FG02-89ER53297 and DE-FC02-04ER54698.

JP8 83 Active Feedback Control of the Current-driven Resistive Wall Mode (RWM) in DIII-D* Y. IN, J.S. KIM, *FARTECH, Inc.* M.S. CHU, A.M. GAROFALO, G.L. JACKSON, R.J. LA HAYE, M.J. SCHAFFER, E.J. STRAIT, *GA* M.J. LANCTOT, H. REIMERDES, *Columbia U.* Y.Q. LIU, *UKAEA* L. MARRELLI, P. MARTIN, *Consorzio RFX* M. OKABAYASHI, *PPPL* Recent DIII-D experiments show that complete RWM feedback stabilization requires good error field correction (EFC), yet the RWM feedback control could not be replaced by EFC. A systematic investigation of feedback response time confirmed that a bandwidth greater than the RWM growth rate is required for direct RWM stabilization. The optimized feedback gain of RWM feedback stabilization was ultimately determined by the minimal level of plasma fluctuations. The parametric dependencies observed for feedback control of current-driven RWMs are consistent with predictions based on pressure-driven RWM models. Additionally, there was an indication of the influence of a second-least stable RWM which had never been identified in experiments. The experimental details are being used to assess the RWM feedback models for prediction of RWM suppression in ITER.

*Work supported in part by the US DOE under DE-FG02-06ER84442, DE-FC02-04ER54698, DE-FG02-89ER53297, and DE-AC02-09CH11466.

JP8 84 Physics Issues at the Initial Phase of Robust RWM Feedback* M. OKABAYASHI, *PPPL* Y. IN, J.S. KIM, *FARTECH, Inc.* G.L. JACKSON, A.M. GAROFALO, R.J. LA HAYE, E.J. STRAIT, *General Atomics* T. BOLZONELLA, L. MARRELLI, P. MARTIN, *Consorzio RFX* M.J. LANCTOT, H. REIMERDES, *Columbia U.* The magnetic feedback process has robustly suppressed low beta $q_{95} \sim 4$ current-driven resistive wall mode (RWM) by direct feedback beyond application of effective error field correction only. Without feedback, the current-driven RWM usually evolved into a resistive wall tearing mode even when the RWM amplitude is less than a few Gauss. There remain several issues in RWM feedback process, such as how it functions near the onset of magnetic island growth and the impact of uncorrected error fields. Another issue is the operational compatibility of fast direct feedback with slow error field correction at the initial phase of feedback. These issues will be discussed to clarify the requirements for robust RWM feedback control in ITER.

*Work supported in part by the US DOE under DE-AC02-09CH11466, DE-FG02-06ER84442, DE-FC02-04ER54698, and DE-FG02-89ER53297.

JP8 85 Development of An Energetic Particle Module and Integration into IMFIT With Initial Applications* W. GUO, *ASIPP* M.S. CHU, L.L. LAO, *General Atomics* Y.Q. LIU, *Culham* Q. REN, G. LI, C. PAN, *ASIPP* D. YADYKIN, *CTH* The performance of future burning tokamak experiments depends critically on the behavior of energetic particles. To facilitate the validation

of energetic particle physics in present-day experiments, an energetic particle physics module is being developed and integrated into the IMFIT Integrated Modeling tool. This IMFIT module provides a convenient platform to facilitate interactions among various physics codes starting from the experimental data to the analysis of stability and transport with the inclusion of energetic particles. Key components of the module include the EFIT, NUBEAM, CONT, ONETWO, and MARS-K codes, in which the effects of fast ions have been implanted. Starting from experimental data, the energetic particle distribution function is obtained by using various birth and transport models, and their subsequent effect on the stability and transport of the background plasma studied. Initial applications using DIII-D experimental data will be presented.

*Work supported by US DOE under DE-FG03-95ER54309 and DE-FC02-04ER54698 and China MOST under 2007DFA01290.

JP8 86 Improvements to IMFIT Integrated Modeling Tool and Initial Release* A. COLLIER, L.L. LAO, G. ABLA, M.S. CHU, H.E. ST. JOHN, R. PRATER, *GA* W. GUO, G. LI, C. PAN, Q. REN, *ASIPP* J.M. PARK, *ORNL* R. SRINIVASAN, *IPR* M. WORRALL, *Colorado School of Mines* The current status of a modern integrated modeling tool named IMFIT used to support key elements of DIII-D and EAST research is summarized. IMFIT is a Python-based GUI tool utilizing a modular framework with a central manager that coordinates tasks between component modules. Different component managers provide access to specific physics codes for equilibrium, stability, and transport analysis. An IMFIT plasma state file and associated translator are being developed to allow efficient inter- and intra-module communication. The IMFIT state file includes all necessary information for transport, stability, equilibrium, and data processing codes. The translator can generate native state files for codes and includes support for bi-directional translation. IMFIT is designed to be portable and includes the capability to dynamically link to codes and also provide source management tools for developers. The first public version of IMFIT has been released.

*Work supported in part by US DOE under DE-FG03-95ER54309 and DE-AC05-00OR22725.

JP8 87 Tearing-Mode Excitation by Counter ECCD for Validation of Resistive MHD Models in DIII-D* L.L. LAO, R. PRATER, R.J. LA HAYE, M.S. CHU, A.W. HYATT, T.C. LUCE, T.H. OSBORNE, E.J. STRAIT, G. ABLA, V.S. CHAN, A. COLLIER, A.D. TURNBULL, *GA* V.A. IZZO, *UCSD* W. GUY, G. LI, C. PAN, Q. REN, *ASIPP* R. SRINIVASAN, *IPR* J.M. PARK, *ORNL* Resistive MHD modes play an important role in tokamak plasma confinement and stability. Although ideal MHD is well established as a reliable predictive tool for takamak stability limit, resistive MHD is less understood. In this DIII-D experiment, 3/2 tearing modes of varying amplitudes are systematically excited and their characteristics documented for validation of their linear stability threshold and saturated island structure against PEST3 and NIMROD predictions. Up to 3 MW of counter ECCD power is injected into H-mode plasmas. 3/2 tearing modes with increasing amplitudes are driven as the amount of injected counter ECCD power is stepped up. Detailed stability analyses using PEST3 and NIMROD are being performed for comparison against experimental observations with accurately reconstructed equilibria that allow for the counter ECCD effects. Results will be presented.

*Work supported by the US DOE under DE-FG03-95ER54309, DE-FC02-04ER54698, and DE-AC05-00OR22725.

JP8 88 Modeling of Plasma Pressure Effects on ELM Suppression With RMP in DIII-D* D.M. ORLOV, R.A. MOYER, S. MORDIJCK, *UCSD* T.E. EVANS, T.H. OSBORNE, P.B. SNYDER, *General Atomics* E.A. UNTERBERG, *ORISE* M.E. FENSTERMACHER, *LLNL* Resonant magnetic perturbations (RMPs) are used to control the pedestal pressure gradient in both low and high (ν_3^*) DIII-D plasmas. In this work we have analyzed several discharges with different levels of triangularity, different neutral beam injection power levels, and with, β_N ranging from 1.5 to 2.3. The field line integration code TRIP3D was used to model the magnetic perturbation in ELMing and ELM suppressed phases during the RMP pulse. The results of this modeling showed very little effect of β_N on the structure of the vacuum magnetic field during ELM suppression using $n = 3$ RMPs. Kinetic equilibrium reconstructions showed a decrease in bootstrap current during RMP. Linear peeling-ballooning stability analysis performed with the ELITE code suggested that the ELMs, which persist during RMP, i.e. ELMing still is observed, are not Type I ELMs. Identification of these D_α spikes is an ongoing work.

*Supported by US DOE under DE-FG02-05ER54809, DE-FG02-07ER54917, DE-FC02-04ER54698, DE-AC05-06OR23100, and DE-AC52-07NA27344.

JP8 89 Pellet ELM Triggering Results and Pacing Prospects for DIII-D* L.R. BAYLOR, T.C. JERNIGAN, N. COMMAUX, *Oak Ridge National Laboratory* T.E. EVANS, P.B. PARKS, *General Atomics* M.E. FENSTERMACHER, *LLNL* R.A. MOYER, J.H. YU, *UCSD* Small deuterium pellets have been injected with high speed and dropped with low speed into DIII-D H-mode plasmas from different locations. ELMs have been triggered by pellets injected from all locations, but not from vertically dropped low speed pellets. Experimental details of the pellet triggering of ELMs show that they are triggered before the injected fueling pellets reach the top of the H-mode pedestal, implying that penetration just inside the separatrix is sufficient to trigger ELMs. Results from 1-mm pellets dropped with a speed of 10 m/s into the edge plasma show a strong toroidal deflection in the scrape off layer with minimal penetration into the plasma and no clear triggering of ELMs. A planned upgrade of the pellet injector and new pellet trajectory for ELM pacing studies will be presented. Implications for controlled ELM triggering on ITER will be discussed.

*Supported by the US DOE under DE-AC05-00OR22725, DE-FC02-04ER54698, DE-AC52-07NS27344, and DE-FG02-07ER54917.

JP8 90 Large, Shattered Pellets for Disruption Mitigation in DIII-D* T.C. JERNIGAN, L.R. BAYLOR, S.K. COMBS, N. COMMAUX, S.J. MEITNER, *ORNL* E.M. HOLLMANN, Y.H. YU, *UCSD* D.A. HUMPHREYS, M.A. VAN ZEELAND, J.C. WESLEY, *GA* A new pellet injector, the "shotgun" pellet injector for disruption mitigation studies, has been installed on the DIII-D tokamak. The large pellets ($\sim$ 15 mm diam. x 22 mm long, 2.3 $\times$ 10^{23} electrons with D_2) are shattered on a series of plates and directed toward the plasma magnetic axis. Previous experiments using massive gas injection (MGI) showed that the gas was stopped at the plasma edge and only penetrated diffusively until an MHD event, triggered by the cooling wave, transported some of the ionized gas from the edge to the interior. While the disruption forces and heat load to the first wall were significantly reduced by MGI, the core density achieved was insufficient to achieve suppression of runaway electrons from the avalanche process. Initial experiments with the new injector have demonstrated direct penetration of some of the shattered pieces deep into the plasma. Details of assimilation, mitigation, and density achieved in subsequent experiments will be presented.

*Work supported by the US DOE under DE-AC05-00OR22725, DE-FG02-07ER54917, and DE-FC02-04ER54698.

JP8 91 3D Field Effects on Disruption-Generated Runaway Electrons in DIII-D* D.A. HUMPHREYS, N.W. EIDIETIS, T.E. EVANS, P.B. PARKS, E.J. STRAIT, J.C. WESLEY, *General Atomics* N. COMMAUX, T.C. JERNIGAN, *ORNL* E.M. HOLLMANN, A.N. JAMES, J.H. YU, *UCSD* A relatively modest conversion of thermal current-carrying electrons to multi-MeV runaway electrons (RE) during a disruption current quench can lead to damage of ITER in-vessel components. Effective mitigation of this conversion process is therefore essential to ITER operation. Injection of large amounts of impurities holds promise for RE mitigation, but has not yet reached the density levels expected to ensure full suppression. Experiments in TEXTOR and other devices have suggested that resonant magnetic perturbations (RMP) may suppress disruption runaways (e.g. [1]). We report on recent experiments in DIII-D applying nonaxisymmetric fields during disruptions with RE current channels, produced in ITER-like lower single null configurations using Ar cryogenic pellet injection. Experimental summaries and analysis of the effects of 3D fields on RE generation and deconfinement are presented.[1] M. Lehnen, *et al.*, Phys. Rev. Lett. **100** (2008) 255003.

*Work supported by the US DOE under DE-FC02-04ER546598, DE-AC02-00OR22725, and DE-FG02-07ER54917.

JP8 92 Modeling and Measurement of Disruption Halo Current Evolution on DIII-D* N.W. EIDIETIS, *GA* E.M. HOLLMANN, *UCSD* D.A. HUMPHREYS, *GA* T.C. JERNIGAN, *ORNL* E.J. STRAIT, J.C. WESLEY, *GA* Disruption halo current $J \times B$ forces present a significant danger to the physical integrity of vessel components in ITER. Understanding the evolution of halo currents is critical to ensuring safe and reliable tokamak operation. A model for halo current evolution was presented in [1] which reliably recreated DIII-D halo current evolution, but it assumes a halo width and temperature, both of which are significant factors in the halo current evolution. A diffusion model for halo width evolution is presented here, and compared to DIII-D data. To better test this model, an upgraded halo current monitoring system with fine toroidal and poloidal resolution is planned for installation in 2010. In addition, the design of an accelerometer array for measuring disruption force asymmetries is presented.[1] D.A. Humphreys and A.G. Kellman, Phys. Plasmas **6**, 2742 (1999).

*Work supported in part by the US DOE under DE-FC02-04ER54698, DE-FG02-07ER54917, and DE-AC05-00OR22725.

JP8 93 Fast Disruptions and Halo Currents in the International Disruption Database* A.W. HYATT, N.W. EIDIETIS, S.M. FLANAGAN, D.A. HUMPHREYS, J.C. WESLEY, *General Atomics* M.D. WALKER, *SDSUF* The International Disruption Database (IDDB) is an International Tokamak Physics Activity (ITPA) sponsored undertaking hosted at GA. It contains information from thousands of disrupted discharges on many tokamaks. Disruptions potentially apply very large forces and thermal loads on tokamak components. Delineating the expected extremes of disruption phenomena is essential to designing a tokamak that is robust to these off-normal events. Examples of database quantities include disruption current quench (CQ) time and the degree of toroidal asymmetry in the disruption halo currents. We present analysis of IDDB data using a simple isolated current ring model that puts all tokamaks on an equal footing, and shows that the fastest CQ times normalized by plasma area are about 0.6 ms/m^2. Some limitations of the simple model are discussed, and recent expansions of the IDDB data set with halo current data from DIII-D are described.

*Work supported in part by the US DOE under DE-FC02-04ER54698.

JP8 94 Development of Off-Normal and Fault Event Detection and Response Techniques for ITER and DEMO* M.L. WALKER, B.S. SAMMULI, D.A. HUMPHREYS, J.R. FERRON, R.D. JOHNSON, B.G. PENAFLOR, D.A. PIGLOWSKI, E.J. STRAIT, *General Atomics* Future devices such as ITER and DEMO will demand a sophisticated collection of actions in response to a set of off-normal and fault events. The number of such response actions is significantly larger than on any presently operating fusion device. The objective of these actions is to allow fusion devices to operate disruption-free, thereby making fusion a more attractive power generating technology. We report on work performed at DIII-D to develop appropriate methods for detection of and response to off-normal and fault events and the software and computational infrastructure needed to support these methods.

*Work supported by the US DOE under DE-FC02-04ER54698.

JP8 95 Recent Investigations of Runaway Electron (RE) Generation and Transport in DIII-D* A.N. JAMES, E.M. HOLLMANN, J.H. YU, G.R. TYNAN, *UCSD* N. COMMAUX, T.C. JERNIGAN, *ORNL* N.W. EIDIETIS, T.E. EVANS, R.J. LA HAYE, E.J. STRAIT, J.C. WESLEY, *GA* C.J. LASNIER, *LLNL* M.E. AUSTIN, *U. Texas* We generated record RE currents in DIII-D of $>$ 500 kA by terminating stationary discharges via frozen Ar pellet injection. The largest measured RE currents evolved from discharges with $q_0 > 0.97$ and $\ell_i > 0.92$. A new scintillator array observed 3 phases of RE escape to the wall: a toroidal band of prompt release to the upper and lower divertors just after the thermal quench, 1 ms later a longer 5-50 ms period where RE drifted upward and escaped via slow diffusion and rapid bursts, and a final rapid strike of remaining RE current on the upper divertor. Visible synchrotron or bremsstrahlung emission appeared

on the fast camera during the 2nd phase near machine center and drifted to the upper divertor. The electron cyclotron emission radiometer recorded a ~ 1 ms spike just before the 1st phase radiation burst, and a broader lower intensity emission during the 2nd phase.

*Work supported by the US DOE under DE-FG02-07ER54917, DE-FC02-04ER54698, DE-AC05-00OR22725, DE-AC52-07NA27344, and DE-FG03-97ER54415.

JP8 96 Fast Imaging of Runaway Electron Beams in DIII-D* J.H. YU, A.N. JAMES, E.M. HOLLMANN, J.A. BOEDO, *UCSD* N. COMMAUX, T.C. JERNIGAN, *ORNL* T.E. EVANS, D.A. HUMPHREYS, E.J. STRAIT, M.A. VAN ZEELAND, J.C. WESLEY, *GA* We present fast visible images of runaway electron (RE) beam formation and evolution following plasma shutdown induced by Ar pellet injection. The RE beam forms when a sufficiently strong toroidal electric field is generated in the cold plasma after the thermal collapse, and visible RE emission is first detected 3 to 10 ms after the pellet injection. The RE beam persists for up to 50 ms and moves upwards toward the top of the vessel with drift velocities ranging from < 5 to 120 m/s. When fast electrons make contact with the vessel, gammas produce scintillations in BGO crystal detectors located around the machine and on the fast camera CMOS chip. The emission from well-developed RE beams is localized to the region of tangency between the camera line of sight and flux surfaces, indicating forward-beamed emission from either bremsstrahlung or synchrotron radiation. The beam location and spatial profile of emission is in good agreement with equilibrium reconstruction of flux surfaces.

*Supported by the US Department of Energy under DE-FG02-07ER54917 and DE-FC02-04ER54698.

JP8 97 Modeling Steady-State DIII-D Plasmas for Tearing Stability Studies* F. TURCO, *ORAU* T.C. LUCE, *General Atomics* D.P. BRENNAN, *U. Tulsa* A.D. TURNBULL, J.R. FERRON, C.C. PETTY, P.A. POLITZER, *General Atomics* L.L. LODESTRO, L.D. PEARLSTEIN, R.J. JAYAKUMAR, T.A. CASPER, C.T. HOLCOMB, *LLNL* M. MURAKAMI, *ORNL* In DIII-D, steady-state high-β discharges are limited by a $n = 1$ tearing mode, causing a radial redistribution of the current density not recoverable with the available noninductive current drive sources. The use of electron cyclotron (EC) current with a broad deposition can prevent the mode onset. The current density profile from an experimental DIII-D equilibrium has been perturbed numerically, mimicking the injection of EC current. The tearing stability index Δ' is evaluated by the PEST3 code as a function of the perturbation amplitude, shape and radial position. The results are compared to the evolution of the experimental current density found previously to characterize discharges unstable to the $n = 1$ tearing instability, and to a previous analytical study performed in cylindrical geometry for similar conditions.

*Work supported in part by the US DOE under DE-AC05-06OR23100, DE-FC02-04ER54698, DE-AC05-00OR22725, and DE-AC52-07NA27344.

JP8 98 Optimization of the Internal Magnetic Configuration for High Bootstrap Current Fraction and High Beta for Steady-state* J.E. FERRON, T.C. LUCE, P.A. POLITZER, J.C. DEBOO, T.W. PETRIE, C.C. PETTY, R.J. LA HAYE, *GA* C.T. HOLCOMB, *LLNL* A.E. WHITE, F. TURCO, *ORISE* E.J. DOYLE, T.L. RHODES, L. ZENG, *UCLA* A systematic scan of the safety factor (q) profile has been used to study the optimum for steady-state operation, which requires the maximum possible beta and bootstrap current fraction (f_{BS}) and good alignment between the total current density and the bootstrap current density (J_{BS}). The n_e, T_e, and T_i profiles at constant $\beta_N = 2.7$ were measured in a scan of the minimum q ($1.1 < q_{min} < 2$) and q at the edge ($4.5 < q_{95} < 6.5$). ∇n_e is largest at the highest q_{min} and the pedestal n and T are highest at $q_{95} = 4.5$. Thus, with the q scaling of J_{BS}, the calculated f_{BS} is maximum at $q_{min} = 2$, but with J_{BS} that locally exceeds the total current density. The maximum achieved β_N was 3.1 at $q_{min} > 2$, and 3.8 at $q_{min} = 1.1$. These opposite trends in β_N and f_{BS}, and the improved current profile alignment for $q_{min} < 2$, point to intermediate q_{min} and q_{95} as optimal for steady-state operation.

*Work supported by the US DOE under DE-FC02-04ER54698, DE-AC52-07NA27344, DE-AC05-06OR23100, and DE-FG03-08ER54984.

JP8 99 Predictions of ITER Steady State Scenario Using Scaled Experimental Edge Profiles in DIII-D* M. MURAKAMI, J.M. PARK, *ORNL* J.E. KINSEY, L.L. LAO, T.C. LUCE, T.H. OSBORNE, G.M. STAEBLER, H.E. ST. JOHN, P.B. SNYDER, *General Atomics* E.J. DOYLE, R.V. BUDNY, D. McCUNE, *PPPL* The DIII-D ITER demonstration shots replicated leading features of the ITER steady state scenario, including noninductive fraction (f_{NI}) above 100%, $q_{95} \sim 5$, plasma shape, aspect ratio and I_p/aB. Integrated modeling with a theory-based (GLF23) model is used to extrapolate these results to the ITER steady state scenarios. The boundary conditions for GLF23 are set at $\rho = 0.8$ while the edge profiles at $0.8 < \rho < 1.0$ are scaled with the experimental local $\beta_N(\rho)$. The predicted values of f_{NI} and fusion gain (Q) using the ITER Day-1 heating and current drive capability are close, but still somewhat short (by ~ 10%) in achieving the $f_{NI} = 100\%$ and $Q = 5$ goal. Sensitivities of f_{NI}, Q, edge and core stability, and gyrokinetic stability to plasma current, density, and density peaking, etc. will be discussed. Possible heating and current drive upgrades will also be explored.

*Work supported by the US DOE under DE-AC05-00OR22725, DE-FC02-04ER54698, DE-FG03-08ER54984 and DE-AC02-09CH11466.

JP8 100 Scaled Experiment of ITER Operational Scenarios on DIII-D and Extrapolation to ITER* J.M. PARK, M. MURAKAMI, *ORNL* T.C. LUCE, P.A. POLITZER, L.L. LAO, P.B. SNYDER, H.E. ST. JOHN, G.M. STAEBLER, *GA* E.J. DOYLE, *UCLA* Scaled experiments of ITER operational scenarios on DIII-D are projected to ITER using theory-based (GLF23) modeling. Time-dependent transport simulations coupled to free-boundary equilibrium calculation reproduce successfully the time evolution of ITER similarity discharges, including stored energy and internal inductance, if the experimental edge pedestal profiles are imposed as boundary conditions. To extrapolate these results to ITER, iterative solution of core transport with MHD stability calculation of peeling-ballooning modes is employed assuming a moderate density peaking, which is consistent with DIII-D dis-

charges and gyrokinetic calculations. Simulation of the baseline scenario shows that ITER can achieve its goal of fusion gain Q = 10 with duration of burn ~ 400 s. ITER performance for the steady state scenario approaches the f_{NI} = 100% and Q = 5 goals but shows a trade-off between f_{NI} and Q with variation in q_{95}. Sensitivities to edge pedestal and density peaking will be discussed.

*Supported by the US DOE under DE-AC05-00OR22725, DE-FC02-04ER54698, and DE-FG03-08ER54984,

JP8 101 Development of Hybrid Scenario on DIII-D for Burning Plasma Devices* C.C. PETTY, J.C. DEBOO, T.E. EVANS, J.R. FERRON, J.E. KINSEY, R.J. LA HAYE, T.C. LUCE, T.H. OSBORNE, P.A. POLITZER, *GA* H. REIMERDES, *Columbia U.* S.L. ALLEN, M.E. FENSTERMACHER, C.T. HOLCOMB, *LLNL* M. MURAKAMI, *ORNL* E.J. DOYLE, *UCLA* R.A. MOYER, *UCSD* Experiments on DIII-D have extended the hybrid scenario towards the burning plasma regime by increasing the noninductive current fraction to nearly 100%, and in separate experiments by incorporating edge localized mode (ELM) suppression. Strong core current drive by neutral beam injection and electron cyclotron heating reduced the loop voltage to 0.01 V in hybrids with normalized beta up to 3.5 and an H_{98} factor of 1.4. This demonstrates the potential for hybrids as a high-beta, steady-state scenario that is not sensitive to alignment of the noninductive current profiles. For the first time, large type-I ELMs have been completely suppressed in hybrids at q_{95} = 3.6 by applying edge resonant magnetic perturbations using n = 3 internal coils. The ELM suppression lasted for 0.5-1.0 times the current redistribution time for normalized beta up to 2.5 and a fusion performance factor equivalent to Q = 10 operation in ITER.

*Work supported by the US DOE under DE-FC02-04ER54698.

JP8 102 Modeling Tokamak Discharges during Startup in DIII-D and Predictions for ITER* R.V. BUDNY, R. ANDRE, C.E. KESSEL, D. McCUNE, *PPPL* G.L. JACKSON, D.A. HUMPHREYS, T.C. LUCE, P.A. POLITZER, *General Atomics* The PTRANSP code is being developed for improving predictions of ITER and future Tokamaks [1]. Important goals are predicting plasma performance as well as safe and efficient startup and termination. PTRANSP is being tested on experiments in DIII-D to explore and optimize plasma startup and termination, and to benchmark of transport. An important aspect is to model the boundary accurately since parameters such as the flux consumption and induction *li* can vary sensitively on the boundary shape. PTRANSP is being modified to allow for direct input of the flux in R, Z space (from EFIT) instead of using Fourier moments of the boundary. PTRANSP will write quantities such as the inductance and surface voltage at the separatrix surface as well as the flux boundary usually used in TRANSP. The predictive capabilities are being improved also. These include models for predicting temperatures, densities, and toroidal momentum. Predictions for ITER will be discussed. [1] R.V. Budny, Nuclear Fusion **49** (2009) 085008.

*Supported in part by DoE contract DE-AC02-09CH1146

JP8 103 Operation of the Complete DIII-D Gyrotron System* J. LOHR, M. CENGHER, J.L. DOANE, Y.A. GORELOV, H.J. GRUNLOH, C.P. MOELLER, D. PONCE, R. PRATER, *GA* The 110 GHz six gyrotron system on the DIII-D tokamak has been completed and is now in routine operation in support of experiments. The gyrotrons can be modulated using preprogrammed waveforms at frequencies greater than 5 kHz or under control of the DIII-D Plasma Control System using feedback on various signals, such as Te from fast ECE and fluctuations from magnetic probes. Full control of the elliptical polarization of the injected rf is provided and the individual rf beams can be steered over 40° both poloidally and toroidally. Reliability of 90% has been achieved. The system has been used for rf pulses up to 5 s in length, injecting over 3 MW into the plasma limited by transmission line efficiency with maximum injected energy over 12 MJ for a single tokamak pulse. The system has been used in instability suppression and to rock the T_e gradient periodically for transport studies. The ECH power has initiated the discharge for breakdown studies and for solenoidless startup and created and maintained H-modes without particle injection. An upgrade to 8 gyrotrons is planned.

*Work supported by the US DOE under DE-FC02-04ER54698.

JP8 104 Operational Experience with the Six Gyrotron System on DIII-D* Y.A. GORELOV, J. LOHR, M. CENGHER, D. PONCE, *General Atomics* For the 2009 experimental campaign, the DIII-D gyrotron system comprised six 110 GHz gyrotrons in the 1 MW class. This marks the completion of a significant upgrade to the ECH system that included the replacement of three short pulse gyrotrons with three long pulse gyrotrons and the acquisition of an additional 3 long pulse tubes, plus the construction of the high voltage power supplies and control infrastructure. As conditioning of the last gyrotron continues during experiments, the rf power from the six tubes has been set at 4.3 MW giving, at 75% transmission efficiency, an injected power of 3.2 MW for the 4 s pulses typically being used. Improved diagnostic capability, such as video monitoring and Langmuir probes at the launchers, external current monitors for the gyrotron magnets and fast fault handling using Field Programmable Gate Array logic, has provided enhanced protection for the system. Calorimetric loading measurements and the thermal performance of the entire system will be presented.

*Work supported by the US DOE under DE-FC02-04ER54698.

JP8 105 Summary of RF power measurements on the ECH System on DIII-D* M. CENGHER, J. LOHR, J.L. DOANE, Y.A. GORELOV, C.P. MOELLER, J.C. DEBOO, A.W. LEONARD, D. PONCE, *General Atomics* For the six 110 GHz, 1 MW class gyrotrons of the ECH system on DIII-D at GA, the power injected at the tokamak by the electron cyclotron heating (ECH) system is measured for every pulse using calorimetry. The relationship between generated rf power and component cooling was determined originally by the manufacturer with 1% total power accountability. Transmission line efficiencies have been measured directly at DIII-D for high power. The injected power calculations resulting from combining the generated power measurements corrected for transmission loss have been verified using synchronous detection of ECE signals of plasma heating using modulated rf injection. Direct measurements of the injected power at the tokamak for pulses up to 5 s in length are being developed. The result from the following techniques will be described: measurements of the response of the DIII-D diagnostic bolometers to rf injection, heating of a leaky waveguide gap monitor, detailed rf power accounting in dummy loads and waveguides, and rf pickoff in a 4 port miter.

*Work supported by the US DOE under DE-FC02-04ER54698.

JP8 106 Local Gas Puff Effects on Fast Wave Antenna Loading in H-mode* A. NAGY, S. DEPASQUALE, E. FREDD, N.L. GREENOUGH, J.C. HOSEA, R. NAZIKIAN, J.R. WILSON, *Princeton Plasma Physics Laboratory* F.W. BAITY, N. COMMAUX, R.H. GOULDING, G. HANSON, A.R. HORTON, M. MURAKAMI, D.A. RASMUSSEN, P.M. RYAN, *Oak Ridge National Laboratory* F. CHAMBERLAIN, C.C. PETTY, R.I. PINSKER, *General Atomics* M. PORKOLAB, *Massachusetts Institute of Technology* Experiments show substantially enhanced resistive fast wave (FW) antenna loading in H-mode plasmas is obtained with a local gas puff during the application of rf. Results with short magnetic field lines connecting the puff orifice and the antenna face are compared with cases with longer field line connections. Scans of gas puff and FW pulse start timing suggest that filling the antenna box with gas prior to the application of rf may lead to antenna breakdown. Effects of the gas puffing on tokamak plasma include increased density, some reduction in confinement time, and strong effects on the edge localized mode character and frequency. The relationships between these results and those obtained in similar experiments elsewhere are discussed.

*Work supported by the US DOE DE-AC02-09CH11466, DE-AC05-00OR22725, and DE-FC02-04ER54698.

JP8 107 Design Concepts for a Long Pulse Upgrade for the DIII-D Fast Wave Antenna Array* P.M. RYAN, F.W. BAITY, J.B.O. CAUGHMAN, R.H. GOULDING, D.A. RASMUSSEN, *ORNL* R.I. PINSKER, *General Atomics* J.C. HOSEA, N.L. GREENAUGH, A. NAGY, J.R. WILSON, *PPPL* A goal in the 5-year plan for the fast wave program on DIII-D [1] is to couple a total of 3.6 MW of RF power into a long pulse, H-mode plasma for central electron heating. The present short-pulse 285/300 antenna array would need to be replaced with one capable of at least 1.2 MW, 10 s operation at 60 MHz into an H-mode (low resistive loading) plasma condition. The primary design under consideration uses a poloidally-segmented strap (3 sections) for reduced strap voltage near the plasma/Faraday screen region. Internal capacitance makes the antenna structure self-resonant at 60 MHz, strongly reducing peak E-fields in the vacuum coax and feed throughs. Calculations using the 3D EM code CST Microwave Studio indicate peak voltages can be reduced by a factor of 3 and peak E-fields by a factor of 5, compared to the present antenna for the same power and load. Alternative designs for the internal capacitance to cope with geometry constraints will be presented. [1] Project Staff, "Five-Year Plan: 2009–2013," General Atomics Report GA-A25889 (2008).

*ORNL is managed by UT-Batelle, LLC, for the U.S. Dept of Energy under contract DE-AC-05-00OR22725.

JP8 108 Fast Ion Transport during Sawteeth in the DIII-D Tokamak* C.M. MUSCATELLO, W.W. HEIDBRINK, *UC-Irvine* YA.I. KOLESNICHENKO, V.V. LUTSENKO, YU.V. YAKOVENKO, *Institute for Nuclear Research* E.A. LAZARUS, *ORNL* M.A. VAN ZEELAND, *General Atomics* J.H. YU, *UCSD* The transport of energetic ions in the presence of sawteeth is an important issue in tokamaks operating with the central safety factor $q < 1$. By altering the plasma cross section between bean and oval shapes, the nature of the sawtooth crash shifts from one dominated by the internal kink to one dominated by quasi-interchange. The q profile is measured by a motional Stark effect diagnostic. The FIDA diagnostic measures the spatial profile of fast ions before and after the crash. Two-dimensional imaging of the FIDA light diagnoses the transport of counter-circulating fast ions. The FIDA data show that fast ions up to the injection energy are redistributed in the bean while, in the oval, only lower energy ions experience appreciable transport. The observations are in qualitative agreement with the theoretical expectation that significant transport occurs when characteristic orbit times are longer than the sawtooth reconnection timescale.

*Work supported in part by the US DOE under SC-G903402, DE-AC05-00OR22725, DE-FC02-04ER54698, and DE-FG02-07ER54917.

JP8 109 Global Geodesic Acoustic Modes Driven by Energetic Particles in the DIII-D Tokamak* R. NAZIKIAN, G.Y. FU, N.N. GORELENKOV, G.J. KRAMER, *Princeton Plasma Physics Laboratory* M.E. AUSTIN, H.L. BERK, *University of Texas-Austin* W.W. HEIDBRINK, *University of California-Irvine* G.R. MCKEE, M.W. SHAFER, *University of Wisconsin-Madison* E.J. STRAIT, M.A. VAN ZEELAND, *General Atomics* Intense axisymmetric oscillations driven by suprathermal passing ions injected in the direction counter to the toroidal plasma current are observed in the DIII-D tokamak. Strong bursting and frequency chirping coincide with large ($10 - 15\%$) drops in the neutron emission, suggesting that the mode is very effective in displacing beam ions from the plasma core. BES measurements of density fluctuations indicate an outward propagating mode of large radial extent. The large density to temperature ratio of the mode confirms a dominant compressional contribution to the pressure perturbation, indicative of the Geodesic Acoustic Mode (GAM).

*Work supported by the US DOE under DE-AC02-09CH11466, DE-FG03-97ER54415, SC-G903402, DE-FG02-89ER53296, DE-FG02-08ER54999, and DE-FC02-04ER54698.

JP8 110 Full-orbit Studies of Alfven Eigenmode Induced Fast-ion Losses in DIII-D* G.J. KRAMER, R. NAZIKIAN, N.N. GORELENKOV, R.B. WHITE, *Princeton Plasma Physics Laboratory* M.A. VAN ZEELAND, *General Atomics* W.W. HEIDBRINK, *UC-Irvine* In recent experiments at DIII-D, cases of a significant discrepancy between measured and predicted fast-ion pressure profiles have been documented. In the region of enhanced fast-ion diffusion strong Alfvènic activity was observed. In this paper we present results of full-orbit simulations of fast-ion transport and investigate to what extend the finite Lamor radius influences fast-ion transport. The simulations are done with the SPIRAL code and include the full magnetic and electrical field fluctuation contributions from the AEs.

*Supported by the US DOE under DE-AC02-09CH11466, DE-FC02-04ER54698, and SC-G903402.

JP8 111 Active and Passive Spectroscopic Imaging in the DIII-D Tokamak* M.A. VAN ZEELAND, *GA* J.H. YU, *UCSD* N.H. BROOKS, K.H. BURRELL, R.J. GROEBNER, A.W. HYATT, T.C. LUCE, M.R. WADE, *GA* N. PABLANT, *UCSD* W.W. HEIDBRINK, *UCI* W.M. SOLOMON, *PPPL* Wide angle, 2D visible imaging of Doppler-shifted, D_α emission from high energy injected neutrals, charge exchange recombination (CER) emission from beam interaction with Carbon VI ions; and visible Bremsstrahlung (VB) from the core of DIII-D plasmas has been carried out using multiple narrowband interference filters combined with a tangentially viewing, fast-framing camera. Measurements of the D_α emission from fast neutrals reveal the vertical

beam profile and the variation with density in its radial penetration. Modeling of the D_α emission using lookup tables in the ADAS database yields qualitative agreement. Active measurements of carbon CER brightness are in agreement with those made independently using DIII-D's multichordal, CER spectrometer system, confirming the potential of this technique for obtaining 2D profiles of impurity density. Passive imaging of VB is also carried out and the obtained images are inverted to obtain local emissivity profiles.

*Work supported by the US DOE under DE-FC02-04ER54698, DE-FG02-07ER54917, SC-G903402 and DE-AC02-09CH11466.

JP8 112 A Fast MSE Measurement of MHD Magnetic Fluctuations on DIII-D* J.D. KING, M.A. MAKOWSKI, S.L. ALLEN, C.T. HOLCOMB, R. GEER, *LLNL* R. ELLIS, *LLNS* E.C. MORSE, *UC-Berkeley* Resolved local magnetic fluctuation measurements, along with other fluctuation diagnostics, could provide a means of accurately measuring magnetic island size and evolution. The ability to make such measurements has significant implications for the detailed analysis of the structure of NTMs and other MHD. A new 16 bit, 500 kS/s data acquisition system has been installed on all channels of the existing MSE diagnostic on DIII-D. In addition to the fundamental $2f_1$ and $2f_2$ signals used for existing MSE polarimetry measurements, the spectrum contains peaks that strongly correlate to MHD fluctuations. Of particular interest are sideband spectral peaks at $2\omega_{1,2} \pm \omega_{MHD}$, which provide information needed for recovering the amplitude of local magnetic field fluctuations. In this work, a brief quantitative validation of the underlying theory of magnetic fluctuation measurements is presented, relationships between spectral harmonics are shown, and a first attempt at a temporally and spatially resolved MHD measurement is discussed.

*Work preformed under the auspices of the US DOE by LLNL under DE-AC52-07NA2734.

JP8 113 Initial Operation of an Improved Thomson Scattering System at DIII-D* B.D. BRAY, T.M. DETERLY, D.M. PONCE, C. LIU, *General Atomics* A redesigned Thomson scattering data acquisition system has been installed for the eight chord, forty channel divertor Thomson system at DIII-D. The new electronics contain significantly faster and quieter analog components which improve the signal to noise ratio of the system by a factor of three. An internal integration and sample and hold circuit has been added to the new detector modules which replaces aging the digitizers and couples to a standard digitizer used throughout DIII-D. This new design improves the maintainability of the system and replaces unreliable, obsolete components. A description of the system and profiles from the initial year of operation will be presented with status of the upgrade of the complete Thomson system.

*Work supported by the US DOE under DE-FC02-04ER54698.

JP8 114 Measurements of the Internal Magnetic Field and n=3 Level Populations of Injected Deuterium Using the B-Stark Motional Stark Effect Diagnostic on DIII-D* N.A. PABLANT, K.H. BURRELL, R.J. GROEBNER, D.H. KAPLAN, *General Atomics* C.T. HOLCOMB, *LLNL* B. DEN HARTOG, *U. Wisconsin-Madison* H.P. SUMMERS, *U. Strathclyde* We describe the latest results from the newly upgraded B-Stark diagnostic system installed on the DIII-D tokamak. This system is a version of a motional Stark effect (MSE) diagnostic based on the relative line intensities and spacing of the Stark-split D_α emission from injected neutral beams. We present a thorough study of the performance of the diagnostic in measuring the magnitude and direction of the internal magnetic field over a range of plasma conditions. Measurements were made with toroidal fields in the range 1.2 − 2.1 T and plasma currents in the range 0.5 − 2.0 MA. We also present results from a study of the level populations of the $n = 3$ state of the injected deuterium neutrals over a range of plasma densities, $1.7 - 9.0 \times 10^{13}\mathrm{m}^{-3}$, and neutral beam voltages, 50 − 81 keV. These results are compared against the calculations from an atomic physics code, part of the ADAS package.

*Work supported in part by the US DOE under DE-FG02-07ER54917, DE-FC02-04ER54698, DE-AC52-07NA27344, DE-FG02-89ER53296 and DE-FG02-08ER54999.

JP8 115 Charge Exchange Recombination Detection of Low-Z Impurities in the Extreme UV using Digital Lock-In Techniques* N.H. BROOKS, *General Atomics* O. MEYER, *CEA-Cadarache* A digital technique has been used to extract that portion of the XUV spectrum which varies synchronously in time with the modulation of the 30-Left neutral beam (NB) viewed by DIII-D's SPRED spectrometer [1]. A scalar product of two temporal vectors is performed for each pixel in the SPRED linear array detector–the first vector is the time history of light intensity at that pixel, the second is a NB-derived correlation function. In the spectra resulting from this pixel-by-pixel manipulation of the temporal data, all light from medium-Z and high-Z metals are strongly suppressed, exposing with great clarity the Rydberg-series lines from the H-like charge states of the low-Z impurities He, B, C and O. Time-averaged relative abundances of the low-Z impurities may be readily deduced. Removal of the beam-correlated component of the detected XUV light will be used as a pre-processing step to improve reliability of emission line time histories calculated from SPRED data. [1] R.J. Fonck et al., Applied Optics **21**, 2115 (1982).

*Work supported in part by the US DOE under DE-FC02-04ER54698.

JP8 116 Advanced Ion Temperature and Velocity Fluctuation Diagnostic Design and Preliminary Measurements* I.U. UZUNKAYMAK, R.J. FONCK, G.R. McKEE, D.J. SCHLOSSBERG, M.W. SHAFER, G. WINZ, Z. YAN, *U. Wisconsin-Madison* A high-efficiency, high-throughput custom spectroscopic system is being designed and implemented at DIII-D to measure localized, long-wavelength ion thermal fluctuations associated with drift wave turbulence. A high-transmission grism (prism-coupled transmission grating) and high-throughput collection optics are employed to observe Doppler-shifted emission from the $n = 8$-7 transition of C VI centered near $\lambda = 529$ nm. The diagnostic achieves 0.25 nm resolution for 2.0 nm spectral band using eight discrete spectral channels. A turbulence-relevant time resolution of 1 μs will be achieved using high-speed photodiodes and low-noise preamplifiers. The system sensitivity should allow for measurements of normalized ion temperature fluctuations on the order of $\tilde{T}_I/T_I \leq 1\%$. These measurements will be combined with

2D BES measurements to determine the local multi-field turbulence dynamics. The predicted signal-to-noise for turbulence measurements, signal analysis techniques, and preliminary data will be presented.

*Work supported by the US DOE under DE-FG02-89ER53296, DE-FG02-09ER54999, and DE-FC02-04ER54698.

JP8 117 Q-band AM Reflectometer on the DIII-D 285°-300° Fast Wave Antenna* G.R. HANSON, N. COMMAUX, F.W. BAITY, A.R. HORTON, J.B. WILGEN, *Oak Ridge National Laboratory* A. NAGY, *Princeton Plasma Physics Laboratory* R.I. PINSKER, *General Atomics* A Q-band AM reflectometer has been re-installed onto the 285°-300° fast wave antenna on DIII-D to measure the local density profile in the scrape-off layer (SOL) at the ICRF antenna. This reflectometer sweeps from 32-54 GHz in 100 microseconds and uses 100 MHz amplitude modulation to allow differential-phase measurements. Initial results during RF operation will be presented, including results during gas puffing at the fast wave antenna to increase antenna loading.

*Work supported by the US DOE DE-AC05-00OR22725, DE-AC02-09CH11466, and DE-FC02-04ER54698.

JP8 118 LASER AND PLASMA BASED ACCELERATORS

JP8 119 Laser Wakefield Electron Acceleration and Frequency-Domain Holography Using the 1.1 PW Texas Petawatt Laser System STEPHEN REED, WATSON HENDERSON, XIAOMING WANG, PENG DONG, SERGUEI KALMYKOV, ERHARD GAUL, MIKAEL MARTINEZ, GENNADY SHVETS, TODD DITMIRE, MICHAEL DOWNER, DEPARTMENT OF PHYSICS, UNIVERSITY OF TEXAS AT AUSTIN, AUSTIN, TX 78712-1081 TEAM, Preparation for multi-GeV electron acceleration in an underdense plasma driven by the 1.1 PW, 160 fs Texas petawatt laser system will be presented. Laser wakefield acceleration (LWFA) experiments have demonstrated 1 GeV electron beams with muilt- TW class lasers and scaling laws suggest, that 3 - 10 GeV electrons can be produced with a short pulse PW system without external guiding. The Texas Petawatt laser uses an F/# 40 focusing geometry creating a long interaction and transverse region while still maintaining intensities above 10[1]9 W/cm2. Such geometry creates an opportunity to "image" the large wakefield structures using the single shot visualization technique of frequency-domain holography (FDH) in the longitudinal direction. The presented material will include details of the Texas petawatt laser systems, experimental setup and designs for electron generation and detection, FDH measurements and PIC simulations of laser wakefield acceleration for the given laser parameters, as well as preliminary results from anticipated test runs during the fall of 2009.

JP8 120 Frequency domain holography of laser wakefield accelerators in the nonlinear bubble regime S.A. YI, S. KALMYKOV, P. DONG, S.A. REED, M. DOWNER, G. SHVETS, *Department of Physics, University of Texas at Austin* We present the theoretical basis of frequency domain holography (FDH), a technique for single-shot visualization of laser driven plasma wakes. In FDH, the nonlinear index modulations of the plasma wake are recorded as phase shifts in a co-propagating probe pulse, and interference with a reference allows for the reconstruction of the wake structure. Earlier experimental work [N. H. Matlis *et al.*, Nature Phys. **2**, 749 (2006)] has shown that reconstruction of the probe phase is sufficient for imaging weakly nonlinear periodic wakes. In the highly nonlinear regime, the laser ponderomotive force blows out plasma electrons and forms a density "bubble" that strongly focuses the probe light. We show that imaging the bubble requires full (amplitude and phase) reconstruction of the probe pulse, and find reconstructions of simulated frequency domain holograms in full agreement with direct PIC modeling of the probe pulse. We also assess the sensitivity of the technique to the spectral bandwidth of the probe and reference pulses. In combination with ray-tracing techniques which help evaluate the localized frequency up- and down-shifts of the probe light ("photon acceleration"), FDH appears to be a unique tool for visualization of plasma wakes. This work is supported by the US DOE grants DE-FG02-04ER41321 and DE-FG02-07ER54945.

JP8 121 Electron self-injection and trapping into an evolving plasma bubble* S. KALMYKOV, S.A. YI, V.N. KHUDIK, G. SHVETS, *Institute for Fusion Studies, The University of Texas at Austin* In the blowout regime of laser wakefield acceleration (LWFA), radiation pressure creates a co-moving bubble of electron density behind the driving laser pulse. Self-injection of initially quiescent electrons into the bubble and their subsequent acceleration are studied both analytically and by particle-in-cell (PIC) simulations. Semi-analytic model treats the bubble as a spherical cavity of electron density moving with a relativistic velocity over an immobile ion background. The non-evolving bubble must be unrealistically large to self- inject quiescent electrons, whereas its slow expansion significantly relaxes this requirement. PIC modeling shows that a defocusing laser may cause self-injection into the expanding bubble, even when a non-evolving pulse would not. This effect is explained in terms of non-stationary Hamiltonian theory. Temporal expansion of the bubble appears to be the dominant mechanism of electron self-injection in rarefied plasmas ($n_0 \sim 10^{17}$ cm^{-3}) relevant to the LWFA with petawatt-class lasers. Combination of bubble expansion and contraction results in monoenergetic electron beams due to the termination of self-injection process and phase space rotation.

*Supported by the U.S. Department of Energy under Contracts No. DE-FG02-04ER41321 and DE-FG02-07ER54945.

JP8 122 Stimulated Raman Scattering (SRS) Driven by 30 fs Laser Pulse in Underdense Plasmas* T. MATSUOKA, Y. HOROVITZ, C. McGUFFEY, P.G. CUMMINGS, V. CHVYKOV, G. KALINTCHENKO, P. ROUSSEAU, F. DOLLAR, S.S. BULANOV, V. YANOVSKY, A.G.R. THOMAS, A. MAKSIMCHUK, K. KRUSHELNICK, *CUOS U. of M.* Propagation of an ultra-short laser pulse in underdense plasma was studied in the parameter range relevant for laser wakefield accelerators (LWFA) at 100 TW laser power. Filamentation of the transmitted laser pulse observed with the transverse interferpmetry was well correlated with stimulated side Raman scattering (SSRS). Experimentally measured scattered light angle relative to the laser axis is well reproduced by an analytic formula for SSRS in the range of the experimental plasma densities. Spectra orthogonal to the laser pulse showed spatially modulated intensity profile and laser intensity dependent shift for Stokes light. 2D-PIC simulation showed the evolution of the laser pulse due to SSRS.

*This work was supported by the NSF grant PHY-0114336.

JP8 123 Acceleration of Cone-Produced Electrons by Double-Line Ti-Sapphire Laser Beating* YOSHITAKA MORI, *Graduate School for the Creation of New Photonics Industries* HAJIME KUWABARA, *IHI Corporation* KIMINORI KONDO, *Kansai Photon Science Institute, JAEA* YONEYOSHI KITAGAWA, *the Graduate School for the Creation of New Photonics Industries* We proposed a new scheme for simultaneously injecting and accelerating electrons. Acceleration and stochastic heating of electrons are demonstrated in a beat wave scheme using a pre-pulse free short-pulse (150 fs) double-line Ti-Sapphire laser. The laser beat wave produces a resonant relativistic plasma wave of field intensity 11 GV/m in a hydrogen plasma of density 2.5 $\times$ $10^{18} cm^{-3}$. To inject electrons, we used a hybrid target composed of a cone-drilled plane and a gas jet, where the cone-produced electrons are accelerated via the resonant plasma wave excited in the gas jet set behind the plane, increasing the slope temperature from 0.05 MeV to 0.15 MeV. A one-dimensional particle-in-cell simulation and a stochastic acceleration model confirm the slope temperature increase.

*This work is supported by the Advanced Compact Accelerator Development of the MEXT, the Grant-in Aid for Scientific Research (B) 16340182-00, and the collabration program of ILE, Osaka University.

JP8 124 Longitudinal Profile of an Electron Beam Generated from a Laser Wakefield Accelerator* DMITRI KAGANOVICH, *Icarus Research Inc.* MICHAEL HELLE, *Georgetown University* DANIEL GORDON, *U.S. Naval Research Laboratory* EDWARD VAN KEUREN, *Georgetown University* ANTONIO TING, *U.S. Naval Research Laboratory* Electron beams produced from a laser wakefield accelerator are predicted to have bunch lengths approximately equal to one quarter of a plasma wavelength. For plasma densities on the order of 10^{19} cm^{-3} this corresponds to lengths of $\sim$ 3μm. Current techniques have proven unable to resolve such a short pulse at relativistic speeds. Work is underway to develop and test a noninvasive single-shot technique to measure the bunch length of high-energy ultrashort electron beams. The technique relies on the mixing of the relativistic beam's transverse electric field with a probe laser within a nonlinear material. The theory of operation and the devices integration into the beam line will be discussed.

*This work is supported by the Department of Energy and Office of Naval Research

JP8 125 Laser Wakefield Accelerator Injection Control and X-Ray Sources C.G.R. GEDDES, E. CORMIER-MICHEL, E.H. ESAREY, T. LE CORRE, C. LIN, N.H. MATLIS, K. NAKAMURA, G.R. PLATEAU, C.B. SCHROEDER, R.A. VAN MOURIK, W.P. LEEMANS, *LBNL* D.B. THORN, *GSI* D.L. BRUHWILER, B. COWAN, K. PAUL, J.R. CARY, *Tech-X* Reduced beam energy spread, fluctuation, and emittance are important to applications of compact, high gradient laser-plasma wakefield accelerators including Thomson gamma sources and high energy colliders. Experiments and simulations will be presented on control of injection to improve beam quality compared to use of self-injection by the wake. Trapping of electrons in the wake can be controlled using the beat between multiple laser pulses to via kick electrons in momentum and phase into the wake accelerating phase. Laser and gas target shaping and control are used to further control the accelerator structure. Simulations demonstrate the tuning of accelerator structure required to accelerate such bunches to high energies while retaining high bunch quality. Electron beam source size and position are measured using betatron X-ray emission produced when electrons oscillate in the focusing field of the wake to improve understanding of beam emittance and stability, while also producing a broadband, synchronized fs source of keV X-rays. Supported by US DOE NA-22 and HEP including DE-AC02-05CH11231, SciDAC, and SBIR.

JP8 126 PIC Simulations of Colliding Pulse Injection for Laser Wakefield Acceleration* DAVID BRUHWILER, BEN COWAN, KEVIN PAUL, JOHN CARY, *Tech-X Corporation* CAMERON GEDDES, ESTELLE CORMIER-MICHELLE, ERIC ESAREY, CARL SCHROEDER, WIM LEEMANS, *LBNL* The use of colliding laser pulses to control the injection of plasma electrons into the plasma wake of a laser wakefield accelerator (LWFA) is a promising approach to obtaining GeV scale electron bunches with orders of magnitude smaller emittance and energy spread. Colliding pulse injection (CPI) is being explored experimentally by groups around the world. We will present recent particle-in-cell (PIC) simulations of colliding pulse injection, using the parallel VORPAL framework, for physical parameters relevant to ongoing experiments of the LOASIS Program at Lawrence Berkeley Laboratory. The details of how particle trapping starts and stops, in the presence of counter-propagating laser pulses and nonlinear beam loading, is sensitive to noise and other errors in the PIC simulation. Hence, we will present results of different algorithmic choices, including high-order particle shapes and spatial smoothing.

*Work supported by U.S. Department of Energy High Energy Physics, including DE-AC02-05CH11231and SciDAC, and by NA-22, and used computational facilities at NERSC.

JP8 127 Plasma wave phase velocity and density tapering in laser-plasma accelerators* CARL SCHROEDER, ERIC ESAREY, WIM LEEMANS, *Lawrence Berkeley National Laboratory* WOLF RITTERSHOFER, FLORIAN GRÜNER, *Ludwig-Maximilians University of Munich* BRADLEY SHADWICK, *University of Nebraska, Lincoln* In a laser-plasma-based accelerator, the laser-driven plasma wave phase velocity (determined in part by the intensity transport velocity and evolution of the short-pulse drive laser) sets the dephasing length of the plasma accelerating structure and, hence, the energy gain of an accelerated particle beam. The phase velocity of a plasma wave driven by a relativistically-intense, short-pulse laser propagating in a cold underdense plasma is investigated, as well as the drive laser evolution. A relativistic beam may be phase-locked to the plasma wave using a plasma density taper, increasing the single-stage energy gain. The expression for the density taper in a plasma channel to maintain a relativistic beam at a constant plasma wave phase is presented. The optimal laser pulse duration for maximizing energy gain in a tapered plasma channel is calculated. Novel quasi-periodic plasma tapering schemes are considered.

*Supported by the U.S. Department of Energy under Contract No. DE-AC02-05CH11231.

JP8 128 Nonlinear Laser Energy Depletion in Laser-Plasma Accelerators* B.A. SHADWICK, *Department of Physics and Astronomy, University of Nebraska – Lincoln* C.B. SCHROEDER, E. ESAREY, *Lawrence Berkeley National Lab* Energy depletion of intense, short-pulse lasers via excitation of plasma waves is investigated numerically and analytically.[1] The evolution of a resonant

laser pulse proceeds in two phases. In the first phase, the pulse steepens, compresses, and frequency red-shifts as energy is deposited in the plasma. The second phase of evolution occurs after the pulse reaches a minimum length at which point the pulse rapidly lengthens, losing resonance with the plasma. Expressions for the rate of laser energy loss and rate of laser red-shifting are derived and are found to be in excellent agreement with the direct numerical solution of the laser field evolution coupled to the plasma response. Both processes are shown to have the same characteristic length-scale. Channel- guided Gaussian laser pulses, in two and three dimensions are modeled and are well-described by this theory.

*Supported by the US DoE

[1]B. A. Shadwick, C. B. Schroeder, and E. Esarey, "Nonlinear laser energy depletion in laser-plasma accelerators," Phys. Plasmas **16**, 056704 (2009).

JP8 129 Physics of a 10 GeV laser-plasma accelerator* E. ESAREY, C.B. SCHROEDER, C.G.R. GEDDES, E. CORMIER-MICHEL, W.P. LEEMANS, *Lawrence Berkeley National Laboratory* D. BRUHWILER, B. COWAN, *Tech-X Corp.* B.A. SHADWICK, *U. Nebraska, Lincoln* The single-stage energy gain in a laser-plasma accelerator is limited by laser diffraction, electron dephasing, and laser depletion. Diffraction can be prevented by using a plasma channel and electron dephasing can be mitigated by increasing the on-axis density as a function of distance, which increases the wake phase velocity. Depletion (loss of laser energy to the wake) ultimately limits the single stage energy gain. Beam loading (modification of the wake by the accelerated electron bunch) limits the bunch charge and affects the energy spread and emittance. Advantages of various wake regimes,such as the quasi-linear or the blow-out regime, will be examined. Simulations of a 10 GeV stage driven by the 40 J BELLA laser will be presented. Also discussed are applications to future light sources and colliders.

*Supported by U.S. Department of Energy HEP Contract No. DE-AC02-05CH11231, NA-22, SciDAC and SBIR.

JP8 130 Full scale quasi-static modeling of the PWFA-based linear collider concept* CHENGKUN HUANG, W.-M. AN, C. CLAYTON, C. JOSHI, W. LU, K. MARSH, W. MORI, *UCLA* T. KATSOULEAS, *Duke University* I. BLUMENFELD, M. HOGAN, N. KIRBY, T. RAUBENHEIMER, A. SERYI, *SLAC* P. MUGGLI, *USC* Plasma Wakefield Acceleration (PWFA) has been proposed as a possible way to reduce the size and cost of the next linear collider. The needs to faithfully simulate the drive beam evolution and the main beam dynamics in the future plasma-based linear collider using Particle-In-Cell codes are extremely challenging. However, the recent progress on the development of quasi-static model and the usage of massive parallel computing resources have enabled simulation studies of the near term PWFA experiments and for the conceptual designs of the next generation facilities in full details with realistic linear collider parameters and including necessary effects such as ion motion. The simulation needs for modelling the plasma-based advanced accelerator at the energy frontier is discussed and a path towards this goal is outlined. Results from full scale simulations that include all particles in real plasma will be reported.

*Work supported by DOE.

JP8 131 Simulation of positron acceleration in Plasma Wake Field Accelerator (PWFA) WEIMING AN, *University of California Los Angeles* WEI LU, CHENGKUN HUANG, WARREN MORI, The Plasma Wake Field Accelerator (PWFA) concept is very attractive because the accelerating gradient can be three orders of magnitude higher than that of a traditional RF accelerator. In this poster the acceleration of positron beams in PWFA is investigated both in the linear and weakly nonlinear regimes. The results show that a beam-loading efficiency around 50% can be achieved both in the linear and weakly nonlinear regime when the spot sizes of both the drive beam and trailing beam are $k_p\sigma_r \sim 1$. In the linear regime the total charge of the accelerated positron beam and the average accelerating gradient are both smaller than those in the weakly nonlinear regime. Issues related to energy spread are also discussed.

JP8 132 Acceleration of polarized electron beams in plasma-based accelerators JORGE VIEIRA, RICARDO FONSECA, LUÍS SILVA, *Instituto Superior Técnico* CHENGKUN HUANG, *University of California, Los Angeles* WARREN MORI, The acceleration of highly polarized particle beams is critical not only to test and validate current physical models, but it is also critical in the search for new physics in high-energy physics (HEP) experiments. Plasma-based accelerators can play an important role in next generations of accelerators, as they can reduce the size of standard acceleration structures by two-three orders of magnitude. However, for high-energy physics applications, and in addition to beam quality requirements such as the emmittance, luminosity, energy, or energy spread, the evolution of the electron beam polarization is also crucial for the use of future linear plasma based colliders in HEP experiments. In this work, the spin-precession in plasma-based acceleration scenarios is examined using the Thomas– Bargmann-Michel-Telegdi equations. Analytical expressions which show that lower depolarizations can be achieved by using narrower beams, with lower initial energies, are derived. In addition, it is found that mildly relativistic regimes lead to lower depolarizations in comparison to strongly relativistic regimes. Our findings are confirmed with 3D particle-in-cell simulations using QuickPIC.

JP8 133 Effect of frequency and phase fluctuations in multi laser beam systems on wakefield excitation* VISHWA BANDHU PATHAK, JOANA MARTINS, RICARDO FONSECA, LUIS SILVA, *GoLP/Instituto de Plasmas e Fusão Nuclear, Instituto Superior Técnico, Lisboa, Portugal* The next generation of ultra high intensity laser systems for laser driven fusion and plasma accelerator facilities will combine multiple lasers beams to achieve very high intensities. These beams may have small frequency and phase mismatches, due to the separate optics involved. We study the effect of random variation in the frequencies and/or the phases of the multiple laser drivers on wakefield generation in underdense plasmas with averages over statistical ensembles of PIC simulations. In our 2D PIC simulations, we have explored the conditions close to optimal excitation of the wake field, by using up to 10 laser pulses. Taking advantage of the absolute reproducibility of the numerical features of the simulations in Osiris, we take ensemble averages over a large number of runs to explore the effects associated with the enhanced laser bandwidth due to frequency fluctuation, and the effects of phase

mismatch. Laser wakefield generation can also be seen as a manifestation of stimulated forward Raman scattering(SFRS) in underdense plasmas. We compare the simulation results with our theoretical model for SFRS by a partially coherent laser pump.

*Work partially supported by FCT (Portugal).

JP8 134 Emittance Preservation in Future Plasma Wakefield Accelerators using Adiabatic Matching* REZA GHOLIZADEH, *University of Southern California* TOM KATSOULEAS, *Duke University* PATRIC MUGGLI, *University of Southern California* CHENGKUN HUANG, WARREN MORI, *University of California, Los Angeles* Plasma Wakefield Accelerator has been proven to be a promising technique to lower the cost of the future high energy colliders by offering orders of magnitude higher gradients than the conventional accelerators. However, it has been shown that ion motion is an important issue to account for in the extreme regime of ultra high intensity and ultra low emittance beams, characteristics of future high energy colliders. In this regime, the transverse electric field of the beam is so high that the plasma ions cannot be considered immobile at the time scale of electron plasma oscillations, thereby leading to a nonlinear focusing force. Therefore, the transverse emittance of a beam matched to the initial linear focusing will not be preserved under these circumstances. However, Vlasov's equation predicts a matched profile even in the nonlinear focusing force case. Furthermore, we extend the idea and introduce a plasma section that can match the entire beam to the mobile-ion regime of plasma by adiabatically reducing the plasma ion mass. We also find the analytic solution for the optimal matching section. Simulation results are presented.

*Work supported by the US Department of Energy.

JP8 135 Plasma and Beam Measurements for Multi-bunch PWFA Experiments* P. MUGGLI, B. ALLEN, *University of Southern California* V. YAKIMENKO, J. PARK, K. KUSCHE, M. BABZIEN, *Brookhaven National Laboratory* We study for the first time the excitation of plasma wakefields by a train of electron bunches. The wakefields amplitude strongly depends on the plasma density and the spacing between the electron bunches. In particular, resonant excitation is expected when the plasma density is such that the plasma wavelength is equal to the drive bunch train spacing. The bunch spacing and plasma density therefore need to be accurately measured. We describe the time resolved measurement of the capillary discharge plasma density using Stark broadening of the hydrogen H_α line. The plasma density is adjusted by varying the delay between the bunch train arrival time and the plasma discharge time. We also describe the method used to produce the electron bunch train, as well as the measurement of the train spacing using coherent transition radiation interferometry. The bunch train consists of a variable number of equidistant drive bunches followed by a witness bunch. The spacing between the drive bunches is $\approx 300\mu$m, and the spacing between the last drive bunch and the witness bunches is $\approx 450\mu$m These spacings can be varied through the beam parameters. Detailed experimental results will be presented.

*Work supported by the US Department of Energy

JP8 136 Numerical Study of the Current Filamentation Instability of an Accelerator Beam in a Capillary Plasma* B. ALLEN, P. MUGGLI, *University of Southern California* V. YAKIMENKO, J. PARK, K. KUSCHE, M. BABZIEN, *Brookhaven National Laboratory* C. HUANG, *University of California Los Angeles* Current Filamentation Instability, CFI, is of central importance for the propagation of relativistic electron beams in plasmas. In the laboratory it could influence the energy deposition by hot electrons in fast-igniter concept for inertial confinement fusion. It could also play an important role in the generation of magnetic fields and of radiation in the after-glow of gamma ray bursts. Using the particle-in-cell code QuickPIC, we simulate the propagation of the BNL-ATF beam in a cm-long plasma produced by a capillary discharge. The occurrence of the instability is investigated as a function of electron beam parameters (including charge and emittance) and plasma parameters (density and length) by evaluating the beam density and magnetic energy. The results show that with beam and plasma parameters achievable at the BNL-ATF the CFI should be observed after only 2 cm of plasma. We present simulation results, discuss further simulation refinements, suggest criteria and threshold parameters for observing the presence of CFI and outline the experiment we will perform at the BNL-ATF.

*Work supported by the US Department of Energy.

JP8 137 Designing Particle-in-Cell Algorithms for Advanced Computer Architectures: Application to GPUs V.K. DECYK, T.V. SINGH, P. ABREU, R.A. FONSECA, L.O. SILVA, *GoLP/Instituto de Plasmas e Fusão Nuclear, Instituto Superior Técnico, Lisboa, Portugal* New emerging multi-core technologies can achieve high performance, but only in special, restricted cases. For example, modern graphic processors units (GPUs) can achieve TFLOP performance in single precision calculations and have low power usage per FLOP. However, the potential performance of GPUs often comes with a price. They are complex and difficult to program effectively. Therefore, algorithms often need to be redesigned to make effective use of these processors. We will describe two approaches to implementing Particle-in-Cell (PIC) codes on GPUs. One is more general and applicable to other emerging multi-core technologies. We will conclude with lessons learned that can be applied to other problems. Some of these lessons will be familiar to those who have programmed vector processors in the past, others will be new. We have also implemented a real-time visualization feature so that the user can interact on the screen with the simulation, watching the virtual particles movement, enabling real time rotation, translation, and zooming of simulation output (EM field intensity, charge density, current). This was implemented as part of a fully relativistic PIC code that runs of CUDA enabled devices using the CUDA API.

JP8 138 Preliminary results on GPU Acceleration of the PIC Simulation Code OSIRIS Using CUDA XIANGLONG KONG, M.C. HUANG, C. REN, *University of Rochester* Modern graphics processing units (GPUs) equipped with NVIDIA's massively multithreaded computing architecture, with their teraflop performance potential and high memory bandwidth, offers an opportunity to greatly improve the performance of Particle-in-cell (PIC) codes. There are a variety of approaches being developed for porting PIC codes to a GPU. In this poster we describe how multi-threaded algorithms were implemented for the key parts (field solver, particle pusher, current deposition, current smoothing) of an existing PIC simulation code (OSIRIS) on a GPU using the programming

environment CUDA. Initial speedups with double-precision operations will be described. Write conflicts in the current-to-gird deposition part are identified as the performance bottleneck. We will compare several different methods of resolving the write conflicts. We acknowledge the OSIRIS Consortium. This work was supported by DoE under Grants Nos. DE-FG02-06ER54879 and DE-FC02-04ER54789.

JP8 139 Ion beam generation experiments: near-critical density plasma proton acceleration using the Omega EP laser and ion source surface investigation using the T-cubed laser LOUISE WILLINGALE, A. MAKSIMCHUK, K. KRUSHELNICK, *CUOS and NERS, University of Michigan, Ann Arbor, MI 48109, USA* P.M. NILSON, T.C. SANGSTER, C. STOECKL, *Laboratory for Laser Energetics, University of Rochester, Rochester, NY 14623, USA* W. NAZAROV, *University of St Andrews, St Andrews, Scotland, UK* G.M. PETROV, J. DAVIS, *Naval Research Laboratory, Plasma Physics Division, Washington, DC 20375, USA* C.D. MURPHY, V. OVCHINNIKOV, *Ohio State University, Columbus, OH 43210, USA* Experiments performed using the Omega EP laser facility (1000 *J* in 10ps) investigating proton acceleration from near-critical density plasma will be presented. The laser propagation is investigated experimentally and with PIC simulation as it is expected to be influential on the proton acceleration. Also presented will be experiments investigating front vs rear surface acceleration of ions using the T-cubed laser at the University of Michigan (4 J in 400 fs). Thin foil targets are coated on the front, rear or both sides with a deuterated plastic layer and the accelerated deuterons are used to diagnose the interaction. PIC simulations are used to model the interactions and the influence of the ion acceleration processes on neutron generation experiments will be discussed.

JP8 140 Ion Acceleration in High Contrast High Intensity Laser Interaction with Thin Film and Membrane Targets* FRANKLIN DOLLAR, TAKESHI MATSUOKA, CHRIS McGUFFEY, LOUISE WILLINGALE, STEPAN BULANOV, VLADAMIR CHVYKOV, GALINA KALINTCHENKO, PASCALE ROUSSEAU, VICTOR YANOVSKY, ALEC THOMAS, ANATOLY MAKSIMCHUK, KARL KRUSHELNICK, *Center for Ultrafast Optical Sciences, Univ. of Michigan* We present the experimental results on ions acceleration from thin film and membrane targets using the 300TW 30fs HERCULES Laser Facility. The utilization of an F/1 parabolic mirror allow for on target intensities of up to 1022 W/cm2. Use of dual plasma mirrors as well as crossed-polarized wave generation allows for the ASE pedestal to peak intensity contrast of over 10-13. We perfomed measurements of protons from the back side of foils as well as ions generated from 20-200 nanometers thickness silicon nitride membranes using a Thomson parabola spectrometer coupled to a microchannel plate with readout to a CCD. Detailed 2D-PIC computer modeling of these interactions will also be presented and compared to the experimental data.

*This work was supported by the NSF grant PHY-0114336.

JP8 141 Parametric Study of Laser Driven Proton Beams from a Critical Density Gas Jet* D. HABERBERGER, F. TSUNG, S. TOCHITSKY, W. MORI, C. JOSHI, *UCLA* Laser driven ion acceleration (LDIA) is studied via particle-in-cell simulations in a novel parameter space for laser-plasma interactions of a relativistic laser pulse with a gas jet target at the critical plasma density (n_c). Previous LDIA studies have been based on the interaction of a 1 μm laser pulse with either a solid foil ($n \sim 100 n_c$) or a gas jet ($n \leq 0.1 n_c$). Here we propose focusing a high power CO_2 laser pulse at a H_2 gas jet which is tunable around the critical plasma density for 10μm radiation ($10^{19} cm^{-3}$). A rectangular H_2 gas jet operated near n_c lends itself to efficient coupling of the laser light to forward directed electrons instigating the target normal sheath acceleration mechanism to produce a beam of protons. Results are presented here on a parametric study of the peak plasma density and plasma profile to find optimal conditions for total charge, divergence, and energy of the accelerated proton beam. These simulations support an ongoing LDIA experiment at the Neptune Laboratory at UCLA using a 3ps 1TW CO_2 laser pulse for the production of collimated proton beams.

*This work is supported by DOE grant DE-FG03-92ER40727.

JP8 142 Hot Electron Confinement in High Intensity Laser-Matter Interactions LEE ELBERSON, *University of Maryland* YUAN PING, SCOTT WILKS, RONNIE SHEPHERD, ANDREW MACKINNON, PRAV PATEL, *LLNL* WENDELL HILL, *University of Maryland* High-intensity ($> 10^{18}$ W/cm^2) lasers can produce relativistic electrons ($\sim$ MeV) when focused onto solid density targets. We present measurements of escaped relativistic electron lifetimes in short pulse laser-irradiated solid experiments. Electron durations measured were significantly longer than the laser pulse length, suggesting the presence of phenomena which confine high energy electrons within the target-plasma volume. Investigating the confinement time of high energy electrons exceeds the limits of any simple plasma expansion models. Utilizing the implicit hybrid particle-in-cell code LSP [D. R. Welch *et al.*, Phys. Plasmas **13**, 063105 (2006)], experimental conditions were simulated to explore the physics of hot electron confinement in laser-irradiated materials. *This work performed under the auspices of the U.S. Department of Energy by Lawrence Livermore National Laboratory under Contract DE-AC52-07NA27344.

JP8 143 Optimization of radiation acceleration regime and the target structure in laser plasma interaction GALINA DUDNIKOVA, CHUAN LUI, DENNIS PAPADOPOULOS, ROALD SAGDEEV, *University of Maryland, College Park, Maryland, USA* ARI ZIGLER, *Hebrew University, Jerusalem, Israel* Recent work [1,2] indicates that under proper conditions the interaction of ultra-short, high power lasers with thin foils can generate ion beams in the 100-200 MeV energy range with relatively low velocity dispersion. This technology can have major implications to medical ion proton cancer therapy since it can provide a relatively inexpensive table-top alternative to the current used traditional cyclotrons. This paper presents a simulation trade-off study of laser driven generation of quasi-monochromatic ion beams in the thin-foil Radiation Pressure Acceleration (RPA) regime. The radiation pressure accelerates the electron cloud, which in its turn transfers accelerates the ions due to the induced longitudinal charge separation fields. A series of two and three-dimensional PIC simulations are presented with emphasis on stabilizing the target plasma against Raleigh-Taylor and modulational instabilities. Such instabilities are known as the main obstacles in achieving monochromatic beams. [1] B. Eliasson, C. Lui, et al. New Jour. Phys., 11, 2009. [2] F. Pegoraro, S.V. Bulanov. Laser Phys., v19, N 2, 2009.

JP8 144 Experimental measure of proton energy loss in short pulse laser generated, proton heated carbon* R. SHEPHERD, H. CHEN, *LLNL* S. FELDMAN, G. DYER, *University of Texas, Austin* S. CHEN, *LLNL* J. FUCHS, M. GAUTHIER, P. AUDEBERT, *Laboratoire d'Utilisation de Lasers Intenses (LULI)* T. DITMIRE, *University of Texas, Austin* P. BEIERSDORFER, *LLNL* M. PURVIS, *Colorado State University* A. HAZI, R. LONDON, *LLNL* M. MURILLO, *Los Alamos National Laboratory* L. BENEDICT, J. DUNN, J. GLOSI, S. HAU-RIEGE, B. LANGDON, R. MORE, *LLNL* J. ROCCA, *Colorado State University* N. ROHRINGER, F. STREITZ, J. WEISHEIT, F. GRAZIANI, *LLNL* We present a new approach to determining stopping power of charged particles in plasmas. We will use short pulse laser-generated protons to heat solid slab targets. The high intensity, short duration laser pulse will generate a burst of protons that isochorically heat the sample, minimizing temperature and density gradients. A second laser-generated proton beam will be sent through the heated target and the relative energy loss will be measured using a proton spectrometer. The heated target thickness will be changed, providing a measure of *dE/dx*. The target conditions will be determined using Frequency Domain Interferometry for density and emissivity for temperature. The target thickness is varied, providing an avenue to determine the *dE/dx*. Preliminary experimental results will be presented.

*This work performed under the auspices of the U.S. Department of Energy by Lawrence Livermore National Laboratory under Contract DE-AC52-07NA27344.

JP8 145 How Can One Maximize the Current Density & Total Electron Density of a Short-Pulse, Approximately Unidirectional, 5-10 MeV Monoenergetic Electron Beam?* G.R. BENNETT, A.B. SEFKOW, B.W. ATHERTON, M. GEISSEL, D.I. HEADLEY, M.C. HERRMANN, M.W. KIMMEL, J.L. PORTER, P.K. RAMBO, M. SCHOLLMEIER, M. SCHWARZ, A Sandia National Laboratories (SNL) program has the goal of attaining the highest possible conversion of Z-Petawatt-Testbed (ZPW-T; up to 120-J in a 0.5-ps pulse) 1054-nm laser light, into an approximately unidirectional, 5-10 MeV, electron beam – with maximum current density & maximum total electron density. If sufficiently successful, the technique will be applied to the larger multikiljoule Z-Petawatt laser, when complete. This paper discusses the early progress/plans to date; including LSP Particle-in-Cell simulations, metrology of ultrathin carbon foils, a Double-Plasma-Mirror system to improve the ZPW-T contrast, a novel linear (LP) to circular polarization (CP) rotator, etc. Results will include: simulation, analytical (a rigorous 1D derivation of the relativistic pondermotive electric field for LP vs. CP light), & experimental progress.

*Sandia is a multi-program laboratory operated by Sandia Corporation, a Lockheed Martin Company, for the United States Department of Energy under contrat DE-AC04-94AL85000. This work is a SNL Laboratory Directed Research and Development project.

JP8 146 Energy Gain of a Free Electron in a Pulsed Electromagnetic Plane Wave with Constant External Magnetic Fields JUSTIN ANGUS, SERGEI KRASHENINNIKOV, *UCSD* We consider free electron interactions with a pulsed plane electromagnetic (EM) wave in the presence of static homogeneous magnetic fields. The main goal of this study is to find the energy gained by the electron after the wave has passed. We use the constants of motion, expressed in terms of the EM vector potential, which can be obtained from the relativistic equation of motion for a charged particle. For a constant magnetic field along the axis of the wave an exact solution is obtained for the energy gain for arbitrarily polarized EM plane wave with a Gaussian amplitude profile. It shows that significant energy gain is possible when the rest mass cyclotron frequency is resonant with the frequency of the wave, but that it decays exponentially when we deter from this resonance. For magnetic fields transverse to the axis of the wave it is shown that the governing equations can be reduced to a two-dimensional Hamiltonian system that when time-averaged in the in the limit where the cyclotron frequency is much less than that of the wave remain in Hamiltonian form. Solutions are sought in this limit for these time-averaged equations using both a Gaussian and step function profile for the wave. For both cases it is found that the maximum energy gain is independent of the size of the transverse magnetic fields and scales with the wave amplitude squared. This work was supported the US DoE under Grant DE-FG02-04ER54739.

JP8 147 DC-like phase space manipulation and particle acceleration using chirped AC fields* PAUL SCHMIT, *Princeton Plasma Physics Labortory* NATHANIEL FISCH, *Princeton Plasma Physics Laboratory* Waves in plasmas can accelerate particles that are resonant with the wave. A DC electric field also accelerates particles, but without a resonance discrimination, which makes the acceleration mechanism profoundly different. We investigate the effect on a Hamiltonian distribution of an accelerating potential waveform, which could, for example, represent the average ponderomotive effect of two counterpropagating electromagnetic waves. In particular, we examine the apparent DC-like time-asymptotic response of the distribution in regimes where the potential structure is accelerated adiabatically. A highly resonant population within the distribution is always present, and we characterize its nonadiabatic response during wave-particle resonance using an integral method in the noninertial reference frame moving with the wave. Finally, we show that in the limit of infinitely slow acceleration of the wave, these highly resonant particles disappear and the response of the bulk distribution becomes identical to the response of a distribution to a uniform DC field.

*This work was supported by US DoE contract No. DE-AC02-76-CH03073. One of us (PFS) was supported by the National Defense Science and Engineering Graduate Fellowship.

JP8 148 White light generation under laser driven avalanche breakdown of air* UPDESH VERMA, *IITD* ASHOK KUMAR SHARMA, A theoretical model of avalanche breakdown of air by a Gaussian laser beam and white light generation is developed. An intense laser beam, below the threshold for tunnel ionization heats the seed electrons to high energy that causes avalanche ionization of the air. However, the plasma density has a maximum on axis and falls off with radial co-ordinates. Such a density profile causes refraction divergence of the beam. However, temporal evolution of plasma density causes self phase modulation of the laser pulse causing frequency broadening of the pulse. The hot plasma thus produced causes strong spectral emission in the visible.

*thanking to CSIR

JP8 149 Terahertz generation by an amplitude modulated Gaussian laser beam in a plasma* DEEPAK TRIPATHI, R. UMA, VIPIN KUMAR TRIPATHI, *IIT Delhi, India* A theoretical model of an analytical formalism of magnetic field generation due to an amplitude modulated intense laser beam in a plasma is de-

veloped. At plasma resonance, where modulation frequency equals the plasma frequency, significant enhancement in the magnetic field is seen. The magnetic field is found to scale directly with laser intensity and plasma frequency, while scaling inversely with laser spot size.

*The author is thankful to UGC, India.

JP8 150 Resonant Excitation of Millimeter Wave by Beating two Lasers in a Plasma Embedded with a Magnetic Wiggler* VIJAY GARG, *Department of Physics, M.M. College, Modinagar-2010004, U.P India* Two high power lasers of frequencies w_1 and w_2, co-propagating in a semiconductor embedded with a magnetic wiggler, produce electromagnetic radiation at the difference frequency (w_1-w_2). The lasers exert a ponder-motive force on the electrons at the difference frequency, giving them longitudinal oscillatory velocity. This velocity beats with the magnetic wiggler to produce a transverse current, driving a millimeter wave at a frequency w_1-w_2 and wave number k_1-k_2+k_w where k $_1$ and k_2 are the wave number of the lasers and k_w is the wave number of the wiggler. For a suitable value of wiggler wave number the process becomes a resonant one, giving high efficiency of millimeter wave generation.

*thankful to UGC for financial support

JP8 151 Asymmetric Self-focusing of a Laser Pulse under Relativistic and Ponderomotive Nonlinearities* AMRITA SINGH, *D.A.V. College, Mujaffarnagar, U.P.* ASHOK KUMAR SHARMA, *CES, IIT Delhi* A short pulse laser beam suffers self-pulse distortion due to combined effects of nonlinearity induced self-focusing and dispersion. Nonlinearity arises due to relativistic mass variation and ponderomotive force. As the beam propagates through plasma, beam width parameter (f)decreases, so intensity of the beam increases. Self focusing of the beam takes place. As time passes, decrease in (f) is smaller and smaller, broadening of pulse takes place. Intensity of the beam decreases with time. Hence due to ponderomotive and relativistic nonlinearities, broadening of the pulse takes place and intensity of the beam decreases due to temporal effect.

*Supported by UGC.

JP8 152 Dependence of Electron Beam Emittance on Electron Gun Controls, and the Description of Electron Dynamics Using Phase Space Diagrams RONALD WILLIAMS, ARNESTO BOWMAN, *Florida A&M University* The designs and test results of devices for measuring the emittance of a low energy electron beam are discussed. The emittance is controlled by varying the electron gun's cathode, grid and anode; with the goal of minimizing the emittance. Scanning wire probes are used initially however non-perturbing optical probes are being developed. The tests are performed using a 5 keV electron beam, however the scaling to higher energy beams will be discussed. Multidimensional phase space diagrams for the emittance measurements will be discussed. Also, similar phase space diagrams for electrons propagating across laser and plasma waves will be discussed. These results are important steps toward developing a diagnostic for plasma waves using a low emittance electron beams.

SESSION JM9: MINI-CONFERENCE ON UNSTEADY RECONNECTION IN LABORATORY AND NATURE II: IMPULSIVE RECONNECTION AND ONSET
Tuesday Afternoon, 3 November 2009
Regency V at 14:00
Tom Intrator, Los Alamos National Laboratory, presiding

14:00
JM9 1 Impulsive Reconnection in the Sun's Atmosphere* SPIRO ANTIOCHOS, *NASA/GSFC* Recent high-resolution observations from the Hinode mission show dramatically that the Sun's atmosphere is filled with explosive activity ranging from chromospheric explosions that reach heights of Mm, to coronal jets that can extend to solar radii, to giant coronal mass ejections (CME) that reach the edge of the heliosphere. The driver for all this activity is believed to be 3D magnetic reconnection. From the large variation observed in the temporal behavior of solar activity, it is clear that reconnection in the corona must take on a variety of distinct forms. The explosive nature of jets and CMEs requires that the reconnection be impulsive in that it stays off until a substantial store of free energy has been accumulated, but then turns on abruptly and stays on until much of this free energy is released. The key question, therefore, is what determines whether the reconnection is impulsive or not. We present some of the latest observations and numerical models of explosive and non-explosive solar activity. We argue that, in order for the reconnection to be impulsive, it must be driven by a quasi-ideal instability. We discuss the generality of our results for understanding 3D reconnection in other contexts.

*This work was supported by the NASA HTP and SR&T programs.

14:25
JM9 2 Impulsive Magnetic Reconnection in Solar Flares and CMEs C.Z. CHENG, Y.H. YANG, *Plasma and Space Science Center, National Cheng Kung University* G.S. CHOE, *Kyung Hee University* Y. ONO, *University of Tokyo* Impulsive magnetic reconnection has been considered as the mechanism responsible for impulsive non-thermal emission in hard X-rays (HXR) and mm/smm waves during soft X-ray (SXR) flare rise phase. The impulsive non-thermal emission also correlates temporarily with impulsive upward acceleration of coronal mass ejection (or flux rope) via the impulsive magnetic reconnection process. The magnitude of impulsive magnetic reconnection rate and magnetic reconnection electric field at the reconnecting X-line can be computed from the rate of change in magnetic flux swept by the evolution of H-alpha ribbons or EUV ribbons or HXR footpoints. By averaging the magnetic flux change rate over the ribbons the peak reconnection electric field during HXR impulsive phase is ~ O(1 kV/m) for X-class flares. Further studies show that the magnetic flux change rate of reconnected field lines varies along the ribbons and the peak value is located near HXR footpoints and can be several times larger than the averaged value. Recent laboratory experiments directly measured the impulsive magnetic reconnection associated with accelerated ejection of flux ropes. Ccombined results from both solar observations and laboratory experiments thus provide strong support of impulsive magnetic reconnection for explaining impulsive phenomena in solar flares and CMEs.

14:45

JM9 3 Onset of Fast Reconnection in Laboratory and Space Plasmas A. BHATTACHARJEE, K. GERMASCHEWSKI, YI-MIN HUANG, *Center for Integrated Computation and Analysis of Reconnection and Turbulence, University of New Hampshire* H. YANG, B. ROGERS, *Center for Integrated Computation and Analysis of Reconnection and Turbulence, Dartmouth College* The onset of fast reconnection is widely studied in laboratory plasmas, satellite measurements in the Earth's magnetosphere, and solar flares. Using high- performance computing tools, based on Hall MHD equations, we will show that important features of such dynamics can be accounted for in one unifying framework. The model also elucidates the role of diamagnetic drifts that can quench nonlinearly the onset of fast reconnection. The problem takes on additional complexity when it is applied to large systems of high Lundquist number. It is shown that the dynamics of thin current sheets in such systems shows qualitative similarities in the collisional and collisionless regimes. In the resistive MHD model, at high-Lundquist number, the thin current sheet becomes near-explosively unstable to secondary tearing, producing plasmoids copiously. The linear instability for an entire class of such super-Alfvenic instabilities can be deduced from the classical tearing mode dispersion relation. In the nonlinear stage, one attains a new regime of fast reconnection in which the reconnection rate exceeds by far the predictions of Sweet-Parker theory, and becomes weakly dependent on the Lundquist number.

15:10

JM9 4 Excitation and Removal of Neoclassical Tearing Mode Islands in Tokamaks* R.J. LA HAYE, *General Atomics* A principal pressure limit in tokamaks is set by the onset of neoclassical tearing modes (NTMs), which are destabilized and maintained by helical perturbations to the pressure-gradient driven "bootstrap" current. The resulting magnetic islands break up the magnetic surfaces that confine the plasma. The NTM is linearly stable but nonlinearly unstable, and generally requires a "seed" to destabilize a meta-stable state. Thus a good analogy is an avalanche. Once excited NTM islands are very robust but can be removed by reducing the plasma pressure (i.e. bootstrap current) sufficiently so that the meta-stable parameter space is gone; self-stabilization then occurs. Examples from the DIII-D tokamak will be presented.

*Work supported by the US Department of Energy under DE-FC02-04ER54698.

15:35

JM9 5 Impulsive Magnetic Reconnection in TS-3 and TS-4 Merging Experiments YASUSHI ONO, *University of Tokyo* TS AND UTST TEAM, Impulsive effects of magnetic reconnection have been investigated in TS-3 and TS-4 tokamak merging experiments for maximizing reconnection speed. Under low guide-field, over-acceleration of two merging tokamaks caused the 3-D local deformation of current sheet. The toroidal asymmetry grew locally around the current sheet only during the reconnection time, increasing the plasma mass ejection from the current sheet. The local compression of current sheet thickness shorter than ion gyroradius triggered its anomalous resistivity, causing significant increase in the reconnection speed. Under high guidefield, the sheet resistivity was almost classical due to the sheet thickness larger than ion gyroradius When we over-accelerated the merging tokamaks under high-guide field, large inflow flux and low current-sheet dissipation caused plasma pileup around the sheet. When the flux pileup exceeded a critical limit, the sheet was ejected mechanically from the squeezed X-point area. The reconnection (outflow) speed was slow during the flux pileup and was fast during the ejection During the ejection, the current sheet was often transformed into several current islands, suggesting that the island size comparable with ion gyrorasius increased the sheet resistivity. Those three fast reconnection mechanisms: anomalous reisistvity, plasmoid (sheet) ejection and 3-D reconnection were observed consistently in TS reconnection experiments.

16:00

JM9 6 Unsteady magnetic reconnection in laboratory experiments with current sheets ANNA FRANK, *Prokhorov General Physics Institute of the Russian Academy of Sciences* According to present notion, unsteady magnetic reconnection in current sheets (CS) is basic to dramatic natural phenomena: solar and stellar flares, substorms in the Earth and other planetary magnetospheres, as well as to disruptive instabilities in tokamak plasmas. We present a review of laboratory experiments studying evolution of CS formed in 3D and 2D magnetic configurations with an X line, in the CS-3D device. Usually CS exists during an extended period in a metastable stage, without essential changes of its structure and parameters. Under certain conditions this stage may be suddenly interrupted by unsteady phase of magnetic reconnection, which manifests itself in a rapid change of the magnetic field topology, current redistribution, excitation of pulsed electric fields, and other dynamic effects. The unsteady phase results in effective conversion of magnetic energy into the energy of plasma and accelerated particles, and may finally bring about the CS disruption. In the context of the solar flares, a metastable CS is associated with a pre-flare situation, while CS disruption – with the flare itself. The physical mechanisms triggering the unsteady magnetic reconnection in the laboratory produced current sheets are discussed. Supported by the Russian Foundation for Basic Research (project # 09-02-00971).

16:25

JM9 7 Impulsive Reconnection and the Role of Hall Physics in the Reversed Field Pinch* T.D. THARP, A.F. ALMAGRI, M.C. MILLER, V.V. MIRNOV, S.C. PRAGER, J.S. SARFF, *University of Wisconsin-Madison* Previous measurements have established that the RFP sawtooth relaxation is characterized by the simultaneous occurrence of multiple impulsive reconnection events. Here, we report measurements of the reconnection Ohm's Law, including the reconnection electric field and terms that balance this field. This analysis is applied to tearing modes with poloidal mode number $m = 0$ and toroidal mode number $n \geqslant 1$. Measurements are performed with probes in the vicinity of the resonant surface, and clearly indicate that single fluid physics is not sufficient to explain this reconnection. In particular, nonlinear three-wave interaction Hall terms are a strong contributor to the dynamics of this reconnection, indicating the substantial role of collective mode phase matching during sawtooth events.

*Work Supported by US DOE and NSF

16:45

JM9 8 Experiments on 3D Onset of Magnetic Reconnection* N. KATZ, J. EGEDAL, W. FOX, A. LE, A. VRUBLEVSKIS, J. BONDE, M. PORKOLAB, *MIT, PSFC* We study collisionless magnetic reconnection in the laboratory using the Versatile Toroidal Facility (VTF) at MIT. In our experiments a parameter regime exists where the reconnection process appears in rapid bursts [1]. This regime provides a unique opportunity to study the unresolved "trigger problem" of magnetic reconnection related to the spontaneous and explosive onset of events observed on the sun, in the

Earth's magneto-tail and in sawtooth oscillations in magnetic fusion devices. Although the reconnection is driven, fast reconnection is not seen immediately: instead, the plasma responds at first by building up current to oppose the drive, and only after a delay of $\sim$ 100 μs is there a burst of spontaneous, fast reconnection. We find that although the experiment is set up axi-symmetrically, the burst of reconnection starts at one toroidal location and propagates along X-line approximately at the Alfvén speed. This burst of fast reconnection is only observed in the presence of a global plasma mode ($q = 2$ or $q = 3$), which is seen both in the current density and in the floating potential and is related to the formation of a magnetic island. [1] J. Egedal et al., Phys. Rev. Lett., **98**, 015003 (2007)

*Supported by DOE Junior Faculty Award DE-F602-06ER54878 and NSF/DOE Award PHY-0613734.

SESSION LE1: TOWN MEETING: A CONVERSATION WITH DR. STEVEN KOONIN

Tuesday Evening, 3 November 2009; Centennial I at 19:30; Steven Koonin, Undersecretary for Science, Department of Energy, presiding

19:30

LE1 1 How Can We Accelerate Scientific Progress Towards Fusion Energy?

STEVEN KOONIN, *Undersecretary for Science, Department of Energy*

SESSION MR1: REVIEW: PHYSICS PROGRESS OF REVERSED FIELD PINCH MAGNETIC CONFINEMENT
Wednesday Morning, 4 November 2009; Centennial I-II at 8:00; Stewart Prager, Princeton Plasma Physics Laboratory, presiding

8:00
MR1 1 Physics progress of Reversed Field Pinch magnetic confinement.
JOHN S. SARFF, *University of Wisconsin-Madison*

Over the last decade, the international RFP community has made large strides understanding key physics challenges for plasma confinement with weak external magnetization. This progress fundamentally changes the fusion outlook for the RFP. In several areas, resolving the RFP's fusion challenges is simultaneously advancing basic plasma physics, with potentially large impact in astrophysics. For example, the magnetic dynamo in the RFP reveals how large-scale instabilities can efficiently transport magnetic energy. An understanding of MHD tearing that supports dynamo action inspired current profile control. This produces a ten-fold improvement in confinement, comparable to a same-size, same-current tokamak. A recent push to higher plasma current reveals remarkable self-organization to a helical equilibrium, or quasi-single-helicity dynamo state, that also exhibits improved confinement. These controlled and spontaneous transitions from high to low levels of magnetic chaos probe transport in a stochastic magnetic field, the natural state of the field in astrophysical settings. High temperature ions > 1 keV are observed, heated during magnetic reconnection events. This is reminiscent of non-collisonal heating in the solar atmosphere. Coupled with current profile control, improved confinement with multi-kilovolt temperature electrons and ions is demonstrated. Active control of the magnetic boundary is now routine to stabilize many resistive wall modes in pulse lengths > 10 times their growth rate, an essential need for the RFP and likely other high beta configurations. Few options exist for steady-state current sustainment in fusion plasmas. One is Oscillating Field Current Drive, based on magnetic helicity conservation principles that underpin magnetic self-organization. Partial OFCD sustainment experiments so far agree with the self-organization physics basis. This work is supported by the US DOE and NSF.

SESSION NI2: ICF CAPSULES AND RAYLEIGH-TAYLOR INSTABILITY
Wednesday Morning, 4 November 2009; Centennial I at 9:30; David Meyerhofer, University of Rochester, presiding

9:30
NI2 1 Capsule Performance Optimization for the National Ignition Facility.
OTTO LANDEN, *Lawrence Livermore National Laboratory*

The overall goal of the capsule performance optimization campaign is to maximize the probability of ignition by experimentally correcting for likely residual uncertainties in the implosion and hohlraum physics used in our radiation-hydrodynamic computational models before proceeding to cryogenic-layered implosions and ignition attempts. This will be accomplished using a variety of targets that will set key laser, hohlraum and capsule parameters to maximize ignition capsule implosion velocity, while minimizing fuel adiabat, core shape asymmetry and ablator-fuel mix. The targets include high Z re-emission spheres setting foot symmetry through foot cone power balance [1], liquid Deuterium-filled "keyhole" targets setting shock speed and timing through the laser power profile [2], symmetry capsules setting peak cone power balance and hohlraum length [3], and streaked x-ray backlit imploding capsules setting ablator thickness [4]. We will show how results from successful tuning technique demonstration shots performed at the Omega facility under scaled hohlraum and capsule conditions relevant to the ignition design meet the required sensitivity and accuracy. We will also present estimates of all expected random and systematic uncertainties in setting the key ignition laser and target parameters due to residual measurement, calibration, cross-coupling, surrogacy, and scale-up errors, and show that these get reduced after a number of shots and iterations to meet an acceptable level of residual uncertainty. Finally, we will present results from upcoming tuning technique validation shots performed at NIF at near full-scale. Prepared by LLNL under Contract DE-AC52-07NA27344. [1] E. Dewald, et. al. Rev. Sci. Instrum. 79 (2008) 10E903. [2] T.R. Boehly, et. al., Phys. Plasmas 16 (2009) 056302. [3] G. Kyrala, et. al., BAPS 53 (2008) 247. [4] D. Hicks, et. al., BAPS 53 (2008) 2.

10:00
NI2 2 Shock-Tuned Cryogenic DT Implosion Performance on OMEGA.
T.C. SANGSTER, *Laboratory for Laser Energetics, U. of Rochester*

Cryogenic-target-compression experiments with low-adiabat ($\alpha \sim$ 1 to 3) continuous and multiple-picket-drive pulses are performed on the OMEGA laser to understand the physics of fuel assembly in inertial confinement fusion. Continuous-drive-pulse designs require accurate modeling of the compression wave generated by the gradual rise in laser intensity. Uncertainties in the ablator/fuel equation-of-state modeling and laser coupling can lead to uncertainties in the predicted shock coalescence and fuel adiabat. The multiple-picket-drive pulse designs replace the gradual intensity rise of the continuous pulse with two or three narrow pickets (each picket is approximately 100 ps long). These picket designs facilitate shock tuning using an experimental cone-in-shell platform[1] developed for the National Ignition Campaign. The coalescing shocks are measured with VISAR. The required shock-timing accuracy is achieved by adjusting the energies of the individual pickets. The shock-tuned, multiple-picket-drive pulses have been used to drive cryogenic DT targets to implosion velocities ($> 3 \times 10^7$ cm/s) that exceed those reached using continuous-pulse designs.[2] This talk will present new multiple-picket shock-timing results and target performance data (yield, areal density, and ion temperature) from shock-tuned implosions on OMEGA. The areal density is inferred from the spectra of knock-on deuterons and the primary neutron down-scattered fraction using a magnetic recoil spectrometer (primary DT neutrons that scatter in the dense fuel end up with energies well below 14 MeV; the ratio of this yield to the primary yield is proportional to the fuel areal density). Properly tuned implosions produce nearly 1-D areal densities. This work was supported by the U.S. Department of Energy Office of Inertial Confinement Fusion under Cooperative Agreement No. DE-FC52-08NA28302.

[1]T. R. Boehly *et al.*, Phys. Plasmas **16**, 056302 (2008).
[2]T. C. Sangster *et al.*, Phys. Rev. Lett. **100**, 185006 (2008).

10:30
NI2 3 Asymmetrically-Driven Implosions.
KELLY VAUGHAN, *Atomic Weapons Establishment*

Techniques to achieve uniform, near-spherical symmetry of radiation drive on a capsule in a laser-heated hohlraum have received detailed attention in the context of ICF. However, much less attention has been paid to the understanding of the hohlraum physics in cases where the radiation drive departs significantly from spherical symmetry. In recent work at the OMEGA laser, AWE has carried out a series of experiments to study the implosion dynamics of a capsule irradiated by a deliberately asymmetric X-ray drive. The experimental data provide a sensitive test of radiation transport in which drive symmetry is modulated by the use of variable albedo layers and asymmetric laser-beam timing. Data from foam-ball and thin-shell capsule experiments are presented, together with modelling using consecutively linked Lagrangian and Eulerian, as well as single-step ALE, calculational schemes. The thin-shell capsules exhibit much stronger sensitivity to asymmetry than foam balls resulting in the formation of a well-defined polar jet. These data are shown to challenge computational modelling in this highly asymmetric, strongly convergent regime.

11:00
NI2 4 Measurements of the down-scattered and TT-neutron spectrum using the Magnetic Recoil Spectrometer.
JOHAN FRENJE, *MIT*

Proper assembly of capsule mass, as manifested through evolution of fuel areal density (ρR), is fundamentally important for achieving hot-spot ignition planned at the National Ignition Facility (NIF). Experimental information about ρR and ρRasymmetries,Ti and yield is therefore absolutely essential for understanding how assembly occurs. To obtain this information, we have built and activated, at OMEGA, a Magnetic−Recoil Spectrometer (MRS) whose objective is to measure the absolute neutron spectrum in the range 5 to 30 MeV, from which ρR, Ti and yield can be directly inferred for energy−scaled cryogenic DT implosions. This allows for experimental validation of the direct−drive ignition −capsule design prior to the first experiments on the NIF. Another MRS is currently being built for the NIF. In this talk, we present the first ever measurements of the down−scattered neutron spectrum, from which ρR was accurately inferred for both CH and cryogenic DT implosions. As much of the OMEGA−MRS R&D is directly applicable to the NIF−MRS, the MRS activities on the NIF are presented as well. In addition, high−resolution measurements of the DT and TT −neutron spectrum have recently been performed to address, for the first time, important science questions regarding non−thermal components in the DT−neutron spectrum, as well as the possible existence of the TT−two−body reaction, at low energies, producing a neutron peak at about 9 MeV. This work was supported in part by the U.S. Department of Energy (Grant No. DE−FG03−03SF22691), LLE (subcontract Grant No. 412160−001G), LLNL (subcontract Grant No. B504974). Contributors: D.Casey, C.Li, F.Séguin, N.Sinenian, R.Petrasso, MIT, V.Glebov, T.Sangster, D.Meyerhofer, LLE−UR, S.Hatchett, S.Haan, C.Cerjan, M.Eckart, H.Kather, O.Landen, M. Moran, LLNL, K. Fletcher, *Suny Geneseo, and* R. Leeper, SNL.

11:30
NI2 5 Strong viscous stabilization of the Rayleigh-Taylor instability at Mbar pressures.*
HYE-SOOK PARK, *Lawrence Livermore National Laboratory*

We report experimental results showing significant reductions from classical in the Rayleigh-Taylor instability (RTI) growth rate due to high pressure effective lattice viscosity. Stabilization of the RT instability by ablation and density gradients has been studied for decades. Stabilization by lattice viscosity (material strength) at Mbar pressures is new. Target samples are compressed and accelerated quasi-isentropically by plasma drives, while maintaining the samples in the solid-state. Provided strong shocks are avoided, the higher the applied peak pressure, the higher the sample strength, and hence, the higher the degree of strength stabilization of RTI [1]. This paper will present our results on vanadium (V) using the Omega long-pulse lasers and tantalum (Ta) using the Omega long pulse and EP short pulse laser in combination. The amount of RTI growth is measured by face-on radiography, utilizing a thermally driven He-α backlighter for V and a high energy ($>$ 20 keV) K-α backlighter driven by the EP petawatt laser for Ta. Comparisons with 2D simulations employing constitutive models for solid state strength suggest that we are in the new stabilization regime of very high effective lattice viscosity caused by phonon drag on dislocation motion. This effective lattice viscosity is predicted to increase with pressure, provided the lattice is maintained, making our results relevant to the fields of ICF and high energy density physics in general. Designs that extend this experiment by an order of magnitude in pressure on NIF will also be shown [1] B.A. Remington, H.S. Park et al., European Physics Journal, in press (2009). [2] H.S. Park et al., J. Phys.: Conf. Ser. 112, 042024 (2008).

*This work was performed under the auspices of the Lawrence Livermore National Security, LLC, (LLNS) under Contract No. DE-AC52-07NA27344.

12:00
NI2 6 Investigations into the Seeding of Instabilities due to X-ray Preheat in Beryllium-Based Inertial Confinement Fusion Targets.
ERIC LOOMIS, *Los Alamos National Laboratory*

The geometry of inertial confinement fusion (ICF) capsules makes them susceptible to various types of hydrodynamic instabilities at different stages during an ICF implosion. From the beginnings of ICF research, it has been known that grain-level anisotropy and defects could be a primary source of instability seeding in solid capsules. This has steered ICF designs to include amorphous materials such as plastic; however, the benefits of low-Z metallic materials, i.e. beryllium, has kept these materials the focus of much research. Recently, experiments were conducted at the Trident laser facility to measure dynamic surface roughening from hard x-ray preheat. M-band emission from laser produced gold plasma was used to heat beryllium targets with different amounts of copper doping to temperatures comparable to National Ignition Facility (NIF) preheat levels. Temporal and spectral x-ray diagnostics were used to estimate the target heating, which was also predicted by multi-dimensional radiation hydrodynamics calculations. Wave profiles of varying complexity due to differences in copper doping were observed with free surface line imaging velocity interferometry. Dynamic roughening measurements were made on the surface away from the plasma at discrete times up to 8 ns after the beginning of the drive pulse using a surface displacement interferometer with nanometer scale sensitivity. Undoped, large-grained targets were measured to roughen between 15 and 50 nm rms depending on variations in x-ray absorption through the target thickness. Fine-grained, copper-doped targets were observed to roughen near the sensitivity limit of the interferometer and approached the Rev2 NIC design point of 0.9 nm. The results of this combined experimental and modeling effort have shed light on the effects of high-Z doping and microstructural refinement on the dynamics of differential thermal expansion and have shown that current NIF capsule designs using beryllium are very effective in reducing preheat related roughening ahead of the first shock. These experiments have raised additional questions, however, such as the possibility of spallation from intense thermal expansion, which will also be discussed.

SESSION NI3: PLASMA ROTATION AND HELICAL EQUILIBRIA
Wednesday Morning, 4 November 2009; Centennial II at 9:30; Eric Fredrickson, Princeton Plasma Physics Laboratory, presiding

9:30
NI3 1 Transport Equations In Tokamak Plasmas.*
J.D. CALLEN, *University of Wisconsin*

Tokamak plasma transport equations are usually obtained by flux surface averaging the collisional Braginskii equations. However, tokamak plasmas are not in collisional regimes. Also, ad hoc terms are added for: neoclassical effects on the parallel Ohm's law (trapped particle effects on resistivity, bootstrap current); fluctuation-induced transport; heating,

current-drive and flow sources and sinks; small B field non-axisymmetries; magnetic field transients etc. A set of self-consistent second order in gyroradius fluid-moment-based transport equations for nearly axisymmetric tokamak plasmas has been developed recently using a kinetic-based framework. The derivation uses neoclassical-based parallel viscous force closures, and includes all the effects noted above. Plasma processes on successive time scales (and constraints they impose) are considered sequentially: compressional Alfvén waves (Grad-Shafranov equilibrium, ion radial force balance); sound waves (pressure constant along field lines, incompressible flows within a flux surface); and ion collisions (damping of poloidal flow). Radial particle fluxes are driven by the many second order in gyroradius toroidal angular torques on the plasma fluid: 7 ambipolar collision-based ones (classical, neoclassical, etc.) and 8 non-ambipolar ones (fluctuation-induced, polarization flows from toroidal rotation transients etc.). The plasma toroidal rotation equation [1] results from setting to zero the net radial current induced by the non-ambipolar fluxes. The radial particle flux consists of the collision-based intrinsically ambipolar fluxes plus the non-ambipolar fluxes evaluated at the ambipolarity-enforcing toroidal plasma rotation (radial electric field). The energy transport equations do not involve an ambipolar constraint and hence are more directly obtained. The resultant transport equations will be presented and contrasted with the usual ones. [1] J.D. Callen, A.J. Cole, C.C. Hegna, "Toroidal Rotation In Tokamak Plasmas," to be published in Nuclear Fusion.

*Collaborators A.J. Cole, C.C. Hegna; research supported by DoE grants DE-FG02-86ER53218 and DE-FG02-92ER54139.

10:00
NI3 2 Generation and Sustainment of Rotation in Tokamaks.*
W.M. SOLOMON, *Princeton Plasma Physics Laboratory*

Recent experiments on DIII-D, NSTX and C-Mod have led to new discoveries related to toroidal rotation in tokamaks, including evidence for an effective torque responsible for "intrinsic rotation" generation and the existence of a strong inward pinch of angular momentum. Measurements on DIII-D using a mix of co- and counter-neutral beam injection show an effective torque in the co-current direction for H-mode plasmas with a profile that is largely localized toward the edge. This shows consistency with theoretical models of non-diffusive momentum transport such as the "residual stress" driven for example by the turbulent Reynolds stress. New data from DIII-D show that the effective torque is modified by electron cyclotron heating, resulting in a counter torque inside of the deposition radius. Application of lower hybrid heating in C-Mod also modifies the intrinsic rotation, again presumably through modifications to the residual stress. In NSTX, experiments have demonstrated the existence of an inward momentum pinch of up 40 m/s, generally showing quantitative agreement with theoretical predications originating from consideration of low-k turbulence. Similar observations have been obtained on DIII-D and C-Mod, although in some cases the experimental pinch can significantly exceed the theoreticallt expected level. Significant inward pinches will directly affect the peakedness of the rotation profile in plasmas with minimal external torque and an edge drive for the intrinsic rotation. In plasmas with large rotation and strong $E \times B$ shear, ion thermal transport can be reduced to neoclassical levels in DIII-D and NSTX; however, diffusive momentum transport still remains highly anomalous. The common physics of momentum transport between the three devices is under investigation.

*Supported by US DOE under DE-AC02-76CH03073 and DE-FC02-04ER54698.

10:30
NI3 3 Comparison of poloidal velocity measurements to neoclassical theory on NSTX.*
R.E. BELL, *Princeton Plasma Physics Laboratory*

Knowledge of poloidal velocity is required for the determination of the radial electric field, which along with its gradient, is linked to turbulence suppression and transport barrier formation. Pitch-angle measurements from the motional Stark effect require knowledge of the radial electric field to obtain accurate current profiles. Measurements of impurity poloidal flow on conventional tokamaks, that differ an order of magnitude from expected neoclassical values, challenge neoclassical theory as presently formulated. In contrast, recent poloidal velocity measurements from a new diagnostic on NSTX are much more similar to neoclassical predictions from the code NCLASS. The novel NSTX charge exchange recombination spectroscopy diagnostic addresses many atomics physics issues that complicate poloidal velocity measurements, e.g. the collisonal energy dependence of the charge exchange cross section and effects due to ion gyro motion, which lead to pseudo velocities not associated with plasma flow. Uncertainties in atomic physics cross sections that can dominant the relatively small impurity poloidal velocity to be measured are virtually eliminated with a novel viewing geometry. Unique active and passive sets of up/down symmetric views are used to isolate charge exchange emission in the beam volume. Each up/down viewing pair yields an independent line-integrated measurement of poloidal velocity that does not rely on any atomic physics, since gyro orbit effects are small due to low magnetic fields on NSTX. Local profiles can be obtained with an inversion of line-integrated measurements in the beam volume. Comparisons between the measured poloidal velocity and neoclassical predictions and the potential implications will be described.

*Supported by U.S. Dept. of Energy Contract DE-AC02-09CH11466.

11:00
NI3 4 Three-dimensional shaping of tokamak plasmas.*
MICHAEL ZARNSTORFF, *Princeton Plasma Physics Laboratory*

Three-dimensional (3-D) shaping of advanced tokamak plasmas is explored to provide resilience against disruptions, eliminate the need for current drive, and stabilize several instabilities without external feedback. The 3-D shaping is constrained to be approximately quasi-axisymmetric, so the orbit and neoclassical properties of the original equilibrium are preserved. Sequences of numerically generated equilibria with β=4% are studied, parametrically varying the shape and aspect ratio to examine the properties achieved at different levels of shaping, and the impact on coil-set complexity. The base axisymmetric equilibrium has elongation of 1.8, high triangularity, and average aspect ratio $\sim$ 4. The 3-D shaping has N=3 periodicity in the toroidal direction. It is found that a small distortion, producing a vacuum rotational transform ι=0.05, stabilizes the vertical instability. With vacuum ι=0.1 and a self-consistent bootstrap current, the need for external current drive is eliminated, while keeping the Shafranov shift less than half the minor radius. Above vacuum ι=0.2, the equilibrium remains inside the vacuum vessel even if the plasma pressure and current disappear. Thus, this should be robust against disruptions, similar to experiments on W7-A. For vacuum ι=0.3, the external kink and resistive wall mode are passively stable. With fixed 3-D shape amplitude, variations of the average two-dimensional plasma shape changed the MHD stability thresholds as in axisymmetric tokamaks. Increased aspect ratio systematically reduces the toroidal excursion of a modular coil set that produces the 3-D shaped magnetic field, giving simpler, smoother coils. Other strategies to simplify the coil shapes will be discussed, including saddle coils combined with planar tokamak coils.

*In collaboration with A. Boozer and L.-P. Ku.

11:30
NI3 5 Transport barriers in helical equilibria: structural change in the reversed field pinch.*
PIERO MARTIN, *Consorzio RFX - Associazione EURATOM-ENEA sulla fusione, Padova, Italy*

Self-organization of RFX plasmas in single helical axis equilibrium, with m=1,n=7 helicity, is a structural change for the reversed field pinch (RFP) [Lorenzini et al., Nature Phys 2009 doi:10.1038/nphys1308]. This happens at high plasma current (I> 1 MA) while axisymmetric boundary conditions are enforced: the helical state has almost conserved magnetic flux surfaces, interpreted as ghost surfaces [Hudson&Breslau PRL 2008], leading to strong core electron transport barriers. Electron temperature Te reaches 1.3keV @1.7MA. Ion temperature Ti is $\sim$ (0.5-0.75)Te, consistent with collisional ion heating. The core barrier extends up to $\sim$ 0.65r/a. Magnetic surfaces quality improves with Lundquist number S, thanks to the simultaneous decrease of magnetic chaos and increase of the helical field strength. Helical equilibria are reconstructed by the 3d code VMEC. The (1,7) helicity acts to hold the core safety factor almost flat and below 1/7. The barrier foot coincides with a zero magnetic shear region, where density of rational surfaces is minimum, as in other configurations. Plasma-wall interaction is smoother. Main gas particle confinement time improves in pellet-fuelled plasmas, with record value $\sim$ 10ms. No core impurity accumulation is evident in Laser Blow Off experiments, which is consistent with numerical simulation results. High current sets a transition also for the edge, where robust Te gradients are observed with a pedestal of $\sim$ 1keV in $\sim$ 3cm, possibly due to improved magnetic topology and synergic with core barrier. As persistence and quality of these improved helical states increase with current, the likelihood of achieving steady helical multi-MA RFPs can be inferred. RFX experiments allow a study of the beneficial effects of non-axisymmetric shaping and may provide a platform for a more general validation of theoretical tools developed for stellarators. Moreover, these results are transformational in supporting the RFP as a low-external field, non-disruptive, ohmic approach to fusion, exploiting self-organization and technological simplicity.

*In collaboration with the RFX-mod team.

12:00
NI3 6 Internal Electron Transport Barrier due to Neoclassical Ambipolarity in the HSX Stellarator.*
JEREMY LORE, *HSX - UW Madison*

Strongly peaked electron temperature profiles are measured in the core of the Helically Symmetric Experiment (HSX) during electron cyclotron heating; with central temperatures of 2.5keV for 100kW of injected power. These measurements, coupled with neoclassical predictions of large "electron root" radial electric fields with strong radial shear, are evidence of a neoclassically driven thermal transport barrier. Neoclassical transport is analyzed using the PENTA code [1], in which parallel momentum is conserved. Momentum conservation, including the effects of parallel flow, has long been known to be important in tokamak neoclassical calculations. Conventional stellarators, on the other hand, typically exhibit strong flow damping in all directions on a flux surface, and the parallel flows can be neglected. In this case, the radial electric field is calculated using a simple ambipolarity constraint: setting the ion flux equal to the electron flux. In stellarators with very low effective ripple, such as HSX, parallel flow and momentum conservation are again expected to be important. Large parallel flow measurements ($\sim$ 20km/s) from the ChERS diagnostic are consistent with reduced damping in the direction of symmetry. In addition to neoclassical transport, a model of Trapped Electron Mode turbulence

is used to calculate the turbulent-driven electron thermal diffusivity. The very peaked T_e profile is reproduced by predictive transport simulations only when turbulent transport quenching via sheared ExB flow is included [2]. ChERS measurements of the radial electric field profile and comparison to the neoclassical calculations will also be presented. [1] D.A. Spong, Phys. Plasmas **12**, 056114 (2005). [2] W. Guttenfelder, J. Lore, *et. al*, Phys. Rev. Lett. **101**, 215002 (2008).

*Work supported by DOE Grant DE-FG02-93ER54222.

SESSION NO4: INTERNATIONAL TOKAMAK RESEARCH AND ITER
Wednesday Morning, 4 November 2009
Regency VI at 9:30
Raffi Nazikian, Princeton Plasma Physics Laboratory, presiding

9:30
NO4 1 Summary of steady-state research during 23 years of JT-60 tokamak experiments MITSURU KIKUCHI, *JAEA* JT-60 TEAM, This talk summarizes the achievement of steady state research during 23 years of JT-60 tokamak experiment. JT-60 was one of 3 large tokamaks, which started its operation in April 1985 and completed in August 2008. Before the modification to JT-60U, up to 80% of plasma current was driven by the bootstrap current and the steady state tokamak reactor concept SSTR was proposed in 1990. Theory of generalized Ohm's law in tokamak was developed. Negative shear configuration was first proposed (1992) and becomes popular in advanced tokamak research now. Formation of internal transport barrier (ITB) in PS(1994) and NS(1997) leads to enhanced bootstrap current fraction in the core region. Physics of NBCD and ECCD was developed using N-NBI and ECCD systems. A current hole (CH) was observed as unique structure formation(2001). Stabilization of RWM with small toroidal rotation $\sim 0.4\%V_A$ is important step to sustain high plasma pressure above no-wall limit(2007). Demonstration of full CD with 75% bootstrap current fraction and rest by NBCD was made under relatively high $q_{95} \sim 8$(2005) and access to low $q_{95} \sim 5$ was reached by the stabilization of RWM(2008). All these results favors the concept of SSTR, but simultaneous sustainment of high bootstrap & high beta operation is left for future study.

9:42
NO4 2 Comparison of long pulse single and double null divertor plasma behaviors in EAST H.Y. GUO, X. GAO, J. LI, G.-N. LUO, S. ZHU, J.F. CHANG, W. GAO, X.Z. GONG, Q.S. HU, Q. LI, T.F. MING, J. OU, Y.J. SHI, B.N. WAN, D.S. WANG, J. WANG, Z.W. WU, B.J. XIAO, Q. XU, L. ZHANG, W. ZHANG, *Institute of Plasma Physics, Chinese Academy of Sciences* EAST TEAM, Divertor performance has been assessed in the new EAST superconducting tokamak for both single null (SN) and double null (DN) configurations. Stable DN discharges over 60 seconds have been achieved for the first time in EAST with active wall conditioning and divertor pumping. Particle and heat fluxes to both inner and outer divertor targets are lower for DN, but with stronger asymmetry favoring outer divertors, as compared to SN. Plasmas exhibit a large amplitude broadband turbulence in the outer divertors for both SN and DN, as indicated by Langmuir probe measurements. The turbulence level is significantly reduced in the inner divertors, especially for DN. DN operation also leads to an up-down asymmetry with higher power and particle fluxes to the divertors with their ∇B drift toward the X-point. Revering B_T shows a strong influence on the observed divertor asymmetries. As an active means to control power and particle fluxes to the target plates, localized divertor puffing has been explored in EAST under long pulse operating conditions. This presentation will highlight these recent advances.

9:54
NO4 3 Real time Suppression MHD with Active Feedback Modulating LHW&IBW on HT-7 Superconducting Tokamak* J.S. MAO, J.R. JUO, H. WANG, Y.W. SUN, B.J. DING, *Institute of Plasma Physics, Chinese Academy of Sciences* A active modulation LHW and IBW have used successfully for real-time measure and suppress MHD on the superconducting tokamak HT-7. DAQ2010 advanced data acquisition card was used. We also did the synergy modulation experiment of LHW & IBW. A feedback system was used which activated modulation only when MHD activity reach a predetermined level so as to optimize the current drive through out the discharge. The LHCD modulation was varied in power and frequency, with the frequency always being less than the resistive skin time (100ms). Optimal MHD suppression was achieved when modulating LHW power $>$ 200kW, and frequency of 50Hz. Details of the MHD suppression will be discussed in this poster. The amplitude, interval and the period of LHW and IBW modulation pulse can be adjusted very conveniently. The modulation LHW & IBW can be delivered very fast at the any time during the discharge. The modulation LHW & IBW period was always much shorter than the plasma resistive time. So the profile of plasma current is changed much fast than the plasma resistive time.

*This work was Support by National Natural Science Fund of China, Contract No. 10675126.

10:06
NO4 4 The Real Mission of ITER* G.A. WURDEN, *Los Alamos National Laboratory* ITER will operate subject to multiple physics and engineering constraints, and to be successful it must satisfy many constraints simultaneously. One of the most serious issues it will face is learning how to handle 100-400 MJ of plasma energy that can be quickly released in the event of a disruption, and the conversion of an additional 500 MJ of stored poloidal magnetic field energy. The number of full energy disruptions that the armor system can survive is very small. The consequences of multi-megaampere beams of runaway electrons (created in a disruption) hitting water-cooled armor tiles will be catastrophic for ITER if not mitigated. A survey of disruption features in existing machines is discussed. A coordinated global effort to avoid, control, and mitigate tokamak disruptions must be developed with the highest priority.

*Supported by DOE Contract DE-AC52-06-NA25396.

10:18

NO4 5 Spectrally resolved measurements of runaway electrons during plasma disruptions in the TEXTOR tokamak* TIMUR KUDYAKOV, OSWALD WILLI, *HHU* KARL HEINZ FINKEN, SADRILLA ABDULLAEV, MICHAEL LEHNEN, *FZJ* SERGEY BOZHENKOV, MARCIN JAKUBOWSKI, *MPI* YU-HONG XU, *LPP* A new diagnostic, a probe, has been developed to provide the absolute number of runaways and their spectrum at the plasma edge. Additionally, measurements of the thermal load from incident runaway electrons in the material were performed by two thermocouples installed in the probe. The probe consists of 9 YSO (Y_2SiO_5 : Ce) crystals. Different thicknesses of stainless steel filters allow to measure the spectrum of runaways with energies between 4 and 30 MeV. Disruptions were provoked by massive gas injection (Ar, Kr, Xe) in to stable TEXTOR discharges. In the thermal quench the loss of runaways produced at the start up of the discharge was detected by the probe. During the current quench a current plateau of runaway electrons is formed. It was found that during the current quench runaway electrons are coming from the plasma as a set of bursts. Such parameters of runaways as their absolute number, the spectrum and the corresponding thermal load in the tungsten plate were measured during thermal and current quenches.

*Funding of this work by GRK1203 is acknowledged.

10:30

NO4 6 Investigation of vapor cloud formation and dynamic behavior during plasma strikes similar to fusion disruptions TRAVIS GRAY, VIJAY SURLA, *University of Illinois at Urbana-Champaign* DAVID RUZIC, *Univeristy of Illinois at Urbana-Champaign* CENTER FOR PLASMA MATERIAL INTERACTIONS, UNIVERSITY OF ILLINOIS TEAM, The Divertor Erosion and Vapor shielding eXperiment (DEVeX) at the University of Illinois at Urbana-Champaign is designed to produce plasmas with densities on the order of 10^{21} m^{-3} with a electron temperature greater than 100 eV. This is accomplished with the rapid discharge of a 64 kJ capacitor bank through a conical shaped θ-pinch coil. This study utilizes a thin lithium film as the target. The expanding lithium vapor cloud is measured with an axial array of calibrated photodiodes. Vapor temperature is deduced from a collisional-radiative model of lithium interactions with energetic ions and electrons from the bombarding plasma and found to be 1-2 eV. The vapor cold is also found to cool adiabatically as it expands into the vacuum chamber after the plasma strike. Furthermore, the thin lithium film reduces the incident energy to the target (compared to a bare, non-lithium coated target) by up to 81%. The result is a significantly cooler target temperature under similar plasma bombardment.

10:42

NO4 7 The Negative Ion based Diagnostic Neutral Beam for ITER B. SCHUNKE, H. DECAMPS, M. DREMEL, R. HEMSWORTH, A. TANGA, *ITER Organization* M. BANDYOPHADHYAY, B. BARUAH, A. CHAKRABORTY, C. ROTTI, S. SHAH, M. SINGH, N. SINGH, *ITER India* The ITER dedicated Diagnostic Neutral Beam (DNB) is under construction. It is the basis for the Motional Stark Effect measurements at the ITER plasma edge and charge exchange spectroscopy. The DNB shares many features of the ITER Heating Neutral Beams (HNBs), but will operate only in hydrogen and inject ~ 2 MW of 100 keV of H^0 into the ITER plasmas. The same Cs seeded RF negative ion source is used as for the HNBs. The strong influence of the residual fields on the H^- and electrons in the accelerator has led to a new design of the magnetic filter in the ion source. Electron dumps consisting of parallel, vertical, cooled, plates between groups of beamlets immediately downstream of the accelerator prevent excessive electron power reaching the DNB cryopumps. The 4 channel gas neutralizer is made of cooled panels with special protection for the leading edges. Residual ions are deflected electrostatically onto cooled panels based on CuCrZr Heat Transfer Elements. A retractable calorimeter allows commissioning and beam profile measurements. It will be shown how imposed commonalities with the HNBs have influenced the design choices. The baseline DNB operating scenario and the engineering issues (lifetime, fatigue etc.), will be discussed.

10:54

NO4 8 The Motional Stark Effect Diagnostic for ITER* E.L. FOLEY, F.M. LEVINTON, H.Y. YUH, *Nova Photonics, Inc* The United States has been tasked with the development and implementation of a Motional Stark Effect (MSE) system on ITER. In the harsh ITER environment, MSE is particularly susceptible to degradation, as it depends on polarimetry, and the polarization reflection properties of surfaces are highly sensitive to thin film effects due to plasma deposition and erosion of a first mirror. We propose a comprehensive approach to the challenges, one which incorporates a sophisticated calibration system for the polarization measurement and also a spectrometer-based system for measurement of the line spacing in the Stark spectrum. The high fields and high beam energy in ITER allow this spectral measurement to be made with good precision for determination of the magnetic field magnitude. Conceptual designs for the MSE system on ITER will be presented.

*Supported By USDOE Contract No. S006930-F.

11:06

NO4 9 ITER IC H&CD system: physics requirements and performance predictions P. LAMALLE, B. BEAUMONT, F. KAZARIAN, A. LOARTE, R. MITTEAU, C. SCHÜLLER, *ITER Organization, CS 90 046, 13067 Saint-Paul-Lez-Durance, France* A. MUKHERJEE, *ITER India, GIDC, Gandhinagar, India* R. GOULDING, F. JAEGER, D. RASMUSSEN, D. SWAIN, *US ITER Project Office, ORNL, Oak Ridge, USA* R. SARTORI, *Fusion for Energy, Barcelona, Spain* M. NIGHTINGALE, *EURATOM/UKAEA Fusion Association, Abingdon, U.K.* E. LERCHE, A. LYSSOIVAN, A. MESSIAEN, D. VAN EESTER, R. WEYNANTS, *ERM-KMS, Association EURATOM-Belgian State, Brussels, Belgium* R. MAGGIORA, D. MILANESIO, *Politecnico di Torino, Torino, Italy* L. COLAS, R. DUMONT, *Euratom-CEA Association, CEA-Cadarache, France* The ITER Ion Cyclotron Heating and Current Drive (IC H&CD) system will deliver 20MW of radio frequency power to the plasma in quasi continuous operation during the different phases of the experimental programme. It must have a high availability and reliably couple to ELMy H-Mode plasmas. It has the additional functionality of performing wall conditioning (ICWC) at powers up to ~ 3MW. The paper will 1) discuss the physics and design requirements on the system, 2) review the main scenarios planned for H&CD and ICWC, 3) describe the main features of the current design, 4) discuss performance predictions based on recent modelling, and 5) present the key measures under implementation to reduce risks on performance.

11:18

NO4 10 SOL Width Studies for ITER Ramp-up* D.L. RUDAKOV, J.A. BOEDO, R.A. MOYER, *UCSD* R.A. PITTS, *ITER* A.W. LEONARD, G.L. JACKSON, *General Atomics* C.J. LASNIER, *LLNL* P.C. STANGEBY, *UTIAS* J.G. WATKINS, *SNL* L. ZENG, *UCLA* The present ITER scenarios contain limiter phases in Ohmic or L-mode for ramp-up and ramp-down. Dependencies of scrape-off layer (SOL) density and temperature e-folding lengths on discharge parameters were studied in inner-wall limited (IWL) and lower single null (LSN) discharges on DIII-D in order to benchmark the currently used power flux scaling based on divertor measurements from a number of tokamaks. Scans of the plasma current (q_{95}), density, and heating power have been performed. The power flux e-folding lengths derived from the reciprocating probe measurements near the outboard midplane in the IWL configuration are on the average a factor of $\sim$ 2 larger than those predicted by the scaling for an outer-wall limited configuration. Probe measurements in LSN configuration were also benchmarked against infrared camera data from the lower divertor.

*Work supported by US DOE under DE-FG02-07ER54917, DE-FC02-04ER54698, DE-AC52-07NA27344, DE-AC04-94AL85000, and DE-FG03-08ER54984.

11:30

NO4 11 Confinement and Pedestal Characteristics in H-mode With ECH Heating* R. PRATER, J.S. DEGRASSIE, P. GOHIL, T.H. OSBORNE, C.C. PETTY, *GA* E.J. DOYLE, *UCLA* B. HUDSON, *ORISE* M. MURAKAMI, *ORNL* Good global confinement in H-mode discharges when electron heating is dominant is critical to the success of ITER, since the proposed heating schemes predominantly heat electrons. Most of the world database is derived from discharges with high power positive-ion neutral beam injection (NBI), which primarily heats the ions. Issues for dominant electron heating include the H-mode power threshold and effect on rotation, density profile, global confinement, pedestal height, and ELM characteristics. In DIII-D the electron cyclotron heating power is 3.5 MW, so observations of these effects can be made at powers well above the threshold. A study of a few relevant discharges suggests that the H-mode pedestal is not much different from that in NBI, and the global confinement relative to balanced NBI-only may be around 10% smaller. The H-mode pedestal and ELM characteristics are also not greatly different than for NBI H-modes, and this will be compared with EPED1 modeling.

*This work was supported by the US DOE under DE-FC02-04ER54698, DE-FG03-01ERF54615, DE-AC05-06OR23100, and DE-AC05-00OR22725.

11:42

NO4 12 Dynamic Confinement of ITER Plasma by X-Mode Driver at Electron Cyclotron Frequency Range* V. ALEXANDER STEFAN, *Institute for Advanced Physics Studies (Stefan University)* Nonlinear interaction of the electron cyclotron X-Mode driver[1] with the ITER plasma leads to the dynamic rf plasma confinement in addition to the rf turbulent heating. The dynamics of unstable dissipative trapped particle modes (DTPM)[2] strongly coupled to Trivelpiece-Gould (T-G) modes is studied for the gyrotron frequency of 170GHz; X-mode power of 24 MW CW; and with on-axis B-field of 10T. In the case of dynamic control of DTPM turbulence and for the heavily damped T-G modes, the energy confinement time scalings are evaluated. The ITER plasma-ignition criterion is analyzed in terms of the X-Mode power.

*Supported by Nikola TESLA Lab., La Jolla, CA.

[1]R. Prater et. al., *Nucl. Fusion* 48, No 3 (March 2008).
[2]V. Alexander Stefan, 2009 APS April Meeting; May 2-5, 2009, Denver, Colorado; Abstract: K1.00028

11:54

NO4 13 ITER Test Blanket Module (TBM) Error Field Experiments in DIII-D* M.J. SCHAFFER, *General Atomics* J.A. SNIPES, *ITER Organization* Proposed ITER tritium breeding TBMs would contain ferromagnetic steel near the plasma and would make a localized peak magnetic perturbation of about 1.6%. While some effects can be computed, e.g. modified ion orbits, other important consequences cannot, such as global energy confinement and the L- to H-mode transition power. Therefore, an approximate scaled mockup of the error field from two TBMs in one port, as planned for ITER, will be installed temporarily in a DIII-D equatorial port to study its effects on plasmas. The mockup uses active electromagnet coils rather than passive steel for experimental flexibility. Numerical calculations show that the TBM error vacuum field has no strong resonant harmonics, but a natural resonant valley instead. However, the field has strong non-resonant harmonics, and non-resonant braking of plasma rotation is anticipated. The experiments will be performed in Autumn 2009, and we plan to report first results at this meeting.

*Work supported in part by the US DOE under DE-FC02-04ER54698 and Economic Stimulus Funds.

12:06

NO4 14 Turbulent impurity transport in ITER based on theory and CMOD data W. HORTON, SEAN FU, *Institute for Fusion Studies* W. ROWAN, I.O. BESPAMYATNOV, S. FUTATANI, *Universite de Provence, Case 321, 13397 Marseille Cedex 20, France* S. BENKADDA, *University of Texas at Austin* INSTITUTE FOR FUSION STUDIES COLLABORATION, INTERNATIONAL INSTITUTE FOR FUSION SCIENCE COLLABORATION, A key ITER issue is the turbulent radial transport from drift waves of impurities, especially beryllium. Impurtiy transport has been important in earlier tokamak transport research TFTR, CMOD and is treated for ITG in Dong and Horton, 1995. A new formulation based on nonlinear interactions of the dim=4 vector field associated with the eigenvalues and eigenvectors is formulated and solved for ITER parameters and for CMOD with Boron impurity. In a low dimensional truncation of the turbulence we find the bifurcations between L, H and ITB confinement regimes. Three-component fluid equations are used to find the eigenmodes and eigenfrequencies of the nonuniform, magnetized plasma with a four dimensional fluctuation vector X(k,n) composed of fluctuations of the electron density, the working gas ion density, the impurity density and the electrostatic plasma potential. The nonlinear dynamics is evaluated in (i) the collisional drift waves appropriate for the scrape off layer (SOL) and the edge plasma in limiter discharges and in (ii) the trapped electron mode-ITG core plasma taken in the limit of a Terry-Horton model. The particle fluxes are a function of the power spectrum of the plasma potential fluctuations and the gradient parameters charactering the L, H and ITB confinment modes. Fluctuation levels are taken from simulation.

12:18
NO4 15 High-Speed Pellet Injection for Ignition Experiments by Ignitor[1] F. BOMBARDA, A. FRATTOLILLO, S. MIGLIORI, *ENEA, Italy* L.R. BAYLOR, *ORNL* B. COPPI, *MIT* he path to ignition chosen by the Ignitor program[2] is based on the outstanding confinement and purity properties of high density plasma regimes. Typically, these correspond to peak densities $n_0 \cong 0.7 - 1 \times 10^{21}\mathrm{m}^{-3}$ and were discovered and investigated originally by axisymmetric high magnetic field machines. Record high values of density and confinement time were obtained on the Alcator C machine following the injection of deuterium pellets that were intended to stabilize modes of the ITG kind. In order to control the density profile during the initial current rise phase of the discharge, which is critical for optimizing the Ohmic and fusion heating rates in Ignitor, a fast pellet injector has been developed in collaboration between ENEA and ORNL. The 4- barrel, two stage injector will deliver pellets of different size and speeds into the plasma from the low field side. The Ignitor Pellet Injector (IPI) has completed two experimental campaigns, reaching pellet speeds up to 2 km/s, and a third campaign is due soon. After reaching the target performances ($\leqslant$ 4 km/s), the injector will be ready for installation on existing experiments. Simulations carried out for JET and LHD indicate that on both devices the IPI could provide much needed deep fueling in high temperature plasmas. [1]Sponsored in part by ENEA of Italy and by the U.S. D.O.E. [2]B. Coppi, A. Airoldi, et al., *Nucl. Fusion* **41(9)**, 1253 (2001)

12:30
NO4 16 High Particle Density Path to Fusion* B. COPPI, *MIT* F. BOMBARDA, P. DETRAGIACHE, *ENEA* A. AIROLDI, G. CENACCHI, *CREATE* A. SESTERO, Experiments by the heliotron LHD machine have confirmed the outstanding confinement and purity properties of plasmas with peak densities $n_0 \sim 10^{21} m^{-3}$ that had been originally discovered and investigated by the high-field line of machines (Alcator and FT). The finding of these regimes opened the way to aim at reaching ignition conditions on the basis of existing knowledge of plasma physics and available technologies. The high field and high particle density approach represented by Ignitor [1] ($R_0 \cong 1.32$ m, $a \times b \cong 0.47 \times 0.86\ m^2$, $B_T \leqslant 13$ T, $I_p \leqslant 11$ MA) remains the only one that can be pursued realistically in the near term in order to reach ignition. The choice of machine parameters have been guided by the criterion of optimizing the Ohmic and α-particle heating process, with the possible assistance of modest amount of RF power, and that of studying the physics and the control of meaningful burning plasmas in regimes sufficiently far from well known operational limits (e.g. density and β limits). Achieving these conditions (including, $t_{pulse} \sim \tau_{crd} \gg \tau_E \gg \tau_{sd}$) will provide the proof of scientific feasibility of power producing reactors. Studies of reactors concepts (e.g. material testing reactors, neutron sources, tritium poor reactors, etc.) based on the Ignitor approach are being reconsidered. *Sponsored in part ENEA of Italy and by the U.S. D.O.E. [1] B. Coppi, A. Airoldi, F. Bombarda, *et al., Nucl. Fusion* **41 (9)**, 1253 (2001).

SESSION NO5: FAST IGNITION
Wednesday Morning, 4 November 2009
Hanover CDE at 9:30
Richard Petrasso, Massachusetts Institute of Technology, presiding

9:30
NO5 1 Anomalous Divergence of Laser-Generated Hot Electrons Generated in a Cone Geometry* R.B. STEPHENS, K.U. AKLI, E.M. GIRALDEZ, *GA* T. MA, M.S. WEI, T. YABUUCHI, F.N. BEG, *UCSD* H.S. McLEAN, A.G. MacPHEE, M.H. KEY, L. DIVOL, D. HEY, A.J. KEMP, D. LASON, S. LE PAPE, A.J. MACKINNON, P.K. PATEL, S.C. WILKS, *LLNL* V.M. OVCHINNIKOV, R.R. FREEMAN, L.D. VAN WOERKOM, *Ohio State U.* C.D. CHEN, *MIT* Y.Y. TSUI, R. FEDOSEJEVS, *U. Alberta* Short pulse, lasers generate hot electrons at the cone tip in a Fast Ignition (FI) target. Previous flat foil studies suggest they propagate forward, diverging by $\sim$ 40° [1]. Those experiments used thin-walled cones in vacuum, allowing electrostatic fields on the outside surface of the cone to redirect errant electrons. In an FI target the cone will be embedded in blow-off plasma, removing those fields. We have emulated such conditions with thick-walled cones. Initial results suggest that electrons produced in such geometry diverge much more widely than seen in flat foils. The size of this effect and its dependence on tip size will be discussed.[1] R.B. Stephens, *et al.*, *Phys. Rev. E* **69**, 066414 (2004).

*Work supported by the US DOE under DE-FG02-05ER54834 and DE-AC52-07NA27344.

9:42
NO5 2 Resistive Stopping of Fast Electrons in Fast Ignition D.P. HIGGINSON, B. WESTOVER, T. BARTAL, S. CHAWLA, T. MA, M.S. WEI, *UCSD* C.D. CHEN, D.S. HEY, P.K. PATEL, H. CHEN, M.H. KEY, A.J. MACKINNON, A.G. MacPHEE, H. McLEAN, S. LE PAPE, *LLNL* K.U. AKLI, R.B. STEPHENS, *GA* R.R. FREEMAN, L.D. VAN WOERKOM, *The Ohio State Univ.* F.N. BEG, *UCSD* The mechanisms of fast electron generation and transport are of critical important to the fast ignition approach to inertial confinement fusion. Fast electrons in multi-layered Al/Cu/Al/Ag/Al targets were created on the Titan Laser (150 J, 0.7 ps, $4\text{x}10^{19}$ W/cm^2). The relative importance of resistive and collisional stopping effects was studied by varying the Ag layer depth. K shell fluorescence from Cu and Ag were measured with a highly oriented pyrolytic graphite spectrometer, which was cross-calibrated with a single photon counting charged coupled device. Analysis is performed with the collisional Monte Carlo code ITS 3.0 by injecting hot electrons into a cold target using the absolutely calibrated K shell yeilds as constraints. A comparison is made with the hybrid/PIC code LSP to demonstrate resistive effects [1]. This work was supported by the US DOE under contracts DE-FC02-04ER54789 (Fusion Science Center) and DE-FG-02-05ER54834 (ACE). [1] M.S.Wei et al., this conference.

9:54

NO5 3 Integrated Fast-Ignition Experiments on OMEGA W. THEOBALD, C. STOECKL, V.YU. GLEBOV, F.J. MARSHALL, K.S. ANDERSON, R. BETTI, R.S. CRAXTON, D.D. MEYERHOFER, P.M. NILSON, T.C. SANGSTER, A.A. SOLODOV, *Laboratory for Laser Energetics, U. of Rochester* J.A. FRENJE, R.D. PETRASSO, *PSFC, MIT* D. HEY, P.K. PATEL, *LLNL* R.B. STEPHENS, *General Atomics* R. LAUCK, *PTB, Germany* P.A. NORREYS, *RAL, UK* Integrated fast-ignition experiments using room-temperature cone-in-shell targets have begun at the Omega/Omega EP Laser Facility. Empty 40-μm-thick CD shells are imploded using 54 UV beams. At the time of peak compression, a short-pulse ($\sim$ 10 ps) IR laser with energy $>$ 1 kJ is focused into the tip of the hollow cone. A three-fold increase in time-integrated 2- to 7-keV x-ray emission was observed, indicating that fast-electron energy is coupled into the core. Neutron detectors are strongly affected by the emission of an intense γ-ray pulse, making it challenging to measure neutron yield. Significant reduction of the γ-ray background has been achieved by gating the MCP detector and using a liquid scintillator to suppress the afterglow. The D_2 neutron yield is being measured. This work was supported by the U.S. Department of Energy Office of Inertial Confinement Fusion under Cooperative Agreement Nos. DE-FC52-08NA28302, DE-FC02-04ER54789, and DE-FG02-05ER54839.

10:06

NO5 4 Integrated Fast ignition Experiments on the NIF* PRAVESH PATEL, PETER AMENDT, DAN CLARK, BRUCE COHEN, DAN HEY, LAURENT DIVOL, DOUG HOMOELLE, NOBUHIKO IZUMI, ANDREAS KEMP, MIKE KEY, DAVID LARSON, BARBARA LASKINSKI, SEBASTIEN LE PAPE, ANDREW MACKINNON, ANDREW MACPHEE, HARRY MCLEAN, DON MEEKER, YUAN PING, HANK SHAY, DAVID STROZZI, MAX TABAK, RICHARD TOWN, SCOTT WILKS, *Lawrence Livermore National Laboratory* The National Ignition Facility at LLNL will provide the first capability for assembling the fuel mass and ρR required for full-scale Fast Ignition. A quad of NIF beams converted to short-pulse operation will provide an ignitor pulse with which to determine the efficiency of fast electron energy coupling to the ignition hot spot. In this talk we review progress in the design of fast ignition core heating experiments that use: (i) 600 kJ of NIF laser energy in indirect-drive to compress DT (cryo) and CD (warm) capsules, and (ii) 8 kJ of ARC at 5 ps duration injected via a Au cone to heat the assembled fuel. We describe 2-D integrated hohlraum and capsule designs that optimize the peak density, ρR and spatial uniformity of the fuel assembly around the cone tip. The interaction of the short-pulse ignitor beam in the cone is simulated with the 3-D PSC explicit particle-in-cell (PIC) code, and the subsequent transport of the electrons and core heating calculated with the LSP hybrid transport code.

*This work performed under the auspices of the U.S. Department of Energy by Lawrence Livermore National Laboratory under Contract DE-AC52-07NA27344.

10:18

NO5 5 Transport Simulations for Fast Ignition on NIF* D.J. STROZZI, M. TABAK, D.P. GROTE, R.P.J. TOWN, A.J. KEMP, *Lawrence Livermore National Lab* Calculations of the transport and deposition of a relativistic electron beam into fast-ignition fuel configurations are presented. The hybrid PIC code LSP is used, run in implicit mode and with fluid background particles. The electron beam distribution is chosen based on explicit PIC simulations of the short-pulse LPI. These generally display two hot-electron temperatures, one close to the ponderomotive scaling and one that is much lower. Fast-electron collisions utilize the formulae of J. R. Davies [S. Atzeni et al., Plasma Phys. Controlled Fusion 51 (2009)], and are done with a conservative, relativistic grid-based method similar to Lemons et al., J. Comput. Phys. 228 (2009). We include energy loss off both bound and free electrons in partially-ionized media (such as a gold cone), and have started to use realistic ionization and non-ideal EOS models. We have found the fractional energy coupling into the dense fuel is higher for CD than DT targets, due to the enhanced resistivity and resulting magnetic fields. The coupling enhancement due to magnetic fields and beam characteristics (such as angular spectrum) will be quantified.

*Prepared by LLNL under Contract DE-AC52-07NA27344.

10:30

NO5 6 Simulations of Directly-Driven Cone-in-Shell Implosions* R.P.J. TOWN, D.S. CLARK, M.M. MARINAK, H.D. SHAY, M. TABAK, D.S. HEY, P.K. PATEL, *Lawrence Livermore National Laboratory* K.S. ANDERSON, R. BETTI, W. THEOBALD, *Laboratory for Laser Energetics, U. of Rochester* In fast ignition a short-pulse high intensity laser is used to generate relativistic electrons that subsequently deposit their energy into the compressed fuel to initiate a propagating burn wave. A high-density cone is often inserted into the capsule to allow a clear path for the ignition laser to the compressed fuel. The presence of the cone alters the dynamics in two ways from a spherically symmetric implosion. First, x-ray preheat can be absorbed by the cone causing the cone material to expand ahead of the imploding fuel leading to mixing of the high-Z cone material into the fuel. Second, the stagnation of the fuel near the cone can launch a jet into the cone increasing the transport distance of the short-pulse generated relativistic electrons. This paper reports on HYDRA simulations of directly driven OMEGA-scale plastic capsule implosions.

*This work performed under the auspices of the U.S. Department of Energy by Lawrence Livermore National Laboratory under Contract DE-AC52-07NA27344.

10:42

NO5 7 Simulations of Electron-Beam Transport in Solid-Density Targets and the Role of Magnetic Collimation A.A. SOLODOV, M. STORM, J.F. MYATT, R. BETTI, D.D. MEYERHOFER, P.M. NILSON, W. THEOBALD, C. STOECKL, *Laboratory for Laser Energetics and FSC, U. of Rochester* Three-dimensional simulations of solid-target electron-transport experiments at the Laboratory for Laser Energetics have been performed, using the hybrid-PIC code *LSP*. The experimentally observed fast-electron divergence half-angle of 16[r] in the target was reproduced assuming an initial divergence half-angle of $\sim$ 56[r], close to the value expected from the simple ponderomotive acceleration formula: $\theta_{1/2} = \tan^{-1}[\sqrt{2/(\gamma-1)}]$, where γ is the electron relativistic factor. The simulations accurately reproduce the details of

the electron transport observed in the experiment. The electron beam propagates as an expanding annulus that breaks into filaments because of the resistive filamentation instability. The electron-beam partial collimation and annular propagation is due to the resistive azimuthal magnetic field generated at the outer edge of the electron beam. Features of the electron-beam transport through the cone tip of fast-ignition cone-in-shell targets will also be discussed. This work was supported by the U.S. Department of Energy under Cooperative Agreement Nos. DE-FC02-04ER54789 and DE-FC52-08NA28302.

10:54

NO5 8 LSP modeling of fast electron transport and K-shell x-ray production in multiple-layer solid targets* H.K. CHUNG, M.S. WEI, B. WESTOVER, D.P. HIGGINSON, B.S. PARADKAR, F.N. BEG, *University of California, San Diego* K.U. AKLI, R.B. STEPHENS, *General Atomics* T. MA, P.K. PATEL, M.H. KEY, H.S. McLEAN, *Lawrence Livermore National Laboratory* J. MYATT, *LLE, University of Rochester* Understanding of fast electrons transport is crucial for Fast Ignition of Inertial Confinement Fusion. In experiments, transport of high intensity laser produced electrons is generally characterized by measuring fast electron produced K-shell photons using x-ray spectroscopic technique. Results from recent experiments performed at the Titan laser show that Ag Kα yield is insensitive to the buried depth in Al/Cu/Al/Ag/Al targets [1]. We have performed a series of 2D hybrid/PIC simulations using LSP code to model fast electron transport and Kα production in such targets to study underlying physics. The details of simulation results along with comparison with experimental data will be presented. [1] D.P. Higginson et al., this conference.

*Work supported by US DOE under contracts DE-FC02-04ER54789 (Fusion Science Center) and DE-FG02-05ER54834 (ACE).

11:06

NO5 9 Numerical study of the effects of preformed plasma on the fast electron transport* B.S. PARADKAR, M.S. WEI, T. YABUUCHI, F.N. BEG, *UCSD* R.B. STEPHENS, *GA* Recent short pulse laser-solid interaction experiments performed at ILE, Japan [T. Yabuuchi et. al., Bull Am Phys Soc 2008.DPP.JP6.113] have reported pre-formed plasma causing a ring-like Kα x-ray emission around the central bright spot from a Cu fluorescence layer buried between Al layers. To explain this, we have performed a series of 2D hybrid/PIC simulations with LSP code to model fast electron transport in pre-formed plasma. The pre-formed plasma and corresponding thermoelectric azimuthal magnetic fields are obtained by simulating the long pulse laser-solid interaction with 2-D radiation hydrodynamic code, h2d [larsen@casinc.com]. The LSP simulations suggest that the ring structure is due to the fast electrons deflected by B-fields into the pre-plasma and then reflected back by electrostatic sheath fields excited near the transverse edge of plasma plume. The details of simulation results along with comparison with experimental data will be presented.

*Work supported by US DOE under contracts DE-FC02-04ER54789 (Fusion Science Center) and DE-FG02-05ER54834 (ACE).

11:18

NO5 10 Resistive filamentation and collimation of relativistic electron beams in the fast ignition scenario JAVIER HONRUBIA, ARNAUD DEBAYLE, *Technical University of Madrid, Spain* EMMANUEL D'HUMIERES, *CELIA, Universite Bordeaux 1, France* SAMUEL MICHEAU, *The Queens University of Belfast, U.K.* VLADIMIR TIKHONCHUK, *CELIA, Universite Bordeaux 1, France* We have reported recently resistive filamentation and magnetic collimation of relativistic electron beams with currents around 1 GA and 10 – 20 ps pulses [J.J. Honrubia and J. Meyer-ter-Vehn, *Nucl. Fus.* **46**, L25 (2006): *Plasma Phys. Control. Fus.* **51**, 014008 (2009).]. Beam collimation due to self-generated magnetic fields reduces significantly the ignition threshold of imploded fuel capsules and depends strongly on the source size and the initial distribution function of relativistic electrons. We will demonstrate fast ignition integrated simulations in 2D axisymmetric geometry including 1) laser-driven relativistic electron sources obtained by 2D PIC simulations for actual laser intensities and pulse durations, 2) optimized configurations of the assembled fuel in re-entrant cone targets, and 3) interaction of fast electrons with the cone tip. The material of the cone tip has been selected as a compromise between hydrodynamic and electron transport requirements to guarantee the cone tip survival and to minimize the electron energy loss and scattering. We will provide estimates for the ignition energies.

11:30

NO5 11 Numerical simulations of laser hole boring for fast ignition fusion* R. TRINES, P. NORREYS, *STFC Rutherford Appleton Laboratory, Didcot, UK* G. SARRI, M. BORGHESI, *Queens University, Belfast, UK* Hole boring fast ignition is an attractive scenario for fast ignition (FI) fusion, as it requires much simpler targets than cone guided FI, a clear advantage for future operations at high repetition rate. In a recent experiment at the Rutherford Appleton Laboratory, hole boring has been investigated in a laser parameter regime (25 ps, 10^{18} W/cm^2) that is relevant to realistic FI scenarios but has scarcely been investigated before. We have conducted particle-in-cell simulations of laser-driven hole boring in plasma that follow the conditions of this experiment, i.e. at the critical density and at 1% of the critical density. At the lower density most of the laser energy is transmitted through the plasma, while at the higher density most of the energy is absorbed, leading to large differences in the evolution of the laser-driven channel. Good agreement between the numerical and experimental results has been obtained. Possible physical mechanisms underlying the hole boring process and the consequences of our findings for hole boring FI will be discussed.

*We gratefully acknowledge the Osiris consortium for the use of Osiris 2.2. This work is supported by the STFC Accelerator Science and Technology Centre.

11:42

NO5 12 Modeling the Modification of Escaping Energetic Electron Spectrum by Target Charging with LSP* A. LINK, R.R. FREEMAN, D.W. SCHUMACHER, L.D. VAN WOERKOM, *The Ohio State University* M.S. WEI, F.N. BEG, *University of California, San Diego* M.H. KEY, A.J. MACKINNON, P.K. PATEL, *Lawrence Livermore National Laboratory* R.B. STEPHENS, *General Atomics* Ultraintense lasers interacting with solid density plasma transfer their energy to electrons at the laser-plasma interface (LPI). The resulting electron spectrum is typically acquired by direct measurement of the electrons which escape the plasma. A 1D capacitor model and 2D LSP simulations

were used to determine the relationship between the externally measured spectrum and the in situ spectrum. A time and space varying electron source was generated consistent with electron temperature scaling laws and experimentally observed laser to electron energy coupling as the input for the models. Results will be presented for the modification of the escaped electron spectrum's energy, angular, and temporal properties for a collisional plasma with pulse durations of 70 fs and 700 fs.

*Work supported by the U.S. Department of Energy under contracts DE-FG02-05ER54834, DE-AC52-07NA27344 and by an allocation of computing time from the Ohio Supercomputer Center.

11:54

NO5 13 Characteristics of fast electrons generated in laser-cone interaction for the HiPER project SAMUEL MICHEAU, *Centre for Plasma Physics, The Queen's University of Belfast, Belfast, United Kingdom* ARNAUD DEBAYLE, *ETSI Aeronauticos, Universidad Politecnica de Madrid, Spain* EMMANUEL D'HUMIERES, *CELIA, Universite Bordeaux 1, CNRS, CEA, Talence, France* JAVIER HONRUBIA, *ETSI Aeronauticos, Universidad Politecnica de Madrid, Spain* MARCO BORGHESI, MICHAEL GEISSLER, *Centre for Plasma Physics, The Queen's University of Belfast, Belfast, United Kingdom* The fast ignition scheme considered for future facilities such as HiPER relies on the efficient generation and propagation of a relativistic electron beam to ignite a pre-compressed fusion pellet. Conical targets have proven to be very attractive to produce high-energy electrons close to the core plasma. However, hybrid PIC simulations have shown that the coupling efficiency between the high-energy electrons and the dense core is highly sensitive to the initial properties of the fast electrons. Here, we present 2D-PIC simulations with the code ILLUMINATION of the laser-cone interaction. We focus on the characteristics of the fast electron beam emitted at the cone tip, such as divergence, temporal evolution, energy and spatial distributions, as a function of the interaction parameters, so as to reach the requirements for fast ignition.

SESSION NO6: COMPLEX PLASMAS
Wednesday Morning, 4 November 2009
Hanover FG at 9:30
Jeremiah Williams, Wittenberg University, presiding

9:30

NO6 1 Observation of frequency cutoff for self-excited dust acoustic waves* V. NOSENKO, S.K. ZHDANOV, G.E. MORFILL, *Max-Planck Institute for extraterrestrial Physics* S.-H. KIM, J. HEINRICH, R.L. MERLINO, *Department of Physics and Astronomy, Univ. of Iowa, Iowa City Iowa 52242* Complex (dusty) plasmas consist of fine solid particles suspended in a weakly ionized gas. Complex plasmas are excellent model systems to study wave phenomena down to the level of individual "atoms." Spontaneously excited dust acoustic waves were observed with high temporal resolution in a suspension of micron-size kaolin particles in a dc discharge in argon. Wave activity was found at frequencies as high as 400 Hz. At high wave numbers, the wave dispersion relation was acoustic-like (frequency proportional to wave number). At low wave numbers, the wave frequency did not tend to zero, but reached a cutoff frequency f_c instead. The value of f_c declined with distance from the anode. We propose a simple model that explains the observed cutoff by particle confinement in plasma. The existence of a cutoff frequency is very important for the propagation of waves: the waves excited above f_c are propagating, and those below f_c are evanescent.

*Work at University of Iowa funded by DOE.

9:42

NO6 2 Laboratory observations of self-excited dust acoustic shock waves* ROBERT L. MERLINO, JONATHON R. HEINRICH, SU-HYUN KIM, *University of Iowa* Dust acoustic waves have been discussed in connection with dust density structures in Saturn's rings and the Earth's mesosphere, and as a possible mechanism for triggering condensation of small grains in dust molecular clouds. Dust acoustic waves are a ubiquitous occurrence in laboratory dusty plasmas formed in glow discharges. We report observations of repeated, self-excited dust acoustic shock waves in a dc glow discharge dusty plasma using high-speed video imaging. Two major observations will be presented: (1) The self-steepening of a nonlinear dust acoustic wave into a saw-tooth wave with sharp gradient in dust density, very similar to those found in numerical solutions [1] of the fully nonlinear fluid equations for nondispersive dust acoustic waves, and (2) the collision and confluence of two dust acoustic shock waves. [1] B. Eliasson and P. K. Shukla, Phys. Rev. E 69, 067401 (2004).

*Work supported by DOE

9:54

NO6 3 Externally driven dust density waves at low and high modulation frequencies* IRIS PILCH, TORBEN REICHSTEIN, ALEXANDER PIEL, *Institute for Experimental and Applied Physics, Christian-Albrechts University, D-24098 Kiel, Germany* An individual dust cloud, confined in an anodic glow discharge, immersed in a radio-frequency-produced plasma, is shown to support self-excited dust density waves (20-30 Hz), if the number of dust grains is sufficiently large. When the anode voltage is modulated at low frequencies (1-15 Hz) the self-excited wave is disturbed by a sloshing and stretching motion of the entire dust cloud. For higher frequencies (16-60 Hz), the self-excited wave is entrained at the external modulation frequency but a spatial wave decay can be found for frequencies above the eigenfrequency of the self-excited wave. If the frequency is further increased, the wave is not anymore entrained at the modulation frequency but the wave propagation is more coherent compared with the self-excited wave. We report on these dynamical features of externally modulated dust density waves.

*This work is supported by Deutsche Forschungsgesellschaft (DFG) under TR24-A2.

10:06

NO6 4 Time-dependent correlation buildup in spherical Yukawa balls* HANNO KAEHLERT, MICHAEL BONITZ, *ITAP, University of Kiel* In recent years it has become possible to create 3D dust crystals in experiments [1], where the particles arrange on concentric spherical shells. Compared to confined ions the interaction between the dust particles is screened, which has been shown to affect the shell occupation of the ground state [2], and the probability of metastable states [3,4]. Here we study dynamical processes in a trapped Yukawa plasma by means of Langevin dynamics simulations, which fully include the Coulomb

correlations, the confinement and friction with the neutral gas. By cooling a weakly correlated initial state towards the strong coupling regime, the formation of concentric shells is observed. While in systems with Coulomb interaction the shells clearly emerge at the cluster boundary, they appear almost simultaneously for sufficiently large screening. Monte Carlo simulations are used to show that the sequence, in which radial order is established, is determined by the confinement potential. [1] O. Arp, D. Block, A. Piel, and A. Melzer, PRL **93**, 165004 (2004) [2] H. Baumgartner et al., New J. Phys. **10**, 093019 (2008) [3] D. Block et al., Phys. Plasmas **15**, 040701 (2008) [4] H. Kählert et al., Phys. Rev. E **78**, 036408 (2008)

*Supported by the DFG via SFB-TR 24.

10:18

NO6 5 On the influence of wakefields on 3D particle arrangement* MATTIAS KROLL, JAN SCHABLINSKI, DIETMA BLOCK, ALEXANDER PIEL, *IEAP CAU Kiel* So far basically two different particle arrangements have been observed in 3D dust clouds. On the one hand,plasma crystals, trapped in the lower plasma sheath, feature among the hexagonal structure within the horizontal plane a distinctive chain structure in vertical direction. On the other hand, Yukawa balls show an isotropic structure of concentric shells [1]. The difference in structure is caused by the directed ion flow in the sheath. Because of this ion flow, the shielded interaction between particles is not the isotropic Yukawa potential, but rather takes the form of a wakefield [2]. However, the picture of either particle chains or hcp- odered dust clouds is too simple. The structure of plasma crystals is strongly affected by the confinement. In this contribution experiments with two particles trapped in the lower plasma sheath are presented. The particles were manipulated by a laser and their response is analyzed. Stereoscopic digital in-line holography as a novel diagnostic for dusty plasmas allows to observe the particle trajectories with high spatial and temporal resolution. The excitation of metastable particle positions will be demonstrated and their role for the 3D particle arrangement in dust clouds is discussed. [1] O. Arp et al., Phys. Rev. Lett. 93, 195002 (2004) [2] A. Melzer et al., Phys. Rev. E, Vol. 54 (1996)

*Financial support by the Deutsche Forschungsgemeinschaft via SFB-TR24 grant A3 is gratefully acknowledged.

10:30

NO6 6 Neutral Wind Effects on 3D-Clusters in RF Plasmas at Low Pressure FRANKO GREINER, JAN CARSTENSEN, LUJING HOU, ALEXANDER PIEL, *IEAP CAU Kiel, Germany* SFB-TR24 A2 TEAM, For the investigation of 2D dust clusters in RF plate reactors the neutral gas pressure is typically around 10Pa. In this regime, the flow is Knudsen like, i.e. the flow regime is between the hydrodynamical and the molecular dynamical flow regime. In this regime, a rotating electrode disk can be used to introduce a shear flow rotation of the neutral gas column. Using 2D dust clusters as high precision velocity detectors we found, that the flow can be described by hydrodynamic equations with no-slip boundary conditions.The fact that viscous neutral gas flows are possible even at low pressure can explain the observation,that the rotation of 2D dust clusters in a magnetic field parallel to the electric field of the plasma boundary, show rotation frequencies which are much higher then predicted. The "standard model" for rotation of dust in a magnetic field by pure ion wind force is based on the assumption, that neutral gas flows are not possible [POP 16, 013702, 2009]. In addition the rotating electrode can be used as a new technique to introduce torque to the dust grains without any drawback of the plasma. This torque can be used to modify horizontal confinement of the dust clusters. In this way the effective screening length in the plasma boundary can be measured without any prior knowledge of the plasma parameters.

10:42

NO6 7 Oscillatory Particle Motion in Dusty Plasma under Microgravity Conditions* JOHN GOREE, BIN LIU, *Univ. of Iowa* V.E. FORTOV, A.M. LIPAEV, V.I. MOLOTKOV, O. PETROV, *JIHT, Russian Acad. of Sciences, 125412 Moscow, Russia* G.E. MORFILL, H.M. THOMAS, R. ROTHERMEL, A. IVLEV, *Max-Planck-Institut für Extraterrestrische Physik, Garching, Germany* In an experiment aboard the International Space Station, performed using the PK-3 Plus instrument, 6.8-micron diameter polymer microspheres were introduced into a neon RF discharge at 0.2 Torr. The microspheres became highly charged in this dusty plasma. Microspheres were tracked by video micrography. The suspension had a void, and on one side there was only a single layer of microparticles. The random motion in this single layer was analyzed by spectral analysis methods, revealing the presence of oscillations. Microspheres oscillate about equilibrium positions determined by confining forces. The transverse, or out-of-plane, motion had a resonance frequency that allows us to compute a force constant $k = 2 \times 10^{-10}$ Nm^{-1} for the radial confining forces. These forces, QE and ion drag, are equal and opposite. Their magnitudes correspond to an acceleration in the range $0.2 - 0.4g$

*Work in Iowa was supported by NASA grant NNX07AD22G. Work in Germany was supported by supported by DLR/BMWi grant no 50WP0203 and by RFBR grant no. 06-02-08100.

10:54

NO6 8 Void formation and closure under microgravity for different gases VICTOR LAND, *Center for Astrophysics, Space Physics and Engineering Research, Baylor University, Waco, TX 76798, USA* DIANA BOLSER, *Participant in Baylor University's Summer Undergraduate Research Program* LORIN MATTHEWS, TRUELL HYDE, A self-consistent 2D dusty plasma fluid model used to model micro-gravity experiments in argon has been extended to allow the modeling of dusty plasmas in additional noble gases, including helium, krypton, neon, and xenon. The electron transport coefficients were obtained using BOLSIG+[1], whereas the ion transport coefficients were obtained from many literature sources, together with the thermal conductivity of the gases and the thermal accommodation coefficients. In this presentation we focus on the formation and closure of voids in microgravity experiments at different pressures and driving potentials, with the different noble gases. The goal is to provide a two-dimensional plot of the pressures and potentials at which 3D dust clouds under microgravity contain a dust-free void, or are void-free, for different carrier gases. This plot could serve as a road map for future experiments. [1] G. J. M. Hagelaar and L. C. Pitchford, Plasma Sources Sci. Technol. 14 (2005) 722-733

11:06
NO6 9 Interparticle Forces Between Dust Particles Confined within a Glass Box in a GEC Chamber JIE KONG, TRUELL HYDE, LORIN MATTHEWS, KE QIAO, ZHUANHAO ZHANG, *CASPER - Baylor University* BRANDON HARRIS, GARY SHETLER, STEVE RAPP, JIMMY SCHMOKE, MIKE COOK, *CASPER-Baylor University* The additional confinement provided by a glass box placed on the lower electrode of a GEC rf reference cell easily allows the generation of individual long vertical dust chains. This extended 1D vertical dust structure is ideal for the investigation of dust crystal vertical dispersion relations. It can also be used as a probe to allow the investigation of plasma parameters within the sheath. In this work, the oscillation spectrum of an extended 1D dust particle chain, driven through the addition of an external DC bias applied to the lower electrode, was examined. The vertical oscillation spectrum obtained using this experimental setup will be discussed and shown to exhibit significant differences as compared to the spectrum obtained for a dust particle pair without the glass box confinement.

11:18
NO6 10 Investigation of the Wakefield Interaction within 3D Dust Particle Clusters in a Complex Plasma KE QIAO, TRUELL HYDE, LORIN MATTHEWS, JIE KONG, JORGE CARMONA REYES, *CASPER - Baylor University* ZHUANHAO ZHANG, JIMMY SCHMOKE, MIKE COOK, *CASPER-Baylor University* Two-dimensional (2D) dust particle systems confined to a horizontal plane within a capacitively coupled rf discharge have been studied extensively over the past decade. However three-dimensional (3D) clusters, where the wake field interaction between particles often plays a major role, have not yet received the same amount of attention. In this research, stable 3D dust particle clusters, consisting of 1-5 particles, were formed in a complex plasma confined within a glass box. These clusters were examined over a range of powers in order to determine the various structural phases allowed by the system. As rf power was increased, the system was observed to exhibit a series of structural phase transitions. (For example, a 3-particle cluster can exist as a linear chain, a triangle in the vertical plane or a triangle in the horizontal plane.) Analysis employing a force-balance method was used to quantitatively determine the wakefield interaction between the particles.

11:30
NO6 11 A Study of the Resonance Frequency of Conductive Grains in a Dusty Plasma ZHUANHAO ZHANG, TRUELL HYDE, LORIN MATTHEWS, JIE KONG, JORGE CARMONA REYES, *CASPER - Baylor University* KE QIAO, JIMMY SCHMOKE, MIKE COOK, *CASPER-Baylor University* Over the past decade, the dynamic behavior of insulating (melamine formaldehyde) dust particles immersed in a complex plasma have been studied extensively. Phenomena such as disordered or ordered structures, the interaction of dust particles with the wake field produced by the ion flow, and the interaction between particles have all been the subject of both experimental and numerical investigation. However, the investigation of conducting materials in dusty plasmas has not yet received the same attention. In this work, the resonance frequency of conductive grains at various pressures and powers within a standard GEC reference cell is examined and the results compared to those for insulating grains (MF). Since the resonance frequency of a dust grain is proportional to its charge-to-mass ratio, such studies are beneficial in helping determine the particle charge. Preliminary results will be presented showing that in similar plasma environments, conducting grains do not exhibit the same behavior as non-conducting grains possibly due to differences in the charging process.

11:42
NO6 12 Layer Splitting in a Complex Plasma BERNARD SMITH, TRUELL HYDE, LORIN MATTHEWS, MEGAN JOHNSON, MIKE COOK, *CASPER - Baylor University* JIMMY SCHMOKE, *CASPER-Baylor University* Dust particle clouds are found in most plasma processing environments and many astrophysical environments. Dust particles suspended within such plasmas often acquire an electric charge from collisions with free electrons in the plasma. Depending upon the ratio of interparticle potential energy to average kinetic energy, charged dust particles can form a gaseous, liquid or crystalline structure with short to longer range ordering. An interesting facet of complex plasma behavior is that particle layers appear to split as the DC bias is increased. This splitting of layers points to a phase transition differing from the normal phase transitions found in two-dimensional solids. In 1993, Dubin noted that as the charged particle density of an initially two-dimensional Coulomb crystal increases the system's layers split at specific charge densities. This work modeled ions in a Paul or Penning trap, but may be applicable to dusty plasma systems as well. This work will discuss this possibility along with splitting observed in the CASPER GEC rf Reference Cell at specific pressures and powers.

11:54
NO6 13 Potential Structure Formation in the Gas-Liquid Interfacial Plasmas* TOSHIRO KANEKO, TAKASHI HARADA, QIANG CHEN, RIKIZO HATAKEYAMA, *Department of Electronic Engineering, Tohoku University* Specific kinds of plasmas composed of ionic liquids and gas phase discharge plasmas are created. These novel gas-liquid interfacial plasmas could contribute to the effective creation and modification of nano-bio materials, where the control of ion behavior in both the gas and liquid phases is desired. In this study, the plasma source containing the ionic liquids is developed for clarifying the effects of the ionic liquids on the plasma generation and the potential structure formed in the gas-liquid interfacial region is investigated for controlling the ion motion A direct current (DC) or a pulsed DC discharge plasma is generated just above the ionic liquid by applying the DC or the pulsed DC voltage to an electrode immersed in the ionic liquid against a grounded electrode set in the gas phase region. The precise potential structure between these electrodes through the gas-liquid interfacial region is clarified, and the dynamics of the plasma ions is found to be controlled using the sheath electric field in the interfacial region. The control of the plasma ion irradiation flux and energy to the ionic liquid leads to the creation of various kinds of nanoparticles.

*Work was supported by a Grant-in-Aid for Scientific Research from the Ministry of Education, Culture, Sports, Science and Technology, Japan.

12:06
NO6 14 Scaling Studies of Pair Production by Ultraintense Lasers EDISON LIANG, ALEXANDER HENDERSON, TAL EINAV, PABLO YEPES, *Rice University* HUI CHEN, SCOTT WILKS, *Lawerence Livermore National Laboratory* Using a combination of particle-in-cell plasma kinetic simulations and the CERN GEANT code for pair production, we systematically study the pair production by ultraintense lasers irradiating gold targets.

We will present results for the pair production yield as a function of laser and target parameters. Using these we will develop road maps for future experiments to optimize the pair yield. Applications of these results to both laboratory astrophysics and high density positronium physics will be discussed.

SESSION NP8: POSTER SESSION V
Wednesday Morning, 4 November 2009
Grand Hall East at 9:30

NP8 1 ELECTRON AND ION BEAMS AND RADIATION GENERATION

NP8 2 Results of the upgraded Neutralized Drift Compression Experiment* STEVEN M. LIDIA, F.M. BIENIOSEK, *Lawrence Berkeley National Laboratory* E.P. GILSON, *Princeton Plasma Physics Laboratory* P.K. ROY, P. NI, P.A. SEIDL, K. VAN DEN BOGERT, W.L. WALDRON, *Lawrence Berkeley National Laboratory* Recent changes to the NDCX beamline offer the promise of higher current compressed bunches, with correspondingly greater fluence delivered to the target plane for ion-beam driven warm dense matter experiments. We report modeling and commissioning results of the upgraded NDCX beamline that includes a new induction bunching module with approximately twice the volt-seconds and greater tuning flexibility, combined with a longer neutralized drift compression channel.

*This work was supported by the Director, Office of Science, Office of Fusion Energy Sciences, of the U.S. Department of Energy under Contract No. DE-AC02-05CH11231.

NP8 3 Simultaneous induction acceleration and bunching in the Neutralized Drift Compression Experiment* PETER SEIDL, G. BAZOUIN,[†]S.M. LIDIA, P.K. ROY, W.L. WALDRON, *Lawrence Berkeley National Laboratory* The Neutralized Drift Compression Experiment uses a ramped, bipolar induction module waveform to compress the beam to nanosecond bunches for the study of warm dense matter (WDM). We have recently explored beam dynamics and possible beamline modifications required to simultaneously compress and accelerate the beam using a unipolar waveform. This has the advantage of a higher energy deposition in the target, and mimics beam manipulations in next-generation ion accelerators for WDM experiments. We report modeling and experimental results of this beam manipulation on the NDCX beamline with the new induction bunching module with approximately twice the volt-seconds.

*This work was supported by the Director, Office of Science, Office of Fusion Energy Sciences, of the U.S. Department of Energy under Contract No. DE-AC02-05CH11231.
[†]Grenoble Institute of Technology

NP8 4 Design Studies for the induction cells for NDCX-II* J.W. KWAN, A. FALTENS, J.Y. JUNG, E.P. LEE, M. LEITNER, B.G. LOGAN, W.L. WALDRON, *LBNL* A. FRIEDMAN, *LLNL* The Heavy Ion Fusion Science Virtual National Lab is funded to build NDCX-II, at LBNL for high energy density (warm dense matter) and IFE target physics research. The goal is to produce Li+ ion beam with pulse length ~ 1 ns, energy ~ 3 MeV, beam charge per pulse ~ 20 nC, and rep rate ~ 0.02 Hz. The linac will reuse induction cells and Blumleins from the decommissioned Advanced Test Accelerator (ATA) at Lawrence Livermore National Laboratory. Among other changes, the original dc solenoid magnets will be replaced with new 2-3 T pulsed solenoids. The machine will have about 30 cells, a neutralized drift compression section, and a final focusing solenoid (8 T) followed by a target chamber. The total length of the machine will be about 15 m. One critical need is to avoid premature saturation of the induction cores due to the stray field generated by the pulsed solenoids. Another issue is beam steering due to misalignment of the magnetic axis. Testing of a prototype cell will be done to characterize the pulsed power and magnetic performance. These results will be presented in the meeting.

*Supported by DOE-OFES.

NP8 5 Multi-Meter-Long Plasma Source for Heavy Ion Beam Charge Neutralization* P.C. EFTHIMION, E.P. GILSON, R.C. DAVIDSON, *Plasma Physics Laboratory, Princeton University, Princeton, NJ* B.G. LOGAN, P.A. SEIDL, W. WALDRON, *Lawrence Berkeley National Laboratory, University of California, Berkeley, CA* Plasmas are a source of unbound electrons for neutralizing heavy ion beams to focus their radial and compress their axial dimensions to achieve high intensity beams for warm dense matter experiments. Long metal plasma columns are produced by the ferroelectric ceramic, $BaTiO_3$. The drift tube inner surface of the Neutralized Drift Compression Experiment (NDCX) is covered with ceramic material. High voltage (~ 8 kV) is applied across the ceramics. A $BaTiO_3$ source comprised of five 20-cm-long sources produced uniform plasma in the $5x10^{10}$ cm^{-3} density range and was used to achieve high beam compression ratios on NDCX. The source was extended to 2 meters and resulted in the heavy ion beam density increasing from $2x10^8$ to $7x10^{11}$ cm^{-3} and reducing the spot size to 1.5 mm. Present research is developing higher density sources by examining smaller diameter ferroelectric sources and flashboard circuits. A ferroelectric source of 2.9 cm ID achieved densities of $6x10^{11}$ cm^{-3}. Flashboards have the potential to achieve densities approaching 10^{13} cm^{-3}.

*Work Supported by US Department of Energy.

NP8 6 Collective Instabilities and Beam-Plasma Interactions for an Intense Ion Beam Propagating Through Background Plasma* RONALD DAVIDSON, MIKHAIL DORF, IGOR KAGANOVICH, HONG QIN, EDWARD STARTSEV, *PPPL* This paper presents a survey of the present theoretical understanding based on advanced analytical and numerical studies of collective interactions and instabilities for intense one-component ion beams, and for intense ion beams propagating through background plasma. The topics include: discussion of the condition for quiescent beam propagation over long distances; the electrostatic Harris instability and the transverse electromagnetic Weibel instability in highly anisotropic, one-component ion beams; and the dipole-mode, electron-ion two-stream instability (electron cloud instability) driven by an unwanted component of background electrons.

For an intense ion beam propagating through a charge-neutralizing background plasma, the topics include: the electrostatic electron-ion two-stream instability; the multispecies electromagnetic Weibel instability; and the effects of a velocity tilt on reducing two-stream instability growth rates. Operating regimes are identified where the possible deleterious effects of collective processes on beam quality are minimized.

*Research supported by the U. S. Department of Energy.

NP8 7 Collective Focusing of a Plasma-Neutralized Intense Ion Beam Propagating Along a Weak Solenoidal Magnetic Field* MIKHAIL A. DORF, IGOR D. KAGANOVICH, EDWARD A. STARTSEV, RONALD C. DAVIDSON, *Princeton Plasma Physics Laboratory, Princeton University* Two schemes are considered for focusing intense ion beams utilizing the collective dynamics of plasma electrons. In the first approach, an ion beam propagates through a neutralizing background plasma along a uniform magnetic field. In the second approach, an ion beam passes through a finite size plasma, extracts neutralizing electrons from the plasma, and then enters a magnetic lens. In the both cases, a strong radial electric field is produced due to the collective electron dynamics. This self-electric field provides the enhanced transverse focusing of the ion beam. Detailed analytical and advanced numerical studies using particle-in-cell simulations are performed for both approaches. The radial focusing force acting on beam ions is calculated for an arbitrary ratio between the electron cyclotron and plasma frequencies. Collective focusing effects are shown to be important for the design of heavy ion drivers for high energy density and warm dense matter physics applications.

*Research supported by the U.S. Department of Energy.

NP8 8 Approximate matched solution of an intense charged particle beam propagating through periodic quadrupole focusing lattice* E. STARTSEV, R. DAVIDSON, M. DORF, *PPPL* The transverse dynamics of an intense charged particle beam propagating through a periodic quadrupole focusing lattice is described by the nonlinear Vlasov-Maxwell system of equations, where the propagating distance plays the role of time. To find matched-beam quasi-equilibrium distribution functions one needs to determine a dynamical invariant for the beam particles moving in the combined applied and self-generated fields. In this paper, we present a perturbative Hamiltonian transformation method which is an expansion in the particle's vacuum phase advance $\epsilon = \sigma_v/2\pi$, treated as a small parameter, which is used to transform away the fast particle oscillations and obtain the average Hamiltonian accurate to order ϵ^3. The average Hamiltonian is an approximate invariant of the original system, and can be used to determine self-consistent beam equilibria that are matched to the focusing channel. In the third-order, the average self-field acquires a octupole component which results in the average motion of some beam particles being non-integrable and their trajectories chaotic. This chaotic behavior of the beam particles may significantly change the nature of the Landau damping (or growth) of collective excitations supported by the beam.

*Research supported by the U.S.Department of Energy.

NP8 9 Generalized Courant-Snyder theory and Kapchinskij-Vladimirskij distribution for high intensity beams in coupled transverse focusing lattices* HONG QIN, RONALD DAVIDSON, *Princeton Plasma Physics Lab, Princeton University* MOSES CHUNG, *Fermi National Accelerator Laboratory* Courant-Snyder (CS) theory for uncoupled transverse dynamics of charged particles is generalized to the case of coupled transverse dynamics with two degree of freedom. The generalized theory has the same structure as the original CS theory for one degree of freedom. The four basic components of the original CS theory, i.e., the envelope equation, phase advance, transfer matrix, and the CS invariant, all have their counterparts, with remarkably similarity, in the generalized theory. The envelope function is generalized into an envelope matrix, and the envelope equation becomes a matrix envelope equation with matrix operations that are non-commutative The generalized theory gives a new parameterization of the 4D symplectic transfer matrix that has the same structure as the parameterization of the 2D symplectic transfer matrix in the original CS theory. For high intensity beams, the generalized Courant-Snyder theory is applied to discover a generalized Kapchinskij-Vladimirskij distribution for high-intensity beams in coupled focusing lattices. This self-consistent distribution, which solves the nonlinear Vlasov-Maxwell equations, is 4D ellipsoid in the phase space. A set of envelope equations are derived to describe the dynamics of the phase space ellipsoid.

*Research supported by US DOE.

NP8 10 Relativistic Electron Beam Propagation in the Presence of Plasma Electron-Ion Collisions CARL SIEMON, VLADIMIR KHUDIK, GENNADY SHVETS, *University of Texas at Austin* The physics of relativistic electron beam propagation through a collisional background plasma and electromagnetic Weibel Instability is described. A reduced hybrid approach treats the beam electrons as macro-particles, plasma electrons as a fluid, and assumes stationary plasma ions. This treatment, along with the assumption of quasi-neutrality, provides a simplified, computationally efficient framework for solving this system. Collisional simulation results are presented, which sharply contrast collisionless dynamics in several areas. One striking feature of these simulations is the enhancement of beam stopping. The most obvious mechanism for this effect is a persistent stopping electric force along the propagation direction. During the merging of filaments, the coupling of Weibel Instability with collisions leads to beam deflection in addition to electric stopping, slowing the beam down further. This coupling occurs because of increased magnetic field strength due to enhanced current imbalance from collisions. The increased field strength decreases filament merging time, thus augmenting transverse thermalization, which occurs when filaments merge. Transverse thermalization results in a loss of beam momentum in the propagation direction. Other interesting phenomena present in collisional simulations include the reversal of the return current direction in selected regions.

NP8 11 Halo characterization of mismatched beams using the theory of violent relaxation* RENATO PAKTER, YAN LEVIN, TARCISIO N. TELES, *Instituto de Fisica - Universidade Federal do Rio Grande do Sul, Brazil* Relaxation to a final stationary state of particles interacting through long-range forces, such as Coulomb, is intrinsically different than that of systems with short-range interactions. While in the latter case it is known that the interparticle collisions drive the system to an equilibrium Maxwell-Boltzmann distribution, in the former case, the collision

duration time diverges and the state of thermodynamic equilibrium is never reached. In this paper, we extend previous results on the relaxation of initially rms mismatched beams,[1] by taking into consideration more general initial beam distributions. We also present results on the beam relaxation and halo formation based on an approximation of the theory that allows simpler analytic expressions for the final stationary state

*Work supported by CNPq, Brazil and the US-AFOSR under Grant No. FA9550-09-1-0283.

[1]Y. Levin, R. Pakter, T.N. Teles, Phys. Rev. Lett., **100**, 040604 (2008).

NP8 12 The controlling role of envelope mismatches in intense inhomogeneous charged beams* FELIPE RIZZATO, EVERTON SOUZA, ANTONIO ENDLER, *IF-UFRGS* RENATO PAKTER, *IF-IFRGS* ROGER NUNES, *FURG* Inhomogeneous cold beams undergo wave breaking as they move along the axis of a magnetically focusing system. All the remaining control parameters fixed, the earliest wave breaking is a sensitive function of the inhomogeneity parameter: the largest the inhomogeneity, the soonest the breaking The present work analyzes the role of the envelope size mismatches in the wave breaking process. The analysis reveals that the wave breaking time is also very susceptible to the mismatch. As mismatched and matched beams are compared, one finds out that judiciously chosen mismatches can largely extend the beam lifetimes. The work is extended to include some recently discussed issues: the presences of fast and slow regimes of wave breaking regimes are identified, and the role of thermal velocity distributions in space-charge dominated beams. In all instances, the theory is shown to be accurate against simulations.

*CNPq, CAPES, AFOSR FA9550-09-1-0283

NP8 13 Vlasov analysis of relaxation of intense inhomogeneous charged beams* ANTONIO ENDLER, EVERTON SOUZA, *IF-UFRGS* ROGER NUNES, *FURG* RENATO PAKTER, FELIPE RIZZATO, *IF-UFRGS* This work analyzes the dynamics of inhomogeneous, magnetically focused high intensity beams of charged particles. Initial inhomogeneities lead to density waves propagating transversely in the beam core, and the presence of transverse waves eventually results in particle scattering. Particle scattering off waves in the beam core ultimately generates a halo of particles with concomitant emittance growth. Emittance growth indicates a beam relaxing to its final stationary state, and the purpose of the present paper is to describe halo and emittance in terms of the Vlasov equation.

*CNPq, FAPERGS, AFOSR FA9550-09-1-0283.

NP8 14 Effect of Accelerator Impedance on Electron Cloud Instability* BRIAN ALLEN, PATRIC MUGGLI, *University of Southern California* WOLFRAM FISCHER, MICHAEL BLASKIEWICZ, *Brookhaven National Laboratory* THOMAS KATSOULEAS, *Duke University* Interaction between a beam and electron clouds (e-cloud) present in circular accelerators is known to limit accelerator performances through instabilities, beam loss, beam-blowup, and the resulting reduced luminosity. The RHIC beam is most susceptible to instabilities as it crosses energy transition (γ_t=22.9) and it is posited that ring impedance could play a role in the development of instabilities during this transition. We use the quasi-static particle in cell code QuickPIC to describe the interaction between the RHIC Au beam and the electron cloud. In QuickPIC the electron cloud density is uniform around the ring and the beam has a constant beta function given by the accelerator circumference and the beam tune. We incorporate in the current QuickPIC version the ring impedance for a circular accelerator and we take a first look at the effect this impedance has on the beam and e-cloud interaction for typical RHIC parameters.

*Work supported by the US Department of Energy

NP8 15 Dispersion characteristics of space-charge waves on elliptic electron beams* KATHLEEN GEYER, ANDREW BRAINERD, CHIPING CHEN, *Massachusetts Institute of Technology* A small-signal theory of space-charge waves on a relativistic elliptic electron beam has been developed recently [A. E. Brainerd, C. Chen and J. Zhou, J. Appl. Phys., in press (2009)]. This paper discusses results of a comprehensive parametric study of dispersion characteristics of space-charge waves on such beams over a wide range of the parameter space, using the MIT Elliptic Beam Small Signal (EBSS) code. Applications of the theory in elliptic-beam klystrons are discussed. Implications of the space-charge wave theory are discussed in the research and development of elliptic- or sheet-beam klystrons.

*Research supported by US Department of Energy, Office of High Energy Physics, Grant No. DE-FG02-95ER40919, and by the MIT Undergraduate Research Opportunity Program Endowment Fund.

NP8 16 Charged-Particle Dynamics in an Adiabatic Thermal Beam Equilibrium* HAOFEI WEI, CHIPING CHEN, *Massachusetts Institute of Technology* The dynamics of charged particles in a recently-discovered adiabatic thermal beam equilibrium [J. Zhou, K.R. Samokhvalova and C. Chen, Phys. Plasmas **15,** 023102 (2008)] are studied. In particular, test particle motion is analyzed numerically, assuming the beam equilibrium fields in a periodic solenoidal focusing channel. Poincare surface-of-section maps are generated to examine the behavior of the test particles in phase space such as nonlinear resonances and chaotic regions. Comparisons are made between the adiabatic thermal and rigid-rotor Vlasov beam equilibria [C. Chen, R. Pakter and R. C. Davidson, Phys. Rev. Lett. **79**, 225 (1997)].

*Research supported by US Department of Energy, Office of High Energy Physics, Grant No. DE-FG02-95ER40919, and by the MIT Undergraduate Research Opportunity Program Endowment Fund.

NP8 17 Piezoelectric Transformer Accelerator Systems for Neutron Interrogation* EMILY BAXTER, SCOTT KOVALESKI, ANDREW BENWELL, TONGTAWEE WACHARASINDHU, JAE KWON, *University of Missouri* The detection of nuclear materials such as highly enriched uranium has become increasingly important. The University of Missouri is developing a compact accelerator system for active neutron interrogation using a piezoelectric transformer with an ion diode for neutron production. The piezoelectric high voltage generator is composed of a rotated y-cut bar of lithium niobate and will ultimately be used to accelerate deuterium ions. When driven near resonance the device is capable of yielding very high voltages. The ion source will be

attached to an electrode on a piezoelectric transformer for subsequent ion acceleration. A number of ion sources are being studied, and relative merits of each will be presented, along with piezoelectric transformer performance results.

*This work is supported by the Nuclear Regulatory Commission and Qynergy.

NP8 18 Electron Beam Coupling to Electrical Metamaterial Structures DON SHIFFLER, *Air Force Research Lab* JOHN LUGINSLAND, JACK WATROUS, *Numerex LLC* DAVID FRENCH, *University of Michigan* Y.Y. LAU, Many authors over many decades have considered the coupling of electron beams to various microwave structures. These structures range from slow wave structures, such as traveling wave tubes, to dielectrics, such as the dielectric Cherenkov maser. In this presentation, we consider the coupling of relativistic electron beams to electronic metamaterials. We consider cylindrical and planar geometries and treat the electron beam as a cold, non-neutral plasma confined by an infinite magnetic field, confining motion of the electrons to the axial direction. We treat the metamaterial, which loads the cylindrical waveguide along its outer wall, using effective medium theory, considering cases of double positive, single positive, and double negative dielectrics. The presentation begins with a review of the cold structure characteristics in the absence of an electron beam and then moves to consider the coupling of the electron beam to the metamaterial. In particular we study the dispersion and small signal growth rate of this system, the frequency range of applicability, and the power handling potential of such structures.

NP8 19 RF power loss and electric and magnetic field enhancements due to surface roughness* PENG ZHANG, YUE YING LAU, RONALD GILGENBACH, *University of Michigan - Ann Arbor* Surface roughness plays an important role in a cavity or slow wave structure. It may cause enhanced RF power absorption. Excessive local electric field enhancement may trigger RF breakdown. In a superconducting cavity, local magnetic field enhancement due to surface roughness may lead to rapid loss of superconductivity. In this work, we analytically compute the power absorption due to a hemispherical protrusion with arbitrary values of ε, μ and σ on a metallic surface. Scaling laws are derived [1]. The local field enhancement factors of both electric and magnetic field on the protrusion are also calculated analytically, and spot-checked against a Maxwell-3D code [1]. The protrusion may represent a foreign object, or is made of the same material as the conducting surface, since its ε, μ and σ may take on arbitrary values. [1] P. Zhang *et al.*, J. Appl. Phys. **105**, 114908 (2009).

*This work was supported by AFOSR Cathode and Breakdown MURI04 grant number FA9550-04-1-0369, and by AFRL, L-3, and Northrop-Grumman Corporation.

NP8 20 Experiments and Simulations on a Discrete Element Nonlinear Transmission Line* DAVID FRENCH, *University of Michigan* DON SHIFFLER, *Air Force Research Laboratory* JOHN LUGINSLAND, *Numerex* RONALD GILGENBACH, Y.Y. LAU, *University of Michigan* Nonlinear transmission lines have been demonstrated to be an effective technique for generating high power ultrawideband or mesoband radiation without the need for a vacuum system, electron beam, or magnet. Preliminary experiments have been performed at AFRL and UM on a discrete element nonlinear transmission line with nonlinear capacitance. Depending on the injected pulse, either pulse sharpening or RF generation could be observed. The differences between these two cases and the threshold for RF generation will be discussed. Time frequency analysis has been applied to analyze the generated RF spectrum. These effects were reproduced in circuit simulations. Results from these preliminary experiments and plans for future high power nonlinear transmission line experiments using LTD technology at UM will be presented.

*Supported by AFOSR and AFRL.

NP8 21 Metal-Dielectric Washer Cathode for Relativistic Magnetron Plasma, Pulsed Power and Microwave Lab, University of Michigan, Ann Arbor, MI 48109-2104* MATTHEW FRANZI, RONALD GILGENBACH, *University of Michigan* BRAD HOFF, *Air Force Research Labs* Y.Y. LAU, ED CRUZ, *University of Michigan* The UM/L-3 relativistic magnetron operates at -300 kV, 2-10 kA, for durations of up to 1 microsecond and generates microwave pulses of 100's MW output power at 1 GHz for 100's ns. Recent research with the magnetron has focused on the exploitation of electrical triple points on the cathode to generate electron avalanching. This Metal-Dielectric Washer (MDW) cathode consists of alternating washers of OFHC-Cu and BN, which vary in radius for each tested triple point configuration. The MDW cathode exhibits high current and fast turn on times and does not degrade under magnetron operating conditions. Initial experimental results of the MDW cathode on the magnetron have shown electron emission currents up to 4 kA and microwave power between 100-200 MW. Experiments will be compared to simulation results. [1] N.M. Jordan, R.M. Gilgenbach, B.W. Hoff, and Y.Y. Lau, Rev. Sci. Inst. 79, 064705 (2008) [2] N. M. Jordan, Y. Y. Lau, D. M. French, R. M. Gilgenbach, and P. Pengvanich,, J. Appl. Phys. 102, 033301 (2007)

*Supported by the AFOSR, AFRL and the AFOSR MURI. Support also received from NG and L -3.

NP8 22 Buneman-Hartree Condition Re-Visited Y.Y. LAU, W. TANG, B. HOFF, R. GILGENBACH, *University of Michigan - Ann Arbor* J. LUGINSLAND, *NumerEx* K. CARTWRIGHT, *Air Force Reserach Laboratory* NUMEREX COLLABORATION, AIR FORCE RESEARCH LABORATORY COLLABORATION, The Buneman-Hartree condition (BHC) is re-examined in a cylindrical, smooth-bore, relativistic magnetron using both the conventional, single particle model, and the Brillouin flow model. These two models yield the same result for the BHC only in the limit of a planar magnetron. When b/a = 1.3, where a is the cathode radius and b ($>$ a) is the anode radius, the difference in BHC for the two models is significant. When b/a = 4, this difference becomes unexpectedly large. Such a difference is always present, whether the gap voltage is relativistic or not. These results are quantified for b/a $>>$ 1 using Davidson's model [1], conveniently cast in terms of the normalized gap voltage and normalized magnetic flux imposed on the cylindrical magnetron. This work is supported by AFOSR, AFRL, L-3, and Northrop-Grumman. [1] R. C. Davidson, Prco. SPIE 1061, p. 186 (1989).

NP8 23 Experimental Verification of Peer-to-Peer Magnetron Locking* EDWARD CRUZ, RON GILGENBACH, YUE LAU, BRAD HOFF, PHONGPHAETH PENGVANICH, *University of Michigan* Injection locking of conventional magnetrons, and other types of oscillators, employing a master-to-slave configuration has been studied theoretically and experimentally [1,2]. We have re-

cently derived the condition for peer-to-peer locking of two conventional magnetrons [3]. This condition reduces to Adler's classical locking condition (master-to-slave) if the coupling is one way. Dependent on the coupling, the frequency of oscillation when locking occurs does not necessarily lie between the free running frequencies of the two isolated, stand-alone magnetrons. Likewise, when the locking condition is violated, the beat frequency is not necessarily equal to the difference between these free running frequencies. These features were revealed in our recent experiments on the peer-to-peer locking of two 1-kW magnetrons. The necessary condition under which the two magnetrons may be locked to a common frequency is also experimentally verified. [1] P. Pengvanich et al., J. Appl. Phys. 98, 114903 (2005). [2] V. B. Neculaes, Ph.D. Dissertation, U. Michigan, Ann Arbor, MI (2005). [3] P. Pengvanich et al., Phys. Plasmas 15, 103104 (2008).

*Work supported by ONR and AFRL.

NP8 24 Effect of Cathode Alignment on Magnetron Operation SARITA PRASAD, MARVIN ROYBAL, C. JERALD BUCHENAUER, *Dept. of Electrical and Computer Engineering, University of New Mexico* KENNETH PRESTWICH, MIKHAIL FUKS, EDL SCHAMILOGLU, *Dept. of Electrical and Computer Engineering, University of New Mexico* Recently, relativistic magnetron experiments were conducted at the University of New Mexico (UNM) to demonstrate the effect of using a transparent cathode on magnetron operation. We fabricated an A6 magnetron at UNM and during the procedure the magnetron got distorted and the result is a slightly elliptical cross-section magnetron. Consequently, the anode-cathode (AK) gap is not uniform. Magnetron operation is known to be sensitive to RF field distribution in the interaction region, which in turn is sensitive to the AK gap. Despite the asymmetry the transparent cathode was still capable of showing overall improvement in magnetron operation, i.e. faster start of microwave oscillations, higher output powers and single mode operation over a wide range of magnetic field. Interestingly, the magnetron operated in the π-mode instead of the expected 2 π-mode. The solid cathode on the other hand showed mode competition and produced very low output powers. The elliptical magnetron geometry was studied using the 3-dimensional particle-in-cell code MAGIC in order to explain the experimental results.

NP8 25 Study of a Simple Gyrotron System MEIXUAN SHI, HAROLD WEITZNER, *New York University* This study surveys a typical coupled equations of the gyrotron system. A hypothetic non-constant media is proposed in order to study different parameter regions of the system. Instead of linearizing the equations, an asymptotic analysis is performed directly onto the Maxwell equation to get the asymptotic waveforms. Results of the linearized equations are recovered at faraway from the transition regions. In two transition regions, one for cut-off, one for resonance, connections forms are obtained. Conditions of getting high amplitude outgoing waves are achieved by substituting the asymptotic waveform back to the momentum distribution equation.

NP8 26 Testing of an Advanced Internal Mode Converter for a 1.5 MW, 110 GHz Gyrotron* D.S. TAX, I. MASTOVSKY, *MIT PSFC* J. NEILSON, *Calabazas Creek Research Inc.* M.A. SHAPIRO, J.R. SIRIGIRI, R.J. TEMKIN, A.C. TORREZAN, *MIT PSFC* Megawatt gyrotrons are under development for the electron cyclotron heating (ECH) of plasmas, including ITER. To optimize the efficiency of gyrotrons and of the transmission lines, the internal mode converter (IMC) should output a perfect Gaussian beam. The $TE_{22,6}$110 GHz IMC we have implemented consists of a helically-cut launcher and three smooth curved mirrors. The theoretically predicted output beam has waist $W_z = W_x = 2.9$ cm at the gyrotron window. Cold test measurements using a VNA and a 3-axis scanner were in good agreement with theory with measured beam waists $W_z = 2.9$ cm and $W_x = 2.7$ cm. We also installed the IMC in a 110 GHz, 1.5 MW, 3 μs pulsed gyrotron and measured the field pattern with over 40 dB signal to noise accuracy using an rf diode on a 2-axis scanner. Measured beam waists $W_z = 4.8$ cm and $W_x = 4.2$ cm compared well with theoretical waists $W_z = W_x = 4.7$ cm at a plane 124 cm from the gyrotron window.

*This research was supported by the DOE, Office of Fusion Energy Sciences.

NP8 27 Precision 0.5 GW X-band rf system for advanced Compton scattering source* T.S. CHU, G. ANDERSON, D. GIBSON, F.V. HARTEMANN, C.P.J. BARTY, *LLNL* A. VLIEKS, S. TANTAWI, E. JONGEWAARD, *SLAC* S.G. ANDERSON, *LLNL* LLNL COLLABORATION, SLAC COLLABORATION, A Mono-Energetic Gamma-Ray (MEGa-Ray) Compton scattering light source is being developed at LLNL. The electron beam for the Compton scattering interaction will be generated by a X-band RF gun and a X-band LINAC at the frequency of 11.424 GHz. High power RF in excess of 500 MW is needed to accelerate the electrons to energy of 250 MeV or greater for the interaction. Two high power klystron amplifiers, each capable of generating 50 MW, 1.5 msec pulses, will be the main high power RF sources for the system. These klystrons will be powered by state of the art solid-state high voltage modulators. A RF pulse compressor, similar to the SLED II pulse compressor, will compress the klystron output pulse with a power gain factor of five. This will give us 500 MW (0.5 GW) at output of the compressor. The compressed pulse will then be distributed to the RF gun and to the LINAC with specific phase and amplitude control points to allow for parameter control during operation. This high power RF system is being designed and constructed. In this paper, we will present the design, layout, and status of this RF system.

*This work performed under the auspices of the U.S. Department of Energy by Lawrence Livermore National Laboratory under Contract DE-AC52-07NA27344

NP8 28 Commissioning of a Compton-Scattering-Based Gamma Ray Source* DAVID GIBSON, FELICIE ALBERT, SCOTT ANDERSON, FRED HARTEMANN, MIKE MESSERLY, MIRO SHVERDIN, DENNIS McNABB, CRAIG SIDERS, CHRIS BARTY, *Lawrence Livermore National Lab* Recently a Compton-scattering based gamma-ray source, in which a high-intensity laser scatters off a high-brightness electron beam and emerges as a narrow-band gamma-ray beam, has been commissioned at Lawrence Livermore National Laboratory. Operating at energies from 0.1 to 0.9 MeV, the source produces fluxes upwards of 10^6 photons/sec with a brightness of 10^{15} photons/s/mm^2/mrad^2/0.1% BW. Presented here is a discussion of the design and performance of the laser and electron subsystems that are used to drive the source, and an overview of the parameters of the generated gamma-ray beam.

*This work performed under the auspices of the U.S. Department of Energy by Lawrence Livermore National Laboratory under Contract DE-AC52-07NA27344.

NP8 29 120-Hz Diode-Pumped Kilowatt Class Laser for Compton Scattering Sources ANDY BAYRAMIAN, GLENN BEER, ROB CAMPBELL, BARRY FREITAS, WILLIAM MOLANDER, STEVE SUTTON, STEVE TELFORD, CHRIS BARTY, *Lawrence Livermore National Laboratory* A Mono-Energetic Gamma-Ray (MEGa-ray) Compton scattering light source is currently based on a 120-Hz electron accelerator. A 120-Hz laser source can increase the current gamma ray production by more than an order of magnitude and further enhancements are possible. Diode pumped solid state lasers (DPSSLs) offer the potential to operate at these higher repetition rates where flash lamp pumped laser systems are currently limited by thermal and lamp lifetime issues. Utilizing LLNL expertise in high energy DPSSLs, a 10-J, 120-Hz diode-pumped Nd:YAG laser architecture has been developed. The laser design makes use of advances in diode packaging, power conditioning, and beam conditioning to provide over 100-kW peak power array. Sapphire heatsinks and longitudinal cooling of the amplifier yields low parasitic loss and low wavefront distortion. An image relayed architecture and adaptive optics will yield a diffraction limited beam ideal for Compton scattering. This work was performed under the auspices of the U.S. Department of Energy by Lawrence Livermore National Laboratory under Contract DE-AC52-07NA27344.

NP8 30 Generating radiation in terahertz frequency range by means of two-stream instability NIKOLAI YAMPOLSKY, KIP BISHOFBERGER, BRUCE CARLSTEN, RICKEY FAEHL, TENGIZ SVIMONISHVILI, *Los Alamos National Laboratory* Generating radiation in the terahertz frequency range using methods developed in electronics is complicated. These methods imply the use of a slow-wave structure which is designed to match the dispersion curves of the electro-magnetic mode and the electron beam traveling slower than the speed of light. Such a slow-wave structure should have the scale on the order of the radiation wavelength, which is 100 μm for 3 THz radiation. Moreover, metal-based structures become ineffective in this frequency range due to high losses. Alternatively, two electron beams having close energies develop the two-stream instability resulting in the beam bunching. The resulting bunched beam can be utilized for generating radiation either by means of transition radiation or through the coupling of the output radiation with the second harmonic of the beam density modulations. The frequency of the output radiation can be easily controlled by adjusting the voltage, current, and spot size of the electron beams coupled by the two-stream instability. Therefore, the proposed scheme can be used for generating high-power radiation in a broad frequency range.

NP8 31 Harnessing the plasma magnetic mode for the generation of brilliant synchrotron radiation LUIS SILVA, FREDERICO FIUZA, SAMUEL MARTINS, RICARDO FONSECA, *GoLP/IPFN - Instituto Superior Tecnico* CHAN JOSHI, *University of California Los Angeles, Los Angeles, USA* The existence of a plasma magnetic mode (PMM), or picket-fence mode, excited in the collision of a light pulse with a relativistic ionization front, has been predicted theoretically, but a clear experimental evidence of this fundamental plasma mode is still missing. We study the possibility to generate ultrashort-wavelength, high-brilliance radiation by using the PMM as a short-wavelength plasma undulator. The synchrotron radiation, generated when a relativistic energy beam traverses this magnetic structure, allows for a clear signature of the PMM. In order to check the validity of our scheme, we have performed simulations both with OSIRIS 2.0, including tunneling ionization, and with GENESIS 1.3, for an equivalent magnetic field structure. Our results demonstrate the possibility for controlled generation of radiation in the PMM, with high brilliance, equivalent to a compact gamma-ray synchrotron source, providing a clear experimental evidence of this plasma mode and opening the way towards the use of short-wavelength magnetostatic structures in plasmas.

NP8 32 Harmonics Generation in the Reflection of a Linearly Polarized Laser Beam Normally Incident on an Overdense Plasma* MAGDI SHOUCRI, *IREQ, Quebec, Canada* BEDROS AFEYAN, *Polymath Research Inc.* We study the harmonics generation in the reflection of a high intensity linearly polarized laser wave normally incident on an overdense plasma. We use an Eulerian Vlasov code for the numerical solution of the one-dimensional relativistic Vlasov-Maxwell equations for both electrons and ions. The oscillation of the laser wave at the plasma edge creates an oscillating space-charge, giving rise to an oscillating electric field. If the intensity of the wave is sufficiently high to make the oscillation of the electrons relativistic, then the plasma edge oscillates nonlinearly in the field of the high intensity laser beam (similar to the relativistic oscillating mirror ROM), which results in an important distortion in the reflected wave associated with the generation of harmonics. The combined effects of the edge electric field with the incident ponderomotive pressure have also important consequences on the ion dynamics, with the ion density profile forming a solitary-like structure close to the plasma edge. We consider the case when the laser beam wavelength is much greater than the scale length of the jump in the plasma density at the edge.

*The work of BA was supported by a DOE NNSA SSAA grant and LANL.

NP8 33 Generation of Phase-Coherent Soft X-Ray Laser Beams by Seeding Plasma Amplifiers DAVID ALESSI, MARK BERRILL, YONG WANG, SCOTT DOMINGUE, DALE MARTZ, DAVID KEMP, BRAD LUTHER, JORGE ROCCA, *Colorado State University* NSF ERC FOR EXTREME ULTRAVIOLET SCIENCE AND TECHNOLOGY TEAM, Injection seeding of soft x-ray plasma amplifiers with high harmonic pulses offers important advances for applications including full spatial and temporal coherence, reduced divergence, shorter pulsewidth, and increased brightness. We report detailed measurements and simulations of the near-field and far-field beam patterns from a 13.9 nm Ni-like Ag seeded soft x-ray laser. A comparison of the ASE and seeded soft x-ray lasers beam characteristics gives insight into the underlying physics of the plasma amplifier, including the extent and duration of the gain. Model results are compared to 2D model simulations. Work supported by the NSF EUV ERC Award #EEC-0310717. M.B. was supported by DOE CSGF Grant #DE-FG02-97ER25308 References Y. Wang et al., Nature Photonics 2, 94-98 (2008) Y. Wang et al., Physical Review A, 79, 023810 (2009)

NP8 34 LOW TEMPERATURE PLASMAS

NP8 35 CVD technologies assisted with millimeter waves ALEXANDER LITVAK, ANATOLY VIKHAREV, SERGEY GOLUBEV, ALEXEY GORBACHEV, PETR SENNIKOV, *Institute of Applied Physics of RAS* INSTITUTE OF APPLIED PHYSICS OF RAS TEAM, Gas discharges supported by quasi-optical millimeter wave beams are considered. Application in the plasma enhanced chemical vapour deposition technologies of such discharges that are characterized by high electron density allow to increase essentially the rate of activation of the gas medium as compared with traditional microwave based reactors with frequencies 2.45 GHz and 0.915 GHz. The results of films deposition in the plasma reactors pumped by 30 GHz gyrotron are presented for two cases: high rate growth of diamond films and production of nanocrystalline silicon films enriched with Si-isotope.

NP8 36 Feature Profile Simulation Taking into Account the Finite Penetration Depth PAUL MOROZ, *Tokyo Electron US Holdings* Feature profile simulations so far were mainly done under an assumption that incoming gas species of all energies physically or chemically interact only with the surface monolayer of the material. In a more advanced studies, a constant-width mixing layer was considered to take into account energetic particles which could go deep inside the material. However, the penetration depth is not a constant and should be different for different particles, because it strongly depends on the particle energy, on the type of the particle, and on the type of the material. In our work, the penetration depth is derived from analytic theory, molecular dynamics simulations, and from stopping and range software. The resulting fitting curves for the finite penetration depth are then used in the FPS feature profile simulator. The proposed simulation is discussed and the results of simulation are presented.

NP8 37 Impact of low pressure plasma discharge on etch rate of SiO_2wafer DUSAN POPOVIC, VLADIMIR MILOSAVLJEVIC, ANDRIJANA ZEKIC, *Faculty of Physics, University of Belgrade* NIALL MACGEARAILT, STEPHEN DANIELS, *National Centre for Plasma Science and Technology, Dublin City University, Dublin-9, Ireland* Low-k materials as SiO_2 play important role in semiconductor industry. In this work a treatment of SiO_2 single crystal by DC plasma discharge is studied in details. Our work is focused on interaction between ions and dielectric surface. The etch rates, surface morphology and chemical composition of modified surface layer obtained by DC plasma etching are reported. Influence of plasma chemistry (SF_6, O_2, N_2, Ar and He), discharge voltage (up to 1.2 kV), gas flow (up to 25 sccm, for each gas) and electrode-wafer geometry on etch rate of SiO_2wafer have been studied. Offline metrology is conducted for SiO_2 wafer by SEM/EDAX technique and Raman scattering. Effects of plasma treatment conditions on integrated intensity of broad Raman peak at around 2800cm^{-1}are reported in the paper. An analysis of this correlation could be a framework for creating virtual etches rate sensors, which might be of importance in managing of plasma etching processes.

NP8 38 Use of a dielectric barrier discharge reactor for hydrogen production ANGEL MARIO FIGUEROA-HERNANDEZ, MARTIN NIETO-PEREZ, GONZALO RAMOS, *Insituto Politecnico Nacional* JOEL PACHECO-SOTELO, *Instituto Nacional de Investigaciones Nucleares* A dielectric barrier discharge reactor is used to produce hydrogen from a methane feed mixed with water vapor. The dielectric barrier reactor uses an anodized electrode to generate a thin oxide layer that serves as a second dielectric barrier, as well as a support for catalytic sites. Diagnostics of the system include optical spectroscopy and gas analysis using a differentially-pumped quadrupole residual gas analyzer, capable of sampling feed, exit and recirculation streams of gas to determine the conversion efficiency and the selectivity towards hydrogen of the system. Results on the initial operation of the system are presented in this work.

NP8 39 Physical and biological aspects of cold plasma jet interaction with tissue ALEXEY SHASHURIN, *George Washington University* M.N. SHNEIDER, A. DOGARIU, R.B. MILES, *Princeton University* M.A. STEPP, M. KEIDAR, *George Washington University* Parameters of helium atmospheric plasma jet are measured by means of microwave scattering, fast photographing and measuring of jet currents. Streamer ("plasma bullet") propagating along with gas flow is generated immediately after the breakdown of the interelectrode gap. It is observed that post-streamer afterglow plasma column remains on the way of streamer passing. Lifetime of this afterglow plasma column is longer (about 3-5 μs) than that for the streamer (about 1 μs). The effects induced in living cells due to treatment with cold atmospheric plasma jet are studied by means of time-lapse microscopy and flow cytometry. We show that treatment of cells with plasma jet affects the cells on sub-cellular level, namely decreases expression of cell surface integrins. This change in integrin expression might be the original cause for the effects observed on cellular level, such as reduced cell migration rate and cell detachment. The living tissue response on treatment with plasma jet may be probably caused by post-streamer plasma column and excited species (due to their longer lifetime) rather than by "plasma bullets." We would like to acknowledge the technical assistance of Dr. Y. Raitses, through the PPPL Offsite University Research Program supported by the Office of Fusion Energy Sciences.

NP8 40 A helicon hydrogen plasma source for PMI studies* R. GOULDING, G. CHEN, S. MEITNER, L. OWEN, F.W. BAITY, J.B.O. CAUGHMAN, M. COLE, *Oak Ridge National Laboratory* Linear plasma devices are important tools for studying phenomena occurring in the plasma material interface (PMI) regions of fusion experiments. An electrodeless rf helicon based plasma source is being designed and constructed at ORNL for possible use in a high power flux ($\sim$ 20 MW/m^2) linear PMI test device. The source will produce high density hydrogen and deuterium plasmas with density $> 10^{19}$ m^{-3}, and total ion production $\geq 10^{21}$s^{-1}. It consists of a 1.3 m long, 15 cm diameter vacuum chamber, with a helical antenna transmitting rf power at f= 10-26 MHz through a cylindrical aluminum nitride (AlN) vacuum window, and four circular coils creating an axial magnetic field with $|B| \leq$ 1T. Preliminary modeling using the EMS2D code indicates that antenna plasma loading $\geq$ 5 Ω should be acheivable, permitting coupled power $P >$ 50 kW. The device will operate for pulse lengths up to

3 s, with data obtained permitting the design of a later steady state version. The design will be reviewed, as well as well as power deposition and electric field profiles calculated using EMS2D and CST Microwave Studio. Thermal stress calculations for the AlN window will also be reported.

*Oak Ridge National Laboratory, managed by UT-Battelle, LLC, for the U.S. Dept. of Energy under contract DE-AC05-00OR22725

NP8 41 Enhanced Output from the High Power Helicon Resulting from Modification of the Downstream Magnetic Field with a Magnetic Nozzle RACE ROBERSON, ROBERT WINGLEE, TIM ZIEMBA, JAMES PRAGER, *University of Washington* The high power helicon plasma source developed at the University of Washington is capable of transferring tens of kilowatts of power into the plasma with source plasma densities near 2x10 $^{20}m^{-3}$. The helicon operates with a B_0 magnetic field of.2 to.6 kG on axis that diverges with axial distance from the source. The addition of a magnetic nozzle downstream of the source region increases the magnetic field along the source axis and limits the divergence of the magnetic field at the source exit. Optical emissions from the plasma show an intense axially peaked central plasma core, typical of a helicon discharge. Light emission occurs outside of the source region within one antenna length downstream, and with the addition of the nozzle the optical emission region extends more than one antenna length. Density along the source axis is increased downstream as expected and time of flight estimates show an increase in bulk plasma velocity downstream of the nozzle. Measurements of plasma density with Langmuir probes and ion energies with a retarding field energy analyzer will be presented.

NP8 42 Performance of a new Extraction Aperture for the Nonambipolar Electron Source* JESSE GUDMUNDSON, NOAH HERSHKOWITZ, *University of Wisconsin - Madison* The Nonambipolar Electron Source (NES) is a radio frequency plasma-based electron source that does not rely on electron emission at a cathode. All electrons are extracted at an electron sheath through a biased ring and all ions are lost radially to a separately biased cylindrical graphite Faraday shield. Plasma density increases and electron confinement at the ring improves by the addition of an axial magnetic field. An electromagnet in the original NES has been replaced by a NdFeB magnet array. Approximately 30% of the electron current was extracted using the magnet array. The remainder was lost to the ring while the electromagnet provided 90% extraction efficiency. A disk with a concentric hole has replaced the ring and the hole diameter was varied to improve extraction efficiency. The disk was separated from the cylinder to prevent shorting between them and previously observed sputtering of graphite on the insulator between the ring and the cylinder. Bulk plasma potential, density, electron temperature, and plume electron energies measurements as well as time resolved ICCD camera images of the plume will be discussed.

*Work supported by DOE Grant No. DE-FG02-97ER54437

NP8 43 Study of OH radical generation in atmospheric pressure microwave plasma jets of Ar, N_2 and O_2 gases using pulsed cavity ringdown spectroscopy* CHUJI WANG, NIMISHA SRIVASTAVA, *Department of Physics & Astronomy, Mississippi State University, MS, US* We employ UV-pulsed laser cavity ringdown spectroscopy, optical emission spectroscopy and visual imaging, to characterize OH radical generation in atmospheric pressure microwave plasma jets created, respectively, by argon, mixture of Ar and N_2, mixture of Ar and O_2, and mixture of Ar, N_2 and O_2. OH radicals were observed in far downstream for all of these plasma jets (Far downstream is referred to as the location where ratio of the distance from the jet orifice to the length of the jet column is $>$ 3).We also investigated the effect of variations in humidity on OH generation in the APJs. Absolute number densities were measured for OH (v" = 0, J"= 3.5) along the plasma column axis. Effects on OH radical concentrations along the plasma column axis with variations of plasma powers, gas flow rates with different mixing ratios and humidity levels were also studied. The rotational T_{rot}, vibrational T_{vib} and electronic excitation temperature T_{elex} were provided by simulations of emission spectra of the plasmas.

*This work is supported by National Science foundation, grant # CTS-0626302.

NP8 44 Laser Assisted Plasma Coatings at Atmospheric Pressure (LAPCAP) ZIHAO OUYANG, VIJAY SURLA, KYONG-NAM KIM, MARTIN NEUMANN, DAVID RUZIC, *University of Illinois at Urbana-Champaign* The Center for Plasma-Material Interactions (CPMI) has developed a new Laser Assisted Plasma Coatings at Atmospheric Pressure (LAPCAP) system that will allow high quality, non-porous and uniform coatings on variety of substrates. The basic principle of LAPCAP is to utilize a pulsed Nd:YAG laser (5-10 ns) with an intensity in the range of 10^{10}– 10^{11} W/cm^2 to ablate target particles and feed them into the plasma torch for deposition. A large range of materials such as metals and ceramics can be ablated using the laser. A new atmospheric pressure plasma torch based on microwave frequency (2.45 GHz) is developed for this purpose, which is characterized using optical emission spectroscopy (OES). The velocity of the plasma jet is measured using a Pitot tube. In addition, the laser ablation of Yttria-stabilized zirconia (YSZ) target material is currently being investigated for different laser operating parameters to optimize the particle flux and distribution as suitable for the coating requirements.

NP8 45 Observing Pseudowaves in a Multi-Species Plasma using an Antenna/Receiver Setup* J.P. SHEEHAN, NOAH HERSHKOWITZ, *University of Wisconsin - Madison* Ion bursts known as pseduowaves are created and detected in a low temperature ($T_e \approx$ 1eV, $n_e \approx 10^8$ cm^{-3}) plasma confined in a multi-dipole chamber. A negative-going square wave on a gridded antenna (14 cm diameter) is used to launch the pseudowaves in an argon/neon plasma. They are detected by a single-sided plate receiver (3.5 cm diameter) collecting ion saturation current. Results show the ability of this technique to create and observe pseudowaves in a multi-ion species plasma. Application in determining ion concentrations in a multi-ion species plasma is presented.

*Work supported by U.S. DOE Grant No. DE-FG02-97ER54437.

NP8 46 Non-Perturbative PlasmaTransducer CARLOS LOBO,* *CMV-affiliated to DESY* High/low energy physics and Biomimmetics computer vision artifacts are used to simulate a femtosecond isomerization of 3D Rhodopsin-humor vitreous neuron subsystem that is triggered by real time 2D nanoplasma reflecting 90% of the incident radiation with a wavefront similar to the initial solid surface. A complex plasma mirror map is created. It's outlined an holographic transducer that is embedded inside

orbital channel superconducting nanorings plasma crystals clusters synchronized by tokamak-like simultaneous regulation controls of injection, electron/proton/neutron retranscript production rate, line density, edge pressure, vortex islands, radiated power fraction in the divertor region, small "spontaneous" discharges and others coherent oscillations. EPICS input/output controller is the injection program source Vorpal assemblies QCD-centric parameters to a special class of plasma accelerator in a cell (PIC). A Rhodopsin-based "computer" accelerator model that produce photoproduct data is presented.

*Invited to ICALEPCS

NP8 47 Imaging with spherically bent crystals or reflectors M. BITTER, K.W. HILL, F. JONES, S. SCOTT, *Princeton Plasma Physics Laboratory, Princeton, NJ* A. INCE-CUSHMAN, M. REINKE, J.E. RICE, *MIT Plasma Science and Fusion Center, Cambridge, MA* P. BEIERSDORFER, M.-F. GU, *Lawrence Livermore National Laboratory, CA* S.G. LEE, *NFRC, Korea Basic Science Institute, Daejeon, Korea* S. MORITA, M. GOTO, *National Institute for Fusion Science, Toki, Japan* This paper deals with the astigmatism of spherically bent crystals or reflectors and presents new imaging schemes, which can be applied to a wide spectrum of the electromagnetic radiation, including x-rays and EUV radiation. In Part I, we describe an x-ray imaging crystal spectrometer, where the astigmatism of a spherically bent crystal is being used with advantage to obtain radial profiles of the ion temperature and toroidal plasma rotation velocity in tokamaks and stellarators. In Part II, we present two new imaging schemes, where the astigmatism has been eliminated by matched pairs of spherical reflectors, enabling point to point imaging with almost arbitrary angles of incidence. Potential applications are the x-ray diagnosis of laser-produced plasmas, imaging of biological samples with monochromatic radiation from synchrotron light sources, and EUV lithography.

*Work supported by US Department of Energy Contracts: DE-FC02-99ER54512 and DE-AC02-09CH11466.

NP8 48 Rotating Spoke in a Cylindrical Hall Thruster* JEFFREY B. PARKER, YEVGENY RAITSES, NATHANIEL J. FISCH, *Princeton Plasma Physics Laboratory* In a cylindrical Hall thruster (CHT)[1], a spoke of increased visible light emission propagates azimuthally and has been imaged with the use of a high speed camera. The spoke frequency is about 15 kHz. The observation of the rotating spoke depends on the magnetic field configuration. When the CHT is configured to have a cusp magnetic field, the rotating spoke is visible, while when it is configured to have an enhanced mirror field, the rotating spoke is not visible. The rotating spoke is also suppressed due to enhancing the cathode electron emission above its self-sustained level. In the regimes where the rotating spoke is not visible, steady-state probe measurements have found the electron cross-field mobility to be reduced[2], indicating the spoke may contribute to anomalous electron transport.

*Work supported by an NSF Graduate Fellowship and USDOE DE-AC02-09CH11466.

[1]Y. Raitses and N. J. Fisch, *Phys. Plasmas* 8, 2579 (2001)
[2]A. Smirnov, Y. Raitses, and N. J. Fisch, *Phys. Plasmas* 14, 057106 (2007)

NP8 49 Negative differential conductivity and discharge current oscillations in Hall thrusters* YEVGENY RAITSES, JEFFREY B. PARKER, NATHANIEL J. FISCH, *Princeton Plasma Physics Laboratory, Princeton, NJ 08543* Large-amplitude, low-frequency, discharge current oscillations invariably occur in the Hall thrusters. The oscillations are thought to result from ionization instability [1]. Increase of the cathode electron emission was recently shown to suppress these oscillations [2]. This suppression correlates with a change in the local V-I characteristics of the discharge. In this regime, there are no plasma regions with negative differential conductivity, which are normally observed for the self-sustained thruster discharge. A similar effect can be achieved by using the thruster channel with low secondary electron emission (SEE) walls. The common feature between enhanced cathode electron emission and low SEE wall effects is that in both cases, the electron cross-field mobility is reduced inside the channel and therefore, the ion accelerating and ionization regions are located mainly in this region of a strong magnetic field. [1] S. Barral, E. Ahedo, Phys. Rev. E 79, 046401 (2009), [2] Y. Raitses, A. Smirnov, N. J. Fisch, Phys. Plasmas 16, 057106 (2009).

*Work supported by USDOE DE-AC02-09CH11466.

NP8 50 Surface Material Deposition on a Ferroelectric Plasma Thruster* B.T. HUTSEL, S.D. KOVALESKI, T. WACHARASINDHU, R. ALMEIDA, J.W. KWON, *University of Missouri* The ferroelectric plasma thruster (FEPT) is being developed for micropropulsion. The FEPT produces thrust by the acceleration of ions from plasma formed at the surface of a ferroelectric disk. Ions are accelerated due to the electrostatic fields generated from an applied RF voltage. The generated surface plasma is composed of electrode material (silver or aluminum) deposited on the crystal. Experiments are being conducted to optimize the material deposition on the FEPT. Finite element simulation software is used to model the materials effect on the generated electrostatic fields. Measurements of total ion currents and plasma composition for various depositions are compared.

*Work supported by the Air Force Office of Scientific Research.

NP8 51 Effects of Secondary Electron Emission on the Two-Stream Instability in Hall Thrusters* ANTON STEPANOV, N.J. FISCH, *Princeton University* In Hall thruster discharges, secondary electron emission (SEE) electrons produced at the chamber wall are accelerated radially into the channel by the sheath potential. The plasma inside the channel moves in the azimuthal direction due to E x B rotation. Next to the channel wall, this rotation could give the bulk plasma a greater azimuthal velocity compared to the SEE beam. The resulting nonmonotonic electron velocity distribution function (EVDF) might be two-stream unstable. In this work we consider the possibility of such a two-stream instability in the combined SEE beam/plasma EVDF in the azimuthal dimension.

*This work supported, in part, by US DOE Contract No. DE-AC02-CH0911466.

NP8 52 Characterization of the Micro Pulsed Inductive Thruster JAMES PRAGER, *University of Washington* TIMOTHY ZIEMBA, *Eagle Harbor Technologies, Inc.* DAVID PETERS, ROBERT WINGLEE, *University of Washington* The micro pulsed inductive thruster (uPIT) is a low mass ($<$ 500 g) pulsed plasma thruster with an inductive drive section that was invented

and developed at Eagle Harbor Technologies, Inc. and investigated at the University of Washington. This thruster is designed for primary propulsion of nanosatellites and satellite missions that require very fine impulse bit for precision pointing. Here we present data demonstrating increased performance with the use of the inductive drive section. Also presented is data to characterize the thruster including spectrometer data, exhaust speed data, preliminary thrust stand data, and long duration operation data. We demonstrate that uPIT is a viable option for a micropropulsion concept that fills an open niche in thruster concepts.

NP8 53 Wave-driven plasma centrifuge* ABRAHAM FETTERMAN, NATHANIEL FISCH, *Princeton University* A method for driving rotation in a fully ionized plasma centrifuge is described. The rotation is produced by radiofrequency waves near the cyclotron resonance. The wave energy is transferred into potential energy in a manner similar to the α channeling effect. By driving the rotation using waves instead of electrodes, physical and engineering issues may be avoided.

*This work was supported by DOE Contracts DE-FG02-06ER54851 and DE-AC0276-CH03073.

NP8 54 Spatially-Resolved Spectroscopic Study of Arcjet Helium Plasmas Expanding through a Rectangular-Shaped Converging-Diverging Nozzle SHINICHI NAMBA, NORIYASU YASHIO, KAZUKI KOZUE, KEISUKE NAKAMURA, TAKUMA ENDO, KEN TAKIYAMA, *Hiroshima University* KUNINORI SATO, *National Institute for Fusion Science* An arcjet discharge device with a rectangular-shaped converging and diverging nozzle has been developed, which allowed us to optically observe high density plasmas inside the anode nozzle. Spectroscopic observation along the plasma expansion axis was carried out to examine the characteristics of plasma parameters inside the nozzle. Analyzing the intense continuum and line emission spectra, we successfully obtained the spatial variations of electron temperature and density. Moreover, it was found that two dimensional optical measurement was of great use in visualizing the transition from the atmospheric thermal plasma to strong non-equilibrium recombining phase due to an adiabatic expansion.

NP8 55 A Zero Dimensional Model of High-Pressure Ablative Capillary Discharge LEONID PEKKER, OKSANA PEKKER, *ERC* The presented model of high-pressure ablative capillary discharge includes: a heat-transfer radiation model based on radiation database constructed using PrismSPECT, a commercially available radiation software, to calculate the radiation heat flux output from a uniform plasma slab; a model of the transition boundary layer between the uniform plasma core and the ablative wall to calculate the thermal and radiation heat fluxes at the capillary wall; capillary wall thermal conduction and radiation absorption; and a RLC circuit. Thus, the model self-consistently calculates plasma parameters of the capillary discharge and distribution of wall temperature vs. time. We show that the radiation grey factor varies from 0.06 to 0.95 with time. This illustrates that the grey factor can change significantly with time in nonsteady operation regime and, therefore, assuming that it is constant can lead to false results. The model also shows that small extinction coefficients of the wall material lead to large energy losses from the capillary discharges (the heat is absorbed by the bulk of the capillary wall or just escapes the capillary) and to spikes in plasma temperature. If the extinction coefficient is too small, the discharge may become extinguished because the temperature of ablative surface does not increase fast enough to compensate the plasma exhaust from the open end of the capillary.

NP8 56 ePLAS modeling of laser induced lightning streamers* W. ATCHISON, R.J. MASON, *Research Applications Corp* J. ZINN, *Sumner Associates* The ePLAS code is a derivative of ANTHEM[1] originally developed to model long pulse laser interactions. The code has been enhanced to treat opening switch plasmas, plasma jets, and short pulse laser interactions with cones and wires.[2] We address new features for application to lightning and guided arcs. ePLAS models collisional background plasma with cold electron and ion components. Self-consistent *E- and B*-fields are determined implicitly for time steps well beyond the plasma period; hybridization permits spatial scales exceeding the Debye length. For lightning studies an initial start-up potential in a strongly ionized region has been added, plus "air chemistry" to create additional plasma in intense, propagating E − field regions at the leading edge of "streamers." We discuss the motion of both positive and negative streamers in nitrogen on nanosecond time scales, showing streamer guidance in added plasma seeded by a laser. *B*-field inclusion permits the study of return strikes.

*Work supported in part by DOE SBIR Grant DE-FG02-07ER84723.

[1]R. J. Mason, J. Comp. Phys. 71, 429 (1987)
[2]R. J. Mason, et al., Bull. Am. Phys. Soc. 53, 152 (2008).

NP8 57 Formation and Radial Propagation of Filaments in a Plasma Ball MICHAEL CAMPANELL, S. VASQUEZ, *PPPL* C. CZARNOCKI, M. BURIN, *CSSM* S.J. ZWEBEN, *PPPL* High speed photography was used to analyze the formation and propagation of the filaments in a commercial plasma ball. Videos made at up to 500,000 frames/sec show that the filaments propagate radially at about 10,000 m/s during each cycle at the 25 kHz driving frequency and follow the same path in consecutive cycles. Just after the initial switching on of the voltage, the filaments develop out of a diffuse glow and self-organize into their final form over about 1 msec. It is also found that the number of filaments varies with applied voltage frequency and the radial length of filaments varies with voltage amplitude. A custom plasma ball apparatus has been built to analyze the dependence of the filamentary behavior on gas composition, pressure, applied voltage waveform and electrode geometry. Initial results will be presented.

NP8 58 PINCHES, EQUATION OF STATE, AND SIMULATIONS

NP8 59 The Affects of Ablation, Two-Dimensional Instability, and Current Losses on K-Shell Emission in Wire Array Z-Pinch Implosions.* J.W. THORNHILL, J.L. GIULIANI, J.P. APRUZESE, Y.K. CHONG, J. DAVIS, A. DASGUPTA, *Plasma Physics Division, Naval Research Laboratory* R.W. CLARK, K.G. WHITNEY, *Berkeley Scholars, Inc.* B. JONES, C.A. COVERDALE, D.J. AMPLEFORD, C.A. JENNINGS, M.E. CUNEO, *Sandia National Laboratories* We present the results of a 2D radiation MHD based theoretical investigation that examines how wire ablation, the level of two-dimensional instability, and current losses in the load region of the pinch affect K-shell radiation for copper and stainless steel wire array implosions on the refurbished Z machine. We find that the broad mass distribution produced by including ablation physics largely overcome the diminishing effects on K-shell yield of two-dimensional instability growth. On the other hand, results of calculations that model suspected current losses near the load region[1] show substantial reductions in K-shell yield.

*Work supported by DOE/NNSA and Sandia (DOE contract DE-AC04-94AL85000).

[1]C. A. Jennings, Invited talk ICOPS (2009).

NP8 60 Ablation studies of low number wire arrays on the GenASIS Linear Transformer Driver (LTD) at 200 kA SIMON BOTT, FARHAT BEG, GILBERT COLLINS IV, MILES ABARR, *University of California San Diego* The ablation of wires in a wire array z-pinch remains one of the critical challenges in scaling these systems to drive currents required for Inertial Confinement Fusion (ICF) ignition. Whilst the dynamical evolution of wire arrays is well understood, and multi-dimensional Magneto-Hydrodynamic (MHD) modeling has demonstrated significant progress, a predictive capability has not been realized to date. In addition, recent experimental investigations have highlighted the need to more closely examine the ablation structure and its dependence on the initial parameters of the array. We present investigations on the ablation in wire arrays on a recently completed generator at UCSD. The radial and axial variation of the plasma density is examined quantitatively using laser interferometry, and temperature estimates are made from time integrated and time-gated emission images. Results are compared to analytical models of the ablation process which show that the effective ablation velocity varies continuously in the axial direction as a result of the ablation process at the wire.

NP8 61 An Investigation of the Radiation and Implosion Performance of Al/Mg Nested Wire Arrays on the Refurbished Z Simulator* Y.K. CHONG, W. THORNHILL, J. GIULIANI, *Plasma Physics Division, NRL* R. CLARK, *Berkeley Research Scholars* D. AMPLEFORD, C. JENNINGS, B. JONES, C. COVERDALE, *Sandia National Laboratories* A set of Al/Mg nested wire array Z-pinch load experiments has been recently performed on the refurbished Z accelerator. The initial 1D predictions display a K-shell yield increasing w/ mass load, but the exp. data showed the opposite trend. In this study, we present the results from the modeling of the exp. using a 1-D non-LTE radiation MHD code with a detailed atomic model and the prob.-of-escape radiation transport. Our focus will be on the characterization of the radiation emission, absorption & transport, & the energetics & dynamics of the Z-pinch plasma as a function of the load mass & wire array distribution. The effects of the current loss & the e-i energy coupling physics on the radiation power & yield and the implosion performance will be investigated. Finally, an examination of the role of multidimensional structures on the radiation & implosion physics will be made using appropriate models w/ relevant improvements suitable for studying the Z-pinch loads in order to help bridge the gap between the exp. & the previous 1-D predictions.

*Work supported by the DOE/NNSA and Sandia National Laboratories.

NP8 62 Analysis of implosion dynamics of nested cylindrical wire arrays of Mo and Al on the Zebra and Cobra generators* M.E. WELLER, M.F. YILMAZ, A.S. SAFRONOVA, V.L. KANTSYREV, A.A. ESAULOV, K.M. WILLIAMSON, I. SHRESTHA, G.C. OSBORNE, N.D. OUART, V. SHYLAPTSEVA, *UNR* Results of experiments with nested cylindrical wire arrays of Mo and Al that were performed on the 1.6 MA, 100 ns Zebra generator and the 1.0 MA, 100 ns Cobra generator are presented. Both the Zebra and Cobra experiments had loads with Al tracer wires with different concentrations in linear mass ($\sim$ 30% Al for Zebra and $\sim$ 15% Al for Cobra). The full set of diagnostics produced data that were compared and analyzed, which include PCD, XRD, and bolo signals, laser shadowgraphy and optical streak images, and time-gated/integrated pinhole and spectra images. Implosion dynamics is analyzed with a wire-ablation dynamics model. Non-LTE kinetic modeling was utilized to derive plasma parameters of electron temperature and density and to estimate opacity effects. The advantage of using Mo wires for future study of L-shell radiators from wire arrays is demonstrated.

*Work was supported by DOE/NNSA under Cooperative Agreements DE-FC52-06NA27588 and DE-FC52-06NA27586, and in part by DE-FC52-06NA27616 and DE-FC03-02NA00057.

NP8 63 Comprehensive Analysis of Implosions of Single Planar Tungsten Wire Arrays with Aluminum Center Wires Produced on a 1-MA generator* G.C. OSBORNE, A.S. SAFRONOVA, V.L. KANTSYREV, A.A. ESAULOV, M.F. YILMAZ, K.M. WILLIAMSON, M.E. WELLER, I. SHRESTHA, *University of Nevada, Reno* An analysis of five-wire W single planar wire array (SPWA) experiments with Al center wires is presented. Comparisons are drawn to previous work which focused on SPWAs with smaller inter-wire gaps of pure W loads and W loads with single Al wires on the edge of the array. Experiments were performed on the 1MA generator "Zebra" at UNR, with data taken on a pulse laser shadowgraphy apparatus, an x-ray time-gated pinhole camera, and both time-integrated spatially resolved and time-gated spatially integrated spectrometers. Utilizing this full suite of plasma diagnostics, comprehensive set of data with staggered timings has been compiled. Non-LTE kinetic modeling is used to describe temperature and density features of the spectral data, while the Wire Ablation Dynamics Model is utilized to better understand implosion dynamics.

*This work was supported by DOE under Grant No. DE-FG02-08ER54951 and in part under NNSA Cooperative Agreements DE-FC52-06NA27588 and DE-FC52-06NA27586.

NP8 64 Magneto-Rayleigh-Taylor Instability Experimental Progress on Thin Foils Driven by a 1-MA LTD* J.C. ZIER, Y.Y. LAU, M.R. GOMEZ, W.W. TANG, M.A. FRANZI, D.M. FRENCH, R.M. GILGENBACH, *U of Michigan* M.G. MAZARAKIS, M.E. CUNEO, M.R. LOPEZ, B.V. OLIVER, T.A. MEHLHORN, *Sandia National Labs* Foils may soon become necessary to achieve the required mass for higher current-driven x-ray sources. They may also offer useful options for x-ray pulse shaping and as imploding liners for magnetized target fusion. This paper reports our latest design and experimental progress on the dominant instability, the magneto-Rayleigh-Taylor instability (MRT). Planar Al foils as thin as 400 nm driven by the 1-MA linear transformer driver (LTD), MAIZE, at the U of Michigan, are used as the dynamic loads for this investigation. A higher inductance feed will be used to lengthen the current drive to achieve $>$ 10 e-foldings of MRT growth for observation with a laser backlighter. Inductance considerations, schlieren and interferometry diagnostics, and experimental progress will be presented along with MRT theory. *This work was supported by US DoE through Sandia National Labs award numbers 240985 and 76822 to the U of Michigan. Sandia is a multiprogram laboratory operated by Sandia Corporation, a Lockheed Martin Company, for the US DoE's NNSA under Contract DE-AC04-94AL85000. JCZ was supported by a NPSC fellowship through Sandia National Labs. MRG was supported by a SSGF fellowship through NNSA.

NP8 65 Development of the Axial Instability in Low Wire Number Wire Array Z-Pinches PATRICK KNAPP, JOHN GREENLY, PIERRE GOURDAIN, CAD HOYT, MATTHEW MARTIN, SERGEI PIKUZ, TANIA SHELKOVENKO, DAVID HAMMER, BRUCE KUSSE, *Cornell University* We investigate the growth of the axial instability in wire-array Z-pinches. In these experiments we image individual wires in aluminum wire arrays using laser shadowgraphy and XUV framing cameras at times ranging from 0 to 100 ns after the start of a 1 MA, 100 ns rise time current pulse. We document the radial growth of the coronal plasma around each wire and the development of the wavelength and amplitude of the instability from the time of plasma formation until the instability stops growing. The ratio of the dominant instability wavelength to the coronal plasma radius is $\sim$ 1 during this time. The magnetic field topology is also probed using small B-dot probes inside the array. The change in topology from local- to global- field dominated near an exploding wire correlates well in time with the moment that the instability stops growing. In addition, preliminary experiments show that perturbations seeded in the coronal plasma using twisted wires grow at the twist wavelength and evolve to much larger amplitude than in the unseeded case. This research was supported by the SSAA program of the National Nuclear Security Administration under DOE Cooperative agreement DE-FC03-02NA00057.

NP8 66 Coronal plasma development in wire-array z-pinches made of twisted-pairs C.L. HOYT, J.B. GREENLY, P.A. GOURDAIN, P.F. KNAPP, S.A. PIKUZ, T.A. SHELKOVENKO, D.A. HAMMER, B.R. KUSSE, *Cornell University* We have investigated coronal and core plasma development in wire array z-pinches in which single fine wires are replaced by twisted-pairs ("cable") on the 1 MA, 100 ns rise time COBRA pulsed power generator. X-ray radiography, employed to investigate dense wire core expansion, showed periodic axial nonuniformity and evidence for shock waves developing where the individual wire plasmas collide. Laser shadowgraphy images indicated that the axial instability properties of the coronal plasma are substantially modified from ordinary wire arrays. Cable mass per unit length, material and the twist wavelength were varied in order to study their effects upon the instability wavelength. Implosion uniformity and bright-spot formation, as well as magnetic topology evolution, have also been investigated using self-emission imaging, x-ray diagnostics and small B-dot probes, respectively. Results from the cable-array z-pinches will be compared with results from ordinary wire-array z-pinches. This research was supported by the SSAA program of the National Nuclear Security Administration under DOE Cooperative agreement DE-FC03-02NA00057.

NP8 67 Embedding magnetic field lines in the plasma jet of an exploding radial foil on COBRA* PETER SCHRAFEL, PIERRE GOURDAIN, JOHN GREENLY, BRUCE KUSSE, *Cornell University* Previous investigations of exploding radial foils have shown the formation of an axial plasma jet in the early stages of the foil explosion. In this case a thin load foil was pressed at an outer annulus held at ground, and contacted in the center by a small straight rod cathode driven by the 1MA COBRA accelerator. The present experiments look at the effects of inducing a transient magnetic field in the region containing the plasma jet. This induced magnetic field is created in one of two ways: twisting the rod cathode to have a helical coil segment near the foil, or putting an inductive current path in parallel to the straight rod cathode. Of great interest is whether this applied magnetic field can be embedded into the plasma jet and influence its development. The jet is diagnosed visually with laser shadowgraphy and observation of XUV emission. B-dot probes measure the magnetic field strength in the region near the jet.

*This work was supported by NNSA Stockpile Stewardship Academic Alliances program under DOE cooperative agreement DE-FC52-02NA00057.

NP8 68 Compression of an Applied Bz field by a z-pinch onto a Tamped DT Fiber for Inertial Confinement Fusion* TOM NASH, *Sandia National Lab* Simulations of a z-pinch compressing an applied 100 kG Bz field onto an on-axis DT fiber tamped with beryllium show the field reaching over 100 MG in the tamp, sufficient to confine DT alpha particles and to form a thermal barrier. The barrier allows the DT plasma to burn at a rho*r value as low as 0.045 g/cm^2, and at temperatures over 50 keV for a 63 MA drive current. Driving currents between 21 and 63 MA are considered with cryogenic DT fiber diameters between 600 μm and 1.6 mm. Pinch implosion times are 120 ns with a peak implosion velocity of 35 cm/μs. 1D simulations are of a foil pinch, but for improved stability we propose a nested wire-array. Simulated fusion yields with this system scale as the sixth power of the current, with burn fractions scaling as the fourth power of the current. At 63 MA the simulated yield is 521 MJ from 4.2 mg/cm of DT with a 37% burn fraction at a rho*r of only 0.18 g/cm^2.

*Sandia is a multiprogram laboratory operated by Sandia Corporation, a Lockheed Martin Company, for the United States Department of Energy's National Nuclear Security Administration under Contract DE-AC04-94AL85000.

NP8 69 Neutron Production in Deuterium Gas-Puff Z-Pinch Implosions on Refurbished Z* R.W. CLARK, *Berkeley Research Associates* A.L. VELIKOVICH, J. DAVIS, J.L. GIULIANI, *Plasma Physics Division, Naval Research Laboratory* C.A. COVERDALE, D. FLICKER, *Sandia National Laboratories* Earlier experiments with deuterium gas puff implosions on Z [Coverdale et al., Phys. Plasmas **14**, 022706 and 056309 (2007)] demonstrated reproducible production of high neutron yields, up to $\sim 3\times 10^{13}$, a large part of which might be of thermonuclear origin. We report a scoping study for such experiments on refurbished Z which can implode deuterium gas-puff loads at high-current, longer pulse ($\sim$ 250 ns) regime. Significantly higher thermal DD neutron yields are predicted for ZR. We discuss the relative roles of kinetic-to-thermal energy conversion and adiabatic compression in heating the central deuterium column to the fusion temperature. We quantify the effect on the thermal neutron yield produced by loading the outer shells of the multi-shell gas-puff with a heavier gas to improve matching of the implosion to the current pulse, by additional heating of the central jet area with a Z-Beamlet laser and by applying an axial magnetic field in order to stabilize the implosion from a large initial radius.

*Work supported by Sandia National Laboratories.

NP8 70 Parallel X pinches on the 1 MA COBRA pulser* S.A. PIKUZ, T.A. SHELKOVENKO, P.F. KNAPP, C.L. HOYT, J.B. GREENLY, H. WILHELM, D.A. HAMMER, *Cornell University* Two standard and nested X pinches have been tested in parallel as the load on the 1MA, 100 ns risetime COBRA pulsed power generator at Cornell University. The spatial, temporal, and spectral parameters of the X pinches were studied using laser-based imaging, time gated XUV-sensitive cameras, a slit-step-wedge and pinhole cameras, X-ray spectroscopy and x-ray radiography. The latter includes testing a new method of point-projection quasi-monochromatic radiography. Electrical cross-talk of the X pinches was studied using very small B-dot probes placed in the space between X-pinches. The experiments show that the parallel nested x-pinches produce smaller, brighter and more stable x-ray source points than the standard configuration.

*This work was sponsored by NNSA under DOE Cooperative Agreement DE-FC03-02NA00057.

NP8 71 X pinch experiments on the table-top MINI-generator* T.A. SHELKOVENKO, S.A. PIKUZ,[†]D.A. HAMMER, *Cornell University* I.N. TILIKIN, A.R. MINGALEEV, *P.N.Lebedev Physical Institute* S.A. CHAIKOVSKY, *P.N.Lebedev Institute* The MINI-generator, a 340 kA peak current, 170 ns risetime, 40-50 kV, pulsed power generator with energy storage of 1 kJ, was designed and built at the High Current Electronic Institute (Tomsk, Russia). The generator is 45 cm diameter, 33 cm high and weights about 80 kg. The main goal was to design a table-top generator for use with X pinches to create a point source of soft x-ray radiation for radiography of plasma and biological objects. The first experiments with X-pinch loads performed in P.N. Lebedev Physical Institute (Moscow, Russia) showed that the MINI-generator has very high efficiency in transformation of a stored energy to radiated energy of an X-pinch hot spots in the range of 1 to 5 μm diameter, depending on the photon energy range. Results obtained in X-pinch experiments on MINI-generator and the XP–generator (0.5 MA, 45 ns risetime) at Cornell University will be compared.

*The work is supported by the grants RFBR 08-02-00993, DSPHS (2.1.1/5470) and NNSA under DOE Cooperative Agreement DE-FC03-02NA00057.

[†]Permanent address:P.N.Lebedev Physical Institute

NP8 72 Axial x-ray backlighting of wire array Z-pinches using X pinches* I.C. BLESENER, J.B. GREENLY, S. PIKUZ, T. SHELKOVENKO, S. VISHNIAKOU, B.R. KUSSE, D.A. HAMMER, *Cornell University* A high resolution axial x-ray imaging system for wire-array Z-pinch experiments has been developed. Calibrated areal density measurements of the Z-pinch plasma; including wire cores, coronal plasma, streaming plasma, and precursor can be obtained. The system uses Mo X pinches in series and below the Z-pinch load to provide point sources of x-rays for point-projection radiography. Images have a 15 mm diameter field of view at the center height of the array and a magnification of about 7.5:1. Ti filters in front of the film transmit continuum radiation in the spectral range of 3-5 keV. A separate film of the same thickness Ti and placed the same distance away with an unobstructed path includes step wedges for calibration of the Z-pinch plasma. The step wedges have thicknesses of W ranging from 0.015 to 1.1 μm to obtain areal density measurements of the W plasma from the wire-array. Images have subnanosecond temporal resolution and about 10 μm spatial resolution. The diagnostic will also be used in the future for imaging thin foil cylinder Z-pinches. Recent calibrated images as well as a discussion of future foil experiments will be presented.

*This research was supported by the SSAA program of the NNSA under DOE Cooperative Agreement No. DE-FC03-02NA00057.

NP8 73 Dynamic measurement of plasma density in wire array z-pinches by using continuum interferometry* A. HABOUB, V.V. IVANOV, *University of Nevada, Reno* G.S. SARKISOV, *Ktech Corp., Albuquerque, NM* UNIVERSITY OF NEVADA, RENO TEAM, KTECH CORP., ALBUQUERQUE, NM COLLABORATION, Measurement of the electron plasma density with regular laser interferometery encounters the zero-number fringe issue on the axis of the z-pinch. From the ablation stage on, the density of the inhomogeneous plasma increases quickly and produces a very complicated structure of fringes. We suggested a new continuous interferometry diagnostic that has been developed for the 1-MA Zebra generator. This diagnostic can record a continuous history of the interferograms and the individual evolution of the streaked fringes. It is based on a Nd:YAG laser with a long probing pulse of 300 ns at either the fundamental wavelength or the second harmonic, a Mach Zehnder interferometer, and an optical streak camera. By using this new diagnostic, the precursor z-pinch plasma density can be precisely measured during the ablation and the implosion phases in wire arrays.

*Work was supported by the DOE/NNSA under UNR grant DE-FC52-06NA27616.

NP8 74 Development of laser based diagnostics for wire array z-pinch experiments on the MAGPIE generator* GEORGE SWADLING, S.V. LEBEDEV, S.N. BLAND, G.N. HALL, F. SUZUKI-VIDAL, N. NIASSE, G. BURDIAK, E. KHOORY, L. PICKWORTH, C. HUTCHISON, *Imperial College* End on Interferometric imaging is a useful technique for diagnosing the electron density distribution in the interior of wire array z-pinches

during their ablation phase. These measurements are limited as there is often no known density reference point in the image. By using a time resolved, CW line integrated interferometry system, we can measure the electron density for a single point on the image. This allows us to calculate the density distribution across the remainder of the image. Two new quadrature interferometry systems are discussed, the first free space and the second fiber based. Also discussed is a new fiber based multipoint Heterodyne Velocimetry (HET-V) system, for the time resolved measurement of large velocities and accelerations, and a new faraday rotation current probe system, to measure rapidly rising currents in new switched mode wire arrays.

*This research was sponsored by the NNSA under DOE Cooperative Agreement DE-FC03-02NA00057.

NP8 75 Development of laser-based diagnostics for 1-MA z-pinch plasmas* V.V. IVANOV, P. HAKEL, R.C. MANCINI, P. WIEWIOR, R. PRESURA, J.M. KINDEL, *University of Nevada, Reno* A.P. SHEVELKO, *Brigham Young University, Provo* O. CHALYY, A. ASTANOVITSKIY, A. HABOUB, S.D. ALTEMARA, D. PAPP, T. DURMAZ, *University of Nevada, Reno* The 50 TW Leopard laser coupled with the 1-MA Zebra generator was used for development of new diagnostics of z-pinch plasmas. Two plasma diagnostics are presented: an x-ray broadband backlighting for z-pinch absorption spectroscopy and parametric two-plasmon decay of the laser beam in dense z-pinch plasma. Implementation of new diagnostics on the Zebra generator and the first results are discussed. The absorption spectroscopy is based on backlighting of z-pinch plasma with a broadband x-ray radiation from a Sm laser plasma. Detailed analysis of the absorption spectra yields the electron temperature and density of z-pinch plasma at the non-radiative stage. The parametric two-plasmon decay of intensive laser radiation generates $3/2\omega$ and $1/2\omega$ harmonics. These harmonics can be used to derive a temperature of z-pinch plasma with the electron density near the quarter of critical plasma density.

*Work was supported by the DOE/NNSA under UNR grant DE-FC52-06NA27616.

NP8 76 Optical Spectroscopy Experiments on the 500 kA XP Pulsed Power Generator* KATE BLESENER, TANIA SHELKOVENKO, SERGEI PIKUZ, ISAAC BLESENER, DAVID CHALENSKI, CAD HOYT, PATRICK KNAPP, JOHN GREENLY, DAVID HAMMER, *Laboratory of Plasma Studies, Cornell University* YITZHAK MARON, *Weizmann Institute of Science* A new diagnostic technique using non-perturbing emission spectroscopy at visible wavelengths is being developed to determine the magnetic field in high energy density plasmas. This technique which makes use of the Zeeman Effect, has been demonstrated in experiments performed at the Weizmann Institute of Science in plasmas with lower energy densities [1]. Experiments on the 500 kA XP pulsed power generator at Cornell University are exploring the properties of optical spectra emitted by single exploding wires, wire-arrays, and X pinches. We are studying the time resolved visible spectra to identify appropriate spectral lines for measuring magnetic field strength. Preliminary results will be discussed. [1] E. Stambulchik, K. Tsigutkin, and Y. Maron. Phys. Rev. Lett. 98, 225001 (2007).

*This research is supported by the NNSA Stockpile Stewardship Academic Alliances program under DOE Cooperative Agreement DE-FC03-02NA00057 and by the DOE/NNSA joint program in HEDLP.

NP8 77 Non-LTE modeling and simulations for spectroscopic analysis of stainless-steel Z-pinch plasma* A. DASGUPTA, J.L. GIULIANI, J. DAVIS, J.W. THORNHILL, *Naval Research Laboratory* R.W. CLARK, *Berkeley Scholars Inc* C.A. COVERDALE, B. JONES, D.J. AMPLEFORD, *Sandia National Laboratories* BERKELEY SCHOLARS INC COLLABORATION, SANDIA NATIONAL LABORATORIES COLLABORATION, We have developed a collisional-radiative spectroscopic model that combines the accuracy of detailed accounting for all important excited states coupling with the completeness of a highly averaged Rydberg state model. The model was used to investigate the implosion dynamics of nested Stainless-Steel (SS) wire arrays and generate K- and L-shell spectra using a 1-D non-LTE radiation hydrodynamics model self-consistently coupled to a transmission line description of the device. We compare our SS spectra with experimental data of shot Z581 and Z1860 on the Z and the refurbished Z accelerators respectively, at Sandia National Laboratories. The simulations self-consistently include the effects of radiation transport and line broadening. We include level-specific dielectronic recombination data in order to investigate the Ly_g satellite lines that are useful for diagnosing line broadening in a Z-pinch plasma at stagnation.

*Work supported by DOE/NNSA and Sandia (DOE contract DE-AC04-94AL85000).

NP8 78 Modeling of Ion Thermalization in a Ne Gas Pinch* J. GIULIANI, J. THORNHILL, A. DASGUPTA, A. VELIKOVICH, J. DAVIS, *Plasma Phys. Div. Naval Res. Lab.* R. CLARK, *Berkeley Res. Assoc.* E. KROUPP, D. OSIN, Y. MARON, A. STAROBINTES, E. STAMBULCHIK, V. FISHER, V. BERNSHTAM, *Weizmann Inst. Sci.* A. FISHER, *Technion Univ.* C. DEENEY, *Depart. of Energy/NNSA* Understanding of the dynamics, population kinetics, and energy budget of a K-shell radiating Z pinch remains a challenging problem in high energy density plasma physics. Large ion kinetic energies have been reported for Ne pinches at $\sim$ 1 MA.[1] The present work examines the dynamics of this pinch with a 1D radial magnetohydrodynamic simulation code including collisional-radiative ionization dynamics and radiation transport. Synthetic spectra from the simulations can match the measured H-like satellite line profiles if the ion-electron equilibration rate is reduced by a factor of $\sim$ 10. In anticipation of further experiments, radially resolved synthetic spectra of the satellite lines will also be presented to analyze the plasma structure at stagnation.

*Work supported by DOE/NNSA.

[1]E. Kroupp, et al., PRL, 98, 115001 (2007), D. Osin, Ph.D. Thesis (2008).

NP8 79 Experimental Post-Hole Convolute Plasma Studies on a 1-MA Linear Transformer Driver (LTD)* M.R. GOMEZ, R.M. GILGENBACH, D.M. FRENCH, J.C. ZIER, Y.Y. LAU, *U. of Michigan* M.E. CUNEO, M.R. LOPEZ, M.G. MAZARAKIS, *Sandia National Labs* Post-hole convolutes are used to combine current from several parallel transmission lines, such that there is a low-inductance path to a single anode-cathode gap at the load. Experimental observations of the post-hole convolute are difficult to make on large systems, such as the Z-Machine at Sandia National Laboratories. A single post-hole convolute has been designed as the load for the 1 MA LTD at U. of Michigan. The geometry of the design allows diagnostic access to the post-hole

region. The goal of these experiments is to monitor plasma formation in the convolute and to measure the current losses as a result of that plasma. Diagnostics under development for this experiment include B-dots for current measurement, optical spectroscopy for plasma composition, temperature and density measurements, and pinhole and laser diagnostics for imaging plasma dynamics. Experimental results will be compared to Particle-In-Cell simulations of this system using MAGIC PIC.* Research supported by Sandia National Labs subcontacts to UM. MRG sponsored by SSGF through NNSA and JZ sponsored by NPSC through DOE. Sandia is a multi-program laboratory operated by Sandia Corporation, a Lockheed Martin Company, for the US DOE's NNSA under contract DE-AC04-94AL85000.

NP8 80 Higher Dimensional Theory of Contact Resistance and Experimental Validation W. TANG, M. GOMEZ, D. FRENCH, J. ZIER, P. ZHANG, Y.Y. LAU, R. GILGENBACH, *University of Michigan - Ann Arbor* UNIVERSITY OF MICHIGAN - ANN ARBOR TEAM, Electrical contact is an important issue to Z-pinches, pulsed power systems, field emitters, and wafer evaluation, etc. Because of the surface roughness on a microscopic scale, true contact between two pieces of metal occurs only on the asperities of the two contacting surfaces, resulting in contact resistance [1]. We recently developed a higher dimensional theory of contact resistance for an asperity of transverse dimension (a) and finite axial length (h) connecting two metal blocks [2]. For asperity of rectangular, cylindrical or funnel shape, the contact resistance is found to be of the form R[1+p(h/a)] where R is the corresponding h=0 "a-spot" theory limit of Holm and Timsit [1], p has a simple form which is geometry-dependent. This scaling law is verified against electrostatic code results [2]. It is also recently validated in a series of controlled experiments [3]. This work is supported by Sandia, AFOSR, AFRL, L-3, and Northrop-Grumman. [1] R. Holm, *Electric Contact* (Springer-Verlag, 1967); R. S. Timsit, *IEEE Trans. Components Packaging Tech.* **22**, 85 (1999). [2] Y. Y. Lau and W. Tang, *J. Appl. Phys.* **105**, 124902 (2009). [3] M. R. Gomez et al., *Appl. Phys. Lett.* (submitted).

NP8 81 Current Switching and 0D-like Implosions Produced Using Inverse Wire Array Z-Pinches* ADAM HARVEY-THOMPSON, SERGEY LEBEDEV, GARETH HALL, SIMON BLAND, GUY BURDIAK, FRANSISCO SUZUKI-VIDAL, GEORGE SWADLING, ESSA KHOORI, JEREMY CHITTENDEN, LOUISA PICKWORTH, *Imperial College* Experiments using an inverse (exploding) wire array setup (where the wires hang down from a central current conductor, acting as a return current cage) to rapidly switch current into a cylindrical wire array have been fielded on the MAGPIE generator (1.5MA, 240ns). The setup has been found to rapidly switch current into the cylindrical array, delivering ~ 1.5MA in 95ns. The implosion of the cylindrical array deviates substantially from the standard snowplough dynamics, suppressing the ablation phase and producing a 0D-like implosion. Data suggests that the change in dynamics is due to a ~ 5kA pre-pulse driven over 10ns into the cylindrical array over 100ns before the current switch operates which preconditions the wires in the array. This paper will focus on the effectiveness of the current switch.

*This research was sponsored by the NNSA under DOE Cooperative Agreement DE-FC03-02NA00057.

NP8 82 Experimental study of features on burn for direct-drive capsules G.R. MAGELSSEN, J.A. COBBLE, I.L. TREGILLIS, M.J. SCHMITT, S.H. BATHA, P.A. BRADLEY, K.A. DEFRIEND OBREY, H.W. HERRMANN, M.D. WILKE, *Los Alamos National Laboratory* The effect of small localized perturbations, such as fill tubes and mounting tents, on the NIF ignition capsule and the effect of hemi-joints on high gain double shell capsules are an important issue in achieving ignition on NIF. To begin the study of defects on yield, an exploding pusher has been designed. In this presentation experimental results and simulations will be presented. Exploding pushers with defect rings 15-17 microns wide and 2.2-2.7 microns deep were shot on the OMEGA laser. The capsules were CH shells 431-436 microns in radius and 8.1-8.5 microns thick. They were filled with a 50-50 ratio of 5 atm DT and were directly driven. These results were compared to thicker shell CH targets. These targets were 440-445 microns in radius and 15.1-15.2 microns thick. The defects were similar to those for the exploding pusher. Calculations with both Eularian AMR and Lagrangian codes were done and compared to the experimental results. For the exploding pushers, the codes predict and the experiments gave about a factor of 2 decrease in the neutron yield over the unperturbed results. The yield for the thicker targets showed at most a factor of 2 loss in yield much higher than predicted.

NP8 83 Multiple Scattering of Slow Ions in a Partially Degenerate Electron Fluid ROMAIN POPOFF, GILLES MAYNARD, CLAUDE DEUTSCH, *LPGP UParis XI* MULSCATT COLLABORATION, We extend former investigations to a partially degenerate electron fluid at any temperature of multiple slow ion scattering at T=0. We implement an analytic and mean-field interpolation of the target electron dielectric function between T=0 (Lindhard) and T→ oo (Fried-Conte). A specific attention is given to multiple scattering of proton projectiles in the keV energy range stopped in a hot electron plasma at solid density.

NP8 84 The ionization balance of gold in the Livermore Electron Beam Ion Trap M. MAY, *LLNL* S. HANSEN, *SNL* H.-K. CHUNG, K. REED, J. SCOFIELD, M. SCHNEIDER, B. WILSON, K. WONG, P. BEIERSDORFER, *LLNL* Spectra have been recorded from gold that has been injected into the Lawrence Livermore Electron Beam Ion Trap (EBIT-II). Both monoenergetic and experimentally simulated Maxwell-Boltzmann (MB) nonlocal thermodynamic equilibrium (NLTE) plasmas were created for these measurements. The beam plasmas had energies of 2.75, 3.0, 3.6, 4.6, 5.5, 6.0 and 6.5 keV. The MB plasmas had electron temperatures of 2.0, 2.5 and 3.0 keV. M-band gold spectra (n = 4-3, 5-3, 6-3 and 7-3 transitions) were recorded between 1-8 keV from K-like to Kr-like ions in the X-ray. The emission of gold was recorded by crystal spectrometers and a micro-calorimeter from the Goddard Space Flight Center. The experimental charge state distribution was inferred by fitting the observed spectra with modelled spectra from the Hebrew University Lawrence Livermore Atomic Code and the Flexible Atomic Code (FAC). The charge state distribution has been modelled using the SCRAM collisional radiative model with FAC atomic data. Fairly good agreement between the experimental and the calculated charge state distributions for several of the beam plasmas has been achieved by including dielectric recombination from high n = 10 to 15 states. This work was done under the auspices of the U.S. Department of Energy by Lawrence Livermore National Laboratory under Contract DE-AC52-07NA27344.

NP8 85 Experiment to determine electrical conductivity and equation of state data from Ohmically exploded tamped planar foils - preliminary diagnostic results and modeling E.L. RUDEN, D.J. AMDAHL, *Air Force Research Laboratory, Directed Energy Directorate* D.J. BROWN, T.C. GRABOWSKI, C.W. GREGG, M.R. KOSTORA, B.M. MARTINEZ, J.V. PARKER, *Science Applications International Corporation* J.F. CAMACHO, S.K. COFFEY, *NumerEx, LLC* P. POULSEN, *CAREN Co.* Diagnostic results from initial nondestructive (thick foil, low current) tests are presented for an experiment to simultaneously determine the electrical conductivity, pressure, density, specific energy, and temperature time histories of a planar metal foil tamped by a well characterized transparent material and exploded by a 36 μF, 50 kV rated capacitor bank discharge. Voltage differentials measure the foil's surface electric field, a B-dot probe measures surface current density, and a laser velocity interferometer (VISAR) measures dynamic foil thickness. From such and future filtered photodiode measurements, the desired properties will be inferred up to a few eV and within an order of magnitude of solid density. The purpose of the present phase of the experiment is to develop and validate diagnostic designs, data analysis techniques, and 2-D MHD simulations of the process using the MACH2 code.

NP8 86 Characteristics of warm dense matter produced by a relativistic electron beam* THOMAS KWAN, MARK SCHMITT, *Los Alamos National Laboratory* MICHAEL BERNINGER, *National Security Technologies, LLC* Accurate equation-of-state theory on warm dense matter is a big challenge to model and good experimental data is difficult to obtain. One of the difficulties is the creation of a warm dense matter (WDM) suitable for experiments to examine its equation of state. We have performed calculations using MCNP and LASNEX to examine the warm dense matter created by a highly energetic electron beam such as the DARHT beam at LANL in a cylindrical sample confined by a collar. Energy deposition by the electron beam in the target and collar of different materials were calculated with different beam profiles. The energy deposition was sourced into LASNEX calculations to examine the dynamic evolution of the target and the generation of radially outward propagating shock waves. Our calculations indicated warm dense matter with a temperature of a few electron volts is achievable and the speed of the shock wave can be determined using photonic Doppler velocimetry technique. We will present results from our calculations for various materials of the target and collar and in different geometries.

*Work supported by US DOE/NNSA, performed at LANL, operated by LANS LLC under Contract DE-AC52-06NA25396.

NP8 87 Effects of Coulomb and Fermi corrections on the equation of state of dense plasmas* IGOR SOKOLOV, ERIC MYRA, ALEXANDER POTASHEV, *University of Michigan* In this presentation, we derive corrections for two frequently neglected or poorly approximated components of the equation of state for dense plasmas: (i) the Coulomb correction, which accounts for electron-electron interactions and (ii) the Fermi correction, which accounts for (frequently important) quantum-mechanical behavior of electrons. We demonstrate a more accurate approach to these calculations and discuss their effects on thermodynamic properties, ionization, and emissivity of dense plasmas.

*This work was supported in part by the US DOE NNSA under the Predictive Science Academic Alliance Program by grant DE-FC52-08NA28616.

NP8 88 Improving predictive simulation of high-energy-density physics experiments: effects of Coulomb and Fermi corrections* ERIC MYRA, IGOR SOKOLOV, ALEXANDER POTASHEV, *University of Michigan* The work of Sokolov et al. (also in this poster session) discusses the important effects of Coulomb and Fermi corrections to the thermodynamic properties and emissivity of dense plasmas. In this presentation, we apply these equation-of-state corrections to a set of test problems to help gauge their importance in the predictive simulation of an HEDP experiment. The simulations are performed with the CRASH code, which is a radiation-hydrodynamic simulation code developed at the Center for Radiative Shock Hydrodynamics at the University of Michigan.

*This work was supported in part by the US DOE NNSA under the Predictive Science Academic Alliance Program by grant DE-FC52-08NA28616.

NP8 89 Platform development of x-ray absorption-based temperature measurements above 100-eV PAUL KEITER, JOHN BENAGE, NICK LANIER, KUNEGUNDA BELLE, GLENN MAGELSSEN, BARBARA DEVOLDER, *Los Alamos National Laboratory* ANDREW COMLEY, JOHN MORTON, MARK TAYLOR, *Atomic Weapons Establishment* Experiments are being performed on the OMEGA laser system at the University of Rochester to develop experimental techniques for measuring the temperature of radiatively heated foams. The development of this technique in the temperature range of 100 – 200 eV is required for future NIF experiments. We will present a current summary of the experimental data as well as direction for the future campaigns. This was performed by the Los Alamos National Laboratory under the auspices of the United States Department of Energy under contract no. DE-AC52-06NA25396.

NP8 90 X-ray emission measurements from implosion experiments with Fe doped glass capsules* FRED WYSOCKI, JOHN BENAGE, GEORGE KYRALA, EVAN DODD, DOUG WILSON, *Los Alamos National Lab* Recent results obtained for glass capsule implosions at the Omega laser indicate that when the gas contains a high z dopant gas, simulations do not match the compression and yield of the capsule, even when using a mix model. A critical time for when the experiments deviate from predictions occurs when the reflected shock hits the imploding shell. We have identified two possible issues that the codes may have incorrect, the density of the shell at this critical time and the density and temperature profile in the gas. To address these questions, we are attempting two new measurements in these experiments. These are x-ray radiography of the shell and temporally and spatially resolved temperature and density measurements in the gas. In this poster, we present our plan for the time and space resolved gas measurements utilizing a new multiframe monochromatic imager (MMI) diagnostic. This diagnostic will utilize emission from Fe ions that have been mixed into the gas from the shell. We will present data from some recent measurements that determine the K-shell Fe emission from the gas as a function of Fe dopant levels in the glass. We will also give results for the impact such mixing has on the performance of the capsules. The implications to obtaining the desired temperature and density profiles will be discussed.

*Work supported by US DOE/NNSA under Contract DE-AC52-06NA25396.

NP8 91 Cone-guided Target Acceleration for Impact Ignition HIDEO NAGATOMO, MASAKATSU MURAKAMI, TOMOYUKI JOHZAKI, HIROSHI AZECHI, *ILE, Osaka University* Various ignition schemes have been proposed in laser fusion. One of the latest concepts is Impact ignition [1], which does not include uncertain physics, such as laser plasma interaction, or core heating by hot electrons. In the Impact ignition scheme, one of the most critical issues is how to achieve very high speed projectile made of fuel. If most of the kinetic energy of the impactor is converted into thermal energy, the impactor velocity needs to be 1100–1500 km/s to achieve the ignition temperature of Te=5-10keV. In addition, impactor is isolated from impactee, a main fuel part by guiding cone in similar way of Fast ignition. In this study, preliminary numerical simulations were performed for the target acceleration in guiding cone, where radiation transport, shock-wall interaction are included. [1] M. Murakami and H. Nagatomo, Nucl. Instrum. Methods, Phys. Res., Sect. A 544, 67 (2005). [2] H. Azechi, et al., Phys. Rev.Lett. 102, 235002 (2009).

NP8 92 Nuclear energy without radioactivity: Laser driven block ignition of hydrogen-lithium7 HEINRICH HORA, *Department of Theoretical Physics* GEORGE MILEY, *Department of Nuclear Plasma and Radiological Engineering* Side-on block ignition of uncompressed solid fusion fuel by multi-petawatt-picosecond laser pulses following the Chu-Bobin scheme may be possible using a drastic anomaly of laser-plasma interaction. It is essential that the laser pulses are extremely clean (contrast ratio 10^8) to avoid relativistic self-focusing[1] as shown for DT with next available laser pulses after updating the Chu-Bobin scheme.[2] Using $p^{11}B$ (HB11) turned out to be only about ten times more difficult for laser fusion by this side-on ignition in contrast to impossible ignition by the usual spherical laser compression. Results for p-7Li fusion are similar to HB11. Controlled laser fusion energy may be produced with less radioactivity per energy than burning coal. [1]H. Hora, J. Badziak et al. Phys. Plasmas, **14**, 072701 (2007); [2]H. Hora, B. Malekynia et al. Appl. Phys. Lett. **93**, 011101 (2008); [3]H. Hora, G.H. Miley et al. Laser & Part. Beams **27**, (2009) doi:10.1017/8S026303460999022X.

NP8 93 Simulations of Targets for Warm Dense Matter and Inertial Fusion Energy Applications on NDCX II* J.J. BARNARD, *LLNL* J. ARMIJO, F.M. BIENIOSEK, *LBNL* A. FRIEDMAN, *LLNL* M. HAY, E. HENESTROZA, B.G. LOGAN, R.M. MORE, P.A. NI, *LBNL* L.J. PERKINS, *LLNL* S.F. NG, *CUHK* S.A. VEITZER, J.S. WURTELE, S.S. YU, A.B. ZYLSTRA, *LBNL* The Neutralized Drift Compression Experiment II (NDCX II) is an induction accelerator now being constructed at LBNL. The baseline design calls for a 3 MeV, 30 A Li+ ion beam, delivered in a bunch with pulse duration of $\sim$ 1 ns, and transverse dimension $\sim$ 1 mm. The purpose of NDCX II is to experimentally study material in the warm dense matter regime and ion beam/hydrodynamic coupling, relevant to heavy ion fusion. In preparation for NDCX II, we have performed hydrodynamic simulations of ion-beam-heated, metallic targets, connecting observable quantities with the simulated density, temperature, and velocity, exploring the sensitivity of EOS on observables. Simulated target geometries include spherical and cylindrical bubbles (to create regions of higher pressure), and planar solid and foam targets. Pulse formats include single pulses of fixed ion energy E, and single and double pulses with variable E to study ion-coupling efficiency. Comparisons are made with simulations of ion driven direct drive capsules that show high coupling efficiencies.

*Work performed under the auspices of the U.S. DOE under contracts DE-AC52-07NA27344 and DE-AC02-05CH11231.

NP8 94 Optimized Ion Energy Profiles for Heavy Ion Direct Drive Targets* MICHAEL J. HAY, *Lawrence Berkeley National Laboratory* JOHN J. BARNARD, L. JOHN PERKINS, *Lawrence Livermore National Laboratory* B. GRANT LOGAN, *Lawrence Berkeley National Laboratory* Recent 1-D implosion calculations [1] have characterized pure-DT targets delivering gains of 50-90 with less than 0.5 MJ of heavy ion direct drive. With a payload fraction of 1/3, these low-aspect ratio targets operate near the peak of rocket efficiency and achieve $\sim$ 10% overall coupling efficiencies (vs. the 15-20% efficiencies analytically predicted for less stable, higher-aspect ratio targets). In Ref. 1, the ion energy is ramped directly from a 50 MeV foot pulse to a 500 MeV main pulse. In this paper, we instead tune the ion energy throughout the drive to closely match the beam deposition with the inward progress of the ablation front. We will present the ion energy and intensity time histories that maximize drive efficiency and gain for a single target at constant integrated drive energy. [1] L. J. Perkins, B. G. Logan, J. J. Barnard, and M. J. Hay. "High Efficiency High Gain Heavy Ion Direct Drive Targets," *Bulletin of the American Physical Society*, vol. 54: DPP, Nov. 2009.

*Work performed under the auspices of the U.S. Department of Energy under contract DE-AC52-07NA27344 at LLNL and University of California contract DE-AC02-05CH11231 at LBNL.

NP8 95 Warm Dense Matter Experiments Driven by Ion Beams* F.M. BIENIOSEK, E. HENESTROZA, J.Y. JUNG, M.A. LEITNER, S. LIDIA, B.G. LOGAN, R.M. MORE, P.A. NI, P.K. ROY, P.A. SEIDL, W.L. WALDRON, *LBNL* J.J. BARNARD, A. FRIEDMAN, *LLNL* Intense beams of heavy ions are capable of heating volumetric samples of matter to high energy density. We present results from warm dense matter (WDM) experiments at NDCX-I. The 0.3 MeV, 30-mA K^+ beam from the NDCX-I accelerator heats foil targets by combined longitudinal and transverse neutralized drift compression of the ion beam to a spot size $\sim$ 1 mm, and compressed pulse length $\sim$ 2 ns. The uncompressed beam flux is $\geqslant$ 500 kW/cm^2, and the compressed pulse flux is $>$ 5 MW/cm^2. Both the compressed and uncompressed parts of the NDCX-I beam heat targets. Future plans include construction of the NDCX-II accelerator, which is designed to heat targets at the Bragg peak using a 3-4 MeV lithium ion beam. We have developed a target chamber and target diagnostics including a fast multi-channel optical pyrometer, optical streak camera, and high-speed gated cameras. We compare measurements of temperature, droplet formation and other target parameters with model predictions. Continued improvements in beam tuning, bunch compression, and other upgrades are expected to yield higher flux on target.

*This work was performed under U.S. DOE Contracts DEAC5207NA27344 and DE-AC02-05CH11231.

NP8 96 Thermal simulations of the NDCX-I target experiments* E. HENESTROZA, F.M. BIENIOSKE, P.A. NI, R.M. MORE, J.J. BARNARD, *Lawrence Berkeley National Laboratory* Experiments on ion-beam target heating use a 0.3 MeV K+ beam from the Neutralized Drift Compression Experiment (NDCX-I) accelerator at LBNL. The NDCX-I delivers a long pulse beam (several microseconds) with a power density of 500 kW/cm^2 over a sampled spot size on the target of several hundred micrometers. With the addition of an imposed velocity tilt from an induction core, the NDCX-I can compress a portion of the long pulse to reach a power density of 25 MW/cm^2 over 2 nanoseconds. Under these conditions, the free-standing thin foil targets used in the experiments go through the melting and vaporization phases to reach temperatures up to 4000 K. Since the targets are thin foils of fractions of a micron in thickness we can model the target thermal dynamics using the equation of heat conduction for the temperature T(x,t) as function of time and the spatial dimension along the beam direction; we also include cooling processes from energy flux from the surface of the foil due to evaporation, radiation, and thermionic (Richardson) emission.

*This work was supported by the Director, Office of Science, Office of Fusion Energy Sciences, of the U.S. Department of Energy under Contract No. DE-AC02-05CH11231 and Contract DE-AC52-07NA27344.

NP8 97 Numerical studies on plasma jets and minirailguns at HyperV LINCHUN WU, F. DOUGLAS WITHERSPOON, *HyperV Technologies Corp.* DALE R. WELCH, *Voss Scientific, LLC* MICHAEL W. PHILLIPS, *Advanced Energy Systems* Computational study of plasma jets using contoured gap coax and parallel plate minirailguns are underway using helium, argon and xenon plasmas with injection speeds of up to 10-20 km/s and plasma density of 10^{15} - 10^{17} cm^{-3}. The study is performed using the recently improved Lsp code, which now implements a new sheath model and direct implicit algorithms enabling more accurate and faster simulations. The new radiation transport model in Lsp, with atomic data from Prism, is used in these 2D simulations. Results are shown and compared between these high-Z plasma species. Blow-by instability and restrike are observed in these simulations and will be discussed. The effects of ion stripping on high-Z plasma acceleration in the railguns will be studied as well using available atomic data. Work supported by the U.S. DOE Office of Fusion Energy Sciences.

NP8 98 3D Kinetic Simulation of Plasma Jet Penetration in Magnetic Field* SERGEI A. GALKIN, I.N. BOGATU, J.S. KIM, *Far-Tech, Inc.* A high velocity plasmoid penetration through a magnetic barrier is a problem of a great experimental and theoretical interest. Our LSP PIC code 3D fully kinetic numerical simulations of high density (10^{16} cm^{-3}) high velocity (30-140 km/sec) plasma jet/bullet, penetrating through the transversal magnetic field, demonstrate three different regimes: reflection by field, penetration by magnetic field expulsion and penetration by magnetic self-polarization. The behavior depends on plasma jet parameters and its composition: hydrogen, carbon (A=12) and C_{60}-fullerene (A=720) plasmas were investigated. The 3D simulation of two plasmoid head-on injections along uniform magnetic field lines is analyzed. Mini rail plasma gun (accelerator) modeling is also presented and discussed.

*Work supported by the US DOE SBIR grant.

NP8 99 IMC Photonics in HYDRA NIF Simulations G.D. KERBEL, M.M. MARINAK, N. GENTILE, *Lawrence Livermore National Laboratory* One option in the radiation hydrodynamics code HYDRA for computing radiation transport is IMC (Implicit Monte Carlo) direct simulation. Well-converged simulations run with IMC spend most of their time doing radiation transport. We desire the run time to be as short as possible for the (NIF) experimental campaign and thus we have focussed efforts on ways to speed the IMC computation. Techniques were implemented to accomplish variance reduction through angular biasing, reducing the amount of computation required for given accuracy. We have improved load balance through multi-level parallelism and dynamic domain data distribution across processes. In addition we have added domain data replication to attain strong scaling with process count as more computing resources become available. This work performed under the auspices of the U.S. Department of Energy by Lawrence Livermore National Laboratory under Contract DE-AC52-07NA27344.

NP8 100 New capabilities in HYDRA for simulations of Inertial Confinement Fusion targets* M.M. MARINAK, G.D. KERBEL, J.M. KONING, M.V. PATEL, S.M. SEPKE, P.N. BROWN, B. CHANG, R. PROCASSINI, D. LARSON, *Lawrence Livermore National Laboratory* A variety of new capabilities have been installed in the HYDRA 2D/3D multiphysics ICF simulation code. We discuss how these enhance its ability to simulate various aspects of inertial confinement fusion targets. A novel polar S_N multigroup radiation transport package now operates on 2D meshes. It converges with second order accuracy without significant ray effects. Simulations of targets illuminated with short pulse lasers are now possible by running HYDRA in conjunction with an explicit relativistic particle in cell code. Data is exchanged between the two codes automatically, enabling the plasma heating and magnetic fields generated by the short pulse laser to be included consistently in the full target simulation. A Monte Carlo burn package has also been incorporated and is being applied to model diagnostic signatures of neutrons, gamma rays and charged particles produced in NIF capsule implosions.

*This work was performed under the auspices of the Lawrence Livermore National Security, LLC, (LLNS) under Contract No. DE-AC52-07NA27344.

NP8 101 The Hydra Magnetohydrodynamics Package* J.M. KONING, G.D. KERBEL, M.M. MARINAK, *LLNL* The Magnetohydrodynamics package of the ALE radiation-hydrodynamics code Hydra is being extended to model the magnetic field and its effect on temperature for ICF targets. The current package capabilities include a fully three-dimensional resistive MHD package in the small Hall limit. An operator split method is used to couple the MHD to the hydrodynamics and is fully implicit in time and second order accurate in space. A three-dimensional vector finite element method is utilized to define a set of spaces and differential operators that maintain the zero divergence of the magnetic field exactly. The Hydra MHD package has been improved by the addition of an exact circuit solution method that enables the potential for multiple circuits. A significant enhancement of Hydra is the addition of a Python interpreter embedded in the code. The Python interpreter allows users to make full use of Python's features in

parallel with full access to the parameters and variables in the simulation. Examples of the Python interpreter used with MHD package and Hydra in general will be presented.

*Prepared by LLNL under Contract DE-AC52-07NA27344.

NP8 102 Simulating NIF Neutron Diagnostics with HYDRA* MEHUL V. PATEL, SCOTT SEPKE, MICHAEL M. MARINAK, MICHAEL S. McKINLEY, MATTHEW O'BRIEN, RICHARD PROCASSINI, *Lawrence Livermore National Laboratory* DOUG WILSON, *Los Alamos National Laboratory* LLNL's 3D radiation hydrodynamics code, HYDRA, is routinely used for modeling laser inertial confinement fusion (ICF) targets (both direct drive and indirect drive). Since neutron and gamma diagnostics will play a critical role in assessing the performance of capsule implosions at the National Ignition Facility (NIF), we have installed a particle Monte Carlo (PMC) package into HYDRA to model the transport of light nuclei (Z=1,2), gammas, and neutrons. The PMC package uses both domain decomposition (using HYDRA's existing computational domains) and dynamic replication of domains to maximize utilization of available computational resources. Recent results from simulations of NIF capsules will be presented to demonstrate our ability to produce realistic simulated neutron images and spectra.

*Prepared by LLNL under Contract DE-AC52-07NA27344.

NP8 103 Modeling ICF Spherical Implosion Instabilities in 3D with Exact Energy Conservation* MILAD FATENEJAD, GREGORY MOSES, *Univ. of Wisconsin - Madison* We will present the results of 3D instability simulations performed on spherically convergent geometries with a new 3D Lagrangian hydrodynamics code, cooper. The code uses a compatible discretization of the conservation equations to ensure that energy is conserved to within machine round off error [Caramana slJCP 146, 227 (1998)]. Modifications are made to the discrete equations to ensure that spherically symmetric implosions can be performed on non-orthogonal Cartesian grids [Caramana slJCP 157, 89 (2000)]. Subzonal restoring forces counteract anomalous grid distortions [Carmana slJCP 142, 521 (1998)] and an edge-centered viscosity is used to capture shocks [Caramana slJCP 215, 385 (2006)]. Cooper is parallelized using domain decomposition. This is necessary due to the large processor and memory requirements associated with simulations in three dimensions. Advanced computational libraries are used to reduce the complexity of the code without sacrificing features. One example is the MOAB library [Tautges slEngr. Comput. 20, 286 (2004)] which manages the mesh and is responsible for communicating information between processes.

*Work Supported By: Laboratory for Laser Energetics, U. of Rochester

NP8 104 Simulation of the Radiative Emission from Plasmas Based on LSP Particle-In-Cell Simulations JOSEPH MacFARLANE, IGOR GOLOVKIN, PAMELA WOODRUFF, *Prism Computational Sciences* DALE WELCH, CARSTON THOMA, *Voss Scientific* DOUGLAS WITHERSPOON, *HyperV Technologies* Particle-in-cell (PIC) simulation codes are valuable tools in simulating the physical properties of plasmas in a wide variety of high energy density laboratory plasma experiments. Two examples of this are short-pulse laser experiments, which are used to study the fast ignition concept for inertial fusion, and plasma jet experiments, which are of interest to magnetic fusion and mageto-inertial fusion studies. The LSP code is a widely-used PIC simulation code that computes the detailed characteristics of electron and ion particle distributions in such experiments. To compute the radiative emission characteristics of plasmas based on PIC simulation predictions, we use the SPECT3D multi-dimensional collisional-radiative package to generate high-resolution spectra and images which can be compared with experimental measurements. SPECT3D includes the effects of energetic particles (including relativistic electrons) in computing non-LTE atomic level populations, emergent spectra, and images for the target plasma. We will present results for the radiative characteristics of plasmas created in short-pulse laser and plasma jet experiments.

NP8 105 Simulation of non LTE opacity with incoming radiation* MARCEL KLAPISCH, MICHEL BUSQUET,† *ARTEP, inc., Ellicott City MD 21042* Simulation of radiative properties of hot plasmas is important for ICF, other laboratory plasmas, and astrophysics. When mid-Z or high-Z elements are involved, the spectra are so complex that one commonly uses LTE approximation. This was recently done in interpreting a carefully calibrated experiment on Fe at 160 eV [1]. However some disagreement remains concerning the ion charge distribution. The newest version of HULLAC [2] has the capability to take into account an incoming radiation field in solving the rate equations of the coronal radiative model (CRM). We will show results with different representation of the radiation field. [1] J.E. Bailey, G.A. Rochau, C.A. Iglesias, et al., Phys. Rev. Lett. 99, (2007) 265002-4. [2] M. Klapisch and M. Busquet, High Ener. Dens. Phys. 5, (2009) 105-9.

*Work supported by USDOE under contract # N00173-05-C-2020 with Laser Plasma Branch, NRL, Washington, DC.
†also at Observatoire de Paris, Meudon, France

NP8 106 Particle-in-Cell Simulations of the High Frequency Hybrid Instability and Two Plasmon Decay* FRANK TSUNG, W.B. MORI, *UCLA* B.B. AFEYAN, *Polymath Research Inc.* A comprehensive set of PIC simulations of laser-plasma interactions at or near the quarter critical density of laser-produced plasmas has been conducted. In order to isolate physical effects, we conduct fixed, mobile ion simulations, and simulations with rapid and adiabatic rise times. In the fixed ion simulations near threshold the instability is dominated by absolute modes with growth rates and ranges of transverse wave numbers in agreement with the theoretical results Afeyan and Williams (1995 & 1997)[1,2]. These include the high frequency hybrid modes (HFHI). Further above threshold, modes with larger transverse wave numbers occur at lower densities and these were identified as convective modes. There can be a strong interaction between the modes at low density and the absolute modes at higher densities on the hot electron spectrum. The role of the adiabatic rise time on the instability will be discussed. Finally, we will also investigate the role of mobile ions on the excitation of the 2wp/HFHI modes, and the subsequent absorption of speckles in regimes relevant to direct ICF and fundamental HEDLP studies. [1] B. B. Afeyan, E. A. Williams, *Phys. Rev. Lett.*, **75** 4218 (1995). [2] B. B. Afeyan, E. A. Williams, *Phys. Plas.*, **4**, 3827 (1997).

*This research is supported by DOE and NRL.

NP8 107 Condensed Matter Deuterium Cluster Target for Study of Pycnonuclear Reactions XIAOLING YANG, MILEY GEORGE, *University of Illinois at Urbana-Champaign* Fusion reactions have two main classes: thermonuclear and the pycnonuclear. Thermonuclear fusion occurs in low density high temperature plasmas, and is very sensitive to the ion temperature due to Columbic repulsion effects. As the density increases, the Columbic potential barrier is depressed by increased electron screening, allowing fusion at lower temperatures. This type of nuclear reaction is termed a pycnonuclear fusion and is the basis for astrophysical fusion. Ichimarua [1] proposed a laboratory study of this process using explosive mechanical compression of H/D to metallic densities, which would be extremely difficult to implement. Instead, our recent research suggests that metallic-like H/D "clusters" can be formed in dislocation loops of thin Palladium foils through electrochemical processes. [2] If this technique is used as a laser compression target, the compressed cluster density would allow study of pycnonuclear reactions. This provides a means of studying astrophysical fusion process, and could also lead to an important non-cryogenic ICF target. [1] S. Ichimaru, H. Kitamura. Phys. Plasmas, 6, 2649 (1999) [2] G. Miley and X. Yang, Deuterium Cluster Target for Ultra-High Density, 18TH TOFE, San Francisco, CA Sep. 28 – Oct. 2, 2008

NP8 108 New features in OSIRIS 2.0 R.A. FONSECA, *DCTI, Instituto Superior de Ciências do Trabalho e da Empresa, Lisboa, Portugal* S.F. MARTINS, P. ABREU, J. MARTINS, F. FIUZA, J. VIEIRA, L.O. SILVA, *GoLP/Instituto de Plasmas e Fusão Nuclear, Instituto Superior Técnico, Lisboa, Portugal* V. DECYK, F. TSUNG, J. TONGE, W.B. MORI, *UCLA Plasma Simulation Group, CA 90095* OSIRIS 2.0 [1] is a state of the art, fully relativistic massively parallel particle in cell code, that is widely used in kinetic plasma modeling for many astrophysical and laboratory scenarios. We report on the new developments done in the code, focusing on the new high performance vector SIMD code (Altivec/SSE3) for single precision calculations, detailing performance and floating point efficiency, and also parallel I/O for diagnostics, allowing for higher performance and scalability on HPC systems. We will also describe the new numerical precision features in the code, and we will also present the new algorithms incorporated into the code, in terms of field solver (4^{th} order Yee solver, etc.), new filtering techniques, perfectly matched layers (PML) boundary conditions, and boosted frame simulations. Finally, we also report on a new diagnostic tool to calculate the radiation produced with wavelengths below the simulation grid resolution. [1] R. A. Fonseca et al., LNCS 2331, 342, (2002)

NP8 109 Progress report in developing a 3D parallel object-oriented Vlasov-Fokker-Planck code MICHAIL TZOUFRAS, ANTHONY BELL, *University of Oxford* RAOUL TRINES, PETER NORREYS, *RAL* FRANK TSUNG, *UCLA* We utilize the expansion of the electron distribution function to spherical harmonics to design an object-oriented VFP code [1]. Using this approach we significantly reduce the size of the computational grid, compared to what is required by standard VFP codes, thereby making it possible to model the entire distribution function in three dimensions. The object-oriented design allows for parallelism and interchangeability of numerical operators. The performance of the most up-to-date version of the code in terms of speed, accuracy and stability is discussed for standard plasma physics problems. [1] A. R. Bell et al., Plasma Phys. Control. Fusion 48 (2006) R37-R57.

NP8 110 Simulating the NDCX-II Physics Design* W.M. SHARP, A. FRIEDMAN, D.P. GROTE, R.H. COHEN, S.M. LUND, *LLNL* M. LEITNER, J.-L. VAY, W.L. WALDRON, *LBNL* The Virtual National Laboratory for Heavy-Ion Fusion is developing a physics design for NDCX-II, an experiment to study warm dense matter heated by ions near the Bragg-peak energy. Present plans call for using thirty-four induction cells to accelerate 30 nC of Li^+ ions to more than 3 MeV. Neutralized drift-compression is then used to compress the beam to the sub-millimeter radius and 1-ns duration needed to attain useful target temperatures. A 1-D particle-in-cell simulation ASP has been used for developing the NDCX-II acceleration schedule, and centroid equations have recently been added to study the effects of transverse-focusing errors. Multidimensional simulations with Warp have validated the ASP model and have been used both to design transverse focusing and to compensate for injection non-uniformities and 3-D effects. Results from this work are presented, and ongoing work to replace the analytic waveforms with output from circuit models is discussed.

*Work performed under the auspices of US Department of Energy by LLNL under Contract DE-AC52-07NA27344 and by LBNL under Contract DE-AC03-76SF00098.

NP8 111 EDGE

NP8 112 Flush-mounted probes smaller than the ion gyroradius* ILON JOSEPH, RON COHEN, DMITRI RYUTOV, *Lawrence Livermore National Lab* When an electrically conducting probe with a cross-section that is smaller than an ion gyroradius but larger than an electron gyro-radius is placed within a magnetized plasma, the electrostatic perturbation that is produced develops an extremely long length scale parallel to field lines. For such small-scale disturbances, collisions play an important role in determining the response of the lowest-order distribution function. In the fluid picture, the ion viscous force dominates and the ions effectively become demagnetized. Kinetically, the dominant non-adiabatic response is generated by electron-ion friction rather than parallel streaming, because the parallel length scale is typically much longer than the mean free path. This study also has direct application to the linear dispersion relation of modes that are dominated by electron-scale physics. For example, divertor leg instabilities can be terminated near an X-point due to the development of fine scales through the action of magnetic shear. The non-adiabatic correction to the dispersion relation of these modes is determined.

*Performed by LLNL under US DOE Contract DE-AC52-07NA27344.

NP8 113 Peeling-Ballooning Mode Analysis in Shifted-Circle Tokamak Equilibria* B. BURKE, *UW-Madison* S.E. KRUGER, *TechX* C.C. HEGNA, *UW-Madison* P.B. SNYDER, *General Atomics* C.R. SOVINEC, P. ZHU, *UW-Madison* Progress in understanding edge localized modes (ELMs) has been made by investigating the stability properties of edge localized peeling-ballooning modes. We focus on the evolution of ideal MHD modes over a large spectrum in two shifted-circle tokamak equilibria, using the extended-MHD code NIMROD. The TOQ-generated

equilibria model a H-mode plasma with a pedestal pressure profile and parallel edge currents. A vacuum region is prescribed by a resistivity profile that transitions from a small to very large value at a specified location. The vacuum model is benchmarked against the linear ideal MHD codes ELITE & GATO. We demonstrate vacuum effects on the stability by adjusting the vacuum location relative to the pedestal pressure region. Ballooning-like instabilities dominate distant vacuum cases, whereas peeling mode physics is expected to dominate as the vacuum approaches the pedestal. Numerical simulations of the early nonlinear stages of edge localized MHD instabilities are presented. Comparisons between equilibria that have "ballooning" dominated instabilities relative to equilibria that are "peeling" dominated are made.

*The research was performed under appointment to the FES Fellowship and supported by the U.S. DOE under grant no. DE-FG02-86ER53218.

NP8 114 Numerical Simulation of Giant Sawteeth in Tokamaks Using the NIMROD Code* D.D. SCHNACK, *University of Wisconsin, Madison, WI* S.E. KRUGER, *TechX Corp., Booulder, CO* C.C. KIM, *University of Washington, Seattle, WA* A.D. TURNBULL, *General Atomics, Sam Diego, CA* A minority population of energetic particles can stabilized the n=1 sawtooth mode in tokamaks. This allows for giant sawteeth with long period and large amplitude. The crash can lead to degradation of confinement, NTM and ELMs, and a significant loss of stored energy. This could have important implications for the design and operation of ITER. In order to evaluate the efficacy of the Porcelli model, extensive linear studies have been performed recently to analyze the sawtooth activity in DIII-D discharge #96043 through a sequence of equilibria reconstructed from experimantal data[1]. The results were consistent with the observed sawtooth crash. Here we begin a computational study of the non-linear consequences of the crash of a giant sawtooth using the NIMROD Extended MHD code[2]. We use the series of equilibrium reconstructions considered in Ref. 2. Initial linear results for both MHD and extended MHD, including energetic particle effects, are presented. [1] M. Choi, A. D. Turnbull, V. S. Chan, et al., Phys. Plasmas 14, 112517 (2007). [2] C. R. Sovinec, et al., J. Phys. Conf. Ser. 16, 25 (2005).

*Work supported by USDOE.

NP8 115 Modeling anomalous radial transport in kinetic transport codes* K. BODI, S.I. KRASHENINNIKOV, *UCSD* R.H. COHEN, T.D. ROGNLIEN, *LLNL* ESL TEAM, Anomalous transport is typically the dominant component of the radial transport in magnetically confined plasmas, where the physical origin of this transport is believed to be plasma turbulence. A model is presented for anomalous transport that can be used in continuum kinetic edge codes like TEMPEST, NEO and the next-generation code being developed by the Edge Simulation Laboratory. The model can also be adapted to particle-based codes. It is demonstrated that the model with a velocity-dependent diffusion and convection terms can match a diagonal gradient-driven transport matrix as found in contemporary fluid codes, but can also include off-diagonal effects. The anomalous transport model is also combined with particle drifts and a particle/energy-conserving Krook collision operator to study possible synergistic effects with neoclassical transport. For the latter study, a velocity-independent anomalous diffusion coefficient is used to mimic the effect of long-wavelength ExB turbulence.

*LLNL contribution prepared for USDOE under contract DE-AC52-07NA27344.

NP8 116 Comparison of cross-magnetic-field drift algorithms in UEDGE.* S.K. NAM, T.D. ROGNLIEN, *LLNL* Inclusion of ExB, gradient-B, and curvature drift terms in 2D edge plasma transport codes typically results in substantially slower convergence or lack of convergence for obtaining steady-state profiles. Those cases where convergence is obtained show that drifts can have a strong effect of the scrape-off layer plasma profiles and flows, and thus improvement of the efficiency and robustness of edge transport codes with drifts is a high priority, especially as these codes become components within integrated whole-device models. Rozhansky *et al.* [Nucl. Fusion 49 (2009) 025007] have proposed a new numerical formulation of the drift terms, and it is shown to improve the SOLPS code performance and accuracy, though an artificial stabilizing diffusive term is still required beyond the physical turbulent diffusive term. While the fully implicit algorithm in UEDGE requires no separate stabilizing term, it often does exhibit convergence difficulties for steep-gradient cases. Results from UEDGE implementation of the Rozhansky algorithm are presented and compared to the original algorithm for performance and accuracy.

*Prepared by LLNL under Contract DE-AC52-07NA27344.

NP8 117 Coupled turbulence and transport simulations for edge plasmas.* T.D. ROGNLIEN, *LLNL* M.V. UMANSKY, R.H. COHEN, X.Q. XU, *LLNL* Coupling between edge turbulence and transport has been demonstrated in the past using a type of Relaxed-Iteration Coupling (RIC) scheme [Shestakov et al., JCP 185 (2003) 399] where time-averaged turbulent fluxes (BOUT) are coupled to a transport code (UEDGE) in a series of time-lagged iteration to find a steady-state solution [Rognlien et al., JNM 337-339 (2005) 327]. A key issue for such a method applied to edge turbulence relates to the fact that here the transport events can be large, intermittent, and have spatial scales comparable to equilibrium gradients. Thus, the long-time averages of the resulting transport fluxes coupled to the transport code may not faithfully represent the actual transport/profile-modifications from large events. This issue is quantified by comparing BOUT/UEDGE simulations using the RIC algorithm to more time-consuming direct simulations where BOUT evolves the edge plasma profiles at each step of the turbulence simulation during the course of a long transport timescale simulation.

*Prepared by LLNL under USDOE contract DE-AC52-07NA27344.

NP8 118 Tests of and plans for the ESL Code* R.H. COHEN, M. DORR, T.D. ROGNLIEN, X.Q. XU, *LLNL* P. COLELLA, D. MARTIN, *LBNL* The Edge Simulation Laboratory (ESL) is a multi-institutional collaboration to develop kinetic edge codes using continuum techniques. A new code, based on fourth-order conservative finite-volume discretization of gyrokinetic equations, has recently become operational. Initially the code is electrostatic, 4D (axisymmetric), with a Miller (core, shaped) geometry, but with the optional addition of a toroidal limiter to provide a scrape-off-layer region. A number of test simulations have been or are being

carried out, including advection and magnetic mirroring of phase space blobs, evolution of steep radial density and temperature profiles, collisional loss to a limiter with a model collision operator, and geodesic acoustic modes in periodic and bounded domains. Results of this test campaign will be reported. In addition we report on progress/plans for adding capability to the code, in particular extending the code to full divertor geometry, 5D, and, ultimately, electromagnetic physics.

*Work performed for USDOE, at LLNL under contract DE-AC52-07NA27344.

NP8 119 Drift-orbit loss at the null-point in a snowflake divertor configuration* M.V. UMANSKY, D.D. RYUTOV, *LLNL* The prompt loss of ion drift orbits at the null point may be an important effect in divertor tokamak edge plasmas [1]. In the snowflake divertor configuration [2], the prompt loss may be quite different from that in the standard X-point configuration, due to a quadratic dependence of the poloidal magnetic field on the distance from the null point. As a result, the zone affected by the prompt loss in snowflake geometry is significantly larger than that in the standard X-point configuration [3]. Continuing the analytic study in [3], here we consider more complicated cases using numerical calculation of drift orbits, including the effects of electric field and collisions. As a special case we include the case of heavy impurity ions in low charge states, where the effect of the vertical drift is the strongest. Results will be presented for realistic snowflake-like configurations based on parameters of existing tokamaks. [1] C.S. Chang, S. Kue, and H. Weitzner, Phys. Plasmas, 9, 3854 (2002). [2] D.D. Ryutov, Phys. Plasmas, 14, 064502, June 2007. [3] D.D. Ryutov and M.V. Umansky, presentation at TTF 2009.

*Work performed for U.S. DOE by LLNL under contract DE-AC52-07NA27344.

NP8 120 Instabilities and coherent structures in long-legged divertors D.D. RYUTOV, R.H. COHEN, I. JOSEPH, T.D. ROGNLIEN, M.V. UMANSKY, *Lawrence Livermore National Laboratory* In some versions of tokamak divertor designs the distance between the strike point and the X-point is large, approaching and even exceeding the tokamak minor radius (e.g., R.W. Conn et al, Nucl. Fusion Suppl., v. 3, p. 203, 1977; P.M. Valanju et al, Phys. Plasmas, 16, 056110, 2009). In such a situation, the plasma propagates from the vicinity of the X-point to the divertor plate along a narrow channel ("divertor leg"). The presence of a large geometrical factor, the length-to-thickness ratio, enhances the role of particle drifts and leads to the appearance of significant parallel currents, thereby enhancing the role of the divertor-plate boundary conditions. The divertor modes associated with the finite-beta effects (R.H. Cohen, D.D Ryutov. PPCF, 47, 1187, 2005) become more virulent and may lead to formation of a specific type of finite-beta blobs. The characteristics of these blobs are evaluated and possible damage to the vacuum chamber in the divertor legs is discussed. Prepared by LLNL under Contract DE-AC52-07NA27344.

NP8 121 Edge gyro-kinetic transport simulations with a kinetic neutral model* X.Q. XU, *Lawrence Livermore National Laboratory* EDGE SIMULATION LABORATORY TEAM, We report on the derivation of a kinetic neutral model for gyro- kinetic continuum codes. The dominant interactions for hydrogen atoms are charge-exchange with proton, ionization by electron impact and three-body-recombination of ion-electron pairs back to neutrals. Since a neutral dynamics is intrinsic 3D in velocity space, while gyro-kinetic ion dynamics are 2D after gyro-averaging. A proper formulation will be presented to ensure that the essential physics is kept and conservation properties are preserved. An efficient numerical mapping between ion velocity coordinates and neutral velocity coordinates will have to be developed. Assuming the charge-exchange with proton to be dominant process, a simplified neutral diffusion model can be derived. In this case, both neutrals and ions could use the same velocity coordinates and therefore no coordinate mapping is needed. The preliminary simulations with the neutral model will be reported for plasma transport and flow dynamics in single- null tokamak geometry, including the pedestal region that can extend across the separatrix into the scrape-off layer (SOL) and private flux region.

*Work performed for U.S. DOE by U.C. LLNL under Contract DE-AC52-07NA27344.

NP8 122 Self-consistent edge-wall simulations with WALLPSI in FACETS A. PIGAROV, S. KRASHENINNIKOV, *UCSD* J. CARY, A. HAKIM, S. KRUGER, M. MIAH, A. PLETZER, S. SHASHARINA, *Tech-X* R. COHEN, T. ROGNLIEN, T. EPPERLY, *LLNL* The Framework Architecture for Core-Edge Transport Simulations (FACETS) is a SciDAC project for self-consistent simulations of core-edge-wall transport in tokamaks using leadership class computers [1]. For analysis of transient peak power load handling, PFC erosion/deposition and lifetime, plasma impurity contamination, and hydrogen retention issues in FACETS, we developed the 1D continuum code WALLPSI [2]. WALLPSI simulates highly non-linear transport, release and trapping of hydrogen species in wall, and calculates the wall temperature and emerging impurity fluxes. We present progress on the development of an interface to allow WALLPSI to be invoked from within the multiple-component FACETS infrastructure. Each wall segment is modeled by WALLPSI instance which are all run concurrently on separate CPUs. FACETS provides the mechanism for coupling the wall to plasma transport code UEDGE. The results are presented showing non-linear variation of hydrogen species wall inventory in response to incident plasma fluxes and abrupt changes in edge plasma parameters caused by wall switching from net pumping regimes to net outgassing ones using an initial slab edge plasma setup. [1] J.Cary et al J.Physics CS 125(2008)012040 [2] A.Pigarov et al JNM 390(2009)192

NP8 123 Kinetic simulation of the plasma edge on high performance computers DAVID TSKHAKAYA,* *University of Innsbruck, Association EURATOM-OEAW, A-6020 Innsbruck, Austria* RALF SCHNEIDER, *Max Planck Institute fuer Plasmaphysik, EURATOM Association, 17491 Greifswald, Germany* SIEGBERT KUHN, *University of Innsbruck, Association EURATOM-OEAW, A-6020 Innsbruck, Austria* In the present contribution we describe results of to our knowledge first fully kinetic simulations of the plasma edge on High Performance Computers (HPC) with more than 500 processors. We demonstrate that these new type of modeling allow to simulate large (few meter size) systems with finest resolution up to Debye length and electron Larmor radius. The developed parallel BIT1 code incorporates new physics-based parallel 1D solver and adaptive processor loading scheme allowig highly scalable parallel runs for strongly non-uniform plasma edge. As an example, we consider kinetic simu-

lations of the 1D plasma, 2D neutral and impurity transport in the tokamak Scrape-of Layer. The developed model includes nonlinear interaction between all particle species and linear plasma recycling and impurity sputtering models.

*Permanent address: Anronikashvili Institute of Physics, 0177 Tbilisi, Georgia

NP8 124 Initial Results from a Coupled Kinetic Plasma - Neutral Transport Code* D.P. STOTLER, *PPPL* C.S. CHANG, G. PARK, *NYU* CPES TEAM, To provide a kinetic neutral simulation capability for the Center for Plasma Edge Simulation, a subroutine interface to the DEGAS 2 Monte Carlo neutral transport code has been implemented and coupled into the XGC neoclassical particle transport code. The neutral transport routine simulates the collision of kinetic neutrals with a fluid plasma background provided by XGC; a complementary collision routine in XGC handles plasma particle collisions with a fluid neutral background. While mass conservation between the plasma and neutral species is ensured, the rates at which momentum and energy are exchanged will not be the same in the two calculations to the degree that the kinetic distributions are non-Maxwellian. We assess non-conservation of the instantaneous and time integrated momentum and energy exchanges in a physically relevant simulation. We will also compare the resulting neutral penetration and pedestal buildup obtained with that computed by the rudimentary Monte Carlo neutral transport routine used in the original XGC code. Extensions, such as the inclusion of molecules and time dependence, will be discussed.

*This work supported by US DOE contract DE-AC02-09CH11466.

NP8 125 Baseline neoclassical scaling law on H-mode pedestal width from XGC0 kinetic simulation* GUNYOUNG PARK, C.S. CHANG, S. KU, *NYU* CPES TEAM, In the H-mode pedestal before the ELM onset, nonlocal neoclassical self-organization is an important physical effect, to set the baseline pedestal width scaling law. Deviation from the neoclassical scaling will define the anomalous scaling. The neoclassical self-organization includes effects from the self-consistent radial electric field shear, strong magnetic field shear, ion-orbit loss across the last closed magnetic surface, finite ion banana width, particle source from neutral ionization, heat flux from the core plasma, and collisional transport. XGC0 code is used to perform an inter-machine study of the neoclassical pedestal scaling law between two representative devices DIII-D (low-B, low collisionality) and C- Mod (high-B, high collisionality). Anomalous scaling component in the experimental pedestal width data will be separated out from the neoclassical component. Prediction for ITER pedestal will be attempted based upon the combined neoclassical (theoretical) and anomalous (empirical) scaling laws obtained in this study. This ion-electron study indicates that the neoclassical pedestal width is broader than the previous ion only study results, closer to experimental pedestal width.

*Work supported by US DOE Office of Fusion Energy and Office of Advanced Scientific Computing Research

NP8 126 Nonlocal theory for the excitation of GAMs in the edge region of tokamak plasmas* R.G. KLEVA, *IREAP, University of Maryland, MD, USA* P.N. GUZDAR, *IREAP, University of Maryland, College Park, MD, USA* N. CHAKRABARTI, *SINP, Kolkata, India* J.J. RASMUSSEN, V. NAULIN, *Association EURATOM - Risø DTU, RNLSE, Technical University of Denmark, Roskilde, Denmark* P.K. KAW, R. SINGH, *IPR, Gandhinagar, India* A nonlocal theory of the excitation of geodesic acoustic modes by drift waves in an inhomogeneous plasma typical of the edge region of tokamaks, has been developed. The continuum GAM modes with coupling to the drift waves can give rise to discrete "global" unstable eigenmodes localized in the edge "pedestal" region of the plasma. These global eigenmodes have a two-space scale character. Inclusion of finite beta effects of the drift waves shows that the excitation of GAMs by the three-wave parametric coupling is stabilized by the Maxwell-Stress component of the nonlinear coupling. We will present comparison of our theoretical/numerical model with observations of GAMs spatial structure observed in various tokamak devices.

*Work partially supported by DOE and the Danish Natural Science Research Council (FNU-272-06-0367).

NP8 127 Modeling on Pellet Injection in Tokamak Plasmas KI MIN KIM, HYUNSUN HAN, YONG-SU NA, SANG HEE HONG, *Seoul National University* P.T. LANG, *Max Planck Institute for Plasma Physics* B. ALPER, A. BOBOC, *Euratom/UKAEA Fusion Association* JET-EFDA CONTRIBUTERS COLLABORATION,* Modeling on pellet injection in tokamak plasmas is conducted with a 1.5D core transport code. The calculated electron density evolution after the sequential pellet injections appear to be in good agreements with the JET measurements. Some discrepancies are observed on the particle transport in the higher density enhanced in each pellet fueling phase. The modeling reproduces the measured data more closely by increasing the plasma transports when approaching the higher density. Based on this simulation, the pellet fueling in KSTAR is predicted to provide the design parameters of a pellet launching system. ELM triggering by pellet is studied with the transport code as well, which discusses that the enhancements of surface-averaged pressures and locally-perturbed pressure gradients by pellets might be responsible for driving the ideal ballooning mode to trigger ELMs. Density-enhanced ELMs in the post pellet phase are presented as additional ELMs induced by pellet injection.

*See the Appendix of F. Romanelli et al., Fusion Energy (Proc. 22nd Int. Conf. Chengdu) IAEA, 2008

NP8 128 On dust grain interactions with fusion plasmas SERGEI KRASHENINNIKOV, ROMAN SMIRNOV, *UCSD* Recently different aspects of dust physics in fusion devices brought additional attention from both theoreticians and experimentalists, which, in part, was motivated by the work on the ITER project. To predict the role of dust in core plasma contamination and material migration we need to use some models describing the processes of the interactions of dust grains with fusion plasmas (including charging, forces and energy deposition). So far the models based on the interactions of collisionless plasma with the grain immersed in the self-consistent ambipolar electric field, which were developed for the study of so-called "dusty plasmas" are utilized. However, rather hot and dense edge plasma environment in fusion devices results in a strong heating of dust grain and subsequent grain sublimation and evaporation. When the vapor density and/or the amount of ionized impurity atoms become large enough they can alter the grain-plasma interactions. Somewhat similar processes occur during pellet injection in fusion plasma and the interactions of comets with sun radiation and Earth atmosphere. In this presentation we discuss: i) dust and plasma parameter range where the role of dust grain evaporation/sublimation and the pro-

cesses associated with it do not have a significant impact on grain-plasma interactions, and ii) statistical issues of the description of dust-pasma interactions. This work was supported the US DoE under Grant DEFG02-04ER54852.

NP8 129 Li Experiments at the Tokamak T-11M Toward PFC Concept of Steady State Tokamak-Reactor S.V. MIRNOV, *TRINITI, Troitsk, Moscow Region, 142190 Russia* As practical method of using a liquid lithium as a renewable plasma-facing component (PCF) for steady state tokamak-reactor the concept of lithium emitter-collector is considered [1]. It is based on lithium filled capillary porous system proposed by V.A. Evtikhin et al. (1996). The lithium circulation process consists of four steps: (1) Li emission from the PFC emitter into the plasma; (2) plasma boundary cooling by non-coronal Li radiation; (3) Li ion capture by the collector (before they are lost to the tokamak chamber wall); (4) Li return from the collector to the emitter. T-11M tokamak experiments have used three local rail limiters made from lithium, molybdenum and graphite as lithium collectors. The lithium behavior was studied by analysis of the witness samples, and by a mobile graphite probe. The key findings are: (1) lithium collection on the ion side of the lithium limiter is 2-3 times larger than on the electron side; (2) total efficiency of Li collection integrated over all three rail limiters can reach 50-70% of the lithium emission during the discharge pulse, while the theoretical limit is about 90%. [1] S.V. Mirnov, J. Nucl. Mat., **390-391**, 876 (2009).

NP8 130 Sputtering and Evaporation Studies of Lithiated Graphite* VIJAY SURLA, KENZO IBANO, MARTIN NEUMANN, DAVID RUZIC, *University of Illinois at urbana-Champaign* To understand the complex system of lithiated ATJ graphite, studies of sputtering and evaporation of lithium and lithiated ATJ graphite are conducted in the Ion InterAction eXperimental (IIAX) facility. The sputtering yields are measured using QCM for both graphite and lithiated graphite targets when bombarded by Li ions with energies ranging from 700 eV-2000 eV. Typical flux of Li ion beam obtained is $\sim$ 4 x 10^{13} ions/ (cm^2- s). Results indicate suppressed amounts of sputtered yields after Li treatment. Deuterium saturation for target samples is also performed to simulate actual divertor conditions; however, no distinct difference in sputter yields is seen after D treatment. The percentage fraction of sputtered Li ions to neutrals is also determined. The thermal evaporation flux studies of Li on stainless steel (SS) and lithiated graphite show that there is an order of magnitude less evaporation from lithiated graphite compared to Li on SS, thereby enhancing the temperature limit on plasma facing components.

*This work is supported by DOE-ALPS contract.

NP8 131 Thermoelectric magnetohydrodynamic (TEMHD) stirring of liquid lithium* M.A. JAWORSKI, WENYU XU, JASON KIM, MATT LEE, MARTIN NEUMANN, VIJAY SURLA, DAVID RUZIC, *University of Illinois at Urbana-Champaign* The Solid/Liquid Lithium Divertor Experiment (SLiDE) was constructed to examine passive flows in liquid lithium under an applied heat load and external magnetic field. The offered explanation for the results of the CDX-U experiment, where liquid lithium was capable of transporting $>$ 50 [MW/m^2] of incident heat flux without rapid evaporation, was thermocapillary (Marangonic) driven flows. The SLiDE apparatus utilizes a line-stripe heat source and external magnetic fields to mimic a divertor scenario to test the thermocapillary hypothesis. Instead of thermocapillary induced flows, TEMHD flows are observed on the order of 10 [cm/s]. The thermoelectric effect was confirmed through a series of qualitative experiments in the apparatus which will be described. A quantitative scaling matching the measured target temperatures and heat fluxes is compared to the measured velocities. A novel plasma facing component based on porous material TEMHD is also presented.

*This work support under DoE grant #DE-FG02-99ER54515.

SESSION NM9: MINI-CONFERENCE ON UNSTEADY RECONNECTION IN LABORATORY AND NATURE III: 3D RECONNECTION AND DIFFUSION REGION

Wednesday Morning, 4 November 2009
Regency V at 9:30
Yasushi Ono, University of Tokyo, presiding

9:30

NM9 1 Satellite observations of lower-hybrid-oscillated magnetic null and related anomalous resistivity CHIJIE XIAO, XIAOGANG WANG, *School of Physics, Peking University* ZUYIN PU, *School of Earth and Space Sciences, Peking University* Here we report two 3D fast reconnection events with magnetic nulls, one located in the geomagnetotail and the other one in dayside magnetopause. The magnetic nulls in both events are oscillated at lower-hybrid frequencies, which imply that lower-hybrid wave may be very important at the center of reconnection current sheet. The power spectrum of the electric field around the lower-hybrid (LH) frequency is measured to compute the anomalous resistivity near the magnetic null. The anomalous resistivity due to lower-hybrid frequency turbulence is in comparison with the effective resistivity calculated from electrical field and current data. Also the fast reconnection rate is estimated from magnetic field and flow data to compare with the reconnection electrical field computed from the current data and anomalous resistivity calculation. It is found that, the anomalous resistivity induced by LH frequency turbulence is sufficient to trigger fast reconnection.

9:55

NM9 2 General Method for Describing Three-Dimensional Magnetic Reconnection* VIACHESLAV TITOV, *Predictive Science, Inc.* TERRY FORBES, *University of New Hampshire* ERIC PRIEST, *University of St. Andrews* ZORAN MIKIC, JON LINKER, *Predictive Science, Inc.* A general method for describing magnetic reconnection in arbitrary three-dimensional magnetic configurations is proposed. The method is based on the field-line mapping technique previously used only for the analysis of magnetic structure at a given time. This technique is extended here so as to analyze the evolution of magnetic structure. Such a generalization is made with the help of new dimensionless quantities called "slip-squashing factors." Their large values define the surfaces that border the reconnected or to-be-reconnected magnetic flux tubes for a given period of time during the magnetic evolution. The proposed method is universal, since it assumes only that the time sequence of evolving magnetic field and the tangential boundary flows are known. We illustrate our method for several examples and compare it with the general magnetic reconnection

theory, proposed previously by Hesse and coworkers. The new method admits a straightforward numerical implementation and provides a powerful tool for the diagnostics of numerical data obtained in theoretical or experimental studies of magnetic reconnection in space and laboratory plasmas.

*Supported by NASA, NSF, AFOSR, and EU Solaire Network.

10:20

NM9 3 Experiments on Three-Dimensional Reconnection* WALTER GEKELMAN, ERIC LAWRENCE, ANDREW COLLETTE, STEPHEN VINCENA, *UCLA, Dept Physics* Magnetic Field Line reconnection is still considered, by some, to be one of the most important topics in plasma physics and has been in this category for close to thirty years. One reason is most of the models for it are still two dimensional. We report on two very different experiments in which 3D reconnection plays a role. In the first experiment two magnetic flux ropes are generated from initially adjacent pulsed current channels in a background magnetoplasma. The currents twist about each other and merge and are observed to filament after merging. Volumetric space-time data show multiple reconnection sites with time-dependent locations. The quasi-separatrix layer (QSL), a concept used in study of solar reconnection has been measured, and its three dimensional development will be shown. In the second experiment three-dimensional currents associated with colliding laser produced plasmas are observed. The currents in this situation are those of shear Alfvén waves. The wave fields are a small fraction of the background field; nevertheless, reconnection regions, multiple magnetic 'X' points (which are three dimensional) and induced electric fields are observed. The role of the guide field is investigated.

*Work supported by the Department of Energy and National Sci. Foundation.

10:40

NM9 4 Energetics of Localized, Transient Reconnection Models in 1, 2 and 3 Dimensions* DANA LONGCOPE, *Montana State University* Fast magnetic reconnection has been proposed to explain how stored magnetic energy might be rapidly converted into other forms. The general prerequisite for local flux transfer to release significant energy is achieved most easily at some form of current sheet where fields of distinct global topologies come into close proximity. In Petschek's steady model magnetic fields are reconnected at a site of localized electric field, initiating energy release far away at standing slow mode shocks. I show that a wide variety of models, both steady and transient, agree qualitatively and quantitatively in the nature and outcome of a basic energy release scenario broadly similar to Petschek's. These include a recently-developed three-dimensional model whereby transient, localized flux transfer across a current sheet creates retracting magnetic flux tubes. This and all other models predict the same total energy release, its apportionment between thermal to kinetic forms, and the final plasma temperature. These quantities depend on initial field line angle and plasma beta and not on details of the flux-transfer electric field due to its assumed localization.

*This work supported by the NSF

11:05

NM9 5 Response of the Chromosphere to Penumbral Dynamics: Reconnection and Bow Shocks MARGARITA RYUTOVA, *LLNL/IGPP* THOMAS BERGER, ZOE FRANK, ALAN TITLE, *LMSAL* We present observations of sunspot penumbrae obtained during the disk passage of AR 10923 (2006 November 10-20) with the SOT instrument on Hinode in 4305 A G band and Ca II H line. These observations allowed us to study new phenomena consisting in the appearance of bright elongated transients having a double structures, and abundantly pervading the entire penumbra. These transients, drifting as a whole in a direction almost perpendicular to their long axes, are clearly associated with the photospheric bright points emerging in a Y-shaped configuration formed by the reconnecting penumbral filaments. We find that a specific character of reconnection and post-reconnection dynamics in the photosphere, determined by a finite plasma beta and sharp stratification, provide necessary conditions for the formation of bow shocks generated by reconnected filaments moving upward with transsonic velocities. We present quantitative analysis, and show that calculated parameters of bow shocks, e.g. velocity, standoff distanse, height of formation, lifetime, length, etc. are in good agreement with observations.

11:30

NM9 6 Unsteady 3D magnetic reconnection in the Reconnection Scaling Experiment* T.P. INTRATOR, *Los Alamos Natl Lab* T.D. OLSON, R.J. OBERTO, Magnetic reconnection changes the topology of magnetic field lines to a lower energy state. This process can liberate stored magnetic field energy and accelerate particles during unsteady, explosive events. This is one of the most important processes in astrophysical, space and laboratory plasmas. The abrupt onset and cessation has been a long standing puzzle. We show the first three-dimensional (3D) laboratory example of onset and stagnation of magnetic reconnection between magnetized and parallel current channels (flux ropes) driven by magnetohydrodynamic (MHD) attraction and an external kink mode, which is a 3D plasma current driven instability. Antiparallel magnetic field lines carried by these colliding flux ropes annihilate and drive an electric field. The inflow soon exceeds a threshold for the formation of a reconnection current layer. Magnetic flux and pressure pile up just outside this layer, and eventually become large enough to support MHD back-reaction forces that stall the inflow and stagnate the reconnection process.

*Supported by LANS Contract No. DE-AC52-06NA25396, and Center for Magnetic Self Organization funded by the National Science Foundation and the Department of Energy

11:50

NM9 7 Kinetic Theory and Petascale 3D Simulations of Magnetic Reconnection with a Guide Field W. DAUGHTON, V. ROYTERSHTEYN, L. YIN, B.J. ALBRIGHT, K.J. BOWERS, *LANL* H. KARIMABADI, *UCSD* In the presence of a finite guide field, current sheets are unstable to a spectrum of collisionless tearing modes at resonant surfaces across the layer. Fully kinetic treatments of this problem have typically focused on the fastest growing modes with resonant surface in the center of the layer. However in large-scale systems, tearing modes can grow at resonant surfaces on both sides of the layer, corresponding to oblique angles relative to the standard 2D reconnection geometry. In hydrogen plasmas, these modes couple to the electron drift wave while in electron-positron plasmas the oblique tearing modes are purely growing. In this work, we review the Vlasov theory for this problem using an exact integro-differential treatment. The theoret-

ical results are used to guide and interpret 3D fully kinetic simulations performed on Roadrunner, the world's first petascale supercomputer. The evolution is highly dynamic and features the formation and interaction of flux ropes over a wide range of angles consistent with linear theory. Over long time scales, new current sheets form which are unstable to additional reconnection instabilities and island (flux rope) formation. The influence of this complex evolution on the dissipation of magnetic energy and particle acceleration is explored.

12:10
NM9 8 3D Magnetic Reconnection of Relativistic Pair Plasmas* WEI LIU, LIN YIN, *LANL* BRIAN ALBRIGHT, *balbright@lanl.gov* KEVIN BOWERS, HUI LI, *LANL* EDISON LIANG, *Rice University* Relativistic plasma physics plays an essential role in a number of famous and longstanding astrophysical problems. Using the ultrafast code VPIC, we present one of the largest scale 3D particle-in-cell (PIC) simulations to date to examine relativistic magnetic reconnection in pair plasmas. These simulations are large enough to accommodate a sufficient number of kink modes. It is demonstrated that multiple, patchy reconnection sites form during the initial stage and then self-organize to form an elongated diffusion region with increased system size. The secondary kinking folds the current sheet in the orthogonal direction. The interaction between kink and tearing instabilities results in plasmoids, which affect the particle acceleration and reconnection rate. The reconnection rate remains fast and time varying. The relativistic effects increase the linear kink mode wavelengths and results in almost identical growth rates for initial linear kink and tearing modes. Relativistic drift kink instability, reconnection, folding of the diffusion region due to the secondary kink and plasmoids all contribute to the particle energization.

*Supported by LANL-LDRD

SESSION PI2: TOKAMAK PHYSICS: EDGE, SCRAPE-OFF LAYER AND WALL
Wednesday Afternoon, 4 November 2009; Centennial I at 14:00; Andrea Garofalo, General Atomics, presiding

14:00
PI2 1 ELMs, Magnetic X-points, and Chaotic Fields.* LINDA E. SUGIYAMA, *M.I.T.*

Edge Localized Modes (ELMs) in a magnetically confined plasma are shown to be a new type of nonlinear plasma instability, in which a coherent plasma structure couples to part of a chaotic magnetic field. Numerical simulation using the M3D code [1] provides a detailed picture. Toroidal magnetic fields can be described as Hamiltonian systems. Under small perturbations, a plasma boundary magnetic surface containing an X-point splits into two, defined asymptotically by the limits of the field lines traced infinitely in each direction. The limiting surfaces overlap to form a homoclinic tangle [2]. The steep pressure gradient near the edge of an H-mode fusion plasma drives ballooning-type plasma instabilities, aligned along the equilibrium magnetic field. These can couple nonlinearly to the "unstable" magnetic surface that ripples the equilibrium boundary. Fingers of plasma grow outwards, above and below the midplane on the outboard side, and the alternating low density regions may penetrate deep into the plasma. The field becomes chaotic over the affected region. Field lines are contained for many toroidal transits, but develop significant radial excursions. Many are eventually lost through the X-point region. The original magnetic boundary is preserved. Over several hundred Alfvén times the plasma heals back towards the original shape, but with relaxed profiles of density and temperature. A complex nonlinear interaction between the plasma instability and a magnetic homoclinic tangle leads to distinct stages in the ELM crash, that are similar to experimental observations. This new picture may help to explain the large range of ELM and ELM-free behavior seen in experiments and suggests a re-examination of H-mode edge confinement and the L-H transition. [1] W. Park, et al., *Phys. Plasmas* **6** 1796 (1999). [2] T. Evans, et al,, *J. Phys. Conf. Series* **7** 174 (2005).

*Work supported by the U.S. Department of Energy.

14:30
PI2 2 ELM mitigation studies in JET and implications for ITER.* ELENA DE LA LUNA, *Laboratorio Nacional de Fusion, Asociacion EURATOM/CIEMAT, Madrid-28040, Spain*

Type I edge localized modes (ELMs) remain a serious concern for ITER because of the high transient heat and particle flux that can lead to rapid erosion of the divertor plates. This has stimulated worldwide research on exploration of different methods to avoid or at least mitigate the ELM energy loss while maintaining adequate confinement. ITER will require reliable ELM control over a wide range of operating conditions, including changes in the edge safety factor, therefore a suite of different techniques is highly desirable. In JET several techniques have been demonstrated for control the frequency and size of type I ELMs, including resonant perturbations of the edge magnetic field (RMP), ELM magnetic triggering by fast vertical movement of the plasma column ("vertical kicks") and ELM pacing using pellet injection. In this paper we present results from recent dedicated experiments in JET focusing on integrating the different ELM mitigation methods into similar plasma scenarios. Plasma parameter scans provide comparison of the performance of the different techniques in terms of both the reduction in ELM size and on the impact of each control method on plasma confinement. The compatibility of different ELM mitigation schemes has also been investigated. The plasma response to RMP and vertical kicks during the ELM mitigation phase shares common features: the reduction in ELM size (up to a

factor of 3) is accompanied by a reduction in pedestal pressure (mainly due to a loss of density) with only minor ($<$ 10%) reduction of the stored energy. Interestingly, it has been found that the combined application of RMP and kicks leads to a reduction of the threshold perturbation level (vertical displacement in the case of the kicks) necessary for the ELM mitigation to occur. The implication of these results for ITER will be discussed.

*JET-EFDA, Culham Science Centre, OX14 3DB, Abingdon, UK

15:00
PI2 3 Modification of Edge Profiles and Stability with Lithium Wall Coatings in NSTX.*
RAJESH MAINGI, *Oak Ridge National Laboratory*

Rapidly growing instabilities known as Edge Localized Modes (ELMs) are commonly observed in high-confinement (H-mode) regimes in many toroidal confinement devices. The reduction or elimination of ELMs with high confinement is essential for ITER, which has been designed for H-mode operation. Large ELMs are thought to be triggered by exceeding either edge current density limits (peeling modes) and/or edge pressure gradient limits (ballooning modes) [1]. Edge stability calculations have indicated that spherical tori should have access to higher pressure gradients and H-mode pedestal heights than higher aspect ratio tokamaks, owing to high magnetic shear and possible access to second stability regimes [2]. Such a regime was recently discovered in the National Spherical Torus Experiment (NSTX) following the application of Lithium onto the graphite plasma facing components [3]. ELMs were eliminated in phases [4], with the resulting pressure gradients and pedestal widths increasing substantially [5]. The modification of the pressure profile originated mainly from reduced recycling and edge fueling, which relaxed the edge density gradients. PEST and ELITE calculations have confirmed that the resulting pressure profiles were further from the stability boundary than reference discharges. The resulting discharges are ELM-free with a 50% increase in normalized energy confinement, up to the global $\beta_N \sim$ 5.5-6 limit. While the ELM-free discharges ultimately suffer radiative collapse, pulsed 3-d magnetic fields are used to trigger ELMs and purge impurities

[1] P. B. Snyder, et. al., *Physics of Plasmas* **9** (2002) 2037. [2] P. B. Snyder, *Plasma Physics Controlled Fusion* **46** (2004) A131. [3] H. W. Kugel, et. al., *Physics of Plasmas* **15** (2008) 056118. [4] D. M. Mansfield, et. al., *J. Nucl. Materials* **390-391** (2009) 764 [5] R. Maingi et. al., *Physical Review Letters* (2009) at press. [6] J.M. Canik, et. al, *Nucl. Fusion* (2009) submitted.

*Supported in part by contracts DE-AC05-00OR22725 and DE-AC02-09CH11466.

15:30
PI2 4 Detached divertor plasma physics with a stochastic magnetic field.
MASAHIRO KOBAYASHI, *NIFS*

Stable detachment control is demonstrated by superposing resonant magnetic perturbation of m/n=1/1 on the stochastic boundary of LHD, which introduces a remnant magnetic island outside the last closed flux surface (LCFS). A strongly radiating region is stabilized in the edge, without core plasma degradation. The diagnostics show, a significant reduction of divertor particle/heat flux, formation of very dense ($\sim 10^{20}$ m^{-3}) and cold (a few eV) plasma outside of LCFS, volume recombination in the hydrogen line emission, and strongly decreased intensity of iron emission (Fe VIII$\sim$ XII). It is also demonstrated that the discharge is compatible with the internal diffusion barrier (IDB) type plasma, and that the detach-attach transition is readily controlled by gas puff adjustment. The field line structure of a remnant island outside the LCFS is considered responsible for stabilizing the radiating region with the core plasma being unperturbed, because of selective cooling at either O or X-point, where the thermal instability can favorably set in. Simulation of 3D edge transport shows a possibility of the radiative condensation around a remnant island structure at the detachment transition. The simulation also indicates that the geometry of low order (m=7$\sim$ 5) remnant islands effectively reduces the parallel temperature gradient by increased cross-field energy transport at high collisionality. This results in suppression of the thermal force that usually drives impurities towards the confinement region. Together with increased outward friction from background parallel plasma flow at high collisionality, the high density edge plasma with stochastic field leads to effective impurity screening. The measurements also indicate better screening for discharges with the m/n=1/1 perturbation.

16:00
PI2 5 Quantification of Chemical Erosion in the DIII-D Divertor.*
ADAM McLEAN

Chemical erosion (CE) yield at the graphite divertor target in DIII-D was measured to be substantially lower in cold near-detached plasma conditions compared to well-attached ones, with major implications for ITER. Current estimates of tritium retention by co-deposition with hydrocarbons (HCs) in ITER place potentially severe restrictions on operation. However, calculations done to date have been based on excessively conservative assumptions, due to limited understanding of cold divertor plasmas (1-5eV) which bridge energy thresholds for complex atomic and molecular processes not present in attached conditions. Hydrocarbon injection through a unique porous graphite plate which realistically simulates secondary reactions of HCs with a graphite surface has been used to measure CE*in-situ*. For the first time in a divertor,

measurements were made at extrinsic CH_4 injection rates comparable to the expected intrinsic CE rate of C, with the resulting spectroscopic emissions separated from those of the intrinsic sources. Under cold plasma conditions the contribution of CE-produced C relative to total C sources in the divertor declined dramatically from $\sim$ 50% to $<$ 15%. Photon efficiencies for products from the breakup of injected CH_4 were greater than previous measurements at higher puff rates, indicating the importance of minimizing perturbation to the local plasma. At 350K, the measured CE yield near the outer strike point was $\sim$ 2.6% in attachment dropping to only $\sim$ 0.5% in cold plasma; results are consistent with some theoretical predications and lab studies. Under full detachment, near total extinction of the CD band occurred, consistent with suppression of net C erosion. These findings have potentially major impact on projected target lifetime and tritium retention in future reactors, and for the PFC choice in ITER.

*Work supported in part by the US DOE under DE-FC02-04ER54698.

16:30
PI2 6 Runaway Electron Transport and Disruption Mitigation Optimization on Alcator C-Mod.*
DENNIS WHYTE, *MIT-PSFC*

Experiments and modeling on Alcator C-Mod have provided new insights into the physics of runaway electron transport and disruption mitigation optimization, both critical issues for ITER. Avalanche amplification of runaway current in disruptions is a concern for ITER since the amplification gain scales exponentially with plasma current. While stochastic transport losses of the fast electrons can effectively eliminate the amplification, such losses have not previously been quantified. C-Mod has investigated runaway production and transport by seeding a suprathermal electron tail using Lower Hybrid heating and then promptly terminating the discharge with a massive gas injection (MGI). This innovative combination assures, through the Dreicer mechanism, a sufficient "seed" population of runaways, $\sim$ 0.1 of the initial plasma current, such that their amplification and transport can be measured. In the experiment electrons accelerate to relativistic velocities but are all lost due to transport on a timescale less than a millisecond, effectively resulting in runaway electron suppression before the current quench. The runaway loss mechanism is confirmed to be stochastic transport by using electron tracing in 3-D resistive MHD simulations (NIMROD), which have also shown the importance of MHD activity in MGI disruption mitigation. Large parallel electric fields and stochasticity appear simultaneously in the model, suggesting that the development of strongly stochastic regions through sufficient impurity radiation cooling is key to both mitigation and runaway avoidance. Particle delivery, mitigation effectiveness, runaway avoidance and overall response time of the system is optimized using mixed-gases of a fast low-Z gas carrier with a trace high-Z radiating species. Mitigation options and optimization for ITER are discussed.

*Supported by US-DOE.

SESSION PT3: TUTORIAL: ICF IGNITION: THE LAWSON CRITERION, AND COMPARISON WITH MFE IGNITION
Wednesday Afternoon, 4 November 2009; Centennial II at 14:00; Debra Callahan, Lawrence Livermore National Laboratory, presiding

14:00
PT3 1 ICF Ignition, the Lawson Criterion, and Comparison with MFE Ignition.*
R. BETTI, *Laboratory for Laser Energetics and FSC, U. of Rochester*

The Lawson criterion, which determines the onset of thermonuclear ignition, is usually expressed through the product $p\tau > 10$ atm $\cdot$ s, where p is the plasma pressure in atm and τ is the energy confinement time in seconds. In magnetic fusion devices, both the pressure and confinement time are routinely measured and the performance of each discharge can be assessed by comparing the value of $p\tau$ with respect to the ignition value (10 atm $\cdot$ s). In inertial confinement fusion, both p and τ cannot be directly measured and the performance of surrogate and/or subignited ICF implosions cannot be assessed with respect to the ignition condition. This makes it difficult to compare the performance of ICF implosions with that of magnetic fusion energy (MFE) discharges. Here, we define the meaning of ignition in ICF implosions and compare it to MFE ignition. We then show that a multidimensional ignition condition for inertial confinement fusion can be cast in a form that depends on three measurable parameters of the compressed-fuel assembly: the hot-spot ion temperature T, the neutron yield normalized to the 1-D prediction (yield over clean or YOC) and the total areal density ρR, which includes the cold shell's contribution. A family of marginal-ignition curves are derived in the ρR–T plane.[1] On this plane, hydrodynamic-equivalent curves show how a given implosion would perform with respect to the ignition condition when the laser-driver energy is varied. Such a criterion can be used to measure the ignition margin[2] of NIF targets and to predict the performance of OMEGA targets when scaled up to NIF energies. This work has been supported by the US Department of Energy under Cooperative Agreement Nos. DE-FC02-ER54789 and DE-FC52-08NA28302.

*In collaboration with P.Y. Chang, R. Nora, K.S. Anderson (LLE, FSC), D. Shvarts (NRCN), B. Spears (LLNL).

[1]C. D. Zhou and R. Betti, Phys. Plasmas **15**, 102707 (2008).
[2]D. S. Clark, S. W. Haan, and J. D. Salmonson, Phys. Plasmas **15**, 056305 (2008).

SESSION QI3: ICF AND IGNITION
Wednesday Afternoon, 4 November 2009; Centennial II at 15:00; Debra Callahan, Lawrence Livermore National Laboratory, presiding

15:00
QI3 1 National Ignition Campaign Hohlraum Energetics.*
NATHAN MEEZAN, *Lawrence Livermore National Laboratory*

The first series of experiments on the National Ignition Facility (NIF), as part of the National Ignition Campaign, will determine the hohlraum path forward for indirect drive ignition. These first experiments will test ignition hohlraum "energetics," a term described by four broad goals:

Measurement of laser absorption by the hohlraum

Measurement of the x-ray radiation flux (T^4_{RAD}) on the surrogate ignition capsule

Quantitative understanding of the laser absorption and resultant x-ray flux

Determining whether initial hohlraum performance is consistent with point design requirements for ignition using either a beryllium or plastic capsule ablator.

In this talk, we summarize the status of NIF hohlraum energetics experiments. We describe the hohlraum target and experimental design, including an overview of the theoretical and computational tools that have been used to design the hohlraums. We explain the validation of these tools on predecessor facilities and describe their performance on the first NIF experiments. We then discuss our current understanding of NIF hohlraum performance and the resulting near-term and long-term plans for NIF ignition hohlraum experiments.

*Prepared by LLNL under Contract DE-AC52-07NA27344.

15:30
QI3 2 Experimental basis for laser-plasma interaction predictions on the National Ignition Facility ignition designs.*
DUSTIN FROULA, *Lawrence Livermore National Laboratory*

Recent laser plasma interaction experiments at OMEGA (LLE, Rochester) using gas-filled hohlraums shed light on the behavior of stimulated Raman scattering (SRS) in the hot, high-density plasma that laser beams will encounter near the capsule in NIF ignition hohlraums. We will present detailed results on the SRS thresholds for densities (10-15% critical) at ignition relevant intensities (10^{14} - 10^{15} W-cm^{-2}). These results follow the expected Landau damping scaling with density and quantitatively agree with full three-dimensional laser propagation simulations (pF3d) that rely on detailed hydrodynamic simulations (HYDRA), providing an experimental basis for forthcoming experiments on NIF. In addition to controlling plasma parameters, the National Ignition Campaign relies on optical beam smoothing techniques to mitigate backscatter. We will show that polarization smoothing, which was previously demonstrated to increase the stimulated Brillouin scattering threshold, is also effective at controlling SRS. Finally, we have performed a scaling of the interaction beam numerical aperture and measured its impact on backscatter, which relates directly to the evolution of a laser beam aperture as it propagates inside an ignition hohlraum. These results will also be compared with 3D simulations. Prepared by LLNL under Contract DE-AC52-07NA27344.

*Collaborators: L. Divol, R. A. London, R. L. Berger, T. Doeppner, N. B. Meezan, J. Ralph, J. S. Ross, L. J. Suter, and S. H. Glenzer.

16:00
QI3 3 Multi-laser beams scattering processes in ignition targets.*
PIERRE MICHEL, *Lawrence Livermore National Laboratory*

Inertial Confinement Fusion experiments in the indirect drive approach rely on efficient deposition of the energy from many laser beams on the interior walls of a cylindrical cavity (the hohlraum). On the National Ignition Facility, 96 laser beams will overlap at each of the two laser entrance holes (LEH) of the hohlraum. As they propagate further into the hohlraum, they can potentially trigger laser plasma instabilities (LPI) such as stimulated Raman or Brillouin scattering (SRS/SBS) where plasma conditions are favorable for LPI. In this talk, we show that the SRS or SBS light exiting the hohlraum can get collectively amplified by multiple overlapping laser beams as it goes through the LEH. Typically, a SRS or SBS seed will be very weakly amplified by each of the overlapping laser beams; however, the total contribution from all 96 beams can lead to a strong amplification. This was analyzed with a steady-state kinetic model accounting for the collective coupling to all the laser beams. The effects of possible plasma turbulence due to superimposition of multiple plasma waves, as well as nonlinear saturation mechanisms, will also be discussed. The LPI amplification process in a NIF hohlraum is thus similar to a two-stage Raman or Brillouin amplifier, with a first pre-amplifier stage inside the hohlraum followed by a post-amplifier at the LEH. We will show that the process can be controlled by separating the range of

frequencies at which the seeds are generated inside the hohlraum, from those that are efficiently amplified at the LEH - i.e. by detuning the pre- and post-amplification stages of the hohlraum. This is achieved by modifying the plasma conditions inside the hohlraum and at the LEH, by appropriately changing the targets designs and compositions. Several targets will be tested on the National Ignition Facility to validate the LPI amplification process as well as its mitigation in the summer of 2009. We will present the experimental data, compare it to our prediction and discuss the results.

*This work was performed under the auspices of the U.S. Department of Energy by Lawrence Livermore National Laboratory under Contract DE-AC52-07NA27344.

16:30
QI3 4 Hohlraum Performance at > 100 TW on the National Ignition Facility.
KLAUS WIDMANN

This abstract not available.

SESSION PO5: HIGH-INTENSITY SHORT-PULSE LASER PLASMA INTERACTIONS
Wednesday Afternoon, 4 November 2009
Hanover CDE at 14:00
Christina Back, General Atomics, presiding

14:00
PO5 1 Initial Results from the OMEGA EP Laser System D.D. MEYERHOFER, R. BETTI, T.R. BOEHLY, J.H. KELLY, S.J. LOUCKS, R.L. McCRORY, S.F.B. MORSE, P.M. NILSON, S.P. REGAN, T.C. SANGSTER, V.A. SMALYUK, C. STOECKL, W. THEOBALD, L.J. WAXER, *Laboratory for Laser Energetics, U. of Rochester* The OMEGA EP Laser, with four NIF-like beams, was completed in April 2008. The beams can be operated at 351 nm, with each ultimately producing 6.5 kJ in a 10-ns pulse into the OMEGA EP target chamber. Two of the beams can be operated as high-energy petawatt lasers (HEPW), each producing up to 2.6 kJ in a 1053 nm, 10-ps pulse. The HEPW beams can be directed into the OMEGA EP target chamber or into the 60-beam OMEGA target chamber for experiments that combine target compression with HEPW capability. Initial experiments include measurements of the duration-dependent HEPW laser-to-fast-electron conversion efficiency, isochoric heating of small-mass targets, radiography of imploding targets, integrated fast ignition, materials physics, and the development of > 10-keV backlighting sources. These results show the effectiveness of OMEGA EP for high-energy-density physics experiments. This work was supported by the U.S. Department of Energy Office of Inertial Confinement Fusion under Cooperative Agreement No. DE-FC52-08NA28302.

14:12
PO5 2 Hot-Electron Generation with Kilojoule Pulses on OMEGA EP P.M. NILSON, J.F. MYATT, C. STOECKL, P.A. JAANIMAGI, W. THEOBALD, J.A. DELETTREZ, J.D. ZUEGEL, R. BETTI, D.D. MEYERHOFER, T.C. SANGSTER, *Laboratory for Laser Energetics, U. of Rochester* K.U. AKLI, *General Atomics* P.K. PATEL, A.J. MACKINNON, *LLNL* Intense laser–solid interactions generate high-current electron sources with relativistic energies that are important for advanced ignition experiments. Applications include rapid heating for fast ignition and energy deposition in solid material for flash radiography, isochoric heating, and x-ray scattering experiments. Results of laser-electron coupling experiments carried out on the OMEGA EP laser with up to 1.3-kJ, 10-ps-long pulses will be presented. Strong (~ 20%) energy coupling to electrons is demonstrated with conversion efficiencies *independent* of the laser pulse duration. This work was supported by the U.S. D.O.E Office of Inertial Confinement Fusion under Cooperative Agreement Nos. DE-FC02-ER54789 and DE-FC52-08NA28302. (P.M. Nilson, R. Betti, and D.D. Meyerhofer also FSC.)

14:24
PO5 3 Temperature measurement of short-pulse heated beryllium using non-collective x-ray Thomson scattering with a Zn K-α line source* T. DOEPPNER, *LLNL* A.L. KRITCHER, *LLNL, UC Berkeley* O.L. LANDEN, *LLNL* H.J. LEE, *UC Berkeley* S.T. LE PAPE, *LLNL* C. STOECKL, W. THEOBALD, *LLE* S.H. GLENZER, *LLNL* Experiments are fielded on the OmegaEP laser facility at the Laboratory of Laser Energetics in Rochester that use the unique capability of sending two kJ-class short pulse beams on target. One of the beams is used to generate hot electrons that isochorically heat a 250 μm Be cube to T_e = 20-100 eV at n_e ~ 3 x 10^{23} cm^{-3}. The second beam creates Zn K-α x-rays at 8.6 keV to measure Thomson scattering in the non-collective regime with time resolution of ~ 10 ps. T_e can be inferred from Doppler-broadening of the Compton feature that is energy down-shifted from the Rayleigh signal. Future experiments will aim at measuring collective scattering from plasmon oscillations. The collisionality can be inferred from broadening of the plasmon signal, allowing measurement of the conductivity at conditions encountered during capsule implosions at the National Ignition Facility.

*This work was performed under the auspices of the U.S. Department of Energy by the Lawrence Livermore National Laboratory under contract DE-AC52-07NA27344. The authors also acknowledge support from LDRD Grant No. 08-LW-004

14:36
PO5 4 Transport of MA electron currents in ultra-fast heated conducting solids* YASUHIKO SENTOKU, *University of Nevada, Reno* JULIEN FUCHS, *LULI, Ecole Polytechnique* EMMANUEL D'HUMIERES, *Universite Bordeuax* Transport of MA currents in conducting high Z solids is crucial for number of applications, e.g. the generation of efficient and fast secondary sources (ions, X-rays, g-rays, etc) or cone-guiding fast ignition of

inertial fusion. We have simulated the ultra-intense ultra-short laser - solid target interaction with a particle-in-cell code, PICLS, which features the relativistic Coulomb collisions, dynamics ionization in gas and solid target, and have studied the MA current transport by irradiating an ultra-intense laser pulse (5×10^{19}W/cm^2, 300fs) in different conducting metal target, such as aluminum, copper, and gold. We found that the strong resistive magnetic fields are excited inside solid, and the fields become stronger in higher Z target because of ∇Z induced by dynamics ionization. The transport of hot electron currents are affected by these magnetic fields, $\sim$ 10 MG in a Al target, and $>$ 50MG in Cu or Au targets. The sheath field at target rear is also modulated because of the transport pattern. Simulations results are consistent with MeV proton beam images observed in experiments.

*This work was supported by DOE/NNSA Grant No. DE-FC52-06NA27616.

14:48

PO5 5 Energy transport and isochoric heating of ultra-fast heated low-Z targets ROHINI MISHRA, YASUHIKO SENTOKU, PETER HAKEL, ROBERTO MANCINI, *University of Nevada, Reno* Ultra-short intense laser pulse generates hot electrons on a target surface. Energy transport and isochoric heating of solid target are important for number of applications, e.g. the generation of secondary sources (ions, X-rays, etc) or the fast ignition of inertial fusion targets. We have performed a particle-in-cell, PICLS, which incorporates the relativistic Coulomb collisions and dynamic ionization in gas and solid targets in order to study the MA current transport and isochoric heating in low Z insulator targets. Our target is a triple layered plastic target ($C_2H_2/C_2H_3Cl/C_2H_2$, 5μm-thick for each layer), inspired by the experiments by Ohshima, Nishimura et al., ILE, Osaka. In the experiment, the 2^{nd} layer is heated up to 50 eV by irradiating a 0.5 PW laser pulse with 250 J in 500fs. We studied the isochoric heating processes in the triple-layered target, and identified three different heating processes, namely, resistive, collisional and diffusive heating, which compete in their different time frames. Re-circulating hot electrons ionize the target, and change the resistivity dynamically. Effects of hot electron recirculation, dynamic ionization, and the resistive magnetic fields are also discussed in this talk.

15:00

PO5 6 Hydrodynamic Simulations and Optical Diagnosis of a Long-Scale-Length Channeling Experiment on OMEGA EP R.S. CRAXTON, W. THEOALD, W. SEKA, S. IVANCIC, G. LI, C. REN, D. WEINER, *Laboratory for Laser Energetics, U. of Rochester* An experiment is planned for OMEGA EP to investigate the channeling concept proposed for fast ignition. A long-scale-length plasma is first produced using long-pulse OMEGA EP beams and then irradiated with a tightly focused, high-intensity, short-pulse ($\sim$ 100 ps) "channeling" beam. An optical probe will be employed to characterize the long-scale-length plasma using the grid image refractometry[1] technique and the channel formed in the underdense plasma using schlieren imaging. Two-dimensional hydrodynamic simulations using *SAGE* will be presented, together with ray-tracing simulations of the optical diagnostics using *SAGE* profiles adjusted to include the channel predicted by particle-in-cell simulations. This work was supported by the U.S. Department of Energy Office of Inertial Confinement Fusion under Cooperative Agreement No. DE-FC52-08NA28302.

[1]R. S. Craxton *et al.*, Phys. Fluids B **5**, 4419 (1993).

15:12

PO5 7 Self- Focusing and Channeling of Relativistic Laser Pulses in Underdense Plasmas NEDA NASERI, WOJCIECH ROZMUS, *Department of Physics-University of Alberta-Edmonton-Canada* We studied in details the ponderomotive channeling of the intense laser pulse in underdense homogeneous plasma using 3D PIC simulations, considering different laser powers and plasma densities. We found limits on plasma density in order to get fully evacuated channels. Also the effects of surface wakes on destruction of electron evacuated channels have been addressed. Evacuation can be lost due to surface wave excitation on the channel edges. The wavelength of the surface waves has been calculated in cylindrical geometry for arbitrary laser intensity on the channel edges. The rise time of the laser pulse plays an important role on the stability of the channels. We also found that the dominant mechanisms in higher densities is hosing and filamentation of the laser pulse. Formation of ring structure, central electron density enclosed by a hollow ring, has been observed in 3D simulations. We have also found that analytical multi-channel solutions are unstable due to the interaction between filaments. The simulation results are in a very good agreement with existing analytical results. [1] Kim et al. Phys. Rev E, 65,036416 (2002)

15:24

PO5 8 Millimeter-scale laser channeling in underdense argon plasma diagnosed with Kα x-ray imaging* N.L. KUGLAND, C.G. CONSTANTIN, *University of California Los Angeles* T. DOEPPNER, A. KEMP, L. DIVOL, S.H. GLENZER, *Lawrence Livermore National Laboratory* C. NIEMANN, *University of California Los Angeles* Two-dimensional x-ray imaging of Kα self-emission from laser-irradiated Ar gas jets has been used to study laser channeling and fast electron transport over millimeter-scale distances. We irradiated high density (10^{20} cm^{-3} atomic density) supersonic Ar gas jets with an ultra-high intensity (10^{19} W/cm^2), high power (100 TW class) 800 nm laser. Kα fluorescence reveals a millimeter-scale laser channel, oriented along the laser axis, which ends in a forward-directed spray of fast electrons. K-shell x-ray spectroscopy diagnoses a spatially averaged mean ionization state of 6 $\pm$ 1 during the Kα emission, implying an electron density of 0.5 n_c. Study of this system can help understand the initial stage of the hole-boring approach to fast ignition, during which an intense laser pulse must propagate through a mm-scale moderately underdense plasma. *This work was performed under the auspices of the U.S. Department of Energy by the Lawrence Livermore National Laboratory under contract DE-AC52-07NA27344. Additional support was provided by LDRD grant 08-LW-004 and the DOE Plasma Physics Junior Faculty Award Program.

15:36

PO5 9 LSP Modeling of Reflection and Absorption of an Intense Laser Pulse from a Solid Target* DOUGLASS SCHUMACHER, ANTHONY LINK, VLADIMIR OVCHINNIKOV, RICHARD FREEMAN, LINN VAN WOERKOM, *The Ohio State University* MINGSHENG WEI, FARHAT BEG, *University of California, San Diego* MICHAEL KEY, ANDREW MACKINNON, PRAVESH PATEL, *Lawrence Livermore National Laboratory* LUJBOMIR NIKOLIC, YING TSUI, ROBERT FEDOSEJEVS, *University of Alberta* We describe the results of LSP modeling of laser reflection from solid-density gold slabs surrounded by lower density plasma (scale length of order 10 μm). We treat p-polarized light at various incident angles, intensities up to 10^{19}W/cm^2 and various pulse widths. We examine absorbed,

specularly reflected, and scattered light, and near and far field spatial and spectral modification of the beam. We find large, regular variation of reflectivity and scatter with all parameters, increased divergence and red chirp in the reflected beam, and other effects. We compare to recent experiment.

*Work supported by the U.S. Department of Energy under contracts DE-FG02-05ER54834, DE-AC52-07NA27344, and by an allocation of computing time from the Ohio Supercomputer Center.

15:48

PO5 10 Efficient Generation of High-Quality Proton Beam in Laser Tailored-Target Interaction* S. KAWATA, K. TAKAHASHI, D. SATOH, D. BARADA, *Utsunomiya Univ.* Y.Y. MA, *National Univ. of Defence Tech., China* Z.M. SHENG, *Shanghai Jio Tong Univ.* O. KLIMO, J. LIMPOUCH, *Czech Tech. Univ. Prague* Q. KONG, P.X. WANG, *Fudan Univ., China* Improvement of energy conversion efficiency from laser to proton beam is demonstrated in a laser-foil interaction. When an intense short-pulse laser illuminates the thin foil target, the foil electrons are accelerated around the target. The hot electrons generate a strong electric field, which accelerates the foil protons, and the proton beam is generated. In this paper a multihole thin-foil target is proposed in order to increase the energy conversion efficiency from laser to protons. The multiholes transpiercing the foil target help to enhance the laser-proton energy conversion efficiency significantly. 2.5-dimensional particle-in-cell simulations present that the total laser-proton energy conversion efficiency becomes 9.3% for the multihole target, though the energy conversion efficiency is 1.5% for a plain thin foil target. The transpiercing multihole target serves a new method to increase the energy conversion efficiency from laser to ions. [1] R. Sonobe, et al., Phys. Plasmas, 12 (2005) 073104. [2] Y. Nodera, et al., Phys. Rev. E78 (2008) 046401.

*Supported in part by JSPS, MEXT and CORE.

16:00

PO5 11 Radiation Pressure Acceleration of Ions A.P.L. ROBINSON, *Plasma Physics Group, Central Laser Facility, STFC Rutherford-Appleton Lab, Oxfordshire, OX11 0QX UK* The possibility of accelerating ions by ultraintense lasers in a regime where the radiation pressure of the laser pulse dominates the interaction has received considerable interest in recent years. Simple analytical models show that this regime of acceleration should be highly tunable and permit scaling to hundreds of MeV for laser intensities in excess of 10^{21} Wcm^{-2}. The use of circularly polarized laser pulses has been very important in these theoretical studies. In this presentation we will describe a simple analytical model for RPA and compare this to numerical simulations. The outstanding question of transverse instabilities will also be discussed, as well as the possibility of the RPA mechanism occurring in underdense plasmas.

16:12

PO5 12 The Effect of Hemispherical Target Diameter on Proton Focusing T. BARTAL,*D.P. HIGGINSON, M.S. WEI, F.N. BEG, *UCSD* D. HEY, S. LE PAPE, M.H. KEY, P.K. PATEL, A.J. MACKINNON, H.S. McLEAN, *LLNL* S.A. GAILLARD,†K. FLIPPO, D.T. OFFERMANN, R.P. JOHNSON, D.S. MONTGOMERY, T. SHIMADA, R. GONZALES, S. REID, F. ARCHULETA, S. LETZRING, T. HURRY, *LANL* R.B. STEPHENS, *GA* Proton focusing from hemispherical targets, to be used in the concept of proton fast ignition, was investigated using the 200TW Trident laser at LANL delivering 80J in 0.5ps with 45% of the energy focused to 7 microns fwhm. High-density carbon hemispherical segments, 0.35-2mm in diameter with 10 miron thick walls, were irradiated at normal incidence. On the rear side of the target, two Cu meshes were placed 1mm and 1.5mm from the opening of the hemispherical segment, one angled with respect to the other. Radiochromic film (RCF) was used to image the proton beam, which carried an imprint of each mesh. The mesh images were used to reconstruct the proton beam and determine the focal plane using a ray tracing technique. Experimental results will be discussed. *Performed for U.S. DOE under contracts FI-ACE, DE-FG-02-05ER54834, DE-AC52-07NA27344.

*Also with LLNL and supported by the Lawrence Scholar Program

†Also with ForschungsZentrum Dresden-Rossendorf

16:24

PO5 13 Simulations of relativistic positron creation using ultra-intense, short pulse lasers* S.C. WILKS, H. CHEN, C.D. CHEN, S.N. CHEN, J. GRONBERG, *LLNL* J. MYATT, D.D. MEYERHOFER, *LLE* G. GREGORI, C.D. MURPHY, J. MITHEN, *CCLR RAL and University of Oxford* D. WELCH, *Voss Sci.* The recent generation of positrons using ultra-intense lasers will be discussed in detail [1]. Although good agreement between theory and experiment for the number of positrons created is obtained [2], the positron peak appears to be shifted in energy by several MeV, depending on the number of electrons that are heated by the laser. We attribute this shift to the TNSA mechanism [3], and will present simulation results consistent with this hypothesis. Indications are that even with targets a few millimeters thick, the electric field on the rear of the target can be $\sim$ 10 MeV/micron. Particle-in-cell and Monte Carlo simulations of the process have been performed in an attempt to maximize the positron production, and these results will be presented. [1] H. Chen, *et al.*, PRL **102**, 105001 (2009). [2] J. Myatt,*et al.*, PRE **79**, 066409 (2009). [3] S.C. Wilks, *et. al.*, Phys. Plasmas **8**, 542 (2001).

*Prepared by LLNL under Contract DE-AC52-07NA27344. LLNL-ABS-414748.

16:36

PO5 14 Using x-ray-free-electron lasers to generate and probe high-energy-density matter STEFAN HAU-RIEGE, RICHARD LONDON, SIEGFRIED GLENZER, *LLNL* JON WEISHEIT, *University of Pittsburg* JIM GLOSLI, DAVE RICHARDS, FRANK GRAZIANI, *LLNL* Recently, lasing has been achieved at the LCLS x-ray free electron laser. Sub-200 fs pulses with a wavelength of 0.15 nm and a pulse energy of 2 mJ have been produced. We have designed an experiment, which utilizes this laser to study ultrafast processes in warm- and hot-dense matter, including ionization, energy transfer, and initial atomic motion. We use the unique high peak-brightness radiation to heat solids isochorically to temperatures up to 100 electron volts, corresponding to pressures up to 20 Mbar. The x-ray free electron laser pulses will also serve as a probe of the state of the material via by Bragg and x-ray Thomson scattering. Elastic Bragg scattering provides ionic properties and structural information about the crystal, while the inelastic Compton and plasmon scattering spectrum reflects the electrical/optical properties, and further provides temperature and density information. We used a new modeling methodology that includes the relevant ionization processes in a massively-parallel molecular dynamics code to simulate the full experiment, including the generation of the high-energy-density material and the formation of the probe-signals.

SESSION PO6: WAVES, TURBULENCE, AND BOUNDARY EFFECTS IN LABORATORY AND SPACE PLASMAS II
Wednesday Afternoon, 4 November 2009
Hanover FG at 14:00
Bill Dorland, University of Maryland, presiding

14:00
PO6 1 Physics of turbulent transport and zonal flows in the edge of fusion plasmas ULRICH STROTH, *University Stuttgart* The understanding of turbulent transport at the plasma edge and on transition to the scrape-off layer is of greatest importance for fusion plasmas. Edge transport sets the values of temperature and density at the pedestal top, parameters which are needed as input for core-turbulence simulations. And SOL transport ultimately defines the peak power density on the divertor plates and the first wall. Furthermore, the interplay between flows and turbulence is one of the most fascinating and rich topics of fusion research. The talk will give an overview of experimental studies on turbulent transport and the interaction of fluctuations with poloidal flows. The studies were carried out on the low-temperature plasma in the TJ-K stellarator which is dimensionally similar to fusion edge plasmas and, hence, a kind of "windtunnel" experiment for fusion devices and testbed for turbulence code. Turbulence is studied with high spatial and temporal resolution and a close comparison of the data with results from the gyro-fluid code GEM shows a great structural similarity. This comparison indicates that drift-waves dominate turbulent transport in the edge plasma. It is also shown how drift waves couple to zonal flows and how they generate intermittent structures (blobs) at the natural edge shear layer. Results are compared with findings from ASDEX Upgrade and other devices.

14:12
PO6 2 Control of drift wave turbulence by driven plasma currents OLAF GRULKE, CHRISTIAN BRANDT, STEFAN ULLRICH, KIAN RAHBARNIA, THOMAS KLINGER, *MPI for Plasma Physics, EURATOM Association, D-17491 Greifswald* The anomalous transport in the plasma edge of fusion devices is believed to be dominated by the drift wave instability, which is inevitable because of the relatively steep radial plasma pressure gradient. Due to its three-dimensional nature the associated parallel plasma currents are a characteristic feature of the drift wave instability. In the present paper we demonstrate that drift waves nonlinearly interact with driven plasma currents in the linear, homogeneously magnetized helicon plasma device VINETA. The intrinsic parallel drift wave currents have an amplitude of typically $100\,mA/cm^2$. If currents are driven mode-selectively by an array of eight electrodes or eight saddle coils on a plasma circumference, respectively, single drift wave modes can be synchronized in frequency, whereas the frequency range of synchronization depends nonlinearly on the amplitude of the driven current. The synchronization is of spatiotemporal nature, i.e. is only achieved if also the propagation direction of the driven current pattern is parallel to the drift wave's phase velocity. In drift wave turbulence the energy of the turbulent fluctuations can be synchronized to a single predefined drift wave mode, which results in an almost complete suppression of the associated fluctuation-induced transport.

14:24
PO6 3 Drift-wave convection in a temperature filament at large Peclet number* J.E. MAGGS, *UCLA* M. SHI, *Courant Inst.* D.C. PACE, *UC Irvine* G.J. MORALES, T.A. CARTER, *UCLA* Heat transport in a narrow elongated temperature filament is governed by conduction at classical rates, and convection due to the ExB flows produced by the potential associated with drift-Alfven waves driven by the filament pressure gradient [Shi, et. al., Phys. of Plasmas, 16, 062306 (2009)]. The results of a study of temperature transport in a model of the temperature filament system due to pure convection (the limit of very large Peclet number) are reported. The model system uses two drift waves, one with azimuthal mode number, m=1 and the other with m=6. The drift wave amplitudes are increased slowly from zero to their maximum value. It is found that convection leads to very fine-scale spatial structures, the larger the final potential amplitude the finer the scale. The power spectrum of a temporal signal taken at a fixed spatial location is found to be exponential at all scale sizes. These spectra arise from Lorentzian-shaped temporal pulses whose temporal widths are consistent with the scale size of associated spatial structures. Although temperature fluctuations produced by pure convection can be quite large, the difference between the initial temperature profile and the azimuthal average of the modified temperature profile is rather modest.

*Supported by BaPSF under NSF/DoE cooperative agreement.

14:36
PO6 4 On the role of an inverse cascade in ion-scale turbulence GABRIEL PLUNK, TOMO TATSUNO, BILL DORLAND, *University of Maryland, College Park* Theoretical works using simplified models of magnetized plasma turbulence have brought a deeper understanding of mechanisms for zonal flow generation and saturation of ion-scale turbulence, and inverse cascade in particular is sometimes cited as an important player. However, these works investigate the Hasegawa–Mima (HM) equation or the Generalized Hasegawa–Mima (GHM) equation that assume cold ions and are thus not applicable for most plasmas. In this work we find a rigorously derived two-dimensional fluid system, valid at finite ion temperature, for turbulence at wavelengths larger than the ion Larmor radius. It is shown that the theoretical basis for an inverse cascade within this model is not present. We also perform the modulational/secondary instability analysis to investigate other mechanisms that are believed to be linked to the growth of a large-scale zonal component. Finally, the results are investigated by direct numerical simulation with AstroGK.

14:48
PO6 5 Non-diffusive transport in collisionless trapped electron mode turbulence YONG XIAO, *UC Irvine* Gyrokinetic simulations of collisionless trapped electron mode (CTEM) turbulence find that the electron heat transport shows a gradual transition from Bohm to gyroBohm scaling when the device size is increased. Radial correlation function shows that CTEM turbulence eddies are mainly microscopic but with a significant mesoscale tail. The mesoscale streamers result from a dynamical process of radial streamers breaking by zonal flows and merging of microscopic eddies. It is further found that the radial profile of the electron heat conductivity only follows the global profile of the fluctuation intensity, whereas the ion transport tracks more sensitively the local fluctuation intensity. This suggests the existence of a nondiffusive component in the electron heat flux, which arises

from the ballistic radial ExB drift of trapped electrons due to a combination of the presence of mesoscale eddies and the weak detuning of the toroidal precessional resonance. In contrast, the ion radial excursion is not affected by the mesoscale eddies due to the parallel wave-particle decorrelation, which is not operational for trapped electrons because of the fast electron bounce motion. This is confirmed by our comprehensive analysis of kinetic and fluid time scales.

15:00

PO6 6 Magnetic island induced ITG instability in multi-scale MHD and micro-turbulence YASUAKI KISHIMOTO, JIQUAN LI, Z.X. WANG, J.Q. DONG, MIHO JANVIER, KENJI IMADERA, *Kyoto University* Multi-scale fluctuations due to different drive force can coexist and interplay with each other in magnetic fusion plasmas such as in tokamak. The cross-scale interaction may provide new energy channels as a drive or sink. As a common and typical multi-scale problem, we have proposed a gyrofluid model to numerically simulate the evolution of mixed-scale electromagnetic (EM) turbulence involving resistive MHD and ion-scale micro-instability[1]. In this work, we investigate the stability of ion temperature gradient (ITG) in a plasma with the excitation of resistive tearing mode (RTM). Our gyrofluid simulations are performed for linear excitation and nonlinear evolution of both RTM and ITG instabilities in a slab geometry. It is observed that due to the nonlinear interaction between RTM and ITG modes, the mixed scale EM fluctuation is first saturated at a lower level. Afterwards, the magnetic island continuously grows with a slow time scale. It is interestingly found that a new fluctuation propagating along ion diamagnetic direction becomes growing when the magnetic island width approaches some size. It is identified as a new ITG instability induced by magnetic island, which is referred to as MITG. [1] Jiquan Li, Y. Kishimoto, et al. Nucl Fusion 49, in printing (2009). [2] Z X Wang, Jiquan Li, J.Q.Dong, Y.Kishimoto, Phys. Plasmas 16, 060703(2009)

15:12

PO6 7 Low-Frequency Fluctuations Driven by Electron Temperature Gradient in Magnetized Plasma CHANHO MOON, SHUICHI TAMURA, TOSHIRO KANEKO, RIKIZO HATAKEYAMA, *Tohoku Univ.* We investigate low-frequency instabilities driven by an electron temperature gradient (ETG), which is generated by using a magnetized electron cyclotron resonance (ECR) plasma. The ECR plasma produced by a microwave (6 GHz, 10 W) passes through mesh grids [grid 1 (ϕ 6 cm, 10 mesh/inch) and grid 2 (doughnut shape, OD:ϕ 6 cm, ID: ϕ 3 cm, 30 mesh/inch)] into an experimental region where low-temperature thermionic electrons (0.2 eV) emitted from a tungsten hot plate (3 kW) are superimposed upon high-temperature electrons (2.5 eV) of the ECR plasma. By applying a bias voltage to the grid 2, a density of the high-energy electrons only in the peripheral region is controlled, and therefore the ETG can be formed easily. In addition, we observe density fluctuations in the frequency domain to find a relation with the ETG and low-frequency instabilities. As a result it can be figured out experimentally that the large ETG excites the fluctuations, but a space potential gradient is also necessary to destabilize the fluctuations.

15:24

PO6 8 GAM shearing feedback loop in turbulence spreading and transport bifurcation KAZUHIRO MIKI, PATRICK H. DIAMOND, *Center for Astrophysics and Space Science, UCSD* ZHIHONG LIN, *Department of Physics and Astronomy, University of California, Irvine* To theoretically discuss the impact of the GAM on turbulence, two synergistic processes are elucidated; zonal flow modulation and the effect of secular wave group propagation on spreading. Using wavekinetic modulational analysis, the response of turbulence to the GAM is calculated. This group speed differs from that for zero-frequency zonal flows due to resonance between drift wave group speed and the GAM strain field, which allows secularity. Finite real frequency and radial group velocity are intrinsic to the GAM, so non-local phenomena at the edge region are likely. To understand the effect of the GAM on turbulence dynamics, a predator-prey model incorporating the turbulence and the GAMs is constructed and analyzed for stability. Three possible states are identified, namely on an L-mode-like stationary, an H-mode-like stationary, and an H-mode-like oscillatory state which reproduces a regime where the GAM shearing regulates the turbulence level. The system is attracted to the state with the minimum turbulence level for the given control parameters. The Doppler-shifted GAM frequency is found as the result of the GAM radiative dissipation. This material is based upon work supported by the Department of Energy under Award Numbers DE-FG02-04ER54738 and DE-FC02-08ER54959.

15:36

PO6 9 Control of turbulent transport by GAMs KLAUS HALLATSCHEK, *IPP-Garching* In principle, geodesic acoustic modes (GAM), poloidal flows in tokamaks oscillating at the system sound frequency, are able to control turbulent transport in a similar way as the better known zonal flows - if certain conditions are met. For once, the GAMs must be weakly damped, restricting the safety factor to the relatively high values of the tokamak edge. The GAM frequency should be significantly lower than the turbulence frequencies to avoid averaging effects, and to allow effective feedback amplification of the GAMs, e.g., by diamagnetic drive. Lastly, the drive is significantly boosted in highly nonlinear situations. Using numerical turbulence studies, the effectivity of GAM drive and the dependence of transport on the GAM properties have been analyzed for varying magnetic geometry, plasma parameters, gradients, and magnitude of nonlinear terms. In particular, in the limit of high gradients and favorable circumstances the GAM activity can become so strong as to virtually suppress the transport in comparison to standard scenarios. The transport is then organized in individual bursts associated with the zero crossings of the flow oscillation.

15:48

PO6 10 Photonic Beam-Plasma Instabilities and Imaging* DMITRY V. DYLOV, JASON W. FLEISCHER, *Princeton University, Princeton, NJ 08544* We consider an all-optical version of the bump-on-tail instability and show that signal-noise interactions can be modeled as a beam-plasma instability. Theoretically, the mapping follows by treating partially-coherent light using a wave-kinetic approach[2]. We analytically derive a Bohm-Gross dispersion relation, showing that optical speckles interact via Langmuir-type modulation waves. Experimentally, we confirm the theory by demonstrating single[2] and multiple[3] bump-on-tail instabilities in a self-focusing photorefractive crystal. We then observe the recovery and amplification of noise-hidden images, showing that the

coherent-incoherent coupling is a photonic beam-plasma instability. Remarkably, the plasma formula recovers a formula from information theory describing stochastic resonance, extended to include the dynamical coupling of transverse modes. The results link the fields of optics, plasma, and information theory in unanticipated ways and suggest new uses for beam shaping in material plasma.

*This work was supported by the NSF, the AFOSR, and the DOE under grant DE-FG02-08ER55001[2] D.V. Dylov and J.W. Fleischer, *Phys. Rev. Lett.* **100**, 103903(2008)[3] D.V. Dylov and J.W. Fleischer, *Phys. Rev. A* **78**, 061804R (2008)

16:00

PO6 11 Orbital angular momentum of photons, plasmons and neutrinos in a plasma J.T. MENDONCA, *Instituto Superior Tecnico, Lisboa, Portugal* BO THIDÉ, *Swedish Institute of Space Physics, Uppsala, Sweden* H. THEN, S. ALI, *Instituto Superior Tecnico, Lisboa, Portugal* We study the exchange of angular momentum between electromagnetic and electrostatic waves in a plasma, due to the stimulated Raman and Brillouin backscatering processes [1]. Angular momentum states for plasmon and phonon fields are introduced for the first time. We demonstrate that these states can be excited by nonlinear wave mixing, associated with the scattering processes. This could be relevant for plasma diagnostics, both in laboratory and in space. Nonlinearly coupled paraxial equations and instability growth rates are derived. The characteristic features of the plasmon modes with finite angular momentum are also discussed. The potential problem is solved and the angular momentum is explicitly calculated [2]. Finally, it is shown that an electron-neutrino beam, propagating in a background plasma, can be decomposed into orbital momentum states, similar to that of photon states. Coupling between different neutrino states, in the presence of a plasma vortex, is considered. We show that plasma vorticity can be transfered to the neutrino beam, which is relevant to the understanding of the neutrino sources in astrophysics. [1] J.T. Mendonca et al., PRL 102, 185005 (2009). [2] S. Ali and J.T. Mendonca, PoP (2009) submitted. [3] J.T. Mendonca and B. Thide, Europhys. Lett. 84, 41001 (2008).

16:12

PO6 12 Turbulence aspects of nonlinearly interacting ion waves in a nonuniform quantum plasma* P.K. SHUKLA, B. ELIASSON, *Ruhr University Bochum, Germany* DASTGEER SHAIKH, *The University of Alabama in Huntsville* By using the inertialess electron momentum equation with the quantum statistical pressure and the quantum Bohm potential, as well as the ion continuity and momentum equations, we derive a pair of nonlinear equations for studying the turbulence properties of 2D nonlinearly interacting ion oscillations in a nonuniform quantum plasma. Computer simulations of the nonlinear quantum ion fluid equations reveal spectrum cascading and the formation of vortical structures. The resulting turbulent spectrum scaling involving nanostructues do not follow the Kolmogorov law. The relevance of our investigation to nanoscale turbulence in the interior of white dwarfs and other compact superdense astrophysical objects is highlighted.

*This work was partially supported by the DFG through the Research Unit 1048.

16:24

PO6 13 Spectral Dependence of Modulation Instability* CAN SUN, DMITRY V. DYLOV, JASON W. FLEISCHER, *Princeton University, Princeton, NJ 08544* We consider the spectral dependence of modulation instability. In addition to the usual Maxwell-Boltzmann, or Gaussian, distribution, we consider Lorentzian, exponential and rectangular power spectra. We show that each distribution gives its own threshold for instability, and that the rectangular spectrum gives the counterintuitive trend of increasing perturbation period as the profile narrows (becomes more coherent). Theoretical results are confirmed experimentally by mapping the plasma problem to the equivalent statistical optics system [2,3].

*This work was supported by the NSF, the AFOSR, and the DOE under grant DE-FG02-08ER55001[2] D.V. Dylov and J.W. Fleischer, *Phys. Rev. Lett.* **100**, 103903 (2008)[3] D.V. Dylov and J.W. Fleischer, *Phys. Rev. A* **78**, 061804R (2008)

SESSION PP8: POSTER SESSION VI
Wednesday Afternoon, 4 November 2009
Grand Hall East at 14:00

PP8 1 C-MOD

PP8 2 Lower Hybrid Wave Induced Rotation on Alcator C-Mod* RON PARKER, YURI PODPALY, JOHN RICE, ANDREA SCHMIDT, *MIT PSFC* Injection of RF power in the vicinity of the lower hybrid frequency has been observed to cause strong counter current rotation in Alcator C-Mod plasmas [1,2]. The spin-up rate is consistent with the rate at which momentum is injected by the LH waves, and also the rate at which fast electron momentum is transferred to the ions. A momentum diffusivity of $\sim$ 0.1 m^2/s is sufficient to account for the observed steady-state rotation. This value is also comparable with that derived from an analysis of rotation induced by RF mode conversion [3]. Radial force balance requires a radial electric field, suggesting a buildup of negative charge in the plasma core. This may be the result of an inward pinch of the LH produced fast electrons, as would be expected for resonant trapped particles. Analysis of the fast-electron-produced bremsstrahlung during LH power modulation experiments yields an inward pinch velocity of $\sim$ 1 m/s, consistent with the estimated trapped particle pinch velocity. [1] A. Ince-Cushman, et.al., Phys. Rev. Lett., **102**, 035002 (2009) [2] J. E. Rice, et. al., Nucl. Fusion **49**, 025004 (2009) [3] Y. Lin, et.al., this meeting

*Work supported by USDoE awards DE-FC02-99ER54512 and DE-AC02-76CH03073.

PP8 3 Integration of Fokker Planck calculation in full wave FEM simulation of LH waves* ORSO MENEGHINI, SYUN'ICHI SHIRAIWA, RON PARKER, *MIT-PSFC* A full wave simulation code based on Finite Element Method (FEM) was developed to solve LH waves in tokamaks [1]. The FEM approach allows a seamless handling of the antenna, first wall, SOL, divertor and core regions. In the region of plasma inside of the separatrix, electron landau damping is modeled by means of an iterative procedure. The code has been recently coupled to a bounce averaged Fokker Planck (FP) solver, which self consistently calculates the electron 2D distribution function resulting from the balance between collisions and RF quasilinear diffusion (DQL) in a toroidal geometry. The evaluation of the DQL term from the full wave fields has been done by integration of the momentum equation of test particles. Results comparing Maxwellian, 1D FP and 2D FP plasmas will be presented for the Alcator C-Mod tokamak. [1] S. Shiraiwa, this conference.

*Work supported by USDOE awards DE-FC02-99ER54512 and DE-AC02-76CH03073.

PP8 4 Investigation of velocity diffusion in the presence of a broad-band Lower Hybrid wave spectrum* JUNGPYO LEE, PAUL BONOLI, JOHN WRIGHT, *MIT-PSFC* ALCATOR C-MOD TEAM, Lower Hybrid (LH) waves are attractive for driving current in Tokamak because of high efficiency. The quasi-linear diffusion coefficient[1] has been used in the past to estimate the current density by electron landau damping. We numerically evaluate the diffusion coefficient taking into account the broad band spectrum of LH wave. The motion of a single electron is simulated by a one dimensional non-linear momentum equation along the magnetic field, and the value of velocity diffusion averaged over initial positions is computed. The electron is accelerated by an electric field whose wavenumber spectrum is broad and discrete due to toroidal geometry. The broad band spectrum induces phase mixing so that it allows only a limited number of kicks every revolution of the electron. We compare the numerically computed diffusion coefficient with the quasi-linear diffusion coefficient[1] as a function of the magnitude of the electric field with Alcator C-Mod LH wave parameters. We also present diffusion coefficient profiles in velocity space overlapped by many resonance modes.

*Work supported in part by a Samsung Fellowship and USDoE awards DE-FC02-99ER54512.

[1]C.F. Kennel and F. Engelmann, Physics of Fluids, 9(1966),2377-2388

PP8 5 Full-Wave Analysis of Lower Hybrid Wave Propagation in the Edge Plasma of a Tokamak* P.T. BONOLI, G.M. WALLACE, J.C. WRIGHT, O. MENEGHINI, R. PARKER, M. PORKOLAB, S. SHIRAIWA, *MIT-PSFC* R.W. HARVEY, *CompX* C.K. PHILLIPS, E.J. VALEO, J.R. WILSON, *PPPL* Recent lower hybrid current drive **(LHCD)** experiments on Alcator C-Mod have revealed a transition density above which LHRF generated fast electrons are no longer detected [1]. This critical density is also well below the threshold density for parametric decay of the LH pump wave. Analysis of these plasmas using a ray tracing-Fokker Planck model shows that poorer wave penetration at higher density, accompanied by increased collisional damping in the Scrape off Layer (SOL) may possibly explain this transition [1]. We have used an electromagnetic field solver TORLH [2] to begin to assess the possible role of full-wave effects in this density limit. Results will be presented, including three-dimensional field reconstructions for varying edge plasma parameters such as SOL density, temperature, and density gradient scale length. [1] G. Wallace *et al*, 18^{th} Topical Conf. on RF Power in Plasmas (Gent, Belgium, June, 2009) Paper B60. [2] J. C. Wright *et al*, Physics of Plasmas **16**, July (2009).

*Work supported in part by the US DOE award DE-FC02-99ER54512.

PP8 6 Full wave/Fokker-Planck analysis of driven current and hard X-ray emission profiles during lower hybrid experiments on Alcator C-Mod* JOHN WRIGHT, *PSFC-MIT* ERNEST VALEO, CYNTHIA PHILLIPS, *PPPL* PAUL BONOLI, *PSFC-MIT* RF-SCIDAC TEAM, Analysis of lower hybrid (LH) wave propagation in the past has been done using ray tracing and the WKB approximation. Advances in algorithms and parallel computer architectures has permitted the solving of the Maxwell-Vlasov system for wave propagation directly [Wright et al., Phys. Plasmas (2009), 16, July]. Self-consistent non-Maxwellian distribution functions are included by coupling the TORIC-LH full wave code with the CQL3D Fokker-Planck code via the export of the quasi-linear diffusion coefficent from TORICLH and the use of the electron distribution function from CQL3D to evaluate the dielectric response in TORICLH following the technique implemented by Valeo [Valeo et al.,18th RF Power in Plasmas Proceedings (2007)]. Using the synthetic HXR diagnostic in CQL3D we will compare self-consistent LH simulations with LH experiments on Alcator C-Mod at several different waveguide phasings. Discussion will include comparisons with ray tracing the relative importance of full wave effects, relativistic effects, and reflections.

*Supported by USDoE award no. DE-FC02-01ER54648.

PP8 7 Analysis and scenario modeling of LHCD on Alcator C-Mod* J.R. WILSON, C. KESSEL, S. SCOTT, E. VALEO, *PPPL* R.R. PARKER, P.T. BONOLI, A.E. HUBBARD, J.W. HUGHES, J.S. KO, O. MENEGHINI, M. PORKOLAB, J.E. RICE, A.E. SCHMIDT, S. SHIRAIWA, G.M. WALLACE, J.C. WRIGHT, *MIT PSFC* Lower Hybrid Current Drive **(LHCD)** on Alcator C-Mod is being used in plasmas with parameters similar to those expected on ITER for the purpose of tailoring the plasma current profile with the ultimate goal of obtaining Advanced Tokamak (AT) operation. New simulation codes have been developed which allow more detailed analysis of the existing data and extrapolation to the final target AT discharges. These codes allow the ability to include the scrape-off plasma, non-Maxwellian electron distribution function and relativistic effects. Scans in the parallel wave-number will be presented and compared to experimental data that have indicated radial broadening of the hard x-ray emission under certain plasma conditions. In addition, scans of the plasma density and temperature will be performed to confirm the optimal approach to achieving AT plasmas.

*This work supported by USDOE awards DE-FC02-99ER54512 and DE-AC02-09CH11466.

PP8 8 Nonthermal ECE as a diagnostic of LH driven fast electrons on Alcator C-Mod* S.G. BAEK, R.R. PARKER, A. HUBBARD, *MIT, Plasma Science and Fusion Center, Cambridge, MA, USA* R.W. HARVEY, *CompX, Del Mar, CA, USA* Down-shifted 2^{nd} harmonic ECE from the outboard horizontal midplane has been measured during Lower Hybrid Current Drive (LHCD) on C-Mod and is a direct indication of the generation of nonthermal electrons. However optical depth and radial magnetic field variation make quantitative analysis difficult. Potential single and multi chord vertical high harmonic ECE measurement systems are investigated with a view to obtaining quantitative information about nonthermal electrons in momentum or physical space. A simple distribution function model is tested to evaluate dependence of emissivity on parallel and perpendicular Maxwellian temperature. A more detailed simulation is done with GENRAY-CQL3D, using its synthetic diagnostic code for nonthermal ECE. Initial results indicate radial emissivity profile and perpendicular temperature can be inferred, but experimental issues originating from optically thin higher harmonic radiation may hinder the realization of vertical ECE diagnostics for Alcator C-Mod.

*Supported by US DoE award DE-FC02-99ER54512.

PP8 9 Detection of Lower Hybrid Waves on Alcator C-Mod with Phase Contrast Imaging Using Electro-Optic Modulators* K. ARAI, M. PORKOLAB, E. EDLUND, P. KOERT, R. PARKER, N. TSUJII, P. WOSKOV, S. WUKITCH, *MIT PSFC, Cambridge, MA 02139* AND ALCATOR C-MOD TEAM, Detection of 4.6 GHz lower hybrid waves with Phase Contrast Imaging (PCI) presents a particular challenge due to the limited frequency response of the photoconductive detectors used for our 10.6 μm CO_2 laser. Acousto-optic modulators have been used to detect ICRF waves in the 80 MHz range through optical heterodyning in Alcator C-Mod [1]. However, the scattering efficiency of the acousto-optic modulators limits modulation frequencies up to 100 MHz. Here we present the design of a waveguide loaded with cadmium telluride (CdTe) to serve as an electro-optic modulator for CO_2 laser amplitude modulation near 4.6 GHz. This amplitude modulator will be installed in the near future on our PCI system to detect lower hybrid waves. The expected signal quality will be discussed. [1] M. Porkolab, et al, IEEE Trans. of Plasma Sci. 34, 229 (2006).

*Work supported by US DOE under DE-FG02-94-ER54235 and DE-FC02-99-ER54512.

PP8 10 Multi-species particle transport in GYRO simulations of low-collisionality, peaked-density H-mode plasmas in C-Mod* D.R. MIKKELSEN, *Princeton University* M. GREENWALD, *MIT* R. WALTZ, J. CANDY, *General Atomics* Experimental results from Alcator C-Mod have confirmed earlier AUG and JET findings that spontaneous peaking of the density profile in H-mode plasmas depends on collisionality. Previously reported nonlinear, 'full-radius' GYRO simulations [1] of low-collisionality, peaked-density H-mode plasmas in C-Mod generated a particle pinch that was produced exclusively by higher-k modes. Nonlinear simulations of AUG have a similar character [2], and recent detailed linear analyses [2,3] suggest that density peaking may be common in low collisionality plasmas. Here we increase the number of ion species in the simulations to determine whether impurity pinches are also expected, and whether the degree of density peaking is predicted to differ for the three hydrogen isotopes. These simulations include experimentally relevant levels of several impurities, and a range of H/D and D/T mixes. [1] D.R. Mikkelsen, et al., Bull. Am. Phys. Soc. 52, (2007) No. 16, 221, NP8.71 [2] C. Angioni, et al., Phys. Plasmas 16 (2009) 060702 [3] M. Maslov, et al., Nucl. Fusion 49 (2009) 075037

*Supported, in part, by DOE Contract Number is DE-AC02-09CH11466

PP8 11 Impurity Transport Studies Using the Multi-Pulse Laser Blow-Off System on Alcator C-Mod* NATHAN HOWARD, MARTIN GREENWALD, JIM TERRY, JOHN RICE, *MIT PSFC* A new laser blow-off system for use in impurity transport studies on Alcator C-Mod was installed for the 2009 run campaign. Its capabilities include: multiple impurity injections during a single plasma pulse, remote manipulation of the ablated spot size, and a laser pulse capable of ablating a wide range in target Z. The use of a 650 mJ, ND:YAG laser operating at up to 10 Hz coupled with fast beam steering via a 2-D piezoelectric mirror mount able to move spot locations in 100 ms, and a remote controllable optical train allow spot sizes to vary from approximately 1 to 5 mm. Alcator C-Mod's extensive diagnostic capabilities (soft X-ray, Vacuum Ultraviolet (VUV), charge exchange spectroscopy, etc.) together with the improvements over standard laser blow-off systems allow for detailed studies of the impurity transport dependencies and mechanisms. An overview of system and results from the 2009 campaign are presented.

*Work supported by US DoE Coop. Agreement No. DE-FC02-99ER54512.

PP8 12 Calculating the Source Terms in the Momentum Diffusion Equation* YURI PODPALY, JOHN RICE, MATT REINKE, YIJUN LIN, *MIT Plasma Science and Fusion Center* DAVID MIKKELSEN, *Princeton Plasma Physics Laboratory* IAN HUTCHINSON, *MIT Plasma Science and Fusion Center* There have been numerous attempts explain the anomalous transport of toroidal momentum in plasmas. Current methods involve the application of diffusive, proportional to gradient v, and convective, proportional to v, terms in the simple momentum conservation equation. Including these terms, however, does not provide a proper representation of the profile shape of the plasma rotation, so other terms must be included, which could be source or off-diagonal residual stress contributions in the momentum conservation equation. Using the spatially resolving soft x-ray spectrometer at Alcator C-Mod which provides temporally and spatially resolved rotation profiles, and solving the momentum conservation equation, it is possible to quantify the effects of diffusion and convection terms and reveal the spatial and temporal shape of a source required to explain the rotation velocity profiles. This poster focuses on running this analysis on discharges with L-H mode transitions, L-mode rotation inversions, and fast SSEP sweeps, which provide strong changes in the rotation profile.

*Supported by USDoE award DE-FC02-99ER54512.

PP8 13 Simulation of turbulent impurity transport in Alcator C-Mod* W.L. ROWAN, I.O. BESPAMYATNOV, K.W. GENTLE, K.T. LIAO, *Fusion Research Center, University of Texas at Austin* W. HORTON, X. FU, *Institute for Fusion Studies, University of Texas at Austin* C.L. FIORE, *MIT-PSFC* S. BENKADDA, S. FUTATANI, *France-Japan Magnetic Fusion Laboratory LIA 336 CNRS* X. GARBET, *CEA, Cadarache, France* Theory/experiment comparisons are presented for impurity transport in H-mode and ITB discharges in Alcator C-Mod. The impurity profiles are hollow in H-mode and peaked for ITB. This range of profiles is a stringent test for theory and represents cases with significant impact on tokamak performance and particular interest for ITER. The data was selected to optimize the comparison: only one impurity charge state must be analyzed and simulated. H-mode is modeled with a new, generalized Hasegawa-Wakatani model that describes on equal footing the fueling ion, the impurity, and the electrons. The ITB is simulated using a 3-D global fluid code which includes two ion species and electrons which are introduced into the plasma with a fixed source. Transport is due to coupled ITG and TEM modes.

*Supported by DOE via grants DE-FG03-96ER54373 and DE-FC02-99ER54512, SciDac-UCSD, and the CEA, France.

PP8 14 CXRS Impurity Density Measurement Techniques in C-Mod* IGOR BESPAMYATNOV, WILLIAM ROWAN, KENNETH LIAO, KENNETH GENTLE, *The University of Texas at Austin, Fusion Research Center* CATHERINE FIORE, ROBERT GRANETZ, *Plasma Science and Fusion Center* DAN THOMAS, *ITER* The wide-view CXRS system installed on C-Mod provides measurements of the time-dependent boron density, temperature, and flow velocity profiles. Conventional technique for CXRS measurement of the absolute impurity density requires accurate characterization of the local neutral beam parameters such as energy, density and excitation states. Currently this data is routinely provided by the set of beam extraction, propagation and penetration codes. A new unifying beam code (ALCBEAM) is being developed to provide the local beam parameters at any point in the plasma. As an alternative to the conventional CXRS system, a new integrated CXRS/BES system is designed and will be installed on the Alcator C-Mod tokamak. In this approach, the BES system serves as an alternative, more accurate, means for measuring of the local beam densities. Advantages and disadvantages of the both approaches will be discussed.

*Supported by USDoE Awards DE-FG03-96ER54373 and DE-FC02-99-ER54512.

PP8 15 Electron thermal transport studies with improved n_e/T $_e$ profiles measured by Core Thomson scattering diagnostic on Alcator C-Mod* YUNXING MA, JERRY HUGHES, DARIN ERNST, MARTIN GREENWALD, JOHN RICE, YURI PODPALY, *MIT PSFC* The Core Thomson scattering (TS) diagnostic on Alcator C-Mod has been upgraded to provide n_e and T_e measurements with improved radial spatial resolution up to 1cm (r/a $\sim$ 0.05) in the range of r/a$<$ 0.6. We present the results from experimental studies of electron thermal transport with the improved n_e and T_e profiles measured by TS and T_i profiles from High Resolution X-ray Spectrometer (HIREX) in Ohmic and RF heated plasma discharges. We also compare the calculated thermal diffusivities from profiles fitted using different combinations of measurements. The purpose of this study is to investigate how the transport coefficients are sensitive to the input profiles. Preliminary results from gyrokinetic and gyrofluid analysis are also presented. Continued profile sensitivity studies and detailed gyrokinetic analysis will be performed in the future.

*Work supported by USDoE award: DE-FC02-99ER54512.

PP8 16 Thomson Scattering Diagnostic for the Scrape Off Layer of Alcator C-Mod* JIEXI ZHANG, J.W. HUGHES, YUNXING MA, *MIT PSFC* In order to study heat and particle transport in the edge plasma of Alcator C-Mod, a new Thomson Scattering (TS) diagnostic for the Scrape-Off-Layer (SOL) has been designed. It will complement the existing Edge TS system, which measures a minimum electron temperature (T_e) of approximately 50 eV. The SOL TS system is designed to resolve the plasma profile of T_e of 10$\sim$ 200 eV and electron density (n_e) as low as 1$\sim$ $2x10^{19}$ m^{-3} with a radial spatial resolution, dR, of about 2 mm (r/a $\sim$ 0.01). With 1064 nm Nd:YAG laser light as the laser source, we used plasma data from the C-Mod Core TS system as a guide in the design of a new spectral configuration for the 4-channel polychromators. The response of the Avalanche Photodiode (ADP) detectors was modeled to estimate the expected signals and signal to noise ratios (SNR). Simulations including the filters show that the system in the new configuration could produce meaningful measurements with SNR$>$ 3 when T_e is 10 eV and n_e is $3x10^{19}$ m^{-3} or less. The spectral location and bandwidth of each filter are optimized to allow calibration using both Raman and Rayleigh scattering in H_2 and D_2.

*Supported by USDoE award DE-FC02-99-ER54512.

PP8 17 Thermal issues and relevant upgrades of the MSE diagnostic on Alcator C-Mod* JINSEOK KO, *MIT PSFC* STEVE SCOTT, *PPPL* SYUN'ICHI SHIRAIWA, BOB MUMGAARD, *MIT PSFC* MARK SMITH, *PPPL* The cause of shot-to-shot drifts in polarization angle measured by the Motional Stark Effect (MSE) diagnostic in Alcator C-Mod has been identified as thermal stress birefringence in the in-vessel optics. Based on a series of bench experiments that characterized the thermal response of the system, a single-layer heat shield with gold plating and a new lens holder which reduces the thermal conduction path to the lens have been designed, fabricated, and installed. These modifications are expected to reduce the temperature variation across the in-vessel lens to less than 0.5 Celsius degrees during C-Mod discharges with high power. The expected reduction in the spurious change in polarization angle is more than a factor of 10. New dielectric mirrors with reduced retardation are expected to reduce the drift by an additional factor of 2 to 4.

*Work supported by the U.S. Department of Energy, Grant No. DE-FC02-99ER54512 and DE-AC02-09CH11466.

PP8 18 Upgraded thermal management of the MSE diagnostic on Alcator C-Mod R. MUMGAARD, *MIT Plasma Science and Fusion Center* S. SCOTT, *Princeton Plasma Physics Laboratory, Princeton, NJ, USA* J. KO, S. SHIRAIWA, *MIT Plasma Science and Fusion Center, Cambridge, MA, USA* M. SMITH, *Princeton Plasma Physics Laboratory, Princeton, NJ, USA* A major upgrade to the Motional Stark Effect (MSE) diagnostic was completed in June 2009 to reduce spurious errors in polarization angle measurements arising from thermal stress birefringence in the in-vessel optics [Thermal issues and relevant upgrades of the MSE diagnostic on Alcator C-Mod, Ko]. The upgrade comprises a gold-plated

thermal shield, a novel thermally-insulating mount mechanism for the in-vessel MSE lenses, and improved dielectric mirrors with low retardance. The thermal and polarimetric performance of these systems will be evaluated over the course of the FY09 Alcator C-Mod experimental campaign. We compare the actual effectiveness of the thermal shield as determined from 20 thermocouple measurements to predicted performance. Reductions in the spurious variation in polarization angle will be evaluated by measuring the pitch angle in identical plasma discharges widely separated in time. Additionally, the effect of retardation in the mirrors and photoelastic modulators on calibration errors will be discussed. Work supported by US DOE Contracts DE-AC02-09CH11466 and DE-FC02-99ER54512.

PP8 19 The Alcator C-Mod FIR Polarimeter* P. XU, J.H. IRBY, J. BOSCO, A. KANOJIA, R. LECCACORVI, E.S. MARMAR, P. MICHAEL, R. MURRAY, Y. ROKHMAN, R. VIEIRA, *MIT* D.L. BROWER, W.X. DING, *UCLA* D.K. MANSFIELD, *PPPL* A multi-chord FIR polarimetry diagnostic is being developed for the Alcator C-Mod Tokamak to be used to determine the q-profile and to study density and magnetic field fluctuations. This poloidally viewing system using retro-reflectors on the inner wall will have geometry and fields similar to those planned for ITER. The full optical layout will be discussed, as well as simulations of the expected Faraday and Cotton-Mouton signal levels. Bench test results from a single chord system including all optical components will be presented, and preliminary experimental results from C-Mod will be compared with simulated Faraday rotation angle calculated using Thomson Scattering density profiles and EFIT reconstructions of actual C-Mod plasmas.

*Supported by US DoE award DE-FC02-99ER54512.

PP8 20 Initial results from divertor heat-flux instrumentation on Alcator C-Mod* B. LABOMBARD, D. BRUNNER, J. PAYNE, M. REINKE, J.L. TERRY, J.W. HUGHES, B. LIPSCHULTZ, D. WHYTE, *MIT PSFC* Physics-based plasma transport models that can accurately simulate the heat-flux power widths observed in the tokamak boundary are lacking at the present time. Yet this quantity is of fundamental importance for ITER and most critically important for DEMO, a reactor similar to ITER but with $\sim$ 4 times the power exhaust. In order to improve our understanding, C-Mod, DIII-D and NSTX will aim experiments in FY10 towards characterizing the divertor "footprint" and its connection to conditions "upstream" in the boundary and core plasmas [2]. Standard IR-based heat-flux measurements are particularly difficult in C-Mod, due to its vertical-oriented divertor targets. To overcome this, a suite of embedded heat-flux sensor probes (tile thermocouples, calorimeters, surface thermocouples) combined with IR thermography was installed during the FY09 opening, along with a new divertor bolometer system. This paper will report on initial experiments aimed at unfolding the heat-flux dependencies on plasma operating conditions. [2] a proposed US DoE Joint Facilities Milestone.

*USDOE Coop. Agree. No. DE-FC02-99ER54512.

PP8 21 Plasma sheath heat flux transmission in the Alcator C-Mod divertor* D. BRUNNER, B. LABOMBARD, J. PAYNE, *MIT PSFC* A new array of embedded sensors has been installed in the Alcator C-Mod divertors to measure plasma heat flux deposition profiles. These include tile thermocouples, calorimeters [2] and a unique set of surface temperature thermocouple probes [3]. The latter sensors have the ability to measure the surface temperature evolution with $\sim$ 10 ms time response during a plasma discharge. From a simple 1-D heat transport model, surface heat fluxes can be computed as a function of time. In addition, embedded Langmuir probes simultaneously record poloidal profiles of plasma density and electron temperature at the divertor surface. Taken together, these data allow sheath heat-flux transmission factors to be inferred – a fundamental quantity of plasma-sheath physics. This paper will report initial observations and estimates of heat flux and heat deposition profiles on C-Mod's outer divertor and the implied plasma-sheath transmission factors. [2] J. Payne, *et al.*, this meeting. [3] S. Gangadhara, *et al.*, Bull. Am. Phys. Soc. **41** (1996), 1550.

*USDOE Coop. Agree. No. DE-FC02-99ER54512.

PP8 22 Design and analysis of divertor calorimetry in Alcator C-Mod* J. PAYNE, D. BRUNNER, B. LABOMBARD, J.L. TERRY, *MIT PSFC* An array of 14 calorimeter sensors was recently installed in a set of specially-design "ramped" tiles in C-Mod's outer divertor. Each sensor consists of a 5 mm diameter molybdenum body, thermally isolated from its host tile, with an embedded type-K thermocouple positioned 5 mm from the plasma-facing end. Optimization of the design was performed by mechanical modeling with SOLID EDGE combined with thermal analysis using the ALGOR package. The plasma-facing surface of the tiles and embedded calorimeters are ramped at 2 degrees in the toroidal direction to eliminate plasma shadowing effects and to improve signal-to-noise by enhancing the local heat flux. Temperature readings taken before and after a plasma discharge allow energy deposition profiles to be inferred. The entire array is viewed by an IR imaging system (ElectroPhysics Titanium 550M Camera), allowing a cross-check between these two diagnostics. This paper will report on the diagnostic design and thermal analysis with data from C-Mod discharges.

*USDOE Coop. Agree. No. DE-FC02-99ER54512.

PP8 23 Interpretation and implementation of an ion sensitive probe (ISP) as a plasma potential diagnostic.* ROMAN OCHOUKOV, DENNIS WHYTE, BRUCE LIPSCHULTZ, BRIAN LABOMBARD, *PSFC MIT* An ISP is being developed as a robust diagnostic capable of measuring space potentials (Φ_P) in the boundary plasma of tokamaks. The ISP relies on the large difference between the ion and electron gyroradii ($\rho_i/\rho_e \sim 60$) to reduce electron collection at a collector which is oriented parallel to the magnetic field, and recessed behind the ISP shield a distance of $\sim \rho_i$. The shield is independently biased. By sweeping the collector voltage, while maintaining a constant voltage difference of a few volts between the shield and the collector (with $V_{WALL} < V_{COLLECTOR}$), we obtain only ion current. The ISP was studied in a magnetized plasma chamber (DIONISOS, B = 0.04 T, $n_e = 10^{16}$-10^{18} m^{-3}, ρ_e = 0.2 mm) at MIT. A model of the ISP potential shows that the collected ion current should reach zero for $V_{WALL} > \Phi_P$ and that space-charge effects are critical to the probe operation. The plasma potentials obtained from the ISP match well the plasma potentials measured with an emissive probe over a wide range of plasma conditions in DIONISOS, yet with a more robust physical design than the emissive probe.

*Supported by USDoE award DE-FC02-99ER54512.

PP8 24 Development of a novel in-situ accelerator-based surface diagnostic for Alcator C-Mod* ZACH HARTWIG, DENNIS WHYTE, *Massachusetts Institute of Technology* Boundary science in magnetic fusion devices is severely hindered by a dearth of in-situ diagnosis of the surfaces of Plasma Facing Components (PFC). The customary laboratory surface diagnostic, nuclear scattering using MeV-range ions, is being adapted to the Alcator C-Mod tokamak. The design features toroidally and poloidally resolved measurements of PFC surface element and isotope compositions on a shot-to-shot basis with 1 cm spatial resolution and sub-micron depth resolution. Several novel design features are described. An RF quadrupole accelerator supplies a high-current 0.93 MeV deuteron ion beam for injection into C-Mod between discharges. The ion beam is steered to a large fraction of the PFC surfaces by applying tokamak toroidal and poloidal fields. The deuterons have high Q, large nuclear-reaction cross-sections with most low-Z isotopes; the resulting high-energy gammas and neutrons are then detected for quantitative analysis of the surface compositions. Numerical modeling of these processes towards PFC measurements of interest are described, including boron film depth, deuterium fuel retention, isotope tracing for transport studies and PFC net erosion.

*Supported by USDoE award(s) DE-FC02-99ER54512.

PP8 25 A Study of Tungsten Migration in the Alcator C-mod Divertor using Particle Induced X-Ray Emission Analysis HAROLD BARNARD, *MIT* DENNIS WHYTE, BRUCE LIPSCHULTZ, FLORENT SAINCT, An ion beam analysis study of campaign integrated, poloidal Tungsten (W) migration patterns in the Alcator C-mod tokamak is presented. Eroded W from a toroidally continuous row of W tiles near the outer divertor strike point is used as a tracer to map W erosion and redeposition onto a set of Mo and W tiles that covered the poloidal extent of the C-Mod lower divertor which were removed following the 2008 experimental campaign. These tiles were examined for W using external (in air) particle induced X-ray emission (X-PIXE) analysis; a highly W sensitive ion beam analysis (IBA) technique in which a characteristic x-ray emission is induced from a material surface as it is exposed to an external proton beam, produced by a electrostatic tandem accelerator. With a set of systematic high spacial resolution measurements ($\sim 3mm$ resolution), complete poloidal profiles of W redeposition have been constructed. These profiles indicate W transport and redeposition of up to 1.5 $\times 10^{21} atoms/m^2$ ($\sim 14nm$ of equivalent W thickness) in several regions including the outer divertor, the inner divertor, and inside the private flux region. A comprehensive description and explanation of these results is presented.

PP8 26 Effect of plasma elongation on disruption runaway electrons* ROBERT GRANETZ, DENNIS WHYTE, *MIT Plasma Science and Fusion Center* VALERIE IZZO, *UCSD* Studies of runaway electron (RE) populations during disruptions on a number of different tokamaks have shown two distinctly different types of behavior: (a) some machines tend to observe RE's during a significant number of current quenches, and (b) some machines rarely observe RE's during the disruption current quench. Of those that do see runaways, a general trait is that they run circular or low elongation and/or limited discharges (FTU, Tore-Supra, TEXTOR, JT-60U), and conversely, those that don't see runaways tend to run elongated, diverted discharges (C-Mod, DIII-D, ASDEX-U). This suggests that elongation and/or vertical stability might play a role in RE confinement during disruptions. An experiment to test this hypothesis on Alcator C-Mod uses lower hybrid current drive to generate a strong RE population, and gas jet injection to trigger reproducible disruptions. Behavior of runaways during disruptions in both low elongation and high elongation equilibria are compared. Experimental findings will be presented and compared to NIMROD modeling predictions, and implications for ITER will be discussed.

*Supported by USDoE award DE-FC02-99ER54512.

PP8 27 Excitation of unstable TAEs and stable n=0 modes in Alcator C-Mod* J. SEARS, A. BADER, R.R. PARKER, *MIT PSFC* G.J. KRAMER, *PPPL* Toroidicity-induced Alfvén Eigenmodes (TAEs) are weakly damped MHD modes in tokamak plasmas. The modes occur at discrete frequencies near $\omega_{TAE} = v_A/2qR$, ($v_A = B/\sqrt{\mu_0 \rho}$) in a gap of the continuous spectrum of Alfvén waves. Unstable TAEs are excited by ICRF heating of at least 3.5 MW in Alcator C-Mod L-mode plasmas. These unstable modes have toroidal mode numbers in the range of $n = -6$ to $n = 6$. In contrast, stable resonant modes that are observed in these plasmas at similar and lower ICRF powers by the Active MHD diagnostic in the TAE frequency range commonly have toroidal mode numbers of $n = 0$, which precludes a TAE or EAE identity. The origin of these modes is explored with the NOVA-K code, and the destabilizing role of the energetic hydrogen tail as measured by the Neutral Particle Analyzer is presented.

*Supported by US DoE contract DE-FC02-99ER54512 and DE-AC02-09CH11466.

PP8 28 The emission spectrum of fast neutrals in Alcator C Mod and its use as a fast ion diagnostic* K.T. LIAO, W.L. ROWAN, I.O. BESPAMYATNOV, *Fusion Research Center, The University of Texas at Austin* A. BADER, R.S. GRANETZ, *MIT-PSFC* The emission spectrum of fast neutrals will be used to investigate the spatial distribution and temporal dynamics of fast ions in Alcator C-Mod. Fast hydrogen ions are formed by wave particle interaction between externally applied radio frequency (RF) fields and the plasma. These charge exchange with the neutrals in a diagnostic beam to form a population of fast neutrals. The newly formed fast neutrals emit a Doppler-shifted H_α spectrum which stands out against the wing of the broad ambient background spectrum of plasma D_α. Competing spectral features are emission from the cold D and H at the edge, the Doppler-shifted, beam emission spectrum, and various continuum emission processes. The unique contribution of this diagnostic is that it measures fast ions inside the plasma. The information derived from this and other fast ion diagnostics will be used to validate the physical models for RF deposition via minority ions.

*Supported by USDoE Awards DE-FG03-96ER54373 and DE-FC02-99-ER54512.

PP8 29 Measurements of Fast Ion Distribution in ICRF Heated Plasmas* A. BADER, J. SEARS, P. BONOLI, R. GRANETZ, R. PARKER, S. WUKITCH, *MIT - Plasma Science and Fusion Center* Alcator C-Mod uses ICRF for the bulk auxiliary heating and relies primarily on hydrogen minority heating scenarios. Measuring the resulting hydrogen ion distribution provides an opportunity to validate upgraded ICRF simulation capability that includes non-Maxwellian ions. The Compact Neutral Particle Analyzer (CNPA) is a diagnostic employed on Alcator C-Mod to measure this fast ion distribution function. The diagnos-

tic can measure the energy distribution of the fast ion tail, serving as a benchmark for simulation results and allowing for an assessment of the simulation algorithm and physics kernel. In this poster, we will present results from the detector in the most recent campaigns, including expanded capabilities in the 2009 campaign. We will discuss the calculation of the fast ion distribution from the measured CNPA distribution and the effective temperature.

*Work supported by USDoE award DE-FC02-99ER54512.

PP8 30 Experimental Studies of ICRF Mode Conversion with Phase Contrast Imaging and Comparison with Full-wave Simulations* N. TSUJII, M. PORKOLAB, E.M. EDLUND, L. LIN, Y. LIN, S.J. WUKITCH, P.T. BONLI, J.C. WRIGHT, *MIT Plasma Science and Fusion Center* E.F. JAEGER, *Oak Ridge National Laboratory* Mode conversion of fast wave to ion Bernstein wave and ion cyclotron wave has been observed with the phase contrast imaging diagnostic (PCI) in D(-^{3}He) plasmas in Alcator C-Mod [1, 2]. The wave electric fields are simulated for the experimentally measured equilibrium profiles using the full- wave codes TORIC [3] and AORSA [4]. Although the predictions of the two codes agree, the simulated PCI signals are larger than the measurements by at least a factor of 10. This could be partially explained by edge losses, which are not accounted for in the simulations, but is not fully understood. Predictions of direct rf flow drive for this scenario will also be presented. [1] E. Nelson-Melby, et al., Phys. Rev. Lett. 90, 155004 (2003). [2] Y. Lin, et al., Phys. Rev. Lett. 101, 235002 (2008). [3] M. Brambilla, Plasma Phys. Control, Fusion 41, 1 (1999). [4] E. F. Jaeger, et al., Phys. Plasmas 8, 1573 (2001).

*Supported by USDoE awards DE-FG02-94-ER54235 and DE-FC02-99-ER54512.

PP8 31 SOL reflectometer CORNWALL LAU, *MIT PSFC* GREG HANSON, *Oakridge National Laboratory* JOHN WILGEN, YIJUN LIN, STEVE WUKITCH, *MIT PSFC* Antenna-plasma interactions during RF heating and current drive are greatly influenced by the SOL density profile. A swept-frequency X-mode reflectometer is being built for Alcator C-Mod to measure the SOL density profiles at top, middle and bottom locations in front of both the new Lower Hybrid Launcher and the new ICRF antenna [1]. The system is planned to operate between 100 and 146 GHz at sweep rates from 10 μs to 1 ms per sweep and will cover a density range of approximately 10^{16} to 10^{20} m^{-3} at 5-5.4 T. Design, test data, and calibration results for the electronics and waveguide runs for both the ICRF and LH antenna will be shown. Preliminary plans for using the reflectometer density profile results to study antenna-plasma interactions such as RF loading and RF sheaths will be discussed. [1] Rev. Sci. Instrum. **79**, 10F114 (2008) This work is supported by U.S. DoE under awards DE-AC05-00OR22725 and DE-FC02-99ER54512.

PP8 32 ICRF Antenna Design Studies for Alcator C-Mod* M.L. GARRETT, S.J. WUKITCH, S. SHIRAIWA, O. MENEGHINI, Y. LIN, P. KOERT, W. BECK, *MIT PSFC* Two major challenges for ICRF utilization are reducing impurity generation and increasing reliability at high voltages. In Alcator C-Mod, we are designing a new 4-strap antenna where we seek to lower E-parallel and improve voltage handling. Simulations were conducted to analyze the effect of antenna orientation on the parallel electric field, which is thought to influence impurity production. ICRF antenna coupling was also simulated using both cold plasma and dielectric models. Previous experiments suggest that improved voltage handling may be obtained through the use of refractory metals compared with copper. A test stand has been designed and built to characterize ICRF relevant voltage breakdown as a function of: antenna material, neutral pressure, and magnetic field orientation. Results from simulations and experiments will be presented along with details of the new design.

*Work supported by USDoE award DE-FC02-99ER54512.

PP8 33 NSTX AND GENERAL SPHERICAL TORUS

PP8 34 NSTX Facility Highlight and Upgrade Plan* MASAAYUKI ONO, *PPPL, Princeton University* THE NSTX TEAM, The new NSTX facility additions included dual lithium (li) dropper to inject li powder directly into the plasma discharge complementing the dual li evaporators for between-shots li coverage of divertor region. Li evaporator together with EF/RWM feedback control enabled the record pulse length, stored energy, and confinement in NSTX. An edge sample probe allowing in-situ surface thermal desorption spectroscopy was introduced. The high harmonic fast wave heating system upgrade was implemented to double the power handling capability to support the current ramp-up and sustainment research. The Coaxial Helicity Injection (CHI) absorber coil was also introduced to form the field null to reduce the absorber arc. The CHI was able to increase the start-up plasma current by 100 kA above the ohmic induction. For the 2010 run, new upgrades are planned including a liquid-li divertor target to achieve lower collisionality and a Beam Emission Spectroscopy diagnostic to extend the localized ion gyro-radius scale turbulence measurements to complement the electron gyro-radius scale high-k scattering system. For the longer term, a new center stack and second NBI system are planned to access lower collisionality, full non-inductive operation, and current profile control.

*This work supported by DoE Contract DE-AC02-09CH11466.

PP8 35 Physics design of the NSTX Upgrade* JONATHAN MENARD, *PPPL* FOR THE NSTX RESEARCH TEAM, Access to low collisionality is important to more fully understand transport, stability, and non-inductive start-up and sustainment in the ST. For example, NSTX and MAST observe a strong (nearly inverse) scaling of normalized confinement with collisionality, and if this trend holds at low collisionality, high fusion neutron fluences could be achievable in very compact ST devices. Such considerations motivate the proposed upgrade of NSTX to higher field, current, and heating power. To enable engineering design of the upgrade, systematic free-boundary equilibrium calculations have been performed to determine the upgrade poloidal field requirements as a function of plasma shape, magnetic balance, internal inductance, and beta. Additional poloidal field coils in the divertor region are proposed to provide very high flux expansion for reduction of high predicted divertor heat flux. TRANSP simulations

indicate that more tangential neutral beam injection (NBI) can increase NBI current drive efficiency by up to a factor of two, enable control of the core q profile, and ramp-up the plasma current to near mega-ampere levels. These and other physics design activities will be discussed.

*This work supported by U.S. DOE Contract DE-AC02-09CH11466

PP8 36 Continuation of Lithium Aerosol Injection Experiments on NSTX* D.K. MANSFIELD, A.L. ROQUEMORE, H. KUGEL, *PPPL* R. MAINGI, *ORNL* J. IRBY, *MIT* Z. WANG, *LANL* PPPL TEAM, ORNL COLLABORATION, MIT COLLABORATION, LLNL COLLABORATION, During the 2008 run campaign, a Li powder dropper was installed on NSTX that successfully injected up to 35 mg/s of Li aerosol into the SOL. Initial improvements in the plasma performance from these initial experiments warranted the installation of a second Li dropper for the 2009 campaign. Design improvements in the dropper have resulted in accurate control of the flux of Li powder injected. The improved duel-dropper system has injected lithium fluxes of from 30 - 140 mg/s. At the highest flux, plasmas of 950 kA with 6 MW off NBI auxiliary heating have been successfully operated. This flux corresponds to 2.5 x106 - 5.8 x106 aerosol particles/s and is stoichiometrically equivalent 80 - 187 Torr L/s of D2. Operation of the Li dropper and the effects of the Li aerosol on the plasma performance will be discussed.

*Supported by DoE contract DE-AC02-09CH11466.

PP8 37 Modifications in divertor and scrape-off layer conditions with lithium coatings in NSTX V.A. SOUKHANOVSKII, *LLNL* H.W. KUGEL, R. KAITA, R.E. BELL, D.A. GATES, J.E. MENARD, D. MUELLER, B.P. LEBLANC, S.F. PAUL, A.L. ROQUEMORE, D.P. STOTLER, *PPPL* R. MAINGI, *ORNL* R. RAMAN, *U. Washington* A. YU. PIGAROV, R. SMIRNOV, *UCSD* Two lithium evaporators were used in NSTX to deposit lithium coatings on graphite plasma-facing tiles in the lower divertor, enabling neutral deuterium pumping and resulting in reduced recycling. This was evident from the reduction by 50% – 80% in D_α poloidal and divertor brightnesses, as well as the ion outfluxes, edge neutral pressure, core and divertor n_e. The two point and multi-fluid UEDGE code modeling suggested a shift of the outer divertor operating space toward the sheath-limited transport regime with lithium. Particle balance calculation showed that the deuteron inventory was well controlled and remained nearly constant in the long (1.2–1.4 s) ELM-free H-mode discharges with lithium coatings. However, n_e rose due to the increasing carbon inventory. The carbon source, estimated from C II and C III intensities and atomic S/XB factors, was reduced, suggesting that impurity accumulation was due to the improved particle confinement. Supported by the U.S. DOE under Contracts DE-AC52-07NA27344, DE-AC02-09CH11466, DE-AC05-00OR22725, DE-FG02-08ER54989, and W-7405-ENG-36.

PP8 38 Dependence of impurity accumulation on Ip and the outer gap in the presence of lithium deposition in NSTX* STEPHEN PAUL, M.G. BELL, S.P. GERHARDT, H.W. KUGEL, J. KALLMAN, R. KAITA, J.A. ROBINSON, *Princeton Plasma Physics Laboratory* NSTX TEAM, Shortly after commencing evaporation of a lithium coating onto the carbon surfaces of the lower divertor and other plasma-facing components in NSTX, a reduction in the frequency of ELMs was observed, eventually resulting in complete suppression for periods up to about 1s as deposition continued. Co-incident with ELM suppression, the effective ion charge increased as a result of a buildup in carbon, though lithium itself remained at a low level in the core. Radiated power steadily increased as medium-Z metallic impurities, notably iron, accumulated in the core of the plasma. This phenomenon may occur in these NBI-heated, deuterium H-mode plasmas because the lithium coating modifies the recycling of hydrogenic species, affecting the plasma's edge and scrape-off layer. Another possibility, the role of sputtering from metal surfaces by fast beam ions introduced by NBI heating, has been investigated by changing the amount of fast beam ion loss by varying the plasma current, neutral beam tangency radius and the gaps between the plasma boundary and surrounding components. Results from bolometry and XUV spectroscopy show that the plasma current affects accumulation of metals much more strongly than the gap between the plasma and the outer limiter.

*Supported by U.S. DOE contract DE-AC02-09CH11466.

PP8 39 Identification and time evolution of impurities in NSTX plasmas J.K. LEPSON, *SSL* P. BEIERSDORFER, *LLNL* M. BITTER, L. ROQUEMORE, G. ZIMMER, S. GERHARDT, J. KALLMAN, R. KAITA, *PPPL* Operation of the NSTX tokamak with lithium-coated plasma facing components has shown many beneficial changes, including MHD quiescence and higher electron temperatures near the edge. Impurity accumulation, however, is of concern, especially during ELM suppression. Spectroscopic diagnostics are important in determining the composition and concentration of plasma impurities, which can vary dramatically between shots and for different run conditions. We present data from the Livermore XEUS and LoWEUS spectrometers, which observe the extreme ultraviolet and soft x-ray regions on NSTX. XEUS and LoWEUS are complementary, and have been set up to cover the 10-250 A range during the most recent run period. Because of their higher spectral resolution than provided by SPRED, the instruments can discern lines from different elements and charge states. We have also implemented time resolved data acquisition, providing the first data on when the particular metal impurities appear in the plasma. The time resolution has been 130 ms. This value is expected to improve in the near future. We present spectra from NSTX exhibiting a wide range of impurities, including lithium, boron, carbon, oxygen, neon, titanium, iron, nickel, and copper, which serve as reference spectra for tracking the different impurities.

PP8 40 Time dependent chemical interactions of lithium, deuterium, and oxygen on lithium-coated graphite surfaces* C.N. TAYLOR, J.P. ALLAIN, B. HEIM, *Purdue University* C.H. SKINNER, H.W. KUGEL, R. KAITA, A.L. ROQUEMORE, *Princeton Plasma Physics Laboratory* PURDUE UNIVERSITY TEAM, PRINCETON PLASMA PHYSICS LABORATORY COLLABORATION, Lithium conditioning of plasma facing components has been used for particle control in fusion devices such as TFTR, CDX-U, FTU, T-11M, TJ-II and NSTX and has yielded improved plasma performance. A PMI probe has been installed on NSTX to provide an in-situ diagnostic for surface chemistry and deuterium retention measurements. Recent controlled laboratory experiments at Purdue University are investigating the chemical functionalities in lithiated graphite and the mechanism by which D is retained. XPS results show that Li reacts readily with residual oxygen in ATJ graphite, and immediately begins to intercalate into

the substrate. Additionally, it has been found that Li-O and Li-C react to D proportional to the lithium thickness, suggesting a D saturation threshold. This work investigates the transient nature of the lithium and oxygen functionalities, their response to time varying D flux, and the implications to NSTX.

*Work supported by USDOE Contract DE-FG02-08ER54990, DE-AC02-09CH11466.

PP8 41 Modeling of low-recycling divertor with lithium coating in NSTX R.D. SMIRNOV, A.YU. PIGAROV, S.I. KRASHENINNIKOV, *UCSD* C.H. SKINNER, D.P. STOTLER, R.E. BELL, H.W. KUGEL, *PPPL* V.A. SOUKHANOVSKII, T.D. ROGNLIEN, M.E. RENSINK, *LLNL* R. MAINGI, *ORNL* We have modeled D-Li-C edge-plasma transport with UEDGE code in support of lithium coating experiments on NSTX. The transition from the usual high-recycling regime (HRR) to low-recycling regimes (LRR) was simulated by varying hydrogen pumping by the Li coated divertor plates. The LRR modeling demonstrates the onset of sheath-limited divertor plasma conditions, flat parallel profile of electron temperature in SOL, and plate thermal loading dominated by parallel heat conduction. The results also show that Li impurities (mainly originating from the coated divertor plates) are well retained in the divertor volume. The modeled core contamination level for Li+3 ions is 0.1% that is consistent with recent experimental NSTX data. At the same time, the simulated and experimental levels of wall-originated C+6 (modeled with anomalous inward pinch in core) can be as high as $\sim$ 10% (maximal Zeff$\sim$ 4). High surface temperatures ($>$ 800K) are predicted to result in a divertor transition from LRR to HRR due to excessive evaporation and recycling of Li. The work is supported by DoE Grant DE-FG02-08ER54989 (UCSD) and Contracts DE-AC02-09CH11466 (PPPL), DE-AC52-07NA27344 (LLNL), DE-AC05-00OR22725 (ORNL).

PP8 42 Modeling of Balmer series deuterium spectra with the Cretin code for diagnosing the inner divertor re-attachment threshold in NSTX discharges with lithium coatings* F. SCOTTI, *Princeton University* V.A. SOUKHANOVSKII, H.A. SCOTT, *LLNL* Application of evaporated lithium coatings on graphite divertor tiles in NSTX led to a reduction of divertor recycling. The inner divertor electron density and recombination rate were also drastically reduced, suggesting that the normally detached inner divertor re-attached in many lithium-assisted ELM-free H-mode discharges. This observation was based on the divertor brightness profiles of Stark-broadened ultraviolet spectral lines from the Balmer series $n = 2 - 7 \ldots 12$ transitions. To understand the divertor transport regimes with reduced recycling and the density thresholds for both the inner divertor detachment and X-point MARFE formation, we are developing a simulation of the NSTX divertor spectra in a realistic viewing geometry using the Cretin code. The non-local thermodynamic equilibrium radiation transport code Cretin uses a 1-D plasma model with neutral diffusion and line shape calculations based on the quasi-static ion microfield approximation and a binary electron impact collision model.

*Supported by the U.S. DOE under Contracts DE-AC52-07NA27344 and DE-AC02-09CH11466.

PP8 43 Study of Thermo-electrically Driven Scrape-Off-Layer Current (SOLC) in NSTX Tokamak* HIRO TAKAHASHI, ERIC FREDRICKSON, JOSH KALLMAN, STEFAN GERHARDT, ROBERT KAITA, DENNIS MANSFIELD, STUART ZWEBEN, *Princeton Plasma Physics Laboratory* RAJESH MAINGI, *Oak Ridge National Laboratory* SOLC flow in ELMing discharges in NSTX has been found qualitatively similar to that in DIII-D [1], with steady small amplitude during a quiescent period leading to a rapid change to much larger values, abruptly beginning just before ELM onset (as detected by D-alpha signal). Current density (spatially averaged normal to divertor plate) in NSTX is comparable to that in DIII-D during the main ELM event, but is much smaller during the quiescent period. The possible thermoelectric origin of the current in the quiescent period will be investigated using flush-mounted Langmuir probes and halo current sensors to see whether observed SOLC distributions can be quantitatively related to sheath parameters at divertor plates. Effect on SOLC of Lithium coating of plasma facing surfaces will also be examined. [1] H. Takahashi, et al., Paper TP6.00033, 50^{th} Ann. Mtg. of APS-DPP, Dallas, TX, Nov., '08.

*Supported by the US DOE under DE-AC02-09CH11466.

PP8 44 Status of National Spherical Torus Experiment Liquid Lithium Divertor* H.W. KUGEL, M. VIOLA, R. ELLIS, M. BELL, S. GERHARDT, R. KAITA, J. KALLMAN, R. MAJESKI, D. MANSFIELD, A.L. ROQUEMORE, H. SCHNEIDER, J. TIMBERLAKE, L. ZAKHAROV, *PPPL* R.E. NYGREN, *SNL* J.P. ALLAIN, *Purdue University* R. MAINGI, *ORNL* V. SOUKHANOVSKII, *LLNL* Recent NSTX high power divertor experiments have shown significant and recurring benefits of solid lithium coatings on plasma facing components to the performance of divertor plasmas in both L- and H- mode confinement regimes heated by high-power neutral beams. The next step in this work is the 2009 installation of a Liquid Lithium Divertor (LLD). The 20 cm wide LLD located on the lower outer divertor, consists of four, 80 degree sections; each section is separated by a row of graphite diagnostic tiles. The temperature controlled LLD structure consists of a 0.01cm layer of vacuum flame-sprayed, 50 percent porous molybdenum, on top of 0.02 cm, 316-SS brazed to a 1.9 cm Cu base. The physics design of the LLD encompasses the desired plasma requirements, the experimental capabilities and conditions, power handling, radial location, pumping capability, operating temperature, lithium filling, MHD forces, and diagnostics for control and characterization.

*Work supported by USDOE Contract DE-AC02-09CH11466.

PP8 45 Development of Operational Scenarios and Edge Diagnostics for the NSTX Liquid Lithium Divertor* J. KALLMAN, R. KAITA, H. KUGEL, E. KOLEMEN, *PPPL* M.A. JAWORSKI, *UIUC* J.W. AHN, D. GATES, S. GERHARDT, *PPPL* R. MAINGI, *ORNL* J. ROBINSON, A.L. ROQUEMORE, *PPPL* V. SOUKHANOVSKII, *LLNL* During the 2010 run campaign, NSTX will continue to investigate the effects of lithium-coated plasma facing components utilizing a Liquid Lithium Divertor (LLD), to be installed at the end of 2009 run operations. In order to balance the pumping capabilities of the LLD (located on the outboard divertor) with the performance benefits of high triangularity discharges (typically with the strike points on the inner divertor), a new intermediate triangularity discharge was developed. Operational LLD-ready scenarios utilizing this shape and new strike point control algorithms were successfully developed. Neu-

tral beam power and current scans were conducted to characterize density and temperature profiles as well as radiated power due to impurities. In addition, new diagnostics will be necessary to better assess the effect of the LLD on edge plasma parameters, key among these is a high density Langmuir probe array for measurements of plasma density and temperature in the vicinity of the LLD.

*Supported by the US DOE under DE-AC02-09CH11466, DE-AC52-07NA27344.

PP8 46 Diagnostics for Evaluating Performance of NSTX Liquid Lihium Divertor* R. KAITA, H. KUGEL, J. KALLMAN, B. LEBLANC, S. PAUL, A.L. ROQUEMORE, C. SKINNER, *PPPL* V. SOUKHANOVSKII, *LLNL* R. MAINGI, J.-W. AHN, J. WILGEN, *ORNL* J.-P. ALLAIN, C. TAYLOR, *Purdue U.* A Liquid Lithium Divertor (LLD) is being installed on NSTX to investigate particle control and power handling with liquid lithium as plasma-facing component (PFC). The LLD is expected to provide a low-recycling plasma-facing component (PFC). To study the effects of such a PFC on plasma performance, a variety of edge measurements are required. Since its surface is highly reflective at visible wavelengths, a Lyman-alpha detector array will be used to monitor the recycling. To understand changes in edge transport, electron temperature and density measurements will be made with Langmuir probes mounted in PFC's near the LLD, and the edge sightlines of a multipoint Thomson scattering system. A frequency-scanning reflectometer will also provide scrapeoff layer electron density profiles. The LLD response to heat loads will be examined with infrared cameras and thermocouples. Diagnostics are also needed to measure the erosion and codeposition of lithium. They include quartz deposition monitors and a retractable probe for exposing samples to the plasma.

*Supported by DOE Contracts DE-AC02-09CH11466, DE-AC52-07NA27344, and DE-AC05-00OR22725.

PP8 47 Characteristics of energy transport of Li- and non-Li-conditioned plasmas in NSTX SIYE DING, *Chinese Academy of Sciences, Inst. of Plasma Physics, Hefei, China* STANLEY KAYE, RON BELL, ROBERT KAITA, HENRY KUGEL, BENOIT LEBLANC, STEPHEN PAUL, *PPPL, Princeton University, Princeton, NJ* BAONIAN WAN, *Chinese Academy of Sciences, Inst. of Plasma Physics* The transport properties of NSTX plasmas obtained during the 2008 experimental campaign have been studied and are reported here. Transport trends and dependences have been isolated, and it is found that both electron and ion energy transport coefficients have strong dependences on local values of n*grad T, which in turn is strongly dependent on local current density profile. Without identifying this dependence, it is difficult to identify others, such as the dependence of transport coefficients on poloidal magnetic field (or q), plasma current and heating power. In addition, a comparison between discharges with and without Lithium wall conditioning has been made. While the trends in the two sets of data are similar, the thermal transport loss, especially in the electron channel, is found to strongly depend on the amount of Lithium deposited, decreasing by up to 50% of its no-Lithium value.

PP8 48 Investigation of Power Balance and Excess Ion Heating in the National Spherical Torus Experiment P.W. ROSS, R.E. BELL, D.A. GATES, S.M. KAYE, B.P. LEBLANC, S.S. MEDLEY, R.B. WHITE, *PPPL* NSTX TEAM, Neutral Beam modulations were used to create a transient heat pulse to investigate power balance of thermal ions in NSTX discharges. The primary effect of the beam modulation is a change in the ion temperature, with very little electron response. Classical neutral beam heating is expected to preferentially heat electrons with only $\sim$ 1/3 of the power going to the ions. Grad-Shafranov reconstructions of the plasma were performed using Thomson scattering, CHERS and MSE to measure the plasma temperature profiles and constrain the current profile. The ion power balance was calculated using the TRANSP time dependent transport calculation code. Assuming ion neoclassical transport, TRANSP calculates excess ion heating for some plasma conditions. This heating is strongest in the presence of high frequency MHD modes. The predicted peak of these modes correlates well with the location of strongest heating. Full orbit calculations of thermal ions in the presence of these modes show that stochastic heating can be sufficient to explain the excess heating. This work was supported by DoE contract No. DE-AC02-09CH11466.

PP8 49 Gyrokinetic studies of neoclassical poloidal rotation with finite orbits. R.A. KOLESNIKOV, W.X. WANG, *PPPL* F.L. HINTON, *UCSD* R.E. BELL, S.M. KAYE, W.M. TANG, W.W. LEE, *PPPL* A significant discrepancy of impurity poloidal rotation from local theoretical predictions is found in tokamak experiments. The amplitude of carbon poloidal velocity is observed to be smaller in NSTX [1] and larger in DIIID [2] and JET [3] devices compared to appropriate neoclassical estimates. We performed global neoclassical simulations of toroidal plasmas using GTC-NEO particle-in-cell delta-f code [4] with a new multiple ion-species capability. In case of large-aspect ratio tokamak with sharp toroidal flow profile, the difference between simulated carbon poloidal flow and neoclassical estimate is found to be due to presence of finite ion orbits. The dominant mechanisms underlying this nonlocal effect are identified to be due to ion orbit shearing and orbit squeezing. Such finite orbit mechanisms result in generation of additional parallel ion flow due to shear in the toroidal rotation and shear in the radial electric field accordingly. We also compare simulations as well as theoretical estimates based on identified nonlocal effects with some experimental data from NSTX as well as other magnetic configurations to clarify the role the nonlocal effects might have on observed poloidal velocity. [1] R.E. Bell, this meeting. [2] W. Solomon, Physics of Plasmas 13, 056116 (2006). [3] K. Crombe, EPS, Sopfia (2009). [4] W.X. Wang, Physics of Plasmas 13, 082501 (2006).

PP8 50 Sensitivity of Tearing Mode Beta Limits to Rotation and Current Profile* R.J. BUTTERY, C.D. CHALLIS, *EURATOM/UKAEA Fusion Assoc.* R.J. LA HAYE, *GA* S.P. GERHARDT, *PPPL* DIII-D TEAM, JET TEAM, NSTX TEAM, Unless carefully controlled, 2/1 tearing modes are likely to limit the β of tokamak plasmas with $q = 2$ surfaces. Mode onset may depend on changes to intrinsic tearing stability (Δ') and external triggers. Studies have probed this underlying physics by perturbing plasma rotation and current profiles to determine how these mechanisms apply. On NSTX, $n = 1$ and $n = 3$ braking have been deployed to change rotation profiles at mode onset, and gauge whether action is through rotation shear and so intrinsic island stability, or differential rotation with respect to external triggers. This also provided key measurements of error field tolerability. On DIII-D saturated mode sizes also show a response to rotation changes. On

JET the role of intrinsic stability was directly tested in hybrid plasmas, with changes to q profile leading to significant differences in 2/1 β_N limit, identifying optimal conditions for stability. Results to be reported show a significant role of intrinsic tearing stability governing mode onset.

*Work by EURATOM, UK EPSRC, and the US DOE under DE-FC02-04ER54698 and DE-AC02-09CH11466.

PP8 51 Study of Error Field Physics in Tokamaks and Implications for ITER JONG-KYU PARK, JONATHAN MENARD, STEFAN GERHARDT, *Princeton Plasma Physics Laboratory* ALLEN BOOZER, STEVE SABBAGH, *Columbia University* MICHAEL SCHAFFER, *General Atomics* STEPHEN WOLFE, *Massachusetts Institute of Technology* Tokamaks are sensitive to a small nonaxisymmetric field. Nonaxisymmetric error fields in tokamaks can cause a disruption by plasma locking, or degrade confinement by Neoclassical Toroidal Viscosity (NTV). Hence, the correction of error field is important to improve plasma performance. Recent NSTX experiments showed that the critical n=1 error field to cause a locking is much smaller at high beta than expected from the standard scaling at low beta, and also that the correction of n=3 field is essential to sustain high toroidal rotation. Both results indicate the importance of error field correction, not only for resonant n=1 field at low beta, but also at high beta and for nonresonant fields. This enlarged parametric space in error field physics requires a deeper understanding of the plasma response. Many useful insights on plasma response effects can be obtained using the Ideal Perturbed Equilibrium Code (IPEC) coupled with NTV theory. IPEC and NTV calculations for the recent NSTX results will be combined with the multi-machine locking scaling at low beta, in order to improve the predictability of error field thresholds and correction in ITER. This work was supported by US DOE Contract # DE-AC02-09CH11466.

PP8 52 Effect of Impurities and Wall Conditioning on the Onset of NTMs in NSTX* F. VOLPE, *U. Wisc.* S. GERHARDT, *PPPL* S. SABBAGH, *Columbia* R. BELL, J. ROBINSON, *PPPL* L. DELGADO-APARICIO, *John Hopkins U.* Neoclassical Tearing Mode (NTM) stability was examined in the NSTX spherical torus as a function of wall conditioning by Lithium evaporation in between discharges and/or of deliberate Neon puffing during the discharge. Lithiumization was found to postpone the appearance of an NTM of toroidal number n=1, whereas Neon puffing had the opposite effect. The effect of error field correction and magnetic feedback on the NTM onset was comparatively small. It has to be noted that Lithium evaporation leads to a hotter plasma edge and to an overall increase of Carbon in the plasma. Both effects modify the global evolution of the discharge. The perturbation associated with Neon, instead, was more localized: USXR, SPRED and charge exchange recombination measurements confirm that Neon reached the mode location and resulted in increased radiation from the island. Possible interpretations of these results in terms of the Modified Rutherford Equation and NTM triggers will be discussed.

*Work supported in part by the US DOE under DE-ACO2-09CH11466.

PP8 53 SXR measurements of Resistive Wall Mode behavior in NSTX LUIS F. DELGADO-APARICIO, K. TRITZ, *The Johns Hopkins University* M. FINKENTHAL, D. STUTMAN, *The Johns Hopkins University* S.A. SABBAGH, J. BERKERY, *Columbia University* S. GERHARDT, R. BELL, B. LEBLANC, J. MANICKAM, J. MENARD, L. ROQUEMORE, *Princeton Plasma Physics Laboratory* A multi-energy soft X-ray (ME-SXR) array has been used for the determination of time and space-resolved emissivity profiles during stabilized resistive wall mode (RWM) experiments in NSTX. The main purpose of this study is to distinguish whether the changes on the plasma response (T_e, n_e, n_Z) correspond to the observation of a stabilized RWM or to the effect of the Resonant Field Amplification (RFA). Kinetic measurements of the RFA due to stable RWMs were tested using a single frequency $n = 1$ traveling waveform in which the peak-to-peak amplitude was changed by an order of magnitude; neon injection was used to increase the signal-to-noise ratio of the ME-SXR diagnostic. The effect of the RFA on the kinetic profiles was observed and correlated with a suite of diagnostics including that of a toroidally displaced SXR array for $n = 1$ RWM identification. This work was supported by the US DoE grant No. DE-FG02-99ER5452 at JHU and DoE-PPPL Contract No. DE-AC02-09CH11466.

PP8 54 Prototype high resolution multi-energy soft X-ray array for NSTX* K. TRITZ, D. STUTMAN, L. DELGADO-APARICIO, M. FINKENTHAL, *Johns Hopkins University* R. KAITA, L. ROQUEMORE, *PPPL* Our previous work has shown the utility of multi-energy filtered SXR data for the fast measurement of electron temperature and impurity profiles in NSTX. A novel diagnostic design with an improved spatial resolution of < 1cm and an increased set of multi-energy SXR profiles allows continuous, fast (1-10kHz) measurements of both T_e and impurity profiles ranging from the plasma core into the steep gradient region of the pedestal. With this, 4-6 filtered SXR profiles as well as an unfiltered bolometric profile will extend the temperature measurement to lower T_e. A single energy prototype system has been implemented on NSTX which is comprised of a filtered X-ray pinhole camera which converts the X-rays to visible light using a CsI:Tl phosphor. The phosphor is mounted on an image intensifier coupled to a high-speed CMOS camera using a fiber optic image bundle. Low noise SXR profiles have been measured in high beta H-mode plasmas at frame rates up to 10kHz. Comparisons to the existing, toroidally displaced tangential multi-energy SXR array will be also presented, aimed at measurements of non-axisymmetric perturbations.

*Supported by DoE Grant DE-FG02-99ER54523 and DE-AC02-09CH11466.

PP8 55 Fast Ion Loss and Search for Current Redistribution due to Energetic Particle Mode Bursts in NSTX* DOUGLASS DARROW, E. FREDRICKSON, *PPPL* N. CROCKER, *UCLA* N. GORELENKOV, *PPPL* M. PODESTA, *UC Irvine* J. KIM, *POSTECH* S. KUBOTA, *UCLA* K.C. LEE, *UC Davis* S. MEDLEY, *PPPL* K. TRITZ, *Johns Hopkins* H. YUH, *Nova Photonics* Bursts of MHD modes driven by neutral beam ions, termed Energetic Particle Modes (EPMs) are frequently observed in NSTX plasmas. These bursts typically comprise multiple n number modes in the 20-100 kHz frequency range and are believed to be beta induced Alfvén acoustic eigenmodes (BAAEs). The bursts produce sizable drops in the neutron rate, up to 36% in a 100 μs

interval in one instance. A simultaneous loss of beam ions over a wide range of pitch angles is often seen. Details of beam ion diagnostic results will be presented. An effort has also been made to determine whether these modes alter the current profile of the discharge. Initial results indicate some changes in MSE pitch angle profiles concurrent with the bursts. However, these are comparable to changes seen with other types of MHD activity and with the general level of fluctuations seen in virtually every NSTX discharge. Consequently, it is inferred that any effect these bursts have on the current profile is no greater than that created by other frequently occurring phenomena.

*Work supported by US DoE contract DE-AC02-09CH11466.

PP8 56 Fishbone-induced fast-ion transport in NSTX* N.A. CROCKER, *UCLA* D. LIU, *UCI* E.D. FREDRICKSON, *PPPL* E. RUSKOV, *UCI* S.S. MEDLEY, *PPPL* W.W. HEIDBRINK, *UCI* G.J. KRAMER, N.N. GORELENKOV, R.B. WHITE, B.P. LEBLANC, R.E. BELL, *PPPL* F.M. LEVINTON, *Nova Photonics* S. KUBOTA, *UCLA* NSTX TEAM, Fast-ions from neutral beams excite bursts of large amplitude ($\delta n/n \sim 1\%$) fishbones – low f ($\sim$ 25 kHz) global modes – in NSTX. The bursts correlate with significant fast-ion loss, indicated by large ($> \sim 10\%$) drops in neutron flux. The role of fishbones in the loss is probed via theoretical tools, measurement and modeling. The radial structure of the fishbone density perturbation – measured with 5 fixed-frequency reflectometers – has been compared to the modeled reflectometer response to eigenmodes found by the NOVA-K ideal stability code. Ideally unstable internal kinks, expected to have structure similar to fishbones, were considered. The best match will be used with the ORBIT guiding-center code to estimate fast-ion redistribution and loss using an intial distribution from the TRANSP Monte Carlo beam deposition code. The perturbation to the population will be compared with measured changes in the flux and spectrum of energetic neutrals via modeling.

*Supported by USDOE Contracts DE-FG03-99ER54527 and DE-AC02-09CH11466.

PP8 57 Experimental studies of TAE dynamics and induced fast ion losses on NSTX* M. PODESTA, W.W. HEIDBRINK, D. LIU, E. RUSKOV, *(UCI)* R.E. BELL, D.S. DARROW, E.D. FREDRICKSON, N.N. GORELENKOV, B.P. LEBLANC, *(PPPL)* N.A. CROCKER, S. KUBOTA, *(UCLA)* The dynamics of toroidicity-induced Alfvén eigenmodes (TAEs) is studied in neutral beam heated NSTX plasmas. The results from similar discharges conducted in helium and deuterium plasmas are compared. Emphasis is put on investigating the transition of the modes from a quasi-stationary behavior into a phase characterized by frequency chirps and amplitude bursts as the injected neutral beam power is increased. The fast ion transport associated with bursting TAE activity is measured through Fast Ion D-Alpha spectroscopic diagnostics, neutral particle analyzers, neutron rate measurements and a fast ion loss probe. In particular, drops of the fast ion profile and neutron rate on time scales of $\sim$ 1ms are observed during so called *TAE avalanches,* i.e. large bursting events accompanied by a frequency down-chirp which involve multiple TAEs.

*Work supported by US DOE contracts DE-AC02-09CH11466, DE-FG02-06ER54867, DE-FG02-99ER54527

PP8 58 Simulation of Ion loss during TAE avalanches in NSTX* E.D. FREDRICKSON, D. DARROW, G. KRAMER, N.N. GORELENKOV, S.S. MEDLEY, B. LEBLANC, R.E. BELL, R.B. WHITE, *PPPL, Princeton, NJ* M. PODESTA, N.A. CROCKER, S. KUBOTA, *UC Irvine, CA* F.M. LEVINTON, H. YUH, *Nova Photonics, Princeton, NJ* Non-linear interactions of multiple Toroidal Alfvén Eigenmodes (TAE) can result in explosive mode growth and enhanced losses of fast ions in a repetitive cycle of TAE bursts called avalanches. Fast ion losses have been documented with NPA diagnostics and fast neutron measurements during strongly bursting TAE on NSTX. The mode structure and mode amplitudes are measured with arrays of reflectometers and Mirnov coils. These experimental data are used to identify and scale the amplitude and frequency evolution of Toroidal Alfvén Eigenmodes simulated with the NOVA code. These scaled eigenmodes are then used in the ORBIT code to simulate the fast ion redistribution during a strong, 1ms, TAE burst. Fast ion redistribution is seen for the energies $>$ 30 keV, consistent with experimental observations. The simulated level of fast ion losses are in good agreement with the observed losses.

*Work supported by U.S. DOE Contract DE-AC02-09CH11466, DE-FG03-99ER54527, DE-FG02-06ER54867, and DE-FG02-99ER54527.

PP8 59 Observation of "Anomalous" Energetic Ion Spectra by the E||B Neutral Particle Analyzer on NSTX* S.S. MEDLEY, R.E. BELL, D.S. DARROW, E.D. FREDRICKSON, N.N. GORELENKOV, B.P. LEBLANC, A.L. ROQUEMORE, *PPPL, Princeton, NJ* M. PODESTA, *UC Irvine, CA* AND THE NSTX TEAM, An "anomalous" increase in E||B NPA charge exchange neutral flux ($\sim$ 4x) localized at the neutral beam (NB) injection full energy, E_b = 90 keV, is observed in NSTX. This so-called "High-Energy Feature (HEF)" appears in discharges only when kink-type modes ($f <$ 10 kHz) are absent, TAE activity ($f \sim$ 10-150 kHz) is weak ($\delta B_{rms} <$ 75 mGauss) and CAE activity ($f \sim$ 400 – 1200 kHz) is robust. The HEF exhibits a growth time of $\sim$ 20-80 ms and develops a slowing down distribution that evolves over 100-400 ms, a time scale long compared with the $\sim$ 50 ms equilibration time of the NB injected particles. Increases of $\sim$ 10-30% in the measured neutron yield and total stored energy are observed to coincide with the HEF along with broadening of the CHERS $T_i(r)$ profile. The HEF is observed only in H-mode (not L-mode) discharges with injected NB power above 4 MW and is suppressed by vessel conditioning using lithium deposition at rates $\sim$ 100 mg/shot sufficient to suppress ELM activity. Though a definitive mechanism has yet to be develop, the HEF appears to be driven by a form of CAE resonance.

*Work supported by U.S. DOE Contract DE-AC02-09CH11466.

PP8 60 Comparison of Fast-ion D-alpha Measurements with Theory in MHD-quiescent Plasmas* E. RUSKOV, W.W. HEIDBRINK, M. PODESTA, *University of California, Irvine* The NSTX fast-ion D-alpha (FIDA) diagnostic measures the Doppler-shifted charge-exchange recombination light from energetic ions that neutralize in a heating beam. The present instrument views the beam nearly vertically. In a spherical tokamak (ST), the large fast-ion gyroradius is expected to cause an asymmetry between the intensity of blue-shifted and red-shifted light. In addition, for near-tangential injection, the large field-line pitch associated with the large poloidal field in an ST should also produce spectral asymmetries. In a dedicated experiment designed to test these predic-

tions, toroidal field and plasma current scans were performed in low-power neutral-beam heated discharges that had little detectable fast-ion driven instabilities or MHD. The TRANSP NUBEAM module calculates the fast-ion distribution function f, which is then used in a FIDA simulation code to predict the spectra. In preliminary analysis, large discrepancies between predicted and experimental spectra are observed.

*Supported by the U.S. Department of Energy.

PP8 61 Anomalous electron transport induced by multiple beam ion driven global Alfven instabilities* NIKOLAI GORELENKOV, *PPPL, Princeton University* ALLEN BOOZER, *Columbia University* DAN STUTMAN, *Johns Hopkins University* ERIC FREDRICKSON, *PPPL, Princeton University* KEVIN TRITZ, *Johns Hopkins University* ROSCOE WHITE, *PPPL, Princeton University* We investigate theoretically the electron thermal transport induced by multiple Global Alfvén Eigenmodes (GAE) in a toroidal plasma recently reported in NSTX when strong $P_{NBI} = 6MW$ NBI heating was applied. A strong GAE activity correlates with such transport. The stochastization of electron longitudinal motion in the presence of the multiple oscillations is responsible for the electron transport. Application of the guiding center code, ORBIT, shows that the required level of the electron heat conductivity, $\chi_e \geqslant 10m^2/sec$ can be achieved in simulations with $\sim$ 20 intermittently unstable GAEs with the local density perturbation amplitudes on the order of $\delta n_e/n_e = 10^{-3}$. Our simulations address the requirements for GAE structure, amplitudes and the number of modes to achieve the electron heat diffusivity inferred from experiments. Results from the comparisons of the theory and recent NSTX experiments will be presented. The above anomalous electron transport potentially can have significant implications for fusion devices.

*This work supported by DoE contract No. DE-AC02-09CH11466.

PP8 62 High-k scattering of low frequency MHD activities in NSTX K.L. WONG, E. MAZZUCATO, *Princeton Plasma Physics Laboratory* D.R. SMITH, *The University of Wisconsin* K. TRITZ, *The Johns Hopkins University* S. KAYE, *Princeton Plasma Physics Laboratory* Low frequency MHD modes in tokamaks usually have long wavelengths outside the detection range of high-k scattering diagnostics. However, data from the NSTX high-k scattering system exhibit many narrow low frequency (10-100 kHz) peaks associated with various low frequency MHD activities, from fishbones to Alfvén eigenmodes. These MHD modes are basically shear Alfvén waves, they can convert into short wavelength kinetic Alfvén waves near Alfvén resonance and thus become detectable by high-k scattering. Such observation was first reported in TFTR.[1] Since the NSTX scattering system mainly detects the radial component of **k**, it can see more detailed features of these mode-converted kinetic Alfvén waves. Corroborating data from soft X-ray camera, Mirnov coils and detailed analysis of these data will be presented.

[1]K.L. Wong et al., Phys. Lett. A **224** (1996) 99.

PP8 63 Modeling polarization of propagating millimeter-waves in NSTX* J. ZHANG, T. CARTER, N.A. CROCKER, W.A. PEEBLES, S. KUBOTA, *UCLA* Magnetized plasma has an anisotropic index of refraction. For propagation perpendicular to the magnetic field, this leads to polarization elliptization via the Cotton-Mouton effect. In contrast, for propagation parallel to the field, the axis of the polarization ellipse rotates: this is known as Faraday rotation. In fusion plasmas millimeter-waves typically experience a combination of these two effects. To date, little attention has been given to the evolution of polarization for radial propagation in a spherical tokamak where a much greater variation of magnetic pitch angle and field strength exists in comparison to conventional tokamaks. This work investigates the polarization modification of millimeter-waves propagating radially in the National Spherical Torus eXperiment. Typical NSTX density and magnetic field profiles are utilized. The calculations provide the basis for optimization of the performance of a planned radial chord polarimeter. Future analysis will assess the sensitivity of polarization modifications to magnetic perturbations such as Alfven eigenmodes and tearing modes.

*Supported by US DOE Contracts DE-FG03-99ER54527 and DE-AC02-09CH11466.

PP8 64 Full-Wave Codes Applied to Reflectometry Measurements of Core-Edge Turbulence in NSTX* S. KUBOTA, W.A. PEEBLES, N.A. CROCKER, *UCLA* B.C. ROSE, *Purdue U.* S.J. ZWEBEN, T.S. HAHM, *PPPL* The interpretation of turbulence properties from reflectometry measurements is often not straightforward and requires full-wave simulations using modeled turbulence and a detailed knowledge of the equilibrium profiles. On NSTX, the unique combination of reflectometry hardware (FM-CW, fixed- frequency, and correlation reflectometers) is well-suited to turbulence measurements in both core and edge plasmas. Here we report on the simulation work required to generate quantitative estimates of turbulence properties (such as turbulence levels, wavenumber spectra, decorrelation times, correlation lengths, flow velocities) from these measurements. We focus on the core-edge region near the L-H transition, where the evolution of the turbulence and density profile characteristics are related to the edge transport barrier formation. Simulations will use the UCLA 1-D and 2-D FDTD full-wave codes. Recently these codes were upgraded to utilize the parallel processing capabilities of the NVIDIA C870 GPU card.

*Supported by U.S. DoE Grant DE-FG03-99-ER54527 and the U.S. DoE National Undergraduate Fusion Fellowship.

PP8 65 Global Gyrokinetic Electron Temperature Gradient Turbulence and Transport in NSTX Plasmas. S. ETHIER, W.X. WANG, *PPPL* F. POLI, *U. of Warwick* T.S. HAHM, S.M. KAYE, W.W. LEE, E. MAZZUCATO, G. REWOLDT, W.M. TANG, *PPPL* Global, nonlinear simulations of electron temperature gradient (ETG) turbulence for experimental discharges have been carried out for the first time for direct validation against high-k scattering measurements of electron gyroradius scale fluctuations in NSTX. Qualitative agreement in the density fluctuation spectra and overall density fluctuation levels between the experiment and the simulation is obtained. The nonlinear generation of zonal flows with fine radial scale is observed during ETG turbulence development although they are too weak to break up the radially-elongated streamers during the nonlinear phase of ETG turbulence, leading to anisotropic fluctuations in the perpendicular wave number space. Comparison of density fluctuation amplitudes based on synthetic diagnosis between simulations and measurements are discussed. Also reported are sensitivity studies of simulated ETG-driven electron thermal transport with respect to the local profiles

of electron temperature gradient, effective charge number Zeff, and safety factor, which are subject to significant experimental errors. Work supported by U.S. DOE Contract DE-AC02-09CH11466 and the SciDAC GPS-TTBP project. F. Poli is funded by UK EPSRC.

PP8 66 Nonlinear Gyrokinetic Turbulence Simulations of the NSTX Spherical Torus J.L. PETERSON, G.W. HAMMETT, D. MIKKELSEN, S. KAYE, *Princeton Plasma Physics Laboratory* J. CANDY, R.E. WALTZ, *General Atomics* Recent progress in the numerical simulation of plasma turbulence has led to a greater understanding of the mechanisms behind anomalous heat and particle losses in tokamaks. However, the source of turbulent transport in machines with smaller aspect ratios, such as the National Spherical Torus Experiment (NSTX), remains elusive. Leading contenders for explaining transport in spherical tori include turbulence driven by the Electron Temperature Gradient (ETG) mode and microtearing modes. We present here nonlinear GYRO[1] simulations of microturbulence in a variety of NSTX discharges and make comparisons between numerically simulated and experimentally measured levels of electron-scale turbulence.

[1]J. Candy, R. E. Waltz et al., J. Phys. Conf. Ser. **78**, 012008 (2007).

PP8 67 Study of boundary diffusion via density fluctuation measurement using the FIReTIP system on NSTX* K.C. LEE, C.W. DOMIER, M. JOHNSON, W.-C. TSAI, N.C. LUHMANN, JR., *UC Davis* H. PARK, *POSTECH* B.P. LEBLANC, R.E. BELL, R. KAITA, *PPPL* S.A. SABBAGH, *Columbia University* The Far Infra Red Tangential Interferometry/Polarimetry (FIReTIP) system on the National Spherical Torus Experiment (NSTX) measured boundary density fluctuations with upgraded time resolution up to 3.3 MHz in 2009. The density fluctuation level compared with the energy confinement from EFIT showed agreement with the turbulence induced diffusion coefficient which was recently introduced [1]. According to the gyrocenter shift theory, the plasma diffusion at the boundary is dependent on the density fluctuation level and the density fluctuation level is dependent on the Reynolds number of the poloidal ion gyrocenter drift arising from collisions with boundary neutrals. FIReTIP density fluctuation data are also compared with various plasma parameters which determine the Reynolds number such as the radial electric field and plasma temperature in the vicinity of separatrix for the study of the L\H transition mechanism. [1] K. C. Lee, Plasma Phys. Control. Fusion, Vol. 51, 065023 (2009)

*This work is supported by U.S. Department of Energy Grant Nos DE-FG02-99ER54518, DE-AC02-09CH11466 and DE-AC05-00OR22725.

PP8 68 Preliminary study of HHFW driven plasma fluctuation measurement using FIReTIP in NSTX* J. KIM, *POSTECH* K.C. LEE, *UC Davis* C.K. PHILLIPS, R. KAITA, *PPPL* C.W. DOMIER, N.C. LUHMANN, JR., *UC Davis* H. PARK, M. CHO, W. NAMKUNG, *POSTECH* NSTX is equipped with an FIR interferometry (FIReTIP) and high k scattering system, which can monitor high frequency density fluctuations driven by RF waves. High Harmonic Fast Wave (HHFW) fields drive localized density fluctuations at 30 MHz that may be detectable by this system. The electronics for 30 MHz signal observations were designed and are being upgraded for FIReTIP. The location of the observed fluctuations will be compared to predictions from the HHFW version of the TORIC code, which solves the Maxwell equations in toroidal geometry, using a quasilocal approximation that retains large $k_{perp}\rho_i$ effects but assumes that only the HHFW fields are excited. The RF induced density perturbation in NSTX discharges heated by the 30 MHz HHFWs will be localized within the field distribution predicted by the TORIC code. In this presentation, the conceptual design including experimental development and the preliminary results of simulation will be presented.

*This work supported by US DoE contract DE-AC02-09CH11466.

PP8 69 Turbulent filaments on the divertor target plates of NSTX* R.J. MAQUEDA, *Nova Photonics, Inc.* S.J. ZWEBEN, J. KALLMAN, *PPPL* C.E. BUSH, *ORNL* NSTX TEAM, Fine structured filaments are seen on the lower divertor target plates of NSTX during H-mode discharges. These filaments, not associated with edge localized modes, correspond to the footprints of the turbulent blobs seen near the midplane of the device with multiple diagnostics. The fluctuation level of the neutral lithium light observed and the skewness and kurtosis of its probability distribution function have similar characteristics than midplane blobs: increasing with increasing radii outside the outer strike point (separatrix). In addition, their toroidal and radial movement agrees with the typical movement of blobs at the midplane. Furthermore, with the appropriate magnetic topology, i.e. mapping between the portion of the target plates being observed into the field of view of the midplane gas puff imaging diagnostic, very good correlation is observed between the midplane blobs and these divertor filaments. The existence of "magnetic shear disconnection" due to the lower X-point, as proposed by Cohen and Ryutov [Nucl. Fusion 37, p. 621, 1997], is analyzed from the measurements obtained.

*Supported by US DOE under grants DE-FG02-04ER54767 and DE-AC-09CH11466.

PP8 70 GPI Measurements of Edge and SOL Turbulence Across the L-H transition in NSTX* A.L. ROQUEMORE, S.J. ZWEBEN, *PPPL* R.J. MAQUEDA, *Nova Photonics* S. KUBOTA, *UCLA* T. MUNSAT, *University of Colorado* S. KAYE, *PPPL* R. MAINGI, *ORNL* B.D. SCOTT, *IPP-Garching* T.S. HAHM, *PPPL* PPPL TEAM, NOVA PHOTONICS COLLABORATION, UCLA COLLABORATION, ORNL COLLABORATION, IPP-GARCHING COLLABORATION, Edge turbulence across the LH transition has been measured using the gas puff imaging (GPI) diagnostic at the outer midplane edge and scrape-off-layer (SOL) of NSTX. The cross-correlation data from the GPI diagnostic has been analyzed to determine the time- and space-dependent radial and poloidal correlation lengths Lr and Lp and flow speeds Vr and Vp across the transition. The local dimensionless poloidal flow shear S=(dVp/dr)(Lr/Lp)t was estimated from these measurements by averaging the turbulence flow speed over a suitable space and time range (t=autocorrelation time). In the SOL this shear ranges between $\pm$ 2 (with a wide scatter), but preliminary results do not show a clear correlation between the magnitude of S and the local fluctuation level across the transition. A comparison will be made between the turbulence seen by GPI and by the UCLA edge reflectometry diagnostic to determine whether the transition begins inside or outside the separatrix, and how the turbulence changes propagate during the transition.

*Work supported by US DOE Contract #DE-AC02-09CH11466.

PP8 71 Turbulent energy transport and parallel heat flux in the SOL* D.A. RUSSELL, J.R. MYRA, D.A. D'IPPOLITO, *Lodestar Research Corporation* J-W. AHN, *ORNL* R. MAQUEDA, *Nova Photonics* D.P. LUNDBERG, D.P. STOTLER, S.J. ZWEBEN, *PPPL, and the NSTX Team* We model the evolution of vorticity, density, temperature and zonal fluid momentum in the outboard midplane of a tokamak with our SOLT code. Our edge region supports the electron drift wave and interchange instabilities, while sheath losses are isolated in the SOL. Curvature- and grad-B-driven charge separation are included everywhere, enabling blob transport of strong fluctuations ($\delta n/n \sim 1$) from the edge into the SOL. Gas-puff imaging (GPI) diagnostics on NSTX are compared with the corresponding *synthetic* GPI diagnostics from the SOLT simulations. Here we study cross-field energy transport and the resulting profile of parallel heat flux to the divertor, in the outboard midplane, and make comparisons with recent NSTX experiments in which variations of the SOL width were studied.

*Supported by the USDOE under grants DE-FG02-02ER54678 and DE-FG02-97ER54392.

PP8 72 Utilization of Two-Point Model to Estimate Separatrix Temperature in NSTX* JOHN RHOADS, *Princeton University* RAJESH MAINGI, *ORNL* A method of estimating the separatrix temperature was developed using a simple two-point model of the scrape-off layer (SOL). Given an input power, neutral density, and connection length, the two point model determines the target temperature, target density, and upstream temperature. Source and sink terms in the model include radiation and volume recombination in the region near the divertor, collisions with neutrals and viscous forces in the SOL, hydrogen recycling, and parallel heat convection effects. Although the connection length at the separatrix is not well defined, this technique uses a finite connection length determined from the magnetic reconstruction of the discharge at a fixed normalized flux, $\hat{\phi}$, slightly outside of the last closed flux surface. Characteristic connection lengths from the midplane to the outboard lower divertor vary from approximately 8 meters at $\hat{\phi} = 1.01$ to 12 meters at $\hat{\phi} = 1.002$. The upstream temperature from the two-point model is then mapped onto the Thomson scattering profile and the separatrix temperature is deduced from the offset in the normalized flux. Typical separatrix temperatures fall within the range 40-100 eV.

*Supported in part by the US DOE under DE-AC05-00OR22725 (ORNL) and DE-AC02-09CH11466 (PPPL)

PP8 73 Investigation of ELM magnetic precursors in NSTX discharges with and without lithium wall coatings* FREDERICK KELLY, *Unaffiliated* ERIC FREDRICKSON, STEFAN GERHARDT, *PPPL* RAJESH MAINGI, *ORNL* JON MENARD, *PPPL* STEVE SABBAGH, *Columbia U.* HIRO TAKAHASHI, *PPPL* NSTX TEAM, The evolution of ELM magnetic precursors in a series of NSTX discharges without lithium and with increasing lithium deposition [1, 2] are examined. Data from the high-n Mirnov array was used to estimate the toroidal mode number (n) of the precursors. ELMs were observed to have n=1 and/or n=2 magnetic precursors with some delayed modes in the range from n=3 to n=6, which persist as the lithium coating is increased and ELMs become partially suppressed. The D-alpha signal of a few ELMs is preceded by a slow growing plateau period which appear to be dominated by n= 3 to n=6 modes, however, n= 1 and/or n=2 modes appear as precursors to the main ELM peak. The observed n=1 precursors may be evidence of SOL currents in NSTX, similar to those observed in DIII-D [3]. [1] R. Maingi, et al., 36th Eur. Phys. Soc. Conf. on Plasma Physics (Sofia, Bulgaria), P2.175. [2] R. Maingi, et al., Phys. Rev. Lett. (2009) at press. [3] H. Takahashi, et al., Nucl. Fusion 44 (2004) 1075.

*Research sponsored in part by US DOE under DE-AC02-09CH114466

PP8 74 Improvements to CHI Plasma Start-up and Ramp-up in NSTX T.R. JARBOE, R. RAMAN, B.A. NELSON, *Univ. of Washington* D. MUELLER, M.G. BELL, L. ROQUEMORE, H.W. KUGEL, *PPPL* V. SOUKHANOVSKII, *LLLNL* Experiments in NSTX have now demonstrated the savings of central solenoid inductive flux after coupling of toroidal plasmas produced by the technique of Coaxial Helicity Injection (CHI) to inductive sustainment and ramp-up of the toroidal plasma current. In these discharges, the central solenoid with zero pre-charge was used to apply an inductive loop voltage to the decaying CHI started discharges. The coupled discharges ramped up to 800kA without the benefit of auxiliary heating. Inductive flux savings was realized as a result of an effort to reduce the influx of low-Z impurities during the plasma start-up phase. This was achieved through the use of 400ms long CHI discharges produced using a DC rectifier power supply to ablate low-Z surface impurities from the lower divertor electrodes, followed by the use of Lithium evaporative coatings and an effort to reduce spurious arcs in the upper divertor region by controlling the extent of CHI plasma growth in the vessel. Previous work on NSTX has shown that CHI started discharges after coupling to neutral beam heated discharges can transition to an H-mode. These important new results from NSTX demonstrate that CHI is a viable solenoid-free plasma startup method for future STs and Tokamaks. This work supported by U.S. DOE Contracts # DE-AC02-09CH11466 and DE-FG02-99ER54519 AM08.

PP8 75 High Harmonic Fast Wave Heating Studies for L and H Mode NSTX Plasmas J.C. HOSEA, R.E. BELL, B.P. LEBLANC, C.K. PHILLIPS, L. ROQUEMORE, G. TAYLOR, J.R. WILSON, *PPPL* R. MAINGI, P.M. RYAN, J. WILGEN, *ORNL* K. TRITZ, *JHU* AND THE NSTX TEAM, Fast wave research on NSTX is directed toward understanding the coupling of some RF power to edge loss processes. These losses are driven in the vicinity of the antenna as opposed to resulting from multi-pass edge damping. PDI edge losses through ion-electron collisions and direct energetic ion losses appear to be significant, the latter possibly causing clamping of the edge rotation. Deuterium H-mode heating studies reveal that core heating is degraded at lower k_ϕ (- 8 m^{-1} relative to 13 m^{-1}) as for the L-mode case at elevated edge density, consistent with edge wave damping depending on the location of the onset density ($n_{onset} \propto B^* k_\parallel^2/\omega$) relative to the position of the antenna. Fast visible camera images clearly indicate that a major fast wave edge loss process is occurring from the plasma scrape off layer (SOL) in the vicinity of the antenna and along the magnetic field lines to the lower outer divertor plate. Large type I ELMs, which are observed at both k_ϕ values, appear after antenna arcs caused by precursor blobs, low level ELMs, or possibly dust. For large ELMs without arcs, the source reflection coefficients rise on a 0.1 ms time scale, suggesting that this rise time might be used to discriminate between ELMs and arcs. Work supported by US-DOE Contract No. DE-AC02-09CH11466.

PP8 76 Comparison of measurements and simulations of fast ion profiles during high harmonic fast wave heating in NSTX* D. LIU, W.W. HEIDBRINK, M. PODESTA, *UC Irvine* S.S. MEDLEY, *PPPL* R.W. HARVEY, *CompX* M. CHOI, *GA* D. GREEN, *ORNL* Combined neutral beam injection (NBI) and high harmonic fast wave (HHFW) heating at cyclotron harmonics accelerate deuterium fast ions in the National Spherical Torus Experiment (NSTX). Acceleration of fast ions above the beam injection energy is evident in the data from neutron, E||B type Neutral Particle Analyzer (NPA), Solid State Neutral Particle Analyzer (SSNPA) array and Fast-Ion D-Alpha (FIDA) diagnostics. The fast-ion spatial profiles measured by the FIDA diagnostic show that the acceleration is at four harmonics (7-10) simultaneously and it is much broader than in DIII-D. This is because of the multiple resonance layers and large orbits in NSTX. The measured spatial profile of accelerated fast ions is farther from the magnetic axis and broader than predicted by the CQL3D Fokker-Planck code, for which we conjecture that finite Larmor radius and banana-width can have significant effects on the fast ions in NSTX. To test this hypothesis, simulations with ORBIT-RF code coupled with full wave code AORSA are in progress.

*This work is supported by US DOE Contract DE-AC02-09CH11466.

PP8 77 Numerical Modeling of HHFW Heating on NSTX* C.K. PHILLIPS, R.E. BELL, J.C. HOSEA, B.P. LEBLANC, G. TAYLOR, E.J. VALEO, J.R. WILSON, *PPPL* L.A. BERRY, E.F. JAEGER, P.M. RYAN, *ORNL* P.T. BONOLI, J.C. WRIGHT, *PSFC-MIT* R.W. HARVEY, *CompX* T. BRECHT, *UMN* AND THE NSTX TEAM, Recent HHFW heating experiments on NSTX indicate that the core heating efficiency depends strongly on the antenna phasing and plasma conditions, and that it improves when the onset for wave propagation is moved away from the immediate vicinity of the launcher. Since the waves are nearly totally damped in a single transit through the plasma core, this degradation is likely due to power losses from collisions, rf sheaths, and sputtering associated with initial interactions of the waves with the antenna and vessel structures. Full wave and ray tracing codes have been used to study the wave propagation and damping characteristics in L-mode and H-mode discharges, and in lower density start-up plasmas. The extent to which significant wave propagation in the edge regions is correlated with the measured core heating efficiency will be presented for a range of discharge conditions.

*Work supported by DE-AC02-09CH11466.

PP8 78 Rotational Control of Plasma in NSTX* KUNIHIKO TAIRA, EGEMEN KOLEMEN, *Princeton University* DAVID GATES, *Princeton Plasma Physics Laboratory* CLARENCE ROWLEY, JEREMY KASDIN, *Princeton University* In an effort to assist the continuous extraction of fusion energy, a plasma model and a controller are developed for a magnetic fusion devise (NSTX). The model is aimed to capture the rotational (toroidal) momentum transport inside the tokamak. The neutral beam injection and the neoclassical toroidal viscosity are considered in the model for their uses as actuator forces. Based on the proposed model, a feedback controller is designed to sustain the toroidal momentum of the plasma in a stable fashion and to achieve desirable plasma geometry. The model reduction and design approaches will be presented along with validation studies.

*This work was supported by DoE contract No DE-AC02-09CH11466.

PP8 79 Design of a Linear-Quadratic-Gaussian controller for resistive wall mode stabilization in NSTX* OKSANA KATSURO-HOPKINS, S.A. SABBAGH, J.M. BIALEK, *Columbia University* S.P. GERHARDT, *PPPL* Stabilization of the resistive wall mode (RWM) in the NSTX is important to achieve and sustain high-beta plasmas. State-space control algorithms for improved RWM control performance using the existing external control coils and off-midplane poloidal magnetic field sensors in NSTX are investigated numerically. At reduced plasma rotation, normalized beta of 5.6 was achieved experimentally with the present proportional gain controller. The proposed linear quadratic Gaussian (LQG) controller is capable of reaching normalized beta of 6.7 for modes with low natural rotation speed and the ideal wall limit normalized beta of 7.1 for plasma modes with higher natural rotation speed. A Kalman filter, an integral part of the LQG controller, is tested using NSTX experimental data off-line and the RWM mode phase and amplitude are compared to results from the present RWM control system using proportional gain. The LQG algorithm is developed for use in real-time NSTX experiments using current control and voltage control methods.

*Supported by U.S. DOE Contracts DE-FG02-99ER54524 and DE-AC02-09CH11466.

PP8 80 NSTX Strike Point Position Control* EGEMEN KOLEMEN, *Princeton University* DAVID GATES, *PPPL* CLARENCE W. ROWLEY, N. JEREMY KASDIN, *Princeton University* This paper presents the new control algorithm for the inner and outer strike point position for NSTX and the performance analysis of the controller. A liquid lithium diverter (LLD) will be installed on NSTX which provides better pumping than lithium coatings on carbon PFCs. The shape of the plasma dictates the pumping rate of the lithium by channeling the plasma to LLD, where strike point location is the most important shape parameter. Simulations show that the density reduction depends on the proximity of strike point to LLD. Experiments were performed to study the dynamics of the strike point, design a new controller to change the location of the strike point to desired location and stabilize it. The most effective PF coil in changing the outer strike point is PF2L. Thus, we use this coil as the sole controller for the outer strike point. In the same way, PF1AL is used for inner strike point control. The PF coil inputs were changed in a step fashion between various set points and the step response of the strike point position was obtained. From the analysis of the step response, PID controllers for the strike points were obtained and the controller was tuned experimentally.

*This work was supported by DoE contract No. DE-AC02-09CH11466.

PP8 81 Study of strike-point and flux-expansion control in diverted NSTX plasmas* HUA WANG, JONATHAN MENARD, *Princeton Plasma Physics Laboratory* Tokamaks commonly use a poloidal divertor to tailor the trajectory and length of open magnetic field lines outside the main plasma volume. Optimization of the magnetic field configuration at the divertor is desirable to control the heat and particle flux to the material surfaces. Such optimization is important in NSTX, in the design of new divertor configuration for the proposed upgrade of NSTX, and for future Spherical Torus (ST) devices. In particular, simultaneous control of the strike point location and the flux expansion at the strike point is highly desirable to control the location and magnitude of peak heat and particle flux at the divertor target. The

free-boundary equilibrium code ISOLVER is utilized and modified to assess the boundary shape implications of controlling the strike point location. The viability of simultaneous strike point and flux expansion control is also assessed.

*This work supported by DOE contract number DE-AC02-09CH11466

PP8 82 Details and Results from the FIReTIP Electronics Upgrade on NSTX* C.W. DOMIER, W.-C. TSAI, K.C. LEE, N.C. LUHMANN, JR., *University of California* R. KAITA, *Princeton Plasma Physics Laboratory* The IF electronics system of the Multichannel Far Infrared Tangential Interferometer/Polarimeter (FIReTIP) system on the National Spherical Torus Experiment (NSTX) was upgraded in July 2009 to greatly extend its ability to monitor high frequency density fluctuations. The measurements are essential in understanding transport physics issues in NSTX as well as for future devices such as ITER in which fundamental understanding of microturbulence MHD issues is essential. The electronics, which were previously limited to $\sim$ 250 kHz, have now been upgraded to $>$ 3 MHz when operating as an interferometry-only configuration, and to $\sim$ 400 kHz when operated as a simultaneous interferometer/polarimeter system. New electronics are also being tested to monitor 30 MHz density fluctuations induced by high harmonic fast wave heating. Experimental details and test results of the new electronics will be presented.

*Work supported by the U. S. DoE grants DE-FG02-99ER54518 and DE-AC02-09CH11466.

PP8 83 Design and status of the NSTX BES diagnostic for fluctuation measurements on the ion gyro-scale D.R. SMITH, R.J. FONCK, G.R. McKEE, I. UZUN-KAYMAK, G. WINZ, *Univ of Wisconsin-Madison* H. FEDER, R. FEDER, G. LABIK, B.C. STRATTON, *Princeton Plasma Phys Lab* A beam emission spectroscopy (BES) diagnostic has been installed on NSTX to investigate density fluctuations on the ion gyro-scale. The BES diagnostic measures the Doppler-shifted D_α emission at 660 nm from neutral deuterium beams. The measurements provide radial and poloidal correlation functions, wavenumber spectra, decorrelation rates, and turbulent flows for investigating core and edge turbulence and energetic particle modes on NSTX@. The initial deployment includes 16 detection channels, and the viewing optics are aligned to the local magnetic field to optimize spatial resolution. Spot sizes on the neutral beam are in the range 2–3 cm. Radial arrays can measure fluctuations from $r/a \approx 0.1$ to beyond the last-closed flux surface, and poloidal arrays are positioned at $r/a \approx 0.4, 0.6, 0.85$, and 1.1. PIN photodiodes and low noise preamplifiers measure fluctuations with high sensitivity, and filtered data is obtained at 2 MS/s@. The BES diagnostic will collect initial data during the 2010 run campaign. *Supported by the U.S. Department of Energy under Contract No. DE-AC02-09CH11466.

PP8 84 The Use of a 28 GHz Gyrotron for EBW Startup Experiments on MAST* J.B. CAUGHMAN, T.S. BIGELOW, S.J. DIEM, Y.K.M. PENG, D.A. RASMUSSEN, *ORNL* V. SHEVCHENKO, J. HAWES, B. LLOYD, *UKAEA Fusion, Culham Science Centre* The use of electron Bernstein waves for non-inductive plasma current startup in MAST has recently been demonstrated [1]. The injection of 100 kW at 28 GHz generated plasma currents of up to 33 kA without the use of solenoid flux, and limited solenoid assist resulted in up to 55 kA of plasma current. A higher power 28 GHz gyrotron, with power levels of up to 300 kW for 0.5 seconds, is currently being commissioned. It is being used to investigate the scaling of startup current with microwave power and power profile as a function of time. Power modulation experiments are also being explored. Gyrotron performance and experimental results will be presented. [1] V. Shevchenko, et al., Proceedings of the 15th Joint Workshop on ECE and ECRH, Yosimite, USA, p. 68 (2009)

*Oak Ridge National Laboratory is managed by UT-Battelle, LLC, for the U.S. Dept. of Energy under contract DE-AC05-00OR22725. Work supported by USDOE with grant DE-FG02-04ER54765.

PP8 85 The PEGASUS Toroidal Experiment Program* R.J. FONCK, M.W. BONGARD, E.T. HINSON, B.A. KUJAK-FORD, B.T. LEWICKI, A.J. REDD, D.J. SCHLOSSBERG, F. VOLPE, G.R. WINZ, *University of Wisconsin-Madison* The PEGASUS program is developing non-solenoidal startup and growth techniques for tokamaks, and exploring plasma stability at near-unity aspect ratio. Helicity injection from localized current sources in the plasma periphery produced $I_p \geq 0.1$ MA, consistent with a simple theory invoking helicity balance and Taylor relaxation constraints. Future efforts will concentrate on accessing $I_p = 0.3$ MA to test theory to the point where parallel conduction losses dominate the helicity loss rate. Plasma growth following startup will be pursued via Higher Harmonic Fast Wave heating (0.8 MW available) and/or Electron Bernstein Wave heating and current drive (0.5-1.0 MW EBW proposed). Proposed upgrades in support of these programs include a new centerstack for increased TF, divertors for separatrix-limited operation, and long-pulse capabilities. Plasma stability is dominated by peeling-like modes at large $\langle j_{edge}/B \rangle$ and large-scale low-$m/n = 1$ core activity. The new capabilities will provide core and edge $j(r)$ manipulation to stably access the unique high I_N, high-β_t regime at $A \approx 1$.

*Supported by U.S. D.O.E. Grant DE-FG02-96ER54375.

PP8 86 Non-solenoidal startup and low-β operations in PEGASUS* D.J. SCHLOSSBERG, D.J. BATTAGLIA, M.W. BONGARD, R.J. FONCK, A.J. REDD, *University of Wisconsin, Madison, WI, USA* Non-solenoidal startup using point-source DC helicity injectors (plasma guns) has been achieved in the scPegasus Toroidal Experiment for plasmas with I_p in excess of 100 kA using $I_{inj} < 4\,kA$. The maximum achieved I_p tentatively scales as $\sqrt{I_{TF} I_{inj}/w}$, where w is the radial thickness of the gun-driven edge. The I_p limits appear to conform to a simple stationary model involving helicity conservation and Taylor relaxation. However, observed MHD activity reveals the additional dynamics of the relaxation process, evidenced by intermittent bursts of n=1 activity correlated with rapid redistribution of the current channel. Recent upgrades to the gun system provide higher helicity injection rates, smaller w, a more constrained gun current path, and more precise diagnostics. Experimental goals include extending parametric scaling studies, determining the conditions where parallel conduction losses dominate the helicity dissipation, and building the physics understanding of helicity injection to confidently design gun systems for larger, future tokamaks.

*Work supported by US DOE OFES, grant DE-FG02-96ER54375.

PP8 87 Edge current and pressure measurements of plasma equilibrium and stability properties in PEGASUS* E.T. HINSON, M.W. BONGARD, R.J. FONCK, B.A. KUJAK-FORD, B.T. LEWICKI, A.J. REDD, G.R. WINZ, *University of Wisconsin-Madison* The plasma edge region in the PEGASUS ST exhibits a range of fluctuation phenomena, from peeling-like modes at high I_p, to standard broadband electrostatic turbulence. Measurements of the edge region will support studies of its equilibrium and stability properties, and provide information for RF coupling (HHFW and EBW) for future heating and current drive studies. Langmuir probes are used to measure the edge pressure gradient with high temporal resolution. Together with measurements of the edge B_z profile from a radial array of Hall probes, the derived $p(r)$ and $j_\parallel(r)$ profiles will support detailed edge stability analyses. Peeling-like modes manifest as edge filamentary structures commonly observed in Ohmic discharges. Scanning Mirnov probes indicate broadband magnetic turbulence when this filamentation occurs. Peeling-mode theory predicts instability for large $\langle j_\parallel/B\rangle$, a condition that PEGASUS may satisfy ($B_t \sim$ 0.1 T, $j_\parallel \sim$ 0.1 MA/m ^{2}). These measurements will enable determination of $\langle j_\parallel/B\rangle$ and $p(r)$ at $r \approx a$, and offer unique tests of peeling-ballooning theory. Future studies will employ divertors to increase magnetic shear and influence edge turbulence.

*Supported by U.S. D.O.E. Grant DE-FG02-96ER54375.

PP8 88 The Lithium Tokamak eXperiment (LTX) – Status and Plans* RICHARD MAJESKI, *Princeton Plasma Physics Lab* L. BERZAK, D. BOYLE, S. GERSHMAN, E. GRANSTEDT, C.M. JACOBSON, A.D. JONES, R. KAITA, T. KOZUB, B. LEBLANC, D.P. LUNDBERG, K. SNIECKUS, T. STRICKLER, J. TIMBERLAKE, L. ZAKHAROV, *PPPL* G.V. PEREVERZEV, *IPP-Garching* V. SOUKHANOVSKII, *LLNL* C.E. THOMAS, *Third Dimension* LTX is a modest spherical tokamak with R=0.4 m, a=0.26 m, =1.5, $B_{toroidal}$= 3.4 kG, $I_P <$ 400 kA, and $\tau_{flattop} >$ 50 msec. The LTX research objective is to investigate modifications to equilibria and transport when global recycling is reduced to very low values (< 50%), by means of a conformal stainless steel clad copper wall coated with liquid lithium. The resistively heated wall is capable of operating at temperatures exceeding 500C, but the nominal operating temperature range will be room temperature to 400C. Initial lithium operation will employ evaporative coatings applied to the heated wall. Pulsed fueling with gas jets and an H_2 cluster injector will be employed to transiently eliminate edge gas. Diagnostic plans are extensive, and are discussed in companion posters by L. Berzak, D. Lundberg, S. Gershman, E. Granstedt, C. M. Jacobson, and C. E. Thomas.

*Supported by US DOE contracts DE-AC02-09CH11466 and DE-AC52-07NA27344.

PP8 89 Operation of Magnetic Diagnostics on the Lithium Tokamak eXperiment* L. BERZAK, R. KAITA, T. KOZUB, R. MAJESKI, J. MENARD, L. ZAKHAROV, *PPPL* The Lithium Tokamak eXperiment (LTX) is designed to investigate the novel, low-recycling lithium wall operating regime for magnetically confined plasmas. LTX reaches this regime through a heated shell coated with liquid lithium internal to the vacuum vessel. This shell provides an area of 5 m^2 of liquid lithium, more than 90% coverage of plasma facing components. An extensive array of unique magnetic diagnostics has been developed to yield detailed magnetic information in the presence of the shell and allow highly-constrained reconstructions of the plasma equilibrium. CDX-U, with a 2000 cm^2 liquid lithium limiter, observed a 5-10 fold increase in energy confinement time from pre-Li discharges with Ohmic loop voltages of only 0.4-0.5 V. The expanded magnetic diagnostics set is designed to permit more accurate evaluation of the global energy confinement time and surface loop voltage for comparison with the results of CDX-U and to perform scaling experiments in order to elucidate the variation in confinement with toroidal field, plasma current, and plasma density.

*Supported by US DOE contract DE-AC02-09CH11466

PP8 90 Turbulent Thermal Insulation of Spheromak Fusion Reactors ROBERT JONES, *Emporia State University* Spheromak fusion plasmas are likely to suffer from stochastic magnetic fields (Phys. Rev. Letts. vol. 91, #4, 045004, 2003) and have confinement: t=(B/dB)(B/dB)(r/v)(r/v)f. This degradation in confinement can be minimized if the collision frequency f is intentionally enhanced by turbulence (see Jones, Plasma Phys. vol. 22, pg 753, 1980) f=(plasma frequency)* (W/nT), up to a level W/nT limited by plasma overheating: T/t = f W/n. (R. Jones, Current Science, vol. 57, #18, pg. 991, 1988)

PP8 91 The Lithium Tokamak Experiment Thomson Scattering Diagnostic* C.M. JACOBSON, R. KAITA, B.P. LEBLANC, R. MAJESKI, T. STRICKLER, *Princeton Plasma Physics Laboratory* The Lithium Tokamak Experiment (LTX) is a spherical tokamak designed to study the low-recycling regime though the use of a liquid-lithium coated shell conformal to the last closed flux surface. A low recycling rate is expected to flatten core electron temperature profiles, raise edge temperatures, and strongly affect electron density profiles. A Thomson scattering diagnostic is used to measure radial T_e and n_e profiles. The system uses a 15 J, 30 ns pulsed ruby laser and measures profiles of up to 16 radial points on the horizontal midplane at a single temporal point for each discharge. Scattered light is imaged though a spectrometer into an intensified CCD. Two transmission gratings are available for the spectrometer to increase temperature range. In order to protect optical windows from becoming coated with lithium, the system uses automated shutters and gate valves.

*Supported by US DOE contract #DE-AC02-09CH11466.

PP8 92 Molecular Cluster Injection for Fueling and Particle Transport Studies on the Lithium Tokamak eXperiment (LTX)* D.P. LUNDBERG, R. KAITA, T. KOZUB, R. MAJESKI, *PPPL* V. SOUKHANOVSKII, *LLNL* LTX is designed to reduce global recycling with a liquid lithium wall. Gas-based fueling systems, such as wall-mounted gas puffers or supersonic gas injectors, are perturbative to low-recycling plasmas, as they source a significant amount of gas into the edge. Following experiments on the HL-2A tokomak by Yao, et al. (Nucl. Fusion 47(2007) 1399), a molecular cluster injector was designed to supply an increased fraction of core fueling on LTX. A fast solenoid valve is cooled with liquid nitrogen, lowering the temperature of the gas in the valve body. As the gas expands into vacuum, additional cooling yields the formation of molecular clusters. This concentrates the hydrogen into a directed, high-density jet, improving penetration into the plasma. This system can be used for fueling and particle transport studies. Details of the design, construction, and initial operation of this system will be presented, and its application to LTX discussed. *Supported by US DOE contracts DE-AC02-09CH11466 and DE-AC52-07NA27344

PP8 93 Density Fluctuation and Transport Studies for the Lithium Tokamak eXperiment* E.M. GRANSTEDT, R. MAJESKI, R. KAITA, G.W. HAMMETT, *PPPL* C.E. THOMAS, *Third Dimension Technologies* Tokamak fusion energy confinement is generally limited by turbulent transport due to temperature-gradient-driven instabilities; however, a low-recycling plasma boundary may permit high edge temperatures to be realized, resulting in a flattened temperature profile and eliminating the drive mechanism for ITG and ETG turbulence. LTX is uniquely suited to study this regime, where the remaining transport is expected to be neoclassical or driven by density gradients. To extrapolate performance to larger devices, the contributions of both mechanisms to the transport must be understood. Characterization of the transport in the low-recycling regime requires measurement of density fluctuation spectra. The statistical nature of density fluctuations in LTX will be investigated with a digital holography diagnostic currently under development. This diagnostic uses a 9.1 μm CO_2 laser and an IR quantum well FPA camera to measure line-integrated plasma density fluctuations with up to 0.3 mm resolution perpendicular to the line-of-sight, exposures > 1 μs, and frame rates < 48 kHz. Measurement predictions for this diagnostic through linear and nonlinear gyrokinetic simulations using the GYRO code are also presented.

*Supported by US DOE contract DE-AC02-09CH11466.

PP8 94 High Speed Digital Holography for Density and Fluctuation Measurements on LTX* C.E. (TOMMY) THOMAS JR., *Third Dimension Technologies* L.R. BAYLOR, S.K. COMBS, S.J. MEITNER, D.A. RASMUSSEN, *Oak Ridge National Laboratory* E.M. GRANSTEDT, R. MAJESKI, *Princeton Plasma Physics Laboratory* Digital holography has been demonstrated as a viable technique for precision measurement and for measuring the development of high-speed gas flow. A digital holography demonstration system has been used on an ORNL disruption mitigation test stand to make extremely high spatial resolution (less than one mm) 2-D density measurements of gas flow. A second generation system with a high-speed infrared camera (320 x 256 pixels) and higher power 9.1 micron CO_2 laser ($\sim$ 20W) is being developed for electron density and fluctuation measurements on LTX. Exposures as short as one microsecond are exspected and frame rates (at reduced pixel window size) of 10,000 frames per second and higher are planned. Elements of the design, components, and expected performance will be presented.

*Partial Support from DOE SBIR Grant DE-FG02-07ER84724 is gratefully acknowledged.

PP8 95 Design and Assembly of a Langmuir Probe for the Lithium Tokamak Experiment (LTX)* SOPHIA GERSHMAN, LAURA BERZAK, DENNIS BOYLE, ERIK GRANSTEDT, CRAIG JACOBSON, ANDREW JONES, ROBERT KAITA, TOM KOZUB, BENOIT P. LEBLANC, DANIEL LUNDBERG, RICHARD MAJESKI, KURT SNIECKUS, T. STRICKLER, JOHN TIMBERLAKE, LEONID ZAKHAROV, *PPPL* G.V. PEREVERZEV, *IPP-Garching* V. SOUKHANOVSKII, *LLNL* C.E. THOMAS, *Third Dimension* The presence of lithium coatings on plasma facing surfaces has been shown to reduce recycling, increase the electron temperature, and significantly improve the energy confinement in a tokamak. LTX is designed for detailed investigation of the transport phenomena and plasma properties in this new low recycling regime. Edge diagnostics are an important part of this study. A swept probe has been designed to determine the plasma temperature and density in the scrape-off layer. The probe is designed to accommodate continued lithium evaporation and the expected low edge densities and high temperatures characteristic to this regime. Data from the probe will support the study of the transport properties and provide input parameters for the codes modeling the edge plasma in lithium boundary tokamaks.

*Supported by US DOE contracts DE-AC02-09CH11466 and DE-AC52-07NA27344

PP8 96 RF Experiments on TST-2 YUICHI TAKASE, AKIRA EJIRI, YOSHIHIKO NAGASHIMA, OSAMU WATANABE, *University of Tokyo* BUNG IL AN, *MIT* KENTARO HANASHIMA, HIROYUKI HAYASHI, JUNICHI HIRATSUKA, HIDETOSHI KAKUDA, HIROAKI KOBAYASHI, HIROKI KURASHINA, HAZUKI MATSUZAWA, TAKUYA OOSAKO, TAKUYA SAKAMOTO, TAKUMA WAKATSUKI, KOTARO YAMADA, TAKASHI YAMAGUCHI, *University of Tokyo* PAUL BONOLI, JOHN WRIGHT, *MIT* RF experiments were performed on the TST-2 spherical tokamak (R= 0.38 m, a = 0.25 m, B_t = 0.3 T, I_p = 0.1 MA) with up to 5 kW of power at 2.45 GHz and up to 400 kW of power at 21 MHz. In HHFW electron heating of inductively produced plasmas, parametric decay instability was often observed. The spatial distribution measured by RF magnetic probes located at different toroidal locations indicated wave propagation effects as well as nonlinear effects. Spontaneous formation of the ST configuration was studied. Sustainment of the ST configuration was accomplished by low frequency (21 MHz) RF power alone for the first time. LHCD and I_p ramp-up experiments are in preparation using up to 400 kW of power at 200 MHz. This experiment will be carried out at B_t = 0.3 T, and the density of the EC produced plasma will be kept low during I_p ramp-up by LHCD. Status of preparation and results of calculations will be presented.

PP8 97 Observation of non-locality of parametric decay during rf injection experiments on TST-2* YOSHIHIKO NAGASHIMA, TAKUYA OOSAKO, YUICHI TAKASE, AKIRA EJIRI, OSAMU WATANABE, HIROAKI KOBAYASHI, TAKASHI YAMAGUCHI, BYUNG IL AN, HIROKI KURASHINA, KOTARO YAMADA, HIROYUKI HAYASHI, HADUKI MATSUZAWA, KENTARO HANASHIMA, JUNICHI HIRATSUKA, HIDETOSHI KAKUDA, TAKUYA SAKAMOTO, TAKUMA WAKATSUKI, *The University of Tokyo* Investigation of linear/nonlinear wave energy transfer in spectral and real spaces of plasma is important for understanding complex plasma structural formation. We present an experimental observation of non-locality of parametric decay instability (PDI) during rf injection experiments in the TST-2 spherical tokamak. The PDI is considered to be mainly associated with pump wave (high harmonic fast wave, HHFW), lower-sideband (HHFW or ion Bernstein wave), and ion cyclotron quasi-mode (ICQM). PDI is a nonlinear and local phenomenon. However, the PDI is widely observed in various locations inside the vessel, and the same frequency matching condition is satisfied beyond difference of local ion cyclotron frequencies at observation locations. We discuss origin of the non-locality in term of wave propagation and coupling phase.

*This work is supported by grant-in-aids for Scientific Research S (21226021) and for Scientific Research A (21246137) of MEXT, Japan.

PP8 98 Spherical tokamak start-up and sustainment experiments on UTST T. YAMADA, R. IMAZAWA, S. KAMIO, R. HIHARA, K. ABE, M. SAKUMURA, Q.H. CAO, T. OOSAKO, H. KOBAYASHI, T. WAKATSUKI, B.I. AN, Y. NAGASHIMA, M. INOMOTO, A. EJIRI, Y. TAKASE, Y. ONO, *Univ. Tokyo* H. SAKAKITA, H. KOGUCHI, S. KIYAMA, Y. HIRANO, *AIST* UTST TEAM, The University of Tokyo Spherical Tokamak (UTST) device was constructed for the purpose of formation and sustainment of ultra-high beta spherical tokamak (ST) plasma using double null plasma merging and radio-frequency (RF) / neutral beam injection (NBI) heatings. The main feature of UTST is that the poloidal field coils are located outside the vacuum vessel in order to demonstrate the start-up in a more reactor relevant situation. Initial operations were carried out using partially completed power supplies to investigate the appropriate conditions for plasma merging. Plasma current of the merged ST was 50 kA, and reached 170 kA by using the central solenoid coil for assistance of plasma formation. Merging of two ST plasmas through magnetic reconnection was successfully observed by using two-dimensional pickup coil arrays, which directly measure the toroidal and axial magnetic fields inside the UTST vacuum vessel. There are two methods, which are now in progress, to sustain the ultra-high beta ST created on UTST; radio-frequency heating (400 kW and 21 MHz) and neutral beam injection (500 kW and 15 ms).

PP8 99 Experimental Demonstration of Double Null Merging Start-up on UTST RYOTA IMAZAWA, SHUJI KAMIO, RYUMA HIHARA, KEITA ABE, MORIO SAKUMURA, QINGHONG CAO, TAKUMA YAMADA, MICHIAKI INOMOTO, YUICHI TAKASE, YASHUSHI ONO, *The University of Tokyo* We made double null merging(DNM) experiments using outer poloidal field(PF) coils on UTST. We successfully generated two STs at two null points by using a washer gun, and succeeded in merging them. The DNM scheme is started by two magnetic null points generated at the upper and lower regions inside the vacuum vessel. Then poloidal flux swing generates two STs at two null points formed by two pairs of outer PF coils. Finally, the coil currents push two STs toward the mid-plane, and merge them into single ST. Since magnetic reconnection during merging transforms a magnetic energy into a thermal energy, this merged ST plasma is expected to have ultra high beta. It must be noted that DNM scheme can make ST without center solenoid coils. The DNM scheme was demonstrated on TS-3/4(JAPAN) and MAST(UKAEA). However these devices have all PF coils inside the vacuum vessel, and initial plasmas were generated around PF coils, not null points. Since the internal coils are not feasible in the fusion reactor, it is important to demonstrate that the outer PF coils induce electric fields for the breakdown and the formation of two STs.

PP8 100 Measurements of HHFW profile in UTST TAKUMA WAKATSUKI, TAKUYA OOSAKO, HIROAKI KOBAYASHI, TAKUMA YAMADA, BYUNG IL AN, RYOTA IMAZAWA, KEITA ABE, AKIRA EJIRI, KENTARO HANASHIMA, HIROYUKI HAYASHI, RYUMA HIHARA, JUNICHI HIRATSUKA, MICHIAKI INOMOTO, HIDETOSHI KAKUDA, SHUJI KAMIO, HIROKI KURASHINA, YOSHIHIKO NAGASHIMA, YASUSHI ONO, TAKUYA SAKAMOTO, MORIO SAKUMURA, QINGHONG CAO, YUICHI TAKASE, OSAMU WATANABE, TAKASHI YAMAGUCHI, KOTARO YAMADA, *University of Tokyo* HHFW (high-harmonic fast wave, f = 21 MHz) experiments were performed on the UTST spherical tokamak (R= 0.38 m, a = 0.25 m, B_t = 0.1 T, I_p = 0.1 MA) [T. Yamada, this session]. The HHFW antenna consists of two poloidal current straps separated in the toroidal direction. The spatial profile of the HHFW field was measured by a 2-dimensional array of magnetic probes inserted into the plasma 45[r] away from the antenna toroidally. 40 channels of RF data can be acquired simultaneously by fast digitizers (1 GHz sampling frequency) out of 81 probes. A comparison of wave fields measured with out-of-phase two-strap excitation (high parallel wavenumbers) and with single strap excitation (low parallel wavenumbers) indicate higher RF fields inside the plasma for the same input power. The experimental data will be compared with results of wave field calculation.

PP8 101 Numerical Simulations of Current Channel Relaxation For Non-Inductive Startup T.M. BIRD, C.R. SOVINEC, D.J. BATTAGLIA, J.B. O'BRYAN, *Univ. of Wisconsin - Madison* Nonlinear resistive MHD computation with anisotropic thermal conduction is used to investigate the relaxation of helical current filaments into tokamak-like plasmas for non-inductive startup of spherical tokamaks. A localized, volumetric current source has been added to the NIMROD code (nimrodteam.org) to model miniature washer-gun current sources in the lower divertor region of the Pegasus Toroidal Experiment at the Univ. of Wisconsin. When the induced magnetic field is smaller than the vacuum field, a helical filamentary current channel forms on open field lines, comparable to experimental results in similar conditions. Relaxation into tokamak-like plasmas has been demonstrated in experiment with induced fields that exceed the vacuum field [N. W. Eidietis, et al., J. Fusion Energy 26, 43 (2007)]. Simulation results show that current channels begin to collect near the injector when reversing the poloidal flux between the injector and inboard wall. Both zero-beta simulations and temperature dependent simulations with anisotropic thermal conduction are presented along with comparison to experiment.

PP8 102 Development of Continuous Plasma Merging Scenario for Start-up and Formation of Spherical Tokamak Plasmas CHOONGKI SUNG, Y.S. PARK, HYUNYEONG LEE, J. KANG, Y.S. HWANG, A new device which can start-up and sustain ST plasmas by means of continuous tokamak plasma injection has been designed. The device with two separated solenoids at both ends has been designed to generate small plasmas inductively, and then the plasmas are merged to the middle region, where main ST plasmas are formed. If the ST plasma could be sustained while two separated solenoids are recharged subsequent injections of inductively formed plasmas from partial solenoids can maintain or increase plasma currents. To make a feasible operation scenario of the device, a circuit model combined with density and power balance equations is developed. In the model, plasma is assumed to be a single filament in a circuit, and evolution of circuit plasma parameters can be evaluated from balance equations. By using the model, an operational scenario utilizing continuous plasma injections from AC operations of partial solenoids is developed to overcome the ST's weakness. Experimental verification of the operation will be demonstrated in near future.

PP8 103 SIMULATION AND MODELING OF BASIC PLASMA PHENOMENA

PP8 104 Plasma Torque and Non-Ambipolar Transport* ALLEN BOOZER, *Columbia University* Poloidal symmetry breaking in toroidal plasmas causes a damping of poloidal rotation and toroidal symmetry breaking a damping of toroidal rotation. These torques are transmitted by the magnetic field to the outside world. An upper limit exists on the torque that can be transmitted by a magnetic perturbation. This limit is enforced by shielding asymmetries from the plasma, which can be an important effect for toroidal asymmetries. The torque interaction of plasmas with magnetic fields can be either through an anisotropic pressure or by the drive for magnetic islands. The physics of both types of interactions are considered and paradoxical effects are clarified.

*Supported by U.S. Dept. of Energy Grants ER54333 and ER54696.

PP8 105 Modeling high-voltage dielectric insulator breakdown* JOHN VERBONCOEUR, SOREN TAVERNIERS, *University of California - Berkeley* Modeling angled dielectric insulator breakdown has been notoriously difficult due to a number of numerical challenges, including inaccuracies in the surfaces and impact angles caused by stair-stepped surfaces, and the small but surprisingly significant effects of rounding end points of structures off to grid locations. In this work, we describe techniques to overcome these challenges using a two-dimensional particle-in- cell model. Recent theoretical work has suggested that electron emission near the triple point due to an enhanced electric field is responsible for initiating flashover in high voltage insulation systems and RF breakdown in high power microwave windows [1]. In this work, 2D particle simulation is employed to calculate the breakdown voltage versus insulator angle for two parallel conductors. The model includes secondary electron emission insulator surface, and space charge effects in the volume and at the insulator surface. The model is verified for analytical cases, and is compared to the theory [1]. [1] N. M. Jordan, Y. Y. Lau, D. M. French, R. M. Gilgenbach, and P. Pengavich, J. Appl. Phys. 102, 033301 (2007).

*Work supported by the AFOSR under Grant No. FA9550-09-1-0086.

PP8 106 PIC simulations of space charge limited flow* MARTIN E. GRISWOLD, NATHANIEL J. FISCH, *PPPL* JONATHAN S. WURTELE, *LBNL* Achieving the maximum possible current density continues to be an important goal with far ranging applications. The space charge limit to current in diodes can be affected by a number of parameters, such as finite emitter size [1] and short pulse length [2]. Here, using a particle-in-cell code, we examine a number of interesting phenomena associated with space charge limited flow, including virtual cathode formation for time-dependent situations. [1] Luginsland, Lau, et. al., Physics of Plasmas 9 (2002) 2371 [2] Valfells et. al., Physics of Plasmas 12 (2002) 2377

*Work supported by US DoE contract No. DE-AC02-76-CH03073. One of us (MG) was supported by a DOE Fusion Energy Science Graduate Fellowship.

PP8 107 Nonlinear effects due to Langmuir waves in densifying plasmas* NAT FISCH, ILYA DODIN, *Princeton University* Electron Langmuir waves in plasma undergoing slow compression or rarefaction respond adiabatically to the modification of the plasma density and the pressure tensor, such that the total number of plasmons is conserved. However, the change in density modifies the ratio of the field energy to the plasma kinetic energy in ways that depend on how the density changes. The changes in field energy affect the ponderomotive forces, which can in turn govern a variety of plasma processes.

*This work was supported by the NNSA under the SSAA Program through DOE Research Grant No. DE-FG52-04NA00139.

PP8 108 Action principle derivation of one-fluid models from two-fluid actions ALEXANDER WURM, *Dept. of Physical & Biological Sciences, Western New England College, Springfield, MA* P.J. MORRISON, *Institute for Fusion Studies and Dept. of Physics, The University of Texas at Austin, Austin, TX* Ideal MHD possesses a well-known action principle formulation when the theory is expressed in terms of Lagrangian (or material) variables.[1] Here we start with a general electromagnetic two-fluid action functional in Lagrangian variables and derive action principles for one-fluid models, including ideal MHD. [1] W.A. Newcomb, Nuclear Fusion: 1962 Suppl. Part 2, p. 451

PP8 109 Magnetization force in plasma physics* ROBERT JOHNSON, *Alphawave Research* The magnetization force is well documented in materials science, thus it needs to be addressed in the context of plasma physics. Generalization of the macroscopic force densities by Lorentz-Kelvin and Korteweg-Helmholtz yields an expression $\mathbf{J} \times \mathbf{B} + \nabla \mathbf{M} \cdot \mathbf{B}$ appropriate for magnetized plasma. Application to the stationary equilibrium equation indicates its presence is necessary to enforce the reduction to the standard form in the limit of vanishing magnetization. A numerical investigation of an axially symmetric configuration confirms this behavior. Application to toroidal geometry indicates that no stationary solution exists for a curved plasma column.

*arXiv: 0806.4698, 0901.0732

PP8 110 The random path of a charged particle in a white noise magnetic field: analysis, simulation, and a physical realization TREVOR LIPSCOMBE, *Johns Hopkins University Press* DON LEMONS, BLAKE JOHNSON, *Bethel College* We derive a set of stochastic differential equations, parameterized with a single diffusion constant, that describes an isotropic, one-dimensional random path embedded in three dimensions. The path variously describes the trajectory of a charged particle in a white noise magnetic field, a photon undergoing weak scattering, and the random orientation of a long chain molecule. The mean and variance of the squared distance between the ends of the path depend only upon the diffusion constant and the path length. We illustrate this dependence with numerical simulations and test it by gathering data on a physical realization consisting of segments of thread suspended in glycerol.

PP8 111 A Hamiltonian electromagnetic gyrofluid model* F.L. WAELBROECK, *Inst. Fusion Studies, Univ. Texas Austin* R.D. HAZELTINE, P.J. MORRISON, *Inst. Fusion Studies, U. Texas at Austin* An isothermal truncation of the electromagnetic gyrofluid model of Snyder and Hammett [Phys. Plasmas 8, 3199 (2001)] is shown to be Hamiltonian. The corresponding noncanonical Lie-

Poisson bracket and its Casimir invariants are presented. The model describes the evolution of the density, the electrostatic potential, and the component of the vector potential along a strong background field. This makes it suitable for describing such phenomena as the propagation of kinetic-Alfvén modons, the nonlinear saturation of drift-tearing modes, and the diamagnetic stabilization of the internal kink. The invariants are used to obtain a set of coupled Grad-Shafranov equations describing equilibria and propagating coherent structures. They also lead to a Lagrangian formulation of the equations of motion that is well suited to solution with the PIC method.

*Supported by U.S. DOE Contract No. DE-FG03-96ER-54346.

PP8 112 Grid-Free Electromagnetic Particle Simulations* BENJAMIN ONG, ANDREW CHRISTLIEB, *Department of Math, Michigan State University* ROBERT KRASNY, *Department of Math, University of Michigan* In this poster, we demonstrate how the existing boundary integral treecode (BIT) framework can be extended to electrodynamic problems. The key idea is a method of lines transpose methodology, where we choose to discretize in time and directly solve the resulting Helmholtz equation using an integral formulation. Using this formulation, the resulting implicit time integrator can be solved efficiently using treecode algorithms, and is able to take time steps much larger than the imposed CFL restrictions for a standard explicit integrator. Also, this method potentially recovers the magneto-static limit.

*Research supported by Air Force Office of Scientific Research, grant number FA9550-07-01-0092.

PP8 113 Fully EM algorithms for the quasi-neutral, zero-electron-inertia model* DENNIS HEWETT, *LLNL* An algorithm has been developed to compute the electromagnetic signature of impulsive currents in quasi-neutral, collisionless plasmas. Such plasmas are common in laser target chambers, space physics, and EMP generating events. Traditional models[1] used in this regime make the Darwin assumption that neglects purely EM waves. Computing electro-magnetic pulse behavior (EMP) requires the solution of the EM wave equations. Other algorithms designed to treat this problem [2] are susceptible to round-off problems in our applications. The current algorithm, based on the same physics model, is to be much more forgiving in regions of low density or low magnetic field. Results and initial V&V analysis will be presented. [1] "Low-frequency EM (Darwin) applications in plasma simulations," Hewett, CPC, 84, pg 243, May 1994 [2] "A fully electromagnetic model for high density plasma simulations" Jones, Thomas, Mason, and Winske, 13^{th} Conference on the Numerical Simulations of Plasmas, 1983.

*Work performed under the auspices of the Lawrence Livermore National Security, LLC, (LLNS) under Contract No. DE-AC52-07NA27344.

PP8 114 Relativistic Electron Scattering by Electromagnetic Ion Cyclotron Fluctuations: Test Particle Simulations KAIJUN LIU, *Los Alamos National Laboratory, Los Alamos, NM, 87545* DON S. LEMONS, *Department of Physics, Bethel College, North Newton, Kansas, 67117* DAN WINSKE, S. PETER GARY, *Los Alamos National Laboratory, Los Alamos, NM, 87545* Relativistic electron scattering by electromagnetic ion cyclotron (EMIC) fluctuations is studied using a test particle simulation code. The EMIC fluctuation input comes from a one dimensional, self-consistent hybrid simulation model and is due to the growth of the ion cyclotron instability driven by the ion temperature anisotropy, $T_{i\perp} > T_{i\|}$, in a magnetized, homogeneous, collisionless plasma with a single ion species. The test particle code follows the motion of relativistic test electron particles in the input EMIC fluctuations. The time evolution of the mean-square pitch angle change is calculated and used to estimate the pitch angle diffusion coefficient. Finally the results are compared with quasi-linear diffusion theory. The present study has applications to relativistic electron dynamics in the terrestrial magnetosphere.

PP8 115 Stochastic Analysis and Numerical Simulation of Velocity Space Diffusion of Charged Particles by Circularly Polarized Magnetic Waves Transverse to a Uniform Magnetic Field DON LEMONS, *Bethel College* KAIJUN LIU, DAN WINSKE, PETER GARY, *Los Alamos National Laboratory* We describe the velocity space diffusion of charged particles in a static magnetic field composed of a uniform field and a sum of transverse circularly polarized magnetic waves. When the wave sum has many terms the auto-correlation time over which particle orbits become effectively randomized is small compared to the time required for the particle distribution to change significantly. In this regime the deterministic equations of motion can be transformed into stochastic differential equations of motion that are valid over the longer time scale. The resulting velocity space diffusion function is consistent with that produced by quasi-linear theory. Numerical solutions of the deterministic equations of motion agree with the theory for all pitch angles, for different wave spectra, and for normalized wave energy densities less one. The theory is applied to the scattering of magnetospheric relativistic electrons from Alfven-cyclotron waves.

PP8 116 Implicit Plasma Kinetic Simulation Using The Jacobian-Free Newton-Krylov Method WILLIAM TAITANO, DANA KNOLL, *Idaho National Laboratory* LUIS CHACON, *Oak Ridge National Laboratory* The use of fully implicit time integration methods in kinetic simulation is still area of algorithmic research. A brute-force approach to simultaneously including the field equations and the particle distribution function would result in an intractable linear algebra problem. A number of algorithms have been put forward which rely on an extrapolation in time. They can be thought of as linearly implicit methods or one-step Newton methods. However, issues related to time accuracy of these methods still remain. We are pursuing a route to implicit plasma kinetic simulation which eliminates extrapolation, eliminates phase-space from the linear algebra problem, and converges the entire nonlinear system within a time step. We accomplish all this using the Jacobian-Free Newton-Krylov algorithm. The original research along these lines considered particle methods to advance the distribution function [1]. In the current research we are advancing the Vlasov equations on a grid. Results will be presented which highlight algorithmic details for single species electrostatic problems and coupled ion-electron electrostatic problems. [1] H. J. Kim, L. Chacón, G. Lapenta, "Fully implicit particle in cell algorithm," 47th Annual Meeting of the Division of Plasma Physics, Oct. 24-28, 2005, Denver, CO

PP8 117 The FACETS project: integrated core-edge-wall modeling with concurrent execution J.R. CARY, *Tech-X Corp.* S. BALAY, *ANL* J. CANDY, *Gen Atomics* J.A. CARLSSON, *Tech-X* R.H. COHEN, T. EPPERLY, *LLNL* D.J. ESTEP, *Colorado State U* M.R. FAHEY, *ORNL* R.J. GROEBNER, *Gen Atomics* A.H. HAKIM, *Tech-X* G.W. HAMMETT, K. INDIRESHKUMAR, *PPPL* S.E. KRUGER, *Tech-X* A.D. MALONEY, *ParaTools* D.C. McCUNE, *PPPL* L. McINNES, *ANL* A. MORRIS, *ParaTools* A. PANKIN, *Lehigh U* A. PLETZER, *Tech-X* A. PIGAROV, *UCSD* T.D. ROGNLIEN, *LLNL* S. SHASHARINA, *Tech-X* S. SHENDE, *ParaTools* S. VADLAMANI, *Tech-X* H. ZHANG, *ANL* FACETS TEAM,* The multi-institutional FACETS project has the physics goals of using computation to understand of how a consistent, coupled core-edge-wall plasma evolves, including energy flow, particle recycling, and the variation of power density on divertor plates with plasma under different conditions. FACETS is being developed to take advantage of Leadership Class Facilities (LCFs), while still being able to run on laptops with reduced fidelity models. This presentation will provide a high-level overview of the project, discussing the issues of componentization, solvers, performance monitoring, testing, visualization and first physics results for core-edge coupling.

*also J Cobb, S. Krasheninnikov, D. Wade-Stein

PP8 118 FACETS – Infrastructure for Integrated Fusion Modeling* SVETLANA SHASHARINA, JOHN CARY, JOHAN CARLSSON, AMMAR HAKIM, SCOTT KRUGER, MAHMOOD MIAH, ALEXANDER PLETZER, SRINATH VADLAMANI, DAVID WADE-STEIN, *Tech-X Corporation* SATISH BALAY, LOIS McINNES, HONG ZHANG, *Argonne National Laboratory* JEFF CANDY, *General Atomics* MARK FAHEY, *Oak Ridge Natioanal Laboratory* RON COHEN, TOM EPPERLY, TOM ROGNLIEN, *Lawrence Livermore National Laboratory* DON ESTEP, *Colorado State University* ALEXEI PANKIN, *Lehigh University* ALLEN MALONY, ALAN MORRIS, SAMEER SHENDE, *Paratools* KESHAVAMURTHY INDIRESHKUMAR, DOUGLAS McCUNE, *Princeton Plasma Physics Laboratory* ALEXANDER PIGAROV, *University of California San Diego* It is desirable that an infrastructure for integrated fusion modeling has support for: legacy and new components used interchangeably; consistent management of components lifecycle; allocating parallel resources consistent with the nature of participating components and the problem scope; components written in multiple programming languages; composition of sequentially and concurrently executing components respecting dependencies; tight and loose coupling of components; testing and validation of separate and integrated components; and use of multiple platforms from desktops to LCFs. In this poster we will describe the status of the FACETS with respect to these features.

*FACETS is funded by the DOE SciDAC program.

PP8 119 Development of an Arbitrary Curvilinear-Coordinate PIC Code CHRIS FICHTL, *UNM/Los Alamos National Laboratory* JOHN FINN, GIAN LUCA DELZANNO, *Los Alamos National Laboratory* We are developing an innovative new PIC code that couples a grid generation strategy to the standard PIC algorithm. This approach is very beneficial for studies of small objects immersed in plasmas. Standard PIC codes model curved surfaces with a stair-stepping technique, which highly distorts the shapes of small objects. This can become quite problematic when calculating forces on the surface of the object. Our grid generation strategy conforms to objects of arbitrary shape, eliminating such problems as stair-stepping along curved boundaries, and thus allows us to simulate complicated physical structures very accurately. Furthermore, we have developed a semi-implicit particle mover for based on a generalization of the leapfrog method to arbitrary (including nonorthogonal) grids. We show our mover to be symplectic and thus it preserves phase-space area exactly. Extensive testing has shown that it also conserves energy to high accuracy. Our new code is validated using OML charging theory for spherical and cylindrical dust grains. Further tests include the charging of an electron-emitting dust grain in a uniform plasma. The final goal is to study the forces between two emitting grains of like charge.

PP8 120 Modeling a short cold cathode DC discharge device with controllable plasma parameters* ANATOLY KUDRYAVTSEV, *SPbSU* STEVEN ADAMS, *AFRL* VLADIMIR DEMIDOV, *UES/WVU* YEVGENY BOGDANOV, *SPbSU* A short (without positive column) DC gas-discharge device with a cold cathode has been modeled. The device consists of the plane disk-shaped cathode and anode while the inter-electrode gap is bounded by a cylindrical wall. The cathode and anode are each 2.5 cm in diameter, and the inter-electrode gap is 12 mm. The wall is made of conducting parts divided by an insulator. The modeling has been performed for argon plasma at 1 Torr pressure. It is demonstrated in the model that spatial distributions of electron density and temperature and argon metastable atom density depend on the DC voltage applied to different conducting parts of the wall. Applied voltage can trap within the device volume energetic electrons arising from atomic and molecular processes in the plasma. This leads to a modification in the heating of slow electrons by energetic electrons and as a result modifies the controlling plasma parameters.

*This work has been supported by AFOSR.

PP8 121 Efficient hybrid algorithms for collisional plasma simulation* A.M. DIMITS, B.I. COHEN, *LLNL* R.E. CAFLISCH, C.M. WANG, Y. HUANG, *UCLA* We report on the development of efficient hybrid simulation algorithms for plasma systems that span a wide range of collisionality. Investigations of their performance, using ion-sheath and electron-transport test problems, are presented. In these schemes the distribution function is decomposed of into kinetic and fluid components. The fluid component is treated via Eulerian fluid simulation methods. In one class of algorithms, the kinetic component is treated using a combination of fixed-weight particle-in-cell (PIC) and binary Monte-Carlo collision methods. Particles are created by sampling from the fluid component, and paired for collisions with the kinetic particles. In the other class of algorithms, the kinetic component is treated using evolving-weight delta-f-PIC schemes and collision-field algorithms. The performance these algorithms depends strongly on the particular sets of criteria for (a) exchange between the particle and fluid components and (b) creation, destruction, and retention of the simulation particles.

*Work performed for U.S. DOE by LLNL under Contract DE-AC52-07NA27344.

PP8 122 A Novel Approach to Solving the Vlasov-Fokker-Planck Equations through Particle-In-Cell Hybridization PAUL CUMMINGS, ALEC THOMAS, *University of Michigan* A new computational method for modeling ultra-fast, ultra-intense laser-solid and laser-plasma interactions is proposed. The method

consists of a hybridization of the particle-in-cell technique and a direct solution to the collisional Vlasov equation with the Krook operator, wherein the Vlasov equation is expanded in velocity space using Cartesian tensors, and the higher-order terms serve as a source of particles and "holes" to be tracked by PIC methods. The mathematics underlying the solution method for a simple implementation are presented and analyzed; this implementation features one spatial dimension and truncates the expansion to first-order. A computational scheme for this implementation of the solution method is presented. More advanced implementations of the solution method, including retaining second- order expansion terms and replacing the Krook model with the Fokker-Planck model, are discussed.

PP8 123 Magnetic Insulation and the Effects of External Magnetic Fields on RF Cavity Operation in Muon Accelerators* KEVIN PAUL, SETH VEITZER, *Tech-X Corporation* ROBERT PALMER, HAROLD KIRK, DIKTYS STRATAKIS, *Brookhaven National Laboratory* High-gradient RF cavities operating in strong external magnetic fields are required for efficient and cost-effective muon ionization cooling for neutrino factories and muon colliders. It has been observed, however, that strong external magnetic fields degrade the maximum achievable gradient of typical RF cavities. One possible explanation for this is that the external magnetic fields focus accelerated surface-emitted electrons within the cavity to localized regions on the cavity surface, increasing the potential for surface damage and breakdown. We present preliminary results of a study to perform simulations of RF cavity operation in the presence of magnetic fields. We perform these simulations with the electromagnetic particle-in-cell code VORPAL, which tracks the emitted particles through the cavity and external magnetic fields, including the effects of space-charge on the emitted particles. The simulations model heating of the cavity surfaces and temperature-dependent field-induced, electron-induced, and ion-induced emission.

*Work supported by the U.S. Department of Energy SBIR program, contract No. DE-SC0000841.

PP8 124 Wavelet-based density estimation for noise reduction in plasma simulations using particles R. NGUYEN VAN YEN, *Ecole Normale Superieure, Paris* D. DEL-CASTILLO-NEGRETE, *Oak Ridge National Laboratory* K. SCHNEIDER, *Universite Aix-Marseille* M. FARGE, *Ecole Normale Superieure, Paris* G. CHEN, *Oak ridge national laboratory* A limitation of particle methods is the inherent noise caused by limited statistical sampling with finite number of particles. Thus, a key issue for the success of these methods is the development of noise reduction techniques in the reconstruction of the particle distribution function from discrete particle data. Here we propose and study a method based on wavelets, previously introduced in the statistical literature to estimate probability densities given a finite number of independent measurements. Its application to plasma simulations can be viewed as a natural extension of the finite size particles (FSP) approach, with the advantage of estimating more accurately distribution functions that have localized sharp features. Furthermore, the moments of the particle distribution function can be preserved with a good accuracy, and there is no constraint on the dimensionality of the system. It is shown that the computational cost of the denoising stage is of the same order as one time step of a FSP simulation. The wavelet method is compared with the recently introduced proper orthogonal decomposition approach in Ref. [D. del-Castillo-Negrete, et al., Phys. Plasma, **15** 092308 (2008)].

PP8 125 Collisionless stochastic electron heating in a plasma slab ALEXEY AREFIEV, VLADIMIR KHUDIK, *Institute for Fusion Studies, The University of Texas at Austin* We find the rate and the saturation energy for stochastic collisionless electron heating by an AC field in a plasma slab. The work is motivated by "two-sided" vacuum heating of radially moving electrons in laser-irradiated microclusters [1]. We consider an ideally conducting slab that freely emits electrons in an AC electric field. The interaction of an emitted electron with the field is analogous to a 1D random walk in velocity space, with the time between the walk steps proportional to the travel time through the slab ($t_s \sim 1/|v|$). The resulting increase of the average electron energy is slower than previously expected (t^2) [1] because of long delays between the interactions for slower electrons. The heating saturates when a considerable number of electrons reach a velocity limit where the Chirikov resonance-overlap criterion is not satisfied. The velocity saturation might alter the resonant heating mechanism proposed in [2], since the travel-time t_s at the limiting velocity can significantly exceed the period of the AC field. [1] Phys. Plasmas 12, 056706 (2005); [2] Phys. Plasmas 12, 056703 (2005).

SESSION PM9: MINI-CONFERENCE ON UNSTEADY RECONNECTION IN LABORATORY AND NATURE IV: TURBULENCE AND MULTIPLE RECONNECTIONS

Wednesday Afternoon, 4 November 2009
Regency V at 14:00
Masaaki Yamada, Princeton Plasma Physics Laboratory, presiding

14:00

PM9 1 Three Dimensional Fast Reconnection in the Magneto-hydrodynamic Limit: Theory* ETHAN VISHNIAC, *McMaster University* ALEX LAZARIAN, *University of Wisconsin* GRZEGORZ KOWAL, KATARZYNA OTMIANOWSKA-MAZUR, *Jagiellonian University* We examine the role of turbulence in mediating fast reconnection in three dimensions. We work in the single fluid MHD limit, appropriate to the interiors of stars and denser parts of accretion disks, although the model we sketch here should be broadly applicable. In the limit of infinitesimal resistivity, turbulence provides a roughness to the flow and to the magnetic field which renders the definition of magnetic field lines and fluid flow lines somewhat problematic. In this context, we generalize the Sweet-Parker current sheet to include turbulence. We note that in three dimensions this leads to a plasma outflow zone which is much wider than the current sheet, and whose width depends only on the properties of the turbulence. If this sets the speed of reconnection, then it is always of order the local turbulent velocity. We briefly discuss numerical tests of this conjecture and conclude that this conjecture is supported by the available evidence.

*Supported in part by the National Science and Engineering Council of Canada.

14:25
PM9 2 Non-stationary Magnetic Reconnection: plasmoids, turbulence, and what it all means DMITRI UZDENSKY,* *Princeton University/CMSO* NUNO LOUREIRO, *IPFN, IST Lisbon* ALEXANDER SCHEKOCHIHIN, *R. Peierls Centre for Theoretical Physics, University of Oxford* In this contribution the recent progress on understanding the role of secondary tearing instabilities and small-scale turbulence in resistive-MHD reconnection with very large Lundquist numbers $S \geqslant 10^4$ is reviewed. It is argued that the resulting formation of multiple plasmoids and their rapid nonlinear evolution greatly affect the basic structure of the reconnection layer and force upon us a total revision of the conventional picture of the reconnection processes. In particular, the very definition of the reconnection rate and its scaling with S are discussed and compared with the results of recent numerical simulations.

*supported by NSF

14:45
PM9 3 Turbulent Reconnection in the Magnetic Reconnection Experiment (MRX) S. DORFMAN, H. JI, M. YAMADA, E. OZ, J. YOO, *CMSO, PPPL* W. DAUGHTON, V. ROYTERSHTEYN, *LANL* One of the key open questions in Magnetic Reconnection is the nature of the mechanism that governs the reconnection rate in real astrophysical and laboratory systems. For collisonless plasmas, the Hall effect removes an important bottleneck to fast reconnection as the heavier ions exit the reconnection layer over a broader region [1]. However, the Hall term cannot balance the reconnection electric field at the layer center, and the 2-D, collisionless expression for the electric field due to particle dynamics [2] has been shown to be insufficient in the Magnetic Reconnection Experiment (MRX) [1,3]. Turbulent 3-D effects such as lower hybrid frequency range fluctuations [4] may play an important role in fast reconnection in MRX. These electromagnetic fluctuations tend to be associated with high local currents and a rapid local reconnection rate. The precise relation of these fluctuations and associated 3-D asymmetries to fast reconnection is a topic of active investigations; the most up to date results will be discussed. This work was supported by NDSEG, DOE, NASA, and NSF. [1] Y. Ren, et al., Phys. Plasmas 15, 082113 (2008). [2] M. Hesse, et al., Phys. Plasmas, 6:1781 (1999). [3] S. Dorfman, et al., Phys. Plasmas 15, 102107 (2008). [4] H. Ji, et al., Phys.Rev.Lett. 92 (2004) 115001.

15:10
PM9 4 Statistical Properties of Magnetic Reconnection in MHD turbulence SERGIO SERVIDIO, *Univ. of Calabria* WILLIAM MATTHAEUS, *Univ. of Delware* PAUL CASSAK, *Univ. of West Virginia* MICHAEL SHAY, *Univ. of Delaware* PABLO DMITRUK, *Univ. of Buenos Aires* Magnetic reconnection is an integral part of MHD turbulence[1] in that the fragmentation of magnetic eddies into smaller structures necessarily involves change of magnetic topology. To better understand this relationship, recently the properties of thousands of magnetic reconnection events in moderate Reynolds number MHD turbulence have been studied [1] using 2D spectral method simulations of compressible and incompressible MHD. Reconnection between magnetic islands, different in size and energy, occurs locally and sporadically in time. The associated reconnection rates are distributed over a wide range of values and scale with the geometry of the diffusion region. Matching classical turbulence analysis with the Sweet-Parker theory, the main statistical features of these multiscale reconnection events are identified. Magnetic reconnection in turbulence can be described through an asymmetric Sweet-Parker model, in which the parameters that control the reconnection rates are determined by turbulence itself. This new and general perspective on reconnection is relevant in space and astrophysical systems, where plasma is generally in a fully nonlinear regime. [1] W. Matthaeus and S. Lamkin, Phys. Fluids, 29, 2513 (1986). [2] S. Servidio et al, PRL, 102, 115003 (2009).

15:35
PM9 5 The time-dependent structure of the electron reconnection layer MICHAEL HESSE, SEIJI ZENITANI, MASHA KUZNETSOVA, ALEX KLIMAS, *NASA GSFC* Collisionless magnetic reconnection is often associated with time-dependent behavior. Specifically, current layers in the diffusion region can become unstable to tearing-type instabilities on one hand, or to instabilities with current-aligned wave vectors on the other. In the former case, the growth of tearing instabilities typically leads to the production of magnetic islands, which potentially provide feedback on the reconnection process itself, as well as on the rate of reconnection. The second class on instabilities tend to modulate the current layer along the direction of the current flow, for instance generating kink-type perturbations, or smaller-scale turbulence with the potential to broaden the current layer. All of these processes contribute to rendering magnetic reconnection time-dependent. In this presentation, we will provide a summary of these effects, and a discussion of how much they contribute to the overall magnetic reconnection rate.

16:00
PM9 6 Unsteady reconnection in MHD models GIOVANNI LAPENTA, *KU Leuven* Within a MHD approach we find magnetic reconnection to progress in two entirely different ways. The first is well known: the laminar Sweet-Parker process. But a second, completely different and chaotic reconnection process is possible [1]. This regime has properties of immediate practical relevance: (i) it is much faster, developing on scales of the order of the Alfvén time, and (ii) the areas of reconnection become distributed chaotically over a macroscopic region. The onset of the faster process is the formation of closed-circulation patterns where the jets going out of the reconnection regions turn around and force their way back in, carrying along copious amounts of magnetic flux. We further investigate the presence of unsteady reconnection regimes in the RSX experiment in Los Alamos [2]. Work in collaboration with: Intrator TP, Sun X, Dorf L and Furno I. [1] Lapenta, G., Self-Feeding Turbulent Magnetic Reconnection on Macroscopic Scales, Phys. Rev. Lett. 100, 235001 (2008) [2] Intrator TP, Sun X, Dorf L, Lapenta G and Furno I, Experimental onset threshold and magnetic pressure pileup for 3D reconnection, Nature-Physics, 5, 521 - 526 (2009)

16:25
PM9 7 Electron scale structures in collisionless magnetic reconnection with multiple reconnection sites SURJALAL SHARMA, NEERAJ JAIN, *University of Maryland, College Park, MD-20742* The early time-dependent phase of collisionless reconnection, which is dominated by electron dynamics, is investigated using electron-magnetohydrodynamic simulations. In EMHD the frozen-in condition of magnetic field breaks down due to electron inertia, which is the dominant non-ideal term in generalized Ohm's law for very thin current sheets (CS) with thicknesses of the order of electron skin depth. This is in contrast with ion-scale current sheets for which divergence of pressure tensor is the dominant term. Simulations initialized with multi-wavelength

perturbations lead to reconnection at multiple sites one of which is dominant and others are secondary. The current sheet bifurcation in the outflow regions limits the length of the reconnecting CS which is further reduced by the secondary instabilities growing on the bifurcated CS. The interaction of inflow to the secondary site and outflow from the central dominant site gives rise to the nested structure of quadrupoles. These structures have important implications for multi-spacecraft missions in Earth's magnetotail.

16:45

PM9 8 A new mechanism for the generation of anomalous cosmic rays: dissipation of the sectored heliospheric magnetic field in the heliosheath J.F. DRAKE, *University of Maryland* M. OPHER, *George Mason University* M. SWISDAK, K. SCHOEFFLER, *University of Maryland* The recent observations of the anomalous cosmic ray (ACR) energy spectrum as Voyagers 1 and 2 crossed the heliospheric termination shock have called into question the conventional shock source of these energetic particles. We suggest that the sectored heliospheric magnetic field, which results from the flapping of the heliospheric current sheet, piles up as it approaches the heliopause, narrowing the current sheets that separate the sectors and triggering the onset of collisionless magnetic reconnection. MHD simulations of the global heliosphere reveal the structure of sectored field and pileup. Particle-in-cell simulations reveal that the current layers break up into a turbulent bath of magnetic islands that merge to release a large fraction of the energy in the sectored magnetic field. Most of the magnetic energy goes into energetic ions with significant but smaller amounts of energy going into electrons. The ACR differential energy spectrum takes the form of a power law with a spectral index slightly above 1.5, which is consistent with the Voyager observations. The model has the potential to explain several other key observations, including the spectra of super-Alfvenic ions seen throughout the heliosphere.

17:10

PM9 9 The Role of Turbulent Outflow Jets in Electron-Positron Plasmas MARC SWISDAK, YI-HSIN LIU, JAMES DRAKE, *U. of Maryland* Numerical simulations of reconnection in electron-positron (pair) plasmas provide an interesting window into the role turbulence plays in current theories of whistler-mediated Hall reconnection. Because of the system's mass symmetry the Hall term vanishes from the generalized Ohm's law, suggesting that perhaps pair reconnection is slow, as in the classic Sweet-Parker picture. Large particle-in-cell simulations of pair reconnection confirm that the reconnection rate remains fast even as the system size changes by a factor of 8. For the largest systems a Weibel-like temperature anisotropy instability in the X-line outflow broadens the current layer and permits fast reconnection. This instability can be suppressed both artificially and for certain parameter choices, leading to non-steady behavior and a decrease in the reconnection rate.

SESSION SR1: MAXWELL PRIZE ADDRESS: TAMING MAGNETICALLY CONFINED PLASMAS WITH RF WAVES: A HISTORICAL PERSPECTIVE

Thursday Morning, 5 November 2009; Centennial I-II at 8:00; Ronald Davidson, Princeton Plasma Physics Laboratory, presiding

8:00

SR1 1 Taming Magnetically Confined Plasmas with RF Waves: A Historical Perspective.*

MIKLOS PORKOLAB, *MIT Plasma Science and Fusion Center, Cambridge, MA 02139*

Heating and profile control by RF waves in magnetic fusion experiments has led to the development of a new area of physics, namely wave propagation and absorption in high temperature plasmas in complex magnetic field geometries. In addition, the development of high power microwave sources as well as novel antenna structures capable of handling high RF powers has also been necessary. In this talk I shall summarize the historical progression of relevant results in three frequency regimes, namely the ion cyclotron range of frequencies (ICRF), the electron cyclotron frequency and its harmonics (ECRH), and the lower hybrid frequency range (LHRF). In the ICRF regime breakthrough heating results were obtained in the 1980s in tokamaks with good confinement of energetic ions, such as PLT, TFTR and JET. In the period of late 1970s to mid 1980s the theory of RF current drive (LHCD, ECCD and that of fast wave, or FWCD) was developed. Soon thereafter efficient lower hybrid current drive was demonstrated in tokamak experiments such as Versator II, Alcator–C and PLT, and later JT60-U, Tore-Supra and JET. High harmonic FWCD has been also demonstrated on DIII-D and NSTX. Long pulse multi-MW LHCD experiments are now in preparation on the new superconducting tokamaks EAST (China) and K-STAR (Korea). ECRH results in the 1980s and beyond progressed rapidly with the development of gyrotron sources at the MW level and subsequently efficient heating and current drive was demonstrated on DIII-D, Asdex-U, JT-60U and TCV, including the stabilization of neoclassical tearing modes. Recent gyrotron tube development at the MW level at 170 GHz ensures the availability of ECH and ECCD on ITER. Finally, new results on RF induced transport phenomena have been discovered, such as enhanced plasma rotation and flow drive that hold promise for optimizing ITER performance.

*Work supported by the US Department of Energy.

SESSION TI2: FLOWS AND TURBULENCE IN LABORATORY AND SPACE

Thursday Morning, 5 November 2009; Centennial I at 9:30; William Amatucci, Naval Research Laboratory, presiding

9:30

TI2 1 How ions really flow to objects in magnetized plasmas.

IAN H. HUTCHINSON, *Plasma Science and Fusion Center, MIT, Cambridge, MA, USA*

A new exact, 3-D, analytic solution has been obtained of the drift equations for the plasma perturbation around an ion-collecting object of essentially arbitrary shape in a flowing strongly-magnetized plasma [1]. It provides a direct rigorous theory of magnetized Langmuir probes, especially Mach probes, and of other diverse plasma-object interactions. The cross-field flow is a combination of external drifts and self-consistent perturbation by the object. This convective calculation is valid for objects smaller than the characteristic size of turbulent plasma flow structures: the usual situation. The Mach probe calibration obtained agrees with prior diffusive theory, but now accounts for cross-field diamagnetic drifts, which are not ignorable. Their contribution is non-intuitive, in that the *electron* diamagnetic velocity is dominant. Consequently, transverse Mach probes measure a combination of ExB and diamagnetic drifts. The analytic fluid solution compares very favorably with numerical kinetic-parallel-distribution calculations [2]. And 3-D PIC calculations for a spherical object, accounting for finite gyro-radius, also verify its regime of applicability. [1] I.H. Hutchinson, Phys Plasmas, 15, 123503 (2008) [2] L. Patacchini and I.H. Hutchinson submitted to Phys Rev E.

10:00
TI2 2 Plasma Experiments and the Environment.*
ALFRED WONG, *Nonlinear Ion Dynamics, LLC*

Laboratory and Field experiments demonstrate nonlinear interactions of Electromagnetic waves and plasma waves in the presence of free energy sources. Viewing the earth's atmosphere immersed in a magnetic mirror, a number of environmental remediation concepts are presented. Waves at ion cyclotron frequencies injected into an auroral ionosphere are used to selectively excite ion species and eject them out through the "magnetic field cusp." The roles of the parametric decay instabilities and the auroral kilometric radiation in the presence of electron and ion loss cone distributions are considered in the presence of solar wind and radiation. There is sufficient convection of CO and CO_2 throughout the atmosphere for the sequestration of greenhouse gases in geospace. Active experiments with atmospheric platforms are presented to illustrate how charge-neutral coupling enhances transports from lower to upper atmosphere. References: Wong, A. Y., J. Chen, L. C. Lee and L. Y. Liu, Phys Rev Lett.102, 105002 (2009); Leyser, T.B. and A, Y, Wong, Rev. Geophys. 47, RG1001 (2009).

*International Foundation for Science, Health and the Environment

10:30
TI2 3 Increased Upstream Ionization Due to Spontaneous Formation of a Double Layer in an Expanding Plasma.*
EARL SCIME, *West Virginia University*

We report observations that confirm a theoretical prediction that formation of a current-free double layer in a plasma expanding into a chamber of larger diameter is accompanied by an increase in ionization upstream of the double layer. The theoretical model argues that the increased ionization is needed to balance the difference in diffusive losses upstream and downstream of the expansion region. In our expanding helicon source, we find that the upstream plasma density increases sharply at the same driving frequency at which a double layer appears. For driving frequencies at which no double layer appears, large electrostatic instabilities are observed. Time resolved laser induced fluorescence and electrostatic probe measurements suggest that the double layer initially forms for all driving frequencies. However, for particularly strong double layers, the instability appears early in the discharge and disrupts the double layer. The double layer is identified in this work through observations of an acceleration population of ions downstream of the plasma source.

*This work was supported by NSF award PHY-0611571.

11:00
TI2 4 Strong magnetohydrodynamic turbulence with cross helicity.*
JEAN C. PEREZ, *University of Wisconsin-Madison*

Magnetohydrodynamics (MHD) is invoked to model different turbulent phenomena in magnetized plasmas. For instance, the energy spectrum of velocity and magnetic fluctuations in the solar wind obeys a power law spanning a broad range of scales, which has been associated to an inertial range of incompressible MHD turbulence. In addition to the total energy, ideal MHD equations conserve cross helicity which also undergoes a turbulent cascade to small scales. However, most of the current understanding of MHD turbulence is limited to the zero cross helicity case. Cross helicity quantifies the energy imbalance in Alfvénic fluctuations oppositely moving along the background magnetic field. Although it is well established that turbulence in the solar wind is dominated by fluctuations moving away from the sun, only in recent years there have been an increased interest in addressing the role of cross helicity in MHD turbulence. Moreover, numerical simulations have also revealed the fundamental role that cross helicity plays in the turbulent cascade. In this talk, we present results from high resolution numerical simulations of steady-state incompressible MHD turbulence, with and without cross helicity. We show that in the zero cross helicity case the configuration space spontaneously develops regions of positive and negative cross-helicity. The obtained scaling of the energy spectrum ($E^{\pm}$) of fluctuations moving in opposite directions is consistent with simulations of incompressible MHD *without* cross-helicity by other groups. When cross helicity is injected, E^+ and E^- maintain the same inertial range scaling, but with differing amplitudes depending on the amount of injected cross-helicity. It is argued that in each of these correlated regions of *imbalance*, the scaling of E^+ and E^- is the same. When the total energy spectrum $E^+ + E^-$ is averaged over those regions, the inertial range scaling is the same regardless of the amount of cross helicity in the system.

*This work was supported by the U.S. DOE under Grant No. DE-FG02-07ER54932, by the NSF Center for Magnetic Self-Organization in Laboratory and Astrophysical Plasmas at the UW-Madison, and in part by the NSF under Grant No. NSF PHY0821899.

11:30
TI2 5 Modification of turbulence and turbulent transport associated with a confinement transition in LAPD.*
TROY CARTER,† *Department of Physics and Astronomy, UCLA*

Azimuthal flow is driven in the edge of the Large Plasma Device (LAPD) through biasing a section of the vacuum vessel relative to the plasma source cathode. As the applied bias exceeds a threshold, a transition in radial particle confinement is observed, evidenced by a dramatic steepening in the density profile, similar to the L- to H-mode transition in toroidal confinement devices. The threshold behavior and dynamic behavior of radial transport is related to flow penetration and the degree of spatial overlap between the flow shear and density gradient profiles. An investigation of the changes in turbulence and turbulent particle transport associated with the confinement transition is presented. Two-dimensional cross-correlation measurements show that the spatial coherence of edge turbulence in LAPD changes significantly with biasing. The azimuthal correlation in the turbulence increases dramatically, while the radial correlation length is little altered. Turbulent amplitude is reduced at the transition, particularly in electric field fluctuations, but the dominant change observed is in the cross-phase between density and electric field fluctuations. The changes in cross-phase lead to a suppression and then apparent reversal of turbulent particle flux as the threshold is exceeded.

*Research supported by NSF and DOE
†In collaboration with J.E. Maggs and P. Popovich

12:00
TI2 6 A second look at zonal flows.*
P.H. DIAMOND,† *Center for Astrophysics and Space Sciences, University of California, San Diego, La Jolla, CA 92093-0424 USA*

Despite the fact that the paradigm of self-regulating drift wave-zonal flow turbulence is over fifteen years old, many relevant fundamental questions remain. In particular, nearly all the theoretical work on zonal flow generation has approached the problem via an essentially linear modulational analysis of some pre-existing turbulent state. In this talk, we report on exact momentum theorems which constrain the zonal flow and wave momentum (pseudomomentum), and relate flow evolution to the driving flux, potential enstrophy, dissipation, etc., as well as flow drag. These theorems are derived for both reduced fluid and gyrokinetic models, and severely constrain possible zonal flow growth, via the zonal momentum budget. Since the zonal momentum balance includes potential enstrophy convergence, turbulence spreading dynamics is intrinsically coupled to zonal flow momentum. Results for spreading, collisionless saturation and zonal flow evolution in flux-driven systems will be discussed. The relation between kinetic pseudomomentum and dynamic pressure in kinetic energy principles for self-gravitating systems has been determined and will be presented, along with implications for phase space granulation evolution.

*This research was supported by U.S Department of Energy Grant Nos. DE-FG02-04ER54738, DE-FC02-08ER54959 and DE-FC02-08ER54983.
†In collaboration with: Y. Kosuga, C. McDevitt, G. Dif-Pradalier, M. Malkov, X. Garbet, O.D. Gurcan, T.S. Hahm

SESSION TI3: RF IN TOKAMAKS AND ITER
Thursday Morning, 5 November 2009; Centennial II at 9:30; Paul Bonoli, Massachusetts Institute of Technology, presiding

9:30
TI3 1 Iterated Finite Orbit Monte Carlo Simulation with Full Wave Fields for Tokamak ICRF Wave Heating Experiments.*
M. CHOI, *General Atomics*

A predictive understanding of ICRF wave heating is important for tokamak experiments and ITER. Finite-orbit effects due to drift motion of non-Maxwellian species may significantly modify the ICRF wave propagation and absorption in the plasma. To self-consistently obtain wave heating and fast-ion velocity space information, the 5D finite-orbit Monte-Carlo plasma distribution solver ORBIT-RF is integrated with the 2D full-wave code AORSA. To evaluate the finite-orbit effects on wave heating, the ORBIT-RF wave absorption model has been validated against linear full-wave zero orbit-width predictions from CQL3D/AORSA and measurements in Alcator C-Mod and DIII-D experiments for various ion cyclotron harmonics. Systematic comparison performed with an initial Maxwellian distribution largely reproduces linear absorption directly evaluated by AORSA dielectric tensor. An inward shift of ORBIT-RF absorption peak for high harmonics compared with that of AORSA has been observed. This inward shift may be indicative of finite orbit effects, which can produce a noticeable change in the radial absorption profile. DIII-D simulations based on combined ray-tracing zero orbit-width calculations using GENRAY/CQL3D show discrepancies with the measured FIDA spectroscopic data. To assess the finite-orbit effects on this difference, the non-Maxwellian plasma distribution evolution calculated by

ORBIT-RF is iterated with wave fields computed from AORSA including quasilinear and collisional orbit diffusion. To accurately start the ORBIT-RF/AORSA iterations, beam-ion distributions computed from PTRANSP from experimental profiles are used as initial conditions. Comparison of ORBIT-RF/AORSA results against FIDA measurements of fast-ion distribution and results from CQL3D/AORSA with zero orbit assumption will be presented.

*Supported by US DOE under DE-FG03-95ER54309.

10:00
TI3 2 Advances in High-Harmonic Fast Wave Physics in the National Spherical Torus Experiment.*
GARY TAYLOR, *Princeton Plasma Physics Laboratory, Princeton University*

Improved core high-harmonic fast wave (HHFW) heating, particularly at longer wavelengths and during low-density start-up and current ramp-up, has now been obtained by lowering the edge density with lithium conditioning, thereby moving the propagation onset away from the vessel wall. Significant core electron heating of deuterium neutral beam injection (NBI) fuelled H-modes has been observed for the first time over a range of launched wavelengths. The observed broadening of the electron heating profile in H-mode relative to L-mode plasmas is consistent with simulations obtained with ray tracing and full wave models. Newly taken camera images indicate that fast wave interactions can deposit considerable RF energy on the outboard divertor plate, especially at longer wavelengths that begin to propagate closer to the vessel walls. Edge power loss can also arise from HHFW-generated parametric decay instabilities that drive ions in the edge onto direct loss orbits that intersect the wall, and may be the cause for an observed drag on edge toroidal rotation in combined HHFW and NBI discharges. Fast-Ion D-alpha emission clearly shows fast-ion profile broadening in the plasma core that is much greater than predicted by Fokker-Planck modeling when HHFW power is applied to NBI-fuelled plasmas, pointing to the need for a full-orbit treatment in the simulation. Large ELMs have been observed immediately following the termination of RF power, whether the power turn off is programmed or due to antenna arcing. RF power has been successfully applied during large ELMs by setting the source reflection coefficient trip levels to relatively high values – an approach potentially important for ITER ICRF heating. Plans for an HHFW ELM-resilience upgrade will be presented.

*Supported by USDOE Contract No. DE-AC02-09CH11466 and DE-AC05-00OR2272.

10:30
TI3 3 Plasma wave simulation based on a versatile FEM solver on Alcator C-Mod.*
SYUN'ICHI SHIRAIWA, *PSFC, MIT*

A new efficient full wave simulation code of the lower hybrid (LH) wave was developed using the finite element method (FEM). A dielectric tensor consisting of the cold plasma contribution and the electron Landau damping (ELD) was used. The non-trivial problem of introducing non-local hot plasma effects into an FEM solver was addressed by iteratively solving the coupled problem of the Maxwell's equations with the convolution integral. With this approach, the EM problem is numerically sparse, and the computational requirements are reduced significantly compared to spectral domain solvers [1]. The simulation of an Alcator C-Mod scale plasma has been done on a desktop computer, suggesting the possibility of an ITER scale plasma simulation. The algorithm was implemented using a general purpose FEM software, COMSOL Multiphysics, and the simulation results of a Maxwellian tokamak plasma showed good agreement with ray tracing calculations in the strong single pass absorption regime. Integration of a Fokker-Planck calculation for a more realistic non-Maxwellian plasma is underway and initial results show reasonable shift of the power absorption towards the plasma edge [2]. Importantly, the FEM approach allows seamless handling of the core, SOL, and antenna regions. This flexibility has been exploited to address issues of antenna-plasma coupling in the LH and ICRF frequency ranges. Techniques to use the FEM package for this purpose were validated by solving the LH grill antenna coupling problem whose analytic solution is known. The code has been applied to a new Alcator C-Mod ICRF antenna to assess the antenna near field pattern [1] J. C. Wright, et. al., Comput. Phys. 4, 545 (2008) [2] O. Meneghini, et. al., this conference [3] M. Garrett, et. al., this conference

*Work supported by USDOE awards DE-FC02-99ER54512 and DE-AC02-76CH03073.

11:00
TI3 4 Understanding and Predicting the Dynamics of Tokamak Discharges during Startup and Rampdown.*
G.L. JACKSON, *General Atomics*

Understanding the dynamics of plasma startup and termination is important for present tokamaks and for predictive modeling of future burning plasma devices such as ITER. We report on experiments in the DIII-D tokamak that explore the plasma startup and rampdown phases, and on the benchmarking of transport models. Key issues have been examined such as plasma initiation and burnthrough with limited inductive voltage and achieving flattop and maximum burn within the technical limits of coil systems and their actuators while maintaining the desired q profile. Successful rampdown requires scenarios consistent with technical limits, including controlled H-L transitions, while avoiding vertical instabilities, additional Ohmic transformer flux consumption, and density limit disruptions. The ITER baseline startup and rampdown scenarios have been demonstrated in DIII-D by scaling the dynamic phases by the ratio of the resistive current

penetration time between the devices while maintaining the same I/aB and scaled shape within the phase. Discharges were typically initiated with an inductive electric field typical of ITER, 0.3 V/m, most with 2nd harmonic electron cyclotron (EC) assist. A fast framing camera was used during breakdown and burnthrough to study the formation physics. An improved "large aperture" ITER startup scenario was developed and aperture reduction in rampdown was found to be essential to avoid instabilities. Extrapolation of these scenarios to burning plasma devices requires model validation. Current evolution using neoclassical conductivity in the Corsica code agrees with rampup experiments, but prediction of the temperature and internal inductance evolution using the Coppi-Tang model for electron energy transport is not yet accurate enough to allow extrapolation to future devices.

*Supported by US DOE under DE-FG03-95ER54309.

11:30
TI3 5 Kinetic theory of geodesic acoustic modes.
ANDREI SMOLYAKOV, *CEA Cadarache/University of Saskatchewan, Canada*

Geodesic Acoustic Modes (GAM are linear eigen-modes of poloidal plasma rotation supported by plasma compressibility in toroidal geometry. GAMs are linearly coupled to drift-waves via toroidal side-bands of plasma pressure, can be nonlinearly driven by Reynolds stress from small-scale fluctuations (similar to Zonal Flows) and therefore expected to play an important role in dynamics of drift-wave turbulence. GAMs have also been prominently featured due to their inherent relation to Beta Alfven Eigen-modes (BAE), particularly in plasmas with highly energetic particles Multiple GAM and BEA modes were observed in high-temperature tokamak plasmas and are currently subject of active experimental and theoretical studies. This talk will describe the currents status of GAM/BEA theory. New results will be presented emphasizing the relation of GAM/BAE modes with neoclassical rotation in a tokamak. It is shown that the GAM intrinsically involve anisotropic perturbations of plasma pressure (corresponding to parallel viscosity). Moreover, the GAMs and standard equilibrium (neoclassical) plasma rotation represent two limit cases of poloidal plasma rotation: high frequency rotational mode (GAM) and the low frequency over damped (damping is larger than the real part of the frequency) mode of the neoclassical equilibrium rotation. Most importantly, new regimes of global GAM/BAE modes will be reported. These regimes occurs as a result of the parallel kinetic response of electrons which has not been included previously. It is shown that in certain regimes (corresponding to global modes), the electron response becomes strongly electromagnetic and GAM/BAE modes have significant electromagnetic component in the side-bands (thus it is not of the Alfven type). Resulting modifications in the mode dispersion and mode damping will be presented and potential consequences for GAM/BAE excitation and electron transport will be discussed.

SESSION TO4: LASER WAKEFIELD ACCELERATORS AND RADIATION SOURCES
Thursday Morning, 5 November 2009
Regency VI at 9:30
David Bruhwiler, Tech-X Corporation, presiding

9:30
TO4 1 Injected wake field acceleration with a 40 MeV electron linac S. KRAFT, A. JOCHMANN, C. ERLER, A. DEBUS, M. BUSSMANN, R. SAUERBREY, U. SCHRAMM, T.E. COWAN, *Forschungszentrum Dresden-Rossendorf* Over the last years multiple research groups achieved multi-MeV to GeV electron beams. Ultrashort bunches and a very low emittance combined with a high bunch charge offer a wide range of applications nevertheless the reproducibility of those beams is one of the main problems. External injection into a plasma wake is a promising concept to separate the influence of different input parameters from each other for more control of experimental results and to improve reproducibility. At the Research Center Dresden-Rossendorf the 150TW laser system DRACO was set up next to an superconducting electron accelerator. This will give the opportunity to study wake field acceleration in more detail. In this talk the present status of the experiment, ongoing upgrades and future plans will be described.

9:42
TO4 2 Injection and Trapping of Tunnel Ionized Electrons into Laser Produced Wakes* A. PAK, *UCLA* K.A. MARSH, S.F. MARTINS, W. LU, W.B. MORI, C. JOSHI, DEPARTMENT OF ELECTRICAL ENGINEERING, UCLA, LOS ANGELES, CALIFORNIA 90095 USA COLLABORATION, DEPARTMENT OF PHYSICS AND ASTRONOMY, UCLA, LOS ANGELES, CALIFORNIA, 90095 USA COLLABORATION, GOLP / INSTITUO DE PLASMAS E FUSAO NUCLEAR, INSTITUTO SUPERIOR TECNICO, LISBON, PORTUGAL COLLABORATION, A method which utilizes the ionization potentials of gases as a mechanism for injecting electrons into a laser produced accelerating wakefields is presented. The properties of accelerated beams created via this injection method will be discussed for various experimental parameters. Experimental results will be supported by theory and simulations.

*Work Supported by DOE Grant DEFG02-92ER40727.

9:54
TO4 3 Ionization induced trapping in a laser wakefield accelerator WILLIAM SCHUMAKER, C. McGUFFEY, A.G.R. THOMAS, T. MATSUOKA, V. CHVYKOV, F.J. DOLLAR, G. KALINTCHENKO, V. YANOVSKY, A. MAKSIMCHUK, K. KRUSHELNICK, *University of Michigan* V. YU. BYCHENKOV, *P. N. Lebedev Physics Institute* I.V. GLAZYRIN, *RFNC-VNIITF* Experimental measurements of electrons accelerated in a laser wake?eld accelerator indicate trapping initiated by an ionization mechanism. By using a range of noble gases and nitrogen as a very small percentage contaminant in helium gas, it is found that tun-

neling ionization of inner shell electrons plays an important role in determining the trapped charge. Although there is a small increase in electron number density due to the higher Z contaminant, it is shown to be insufficient to account for the increase in charge in the trapped bunch. The behavior of the trapping with laser intensity is also consistent with the tunnel-ionization thresholds for the gases used. This mechanism is likely to allow lower power laser systems to be used to generate comparably high-energy and low-emittance monoenergetic electron beams than in pre-ionized gas configurations. 2D particle-in-cell simulations including an ADK ionization model were used to correlate with experimental results.

10:06

TO4 4 High-brightness near-GeV energy electron beams from a laser wakefield accelerator for long-standoff nuclear interrogation* NATHAN POWERS, SUDEEP BANERJEE, VIDYA RAMANATHAN, NATHANIEL CUNNINGHAM, NATE CHANDLER-SMITH, DONALD UMSTADTER, *University of Nebraska-Lincoln* RANDY VANE, DAVID SCHULTZ, *Oak Ridge National Laboratory* SHAUN CLARKE, SARA POZZI, *University of Michigan* UNIVERSITY OF NEBRASKA-LINCOLN TEAM, OAK RIDGE NATIONAL LAB TEAM, UNIVERISTY OF MICHIGAN TEAM, High-brightness monochromatic electron beams are generated in a wakefield accelerator driven by a 100 TW laser. The energy can be varied from 20-800 MeV by varying laser and plasma parameters. Stable electron beams are obtained using self-injection and optical injection. The ability of these beams to penetrate large thicknesses of dense material and an angular spread of < 5 mrad makes them suitable as active interrogation probes for long standoff nuclear activation of concealed nuclear materials. A series of (γ,xn) activation measurements were performed to demonstrate the viability of this technique. MCNP and GEANT Monte Carlo simulations are used to aid experiment design and interpretation.

*Work Supported by Defense Advanced Research Projects Agency, Department of Energy, and Domestic Nuclear Detection Office DHS

10:18

TO4 5 Laser plasma generated electron beams for high resolution long range radiography VIDYA RAMANATHAN, SUDEEP BANERJEE, NATHAN POWERS, KUN ZHAO, NATE CHANDLER-SMITH, NATHANIEL CUNNINGHAM, DONALD UMSTADTER, *University of Nebraska* SHAUN CLARKE, SARA POZZI, *University of Michigan* Applications of tunable, collimated, high energy, monochromatic electron beams generated from a laser-plasma based accelerator are explored as active interrogation probes for long stand-off electron beam radiography. Besides being highly penetrating in nature the low-divergence of these electron beams, provides for an efficient delivery of the beam energy to a distant target. Laser wakefield accelerators are advantageous in that, they give rise to electron beams with micron-scale source size (comparable to the waist of the laser beam), which can provide superior image resolution. For the first time, electron beams are shown to resolve sub-millimeter (250 μm) structures that are embedded in thick and dense materials placed at a long standoff distance ($\sim$ 2m) from the source. Monte-Carlo simulations of the experimental results are also presented.

10:30

TO4 6 Generation and characterization of high-field, short-pulse THz emission from the Berkeley Laser Plasma Accelerator NICHOLAS MATLIS, GUILLAUME PLATEAU, JEROEN VAN TILBORG, CARL SCHROEDER, CAMERON GEDDES, CSABA TOTH, WIM LEEMANS, *Lawrence Berkeley National Lab* We present progress on the generation of sub-ps THz pulses in the MV/cm regime from a Laser Plasma Accelerator (LPA) and their use as an accelerator diagnostic. The THz pulses serve the dual purpose of acting as a high-field short pulse source for pump-probe studies as well as a diagnostic of the bunch duration of electrons from the LPA. Characterization of the focused THz spatial and temporal mode properties was done using state-of-the-art electro-optic (EO) sampling methods. A new technique was also implemented which allows single-shot acquisition of the THz spatio-temporal waveform. Preliminary results showing spatio-temporal features of the THz pulses will be presented, as well as a preliminary demonstration of correlation between electron bunch properties and the THz spectrum.

10:42

TO4 7 Betatron radiation from the self-injected electrons in a laser wakefield SEOK WON HWANG, SANG-YOUNG CHUNG, HAE JUNE LEE, *Pusan National University* When self-injected electrons in a laser wakefield are accelerated to a hundred MeV or 1 GeV, the electrons also oscillate by the focusing fields of the wakefield which are composed of transverse electric field and azimuthal magnetic field. This oscillation is called betatron oscillation. The oscillating electrons emit betatron radiation per a half period of the oscillation. The number of oscillations is dependent on the propagation length and the strength of the wakefields. The radiation has a broad spectrum with an energy band from a few eV to several keV and a beam divergence of tens of mrad. In this presentation, the self-injected electrons are traced using a relativistic electromagnetic particle-in-cell (EM-PIC) code, and the radiaitons emitted from the electrons are calculated from the particle motion. The characteristics of the radiations are compared with the results from a single electron simulation which was calculated with an assumption that the wakfields did not change for the propagation of the electron.

10:54

TO4 8 Laser Plasma Wiggler S. KNEIP, S.P.D. MANGLES, C.A.J. PALMER, S.R. NAGEL, C. BELLEI, J. SCHREIBER, Z. NAJMUDIN, *Imperial College London, UK* C. McGUFFEY, V. CHVYKOV, F. DOLLAR, C. HUNTINGTON, G. KALINTCHENKO, G. MAKSIMCHUK, T. MATSUOKA, A.G.R. THOMAS, V. YANOVSKY, K. KRUSHELNICK, *University of Michigan, USA* J. MARTINS, S.F. MARTINS, R. FONSECA, S.O. SILVA, *Instituto Superior Tecnico, Portugal* K. TA PHUOC, *Laboratoire Optique Appliquee, France* A high quality beam of X-rays is measured when electrons perform transverse oscillations in a Laser-Wakefield Accelerator. The radiation is spatially coherent, originates from a micron-sized source, has mrad divergence, 10 to 100 keV energy range and a peak brightness comparable to 3rd generation conventional light sources. Radiation post-processing of electron trajectories obtained from PIC modeling is in excellent agreement with the experimental results. Electron trajectories resemble the scenario of an electron in a wiggler-type insertion device. This is an important step on a route to realize a single stage table-top all optical x-ray source with unique characteristics and interests over the whole spectrum of scientific studies.

11:06

TO4 9 Algorithm for calculating coherent radiation from many particles ALEC THOMAS, *University of Michigan* An efficient algorithm for calculating coherent radiation in the far-field is described. Direct integration of the Lienard-Wiechert potentials for extremely high photon energies and many particles is made computationally feasible by a mixed analytic and numerical method. Exact integrals of spectral intensity are made between discretely sampled trajectories by assuming the space-time four-vector is a quadratic function of proper time. The integral of the trajectory with respect to time, the modulus squared of which comprises the spectral intensity, can then be formed by piecewise summation of exact integrals between discrete points. Because of this, the calculation is not restricted by discrete sampling bandwidth theory, and time- steps much larger than the inverse of the maximum frequency can be taken. The technique is incorporated into a radiation code *Radampeltrac*. Calculations of non-linear Thomson back-scattering of a 150 MeV electron bunch from the HERCULES laser system show angularly resolved spectral intensity photon distributions extending to 10 MeV in a well collimated beam. An experimentally measurable difference in the photon spectral distribution with and without radiation damping is demonstrated.

11:18

TO4 10 Spectral Analysis of Forward Scattered Radiation in a Laser Wakefield Acceleration Experiment* MICHAEL HELLE, *Georgetown University* DMITRI KAGANOVICH, *Icarus Research Inc.* DANIEL GORDON, *U.S. Naval Research Laboratory* BAHMAN HAFIZI, *Icarus Research Inc.* ANTONIO TING, *U.S. Naval Research Laboratory* We have characterized the forward scattered radiation generated from a LWFA experiment at the U.S. Naval Research Laboratory. High-order, large amplitude, anti-Stokes radiation was produced from the interaction of an intense laser pulse propagating through an $\sim$ 1% critical density plasma. Evidence of relativistic cross-phase modulation and previously unreported conical emission of Stokes radiation has also been observed. The Stokes radiation can be the consequence of a third order nonlinear mixing of two fundamental photons with an anti-Stokes photon. This nonlinear electromagnetic four wave mixing process is usually not permissible owing to phase matching considerations. However, the matching condition can become satisfied when modification of the plasma dispersion relation due to plasma channel guiding is considered. Discussion of these novel experimental results in relation to the underlying nonlinear effects will be presented.

*This work is supported by the Department of Energy and Office of Naval Research.

11:30

TO4 11 Formation of optical bullets in laser-driven plasma bubble accelerators P. DONG, S.A. REED, S. YI, S. KALMYKOV, G. SHVETS, *Physics Department, U. of Texas at Austin* N.H. MATLIS, W.P. LEEMANS, *LBNL* C. MCGUFFEY, S.S. BULANOV, V. CHVYKOV, G. KALINTCHENKO, K. KRUSHELNIK, A. MAKSIMCHUK, T. MATSUOKA, A.G.R. THOMAS, V. YANOVSKY, *CUOS, U. of Michigan* We show that luminal velocity electron density bubbles produced by relativistically intense ultrashort drive laser pulses propagating through near-atmospheric-density plasma re-shape co-propagating probe pulses into optical "bullets" that we reconstruct using frequency-domain interferometric techniques and use to visualize the spatio-temporal profile of the plasma bubble. A study of bubble-compressed bullets together with bubble-accelerated electrons reveals three regimes: (I) bullets of sub-plasma-wavelength (sub-λ_p) size, trapped and compressed inside plasma bubbles, appear at $1 < n_e < 1.5 \times 10^{19}$ cm^{-3} without production of relativistic electrons; (II) enlongated bullets spanning $\sim 2\lambda_p$, signifying temporary merging of sequential bubbles, are observed frequently at $n_e > 2 \times 10^{19}$ cm^{-3} together with poly-energetic relativistic electrons; (III) mono-energetic electrons are observed only in conjunction with intense sub-λ_p bullets signifying stable or contracted bubbles, generally at $n_e > 2.5 \times 10^{19}$ cm^{-3}. The results help to relate bubble structure to the properties of laser-wakefield-accelerated electrons in the blowout regime.

11:42

TO4 12 Laser Wakefield Simulation Using a Speed-of-Light Frame Envelope Model* BENJAMIN COWAN, DAVID BRUHWILER, PETER MESSMER, KEVIN PAUL, *Tech-X Corporation* ESTELLE CORMIER-MICHEL, ERIC ESAREY, CAMERON GEDDES, *Lawrence Berkeley National Laboratory* Simulation of laser wakefield accelerator (LWFA) experiments is computationally highly intensive due to the disparate length scales involved. Current experiments extend hundreds of laser wavelengths transversely and many thousands in the propagation direction, making explicit FDTD/PIC simulations enormously expensive. We present a model which substantially improves the performance of LWFA simulations by modeling the envelope modulation of the laser field rather than the field itself. This allows for much coarser grids, since we need only resolve the plasma wavelength and not the laser wavelength, and this also allows larger timesteps. We show that this envelope model has much lower numerical dispersion error than FDTD, while maintaining second-order convergence. We demonstrate a complete 3D simulation of a meter-scale LWFA stage with over 10^5 speedup over explicit FDTD. In addition, we show studies of kinetic interpolation errors and simulations of particle trapping.

*Work supported by U.S. Department of Energy grants DE-FC02-07ER41499 (ComPASS SciDAC) and DE-SC0000840 (SBIR), and by Tech-X Corporation.

11:54

TO4 13 Modeling 10 GeV laser-plasma accelrators and conventional accelerators using boosted computational frames* J.-L. VAY, W.M. FAWLEY, M.A. FURMAN, C.G. GEDDES, E. CORMIER-MICHEL, *LBNL, CA, USA* D.P. GROTE, *LLNL, CA, USA* It can be computationally advantageous to perform computer simulations in a Lorentz boosted frame for a certain class of particle acceleration devices or problems such as: free electron laser, laser-plasma accelerator, particle beams interacting with electron clouds [1]. Complications arising from calculating in a Lorentz boosted frame and respective solutions have now been further analyzed, supporting more successful applications of the method to these problems. Most notably, full PIC 3D simulations of 10 GeV laser acceleration stages were enabled, with demonstrated convergence at a few percent level at various gammas, with speed-

ups of 1,000 or more. Such simulations are important to the design of next generation accelerators. We will present and discuss the latest developments of the method illustrated with various examples of its application. [1] J.-L. Vay, Phys. Rev. Lett. **98**, 130405 (2007)

*Supported by US-DOE Contracts DE-AC02-05CH11231 and DE-AC52-07NA27344, US-LHC program LARP, and US-DOE SciDAC program ComPASS. Used resources of NERSC, supported by US-DOE Contract DE-AC02-05CH11231.

12:06

TO4 14 Laser Wakefield Acceleration with Shaped Laser Modes* ESTELLE CORMIER-MICHEL, ERIC ESAREY, CAMERON G.R. GEDDES, CARL B. SCHROEDER, *Lawrence Berkeley National Laboratory* DAVID L. BRUHWILER, BEN COWAN, KEVIN PAUL, *Tech-X Corporation* WIM P. LEEMANS, *Lawrence Berkeley National Laboratory* LBNL is currently pursuing a collider design based on meter-long 10 GeV laser-plasma accelerator stages, and Thomson gamma source designs at ~ 1 GeV, that will operate in the quasi-linear regime. This regime allows symmetric acceleration of electrons and positrons and has the property that the transverse fields are proportional to the transverse gradient of the laser intensity profile. We show that higher order laser modes can tailor this gradient and hence the focusing forces in the plasma, allowing control over the radius and the emittance of the accelerated bunch. We present simulations, using the VORPAL framework, of the design of 1-10 GeV stages. In particular, we show that, by using shaped laser modes, it is possible to increase the matched electron beam radius and hence the total charge in the bunch while preserving the low bunch emittance required for applications.

*Work supported by the U.S. Department of Energy NA-22 and HEP Contract No. DE-AC02-05CH11231, SciDAC, and SBIR.

12:18

TO4 15 Plasma Wakefield Accelerator Driven by a Train of Electron Bunches* PATRIC MUGGLI, BRIAN ALLEN, *University of Southern California* VITALY YAKIMENKO, JANGHO PARK, KARL KUSCHE, MARCUS BABZIEN, *Brookhaven National Laboratory* We study experimentally the physics of the interaction between a train of electron bunches and a plasma whose density can be varied. The train of electron bunches consists of equidistant (~ 300 microns) drive bunches followed by a witness bunch (~ 450 microns from the last drive bunch). Each bunch length is about half the drive bunch spacing (~ 150 microns). The bunch train is produced using a masking technique recently demonstrated (P. Muggli et al., Phys. Rev. Lett. 101, 054801, 2008). The plasma density is varied by changing the arrival time of the bunch train with respect to the capillary discharge. At low density (< 1e16/cc) the wakefields are driven by the envelope of the bunch train. At resonance, when the plasma density is such that the plasma wavelength is equal to the drive bunches spacing, large energy loss and energy gain is observed. The resonance also disappears at higher densities, or when the bunch train is replaced by a continuous electron bunch with a length equal to that of the train. Detailed experimental results will be presented.

*Work supported by the US Department of Energy.

SESSION TO5: ICF SIMULATIONS AND TARGET FABRICATIONS

Thursday Morning, 5 November 2009
Hanover CDE at 9:30
Chuang Ren, University of Rochester, presiding

9:30

TO5 1 NIF ignition target requirements, margins, and uncertainties: Status Nov. 2009 S.W. HAAN, J.D. SALMONSON, D.S. CLARK, D.D. HO, B.A. HAMMEL, D.A. CALLAHAN, C.J. CERJAN, M.J. EDWARDS, S.P. HATHCETT, O.L. LANDEN, J.D. LINDL, B.J. MacGOWAN, M.M. MARINAK, D.H. MUNRO, H.F. ROBEY, B.K. SPEARS, L.J. SUTER, R.P. TOWN, S.V. WEBER, *Lawrence Livermore National Laboratory* D.C. WILSON, *Los Alamos National Laboratory* We describe simulations of NIF ignition targets, including Be, CH, and C-ablator designs. Requirements define all aspects of the experiment: fabrication, laser pulse, and features of pre-ignition experiments. We describe a model, normalized to simulations, that characterizes the margin of the target as a function of input parameters and uncertainties. The model is used to quantify the impact of each requirement, and to project the probability of ignition, both shot-to-shot variations and given systematic errors. This presentation emphasizes changes in the requirements and margin modeling in the last year, and the relative performance of the final CH, Be, and C designs. Recent work has concentrated on surface perturbations on the CH ablator, and composition variations in the Be shells. LLNL-ABS-414529. Prepared by LLNL under Contract DE-AC52-07NA27344.

9:42

TO5 2 High Gain High Efficiency Heavy-Ion Direct Drive Targets L.J. PERKINS, J. BARNARD, *LLNL* B.G. LOGAN, *LBNL* M. HAY, *UC Berkeley* New simulations of heavy ion (HI) direct drive fusion targets indicate that fusion gains of 50-80 may be achievable with less than 0.5MJ of heavy-ion drive energy. The inherently high efficiency of HI direct drive (15-20% incident beam energy to shell kinetic energy) permit very simple all-DT targets with thick, low aspect ratio (A=2) shells that should exhibit high ablative R-T stabilization with robust in-flight stability characteristics. Beam symmetry studies show that 60 beams may suffice with rotated beam spots on the ablator. Present work is directed to obtaining target gain curves (i.e., target fusion energy gain versus HI drive energy), optimum HI pulse shapes in both ion kinetic energy and intensity, hydrodynamic stability, and the prospects of driving such targets with two-sided beam geometry as opposed to conventional 4-pi spherical symmetry that would permit simplified, more attractive target chamber geometries. Application to small heavy ion fusion test reactors with 10's MW average fusion powers, and to small fission fusion hybrids will be addressed. (Work performed by LLNL under Contract DE-AC52-07NA27344 on behalf of the Heavy Ion Fusion Virtual National Laboratory)

9:54

TO5 3 Simulations of the Shock-Timing Diagnostic Commissioning Experiments at the National Ignition Facility T.J.B. COLLINS, P.W. McKENTY, K.S. ANDERSON, T.R. BOEHLY, M.A. BARRIOS, *Laboratory for Laser Energetics, U. of Rochester* P.M. CELLIERS, D.G. BRAUN, M.M. MARINAK, *LLNL* As inertial confinement fusion targets are imploded, they generate several shock waves. The shock waves must be precisely timed to

maintain a low target adiabat while achieving the necessary fuel compression. Shock timing of ignition experiments for the National Ignition Facility (NIF) will be confirmed using surrogate targets that allow one to determine shock speeds. The shock speeds are measured using an optical interferometer (VISAR) and a streaked optical pyrometer (SOP). This NIF platform will be tested with direct drive using impedance-matching experiments of a quartz sample and a stepped aluminum layer as a standard, based on previous experiments on OMEGA. These experiments have been simulated in three dimensions using the radiation hydrodynamics code *HYDRA*. The results of these simulations will be presented and compared to initial experimental data. This work was supported by U. S. Department of Energy Office of Inertial Confinement Fusion under Cooperative Agreement No. DE-FC52-08NA28302.

10:06

TO5 4 A Measurable Three-Dimensional Lawson Criterion and Hydro-Equivalent Curves For Inertial Confinement Fusion* P. CHANG, K. ANDERSON, R. BETTI, *University of Rochester* It is shown that a multi-dimensional ignition condition (Lawson criterion) can be cast in a form that depends on three measurable parameters of the compressed fuel assembly: the hot-spot ion temperature T, the neutron yield normalized to the 1-D prediction (Yield-Over-Clean, YOC) and the total areal density ρR including the cold shell contribution. A family of marginal-ignition curves is derived in the ρR-T plane. They are parameterized according to the YOC, and hydrodynamic simulations are compared with the ignition curves. On this plane, hydrodynamic equivalent curves show how a given implosion would perform with respect to the ignition condition when the laser-driver energy is varied. For $3 < T < 6$ keV, the 3D ignition condition can be approximated by a simple formula : $\rho R \cdot T^{2.6} \cdot YOC > 50 g/cm^2 keV^{2.6}$, where ρR, T and YOC are the measured, neutron-averaged total areal density, hot-spot ion temperature and the neutron yield normalized to the 1-D prediction respectively. All quantities are calculated without accounting for the α-particle energy deposition. Such a criterion can be used to measure the Margin in the THD (Tritium, Hydrogen, Deuterium-poor targets) campaign on the National Ignition Facility and to determine how surrogate D_2,THD, and sub-ignited DT target implosions perform with respect to the ignition threshold.

*This work has been supported by the US Department of Energy under Cooperative Agreement DE-FC02-ER54789 and DE-FC03-92SF19460.

10:18

TO5 5 Enhancing the SRS model in pF3d to simulate off-resonant backscatter in NIC targets C.H. STILL, E.A. WILLIAMS, D.E. HINKEL, A.B. LANGDON, P.A. MICHEL, *LLNL* Of particular interest to the National Ignition Campaign (NIC) is the amplification of laser backscatter, which is generated near the target wall, by crossing laser beams in the plasma region near the laser entrance hole (LEH)[1] of an ignition target. We study here the amplification of stimulated Raman scatter (SRS), where laser light scatters off self-generated electron plasma waves. Recently, we have incorporated an SRS model that supports two electron plasma waves at different frequencies (and hence two reflected light waves) into the laser beam propagation code pF3d.[2] This enables simulations which include a secondary SRS wave matched to the least damped mode in the LEH as determined by post-processing radiation-hydrodynamics simulations. Such a simulation also entails calculating the off-resonant amplification. Thus, we have enhanced the SRS model in pF3d to improve the accuracy of modeling the off-resonant response. We report on the enhancements to the SRS model, implementation, and the results of two SRS group simulations with one mode the primary SRS backscatter and one matched in the LEH plasma. LLNL-ABS-414822 prepared by LLNL under contract DE-AC52-07.

[1]P. A. Michel, private communication.
[2]C. H. Still, *et al.* IFSA Proceedings (2009)

10:30

TO5 6 Nonlinear Plasma Wave Behavior in Multiple Dimensions Relevant to Stimulated Raman Scattering JAY FAHLEN, *UCLA* BEN WINJUM, THOMAS GRISMAYER, VIKTOR DECYK, WARREN MORI, Recent particle-in-cell (PIC) simulations (L. Yin *et al.*, PRL **99**, 265004 (2007) and B. Winjum's poster) of stimulated Raman scattering (SRS) in multiple dimensions indicate that plasma wavefront bowing and localization are important potential nonlinear saturation mechanisms. We present here the results of detailed PIC simulations in which an external, ponderomotive impulse driver generates finite-width plasma waves. These simulations allow careful study of wave behavior over a wide range of parameters. We find that local, kinetic damping effects operate in conjunction with wavefront bowing to localize large-amplitude plasma waves along their axis. The simulations are performed using an electrostatic PIC code, and also a PIC code using the Darwin approximation to solve for the electric and magnetic fields without radiation. This work was supported by DOE under Grant Nos. DE-FG52-03-NA00065, DE-FG52-06NA26195, and DE-FG02-03ER54721.

10:42

TO5 7 STUD Pulses: Spike Train of Uneven Duration and Delay for the Control of Laser-Plasma Instabilities in ICF, IFE and HEDLP BEDROS AFEYAN, *Polymath Research Inc.* It is possible to stop the runaway growth of parametric instabilities by breaking up multi-nanosecond laser pulses into a train of spikes on the psec time scale whose amplitudes, durations and inter-spike delays are design parameters adjusted to keep laser plasma instabilities (LPI) from undergoing too many e-foldings (which would be determined experimentally, under given plasma conditions). This new approach also addresses multiple overlapping laser beam (direct drive) and intercone beam crossing (indirect drive) effects which are major concerns for all options for ICF and IFE to date. With STUD pulses, multi-beam interactions are kept under control or disallowed outright by interleaving in time the spikes in different beams. Most importantly, STUD pulses usher in the possibility of the use of green (0.53 μm) or even 1 μm radiation as ICF drivers since LPI will now be actively controlled. STUD pulses can be implemented on the NIF by just changing the front end with no need for changes to the amplifier chain. Finally, in the million or more (wide bandwidth) fiber laser approach to IFE in the future, STUD pulses are a natural mechanism to ensure LPI control since the speckle patterns of overlapped randomly timed beams will be naturally independent from spike to spike with very long recurrence times, guaranteeing linear and modest growth in time of instabilities.

10:54

TO5 8 A 3D, Parallel, Solution-Adaptive Model for Radiative Shocks* KENNETH POWELL, PAUL DRAKE, JAMES HOLLOWAY, BART VAN DER HOLST, SMADAR KARNI, WILLIAM MARTIN, ERIC MYRA, IGOR SOKOLOV, QUENTIN STOUT, G. TOTH, *Center for Radiative Shock Hydrodynamics, University of Michigan* In this talk, a radiation hydrodynamics code for simulating radiative shocks will be described. The high-level validation problem for the code is one in which a 1 ns, 4 kJ laser pulse irradiates a Be disk, driving a shock into a Xe-filled plastic tube. The radiative precursor to the shock heats the wall of the tube, so that the there is a complex interaction among the shock driven by the ablated material from the wall, the laser driven shock, and the Be-Xe interface. The code is three-dimensional, solution-adaptive, and parallel. The radiation transport model in the current code is based on gray diffusion; work is underway to support higher-fidelity radiation transport models. The methodology used in the code and preliminary results of simulations will be presented.

*This work was supported in part by the US DOE NNSA under the Predictive Science Academic Alliance Program by grant DE-FC52-08NA28616.

11:06

TO5 9 Kinetic simulation of neutron production in a deuterium z-pinch* DALE WELCH, DAVID ROSE, *Voss Scientific, LLC* WILLIAM STYGAR, *Sandia National Laboratories* RAMON LEEPER, *Sandia National Laboratories* Fully kinetic particle-in-cell (PIC) modeling of a deuterium gas puff z-pinch can provide insight into the physical mechanisms for D-D fusion neutron production. Experiments with 15-MA current pinches on the Z accelerator have suggested that the dominant neutron-production mechanism is thermonuclear. The non-linear evolution of the Rayleigh Taylor instability as the pinch coalesces on axis, however, induces large electric fields capable of driving a significant number of high energy ions similar to that reported in dense plasma focus machines where measured ion spectra exhibit power-law dependence. In order to gain further insight, we have performed 2D PIC simulations of deuterium z-pinch implosions that permit non-Maxwellian particle distributions, finite mean-free-path effects, self-consistent anomalous resistivity, and charge separation. The calculated neutron yields largely follow the predicted thermonuclear I^4 current scaling [A. L. Velikovich, et. al, Phys. of Plasmas 14, 022701 (2007)], but also exhibit the power law ion distribution and significant non-thermal neutron production. We will discuss both production mechanisms and impact on the scaling of neutron yield at higher current.

*Work support by the DOE through Sandia National Laboratories.

11:18

TO5 10 Surface Roughness Reduction on Divinylbenzene Foam Shells* JON STREIT, JOHN KARNES, BRIAN MOTTA, NICOLE PETTA, *Schafer Corporation* Inertial fusion energy targets for the Naval Research Laboratory's High Average Power Laser Program require millimeter-scale, low density foam capsules with a gas permeation barrier and an outer surface roughness less than 50 nm RMS. Divinylbenzene (DVB) foam is a candidate for the capsule wall material, but its porous, open celled surface has been both too rough and difficult to seal. To overcome this difficulty we have repurposed a previously reported dual stage initiator emulsion microencapsulation method, adding an additional step that enhances the surface of the foam capsules. Using both low and high temperature initiators allows the DVB foam to gel in the low temperature stage and a water soluble monomer to be added and polymerized during the high temperature stage without breaking down the emulsion. This method forms a submicron skin that covers the open celled DVB foam surface, resulting in a superior substrate for gas permeation barrier deposition.

*This work was performed under the auspices of the U.S. Department of Energy by Schafer Corporation under contract numbers DE-AC52-06NA27472 and N00173-06-C-6010.

11:30

TO5 11 Progress toward an air-dried HAPL target capsule* JOHN KARNES, JONATHAN STREIT, BRIAN MOTTA, NICOLE PETTA, *Schafer Corporation* SHANNAN DOWNEY, MICHAEL DROEGE, *Ocellus Inc.* NRL's High Average Power Laser (HAPL) Program works to design an inertial fusion energy power plant based on a modular laser system and direct drive targets. One task of this project is the development of a coated low density foam shell to contain the cryogenic deuterium-tritium (DT) fuel. An economic model of the HAPL fusion power plant requires that these foam capsules must be produced at a cost of less than 25¢ each for the plant to produce competitively priced energy. Capsule materials of interest are open celled structures with submicron-scale pores. If allowed to "air-dry," capillary forces at air-liquid interfaces within the pores destroy the capsule's morphology. Critical point drying, a costly production step, is used to avoid this problem. We present recent work towards developing a low density HAPL capsule prototype that avoids this processing step by synthesizing a low density material that survives "air-drying."

*This work was performed under the auspices of the U.S. Department of Energy by Schafer Corporation under contract numbers DE-AC52-06NA27472 and N00173-06-C-6010.

SESSION TO6: LABORATORY ASTROPHYSICS
Thursday Morning, 5 November 2009
Hanover FG at 9:30
Bruce Remington, Lawrence Livermore National Laboratory, presiding

9:30

TO6 1 Super-Alfvénic Expansion of a Laser-Plasma through an Ambient Magnetized Plasma ERIK EVERSON, CARMEN CONSTANTIN, LUCAS MORTON, DEREK SCHAEFFER, NATHAN KUGLAND, WALTER GEKELMAN, CHRISTOPH NIEMANN, *University of California, Los Angeles* In recent experiments on the Large Plasma Device (LAPD) several diagnostics have been implemented to investigate the super-Alfvénic flows created by the rapid expansion of a high-density, energetic laser-plasma through the ambient magnetized, helium plasma of the LAPD. The laser-plasma is created by a 25 J, 5 ns FWHM laser pulse of 1064 nm light incident on a graphite target and is allowed to expand a distance > 30 cm across the magnetic field lines. With the laser-plasma expansion imparting enough energy to the low-density ambient plasma ($n \sim 2 \times 10^{-12}$ cm^{-3}, $T_e \sim 6$ eV,

$T_i \sim 1$ eV, $B_o = 300$ G), super-Alfvénic flows can be created. The magnetic structure of these flows has been measured using a 1 mm, 3-axis differential magnetic probe (B-dot probe). A measurement of the energy distribution of ions has also been attempted using an energy analyzer.

9:42

TO6 2 Generation of intense magnetosonic waves by erupting laboratory simulations of solar coronal loops* SHREEKRISHNA TRIPATHI, WALTER GEKELMAN, *Department of Physics and Astronomy, UCLA* Eruption of coronal loops in the ambient plasma of the sun is simulated in a laboratory experiment at UCLA. The laboratory plasma loops (simulations of coronal loops) are produced using an annular LaB_6 cathode and an annular anode mounted on two movable shafts in a large vacuum chamber. Two electromagnets produce a vacuum magnetic field along the arched axis of the plasma loop. Controlled flows of dense plasma are generated from the foot-points of the electrodes using laser beams that strike movable targets (C, LaB_6) placed behind the holes in the electrodes. This novel approach provides flexibility in independently controlling the timing and intensity of the flows. The vacuum chamber has an additional source to produce ambient magnetized plasma. In recent experiments, dramatic eruption of the loop plasma was observed following generation of super-Alfvénic flows ($V_{flow} \sim 2 - 5\ V_a$) from the foot-points. The erupting plasma loop sets up intense magnetosonic waves in the ambient plasma. We will present initial results on the loop eruption and excitation of the magnetosonic wave.

*Work supported by US DOE and NSF.

9:54

TO6 3 Episodic Magnetic Tower Jets in Laboratory Experiments* F. SUZUKI-VIDAL, S.V. LEBEDEV, S.N. BLAND, G. BURDIAK, J.P. CHITTENDEN, G.N. HALL, A.J. HARVEY-THOMPSON, E. KHOORY, L. PICKWORTH, G. SWADLING, *Imperial College London* A. CIARDI, *Ecole Normale Superieure* C. STEHLE, *Observatoire de Paris* Results from laboratory astrophysics experiments showing the formation of episodic plasma jets will be presented. The jets are highly supersonic, radiatively cooled and driven by the pressure of the toroidal magnetic field in a 'magnetic tower' configuration. The 1 MA, 250 ns current pulse from the MAGPIE generator is introduced into a radial foil, an aluminium disc held between two concentric electrodes. The ablation of plasma from the foil close to the central electrode forms a radial gap which triggers the formation of the jets. Several diagnostics including magnetic and inductive probes were used to study their dynamics, particularly their launching mechanism. The similarities with previous single-episode magnetic tower jets from radial wire arrays together with new measurements of dimensionless parameters such as the magnetic Reynolds number ($Re_M > 400$) indicate that the experiments can be scaled to astrophysical jets.

*This research was sponsored by the NNSA under DOE Coop. Agreement DE-F03-02NA00057 and by a Marie Curie RTN fellowship as part of the JETSET project.

10:06

TO6 4 Spike penetration in blast-wave-driven instabilities R.P. DRAKE, *University of Michigan* Recent experiments by C. Kuranz and collaborators, motivated by structure in supernovae, have studied systems in which planar blast waves encounter interfaces where the density decreases. During the Rayleigh-Taylor (RT) phase of such experiments, they observed greater penetration of the RT spikes than tends to be seen in simulations. Here we seek to employ semi-analytic theory to understand the general nature and regimes of spike penetration for blast-wave-driven instabilities. This problem is not trivial as one must account for the initial vorticity deposition at the interface, for its time-dependent deceleration, for the expansion of the shocked material in time and space, and for the drag on the broadened tips of the spikes. One can hope that such models will increase our ability to interpret the behavior of simulations of such systems, in both the laboratory and astrophysics. Supported by the US DOE NNSA under the Predictive Sci. Academic Alliance Program by grant DE-FC52-08NA28616, the Stewardship Sci. Academic Alliances program by grant DE-FG52-04NA00064, and the Nat. Laser User Facility by grant DE-FG03–00SF22021.

10:18

TO6 5 Shock Wave Structure in a Fully Ionized Plasma THOMAS MASSER, JOHN WOHLBIER, ROBERT LOWRIE, *Los Alamos National Laboratory* We study the structure of planar shock waves in a two-temperature model of a fully ionized plasma that includes electron heat conduction and energy exchange between electrons and ions. For steady flow in a reference frame moving with the shock, the model reduces to an autonomous system of ordinary differential equations which can be numerically integrated. A phase space analysis of the ODEs provides additional insight into the structure of the solutions. For example, below a threshold mach number the model produces fully dispersed shocks; while above the threshold, the solutions contain embedded hydrodynamic shocks. We also find that the ion temperature may continue to increase after the shock and reaches a maximum near the isothermal sonic point. We summarize the methodology for solving for two-temperature shocks, and show results for several values of shock strength and material parameters to quantify the shock structure and explore the range of possible solutions. Such solutions may be used to verify hydrodynamic codes that use similar plasma physics models.

10:30

TO6 6 Accelerating aluminum foils for shock wave experiments* STEPHAN NEFF, SANDRA STEIN, DAVID MARTINEZ, CHRISTOPHER PLECHATY, RADU PRESURA, *University of Nevada, Reno* The interaction of shock waves with inhomogeneous background media is ubiquitous in astrophysics, taking place for expample when supernova remnants move through interstellar gas clouds. Scaled experiments of such interactions are possible by launching shock waves into inhomogeneous low-density foam targets.Using a pulsed-power accelerator (Zebra) with a short-circuit load, we are currently developing the methods and diagnostics necessary for such experiments at the Nevada Terawatt Facility. So far, we have successfully accelerated flyers (50 micron thick, 6 mm in diameter) to velocities of up to 8 km/s with a 1 MA current. We have also impacted these flyers on transparent Plexiglas targets and imaged the resulting shock with shadowgraphy. We are currently implementing improvements to be ready for scaled experiments. These improvements include using a current-multiplier (currents of up to 1.6 MA) to achieve higher velocities and implementing velocity interferometry (VISAR) to obtain a more accurate and time-resolved velocity measurement. In addition, we are currently implementing x-ray backlighting using a 50 TW short-pulse laser.

*This work was supported by DOE/NNSA under UNR grant DE-FC52-06NA27616.

10:42

TO6 7 Radiation effect and relaxation layer in electromagnetically driven strong shock waves* KOTARO KONDO, MITSUO NAKAJIMA, TOHRU KAWAMURA, KAZUHIKO HORIOKA, *Tokyo Institute of Technology* Strong shock waves play a crucial role in many astrophysical phenomena. Ion-electron relaxation process and radiation affect the structure of strong shock waves. Since the non-linear nature of the relaxation process makes the plasma behavior extremely complicated, it requires well-defined shock wave formation to estimate the structure. We investigate electro-magnetically driven shock in laboratory experiments. The pulse power device with tapered electrodes can generate a quasi steady and 1-D shock [1], which allows for analysis of ion-electron relaxation and radiation processes. We will show results of electron temperature measurement by a line pair method and radiative cooling, which restricts the increase of electron temperature. [1] K. Kondo, M. Nakajima, T. Kawamura and K. Horioka, Rev. Sci. Instr. **77**, 036104 (2006).

*Support by JSPS.

10:54

TO6 8 Structure in Radiative Shock Experiments F.W. DOSS, R.P. DRAKE, *University of Michigan* H.F. ROBEY, *Lawrence Livermore National Laboratory* Astrophysical systems in which radiation transport across a shock front contributes substantially to the properties and dynamics of the system may be modeled in laboratory experiments under high-energy-density conditions. Recent experiments on the Omega laser facility have launched Be discs into shock tubes of Xe gas at atmospheric pressure, producing radiative shocks with speeds over 100 km/sec that are then diagnosed by x-ray pinhole radiography. These experiments are found to develop rich internal structure. First, heating and ablation of the shock tube material ahead of the radiative shock drives a secondary, inwardly directed radial shock, which we call a wall shock. Second, these radiating shock systems become susceptible to hydrodynamic instabilities of thin shocked layers. This research was supported by the DOE NNSA under the Predictive Science Academic Alliance Program by grant DE-FC52-08NA28616, the Stewardship Sciences Academic Alliances program by grant DE-FG52-04NA00064, the National Laser User Facility by grant DE-FG03-00SF22021, and by the Stewardship Science Graduate Fellowship program.

11:06

TO6 9 Measurements of Radiative Shock Properties using Thomson scattering* A. VISCO, R.P. DRAKE, M.J. GROSSKOPT, *University of Michigan* D.H. FROULA, S.H. GLENZER, *LLNL* G. GREGORI, *University of Oxford* Radiative shocks are shock waves whose structure has been altered by radiation transport. Recent experiments have used the Omega laser to study radiative shock systems that are optically thin upstream and optically thick downstream. In these systems, a radiative precursor and high density cooling layer are formed in response to radiation. To create these shocks, a thin slab of berylium is driven into cylinder of argon gas at speeds $>$ 100 km/s, producing strong radiative effects. Thomson scattering is employed to measure the electron temperature and ionization in the system. The experiment used emission from a Mn x-ray source and the x-ray spectrum was detected using a crystal spectrometer and a gated, multi-strip, microchannel-plate detector. Measured results the will be shown, and the inferred properties will be compared with simulations and analytic estimates.

*Supported by the US DOE NNSA under the Predictive Sci. Academic Alliance Program by grant DE-FC52-08NA28616, the Stewardship Sci. Academic Alliances program by grant DE-FG52-04NA00064, and the Nat. Laser User Facility by grant DE-FG03-00SF22021.

11:18

TO6 10 Laboratory Tests of Stellar Interior Opacity Models* J.E. BAILEY, G.A. ROCHAU, S.B. HANSEN, P.W. LAKE, T.J. NASH, D.S. NIELSEN, R.D. THOMAS, *Sandia* C.A. IGLESIAS, *LLNL* J. ABDALLAH JR., M.E. SHERRILL, *LANL* J.J. MacFARLANE, I.E. GOLOVKIN, P. WANG, *Prism* R.C. MANCINI, *UNR* C. BLANCARD, PH. COSSE, G. FAUSSURIER, F. GILLERON, J.C. PAIN, *CEA* A.K. PRADHAN, S.N. NAHAR, M. PINSONNEAULT, *OSU* The internal structure of stars depends on the radiative opacity of the stellar matter. However, opacity models have never been experimentally tested at the conditions that exist inside stars. Experiments at the Sandia Z facility are underway to measure the x-ray transmission of iron, an important stellar constituent, at temperature and density high enough to evaluate the physical underpinnings of stellar opacity models. Initial experiments provided information on the charge state distribution and the energy level structure for the iron ions that exist at the solar radiation/convection boundary. Data analysis and new experiments at higher densities and temperatures will be described.

*Sandia is a multiprogram laboratory operated by Sandia Corporation, a Lockheed Martin Company, for the United States Department of Energy under contract DE-AC04-94AL85000.

11:30

TO6 11 Radiation from plasmas with sub-Larmor scale magnetic fields – generalized jitter radiation* MIKHAIL MEDVEDEV, *University of Kansas* Radiation produced by relativistic electrons in random magnetic fields of a sub-Larmor scale is referred to as the jitter radiation. It has been predicted to be produced from high- energy density environments which naturally generate such fields via Weibel-type (e.g., streaming) instabilities. Thus, it was argued to be a new diagnostic of Weibel turbulence in relativistic collisionless shocks, in reconnection in electron- positron plasmas and in laser-produced plasmas, the latter is of interest to both laser-plasma applications (e.g., Fast Ignition) and to Laboratory Astrophysics. The spectral characteristics of jitter radiation are markedly different from those of synchrotron and carry information about the magnetic fields structure (e.g., its spatial spectrum). Conventional treatment of jitter radiation assumes negligibly small deflections of particles in the magnetic fields, which is not always the case. Here we relax this assumption and discuss the transition between jitter and synchrotron regimes. Although the full treatment is model-dependent, certain important conclusions can be drawn. We will also address applications to both laboratory studies of the Weibel turbulence and astrophysical phenomena.

*This work is supported by grants DE-FG02-07ER54940 (DOE), AST-0708213 (NSF), NNX08AL39G (NASA)

11:42

TO6 12 Fully relativistic form factor for Thomson scattering in umagnetized plasmas* J.P. PALASTRO, J.S. ROSS, B. POLLOCK, E.A. WILLIAMS, L. DIVOL, D.H. FROULA, S. GLENZER, *Lawrence Livermore National Laboratory* We derive a fully relativistic form factor for Thomson Scattering in umagnetized plasmas valid to all orders in the normalized electron velocity, beta=v/c. The form factor is compared to a previously derived expression where the lowest order electron velocity, beta, corrections are included [J. Sheffield, "Plasma scattering of electromagnetic radiation," Academic Press (1975)]. The beta expansion approach is sufficient for electro-static waves with small phase velocities such as ion-acoustic waves, but for electron plasma waves the phase velocities can be near luminal. At high phase velocities, the electron screening acquires relativistic corrections including effective electron mass, relative motion of the electrons and electromagnetic wave, and polarization rotation. These relativistic corrections alter the scattered emission of thermal plasma waves, which manifest as changes in both the peak and width of the observed Thomson scattered spectra.

*Prepared by LLNL under Contract DE-AC52-07NA27344; Tracking Number ERD-08-017.

11:54

TO6 13 Observation of relativistic, collective Thomson scattering from electron plasma waves JAMES ROSS, *University of California, San Diego* SIEGFRIED GLENZER, LAURENT DIVOL, JOHN PALASTRO, *Lawrence Livermore National Laboratory* BRADLEY POLLOCK, GEORGE TYNAN, *University of California, San Diego* DUSTIN FROULA, *Lawrence Livermore National Laboratory* We present collective Thomson-scattering measurements of light scattered from electron plasma fluctuations with relativistic phase velocities. Phase velocities (v/c) between 0.06 and 0.12 have been achieved in a N2 gas jet plasma by varying the gas jet backing pressure. These plasmas are heated by a 330 J, 527 nm laser beam resulting in plasmas with electron temperatures ranging from 200 to 700 eV and electron densities ranging from $1\times\ 10^{19}$ cm^{-3} to $7\times\ 10^{19}$ cm^{-3}. For these conditions, the classical Thomson-scattering description is inadequate to analyze the measured spectra due to the large phase velocities. A fully relativistic treatment of the Thomson-scattering form factor has been developed and shows excellent agreement with the experimental data. This work was performed under the auspices of the U.S. Department of Energy by Lawrence Livermore National Laboratory under Contract DE-AC52-07NA27344 and was partially funded by the Laboratory Directed Research and Development Program under project tracking code 08-LW-070.

12:06

TO6 14 Off-Hugoniot measurements for alpha-quartz* NORIMASA OZAKI, *Graduate school of Engineering, Osaka University* TAKAYOSHI SANO, TSUTOMU MASHIMO, TOMOAKI KIMURA, KOHEI MIYANISHI, TOMMASO VINCI, FRANCIS REE, TAKASHI ENDO, TATSUYA JITSUI, MIHCEL KOENIG, RYOSUKE KODAMA, In order to accurately obtain unknown material's EOS, off-Hugoniot information of standard material, including re-shock and release isentrope, is required. For this purpose, we performed sapphire EOS measurements with using quartz base, obtaining new sapphire data in TPa (10 Mbar) pressure regime. Moreover, a novel experimental scheme will be discussed to accurately determine quartz release curve for low-density, soft materials EOS experiments.

*This work was performed under the joint research project of the ILE, Osaka University. This research was partially supported by grants for the Global COE Program, "Center for Electronic Devices Innovation," from the MEXT of Japan.

12:18

TO6 15 A New Candidate for Magnetic Energy Dissipation in Neutron Star Binary Systems STEVEN BEKHOR, *Michigan Plasma Physics Research Institute* Magnetic mountains, which build up against the confining stress of compressed equatorial magnetic fields through accretion over many Alfvén times, in low-mass X-ray binary neutron stars are likely sources of gravitational waves. In spite of the susceptibility of magnetic mountains to transient, toroidal ideal inviscid magnetohydrodynamic (MHD) instabilities, none of these is sufficient to disrupt the confinement of accreted matter to the poles. Nonetheless, magnetic relaxation is believed to occur on time scales comparable to the fiducial accretion time scale on the order of 10^5 to 10^8 years. In this study, a new mechanism for the dissipation of magnetic fields in systems of neutron star binaries via the coupling of large-amplitude gravitational waves to the background plasma flow is postulated. The mechanism invokes power loss in the Alfvén wave energy spectrum due to Joule heating as the waves accelerate upward in a gravitational potential field. This mechanism may account for much of the magnetic energy released by the stars without recourse to resistive effects. As a consequence, an analysis of the evolution of the global magnetic field's structure may provide some insight about the frequency and intensity of burst oscillations.

SESSION TO7: SHOCK IGNITION, DIAGNOSTICS, AND X-RAY SOURCES
Thursday Morning, 5 November 2009
Regency VII at 9:30
Roberto Mancini, University of Nevada, presiding

9:30

TO7 1 Design of laser-driven shock ignition targets ANDREW J. SCHMITT, J.W. BATES, S.P. OBENSCHAIN, *Plasma Physics Division, Naval Research Lab* D.E. FYFE, *LCP & FD, Naval Research Lab* S.T. ZALESAK, *Berkley Research Associates* Shock ignition target designs can produce high gains at modest driver energies.[1] High resolution 2D simulations that include nominal pellet perturbations have shown that gains well over 100 can be generated with targets driven by short-wavelength sub-megajoule KrF lasers.[2] A key feature of shock ignition is the separation of the compression and ignition parts of the target assembly. allowing independent control. We use a simple theoretical model of the assembled pellet to demonstrate how to optimize this separation, and show how it differs from optimized fast ignition and conventional central ignition designs. We also address the issue of high convergence ratios found in previous simulations of shock

ignition targets,[2] which can lead to greater sensitivity of the target gain to low-mode pellet asymmetries. We investigate techniques to minimize both this sensitivity, and present 2D simulations that demonstrate the effectiveness of these strategies. Work supported by US DoE/NNSA.

[1]R. Betti, C.D. Zhou, K.S. Anderson, *et al.*, Phys. Rev. Lett. **98**, 155001
[2]A.J. Schmitt, J.W. Bates, S.P. Obenschain *et al.*, Fusion Sci.Tech. **56**, 377 (2009).

9:42
TO7 2 Shock-Ignition Experiments at High Intensity on OMEGA C. STOECKL, W. THEOBALD, R. BETTI, R.S. CRAXTON, J.A. DELETTREZ, O.V. GOTCHEV, V.YU. GLEBOV, F.J. MARSHALL, D.D. MEYERHOFER, W. SEKA, T.C. SANGSTER, *Laboratory for Laser Energetics, U. of Rochester* C.D. ZHOU, *Laboratory for Laser Energetics and FSC, U. of Rochester* J.A. FRENJE, R.D. PETRASSO, *PSFC, MIT* Shock ignition is a two-step concept in which a strong spherically convergent shock wave is launched at the end of the laser pulse to ignite the compressed core of a low-velocity implosion. Spherical plastic-shell targets were used in experiments on the OMEGA laser at low implosion velocity. A strong shock wave was sent into the converging capsule using an intensity spike at the end of the laser pulse. Both the neutron yield and the areal density improved significantly with an optimized spike pulse. In a second experiment, the 60 OMEGA beams were split into 40 low-intensity beams used for fuel assembly and 20 delayed beams focused to a high intensity (up to 1×10^{16} W/cm^2) for shock generation. Preheat and laser absorption during the high-intensity spike were studied using hard x-ray detectors and scattered-light measurements. This work was supported by the U.S. Department of Energy Office of Inertial Confinement Fusion under Cooperative Agreement Nos. DE-FC52-08NA28302, DE-FC02-04ER54789, and DE-FG02-05ER54839.

9:54
TO7 3 Dynamics of Laser-Driven Shock Waves in Solid Targets* Y. AGLITSKIY, M. KARASIK, *SAIC* A.L. VELIKOVICH, V. SERLIN, J. WEAVER, A.J. SCHMITT, S.P. OBENSCHAIN, J. GRUN, *Plasma Physics Division, NRL* N. METZLER, *Artep, Inc.* S.T. ZALESAK, J.H. GARDNER, *Berkeley Research Associates* J. OH, *RSI* E.C. HARDING, *University of Michigan* Accurate shock timing is a key issue of both indirect- and direct-drive laser fusions. The experiments on the Nike laser at NRL presented here were made possible by improvements in the imaging capability of our monochromatic x-ray diagnostics based on Bragg reflection from spherically curved crystals. Side-on imaging implemented on Nike makes it possible to observe dynamics of the shock wave and ablation front in laser-driven solid targets. We can choose to observe a sequence of 2D images or a continuous time evolution of an image resolved in one spatial dimension. A sequence of 300 ps snapshots taken using vanadium backlighter at 5.2 keV reveals propagation of a shock wave in a solid plastic target. The shape of the shock wave reflects the intensity distribution in the Nike beam. The streak records with continuous time resolution show the $x - t$ trajectory of a laser-driven shock wave in a 10% solid density DVB foam.

*Work supported by DoE, Defense Programs.

10:06
TO7 4 Neutron imaging development for inertial confinement fusion experiments TONY CAILLAUD, OLIVIER LANDOAS, ISABELLE THFOIN, FRANCK PHILIPPE, ALEXIS CASNER, JEAN-LUC BOURGADE, *CEA, DAM, DIF, F-91297 Arpajon, France* VLADIMIR GLEBOV, FREDERIC J. MARSHALL, CRAIG SANGSTER, *LLE, University of Rochester, NY 14623, USA* HYE SOOK PARK, HARRY ROBEY, PETER AMENDT, *LLNL, Livermore, CA 94550, USA* Various failure mechanisms may limit fuel compression and ignition during Inertial Confinement Fusion (ICF) experiments with MegaJoule class lasers (e.g., the Laser MégaJoule: LMJ and the National Ignition Facility: NIF). A Neutron Imaging System (NIS) may be used to determine the asymmetries in the hot core and the surrounding cold fuel shell. To reveal such asymmetries, a NIS must record both a primary (14 MeV) and a down-scattered (5-10 MeV) neutron image with high SNR and an image plane spatial resolution as low as 5 μm. We report on the continuing development of an NIS diagnostic at the OMEGA laser facility, using coded apertures. A new large neutron camera (150 mm entrance diameter: scaled for LMJ/NIF design) has been activated at OMEGA. This camera will allow 5 μm resolution for LMJ neutron source. We have tested a set of three detectors that can be used for various NIS diagnostic experiments on OMEGA from low yield (10^9-10^{10} neutrons) low resolution (32 μm) measurements at 4 m from the neutron source to high yield (10^{12}-10^{14} neutrons) high resolution (15 μm) measurements at 13 m. The low yield configuration allowed us to record, the first neutron image on an indirect drive shot with pure deuterium filled capsules.

10:18
TO7 5 Self-generated electric fields in imploding capsules due to shock-front polarization* PETER AMENDT, JOSE MILOVICH, SCOTT WILKS, *LLNL* CHIKANG LI, RICH PETRASSO, FREDRICK SEGUIN, *PSFC MIT* The generation of strong, self-generated electric fields in direct-drive, inertial-confinement-fusion capsules has been reported using 15 MeV proton radiography [1]. A model incorporating charge separation at a shock front [2] is shown to provide good agreement with the measured proton deflections. A simple proton deflectometry model is developed to further assess the origin of the fields and the sensitivity to thickness of the annular field-generating region in an imploding capsule. The strength of the field in a polarized shock front is calculated to be $\approx 10^{10}$ V/m or higher, and is competitive with the criterion for runaway electron generation. Collisional particle-in-cell simulations of a shock front are performed to gauge such kinetic effects and their potential role on shock-front broadening. [1] J.R. Rygg *et al.*, Science **319**, 1223 (2008); C.K. Li *et al.*, PRL **100**, 225001 (2008). [2] Ya. Zel'dovich and Yu. Raizer, *Physics of Shock Waves* (Dover, Mineola NY, 2002), p. 522.

*Prepared by LLNL under Contract DE-AC52-07NA27344.

10:30
TO7 6 Development of Scintillator Detectors for Fast-Ignition Experiments and Down-Scattered Neutron Measurements on OMEGA V.YU. GLEBOV, C. STOECKL, W. THEOBALD, T.C. SANGSTER, K.L. MARSHALL, M.J. SHOUP III, T. BUCZEK, A. PRUYNE, M. FOX, T. DUFFY, *Laboratory for Laser Energetics, U. of Rochester* M.J. MORAN, *LLNL* R. LAUCK, *PTB, Germany* A small signal must be recorded after very large DT or hard x-ray signals in a neutron time-of-flight detector to measure down-scattered neutrons in cryogenic DT implosions or to measure neutron yield in the presence of hard x-ray background from

an ultrahigh-intensity laser. Several detectors with plastic and liquid scintillators were developed and tested at the Omega/Omega EP Laser Facility in cryogenic DT implosions and integrated fast-ignition experiments. A gated photomultiplier tube was used to eliminate large DT or hard x-ray signals. The liquid scintillator consists of 0.4% PPO, 0.04% MSB dissolved in xylene and saturated with oxygen. The afterglow (long decay constant) with this scintillator is $\sim 100\times$ less than conventional scintillators. This is an essential property to mitigate the residual scintillator signal in down-scattered neutron measurements and fast-ignition experiments. Detector designs and responses with the different scintillators will be presented. This work was supported by the U.S. Department of Energy Office of Inertial Confinement Fusion under Cooperative Agreement Nos. DE-FC52-08NA28302, DE-FC02-04ER54789, and DE-FG02-05ER54839.

10:42

TO7 7 Opacity Measurements on Fully Characterized 1.3 MK Titanium Plasmas ROBERT HEETER, SCOTT ANDERSON, GREG BROWN, JOHN CASTOR, JIM EMIG, KEVIN FOURNIER, CARLOS IGLESIAS, STEPHAN MACLAREN, ROSS MARRS, MARILYN SCHNEIDER, CHARLES SORCE, BRIAN WILSON, PETER BEIERSDORFER, *Lawrence Livermore National Laboratory* X-ray transmission spectra from fully characterized, high temperature plasmas provide validation benchmarks for high-energy-density physics models of interest to stellar astrophysics. This work presents new data from experiments at the Omega laser. 24 beams (at $\approx$ 500J/beam) heat the outer chambers of a 3-part (shine-shielded), 1.6 mm diameter hohlraum. The outer chambers radiatively heat a CH-tamped Ti foil in the center. Other beams drive 2 backlighters: a rear wall burnthrough halfraum, and a Kr-filled CH capsule implosion. Looking through the sample to these backlighters, 2 spectrometers measure the sample transmission from 250-1600 eV and 3000-5500 eV, respectively. The lower energy band encompasses the Rosseland mean opacity, governing radiation flow in stellar interiors. Plasma density of 0.05 g/cc, measured by expansion radiography, agrees with pre-shot calculations. Plasma temperature of 110-125 eV (1.3 MK), inferred from n=1 to n=2 titanium absorption lines, is 10-30% below predictions. Use of similar techniques on the National Ignition Facility could validate stellar models in stellar core conditions.

10:54

TO7 8 Anomalous fluorescence line intensity in megavoltage bremsstrahlung* NINO PEREIRA, *Ecopulse. Inc* MARC LITZ, GEORGE MERKEL, *Army Research Laboratory* JOSEPH SCHUMER, JOHN SEELY, *Naval Research Laboratory* JEFF CARROLL, *Youngstown State University* A Cauchois transmission crystal spectrometer intended for laser plasma diagnostics has measured an anomalous ratio between the fluorescence lines in megavoltage bremsstrahlung. When observed in reflection, $K\alpha_1$ fluorescence is twice as strong as the $K\beta$ line, as is usual. However, in forward-directed bremsstrahlung from a 2 MV end point linear accelerator with a tungsten converter, the $K\alpha_1$ and $K\beta$ fluorescence are approximately equal. The anomalous fluorescence line ratio, unity, reflects the large amount of fluorescence generated on the side of the converter where the electrons enter, and the differential attenuation of the fluorescence photons as they pass through the converter to opposite side. Understanding of fluorescence in megavoltage bremsstrahlung is relevant to the explanation of anomalous line ratios in spectra produced by high-energy electrons generated by intense femtosecond laser irradiation.

*Supported by ARL and DTRA.

11:06

TO7 9 X-ray sources such as metallic liner inside plastic cavities are used to test atomic physics models for LMJ simulations FREDERIC GIRARD, L. JACQUET, M. PRIMOUT, D. BABONNEAU, B. VILLETTE, PH. STEMMLER, *CEA/DAM/DIF* Bright multi-keV K-shell emission sources [1-3] are necessary for ICF studies such as radiography of dense materials. Our recent works with titanium (He_α at 4.7 keV) and germanium (He_α at 10.3 keV) lined cavities showed very high multi-keV x-ray conversion efficiencies up to 14.0% and 0.8% (respectively) [3]. Cavities with a titanium, copper or germanium liner have been used on the OMEGA laser facility in Rochester to test specifically atomic physics models coupled to hydrodynamic codes. Simulation results differ significantly from experimental conversion efficiencies for titanium liner but they are close together for germanium one. Atomic physics models do have great impact on X-ray output. The need for accurate predictive simulation is important in order to set up relevant radiography sources for experiments on the path to ignition. Multi-keV emission is diagnosed by a full set of diagnostics giving conversion efficiencies, time dependant x-ray power and imaging, time integrated imaging and high resolution spectra of titanium. [1] D. Babonneau et al., Phys. Plasmas, **15**, 092702, 2008 [2] K. B. Fournier et al., Phys. Plasmas, **16** 052703, 2009 [3] F. Girard et al., Phys. Plasmas, **16**, 052704, 2009

11:18

TO7 10 A Computational Study of X-ray Emissions from Laser-Irradiated Under-dense High-Z X-ray Sources* JEFFREY COLVIN, MARK MAY, KEVIN FOURNIER, STEPHEN MOON, HOWARD SCOTT, *Lawrence Livermore National Laboratory* We generate x-rays from plasmas that are not in local thermodynamic equilibrium (LTE). We first discuss simulations of the x-ray spectral emissions from laser-irradiated very low-density Ge-doped aerogel targets using a 2D radiation-hydrodynamics code incorporating a modern Detailed Configuration Accounting atomic model in non-LTE. We present the details of the computational model and show that, for the $\sim$ 2 keV long-scale-length sub-critical-density plasmas created in experiments at the Omega laser facility, the simulations get both the measured Ge L-shell emission ($\sim$ 1-1.5 keV) and the measured Ge K-shell emission ($\sim$ 10-11 keV) about right, but only by properly accounting for non-local thermal conduction. The older average-atom atomic model is shown to be inadequate for these non-LTE plasmas. We then use the preferred model in the design of larger-scale experiments planned for the National Ignition Facility, in which we will use 350 kJ of laser beam energy to heat a mixture of Ar and Xe gas to peak temperatures $>$ 5 keV. We predict 20% x-ray conversion efficiency into Ar K-shell and Xe L-shell emission.

*This work was performed under the auspices of the U.S. Department of Energy by LLNL under Contract No. DE-AC52-07NA27344.

11:30

TO7 11 Spectroscopic study of z-pinch K-shell x-ray sources* B. JONES, G.A. ROCHAU, J.E. BAILEY, D.J. AMPLEFORD, C.A. COVERDALE, S.B. HANSEN, C.A. JENNINGS, M.E. CUNEO, *Sandia National Laboratories* Y. MARON, V. FISHER, V. BERNSHTAM, A. STAROBINETS, L. WEINGARTEN, *Weizmann Institute* J.P. APRUZESE, A. DASGUPTA, R.W. CLARK, J.W. THORNHILL, K.G. WHITNEY, J.L. GIULIANI, J. DAVIS, *Naval Research Laboratory* Fast z-pinches provide intense 1-10 keV photon energy radiation sources. Analysis of time-integrated K-shell x-ray spectra indicates electron temperatures up to 5 keV

and ion densities of order 10^{20} cm^{-3} in the stagnated plasma created from wire array implosions on Sandia's Z machine pulsed power driver. Elliptical crystal spectrometers coupled to microchannel plate detectors, fielded previously on Z, have recently provided time-resolved spectral measurements for Al (~ 2 keV), stainless steel (~ 6.7 keV), and Cu (~ 8.4 keV) sources. We discuss implosion and stagnation dynamics, plasma conditions, and spectral analysis in the presence of opacity and Doppler effects.

*Sandia is a multi-program laboratory operated by Sandia Corporation, a Lockheed Martin Company, for the United States Department of Energy's National Nuclear Security Administration under contract DE-AC04-94AL85000.

11:42

TO7 12 Searching for efficient Z-pinch L-shell Radiators using Cu, Mo, and Ag Single Planar Wire Arrays on 1.6 MA ZEBRA at UNR A.S. SAFRONOVA, V.L. KANTSYREV, A.A. ESAULOV, N.D. OUART, M.F. YILMAZ, V. SHLYAPTSEVA, I. SHRESTHA, K.M. WILLIAMSON, M.E. WELLER, G.C. OSBORNE, *UNR* C.A. COVERDALE, *SNL* C. DEENEY, *DOE* The comparative analysis of the results of recent experiments with single planar wire array (SPWA) loads made from Cu, Mo, and Ag performed on 1.6 MA Zebra at UNR is presented. The diagnostic set included a bolometer, x-ray detectors, laser shadowgraphy, x-ray time-gated and integrated imaging, and x-ray time integrated spatially resolved and time-gated spatially integrated spectrometers. The x-ray yields from such mid-Z_a SPWAs exceed twice those from low-Z_a wire arrays such as Al PWAs, increase with Z_a, and reach more than 24 kJ for Ag. The size of the x-ray source decreases as Z_a increases, which lowers the opacity effects. The maximum L-shell plasma electron temperature increases as Z_a increases, up to 1.4 keV for Mo and Ag. These results and the developed models have much broader application, not just only for SPWAs on Zebra, but for higher current Z-pinch generators such as Z at SNL. This work was supported by NNSA under DOE CA DE-FC52-06NA27588, DE-FC52-06NA27586, and in part by DE-FC52-06NA27616. Sandia is a multi-program laboratory operated by Sandia Corporation, a Lockheed Martin Company, for the US DOE under Contract DE-AC04-94AL85000.

11:54

TO7 13 X-Ray Emission Trends with Atomic Number and Initial Array Radius from K-Shell Z Pinches C.A. COVERDALE, B. JONES, D.J. AMPLEFORD, M.E. CUNEO, *Sandia National Labs* C. DEENEY, *NNSA/DOE* P.D. LEPELL, *Ktech Corp.* K.G. WHITNEY, *Berkeley Research Associates* J.W. THORNHILL, J. GIULIANI, J. DAVIS, J.P. APRUZESE, A. DASGUPTA, *NRL* Experiments at the pre-refurbished Z facility covered a wide range of K-shell x-ray sources, including Ti (4.7 keV), SS (6.7 keV), and Cu (8.4 keV). The initial wire array radius of single and nested configurations was varied for each of these materials. The total x-ray emission decreased with larger diameter wire arrays for all materials, and nested arrays generally produced higher powers than single arrays. The K-shell emission for Ti behaved as expected based on the K-shell scaling theory [J.W. Thornhill et al., Phys. Plasmas **1**, 321 (1994)], with decreases in K-shell output observed for $\eta < 2$ and for mass < soft mass breakpoint (m_{bp}). For SS, the scaling theory would predict inefficient K-shell emission for all the loads fielded ($\eta > 2$, but mass < soft m_{bp}), although the K-shell output increased for larger diameter loads, even with masses < soft m_{pb}. Emission from the higher atomic number arrays appears to be dominated by regions of brightly emitting plasma. Sandia is a multi-program laboratory operated by Sandia Corporation, a Lockheed Martin Company, for the United States Department of Energy under Contract DE-AC04-94AL85000.

12:06

TO7 14 Analysis of space- and time-resolved Ar K-shell emission in ICF experiments and determination of plasma spatial structure I.E. GOLOVKIN, J.J. MACFARLANE, P.R. WOODRUFF, *Prism Computational Sciences, Inc.* J.E. BAILEY, G.A. ROCHAU, R.J. LEEPER, *Sandia National Laboratories, Albuquerque* We present a novel method to determine spatial distributions of the plasma temperature, density and relative fuel-pusher material fractions (mix) based on the analysis of space- and time-resolved spectroscopic data obtained in ICF implosion experiments. The determination of space-dependent plasma characteristics provides important constraints for radiation- hydrodynamics calculations and improves the understanding of implosion physics. Determination of the plasma spatial structure is a complex inverse problem with a non-trivial dependence of spectroscopic observables on the plasma distributions. We will present the genetic-algorithm-based analysis of the data and demonstrate that the plasma conditions can be successfully determined. All spectral simulations are performed using a suite of codes contained in the SPECT3D Imaging and Spectral Analysis package. We will discuss the details of the calculations based on the analysis of synthetic experimental data generated with known plasma distributions.

SESSION TP8: POSTER SESSION VII
Thursday Morning, 5 November 2009
Grand Hall East at 9:30

TP8 1 DIII-D TOKAMAK III

TP8 2 Effect of Self-consistent Poloidal Electric Field on Neoclassical Angular Momentum Transport* S.K. WONG, V.S. CHAN, *General Atomics* Existing calculations of toroidal angular momentum flux in the banana regime of neoclassical transport theory have neglected the self-consistent electric field, or the poloidal variation of the electric potential, that arises from quasi-neutrality. Recently, it has been shown that this variation cannot be neglected in the Pfirsch-Schluter regime, where it in fact gives the dominant contribution for large aspect ratio flux surfaces. We show that the same conclusion applies in the banana regime. We have revisited the calculation of this variation in the banana regime, and found an analytic expression that does not have the divergence at the inner most point of the flux surface noted in an earlier work, although it is still discontinuous there. Using this expression, and an analytic solution of the linearized drift kinetic equation based on a model collision operator, we have obtained a closed form for the angular momentum flux to leading order of an expansion in inverse aspect ratio. The result is larger than the existing one by the order of square root of inverse aspect ratio.

*Work supported by US DOE under DE-FG03-95ER54309.

TP8 3 Toroidal Rotation With Near-Balanced NBI in DIII-D H-Mode Discharges* J.S. DEGRASSIE, K.H. BURRELL, R.J. GROEBNER, *General Atomics* W.M. SOLOMON, *PPPL* Intrinsic rotation exists in the tokamak with no applied auxiliary torque and is important to understand for projection to burning plasmas and ITER. Rice's scaling, that $V \sim W/I_p$ [1], exists in other tokamaks, including DIII-D, where V is toroidal velocity, and W the stored energy. A dimensionless casting of this scaling is being sought [1]. Heating by rf waves is the primary tool to investigate intrinsic rotation in H-mode conditions. It is difficult to attain ITER-relevant values of $\beta_N \sim 2$ simply due to the typical rf power capabilities installed, compared with neutral beam injection (NBI). In DIII-D we are using the balanced beam capability to investigate the intrinsic rotation scaling at these β_N values. An issue is the localized remnant torque density that exists to some extent with mirrored beam injection, because of the opposite radial drift of co- and counter-injected fast ions. We will show how these higher β_N conditions compare with the Rice scaling and account for remnant torque. [1] J.E. Rice, Nucl. Fusion **47**, 1618 (2007).

*Work supported by the US DOE under DE-FC02-04ER54698 and DE-AC02-09CH11466.

TP8 4 H-mode Power Threshold, ELM Characteristics and Control, and Plasma Startup in Helium Plasmas in DIII-D* P. GOHIL, *General Atomics* AND THE DIII-D HELIUM PLASMA TEAM, Determining the physics of helium plasmas and comparing with hydrogen and deuterium plasmas is important for the validation of key issues in plasma physics. This is also important for the first operational phase of ITER, which will use helium or hydrogen plasmas. Physcs issues for helium plasmas include: (a) the H-mode power threshold and the H-mode pedestal and ELM characteristics; (b) ELM suppression by resonant magnetic perturbations; (c) requirements for ITER plasma start-up and ramp-down. There is also the question of whether recent results from deuterium and hydrogen plasmas hold for helium plasmas. For example, recent studies of the H-mode power threshold in hydrogen and deuterium indicate that the power required to induce the L-H transition is dependent on the applied beam torque, and the H-mode power threshold using ECH (or a combination of ECH +NBI) is 20%-40% lower than that for discharges using NBI alone. Results from experiments to investigate issues (a) to (c) above in helium plasmas will be presented.

*Work supported by the US DOE under DE-FC02-04ER54698.

TP8 5 Core Turbulence and Flow Dynamics Across L-H Transition on DIII-D* G. WANG, W.A. PEEBLES, T.L. RHODES, J.C. HILLESHEIM, E.J. DOYLE, L. SCHMITZ, L. ZENG, *UCLA* A.E. WHITE, *ORISE* G.R. McKEE, *U. Wisc.* C.C. PETTY, K.H. BURRELL, *General Atomics* W.M. SOLOMON, *PPPL* First measurements of core low and intermediate-k correlation lengths as well as the dynamic turbulence amplitude behavior across near-balanced NBI-heated L- to H-mode transitions have been obtained on DIII-D. In these discharges, poloidal turbulence flow increases with little change in its shear as the L-H transition is approached. Leading up to the transition, fluctuation levels ($\tilde{n}/n$) of low-k (< 3 cm^{-1}) show little variation, while that of intermediate- (3 $-$ 6 cm^{-1}) and high-k ($\sim$ 35 cm^{-1}) increase. At the same time, core radial correlation lengths of both low and intermediate-k decrease. In contrast, electron temperature fluctuation levels ($\tilde{T}_e/T_e$) first increase then drop. With these data a multi-scale and multi-field picture of the L to H transition dynamics is being developed allowing detailed comparison to theory and simulation (e.g. linear gyrokinetic stability simulations, TGLF).

*Work supported by the US DOE under DE-FG03-08ER54984, DE-AC05-06OR23100, DE-FG02-89ER53296, DE-FG02-08ER54999, DE-FC02-04ER54698 and DE-AC02-09CH11466.

TP8 6 Turbulence and Transport Dependence on Plasma Shape in DIII-D* T.L. RHODES, W.A. PEEBLES, L. SCHMITZ, J.C. HILLESHEIM, G. WANG, L. ZENG, E.J. DOYLE, *UCLA* C. HOLLAND, *UCSD* G.R. McKEE, *U. Wisc.* A.E. WHITE, *ORISE* J.C. DEBOO, K.H. BURRELL, C.C. PETTY, *General Atomics* Using a unique array of diagnostics the dependence of turbulence and transport on plasma shape (elongation, elongation shear, and triangularity) is studied. The diagnostic set includes FIR scattering, Doppler backscattering, correlation ECE, BES, reflectometry, and high-k backscattering. This covers a broad range in wavenumber ($0 \leqslant k\rho_s \leqslant 10$) and fields (density, temperature, flows). The measurements concentrated primarily on L-mode plasmas, although, H-mode was obtained in one shape. Data were obtained using two different heating methods, neutral beam and EC heated. Initial results show strong decreases in density and temperature fluctuation levels as the plasma elongation is increased at fixed q_{95}. Thermal transport is reduced as well. This data set was acquired in order to make detailed comparisons to turbulence and transport models such as GYRO and TGLF.

*Work supported by the US DOE under DE-FG03-08ER54984, DE-FG02-07ER54917, DE-FG02-89ER53296, DE-FG02-08ER54999, DE-AC05-06OR23100, and DE-FC02-04ER54698.

TP8 7 2D Core Turbulence Properties on DIII-D* M.W. SHAFER, G.R. McKEE, R.J. FONCK, D.J. SCHLOSSBERG, Z. YAN, *U. Wisconsin-Madison* C. HOLLAND, *UCSD* A.E. WHITE, *ORISE* Quantitative measurements of the inherently 2D turbulence characteristics in magnetized plasmas are compared with nonlinear simulation. This comparison substantiates key aspects of the $E \times B$ shear model of turbulence suppression that explains enhanced confinement. The critical dynamics underlying turbulent transport occur in the plane perpendicular to the magnetic field ($k_\parallel \ll k_\perp$). These localized long-wavelength ($k_\perp \rho_i < 1$) density turbulence measurements are obtained in the core ($0.3 < r/a < 0.9$) of DIII-D L-mode plasmas with a 2D rectangular array of Beam Emission Spectroscopy channels. Radial and poloidal correlation lengths are found to scale with the ion gyroradius and demonstrate a poloidally elongated eddy structure. $S(k_r, k_\theta)$ spectra are compared with GYRO simulations: key features (wavenumber peak, correlation lengths) compare well, however the simulations indicate a sheared eddy structure at outer radii that is not observed. Measured local decorrelation and shearing rates are also compared.

*Work supported by the US DOE under DOE under DE-FG02-89ER53296, DE-FG02-08ER54999, DE-FG02-07ER54917, and DE-AC05-06OR23100.

TP8 8 Density Fluctuation Enhancement During RMP ELM-Suppressed Discharges* G.R. McKEE, R.J. FONCK, D.J. SCHLOSSBERG, M.W. SHAFER, Z. YAN, *U. Wisconsin-Madison* T.E. EVANS, *General Atomics* R.A. MOYER, *UCSD* Fluctuation behavior changes dramatically over the radial range $0.6 < r/a < 1.0$ during ELM-suppressed phases of H-mode discharges with externally applied resonant magnetic perturbations (RMPs) on DIII-D. The 2D spatiotemporal characteristics of density fluctuations during ELM suppression are characterized with beam emission spectroscopy and exhibit a broadband structure from 80− 400 kHz. The fluctuation power increases by up to one order of magnitude in the mid-core region ($0.6 < r/a < 0.8$), with more modest increases in the pedestal region. The increase in turbulence coincides with the ELM-suppressed phases, which typically start a few 100 ms after the application of a radial magnetic field. The radial and poloidal correlation lengths of the increased fluctuations are a few centimeters, typical of long-wavelength turbulence. The increased fluctuations appear to be related to observed profile changes, reduction of the line integrated density, and increased radial particle transport.

*Work supported by the US DOE under DE-FG02-89ER53296, DE-FG02-08ER54999, DE-FC02-04ER54698 and DE-FG02-07ER54917.

TP8 9 Transport of Energetic Ions Due to Interaction With Microturbulence in DIII-D* D.C. PACE, W.W. HEIDBRINK, Z. LIN, W. ZHANG, *U. California-Irvine* G.R. McKEE, *U. Wisconsin-Madison* M. MURAKAMI, J.M. PARK, *ORNL* C.C. PETTY, M.A. VAN ZEELAND, *General Atomics* Cross-field diffusion of energetic ions due to microturbulence is observed during neutral beam injection in the DIII-D tokamak. The energetic ion energy spectrum and radial density profile are measured with fast-ion D_α, neutron detection, and motional Stark effect systems. DIII-D discharges study the range $5 < E/T_e < 20$, where E is the energy of the energetic ions injected by neutral beams and T_e is the electron temperature, in order to test theoretical results [1] that show energetic ion diffusion increasing as this ratio decreases. The parameter space is relevant to energetic ions in present tokamaks and helium ash in ITER. Density fluctuations related to the microturbulence are measured with beam emission spectroscopy and are consistent with ion-temperature gradient and trapped electron modes. Progress on simulating this phenomenon with the gyrokinetic codes GYRO and GTC will be presented. [1] W. Zhang, et al., Phys. Rev. Lett. **101** (2009) 095001.

*Work supported by the US DOE under SC-G903402, DE-FG02-89ER53296, DE-FG02-08ER54999, DE-AC05-00OR22725, and DE-FC02-04ER54698.

TP8 10 Modeling the H-mode Barrier with TGLF* G.M. STAEBLER, J.E. KINSEY, R.E. WALTZ, *General Atomics* The trapped gyro-Landau fluid (TGLF) transport model was designed to be valid in the near separatrix region of tokamaks and spherical tori. Since the last published version [1], a number of improvements have been made to TGLF: general numerical equilibrium magnetic geometry, improved electron-ion collision model, improved saturation rule. Most importantly, momentum transport has been added. Both the parallel and $E \times B$ velocity shear and the coriolis drift are now included in the eigenmode calculation so that the linear wavefunction and viscous stress matrix can be computed quasi-linearly. The $E \times B$ velocity shear is included using a generalization of the successful quench rule that includes a model for the radial wavenumber induced by the $E \times B$ velocity shear. With these improvements, the TGLF model is ready to push out to the edge of the closed flux surface region. The first TGLF results of linear stability calculations and particle, energy and momentum transport simulations of H-mode and L-mode near edge regions of the DIII-D tokamak will be reported. [1] J.E. Kinsey, et al., Phys. Plasmas **15**, 055909 (2008).

*Work supported by the US DOE under DE-FG03-95ER54309.

TP8 11 Predictions of the Confinement in DIII-D Hybrids Using the TGLF Transport Model* J.E. KINSEY, G.M. STAEBLER, R.E. WALTZ, J. CANDY, *General Atomics* In previous work, the TGLF gyro-Landau-fluid transport model [1,2] was validated against a profile database of 96 L- and H-mode discharges. This work focuses on modeling hybrid discharges using an upgraded collision model in TGLF. Recent comparisons between TGLF and GYRO [3] nonlinear simulations of long wavelength driftwave turbulence with collisions motivated improving the collision model in TGLF. Using a newly developed collision model results in the TGLF diffusivities more accurately fitting a database of 35 nonlinear GYRO runs performed with collisions and Miller geometry. TGLF transport simulations of 32 DIII-D hybrid discharges show good agreement with both the ion and electron experimental temperature profiles. The transport simulations show the ion transport tends to be close to the neoclassical level while the electron transport tends to be dominated by short wavelength ETG modes. [1]J.E. Kinsey, et al., Phys. Plasmas **15**, 055908 (2008). [2]G.M. Staebler, et al., Phys. Plasmas **12**, 102508 (2005). [3]J. Candy, R.E. Waltz, Phys. Rev. Lett. **91**, 45001 (2003).

*Work supported by the US DOE under DE-FG03-95ER54309.

TP8 12 Experimental Tests of Elongation Scaling in Gyrokinetic Turbulence Simulations* C. HOLLAND, G.R. TYNAN, *UCSD* T.L. RHODES, W.A. PEEBLES, L. SCHMITZ, J.C. HILLESHEIM, G. WANG, L. ZENG, E.J. DOYLE, *UCLA* G.R. McKEE, Z. YAN, M.W. SHAFER, *U. Wisc.* A.E. WHITE, *ORISE* J. CANDY, R.E. WALTZ, J.E. KINSEY, G.M. STAEBLER, J.C. DEBOO, R. PRATER, K.H. BURRELL, C.C. PETTY, *General Atomics* M.A. MAKOWSKI, *LLNL* Comparisons of nonlinear GYRO simulations of DIII-D discharges with low and high elongation against experimental measurements are presented. Comparisons of measured low-k density spectra (from beam emission spectroscopy), intermediate-k density spectra (from Doppler backscattering), and low-k electron temperature spectra (from correlation electron cyclotron emission radiometry) to synthetic spectra predictions at multiple flux-surfaces are shown. Results using both direct fits to profile measurements and flux-matching profiles predicted by the new TGYRO code [1] are presented, with agreement between model and experiment assessed via a simple set of newly developed validation metrics. [1] J. Candy, et al., General Atomics Report GA-A26380 (2009).

*Work supported by US DOE under DE-FG02-07ER54917, DE-FG03-08ER54984, DE-FG02-89ER53296, DE-FG02-08ER54999, DE-AC05-06OR23100, DE-FG03-95ER54309 and DE-AC52-07NA27344.

TP8 13 Study of the Variation of Turbulence with Poloidal Angle on DIII-D Using Phase Contrast Imaging* J.C. ROST, M. PORKOLAB, J.R. DORRIS, *MIT* K.H. BURRELL, *General Atomics* The Phase Contrast Imaging (PCI) diagnostic on DIII-D, which measures density fluctuations with $k < 30$ cm^{-1}, has operated with three different beam paths; vertical through the last closed flux surface at the outboard midplane (edge), 11 deg from vertical through the outer plasma reaching $r/a = 0.75$ (Phase I), and now vertical through $r/a = 0.4$ (Phase II). PCI measures modes propagating perpendicular to the beam path, i.e. $k_\theta < 0.1k_r$ with the edge path and $k_\theta \sim k_r$ at the edge in Phase I and II. The beam paths also sample the turbulence at different poloidal angles. Results from the three beam paths combined provide a more complete description of the turbulence. Results from the edge and Phase I paths show that the turbulence phase velocity varies more with k_θ/k_r than is accounted for by Doppler shifts. Also, the spectra $S(k)$ show a complex variation in shape with θ and k_θ/k_r. Initial results from Phase II will be presented to help disambiguate the various possible dependencies.

*Work supported by the US DOE under DE-FG02-04ER54235 and DE-FC02-04ER54698.

TP8 14 Measurements of the Wavenumber Spectrum of Multi-scale Turbulence in the Core of DIII-D H-mode Plasmas* L. SCHMITZ, G. WANG, J.C. HILLESHEIM, W.A. PEEBLES, T.L. RHODES, E.J. DOYLE, L. ZENG, *UCLA* C. HOLLAND, *UCSD* A.E. WHITE, *ORISE* G.R. McKEE, *U. Wisconsin-Madison* J.C. DEBOO, J.S. DEGRASSIE, K.H. BURRELL, C.C. PETTY, *General Atomics* The wavenumber spectrum and spectral index of multi-scale turbulence ($0.5 \leq k_\theta\rho_s \leq 6$) in the core of L- and H-mode DIII-D plasmas have been determined by Doppler Backscattering (DBS). A comparison is made to quasi-linear spectra from the trapped gyro-Landau fluid code (TGLF) to assess the contributions of ITG and TEM/ETG turbulence to transport fluxes ($0.4 \leq r/a \leq 0.8$). Initial results of comparisons to spectra calculated via nonlinear gyrokinetic (GYRO) simulations are also presented. In high temperature, low density plasmas, ITG-scale and intermediate-scale core turbulence is found reduced by at least an order of magnitude across the L- to H-mode transition ($T_i/T_e \geq 2$). This reduction is attributed to the combined effects of reduced turbulence drive and increased core $E \times B$ flow shear in H-mode.

*Work supported by the US DOE under DE-FG03-08ER54984, DE-FG02-07ER54917, DE-AC05-06OR23100, DE-FG02-89ER53296, DE-FG02-08ER54999 and DE-FC02-04ER54698.

TP8 15 High Resolution Density Profile Measurement for Electron Transport Studies in DIII-D* L. ZENG, E.J. DOYLE, T.L. RHODES, W.A. PEEBLES, *UCLA* C.C. PETTY, J.C. DEBOO, *General Atomics* W.M. SOLOMON, *PPPL* T. TALA, *VTT/JET* High temporal (to 10 μs) and spatial ($\sim$ 0.5 cm) resolution measurements of density profile evolution via profile reflectometry have been performed in a variety of plasma conditions in DIII-D. These measurements are currently applied to study particle transport. As one example, in a D_2 gas puffing modulation experiment, it is observed that the n_e modulation can propagate from the edge inward to $\rho \sim 0.4$. The dependence of the modulations on q and collisionality is under investigation. In an experiment with EC power alternately deposited at two close positions, it has been seen that the n_e profile is significantly modulated by the EC modulations when the EC power at two locations is unbalanced. The n_e modifications become smaller when the EC power is balanced. For these n_e modulation datasets, an FFT transport analysis technique will be applied to investigate transport coefficients and particle pinch velocity. In addition, the associated n_e fluctuations over a broad range of k will be presented.

*Work supported by the US DOE under DE-FG03-08ER54984, DE-FC02-04ER54698, and DE-AC02-09CH11466.

TP8 16 Analysis of Particle Transport in DIII-D H-mode Plasma with a Generalized Pinch-Diffusion Model* L.W. OWEN, *Oak Ridge National Laboratory* W.M. STACEY, *Georgia Tech* R.J. GROEBNER, *General Atomics* J.D. CALLEN, *U. Wisconsin-Madison* X. BONNIN, *LIMHP* Interpretative analyses of particle transport in the pedestal region of H-mode plasmas typically yield diffusion coefficients that are very small (< 0.1 m^2/s) in the steep gradient region when a purely diffusive particle flux is fitted to the experimental density gradients. Previous evaluation of the particle and momentum balance equations using the experimental data indicated that the pedestal profiles are consistent with transport described by a pinch-diffusion particle flux relation [1]. This type of model is used to calculate the diffusion coefficient and pinch velocity in the core for an inter-ELM H-mode plasma in the DIII-D discharge 98889. Full-plasma SOPLS simulations using neutral beam particle and energy sources from ONETWO calculations and the model transport coefficients show good agreement with the measured density pedestal profile. [1] W.M. Stacey and R.J. Groebner, Phys. Plasmas **12**, 042504 (2005).

*Work supported by US DOE under DE-AC05-00OR22725, DE-FG02-00ER54538, DE-FC02-04ER54698, DE-FG02-92ER54139 and DE-FG02-08ER54999.

TP8 17 Analysis of Pedestal Transport* J.D. CALLEN, *U. Wisconsin-Madison* R.J. GROEBNER, T.H. OSBORNE, *General Atomics* J.M. CANIK, L.W. OWEN, *ORNL* A. PANKIN, T. RAFIG, *Lehigh University* T.D. ROGNLIEN, *LLNL* W.M. STACEY, *Georgia Tech.* To clarify plasma transport properties in the pedestal, we have undertaken an H-mode Edge Pedestal (HEP) Benchmarking Exercise (BE) for a single DIII-D pedestal. Codes used include 1.5D interpretive (ONETWO, WMS), 1.5D predictive (ASTRA) and 2D (SOLPS, UEDGE) codes. The particular DIII-D discharge considered is 98889, which has a typical low density H-mode pedestal. Transport properties are analyzed in near transport equilibrium between Type I ELMs. Both 2D and 1.5D transport properties are obtained and compared. Inferred radial diffusivities are smallest near the midpoint of the pedestal, about $0.1 - 0.3$ m^2/s for electron and ion heat but 10 times smaller for net particle transport. The small effective particle diffusivity could be the result of an inward particle pinch nearly balancing a diffusive outward radial particle flux. These and other pedestal plasma transport properties will be discussed.

*Work supported by US DOE under DE-FG02-92ER54139, DE-FG02-08ER54999, DE-FC02-04ER54698, DE-AC05-00OR22725, DE-FG02-92ER54141, DE-AC52-07NA27344 and DE-FG02-00ER54538.

TP8 18 Further Development of a Predictive Pedestal Model* P.B. SNYDER, R.J. GROEBNER, A.W. LEONARD, T.H. OSBORNE, *General Atomics* H.R. WILSON, *University of York* The pressure at the top of the edge transport barrier (or "pedestal height") strongly impacts tokamak fusion performance, and first

principles prediction of the pedestal height remains an important challenge. A recently developed model, EPED1, combines a calculated peeling-ballooning stability constraint with a simple equation describing kinetic ballooning mode (KBM) onset to yield a predictive model of the pedestal height and width. The model has been successfully tested under a wide range of conditions on several tokamaks, included in a dedicated experiment where predictions were made before the experiment was conducted. Here we discuss continuing development of the model, including a more comprehensive KBM model based directly on gyrokinetic calculations, and improved treatment of diamagnetic stabilization.

*Work supported in part by the US DOE under DE-FG03-95ER54309.

TP8 19 Test of a Model for Limits to Pedestal Pressure Gradient in DIII-D* R.J. GROEBNER, P.B. SNYDER, T.H. OSBORNE, A.W. LEONARD, *General Atomics* T.L. RHODES, L. ZENG, *UCLA* Z. YAN, G.R. McKEE, *University of Wisconsin-Madison* The EPED1 pedestal model predicts that kinetic ballooning modes (KBM) limit the magnitude of the H-mode pedestal pressure gradient, prior to the onset of the ELM instability. Time-resolved measurements of the total pedestal pressure profile are used to test this hypothesis in Type I edge localized mode (ELM) discharges in DIII-D. These measurements show that there is a significant spatial and temporal variation of the pedestal pressure gradient as the pedestal builds up between ELMs. In some regions of the pedestal, particularly in the outer half of the pedestal, the pressure gradient becomes nearly time-stationary long before an ELM crash. When this happens, increases of pressure gradient often are observed in other regions of the pedestal. Thus, the entire pedestal pressure gradient does not usually saturate at one time. The observed pressure gradients will be examined to see if they scale with predictions of linear theory for ballooning modes.

*Work supported by the US DOE under DE-FC02-04ER54698, DE-FG03-08ER54984, DE-FG03-08ER54999 and DE-FG02-89ER53296.

TP8 20 Quiescent H-mode Plasmas in DIII-D with Strong, Co-Current Edge Rotation* K.H. BURRELL, T.H. OSBORNE, P.B. SNYDER, R.J. GROEBNER, P. GOHIL, *General Atomics* M.E. FENSTERMACHER, *LLNL* W.M. SOLOMON, *PPPL* For the first time in any tokamak, quiescent H-mode (QH-mode) plasmas have been created with neutral beam injection in the direction of the plasma current (co-injection) and with edge rotation in the co-current direction. Previous QH-mode plasmas have always exhibited counter-current rotation of the plasma edge. The existence of QH-mode with strong edge co-rotation is a confirmation of the theoretical prediction that QH-mode should exist with either sign of the edge rotation provided the magnitude of the shear in the edge rotation is sufficiently large. In addition, detailed comparison of the edge plasma conditions with peeling-ballooning mode stability theory shows good agreement with that theory. This extends the previous detailed confirmation of the theory to co-rotating QH-mode plasmas. Furthermore, the existence of QH-mode with edge co-rotation demonstrates that counter NBI and counter edge rotation are not essential conditions for QH-mode.

*Work supported by the US DOE under DE-FC02-04ER54698, DE-AC52-07NA27344 and DE-AC02-09CH11466.

TP8 21 H-Mode Pedestal Structure and Transport in Hybrid Plasmas During Magnetic Perturbation in the DIII-D Tokamak* B. HUDSON, *ORISE* A.W. LEONARD, T.E. EVANS, T.H. OSBORNE, C.C. PETTY, P.B. SNYDER, *General Atomics* The effect of resonant magnetic perturbation (RMP) on the H-mode pedestal structure is studied in hybrid discharges in the DIII-D tokamak. The empirical window for complete edge localized mode (ELM) suppression appears to be the same as in standard H-mode plasmas, which is $3.5 < q_{95} < 3.9$. A reduction in the pedestal bootstrap current during RMP is inferred through a decrease in q_{95}, at fixed I_p/aB_T, consistent with the measured reduction in the edge pressure gradient. Statistical analysis indicates that magnetic and MSE measurements are consistent with an edge parallel current profile given by the Sauter bootstrap current model. Small amplitude ELMs are observed to return, when the rotation frequency becomes small or when q_{95} is outside the resonance window for ELM suppression, associated with an increase in pedestal electron temperature and a decrease in the calculated magnetic field line diffusion. The EPED1 model and ELITE code are used to predict the pedestal height and determine ELM stability.

*Work supported by the US DOE under DE-AC05-06OR23100 and DE-FC02-04ER54698.

TP8 22 Non-Ideal ELM Stability and Non-Axisymmetric Field Penetration Calculations with M3D-C1* N.M. FERRARO, M.S. CHU, P.B. SNYDER, *General Atomics* S.C. JARDIN, *PPPL* X. LUO, *Rensselaer Polytechnic* Numerical studies of ELM stability and non-axisymmetric field penetration in diverted DIII-D and NSTX equilibria are presented, with resistive and finite Larmor radius effects included. These results are obtained with the nonlinear two-fluid code M3D-C1, which has recently been extended to allow linear non-axisymmetric calculations. Benchmarks of M3D-C1 with ideal codes ELITE and GATO show good agreement for the linear stability of peeling-ballooning modes in the ideal limit. New calculations of the resistive stability of ideally stable DIII-D equilibria are presented. M3D-C1 has also been used to calculate the linear response to non-axisymmetric external fields; these calculations are benchmarked with Surfmn and MARS-F. New numerical methods implemented in M3D-C1 are presented, including the treatment of boundary conditions with C^1 elements in a non-rectangular mesh.

*Work supported in part by the US DOE under DE-FG02-95ER54309 and DE-AC02-09CH11466.

TP8 23 3D Equilibria for DIII-D ELM Suppression Experiments E.A. LAZARUS,* *Oak Ridge National Laboratory* 3D equilibria have been successfully calculated for DIII-D ELM-suppression experiments in the n=3 configuration using the VMEC equilibrium code. These include the usual poloidal coils as well as the I-coils that produce the perturbation suppressing the ELMs, the error correction coils (C-coils) and the 24 discrete B-coils that produce the TF ripple. No stellarator symmetry is assumed. Relatively minor changes to VMEC enabled such solutions to be obtained, Details of the solutions will be discussed. Solutions take of order a cpu-day per case. Thus far we have used $N_{fp} = 3$, and obtained solutions with toroidal mode numbers $-24 \leq n \cdot N_{fp} \leq 24$, poloidal mode numbers $0 \leq m \leq 12$, and

193 radial zones. We expect to increase the radial resolution and poloidal mode upper bound. Such solutions allow investigation of the possibility that the interaction of the I-coils with the TF ripple plays a role in the observed phenomenology. Results will be presented.

*Work supported in part by the U.S. DOE under contract DE-AC05-00OR22725.

TP8 24 Simulations of Nonlinear ELM Instabilities in Tokamaks* T.E. EVANS, *General Atomics* A. WINGEN, K.H. SPATSCHEK, *Heinrich-Heine University* C.J. LASNIER, *Lawrence Livermore National Laboratory* A model describing the 3D nonlinear evolution of ELMs in DIII-D has been developed. The model invokes field-aligned currents flowing through short flux tubes embedded in the pedestal plasma that connect the outer to the inner target plate. These flux tubes are initially formed by field-errors and a field-error correction coil. Magnetic perturbations due to these currents cause the separatrix topology to evolve which increases the area of the flux tubes and the magnitude of the current. This creates a positive feedback loop. Simulation results are compared to fast IR camera images of ELM heat flux in the divertor. Good agreement between the calculated magnetic structures on the divertor components and camera images during an ELM cycle is found. The simulation predicts a bifurcation from an $n = 1$ homoclinic tangle and an $n = 2$ heteroclinic tangle as the separatrix topology evolves during the growth of an ELM. Implications for suppressing ELMs with external magnetic perturbations are also discussed.

*Work supported in part by the US DOE under DE-FC02-04ER54698 and DE-AC52-07NA27344.

TP8 25 Initial Results from Radiating Divertor Experiments with RMP ELM Suppression* T.W. PETRIE, N.H. BROOKS, T.E. EVANS, J.R. FERRON, A.W. HYATT, T.C. LUCE, P.A. POLITZER, C.C. PETTY, M.J. SCHAFFER, *General Atomics* M.E. FENSTERMACHER, C.J. LASNIER, G.D. PORTER, *Lawrence Livermore National Laboratory* J.G. WATKINS, *Sandia National Laboratory* S. MORDIJCK, *University of California-San Diego* The"radiating divertor" has been posited as an important way of controlling heat flux at the divertor targets. Significant theoretical and experimental progress has been made during previous campaigns at DIII-D at identifying conditions leading to optimal radiating divertor operation [1]. During this same period, several studies at DIII-D clearly demonstrated that eliminating edge localized modes (ELMs) from H-mode plasmas using the resonant magnetic perturbation (RMP) approach could be an attractive possibility for solving the "ELM-issue" in ITER. Whether this ELM suppression approach is compatible with radiating divertor scenarios, however, has been an open question. In this presentation, we present results from the first attempts at combining active ELM by RMP suppression with radiating divertor scenarios. [1] T.W. Petrie, et al., Nucl. Fusion **49** (2009) 065013.

*Work by the US DOE under DE-FC02-04ER54698, DE-AC52-07NA27344, DE-AC04-94AL85000, and DE-FG02-07ER54917.

TP8 26 Particle Exhaust and Scrape-off Layer Conditions During RMPs in Deuterium and Helium Discharges on DIII-D* E.A. UNTERBERG, *ORISE* T.E. EVANS, *General Atomics* J.M. CANIK, *ORNL* O. SCHMITZ, *Forschungszentrum Julich* R. MAINGI, *ORNL* N.H. BROOKS, *General Atomics* The complete suppression of ELMs in a tokamak using the resonant component of a 3D magnetic perturbing field (RMP) has been demonstrated on DIII-D at ITER similar pedestal-ν_e^* and cross-sectional shapes. Recent analysis using global particle balance and measurements of the D_α poloidal distribution show that the wall inventory can be strongly affected by changing the average triangularity of the plasma. Further investigations using vacuum field-line tracing identified a bifurcation in edge plasma conditions and divertor pumping due to a difference in the perturbed separatrix in the two configurations and an apparent increase in the scrape-off layer neutral density. Comparisons with helium discharges will also be made. These results support a goal of understanding the role of particle sources and sinks during the RMP and demonstrate ELM suppression without significant wall pumping, a feature that is essential in long-pulse reactors with saturated walls.

*Work supported in part by the US DOE under DE-AC05-06OR23100, DE-FC02-04ER54698 and DE-AC05-00OR22725.

TP8 27 Scaling of Type-I ELM Divertor Energy, Heat Flux, and Profile Width in DIII-D* C.J. LASNIER, M.A. MAKOWSKI, *Lawrence Livermore National Laboratory* J.A. BOEDO, *University of California-San Diego* N.H. BROOKS, A.W. LEONARD, W.P. WEST, *General Atomics* J.G. WATKINS, *Sandia National Laboratory* In this paper, we show scaling of divertor plate energy per ELM, peak heat flux and heat flux profile width of Type-I ELMs in DIII-D. We obtained data using an IR camera that viewed the divertor during discharges with large low-frequency ELMs. We independently varied the input power P_{in}, line-averaged density $\bar{n}_e$, and toroidal field B_T at constant q_{95}, with other parameters (nearly) fixed. We also scanned I_p while allowing the natural $\bar{n}_e$ (i.e., no gas puffing during the H-mode), with other quantities fixed. Previous scaling efforts have examined the pedestal energy loss during ELMs. We compare the deposited divertor energy with those analyses. We examine the fraction of total ELM energy reaching the target, the variation of ELM heat flux rise time, and the fraction of ELM energy deposited before the surface temperature peak. [1] A.W. Leonard et al., Plasma Phys. Control. Fusion **44**, 945 (2002). [2] A. Loarte et al., J. Nucl. Mater. **313-316**, 962 (2003).

*Work performed under the auspices of the US DOE under DE-AC52-07NA27344, DE-FG02-07ER54917, DE-FC02-04ER54698, and DE-AC04-94AL85000.

TP8 28 Characterization and Scaling of Heat Flux Transport in the DIII-D SOL* M.A. MAKOWSKI, C.J. LASNIER, *Lawrence Livermore National Laboratory* A.W. LEONARD, *General Atomics* J.A. BOEDO, *University of California-San Diego* In this study, we compare the divertor heat flux profile (width) to the upstream T_e profile in DIII-D. It is generally thought that the parallel heat flow in the scrape off layer (SOL), in competition with cross-field transport, governs the heat flux to the divertor. The relative importance of conduction versus convection within the SOL is not yet completely quantified for many operating regimes. In this study, we focus on an operational regime that generates Type I edge localized modes (ELMs). Two diagnostics, a fast framing IRTV and a Thomson scattering system, allow us to ex-

amine the relative role of conduction and convection of the T_e channel by comparing the upstream T_e width with the heat flux width in the divertor. We will present data scalings for a number of parameters scans including variations of plasma current, plasma density, and toroidal field at constant safety factor and input power.

*Work supported by the US DOE under DE-AC52-07NA27344, DE-FC02-04ER54698, and DE-FG02-07ER54917.

TP8 29 Characteristics of the Secondary Divertor on DIII-D* J.G. WATKINS, *Sandia National Laboratory* C.J. LASNIER, *Lawrence Livermore National Laboratory* A.W. LEONARD, T.E. EVANS, *General Atomics* R. PITTS, *ITER* P.C. STANGEBY, *University of Toronto* J.A. BOEDO, R.A. MOYER, D.L. RUDAKOV, *University of California-San Diego* In order to address a concern that the ITER secondary divertor strike plates may be insufficiently robust to handle the incident pulses of particles and energy from ELMs, we performed dedicated studies of the secondary divertor plasma and scrape-off layer (SOL). Detailed measurements of the ELM energy and particle deposition footprint on the secondary divertor target plates were made with a fast IR camera and Langmuir probes and SOL profile and transport measurements were made with reciprocating probes. The secondary divertor and SOL conditions depended on changes in the magnetic balance and the core plasma density. Larger density resulted in smaller ELMs and the magnetic balance affected how many ELM particles coupled to the secondary SOL and divertor. Particularly striking are the images from a new fast IR camera that resolve ELM heat pulses and show spiral patterns with multiple peaks during ELMs in the secondary divertor.

*Work supported by the US DOE under DE-AC04-94AL85000, DE-AC52-07NA27344, DE-FC02-04ER54698, and DE-FG02-07ER54917.

TP8 30 OEDGE Modeling of Deuterium Recycling in DIII-D* J.D. ELDER, P.C. STANGEBY, *University of Toronto* S. LISGO, *ITER* A.W. LEONARD, B.D. BRAY, N.H. BROOKS, *General Atomics* M.E. FENSTERMACHER, M. GROTH, *Lawrence Livermore National Laboratory* J.A. BOEDO, D.L. RUDAKOV, *University of California-San Diego* J.G. WATKINS, *Sandia National Laboratory* E.A. UNTERBERG, *ORISE* The OEDGE code is used to examine the role of deuterium recycling on core and pedestal fueling. In a previously modeled DIII-D discharge, 119925, with a partially detached inner divertor, attached outer divertor and significant plasma wall interaction, it is found that the core fueling is dominated by target and volume recombination sources in the inner divertor where 53% of the neutral deuterium source accounted for 61% of the core influx. In addition, main chamber recycling accounts for 24% of the core influx but only 11% of the source. Sensitivity studies assess the effect of physically plausible variations of the "plasma background." The spatial distribution of the core neutral deuterium influx is reported for representative plasma solutions for attached, partially detached and fully detached divertors.

*Work supported in part by US DOE under DE-FC02-04ER54698, DE-AC52-07NA27344, DE-FG02-07ER54917, DE-AC04-94AL85000, and DE-AC05-06OR23100.

TP8 31 Some Divertor Scaling Considerations* P.C. STANGEBY, *University of Toronto* A case is advanced for "divertor non-scaling," viz that absolute values of divertor density $n_d \sim 10^{21}$ m^{-3} and temperature $T_d \sim$ 5 eV need to be achieved for optimal demo/reactor-relevant studies. For $T_d >$ 10 eV sputtering is very strong; for $T_d <$ 2 eV there is risk of detachment and density limit. High n_d is required for high power, high duty cycle devices so that net erosion $\ll$ gross erosion via prompt local re-deposition of sputtered material. This occurs when impurity neutral ionization mean free path $\ll$ fuel ion gyro-radius (magnetic pre-sheath thickness); for $B \sim$ 5 T this requires $n_d > \sim 10^{21}$ m^{-3}. Thus peak parallel power flux density $\sim 0.1 - 0.5$ GW/m^2. Modified two-point modeling then gives that: (a) "upstream" (e.g. outside midplane, separatrix), conditions, n_{eu}, T_u, are almost fixed, independent of R (device size) and P_{SOL} (power entering the SOL), and (b) the required $P_{SOL} \sim R^1$, $R^{1.5}$ or R^2, depending on assumptions about target power width; the latter are discussed. A test device with these absolute n_d, T_d values will reproduce the most critical edge aspects of demo/reactors including power handling and material erosion/migration.

*Work supported by the NSERC DG and the US DOE under DE-FC02-04ER54698.

TP8 32 Neutral Fueling From Recycling and Contributions to Pedestal Density Profiles in DIII-D* A.W. LEONARD, R.J. GROEBNER, *General Atomics* G.D. PORTER, *Lawrence Livermore National Laboratory* Pedestal density widths in DIII-D are compared with the ionization profiles due to recycled neutrals. The neutral ionization profile is determined by neutral Monte-Carlo calculations based on ion flux measurements to the divertor and a plasma background reconstruction constrained by measurements. Previous studies have indicated that pedestal ionization is dominated by the inboard divertor neutral sources with smaller contributions from the main chamber in DIII-D. A density scan in H-mode is examined where the pedestal density width remains constant. The pedestal ionization rate increases at high density and inboard divertor detachment due to a longer mean free path for neutrals and an increased recombination source for neutrals. The possibility of an inward plasma pinch is explored as a possible explanation for the nearly constant pedestal density width under changing conditions of neutral sources and divertor plasma parameters.

*Work supported by the US DOE under DE-FC02-04ER54698 and DE-AC52-07NA27344.

TP8 33 Analysis of Neutral Recycling Fueling of the DIII-D Edge Pedestal* Z.W. FRIIS, W.M. STACEY, *Georgia Tech* A.W. LEONARD, *General Atomics* M.R. RENSINK, *Lawrence Livermore National Laboratory* A detailed analysis of neutral atom recycling and pedestal fueling in a DIII-D high-confinement mode discharge is presented. Experimental data and 2D edge plasma fluid code (UEDGE) calculations are employed to provide ion wall recycling and recombination neutral sources and background edge plasma parameters for a 2D edge neutral code (GTNEUT) calculation of detailed neutral density, ionization and charge-exchange distributions throughout the edge pedestal, scrape-off layer and surrounding halo region, divertor, and private flux regions. The relative effectiveness of the different neutral sources recycling from the divertor and baffles for fueling the confined plasma is evaluated.

*Work supported in part by the US DOE under DE-FG02-00ER54538, DE-FC02-04ER54698 and DE-AC52-07NS27344.

TP8 34 Generalized Diffusion Theory Calculations of the Edge Pedestal Density Profile* J.-P. FLOYD, W.M. STACEY, *Georgia Tech* It has been shown [1] that momentum balance requires a pinch-diffusion form of the radial particle flux in the edge plasma. Combined with the particle conservation requirement, this implies that the particle density satisfies a generalized diffusion equation with a convective term. This equation will be solved numerically and compared with the measured density profile in a DIII-D H-mode shot. [1] W.M. Stacey, Contrib. Plasma Phys. **48**, 94 (2008).

*Work supported in part by the US DOE under DE-FG02-00ER54538 and DE-FC02-04ER54698.

TP8 35 Evaluation of Particle Pinch and Diffusion Coefficients in the Edge Pedestal of DIII-D H-mode Discharges* W.M. STACEY, *Georgia Tech* R.J. GROEBNER, *General Atomics* Momentum balance requires that the radial particle flux satisfy a pinch-diffusion relationship. The pinch can be evaluated in terms of measurable quantities (rotation velocities, E_r, etc.) by the use of momentum and particle balance [1,2], the radial particle flux can be determined by momentum balance, and then the diffusion coefficient can be evaluated from the pinch diffusion relation using the measured density gradient. Applications to several DIII-D H-mode plasmas are presented. [1] W.M. Stacey, Contr. Plasma Phys. **48**, 94 (2008). [2] W.M. Stacey and R.J. Groebner, Phys. Plasmas **15**, 012503 (2008).

*Work supported in part by the US DOE under DE-FG02-00ER54538 and DE-FC02-04ER54698.

TP8 36 Intrinsic Rotation of Pellet Ablation Clouds* P.B. PARK, *General Atomics* T. LU, R. SAMULYAK, *Brookhaven National Laboratory* The finite resistivity code Frontier-MHD [1] is used to simulate the ablation rate of refueling pellets, including the effect of electrostatically induced $E \times B$ rotation of the ablation cloud about its symmetry axis parallel to the magnetic field [2]. The radial electric field E is set up as a consequence of charge and current neutralization at the end sheaths of the ablation column. The key finding is that the centrifugal force of cloud rotation pushes the cloud density radially outwards, creating a more "transparent" ablation channel. With reduced shielding, the *steady-state* ablation rate of a deuterium pellet significantly increases by 35% to 100%, depending on the B-field strength. This effect brings the ablation rate into better accord with a known theoretical scaling law, which agrees with most current experiments. However, the *transient* ablation rate is shown under the rather extreme situation of a fast pellet traveling across the steep-gradient pedestal region of ITER, to be a factor of 2 lower than predictions from the quasi-steady models. [1] R. Samulyak et al., Nucl. Fusion **47**, 103 (2007). [2] P.B. Parks et al., Phys Plasmas **16**, 060705 (2009)

*Work supported by US DOE under DE-FG03-95ER54309.

TP8 37 Shell Pellet Experiments on DIII-D* E.M. HOLLMANN, A.N. JAMES, J.H. YU, *University of California-San Diego* N. COMMAUX, T.C. JERNIGAN, *Oak Ridge National Laboratory* T.E. EVANS, D.A. HUMPHREYS, G.L. JACKSON, P.B. PARKS, E.J. STRAIT, W. WU, *General Atomics* Injection of hollow shell pellets filled with a dispersive payload is a possible method for rapid shutdown of future large tokamaks to avoid wall damage during disruptions. Preliminary shell pellet experiments have been performed in the DIII-D tokamak by firing small (OD $\sim$ 2 mm) polystyrene shells filled with either pressurized (10 atm) argon gas or with boron powder into quiescent discharges. Pellet slowing from 350 m/s down to 100 m/s was observed, which is not well-understood at present. Using the measured pellet velocity, the observed pellet burn up at $r/a \sim 0.5$, appears consistent with ablation rate calculations. Successful delivery and rapid (< 15ms) dispersal of the pellet payloads into the plasma core was observed. Negligible plasma current contraction or MHD onset were seen as a result of the shell burn up in the plasma edge, consistent with calculations. Planned experiments with large (OD $\sim$ 1 cm) shell pellets will also be discussed.

*This work was supported by the US DOE under DE-FG02-07ER54917, DE-AC05-00OR22725, and DE-FC02-04ER54698.

TP8 38 Development of a Robust Current Profile Feedback Controller in DIII-D* Y. OU, E. SCHUSTER, *Lehigh University* J.R. FERRON, T.C. LUCE, M.L. WALKER, D.A. HUMPHREYS, *General Atomics* T.A. CASPER, W.H. MEYER, *LLNL* Setting up a suitable current profile has been demonstrated to be a key condition for one candidate advanced tokamak scenario with improved confinement and steady-state operation. A control-oriented model of the current profile evolution in DIII-D was recently developed for the plasma current ramp-up and early-flattop phases [1] and used to synthesize open-loop control schemes tested both in simulations and experiments [2]. A robust closed-loop controller is proposed to regulate the current profile under the presence of model uncertainties in the plasma resistivity. Using the POD/Galerkin technique, the control-oriented PDE model is reformulated into a low-dimensional ODE model that preserves the dominant dynamics, and an H_∞ controller is designed to minimize the regulation/tracking error. A Corsica-based simulation assessment is presented. [1] Y. Ou, et al., Fusion Engin. Design **82** (2007) 1153. [2] Y. Ou, et al., Plasma Phys. Control. Fusion **50** (2008) 115001.

*Supported by the NSF CAREER award program (ECCS-0645086) and the US DOE under DE-FC02-04ER54698 and DE-AC52-07NA27344.

TP8 39 Model-based Adaptive Control of Resistive Wall Modes in DIII-D* F. XIE, E. SCHUSTER, *Lehigh University* D.A. HUMPHREYS, M.L. WALKER, *General Atomics* One of the major non-axisymmetric instabilities under study in the DIII-D tokamak is the resistive wall mode (RWM), a form of plasma kink instability whose growth rate is moderated by the influence of a resistive wall. The General Atomics/FARTECH DIII-D/RWM dynamic model represents the plasma surface as a toroidal current sheet and the wall using an eigenmode approach. We report first on the experimental validation and reconciliation of the proposed dynamic model, which is a required step previous to the potential implementation in the Plasma Control System (PCS) of any model-based controller. The dynamic model is then used to synthesize an adaptive control law for the stabilization of the RWM under time-varying β conditions. Simulation results are presented comparing the performance of the model-based adaptive controller and present non-model-based PD controllers.

*Supported by the NSF CAREER award program (ECCS-0645086) and the US DOE under DE-FC02-04ER54698 and DE-FG02-06ER54442.

TP8 40 MST, RFP, AND STELLARATOR

TP8 41 Overview of MST Results and Plans J.A. GOETZ, *UW - Madison and the Center for Magnetic Self Organization* MST TEAM, MST progress in basic and fusion plasma physics investigations and the development of the RFP fusion configuration is reported. Pellet injection into high current, improved confinement plasmas allows the empirical density limit to be surpassed. The reduction in magnetic fluctuations and enhancement in energy confinement is not quite as large as for low-density plasmas. A heavy ion beam probe is providing measurements in the plasma interior to assess electrostatic turbulence when magnetic fluctuation-induced transport is reduced. A multi-pulse Thomson scattering diagnostic allows electron temperature dynamics to be investigated at up to 25 kHz. This new capability has been used for measurement of electron thermal transport through the sawtooth cycle. In addition, temperature fluctuations correlated with magnetic islands have been identified. The ion mass dependence and anisotropy (parallel vs. perpendicular) in non-collisional ion heating have been measured and are useful in testing proposed heating mechanisms. A new 1 MW, 20 ms, 25 keV neutral beam injector will be used to investigate energy and momentum deposition, MHD stability and the beta limit, and super-Alfvenic ion effects on tearing and kinetic instabilities. Progress on lower hybrid and electron Bernstein wave injection for current drive and heating, and on oscillating field current drive for current sustainment will be described. Work supported by USDoE and NSF.

TP8 42 Advances in pellet-fueled, improved confinement MST plasmas K.J. CASPARY, B.E. CHAPMAN, A.F. ALMAGRI, J.K. ANDERSON, D.J. CLAYTON, D.J. DEN HARTOG, F. EBRAHIMI, A.F. FALKOWSKI, G. FIKSEL, J.A. GOETZ, S. KUMAR, S.T. LIMBACH, R.M. MAGEE, M.B. McGARRY, S.P. OLIVA, E. PARKE, J.A. REUSCH, J.S. SARFF, H.D. STEPHENS, *UW-Madison* P. FRANZ, *Consorzio RFX* W.F. BERGERSON, D.L. BROWER, W.X. DING, L. LIN, T. YATES, *UCLA* S.K. COMBS, C.F. FAUST, *ORNL* Pellet injection fueling of improved confinement MST plasmas has led to a seven-fold increase in line-averaged density with a core density now exceeding $9x10^{19}$ m^{-3}. This has been achieved by more than doubling the size of the injected pellets, relative to previous work on MST. The improved confinement is achieved using inductive current profile control. As was previously observed at low toroidal current (0.2 MA) in MST, pellet fueling has now allowed the Greenwald density to be surpassed at high current (0.5 MA). Utilizing new Thomson scattering capability for measurement with a 2 kHz repetition rate, the central electron temperature is observed to rise from 0.4 keV to a maximum 1 keV in only a few ms after pellet ablation. Some plasmas exhibit an increased core temperature lasting longer than the nominal duration of the auxiliary inductive current drive. Work supported by DOE.

TP8 43 Electron density and toroidal current density profile evolution in high-performance pellet-fueled MST plasmas* L. LIN, D.L. BROWER, W.X. DING, W.F. BERGERSON, T.F. YATES, *UCLA* K.J. CASPARY, B.E. CHAPMAN, J.S. SARFF, *UW-Madison* High-density, high-β plasmas have been achieved in MST using pellet injection in conjunction with inductive current profile modification. Here, we present measurements during such plasmas of the electron density (n_e) and toroidal current density (j_{tor}) profiles obtained using a three-wave far-infrared (FIR) laser polarimetry-interferometry diagnostic. Electron density profiles are obtained by inverting the line-integrated interferometry measurements. However, simultaneous measurements of the electron density gradient from a differential interferometry configuration are used to assist in removal of interferometric fringe jumps during the pellet ablation and improve the overall accuracy of the inverted density profiles. Toroidal current density profiles are measured by handling the polarimetry measurements with a parameterized functional fitting method. The evolution of n_e and j_{tor} during pellet ablation is resolved, and profile dynamics will be presented.

*Work supported by the U.S. Department of Energy.

TP8 44 Quasi-Single-Helicity Structures in the MST Reversed-Field Pinch W.F. BERGERSON, W.X. DING, D.L. BROWER, *UCLA* B.E. CHAPMAN, J.S. SARFF, J.K. ANDERSON, D.J. DEN HARTOG, J.A. REUSCH, H.D. STEPHENS, *University of Wisconson-Madison* Tearing modes produce a stochastic magnetic field, which degrades particle confinement in the reversed-field pinch (RFP), and characterize the multiple helicity (MH) state. MHD simulations predict an alternate to the MH state where the tearing modes condense into a single helical mode (SH). The term quasi-single helicity (QSH) describes plasmas with a dominant mode and smaller secondary modes. Studies have been carried out in the MST on both MH and QSH plasmas to investigate the fluctuation and confinement properties. For the first time the internal magnetic topology as well as magnetic and density fluctuations associated with these modes are measured directly in the plasma core using a high-speed, laser-based, polarimetry-interferometry diagnostic. The density and radial magnetic field fluctuations have been correlated in order to evaluate the magnetic-fluctuation-induced particle flux in the high-temperature core region. The electron temperature profile is 50 eV hotter in the region $0< r/a < 0.75$ in the poloidal plane of the island O-point in QSH plasmas, as opposed to the X-point. Global particle confinement measurements are underway to identify properties of the QSH and MH states. This work is supported by the DOE.

TP8 45 Role of Electron Density Fluctuations in Momentum Transport in a Stochastic Magnetic Field W.X. DING, D.L. BROWER, W.F. BERGERSON, L. LIN, T.F. YATES, *University of California, Los Angeles* A. ALMAGRI, G. FIKSEL, D.J. DEN HARTOG, S.C. PRAGER, J.A. REUSCH, J.S. SARFF, *University of Wisconsin, Madison* Plasma density fluctuations associated with magnetic fluctuations are not simply the result of passive advection. They can feed back on the plasma flow through fluctuating pressure, causing parallel momentum transport. The pressure fluctuations resulting from density fluctuations have been measured by using a high-speed polarimetry-interferometry (for both radial magnetic field and density fluctuations), Thomson scattering (for mean electron temperature), Rutherford scattering (for mean ion temperature). Measurements show that the density-fluctuation-induced momentum flux is comparable to the total momentum flux during a sawtooth crash. The temperature fluctuation-induced momentum flux is yet to be measured. Work supported by US DOE and NSF.

TP8 46 Measuring Density Fluctuations And Particle Transport On MST Using Laser Polarimetry-Interferometry* TRAVIS YATES, WEIXING DING, TROY CARTER, DAVID BROWER, *UCLA* Simultaneous interferometry-polarimetry measurements with a bandwidth ~ 500 kHz and 8 cm chord spacing have been utilized to determine the core density and magnetic field

fluctuations in MST. Density fluctuations arising from magnetic fluctuations contribute to electron particle transport. An outward radial flux of particles is caused by a non-zero correlation between velocity and density fluctuations. It is also possible to measure the energy balance, proportional to $\tilde{n}^2$, of density fluctuations during a sawtooth event where the stochasticity of the magnetic field is largest. Measurements show that density fluctuations cannot be balanced by the energy coming from the gradient in the mean plasma density profile. Initial results indicate that, for core modes, density fluctuations are unstable and likely damped by nonlinear coupling, proportional to the gradient of the fluctuating plasma density. Measurements will focus on nonlinear interactions between the dominant, core-resonant modes, (m,n): (1,7)-(1,6) =(0,1). At the sawtooth, a burst of (0,1) mode activity acts to enhance the 3-wave interaction.

*Work supported by U.S. Department Of Energy

TP8 47 Characterization of density and potential fluctuations with a Heavy Ion Beam Probe in MST improved confinement RFP plasmas* X. CHEN, P.M. SCHOCH, D.R. DEMERS, *Rensselaer Polytechnic Institute* P.J. FIMOGNARI, B.E. CHAPMAN, *University of Wisconsin-Madison* In improved confinement (pulsed poloidal current driven) plasmas in MST, magnetic fluctuations are suppressed, and electrostatic fluctuations may be the dominant transport mechanism. We have acquired measurements in these plasmas of the fluctuating electron density ($\tilde{n}_e/n_e$) and potential ($\tilde{\phi}$) at multiple locations in the plasma interior with a heavy ion beam probe (HIBP). This allows us to evaluate the frequency spectra of the fluctuations up to 500kHz, assess wavenumbers, and estimate the electrostatic-fluctuation induced particle flux. Our analysis shows that the spectra of both $\tilde{n}_e/n_e$ and $\tilde{\phi}$ are broadband, and decrease with frequency, with most power below 100kHz. The features of the computed coherence and phase of $\tilde{n}_e/n_e$ at two spatial points are different than that of simultaneously acquired $\tilde{\phi}$. Fluctuation data acquired during improved confinement discharges, results of this analysis, and the role played by electrostatic fluctuations will be presented.

*Work supported by US-DOE.

TP8 48 Heavy Ion Beam Probe Measurements of Equilibrium Potential in the Interior of the MST RFP* D.R. DEMERS, X. CHEN, P.M. SCHOCH, *Rensselaer Polytechnic Instutute, Troy, NY* P.J. FIMOGNARI, *University of Wisconsin, Madison* The 200keV HIBP in operation on MST is being used to measure the equilibrium plasma potential in the interior of standard and improved confinement plasmas with 40-45keV K^+ beams. The injected beam angle is varied by an electrostatic sweep system which allows us to alter the sample volume location during a single shot. Simultaneous measurements at two sample locations within the plasma are obtained using two apertures to the high voltage electrostatic analyzer; high levels of UV radiation from the RFP plasma require use of the third detector set for noise subtraction. Toroidal and poloidal displacement of the sample volumes allows for inference of the electric field. Improved beam operation is enabling us to obtain increased ion current, and measurements as a function of time throughout the improved confinement period. Measurements in the interior of 380kA standard and improved confinement discharges reveal a positive electric potential. Variations in the potential as a function of discharge condition and individual characteristics will be presented.

*Work supported by US-DOE.

TP8 49 Characterization of the Heavy Ion Beam Probe ion trajectory and sample volume in the MST RFP* P.J. FIMOGNARI, J.K. ANDERSON, J.A. REUSCH, *Univ. of WI - Madison* D.R. DEMERS, X. CHEN, *Rensselaer Polytechnic Institute* Operation of an HIBP on MST is complicated by temporal and spatial variations of the beam trajectory and sample volume. The foremost contributors are the uncertainty and temporal changes of the equilibrium magnetic field, throughout a sawtooth cycle in standard discharges, or with edge current drive during improved confinement discharges. Other contributors include edge magnetic field errors, plasma suppression structure magnetic fields, and magnetic mode activity. Accurate modeling of each feature is crucial to sample volume shape and localization calculations used for the analysis of equilibrium plasma potential and fluctuations in electron density and potential. A finite element model of the primary and secondary beamline electrostatic sweep systems has also been developed. This simulation also enables studies of finite-cross-section beams and associated scrape-off effects. An overview of the HIBP system on MST and in-depth spatial and temporal characterization of the trajectory and sample volumes will be presented.

*This work supported by the US-DOE.

TP8 50 Simulated and Measured Electron Thermal Transport with Varying Stochasticity in the MST RFP J.A. REUSCH, J.K. ANDERSON, D.J. DEN HARTOG, F. EBRAHIMI, C.B. FOREST, R. O'CONNELL, D.D. SCHNACK, H.D. STEPHENS, *UW - Madison* Recent results show that the MST RFP exhibits Rechester-Rosenbluth thermal transport only at the sawtooth crash, when the MHD activity peaks. This is in contrast with previous results [Biewer, 2003], which suggested stochastic transport between sawteeth. Results from a new set of first principles simulations using the resistive MHD code DEBS will be presented. The simulations are designed to match experimental conditions as closely as possible. Both Spitzer and neoclassical resistivity models were tried for the case of a fixed, experimentally measured resistivity at a central Lundquist number of 3.8×10^6. The measured electron thermal diffusion, χ_e, obtained through power balance is compared to the Rechester-Rosenbluth electron thermal diffusion obtained from DEBS, $\chi_{RR} = v_{T_e} \pi L_{eff} \tilde{b}^2/B^2$, and the expected thermal diffusion from the field line tracing code MAgnetic Lines (MAL), $\chi_{MAL} = v_{T_e} D_{mag}$ where $D_{mag} = (\Delta r)^2/(2\Delta l)$, where the traced magnetic field is also from DEBS. χ_{RR} is generally found to be an order of magnitude larger than χ_e except at the sawtooth crash, where the two are in agreement, suggesting that while magnetic fluctuations are always the dominant transport mechanism, the magnetic field is only fully stochastic at the sawtooth crash. This work is supported by the U.S. DOE.

TP8 51 Initial results from 2 kHz Thomson scattering measurements on MST* Y.M. YANG, B.E. CHAPMAN, D.J. DEN HARTOG, E. PARKE, J.A. REUSCH, H.D. STEPHENS, *Department of Physics, University of Wisconsin-Madison* The laser system for the Thomson scattering diagnostic on the MST RFP has been upgraded to a pulse-burst system enabling operation at a 2

kHz repetition rate. Single-shot evolution of the electron temperature (Te) profile can now be recorded. This capability is especially useful for analysis of plasmas with shot-to-shot variation, such as those with Enhanced Confinement (EC) or Pulsed Poloidal Current Drive (PPCD). In discharges with PPCD at toroidal plasma current (0.5 MA), the central Te increases by $\sim$ 1500 eV in 10 ms, reaching a maximum $>$ 2000 eV. Simultaneously, Te closer to the plasma boundary remains at a few hundred eV. For reasons not yet understood, the time evolution of the Te profile and maximum central Te can vary substantially shot to shot. A global transport analysis for 0.4 MA standard, non-reversed, EC, and PPCD plasmas will also be presented. The energy confinement time during EC and PPCD plasmas is calculated for specific shots and shows a factor 2-3 improvement during EC and $\sim$ 6 during PPCD, relative to standard discharges.

*This work is supported by the U. S. Department of Energy.

TP8 52 Pulse-Burst Laser Systems for Thomson Scattering on MST* D.J. DEN HARTOG, *University of Wisconsin–Madsion, and Center for Magnetic Self-Organization in Laboratory and Astrophysical Plasmas* M.T. BORCHARDT, W.S. HARRIS, J.A. REUSCH, *University of Wisconsin-Madison* Y.M. YANG, *University of Wisconsin–Madison* A new purpose-built "pulse-burst" laser system is being constructed for the Thomson scattering diagnostic on the MST reversed-field pinch. This new laser will produce a burst of 1–2 J Q-switched pulses at repetition rates 5–250 kHz. It will operate at 1064 nm and is a master oscillator, power amplifier (MOPA) system. Variable pulse-width drive (0.15–20 ms) of the flashlamps in this laser will be accomplished by IGBT switching of large electrolytic capacitor banks. A subset of these power supplies has already been constructed and is currently being used to drive the flashlamps in the two existing commercial Nd:YAG lasers used for Thomson scattering on MST. Each of these upgraded lasers now produces a burst of up to fifteen 2 J Q-switched pulses (1064 nm) at repetition rates 1–12.5 kHz. Direct control of the laser Pockels cell drive enables optimal pulse energy extraction, and up to four 2 J laser pulses during one flashlamp pulse. These lasers are currently being used to study the dynamic evolution of electron temperature in MST. The new purpose-built "pulse-burst" laser system will further expand this capability.

*This work is supported by the U. S. Department of Energy and NSF.

TP8 53 Two-Color SXR Tomography on MST M.B. McGARRY, J.A. GOETZ, D.J. DEN HARTOG, *University of Wisconsin - Madison* P. FRANZ, *Consorzio RFX - Padova, Italy* Recent improvements in the analysis technique used to calculate plasma electron temperature using a soft-x-ray (SXR) tomography diagnostic on MST are presented. The diagnostic is comprised of four 20-channel cameras at the same toroidal angle but different poloidal angles. The two-color configuration uses two pairs of Be filters in the four cameras, giving measurements of two distinct energy ranges dominated by bremsstrahlung radiation. The ratio of emissivity in these two energy ranges gives a poloidal map of electron temperature. Improvements to the original inversion technique have reduced numerical oscillations. The model used to simulate SXR emission from the plasma has also been improved to incorporate measured density and temperature profiles. The model can also simulate line and recombination radiation. Furthermore, the model includes a radially dependent enhancement factor that can be used to assess other sources of radiation, as well as possible radial variations in Z_{eff}. Persistent artifacts in the temperature calculation are being investigated, and the improved technique will be applied to recent experimental results. Work supported by U.S.D.O.E.

TP8 54 Tomographic SXR emissivity measurements on MST* P. FRANZ, F. BONOMO, *Consorzio RFX, Padova, Italy* M.B. McGARRY, B.E. CHAPMAN, J.A. GOETZ, D.J. DEN HARTOG, *University of Wisconsin-Madison* We present a survey of soft x-ray (SXR) measurements in standard and improved confinement plasmas in MST. Data are collected by a SXR tomographic diagnostic made of four 20-channel probes installed on a cross-section of the MST torus. The plasma has been analyzed using different thicknesses of Be foil filters, with values ranging between 15 and 821 microns, in order to select various energy ranges in the SXR spectrum. Correlation of the reconstructed SXR emissivity distributions with magnetic mode measurements enables investigation of MHD core dynamics in MST plasmas. For example during QSH (when one $m = 1$ tearing mode dominates the MHD magnetic spectrum and all remaining modes have reduced amplitudes), SXR tomographic reconstruction shows a more emissive structure on top of a symmetric profile. Data have been taken in the *one-color* configuration (same Be filter in all probes), *two-color* (two pairs of Be foils in the four cameras) and *multicolor* (four different Be filters). The *one-color* configuration measures only SXR emissivity, while the *two-color* configuration with thicker filters allows a reconstruction of the electron temperature from measurement of bremsstrahlung.

*This work is partially supported by the U.S. Department of Energy.

TP8 55 Similarities in QSH thermal measures in RFX-mod and MST experiments in high current regimes* ALBERTO ALFIER, ALESSANDRO FASSINA, PAOLO FRANZ, *Consorzio RFX - Padova, Italy* JOSHUA A. REUSCH, HILLARY STEPHENS, MEGHAN McGARRY, DANIEL J. DEN HARTOG, JAY K. ANDERSON, *University of Wisconsin-Madison* In the two RFP devices, Madison Symmetric Torus (MST) and RFX-mod, experiments have been recently performed at the aim of characterizing and comparing quasi single helicity (QSH) thermal properties. They have been dedicated to study the appearance of helical structures in the core region and to its transient evolution. Shots have been run at an electron density and current in the two devices such that the I/N parameter (I plasma current, N line averaged density) was in the range 3-9*10-14Am. Both spontaneous and induced QSH have been considered. Hot temperature structure, in some cases occupying most of the plasma core, is measured on both devices, corresponding to a more emissive plasma detected through the X-ray tomography. Their occurrence is found to be statistically related to the I/N values. Heat transport analysis in similar cases provides similar heat diffusivity profiles.

*This word was partially supported by the U. S. Department of Energy.

TP8 56 Measurement of Z_{eff} and Particle Diffusion via X-ray Spectroscopy in MST D.J. CLAYTON, A.F. ALMAGRI, J.K. ANDERSON, D.R. BURKE, B.E. CHAPMAN, C.B. FOREST, R. O'CONNELL, *UW-Madison* R.W. HARVEY, *CompX* Measured x-ray spectra constrain Fokker-Planck modeling of MST discharges and provide a means to determine the effective ionic

charge Z_{eff} and the radial particle diffusion coefficient D_r. A new radial array of Si photodiode detectors measures 2-10 keV x rays from thermal and runaway electrons in most plasma conditions. An array of CdZnTe detectors measures 10-150 keV x rays from high energy runaway electrons present only in plasmas with reduced stochasticity and improved particle confinement. The Fokker-Planck code CQL3D models the electron distribution function and predicts the resulting bremsstrahlung emission expected along each detector's line of sight. The code is run iteratively to find the $Z_{eff}(r)$ and $D_r(r)$ that produce the best fit to the data. Tests of this measurement technique with various plasma conditions will be presented, including largely stochastic plasmas with locally improved confinement within a magnetic island, and plasmas with reduced tearing modes and globally improved confinement. In the core of a typical high-temperture, low-density, improved-confinement plasma, Z_{eff} = 4-6 and D_r = 1 m^2/s. Work supported by the USDOE.

TP8 57 Parallel and perpendicular ion heating in the MST RFP* RICHARD MAGEE, DANIEL DEN HARTOG, GENNADY FIKSEL, SANTHOSH KUMAR, *University of Wisconsin - Madison* DARREN CRAIG, *Wheaton College* CMSO COLLABORATION, The anomalous energization of plasma ions during magnetic reconnection has long been observed in numerous laboratory and astrophysical plasmas. In the MST reversed-field pinch, the reconnection impulsively heats the ions, more than doubling their temperature in $\sim$ 100 μsec. A critical outstanding question has been whether or not this heating is isotropic with respect to the magnetic field, which we attempt to address here with charge exchange recombination spectroscopy measurements. A new toroidal view allows localized measurements of the impurity ion (C^{+6}) temperature both perpendicular and parallel to the mean magnetic field. We observe that in the core of low-density discharges, the parallel temperature rise is comparable to the perpendicular rise, and a large increase in neutron flux occurs at the time of reconnection. In high-density discharges, the perpendicular temperature increase is the same as in low, but there is almost no heating seen in the parallel direction, and no increase in neutron flux is observed. Possible mechanisms will be discussed.

*This work has been supported by the U.S. DoE and the N.S.F.

TP8 58 C^{+6} impurity profiles in MST plasmas* SANTHOSH T.A. KUMAR, D.J. DEN HARTOG, R.M. MAGEE, G. FIKSEL, *Department of Physics, University of Wisconsin-Madison, USA* D. CRAIG, *Wheaton College, Wheaton, IL, USA* Temporally-resolved radial profiles of Doppler broadened C^{+6} emission (343.4 nm) have been measured on the MST reversed-field pinch using Charge-Exchange Recombination Spectroscopy. Experimental observations indicate a hollow C^{+6} density profile for both standard and improved confinement plasmas, throughout the duration of the diagnostic neutral beam pulse, even though the C^{+6} ion temperature profile peaks at the center. Measurements are made on deuterium plasmas with density $\sim 1 \times 10^{19} m^{-3}$ and plasma current $\sim$ 400 kA. Experimental results are presented.

*This work is supported by the U.S. Department of Energy.

TP8 59 High Power Neutral Beam Injection on the MST* GENNADY FIKSEL, J.K. ANDERSON, B.E. CHAPMAN, S. LIMBACH, M. NORNBERG, S.P. OLIVA, J.S. SARFF, J. WAKSMAN, *University of Wisconsin-Madison* G.F. ABDRASHITOV, V.P. BELOV, V.I. DAVYDENKO, P.P. DEICHULI, A.A. IVANOV, V.A. KAPITONOV, V.V. KOLMOGOROV, A.N. SELIVANOV, A.V. SOROKIN, N.V. STUPISHIN, R.V. VOSKOBOINIKOV, *Budker Institute of Nuclear Physics, Novosibirsk, Russia* A high power neutral beam injection system has been installed on the MST RFP. The hydrogen beam is designed for a power of 1 MW, an energy of 25 keV, and a duration of 20 ms. The goals for the system include investigation of the beam energy and momentum deposition into the plasma, studying the dependence of MHD stability on the plasma pressure, and investigation of fast particles effects on tearing and kinetic instabilities in the MST. First tests of this system on MST are expected shortly.

*This work is supported by the USDOE.

TP8 60 Computational Simulation Of Neutral Beam Injection On MST JEFF WAKSMAN, JAY ANDERSON, GENNADY FIKSEL, *UW-Madison* MST has recently installed a 1 MW, 20 ms tangential neutral beam injection system. Understanding of initial measurements and guidance of future diagnostics relies heavily on accurate calculations of the beam characteristics. The transport code TRANSP was used to simulate the beam's effect on the plasma, such as shine-through, power and momentum deposition and current drive. While the code was originally developed for tokamaks, its Monte Carlo Beam Deposition and Slowing-Down Model is of particular interest for MST. Initial studies used real Grad-Shafranov equilibrium reconstructions of MST discharges without field reversal, satisfying a TRANSP requirement that the toroidal flux be a monotonic function of radius. Subsequent computations were performed on RFP equilibria modified in one of two different ways: either the plasma boundary was defined to be inside of the reversal surface, or a small artificial toroidal field was added near the boundary. Results from the simulations will be compared with the initial data from NBI operation on MST. Work supported by the U.S.D.O.E.

TP8 61 Oscillating Field Current Drive Experiments on MST K.J. McCOLLAM, J.K. ANDERSON, D.J. DEN HARTOG, F. EBRAHIMI, J.A. REUSCH, J.S. SARFF, D.R. STONE, H.D. STEPHENS, *UW-Madison* D.L. BROWER, W.X. DING, *UCLA* Oscillating field current drive (OFCD) is a proposed method of efficient, steady-state RFP sustainment in which applied AC poloidal and toroidal loop voltages interact with magnetic relaxation to produce a DC plasma current. OFCD is added to a standard RFP in the MST device, increasing the net plasma current by up to about 10%, with Ohmic efficiency and without a net decrease in energy confinement or beta ($\beta \propto p/B^2$). The total current can be increased or decreased according to the phase between the two AC voltages. Time series of equilibria are reconstructed using internal measurements for the cases of OFCD with different phases and of OFCD off. Of these the OFCD case with the most added current is calculated to have, on cycle average, the highest confinement time and beta, the lowest fluctuation-induced dynamo electric field, and the lowest magnetic helicity decay rate. To date, increases in input power have not led to further increases in the OFCD-added current, perhaps due to discrete magnetic fluctuation events often observed at increased input power. This work is supported by the US DOE.

TP8 62 Magnetic Relaxation with Oscillating Field Current Drive on MST D.R. STONE, A.F. ALMAGRI, G. FIKSEL, K.J. McCOLLAM, M.C. MILLER, R.M. MAGEE, S.T.A. KUMAR, J.S. SARFF, *UW-Madison* D.C. BROWER, W.X. DING, W.F. BERGERSON, *UCLA* In oscillating field current drive (OFCD), poloidal and toroidal frequency-matched ac magnetic fields are inductively applied to the plasma to drive dc plasma current through magnetic relaxation. Measurements of the MHD [$< \tilde{v} \times \tilde{B} > = < \tilde{E}_\perp \times \tilde{B}_\perp >$] and Hall [$< \tilde{j} \times \tilde{B} > /ne$] dynamo mechanisms associated with magnetic relaxation are conducted during OFCD both to better understand the relaxation dynamics and to aid in optimizing OFCD performance. Initial measurements of the MHD and Hall dynamo in the core and edge are reported. Charge exchange recombination spectroscopy and far-infrared interferometry-polarimetry are used in the core. Insertable probes are used in the edge, including a secondary emission capacitive probe developed to measure the electric fields. The fluctuation-induced magnetic helicity flux [$< \tilde{\phi}\tilde{B}_r >$] associated with magnetic relaxation is also measured in the edge. This flux is enhanced during OFCD by $\sim$ 100% relative to standard RFP operation. This work is supported by the US DOE.

TP8 63 Lower Hybrid Antenna Coupling on MST* M.C. KAUFMAN, D.R. BURKE, J.A. GOETZ, C.B. FOREST, *University of Wisconsin-Madison* The particular constraints of MST lead to the use of a novel interdigital-line structure rather than the traditional waveguide grill antenna for launching lower hybrid waves. The antenna has been designed to launch the slow wave at 800 MHz and an $n_{||}$ of 7.5 with maximum absorption at r/a $\sim$ 0.8 for current drive scenarios. While there are several drawbacks to this type of antenna including the lack of fine phasing control, the launched spectrum displays fairly good directivity. Loading studies indicate that the antenna operates well in a variety of plasma conditions, and agrees well with theory. With LH wave injection, toroidally localized hard x-rays in standard plasmas with energies up to 50 keV have been observed. Additional x-ray measurements at the antenna indicate that the progenitor fast electrons are lost more quickly than the ohmic field can accelerate them to the inferred velocities. Monte Carlo modeling shows that the emission is likely the result of edge interaction of electron gyro-orbits with gradients in the antenna near field.

*Work supported by US DOE.

TP8 64 Lower hybrid wave absorption on the MST* D.R. BURKE, A.F. ALMAGRI, D.J. CLAYTON, C.B. FOREST, J.A. GOETZ, M.C. KAUFMAN, *UW Madison* Rf waves near the lower hybrid frequency have long been used to accelerate electrons in tokamaks. Lower hybrid wave injection experiments are underway on the MST RFP targeting electrons at r/a $\sim$ 0.8 (where $\nabla J_{||}$ is steep) with the goal of stabilizing tearing fluctuations. Fast electrons are observed through bremsstrahlung emission using an Amptek Si-PIN photodiode to measure x rays from 3-10 keV. Increased x ray flux is observed during rf experiments, toroidally localized near the antenna. This is believed to be caused by the high field winding ($q \simeq 0$) and the high radial diffusion in the RFP edge. Bremsstrahlung emission is enhanced by inserting a probe with a molybdenum tip into the edge, which provides a higher Z target than the plasma, making edge emission more prominent relative to core emission. This probe has been refined, providing a plasma-free line of sight, and an interchangeable target. These probe studies reveal more about the local electron distribution function. Computational studies of wave propagation and absorption have also been undertaken for various plasma conditions, using a Grad-Shafranov fitter coupled with GENRAY (a ray-tracing code) and CQL3D, a Fokker-Planck equation solver. Results from target and computational studies are presented.

*Work supported by US DOE Contract DE-FC02-05ER54814.

TP8 65 Development of a MW-Level EBW Heating and Current Drive Experiment on the MST* JAY ANDERSON, *University of Wisconsin* CARY FOREST, ANDREW SELTZMAN, The electron Bernstein wave experiment on MST is motivated by its potential to deposit heat and drive off-axis current in the RFP plasma. Positive results of emission, coupling and 100kW-level injection experiments compel the development of a new megawatt-level heating and current drive experiment. A 1.2 MW klystron which operates at 5.5 GHz has been selected as a transmitter. Construction is underway on an 80kV 40A IGBT-based modulated power supply to drive the tube, following the design and utilizing spare parts from the Los Alamos National Laboratory on a similar pulsed supply. A half-wavelength quartz window is designed and has been bench-tested, and a cylindrical molybdenum antenna will be used as the initial launching structure. This experiment is at higher frequency (shorter wavelength) than the previous MST injection experiments (3.6 GHz) and therefore the characteristic size of the antenna is reduced. This is favorable from the standpoint of small ports in the vacuum vessel and extension to multiple tubes and multiple antennas in the future. Initial coupling data from the molybdenum launcher are presented.

*Work supported by USDOE.

TP8 66 Electron Bernstein Wave Injection and Heating in MST* ANDREW SELTZMAN, JAY ANDERSON, CARY FOREST, *University of Wisconsin-Madison* The electron Bernstein wave (EBW) has been suggested as a potential means of further improving RFP confinement with sustained, off-axis current drive to stabilize the resistive tearing modes which govern thermal transport. An S-band EBW heating system was tested on MST resulting in measurement of localized soft-x-ray emission concurrent with rf injection. In order to further investigate coupling, an insertable rf probe was constructed. This allowed measurement of the transverse electric field of the x-mode wave as it crossed the right-hand cutoff layer and showed evanescent decay of the electric field amplitude. This motivated the fabrication of an improved RF probe with a dual axis pair of dipole antennas and pair of loops to measure the electric and magnetic components, respectively, of the injected wave. Upcoming analysis will enable verification of conversion of the injected x-mode wave to the electron Bernstein wave at the upper hybrid resonance layer. Further, the rf probe may measure the parametric decay instability, providing further evidence of coupling to the EBW mode.

*Work supported by USDOE.

TP8 67 Modeling of EBW Propagation and Damping in MST* S.J. DIEM, *Oak Ridge National Laboratory* J.K. ANDERSON, C. FOREST, A. SELTZMAN, *University of Wisconsin - Madison* R.W. HARVEY, *CompX* Edge current profile modification is being explored to improve particle and energy transport in the Madison Symmetric Torus (MST) reversed field pinch (RFP). To this end, we report on modeling results of an electron Bernstein wave experiment under development in MST. Numerical modeling of

EBW propagation and damping has been explored using the GENRAY ray-tracing and CQL3D Fokker-Planck codes in support of this upgraded 5.55 GHz EBW heating and current drive system. Calculations were performed for EBWs launched with a 4.5 cm poloidal extent, -19 degrees below the midplane, to investigate off-axis current drive. Current was driven at $\rho/a > 0.65$ with current drive efficiency $>$ 10 kA/MW via the Ohkawa current drive method. The effect of high RFP diffusion on the current drive efficiency was investigated by varying the radial transport coefficient included in CQL3D. Additionally, CQL3D has been used to model the soft x-ray flux resulting from the EBW distortion of the electron distribution function, for comparison with experimental data.

*Work supported by USDOE

TP8 68 Flow Dynamics and Transport in the Edge of MST M.C. MILLER, A.F. ALMAGRI, *University of Wisconsin - Madison* D. CRAIG, *Wheaton College* D.A. ENNIS, G. FIKSEL, S. GANGADHARA, A. KURITSYN, S.C. PRAGER, D. STONE, T.D. THARP, *University of Wisconsin - Madison* CMSO COLLABORATION, Understanding plasma flow dynamics is important to the study of reconnection, momentum transport, and particle transport. In MST, abrupt changes in flow patterns occur during quasi-periodic magnetic reconnection events (sawteeth). During these events, fluctuation levels are observed to increase in many measurable quantities and can lead to the transport of particles, momentum, and energy. Probes have been used in the edge to measure the three components of velocity and magnetic field, as well as density and temperature. This poster presents first time measurements of plasma flows associated with tearing reconnection. In momentum transport studies, the fluctuation-induced Maxwell and Reynolds stresses were unexpectedly found to be much larger than the rate of change in plasma momentum but approximately in balance with each other. Fluctuation-induced particle transport, measured directly as $\langle \widetilde{nv}_r \rangle$, increases dramatically during a reconnection event, reaching several times its initial value. From these measurements we can begin to understand the plasma dynamics that lead to transport. Work is supported by the US DOE and the NSF.

TP8 69 Experimental study of anisotropic magnetic turbulence in a reversed field pinch Y. REN, A.F. ALMAGRI, G. FIKSEL, S.C. PRAGER, J.S. SARFF, P.W. TERRY, *UW-Madison, CMSO* In many space and laboratory plasmas with a background magnetic field, magnetic turbulence is predicted to be anisotropic, *i.e.* the turbulence structure has a large perpendicular wavenumber ($k_\perp$) and much smaller parallel wavenumber ($k_{||}$). The observed small scale turbulence is often thought to cascade from large scale perturbations, forming inertial and dissipation ranges in the wavenumber power spectrum characterized with power and exponential laws, respectively. We carried out our experimental study of magnetic turbulence in MST, a medium-sized reversed- field pinch. MST plasmas exhibit a broad spectrum of magnetic fluctuations, ranging from low frequency coherent tearing modes (10-20 kHz) to high frequency fully developed turbulence (hundreds of kHz), and are ideal for studying magnetic turbulence. Radial profile measurements using a magnetic probe array show that the observed magnetic turbulence has a locally resonant feature, $\vec{k} \cdot \vec{B}$, and exhibits strong anisotropy with $k_\perp \gg k_{||}$ and $\delta B_\perp \gg \delta B_{||}$. We identified power and exponential law dependencies in the $k_\perp$ and $k_{||}$ spectra, which indicates a cascade picture for the origin of the small scale magnetic fluctuations, and the turbulence is shown to have a radial standing wave structure. We will discuss the observed magnetic fluctuation polarization and possible types of high frequency fluctuations. This work is supported by NSF and DoE.

TP8 70 Measurements of Hall Reconnection in MST* T.D. THARP, A.F. ALMAGRI, M.C. MILLER, V.V. MIRNOV, S.C. PRAGER, J.S. SARFF, Previous measurements in MST have established that two-fluid Hall effects produce a dynamo EMF during magnetic relaxation events (sawteeth), and therefore two-fluid dynamics are important to the macroscopic effects of reconnection. This Hall dynamo was established by measuring the nonlinear Hall term ($\tilde{J} \times \tilde{B}$) in the axisymmetric (flux-surface-averaged) Ohm's Law. Here, we report measurements of terms in the *non*-axisymmetric Ohm's Law, including the reconnection electric field and terms that balance this field. This analysis is applied to tearing modes with poloidal mode number $m = 0$ and toroidal mode number $n \geq 1$. Measurements are performed with probes in the vicinity of the resonant surface, and clearly indicate that single fluid physics is not sufficient to explain this reconnection. In particular, nonlinear three-wave interaction Hall terms are a strong contributor to the dynamics of this reconnection and the associated island formation.

*Work Supported by US DOE and NSF

TP8 71 Numerical Studies of Two-Fluid Tearing and Dynamo in a Cylindrical Pinch* JACOB KING, CARL SOVINEC, VLADIMIR MIRNOV, *University of Wisconsin - Madison* The nonlinear evolution of two-fluid tearing modes in a cylindrical pinch is investigated with the NIMROD code. Nonlinear single helicity evolution is examined by constraining the number of unstable modes with a small aspect ratio. Without ion gyroviscosity, the saturated island size and the combined nonlinear Hall and MHD dynamo profile are relatively independent of the ion sound gyroradius, ρ_s, and the Hall dynamo is broad relative to a linear prediction. However, at large ρ_s, the electron flow is modified into a more global structure, with the characteristic m=1 shift across the axis. This effect is not observed at small ρ_s. With ion gyroviscosity, the saturated island width decreases as ρ_s is increased, indicating that the gyroviscous force opposes the driving forces. The saturation mechanism in the simulations is analyzed, and the amplitude and structure of the dynamo are compared with MST experimental results. Mode coupling and modal energy exchange are examined in a multihelicity case with an experimentally realistic aspect ratio.

*Work supported by U.S. D.O.E.

TP8 72 Extended MHD Simulations of Tearing Instabilities and the Dynamo Effect in the Reversed-Field Pinch K. GERMASCHEWSKI, J. DEARBORN, A. BHATTACHARJEE, *Center for Integrated Computation and Analysis of Reconnection and Turbulence, University of New Hampshire* Observations on MST indicate the importance of the Hall current in sawtooth crashes and the dynamo effect in a RFP. We employ our Magnetic Reconnection Code (MRC) to perform fully 3D extended MHD simulations in the RFP, including the Hall current and electron pressure gradient in a generalized Ohm's law. The MRC is an MPI-parallelized finite-volume based simulation code that integrates the extended MHD equations. It supports arbitrary curvilinear coordinate mappings, allowing it to be adapted to cylindrical and toroidal geom-

etries. In order to overcome restrictive time-step limits, it uses implicit time integration. We have benchmarked the code for linear tearing instabilities, and performed fully nonlinear simulations. Due to the presence of the Hall current, novel vortical flows are seen in the vicinity of rational surfaces, akin to those seen in recent sawtooth studies in tokamaks, when the peak of the current density separates from the stagnation point of the flow. We calculate the dynamo field by averaging, and compare simulations with observations.

TP8 73 Relaxed states and finite pressure effects in the reversed field pinch IVAN KHALZOV, FATIMA EBRAHIMI, DALTON SCHNACK, VLADIMIR MIRNOV, *Center for Magnetic Self-Organization, University of Wisconsin, Madison, WI* Two-fluid relaxation and finite pressure effects in the reversed field pinch (RFP) are studied. First, we analytically find the relaxed states of a cylindrical plasma column in standard (single-fluid) and Hall (two-fluid) MHD minimizing the energy with constraints imposed by invariants inherent in corresponding models. The relaxed state in Hall MHD is the force-free magnetic field with uniform axial flow and/or rigid azimuthal rotation. The relaxed states in standard MHD are more complex due to the coupling between velocity and magnetic field. $F - \Theta$ diagrams (reversal parameter vs. pinch) are obtained for different values of cross helicity and total angular momentum. Analytical results are also compared with numerical simulations performed with the extended MHD code NIMROD (nimrodteam.org). Second, we examine the behavior of resistive interchange instability at high beta RFP plasma. Equilibrium profiles from MSTFIT for high beta plasma are loaded into the Grad-Shafranov solver NIMEQ. Two-fluid and MHD stability analysis of the high beta MST plasma is then performed using NIMROD. The growth rate of high-n localized interchange modes is found to be significantly reduced by finite Larmor radius effect. The work is supported by NSF and DOE.

TP8 74 The role of Nonlinear Ion Temperature Gradient Driven Drift Modes in a Reversed Field Pinch Plasma VARUN TANGRI, PAUL TERRY, *University of Wisconsin-Madison* R.E. WALTZ, *General Atomics, San Diego, California 92186, USA* The Ion Temperature gradient (ITG) mode has been rarely investigated in Reversed Field pinch (RFP) plasmas, although its role tokamak turbulence has been studied extensively. In this work, we investigate if it is plausible that ITG may play a role in particle and heat confinement in such devices. The linear stability and nonlinear saturation of ITG is investigated in the RFP geometry by modifying the gyrokinetic code GYRO[1] in a low beta, collisionless limit with and without non-adiabatic electrons. A simple toroidal equilibrium has been devised that is specified by just two parameters: the pinch parameter and the radial position. The level of transport is shown to be sensitive to temperature and density gradients and the threshold is found. To determine the nature of the instability, we study parametric scaling and also compare results with the well-known CYCLONE base case for tokamak simulations. We also estimate mixing level transport for MST parameters using linear simulations to determine if the instability is relevant to the small-scale turbulence observed in MST.

[1]J. Candy and R.E. Waltz, J. Comp. Phys. 186, 545 (2003).

TP8 75 Gyrokinetic simulations of ITG turbulence in the Reversed Field Pinch I. PREDEBON, *Consorzio RFX, Padova, Italy* C. ANGIONI, *Max Planck Institut fur Plasmaphysik, Garching, Germany* S.C. GUO, *Consorzio RFX, Padova, Italy* The Reversed Field Pinch geometry has been implemented in the gyrokinetic code GS2[1,2], to investigate the instability of ion temperature gradient (ITG) modes in typical plasmas of the RFX-mod device. The numerical results are found in agreement with previous analytical[3] and numerical[4] estimates, in the appropriate limits. Consistently, ITG modes are found to be only marginally unstable, in correspondence to the steep temperature gradients at the boundary of the helical structure in the quasi-single helicity states. We discuss the dependence of the ITG instability threshold on the relevant parameters, like density gradient and magnetic shear. The excitation of trapped electron mode (TEM) turbulence is also considered.

[1]M. Kotschenreuther *et al.*, Comput. Phys. Commun. **88**, 128 (1995)
[2]W. Dorland *et al.*, Phys. Rev. Lett., **85**, 5579 (2000)
[3]S. C. Guo, Phys. Plasmas **15**, 122510 (2008)
[4]F. Sattin *et al.*, Easter Plasma Meeting 2009, Torino, Italy

TP8 76 Overview of RFX-mod Results PIERO MARTIN, MARIA ESTER PUIATTI, *Consorzio RFX - Associazione EURATOM-ENEA sulla fusione, Padova, Italy* THE RFX-MOD TEAM, RFX-mod (R=2m, a=0.457m) is proceeding in its mission to explore RFP confinement in the plasma current range $>$ 1MA, to extend the knowledge base on MHD stability active control and to contribute to fusion science, in particular in the low-magnetic field regime. The main recent results is the discovery, at high plasma current (I$>$ 1 MA), of plasma self-organization in a 3d single helical axis equilibrium, with m=1,n=7 helicity [Nature Phys 2009]. The helical state has almost conserved magnetic flux surfaces, with strong core electron transport barriers. Electron temperature Te reaches 1.3keV @1.7MA. Ti is $\sim$ (0.5-0.7)Te, consistent with collisional ion heating. Magnetic surfaces quality improves with current. Together with a global overview of the recent results, advances on active feedback control of tearing modes and RWM will be presented (RFX has a system of 192 independent feedback coils), as well as, in particular, the progress in understanding density limit and plasma edge physics. At the plasma edge temperature barriers are also observed and current density fluctuations are measured and interpreted as Drift-Alfven vortices, similarly to what happens in Earth magnetosphere. First wall lithization is under development. The flexibility of the device allows for low-current tokamak operation, for both edge turbulence and active MHD stability control studies.

TP8 77 Initial Exploitation of RFX-mod at 1.8 MA Plasma Current R. CAVAZZANA, S. DAL BELLO, P. FRANZ, R. LORENZINI, G. MARCHIORI, G. SPIZZO, M.E. PUIATTI, M. SPOLAORE, D. TERRANOVA, N. VIANELLO, L. ZANOTTO, *Consorzio RFX - Padova, Italy* RFX-MOD TEAM, The recent remarkable results [1] of RFX-mod in the 1.5 MA range push forward the exploration of the confinement properties of Reversed Field Pinch (RFP) magnetic configuration at even higher current. During the first exploration campaigns aimed at increasing the plasma current, discharges beyond 1.8 MA have been obtained, highlighting the key issues needed to bring RFX-mod in the 2 MA current range: the most effective start-up and current ramping scheme; the conditioning of the graphite first wall in order to limit the hydrogen influx and the impurity concentration; the optimization strategy needed for tuning the active MHD mode control system (192 actuators, full coverage), aiming at the mitigation of plasma wall interaction still preserving the Helical States and their good confinement properties. [1] Lorenzini R. et al. *Self-organized helical equilibria as a new paradigm for ohmically heated fusion plasmas* Nat.Phys. 2009 - doi:10.1038/nphys1308.

TP8 78 Existence of single helicity ohmic states in the RFP DOMINIQUE ESCANDE, *des Interactions Ioniques et Moléculaires CNRS* D. BONFIGLIO, S. CAPPELLO, P. ZANCA, *Consorzio RFX* The existence of ohmic single helicity (SH) stationary states for the reversed field pinch (RFP), a longstanding issue [1,2,3,4], is analytically proved in the frame of resistive MHD in cylindrical geometry by using perturbation theory for a paramagnetic pinch with a low edge axial magnetic field. A necessary criterion for this existence involves the radial profile of the logarithmic derivative of the Newcomb eigenfunction of the pinch. It suggests that imposing the radial magnetic field to vanish at the plasma edge is not optimal. Numerical simulations with the SpeCyl code check the dependence of the SH RFP states on the boundary radial magnetic field. The existence criterion is checked against the data of RFX-mod discharges in quasi SH states. [1] V. D. Pustovitov, Pis'ma Zh. Éksp. Teor. Fiz. 35, 3 (1982) [JETP Lett. 35,1 (1982)] [2] P. N. Vabishchevich et al., Fiz. Plazmy 9, 484 (1983) [3] J. M. Finn et al., Phys. Fluids B4, 1262 (1992) [4] S. Cappello et al., 26th EPS conference on Controlled Fusion and Plasma Physics, Maastricht 1999, p. 981.

TP8 79 Numerical reconstruction of spontaneous helical equilibria in RFX-mod M. GOBBIN, *Consorzio RFX, Padova, Italy* A.H. BOOZER, *PPPL, Princeton, NJ, USA* S.P. HIRSCHMAN, *ORNL, Oak Ridge, TN, USA* L. MARRELLI, *Consorzio RFX, Padova, Italy* N. POMPHREY, *PPPL, Princeton, N, USA* D. TERRANOVA, *Consorzio RFX, Padova, Italy* The Reversed Field Pinch (RFP) plasmas can spontaneously access regimes in which a single mode dominates the magnetic perturbation spectrum (Quasi Single Helicity, QSH) [1]. For sufficiently large values of the dominant mode the magnetic island separatrix is expelled and a helical magnetic axis appears. This regime is called SHAx (Single Helical Axis) and is characterized by a helically symmetric plasma, with the periodicity of the dominant mode [2]. In order to describe the SHAx regime, the VMEC code has been adapted to the RFP configuration by using as flux coordinate the poloidal flux instead of the toroidal flux. In this work we present the first results obtained with the VMEC code reproducing the magnetic topology of a SHAx plasma in a fixed boundary approach by providing as input the safety factor profile, the shape of the last closed flux surface and taking into account also the effect of pressure. [1] P.Martin et al., Plasma Phys. Control. Fusion 49 (2007) A177-A193 [2] R. Lorenzini et al., to be published on Nature Physics, DOI 10.1038/NPHYS1308

TP8 80 Reversed Field Pinch helical self-organization studies with the volume preserving field line tracing code NEMATO D. BONFIGLIO, M. VERANDA, S. CAPPELLO, *Consorzio RFX, Italy* L. CHACON, *ORNL-USA* D.F. ESCANDE, P. PIOVESAN, *Consorzio RFX* The existence of a Reversed Field Pinch (RFP) dynamo as a (laminar) helical self-organization was anticipated by MHD numerical studies [1]. High current operation in RFX-mod experiment shows such a helical self-organization: strong internal electron transport barriers (ITB) appear and magnetic chaos healing is diagnosed when Single Helical Axis (SHAx) regimes are achieved [2]. We present results of the field line tracing code NEMATO [3] applied to study the magnetic topology resulting from 3D MHD simulations, with the aim of clarifying the conditions for chaos healing in SHAx states. First tests confirm the basic picture: the magnetic chaos due to island overlap is significantly reduced after the expulsion of the dominant mode separatrix. The possible synergy with the presence of magnetic and/or flow shear at the SHAx ITB will also be discussed [1] S. Cappello, Plasma Phys. Control. Fusion (2004) & references therein [2] R. Lorenzini et al., Nature Phys. (2009) [4] M.E. Puiatti et al invited presentation EPS 2009 conference, submitted to Plasma Phys. Control. Fusion

TP8 81 Neoclassical transport in the helical Reversed-field pinch G. SPIZZO, M. GOBBIN, L. MARRELLI, *Consorzio RFX, Padova - Italy* R.B. WHITE, *Plasma Physics Laboratory, P.O.Box 451, Princeton, NJ 08543* In this work we study particle transport in the Reversed-Field Pinch magnetic field topology. The guiding centre test particle code scOrbit is used. We find that passing particles, which in the chaotic multiple helicity (MH) state experience long-correlation Lévy flights, in the low-chaos, Single Helical Axis (SHAx) regime[1] remain well confined within magnetic surfaces. Residual diffusion is given by trapped particles and the associated neoclassical diffusion coefficient D is explored as a function of collisionality. Helically trapped (superbanana) particles appear to provide negligible contribution[2]. As a result, we recover the classical Tokamak and Stellarator transition from the banana to the plateau and Pfirsch-Schlüter regimes, but without the $1/\nu$ dependence at low collisionality which is typical of the unoptimized stellarator.

[1]R.Lorenzini, E.Martines, P.Piovesan *et al*, Nature Physics in press
[2]M. E. Puiatti, In *Proc. of the 36th EPS Conference on Controlled Fusion and Plasma Physics, Sofia (Bulgaria), 29 June- 3 July, 2009*

TP8 82 Progresses in resonant modes control in RFX-mod LIONELLO MARRELLI, FEDERICA BONOMO, PAOLO PIOVESAN, LIDIA PIRON, GIANLUCA SPIZZO, PAOLO ZANCA, BARBARA ZANIOL, *Consorzio RFX-EURATOM ENEA Association, Corso Stati Uniti, 4- 35127-Padova, Italy* The RFX-mod device is equipped with a sophisticated active feedback system which can produce non axisimmetric magnetic field aimed at controlling both MHD modes and reducing error fields. Due to its flexibility, the system can deal simultaneously with multiple harmonics. A proper tuning of the feedback laws on resonant $m = 1$ modes allowed to put them into rotation and to reduce edge values of the radial fields, allowing to explore the high current regime ($I_p \leqslant 1.8$MA). A recently developed model of the nonlinear dynamics of resonant modes (also named Tearing Modes) has been used to try to further improve the feedback law. The simulated dependence of the edge radial field associated to Tearing harmonics has been compared to the results of a PID parameter scan campaign at $0.8 \div 1.1$ MA, confirming the presence of a minimum value for the edge radial field for optimal PID parameters. Statistical analysis of two important inputs of the code, namely $m = 0$ modes phase relations and plasma flow velocity, as measured by passive spectroscopy of intrinsic impurities, will also be presented.

TP8 83 Pseudo-decoupler approach to error field correction in RFX-mod PAOLO PIOVESAN, MARCO GOBBIN, LUCA GRANDO, GIUSEPPE MARCHIORI, LIONELLO MARRELLI, LIDIA PIRON, ANTON SOPPELSA, DAVID TERRANOVA, *Consorzio RFX, Euratom-ENEA Association* An optimal design of feedback schemes for error field and mode control in fusion plasmas has to take into account the electromagnetic effects of real walls. The 3D wall structure introduces significant couplings among the plasma modes, affecting their stability and the feedback

performance. A dynamic decoupling scheme, based on the experimentally identified mutual inductances among active coils and sensors, has been developed in the RFX-mod reversed-field pinch. RFX-mod is equipped with an advanced feedback system made of 192 saddle coils and 192 sensors fully covering the torus. A large subset of the 192× 192 mutual inductances was identified from vacuum shot measurements and a decoupling scheme based on a pseudo-inverse of this matrix was developed. Control schemes based on this approach were tested in the experiment. Error fields due to the non-uniform penetration of the vertical magnetic field through the shell gaps have been reduced. A similar strategy is being developed for tearing mode control, which may allow reducing their edge radial magnetic field component.

TP8 84 Characterization of magnetic field profiles at RFX-mod by Faraday rotation measurements FULVIO AURIEMMA, *Consorzio RFX, Padova Italy* MATTEO BROMBIN, *Department of Electrical Engineering, Padova, Italy* ALESSANDRA CANTON, LEONARDO GIUDICOTTI, PAOLO INNOCENTE, ENRICO ZILLI, *Consorzio RFX, Padova Italy* A multichannel far-infrared (FIR, $\lambda = 118.8$ μm) polarimeter has been recently upgraded and re-installed on RFX-mod to measure the Faraday rotation angle along five vertical chords. Polarimetric data, associated with electron density profile, allow the reconstruction of the poloidal magnetic field profile. In this work the setup of the diagnostic is presented and the first Faraday rotation measurements are analyzed. The measurements have been performed at plasma current above 1.2 MA and electron density between 2 and $6x10^{19}$ m $^{-3}$. The actual S/N ratio is slightly lower than the expected one, due to electromagnetic coupling of the detectors with the saddle coils close to the polarimeter position. Due to this limit, only average information in the flat-top phase of the discharge could be so far obtained. The experimental data have been compared with the result of the μ&p equilibrium model [1], showing a good agreement between experiment and model, whereas the main differences are in the external region of the plasma. A different parameterization of the $\mu = \mu_0 J \cdot B/B^2$ profile has been proposed to enhance the agreement between model and experiment. [1] Ortolani and Snack, World Scientific (1993) Singapore

TP8 85 Experimental background emissivity at the transitions useful for the active CXRS in RFX-mod F. BONOMO, M. VALISA, L. CARRARO, M.E. PUIATTI, B. ZANIOL, *Consorzio RFX, Padova, Italy* We present the investigation of the background emissivity of the transitions useful for active charge exchange (CX) spectroscopy. In particular, we focused on the Carbon and Oxygen emissivities at those transitions which could be attractive for the neutral beam diagnostic installed in RFX-mod. These transitions are: the n=8→ 7 (529.0nm), n=7→ 6 (343.4nm), and n=6→ 5 (207.0nm) for C VI; the n=10→ 9 (606.8nm) for O VIII. Their experimental background emissivities have been studied and compared to those predicted by an active CX simulation code (M.von Hellermann), in order to highlight which transition features the best signal to background ratio and to set up the most effective experimental arrangement for a charge exchange diagnostic on RFX-mod.

TP8 86 Transport and linear stability studies for PPCD optimization in RFPS GIAN LUCA DELZANNO, JOHN M. FINN, *LANL* JOHN SARFF, *U. Wisconsin* We have combined 1D transport simulations of pulsed poloidal current drive (PPCD) together with linear stability studies for a wide spectrum of m=1 and m=0 modes. The present model assumes zero beta and a specified form of resistivity increasing near the edge. The model includes a "dynamo" term in Ohm's law which is gradually decreased to zero during the early part of the PPCD cycle, simulating the decrease in tearing mode activity as PPCD progresses. We present several initial studies with ad-hoc waveforms in time for the wall electric field, and measure the fraction of time over which m=1, m=0 stability is achieved. We have also developed a more systematic scheme by which we decrease the toroidal electric field at the wall and determine the poloidal electric field there by requiring the parallel electric field to be zero there. (This ensures zero helicity dissipation at the edge.) This programming is designed to match at a specific time a self-similar rampdown (SSRD) state [1]. After this time the wall electric field components are then programmed to decay exponentially. We have mapped out the full parameter space of these SSRD states and their linear stability to m=1 and m=0 modes. A PPCD scenario is considered optimal if it has a slow decay rate and develops into a SSRD state well inside the stable SSRD regime. [1] R. Nebel, D. Schnack, and T. Gianakon, Phys. Plasmas 9, 4968 (2002).

TP8 87 High frequency MHD activity due to resistive interchange modes in a reversed field pinch plasma MATTEO ZUIN, *Consorzio RFX, Associazione EURATOM-ENEA sulla Fusione, Padova, Italy* SILVIA SPAGNOLO, *Consorzio RFX, Padova,Italy* ROBERTO PACCAGNELLA, EMILIO MARTINES, ROBERTO CAVAZZANA, GIANLUIGI SERIANNI, MONICA SPOLAORE, NICOLA VIANELLO, *Consorzio RFX, Associazione EURATOM-ENEA sulla Fusione, Padova, Italy* The results of an experimental activity aimed at investigating the origin of high frequency, high toroidal mode number (n> 20) magnetic fluctuations in the RFX-mod reversed field pinch device are presented. The space-time properties of the fluctuations are characterized by means of 2 arrays of in-vessel toroidal and poloidal pick-up coils covering the whole toroidal torus, and by means of an insertable edge probe, housing two radial arrays of triaxial pick-up coils, closely spaced in the toroidal direction. High levels of magnetic fluctuation at frequencies above 30 kHz are observed when the reversal of the magnetic field at the edge is driven to deep values. These fluctuations are due to rotating coherent modes whose resonant radii are located between the plasma edge and the reversal surface. A comparison of the experimental spectral properties to the theoretical predictions by a linear MHD stability analysis for a RFP plasma allows to interpret the observed instabilities as resistive interchange modes.

TP8 88 Resistive g-modes and RFP confinement JAN SCHEFFEL, *Division of Fusion Plasma Physics, Alfvén Laboratory, Royal Institute of Technology, Association EURATOM-VR, Stockholm, Sweden* AHMED MIRZA, *Division of Fusion Plasma Physics, Alfvén Laboratory, Royal Institute of Technology, Stockholm, Sweden* The role of pressure driven resistive modes in the reversed-field pinch remains unclear. It was early shown that unstable resistive g-modes would always exist for an inwardly directed pressure gradient. It now appears that pressure profile smoothing, due to inclusion of heat conductivity terms in the energy equation, enables completely stable RFP states at moderate plasma beta. These calculations, apart from being restricted to linearized perturbations, suffer from the use of rather forced scalings, thus their accuracy can be questioned. Also, they have so far only been applied to conventional RFP states, where confinement-limiting tearing fluctuations maintain the reversed axial magnetic

field. In the advanced RFP, current profile control has largely eliminated current driven tearing modes. Fully nonlinear, numerical studies have shown that energy confinement and poloidal beta increase substantially, but that weak residual modes usually remain. The nature of these residual modes, which limit energy confinement, is studied using a novel semi-analytical, spectral scheme for solving the resistive MHD equations; the generalized weighted residual method (GWRM). Results from the analysis as well as comparisons with the competing linear resistive g-mode theories will be presented.

TP8 89 Progress in Low-Aspect-Ratio RFP Research in RELAX* S. MASAMUNE, A. SANPEI, R. IKEZOE, T. ONCHI, K. OKI, M. SUGIHARA, Y. KONISHI, S. FUJITA, M. NAKAMURA, A. FUJII, H. MOTOI, H. HIMURA, *Kyoto Institute of Technology* R. PACCAGNELLA, *Consorzio RFX* A. EJIRI, *Univ. Tokyo* D. DENHARTOG, *Univ. Wisconsin* RELAX is a low-aspect-ratio RFP experiment with R=0.51m/a=0.25m (A=2). Initial results have shown the advantages of low-A RFP configuration with I_p of up to 100kA and V_l of down to $\sim$ 30V; the configuration tends to relax to a quasi-single helicity (QSH) state. A high-speed camera diagnostic has revealed simple helix structure. In the extreme case, rotating Helical Ohmic equilibrium state has been realized. The pressure driven bootstrap current fraction is shown to be less than 5% of the total current in the present RELAX plasmas. Recent progress includes a test of field error compensation; the control system will also be used in feedback control of RWM. The electron density measurements with a 104 GHz microwave interferometer show that the density lies in the range from $\sim 5 \times 10^{18}$m^{-3} to $\sim 10^{19}$m^{-3}. Design study of Thomson scattering system is also in progress.

*Work supported by NIFS Collaboration Program NIFS07KOAH022.

TP8 90 Imaging Diagnostics for MHD Studies in Low-Aspect-Ratio Machine RELAX* T. ONCHI, R. IKEZOE, K. OKI, Y. KONISHI, M. SUGIHARA, S. FUJITA, A. SANPEI, H. HIMURA, S. MASAMUNE, *Kyoto Institute of Technology* N. NISHINO, *Hiroshima University* RELAX TEAM, Visible-light and soft-X ray imaging diagnostics have been applied to a low-aspect-ratio RFP machine RELAX for the study of MHD dynamics. The visible-light images with a high-speed (80,000fps) camera from a tangential port of RELAX have revealed time evolution of the simple helical structure for the first time in the RFP. The visible-light helical structure agrees well with magnetic structure of the helically deformed RFP (Helical Ohmic RFP), rotating toroidally in the same direction as the magnetic fluctuation. The simple helical structure is one of the results of low-A nature of RELAX. A soft-X ray (SXR) imaging diagnostic technique has also been developed for MHD studies in RELAX. In this diagnostic, a 3-D magnetic structure in the low-A RFP plasma is reconstructed from simultaneously measured tangential and vertical SXR images. Initial results from tangential SXR imaging will be reported, in comparison with the visible-light images of the simple helical structure.

*This work is supported by the NIFS Collaboration Program No.NIFS07KOAH022 and JSPS Grant-in-Aid for Scientific Research No.21009943.

TP8 91 Rotating Helical Ohmic Configuration in a Low-Aspect-Ratio Reversed Field Pinch* KENSUKE OKI,[†]RYUYA IKEZOE, TAKUMI ONCHI,[‡]SHIN-ICHI FUJITA, AKIO SANPEI, HARUHIKO HIMURA, SADAO MASAMUNE, *Kyoto Institute of Technology* ROBERTO PACCAGNELLA, *Consorzio RFX* Recent theoretical studies have shown that a low-aspect-ratio Reversed Field Pinch (RFP) may have several advantages. In a low- aspect-ratio RFP machine "RELAX," inner magnetic field profiles have been measured by a radial array of magnetic probes inserted to the magnetic axis. In a type of plasma, the profiles largely oscillate and are good agreement with rotating "helical Ohmic equilibrium" (helical RFP configuration with a helical magnetic axis). The helical structure indicated by edge magnetic fields at various places corresponds to a helical instability mode having a singular surface in the core region. Thus, the helical deformation may be caused by growth of the single helical mode at the singular surface. It appears that this growth is enhanced by increase in separation of major singular surfaces due to low-aspect-ratio.

*This work was supported by a NIFS Collaboration Program No. NIFS07KOAH022 and JSPS Grant-in-Aid for Scientific Research No. 21009943.
[†]JSPS Research Fellow
[‡]JSPS Research Fellow

TP8 92 Toroidal rotation of localized dynamo event in a low-aspect-ratio RFP plasma* R. IKEZOE, T. ONCHI, K. OKI, Y. KONISHI, M. SUGIHARA, S. FUJITA, A. SANPEI, H. HIMURA, S. MASAMUNE, *Kyoto Institute of Technology* RELAX TEAM, A burst of the edge magnetic fields has been observed in low density discharges in the low-aspect-(A) ratio RFP machine, RELAX. The burst occurs at a toroidally localized position, then rotating in the opposite direction to the plasma current at 10-20 km/s. The evolutions of the edge toroidal field and the toroidal flux in the toroidal section where the burst occurs show that the toroidal flux increases at the burst and the toroidal field profile is modified accordingly; the burst will be referred to as a localized dynamo event. The toroidal flux keeps rising between the bursts at much slower rate than at the burst. This indicates that the discrete dynamo event may be superimposed on the mild continuous dynamo in RELAX. The time evolution of soft-x-ray and H_α emissions, has indicated that the localized dynamo is closely related to particle and energy transport. We present the detailed characteristics of this burst phenomenon with emphasis on the effect of low aspect ratio.

*Work is supported by the NIFS Collaboration Program No. NIFS07KOAH022.

TP8 93 Simultaneous measurement of electron temperature and density by a line pair method in the RFP plasma MASAYUKI WATANABE, S. SHIMIZU, H. OGAWA, T. SHINOHARA, *Nihon University* A line-pair-method has been applied for a simultaneous measurement of the electron temperature and density in ATRAS RFP plasma. Three helium spectrum lines (668nm, 706nm, 728nm) were measured during the discharge at the same time and the electron temperature and density is estimated by using a Collision-Radiation model. To get the signal of the helium impunity line from the RFP discharge, the RFP plasma in the hydrogen gas with a few mixed helium gas was formed. In the typical ATRAS RFP discharge of the plasma current of 60kA, the electron temperature was approximately 50-150 eV and the elec-

tron density is the order of 10^{18} m^{-3}. During the discharge, the change of the temperature and density are mutually related and this correlation was the almost reverse phase. The periodically change of the temperature and density were also observed. This change synchronizes with a periodically increase of the averaged toroidal magnetic field, which is caused by the toroidal rotation of the increase of the toroidal magnetic field. This rotation, which is deeply related with dynamo effect, makes the plasma energy lose and particles also diffuse toward the plasma edge. As a result, the recycling of the particle and energy are occurred at the same time.

TP8 94 Effect of a strong equilibrium electric field on the zonal flow residual in quasisymmetric stellarators MATT LANDREMAN, PETER CATTO, *MIT PSFC* It was recently shown [1] that several neoclassical formulae for tokamaks can be significantly modified if the radial electric field is as large as that observed in a pedestal – specifically, if $d\Phi/dr \sim T/(e\rho_{\rm pol})$, where $\rho_{\rm pol}$ is the poloidal ion gyroradius. In the present work, we consider the same modification of neoclassical quantities in quasisymmetric stellarators, beginning with the zonal flow residual [2]. The tokamak analysis in [1] exploited the conservation of canonical angular momentum. The analysis therefore requires modification in stellarators, in which canonical angular momentum is not conserved. In its place, one can use the "helical momentum" which is known to be conserved if the magnetic field is quasisymmetric [1] Kagan and Catto, *Phys. Plasmas* **16**, 056105 (2009). [2] Rosenbluth and Hinton, *Phys. Rev. Lett.* **80**, 724 (1998). [3] Boozer, *Phys. Fluids* **26**, 496 (1983).

TP8 95 Transport in a stellarator with imperfect flux surfaces and quasisymmetry* HAROLD WEITZNER, *New York University, Courant Institute Mathematical Sciences* With the use of techniques developed in Refs. 1 it is possible to study low shear stellarator steady states. A steady state near a magnetic field with flux surfaces and approximate quasisymmetry is modified by the addition of small magnetic fields restricted only by the condition that the perturbation preserve the underlying stellarator symmetry. The perturbations constrain the profile functions of the electrons and ions. Equations for the profile functions are given and a simple model of a linearized collision operator is used to obtain further results. [1] Phys. Plasmas 1, 3942 (1994); 4, 575 (1997); and 5, 417 (1998).

*This work is supported by U.S. Dept. of Energy Grant No. DE-FG02-86ER53223.

TP8 96 Rotation roots and neoclassical viscosity in quasi-symmetry* A.J. COLE, C.C. HEGNA, J.D. CALLEN, *University of Wisconsin* In a quasi-symmetric device, there exists a symmetry angle $\alpha_h = \theta - N\zeta/M$, such that $|B| = B_0(1 - \epsilon_h \cos M\alpha_h)$ along a field-line, with several much smaller helical 'sidebands.' Provided the departure from symmetry is small, i.e. $\delta B_{\rm eff}/B_0 \ll \epsilon_h$ where $\delta B_{\rm eff}/B_0$ is the effective helical sideband strength, flow damping and thus flow evolution along and 'cross' the direction of symmetry in a flux surface decouple [1,2], and can be determined successively. In the context of a fluid-moment approach [3], the momentum equation in the symmetry direction is equivalent to the ambipolarity condition. Steady state rotation solutions of this equation are equivalent to ambipolar radial electric field 'roots' in conventional stellarator theory and will be presented for various banana-drift neoclassical flow damping regimes [1] J. D. Callen, A. J. Cole, and C. C. Hegna, Tech. Rep. UW-CPTC 08-7, Univ. of Wisconsin, http://www.cptc.wisc.edu (2009). [2] A. J. Cole, C. C. Hegna, and J. D. Callen, Tech. Rep. UW-CPTC 08-8, Univ. of Wisconsin, http://www.cptc.wisc.edu (2009). [3] K. C. Shaing and J. D. Callen, Phys. Fluids 26, 3315 (1983).

*This research was supported by the U.S. Department of Energy under Grant Nos. DE-FG02-86ER53218, DE-FG02-92ER54139 and DE-FG02-99ER54546.

TP8 97 Characterization of magnetic configurations of LHD in terms of boundary shape and the direction of their improvements SHOICHI OKAMURA, *National Institute for Fusion Science* LHD in Japan is the largest stellarator / heliotron device with superconducting magnetic coils (major radius is 3.9 m with 3 T magnetic field). It has been demonstrating good confinement properties comparable to major tokamaks. For the magnetic configuration control, the vertical field control is very effective with which the confinement characteristics such as the magnetic field curvature and trapped particle trajectories are largely changed. For high temperature discharge experiments or high density discharge experiments, two distinct configurations have been used respectively: inward shifted configuration and outward shifted configuration which are produced by selecting different vertical field. In this paper, these two configurations are analyzed in terms of Fourier components of boundary shape for the purpose of understanding them with general physical quantities rather than specific device parameters. The direction of improving magnetic configurations for better confinement properties will be discussed.

TP8 98 New QP/QI optimized stellarator configurations* D.A. SPONG, J.H. HARRIS, *ORNL* A unique characteristic of the quasi-poloidal/isodynamic transport optimization strategy is that it can lead to stellarators that deviate from the usual "doughnut" shape; i.e., they can have extended relatively straight cylindrical sections of plasma (connected by corner regions). This offers a number of potential design advantages, including simplified coil geometries, novel divertor approaches, low bootstrap current (less potential for ELMs and disruptions), more acceptable wall heat fluxes, and demountable blankets for reactors. The STELLOPT approach has been used to develop optimized configurations of this type for two, three and four field periods; the primary optimization targets used so far have been: effective ripple, J* closure and aspect ratio. From a top view, the two field period device is an extended racetrack with $- \; -i = 0.2 - 0.25$, $\varepsilon_{eff}^{3/2} = 8 \times 10^{-4} - 3 \times 10^{-3}$ and outboard $R_{max}/R_{min} \sim 3$; $\langle R \rangle / \langle a \rangle$'s in the range of 9 to 20 have been examined so far. The physics characteristics and remaining optimization targets that are under consideration for such devices will be discussed.

*Research sponsored by the U.S. Department of Energy under Contract DE-AC05-00OR22725 with UT-Battelle, LLC.

TP8 99 Neoclassical and anomalous flows in stellarators* A.S. WARE, T. MARINE, *University of Montana* D.A. SPONG, *Oak Ridge National Laboratory* The impact of magnetic geometry and plasma profiles on flows and viscosities in stellarators is investigated. This work examines both neoclassical and anomalous flows for a number of configurations including a particular focus on the Helically Symmetric Experiment (HSX) and other quasi-symmetric configurations. Neoclassical flows and viscosities are calculated using the PENTA code [1]. For anomalous flows, the

neoclassical viscosities from PENTA are used in a transport code that includes Reynolds stress flow generation [2]. This is done for the standard quasi-helically symmetric configuration of HSX, a symmetry-breaking mirror configuration and a hill configuration. The impact of these changes in the magnetic geometry on neoclassical viscosities and flows in HSX are discussed. Due to variations in neoclassical viscosities, HSX can have strong neoclassical flows in the core region. In turn, these neoclassical flows can provide a seed for anomalous flow generation. These effects are shown to vary as the ratio of electron to ion temperature varies. In particular, as the ion temperature increases relative to the electron flow shear is shown to increase. [1] D. A. Spong, Phys. Plasmas 12, 056114 (2005). [2] D. E. Newman, et al., Phys. Plasmas 5, 938 (1998).

*Work supported by U.S. DOE under Grant DE-FG02-03ER54699.

TP8 100 Linear and nonlinear gyrokinetic studies of turbulence in stellarator geometry with the GS2 code* J.A. BAUMGAERTEL, G.W. HAMMETT, D.R. MIKKELSEN, *Princeton Plasma Physics Laboratory* W. DORLAND, *University of Maryland* E.A. BELLI, *General Atomics* The GS2 gyrokinetic code is being used to study microinstabilities and turbulence in flux-tubes in non-axisymmetric geometries, including stellarators. Stellarators have a number of interesting features, such as natural negative magnetic shear and a large number of shaping parameters, which offer possibilities for reducing microturbulence and improving performance. GS2 traditionally uses numerical equilibria for these studies, but recently an analytical stellarator equilibrium model[1] has been implemented for benchmarking with the GKV and GENE gyrokinetic codes. In addition to studying ITG modes, we will present results on kinetic ballooning mode growth rates and instability thresholds, using both the analytical model and numerical stellarator equilibria from recent design studies. Nonlinear results will also be discussed.

*Supported by the DOE Fusion Energy Sciences Fellowship and DOE Grant DE-FC02-04ER54784, the Center for Multiscale Plasma Dynamics.

[1]SUGAMA, WATANABE, and FERRANDO-MARGALET, Plasma and Fusion Research, Vol. 3, p.041 (2008)

TP8 101 Use of High Temperature Superconducting Monoliths for Field Shaping in Stellarators and Tokamaks* THOMAS BROWN, *PPPL* LESLIE BROMBERG, *MIT* ALLEN BOOZER, PHIL HEITZEROEDER, MICHAEL ZARNSTORFF, *PPPL* JOSEPH MINERVINI, *MIT* Monolithic High Temperature Superconductors (HTS) can be used for field shaping. Design issues relevant to stellarator magnets using single crystal or highly textured YBCO monoliths will be discussed. The excellent properties of YBCO operating at elevated temperatures ($>$ 10 K) will be summarized. High field, cryo-stable, highly complex magnet field topologies can be generated using the techniques discussed in this paper. Engineering constraints, such as stresses in the superconducting monoliths, support, quench protection, superconducting stability of the monoliths and required external support structure will be described. The limitations imposed by different fusion environments on the performance and lifetime of the HTS monoliths will be reviewed, both for near term experiments as well as long term stellarator fusion reactors. Since the HTS monoliths require no insulation or copper for stability/quench protection, some of the irradiation limits on these components are eliminated.

*Supported by US DOE OFES.

TP8 102 Overview of HSX Results and Future Directions* D.T. ANDERSON, *University of Wisconsin-Madison* FOR THE HSX TEAM, HSX is a quasihelically symmetric (QHS) stellarator with minimal toroidal curvature and high effective transform. We present recent results at 1 Tesla operation which highlight the unique features of the bootstrap and Pfirsch-Schlueter currents. Large parallel flows, usually neglected in stellarator calculations, have been observed by CXRS in qualitative agreement with results first predicted by the PENTA code [1]. Electron temperatures in the core during ECRH are up to 2.5 keV with 100 kW input power and drop to 1.5 keV when the symmetry is intentionally degraded. The steep temperature gradient in the core is indicative of a core electron root confinement (CERC) mode. PENTA calculations support the conclusion that even with small symmetry-breaking, it is possible to achieve a neoclassical ITB based on the proximity of an electron root near an ion root. A Weiland ITG/TEM tokamak model for anomalous transport supports the conclusion that E x B suppression of turbulence is responsible for the improved confinement in the plasma core. At a lower field of 0.5 Tesla, an instability due to fast electrons is observed, which disappears when the symmetry is broken. Experimental measurements indicate that the mode is acoustic. We will also briefly summarize topics of current research and future plans.

*Supported by USDOE under Grant DE-FG02-93ER54222

TP8 103 Modeling and Measurement of Toroidal Currents in the HSX Stellarator J.C. SCHMITT, *HSX Plasma Laboratory* J.N. TALMADGE, J. LORE, HSX PLASMA LABORATORY TEAM, A set of magnetic diagnostics are installed to measure the magnetic field at several locations around HSX. Rogowski coils and diamagnetic loops measure the toroidal current and toroidal flux, and two poloidal belts, separated by $\sim$ 1/3 of a field period measure the magnetic field vector at 16 poloidal locations at each toroidal angle. A self-consistent calculation of the Pfirsch-Schlüter (PS) and bootstrap currents is found with VMEC and BOOTSJ, and the 3D equilibrium reconstruction code, V3FIT calculates the expected signal of the magnetic diagnostics. The lack of toroidal curvature in HSX results in a dipole PS current that has a helical rotation and nearly reverses at the two toroidal locations. Also, the bootstrap current reduces the rotational transform ($\sim$ 1) but increases the effective transform ($\sim$ 3). Compared to a tokamak, the magnitude of each current is reduced by $\sim$ 3. Improvements in the modeling include: 1) Comparison of the measured bootstrap current to the PENTA code which includes the effects of parallel momentum conservation and finite electric field. 2) Comparison of the evolution of the net toroidal current to a 3D model involving the susceptance matrix. 3) Analysis of the sensitivity of the diagnostic set and the ability of the V3FIT code to reconstruct the plasma pressure and current profiles based on the magnetic signals.

TP8 104 Determining the Radial Electric Field in HSX Using Impurity Ion Velocity Measurements from CHERS* A. BRIESEMEISTER, K. ZHAI, D.T. ANDERSON, F.S.B. ANDERSON, J. LORE, J.N. TALMADGE, *HSX Plasma Laboratory, University of Wisconsin, Madison* A Charge Exchange Recombination Spectroscopy (CHERS) system is used to measure the velocity, density, and temperature of fully stripped carbon impurities in the Helically Symmetric Experiment (HSX), a quasi-helically symmetric stellarator. Velocity measurements are obtained by reversing the magnetic field between sets of shots in order to reverse the plasma flow velocity. This doubles the distance the measured photons are Doppler shifted and eliminates the need to accurately determine the value of the unshifted emission line which can depend on plasma conditions. Since two viewing angles (one approximately poloidal and the other approximately toroidal) are used at each radial location, the velocity magnitude and direction can be determined. The measured velocity is used to determine the radial electric field from force balance. A comparison of the measured values to those calculated using a momentum-conserving neoclassical transport model will be presented.

*Supported by DOE grant number DE-FG02-93ER54222.

TP8 105 Disruptions in current-driven discharges in the Compact Toroidal Hybrid experiment* S. KNOWLTON, G. HARTWELL, J. HANSON, B. STEVENSON, J. ECKBERG, *Auburn University* K. KAMDIN, *University of Chicago* Disruption avoidance in stellarators is relevant to helical configurations with tokamak-like levels of bootstrap current, e.g. quasi-axisymmetric devices, and stellarator-tokamak hybrids. Disruptions are investigated in the Compact Toroidal Hybrid (CTH) experiment (R_0 = 0.75 m, a ~ 0.2 m, $B_0 \leq$ 0.7 T, $\bar{n}_e = 0.2 - 1.5 \times 10^{19}$ m^{-3}), a flexible heliotron operating with significant ohmic current. At B_0 = 0.5 T, the edge vacuum rotational transform is variable from $\iota_{VAC}(a) = 0.05$ to 0.5gnd plasma currents up to 40 kA are driven in plasmas generated by electron-cyclotron resonant heating at 14 GHz. At the lowest vacuum transform $\iota_{VAC}(a) = 0.05$, current-driven disruptions leading to a complete loss of plasma can be induced for a total rotational transform $\iota_{TOT}(a) > 0.3$ at plasma densities $\bar{n}_e \geq 0.8 \times 10^{19}$ m^{-3}. Disruptions are preceded by m = 2 tearing activity. Complete disruptions have not yet been observed in CTH with h $\iota_{VAC}(a) \geq 0.2$, although partial current collapses can take place. Efforts are underway to study the transitional behavior of the disruptions as the vacuum transform is continuously raised.

*Supported by US DoE Grant No. DE-FG02-00ER54610. Co-author K.K. supported by a DoE summer National Undergraduate Fellowship.

TP8 106 Soft X-Ray Diagnostics on the Compact Toroidal Hybrid Experiment* G.J. HARTWELL, J. ECKBERG, J.D. HANSON, S.F. KNOWLTON, *Auburn University* K. KAMDIN, *University of Chicago* Soft X-Ray (SXR) Diagnostics are used on the Compact Toroidal Hybrid (CTH) torsatron experiment (R = 0.75 m, a ~ 0.2 m, B $\leq$ 0.7 T, $n_e \leq 10^{19}$ m^{-3}, $T_e \leq$ 250 eV) for tomographic reconstruction of the emissivity profile, electron temperature measurement, and as input to a 3D reconstruction code. SXR tomography is performed with three cameras with up to 60 chords viewing a poloidal cross-section. Each camera consists of a 20-channel AXUV-20EL photo-diode array filtered with 500nm Al foil. Electron temperatures are being measured with an Amptek X123-SDD spectrometer. The spectrometer views the Bremsstrahlung emission along a single chord through the plasma in the energy range from 1-10 keV. Signals from the 60 channel tomographic camera system and signals from similar cameras located at other toroidal locations are being incorporated into the V3FIT reconstruction code[1]. [1]. J. D Hanson et. al., Nucl. Fusion **49**, 075031 (2009)

*This work is supported by US. Department of Energy Grant No. DE-FG02-00ER54610. Co-author (K.K.) supported by a Department of Energy National Undergraduate Fellowship.

TP8 107 Reconstruction of current-driven equilibria in the Compact Toroidal Hybrid using magnetic diagnostics* B.A. STEVENSON, *Physics Dept, Auburn University* M. CIANCIOSA, J. HANSON, G. HARTWELL, J. HEBERT, S. KNOWLTON, There is a growing need for rapid reconstruction capability of fully three-dimensional equilibria in toroidal confinement experiments. Test and validation of the new V3FIT 3D magnetic equilibrium reconstruction code are underway on the Compact Toroidal Hybrid (CTH). The CTH is a heliotron-type device in which the magnetic configuration can be strongly modified by plasma current. The present suite of magnetic diagnostics includes internal and external 8-part and full Rogowski coils, four flux loops, and a diamagnetic loop. The measured signals from these diagnostics include contributions from the plasma current, externally applied currents, vacuum vessel current, and various sources of pickup and drift. The induced vacuum vessel current (< 15kA) also contributes to the magnetic diagnostic signals. In order to include this contribution in the reconstruction process, the VALEN code was used to model the time varying vacuum vessel current distribution. For reconstructions, the plasma contribution is extracted from the total signal to provide the experimental input to V3FIT which utilizes least-squares fitting and the VMEC equilibrium code to reconstruct 3D plasma equilibria.

*Supported by US DOE Grant DE-FG02-00ER54610

TP8 108 Plasma Equilibrium in a Magnetic Field with Stochastic Regions* A. REIMAN, J. KROMMES, D. MONTICELLO, M. ZARNSTORFF, *Princeton Plasma Physics Laboratory* The nature of plasma equilibrium in a magnetic field with stochastic regions is examined, with particular application to the reconstruction of equilibria for the W7AS stellarator. It is shown that the magnetic differential equation that determines the equilibrium Pfirsch-Schlüter currents can be cast in a form similar to various nonlinear equations for a turbulent plasma, allowing application of the mathematical methods of statistical turbulence theory. An analytically tractable model, previously studied in the context of resonance- broadening theory, is applied with particular attention paid to the periodicity constraints required in toroidal configurations. It is shown that even a very weak radial diffusion of the magnetic field lines can have a significant effect on the equilibrium in the neighborhood of the rational surfaces, strongly modifying the near-resonant Pfirsch-Schlü ter currents. Implications for the numerical calculation of 3D equilibria are discussed, with specific application to the calculation of equilibria for the W7AS stellarator.

*Work supported by DOE contract DE-AC02-09CH11466.

TP8 109 MAGNETIC RECONNECTION

TP8 110 Laboratory Study of Magnetic Reconnection with Variable Collisionality and its Application to Space Astro-physics* M. YAMADA, D. UZDENSKY, R. KULSRUD, H. JI, S. DORFMAN, E. OZ, J. YOO, *Center for Magnetic Self-Organization, PPPL, Princeton U* The fundamental physics of magnetic reconnection derived from the recent MRX experiment [1] is presented focusing on the different dynamics of electrons and ions during reconnection. Both local and global physics issues for reconnection and magnetic field dissipation are discussed. In the MRX scaling [1], the reconnection rate increases rapidly when the ion skin depth becomes larger than the Sweet-Parker width; the rate depends linearly on λ_{mfp}/L, a ratio of the electron mean free path to the scale length. This scaling can guide comparisons between laboratory results and astrophysical plasmas [2]. The recent experimental study of the global dynamics of line-tied solar flux ropes in a half-toroid plasma arc is also presented. [1] M. Yamada et al, Phys. Plasmas, 13, 052119 (2006) [2] D. A. Uzdensky, Phys. Rev. Lett., v.99, 261101 (2007).

*Supported by DoE, NSF, and NASA.

TP8 111 A Next-Generation Experiment To Study Magnetic Reconnection and Related Explosive Phenomena in Large and Collisionless Plasmas H. JI, M. YAMADA, S. PRAGER, *PPPL* W. DAUGHTON, V. ROYTERSHTEYN, *LANL* Magnetic reconnection, a topological change in magnetic field in plasmas, often occurs explosively leading to rapid conversion of magnetic energy to plasma particle energy in space, astrophysical and laboratory fusion plasmas. The Magnetic Reconnection Experiment (MRX, http://mrx.pppl.gov) is a primary dedicated experiment to study reconnection in a controlled environment. However, further critical understanding and contributions to space and astrophysical plasmas are limited by the parameters achievable in MRX and other dedicated experiments. The MRX plasmas are relatively collisional (Lundquist numbers $S \sim 10^3$) and effectively small (plasma size normalized by ion skin depth or ion sound radius ~ 10). In this paper, we discuss plans for a next-generation reconnection experiment based on MRX. By a combination of larger physical size, stronger magnetic field, and higher heating power, we aim to increase S by a factor of 100 and effective size by a factor of 10, representing a very large jump in the laboratory capabilities. Kinetic simulations in realistic boundaries will be used to guide the experimental design. Research topics include: (1) transition of collisional to collisionless reconnection and its scaling with collisionality and size, (2) interacting multiple reconnections as a possible cause of explosive phenomena, (3) particle energization by reconnection, (4) relation between local reconnection and global magnetic self-organization in 3D realistic geometry and boundary.

TP8 112 Local and Global 3-D Effects in the Magnetic Reconnection Experiment (MRX) S. DORFMAN, H. JI, M. YAMADA, E. OZ, J. YOO, *CMSO, PPPL* W. DAUGHTON, V. ROYTERSHTEYN, *LANL* One of the key open questions in Magnetic Reconnection is the nature of the mechanism that governs the reconnection rate in real astrophysical and laboratory systems. Comparisons between fully kinetic 2-D simulations of the Magnetic Reconnection Experiment (MRX) and experimental data show that the 2-D, collisionless expression for the electric field due to particle dynamics [1] does not match MRX data; related to this is a factor of 3-5 discrepancy in the layer width [2,3]. Adding collisions to the simulation leads to a broadening of the layer, but the level of collisionality present in MRX may not be high enough to resolve the discrepancy. Ongoing research on MRX explores the role of fluctuations and 3-D effects in the force balance. Significant toroidal asymmetries have been found, manifested by regions of high inductive electric field moving in the electron flow direction within the layer. Electromagnetic fluctuations in the lower hybrid frequency range [4] tend to occur in discharges with high local currents and a rapid local reconnection rate. The precise relation of these phenomena to fast reconnection is actively being investigated. [1] M. Hesse, et al., Phys. Plasmas, 6:1781 (1999). [2] Y. Ren, et al., Phys. Plasmas 15, 082113 (2008). [3] S. Dorfman, et al., Phys. Plasmas 15, 102107 (2008). [4] H. Ji, et al., Phys.Rev.Lett. 92 (2004) 115001. Supported by NDSEG, DOE, NASA, and NSF.

TP8 113 Measurement of an Electrostatic Potential Well during Magnetic Reconnection in MRX* JONGSOO YOO, MASAAKI YAMADA, HANTAO JI, SETH DORFMAN, ERDEM OZ, *PPPL* Numerical simulations and space observations have demonstrated that an electrostatic potential well develops during magnetic reconnection, along the direction normal to the current sheet. The existence of an electrostatic potential well is evidence of two-fluid effects in the diffusion region. Electrons and ions have different heating mechanisms, due to the difference in their fundamental length scales. Unmagnetized ions are considered to obtain energy from the electrostatic potential as they approach the X line. Thus, it is important to measure the magnitude of the potential well to study how ions are accelerated and heated during reconnection. With the help of a 10-tip floating potential probe and Langmuir probes, electrostatic potential wells are observed during 'Pull' reconnection in the Magnetic Reconnection eXperiment (MRX). The measured potential drop across the current sheet is on the order of 10 V. The location and width of the current sheet are measured by a nearby magnetic probe. The relationship between the magnitude of the potential drop and ion temperature is under investigation.

*Supported by US DOE contract #DE-AC02-76CH-03073.

TP8 114 Study of Ion heating and acceleration in magnetic reconnection and laboratory flux loop experiments at MRX ERDEM OZ, MASAAKI YAMADA, SETH DORFMAN, HANTAO JI, JONGSOO YOO, *Princeton Plasma Physics Laboratory* Although it has been studied for many decades there is no comprehensive theoretical model that describes particle heating and acceleration commonly observed in space and astrophysical plasmas. Magnetic reconnection is considered to be the main process that causes ion heating and acceleration; however, the fundamentals of reconnection heating mechanism is not yet well understood. In the Magnetic Reconnection Experiment, we recently built a new type of ion Doppler spectroscopy probe in order to measure local ion temperature and flow velocity. The light from the plasma is collected by an optical fiber bundle and transported to a high resolution spectrometer where spectral images of 4 slits are recorded using an intensified gated camera capable of recording 2 images in a single plasma shot. The new light collection system gives an order of magnitude improvement in signal intensity compared to previous studies on MRX [1]. Initial results from this

probe in two specific experimental campaigns, the "pull" reconnection experiments, and the laboratory flux loop experiment [2], will be reported. [1] S. C. Hsu, et al, Phys. Plasmas 8, 1916 (2001) [2] Abstract APS 2008 DPP GP6.19

TP8 115 Fully kinetic 3D simulations of magnetic reconnection in MRX-relevant geometry including Coulomb collisions V. ROYTERSHTEYN, W. DAUGHTON, L. YIN, B.J. ALBRIGHT, K.J. BOWERS, *LANL* S. DORFMAN, H. JI, M. YAMADA, *PPPL* H. KARIMABADI, *UCSD* Considerable progress has been made in understanding of quasi-stationary reconnection in 2D systems. In contrast, 3D reconnection and, in particular, the role of current-aligned instabilities is less understood. This work investigates the effects of these instabilities on reconnection using fully kinetic simulations with a Monte-Carlo model for Coulomb collisions and boundary conditions mimicking Magnetic Reconnection Experiment (MRX) [1]. The motivation comes from a) experimental observations of both electrostatic and electromagnetic fluctuations in the current sheet made in MRX [2,3] and b) our previous 2D simulations demonstrating a discrepancy in the thickness of the current sheet between both collisionless [1] and weakly collisional simulations and the experimental observations. We describe 3D simulations performed at MRX-relevant levels of collisionality that demonstrate the existence of both short-wavelength Lower-Hybrid Drift Instability with $k\rho_e \sim 1$ localized at the edge of the current layer and long-wavelength electromagnetic modes localized at the center. The role of these instabilities in global reconnection dynamics is discussed. [1] S. Dorfman, et al., Phys. of Plasmas **15**, 102107 [2] T. Carter, et al., Phys. Plasmas, **9**, 3272 [3] H. Ji, et al., Phys. Rev. Letters **92**, 115001

TP8 116 Fast Reconnection in High-Lundquist-Number Plasmas Due to Secondary Tearing Instabilities YI-MIN HUANG, AMITAVA BHATTACHARJEE, *Center for Integrated Computation and Analysis of Reconnection and Turbulence, University of New Hampshire* HONGANG YANG, BARRETT ROGERS, *Center for Integrated Computation and Analysis of Reconnection and Turbulence, Dartmouth College* Thin current sheets in systems of large size that exceed a critical value of the Lundquist number are unstable to a super-Alfvénic tearing instability. The scaling of the growth rate of the fastest growing instability with respect to the Lundquist number is shown to follow from the classical dispersion relation for tearing modes. As a result of this instability, the system realizes a nonlinear reconnection rate that appears to be weakly dependent on the Lundquist number, and larger than the Sweet-Parker rate by an order of magnitude (for the range of Lundquist numbers considered). This regime of fast reconnection appears to be realizable in a dynamic and highly unstable thin current sheet, without requiring the current sheet to be turbulent.

TP8 117 Two-dimensional Studies of Super-Alfvenic Instabilities of Thin Current Sheets L. NI, K. GERMASCHEWSKI, A. BHATTACHARJEE, YI-MIN HUANG, H. YANG, *Center for Integrated Computation and Analysis of Reconnection and Turbulence, University of New Hampshire* In large systems such as the solar corona or the magnetotail, extended thin current sheets are formed in situations involving free or forced reconnection. These current sheets are characterized by large values of the tearing instability parameter delta- prime, which is strongly destabilizing, and shear in the outflow velocity along the current sheet, which can be stabilizing. We have carried out a systematic analytical and computational study of this problem in resistive MHD, including the effect of finite plasma compression. When the shear in the outflow velocity is weak, we obtain an entire class of super-Alfvenic instabilities in the high-S regime, predicted by Lourerio et al., and generalized recently by Bhattacharjee et al. In the presence of strong velocity shear along the current sheet, the system tends to be more stable, and the wave number of the fastest growing instability itself evolves as a function of time. In the regime of small growth rates, it is possible to define a critical length below which the system is stable. The parametric dependence of this critical length is determined by analysis and simulations.

TP8 118 Current sheet extension and reconnection scaling in collisionless, hyperresistive, Hall MHD* B.P. SULLIVAN, A. BHATTACHARJEE, Y.M. HUANG, *Center for Integrated Computation and Analysis of Reconnection and Turbulence, UNH, Durham, NH* We present Sweet-Parker type scaling arguments in the context of collisionless, hyper-resistive, Hall magnetohyrdodynamics (MHD). The predicted steady state scalings are consistent with those found by Chacón et al. [PRL 99, 235001 (2007)], and Uzdensky, [PoP 16, 040702 (2009)], though our methods differ slightly. As with those studies, no prediction of electron dissipation region length is made. Numerical experiments confirm that both cusp like & extended geometries are realizable. Importantly, the length of the electron dissipation region (taken as a parameter by several recent studies) is found to depend on the level of hyperresistivity. Although hyper-resistivity can produce modestly extended dissipation regions, the dissipation regions observed here are much shorter than those seen in many kinetic studies. The thickness of the dissipation region scales in a similar way as the length,so that the reconnection rate is not strongly sensitive to the level of hyperresistivity. The length of the electron dissipation region depends on electron inertia as well.The limitations of scaling theories that do not predict the length of the electron dissipation region are emphasized.

*DOE Grant No.DE-FG02-07ER54832, & NSF Grant No. ATM0802727

TP8 119 Fast magnetic reconnection and particle acceleration in pair plasmas NAOKI BESSHO, A. BHATTACHARJEE, *Center for Integrated Computation and Analysis of Reconnection and Turbulence, University of New Hampshire* Magnetic reconnection without a guide field in both non-relativistic and relativistic regimes has been studied in pair plasmas by 2D PIC simulations. We have found that in both regimes, particle acceleration enhances reconnection rates by an interesting feedback effect. Reconnection rates in the impulsive phase become of the order of 1 when the background density in a Harris sheet equilibrium is of the order of 0.01 of the density in the current sheet. Fast reconnection becomes possible not only because of increase of the time derivative part of the inertial term in the generalized Ohm's law, but also by a positive feedback on the pressure tensor term, bootstrapped by particle acceleration that produces a reduction in the particle density in the diffusion region. In this impulsive phase, the extension of the diffusion region along the outflow region is accompanied by a broadening of the width of the current sheet in the inflow region, keeping the aspect ratio small and sustaining a large reconnection rate. The collisionless resistivity originating from non-ideal terms in the generalized Ohm's law becomes large and nearly spatially uniform along the diffusion region even after the extension of the diffusion region, and can account quantitatively for the fast reconnection rate. We will compare and contrast this with reconnection and particle acceleration in hydrogen plasmas.

TP8 120 Plasmoid generation in resistive-MHD reconnection RAVI SAMTANEY,* *PPPL* NUNO LOUREIRO, *IPFN, IST Lisbon* DMITRI UZDENSKY,† *Princeton University/CMSO* ALEXANDER SCHEKOCHIHIN, *R.Peierls Centre for Theoretical Physics, University of Oxford* STEPHEN COWLEY, *EURATOM/UKAEA Culham Science Centre* A detailed numerical study of resistive-MHD magnetic reconnection for very large, previously inaccessible, Lundquist numbers ($10^4 \leqslant S \leqslant 10^8$) is reported. Large-aspect-ratio Sweet-Parker current sheets are shown to be unstable to super-Alfvénically fast formation of plasmoid (magnetic-island) chains. The plasmoid number scales as $S^{3/8}$ and the linear growth rate of the instability as $S^{1/4}$, in agreement with the theory by Loureiro et al. [Phys. Plasmas **14**, 100703 (2007)]. In the nonlinear regime, plasmoids continue to grow faster than they are ejected and completely disrupt the reconnection layer. These results suggest that high-Lundquist-number reconnection is inherently time-dependent and thus call for a substantial revision of the standard Sweet-Parker quasi-stationary picture for $S > 10^4$.

*supported by DoE
†supported by NSF

TP8 121 Analytical model for fast reconnection in large guide field plasma configurations A.N. SIMAKOV, *Los Alamos National Laboratory* L. CHACÓN, *Oak Ridge National Laboratory* D. GRASSO, *CNR-INFM, Italy* D. BORGOGNO, *Politecnico di Torino, Italy* A. ZOCCO, *Culham Science Centre, UK* Significant progress in understanding magnetic reconnection *without a guide field* was made recently by deriving quantitatively accurate analytical models for reconnection in electron [1] and Hall [2] MHD. However, no such analytical model is available for reconnection *with a guide field*. Here, we derive such an analytical model for the large-guide-field, low-β, cold-ion fluid model [3] with electron inertia, ion viscosity μ, and resistivity η. We find that the reconnection is Sweet-Parker-like when the Sweet-Parker layer thickness $\delta_{SP} > (\rho_s^4 + d_e^4)^{1/4}$, with ρ_s and d_e the sound Larmor radius and electron inertial length. However, reconnection changes character otherwise, resulting in reconnection rates $E_z/B_x^2 \approx \sqrt{2\eta/\mu}(\rho_s^2 + d_e^2)/(\rho_s w)$ with B_x the upstream magnetic field and w the diffusion region length. Unlike the zero-guide-field case, μ plays crucial role in manifesting fast reconnection rates. If it represents the perpendicular viscosity [3], $\sqrt{\eta/\mu} \sim \beta^{-1}\sqrt{(m_e/m_i)(T_i/T_e)}$ and E_z becomes dissipation independent and therefore potentially fast. [1] L. Chacón, A. N. Simakov, and A. Zocco, *PRL* **99**, 235001 (2007). [2] A. N. Simakov and L. Chacón, *PRL* **101**, 105003 (2008). [3] D. Biskamp, *Magnetic reconnection in plasmas*, Cambridge University Press, 2000.

TP8 122 Influence of Current Aligned Instabilities on Magnetic Reconnection in Neutral Sheet Geometry W. DAUGHTON, V. ROYTERSHTEYN, L. YIN, B.J. ALBRIGHT, K.J. BOWERS, *LANL* H. KARIMABADI, *UCSD* The influence of current aligned instabilities on collisionless reconnection is studied within neutral sheet geometry using petascale 3D kinetic simulations, which permit ion to electron mass ratios in the range $m_i/m_e = 200 - 400$. Open boundary conditions are employed to avoid artificial recirculation effects and better mimic large-scale systems in nature. During the onset and initial evolution, intense lower-hybrid drift activity is observed immediately upstream of the electron diffusion region and along the separatrices, with characteristic wavelength on the electron gyroscale $k_y\rho_e \sim 1$. These fluctuations do not penetrate into the central electron layer, and are gradually weakened as the upstream density gradients relax and a highly elongated electron-scale current layer is formed. At later times, an electromagnetic instability is observed within the elongated electron layer with wavelength $k_y(\rho_i\rho_e)^{1/2} \sim 1$ roughly consistent with previous predictions from Vlasov theory[1]. This instability gives rise to a pronounced kinking or undulation of the electron layer in a manner qualitatively similar to large-scale electron-positron plasmas[2]. The possible influence of these instabilities on the dissipation rate and energy partition is discussed.

[1]Daughton, Phys. Plasmas, **10**, 3103, 2003
[2]Yin et al, PRL **101**, 125001, 2008

TP8 123 Bi-directional Beams by Electron Trapping during Anti-parallel Reconnection* JAN EGEDAL, A. LE, N. KATZ, *MIT, PSFC* L.-J. CHEN, B. LEFEBVRE, *UNH* W. DAUGHTON, *LANL* So-called bi-directional electron beams have been observed by a number of spacecraft missions in the inflow regions of anti-parallel reconnection. Here we analyze electron distribution functions measured by the four Cluster spacecraft and we show that the beam features can be accounted for by electron trapping mainly by parallel electric fields. In turn, the parallel electric fields can be described by a parallel acceleration potential $\Phi_\parallel$ (defined in Ref [1]). In the analysis we determine the profiles of $\Phi_\parallel$ along the paths of the Cluster spacecraft during their encounter with a reconnection region. $\Phi_\parallel$ is typically in excess of 1kV and therefore all thermal electrons are trapped. This is important for the internal structure of the Hall current system because extended trapping significantly alters the pressure tensor of the electron fluid [2]. [1] J. Egedal, W. Daughton, J. Drake, N. Katz, and A. Le, *Physics of Plasmas*, **16**, 050701 (2009). [2] A. Le, J. Egedal, W. Daughton, W. Fox, and N. Katz, *Phys. Rev. Lett.*, **102**, 085001 (2009).

*Supported by: DOE Junior Faculty Award DE-F602-06ER54878 and NSF/DOE Award PHY-0613734.

TP8 124 Observation of electron holes and lower-hybrid turbulence during magnetic reconnection experiments on VTF* W. FOX, M. PORKOLAB, J. EGEDAL, N. KATZ, A. LE, *MIT PSFC* We report a detailed study of electrostatic turbulence observed during magnetic reconnection experiments on the Versatile Toroidal Facility (VTF) [1], including identification of modes, exploration of instability mechanisms, and studies of correlation with the reconnection events and electron energization. Electrostatic fluctuations are observed by arrays of small, high-bandwidth, impedance-matched Langmuir probes. Broadband fluctuations are found, including lower-hybrid (LH) waves and higher-frequency Trivelpiece-Gould (TG) waves. Strong nonlinear turbulence, consisting of large-amplitude, positive-potential spikes identified as electron phase-space holes, is also observed [2]. We believe that the LH modes are driven unstable by steep electron temperature gradients, while TG and electron holes arise from bump-on-tail instability of high energy electrons. In both cases, it is believed that the modes arise as a consequence of electron energization by the reconnection events. [1] J. Egedal, *et al.*, *PRL* **98**, 015003 (2007). [2] W. Fox, *et al.*, *PRL* **101**, 255003 (2008).

*Support by Center for Multiscale Plasma Dynamics (Award DE-FC02-04ER54786) and DOE Junior Faculty Award DE-FG02-06ER54878.

TP8 125 Rogowski Coil Array for Collisionless Magnetic Reconnection Experiments at VTF* A. LE, J. EGEDAL, W. FOX, N. KATZ, A. VRUBLEVSKIS, M. PORKOLAB, *MIT, PSFC* Recent experiments on magnetic reconnection at the Versatile Toroidal Facility (VTF) indicate that the electron current may become filamented during spontaneous reconnection events [1]. A new array of Rogowski coils, which has centimeter-scale resolution, will measure the parallel currents driven by fast reconnection in the presence of a guide magnetic field. The diagnostic should confirm the filamentary structure of the current profile, determine the distribution of filaments around the X-line, and reveal when the filaments are generated with respect to the onset of reconnection. In addition, multi-shot scans performed by moving the Rogowski coil array across a poloidal section and to several different toroidal angles will yield high-resolution measurements of the reproducible features of the current profile that develops during three-dimensional reconnection at VTF. Preliminary data will be presented if available. [1] J. Egedal et al., Phys. Rev. Lett., **98**, 015003 (2007)

*Supported by DOE Junior Faculty Award DE-F602-06ER54878 and NSF/DOE Award.

TP8 126 Washer-Gun Plasma Source for Magnetic Reconnection Experiments on VTF* A. VRUBLEVSKIS, J. EGEDAL, W. FOX, N. KATZ, A. LE, M. PORKOLAB, *MIT, PSFC* We present a recently built electrostatic washer-gun plasma source for the Versatile Toroidal Facility (VTF). The source produces plasmas with estimated densities of $\sim 10^{19}$ m^{-3} and electron temperatures of $\sim 5 - 20$ eV. The present plasma source for VTF is microwave-induced electron cyclotron resonant breakdown and requires a strong toroidal magnetic field, which acts as a guide field in reconnection experiments. The gun will allow reconnection experiments with no guide field. The source is based on the design developed by Sterling Scientific [1, 2]. To operate, gas is injected into a channel formed by a stack of alternating molybdenum and boron nitride washers with a molybdenum electrode washer at each end. A capacitor bank is discharged through these electrodes and the gas. The resulting plasma escapes the channel into the main chamber of the experiment. If available, we will present data on argon plasma produced by the gun inside the VTF. [1] G. Fiksel, et al., Plasma Sources Sci. Technol., **5**, 78 (1996) [2] D. Hartog et al., Plasma Sources Sci. Technol., **6**, 492 (1997)

*Supported by DOE Junior Faculty Award DE-F602-06ER54878 and NSF/DOE Award PHY-0613734.

TP8 127 Reconnection properties in Hall MHD Plasmas* ZHIWEI MA, XING-QIANG LU, YA-WEI HOU, *Zhejiang University* Dynamics and properties of magnetic reconnection with an asymmetry initial condition are studied by using Hall MHD simulation. In the early phase of the magnetic reconnection, the geometry of the magnetic field in the near reconnection region tends to form a Y-type structure under an asymmetry initial condition instead of to exhibit an X-type structure in the symmetry initial condition. The growth rate of the current density in the early stage is proportional to the square of the ion inertial length. In the late phase, the thin elongated current sheet associated with the Y-type geometry of the magnetic field breaks-up to form a magnetic island due to the secondary tearing instability. It is found that the onset time of the secondary tearing instability is inversely dependent on the square root of the ion inertia length. The generated Hall electric field and net charge are larger in the region inside than outside the magnetic island. The strengths of the Hall electric field and net charge density linearly increase with the increase of the ion inertia length.

*Supported by National Science Foundation of China under Grant No. 40536030, and the National Basic Research Program of China under Grant No 2008CB717806.

TP8 128 Suppression of Double-Tearing Modes by Poloidal Shear Flows* XIAOGANG WANG, *Peking University* WENBIN XU, ZHENGXIONG WANG, YUE LIU, *Dalian University of Technology* Suppression effects of shear flows on double tearing modes are investigated in a reduced resistive magnetohydrodynamics model. It is found that as poloidal flow shear increased, the growth of the magnetic island generated by the double tearing mode can be greatly suppressed.

*This work is supported by NSFC and MOST.

TP8 129 The origin of the abrupt nonlinear growth in Double Tearing Mode MIHO JANVIER, YASUAKI KISHIMOTO, JIQUAN LI, *Graduate School of Energy Science, Kyoto University* Reversed shear configuration represents an effective way to achieve a better confinement of the plasma inside tokamaks via the formation of Internal Transport Barriers (ITB). However, this configuration leads to MHD instabilities such as the Double Tearing Mode, where the dynamics are enhanced due to the presence of two rational surfaces. Kink type or tearing type evolutions of the DTM have been investigated and recently, an evolution in three regimes (linear, slowdown and fast growth) has attracted much attention [1][2]. However, there is still no clear explanation on the triggering mechanism leading to the nonlinear growth of the DTM and fast reconnection. Here, we investigate the physical process that leads to the fast growth regime and we try to understand the trigger mechanism as a result of secondary instability evolving at different time scales. We perform numerical simulations for the DTM in slab geometry by solving the 2-field reduced MHD equations and investigate the stability of the developed magnetic island with flow in the slowdown regime as a quasi-steady equilibrium with slow time scale. The high order magnetic structure is therefore found to play an important role in triggering the abrupt growth of the DTM flows. [1] Y.Ishii, *et al,* Phys. Rev. Lett., Vol.89,**20** (2002) [2] Z.X.Wang, *et al,* Phys. Plasmas, **15** 082109 (2008)

TP8 130 Turbulence driven magnetic reconnections causing magnetic islands with long wavelengths AKIHIRO ISHIZAWA, NORIYOSHI NAKAJIMA, Numerical simulations of reduced two-fluid equations show that micro-turbulence produces magnetic reconnection and magnetic islands with long wavelengths even if the equilibrium is stable against tearing modes. Thus, the turbulence modifies the threshold of magnetic island formation against stability parameter of tearing mode. The length of magnetic islands is the same order as the system size and the width is several times of ion Larmor radius. This suggests that micro-turbulence can cause seed magnetic islands of neoclassical tearing modes which are nonlinear instability and are considered to give the main limitation to plasma pressure in magnetically confined plasmas.

TP8 131 Ion heating during magnetic reconnection with a guide field: a threshold for pickup behavior J.F. DRAKE, *University of Maryland* P.A. CASSAK, *West Virginia University* M.A. SHAY, *University of Delaware* M. SWISDAK, *University of Maryland* E. QUATAERT, *U. C. Berkeley* The acceleration of ions during magnetic reconnetion with a guide field is explored with simulations and analytic analysis. Ions crossing into Alfvénic reconnection outflows can behave like pickup particles and gain an effective thermal velocity equal to the Alfvén speed. However, with a sufficiently strong ambient out-of-plane magnetic field, which is the relevant configuration for most laboratory experiments and astrophysical systems, the ions can become adiabatic and their heating is then dramatically reduced. The threshold for non-adiabatic behavior, where ions are strongly heated, becomes a condition on the ion mass-to-charge-ratio, $m_i/m_pZ_i > 10\sqrt{\beta_{0x}/2}/\pi$, where m_i and Z_i are the ion mass and charge state, m_p is the proton mass and $\beta_{0x} = 8\pi nT/B_{0x}^2$ is the ratio of the plasma pressure to that of the reconnecting magnetic field B_{0x}. Thus, during reconnection high mass-to-charge particles gain energy more easily than protons. A simple model reveals that in the case of flares the abundances of high mass-to-charge ions are enhanced, which is consistent with observations. Implications for understanding ion heating during sawtooth events in the MST reversed field pinch are also discussed.

TP8 132 Lower Hybrid Instability and Coherent Formation of Electron Holes HAIHONG CHE, JAMES DRAKE, *University of maryland* MARC SWISDAK, PETER H. YOON, *University of Maryland* Using particle-in-cell simulations and kinetic theory, we discover that lower hybrid instability can form not only oblique localized structures but also much stronger and more stable bipolar structures parallel to magnetic field. This is a direct result of nonlinear coupling between waves and particles which allows the perpendicular phase speed of lower hybrid waves to be in pace with the undergoing cross-field $\mathbf{E} \times \mathbf{B}$ drift of its trapped electrons. The coherent increasing of phase and group velocity strengthen the stability of the electron holes. The increasing phase speed of lower hybrid waves transfer the momentum from high velocity electrons to ions.

TP8 133 Effects of Plasma Beta on Multiple Island Ion Acceleration KEVIN SCHOEFFLER, JAMES DRAKE, MARC SWISDAK, *University of Maryland* Magnetic reconnection has been found to be associated with energetic ions and electrons. Gamma ray emission from the solar photosphere, and energetic particles found by Wind in the magnetosphere confirm this association. One explanation for the acceleration of these particles is by 1st order Fermi acceleration of particles bouncing in contracting magnetic islands. The contracting islands heat up particles in the direction of the magnetic fields, causing a temperature anisotropy with $T_\parallel > T_\perp$. When the anisotropy reaches the marginal fire hose condition, this mechanism should end. Larger initial values of β might cause the fire hose condition to be reached more quickly. Using a particle-in-cell code, we investigate the effects of β by simulating island growth with initial equilibria with multiple Harris current sheets.

TP8 134 Kinetic effects in gyrokinetic tearing instability* RYUSUKE NUMATA, WILLIAM DORLAND, *University of Maryland* NUNO LOUREIRO, *Technical University of Lisbon* BARRETT ROGERS, *Dartmouth College* ALEXANDER SCHEKOCHIHIN, *University of Oxford* TOMOYA TATSUNO, *University of Maryland* We present numerical results of tearing instability simulations in a strong guide magnetic field limit using the ttAstroGK astrophysical gyrokinetics code. The tearing growth rates from the gyrokinetic simulations show quantitative discrepancy with those of the fluid model based on the compressible two-fluid MHD model [1], which may be ascribed to the treatment of pressure. In the kinetic model, the pressure tensor cannot be described one single relation to the density. Moreover, the behavior of the pressure can be very different in the inner current layer and the outer ideal MHD region. In this presentation, we show results of pressure tensor diagnostics, and discuss the effect of the pressure tensor on the linear tearing instability. Preliminary results from nonlinear simulations will also be presented. [1] E. Ahedo and J.J. Ramos, Plasma Phys. Control. Fusion 51, 055018 (2009).

*This work is supported by the DOE Center for Multiscale Plasma Dynamics, and the Leverhulme Trust Network for Magnetized Turbulence in Astrophysical and Fusion Plasmas.

TP8 135 Progress in kinetic MHD simulation of magnetic reconnection in Harris sheet equilibrium JIANHUA CHENG, YANG CHEN, SCOTT PARKER, *University of Colorado* We have developed a Lorentz force ion, fluid electron kinetic MHD hybrid model [D. Barnes, *et al*, Phys. Plasmas **15**, 055702 (2008)]. Here we focus on the implementation of an isothermal fluid electron model in the GEM turbulence code. A second-order accurate implicit scheme that generalizes the previous implicit scheme for Vlasov ions and drift kinetic electrons [Yang Chen and Scott E. Parker, Phys. Plasmas **16**, 052305 (2009)] has been implemented. The generalized Ohm's law is solved for the Harris sheet equilibrium configuration by Fourier decomposing the electric field along the equilibrium field and solving for each Fourier component in the direction perpendicular to the current sheet using direct matrix inversion. This presentation focuses on the linear instabilities for Harris sheet equilibrium. We will also provide some preliminary reconnection results and their direct comparison with MHD simulations.

TP8 136 3D Ion Temperature Reconstruction HIROSHI TANABE, SETTHIVOINE YOU, ALEXANDER BALANDIN, MICHIAKI INOMOTO, YASUSHI ONO, *University of Tokyo* The TS-4 experiment at the University of Tokyo collides two spheromaks to form a single high-beta compact toroid. Magnetic reconnection during the merging process heats and accelerates the plasma in toroidal and poloidal directions. The reconnection region has a complex 3D topology determined by the pitch of the spheromak magnetic fields at the merging plane. A pair of multi-chord passive spectroscopic diagnostics have been established to measure the ion temperature and velocity in the reconnection volume. One setup measures spectral lines across a poloidal plane, retrieving velocity and temperature from Abel inversion. The other, novel setup records spectral lines across another section of the plasma and reconstructs velocity and temperature from 3D vector and 2D scalar tomography techniques. The magnetic field linking both measurement planes is determined from in situ magnetic probe arrays. The ion temperature is then estimated within

the volume between the two measurement planes and at the reconnection region. The measurement is followed over several repeatable discharges to follow the heating and acceleration process during the merging reconnection.

TP8 137 Local and Global Transient Effect of Magnetic Reconnection* YOSHINORI HAYASHI, TORU II, MICHIAKI INOMOTO, YASUSHI ONO, *University of Tokyo* Transient effect of magnetic reconnection has been investigated in the TS-4 torus plasma merging device. We found axial mergings of two and three loops, which were caused by local and global effect, respectively. The two loop merging with pull reconnection converts one common flux to two private fluxes. Under strongly driven inflow, the plasma and magnetic flux inflow exceeded the outflow ones, causing flux and density piled-up in the current sheet. This pile-up effect was found to increase the inflow speed without anomalous resistivity effect. Under strong guiding field, a plasmoid grew in the current sheet during plasma pile-up. When flux pile-up reached critical value, a plasmoid was ejected from reconnection region and reconnection speed transiently increased. The plasmoid ejection made the reconnection rate maximum when its acceleration was maximized. In the case of three loop merging, two parallel loops stays for a while in a stable state because of another anti-parallel loop. When global magnetic configuration change, two loop reconnected into one loop impulsively forming another equilibrium state. We fond both of these local and global effect cause fast but unsteady magnetic reconnection.

*Supported by Japan Society for Promotion of Science.

TP8 138 Experimental Study of Three-Dimensional Localized Magnetic Reconnection by Use of Merging Torus Plasmas TORU II, YOSHINORI HAYASHI, MICHIAKI INOMOTO, YASUSHI ONO, *University of Tokyo* Three-dimensional (3-D) localized magnetic reconnection was studied experimentally in the University of Tokyo Spherical Torus (TS-4) plasma merging device using controlled external compression force and guide field. We found two unsteady effects: 3-D deformation and ejection of current sheet cause fast magnetic reconnection. When strong compression force $I_{\mathrm{Acc}} \sim 60$ kA compressed two compact toroids with low guide field $B_t \sim B_{\parallel}$ ($B_{\parallel}$ is reconnecting field component), toroidal modes $n = 1-3$ of current sheet was observed to grow only during their reconnection. A new finding is that 3-D deformation of current sheet promotes mass ejection from current sheet and causes the reconnection rate as well as the reconnection outflow to increase. When weak compression force $I_{\mathrm{Acc}} \sim 0$ kA compressed two compact toroids with high guide field $B_t \sim 7B_{\parallel}$, their reconnection rate was maintained small. These phenomena indicate that 3-D localized reconnection is one of fast reconnection mechanisms.

TP8 139 Pulsed High-Power Heating of Magnetic Reconnection for Spherical Torus Plasmas YASUSHI ONO, *University of Tokyo* MICHIAKI INOMOTO, TAKUMA YAMADA, TS AND UTST TEAM, The merging/ reconnection heating of spherical torus plasmas (ST, Spheromak, RFP, FRC) has been developed in the TS-3 TS-4 and UTST experiments, leading us to its new extension to their pulsed high-power heating. Two spherical torus plasmas were produced inductively by two or four PF coil currents without using any center solenoid (CS) and they were merged together for high-power reconnection heating. The reconnection outflow speed was observed to be equal to the Alfven speed under no guiding field condition. The outflow energy is converted mostly into ion thermal energy through ion viscosity and/or fast shock. This fact indicates that the ion temperature increment (and thermal energy) scales with squares of reconnecting magnetic field (Alfven speed). This unique method enables us to utilize the highest heating power MW-GW among all CS-less startups and the heating time much shorter than the energy confinement time and the electron-ion collision time. These facts indicate that the merging of two spherical torus plasmas possibly provides a direct path to the burning plasma formation. The TS-3 and TS-4 scaling data suggest that two merging spherical torus with B=1-3T, $n=10^{20}\mathrm{m}^{-3}$ will increase its ion temperature into the ITER regime plasma of $T \approx 20\mathrm{keV}$

TP8 140 Simulated and experimental compression of a compact toroid* JEFFREY JOHNSON, *UC Davis* We present simulation results and experimental data for the compression of a compact toroid by a conducting nozzle without a center electrode. In both simulation and experiment, the plasma flow is obstructed by even modest magnetic fields. A simple mechanism for this obstruction is suggested by our simulations. The configuration of the plasmoid's magnetic field plays a significant role in its compression. We analyze two types of plasma configurations under compression and demonstrate that the results from the simulations match those from the experiments, and that the mechanism predicts the different behaviors observed in the two cases.

*J.J. is supported by the Lawrence Scholar Program at LLNL.

TP8 141 Mass dependent ion heating in the SSX reconnection device* M. BROWN, T. GRAY, J. SANTNER, M. KOREIN, D. WEINHOLD, *Swarthmore College* Ion heating due to magnetic reconnection is measured in the SSX plasma merging device for a variety of ion masses and charge states with a high resolution ion Doppler spectrometer. The SSX IDS instrument measures the width and Doppler shift of the nascent C_{III} impurity $229.7nm$ line, a doped He_{II} impurity $468.6nm$ line, or a doped Ar_{II} impurity line to determine the temperature and line-averaged flow velocity. The velocity resolution of the instrument is $\leq 5km/s$. There is enough signal to resolve the full line within an MHD dynamical time (about $1\mu s$ in SSX). Peak ion temperatures of $80eV$ have been recorded during reconnection events as well as flows up to $40km/s$. Spheromak merging in a new slightly prolate flux conserver ($R = 0.2m, L = 0.4m$) often results in excitation of several unstable MHD modes. After reconnection and instability, we measure a period of reconnection driven ion heating with peak temperatures for carbon $T_C \cong 50eV$ and for helium $T_{He} \cong 70eV$ (averaged over many shots). During the decay phase, we observe rapid ion cooling likely due to energetic ion loss. Results from a new ion energy analyzer and Mach probe will be presented.

*Work supported by DOE and NSF.

TP8 142 MAGNETO-INERTIAL-FUSION

TP8 143 Field Reversed Configuration (FRC) formation and compression using liners J.H. DEGNAN, P. ADAMSON, D.J. AMDAHL, R. DELANEY, M. DOMONKOS, F.M. LEHR, E.L. RUDEN, W. TUCKER, W. WHITE, *Air Force Research Laboratory, Directed Energy Directorate, Kirtland AFB, NM 87117, USA* C. GRABOWSKI, D. GALE, M. KOSTORA, J. PARKER, W. SOMMARS, *SAIC, Albuquerque, NM USA* M.H. FRESE, S.D. FRESE, J.F. CAMACHO, S.K. COFFEY, V. MAKHIN, *NumerEx LLC, Albuquerque, NM USA* T.F. INTRATOR, G.A. WURDEN, P.J. TURCHI, *Los Alamos National Laboratory, Los Alamos, NM USA* R.E. SIEMON, *University of Nevada Reno, Reno, NV USA* A.G. LYNN, N.F. RODERICK, *University of New Mexico, Albuquerque, NM USA* FRC capture, field and compression experiments all use 2 T guide and mirror fields established inside the liner. A 12 MA, 4.5 MJ discharge drive the liner implosion. The capture experiments use 3 capacitor discharges into a segmented theta coil surrounding the formation region to form a bias field, pre-ionize the deuterium gas, and provide the reverse field theta discharge which forms the FRC. Two cusp field discharges aid this. The guide and mirror fields enable translation and capture of the FRC. Diagnostics include field exclusion, interferometry, radiography, and radiation detection. Design and parameters are guided by MHD simulations. Supported by DOE-OFES.

TP8 144 Progress on Field Reversed Configuration target for Magnetized Target Fusion* T. INTRATOR, *Los Alamos Natl Lab* G.A. WURDEN, P.E. SIECK, W.J. WAGANAAR, R. OBERTO, T.D. OLSON, D. SUTHERLAND, J.H. DEGNAN, *AFRL-Kirtland* E.L. RUDEN, M. DOMONKOS, P. ADAMSON, C. GRABOWSKI, *SAIC-Albuquerque* D.G. GALE, W. SOMMARS, M. KOSTORA, M.H. FRESE, *NumerEx* S.D. FRESE, J.F. CAMACHO, S.K. COFFEY, N.F. RODERICK, D.J. AMDAHL, P. PARKS, *General Atomics* R.E. SIEMON, *University of Nevada, Reno* T. AWE, A.G. LYNN, *University of New Mexico, Albuquerque* We overview the experimental high density Field Reversed Configuration (FRC) approach for a LANL AFRL collaborative physics demonstration of Magnetized Target Fusion (MTF). We show some initial translation data from the Los Alamos FRC experiment FRXL that characterize the MTF translated target plasma. The conical theta coil is expected to generate toroidal magnetic field, helicity, and good curvature field lines, and should increase stability and lifetime. The suitability of the present FRXL data for MTF implosion at AFRL Kirtland will be discussed, along with the hardware, diagnostics, and pre-compression plasma formation and trapping experiments.

*Supported by DOE, OFES, DE-AC52-06NA25396.

TP8 145 Translation and Capture of High-Density Field Reversed Configurations for Magnetized Target Fusion P.E. SIECK, T.P. INTRATOR, G.A. WURDEN, W.J. WAGANAAR, *Los Alamos National Laboratory* R.J. CORTEZ, *University of Alabama, Huntsville* R.J. OBERTO, *University of Washington* A physics demonstration of Magnetized Target Fusion (MTF) is being pursued by a collaborative team from Los Alamos National Laboratory and Air Force Research Laboratory. The LANL facility, known as the Field Reversed eXperiment — Liner (FRX-L), focuses on the physics of producing high-density Field Reversed Configurations (FRCs), translating them, and capturing them in a static flux conserver. Observations of FRCs in translation and capture will be presented. The data suggest FRCs are formed at density above $10^{22}/m^3$, translate over the one meter chamber at 97 km/s, and a captured portion having radius 4 cm lives for $10\mu s$. The repeatability of FRC capture will be discussed in context of that necessary for MTF. This work is supported by the Office of Fusion Energy Sciences, and DOE/LANL contract DE-AC52-06NA25396.

TP8 146 Proposed profile measurements of internal B, ne and Te on the Magnetized Target Fusion (MTF) plasmas using Pulsed Polarimetry R.J. SMITH, *University of Washington* G.A. WURDEN, *LANL* The novel pulsed polarimetry technique combines both the Faraday effect and Thomson scattering into a comprehensive Lidar-like diagnostic that measures the sightline parameters, B(s), ne(s) and Te(s) remotely and non-perturbatively. The target FRC: FRX-L at LANL (development of formation and translation hardware and scenario for MTF) and FRCHX at AFRL, Kirtland AFB (formation + translation + liner implosion) have sufficiently large optical activity to allow polarimetric measurements in the near infrared. The proposed diagnostic is based on an ultra-short pulsed NdYag laser with streak camera detection. Magnetic field spatial resolutions of several *cms* are possible on FRX-L and sub-cm on FRCHX. The pulsed polarimeter system and the relevance of the internal measurements to the MTF program will be described.

TP8 147 Visibility Measurements on a Fiber-Optic Probe Interferometer System* J.F. CAMACHO, *NumerEx, LLC* A.G. LYNN, *University of New Mexico* E.L. RUDEN, *Air Force Research Laboratory, Directed Energy Directorate* A HeNe laser interferometer operating at 632.8 nm with several single-mode optical fiber probe beams has been assembled to measure the electron density of a field-reversed configuration for a magnetized target fusion experiment. Our system features probe beams whose path lengths are many times longer than the reference beam paths. We have generalized the condition for maximum interference visibility to the case of a heterodyned interferometer in which portions of the probe and reference beams propagate through different lengths of single-mode fiber. This analytic development also takes into account the effect of the line width of the individual modes of our multimode laser on mode coherence, which imposes an upper bound on the fiber length for which a good interference signal can be obtained. When this maximum fiber length is exceeded, an interference signal can still be observed, but the signal is amplitude modulated at frequencies much lower than the 80-MHz carrier signal. This modulation is likely due to "mode pulling" that occurs because of fluctuations in laser cavity length arising from acoustic modes of the laser tube. Visibility measurements establishing the viability of our design will be presented.

*Work supported by the DOE Office of Fusion Energy Sciences.

TP8 148 Time resolved visible spectroscopy of surface plasma radiation* TASHA GOODRICH, THOMAS AWE, STEPHAN FUELLING, RICHARD SIEMON, *University of Nevada, Reno* Experiments at UNR demonstrate that interesting multiply ionized aluminum plasma (T=1-30 eV, n $\sim$ 10^{18} cm^{-3}, Z $\sim$ 3) can be created on the surface of mm-diameter aluminum rods by MA pulses of current. Surface temperature has been estimated by mea-

suring the surface brightness in the green part of the visible spectrum (Awe et al., this conference). To investigate the spectral distribution throughout the visible region, which should vary as one over wavelength to the fourth power for temperatures above about 2 eV, a Jobin-Yvon f/2 spectrometer has been coupled with a linear array of silicon photodiodes. This instrument has spectral resolution of 30 nm on each of ten array elements covering the spectrum between 400 – 700 nm and uses a Nikon lens/fiber optic collection system to enable observation of temperatures ranging from 1-30 eV. Experimental data with comparisons to the blackbody spectrum will be presented.

*Supported by DOE contract DE-FG02-04ER54752.

TP8 149 Overview of the Plasma Liner Experiment (PLX) S.C. HSU, *LANL* F.D. WITHERSPOON, *HyperV Tech.* M.A. GILMORE, *UNM* J.T. CASSIBRY, *UAH* THE PLX TEAM, The Plasma Liner Experiment (PLX), to be built at LANL, will explore and demonstrate the feasibility of forming imploding spherical "plasma liners" that can reach peak pressures ~ 0.1 Mbar upon stagnation. The liners will be formed via merging of 30 dense, high Mach number plasma jets ($n \sim 10^{17}$ cm^{-3}, $M \sim 10$–35, $v \sim 50$–70 km/s, $r_{jet} \sim 5$ cm) in spherically convergent geometry. This is a staged, exploratory project where scientific issues will be studied first at modest stored energies (~ 300 kJ) before attempting to reach HED-relevant pressures (requiring ~ 1.5 MJ)@. We have arrived at these numbers via extensive 3D hydrodynamic simulations. The primary scientific goals are to identify/resolve physics issues and to develop a predictive understanding of plasma liner formation, liner ram pressure amplification during liner convergence, conversion of liner kinetic energy to thermal/radiation energy of the stagnated system, and confinement time of this energy. We are aiming for two scaled-up follow-on applications for this work if it is successful: (1) assembling repetitive, macroscopic (cm and μs scale) plasmas suitable for fundamental HEDP studies and (2) a standoff driver solution for magneto-inertial fusion. This poster provides an overview of the project and the research plan. Supported by the DOE Joint Program in HEDLP.

TP8 150 Plasma Guns for the Plasma Liner Experiment (PLX)* F.D. WITHERSPOON, R. BOMGARDNER, A. CASE, S.J. MESSER, S. BROCKINGTON, L. WU, R. ELTON, *HyperV Technologies Corp.* S.C. HSU, *LANL* J.T. CASSIBRY, *UAH* M.A. GILMORE, *UNM* THE PLX TEAM, A spherical array of minirailgun plasma accelerators is planned for the Plasma Liner Experiment (PLX) to be located at LANL. The plasma liner would be formed via merging of 30 dense, high Mach number plasma jets ($n \sim 10^{16-17}$ cm^{-3}, $M \sim 10$–35, $v \sim 50$–70 km/s, $r_{\rm jet} \sim 5$ cm) in a spherically convergent geometry. Small parallel-plate railguns are being developed for this purpose due to their reduced system complexity and cost, with each gun planned to operate at ~ 300 kA peak current, and launching up to ~ 8000 μg of high-Z plasma using a ~ 50 kJ pfn. We describe experimental development of the minirailguns and their current and projected performance. Fast operating repetitive gas valves have recently been added to allow injection of high density gases including helium, argon, and (eventually) xenon. We will present the latest test results with the high-Z gases, and discuss future plans for augmenting the rails, optimizing the nozzle configuration, preionizing the injected gas, and configuring the pulse forming networks with the capacitors available to the program.

*Supported by the U.S. DOE Joint Program in HEDLP.

TP8 151 Hydrodynamic Modeling of the Plasma Liner Experiment (PLX)* JASON CASSIBRY, *University of AL in Huntsville* SCOTT HSU, *Los Alamos National Laboratory* DOUG WITHERSPOON, *HyperV Technologies, Inc.* MARC GILMORE, *University of New Mexico* UNIVERSITY OF AL IN HUNTSVILLE TEAM, LOS ALAMOS NATIONAL LABORATORY TEAM, HYPERV TECHNOLOGIES TEAM, UNIVERSITY OF NEW MEXICO TEAM, Implosions of plasma liners in cylindrically or spherically convergent geometries can produce high pressures and temperatures with a confinement or dwell time of the order of the rarefaction timescale of the liner. The Plasma Liner Experiment (PLX), to be built at LANL, will explore and demonstrate the feasibility of forming imploding plasma liners with the spherical convergence of hypersonic plasma jets. Modeling will be performed using SPHC and MACH2. According to preliminary 3D SPHC results, high Z plasma liners imploding on vacuum with ~ 1.5MJ of initial stored energy will reach ~ 100kbar, which is a main objective of the experimental program. Among the objectives of the theoretical PLX effort are to assist in the diagnostic analysis of the PLX, identify possible deleterious effects due to instabilities or asymmetries, identify departures from ideal behavior due to thermal and radiative transport, and help determine scaling laws for possible follow-on applications of ~ 1 Mbar HEDP plasmas and magneto-inertial fusion. An overview of the plan to accomplish these objectives will be presented, and preliminary results will be summarized.

*This work is supported by the OFES-NNSA HEDLP Joint Program.

TP8 152 Diagnostics for the Plasma Liner Experiment (PLX) ELIZABETH MERRITT, MARK GILMORE, ALAN LYNN, *University of New Mexico* JASON CASSIBRY, *University of Alabama Huntsville* F. DOUGLAS WITHERSPOON, *HyperV Technologies* SCOTT HSU, *Los Alamos National Laboratory* PLX TEAM, High pressure imploding plasma liners are possible sources for assembling plasmas suitable for scientific studies of HEDP and a potential stand-off driver solution for magneto-inertial fusion (MIF). The Plasma Liner Experiment (PLX) will merge 30 dense, high Mach number plasma jets to study plasma liner formation and convergence dynamics. Measurements of the ion and electron densities, temperatures, and velocities will be crucial for characterizing the thermodynamic state of the liner from formation through stagnation. Hydrodynamic simulations predict widely varying density and temperature ranges in the liner over its evolution, from 10^{15} - 10^{19} cm^{-3} and a few to hundreds of eV. To examine the plasma over this wide range of parameters, we will employ laser interferometry, Schlieren imaging, visible imaging, visible and VUV spectroscopy, pressure probes, x-ray photodiodes and bolometry. Simulation results for the proposed interferometers and Schlieren imaging are presented as well as an overview of the entire diagnostic suite.

TP8 153 Optical Measurements of Dense Hypervelocity Plasmoids from Coaxial and Railgun Plasma Accelerators* ANDREW CASE, SARAH MESSER, RICHARD BOMGARDNER, SAMUEL BROCKINGTON, DOUGLAS WITHERSPOON, *HyperV Technologies Corporation* RAY ELTON, *University of Maryland* High velocity dense plasma jets are under continued experimental development for fusion applications including refueling, disruption mitigation, momentum injection/rotation drive, and magnetized target fusion. We present measurements taken on the plasmoids produced by a half-scale coaxial plasmoid accelerator, a full scale coaxial plasmoid accelerator, and a novel minirailgun accelerator. The data presented includes spectroscopic measurements of velocity and density, two point interferometric measurements of line integrated density and velocity, and fast framing camera imaging. Results from these measurements are in agreement with each other and with time of flight measurements taken using photodiodes, as well as total plasmoid momentum measurements taken using a ballistic pendulum technique. Plasma density is greater than 5×10^{15} cm^{-3}, and velocities range up to 100 km/s, with a small component in some cases exceeding 120 km/s.

*Work supported by the U.S. DOE Office of Fusion Energy Sciences

TP8 154 The HyperV Full-Scale Contoured-Gap Coaxial Plasma Railgun SAMUEL BROCKINGTON, ANDREW CASE, SARAH MESSER, RICHARD BOMGARDNER, RAYMOND ELTON, LINCHUN WU, F. DOUGLAS WITHERSPOON, *HyperV Technologies Corp.* HyperV has been developing pulsed plasma injected coaxial railguns with a contoured gap profile designed to mitigate the blowby instability. Previous work using half-scale guns has been successful in launching 150 μg plasmas at 90 km/s [1]. In order to meet the original goal of 200 μg at 200 km/s the full-scale coaxial plasma gun has been constructed, and initial testing is beginning. This new plasma gun consists of two machined aluminum electrodes and a UHMW polyethylene breech insulator. The gun is breech fed by 64 ablative polyethylene capillary discharge units identical to the half-scale gun units. Maximum accelerator energy storage has also been increased 50%. Refractory coatings may be necessary to allow full current ($\sim$ 800 kA) operation. The outer electrode includes 24 small diagnostic ports for optical and magnetic probe access to the plasma inside the gun to allow direct measurement of the plasma armature dynamics. Initial test data from the full-scale coax gun will be presented along with plans for future testing. Work supported by the U.S. DOE Office of Fusion Energy Sciences. [1] F. D. Witherspoon, A. Case, S. Messer, R. Bomgardner, M. Phillips, S. Brockington, R. Elton, "Contoured Gap Coaxial Plasma Gun with Injected Plasma Armature" Rev. Sci. Instr. submitted (2009)

TP8 155 One-Dimensional Burn Dynamics of Plasma-Jet Magneto-Inertial Fusion* JOHN SANTARIUS, *University of Wisconsin* This poster will discuss several issues related to using plasma jets to implode a Magneto-Inertial Fusion (MIF) liner onto a magnetized plasmoid and compress it to fusion-relevant temperatures [1]. The problem of pure plasma jet convergence and compression without a target present will be investigated. Cases with a target present will explore how well the liner's inertia provides transient plasma stability and confinement. The investigation uses UW's 1-D Lagrangian radiation-hydrodynamics code, BUCKY, which solves single-fluid equations of motion with ion-electron interactions, PdV work, table-lookup equations of state, fast-ion energy deposition, and pressure contributions from all species. Extensions to the code include magnetic field evolution as the plasmoid compresses plus dependence of the thermal conductivity and fusion product energy deposition on the magnetic field. [1] Y.C. F. Thio, et al.,"Magnetized Target Fusion in a Spheroidal Geometry with Standoff Drivers," in Current Trends in International Fusion Research, E. Panarella, ed. (National Research Council of Canada, Ottawa, Canada, 1999), p. 113.

*Research funded by the DOE Office of Fusion Energy Sciences, grant DE-FG02-04ER54751.

TP8 156 Laser-driven preheat simulations of magnetized fusion fuel for magnetically-driven liner implosions on pulsed power accelerators A.B. SEFKOW, M.C. HERRMANN, S.A. SLUTZ, R.A. VESEY, *Sandia National Laboratories* Magnetically-driven implosions of cylindrical metal liners containing magnetized and preheated fuel are being studied to determine whether significant inertial confinement fusion yields can be economically obtained on pulsed power accelerators. Preliminary radiation-MHD simulations of dense (1-5 mg/cc), axially-magnetized (3-30 T), and preheated (200-500 eV) deuterium-tritium (DT) fuel driven by a pulsed power accelerator similar to Z (25-60 MA) indicate fast implosions (100-300 ns) and high yields (100s kJ - 10s MJ) may be feasible. Efficient alpha particle trapping for self-heating and reduced heat conduction losses in the radial direction can be provided by compression of the axial magnetic field (to $\sim$ 10 kT), which substantially reduces the traditional threshold value of the fuel ρR at ignition. Preheating the fuel before compressing it is advantageous because ignition temperatures can thereby be accessed without requiring extraordinarily large convergence ratios or implosion velocities. A few kJ of 2ω laser light delivered over a few ns by Z Beamlet (ZBL) may sufficiently preheat the fuel, and Z and ZBL experiments are planned to test the various components of this concept.

TP8 157 Simulation of laser-driven magnetic flux compression in inertial confinement fusion CHUANDONG ZHOU, AMMAR HAKIM, JOHN LOVERICH, PETER STOLTZ, *Tech-X Corporation* Laser-driven magnetic-flux compression is an innovative approach to achieve magneto-inertial fusion (MIF). A cylindrical target with initial seed magnetic field is compressed by energetic laser beams. The magnetic field that is "frozen-in" plasma gets compressed with the target. The resulting high magnetic field reduces electron thermal conductivity and improves alpha particle confinement, thus providing an additional thermal insulation of the fuel forming the hot spot. Computer simulation is a main tool in this area, but an easy-to-use and easy-to-access, parallel, 3D code is not available to this community. New features, including laser energy deposition in under-dense plasma, are incorporated into the Tech-X fluid framework, TxFluids. We discuss our approach to determine the best algorithms for properly modeling laser-driven shock implosions with magnetic fields in conditions relevant to cylindrical MIF and benchmark magnetic compression with one-dimensional simulation.

TP8 158 Progress in plasma liner modeling for MIF JOHN LOVERICH, AMMAR HAKIM, SEAN ZHOU, *Tech-X* Magnetic confinement fusion and inertial confinement fusion represent the two extremes in terms of density and confinement time in fusion energy research. Both approaches have been studied extensively through the decades pushing technology to the limits. An alterna-

tive fusion approach exists between these regimes called magnetized target fusion. In magnetized target fusion longer confinement times are achieved than in ICF through the use of strong magnetic fields, the long confinement time reduces the required plasma density to reach ignition–the approach has advantages over MFE in that it is much more compact and higher density. This work explores computationally a form of magnetized target implosion using a plasma liner. This concept is to be compared with solid liner implosion approach which may not be commercially viable as a reactor due to the "standoff" problem, portions of the device are destroyed with each target implosion. We present simulation results of plasma liner formation, jet merging, and plasma jet magnetized target interaction using a fluid plasma code (TxFluids) developed at Tech-X corporation.

TP8 159 Hybrid-PIC Algorithms for Simulation of Large-Scale Plasma Jet Accelerators* CARSTEN THOMA, DALE WELCH, *Voss Scientific, LLC* PLASMA SIMULATION TEAM, Merging coaxial plasma jets are envisioned for use in magneto-inertial fusion schemes as the source of an imploding plasma liner. An experimental program at HyperV is considering the generation of large plasma jets (length scales on the order of centimeters) at high densities (10^{16}-10^{17} cm^{-3}) in long coaxial accelerators. We describe the Hybrid particle-in-cell (PIC) methods implemented in the code LSP for this parameter regime and present simulation results of the HyperV accelerator. A radiation transport algorithm has also been implemented into LSP so that the effect of radiation cooling on the jet mach number can be included self-consistently into the Hybrid PIC formalism.

*Work supported by U.S. Department of Energy, Office of Fusion Energy Science (OFES).

TP8 160 Plasma Formation and Evolution from Thick Metal Pulsed with Megagauss Magnetic Field* THOMAS AWE, BRUNO BAUER, STEPHAN FUELLING, RICHARD SIEMON, JASPREET BILLING, TASHA GOODRICH, *University of Nevada, Reno* UNIVERSITY OF NEVADA, RENO TEAM, The threshold for plasma formation on the surface of thick metal, in response to a pulsed multi-megagauss magnetic field, is experimentally measured. Thick Aluminum rods with initial diameters ranging from 0.5 to 2.0 mm are pulsed with the 1.0 MA, 100-ns Zebra generator. Surface magnetic field rise rates vary from 30 to 80 MG per microsecond, with corresponding peak fields of 1.5 to 4 MG. The onset of thermal plasma is observed through an abrupt increase in the rate of surface heating when the surface temperature reaches about 0.7 eV. Plasma forms when the surface magnetic field exceeds 2 MG, independent of the rise rate of the applied field. High resolution (30 micron, 2 ns) images detail surface dynamics during this transition from warm-dense-aluminum to plasma. Measurements of magnetic field, brightness temperature, spectrum of emitted radiation, time of plasma formation, expansion velocity, and growth of instabilities are presented.

*Supported by DOE grants DE-FG02-04ER54752, DE-FG02-06ER54892, and DE-FC52-01NV14050

TP8 161 Modeling of an aluminum wall-confined plasma created by MG magnetic fields RICHARD SIEMON, IRVIN LINDEMUTH, *Univ. of Nevada, Reno* Experiments at UNR demonstrate that interesting fully ionized aluminum plasma (T=1-30 eV, $n \sim 10^{18}$ cm^{-3}, $Z \sim 3$) can be created on the surface of mm-size aluminum rods by MA pulses of current. The transport properties of such plasma and nearby wall material at higher density and lower temperature are not well established, but numerical modeling using SESAME tables or Russian material model gives surprisingly good agreement with experimental observations. During the experimental time of current rise, the observed plasma temperature typically increases from 1-eV to 15 eV or more. In order for that to happen the plasma must be sufficiently dense and in a layer sufficiently thick for Ohmic heating to be larger than conduction cooling. That requirement is equivalent to saying that the electron omega-tau must be less than a small number that depends weakly upon plasma Z. This demonstration that a fully ionized plasma can be held by magnetic pressure against a solid surface in what is known as a "wall confined" geometry supports one of the basic assumptions often made in the context of magneto-inertial fusion.

TP8 162 Simulation of Formation and Implosion of Plasma Liners for Magnetized Target Fusion ROMAN SAMULYAK, LINGLING WU, *Stony Brook University* PAUL PARKS, *General Atomics* Spherically symmetric simulations of the implosion of plasma liners and compression of plasma targets in the concept of Magnetized Target Fusion have been performed using the method of front tracking. The cases of single deuterium and xenon liners and double liners containing both deuterium and xenon layers have been investigated. Simulations have been compared with recent theoretical works. In most favorable setups, the state of ignition and large fusion burn up fraction and energy gains have been achieved. The main conclusion of the study is that the efficiency of the method significantly increases if a large initial target (up to 30 cm in radius) is compressed by a high Mach number liner containing a heavy gas layer (xenon). Full 3D simulations of the propagation and merger of high Mach number deuterium jets and the formation of liner have also been performed. It has been shown that the jet merger reduces the Mach number. After the 5 m propagation and full merger of 144 jets with initial Mach number 60, the average Mach number of the liner was approximately 10.

SESSION UI2: LASER WAKEFIELD ACCELERATION AND SOLID TARGET INTERACTIONS
Thursday Afternoon, 5 November 2009; Centennial I at 14:00; Michael Downer, University of Texas, presiding

14:00
UI2 1 Controlled electron injection in laser wakefield accelerators using axially tailored plasmas.*
ANTHONY GONSALVES, *Lawrence Berkeley National Laboratory*

Controlling injection of electrons in laser plasma accelerators (LPA's) is crucial for improving the beam quality and enabling applications such as free electron lasers (FEL's). In addition, techniques are needed to control the amount of charge, energy and energy spread. To date, LPA's have typically operated in a highly nonlinear regime in which electrons are self-injected into a laser-excited plasma density wave. Although percent level energy spread beams have been demonstrated experimentally [1-4], production of lower energy spread beams will require accurate control of the injection process. In order to avoid self-trapping, an LPA would have to operate with lower wake amplitude, whether linear or non-linear. This also necessitates the use of a laser guiding structure to overcome diffraction of the laser beam. Such guiding structures have been obtained by transversely shaping the plasma density profile and they have successfully been used in experiments using laser-produced [2] or capillary-based channels [4]. In this talk, experimental results are presented that demonstrate the use of a longitudinally tailored plasma density profile in a capillary discharge waveguide to control trapping, significantly improving LPA performance. A gas jet was embedded in the capillary to locally alter the plasma density. It was found that electrons can be trapped and accelerated to hundreds of MeV using plasma densities in the capillary lower than in previous experiments, where no stable self-trapped electron beams were obtained in previous experiments [5]. It is found that using a longitudinally tailored density profile improves and increases control over electron beam properties. [1] Mangles et al., Nature 431, 535 (2004) [2] Geddes et al., Nature 431, 538 (2004) [3] Faure et al., Nature 431, 541 (2004) [4] Leemans et al., Nat. Phys. 2, 696 (2006) [5] Nakamura et al., Phys. Plasmas 14, 056708 (2007)

*Supported by US DOE grant DE-AC02-05CH11231 and DARPA.

14:30
UI2 2 Laser Wakefield Acceleration in the Self-Guided Regime.
JOSEPH RALPH, *Lawrence Livermore National Laboratory*

Recent experimental results of laser wakefield acceleration demonstrate self-guiding as means to achieve GeV scale electron energies. Experimental results using Helium gas jet and gas cell targets ranging in length from 3 mm to 14 mm produced electron energies to beyond 700 MeV. Energy measurements relied on a unique two-screen method to eliminate error due to angular deviation of the electron beam. To achieve such high-energy electrons in the self-guided regime, a 200 TW 60 fs laser pulse was focused to a spot size of 15 microns and propagated through underdense plasmas with densities ranging from 10^{18} to 10^{19}cm^{-3}. The power threshold for self-trapping of electrons was found to be a strong function of the laser pulse power compared with the critical power for relativistic self-focusing in plasmas. Full 3D Particle-In-Cell simulations show excellent agreement with experimental results. This work was performed under the auspices of the U.S. Department of Energy by Lawrence Livermore National Laboratory under Contract DE-AC52-07NA27344 and a Department of Energy Grant No. DEFG02-92ER40727 and was partially funded by the Laboratory Directed Research and Development Program under tracking code 06-ERD-056.

15:00
UI2 3 Boosted frame PIC simulations of LWFA: ultra-fast modeling of current experiments and first studies of acceleration towards the energy frontier.*
SAMUEL MARTINS, *GoLP, Instituto de Plasmas e Fusao Nuclear - Instituto Superior Tecnico, Lisbon, Portugal & University of California Los Angeles, Los Angeles, USA*

The development of new laser systems, in the 10PW range, will push Laser Wakefield Accelerators (LWFA) to a new qualitative regime, for which theoretical scalings predict the possibility to accelerate electron bunches close to the energy frontier, with self-injected electrons in excess of 10 GeV, and above 50GeV bunches with externally injected electrons. As in the past, numerical simulations will certainly play an important role in testing, probing and optimizing the physical parameters and setup of these upscale experiments. The distances involved in these numerical experiments, however, are very demanding in terms of computational resources, so that three-dimensional fully kinetic simulations are not yet possible to (easily) accomplish. Following the work on optimized Lorentz frames by J.-L. Vay [PRL 98, 130405 (2007)], the Lorentz transformation for a boosted frame was implemented in OSIRIS [R. A. Fonseca et al, LNCS 2329, III-342 (Springer-Verlag, 2002)], leading to a dramatic change in the computational resources required to model LWFA. The critical implementation details will be described, and the main difficulties discussed. Quantitative benchmarks will be

presented between boosted frame and laboratory frame simulations, and also with experimental results from Imperial College and Lawrence Livermore National Laboratory, with emphasis on the boosted frame scheme as a tool for faster design and modeling of current experiments. Finally, simulations for the scenarios possible with the next generation of laser systems will be presented, including the confirmation of electron bunch acceleration to the energy frontier.

*Work partially supported by F.C.Gulbenkian, FCT [SFRH/BD/35749/2007, PTDC/FIS/66823/2006 (Portugal)], and European Community - New and Emerging Science and Technology Activity, FP6 program (project EuroLeap, contract #028514).

15:30
UI2 4 Measurements and modeling of radiation from laser wakefield accelerators.
ALEC THOMAS, *University of Michigan*

Electron beams produced by laser wakefield acceleration are characterized by having relatively high current density in short and quasi-monoenergetic bunches. Oscillations of these electrons, in the electromagnetic fields of electron plasma cavities, created by laser driven ponderomotive expulsion, can lead to extremely bright sources of x-rays. Radiation is also emitted in the form of coherent scattering of the background electrons and other emission from the highly dynamic electron motions in the field structure. Presented here is a summary of recent experimental measurements and numerical modeling towards laser wakefield driven compact radiation sources, conducted at the Center for Ultrafast Optical Science at the University of Michigan. Experiments, on the 30 fs, 300 TW HERCULES laser, studying tunneling ionization assisted electron trapping, demonstrate an enhancement to the electron beam through the addition of a high-Z contaminant to the Helium background gas. The nature of the effect of the ionization depends on the energy level structure of the contaminant. Electron beams are also measured and characterized from structured gas density profiles, including a density step-function to increase trapping. Measurements of x-rays produced by betatron oscillations in the wakefield demonstrate x-rays with peak brightness comparable to third generation synchrotron sources, from a micron-scale source size. Experimental measurements of side-scattered light from the wakefield interaction yields information on the evolution of the pulse and plasma bubble. Numerical models of radiation emission are compared with the experimental results. These include calculations using the radiation code *Radampeltrac*, which indicate the role of the laser pulse in modifying the radiation distribution.

16:00
UI2 5 Generation and Transport of Hot Electrons in Cone-Wire Targets.*
FARHAT BEG, *University of California San Diego*

We present results from a series of experiments where cone-wire targets in various configurations were employed both to assess hot electron coupling efficiency, and to reveal the source temperature of the hot electrons. Initial experiments were performed on the Vulcan petawatt laser at the Rutherford Appleton Laboratory and Titan laser at the Lawrence Livermore National Laboratory. Results with aluminum cones joined to Cu wires of diameters from 10 to 40 μm show that the laser coupling efficiency to electron energy within the wire is proportional to the cross sectional area of the wire. In addition, coupling into the wire was observed to decrease with the laser prepulse and cone-wall thickness. More recently, this study was extended, using the OMEGA EP laser. The resulting changes in coupling energy give indications of the scaling as we approach FI-relevant conditions. Requirements for FI scale fast ignition cone parameters: tip thickness, wall thickness, laser prepulse and laser pulse length, will be discussed. In collaboration with T. Yabuuchi, T. Ma, D. Higginson, H. Sawada, J. King, M.H. Key, K.U. Akli, Al Elsholz, D. Batani, H. Chen, R.R. Freeman, L. Gizzi, J. Green, S. Hatchett, D. Hey, P. Jaanimagi, J. Koch, K. L. Lancaster, D.Larson, A.J. MacKinnon, H. McLean, A. MacPhee, P.A. Norreys, P.K Patel, R. B. Stephens, W. Theobald, R. Town, M. Wei, S. Wilks, Roger Van Maren, B. Westover and L. VanWoerkom.

*Work supported by US DOE under contracts DE-FC02-04ER54789 (Fusion Science Center) and DE-FG02-05ER54834 (ACE).

16:30
UI2 6 Integrated Kinetic Simulation of Laser-Plasma Interactions, Fast-electron Generation and Transport in Fast Ignition.*
ANDREAS KEMP, *Lawrence Livermore National Laboratory*

We present new results on the physics of short-pulse laser-matter interaction of kilojoule-picosecond pulses at full spatial and temporal scale, using a new approach that combines a 3D collisional electromagnetic Particle-in-Cell code with an MHD-hybrid model of high-density plasma. In the latter, collisions damp out plasma waves so the displacement current can be neglected; and an Ohm's law with electron inertia effects neglected determines the electric field. In addition to yielding orders of magnitude in speed-up while avoiding numerical instabilities, this allows us to model the whole problem in a single unified framework: the laser-plasma interaction at sub-critical densities, energy deposition at rela-

tivistic critical densities, and fast-electron transport in solid densities. Key questions such as the multi-picosecond temporal evolution of the laser energy conversion into hot electrons, the impact of return currents on the laser-plasma interaction, and the effect of self-generated electric and magnetic fields on electron transport will be addressed. We will report applications to current experiments at LLNL's Titan laser and Omega EP, and to a Fast-Ignition point design for forthcoming experiments on NIF-ARC.

*This work was performed under the auspices of the Department of Energy/NNSA by the Lawrence Livermore National Laboratory (LLNL) under Contract No. DE-AC52-07NA27344.

SESSION UI3: BASIC PLASMAS: NOVEL PLASMAS IN LABORATORY AND SPACE
Thursday Afternoon, 5 November 2009; Centennial II at 14:00; Matthew Stoneking, Lawrence University, presiding

14:00

UI3 1 Measurements of Correlation-Enhanced Collision Rates.*

C. FRED DRISCOLL,† *University of California at San Diego*

This talk presents the first detailed experimental measurements of the Salpeter collisional enhancement factor $g(\Gamma)$ in strongly correlated plasmas. This factor is predicted to enhance the nuclear reaction rate in dense strongly-correlated plasmas, such as in giant planet interiors, brown dwarfs and degenerate stars;[1] and recent theory establishes that it also applies to the perpendicular-to-parallel collisions in magnetized plasmas described here.[2] The enhancement is caused by plasma screening of the repulsive Coulomb potential between charges, allowing closer collisions for a given particle energy. The enhancement factor is predicted to be large when the plasma correlation parameter $\Gamma \equiv e^2/aT$ is larger than unity, scaling as $g(\Gamma) \sim e^{\Gamma}$. The perp-to-parallel collision rate is then $\nu_{\perp\|} = n\bar{v}b^2\, I(\bar{\kappa})\, g(\Gamma)$, where $I(\bar{\kappa})$ decreases precipitously below $(8\sqrt{\pi}/15)\ln\Lambda$ in the highly magnetized regime of $\bar{\kappa} \equiv \sqrt{2}\, b/r_c \gg 1$. ● Our measurements[3] of $\nu_{\perp\|}$ in Mg^+ pure ion plasmas are consistent with the predicted Salpeter correlation enhancement, with the comparison limited mainly by systematic spatial variations in the plasma temperature. The plasma temperatures are controlled over the range $4 \times 10^{-6} < T < 1$eV, with the outer radii being up to 2× hotter. Bulk-averaged collision rates of $1 < \nu_{\perp\|} < 2 \times 10^4$ sec^{-1} are measured by 2 techniques: for slow collisions, $T_{\|}$ is heated or cooled, and the subsequent relaxation is directly observed; for rapid collisions, sinusoidal modulation of the plasma length at frequency f_{mod} gives maximal heating when $f_{mod} = \nu_{\perp\|}/2\pi c(\Gamma)$, where $c(\Gamma)$ is the specific heat. Two densities are used, 2.0 and 0.12×10^7 cm^{-3}; the lower density has ~ 2.5 × less correlation at any temperature. Experiments clearly show the expected $\nu_{\perp\|} \propto T^{-3/2}$ regime at high temperatures, and show the strong $I(\bar{\kappa})$ suppression of $\nu_{\perp\|}$ for $b/r_c \gg 1$. At low temperatures and high density, the measured $\nu_{\perp\|}$ is enhanced by up to $g \sim 10^{12}$ over the uncorrelated prediction, consistent with the Salpeter-enhanced prediction. At low (uncorrelated) densities, no enhancement is observed. Future experiments may be able to image "burn fronts" propagating from hot regions to cold regions.

*Supported by NSF grant PHY-0903877 and NSF/DOE grant PHY-0613740.
†In collaboration with F. Anderegg, D.H.E. Dubin and T.M. O'Neil.

[1]E.E. Salpeter and H.M. Van Horn, Astrophys. J. **155**, 183 (1969).
[2]D.H.E. Dubin, Phys. Rev. Lett. **94**, 025002 (2005).
[3]F. Anderegg *et al.*, Phys. Rev. Lett. **102**, 185001 (2009); F. Anderegg *et al.*, Phys. Plasmas **16**, 055705 (2009).

14:30

UI3 2 Noninvasive technique for studying plasma modes of ion Coulomb crystals using cavity quantum electrodynamics.

MICHAEL DREWSEN, *QUANTOP - Danish Research Foundation Center for Quantum Optics, Department of Physics and Astronomy, University of Aarhus, DK-8000 Aarhus C, Denmark*

Cavity Quantum ElectroDynamics (CQED) is a research field which focuses on understanding the interactions between matter and the electromagnetic field in cavities at the quantum level. Currently, CQED is a very active research field due to the prospect of creating efficient light-matter quantum interfaces at the single photon level for quantum information science. Ion Coulomb crystals have a series of properties of particular interest for CQED studies, as demonstrated in recent CQED experiments [1]. The coupling strength between ions in the crystals and photons in the cavity strongly depend on the motion of the ions due to the Doppler-effect. Consequently, the CQED signals can be exploited to learn about excitations of plasma modes in ion Coulomb crystals. Since the method relies on having one or less photons in the cavity at any time, it constitutes a noninvasive alternative to the Doppler-fluorescence method previous demonstrated in Penning trap experiments [2]. So far, CQED signal has been used to characterize how several normal mode frequencies depend on the aspect ratio of Coulomb crystals, and how the so-called micromotion of ions confined in rf traps influences

the damping of the mode [3]. The observed mode frequencies are in remarkable agreement with theoretical prediction based on uniformly charged fluids [1] P. F. Herskind, A. Dantan, J. P. Marler, M. Albert, and M. Drewsen, to appear in Nature Physics (2009). [2] T. B. Mitchell, J. J. Bollinger, X.-P. Huang, and W. M. Itano, Opt. Express **2**, 314 (1998). [3] J. P. Marler, M. Albert, D. Guenot, P. F. Herskind, A. Dantan and M. Drewsen, manuscript in preparation. [4] D. H. E. Dubin, Phys. Rev. Lett. **66**, 2076 (1991).

15:00
UI3 3 Shock Experiments on Pre-Compressed Fluid Helium.*
JON EGGERT, *Lawrence Livermore National Laboratory*

Hugoniot data were obtained for ?uid He in the 100 GPa pressure range by shock compression of samples statically pre-compressed in diamond-anvil cells. The initial (pre-compressed) He density for each experiment was tuned to a value between 1 and 3.3 times the cryogenic liquid density. Maximum observed shock-compression ratios range from 4 to 6 and show an increase in compressibility at the onset of ionization, similar to theoretical predictions. Simultaneous temperature and reflectivity data suggest that ionization is primarily temperature driven, but has an identifiable and significant density component. Fits to a modified Drude model to allow for forbidden electronic energy gaps suggest that the energy gap is relatively independent of temperature and closes with density at about 1.8 g/cc.

*This work performed under the auspices of the U.S. DOE by LLNL under Contract DE-AC52-07NA27344.

15:30
UI3 4 High Energy Plasmas in the Surroundings of Black Holes: Composite Disk Structures and Characteristic Modes.*
BRUNO COPPI, *MIT*

Theoretically finding of composite disk structures around compact objects (e.g. black holes) and recent experimental observations indicate that highly coherent and dynamically important magnetic field configurations exist in the core of these structures [1]. These coherent configurations provide a means to resolve the "accretion paradox" for a magnetized disk [2] while the formation of jets that are emitted in the close vicinity of the compact object is related to them. The absence of vigorous accretion activity in the presence of black holes in old galaxies can be attributed to the loss of the surrounding coherent magnetic configurations during their history. As for relevant dynamics, axisymmetric (ballooning) modes as well as tri-dimensional spirals can be excited from disks with a "seed" magnetic field, under the effects of differential rotation and of the vertical plasma pressure gradient. The properties of these spirals are strongly dependent on their vertical structure. Axisymmetric modes can produce vertical flows of thermal energy [3] and particles in opposing directions that can be connected to the winds emanating from disks in Active Galactic Nuclei (AGN's). A similarity with the effects of temperature gradient driven modes in magnetically confined laboratory plasmas is pointed out. Spiral modes that are oscillatory in time and in the radial direction can produce transport of angular momentum toward the outer region of the disk structure, a necessary process for the occurrence of accretion [3]. The excitation of radially localized density spirals co-rotating with the plasma, at a distance related to the Schwartzchild radius $R_S = 2GM_*/c^2$ where M_* is the black hole mass, is proposed [4] as the explanation for High Frequency Quasi Periodic Oscillations (HFQPOs) of non-thermal X-ray emission from compact objects. *Sponsored in part by the U.S. Department of Energy. [1] B. Coppi and F. Rousseau *Ap. J.* **641** 458 (2006) [2] B. Coppi to be published in *Pl. Phys. Cont. Fus.* (2009) [3] B. Coppi *Europhys. Letters* **82** 19001 (2008) [4] Coppi B and P. Rebusco, Paper P5.154, EPS Int. Conf. Pl. Phys. (Crete, Greece, 2008).

16:00
UI3 5 Astrophysically relevant radiatively cooled hypersonic bow shocks in nested wire arrays.*
DAVID AMPLEFORD, *Sandia National Laboratories*

We have performed laboratory experiments which introduce obstructions into hypersonic plasma flows to study the formation of shocks. Astrophysical observations have demonstrated many examples of equivalent radiatively cooled bow shocks, for example the head of protostellar jets or supernova remnants passing through the interstellar medium or between discrete clumps in jets. Wire array z-pinches allow us to study quasi-planar radiatively cooled flows in the laboratory. The early stage of a wire array z-pinch implosion consists of a steady flow of the wire material towards the axis. Given a high rate of radiative cooling, these flows reach high sonic- Mach numbers, typically up to 5. The 2D nature of this configuration allows the insertion of obstacles into the flow, such as a concentric "inner" wire array, as has previously been studied for ICF research. Here we study the application of such a nested array to laboratory astrophysics where the inner wires act as obstructions perpendicular to the flow, and induce bow shocks. By varying the wire array material (W/Al), the significance of radiative cooling on these shocks can be controlled, and is shown to change the shock

opening angle. As multiple obstructions are present, the experiments show the interaction of multiple bow shocks. It is also possible to introduce a magnetic field around the static object, increasing the opening angle of the shocks. Further experiments can be designed to control the flow density, magnetic field structure and obstruction locations. In collaboration with: S.V. Lebedev, M.E. Cuneo, C.A. Jennings, S.N. Bland, J.P. Chittenden, A. Ciardi, G.N. Hall, S.C. Bott, M. Sherlock, A. Frank, E. Blackman

*Work supported by DOE/NNSA. Sandia is a multi-program laboratory operated by Sandia Corporation, a Lockheed Martin Company, for the US Department of Energy's NNSA under contract DE-AC04-94AL85000.

16:30
UI3 6 Experimental and numerical investigation of auroral cyclotron maser processes.
DAVID SPEIRS, *Department of Physics, University of Strathclyde, Glasgow, Scotland, G4 0NG, U.K.*

When an electron beam with initial spread in rotational velocity is subject to significant magnetic compression, conservation of magnetic moment results in the formation of a horseshoe shaped velocity distribution. It has been shown that such a distribution is unstable to cyclotron emission [1] and may be responsible for the generation of Auroral Kilometric Radiation (AKR) – an intense RF emission sourced at high altitudes in the terrestrial auroral magnetosphere. In a scaled laboratory reproduction of this process, a 75-85keV electron beam of 5-40A was magnetically compressed by a system of solenoids and electromagnetic emissions observed for cyclotron frequencies of 4.42GHz and 11.7GHz [2]. A comparison of these experimental measurements with the results of 2D and 3D numerical simulations will be presented, showing the effect of cyclotron-wave detuning on the efficiency of forward and backward wave coupling. The experiment presently differs from the astrophysical case in that it has a well defined radiation boundary. PiC code calculations have been undertaken to investigate the dynamics of the cyclotron emission process in the absence of such metallic boundaries and incorporating a background plasma of variable density. Computations reveal that the cyclotron emission process persists although its spatial growth is reduced. A quenching of the instability is also apparent as the ratio ω_{ce} / ω_p is reduced to be $<$ 1. This is consistent with the predictions of theory [3] and satellite observations that suggest AKR emission is localized within a region of plasma depletion where ω_{ce} / ω_p $>$ 1. [1] D. Gurnett, "Waves in Space Plasmas," 50th Annual meeting of the APS Division of Plasma Physics, 2008. [2] K. Ronald et al, Physics of Plasmas, 15, 056503, 2008. [3] R. Bingham and R. A. Cairns, Physics of Plasmas, 7, 3089, 2000.

SESSION UO4: RESEARCH IN SUPPORT OF ITER
Thursday Afternoon, 5 November 2009
Regency VI at 14:00
Rich Hawryluk, Princeton Plasma Physics Laboratory, presiding

14:00
UO4 1 ITER Research Plan DAVID CAMPBELL, *ITER Organization* The ITER Research Plan (IRP) is being developed to provide a guide to the research activities which should be undertaken within the framework of the ITER Project and will encompass both physics and technology research during ITER construction and operation. The Plan provides a framework linking and integrating the current research priorities of the Project with the preparation for future exploitation. Recent analysis has focused on the adaptation of the IRP to the Project's updated construction and operation schedule with the aim of developing an operational programme which makes the most rapid transition, within the overall Project constraints, to DT fusion energy production. The programme evolves through a period of non-active (hydrogen and helium) operation to allow full commissioning of the facility, a phase of deuterium operation in which operation with all-metallic PFCs will be established, followed by the transition to full DT operation and the production of plasmas with significant fusion energy gain. Identification of the key elements in the experimental programme leading to burning plasma studies allows priorities for R&D activities required to prepare the efficient exploitation of the ITER device to be defined.

14:12
UO4 2 Disruption mitigation and avoidance at ASDEX Upgrade M. MARASCHEK, *MPI for plasmaphysics, Germany* G. PAUTASSO, B. ESPOSITO, *ENEA-Frascati, Italy* G. GRANUCCI, *IFP-CNR, Italy* J. STOBER, W. TREUTTERER, *all EURATOM Ass.* ASDEX UPGRADE TEAM, Disruptions are a major concern for tokamaks and in particular for ITER. They cause high heat loads during the thermal quench and high mechanical forces during the subsequent current quench. The generation and loss of runaway electrons (highly accelerated electrons carrying large fractions of the plasma current) can produce damage to the vessel structures. Therefore, schemes are implemented in present tokamaks to mitigate or to even avoid them. Mitigation has been proven to be effective through the injection of noble gases causing a reduction of the thermal heat load by radiation and a reduction of the mechanical forces. In addition 25% of the required density for the collisional suppression of runaways in ITER has been reached. For the trigger of the noble gas injection a locked mode detector is routinely used at ASDEX Upgrade. An extension to more complex precursors is planed. A different approach has been used for disruption avoidance by injecting ECRH triggered by the loop voltage increase before the disruption. The avoidance of an ongoing density limit disruption has been achieved when the ECRH is deposited at resonant surfaces where MHD modes, such as the m=2/n=1, occur. Present schemes for the mitigation and eventually avoidance of disruptions will be discussed.

14:24
UO4 3 3-D radiation dynamics during gas jet mitigated disruptions on Alcator C-Mod* MATTHEW REINKE, ROBERT GRANETZ, IAN HUTCHINSON, DENNIS WHYTE, PLASMA SCIENCE AND FUSION CENTER, MIT TEAM, Demonstrating and understanding disruption mitigation (DM) techniques on present tokamaks is critical to the design of similar tools for ITER

and beyond where a near zero-tolerance policy on unmitigated disruptions is envisioned. Efficient mitigation requires the bulk of the thermal and magnetic stored energy to be converted into radiation that is spread uniformly over the walls. Such uniformity has yet to be conclusively demonstrated or understood well enough to confidently design ITER's DM system. Using multiple AXUV diode arrays and spectroscopy, the toroidal and poloidal radiation distribution is investigated on Alcator C-Mod for DM experiments employing a high pressure gas jet. While large, time varying asymmetries in the radiation are observed, the total energy loss is shown to be nearly uniform. Prior to the onset of the thermal quench (TQ) it is shown that both radiation local to the gas jet and axisymmetric radiation are important in shedding the stored energy necessary to destabilize the MHD thought to trigger the TQ. The variation of this pre-TQ period with gas jet species and target plasma are discussed.

*Work supported by DoE Coop. Agree. No. DE-FC02-99-ER54512.

14:36

UO4 4 Disruption Mitigation Experiments Carried Out on DIII-D* N. COMMAUX, L.R. BAYLOR, T.C. JERNIGAN, *ORNL* T.E. EVANS, D.A. HUMPHREYS, P.B. PARKS, M.A. VAN ZEELAND, J.C. WESLEY, *GA* E.M. HOLLMANN, A.N. JAMES, J.H. YU, *YCSD* Disruptions are an important issue for ITER. Major and vertical displacement disruptions in ITER are predicted to generate multi-MeV runaway electron beams (RE) as well as high energy flux to the plasma facing components and high halo currents in the structures that could potentially damage the machine. To mitigate these phenomena, several techniques have been studied on DIII-D: massive gas injection (MGI), external magnetic perturbation, and injection of large shattered cryogenic pellets. MGI, which is proven to mitigate heat fluxes and halo currents, has been tested on DIII-D in terms of impurity radiation toroidal symmetry and optimization of the gas pulse length. Other techniques expected to mitigate the RE have also been tested on DIII-D: deconfinement of the RE using external magnetic fields and collisionally damping the avalanche multiplication process by rapidly increasing the electron density in the core by several orders of magnitude using a new shotgun pellet injector built by ORNL.

*Supported by the US DOE under DE-AC05-00OR22725, DE-FC02-04ER54698, and DE-FG02-07ER54917.

14:48

UO4 5 JET experiments on massive gas injection S.A. BOZHENKOV, R.C. WOLF, *MPI* S. BREZINSEK, A. HUBER, U. KRUEZI, M. LEHNEN, *FZJ* S. JACHMICH, *ERM/KMS* G. ARNOUX, P.D. MORGAN, *UKAEA* JET EFDA COLLABORATION, We present JET experiments on massive gas injection for disruption mitigation. Stable plasmas were terminated by Ne, Ar or their D_2 mixtures. Reaction time of the method consists of vacuum gas flow and plasma edge cooling. This time depends on the injection and plasma parameters. In the following thermal quench the plasma is rapidly cooled, with up to 50% of the energy being radiated. Finally, the plasma current is ohmically dissipated. Since the current decay rate depends on the species, control of the halo currents is possible. Ar and Ne cause runaway generation in the current quench. The runaway conversion exceeds 50% for Ar, while a lower one is found for Ne and no runaways are observed for mixtures. Runaways can locally heat the wall above 1500°C. For suppression of runaways the fueling efficiency is important. It decreases with the gas mass from 25% for Ne/D_2 to 3% for Ar. Our results suggest that for ITER: a further increase of the energy radiated in the thermal quench to 90% is necessary; the halo current control is feasible; and the runaway suppression remains an issue.

15:00

UO4 6 NSTX ELM Pacing and L-H Threshold Experiments for ITER* J.M. CANIK, R. MAINGI, A.C. SONTAG, *ORNL* S.P. GERHARDT, S. KAYE, R.E. BELL, D. GATES, R. GOLDSTON, B.P. LEBLANC, J. MENARD, J.-K. PARK, *PPPL* T. EVANS, T. OSBORNE, *GA* S. SABBAGH, *Columbia U.* E.A. UNTERBERG, *ORISE/ORNL* We present a summary of recent edge-localized mode (ELM) pacing and L-H power threshold (P_{LH}) experiments performed in NSTX in support of ITER. ELM triggering using 3D magnetic perturbations was used to perform pacing during ELM-free H-modes induced by lithium conditioning, mitigating the impurity accumulation typically observed in these conditions. The waveform of the applied field has been tailored to provide high reliability triggering at frequencies of > 60 Hz to reduce the average ELM size. ELM pacing was also performed using vertical position oscillations, with the ELM frequency increased to $\sim$ 30 Hz from a natural frequency of $\sim$ 15 Hz. P_{LH} is reduced by $\sim$ 50% at low triangularity, and also decreased by $\sim$ 50% during discharge with thick lithium wall coatings. P_{LH} was observed to increase strongly with plasma current during sustained H-modes. The influence of heating method, non-axisymmetric fields, and magnetic balance on P_{LH} will be presented.

*Work supported by U.S. DOE Contracts DE-AC05-00OR22725, DE-AC02-09CH11466, DE-FC02-04ER54698, and DE-FG02-99ER54524

15:12

UO4 7 Impurity Behaviour in the H-mode Edge Barrier: Neoclassical Transport and ELM Flushing T. PUETTERICH, R. DUX, M.A. JANZER, *MPI f. Plasmaphysik, EURATOM Association, 85748 Garching, Germany* ASDEX UPGRADE TEAM, In H-mode discharges an edge transport barrier (ETB) exists and steep gradients are observed in density, temperature of electrons, ions and impurities forming an edge pedestal which is briefly but frequently disturbed and degraded by the occurrence of edge localized modes (ELMs). This edge pedestal sets the boundary conditions for the performance of a fusion plasma. In the actual work, the impurity transport in the ETB is measured by CXRS. It is found that the gradients and the dynamics in impurity densities for (He, C, Ne and Ar) are in agreement with neoclassical transport coefficients at the ETB (i.e. small diffusion and inward convection). Furthermore, a model for the ELM cycle was developed, which treats an impurity mix self-consistently, such that for each time step the neoclassical transport is reevaluated according to the actual impurity densities and gradients. For plasma radii inside the ETB turbulent transport is taken into account by additional diffusion. The impurities are expelled by the ELM and then sputter W at the plasma facing components which enters the plasma after losses by prompt re-deposition are taken into account. The model consistently combines the dominant effects into a picture which agrees with the experimental behavior of W in ASDEX Upgrade.

15:24

UO4 8 Impact of large type I ELMs on plasma radiation in JET A. HUBER, S. BREZINSEK, PH. MERTENS, V. PHILIPPS, U. SAMM, B. SCHWEER, G. SERGIENKO, *FZJ* G. ARNOUX, M.N.A. BEURSKENS, W. FUNDAMENSKI, *UKAEA* T. EICH, *MPI* S. JACHMICH, *ERM/KMS* R.A. PITTS, *ITER Organisation* JET-EFDA TEAM, To prevent an unacceptable erosion of divertor targets due to ELMs in ITER, the loss in plasma stored energy should be restricted to $\Delta W_{ELM} \sim$ 1 MJ for a single ELM. Only the JET tokamak, thanks to its size, can produce ELMs in the order of 1 MJ with energy densities comparable to those found in ITER. This contribution examines the impact of large Type I ELMs in high current H-mode JET discharges on plasma radiation and on power load. The production of large Type I ELMs with ΔW_{ELM} in the range 0.25-1.3 MJ has been demonstrated. The ELMs provoke strong radiation losses, mostly confined to the inner divertor region. Large Type I ELMs with $\Delta W_{ELM} \geq 0.72$ MJ show enhanced radiation losses which are associated with the ablation of carbon layers in the inner divertor. Such large ELMs are often followed by a phase of Type III ELMs with an increased radiation in the plasma core. In this contribution, the impact of large Type I ELMs on plasma radiation in JET is summarized and implications of these results for ITER are discussed.

15:36

UO4 9 Simulation of the ITER Rampdown Scenario on DIII-D* P.A. POLITZER, G.L. JACKSON, D.A. HUMPHREYS, T.C. LUCE, A.W. HYATT, *General Atomics* Safe termination of a tokamak discharge becomes increasingly important as the energy stored in the plasma and in the poloidal magnetic field increases ($>$ 750 MJ in ITER). In DIII-D, we simulate the initiation, rampup, and rampdown phases of the proposed ITER discharge scenario, to identify potential issues and problems, to mitigate difficulties and to improve performance. The issues for rampdown are maintaining the separatrix strike point locations on the armored divertor, avoiding additional consumption of transformer flux, and maintaining the density and internal inductance within controllable limits while reducing the current to a negligible level. In these experiments dimensions are reduced by a factor of 3.7 and the current by 10 relative to ITER. We have simulated the ITER rampdown scenario to $I_p <$ 1 MA (equivalent) while controlling the strike points to better tolerance than required. The density falls fast enough to avoid density limits, and ℓ_i remains within control limits. The current ramp rate must be increased beyond the ITER reference value to avoid additional flux consumption.

*Work supported by the US DOE under DE-FC02-04ER54698.

15:48

UO4 10 Recovery of retained fuel through disruptions: implications for ITER* BRUCE LIPSCHULTZ, ROBERT GRANETZ, JAMES IRBY, BRIAN LABOMBARD, DENNIS WHYTE, *MIT Plasma Science and Fusion Center* Single discharge retention of injected gas in current tokamaks ranges from 3-50% of the injected gas raising concerns of excessive tritium retention for ITER. As part of a recent study of fuel retention in Alcator C-Mod it was found that, averaged over a run period, the fuel retained, normalized by ion fluence to divertor surfaces, was 100-1000x lower than for the same normalized retention in a single, non-disruptive discharge. Analyzing all disruptions for a run campaign it was found that the average disruption during plasma current flattop (15% of all discharges), led to fuel recovery 5-6x that retained in a single, non-disruptive discharge; Disruptions appear to remove all the fuel retained in non-disruptive discharges. Analysis of the fuel recovery dependence on disruption characteristics gave a scaling linear in plasma thermal energy and as the square of the magnetic energy. In this presentation we review the above information, discuss the role of the high-Z plasma facing components, and examine possible scalings to the use of disruptions for fuel recovery in ITER.

*USDOE Coop. Agree. No. DE- FC02-99ER54512.

16:00

UO4 11 Physics Requirements for the ITER Plasma Control System J.A. SNIPES, Y. GRIBOV, A. WINTER, *ITER Organization* The Plasma Control System (PCS) on ITER will control the evolution of the plasma parameters necessary to operate ITER throughout all phases of the discharge including plasma termination following off-normal events and plant system faults. The PCS is composed of six closely coupled subsystems that control specific physical quantities comprising: 1) wall conditioning and tritium removal, 2) plasma axisymmetric magnetic control, which includes plasma initiation, inductive plasma current, position, and shape control, 3) power and particle flux control to the first wall and divertor, 4) plasma kinetic control, including fuelling, non-inductive plasma current, plasma pressure and fusion burn control, 5) non-axisymmetric stability control, which includes sawteeth, edge localized modes (ELMs), neoclassical tearing modes (NTMs), error fields and resistive wall modes (RWMs), Alfven eigenmodes, etc., and 6) disruption mitigation and controlled plasma termination. The PCS is the first of a three layered system for machine protection that will decide the course of action to take following off-normal events or plant system faults during plasma operation together with the Central Interlock System (CIS) and the Central Safety System (CSS) for safety related events. Only if the PCS cannot control the plasma within specified operating limits and conditions will the disruption mitigation system by triggered by the CIS.

16:12

UO4 12 Development of a Spatially Resolving X-Ray Crystal Spectrometer (XCS) for Measurement of Ion-Temperature (Ti) and Rotation-Velocity (v) Profiles in ITER* K.W. HILL, M. BITTER, D. JOHNSON, R. FEDER, *Princeton University PPPL* P. BEIERSDORFER, J. DUNN, K. MORRIS, *LLNL* M. REINKE, Y. PODPALY, J.E. RICE, *MIT PSFC* R. BARNSLEY, *ITER Organization* M. O'MULLANE, *Univ. Strathclyde* S.G. LEE, *NFRC, Korea Basic Science Institute* An imaging XCS is being developed as a US-ITER activity for Doppler measurement of Ti and v profiles of impurities (W, Kr, Fe) with $\sim$ 7 cm (a/30) and 10 ms resolution in ITER; the instrument is modeled after the very successful imaging XCS on the C-Mod tokamak, which was developed through a PPPL-MIT collaboration and is a prototype for the ITER instrument. The imaging XCS uses a spherically bent crystal and 2d imaging x-ray detectors to achieve high spectral resolving power ($>$ 6000) in the horizontal dimension and spatial imaging vertically. Two XCS arrays will measure Ti and both poloidal and toroidal rotation velocity profiles. Simultaneous measurement of many spatial views permits tomographic inversion for determination of local parameters. The design of the ITER instrument, predictions of performance, and interesting measurements from C-Mod will be presented.

*Work supported by US DoE under contract DE-AC02-09CH11466.

16:24
UO4 13 On the JET ITER-Like ICRF antenna and implications for the ICRF system for ITER FREDERIC DURODIE, *Laboratory for Plasma Physics, Royal Military Academy, Association Euratom - Belgian State, BE* MARK NIGHTINGALE, *Euratom/UKAEA Fusion Association, UK* JET-EFDA COLLABORATION, A new "ITER-Like" Ion Cyclotron Resonance Frequency (ICRF) antenna was installed on the JET tokamak in 2007 and extensively operated on plasma since May 2008 for a wide range of conditions (frequencies: 33, 42 and 47 MHz, L- and ELMy H-mode plasmas, antenna strap - plasma separatrix distances from 9 to 17 cm). Aspects relating to the potential performance and design of the ITER system, will be discussed: (i) the wave coupling performance and validation of the TOPICA modelling code used to predict the coupled power in ITER; (ii) the operation at high coupled power density (up to 6.2 MW/m^2 in L-mode, 4.1 MW/m^2 in H-mode) and high RF voltage on the antenna structure (up to 42 kV); (iii) the coupling of ICRF power during fast variations (ms) in coupling occurring during ELMs and (iv) antenna control in the presence of high mutual coupling between antenna straps.

16:36
UO4 14 Simulations of ITER-like Discharges on Alcator C-Mod C.E. KESSEL, *PPPL* S.M. WOLFE, *PSFC MIT* A.C.C. SIPS, *EURATOM/UKAEA* I.H. HUTCHINSON, *PSFC MIT* Discharges in Alcator C-Mod are being used to examine the plasma evolution under ITER-like conditions in order to benchmark calculations for ITER. These include equivalent current diffusion timescales, q95, betaN, lower single null and ITER shape, at ITER's toroidal field of 5.4 T, and with ICRF heating. Rampup experiments with both ohmic and with ICRF heating were performed. Simulations, with the time-dependent free-boundary plasma evolution code TSC, of these discharges showed that predictions of the Coppi-Tang L-mode energy transport gave rise to too low a temperature near the plasma edge, which consequently caused the current profile to be too peaked. The model, based on profile consistency, was adjusted to broaden the electron temperature profile producing much better agreement with the temperature profile, sawtooth onset, and li. Simulations with GLF23, which has only a boundary condition, showed some difficulties in the L-mode phase. ICRF and LH in the rampup phase of C-Mod was examined with simulations showing that volt-second savings were resistive, similar to the result from ITER simulations. In rampdown experiments, the transition from H-mode to L-mode and the ramp rate were controlled but demonstrated some complex H-L-H behavior with ICRF power reductions. Supported by DE-AC02-09CH11466, DE-FC02-99ER54512.

16:48
UO4 15 Progress in Developing ITER Operational Scenarios on DIII-D* E.J. DOYLE, *UCLA* J.C. DEBOO, J.R. FERRON, R.J. LA HAYE, J.E. KINSEY, T.C. LUCE, P.A. POLITZER, *General Atomics* DIII-D ITER DEMONSTRATION WG TEAM, The DIII-D program has initiated an effort to provide experimental evaluations of four ITER operational scenarios: baseline ELMy H-mode, advanced inductive, hybrid, and steady-state. Discharges in 2008 matched the anticipated ITER design for plasma shape, aspect ratio and value of I/aB, with size reduced by a factor of 3.7, while matching key performance targets for β_N and H_{98y2}. In 2009, attention has focused on improving the match to anticipated ITER parameters: Baseline scenario plasmas have been operated with reduced densities to match the anticipated ITER edge pedestal collisionality, while maintaining target values for β_N and H_{98y2}. These plasmas have enabled a demonstration of 2/1 NTM mode suppression at low q_{95} using ECCD, as planned for ITER. Additional experiments are planned to investigate operation of baseline scenario plasmas with low torque input (low rotation), as well as rf-dominated operation. Comparison of experimental profiles to those from transport modeling will be shown.

*Work supported by the US DOE under DE-FG02-01ER54615 and DE-FC02-04ER54698.

SESSION UO5: COMPRESSION AND BURN
Thursday Afternoon, 5 November 2009
Hanover CDE at 14:00
Richard Town, Lawrence Livermore National Laboratory, presiding

14:00
UO5 1 Shock-Timing Measurements in Directly Driven Spherical Inertial Confinement Fusion Targets T.R. BOEHLY, V.N. GONCHAROV, W. SEKA, D.E. FRATANDUONO, M.A. BARRIOS, S.X. HU, J.A. MAROZAS, T.C. SANGSTER, D.D. MEYERHOFER, *Laboratory for Laser Energetics, U. of Rochester* D.G. HICKS, P.M. CELLIERS, *LLNL* The timing of multiple shock waves in an inertial confinement fusion (ICF) target is critical to its performance. A series of experiments at the Omega Laser Facility used velocity interferometry to measure shocks in directly driven warm and cryogenic targets. Multiple spherical shocks were observed propagating in plastic and liquid deuterium. We report the measured shock velocities and shock coalescence times and compare them to simulations by hydrodynamic codes. This work was supported by the U.S. Department of Energy Office of Inertial Confinement Fusion under Cooperative Agreement No. DE-FC52-08NA28302.

14:12
UO5 2 Multiple-Picket Cryogenic Target Designs and Performance for OMEGA and the National Ignition Facility V.N. GONCHAROV, T.C. SANGSTER, T.R. BOEHLY, R.L. McCRORY, D.D. MEYERHOFER, P.B. RADHA, V.A. SMALYUK, S. SKUPSKY, *Laboratory for Laser Energetics, U. of Rochester* J.A. FRENJE, R.D. PETRASSO, *PSFC-MIT* Low-adiabat cryogenic-target-compression experiments are currently performed on the OMEGA laser. Multiple-picket designs have several advantages over the continuous-drive pulses. First, as shown in recent shock-velocity measurements performed on OMEGA,[1] the shock tuning can be facilitated by replacing the region of gradual intensity rise in the continuous-pulse designs with three pickets. The required shock-timing accuracy can be achieved in this case by adjusting energies of individual pickets. Second, the main pulse's contrast ratio is reduced from 40 to 100 in the continuous designs to 2 to 5 in multiple-picket designs. The latter are also less susceptible to Rayleigh–Taylor instability since the intensity pickets produce an enhanced adiabat steepening at the ablation front, increasing the ablative stabilization. This talk will summarize details of the multiple-picket designs and modeling validation with the experimental data. This work was supported by the U.S. Department of Energy Office of Inertial Confinement Fusion under Cooperative Agreement No. DE-FC52-08NA28302.

[1]T. R. Boehly *et al.*, Phys. Plasmas **16**, 056302 (2008).

14:24

UO5 3 Simulation and Analysis of Backlit Images of Cryogenic Implosions on OMEGA R. EPSTEIN, V.A. SMALYUK, F.J. MARSHALL, J.A. DELETTREZ, V.N. GONCHAROV, P.W. MCKENTY, D.D. MEYERHOFER, P.B. RADHA, S.P. REGAN, T.C. SANGSTER, W. THEOBALD, *Laboratory for Laser Energetics, U. of Rochester* Radiographs of cryogenic implosions on OMEGA have been obtained using short-pulse backlighters driven by the OMEGA EP laser. Computer simulations of an implosion and its x-ray images are used to assess the implosion performance. The radiograph simulation takes into account spatial and temporal resolution, camera spectral response, and the backlighter spectrum. Radial mass distributions are obtained from the radiographs using Abel inversion and the known temperature and density dependence of the free-free opacity of the hydrogen shell. This extends similar analyses of warm-shell radiographs based on the simpler temperature and density dependence of the CH bound-free opacity. The first measurements (which were short of peak compression) are consistent with simulations. More-recent measurements closer to peak compression will be presented. This work was supported by the U.S. Department of Energy Office of Inertial Confinement Fusion under Cooperative Agreement No. DE-FC52-08NA28302.

14:36

UO5 4 Single- and Multidimensional Robustness Studies of the NIF Ignition Point Design K.S. ANDERSON, R. BETTI, P.Y. CHANG, R. NORA, *Laboratory for Laser Energetics and FSC, U. of Rochester* D. SHVARTS, *NCRN* M. FATENEJAD, *U. of Wisconsin* A robustness study of the NIF ignition point-design target is carried out using hydrodynamically equivalent, all-DT direct-drive targets. The direct-drive targets have similar final mass, kinetic energy, implosion velocity, and adiabat of the indirect-drive point design. The direct-drive target has an equivalent one-dimensional ignition-threshold factor [ITF (1-D)] to the indirect-drive point design. A 1-D sensitivity study of ignition is carried out for various hot-spot conditions, gas pressures, and preheat levels. The hot-spot conditions are varied by changing the thermal conductivity. Two-dimensional studies were performed relating the yield over clean (YOC) of a hydro-equivalent THD surrogate target to fusion gain in the DT ignition target. From these studies is found the minimum THD YOC required to demonstrate ignition in the DT campaign. This work was supported by the U.S. Department of Energy Office of Inertial Confinement Fusion under Cooperative Agreement Nos. DE-FC02-ER54789 and DE-FC52-08NA28302.

14:48

UO5 5 2-D Simulations of a 1-MJ CH-Foam Ignition Target on the NIF with 0.5 THz of 1-D Multi-FM SSD Bandwidth Using an Analytic Model J.A. MAROZAS, J.D. ZUEGEL, T.J.B. COLLINS, *Laboratory for Laser Energetics, U. of Rochester* The 1-D multiple-frequency-modulator (Multi-FM) smoothing by spectral dispersion (SSD) system smoothes efficiently by taking advantage of multiple color cycles dispersed across the laser-beam cross section. An analytic SSD model has been enhanced to handle multiple modulators in one or both orthogonal directions. Previously, modeling Multi-FM required an ensemble of simulations that employed random flipping of phase states at every coherence time. The analytic model incorporates the necessary statistical averaging, so only a single simulation is required. An ensemble of random flipping simulations is compared to a simulation of the analytic model. The simulations use the 2-D radiation-hydrodynamics code *DRACO* of a 1.0-MJ CH-foam ignition target on the NIF with 0.5 THz of bandwidth. Dynamic bandwidth reduction is used to increase the angular divergence during the foot of the pulse. This work was supported by the U.S. Department of Energy Office of Inertial Confinement Fusion under Cooperative Agreement No. DE-FC52-08NA28302.

15:00

UO5 6 Validating Inertial Confinement Fusion (ICF) predictive capability using perturbed capsules* MARK SCHMITT, GLENN MAGELSSEN, IAN TREGILLIS, SCOTT HSU, PAUL BRADLEY, EVAN DODD, JAMES COBBLE, KIRK FLIPPO, DUSTIN OFFERMAN, KIMBERLY OBREY, YI-MING WANG, ROBERT WATT, MARK WILKE, FREDERICK WYSOCKI, STEVEN BATHA, *Los Alamos National Laboratory* Achieving ignition on NIF is a monumental step on the path toward utilizing fusion as a controlled energy source. Obtaining robust ignition requires accurate ICF models to predict the degradation of ignition caused by heterogeneities in capsule construction and irradiation. LANL has embarked on a project to induce controlled defects in capsules to validate our ability to predict their effects on fusion burn. These efforts include the validation of feature-driven hydrodynamics and mix in a convergent geometry. This capability is needed to determine the performance of capsules imploded under less-than-optimum conditions on future IFE facilities. LANL's recently initiated Defect Implosion Experiments (DIME) conducted at Rochester's Omega facility are providing input for these efforts. Recent simulation and experimental results will be shown.

*Work sponsored by US DOE/NNSA, performed at LANL, operated by LANS LLC under contract DE-AC52-06NA25396.

15:12

UO5 7 Design of High-Neutron-Yield Polar-Drive Experiments for Diagnostic Activation on the NIF P.W. MCKENTY, R.S. CRAXTON, J.A. MAROZAS, A.M. COK, D.D. MEYERHOFER, R.L. MCCRORY, *Laboratory for Laser Energetics, U. of Rochester* J.D. KILKENNY, A. NIKROO, M.L. HOPPE, M.J. EDWARDS, *General Atomics* D.H. MUNRO, *LLNL* Polar-drive (PD)[1] target implosions have been designed for neutron diagnostic development on the NIF. These experiments use thin, room-temperature glass shells filled with low pressures of DT. Initial target implosions on the NIF will produce DT yields in the range of a few 10^{14} neutrons. The predicted yields are consistent with earlier data (10^{14} neutrons at 30 kJ) and recent PD scoping experiments performed on OMEGA. The experiments will use existing x-ray-drive phase plates with judicious repointing and defocusing to drive the implosions as uniformly as possible. Current simulation results indicate that the required yields will be obtained using up to 200-kJ UV light. Large-diameter glass shells ($\sim$ 1500-μm OD) are under development and fabrication at General Atomics. As tritium and environmental conditions evolve, similar target designs are expected to produce thermonuclear yields approaching 10^{16} neutrons. This work was supported by the U.S. Department of Energy Office of Inertial Confinement Fusion under Cooperative Agreement No. DE-FC52-08NA28302.

[1]A. M. Cok, R. S. Craxton, and P. W. McKenty, Phys. Plasmas **15**, 082705 (2008).

15:24
UO5 8 Polar-Driven Implosions on OMEGA: Observations and Simulations of Low-Mode Perturbations in the Main Fuel Layer and Hot Spot F.J. MARSHALL, R.S. CRAXTON, R. EPSTEIN, V.YU. GLEBOV, V.N. GONCHAROV, J.P. KNAUER, P.W. McKENTY, P.B. RADHA, A. SHVYDKY, *Laboratory for Laser Energetics, U. of Rochester* J.A. FRENJE, C.K. LI, R.D. PETRASSO, F.H. SÉGUIN, *PSFC, MIT* Low-adiabat, directly driven implosion experiments have been performed on OMEGA using 40 beams in the polar-drive configuration, emulating the configuration of the beams of the NIF. The targets are noncryogenic, D_2-gas-filled CH capsules. The areal-density time history of the CH shell and its low-mode perturbations are determined from x-ray radiographs. The conditions of the central fuel region are diagnosed with particle measurements including neutron yield and time history, while low-mode perturbations of the hot spot are determined from framed images of the hot spot's x-ray emission. The observed perturbations are compared with simulations using the 2-D hydrocode *DRACO*. This work was supported by the U.S. Department of Energy Office of Inertial Confinement Fusion under Cooperative Agreement No. DE-FC52-08NA28302.

15:36
UO5 9 Numerical Investigation of the Effects of Cross-Beam Energy Transfer on the Drive Uniformity of OMEGA Implosions A. SHVYDKY, P.W. McKENTY, J.A. DELETTREZ, I.V. IGUMENSHCHEV, D.H. EDGELL, S. SKUPSKY, R.L. McCRORY, *Laboratory for Laser Energetics, U. of Rochester* Evaluation of the scattered light in OMEGA implosions indicates that cross-beam energy transfer caused by stimulated Brillouin scattering (SBS) may explain the observed reduction in the absorbed energy and the details of the spectral shifts in the scattered light. Recently, an *ad-hoc* model of the cross-beam energy transfer has been implemented that scatters light from the central portions of laser beams to reflected, outgoing rays before reaching the critical region. Such a process decreases the total absorption and increases laser deposition nonuniformities. In this paper, using the 2-D radiation-hydrodynamics code *DRACO*, we investigate these two effects and how they affect the implosion uniformity and target performance in OMEGA implosions. High- and low-adiabat plastic and cryogenic implosions are considered, and the simulation results are compared with available OMEGA experiments. This work was supported by the U.S. Department of Energy Office of Inertial Confinement Fusion under Cooperative Agreement No. DE-FC52-08NA28302.

15:48
UO5 10 Analysis of the Effect of a High-Z-doped CH Ablator and Glass Ablators on Preheat and Hard X-Ray Radiation from Two-Plasmon Decay Electrons J.A. DELETTREZ, J.P. KNAUER, V.N. GONCHAROV, P.B. RADHA, C. STOECKL, A.V. MAXIMOV, *Laboratory for Laser Energetics, U. of Rochester* J.A. FRENJE, *PSFC, MIT* D. SHVARTS, *NRCN* The generation of preheating electrons from two-plasmon decay (TPD) can be mitigated by doping CH shells with Si or Ge or by using glass ablators. Simulations were carried out with a recent model for the source of the TPD fast electrons based on the results of warm-CH-shell implosions. The source energy varies as the threshold parameter $\sim I \times L/T_e$ at quarter critical. The presence of high-Z dopants increases the temperature, which leads to a decrease in the energy deposited into the fast electrons and a reduction in the resulting preheat. The presence of high-Z dopants, however, leads to higher radiation preheat. This presentation will discuss the effect of the dopants on the fast-electron source and the trade-off between the two forms of preheat in terms of the expected ρR's for both warm-CH and cryogenic implosions. This work was supported by the U.S. Department of Energy Office of Inertial Confinement Fusion under Cooperative Agreement No. DE-FC52-08NA28302.

16:00
UO5 11 Intensity Dependence of Target Performance in Low-Adiabat, Warm Implosions on OMEGA P.B. RADHA, C. STOECKL, V.N. GONCHAROV, J.A. DELETTREZ, T.C. SANGSTER, R. BETTI, R.L. McCRORY, D.D. MEYERHOFER, S.P. REGAN, W. SEKA, S. SKUPSKY, V.A. SMALYUK, *Laboratory for Laser Energetics, U. of Rochester* D. SHVARTS, *NRCN* Low-adiabat cryogenic implosions on OMEGA indicate degraded areal densities with increasing intensity. Possible causes include shock mistiming, preheat attributable to coronal fast electrons, and the shadowing of laser illumination caused by silks used to suspend cryogenic targets. Low-adiabat, warm implosion experiments have been designed to study compression in capsule implosions. The adiabat in the shell is set primarily by the foot of the laser pulse and is relatively insensitive to shock mistiming. The plastic ablator in these implosions is similar to the ablator in cryogenic implosions, yielding a very similar density scale length, temperature, and intensity at the quarter-critical surface. Target performance including areal density, yield, bang time, and coronal emission is studied as a function of intensity on OMEGA. Analysis and comparison of experimental observations with 1-D and 2-D simulations will be presented. This work was supported by the U.S. Department of Energy Office of Inertial Confinement Fusion under Cooperative Agreement No. DE-FC52-08NA28302.

16:12
UO5 12 The effects of laser absorption and mix on direct-drive capsule experiments at OMEGA E.S. DODD, J.F. BENAGE, G.A. KYRALA, I.L. TREGILLIS, D.C. WILSON, F.J. WYSOCKI, *LANL* W. SEKA, V. YU. GLEBOV, *LLE, UR* J.A. FRENJE, *MIT* The yield of an ICF capsule can be affected by the inclusion of high-Z material in the fuel, either as a diagnostic or from hydrodynamic mixing. A series of experiments have been fielded at the OMEGA laser to better understand these effects. The targets are glass shells filled with a mixture of D_2 and ^{3}He, and with controlled amounts of a dopant, Ar, Kr, and/or Xe. These targets are then directly driven with a 1.0 ns (0.6 ns) square laser pulse having a total energy of 23 kJ (13.8 kJ), and the data compared with yield and burn-temperature predictions from 1-d radiation-hydrodynamics calculations. However, our calculated yields are typically a factor of two greater than the measured yield, while the calculated burn-weighted temperatures are lower. Estimates for the amount of absorbed laser energy indicate that only 65% to 70% is absorbed. However, our calculations absorb 85% of the energy. The ratio of D^3He-protons to DT-neutrons also indicates that mixing of shell material has occurred. We will discuss the results of recent 1-d calculations where the incident energy and flux limiter have been varied to match the absorption data. We will also discuss the use of a mix-model to match the charged particle data. Supported by US DOE and LANS, LLC under contract DE-AC52-06NA25396. LA-UR-09-04488

16:24
UO5 13 Measurements of Low-Deuterium Surrogates for the Prediction of Ignition Implosion Performance BRIAN SPEARS, S. BRANDON, D. CLARK, C. CERJAN, J. EDWARDS, O. LANDEN, J. LINDL, S. HAAN, S. HATCHETT, J. SALMONSON, P. SPRINGER, S. WEBER, *LLNL* D. WILSON, *LANL* The National Ignition Campaign (NIC) will use non-igniting "THD" capsules to study and optimize the hydrodynamic assembly of the fuel without burn. These capsules are designed to simultaneously reduce DT neutron yield and to maintain hydrodynamic similarity with the DT ignition capsule. We have developed an experimentally observable ignition threshold factor (ITFX) that uses measurements from THD experiments to predict DT ignition implosion performance. The ITFX metric was developed using a database of 2D radhydro simulations of twin DT and THD implosions with a variety of physical failure mechanisms – drive asymmetry, capsule roughness, continuum mixing, fabrication errors, among others. The ITFX encodes all of these failure mechanisms into a single observable metric. The ITFX metric has also allowed us to develop a capability to estimate the probability of DT capsule ignition based on THD experiments. Prepared by LLNL under Contract DE-AC52-07NA27344. LLNL-ABS-414651

16:36
UO5 14 The Use of Tritium Rich Surrogate Capsules with High Deuterium Concentrations to Diagnose Ignition* D.C. WILSON, *Los Alamos National Laboratory* B.K. SPEARS, S.P. HATCHETT II, C.J. CERJAN, P.T. SPRINGER, D.S. CLARK, *Lawrence Livermore National Laboratory* M.J. EDWARDS, J.D. SALMONSON, S.V. WEBER, B.A. HAMMEL, *Lawrence Livermore National Laboratory* G.P. GRIM, H.W. HERRMANN, M.D. WILKE, *Los Alamos National Laboratory* The path to ignition at the National Ignition Facility (NIF) relies upon experimentally tuning target conditions. Capsules with mixtures of Tritium, Hydrogen, and Deuterium (THD) can be made hydrodynamically equivalent to 50:50 DT capsules, up to the time when the alpha particle heating becomes significant. Above about 10% deuterium alpha heating, thermal conduction, and electron-ion disequilibria begin to be important. The ion temperature increases and both X-ray and neutron images become larger and more symmetric. As ignition is approached, the fraction of neutrons scattered by the fuel and the burn duration decrease. The high yields from these capsules preclude time resolved X-ray imagers, but allow time resolution of gamma ray emission. The large variation in neutron yield between capsules that would ignite and those that fail improves the ability to predict ignition with 50% deuterium.

*Supported by the USDOE through LANL and LLNL.

16:48
UO5 15 NIF Ignition Target with High-Density Carbon (HDC) Ablator* DARWIN HO, STEVEN HAAN, JAY SALMONSON, LORIN BENEDICT, JUERGEN BIENER, *Lawrence Livermore National Laboratory* MARK HERRMANN, *Sandia National Laboratory* High-density carbon as an NIF ignition capsule ablator material has several advantages including a very smooth surface finish and small grain structure. Recent Omega experiments[1] show that if the first shock in the ablator is higher than about 6.5 Mbar, which is in the liquid/solid 2-phase region of the carbon phase diagram, then the shock uniformity becomes comparable to that of the Be ablator. Consequently, this is the strength that we adopt for the first shock in our latest HDC capsule design. Using various scanning techniques, the capsule configuration and drive temperature profile are optimized. We describe the 1-D margin and 2-D stability behavior of the optimized point design.

*This work was completed under the auspices of the U.S. Department of Energy by Lawrence Livermore National Laboratory under Contract DE-AC52-07NA27344.

[1]P. M. Celliers private communication

SESSION UO6: BASIC PLASMA PHENOMENA: THEORY AND SIMULATION
Thursday Afternoon, 5 November 2009
Hanover FG at 14:00
Gurudas Ganguli, Naval Research Laboratory, presiding

14:00
UO6 1 Stochastic Flux-Freezing for Non-Ideal Hydromagnetic Plasmas* GREGORY EYINK, *Applied Math and Statistics, Johns Hopkins University* Non-ideal (viscous and resistive) magnetohydrodynamic plasmas are shown to possess stochastic versions of ideal flux-freezing laws. The magnetic field at a point is equal to the average of an infinite ensemble of field-lines advected to that point by the plasma velocity perturbed with a random white-noise (stochastic Lundquist formula). This implies a stochastic Alfvén theorem, valid for any value of the magnetic Prandtl number. At unit Prandtl number there is also a random version of the generalized Kelvin theorem derived by Bekenstein-Oron for ideal MHD. These stochastic conservation laws are not only consequences of the non-ideal MHD equations, but are in fact equivalent to those equations. Similar results hold for Hall magnetohydrodynamics and the two-fluid plasma model. We argue that flux-conservation remains stochastic for turbulent MHD plasmas in the limit of infinite Reynolds numbers. Infinitely-many field lines are advected to each point by turbulent Richardson diffusion. The reconnection speed for pairs of field lines is the relative velocity of the turbulent fluid at their initial locations. Small-scale turbulent dynamo effect is rigorously related to angular correlation of the individual field vectors before reconnection.

*This work was supported by NSF grant AST-0428325

14:12
UO6 2 Scale-locality of energy transfer in magnetohydrodynamic turbulence.* HUSSEIN ALUIE, GREGORY L. EYINK, *Johns Hopkins University* We investigate scale-locality of energy cascade in magnetohydrodynamic (MHD) turbulence at high kinetic and magnetic Reynolds numbers. There is a growing consensus that large-scale flow can transfer energy to the magnetic field at arbitrarily small scales in the inertial range (Alexakis et al. (2005,2007), Carati et al. (2006), Yousef et al. (2007), Schekochihin et al. (2008), etc.) However, we rigorously prove that such non-local transfer cannot occur, under very weak scaling conditions for velocity and magnetic-field increments accepted to hold in the inertial-inductive range of turbulent MHD flows. Our analysis shows that inter-scale fluxes of two conserved quantities, total energy and cross helicity, are dominated by local triadic interactions. Nonlocal triads make an asymptotically negligible contribution, decaying as a power of the scale-disparity. Furthermore,

nonlocal-in-scale triads may dominate in field-line stretching, but energy conversion by stretching is primarily between velocity and magnetic-field modes at comparable scales. To verify our analytical results, we present data of forced MHD turbulence from a pseudospectral simulation on a grid of 1024^3 points with phase-shift dealiasing.

*Computer time provided by DLMS at the Johns Hopkins University and support from NSF grant # ASE-0428325 are gratefully acknowledged.

14:24

UO6 3 New approach to MHD spectral theory of stationary plasma flows HANS GOEDBLOED, *FOM-Institute for Plasma Physics* The basic equations of MHD spectral theory date back to 1958 for static plasmas (Bernstein et al.) and to 1960 for stationary plasma flows (Frieman and Rotenberg). The number of papers on the two subjects appears to be inversely proportional to their complexity, with the vast majority of contributions to MHD stability of tokamaks being restricted to static equilibria and stationary equilibrium flows mostly being discussed analytically for trivial equilibria or numerically for complicated geometries. The problem with the latter is not that numerical approaches are inaccurate, but that they suffer from lack of analytical guidance concerning the structure of the spectrum. One of the reasons is the usual misnomer of "non-self adjointness" of the stationary flow problem. In fact, self-adjointness of the two occurring operators was proved right away. Based on the two quadratic forms corresponding to these operators, (a) we constructed an effective method to compute the eigenvalues in the complex plane, (b) we found the counterpart of the oscillation theorem for eigenvalues of static equilibria (Goedbloed and Sakanaka, 1974) for the eigenvalues of stationary flows, enabling one to map out sequences of eigenvalues in the complex plane. Examples will be given for Rayleigh-Taylor, Kelvin-Helmholtz and magneto-rotational instabilities.

14:36

UO6 4 Variational principle for multi region three dimensional relaxed magnetohydrodynamic equilibria* R.L. DEWAR, *Plasma Research Laboratory, Australian National University (ANU)* S.R. HUDSON, *Princeton Plasma Physics Laboratory* M.J. HOLE, M. McGANN, *ANU* Z. YOSHIDA, *University of Tokyo* Relaxed-magnetohydrodynamic (RXMHD) plasma equilibria are force-free states obtained by minimizing the magnetic energy subject to the constraint of constant magnetic helicity and magnetic fluxes within perfectly conducting toroidal boundaries, giving rise to the Beltrami equation, $\nabla \times \mathbf{B} = \mu \mathbf{B}$, with $\mathbf{B}$ the magnetic field and μ const. The Beltrami equation being consistent with the existence of field-line chaos, such a principle is suitable as a starting point for three-dimensional equilibrium theory. An extension of this variational principle to finite-pressure *multi-region* relaxed MHD (MRXMHD) is developed, in which the total plasma energy, magnetic plus kinetic, is to be minimized assuming arbitrarily thin, ideal-MHD toroidal interfaces act as flexible barriers to thermal and magnetic relaxation. Formal expressions for the variations of total energy with respect to Lagrangian displacements of the barrier interfaces are derived. Generalized magnetic coordinates and the need for control of rotational transforms on the surfaces of the interfaces are discussed.

*Research supported by Australian Research Council and DOE.

14:48

UO6 5 Discontinuous Galerkin Methods for Magnetohydrodynamics JAMES ROSSMANITH, *University of Wisconsin - Madison* Standard shock-capturing numerical methods fail to give accurate solutions to the equations of magnetohydrodynamics (MHD). The essential reason for this failure is that by ignoring the divergence-free constraint on the magnetic field, these methods can be shown to be entropy unstable. In this talk we will briefly review the entropy stability theorem for discontinuous Galerkin (DG) methods. We will then present a class of constrained transport (CT) methods that we will show give both stable and accurate results on several test cases. The proposed CT approach can be viewed as a predictor-corrector method, where an approximate magnetic field is first *predicted* by a standard DG method, and then *corrected* through the use of a magnetic potential. Finally, we will briefly describe efforts to extend this approach to Hall MHD and genuinely two-fluid plasma models.

15:00

UO6 6 Two Dimensional Computer Modeling of Plasmas Using Adaptive Mesh Refinement MARK BERRILL, JORGE ROCCA, *Colorado State University* NSF ERC FOR EXTREME ULTRAVIOLET SCIENCE AND TECHNOLOGY TEAM, An understanding of the physics of laser-created plasma which is important for a wide range of applications often requires a detailed modeling of multi-dimensional effects. We report on a new 2D hydrodynamic plasma model to simulate laser created plasmas. The computer model simulates the plasma by solving the hydrodynamic equations with an atomic model. The equations are discretized on a rectangular Eulerian grid using adaptive mesh refinement (AMR). Multiple levels of refinement with an automatic grid generation allows for accurate simulations while minimizing the run time. The model is capable of running on high performance computers. The current capabilities of the model will be discussed and results of simulations performed to model plasma-based tabletop soft x-ray lasers. Work supported by the NSF EUV ERC Award #EEC-0310717 and the NNSA SSAA program through DOE Grant #DE-FG52-060NA26152. M.B. was support by DOE CSGF Grant #DE-FG02-97E.

15:12

UO6 7 Vlasov simulation in multiple spatial dimensions HARVEY ROSE, WILLIAM DAUGHTON, *Los Alamos National Laboratory* One of the outstanding challenges encountered in modeling plasma is simulating the Vlasov equation over length and time scales that are physically relevant to real experiments. Plasma processes that depend sensitively on spatial dimension include linear ones such as diffraction and its nonlinear variant, self-focusing, cannot be simulated in one spatial dimension (1D). Direct multi-D Vlasov simulations are prohibitive while unphysical particle noise and Debye length resolution may severely constrain multi-D particle in cell (PIC) simulations. We have developed a Vlasov Multi-Dimensional (VMD) model that is specifically designed to take advantage of solution properties in regimes when plasma waves are confined to a narrow cone. Perpendicular grid spacing large compared to a Debye length is then possible without instability, enabling a factor of order 10 decrease in required computational resources compared to standard PIC methods in 2D and another factor of that order in 3D. Further advantage accrues in regimes where particle noise is an issue. VMD and PIC results in a 2D model of localized Langmuir waves are in quantitative agreement.

15:24

UO6 8 Enabling Global Kinetic Simulations of the Magnetosphere via Petascale Computing H. KARIMABADI, H.X. VU, Y.A. OMELCHENKO, *SciberQuest, Inc/UCSD* M. TATINENI, A. MAJUMDAR, *UCSD* U.V. CATALYUREK, E. SAULE, *OSU* The ultimate goal in magnetospheric physics is to understand how the solar wind transfers its mass, momentum and energy to the magnetosphere. This problem has turned out to be much more complex intellectually than originally thought. MHD simulations have proven useful in predicting eminent features of substorms and other global events. Given the complexity of solar wind-magnetosphere interactions, hybrid (electron fluid, kinetic ion) simulations have recently been emerging in the studies of the global dynamics of the magnetosphere with the goal of accurately predicting the energetic particle transport and structure of plasma boundaries. We take advantage of our recent innovations in hybrid simulations and the power of massively parallel computers to make breakthrough 3D global kinetic simulations of the magnetosphere. The preliminary results reveal many major differences with global MHD simulations. For example, the hybrid simulations predict the formation of the quadruple structure associated with reconnection events, ion/ion kink instability in the tail, turbulence in the magnetosheath, and formation of the ion foreshock region.

15:36

UO6 9 A Multifluid Interpenetration Mix Model* BAOLIAN CHENG, ANTHONY SCANNAPIECO, *Los Alamos National Lab* In this work, we present a multifluid interpenetration mix model that consists of a set of multifluid moment equations, with and without both internal and external fields. This model is derived from the collisional Boltzmann equation in a self-consistent manner. The external fields can be either grativational as in astrophysics and Rayleigh-Taylor (RT) mixing problems, or shock acceleration as in Richtmyer-Meshkov (RM) mixing problems, electric and magnetic fields as in magnetic confinement fusion, and rotational forces as in chemical applications. The model equations are mathematically closed and physically consistent with one free parameter, contained in a phenomenological closure for the collisional frequency, which is determined by experimental data. The set of model equations provide a theoretical foundation for a large fraction of phenomenological mix models. They contain all the physical terms, particularly the terms associated with the Reynolds stress due to both species interpenetrations and random chaotic motions. Under certain assumptions, these model equations successfully reduce to the various other mix models. The successful applications of this model in both direct drive and radiatively driven inertial confinement fusion (ICF) capsule implosions are discussed.

*This work was performed under the auspices of the U.S. Department of Energy by the LANL under contract number W-7405-ENG-36.

15:48

UO6 10 Wave Packet Molecular Dynamics and Radiation in Hot Dense Plasmas* FRANK GRAZIANI, RICHARD MORE, *Lawrence Livermore National Laboratory* MICHAEL MURILLO, *Los Alamos National Laboratory* Wave packet molecular dynamics (WPMD) has proven to be a valuable computational tool l for modeling dense plasmas where large scale collective effects are determined by classical processes (screening) and short distances are determined by quantum mechanical processes (diffraction and Pauli blocking). For hot dense fully ionized plasmas in the keV or greater temperature regime, free-free transitions dominated by bremsstrahlung and inverse- bremsstrahlung need to be included. We extend the current WPMD formalism to include both classical and quantum mechanical radiation fields. In the latter case, both spontaneous and stimulated emission is included in the wave packet dynamics. The implementation of this technique into a massively parallel MD code is briefly discussed.

*This work performed under the auspices of the U.S. Department of Energy by Lawrence Livermore National Laboratory under Contract No. DE-AC52-07NA27344.

16:00

UO6 11 Dynamics and Melting of Finite Plasma Crystals PATRICK LUDWIG, HANNO KÄHLERT, HENNING BAUMGARTNER, HAUKE THOMSEN, MICHAEL BONITZ, *University of Kiel* Interacting few-particle systems in external trapping potentials are of strong current interest since they allow to realize and control strong correlation and quantum effects [1]. Here, we present our recent results on the structural and thermodynamic properties of the crystal-like Wigner phase of complex plasma confined in a 3D harmonic potential. We discuss the linear response of the strongly correlated system to external excitations, which can be described in terms of normal modes [2]. By means of first-principle simulations the details of the melting phase transitions of these mesoscopic systems are systematically analysed with the melting temperatures being determined by a modified Lindemann parameter for the pair distance fluctuations [3]. The critical temperatures turn out to be utmost sensitive to finite size effects (i.e., the exact particle number), and form of the (screened) interaction potential. [1] PhD Thesis, P. Ludwig, U Rostock (2008) [2] C. Henning et al., J. Phys. A 42, 214023 (2009) [3] Böning et al., Phys. Rev. Lett. 100, 113401 (2008)

16:12

UO6 12 Thermodynamic Theory of Spherically Trapped Coulomb Clusters JEFFREY WRIGHTON, JAMES DUFTY, *University of Florida* MICHAEL BONITZ, HANNO KÄHLERT, *Christian-Albrechts-Universität zu Kiel* The radial density profile of a finite number of identical charged particles confined in a harmonic trap is computed over a wide ranges of temperatures (Coulomb coupling) and particle numbers. At low temperatures these systems form a Coulomb crystal with spherical shell structure which has been observed in ultracold trapped ions and in dusty plasmas. The shell structure is readily reproduced in simulations. However, analytical theories which used a mean field approach[1] or a local density approximation[2] have, so far, only been able to reproduce the average density profile. Here we present an approach to Coulomb correlations based on the hypernetted chain approximation with additional bridge diagrams. It is demonstrated that this model reproduces the correct shell structure within a few percent and provides the basis for a thermodynamic theory of Coulomb clusters in the strongly coupled fluid state.[3]

[1]C. Henning et al., Phys. Rev. E 74, 056403 (2006)
[2]C. Henning et al., Phys. Rev. E 76, 036404 (2007)
[3]J. Wrighton, J.W. Dufty, H. Kählert and M. Bonitz, J. Phys. A 42, 214052 (2009) and Phys. Rev. E (2009) (to be submitted)

16:24
UO6 13 Breathing is different in the quantum world* MICHAEL BONITZ, SEBASTIAN BAUCH, KARSTEN BALZER, CHRISTIAN HENNING, DAVID HOCHSTUHL, *Kiel University, Inst. Theoretical Physics and Astrophysics* Interacting classicle particles in a harmonic trap are known to possess a radial collective oscillation – the breathing mode (BM). In case of Coulomb interaction its frequency is universal – it is independent of the particle number and system dimensionality [1]. Here we study strongly correlated quantum systems. We report a qualitatively different breathing behavior: a quantum system has *two BMs* one of which is universal whereas the frequency of the other varies with system dimensionality, the particle spin and the strength of the pair interaction. The results are based on exact solutions of the time-dependent Schrödinger equation for two particles and on time-dependent many-body results for larger particle numbers. Finally, we discuss experimental ways to excite and measure the breathing frequencies which should give direct access to key properties of trapped particles, including their many-body effects [1] C. Henning et al., Phys. Rev. Lett. 101, 045002 (2008) [2] S. Bauch, K. Balzer, C. Henning, and M. Bonitz, submitted to Phys. Rev. Lett., arXiv:0903.1993

*Supported by Deutsche Forschungsgemeinschaft via SFB-TR 24.

16:36
UO6 14 Thomson scattering in warm dense matter R. THIELE, T. BORNATH, *University of Rostock* R.R. FÄUSTLIN, *DESY Hamburg* C. FORTMANN, *University of Rostock* S. GLENZER, *LLNL* G. GREGORI, *University of Oxford* B. HOLST, *University of Rostock* T. TSCHENTSCHER, *XFEL Hamburg* V. SCHWARZ, R. REDMER, *University of Rostock* Free electron lasers employing scattering of high-brilliant, coherent photons in the extreme ultraviolet (VUV), e.g. at FLASH (DESY Hamburg) or LCLS (Stanford), allow for a systematic study of basic plasma properties in the region of warm dense matter (WDM). WDM is characterized by condensed matter-like densities and temperatures of several eV. Collective Thomson scattering with VUV or x-ray has demonstrated its capacity for robust measurements of the free electron density and temperature in WDM. Collective excitations like plasmons ("electron feature") appear as maxima in the scattering signal. The respective frequencies can be related to the free electron density. Furthermore, the asymmetry of the red- and blue shifted plasmon intensity gives the electron temperature due to detailed balance. We treat collective Thomson scattering in the Born-Mermin-approximation which includes collisions and present a generalized Gross-Bohm dispersion for plasmas. The influence of plasma inhomogeneities on the scattering spectrum is studied by comparing density and temperature averaged scattering signals with calculations assuming homogeneous targets. For the "ion feature," results of semi-classical hypernetted chain (HNC) calculations and of quantum molecular dynamics simulations are shown for dense beryllium.

16:48
UO6 15 Molecular dynamics simulations of electron-ion temperature equilibration in an SF6 plasma LORIN X. BENEDICT, JAMES N. GLOSLI, DAVID F. RICHARDS, FREDERICK H. STREITZ, STEFAN P. HAU-RIEGE, RICHARD A. LONDON, FRANK R. GRAZIANI, *Lawrence Livermore National Lab* MICHAEL S. MURILLO, JOHN F. BENAGE, *Los Alamos National Lab* We describe classical non-equilibrium molecular dynamics simulations aimed at studying electron-ion temperature equilibration in a two-temperature SF_6 plasma. We choose a density of 1.0×10^6 (dissociated) SF_6 molecules per cm ^{3} and initial temperatures of $T_e = 100$ eV and $T_S = T_F = 15$ eV, in accordance with experiments currently underway at Los Alamos National Lab. Our computed relaxation time lies between two oft-used variants of the Landau-Spitzer relaxation formula. Discrepancies are also found when comparing to the predictions of more recent theoretical approaches. These differences should be large enough to be measured in the upcoming experiments. We highlight one particular source of discrepancy arising from the strong ion-ion coupling: the time-dependent specific heat of the screened ion subsystem.

SESSION UO7: MAGNETO INERTIAL FUSION AND NEUTRON GENERATION
Thursday Afternoon, 5 November 2009
Regency VII at 14:00
James Degnan, Kirtland AFRL, presiding

14:00
UO7 1 Effects of external and self-generated magnetic fields on laser-driven implosions* O. POLOMAROV, P. CHANG, O. GOTCHEV, R. BETTI, *FSC/LLE, U. of Rochester* The magnetized laser-driven implosions are studied using ALE hydro-code DRACO coupled with the newly developed MHD block (with anisotropic, B-dependent transport coefficients). Considered: i) compression of an externally imposed magnetic field and ii) self-generation of the magnetic field by non-collinear density and pressure gradients. For the first case, it is shown that the moderate external magnetic field of ($<$ 10 Tesla) can be compressed to hundreds of Mega-Gauss at the implosion stagnation [O. Gotchev et al., submitted to PRL, (2009)]. The field of such amplitude can influence the thermal flux from the target core and results in noticeable effects on the target hydro-dynamics. For the second case, it is shown that the self-generated magnetic field can be amplified to the multi-mega-gauss level at the different implosion stages by at least three MHD-related mechanisms: i) the Tidman instability due to a lateral B-dependent heat flux, ii) the Rayleigh-Taylor instability at the ablation front and, iii) the corrugation instability of spherical shock fronts. It is also shown that the magnetic field initially produced at the critical surface significantly reduces the imprinting of laser irradiation non-uniformities onto the ablation surface.

*Supported by Grants DEFG02-04ER54768 and DE-FC02-ER54789.

14:12
UO7 2 Foil Liner Compression of FRCs to Megagauss Fields* JOHN SLOUGH, DAVID KIRTLEY, CHRIS PIHL, GEORGE VOTROUBEK, *MSNW LLC* RICHARD MILROY, GEORGE MARKLIN, *University of Washington* The Foil Liner Compression Experiment will explore the metallic liner compression of the FRC where a theta pinch compression coil will be employed to drive a thin foil liner. The intention is to reduce the complexity and enhance the survivability of the apparatus, as well as minimize the kinetic energy required to reach fusion conditions. It is believed that it is possible to accomplish this at sub-megajoule energies. This however will require operation at very small scale. At small scale the implosion speed must be reasonably fast to maintain the

magnetized plasma (FRC) equilibrium during compression. These additional considerations imply that a relatively thin liner must be employed. For limited liner kinetic energy, it becomes clear that the thinnest liner imploded to the smallest radius consistent with the requirements for FRC equilibrium lifetime is desired. For the experiments planned, existing facilities for FRC target creation will be adapted for insertion into an aluminum foil liner with a radius of 70 mm and a thickness of 0.1 mm. A key component of this work will be advancement of the numerical codes to provide accurate and predictive capabilities of the plasma/foil liner compression. These efforts will also be discussed.

*Work supported by the DOE OFES

14:24

UO7 3 Plasma Liner Formation and Compression Experiments on PLC* GEORGE VOTROUBEK, JOHN SLOUGH, CHRIS PIHL, DAVID KIRTLEY, *MSNW, LLC* To make fusion practical at small scale, an efficient method for repetitively compressing the FRC to fusion gain conditions is required. A promising approach that is being explored at the MSNW facility employs a plasma shell to radially compress and heat the FRC plasmoid to fusion conditions. The energy that is required for the implosion compression and heating of the FRC plasmoid is derived from both the radial kinetic energy of the plasma liner used to compress it, and the axial kinetic energy of the FRC's motion prior to compression. The design, construction testing of the large array (32) of MPD plasma sources has been completed and initial testing of the liner formation and implosion are underway. Liner masses of 3 mg have been formed in Xenon and have been accelerated to a velocity of 36 km/s employing a theta pinch compression coil at 0.5 T. In these experiments roughly half of the compression bank energy is transferred to the plasma liner. Details of the liner dynamics and future plans for FRC compression with the liner will be discussed.

*This research supported by US DOE.

14:36

UO7 4 ICF Hybrid Burner Using Tritium-Lean Targets GEORGE MILEY, XIAOLING YANG, SUNG-JIN KIM, *University of Illinois* HEINRICH HORA, *U of New South Wales, Australia* A near-term ICF driven actinide burner has gained much interest. However, the D-T ICF approach with tritium breeding gives a low support ratio. We propose here using fast ignition of tritium-lean targets to obtain a higher fraction of useful neutrons by reducing tritium-breeding requirements while lowering neutron-induced material damage [1]. This approach appears feasible as simulations show fast ignited tritium-lean targets use only a modest added input-energy over DT targets [2, 3]. Further, discovery of the "block ignition" concept is even more encouraging [3]. Thus we suggest the added time to go directly to tritium lean ICF burners (vs. D-T) is minimal. The presentation reviews physics and technology issues for development of a competitive actinide burner. [1] M. Ragheb, et al., "Alternate approach to ICF with low tritium inventories and high power densities," *J. Fus. Energy* **4**, 339-351 (1985). [2] G. N. Miley, "Tritium-Lean Fusion Reactors Revisited," *ANS TOFE Conference*, San Francisco, CA, Sept. 2008. [3] G.H. Miley, et al., "Reduction of Threshold for Laser Fusion Ignition at Nonlinear Force Driven Block Acceleration," *ANS TOFE Conference*, San Francisco, CA, Sept. 2008

14:48

UO7 5 Compact, Energy Efficient Neutron Source: Enabling Technology for Thorium Breeder and Accelerator Transmutation of Waste* A. HERSHCOVITCH, W. HORAK, *BNL* B. JOHNSON, M. TODOSOW, T. ROSER, *BNL* M. DRISCOLL, *MIT* A novel neutron source concept, in which a deuterium beam (energy of about 100 keV) is to be injected into a tube filled with tritium gas or tritium plasma, is described. At the opposite end of the tube, the energy of deuterium ions that did not interact is recovered. Be walls of proper thickness will absorb 14 MeV neutrons and release 2 – 3 lower energy neutrons. Each ion source and tube forms a module. Larger systems can be formed from multiple units. Beam propagation can be further enhanced with vortex-stabilized discharges, electron beams in opposite direction (with energy recovery) or magnetic fields. Deuterium ions propagating through tritium plasma are slowed down and deposit significant energy in the tritium target. Plasma heating results in high temperature electron, thus reducing deuterium ion energy loss. Equilibrium electron temperature exceeding 200 eV can be achieved. Unlike current methods, where accelerator based neutron sources require large amounts of power for operation, this neutron source is compact and can generate neutrons at higher power efficiency. Being modular, the concept can be tested in tabletop experiments.

*Work supported by US DOE

15:00

UO7 6 SABR fusion-fission hybrid transmutation reactor design concept WESTON STACEY, *Georgia Tech* A conceptual design has been developed for a sub-critical advanced burner reactor (SABR) consisting of i) a sodium cooled fast reactor fueled with the transuranics (TRU) from spent nuclear fuel, and ii) a D-T tokamak fusion neutron source based on ITER physics and technology. Subcritical operation enables more efficient transmutation fuel cycles in TRU fueled reactors (without compromising safety), which may be essential for significant reduction in high-level waste repository requirements. ITER will serve as the prototype for the fusion neutron source, which means SABRs could be implemented to help close the nuclear fuel cycle during the 2^{nd} quarter of the century.

15:12

UO7 7 Nuclear fuel cycle analysis of the SABR fusion-fission hybrid transmutation reactor CHRIS SOMMER, *George Tech* WESTON STACEY, BOJAN PETROVIC, *Georgia Tech* Various fuel cycles have been designed and analyzed for the Subcritical Advanced Burner Reactor (SABR). SABR is a sodium cooled fast reactor fueled with transuranics (TRU) from spent fuel of light water reactors and driven by a tokamak fusion neutron source based on ITER physics and technology. SABR employs a four batch fuel cycle using an out-to-in shuffling pattern, with the fuel being reprocessed at the end of each cycle. The reprocessing method assumes recovery rates of 99.9% of the actinides and 0.1% of the fission products remain in the recycled fuel. The reprocessing fuel cycles were analyzed to find an optimal cycle length in terms of burn up, power distribution, and materials limitations. Fuel cycles are analyzed using CEA's ERANOS2.0 code, with fuel residence times limited by radiation damage at 100, 150 and 200 dpa.

15:24

UO7 8 Dynamical Safety Analysis of the SABR Fusion-Fission Hybrid Reactor TYLER SUMNER, WESTON STACEY, SEYED GHIAASSIAN, *Georgia Tech* A hybrid fusion-fission reactor for the transmutation of spent nuclear fuel is being developed at Georgia Tech. The Subcritical Advanced Burner Reactor (SABR) is a 3000 MWth sodium-cooled, metal TRU-Zr fueled fast reactor driven by a tokamak fusion neutron source based on ITER physics and technology. We are investigating the accident dynamics of SABR's coupled fission, fusion and heat removal systems to explore the safety characteristics of a hybrid reactor. Possible accident scenarios such as loss of coolant mass flow (LOFA), of power (LOPA) and of heat sink (LOHSA), as well as inadvertent reactivity insertions and fusion source excursion are being analyzed using the RELAP5-3D code, the ATHENA version of which includes liquid metal coolants.

SESSION UP8: POSTER SESSION VIII: ALTERNATES; TURBULENCE, TRANSPORT, AND STABILITY; SPACE AND ASTROPHYSICAL PLASMAS
Thursday Afternoon, 5 November 2009
Grand Hall East at 14:00

UP8 1 ALTERNATES

UP8 2 Overview of the TCS-Upgrade device J.A. GROSSNICKLE, R.D. BROOKS, C.L. DEARDS, A.L. HOFFMAN, P.A. MELNIK, K.E. MILLER, R.D. MILROY, A. TANKUT, K.M. VELAS, G.C. VLASES, *University of Washington, Redmond Plasma Physics Laboratory* The Translation, Confinement, and Sustainment Upgrade (TCSU) device is a facility to form and sustain field-reversed configurations (FRC) in steady-state using rotating magnetic fields (RMF). Recent campaigns include Ti gettering as well as the installation of a set of internal flux rings. The Ti gettering campaign was carried out to reduce impurities and to reduce deuterium recycling from the walls. This was successful, and for the first time FRCs were sustained using external gas puffs instead of wall recycling for fuelling. These plasmas had very little impurity radiation, and it was possible, with better inventory control, to form hotter FRCs by operating at lower densities. Internal flux rings have been installed to provide a uniform flux surface and minimize plasma-wall contact. Experiments will be performed with the external magnetic field tailored to direct the plasma exhaust to 'divertor' sections where Ta bands have been placed as divertor targets. Results from the Ti gettering and internal flux ring campaigns will be reported.

UP8 3 Ion Spin-Up, Temperature, and Flow Measurements in the TCSU Experiment C.L. DEARDS, J.A. GROSSNICKLE, L.C. STEINHAUER, P.A. MELNIK, R.D. MILROY, *University of Washington, Redmond Plasma Physics Laboratory* The Translation, Confinement, and Sustainment Upgrade (TCSU) experiment employs a bakeable ultra-high vacuum chamber to reduce impurities and overall recycling. In recent experiments with Ti gettering applied to the plasma tube, radiation from impurities was dramatically reduced and recycling was almost eliminated. Ion temperature and azimuthal rotation velocities data from the resulting lower density, higher temperature FRC will be presented. The data comes from Doppler-broadening and Doppler-shifted measurements of Si III, C III, and O III, the dominant impurities in the TCSU plasma. Additionally, plans and initial data will be presented on azimuthal and poloidal velocity shear. Velocity shear is thought to improve stability and transport. All data measurements are made using an Acton Research SpectraPro 500i Czerny-Turney type spectrograph.

UP8 4 Miniaturization of a Combination Langmuir/Mach Probe P.A. MELNIK, T. DEHART, D. LOTZ, *University of Washington, Redmond Plasma Physics Laboratory* A combination Langmuir/Mach probe has been developed to measure electron temperature and density as well as ion flow speed in TCSU. The probe is fully translatable allowing it to diagnose all radial locations of the FRC at either the mid-plane, end section, or in the exhaust jets. The 1/4" probe stalk consists of interlocking boron nitride cylinders which encompass a 1/8" diameter stainless steel tube that houses the probe wires. In addition to the stainless steel jacket the probe wires are twisted to minimize electromagnetic noise pickup. The tip of this combo probe is composed of a boron nitride housing and eight.020" diameter tungsten collection leads. In TCSU, the RMF used to form and sustain the FRC makes Langmuir probe measurements difficult. To this end we have developed a drive circuit that will generate the bias voltages necessary for Langmuir probe operation. This bipolar power supply can produce steady voltages up to 200 volts at loads over 1 amp and can be swept at any frequency up to 1.5 MHz. The probe current and bias voltage will be recorded with an amplifier and transmitted via fiber optic to a receiver allowing the signals to be digitized.

UP8 5 Plasma-Wall Interactions in TCSU with New First-Wall Materials A. TANKUT, K.E. MILLER, G.C. VLASES, *University of Washington, Redmond Plasma Physics Laboratory* Surface analysis studies carried out during the first two years of operation of the Translation, Confinement, and Sustainment Upgrade (TCSU) Experiment proved to be valuable in understanding some of the fundamental processes that occur at the first wall. With the recent modifications in the system including the insertion of Ta/Al flux conserving rings to minimize plasma-wall contact, placement of Ta shields at the scrape-off layer strike points, and an emphasis placed on Ti-gettering, new materials science related phenomena are expected. To study these effects, surface analysis samples representing the various plasma-facing surfaces are being placed in TCSU. This study will present some of the initial observations from the recently modified TCSU first wall. The effect of plasma discharges and wall-conditioning techniques on the plasma-facing surfaces will be discussed in relation to our previous studies.

UP8 6 Magnetic Field Measurements in the TCSU RMF Current Drive Experiment K.M. VELAS, K.E. MILLER, R.D. MILROY, *University of Washington, Redmond Plasma Physics Laboratory* Detailed magnetic measurements from the Translation Confinement Sustainment Upgrade (TCSU) experiment will be presented. A two-axis probe inserted transversely at the axial midplane provides 24 independent measurements of B_z and B_x as a function of radius and two single-axis 29 channel probes provide axial profiles at the plasma edge. The $B_x(r)$ field profiles provide

details about penetration of the Rotating Magnetic Field (RMF) Current Drive. The $B_z(r)$ profiles, when combined with the high beta nature of the FRC, interferometric density measurements, and the assumption of uniform temperature, yield radial density and pressure profiles. Time evolution of these profiles gives plasma dynamics during formation, quiescence, and decay as well as new insight into wobble and n = 2 instabilities. The $B_z(z)$ data, combined with external field measurements, allow the separatrix radius to be inferred as a function of axial position. Magnetic measurements have been crucial in evaluating the impact of the recently installed inner flux rings.

UP8 7 Design and Calibration of Thomson Scattering Diagnostic for TCSU K.Y. LEE, R.P. GOLINGO, *University of Washington, Redmond Plasma Physics Laboratory* A single pulse ruby laser Thomson scattering system is being designed and installed to measure the electron temperature T_e and density n_e profiles in a Rotating Magnetic Field (RMF) driven FRC plasma. Based on measurements that show the total temperature is about 150 eV and the density is about 10^{19} m^{-3} in the Translation, Confinement and Sustainment Upgrade (TCSU) experiment, a T_e of about 100 eV is expected. The system allows observation of 5 points on the bottom half section of the 40 cm radius TCSU device. Each spatial point is resolved with a GA polychromator attached to three PPPL preamplifier modules. A model to relate the fast and slow channel of the pre-amplifier followed by a spectral calibration of the polychromator characterizing the transmission of the bandpass interference filters is described. The overall system design will be discussed and initial results may be presented.

UP8 8 Effect of Magnetic Field Configuration on n = 1 Instabilities in Rotamak XIAOKANG YANG, YURI PETROV, TIAN-SEN HUANG, *Prairie View A&M University* The n = 1 tilt/radial shift modes are observed in rotating magnetic field (RMF) driven FRC plasmas. Experiments studying on the response of n = 1 instabilities to the changes of magnetic field structure have been conducted in 40 ms Rotamak discharges. In one series of experiments the axial current I_z (which produces toroidal field) ramps linearly in time from 0 to 2 kA, leading to transition from FRC to ST configuration. The amplitude of the tilt mode is suddenly doubled when I_z reaches 0.5 kA (compare to 2 kA plasma current); the amplitude remains at this level when I_z is in the range of 0.5-1 kA. The tilt instability disappears when I_z exceeds 1 kA. In other series of experiments, by using a middle shaping coil with a moderate current of 0.25-0.5 kA, the doublet-FRCs are formed which are completely free from both the tilt and radial shift modes.

UP8 9 Analysis of the active equilibrium control experiments in Rotamak YURI PETROV, XIAOKANG YANG, TIAN-SEN HUANG, *Prairie View A&M University* A model is presented that describes the change of plasma shape, plasma current and pressure under the effect of active equilibrium coils in Rotamak. In recent experiments, energizing the active coils with total current 1 kA resulted in plasma current increase from 2 to 4-5 kA. The peak plasma pressure was changing from 3-4 Pa to 5-6 Pa. The elongation of plasma was changing from 1 to 2, but the plasma volume was increasing by only 50% because of reduction in separatrix radius. We show that all these changes can be described by a model based on Solov'ev equilibrium and global power balance, with one input parameter: the value of magnetic field at the boundary.

UP8 10 Overview and Current Status of the Pulsed High Density Experiment* SAMUEL ANDREASON, JOHN SLOUGH, *University of Washington - Plasma Dynamics Laboratory* The goal of the Pulsed High Density (PHD) experiment is to produce a large Field Reversed Configuration (FRC) of approximately 10 mWb flux that can be accelerated and compressed to reach breakeven conditions. The formation section is 0.4 m in radius with a length of 2.5 m. The primary challenge in the formation section is achieving an FRC with sufficient flux while remaining kinetically stable for the necessary lifetime. Earlier efforts were focused on using one on-axis MPD plasma source for initial ionization. Current work is being done with an MPD array inserted near the wall, past the bias field cusp region. There has been some success with this approach for 'dynamic' formation shots. "In situ" shots have proven more problematic. Less than half the intended complement of MPD guns has been manufactured and installed. We are not certain whether current difficulties result from this fact or individual variation in the MPD characteristics. Ionization by rotating magnetic field (RMF) and ringing theta pinch will be attempted as alternatives and supplements to the MPD sources.

*Work supported by DOE OFES.

UP8 11 Ion energy distribution function measurements in the Irvine Field Reversed Configuration THOMAS ROCHE, EUSEBIO GARATE, WAYNE HARRIS, WILLIAM HEIDBRINK, ROGER McWILLIAMS, ERIK TRASK, *UCI* A gridded ion energy analyzer has been constructed to measure the ion energy distribution function in the Irvine Field Reversed Configuration (IFRC). Three grids provide Debye shielding, electron rejection and ion energy selection, respectively. It has an acceptance angle of $\sim$ 20 degrees. Due to a large, negative, floating potential a fast (17 MHz bandwidth) optocoupler is used to decouple the signal from earth ground. A dummy collector is also used to subtract background noise pickup. Ion current flows in the negative theta direction in the IFRC. Measurements have been taken both parallel and anti-parallel to the current near the magnetic null. These measurements have shown that a shifted Maxwellian, with peak energy of $\sim$ 18 eV, can be fit to the ion energy distribution function. This number agrees with the upper limit of 20 eV previously placed on the peak by a time of flight diagnostic[1]. Coupling of the distribution function measurements with magnetic field measurements will determine the distribution of orbit types in the IFRC, specifically the ratio of betatron to drift type particle orbits.

[1]W. S. Harris et al., Rev. Sci. Instrum. **79**, 10F313 (2008)

UP8 12 Ion Flow Measurements and Plasma Current Analysis in the Irvine Field Reversed Configuration WAYNE HARRIS, ERIK TRASK, THOMAS ROCHE, EUSEBIO GARATE, WILLIAM HEIDBRINK, ROGER McWILLIAMS, *University of California - Irvine* The contribution of the ion current in the lab frame to the total plasma current is studied in the Irvine Field Reversed Configuration (IFRC). A charge-exchange neutral particle analyzer chops the emitted neutrals at a rate of 13 kHz and shows that the peak energy is below the 20eV minimum detectable energy threshold. A modified monochromator that is used to measure Doppler shifts of impurity lines indicates that there is a flow in the range of 5-7km/s in IFRC. By evaluating the collision times between the impurities and hydrogen, the dominant plasma ion species, it is concluded that the ions rotate with an angular frequency of $\sim 4 \times 10^4$ rad/s. Estimates of the ion current in the lab frame are accomplished by determining the ion density distribu-

tion using pressure balance, and by fitting the measured magnetic probe data to a theoretical equilibrium. The results from these estimates indicate that the ion current is 1-2 orders of magnitude larger than the measured plasma current of 15kA. Calculations of electron drifts from the equilibrium fields show that the electrons cancel most of the ion current.

UP8 13 Progress on the Colorado FRC Experiment* A. LIGHT, C.L. ELLISON, T. MUNSAT, M. SCHMIDT, *University of Colorado at Boulder* Here we present the latest results from the Colorado FRC Experiment. Designed for the study of turbulence, flow, stability, and cross-field transport in a prolate field-reversed configuration, the project places emphasis on the investigation of spontaneous and driven flows. The experiment is a merged-spheromak device driven by magnetized coaxial guns. We have designed and constructed a two-point biasing probe for driving E x B flows at close to Mach 1. Diagnostics in use include a multi-chord CO2 quadrature interferometer, a compact 48-channel (16-position, three-axis) magnetic probe, a triple-probe, a two-dimensional Mach probe, gun-current Rogowski coils, and loops for measuring the flux ejected from each gun. All measurements are designed to be frequency-limited only by the data acquisition rate (40 MS/s) for recovery of fast phenomena. Details of the instruments and early results from experiments on merging and attempts to measure bulk rotation are presented.

*This research supported by DOE grant DE-FG02-05ER54841.

UP8 14 Detection of electric field around field-reversed configuration plasma TAEKO IKEYAMA, MASANORI HIROI, TOMOHIKO ASAI, TSUTOMU TAKAHASHI, *College of Science and Technology, Nihon University* YASUNORI OHKUMA, *College of Industrial Technology, Nihon University* YASUYUKI NOGI, An electric field around a field-reversed configuration plasma is tried to measure by detecting electric charges induced on a surface of conductor. For this measurement, eight copper plates, each of which has a 10 cm length, 2 cm width and 0.2 mm thickness, are installed on a vacuum vessel in the NUCTE-III device. Experiments show that fluctuating electric fields with a strength of 50~ 100 V/m and a frequency 50~ 200 kHz are detected through a discharge. To investigate a generating mechanism of the electric field, a time evolution and spatial profile of the electric field are compared with those of MHD motions of the plasma obtained from an optical and magnetic measurements. From this comparison, it is found that the generation of the electric field with an n=2 mode correlates with a growth of a rotational instability. However, the electric field with an n=1 mode cannot be found any correlation with a wobble motion which is a very common n=1 mode one in the NUCTE-III device.

UP8 15 Flow and dynamo measurements during the coaxial helicity injection on HIST K. ANDO, T. HIGASHI, M. NAKATSUKA, Y. KIKUCHI, N. FUKUMOTO, M. NAGATA, *University of Hyogo* The current drive by Coaxial Helicity Injection (CHI-CD) was performed on HIST in a wide range of configurations from high-q ST to low-q ST and spheromak generated by the utilization of the toroidal field. It is a key issue to investigate the dynamo mechanism required to maintain each configuration. To identify the detail mechanisms, it is needed to manifest a role of plasma flows in the CHI-CD. For this purpose, we have measured the ion flow and the dynamo electric field using an ion Doppler spectrometer (IDS) system, a Mach probe and a dynamo probe. The new dynamo probe consists of 3-axis Mach probes and magnetic pick-up coils. The flow measurements have shown that the intermittent generation of the flow is correlated to the fluctuation seen on the electron density and current signals during the driven phase. At this time, the toroidal direction of the ion flow in the central open flux column is opposite to that of the toroidal current there, i.e. the same direction as electrons. After the plasma enters to the resistive decay phase, the toroidal flow tends to reverse to the same direction as the toroidal current. The results are consistent with the model of the repetitive plasmoid ejection and coalescence proposed for CHI-CD. The plasma jet emanating from the gun source and magnetic field generations through reconnection during the driven phase is well reflected in the 3D MHD simulation.

UP8 16 Hybrid FRC equilibria* LOREN STEINHAUER, *University of Washington* Field-reversed configurations (FRC) have long been known to be highly-kinetic. This has been investigated in the context of stability. However, their kinetic nature affects FRC equilibria, a fact long overlooked. Ion kinetic effects are especially important near the separatrix and in the scrape-off-layer. These equilibria are investigated using a hybrid formulation, i.e. ions governed by the Vlasov equation and electrons as a warm, massless fluid. In axisymmetric equilibria, the ion distribution is expressible as a function of the Hamiltonian and the canonical angular momentum. This approach was originally used in the context of an Astron plasma [1]. The form distribution form has a "thermal" dependence on the Hamiltonian and a two-part dependence on the canonical angular momentum, the latter accounting for the ion confinement boundary in velocity space. Using this formalism the azimuthal current density is an analytic function of the magnetic flux variable. Equilibrium is found by combining this result with Ampere's law, solvable in 1D or 2D by an iterative procedure. Solutions for elongated FRCs (1D) are presented and the implications discussed. [1] R.V. Lovelace et al., Phys. Fluids (1978).

*Supported by USDOE Grant No. DE-FG02-98ER54480.

UP8 17 Effects of Energetic Beam Ions on Stability Properties of Field-Reversed Configurations* E.V. BELOVA, R.C. DAVIDSON, *PPPL* Stability properties of prolate Field-Reversed Configurations (FRCs) have been studied numerically using the nonlinear hybrid and MHD simulation code HYM, including the effects of energetic neutral beam ions. It is shown that the beam ions can have a stabilizing or destabilizing effect on the global modes in FRCs, depending on the toroidal mode number n, the mode polarization, and the beam parameters. Linear simulation results are compared with a qualitative analysis based on a generalized energy principle. Nonlinear simulations are used to study the nonlinear saturation of the beam-driven instabilities due to nonlinear changes in the distribution function of the beam ions.

*Supported by DE-AC02-09CH11466.

UP8 18 Three-Dimensional MHD Simulations of Co- and Counter-Helicity Spheromak Merging in SSX using the HYM Code* CLAYTON E. MYERS, E.V. BELOVA, *Princeton Plasma Physics Laboratory* The HYM (Hybrid MHD) code has been used to perform 3D MHD simulations of co- and counter-helicity spheromak merging. These simulations aim to understand relaxation and stability phenomena that have been observed in

merging experiments on the Swarthmore Spheromak Experiment (SSX). In simulating a novel co-helicity merging configuration with counter-directed toroidal fields, the two spheromaks are observed to tilt prior to forming an asymmetric, three-dimensional reconnection layer and relaxing to a stable and fully tilted final state. In simulating a more conventional counter-helicity merging configuration, we are attempting to reproduce the Doublet CT (Compact Torus) configuration that has been observed in SSX experiments. The visualization of both simulated and experimental data has been improved using the 3D visualization software VisIt. The HYM code is also being modified to incorporate collisional and radiative heat loss mechanisms to more accurately characterize the evolution of the temperature and density profiles in the plasma.

*This work is supported by DOE Contract Number DE-AC02-09CH11466.

UP8 19 Overview of HIT-SI Results and Plans D.A. ENNIS, C. AKCAY, M.A. CHILENSKI, W.T. HAMP, A.C. HOSSACK, T.R. JARBOE, G.J. MARKLIN, B.A. NELSON, R.J. SMITH, B.S. VICTOR, J.S. WROBEL, *University of Washington* Recent experiments in the Helicity Injected Torus-Steady Inductive (HIT-SI) have yielded improved current amplification, a new understanding of the injector–spheromak interaction, and a clear direction for future campaigns. HIT-SI investigates steady inductive helicity injection in a high-beta spheromak geometry using two semi-toroidal injectors. The HIT-SI diagnostic suite includes: FIR interferometry, IDS, bolometry, internal and surface magnetic probes. Results of operations with unequal injector helicity (differing voltage and flux demands) produced the highest spheromak current (34 kA) and current amplification ($I_{tor}/I_{inj} \approx 2$) to date. Single injector operations established opposing directions of preferred spheromak current for each injector determined by the sign of the helicity and its orientation relative to the confinement volume. Observation of decaying spheromak current is thought to result from equilibrium field loss into the flux conserver eventually leading to spheromak current flipping. Future HIT-SI plans include installation of equilibrium flux control to reduce spheromak degradation and provide favorable boundary conditions. Additionally, mounting the injectors on the same side of the confinement volume will allow all injectors to operate more efficiently in their preferred direction. Work supported by USDoE.

UP8 20 Spheromak Current Drive Direction and Flipping in HIT-SI* B.S. VICTOR, D.A. ENNIS, T.R. JARBOE, B.A. NELSON, R.J. SMITH, A.M. KIRKPATRICK, *University of Washington* The Helicity Injected Torus with Steady Inductive current drive (HIT-SI) experiment uses two inductive plasma injectors to drive magnetic helicity into the confinement region. The direction of the spheromak current in the confinement region is dependent upon the sign of the helicity and the orientation of the injector with respect to the confinement region. Injectors driving helicity of the same sign and positioned on opposite sides of the confinement region have opposing directions of preferred spheromak current direction. However, helicity balance dominates the preferred direction of current drive. Operating the injectors with the same helicity sign produces higher spheromak currents than single-injector operation, but with reversals in the spheromak current direction on time intervals long compared to the injector frequency. A newly constructed, three-pronged probe containing arrays of 3D pickup coils, inserted to the magnetic axis, is used to measure the effects of the helicity sign on the magnetic field profile. Ratios of current density to electron density, as measured by an FIR interferometer, approaching 10^{-14} A$\cdot$ m have been measured, demonstrating improvement from past plasma performance.

*Work supported by USDoE.

UP8 21 Edge Magnetic Activity in the HIT-SI Experiment J.S. WROBEL, D.A. ENNIS, T.R. JARBOE, G.J. MARKLIN, B.A. NELSON, R.J. SMITH, *University of Washington* Arrays of surface magnetic probes embedded in the HIT-SI flux conserver have resolved plasma dynamics in the 10Hz-200kHz frequency range. Four separate Amperian loops formed by the surface magnetic arrays measured the toroidal plasma current with rise times as well as reversals in the current direction on a 100μs time scale. Studies of the reversal process will be presented. Global magnetic field oscillations at the 5.8kHz injector driving frequency are also observed and the distribution of oscillations suggests twisted injector prominences in the confinement region. Data from surface probe arrays along the midplane gap together with external flux loops have shown substantial spheromak flux is driven out the gap characterized by toroidal mode numbers $n = 1$ and $n = 2$. The new magnetic data is providing guidance for eliminating the loss of flux at the gap and for future injector designs. A comparison to Taylor models will also be presented. Work supported by USDoE.

UP8 22 Flux Conserver Improvements to HIT-SI and Ion Temperature Measurements A.C. HOSSACK, C. AKCAY, D.A. ENNIS, T.R. JARBOE, B.A. NELSON, J.A. ROGERS, R.J. SMITH, B.S. VICTOR, J.S. WROBEL, *University of Washington* Significant flux leakage from the mid-plane of the HIT-SI experiment has been observed, which decreases the spheromak helicity decay time. The HIT-SI flux conserver is joined at the mid-plane by a chromium copper ring and flexible spiral wrap electrically connecting the ring to each half of the flux conserver. A series of materials tests were undertaken to explore improvements to the electrical conductivity of the mid-plane junction. Nearly two orders of magnitude improvement was observed when the beryllium copper spiral wrap was plated with silver and the stainless steel flux conserver surface was plated with either silver or copper. These improvements have been implemented on the HIT-SI flux conserver and the results will be presented. Ion temperature data in the spheromak region collected with the Ion Doppler Spectrometer diagnostic are also presented. Overall trends indicate that ion temperature scales with injector voltage demand, but temperature scales inversely with injector flux demand. Work supported by US DoE.

UP8 23 NIMROD Simulations of HIT-SI Plasmas C. AKCAY, C.C. KIM, T.R. JARBOE, B.A. NELSON, *University of washington* V.A. IZZO, *UCSD* We present NIMROD simulation studies of current-drive, magnetic reconnection and relaxation behavior of the HIT-SI experiment. HIT-SI (Steady Inductive Helicity Injected Torus) is a spheromak that uses two semi-toroidal injectors to provide steady inductive helicity injection (SIHI). SIHI produces and sustains a spheromak by generating poloidal flux using relaxation current drive. The helicity injectors of the experiment are modeled as flux (ψ_{inj}) and current (I_{inj}) boundary conditions. Our study uses a zero β resistive MHD model with uniform density. Lundquist number S and injector lambda, $\lambda_{inj}(= \mu_0 I_{inj}/\psi_{inj})$ characterize the parameter space. $S(= \sqrt{\mu_0/\rho}\, B/2\pi R_0 \eta \lambda_{sp}^2)$ is the ratio of resistive diffusion to Alfvén transit time, ρ and η are

the plasma density and resistivity, R_0 is the magnetic axis and λ_{sp}($= \mu_0 j_{//}/B$) is the spheromak lambda, 10.3 m^{-1} for HIT-SI. For our current simulations we set λ_{inj}=30, and perform a scan in S for low values ($\sim$ 10 $-$ 100). Our results to date at S = 22 and 35 show little relaxation during sustainement but growth of the n=0 magnetic energy and an increase in plasma current during the decay phase. Upon completion of this study at λ_{inj}=30 we will repeat the resistive MHD simulations at a lower λ_{inj} ($\sim$ 20) in order to chart the relaxation behavior as a function of λ_{inj}.

UP8 24 Implementation of digital feedback control system for switching power amplifiers on HIT-SI Y. KIKUCHI, *University of Hyogo* B.A. NELSON, A.S. NELSON, D.A. ENNIS, J.S. WROBEL, T.R. JARBOE, *University of Washington* M. NAGATA, *University of Hyogo* Recent developments in high-power switching devices such as insulated gate bipolar transistors (IGBTs) have greatly reduced feedback-controlled power supply costs for fusion plasma experiments. The HIT-II experiment has successfully used a pulse width modulation (PWM) method for analog-based feedback control of switching power amplifiers (SPAs). However, the analog-based feedback controllers are not suited to modification of different feedback methods and applications for the other experimental devices. In the present work, a micro-controller (Analog Devices Inc. Blackfin model 537) was used as a digital feedback controller for SPAs in HIT-SI. The Blackfin 537 is available in an inexpensive ($200) evaluation board (BF537-STAMP) that has a 500 MHz processor clock, 125 MHz peripheral clock, 64 MB of SDRAM, 8 programmable timers, and can host an inexpensive ($40) daughter card with a 12-bit 1 MHz digitizer. The present new feedback controller was successfully implemented for flux coil circuits in HIT-SI. The measured flux coil signal was much better than that based on the analog feedback control by adjusting the feedback gains. The detail technical information about the digital feedback control system and the experimental results will be shown.

UP8 25 Refluxing physics for quasisteady state spheromak sustainment* E.B. HOOPER, *LLNL* "Refluxing" for spheromak sustainment injects helicity during formation, followed by a slowly-decaying, high confinement phase. The plasma is rebuilt before the magnetic flux fully decays, and the cycle repeated as demonstrated in the SSPX experiment [1]. Numerical simulations (NIMROD code) and axisymmetric modeling including transport (CORSICA code) extend the experimental study, improving the confinement phase using bias flux reduction [2]. The free energy in the injected current is reduced, lowering the level of magnetic fluctuations. Flux amplification during buildup is increased above SSPX, achieving higher Te and lengthening the confinement phase duration. Calculations use the SSPX flux-conserver geometry to maintain contact with experiment; some issues with this geometry at high flux amplification are analyzed. Current profile control including edge boundary condition on j/B is considered for limiting internal magnetic mode amplitudes. Opportunities for further improvement of this scenario are identified. [1] B. Hudson, et al., Phys. Plasmas 15, 056112 (2008). [2] E. B. Hooper, et al., Nucl. Fusion 47, 1064 (2007).

*Work performed under the auspices of the U.S. Department of Energy under contract DE-AC52-07NA27344 at LLNL.

UP8 26 NIMROD Simulation of multipulsed edge-current drive in SSPX* L.L. LODESTRO, B.I. COHEN, E.B. HOOPER, H.S. McLEAN, R.D. WOOD, *LLNL* Flux amplification (A)—the ratio of poloidal magnetic flux enclosed by a spheromak's toroidal core to an applied edge flux—is a critical parameter for an economic spheromak-based fusion reactor. In [1], measurements of A in SSPX and NIMROD simulations [2] were found to be in good agreement over a range of discharge parameters while $A < 3$. Experiments to study A performed subsequently with the modular capacitor bank gave some indication that $|dI_{gun}/dt|$ played a role and that increasing it might build magnetic field more efficiently, but were limited by gun discharge circuit inductance. In [3], multipulsed gun injection was investigated numerically and the results compared to SSPX. Here we report the continuation of those simulations to longer times. We find trends on timescales much longer than could be studied in SSPX, negligible effect on A of multipulsed injection at frequencies smaller than the fundamental SSPX reconnection frequency, and small increases in A for large frequencies. [1] B. Hudson et al., Phys. Plasmas **15**, 056112 (2008). [2] E.B. Hooper et al., Nucl. Fusion **47**, 1064 (2007). [3] L.L. LoDestro et al., 50th DPP, TP6-93 (2008).

*Work performed by LLNL under U.S. DoE Contract DE-AC52-07NA27344.

UP8 27 The importance of mass injection boundary conditions for spheromaks, astrophysical jets, and solar coronal loops* PAUL BELLAN, *Caltech* Spheromak formation physics, astrophysical jets, and solar coronal loops all involve electric current flow from a bounding surface (electrode) into an open magnetic flux tube. This current creates an azimuthal magnetic field that twists up the flux tube, i.e., magnetic helicity is injected. Because this process involves injection of azimuthal magnetic flux and because plasma is frozen to magnetic flux, there must be an associated mass flux from the boundary into the flux tube. This required mass source at the boundary is provided by gas puffing in our experiments. MHD forces accelerate mass into the flux tube resulting in an Alfvenic jet [1]. Axial compression of the azimuthal flux frozen into the jet frame pinches the jet and collimates it. The velocity, density, and magnetic profile of experimentally observed collimated jets depend on the ingested mass flux, the normal magnetic flux, and the current. Paschen breakdown constraints impose an undesirable lower bound for the mass flux in our existing experiments. Consideration is being given to pre-ionization schemes inside the gas injection nozzles to overcome the Paschen constraint and so enable access to regimes having lower densities, faster jets, and hotter plasmas. [1] D. Kumar and P. M. Bellan, submitted for publication

*Supported by USDOE, NSF, and AFOSR.

UP8 28 New pulse forming network power supply for the Caltech Spheromak Formation Experiment* A.L. MOSER, P.M. BELLAN, *Caltech* Past experiments on the Caltech Spheromak Formation Experiment produced plasmas with a 120 μF capacitor bank charged to 4–7 kV and supplying a 150 kA peak current with a FWHM of $\sim$ 10 μs. We recently completed construction of a pulse forming network (PFN) having two parallel sections of five 120 μF capacitors, designed to produce a 150 kA peak current pulse with FWHM of $\sim$ 50 μs. Preliminary experiments using only the PFN show the effect of the five–fold increase in current pulse length on the collimated jet precursor to spheromak formation: the jet extends to 55 cm, a length $\sim$ 1.5 times that

previously seen, and can develop two visible twists upon onset of the kink instability. Future experiments will use the 120 μF capacitor bank for plasma breakdown and the PFN for sustainment. A recently constructed capacitively coupled probe and axial 60–channel magnetic probe array will be used to study critical ionization velocity limited collisions between the magnetized jet and a neutral target gas cloud.

*Supported by USDOE.

UP8 29 Alfvénic jets associated with spheromak formation* DEEPAK KUMAR, PAUL BELLAN, *California Institute of Technology* Collimated plasma jets flowing away from the electrodes are produced in the Caltech spheromak experiment. The jet formation stage precedes the spheromak formation and serves as a mechanism for feeding particles, magnetic helicity, energy and toroidal flux into the system. Detailed density and flow velocity measurements of hydrogen and deuterium plasma jets reveal that the flow velocity of these jets is Alfvénic with respect to the the toroidal magnetic field produced by the axial current within the plasma. A MHD model predicts how the flow velocity and plasma density scales with the electric current (D. Kumar and P. M. Bellan, Phys. Rev. Lett., to appear.). Visual images and magnetic field measurements indicate that the jet core is dense ($\beta \sim 1$), while the edge plasma is approximately force-free ($\beta \rightarrow 0$). These laboratory jets also provide useful insight into the acceleration and collimation of astrophysical jets associated with star formation.

*Supported by USDOE.

UP8 30 3D Canonical Momentum Measurements During the Merging of Two Counter-Helicity Spheromaks* SETTHIVOINE YOU, *University of Tokyo* ALEXANDER BALANDIN, *Institute of Systems Dynamics and Control Theory, Irkutsk, Russia* HIROSHI TANABE, YASUSHI ONO, *University of Tokyo* A pair of counter-helicity spheromaks can merge in two possible ways to form a single final compact toroid depending on their toroidal magnetic field direction. Magnetohydrodynamically, no difference should be expected but experimentally, a positive/negative merging or negative/positive merging will generate final compact toroids with different lifetimes and sizes. A pair of multichannel spectroscopic diagnostics have been installed on the TS-4 experiment with view chords designed for measuring 3D ion velocities and temperature. One set retrieves toroidal velocities and temperature from conventional Abel inversion. The second, novel arrangement retrieves poloidal velocities from 3D vector tomography reconstruction and temperature from scalar tomography. With in situ magnetic probe arrays, the ion canonical momentum is thus determined in the complete volume. The ion temperature at the reconnection plane is also evaluated [1]. Both sets of measurements are followed over several repeatable shots during the spheromak merging to also track the evolution of ion self-helicity.[1] Tanabe, You, Balandin, Ono, poster this meeting.

*First author supported by Japanese Society for Promotion of Science

UP8 31 Optical Beat-Wave Experiment on CTIX* ROBERT HORTON, *UC Davis* DAVID HWANG, FEI LIU, BEN ZHU, RUSSELL EVANS, By launching intense electromagnetic waves at differing frequencies, a wave at the beat (difference) frequency can be created within a region of plasma. The beat wave is efficiently damped, and electron current generated, if the beat frequency is close to local plasma frequency, and if phase velocity is close to electron thermal velocity. Beat-wave acceleration of plasma electrons was previously demonstrated at low plasma density [1]. At the higher densities of the CTIX compact-toroid accelerator, plasma frequencies are such that CO2 lasers (f 30 THz) are a cost-effective driver. An experiment is being prepared to test beat-wave current drive using two TEA CO2 lasers on CTIX. The experiment will test models of wave mixing, quasilinear modification of the velocity distribution, and amplification of seed current by plasma kinetic effects. An application of the methods developed may be standoff current generation in a target plasma. Experimental issues to be addressed include: precisely-timed production of the compressed, target plasma; grating tuning of the CO2 lasers for frequency selection; high-peak-power, simultaneous operation of TEA lasers, design of optics; optical and plasma diagnostics. Initial results will be presented. [1] Rogers, J. H. and Hwang, D. Q., Phys. Rev. Lett. v68 p3877 (1992).

*This work supported by U.S. DOE Grant DE-FG02-03ER54732.

UP8 32 Development of Low-Power CO_2 Laser for CTIX Beat-Wave Experiment* BEN ZHU, ROBERT HORTON, DAVID HWANG, FEI LIU, RUSSELL EVANS, *Dept. of Applied Science, UC Davis* To enhance the flexibility of the two high-power Lumonics CO_2 TEA lasers to be used on our beat-wave current drive experiment, we are in the process of restoring two low-power CO $_2$ lasers previously used as drivers for FIR experiments. [1] The expected laser characteristics from previous operation are 10W steady-state and up to 5kW pulsed at 200nsec with Q switching. The frequencies of the high-power lasers are critical for the beat-wave current drive experiment. At low power, the operating wavelength may be accurately tuned using a rotatable diffraction grating. Upon completion of the restoration, the CO_2 lasers will initially be used for gain testing of the Lumonics pulsed lasers. Later, the low-power lasers will be used for mode locking operation of the Lumonics lasers. The low-power CO_2 lasers have many other applications; for instance, they can also be used for scattering diagnostics. The results of steady-state operation and gain testing of the high-power CO_2 laser will be presented. [1] M. M. T. Loy and P. A. Roland, Rev. Sci. Instrum., Vol. 48 #6 May 1977

*Supported by U.S. DOE Grant DE-FG02-03ER54732.

UP8 33 Experimental Estimation for Beat-Wave Current Generation in an Unmagnetized Plasma and Preliminary Results* FEI LIU, *UC Davis* ROBERT HORTON, DAVID HWANG, BEN ZHU, RUSSELL EVANS, Beat-wave current generation experiment in a high density compact torus (CT) is being conducted on CTIX using CO_2 lasers. Tunability of the CO_2 lasers provides many options for the wave-particle interaction experiment at a variety of plasma densities with plasma frequency in THz range. For example strong lines such as 9R(12) and 9R(30) could be chosen for an easily obtainable density of $1.28 \times 10^{15} cm^{-3}$. After restoration, two Lumonics CO_2 lasers are expected to produce approximately 100MW output power in a 50ns pulse. The amount of energy transfer from laser to plasma is determined by the laser power intensity, and by the CT density scale length [1]. The desired power density can be achieved by designing a suitable optical focusing system. In addition, the CT density can be matched to the beat-wave frequency by appropriately selecting the plasma operating conditions and timing. Extensive testing of the Marx

banks and pre-ionization boards was done under a variety of operating conditions. Other preliminary results and plans for the wave-particle interaction experiment will also be reported. [1] A. N. Kaufman, B. I. Cohen, PRL, 30 1306 (1973)

*Supported by U.S. DOE Grant DE-FG02-03ER54732.

UP8 34 Extended MHD Simulations of Interchange Modes in Spheromak Equilibria* E.C. HOWELL, C.R. SOVINEC, *University of Wisconsin-Madison* Numerical computation is applied to investigate two-fluid effects on resonant modes in spheromak equilibria using the NIMROD code (nimrodteam.org). Equilibria represent decaying spheromak conditions, when pressure profiles are peaked and MHD stability has a strong effect on confinement [E.B. Hoper etal., POP **15**, 032502 (2008)]. Both linear growth rate scaling studies and mode structure indicate ideal behavior. Linear growth rates are computed using both ion gyroviscosity and a two-fluid Ohm's law and compared with growth rates computed using resistive MHD. For smaller toroidal mode numbers (n< 15) the two-fluid physics has minimal effect on the growth rate (1-5%) and can be either stabilizing or destabilizing. For intermediate toroidal mode numbers (n=16-30) the two-fluid physics has predominantly stabilizing effects and growth rates are damped by 10-75%. Maximum damping is observed when the mode rotation rate is grater than the resistive MHD growth rate. The effects of altering the equilibrium density and of equilibrium diamagnetic flows are investigated.

*Work supported by U.S. Department of Energy.

UP8 35 Nonlinear MHD simulation of magnetic relaxation during DC helicity injection in spherical torus plasmas TAKASHI KANKI, *Japan Coast Guard Academy* MASAYOSHI NAGATA, *University of Hyogo* YASUHIRO KAGEI, *RIST* Recently, the intermittent plasma flow has been observed to be correlated with the fluctuations of the toroidal current I_t and $n=1$ mode in the HIST spherical torus device. During the partially driven phase mixed with a resistive decay, the toroidal ion flow velocity ($\sim$ 40 km/s) in the opposite direction of I_t is driven in the central open flux region, and the oscillations in $n=1$ mode occur there, while during the resistive decay phase, this flow velocity reverses and results in the same as that of I_t, and the oscillations in $n=1$ mode disappear there. The purpose of the present study is to investigate the plasma flow reversal process and the relevant MHD relaxation by using the 3-D nonlinear MHD simulations. The numerical results exhibit that during the driven phase, the toroidal flow velocity ($\sim$ 37 km/s) is in the opposite direction to I_t, but in the same direction as the $E\times B$rotation induced by an applied voltage. This flow is driven by the magnetic reconnection occurring at the X-point during the repetitive process of the non-axisymmetric magnetized plasmoid ejection from the helicity injector. The oscillations of poloidal flux Ψ_p are out of phase with those of toroidal flux Ψ_t and magnetic energy for the dominant $n=1$ mode, indicating the flux conversion from Ψ_t to Ψ_p. The effect of the vacuum toroidal field strength on the plasma dynamics is discussed.

UP8 36 ZaP Flow Z-Pinch: Overview and Recent Results U. SHUMLAK, D.J. DEN HARTOG, R.P. GOLINGO, S.D. KNECHT, B.A. NELSON, R.J. OBERTO, J.L. ROHRBACH, G. SHAH, G.V. VOGMAN, *Aerospace and Energetics Research Program, University of Washington* The ZaP Flow Z-pinch experiment at the University of Washington investigates the effect of sheared flows on MHD stability. An axially flowing Z-pinch plasma is produced that is 1 m long with a 1 cm radius. After assembly the plasma is magnetically confined for an extended quiescent period where the mode activity is significantly reduced when the plasma flow shows a sheared profile. The experimental flow shear exceeds the theoretical threshold for stability during the quiescent period and the flow shear is lower than the theoretical threshold at other times. Recent experimental modifications have increased the size of the inner electrode to improve neutral gas injection control and to increase the adiabatic compression of the Z-pinch plasma. Equilibrium consistency is evaluated by comparing interferometry measurements of density, Doppler line broadening for ion temperature, Thomson scattering for electron temperature, Zeeman splitting of impurity radiation lines for internal magnetic field measurements, and probes for external magnetic field measurements. The Z-pinch equilibrium is completely described by a radial force balance. An overview of the experimental program, results, and future work will be presented.

UP8 37 Electron Temperature Measurements on the ZaP Experiment R.P. GOLINGO, U. SHUMLAK, B.A. NELSON, D.J. DEN HARTOG, R.J. OBERTO, *Aerospace and Energetics Research Program, University of Washington* The ZaP Flow Z-Pinch Experiment is presently studying the effect of sheared flow on gross plasma stability. During a quiescent period in the magnetic mode activity, a dense Z-pinch with a sheared flow is observed on the axis of the machine. A better comparison between the experimental and analytic results can be made once the pressure profile is known. A single-point Thomson scattering system has been installed on the machine to directly measure the local electron temperature in the Z-pinch. Available components have been used to build the system, reducing the cost. The system has a 3 mm radial resolution and can collect scattered light up to 4 cm off the axis of the machine (The Z-pinch has a 1 cm characteristic radius). The temporal evolution of the background and scattered light is recorded on each pulse. The design and hardware allow the system to be upgraded to a multipoint system. More accurate temperatures are found with a complete calibration of the collection system. The measured electron temperatures are consistent with previous estimates from pressure balance.

UP8 38 Equilibrium and Stability Properties for Long Stability Period and High-Field Regimes in the ZaP Flow Z-Pinch S.D. KNECHT, U. SHUMLAK, R.P. GOLINGO, B.A. NELSON, *University of Washington* The ZaP Flow Z-Pinch experiment investigates the effect of sheared axial flows on the gross stability of a Z-pinch. The cathode is replaced with a larger version to increase heating through increased adiabatic compression and to increase flexibility of gas injection through a greater number of gas valves. Two operational regimes are identified with the electrode configuration: long stability period; high peak magnetic field. The long stability regime results in a well-centered pinch with little magnetic mode activity for an extended period of time which appears to be limited by the current pulse. The high-field regime results in a ramp-up of magnetic field by a factor of two. Loss of stability is typically correlated with the magnetic field peak. Radial density profile is calculated using a four-chord HeNe interferometer, magnetic field and mode activity are measured with an azimuthal array of probes and total temperature is estimated from these values. Equilibrium and stability properties are calculated and reported.

UP8 39 MCX Results and Plans* RICHARD ELLIS, RYAN CLARY, RAYMOND ELTON, ADIL HASSAM, CARLOS ROMERO-TALAMAS, CATALIN TEODORESCU, ILKER UZUN-KAYMAK, WILLIAM YOUNG, *University of Maryland* SARAH MESSER, SAMUEL BROCKINGTON, ANDREW CASE, DOUGLAS WITHERSPOON, *HyperV Technologies* An overview of the Maryland Centrifugal Experiment (MCX) and recent results are described. Major results include: a) IR interferometers at two axial locations and an axial array of diamagnetic loops demonstrate centrifugal confinement at higher mirror ratio; b) diamagnetic loop and magnetic pickup coil data are compared to an MHD equilibrium model; c) an extensive study of the maximum rotational velocity shows it is limited from above by the Alfven velocity and the critical ionization velocity(CIV) ; d) attempts to inject momentum into MCX using plasma guns have not been successful - experiments will be reported; e) a multi chord Halpha array has measured the radial profiles of neutral hydrogen which are dominated by neutrals at the edge and are hollow at plasma center. Efforts to measure impurity concentrations will also be described. Upgrade plans include a central vessel of 1m diameter, new larger and higher field magnets for the center region, and a discharge capacitor bank of 40kV.

*Work supported by USDOE.

UP8 40 Experimental evidence for MHD plasma centrifugal confinement in open magnetic field configuration CATALIN TEODORESCU, *University of Maryland* RICHARD ELLIS, ADIL HASSAM, CARLOS ROMERO-TALAMAS, WILLIAM YOUNG, In the Maryland Centrifugal Experiment, the plasma is created in a shaped open-field magnetic configuration. Plasma rotation perpendicular to the magnetic field at supersonic speeds (sonic Mach number larger than unity) is controlled by an externally-applied E.× B drift. This work documents the centrifugal confinement effect produced by the plasma rotation from interferometric measurements of plasma density at the magnetic minimum (midplane) and 85 cm off-midplane. Complete time histories of density at these two locations are obtained and compared to deduce the efficacy of axial confinement. Other key parameters are also directly measured at midplane (rotation velocity profiles, ion temperature, and diamagnetic flux) and off-midplane (diamagnetic flux). The observed scaling of the average density ratio at midplane and off-midplane is obtained as a function of the shape of the magnetic field (mirror ratio) and the data are compared with the MHD (Grad-Shafranov equation) solution of the centrifugally confined density. The theory depends on the sonic Mach number and mirror ratio and the data are shown to be in agreement with the predictions of the ideal MHD equilibrium theory.

UP8 41 The Diamagnetism of Rotating Plasmas in Shaped Magnetic Fields* WILLIAM YOUNG, M.R. CLARY, R.F. ELLIS, A. HASSAM, G. SWAN, C.A. ROMERO-TALAMÁS, C. TEODORESCU, I. UZUN-KAYMAK, *University of Maryland* MCX TEAM, A combination of diamagnetic and magnetic pick up loops external to the Maryland Centrifugal Experiment's (MCX) vacuum vessel measure changes in the local radial magnetic field and the averaged axial magnetic field. The measurements provide an axial profile of the rotating plasma's diamagnetism on a millisecond timescale, limited by the L/R time of the vacuum vessel. The results are compared to an MHD equilibrium model by numerically solving for a perturbative solution to the Grad-Shafranov equation which includes supersonic rotation. Combined with density measurements from a midplane interferometer, the numerical model provides an estimate of the plasma temperature and constitutes a test for the efficacy of centrifugal confinement, a central goal of the MCX experiment. The data also provide some insight into various parameter profiles and symmetry. Preliminary analysis shows remarkable agreement for the magnitudes and axial profiles of plasma diamagnetism across broad parameter variations.

*Work supported by USDOE.

UP8 42 Magnetic Spring Experiment R. REID, A. HASSAM, J.C. RODGERS, *University of Maryland* A novel fusion concept, the Thermoelectric Rotating Torus [Hassam et al, this meeting], consists of a supersonic, toroidally rotating toroidal Z-pinch. This concept requires momentum sources that can drive supersonic rotation at high beta with a strong field. Marshall guns work by simultaneously creating a plasma and a magnetic field such that the magnetic pressure accelerates the plasma. The maximum magnetic field is, however, limited by the increased plasma resistance at high B when the electrons become magnetized. The Magnetic Spring Experiment seeks to overcome this limitation by creating a strong magnetic field before plasma formation. This is done using a thin metallic foil to carry the initial current. The foil breaks at high magnetic pressure and a plasma is formed; the device then acts as a Marshall gun but with a pre-established magnetic field. A prototype device has been constructed, and preliminary results demonstrate mechanical breaking of the foil and delayed plasma formation. Data will be presented from arrays of magnetic pickup coils and photodiodes. Numerical simulations will also be presented. Work supported in part by the CMPD and the USDOE.

UP8 43 Plasma Impurity Estimations Using Residual Gas Analysis at MCX* C.A. ROMERO-TALAMAS, W.C. YOUNG, G. TAYLOR, R.F. ELLIS, A.B. HASSAM, C. TEODORESCU, *University of Maryland, College Park, MD 20742* A methodology to characterize impurity concentrations created during plasma shots is being tested at the Maryland Centrifugal Experiment (MCX) [R.F. Ellis, et al., Phys. Plasmas 12, 055704 (2005)]. The methodology consists of measurements every 2 seconds of mass spectra with a residual gas analyzer (RGA) before, during, and after plasma shots (10 ms), and fitting the measured signals to the heat load equation for a fixed volume and time varying pressure. An extrapolation of this equation is then made to the plasma time in order to find the maximum pressure, which is otherwise too high and short-lived for reliable RGA measurements. Ratios of hydrogen or helium to impurities are then estimated and used in MCX theory models, in tracking effects of new instruments installed in the MCX vessel, and in assessing the efficacy of cleaning campaigns on plasma shots.

*Work supported by the U.S. Department of Energy.

UP8 44 Axisymmetric Magnetic Mirrors* THOMAS SIMONEN, *simonen42@yahoo.com* MAGNETIC MIRROR STUDY GROUP COLLABORATION, Linear magnetic mirror confinement systems offer key advantages in construction, operation and maintenance, as well as an absence of disruptions. While simple magnetic mirror systems are MHD unstable: minimum-B Ioffe coil systems are robustly stable and therefore have been the work horse of most past experiments. However Minimum-B coils tend to be larger and have weaker magnetic fields than simple circular coils. They also lead to resonant and neoclassical radial transport.

Consequently the power balance of minimum-B systems is less favorable than can be achieved in axisymmetric mirrors. Over the past years several ways of providing MHD stability have been demonstrated in axisymmetric mirror experiments and other methods have been proposed. The emergence of these methods raises the interest in magnetic mirrors as a potential neutron source for material testing or as a fusion-fission hybrid. This paper describes ten methods that provide MHD stability to axisymmetric mirrors.

*Supported in part by DOE - ORAU

UP8 45 Gas Dynamic Trap Neutron Source (DTNS) – a key to fusion energy* ARTHUR MOLVIK, THOMAS SIMONEN, *ORAU* DMITRI RYUTOV, *LLNL* The DTNS is based on the Gas Dynamic Trap at the Budker Institute of Nuclear Physics – which has stable operation to $\beta \sim 60\%$, T_e increasing with neutral beam power to > 200 eV, and classical behavior of hot ions (Ivanov and Beklemishev, this conf.). The DTNS provides ~ 2 MW/m^{2}neutron flux in a 2.5 cm thick annular 20 l irradiated volume to enable aggressive programs in fusion materials development, tritium-breeding blankets (which do not have to breed initially because the DTNS burns less than 200 g/yr of T), and hybrid fission blankets. Together with the present OFES plasma science program, this would form an aggressive fusion energy program. The major issue is steady-state operation of a configuration that has been demonstrated during 5 ms pulses. The known issues are all engineering: cooling components impinged by beams, pumping the gas and regenerating the pumps. Any plasma physics issues, which appear on longer time scales, can be suppressed to low levels.

*This work performed under the auspices of the U.S. Department of Energy by ORAU and by Lawrence Livermore National Laboratory under Contract DE-AC52-07NA27344.

UP8 46 Anomalous Ambipolar Trapping at Intermediate Collision Frequencies* ALEXEI BEKLEMISHEV, PETER BAGRYANSKY, VLADIMIR MAKSIMOV, *Budker Institute of Nuclear Physics* DMITRIY SKOVORODIN, *Novosibirsk State University* VADIM PRIKHODKO, *Budker Institute of Nuclear Physics* GDT TEAM, Unexpectedly high suppression of axial losses by the ambipolar plug has been observed during compact-plasmoid experiments in the Gas Dynamic Trap. Suppression exceeded factor of 5, while the ambipolar potential was only of the order of 0.5 of the ion and electron temperatures. Meanwhile, theories of ambipolar plugging for both collisional and weakly collisional plasmas predict much smaller effect. Our explanation is based on the fact that the GDT operates in the transitional regime from the gas-dynamic to the standard mirror confinement, i.e., the mean free path is of the order of the length of the trap. It means that the loss cone is full for low-energy particles, and almost empty for particles above temperature. Even a low-potential barrier is able to trap the low-energy ions, hence, application of such barrier effectively drives the trap into the standard-mirror regime with an empty loss cone, i.e., with much lower axial losses. The poster will contain experimental data, simplified analytic theory, and a full kinetic simulation of ambipolar axial confinement at intermediate collision frequencies.

*Supported by RNP 2.1.1/579, RFFI 09-08-00137.

UP8 47 Thermoelectric Rotating Torus (TROT): A Concept for Fusion A. HASSAM, *University of Maryland* The plasma thermoelectric effect (Braginskii, Sakharov) arises because of the $1/v^3$ dependence of the collision operator and drives a B x grad[T] current in a magnetized plasma. This current can maintain a magnetic field in steady state against resistive diffusion if the central electron temperature is maintained by auxiliary heating. The effect is akin to the bootstrap current and is best realized in the creation of a steady state Z-pinch plasma. A Z-pinch is, of course, MHD unstable but a toroidal Z-pinch made to rotate toroidally at supersonic speeds can be made both steady state and stable. This is the idea behind the TROT. The system has two novel advantages: (1) there are practically no major coil systems needed (all the field is internally generated); and (2) there is no technological limit to B, and hence to density (the thermoelectric effect can be used to even pump up an initially weak magnetic field). The overarching questions are: (a) is the effect realizable experimentally and (b) what is an appropriate rotation drive for an initial small experiment? A novel rotation drive is presented elsewhere at this meeting (R. Reid, et al).

UP8 48 Experiments on Plasma Injection into a Centrifugally Confined System* S. MESSER, R. BOMGARDNER, S. BROCKINGTON, A. CASE, F.D. WITHERSPOON, *HyperV Technologies* I. UZUN-KAYMAK, R. ELTON, W. YOUNG, C. TEODORESCU, C.H. MORALES, R.F. ELLIS, *University of Maryland - IREAP* We describe the cross-field injection of plasma into a centrifugally-confined system. Two different types of plasma railgun have been installed on the Maryland Centrifugal Experiment (MCX) in an attempt to drive that plasma's rotation. The initial gun was a coaxial device designed to mitigate the blowby instability. The second one was a MiniRailgun with a rectangular bore oriented so that the MCX magnetic field augments the railgun's internal magnetic field. Tests at HyperV indicate this MiniRailgun reaches much higher densities than the original gun, although muzzle velocity is slightly reduced. We discuss the impact of these guns on MCX for various conditions. Initial results show that even for a 2 kG field, firing the MiniRailgun modifies oscillations of the MCX diamagnetic loops and can impact the core current and voltage. The gun also has a noticeable impact on MCX microwave emissions. These observations suggest plasma enters the MCX system. We also compare diagnostic data collected separately from MCX for these and other guns, focussing primarily on magnetic measurements.

*Supported by a grant from U.S. Department of Energy.

UP8 49 A Robust Modular IGBT Power Supply for Magnetic Confinement Concepts* TIMOTHY ZIEMBA, *Eagle Harbor Technologies* KEN MILLER, *Redmond Plasma Physics Laboratory* JOHN CARSCADDEN, JIM PRAGER, *Eagle Harbor Technologies* Among current challenges in fusion science, and in particular within the Innovative Confinement Concepts (ICC) community, is the ability to generate increased power levels for pulsed magnets, arc plasma sources, radio frequency (RF) heating and current drive schemes at reasonable cost with current generation solid state devices. Continuous wave (CW) tube based power supplies are typically large and expensive, making them prohibitive for smaller experimental facilities or not cost effective when only pulsed input power is required. Next generation solid state power supplies could allow for multiple use applications with a single well developed module that can be easily reconfigured. As such, this type of robust power supply could be beneficial to several important fusion applications including high power RF heating and current drive schemes, high current pulsed magnets and plasma pre-ionization sources. Data will be presented on design characteristics and testing of a modular robust solid state power

supply based on Insulate Gate Bi-polar Transistor (IGBT) technologies and developed by Eagle Harbor Technologies, INC. The modular power supply system can be assembled in multiple ways to address a wide range of applications and needs for the magnetic confinement community.

*Work Supported by DOE SBIR Phase I Grant

UP8 50 Overview of the Levitated Dipole Experiment D.T. GARNIER, M. DAVIS, M.E. MAUEL, *Columbia University* R.M. BERGMANN, J.L. ELLSWORTH, B. KARDON, J. KESNER, P.C. MICHAEL, P. WOSKOV, *MIT PSFC* The Levitated Dipole Experiment (LDX) investigates plasmas confined in the closed field line dipole magnetic geometry where the plasma stability is provided by compressibility and where plasma convection leads to peaked profiles and may allow for $\tau_E > \tau_p$. In the past year, we have continued to investigate the improved energy and particle confinement when the supports are removed from the plasma. Of most significance, we observe that: 1) A large fraction of the stored energy in levitated plasmas is contained in the bulk electron population. 2) Eliminating plasma losses along field lines allows observations of a strong particle pinch leading to a density profile with near equal number of particles per flux tube. 3) The previously observed low frequency fluctuations are consistent with the required turbulent convection to drive the observed particle pinch. In future experiments, an optimal levitation control system will be implemented, reflectometer and soft x-ray spectrometer diagnostics will be added, and a higher frequency (28GHz) electron cyclotron heating source will be added to increase the density of LDX plasmas. In preparation for installing a 1MW ICRF transmitter, initial ion cyclotron heating experiments will also be performed.

UP8 51 Investigation of the Variation of Measured Particle Diffusion Coefficient* M. MAUEL, D. GARNIER, M. DAVIS, *Columbia University* J. ELLSWORTH, R. BERGMANN, J. KESNER, P. WOSKOV, *MIT* Measurements of the time evolution of the plasma density profile with a levitated dipole in LDX determine the radial particle diffusivity, provided the ionization source is known. In discharges where the particle ionization source appears to be at the outer plasma edge, we observe an anomolous inward particle pinch leading to centrally peaked plasma profiles. The observed inward pinch corresponds to a particle diffusivity that is independent of or varies weakly on radius. In these circumstances, the magnitude of the diffusion coefficient is equal to the value estimated from the turbulent electric field fluctuations measured at the edge with an array of floating potential probes, or $D \approx R^2\langle E_\varphi^2\rangle\tau_c$, where τ_c is the correlation time. The fluctuation level varies as the plasma density, gas fueling, and microwave heating power changes. We discuss the relationship between fluctuations and particle transport and describe the relationship between particle diffusivity and fluctuation level for several conditions.

*Supported by US DOE Grants: DE-FG02-98ER54458/9.

UP8 52 The Levitated Dipole Experiment: Experiment and Theory* J. KESNER, R.M. BERGMANN, J.E. ELLSWORTH, B. KARDON, P.P. WOSKOV, *MIT PSFC* M.S. DAVIS, D.T. GARNIER, M.E. MAUEL, *Columbia University* A closed field line confinement system such as a levitated dipole is shear-free and the plasma compressibility provides stability. Theoretical considerations indicate the possibility of both MHD and electrostatic instability that can create turbulent driven transport. Importantly, the resulting transport is expected to create "stationary," inwardly-peaked density and pressure profiles. In LDX, ECH is used to create a low density hot-electron species embedded in a background plasma which, during levitation is seen to contain approximately half of the stored energy. When the floating coil is levitated, competing along-the-field-line losses disappear (all losses become cross-field) and near-stationary density profiles are observed. For edge fueling this inwardly peaked density requires an inward pinch which is also observed. Low frequency kHz range fluctuations appear [Garnier et al., J. Pl. Phys. (2008)] that presumably maintain these profiles. The plasma edge is turbulent and for stationary profiles the edge parameters provide boundary conditions which determine the core parameters.

*Supported by US DOE Grants: DE-FG02-98ER54458/9.

UP8 53 Spatial structure of low-frequency plasma fluctuations in a laboratory dipole experiment* J.L. ELLSWORTH, *MIT PSFC* R.M. BERGMANN, J. KESNER, *MIT PSFC* M. DAVIS, D.T. GARNIER, M.E. MAUEL, *Columbia University* Plasma confined in the field of a levitated dipole-like magnet has been shown to undergo a strong, inward particle pinch that leads to centrally peaked density profiles. This pinch may be driven by turbulent transport. Density fluctuations are observed on the interferometer chords. Visible light emission also fluctuates when plasma density fluctuates. In order to better understand the structure of these fluctuations, two 16-channel photodiode arrays have been constructed. They measure the radial and toroidal variations in fluctuations of visible light emission from the plasma. These measurements are chord integrated so a synthetic diagnostic is used to interpret the fluctuation structure. The observed fluctuations fall into three groups: very low frequency ($f \sim$ 100Hz) coherent mode with an azimuthal mode number n=0 and large radial extent; low frequency ($f \sim$ 1kHz), quasi-coherent, n=1 modes which exhibit different radial structure depending on plasma conditions; and broadband turbulent fluctuations. The structure of the fluctuations for different density profiles will be presented.

*Supported by grants from US DOE.

UP8 54 Soft X-ray Measurement of the Thermal Electron Temperature on the Levitated Dipole Experiment (LDX)* MATTHEW DAVIS, DARREN GARNIER, MICHAEL MAUEL, *Columbia University* JENNIFER ELLSWORTH, *PSFC MIT* The Levitated Dipole Experiment studies plasma confinement in a magnetic dipole field. Measurement of the plasma pressure profile is of particular interest in determining whether the dipole geometry is suitable for magnetically confined fusion. Interferometer measurements on LDX have shown the density profile to be "peaked" during levitation but while edge probe temperature measurements and measurements of the hot electron temperature have been made the thermal electron temperature profile has not been determined. Preliminary soft X-ray measurements have approximated a thermal electron temperature of 800 eV. Here we present further soft X-ray measurements made with a Si-PIN diode and pulse height analysis system. By comparing levitated shots with similar supported shots, in which the thermal population is largely absent due to end losses, we deduce the thermal electron temperature.

*This work is supported by DoE grants: DE-FG02-98ER54458/9.

UP8 55 Eddy Currents and Magnetic Reconstruction in LDX* D.P. BOYLE,† *PPPL* M.E. MAUEL, D.T. GARNIER, *Columbia Univ* J. KESNER, *MIT PSFC* Operations of the Levitated Dipole Experiment (LDX) (http://psfcwww2.psfc.mit.edu/ldx/) in which the superconducting current ring is magnetically levitated by a fixed external coil, rather than mechanically supported, have improved plasma confinement and created peaked plasma profiles. However, since the floating coil is vertically unstable and is maintained in position by feedback, small fluctuations in ring and plasma altitude and current are present. The eddy currents induced in the vacuum vessel by the plasma diamagnetic current and by ring motion must be measured and properly included in order to perform accurate plasma equilibrium magnetic reconstruction. The eddy currents produced by the current ring and external coil are measured by imposing vertical jogs on the ring during vacuum shots. In order to estimate eddy currents produced by the plasma, coils of wire with dimensions similar to the peak plasma current were temporarily installed in vessel and excited by trapezoidal current pulses. Results of the eddy current measurements will be presented, as well as reconstructions of levitated plasma current and pressure profiles.

*Supported by US DOE Grants DE-FG02-98ER54458/9.
†Supported by DOE Fusion Energy Sciences fellowship

UP8 56 2-D modeling of eddy currents in the conducting shell of the Lithium Tokamak Experiment (LTX)* A.D. JONES, L. BERZAK, J. MENARD, R. KAITA, *Princeton Plasma Physics Laboratory* LTX is a low aspect-ratio tokamak with a heated metal shell designed to be coated with liquid lithium. While magnetic fluxes through diagnostic Mirnov coils and flux loops on the LTX machine yield data which may be used to constrain plasma parameters during reconstruction, the measured signals are often highly sensitive to magnetically induced eddy currents in the conducting shell. A meshed representation of the conducting metal shell around the LTX machine is implemented into the 2D, axisymmetric LRDFIT code and used to reconstruct sensor behavior in the presence of eddy currents. The resultant model-predicted signals are compared to the measured diagnostic signals, as well as to model-predicted signals from LRDFIT in the absence of the conducting shell mesh. Alternative methods for the inclusion of the conducting shell in reconstruction codes are discussed.

*Supported by US DOE contract DE-AC02-09CH11466

UP8 57 Modifying interchange turbulence by application of rotating perturbations to a dipole-confined plasma* M.W. WORSTELL, M.E. MAUEL, *Columbia University* B.A. GRIERSON, *PPPL* Measurements using the Collisionless Terella Experiment (CTX) determined the structure of turbulent and unstable interchange mixing. An ERCH generated plasma, in the low density regime the Hot Election Interchange instability dominates, while through the application of axisymmetric biasing at the inner boundary Centrifugal Interchange modes can be excited. With additional gas fueling the plasma undergoes a dramatic transition to a turbulent state. Statistical analysis of global and local measurements of the plasma fluctuations show plasma dynamics to be consistent with predictions of two-dimensional turbulence and with the presence of the nonlinear inverse-energy cascade to larger spatial scale. We report new experiments to directly modify the turbulent spectrum by amplifying or controlling individual wavelengths through the application of electrostatic perturbations. Rotating perturbations with both feedback phase-controlled and with constant frequency open-loop perturbations will be discussed.

*This work is supported by U.S. DOE Grant DE-FG02-00ER54585.

UP8 58 Identification of Large Scale Convective Structures in a Dipole Confined Plasma B.A. GRIERSON,* *Princeton University* MIKHAIL KLASSEN, M.W. WORSTELL, M.E. MAUEL,† *Columbia University* The dipole magnetic field has closed field-lines without magnetic shear, and this confinement configuration allows large fluting instabilities. When dipole-confined plasma is produced with ECRH, fast Hot Electron Interchange (HEI) instabilities appear at low densities, and slower turbulent fluctuations occur at higher densities. The global mode structures of the fast HEI instability and driven centrifugal interchange are understood and have been measured accurately. However, the fluctuations of the turbulent interchange modes are less well understood. These turbulent fluctuations are generated when the plasma is maintained at marginal stability to interchange modes. The turbulent fluctuations are characterized by non-steady rotation and a chaotic temporal evolution of the dominant modes in the system. The convective nature of the turbulent fluctuations by $\mathbf{E} \times \mathbf{B}$ motion is investigated by a spatially and temporally resolved diagnostic measuring the plasma density. Using the time evolution of the density, the plasma continuity equation is inverted for the potential. The global density and potential, as well as the particle transport by $\mathbf{E} \times \mathbf{B}$ are visualized. Transport rates are calculated and compared to transport measurements by probes.

*This work is supported by U.S. DOE Grant DE-AC02-09CH11466.
†This work is supported by U.S. DOE Grant DE-FG02-00ER54585.

UP8 59 28 GHz Gyrotron ECRH Upgrade for LDX* P.C. MICHAEL, P.P. WOSKOV, J.L. ELLSWORTH, J. KESNER, *PSFC-MIT* D.T. GARNIER, *Columbia University* M.E. MAUEL,† R.F. ELLIS, *University of Maryland* A 10 kW, CW, 28 GHz gyrotron is being implemented on LDX to increase the plasma density and to more fully explore the potential of high beta plasma stability in a dipole magnetic configuration. Higher density increases the heating of ions by thermal equilibration and allows for improved wave propagation in planned ICRF experiments. This represents over a 50% increase in the 17 kW ECRH from sources at 2.45, 6.4, and 10.5 GHz. The higher frequency will also make possible access to plasma densities of up to 10^{13} cm^{-3}. The 1 Tesla resonances are located above and below the floating coil near the dipole axial region. The gyrotron beam will be transmitted in TE_{01} mode in 32.5 mm diameter guide using one 90[r] bend and a short $<$ 5 m straight waveguide run. A Vlasov launch antenna in LDX will direct the beam to the upper 1 Tesla resonance region. A layout of the planned system will be presented.

*Supported by U. S. DOE
†Columbia University

UP8 60 Inertial-Electrostatic Confinement Modeling, Parametric Variation, and Comparison to Experiments* GILBERT EMMERT, JOHN SANTARIUS, DAVID DONOVAN, *University of Wisconsin* In inertial-electrostatic confinement (IEC), a high voltage accelerates ions between concentric, nearly transparent grids, usually in spherical geometry. For typical parameters

(~ 0.3 Pa≈ 2 mTorr, ~ 100 kV, ~ 30 mA, ~ 0.5 m anode diameter), atomic and molecular processes dominate operation. A numerically solved integral equation approach to modeling D^+, D_2^+, and D_3^+ ions passing radially through D_2 background gas [1] will be summarized. The approach yields the energy spectra of ions and neutrals plus the neutron production. Parametric surveys and comparisons with experimental data for a University of Wisconsin IEC device will be presented. [1] G.A. Emmert and J.F. Santarius, "Atomic and Molecular Effects on Spherically Convergent Ion Flow I: Single Atomic Species" and "Atomic and Molecular Effects on Spherically Convergent Ion Flow II: Multiple Molecular Species," submitted to *Physics of Plasmas* (2009).

*Research supported by the US Dept. of Energy under grant DE-FG02-04ER54745.

UP8 61 Spatial and Energy Profiling of D-D Fusion Reactions in an Inertial Electrostatic Confinement Fusion Device* DAVID DONOVAN, DAVID BORIS, *University of Wisconsin-Madison* The University of Wisconsin-Madison Inertial Electrostatic Confinement (IEC) Group utilizes highly transparent, concentric spherical electrodes to create a potential well that is used to accelerate charged particles towards the center of the spheres. The cathode is placed at a sufficiently high voltage to accelerate deuterium ions to such a speed as to allow fusion to occur with background, embedded, and other fast particles. A new diagnostic has been developed that uses the time of flight (TOF) of the resulting fusion products to determine where along a radial line through the electrodes the fusion event occurred. The diagnostic is also capable of collecting the energy of the fusion reactants using the magnitude of the Doppler shift of the fusion products. The TOF diagnostic will be used to collect spatial and energy profiles of the fusion reactions occurring along a radial line through a spherical IEC device while varying parameters such as background pressure, cathode voltage, ion current, and spacing between electrodes with levels of accuracy never before achieved on an IEC device.

*Research generously supported by the Grainger Foundation.

UP8 62 TURBULENCE, TRANSPORT, AND STABILITY

UP8 63 Bias voltage effects on plasma turbulence reductions in the Helimak: simulation and experiment* BO LI, BARRETT ROGERS, *Dartmouth College* PAOLO RICCI, *CRPP-EPFL* KENNETH GENTLE, *University of Texas at Austin* The Helimak produces toroidal plasmas with open helical field lines and allows for a controlled study of the relation between flow shear and turbulence in a simple geometry with good diagnostics. Above a threshold in applied bias voltage, the turbulence amplitude is reduced and the radial profiles of the flow velocity and shear are modified. Here the bias observations are simulated numerically with a two-dimensional electrostatic fluid model that evolves the full radial profiles of plasma density, potential and electron temperature. The spatial structures of the density, temperature, potential, flow shear, radial particle transport, and density fluctuation amplitude for the biased and unbiased states are presented. The physical implications of the observations in the simulation and experiment are discussed.

*This work was supported by Center for Integrated Computation and Analysis of Reconnection and Turbulence, the U.S. Department of Energy.

UP8 64 Turbulence and Turbulence Suppression in the Helimak* KENNETH GENTLE, W. ROWAN, K. LIAO, B. COVELE, *University of Texas at Austin* BO LI, *Dartmouth College* The Helimak is an approximation to the infinite cylindrical slab, but with open field lines of finite length. Radially segmented isolated end plates allow application of radial electric fields that drive radial currents. Above a threshold in applied voltage (driven current), the fractional turbulent amplitude is greatly reduced, as is the radial turbulent particle transport in the region of applied bias. Stabilization is observed for both positive and negative bias. Concurrent measurements of the ion flow velocity are made by Doppler spectroscopy. The turbulence – density, potential, and temperature fluctuations and their relations, will be compared with simulations from a fluid model for this geometry. Local comparisons of turbulence reduction with changes in radial correlation length and flow shear will be given.

*Work supported by the Department of Energy OFES DE-FG02-04ER54766.

UP8 65 Edge Turbulence Saturation, Sheared Flow and Blobs* D.A. D'IPPOLITO, J.R. MYRA, D.A. RUSSELL, *Lodestar Research Corporation* Simulations with the Lodestar Scrape-Off-Layer Turbulence (SOLT) code are used to study (i) saturation mechanisms for edge turbulence (viz. sheared flow and profile flattening), (ii) the existence of a critical gradient due to the Kelvin-Helmholtz (KH) instability, and (iii) the effect of the saturated turbulence on blob creation. Source terms for particles and heat are balanced by the turbulent transport of particles, energy and momentum across the edge and SOL. This results in the development of sheared flows, which can be limited by the KH instability. This process is studied for electrostatic curvature-driven interchange turbulence. Because the simulation allows full profile evolution, a sharp transition is observed from saturation by sheared flows to saturation by profile flattening as the turbulence drive increases and the linear growth rate exceeds the maximum velocity shear allowed by the KH instability. The effect of the sheared flow on blob creation and transport will also be assessed.

*Work supported by USDOE grant DE-FG02-97ER54392.

UP8 66 Transport with Reversed Er in Gamma -10, LAPD and the Sao Paulo Tokamak SEAN FU, P.J. MORRISON, W. HORTON, *Institute for Fusion Studies* IBERE CALDAS, *USP/Sao Paulo/ Brazil* INSTITUTE FOR FUSION STUDIES TEAM, UNIVERSITY OF SAO PAULO TEAM, The understanding of how and when the reversed radial electric field produces an internal transport barrier is still poorly understood. There are two linked aspects to the problem: (i) the change in the plasma instabilities and thus the fluctuation spectrum from changes away from or towards the generalized Rayleigh condition for destabilizing the drift wave/ Rossby wave instabilities and (2) for a fixed fluctuation spectrum the role of the E_r reversal in creating a layer where the resonant surfaces do not overlap so the condition for the onset of diffusion from overlapping resonances in phase space is not satisfied. We look at a model that is representative of the externally controlled E_r shear in the G-10 Tsukuba tandem mirror and in the wall biasing experiments in the LAPD and the Sao Paulo Tokamak to ask when the effects are dominant and how they may compete with each other to determine the conditions for the transport suppression that is reported in numerous plasma experiments.

UP8 67 Toroidal and Poloidal Flow Evolution C.J. McDEVITT, P.H. DIAMOND, *UCSD* O.D. GURCAN, *CNRS* T.S. HAHM, *PPPL* We present recent results in the theory of turbulent momentum transport pertinent to the description of intrinsic rotation. Emphasis is placed on the self-consistent evolution of poloidal and toroidal flows. Both turbulent and neo-classical stresses are considered, allowing for the recovery of purely neo-classical flows, as well as the description of deviations induced by the background turbulence. Along with radial force balance, toroidal and parallel force balance are utilized to constrain the evolution of poloidal and toroidal momentum. Within the turbulent toroidal momentum flux, in the limit of small but finite inverse aspect ratio, two distinct non-diffusive contributions capable of spinning up a plasma from rest are identified. The first results from E $\times$ B shear induced symmetry breaking of the underlying wave population, whereas the second follows from charge separation induced by the polarization drift. An expression for the poloidal flow, including both neo-classical and turbulent stresses, is obtained from parallel force balance. Potentially significant deviations from neo-classical poloidal rotation are found, which are in turn seen to provide a robust means of enhancing toroidal flow generation. Ongoing work is devoted to the development of a self-consistent model describing the coupled poloidal and toroidal flow evolution.

UP8 68 Edge coherent structures in RFX-mod high current regimes PAOLO SCARIN, MATTEO AGOSTINI, ROBERTO CAVAZZANA, FABIO SATTIN, GIANLUIGI SERIANNI, MONICA SPOLAORE, NICOLA VIANELLO, *Consorzio RFX* The Reversed Field Pinch Experiment RFX-mod is characterized by a complex edge magnetic topology which is correlated with strong pressure gradients. It features also the presence of coherent electron pressure structures, resulting from nonlinear couplings between electron density, temperature and magnetic field. In this work we present measurements of edge parameters by an optical non-perturbing diagnostic (Thermal Helium Beam), which allows the studying of the edge turbulence up to 0.5MHz of high plasma current. The high-frequency HeI emission line has characterized from a Gas Puffing Imaging diagnostic, so it is possible to measure the electron density and temperature of the turbulence structures down to $2\mu s$ scale. From these measurements it appears that there is a clear correlation between better magnetic boundaries (SHAx states) and steeper electron pressure profiles. This has an impact upon global plasma performances since the dimension of edge coherent structures is also correlated with the characteristic pressure length.

UP8 69 Effect of the helical ripple on the confinement via zonal flows in helical plasmas S. TODA, K. ITOH, *National Institute for Fusion Science* The control of zonal flows is the key issue in fusion research. We have examined the reduction of the anomalous transport due to the excitation of zonal flows by the transport code analysis in the core region [1]. The electron Internal Transport Barrier in helical plasmas was shown to be formed by the mechanisms of (i) the bifurcation of the ambipolar electric field and (ii) the reduced damping of zonal flows which causes the suppression of the turbulent transport. In the collisionless plasmas of the Large Helical Device (LHD) (in the region of the negative electric field), if the helical ripple becomes smaller, the level of the anomalous transport gets lower. We focus on the effect of the helical ripple related with zonal flows on the confinement in the helical plasmas. The reduction of the effective helical ripple causes the smaller damping rate of zonal flows in the helical plasmas even in the branch of the ion root, which means that the reduction of the anomalous transport can be obtained. For the cases of the different values for the helical ripple, the calculation results including the effects of zonal flows will be shown. This study is to investigate the impact of shifting axis positions, because the value of the helical ripple changes due to the variation of the experimental magnetic axis positions in LHD. This calculation result will explain the observations on LHD. [1] S. Toda et al., Nucl. Fusion Vol. 47 (2007) 914-919

UP8 70 Gyrokinetic simulation of zonal-flow response in LHD plasma with equilibrium-scale radial electric field TOMOHIKO WATANABE, HIDEO SUGAMA, *National Instituite for Fusion Science* For the anomalous transport reduction, it is important to seek a magnetic configuration with strong zonal-flow generation. The zonal-flow response is enhanced in a neoclassically-optimized helical configuration with slower radial drift of trapped particles, such as the inward-shifted LHD plasma. It is also pointed out that an equilibrium-scale radial electric field (E_r) leads to further increase of zonal flows in helical systems [1]. Our gyrokinetic simulations show increase of the residual zonal flows in case with the poloidal Mach number of 0.1-0.3, and support the theoretical prediction. The residual zonal-flow amplitudes are weakly dependent on the radial wavenumbers in the inward-shifted LHD plasma, while, in case without E_r, the lower residual level is found for the longer radial wavelength. In the standard LHD configuration, furthermore, the zonal-flow response shows an oscillatory behavior. It is also noteworthy that, under the identical conditions on the magnitude of E_r and the magnetic geometry, using ions with a heavier mass gives rise to a higher zonal-flow response. Therefore, the turbulent transport is expected to show a more favorable ion-mass dependence than the conventional gyro-Bohm scaling. [1] H. Sugama and T.-H. Watanabe, Phys. Plasmas **16**, 056101 (2009).

UP8 71 Effects of unsteady sheared E×B flow on slab ITG turbulence SHINYA MAEYAMA, SHUNJI TSUJI-IIO, HIROAKI TSUTSUI, *Tokyo Institute of Technology* AKIHIRO ISHIZAWA, TOMOHIKO WATANABE, MILOS SKORIC, NORIYOSHI NAKAJIMA, *National Institute for Fusion Science* Effects of unsteady sheared **E×B** flow on drift wave turbulence and heat transport driven by slab ion temperature gradient (ITG) instability are investigated by means of Landau fluid simulations. Here, the **E×B** flow, which consists of stationary and time-periodic oscillatory parts, is externally applied to the turbulence. The dependence on the amplitude and frequency of **E×B** flow are examined in the case where the energy of **E×B** flow is the same or larger than the energy of turbulence. In the case above, the transport oscillates with the same period as the **E×B** flow and the time-averaged transport coefficient is larger than the coefficient which is evaluated without oscillatory part of **E×B** flow. The time-averaged coefficient is maximized at the point where the amplitude of oscillatory part is equal to that of stationary part. As the frequency of **E×B** flow increases, the time-averaged coefficient decreases and is close to the coefficient which is evaluated without oscillatory part. These mechanisms are explained.

UP8 72 Natural Fueling of a Tokamak Fusion Reactor WEIGANG WAN, SCOTT PARKER, YANG CHEN, FRANCIS PERKINS, *Center for Integrated Plasma Studies, University of Colorado, Boulder, CO 80309* A plausible natural fueling mechanism for tokamak fusion reactors is discussed. In H-mode plasmas dominated by ion-temperature gradient driven turbulence, cold

deuterium and tritium ions near the edge naturally pinch radially inward towards the core. This may lower some of the pellet acceleration requirements on the pellet injection system on ITER. The natural fueling mechanism is shown using the three-dimensional toroidal electromagnetic gyrokinetic turbulence code GEM. Realistic Tokamak profiles relevant to ITER are tested. A quasi-linear theory is presented explaining the mechanism. Both a non-adiabatic electron response and the effects of toroidal geometry are found to be favorable for natural fueling. Additionally, it is shown that helium ash diffuses radially outward as the cold fuel moves radially inward.

UP8 73 Coupling of turbulent energy and momentum transport A.I. SMOLYAKOV,*X. GARBET, C. BOURDELLE, *CEA Cadarache, IRFM. Saint Paul Lez Durance, France* The parallel momentum balance in low pressure tokamak plasma is analyzed in the framework of fluid theory. It is shown that inertial effects and gyroviscosity lead to coupling of parallel momentum balance with fluctuations of electrostatic potential and plasma pressure [1]. Such coupling, mediated by magnetic field curvature, was earlier identified in gyrokinetic theory [2, 3]. Set of evolution equations for plasma density, energy and parallel momentum are formulated in the form of the conservation laws for Lagrange invariants r_1=ln(n/B^2), $r_2 = ln(p^{3/2}/B^5)$ and $r_3 = ln(V_\parallel/B)$. Coupling of the evolution of parallel momentum to fluctuations of the potential and pressure leads to the modification of the Lagrange invariants. In linear theory, the gradients of the equilibrium profiles of r_1, r_2 and r_3 serve as generalized thermodynamic forces responsible for the slab ITG, toroidal ITG, and parallel flow shear instabilities. Coupled equations for energy and momentum transport are derived in quasilinear approximation. [1] A.I. Smolyakov, X. Garbet, C. Bourdellle 2009, Nuclear Fusion [2] Hahm T S, Diamond P H, Gurcan O D and Rewoldt G 2007 Physics of Plasmas 14 072302 [3] Peeters A G, Angioni C and Strintzi D 2007 Physical Review Letters 98 265003

*Also at University of Saskatchewan, Saskatoon, Canada

UP8 74 Gyrokinetic particle simulations of microturbulence in reversed shear plasmas WENJUN DENG, ZHIHONG LIN, *University of California, Irvine* Electrostatic ion temperature gradient (ITG) and trapped electron mode (TEM) turbulence in tokamak plasmas with reversed magnetic shear is studied by particle-in-cell (PIC) simulations using Gyrokinetic Toroidal Code (GTC). In the ITG turbulence, electrostatic potential gaps are observed in the minimum-q region in the linear phase when $q_{\min}$ is an integer. The mode rational surface distributions are investigated. When $q_{\min}$ is an integer, some rational surfaces degenerate at the minimum-q position, forming two gaps in which there's no rational surface. The potential gap has similar size as the rational surface gaps, confirming previous theories of weakening of toroidal coupling by rarefaction of rational surfaces, which generates a gap in the global mode structure. In the TEM turbulence, the mode grows only in the positive-shear side in the linear phase, because electron precession drift velocity is decreased or reversed in the negative-shear side, breaking the precessional resonance. In the non-linear phase of both ITG and TEM turbulence, turbulence spreads into linearly stable regions. Whatever structure formed in the linear phase is destroyed. The fluctuation and transport have no significant gap across the $q_{\min}$ region even when $q_{\min}$ is an integer.

UP8 75 Streamers and zonal flows in interchange-unstable Boussinesq plasmas* MIKHAIL MALKOV, PATRICK DIAMOND, *UCSD* The interchange instability can be described in the framework of two-dimensional Boussinesq fluid approximation. Assuming very low viscosity and thermoconductivity for such a plasma, we reduce the Boussinesq system to simple moment (Galerkin) equations. However, in contrast to conventional treatments of moment systems that invoke truncations an ad hoc closures, we propose an incomplete closure. It is based on integral inequalities and is in that sense exact even though not fully determined. Nevertheless, the proposed closure constraints the system dynamics to allow predictions of streamers or zonal flows as time asymptotic states depending on the initial conditions. These findings are instrumental in constructing the time asymptotic quasi-stationary solutions of the original Boussinesq equations which are also discussed.

*Supported by the US DoE

UP8 76 Influence of the internal magnetic fluctuation and the dynamic ergodic divertor on the transport of runaways in the TEXTOR tokamak* OSWALD WILLI, TIMUR KUDYAKOV, *HHU* KARL HEINZ FINKEN, SADRILLA ABDULLAEV, MICHAEL LEHNEN, *FZJ* SERGEY BOZHENKOV, MARCIN JAKUBOWSKI, *MPI* YUHONG XU, *LPP* Influence of the internal magnetic fluctuations and resonant magnetic perturbation on the transport of runaway electrons has been studied during the low density discharges at the TEXTOR tokamak. The diffusion coefficient was derived as a function of Bt by means of synchrotron radiation measurements. Applying the model which includes the transport reducing effect of the electron orbit shift the magnetic fluctuation level was estimated from the measured diffusion coefficient. It was found that an increase of runaway losses with the decreasing toroidal magnetic field is accompanied with a growth of the magnetic fluctuations in the plasma. The energy resolved measurements confirm that runaway loss occurs predominantly for low energy runaways (few MeV) and considerably less for high energy ones. Externally applied magnetic perturbations show the same behaviour: confinement of highly relativistic electrons is less affected by the magnetic perturbations as compared to low energetic ones.

*Funding of this work by GRK1203 is acknowledged.

UP8 77 Drift waves in finite beta plasmas and the thermoelectric effect CHINGPUI HUNG, ADIL HASSAM, *IREAP, University of Maryland* The plasma thermoelectric effect generates a B x grad[T] current in a magnetized plasma and is of the same order as the plasma resistivity limited current in a finite beta plasma. Since drift waves are driven by resistivity, it is of interest to know how thermoelectricity affects drift wave stability and, in turn, how drift wave turbulence would influence the (dissipative) thermoelectric effect. In particular, can current generated from thermoelectricity survive turbulence? We study drift waves in beta $\sim$ O(1) systems (e.g., FRCs). At this level, the sonic and Alfven DWs are strongly coupled. For isothermal perturbations, we find that finite beta is strongly stabilizing. With temperature perturbations, we find a new local instability, which is mediated by the Braginskii thermal force; also heat conductivity and resistivity may be stabilizing and this will be discussed. The nonlocal theory and universality of this mode is under investigation. A finite beta 3D 2-fluid code will be used to investigate these various situations and the ensuing turbulence will be studied.

UP8 78 Neoclassical ion heat flux and poloidal flow in a tokamak pedestal* GRIGORY KAGAN, *Massachusetts Institute of Technology* PETER J. CATTO, *Plasma Science and Fusion Center, MIT* In the core of a tokamak, neoclassical transport normally dominates over classical while itself being dominated by turbulent transport. The situation may be different in a high confinement (or H) mode pedestal, where the latter is effectively suppressed by a strongly sheared equilibrium electric field. On the other hand, this very field makes conventional neoclassical results inapplicable in the pedestal by significantly modifying ion drift orbits. We present the first calculation of the banana regime neoclassical ion heat flux and poloidal flow in the pedestal accounting for the strong *ExB* drift inherent to this tokamak region. Interestingly, the fact that ion heat conductivity depends on the local values of the electric field and its shear allows us to hypothesize about possible shapes of the global electric field and density profiles in the pedestal. We also find that due to the electric field the pedestal poloidal ion flow is likely to change its direction as compared to its core counterpart. This result elucidates the discrepancy between the conventional banana regime predictions and recent experimental measurements of the impurity flow performed at Alcator C-Mod.

*Work supported by U.S. DoE

UP8 79 Development of drift ballooning transport model for tokamak edge plasmas T. RAFIQ, A.H. KRITZ, G. BATEMAN, A.Y. PANKIN, *Lehigh U.* A model is developed for transport driven by drift resistive ballooning modes (RBMs). These modes are expected to have a significant role in the lower temperature edge regions of Ohmic and L-mode discharges. A unified theory that includes both resistive and electron inertial ballooning modes is derived using a two fluid model for electron and ion plasmas. The derivation includes finite beta and diamagnetic effects, parallel electron and ion dynamics, electron inertia, transverse particle diffusion, perpendicular gyro-viscous stress terms, electron and ion equilibrium temperature gradients and temperature perturbations. Electron trapping and impurity perturbations are ignored for simplicity. Transport coefficients driven by RBMs are computed using a quasi-linear theory. A prediction for the saturation level is obtained by balancing the resistive ballooning mode growth rate against the nonlinear $\mathbf{E} \times \mathbf{B}$ convection. The dependence of the modes as a function of various plasma parameters is explored. It is anticipated that transport associated with this RBM model will become a component of a multi-mode transport model for use in predictive modeling of tokamak discharges.

UP8 80 Progress on the development and integration of the Framework for Modernization and Componentization of Fusion Models (FMCFM)* ALEXANDER PLETZER, SRINATH VADLAMANI, *Tech-X Corp* ALEXEI PANKIN, *Lehigh U* SCOTT KRUGER, JOHAN CARLSSON, JOHN CARY, *Tech-X Corp* The Framework for Modernization and Componentization of Fusion Models (FMCFM) is an SBIR funded project aimed at offering multiple, anomalous and neoclassical transport flux models within a single, multi-species and multi-language (Fortran, C/C++) friendly interface. FMCFM has been extended in the past year to include the GYRO, TGLF, KAPISN, MMM08, and NCLASS models in addition to the existing GLF23 and MMM95 models, prompting a complete rewrite of the interface. The new FMCFM interface will be described from the point of view of its integration within the Framework Architecture for Core-Edge Transport Simulation (FACETS). Also discussed will be future FMCFM plans for computing momentum transport terms and other user driven extensions.

*Funded by Grant DE-FC02-07ER54907

UP8 81 First temporally dynamic simulation of core transport using the FACETS framework with GYRO and NUBEAM* SRINATH VADLAMANI, *Tech-X Corp.* JEFF CANDY, AARON COLLIER, *General Atomics* AMMAR HAKIM, SCOTT KRUGER, ALEX PLETZER, *Tech-X Corp.* FACETS TEAM, Motivated by the need to accurately predict the time evolution of profiles in tokamaks, we present initial results of core transport simulations using first principle anomalous and neoclassical flux calculations obtained from the GYRO and NEO codes, respectively. Sources are provided by NUBEAM. All three components (GYRO, NEO, and NUBEAM) are executed concurrently using the Framework Architecture for Core-Edge Transport Simulations (FACETS). Progress on the development of a new core solver, which is sufficiently robust to implicitly advance distributed kinetic components, each running on 100-1000s cores, will be presented.

*DE-FC02-07ER54907, DE-FC02-07ER54921

UP8 82 Continuum solution of the drift kinetic equation in NIMROD* ERIC HELD, JEONG-YOUNG JI, MUKTA SHARMA, *Utah State University* NIMROD TEAM, Efforts to incorporate the nonlocal transport of heat and momentum along magnetic field lines in simulations of high-temperature plasmas have focused on integral (nonlocal) forms for the parallel heat flow and stress closures. Although such closures can be rigourously derived, their efficient computation in plasma fluid codes remains a formidable numerical challenge. In this work, we describe a complementary approach to computing closures that uses a continuum solution to the plasma kinetic equation. The closures constructed from these solutions are coupled to the evolving fluid moment equations of the NIMROD code. In addition to capturing the parallel free-streaming and accurate collisional effects of the integral closures, the continuum solution also includes time-dependence, particle trapping and acceleration physics. In this approach, we solve for the coefficients of an expansion in Legendre polynomials on a grid in speed, $s = v/v_T$, throughout the computational domain. Examples of heat and momentum transport in the vicinity of magnetic islands are discussed including comparisons between the integral and continuum closures in the steady state limit. We also compare the continuum and integral closures applied to the problem of sound wave damping as collisionality varies.

*Research supported by the U. S. DOE under grants nos. DE-FG02-04ER54746, DE-FC02-04ER54798 and DE-FC02-05ER54812.

UP8 83 Effect of Trapped Electrons on Turbulence driven Toroidal Momentum and Heat Transport W.X. WANG, T.S. HAHM, P.H. DIAMOND, *UCSD* S. ETHIER, W.M. TANG, W.W. LEE, G. REWOLDT, W. SOLOMON, S.M. KAYE, J. LANG, R. KOLESNIKOV, *PPPL* Using global gyrokinetic simulation, a robust residual stress is found to be nonlinearly generated in both ion temperature gradient (ITG) and trapped electron mode (TEM) tur-

bulence via symmetry breaking in the parallel wave number spectrum, which is induced by turbulence self-generated flow shear. This residual stress represents a significant, universal, non-diffusive component of toroidal momentum transport, which may play an important role for the generation of intrinsic rotation in tokamak experiments. In the ITG marginality regime, trapped electron physics is shown to play a critical role in determining plasma transport, not only producing the proper ion heat flux in experiments but also largely enhancing the residual stress generation. However, trapped electrons do not change the qualitative phase space structure of ITG driven momentum and heat fluxes. On the other hand, TEM driven momentum transport is made by ions from different regions and in a different way in the phase space. Determination of the non-diffusive momentum transport direction (inward or outward) is also examined in connection with the characteristics of the turbulence spectrum. Further, a momentum pinch is shown via simulations using different rigid rotations. Finally, very impressive observations of large eddy formation from earlier phase fine streamers, along with dramatic nonlinear energy cascades to longer wavelengths, in electron temperature gradient driven TEM turbulence is reported. Work supported by U.S. DOE Contract DE-AC02-09-CH11466 and the SciDAC GPS-TTBP project.

UP8 84 Current interchange tearing modes as explanation of tokamak anomalous transport: intermittent/blob formation and transport barrier* L.J. ZHENG, J.W. VAN DAM, *University of Texas at Austin, Institute for Fusion Studies* We show that, in addition to usual neoclassical tearing modes, another type of non-classical tearing mode exists in tokamaks: viz., current interchange tearing modes (CITMs). CITMs are directly driven by unstable electromagnetic and electrostatic modes of the interchange type (e.g., interchange/ballooning modes, drift waves, etc.). Since interchange-type modes exchange not only thermal and magnetic energies, but also current, between flux tubes, a current sheet can be created at a mode resonance surface and a CITM can be excited. The CITMs might provide an alternative explanation for certain aspects of tokamak anomalous transport. Instabilities of the interchange type could be directly converted into CITMs, instead of forming turbulent eddies through nonlinear coupling as in conventional transport theories. In that case, the radial transport step-size would be enlarged via the formation of magnetic islands and their reconnection. In particular, CITMs could help explain the formation of blob filamentary (or intermittent) structures and of transport barriers in reversed-shear configurations, as observed experimentally.

*Research supported by USDOE grant DE-FG02-04ER54742.

UP8 85 Destabilization mechanism of edge-localized MHD modes by a toroidal rotation in tokamaks NOBUYUKI AIBA, *Japan Atomic Energy Agency* MASARU FURUKAWA, *University of Tokyo* MAKOTO HIROTA, SHINJI TOKUDA, *Japan Atomic Energy Agency* In JT-60U, some experimental results showed that the ELM frequency depends on the toroidal rotation, and the rapid rotation in the counter direction of the plasma current changes from Type-I ELM to Grassy ELM, whose frequency is high and the amplitude is small [1]. Since both Type-I and Grassy ELMs are considered as ideal MHD modes destabilizing near the plasma surface, theoretical and numerical analyses about the toroidal rotation effects on the edge localized MHD mode are important to understand this dependence of the ELM frequency on the toroidal rotation frequency. Our previous works have illustrated that the toroidal rotation with shear can destabilize low/intermediate-n (<50) modes [2], but the mechanism of this destabilization is not still clarified. In this paper, we investigate numerically the destabilizing effect of a toroidal rotation on the edge localized MHD mode with the MINERVA code [2], which solves the Frieman-Rotenberg equation. Particularly, we pay attention to the destabilizing effects of the toroidal rotation shear and the centrifuged force on not only equilibrium but also change of equation of motion. [1] N. Oyama et al., Plasma Phys. Control. Fusion 49, 249 (2007). [2] N. Aiba et al., Nucl. Fusion 49, 065015 (2009).

UP8 86 Rotation and rotation shear effects on resistive wall mode stability JUNYA SHIRAISHI, SHINJI TOKUDA, NOBUYUKI AIBA, *Japan Atomic Energy Agency* To study the rotational effects on resistive wall mode (RWM) stability, especially to clarify where the effects are essential for stabilizing RWM (rational surface, Alfven resonant surface, plasma surface, etc), the historic matching problem for magnetohydrodynamic stability analysis [1] is revisited. The existence of the rotation requires the generalization of the Newcomb equation, which plays an essential role in the matching problem. The rotation brings about the split of singularity in the generalized Newcomb equation due to the Doppler shift. We point out that the resonant surface can deviate from the singularities if the mode has a real frequency, which indicates that the locations where the resonance occurs cannot be determined a priori. If the mode frequency is limited in a certain range, such as the RWM case, the range in which the resonance occurs is finite around the singularity. Hence the classical asymptotic matching method becomes invalid. In this study, it is shown that a newly proposed matching method [2], which generalizes the asymptotic one to use the layer with finite width, can resolve the difficulty. [1] H.P. Furth, J. Killeen and M.N. Rosenbluth, Phys. Fluids 6, 459 (1963). [2] S. Tokuda, J. Shiraishi et al., 22nd IAEA FEC TH/P9-20 (2008).

UP8 87 Two-dimensional magnetohydrodynamic simulations of time-dependent poloidal flow.* LUCA GUAZZOTTO, RICCARDO BETTI, *University of Rochester* Poloidal flows in tokamaks are receiving an increasing attention, as newer and better flow measurements keep increasing the amount of available experimental information. In particular, finite poloidal flows are routinely observed in experiments in the edge region of the plasma. MHD theory predicts that when the poloidal velocity is transonic with respect to the poloidal sound speed ($c_{sp} \equiv c_s B_p/B$, where B_p is the poloidal field) shocks will develop in the transonic region. Such shocks will then move in the poloidal direction and disappear once they reach the location of the minimum transverse flow cross section (typically the inboard midplane in a low-β plasma). In the aftermath of the shock disappearance, a pedestal in plasma density and pressure is left, with the height of the pedestal depending on the poloidal location. In this work, we present the result of time-dependent simulations aimed at reproducing the theoretical prediction. Simulation results show how an initial condition with transonic flow evolves, creating a train of shocks near the transonic surface, which eventually result in sharp transitions in (e.g.) density profiles, not dissimilar from what is predicted by theory.

*This work was supported by the US Department of Energy under Contract No. DE-FG02-93ER54215.

UP8 88 Influence of a Nonuniform Resistive Wall on the RWM Stability in a Tokamak CALIN V. ATANASIU, *MEdC EURATOM Association, Bucharest, Romania* AUGUSTIN MORARU, *University Politehnica of Bucharest, Romania* LEONID E. ZAKHAROV, *Princeton University, Plasma Physics Laboratory, Princeton, USA* Writing the expression for the potential energy in terms of the perturbation of the flux function, and performing an Euler minimization, one obtains a system of ordinary differential equations in that perturbation. For a toroidal geometry with a separatrix, natural boundary conditions for the perturbed flux function, just at the plasma boundary have been determined by replacing the vanishing boundary conditions at infinity. By adding the wall, in its thin approximation, but with a realistic geometry with access holes, new boundary conditions for the external kink mode, now a resistive wall mode, due to the field produced by the eddy currents in the wall and due to feedback coils have been determined. The present work is devoted to the presentation of a very fast and reliable numerical tool to calculate the influence of the eddy currents on the boundary conditions with the help of a scalar stream function for the induced surface currents.

UP8 89 A Feasibility Study of ELM Control Coils for JET C.G. LOWRY, *EFDA JET* A. BROOKS, *PPPL* M. COLE, *ORNL* T. EDLINGTON, *UKAEA* T. EVANS, *GA* J. HARRIS, *ORNL* R. HAWRYLUK, *PPPL* L. HORTON, *EFDA JET* D. HOWELL, *UKAEA* R. KOSLOWSKI, Y. LIANG, *FZ Juelich* A. LOVING, E. NARDON, *UKAEA* G.H. NEILSON, *PPPL* H. OMRAN, D. RENDELL, *UKAEA* M. SCHAFFER, *GA* J. STRACHAN, *PPPL* Y. SUN, *FZ Juelich* T.N. TODD, *UKAEA* I. ZATZ, *PPPL* As part of its efforts in preparing for ITER operations, JET is investigating the feasibility of including RMP coils for ELM control. The objective is to provide a system which will make scenario development more ITER relevant, and extend the experimental basis for the physics understanding of ELM suppression, in particular towards conditions close to those of ITER. The study, being conducted under an EU-US collaboration, has considered various coil configurations, including in- and ex-vessel coils. Vacuum field calculations show that in-vessel configurations can produce a much higher fraction of resonant to non-resonant perturbations, but present difficulties related to feedthroughs, vacuum compatibility, and remote handling, although the lower required currents are beneficial. The paper will present the physics criteria used to choose the configuration and outline the technical solutions adopted.

UP8 90 Nonlinear magnetic island dynamics and neoclassical toroidal viscosity in quasi-symmetric configurations* C.C. HEGNA, *University of Wisconsin* In a general 3-D magnetic confinement device, singular Pfirsch-Schlüter currents arise at rational surfaces in the plasmas due to pressure gradients and resonant components of $1/B^2$. These singular currents can be resolved by allowing magnetic islands to form. Additionally, 3-D magnetic fields produce net radial particle drifts that give rise to viscous forces on the plasma. These effects are included in an analytic calculation for isolated magnetic islands using drift kinetic theory for magnetic configurations that are quasi-symmetric, i. e., $|B| = B_o[1 - \epsilon_h \cos(M\theta - N\zeta)] + \delta B(\psi,\theta,\zeta)$ where $M\theta - N\zeta$ denotes the dominant helical symmetry angle and the 3-D helical sidebands are assumed small ($\delta B/B_o \ll \epsilon_h$). The viscous force produces contributions to the island dynamics that have both 'inertial' and 'dissipative' components. The dissipative component yields non-ambipolar particle transport and torques on the plasma in the symmetry direction that influence the island rotation properties. The inertial contribution produces no net torque but does produce a localized current that may partially oppose the singular Pfirsch-Schlüter current and reduces its effect on the self-consistent magnetic island width.

*Research supported by U. S. DoE under grant no. DE-FG02-86ER53218 and DE-FG02-99ER54546.

UP8 91 Studies of Alfvénic instabilities by a kinetic-fluid model Y. NISHIMURA, C.Z. CHENG, *Plasma and Space Science Center, National Cheng Kung University, Tainan 70101, Taiwan* Employing a kinetic-fluid simulation model[1], Alfvénic instabilities driven by energetic particles are studied in tokamak plasmas. The kinetic-fluid model incorporates all the particle dynamics through the pressure tensor by taking the second order moment of the particle simulation while the electromagnetic field quantities are evolved in the fluid equations. The kinetic-fluid model retains the ion and electron wave-particle interaction for both the bulk and the energetic plarticle components. Global Alfven oscillation, continuum damping, and the generation of the TAE gap[2] in the toroidal geometry are demonstrated in the MHD limit.[3] Kinetic particles[4,5] are then incorporated into the fluid set of equations to excite the instabilities (bulk ions/electrons replace the pressure evolution equation). This work is supported by National Cheng Kung University Top University Project.

[1]C.Z.Cheng and J.R.Johnson, J. Geophys. Res. 104, 413 (1999).
[2]C.Z.Cheng and M.S.Chance, Phys. Fluids 29, 3695 (1986).
[3]Y.Nishimura, J.D.Callen, C.C.Hegna, Phys. Plasmas 6, 4685 (1999).
[4]Y.Nishimura and M.Azumi, Phys. Plasmas 4, 2365 (1997).
[5]Y.Nishimura, Contrib. Plasma Phys. 48, 224 (2008).

UP8 92 Nonlinear Ballooning Instability in the Vicinity of a Separatrix* P. ZHU, C.C. HEGNA, C.R. SOVINEC, *University of Wisconsin-Madison* A recent study suggests the presence of a magnetic separatrix may have a unique role in ELM dynamics [1]. More generally, it is not clear if the presence of magnetic separatrix is a prerequisite for the onset of ELMs. In this work, we examine the effects of the magnetic separatrix on the nonlinear dynamics of ballooning instabilities in the H-mode pedestal region of a divertor tokamak, and compare the results to similar analyses applied to limiter tokamaks. Both MHD theory and simulations are being developed to model the linear and nonlinear properties of the ballooning instability in the vicinity of a separatrix. Previous work on the intermediate nonlinear ballooning regime [2] is extended to include the geometry effects of the magnetic separatrix and X-point. The physical significance of the field line stochasticity induced by the separatrix configuration during the late nonlinear stage of ballooning instability will be discussed. [1] L. Sugiyama and H. Strauss, ELMs: A new type of plasma instability, CEMM Workshop, May 2 2009, Denver, CO. [2] P. Zhu, C.C. Hegna, and C.R. Sovinec, Phys. Rev. Lett. 102, 235003 (2009).

*Supported by Grants DE-FG02-86ER53218 and DE-FC02-08ER54975.

UP8 93 Effect of FLR Nonlocality of Fast Ions on Tearing Mode Stability in the RFP* V.V. MIRNOV, *University of Wisconsin-Madison* Interaction of high-energy ions with the background plasma is a long-standing problem of fusion research. In tokamaks, the high energy component decouples due to the large banana width. In the RFP, the gyroradius is much larger than in a tokamak and FLR effects become dominant. Previously, the problem was treated semi-analytically by integrating along particle trajectories in a uniform magnetic field, and numerically using NIMROD, modified for full orbit kinetics. To benchmark these two approaches we develop an analytical model based on the asymptotic limit of large Larmor orbits. In this limit, the fast ion current is ignored. The bulk ion ExB current is compensated by the current of ExB drifting electrons. Due to plasma quasineutrality there is an uncompensated ExB electron current carried by the population of electrons with the density equal to the fast ion density. This current and the bulk ion polarization current lead to a system of differential equations where the effect of the high energy component is expressed locally in terms of the fast ion density. The boundary layer problem for tearing mode stability is treated analytically yielding the effect of high energy ions on the instability threshold.

*The work is supported by the U.S. D.O.E.

UP8 94 Effects of continuous spectra due to plasma rotation on numerical computation of tearing mode stability* M. FURUKAWA, T. NAKATSU, *Grad. Sch. Frontier Sci., U. Tokyo* When we solve the eigenmode equation numerically for resistive MHD tearing modes in cylindrical plasmas with sheared poloidal rotation, we observe that the growth rate of the tearing mode in the absence of the plasma rotation can be increased by the sheared plasma rotation. If the plasma rotation frequency is increased further, we observe that the growth rate starts to decrease. At the same time, we also observe other unstable modes with their growth rates smaller than the tearing mode. Those growth rates increase as the plasma rotation frequency is increased, and merge with the growth rate of the tearing mode eventually. When we solve the so-called inner-layer equation of the asymptotic matching theory for resistive MHD tearing modes including sheared plasma rotation numerically, we also observe similar phenomena. These phenomena are considered as an artificial instability. The relationship between these phenomena and the continuous spectra due to the plasma rotation is discussed.

*This work was supported by KAKENHI(19760595).

UP8 95 Global magnetohydrodynamic stability with COOL finite elements* W. ANTHONY COOPER, RALF GRUBER, *Ecole Polytechnique Federale de Lausanne CRPP, Association Euratom-Confederation Suisse, Lausanne, Switzerland* The COOL finite element scheme relies on the construction of basis functions using variable order Legendre polynomials [1]. We have implemented this approach in the global linear ideal magnetohydrodynamic code TERPSICHORE [2]. The standard version of this code uses a hybrid method that combines piecewise constant and piecewise linear basis elements. The COOL method with Legendre polynomial order $p = 1$ exactly recovers the original formulation. So far, we find that the optimal polynomial order lies around $p = 3$ to 4 (cubic to quartic). At higher order, numerical problems develop in the regions within half-interval mesh points of the magnetic axis and the edge of the plasma because extrapolation of poorly resolved equilibrium quantities at the Gauss-points of the Legendre polynomial can drive very local fictitious near-axis and/or edge mode structures. [2] D. V. Anderson, W. A. Cooper, R. Gruber, S. Merazzi, U. Schwenn, Int. J. Supercomp. Appl. **4** (1990) 34-47.

*Partially supported by the Swiss National Science Foundation.

UP8 96 The effects of sheared flow and parallel viscosity on the RWM stability boundaries* S.P. SMITH, S.C. JARDIN, *PPPL* J.P. FREIDBERG, *MIT* L. GUAZZOTTO, *U. Rochester* The complete spectrum of ideal MHD modes is computed for a flowing circular cylindrical plasma surrounded by a resistive wall. The formulation for the computation casts the MHD stability problem in the standard form $\omega Ax = Bx$ by coupling the resistive wall to the surface plasma perturbations using a Green's function technique. In looking at the complete spectrum, it is shown that the unstable resistive wall mode (RWM) can be stabilized by uniform flow when i) The damped RWM in the absence of flow resonates with the sound continuum and ii) The Doppler shift associated with the flow is greater than the damped mode's real frequency in the absence of flow. By introducing flow shear, it is shown that the value of the flow at the sound resonant surface is the parameter which most determines stabilization (as opposed to the flow shear at the sound resonant surface or the value of the flow at the edge of the plasma.) Convergence studies demonstrate complete stabilization in the limit of zero grid size even in the absence of parallel viscosity. Introducing explicit parallel viscosity reduces the resolution requirements for convergence, but does not affect the region of stability.

*This work was partly performed under contract DE-AC05-06OR23100 between the US DOE and ORAU.

UP8 97 Initial application of the M3D-C^1 code to the study of non-ideal modes in NSTX S.C. JARDIN, J. BRESLAU, J. CHEN, S. GERHARDT, *PPPL* N. FERRARO, *General Atomics* X. LUO, K. JANSEN, M. SHEPHARD, *SCOREC Center, RPI* The M3D-C^1 code is a two-fluid toroidal magnetohydrodynamic code based on high-order, compact finite elements with C^1 continuity on an unstructured adaptive triangle-based grid. The code is built upon and extends many of the favorable features of the M3D approach to solving the MHD equations in a highly magnetized toroidal plasma. The vector fields use a physics-based decomposition that explicitly conserves energy and which allows for two energy-conserving subsets of the full equations (reduced MHD). The efficient split-implicit time advance is closely related to the ideal MHD energy principle, and allows time steps several orders of magnitude in excess of the Courant condition based on the Alfven or whistler waves. The present application is to apply the linearized code to study the onset of non-ideal instabilities in NSTX. The computational model has a physically based resistivity profile such that the Lundquist number S varies from 10^8 in the plasma center to $\sim 10^0$ in the surrounding 'vacuum' region. Special adaptive meshing algorithms have been utilized to allow high resolution both in the regions where the resistivity transitions rapidly and around mode rational surfaces. We also illustrate the differences in stability boundaries and growth rates for an ideal and non-ideal description of the plasma for different plasma profiles.

UP8 98 Marginal stability analysis for the interchange mode in a constant transverse magnetic field* JUPITER BAGAIPO, PARVEZ GUZDAR, ADIL HASSAM, *University of Maryland, College Park* The ideal interchange instability in a plasma immersed in a constant transverse field is studied near marginal stability. Reduced equations for a strong axial field are used to find the tradeoff between the deviation from marginality and residual convection. Nonlinear numerical simulations of this system in dissipative MHD showed a neighbouring equilibrium with weak convection. This has motivated calculations to find a method to predict $|\vec{B}_\perp - \vec{B}_{crit}|$, the deviation of the field from marginality, as a function of residual convective flux. Such a formulation would find application in assessing the B-field tolerances in stellarator coil design. We carry out an expansion in small perturbations in the field amplitude about marginality to find nonlinear analytic solutions. To lowest order, solving an eigenvalue equation yields the critical field for marginal stability, $\vec{B}_{crit}$. To third order, a time-evolution equation for the amplitude is found (for $kL \sim \mathcal{O}(1)$). We attempt to solve for the short and long wavelength evolution and compare the result to a numerical solution. Our results and method are compared with previous works by Beklemishev, Cowley, and Waelbroeck.

*Work supported by the USDOE.

UP8 99 One size fits all: analytic MHD equilibrium for tokamaks, spherical torii, FRCs and spheromaks ANTOINE CERFON, JEFFREY FREIDBERG, *MIT PSFC* We present a new family of analytical solutions of the Grad-Shafranov equation with Solov'ev type profiles. These solutions, which are extensions of the ones previously proposed in [1] and [2], can be used to describe equilibria in any toroidally axisymmetric device. As compared to [1] and [2], our addition of a new polynomial term to the flux function gives an additional degree of freedom to satisfy the boundary conditions. The advantages are two folds: 1) Our solutions can describe FRC and spheromak equilibria, and 2) For tokamaks and spherical torii, we obtain equilibria at the equilibrium beta limit, characterized by the appearance of a poloidal field null on the inboard side of the plasma, for a wide range of aspect ratios, elongations, and triangularities. Using these new solutions, we will investigate several scalings with the different parameters of interest. [1] R. H. Weening, Phys. Plasmas 7, 3654 (2000) [2] B. Shi, Phys. Plasmas 12, 122504 (2005)

UP8 100 Toroidal flow effects in 3/2 and 2/1 resistive modes nonlinearly driven by a 1/1 internal kink* D.P. BRENNAN, *University of Tulsa* S.E. KRUGER, *Tech-X Corporation* R.J. LA HAYE, *General Atomics* The nonlinear drive from an unstable m/n=1/1 internal kink mode to reconnecting modes on surrounding low order rational surfaces is studied with a varying imposed toroidal flow shear in equilibria which accurately model the DIII-D tokamak. The flow is linear in poloidal flux, and is varied from 0 to $\Omega\tau_A \approx 0.1$. The simulations are described in three stages; the linear, nonlinearly driven and nonlinearly saturated stages. In the linear stage the independent modes exhibit classic flow effects. In the nonlinear driven stage, while below the threshold for locking, small components driven by toroidal coupling exhibit damping and phase shifts with small torques. In the nonlinear saturated stage the n=0 flow is strongly modified as various components lock to each other and phases exhibit long timescale oscillations, the details of which depend on the linear stability and equilibrium flow. The nonlinear 3-D resistive magnetohydrodynamic code NIMROD is used for the analysis, which includes the effects of strong anisotropic heat conduction.

*Supported by US DOE Grant DE-FG02-08ER54950

UP8 101 Resistive Wall Mode Studies in NIMROD* ANDREA MONTGOMERY, CHRIS HEGNA, ANDREW COLE, *University of Wisconsin, Madison* SCOTT KRUGER, *Tech-X Corp.* Resistive wall kink stability is considered using both ideal and resistive MHD models. A simple equilibrium with no pressure, a flat current profile and either a vacuum or a resistive plasma between the plasma and the wall is studied using the NIMROD code. Resistive wall boundary conditions for a periodic cylinder with this equilibrium are implemented in NIMROD through the inclusion of a surface electric field in the induction equation. Simulation results are compared with analytic predictions for the effect of a thin resistive wall on ideal MHD and resistive MHD stability [J. M. Finn, Phys. Plasmas **2**, 198 (1995).] The NIMROD code is also used to study the effects of rigid plasma rotation on resistive wall modes. The effects of rotation on ideal plasma resistive wall modes and resistive tearing modes are compared and contrasted. Further plans for generalization of this work to toroidal tokamak equilibria will be discussed.

*Research supported by U.S. DoE under grant no. DE-FG02-86ER53218

UP8 102 Temperature Fluctuations during Sawtooth Crashes in TEXTOR TOBIN MUNSAT, *University of Colorado* I.G.J. CLASSEN, C.W. DOMIER, A.J.H. DONNE, N.C. LUHMANN, JR., H.K. PARK, B. TOBIAS, AND THE TEXTOR TEAM, Recent 2-D spatially and temporally resolved measurements of electron temperature fluctuations in the tokamak core have revealed new information on the complex mechanisms and dynamics of the sawtooth crash. Here we present fluctuation analysis of TEXTOR plasmas using data from the Electron Cyclotron Emission Imaging (ECEI) diagnostic. Maps of electron temperature are measured in the poloidal plane in the vicinity of the q=1 surface on both the high-field and low-field side, and are characterized during sawtooth precursor, crash, and recovery stages. Previous studies have presented studies of global and local topology, and extended coherence and correlation analyses are presented in addition to fundamental spectral characteristics.

UP8 103 Wall force produced during disruptions* H. STRAUSS, *HRS Fusion* R. PACCAGNELLA, *Consorzio RFX and Istituto Gas Ionizzati del C.N.R* J. BRESLAU, *PPPL* The study of disruptions is of great importance for ITER. Previous work on disruptions [1] is extended to compute toroidally asymmetric wall force in ITER, using the M3D code. The disruptions are produced by n = 1 resistive wall modes or external kink modes. A thin wall resistive boundary model is used to calculate the wall forces. The symmetric wall force, produced by a VDE, and the asymmetric wall force, produced by n = 1 modes, are comparable in magnitude. It is found that the asymmetric and axisymmetric forces scale with the growth rate of the instability multiplied by the square of the current divided by magnetic field. A similar scaling was reported for VDEs in JET [2]. Numerically, the study of disruptions is very challenging. In the M3D extended MHD code, dealiasing was applied in the toroidal direction. Ad-

vection terms were treated with a numerical upwind method. These techniques provided sufficient numerical stability to simulate entire disruption events. [1] R. Paccagnella, H. R. Strauss, and J. Breslau, Nucl. Fusion (2009) **49** 035003. [2] V. Riccardo, T. C. Hender, P. J. Lomas, *et al.,* Plasma Phys. Control. Fusion (2004)

*Supported in part by USDOE.

UP8 104 Development of non-axisymmetric structures during MHD disruptions in tokamak plasmas ROBERTO PACCAGNELLA, *Consorzio RFX, Associazione Euratom-ENEA sulla Fusione, Padova, Italy* H.R. STRAUSS, *Institute for Mathematical Sciences, New York University, New York, USA* JOSHUA BRESLAU, *Princeton University Plasma Physics Laboratory, Princeton, USA* Recently the problem of 3D simulations of vertical displacement events (VDEs) and disruptions in tokamak plasmas has been addressed [R.Paccagnella, H. Strauss, J. Breslau, Nucl. Fusion 49 (2009) 035003] by using the M3D code, in the relatively "benign" cases where the on-axis q is above 1 and vertical plasma movement is mainly driven by a resistive wall mode (RWM) on the time scale of the magnetic field penetration of the conducting wall. In this paper we extend the previous simulations to cases in which the on-axis q is below 1 and the driving mode is an external resistive kink able to drive a reconnection process in the central plasma region. In these cases the disruptions are faster and evolve on the Alfvén time scale. Amplitudes and asymmetries of the halo currents and forces at the wall are calculated in both cases. Comparisons with tokamak experimental data and predictions for ITER are also given.

UP8 105 Interaction between fast particles and magnetohydrodynamical waves in the presence of toroidal flow* J.W.S. BLOKLAND, *FOM Institute for Plasma Physics Rijnhuizen, Assocation EURATOM-FOM, Nieuwegein, The Netherlands* S.D. PINCHES, *EURATOM/UKAEA Fusion Association, Culham Science Centre, Culham, Abingdon, OX14 3DB, United Kingdom* In many tokamak experiments, neutral beam injection is used for additional heating. The injected particles induce a net rotation on the plasma. This rotation plays an important role in the stability and in the interaction between the fast particles and the bulk plasma. However, in the next generation tokamaks the plasma will most likely rotate significantly slower and therefore the influence of the rotation in present devices needs to be investigated in detail. We present a fully consistent model of the bulk plasma, the fast particles and their interaction. The bulk is described by the MHD equations, whilst for the fast particles a kinetic description is used. The equilibria are computed using the FINESSE code and their stability is analysed using the PHOENIX code. Both codes take toroidal flow into account. The HAGIS code, extended with toroidal flow, is used to simulate the fast particles. Tests of the model against experimental data from various tokamaks including MAST will be presented.

*This research is financially supported by Fusion Researcher Fellowship grant provided by EURATOM.

UP8 106 Is There a Nonlinear Subcritical MHD Beta Limit?* R.E. WALTZ, *General Atomics* Since the 2005 beta scan on Cyclone case [1], the GYRO code has not been able to operate past about half the ideal MHD critical beta limit with finite stationary transport levels. There appears to be a nonlinear subcritical MHD beta limit [2] which maybe induced by the increased effective pressure gradients from the nonlinearly driven zonal flows. The high-n ideal beta limit is defined as the point where the growth rate extrapolated to the lowest possible wave number is greater than zero. The subcritical point for Cyclone case is about 0.5 the ideal limit (β_{crit} = 3.0%). Some GA-std cases with β_{crit} = 1.4% have the subcritical beta at 0.42-0.35 the ideal. However, some very high beta DIII-D shot manage to get past the usually lower external kink beta limit and close to the ideal high-n limit with good confinement. The remedy appears to be the addition of $E \times B$ shear sufficient to reduce the transport at near zero beta by about half. GYRO simulations of the shots reasonably match the low transport when the high experimental level of $E \times B$ shear is applied.[1] J. Candy, Phys. Plasmas **12**, 072307 (2005).[2] R.E. Waltz, Phys. Rev. Lett. **55**, 1098 (1985).

*Work supported by the US DOE under DE-FG02-95ER54309.

UP8 107 SPACE AND ASTROPHYSICAL PLASMAS

UP8 108 Ray tracing studies of ionospheric effects on the Long Wavelength Array* CHRISTOPHER WATTS, *University of New Mexico* K.F. DYMOND, *Naval Research Lab* MASAYA KUNIYOSHI, *University of New Mexico* LONG WAVELENGTH ARRAY TEAM, The Long Wavelength Array (LWA) is a new telescope/interferometer facility being established to do astrophysical observations in the frequency range 10 MHz to 90 MHz. As such, measurements will be strongly affected by the ionosphere. In fact, part of the LWA mandate is to make highly precise measurements of the ionosphere. We present modeling results from a ray tracing code on the ionospheric effects on a multi-station interferometer system. The purpose is to test a proposed calibration scheme, whereby the LWA scans ~ 100 "calibrator" sources every 10 seconds. It is found that, while generally this scheme is sufficient for basic calibration, refractive effects near the edge of the field of view are of concern.

*Supported by contract N00014-07-C-0147 with the Office of Naval Research. Basic research in ionospheric science at NRL is supported by the Office of Naval Research.

UP8 109 3D Ionospheric Tomography using GPS and VLA JEFFREY KARLE, CHRISTOPHER WATTS, *University of New Mexico* KEN DYMOND, *Naval Research Laboratory* LONG WAVELENGTH ARRAY TEAM, Research is being carried out at UNM to recreate a three dimensional model of the Earth's ionosphere by incorporating data from GPS and GPS occultation and combining it with data from the Very Large Array (VLA) radio telescope. For three days in September of 2007, the VLA recorded data at 73.8 MHz in its largest configuration. The VLA proves to be highly sensitive to total electron content variations of the ionosphere within about a 30 km area. In addition, there are hundreds of GPS receiver stations spread throughout the U.S., each of which provide detailed information on the slant and vertical total electron content (TEC) that modifies the carrier phase signal from the satellites. Our goal is to combine TEC measurements from these GPS receiver stations that are localized around the southwestern United States with the data taken from the VLA to model the ionosphere in a three dimensional regional scale.

UP8 110 Laboratory investigation of auroral cyclotron emission in the presence of background plasma SANDRA McCONVILLE, DAVID C. SPEIRS, KEVIN RONALD, ALAN PHELPS, KAREN GILLESPIE, ADRIAN CROSS, ROBERT BINGHAM, CRAIG ROBERTSON, COLIN G. WHYTE, *SUPA Department of Physics, University of Strathclyde* IRENA VORGUL, ALAN CAIRNS, *University of St Andrews* BARRY KELLETT, *Space Physics Division, CCLRC, Rutherford Appleton Laboratory* In the auroral regions of the Earth's magnetosphere, particles are accelerated downwards into an increasing magnetic field. Due to conservation of the magnetic moment, magnetic compression leads to the formation of a horseshoe velocity distribution. This process is associated with the emission of **A**uroral **K**ilometric **R**adiation (AKR), polarised in the X-mode. A cyclotron maser instability driven by the horseshoe distribution is thought to be the generation mechanism of **AKR**. To simulate this naturally occurring phenomenon, a scaled laboratory experiment was created. Measurements of radiation conversion efficiency, mode and spectral content previously obtained were seen to be in close agreement with numerical predictions and satellite observations in the magnetosphere. To further replicate the magnetospheric conditions, a Penning trap was constructed and inserted into the interaction region of the experiment to generate a background plasma. The latest results from this modification shall be presented including characteristics of the background plasma.

UP8 111 Hybrid Simulation of Mode Conversion at the Magnetopause YU LIN, *Auburn University* JAY JOHNSON, *Princeton Plasma Physics Laboratory* XUEYI WANG, *Auburn University* Hybrid simulations are used to investigate how fast-mode compressional waves incident on a magnetopause current layer mode convert both linearly and nonlinearly to short wavelength ($k_\perp \rho_i \sim 1$) kinetic Alfvén waves near the Alfvén resonance surface. The background magnetic fields on both sides of the current layer are parallel and tangential to the magnetopause normal, corresponding to a northward IMF. The simulations are performed in a 2-D xz plane, which is tilted by an angle, θ, relative to the magnetic field. We examine how the mode conversion depends on wave frequency, wave vector, Alfvén velocity profile (particularly the magnetopause width), ion β, T_e/T_i, and incident wave amplitude. Kinetic effects resolve the resonance, and KAWs radiate back to the magnetosheath side. The compressional wave absorption rate is estimated and compared with linear theory. Unlike the prediction from low-frequency theory, KAWs are generated also in cases with $\theta = 0°$, provided $\omega_0 > 0.1\Omega_0$. As the incident wave amplitude is increased several nonlinear wave properties are manifest in the mode conversion process. Harmonics of the driver frequency are generated, and as a result, the mode conversion region and its spectral width are broadened. The nonlinear waves provide a significant momentum transport across the magnetopause and a significant ion heating in the resonant region.

UP8 112 Hybrid Simulation of Foreshock Waves and Ion Spectra and Their Linkage to Cusp Energetic Ions XUEYI WANG, YU LIN, *Auburn University* SHEN-WU CHANG, *Center for Space Plasma and Aeronomic Research, University of Alabama in Huntsville* A three-dimensional global hybrid simulation is carried out to investigate energetic ions and electromagnetic waves in the quasi-parallel (Q-||) bow shock and cusp for a typical IMF configuration during the cusp energetic particle events. The bow shock, magnetosheath, and dayside magnetosphere form by interaction between the solar wind and geomagnetic dipole field. Ions of solar wind characteristics injected into the system evolve along with electromagnetic waves in a self-consistent manner. Several important features are yielded from the simulation. Solar wind ions are accelerated by the waves and turbulence at the bow shock and foreshock as indicated by the ion distribution. The shock-accelerated ions possess an exponential energy spectrum with their differential flux scaled by the field-aligned distance to the bow shock, consistent with satellite observations. Second, the compressive and transversal waves in the foreshock are strongly correlated with the diffuse ion dynamics. Third, energetic ions in the magnetosheath and cusp downstream from the Q-|| shock also exhibit a spectrum similar to those at the shock. By tracing trajectories of cusp energetic ions in the simulation, the origin of these ions is revealed. Their source is predominantly associated with the Fermi acceleration at the Q-|| shock and foreshock.

UP8 113 First Ion Temperature Images from TWINS Data AMY KEESEE, EARL SCIME, *West Virginia University* Ion heating has been correlated with several magnetospheric phenomena, including magnetic reconnection, instabilities, and convection of plasma through different regions of the magnetosphere. Thus, it is important to be able to measure ion temperatures throughout the magnetosphere to better understand the physics of these phenomena. Effective ion temperatures based on the charge-exchange cross section-corrected energetic neutral atom (ENA) flux versus energy spectrum can be calculated from TWINS data. Effective ion temperatures calculated from the Medium Energy Neutral Atom (MENA) imager on the IMAGE spacecraft using this technique were shown to have excellent (within $\sim$ 30%) agreement with *in-situ* measurements from MPA instruments on LANL geosynchronous spacecraft and GEOTAIL. In order to achieve adequate statistics for reliable ion temperature calculations, we can use either data with significant ENA flux rates, such as during geomagnetic storms, or superpositions of multiple data sets. We present ion temperature images from the few small storms that have occurred so far in the TWINS mission as well as preliminary results of a superposition study of the quiet-time magnetosphere.

UP8 114 Gyrokinetic Particle Simulation Of Drift Compressional Mode In Magnetic Dipole Geometry PETER PORAZIK, ZHIHONG LIN, *University of California, Irvine, Department of Physics and Astronomy* The Pc5 magnetic pulsations dominated by compressional modes have been regularly observed in the Earth's magnetosphere. The objective of this project is to study the linear excitation and nonlinear evolution of these ultra low frequency pulsations, focusing on unstable magnetic trapped particle modes, with kinetic effects due to wave-particle resonance and finite Larmor radius. The method is to develop a three dimensional gyrokinetic particle simulation, with the dipole equilibrium field modelling the Earth's magnetosphere. Results of drift-kinetic simulations will be presented. Currently the code is being benchmarked against analytic results in the gyrokinetic regime.

UP8 115 A Gyrofluid Model for Space Plasmas KATE DESPAIN, WILLIAM DORLAND, *University of Maryland* We continue our quest for a gyrofluid model that includes effects from $\delta B_\parallel$ at arbitrary ρ_i scales. Such a model requires that special care be taken with respect to the ion and electron flows. We predict that such a model would capture the relevant physics to explain the behavior of the solar wind power spectra, including the break near the ion Larmor radius. Such a model would serve as a less-computationally expensive tool to explore the role of driving, dissipation, temperature ratio, and β on the overall spectrum.

UP8 116 Coronal Heating and Turbulence from Drift-Alfven Structures by Current Loops and Instabilities C.E. CORREA, W. HORTON, S.M. MAHAJAN, *Institute for Fusion Studies* H. MIURA, *National Institute for Fusion Science* INSTITUTE FOR FUSION STUDIES TEAM, NATIONAL INSTITUTE FOR FUSION SCIENCE TEAM, Theory and simulations are used to investigate the Drift-Alfven waves and coherent structures launched by flux tube loops of various heights/diameters and collisionality regimes from the photosphere through the transition layer and into the corona. Collisional terms, electron inertia dispersion and ion polarization currents are included in the dynamical equations. Energy densities and Alfvenic Poynting fluxes are evaluated. The coherent interaction between a large number of neighboring current loops is studied and the reconnection rate reported. We attempt to estimate many hours it takes for a set of neighboring flux tubes to reconnect and estimate the fractions of the released magnetic energy that goes into plasma flows, plasma heating and radiation.

UP8 117 Short-Wavelength Solar Wind Turbulence: Kinetic Alfven vs. Whistler Fluctuations S. PETER GARY, *Los Alamos National Laboratory* The inertial range of solar wind turbulence corresponds to magnetic power spectra which scale as $f^{-\alpha}$ with $\alpha \simeq 5/3$. Many observations show, however, that at observed frequencies $f \sim 0.2$ Hz, there is a "breakpoint" such that power spectra at higher frequencies follow a steeper power-law dependence with $\alpha > 5/3$. The constituent modes of this high-frequency, short-wavelength regime are often attributed to kinetic Alfvén modes which propagate at strongly oblique directions relative to the background magnetic field. However, whistler fluctuations represent an alternative hypothesis to describe short-wavelength turbulence in the solar wind and, indeed, in any collisionless, magnetized, homogeneous plasma. Particle-in-cell simulations have shown that the whistler cascade yields steep power-law power spectra consistent with observations [1]. This poster will describe a comparison of linear theory properties of kinetic Alfvén waves and whistler fluctuations, and will apply these results to recent simulations and observations of short-wavelength turbulence in the solar wind. [1] Saito, S., S. P. Gary, H. Li, and Y. Narita (2008), Whistler turbulence: Particle-in-cell simulations, *Phys. Plasmas*, *15*, 102305.

UP8 118 The Princeton MRI experiment: an overview ERIK SPENCE, AUSTIN ROACH, KRISTINE GAROT, MARK NORNBERG, ETHAN SCHARTMAN, ERIC EDLUND, HANTAO JI, *Princeton Plasma Physics Laboratory* The Princeton MRI experiment is used to study the magnetorotational instability (MRI), the instability believed to be responsible for the transport of angular momentum in accretion disks. The MRI is excited when a background magnetic field causes a radially-decreasing angular velocity field to become a source of free energy. The experiment consists of a Taylor-Couette apparatus with independently-rotating split endcaps filled with the gallium eutectic GaInSn. When operated in the stable regime the flow has an outwardly-decreasing angular velocity profile and is hydrodynamically stable up to a Reynolds number on the order of one million, as determined during the water stage of the experiment. An axial magnetic field, up to 5 kG, is applied to the experiment. Magnetic perturbations are measured using an array of Mirnov Coils and the velocity field is measured using a new ultrasonic velocimetry (UDV) system. Initial UDV measurements will be presented. When turbulent flows are generated, and a magnetic field is applied, evidence for magneto-Coriolis waves is found. The hydrodynamically stable flows are expected to become unstable due to the MRI. The latest results of the search for the MRI will be presented.

UP8 119 Internal velocity measurements in the Princeton MRI experiment A.H. ROACH, M.D. NORNBERG, E.J. SPENCE, H. JI, *Princeton Plasma Physics Laboratory, Center for Magnetic Self-Organization* The Princeton MRI experiment seeks to understand the effect of the magnetorotational instability on angular momentum transport in rotating MHD systems. Previous work has focused on observations of magnetic field fluctuations using external pickup coils. An effort is now underway to make local measurements inside the GaInSn working fluid. Ultrasound Doppler Velocimetry (UDV) will allow for the noninvasive measurement of single-component velocity profiles, and later the measurement of multi-component velocity fluctuations to yield the Reynolds stress. A single-component UDV system has been successfully tested with a stationary outer cylinder. The test showed the importance of the concentration of ultrasound-reflecting oxides in the fluid. Work is being done to give better control of the oxide concentration and to allow measurements to be made with a rotating outer cylinder. Preliminary results will be presented.

UP8 120 Free-surface MHD channel flow experiments M.D. NORNBERG, J.R. RHOADS, H. JI, *PPPL* B. BARTELL, *Union College* Surface waves and turbulence are essential components to processes in both astrophysical and laboratory plasmas. Energetic events such as X-ray bursts from neutron stars are thought to be related to the waves generated by accretion of material onto the dense plasma ocean on the star surface. In fusion devices, interest in using liquid metals as a first-wall raises important questions about surface stability with strong magnetic fields and high heat flux. A liquid metal channel experiment is used to study the basic physics of free-surface MHD effects in turbulent channel flow. Surface wave turbulence is characterized by measuring the deflection of a laser beam reflected off the surface of the liquid metal using a position sensitive photodiode. The frequency spectrum of measured fluctuations satisfy a power law whose slope is altered by applying a magnetic field orthogonal to the flow due to damping of waves parallel to the field. The changes to the turbulent spectrum are further characterized by calculating the wavenumber spectrum using two-point correlation analysis of measurements from a pair of reflected lasers to demonstrate the magnetic damping.

UP8 121 MRI in Helicon Plasma C. COLLINS, *UW-Madison* H. JI, *PPPL* C. KAITA, *U. Michigan* Magnetorotational instability (MRI) theory is a basis for explaining efficient angular momentum transport and magnetic field amplification in accretion disks. Observation of MRI in a laboratory plasma would enhance our understanding of how accretion occurs in a range of astrophysical objects, including planet and star forming systems, galactic nuclei, and black holes. Depending on plasma parameters, it may be possible to experimentally identify effects beyond ideal MHD in MRI theory. Here, a helicon plasma is produced by a flat spiral RF antenna in weak ($<$ 250 Gauss) axial magnetic field. Ring electrodes are biased to create a radial electric field that induces plasma rotation through ExB drift. To study plasma responses to such biases, plasma potential and ion flow velocities are measured with emissive and Mach probes. When the ions are unmagnetized,

the Hall effect becomes important. This leads to growth rates that depend on whether the magnetic field is parallel or anti-parallel to the rotation axis. An initial analysis to experimentally decipher signatures of incompressible, dissipative two-fluid MRI from other phenomena in a rotating plasma will be presented.

UP8 122 Strategies for Observing Self-excitation in the Madison Dynamo Experiment N.Z. TAYLOR, C.B. FOREST, E.J. KAPLAN, R.D. KENDRICK, A.M. RASMUS, *University of Wisconsin-Madison* In the Madison Dynamo Experiment two counter-rotating impellers drive a turbulent flow of liquid sodium in a one meter-diameter sphere. One of the goals of the experiment is to observe the spontaneous generation of magnetic field. Initial runs of the Madison Dynamo Experiment saw intermittent bursts of a transverse dipole field similar to the induced field predicted by laminar kinematics, but no sustained self-excited field was observed. Recent numerical simulations have shown that turbulent fluctuations strongly increase the critical magnetic Reynolds number required for self-excitation, beyond the design parameters of the experiment. Three different techniques for accessing dynamos are currently being implemented on the experiment. First, the addition of an equatorial and poloidal baffles to the experiment will help in the reduction of large-scale turbulence and optimization of the helicity of the mean flow. Second, freely rotating segments of a symmetric airfoil will be added to the internal probe tubes to reduce vibration that prevented operation at full speed. Third, the externally applied field will be strengthened to explore a subcritical dynamo transition that has recently been discovered using numerical simulations.

UP8 123 Perturbative Transport studies of Turbulent EMFs in the Madison Dynamo Experiment E.J. KAPLAN, C.B. FOREST, R.D. KENDRICK, A.M. RASMUS, N.Z. TAYLOR, *UW Madison* Previous experiments on the MDE have demonstrated the need for a turbulent electromotive force to describe the dynamics of the magnetic field evolution. In these experiments a weak, DC external seed field—sharing the symmetry axis of the mean flow—was applied to a flowing sodium. Data modeling showed that the currents measured in the sodium could not be explained from the mean flow alone. However, the overall trend was not inconsistent with an enhanced resistivity (a beta effect). Two new experiments are underway to better characterize this turbulent EMF. First, time varying magnetic fields will be applied to perturbatively measure current transport. Second, an internal velocity probe is being developed to directly measure the correlation between magnetic and velocity fluctuations at a given location. This poster will present numerical models which study the degree to which a spatial variation in the resistivity can be determined from measured responses in a range of frequencies. A high current H-bridge amplifier has been constructed to apply 500 gauss, sinusoidal fields with frequencies up to 10 hz. The profile of the response will be measured by an internal array of 3D hall probes. This profile should provide a measure of the turbulent enhancement to resistivity, and the degree to which it is reduced by the presence of a mean magnetic field.

UP8 124 Numerical simulations of the Plasma Couette Flow Experiment F. EBRAHIMI, C.B. FOREST, I.V. KHALZOV, D.D. SCHNACK, *Center for Magnetic-Self Organization in Laboratory and Astrophysical Plasmas, University of Wisconsin-Madison* We have performed numerical simulations of the Plasma Couette Flow Experiment using the extended MHD code NIMROD (nimrodteam.org). The plasma Couette flow experiment has recently been constructed at UW-Madison to study magnetorotational instability (MRI) in a hot, unmagnetized and fast flowing plasma. Plasma is confined by strong multipole magnetic field at the plasma surface, and it rotates through the generated toroidal ExB flow at the boundaries. The goals of the experiment are to study MRI and possible self-generation of the magnetic field by MRI-driven turbulence at high magnetic Reynolds numbers. As proof of principle we first numerically obtain an experimentally relevant flow, a Taylor-Couette flow generated by tangential electric field using the boundary condition ExB. Stability and the dynamo action in this configuration will be discussed. We also study the possibility of self-generation of magnetic field through hydrodynamic turbulence generated by counter-rotating von Karman flows. This work is supported by NSF.

UP8 125 First Results from the Wheaton Impulsive Reconnection Experiment D. CRAIG, D. BLASING, D. COSTER, J. DAHLIN, D. STAPLETON, *Wheaton College, Wheaton IL USA* A new experiment for the study of impulsive magnetic reconnection in three dimensions began operation in Spring 2009. The experiment is composed of two parallel electrodes, linked by a magnetic arcade that is generated by a coil surrounding the electrodes. Plasma current I has been varied from 0.5 kA to 11 kA and the startup magnetic field B has been independently varied from 0 to 400 Gauss. A large ratio of I/B is expected to result in instability and potentially reconnection. As this ratio is increased, we observe a sharp transition towards higher fluctuation levels. Two different fueling configurations have been explored - distributed fueling along the cathode and fueling from one end of the cathode. Distributed fueling resulted in discharges extending further down the length of the electrodes. Intensified CCD cameras explore the formation and subsequent evolution of the discharge. Pinhole photodiode array cameras are being constructed to measure emission profiles throughout a single shot. Work supported by U.S.D.O.E. grant DE-FG02-08ER55002.

UP8 126 Simulations of Kinetic Alfvén Wave Turbulence Over a Range of Outer Length Scales* KURT SMITH, PAUL TERRY, *University of Wisconsin-Madison, CMSO* We compare a three-field model for kinetic Alfvén Wave turbulence with a two-field model that is the small-scale limit of the three-field system. The three-field system couples electron density fluctuations with the bulk flow and magnetic fields, and the two-field simplification, studied in previous work, couples electron density and magnetic fields only. The two-field system has been shown in simulations to yield non-Gaussian electron-density perturbations under a range of dissipation parameters (diffusivity and resistivity). The non-Gaussian statistics have enhanced tails, consistent with Lévy-tailed distributions inferred from pulsar scintillation measurements. Landau damping is expected to be significant in the small-scale regime, which motivates our study of the larger-scale three-field system to determine whether non-Gaussian statistics can result in a regime not expected to be as strongly damped. We present simulations of the three-field system with a variety of outer length scales relative to the ion-sound gyroradius, and compare the results to the small-scale limit.

*Work supported by the NSF.

UP8 127 Gyrokinetic Particle Simulation of Kinetic Alfven Wave XI CHENG, ZHIHONG LING, Random magnetic fluctuations resembling Alfven waves are ubiquitously observed in laboratory, space and astrophysical plasmas. The issue of spectral cascade and plasma heating in Alfvenic turbulence is a major unsolved problem in space plasma physics. Gyrokinetic particle simulation is applied in this work to study the cascade and heating in Alfvenic turbulence with fully self-consistent nonlinear kinetic effects. A Coarse-grained MPI/openMP parallelization strategy has been used for large scale simulation. A massively parallel, electromagnetic, kinetic, non-linear, particle-in-cell code with gyrokinetic ions and fluid-kinetic hybrid electrons is being developed to study the coupling between shear Alfven wave and ion acoustic wave, which lead to energy exchange between waves and particles.

UP8 128 X-ray Measurements and Analytic Models of a Laboratory Solar Coronal Loop Merging Simulation RORY PERKINS, PAUL BELLAN, *California Institute of Technology* Solar coronal loops typically erupt abruptly after long quiescent periods. Such eruptions might be initiated by interactions between two adjacent loops; this idea was explored experimentally in a laboratory simulation where two plasma-filled flux tubes merge in either a co-helicity or counter-helicity arrangement (J.F. Hansen, S.K.P. Tripathi, and P.M. Bellan, Phys. Plasma 2, 3177(2004)). The counter-helicity arrangement produces a bright region with enhanced soft x-ray emission. We are investigating such mergings with a new diagnostic array of EUV photo-detectors of the type described by S.J. Zweben, R.J. Taylor, Plasma Physics, Vol. 23, No. 4(1981), and with analytic studies of particle orbits in the regions between two flux tubes. The EUV array provides means for obtaining spatially and temporally resolved measurements of radiation between 10 and 120 nm. Such resolution is needed to observe the bright regions. Special precautions are taken against capacitive coupling, incoming plasma, and electrical noise. We model the orbits of individual particles in our experiment to understand the merging process. These models suggest that particle trajectories divide into two classes: those confined to a single flux tube and those that freely move between adjacent flux tubes. These models also suggest how trajectories transition from the former to the latter.

UP8 129 Magnetic structures and corresponding flows in current-carrying arched flux tubes* EVE STENSON, PAUL BELLAN, *Caltech* Arched, plasma-filled flux tubes are created with a magnetized plasma gun. First, external coils generate an initial vacuum magnetic field in the shape of an arch, as between the poles of a horseshoe magnet. Gas is supplied to nozzles at the arch footpoints, each located on an electrode. A voltage is then applied across the electrodes, ionizing the gas and driving a current through the plasma. The resulting plasma structure influences and is influenced by the frozen-in magnetic field. From the outset, $\mathbf{J} \times \mathbf{B}$ forces generate flows along the axis of the arched vacuum field, traveling from the footpoints into the apex. The flows fill the arch with plasma so that it becomes a nearly collimated loop. Both flows and collimation persist as the loop expands due to magnetic forces. "B dot" probe measurements show comparable axial and azimuthal magnetic field strengths, with a structure approximating a force-free Bessel function solution. Further insight has been obtained by altering or eliminating the vacuum field altogether. These experiments demonstrate diminished and incoherent flows, loss of collimation, and weak magnetic fields.

*Supported by: NSF, AFOSR, DOE.

UP8 130 Experiment to Study Alfvén Wave Propagation in Plasma Loops* MARK KENDALL, PAUL BELLAN, *California Institute of Technology* Solar coronal loops are simulated in the laboratory using pulsed power techniques [1]. We are now developing a method to excite propagating Alfvén wave modes by superposing a current pulse of roughly 10kA and width 100ns upon the ~ 50kA, 10 microsecond main discharge current that flows along the ~ 10cm long, 1cm diameter arched flux tube. To achieve this short 100ns pulsed timescale at such high power, a magnetic pulse compression technique based on saturable reactors will be employed. A low power prototype has been successfully tested, and design and construction of a full-power device is underway. Upon completion, the fast current pulse device will be used to investigate interactions between the Alfvén waves and the larger-scale loop evolution. Particular attention will be paid to wave propagation including dispersion and reflection, as well as dissipation mechanisms and possible energetic particle generation. [1] J. F. Hansen, S. K. P. Tripathi, P. M. Bellan, "Co- and Counter-helicity Interaction Between Two Adjacent Laboratory Prominences," *Phys. Plasmas*, vol. 11, issue 6, p. 3177 (2004)

*Research supported by NSF, AFOSR, DOE.

UP8 131 X-ray Imaging System and Charged Particle Energy Analyzer for a Laboratory Plasma* VERNON CHAPLIN, PAUL BELLAN, DEEPAK KUMAR, *California Institute of Technology* We report on the development of two new diagnostics for the solar coronal loop experiment at Caltech. A gated x-ray imaging system sensitive to photons with energies 5 eV and above has been designed to complement the fast visual camera in use at the experiment. The shutter mechanism is provided by a high-voltage pulse applied to a micro-channel plate (MCP), allowing for exposure times as short as 10 ns. Spatially resolved images of x-ray emission at specific times during plasma discharges have the potential to provide a greater understanding of the magnetic reconnection that occurs when two plasma loops merge. A charged particle energy analyzer consisting of a pair of coaxial conducting cylinders held at a variable potential difference has also been designed and tested. Optimal refocusing of slightly off-axis particle orbits occurs $\pi/\sqrt{2}$ radians from the entrance slit [1], thus we measure the output current at this point. [1] A. L. Hughes and V. Rojansky, *Phys. Rev.* **34** 284-290 (1929).

*This work was supported by grants from the NSF, DOE, and AFOSR.

UP8 132 Strapping field profile to reproduce transition from slow rise to fast eruptions* BAO NGUYEN QUOC HA, PAUL BELLAN, *California Institute of Technology* In solar coronal loop experiments at Caltech, the hoop force causes plasma loops to expand unless additional forces are applied. By applying a strapping magnetic field of proper polarity, Hansen and Bellan [1] slowed and even inhibited this expansion. Kliem and Torok [2] predicted that a transition from slow rise to fast eruption occurs if the magnetic field's rate of decay with increasing altitude meets an instability criterion. If the restoring force due to the strapping field decays faster than the hoop force, then the plasma will move from a region where its expansion is decelerated to one where its expansion is accelerated. We have calculated magnetic profiles which attain the instability criterion within the length scale of the

Caltech experiment and are constructing an auxiliary coil with independent power supply designed to match the calculated profiles. [1] J. F. Hansen and P. M. Bellan, Astrophys. J. Lett. **563**, L183 (2001) [2] B. Kleim and T. Torok, Phys. Rev. Lett. **96**, 255002 (2006)

*Work supported by the NSF and AFOSR.

UP8 133 Magnetic Bubble Expansion Experimental Investigation Using a Compact Coaxial Magnetized Plasma Gun YUE ZHANG, ALAN LYNN, *University of New Mexico* SCOTT HSU, HUI LI, WEI LIU, *Los Alamos National Laboratory* MARK GILMORE, CHRISTOPHER WATTS, *University of New Mexico* UNIVERSITY OF NEW MEXICO COLLABORATION, LOS ALAMOS NATIONAL LABORATORY COLLABORATION, The poster will first discuss the construction and improved design of a compact coaxial magnetized plasma gun. The plasma gun is used for experimental studies of magnetic bubble expansion into a lower pressure background plasma, which as a model for extragalactic radio lobes and solar coronal mass ejections. In this experiment, the plasma bubble's density, electron temperature, and propagation speed are measured by using a multiple-tipped langmuir probe. Also a three axis B-dot probe array is used to measure the magnetic field in three dimensions during the expansion process. In this poster experiment setup and data will be provided. Finally the comparison with the simulation result will be made.

UP8 134 Laboratory generated magnetized plasma bubbles as a means to understanding coronal mass ejections A.G. LYNN, C. WATTS, *University of New Mexico* W. MANCHESTER, *University of Michigan* The goal of this research is to substantiate, through a series of basic plasma experiments and corroborative numerical modeling, the fundamental physics of coronal mass ejection (CME) interaction with the solar wind flow in the Sun's outer corona. We have begun a series of laboratory experiments using the combined Helicon-Cathode (HelCat) and Plasma Bubble Experiment (PBEX) instruments, which can generate CME like structures injected into a background plasma medium. Results of these experiments are compared with the University of Michigan state-of-the-art 3D BATS-R-US MHD numerical code, which has been used to perform simulations of the propagation of CMEs into a background solar wind. The results will be compared in a systematic way to validate the numerical model, and to further our understanding of CME propagation through the solar wind. The objective is to validate the numerical code under controlled laboratory settings, allowing it to be applied with greater confidence to a more realistic but less well-understood solar setting.

UP8 135 Waves and Fine Structure in Expanding Laser-Produced Plasmas* ANDREW COLLETTE, WALTER GEKELMAN, *University of California, Los Angeles* The behavior of expanding dense plasmas has long been a topic of interest in space plasma research, particularly in the case of expansion within a magnetized background. Previous laser-plasma experiments at the UCLA Large Plasma Device have observed the creation of strong ($\Delta B/B > 50\%$) diamagnetic cavities, along with large-scale wave activity and hints of fine-scale structure. A new series of experiments conducted recently at the LaPD performs direct measurement of the fields inside the expanding plasma via a novel 2D probe drive system. This system combines small-scale (0.5mm-1mm) magnetic and electric field probes with high-accuracy vacuum ceramic motors, to allow measurement of the plasma volume over a 2000-point grid at 1mm resolution. The data reveal both coherent high-amplitude waves associated with the formation of these magnetic features, and complicated small-scale structure in both the magnetic field and floating potential. In addition, we will present correlation techniques using multiple independent B and E field probes. This reveals behavior of turbulent, non-phase-locked phenomena. Both the case of a single expanding plasma and two colliding plasmas were studied.

*Performed at the UCLA BaPSF with support from the U.S. Department of Energy and the National Science Foundation.

UP8 136 Energy Transfer via Ion-Beam Driven Weibel and Two-stream instabilities in Two-Temperature Electron-Ion Plasmas JAEHONG PARK, CHUANG REN, ERIC BLACKMAN, XIANGLONG KONG, *University of Rochester* Whether a collisionless faster-than-Coulomb energy transfer mechanism exists in two-temperature accretion flows is an open question. Using 2D PIC simulations, we generalize Ren et al.2007 (Phy.Plasmas 012901) into counter-streaming ion beam-driven oblique instabilities where Weibel, two-stream, and oblique modes coexist. We explain in detail the evolution patterns in both linear and nonlinear regimes, and how to reach saturation. To compare with simulations, we solve a set of 1+1D quasi-linear calculations. In a real mass ratio, $M/m = 1836$, we estimate that electrons gain 3.2% of initial ion energy for the case, $T_e = 0.2$KeV, $T_i = 375$KeV, and $v_{id} = 0.7c$. While this gain of 3.2% does not threaten the existence of two-temperature accretion flow models per se, one might ask whether it threatens the subset of models (Narayan et al.1998 (ApJ492,554)) which employ less than this percentage of energy to be transferred from ions to electrons on an infall time scales. However, in the solution of Narayan et al.1998, the electron and ion temperature are much larger than ours and ion beam drifts as high as $0.7c$ would probably occur at most in localized regions. As a result, the electron-ion coupling could be smaller than 3.2%. At present, our results do not therefore definitively rule out existing two-temperature accretion solutions.

UP8 137 Radiation emission in electron/proton Weibel scenarios J.L. MARTINS, S.F. MARTINS, R.A. FONSECA, L.O. SILVA, *GoLP / Instituto de Plasmas e Fusao Nuclear, Instituto Superior Tecnico, Portugal* The Weibel instability is common in astrophysical and laboratory scenarios. The features of the radiation associated with the electrons dynamics in such scenarios are relevant for the interpretation of astrophysical observations and of future experiments. We performed 3D PIC simulations with OSIRIS 2.0 to explore scenarios where Weibel turbulence occurs. We leverage on the code particle tracking feature to determine the spectral features of the radiation using a post-processing code. We compare scenarios with streaming electron/positron plasmas versus scenarios with electrons/protons. We focus on the evolution of the spectral features of the radiation when going from the initial growing stage of the instability where electron filamentation occurs, to a time-scale of the order of the inverse of the ion plasma frequency. At these later times, the filamentation of the ions leads to a change in the spatial scale of the electron dynamics. This translates into a broadening of the spectrum peak. Our results are compared with a theoretical model for the temporal evolution of the filamentary structure.

UP8 138 Wavelet analysis approach for radiation from rapidly-evolving astrophysical plasmas SARAH REYNOLDS, MIKHAIL MEDVEDEV, SRIHARSHA POTHAPRAGADA, *University of Kansas* High-energy astrophysical phenomena frequently emit strongly from localized regions of particle acceleration in which field configuration and plasma energy distribution can vary rapidly. Developing radiative modeling techniques suited to tracking these systems' evolution on various scales is an important problem in linking kinematic simulations with astronomical observations. Wavelet analysis, which improves upon Fourier analysis by being able to simultaneously track time and frequency information, has potential as a method of modeling and analyzing the radiative output of such systems. We develop the applicability of wavelet analysis to transient and explosive astrophysical phenomena such as supernovae, GRBs, and solar flares. We highlight features observed in wavelet spectral analysis of observations from such systems and explore the implications of such analysis for associated simulations.

UP8 139 The nonlinear phase of the non-resonant cosmic ray-driven Bell instability LUIS GARGATE, *GoLP/IPFN Instituto Superior Tecnico* RICARDO FONSECA, *DCTI Instituto Superior de Ciencias do Trabalho e da Empresa* JACEK NIEMIEC, *Instytut Fizyki Jadrowej PAN* ROBERT BINGHAM, *SSTD Rutherford Appleton Laboratory* LUIS O. SILVA, *GoLP/IPFN Instituto Superior Tecnico* Cosmic rays (CR) with very high energies are produced in Supernova Remnant (SNR) shocks, via Diffusive Shock Acceleration. The typical interstellar magnetic field present, however, is too low to explain the highest energy particles observed, implying that a magnetic field amplification mechanism is operating. We analyze Bell's instability [1], in which small-scale non-resonant wave modes are driven by cosmic ray ions streaming in the shock precursor along a background magnetic field B0, and driving a current. We use hybrid simulations to study the feedback of magnetic turbulence produced on cosmic ray trajectories. Our results show an amplification of $\sim$ 10 relative to B0. On the nonlinear phase, the background plasma cavitates, gaining a bulk velocity in the CR propagation direction. The nonlinear phase of the instability is explored in detail, and the reaction of the background plasma, along with the isotropization of the CR population is shown to be relevant for the saturation mechanism. The relevance of the mechanism for the acceleration of CRs is also thoroughly discussed.

[1] A. R. Bell, Mon. Not. R. Astron. Soc. 353, 550, 2004

UP8 140 Hybrid simulations of collisionless shocks in exponential density gradients* DAVID LARSON, DENNIS HEWETT, *LLNL* STEPHEN BRECHT, *Bay Area Research Corporation* We present simulations of a strong 3-D collisionless shock transitioning into sub-Alfvénic waves. The transition occurs due changes in the background plasma parameters. The Alfvén speed eventually exceeds the shock speed as the background plasma density falls with altitude; the shock does not run out of energy. At this velocity transition, the shock disassembles into two types of waves: the usual compressional Alfvén wave and a left-hand polarized electromagnetic shear Alfvén wave. This later wave shows remarkable 3-D coherence. Analysis suggests that there are two possible sources of energy: (1) coupling to the strong electromagnetic waves that exist within the collisionless shock and (2) the density and magnetic field gradients at the interface. Results from recent simulations using our three dimensional parallel hybrid plasma code will be presented and discussed.

*This work performed under the auspices of the U.S. Department of Energy by Lawrence Livermore National Laboratory under Contract DE-AC52-07NA27344.

UP8 141 Effect of Pressure Anisotropy on Relativistic Slow-Mode Shocks JASON TENBARGE, *University of Iowa* RICHARD HAZELTINE, SWADESH MAHAJAN, *University of Texas - Austin* Shock mediated reconnection is a possible source for the high-energy non-thermal emissions observed in astrophysical systems such as pulsars and magnetars, gamma-ray bursts, and active galactic nuclei. In such strongly magnetized environments, strong gyrotropic anisotropy in the pressure is expected to occur due to synchrotron emission and various instabilities. A newly developed covariant fluid model[1] for magnetized plasmas, incorporating pressure anisotropy but neglecting heat flow, is used to study Petschek type reconnection in a pair plasma governed by slow-mode shocks. The plasma parameters are found to be strongly modified by anisotropy on both sides of the shock.

[1] J. M. TenBarge, R. D. Hazeltine, and S. M. Mahajan, Phys. Plasmas **15**, 062112 (2008).

UP8 142 Automatic Detection of Shock Wave Features* NICK PATTERSON, R.P. DRAKE, KATSUYO THORNTON, *U of Michigan* An image analysis algorithm and procedure are developed to analyze the radiographs of shock waves to automatically detect features necessary to quantitatively characterize their dynamics. We examine a high-intensity laser-driven nearly planar shock wave to study the shock structure and radiation hydrodynamics. The experimental parameters are relevant to astrophysical systems with dynamics influenced by radiative effects. The image analysis program is also applicable to structures predicted by simulations. The three primary features detected are the wall boundaries, the position of the shock front, and the angle of the wall shock. The program requires very little human input and is a significant improvement over the manual method. Furthermore, the procedure allows consistent characterization of shock waves, both experimental and simulated, which is necessary for uncertainty quantification.

*Supported by the US DOE NNSA under the Predictive Sci. Academic Alliance Program by grant DE-FC52-08NA28616, the Stewardship Sci. Academic Alliances program by grant DE-FG52-04NA00064, and the Nat. Laser User Facility by grant DE-FG03-00SF22021.

UP8 143 Collisionless shock generation in counter-streaming plasmas produced by a high-power laser system YOUICHI SAKAWA, *ILE, Osaka Univ.* Y. KURAMITSU, T. MORITA, H. AOKI, H. TANJI, S. SHIBATA, T. IDE, N. OZAKI, R. KODAMA, A. SHIROSHITA, K. SHIGEMORI, T. SANO, T. NORIMATSU, T. KATO, H. TAKABE, *Osaka Univ, Japan* J. WAUGH, N. WOOLSEY, *York Univ. UK* B. LOUPIAS, *CEA France* C. GREGORY, M. KOENIG, *LULI France* Laboratory experiments to study collisionless shock generation in counter-streaming plasmas have been investigated using Gekko XII HIPER laser system (352 nm (3ω), 500 ps, $\sim$ 100 J / beam, one or four beams, $< 10^{15}$ W/cm^2) at ILE. Two types of double-plane

targets, Jet and Ablation types were used. In the Jet (Ablation) type, 10 μm (60 μm) and 60 μm thick CH planes were placed with the separation of 4.5 mm; beams were irradiated on the 1st CH and a rear-side (an ablation) plasma is formed, and the plasma from the 2nd CH is created by radiation and/or plasmas from the1st CH. The plasmas and shocks were diagnosed transverse to the main laser propagation direction; shadowgraphy and modified Nomarski interferometry using a probe laser with ICCD and streak cameras, and SOP and GOI using a visible (450 nm) self-emission. Counter-streaming plasmas were produced, and shock waves were observed. The width of the transition region is much shorter than ion-ion mean-free-path. A particle-in-cell simulation has predicted generation of an electrostatic shock.

UP8 144 Radiation cooling of dense laboratory plasma jets studied using soft x-ray laser interferometry and simulations MICHAEL PURVIS, JONATHAN GRAVA, JORGE FILEVICH, DUNCAN RYAN, MARIO MARCONI, VYACHESLAV SHLYAPTSEV, JORGE ROCCA, *Colorado State University* STEPHEN MOON, JAMES DUNN, *Lawrence Livermore National Laboratory* The physical mechanisms responsible for the collimation of laboratory plasma jets created with short laser pulses of $\sim$ 0.5-1 J energy were studied using soft x-ray interferometry and hydrodynamic code simulations. Plasma jets with peak densities of $\sim 10^{20}$cm^{-3} were created by irradiation of C, Al, Cu, and Mo 90[r] triangular grooved targets with I = 1 x 10^{12} Wcm^{-2}, 120 ps duration laser pulses. Also, plasma jets with a much higher electron density, $> 10^{21}$cm^{-3}, were created by irradiation of Cu cone shaped targets with I = 3 x 10^{13} Wcm^{-2}. The results were compared with simulations conducted with the code HYDRA. Plasma radiation cooling was found to play a significant role in increasing the collimation of the higher Z jets. In addition, at any instance in the evolution the higher Z jets appear to be more collimated due to their slower plasma expansion velocity associated with their higher mass. Work supported by the NNSA SSAA program through DOE Grant # DE-FG52-060NA26152 and the U.S. Department of Energy by Lawrence Livermore National Laboratory under Contract DE-AC52-07NA27344.

UP8 145 Manson X-Ray Source Characterization and Pre-Shot Radiography for Laboratory Astrophysics Experiments* D.C. MARION, R.P. DRAKE, T.P. REMINGTON, E.C. HARDING, M.E. LOWENSTERN, C.C. KURANZ, M.J. GROSSKOPF, N. JASSEM, D. FISHER, *University of Michigan* We report the results of measurements characterizing the spectrum of our Manson x-ray source and developments in the use of the source for x-ray radiography. X-Ray radiography has proved a useful diagnostic tool in laser experiments; the value of these measurements could be improved with pre-shot radiography, which would allow us to determine the structure of as-built laser targets. We have assembled a pre-shot radiography system and are developing the techniques needed to optimize magnification and resolution. The output from the x-ray source must be well characterized in order to interpret in detail signals from microchannel-plate detectors. An x-ray photodiode and x-ray filters will be used to measure the spectrum of the x-ray source over a range of fluxes.

*Supported by the US DOE NNSA under the Predictive Sci. Academic Alliance Program by grant DE-FC52-08NA28616, the Stewardship Sci. Academic Alliances program by grant DE-FG52-04NA00064, and the Nat. Laser User Facility by grant DE-FG03-00SF22021.

UP8 146 Experiments to assess preheat in blast-wave-drive instability experiments* CHRISTINE KRAULAND, PAUL DRAKE, CAROLYN KURANZ, MICHAEL GROSSKOPF, *University of Michigan* TOM BOEHLY, *Laboratory for Laser Energetics, University of Rochester* The use of multi-kilojoule, ns lasers to launch shock waves has become a standard method for initiating hydrodynamic experiments in Laboratory Astrophysics. However, the intense laser ablation that creates moving plasma also leads to the production of unwanted energetic x-rays and suprathermal electrons, both of which can be sources of material preheating. In principle, this preheat can alter the conditions of the experimental setup prior to the occurrence of the intended dynamics. At the University of Michigan, ongoing Rayleigh-Taylor instability experiments are defined by precise initial conditions, and potential deformation due to preheat could greatly affect their accuracy. An experiment devised and executed in an attempt to assess the preheat in this specific case will be presented, along with the quantitative analysis of the data obtained and comparison with 2D simulations.

*Supported by the US DOE NNSA under the Predictive Sci. Academic Alliance Program by grant DE-FC52-08NA28616, the Stewardship Sci. Academic Alliances program by grant DE-FG52-04NA00064, and the Nat. Laser User Facility by grant DE-FG03-00SF22021.

UP8 147 Sensitivity Analysis of Laboratory Astrophysics Experiments using 2D HYADES* M.J. GROSSKOPF, R.P. DRAKE, C.C. KURANZ, B. FRYXELL, F.W. DOSS, A.J. VISCO, *University of Michigan* We will show results of a series of simulations using 2D HYADES (or H2D) to examine the sensitivity of various physical quantities to the variability of initial parameters. Computer simulations play a critical role in experimental design in order to maximize the quality of results from campaigns at large high-energy-density facilities. Codes such as H2D must be well characterized for each experimental regime before they can be used as a reliable design tool. Designs from experiments carried out on the Omega Laser are used as the basis of the simulation set. Code results are analyzed at 1.3 ns, the time just after the laser deposition phase has finished, and at a later time to follow the hydrodynamic evolution of the experiment. Conducting an initial sensitivity study in 2D is critical for quantifying the predictive capability of H2D and codes coupled to H2D output.

*Supported by the US DOE NNSA under the Predictive Sci. Academic Alliance Program by grant DE-FC52-08NA28616, the Stewardship Sci. Academic Alliances program by grant DE-FG52-04NA00064, and the Nat. Laser User Facility by grant DE-FG03-00SF22021.

UP8 148 Characterization of initial state of radiative shock experiments on Omega C.C. KURANZ, R.P. DRAKE, F.W. DOSS, A.J. VISCO, C.M. HUNTINGTON, M.J. GROSSKOPF, D.C. MARION, *University of Michigan* Radiative shocks, which exist in a regime where most of the incoming energy flux is converted into radiation, can be created in a laboratory using a high-powered laser. We have performed experiments on the Omega Laser that irradiate a 20μm thick Be disk with $\sim$ 4 kJ of laser energy. This shocks and accelerates the disk into a Xe or Ar gas at 1.1 atm. These radiative shocks reach velocities well above 100 km/s. Diagnostics for this experiment have included x-ray radiography, x-ray Thomson scattering, optical pyrometry, and UV Thomson scattering. A 3D, MHD code with a radiation solver is

being developed by the Center for Radiative Shock Hydrodynamics to model this experiment. It is important for this modeling effort that the initial pressure deposited by the laser and the initial state of the Be plasma be well characterized. The design of a new experiment that will use VISAR and optical pyrometry for early time diagnosis of this initial state will be presented. Supported by the US DOE NNSA under the Predictive Science Academic Alliance Program by grant DE-FC52-08NA28616.

UP8 149 Analysis of Radiative Shock Experiments and Simulations Using Uncertainty Quantification Techniques* BRUCE FRYXELL, JASON CHOU, MIKE GROSSKOPF, VIJAY NAIR, ZACH ZHANG, *University of Michigan* DEREK BINGHAM, *Simon Fraser University* BANI MALLICK, DUCHWAN RYU, *Texas A&M University* The CRASH Center at the University of Michigan was established to study the properties of radiative shocks, using both radiation hydrodynamic simulations and experiments at the Omega Laser Facility. Comparison of the experimental results with the numerical simulations provides an excellent opportunity to do not only standard verification and validation studies, but to go one step further and provide a formal quantification of the errors and uncertainties in the numerical simulations using statistical uncertainty quantification techniques. The goal is to provide a formal framework for the quantification of errors and uncertainties in the numerical simulations. Instead of obtaining a single answer to a calculation, one ends up with a probability distribution for each quantity of interest. Thus each computed value has an associated error bar.

*Supported by the US DOE NNSA under the Predictive Sci. Academic Alliance Program by grant DE-FC52-08NA28616, the Stewardship Sci. Academic Alliances program by grant DE-FG52-04NA00064, and the Nat. Laser User Facility by grant DE-FG03-00SF22021.

UP8 150 Measure of the albedo of a warm plasma in the XUV range MICHEL BUSQUET, *Observatoire de Paris-LERMA, (Meudon, France)* FREDERIC THAIS, *CEA/DSM/IRAMIS (Saclay,France)* GHITA GEOFFROY, *CELIA (Bordeaux, France)* DIDIER RAFFESTIN, *CEA/DAM/CESTA/DLP (Bordeaux-,France)* It has been shown in a recent experience at PALS [1] that the radiative precursor celerity in front of a strong radiative shock is sensitive to the lateral radiative losses, thus to the albedo of the wall of a "radiative shock tube." In the experiment presented here, we measure the albedo of various materials (Al, Cu, Au) heated by a Xenon gaz at temperature around 30 eV. The Xenon gas was heated by the ALISE laser in CESTA in Bordeaux (France). The emission of Xenon with and without the reflecting samples is measured with a spatially resolving XUV spectrograph in the 30-250 eV range. [1] M. Busquet et al, HEDP 3, 8 (2007)

UP8 151 Electronic Measurement of Microchannel Plate Pulse Height Distribution ELISEO GAMBOA, CHANNING HUNTINGTON, ERIC HARDING, MARIANO LOWERNSTERN, R. PAUL DRAKE, *University of Michigan* Microchannel plates are a central component to the x-ray framing cameras used in many plasma experiment diagnostic systems. The microchannel plate serves as an amplifying element, increasing the electronic signal from incident radiation by a factor of $10^3 - 10^5$, with a broad pulse-height distribution. Seeking to improve the photon-to-electron conversion efficiency of x-ray cameras, we will characterize the pulse-height distribution of the electron output from a single microchannel plate. Replacing the framing camera's phosphor-coated fiber optic screen with a charge-collection plate and coupling to a low-noise multichannel analyzer, we will quantify the total charge generated per photon event over a range of x-ray energies and incident fluxes. Hypothesizing that the plate saturation is a function of incident photon flux, we will calculate the saturation regime for microchannel plates operated in a single-plate configuration. The electronically-measured pulse height distribution will be compared to the same data collected via a purely-optical method, as described previously (E. C. Harding and R. P. Drake, Rev. Sci. Instrum. 77, 10E312 (2006)).

UP8 152 Supersonic flow through clumpy environments: simulations and experiments M.R. DOUGLAS, B.H. WILDE, *LANL* B.E. BLUE, J.F. HANSEN, *GA* J.M. FOSTER, P.A. ROSEN, R.J.R. WILLIAMS, *AWE* P. HARTIGAN, *Rice University* A. FRANK, *University of Rochester* Over the past decade, high resolution images of a number of Herbig-Haro objects using the Hubble Space Telescope have revealed complex, chaotic, evolving morphologies of bow shocks, knots, and filamentary structure. Such morphologies are likely a consequence of internal and terminal working surfaces moving into a medium that is highly inhomogeneous. To investigate how inhomogeneities play a role in shaping the morphology of such objects, laboratory experiments have been proposed to examine bow shock evolution as it propagates through a clumpy environment and subsequent development of small scale structure after shock passage. The experiments will be carried out at the Omega Laser Facility utilizing an existing platform which launches a near planar shock into an RF ($C_{15}H_{12}O_4$) cylinder. Two types of downstream targets will be embedded in the RF cylinder: a clumpy target consisting of a 1mm-diameter RF foam sphere containing $\sim$ 47 randomly distributed 127-μm diameter ruby microspheres, and a 1 mm-diameter sphere target of "uniformly" mixed RF foam with sapphire nanopowder. Calculations pertaining to the experimental configuration will be presented and compared to experimental data, if available.

UP8 153 3D-Spirals Emerging from Plasma Disk Structures and High Frequency QPOs* P. REBUSCO, B. COPPI, *MIT* M. BURSA, *C.U.* An interpretation based on a novel kind of plasma modes[1] emerging from axisymmetric disks is proposed for High-Frequency Quasi-Periodic Oscillations (HFQPOs) in low mass X-ray binaries supporting the fact that QPOs can be a probe of strong field gravity. Tri-dimensional, tightly wound spirals are considered that co-rotate with the magnetized plasma disk structure surrounding a black hole at a radial distance that is related to the radius of the marginally stable orbit. These modes can be excited under the combined effects of the differential rotation and the vertical gradients of the plasma density and temperature. The spirals are localized over relatively narrow radial widths and have frequencies that are multiples of the plasma rotation frequency. The high toroidal number m_ϕ modes are considered to decay into $m_\phi = 2$ and $m_\phi = 3$ modes, explaining the observed twin peak QPOs spectra with the 3:2 ratio. The modulation of the observed radiation associated with general relativistic effects is analyzed, considering different emission processes. These are connected to strong variations of the plasma collisionality parameters corresponding to a local rarefaction and heating, or to a local increase of plasma density and cooling due to the considered spirals. *Sponsored in part by the U.S. DOE and the Pappalardo Fellowship program. 1.B. Coppi, MIT-LNS Report 08/08, to be published in *A&A* (2009).

UP8 154 Gravitational Influences on Magnetic Field Structure in Accretion Disks* K. SCHNECK, B. COPPI, *MIT* The structure of the magnetic fields associated with plasma disks surrounding black holes is identified when the effects of gravitational and Lorentz forces on the dynamics of the disk are comparable. The effects of corrections to the radial gravitational forceare explored within the geometry of a thin disk. A significant external magnetic field component is considered, along with an internal component due to the azimuthal current configuration. The relation of the resulting configuration to the field structure when the gravitational force can be neglected[1,2] is discussed. The relevant equations for the pseudo-Newtonian potential[3] describing the physics near the event horizon of the black hole are also derived and the physical consequences are explored. *Sponsored in part by the U.S. Department of Energy and the MIT Undergraduate Research Opportunities Program.

[1]B. Coppi, *Phys. Plasmas* **12**, 057302 (2005)
[2]Coppi, B. and Rousseau, F. *Astrophysical Journal*, 641: 458-470 (2006)
[3]Paczyński, B. and Wiita, P. J. *Astron. Astrophys.* 88: 23 (1980)

UP8 155 Simulations of Cluster Magnetic Fields from AGNs HAO XU, HUI LI, *Los Alamos National Laboratory* We will report our research on magnetic fields and MHD turbulence in galaxy clusters using Cosmological Adaptive Mesh Refinement(AMR) MHD simulations of cluster formation with seed magnetic fields from Active Galactic Nuclei(AGNs). In our simulations, magnetic fields with energy between $\sim 10^58$ to 10^60 erg are put into the center of forming clusters at z=3 to mimic the magnetic feedbacks from AGNs. The injected local magnetic fields then spread throughout the whole cluster by the processes of cluster mergers and turbulent mixing. The magnetic fields are amplified and maintained by the bulk motions of the Intra-cluster medium (ICM) at large scales and by the ICM turbulence, which is driven by the continuous mergers and merger shocks, at small scales. The magnetic energy increases to $\sim 10^61$ erg and the strength of the final fields is at micro Gauss level extended to 1 Mpc from the cluster center. We will show the distributions of the simulated magnetic fields and the Faraday rotation measures of the clusters related to the ICM MHD turbulence. We will further discuss properties of the MHD turbulence and small-scale dynamo on the amplification and saturation of the magnetic fields.

UP8 156 Modeling Spectral Variability of Prompt GRB Emission with the Jitter Radiation Paradigm SRIHARSHA POTHAPRAGADA, MIKHAIL MEDVEDEV, SARAH REYNOLDS, *University of Kansas* We present a theoretical model of prompt GRB emission based on jitter radiation - electron emission in small scale magnetic fields, such as those produced in relativistic collisionless shocks mediated by the Weibel instability. We show that the combination of anisotropy in jitter radiation and relativistic shell kinematics of internal shocks produce well known features of time resolved prompt GRB spectra, e.g., the distinct "tracking" of the low energy spectral index α and the photon flux at peak energy $F_{ph}(E_{peak})$ and the presence of synchrotron violating hard spectra at the onset of individual spikes in lightcurves. We derive spectral evolution in time of individual spikes as well as full model lightcurves. We present agreement with observations and discuss predictions that can be made thereof.

UP8 157 Spectroscopic data of methane for astrophysics ROBERT WARMBIER, RALF SCHNEIDER, *Max-Planck-Institute for plasmaphysics* AMIT R. SHARMA, BASTIAAN J. BRAAMS, JOEL M. BOWMAN, *Emory University* STUART CARTER, *University of Reading* PETER H. HAUSCHILDT, *Hamburger Sternwarte* Adequate spectroscopic information of small to medium size molecules is a vital part for the understanding of processes in plasma physics and astrophysics. The demands for this information vary in terms of resolution/accuracy, completeness and consistence, depending on the task. While for many molecules experimental and/or theoretical data is available, these do not always fit the prerequisites. We showed for the example of methane (Warmbieret al. A&A 495, 655-661 (2009)) that we can calculate complete and consistent datasets of rovibrational transitions for a large temperature range with a sufficient accuracy for applications like atmospheric radiation transport. We are going to present an improved potential energy surface. The higher accuracy of the rovibrational energies levels allows line-by-line comparisons with experimental data. We will use an improved version of the quantum chemistry code MULTIMODE (publication pending;S. Carter, A. R. Sharma, P. Rosmus, and J.M. Bowman) to test the adiabatic dipole transition moments used before against the full rotational ones. This will offer a generic approach to calculate spectroscopic information of polyatomic molecules fitting a wide range of requirements.

SESSION WR1: REVIEW: APPLIED SPECTROSCOPY IN PULSED POWER PLASMAS
Friday Morning, 6 November 2009; Centennial I-II at 8:00; Amitava Bhattacharjee, University of New Hampshire, presiding

8:00
WR1 1 Applied Spectroscopy in Pulsed Power Plasmas.*
GREGORY ROCHAU, *Sandia National Laboratories*

Applied spectroscopy is a powerful diagnostic tool for high energy density plasmas produced with modern pulsed power facilities. These facilities create unique plasma environments with a broad range of electron densities (10^{13} – 10^{23} cm^{-3}) and temperatures (10^{0} – 10^{3} eV) immersed in strong magnetic (up to 10 T) and electric (up to 1 GV/m) fields. This paper surveys the application of plasma spectroscopy to diagnose a variety of plasma conditions generated by pulsed power sources including: magnetic field penetration into plasma, measuring the spatial distribution of 1 GV/m electric-fields, opacity measurements at stellar interior conditions, characteristics of a radiating shock propagating at 330 km/s, and determination of plasma conditions in imploded capsule cores at ~ 150 Mbar pressures. These applications provide insight into fundamental properties of nature in addition to their importance for addressing challenging pulsed power science problems.

*Sandia is a multiprogram laboratory operated by Sandia Corporation, a Lockheed Martin Company, for the United States Department of Energy under contract DE-AC04-94AL85000.

SESSION XI2: HIGH ENERGY DENSITY PHYSICS AND HIGH PERFORMANCE CAPSULE IMPLOSIONS
Friday Morning, 6 November 2009; Centennial I at 9:30; Gail Glendinning, Lawrence Livermore National Laboratory, presiding

9:30
XI2 1 Compressing Magnetic Fields with High-Energy Lasers.
J.P. KNAUER, *Laboratory for Laser Energetics, U. of Rochester*

Laser-driven, magnetic-field compression producing a magnetic field of many tens of megagauss (MG) is reported for the first time. A shock wave formed during the implosion of a cylindrical target traps an initial magnetic field that is amplified via conservation of magnetic flux. Such large fields are expected to magnetize the electrons in the hot central plasma leading to a cyclotron frequency exceeding the collision frequency. The Omega Laser Facility was used to implode cylindrical CH targets filled with deuterium gas and seeded with an external field (> 50 kG) from a magnetic pulse generator. This seed field is trapped and rapidly compressed by the imploding shell, minimizing the effect of resistive flux diffusion. The compressed field was predicted to achieve values of several tens of MG and was probed via proton deflectrometry using the 14.7-MeV protons from the D + ^{3}He fusion reaction emitted by an imploding glass microballoon. Protons crossing the hot spot of the imploded cylindrical target undergo the largest deflection since the compressed field peaks within the hot spot. Line-averaged magnetic fields of the imploded core were measured to between 30 and 40 MG. Experimental data were analyzed with both an MHD version of the 1-D hydrocode *LILAC* and the particle propagation code Geant4. This work supported by the U.S. DOE Office of FES under Grants DEFG02-04ER54768 and DE-FC02-ER54789 and by the Office of ICF under Cooperative Agreement No. DE-FC52-08NA28302. In collaboration with O.V. Gotchev, P.Y. Chang, R. Betti, D.D. Meyerhofer, O. Polomarov (LLE), F.H. Séguin, J.A. Frenje, C.K. Li, M.J.-E. Manuel, R.D. Petrasso (MIT), and J.R. Rygg (LLNL).

10:00
XI2 2 Observations of subsonic and supersonic shear flows in laser driven high-energy-density plasmas.*
E.C. HARDING, *University of Michigan, Ann Arbor, MI 48109 USA*

Shear layers containing strong velocity gradients appear in many high-energy-density (HED) systems and play important roles in mixing and the transition to turbulence. Yet few laboratory experiments have been carried out to study their detailed evolution in this extreme environment where plasmas are compressible, actively ionizing, often involve strong shock waves and have complex material properties. Many shear flows produce the Kelvin-Helmholtz (KH) instability, which initiates the mixing at a fluid interface. We present results from two dedicated shear flow experiments that produced overall subsonic and supersonic flows using novel target designs. In the subsonic case, the Omega laser was used to drive a blast wave along a rippled interface between plastic and foam, shocking both the materials to produce two fluids separated by a sharp shear layer. The interface subsequently rolled-upped into large KH vortices that were accompanied by bubble-like structures of unknown origin. This was the first time the evolution of a well-resolved KH instability was observed in a HED plasma in the laboratory. We have analyzed the properties and dynamics of the plasma based on the

data and fundamental models, without resorting to simulated values. In the second, supersonic experiment the Nike laser was used to drive a supersonic flow of Al plasma along a rippled, low-density foam surface. Here again the flowing plasma drove a shock into the second material, so that two fluids were separated by a shear layer. In contrast to the subsonic case, the flow developed shocks around the ripples in response to the supersonic flow of Al. Collaborators: R.P. Drake, O.A. Hurricane, J.F. Hansen, Y. Aglitskiy, T. Plewa, B.A. Remington, H.F. Robey, J.L. Weaver, A.L. Velikovich, R.S. Gillespie, M.J. Bono, M.J. Grosskopf, C.C. Kuranz, A. Visco.

*Sponsored by the Naval Res. Lab. contract NRL N00173-06-1-G906, DOE NNSA Stewardship Sci. Acad. Alliances grant DE-FG52-04NA00064, NNSA Predictive Sci. Acad. Alliance Prog. grant DE-FC52-08NA28616, and Nat. Laser User Facility grant DE-FG03-00SF22021

10:30
XI2 3 Measurement of fast electrons inside the dielectric material via observation of its Cherenkov radiation.
HIDEAKI HABARA, *Osaka University*

Direct measurement of extremely high energy density electrons created in ultra-intense laser plasma interactions is crucial issue for Fast Ignition. Cherenkov radiation is studied to obtain the energy distribution of electrons because the emission angle depends on the electron energy. However in the previous studies [F. Brandl et al. Europhys. Lett. 61, 632 (2003), M. Manclossi et al. Phys. Rev. Lett. 96, 125002 (2006)], the experimental configurations using a planer target raised issues of spatially overlapping among the light from the different energy electrons as well as the other emissions such as transition radiation. We developed a novel prism shaped target in which Cherenkov light emitted from different energy electrons are spatially separated, realizing an absolute measurement of the energy spectrum by counting the light intensities in each observed position. In the experiment we observed a clear expected horseshoe pattern indicating a portion of Cherenkov ring image. In addition, we found that many parts of electrons are considered to propagate along laser axis from the blur of the outer edge of the pattern. The calibrated energy spectrum agrees extremely well with a PIC calculation qualitatively. A large discrepancy between the magnetic electron spectrometer and the Cherenkov results infers the strength of the electrostatic sheath potential at the rear boundary which also well agrees with the calculation.

11:00
XI2 4 High Performance Capsule Implosions on the Omega Laser Facility with Rugby Hohlraums.*
HARRY F. ROBEY, *Lawrence Livermore National Laboratory*

Rugby-shaped hohlraums have been proposed as a method for x-ray drive enhancement for indirectly-driven capsule implosions [1]. This concept has recently been tested in a series of shots on the OMEGA laser facility at the Laboratory for Laser Energetics at the University of Rochester. In this talk, experimental results are presented comparing the performance of D_2-filled capsules between standard cylindrical Au hohlraums and rugby-shaped hohlraums. Not only did the rugby hohlraums demonstrate 18% more x-ray drive energy as compared with the cylinders, but the high-performance design of these implosions (both cylinder and rugby) also provided $\approx$ 20X more DD neutrons than any previous indirectly-driven campaign on Omega (and $\approx$ 3X more than ever achieved on Nova implosions driven with nearly twice the laser energy). This increase in performance enables, for the first time, a measurement of the neutron burn history of an indirectly-driven implosion. Previous DD neutron yields had been too low to register this key measurement of capsule performance and the effects of dynamic mix. A wealth of additional data on the fuel areal density from the suite of charged particle diagnostics was obtained on a subset of the shots that used D^3He rather than D_2 fuel. Comparisons of the experimental results with numerical simulations are shown to be in excellent agreement. The design techniques employed in this campaign, e.g., smaller NIF-like laser entrance holes and hohlraum case-to-capsule ratios, provide added confidence in the pursuit of ignition on the National Ignition Facility. [1] P. Amendt, C. Cerjan, D. E. Hinkel, J. L. Milovich, H.-S. Park, and H. F. Robey, "Rugby-like hohlraum experimental designs for demonstrating x-ray drive enhancement," *Phys. Plasmas* **15**, 012702 (2008).

*Prepared by LLNL under Contract DE-AC52-07NA27344.

SESSION XI3: ENERGETIC PARTICLES
Friday Morning, 6 November 2009; Centennial II at 9:30; Nikolai Gorelenkov, Princeton Plasma Physics Laboratory, presiding

9:30
XI3 1 Marginal Stability Dynamics for Energetic Particles.*
HERBERT BERK, *Univerisity of Texas at Austin*

Marginal stability in plasmas characteristically sets a stiff limit to the range of that can be achieved. Below this limit, the system is governed by classical. Near marginal stability, however, plasmas may be subject to rapid processes, resulting in a system that hovers near marginality. This scenario emerged from nonlinear studies of energetic particle relaxation and

may be to more general plasma transport. We describe results from several such which include. [1] Avalanches—Near marginal stability, an important point is whether an instability driven by resonant particles where the distribution function has "free energy" will cause global radial diffusion. For that,modes need to overlap. This process can be continuous or bursty, the latter having been recently observed in NSTX and DIII-D. [2] Frequency chirping—Recent simulations by Vann showed that marginal stability can be sustained when there is only one unstable linear mode, due to the mechanism of spontaneous frequency sweeping. Although a single mode near stability should not cause dramatic relaxation, nevertheless in the Vann simulations, the achievement of marginal stability induced a continual chirping of that had removed energy from the bulk of the region where the external beam to deposit free energy. The distribution was then found to hover near stability. This mechanism may apply to the n=0 GAM where frequency sweeping might be a mechanism for extracting energy from alpha particles in a burning plasma, thereby reducing the stored alpha particle pressure. One way to implement this is to have the n=0 geodesic acoustic modes (GAM) be preferentially excited, since energy rather than momentum (leading to spatial diffusion) is then primarily extracted from alpha particles.

*Supported by U. S. Department of Energy

10:00
XI3 2 Gyrokinetic Simulations of Enhanced Alpha Transport by De-stabilized Alfvèn Turbulence.*
E.M. BASS, *General Atomics*

Alfvèn turbulence, destabilized by fusion-produced α-particles, is expected to greatly enhance transport of these hot fusion products. Previously, the gyrokinetic code GYRO [1] was used to simulate the convective transport of fusion alpha particles by electrostatic ($\beta = 0$) ITG/TEM turbulence driven at low k ($0 < k_\theta \rho_s < 1$) by density and temperature gradients in the background plasma for the GA-standard case [2]. The present study, at $\beta_e = 0.002$, includes electromagnetic effects, allowing for driven Alfvèn turbulence. The alpha particles are modeled by a hot Maxwellian ($T_\alpha = 100\,T_e$) superimposed at trace density ($0.005 < n_\alpha/n_e < 0.025$ and $a/L_\alpha = 4$ fixed) on the background plasma. Linear stability studies show two high-frequency modes driven unstable at very long wavelength ($0 < k_\theta \rho_s < 0.14$) by a radial density gradient in the alpha population. A new eigenvalue solver within GYRO shows that the leading modes, identified as the toroidal Alfvèn eigenmode (TAE) and the energetic particle mode (EPM), exhibit hybrid "drift-Alfvèn" frequency scaling with $k_\theta \rho_s$ and n_α. At densities below the Alfvèn linear stability threshold ($n_\alpha/n_e \leq 0.005$), ITG/TEM turbulence dominates nonlinear simulations. In this limit, the transported alpha particles are passive tracers and ion and electron transport agrees well with $n_\alpha = 0$ results. Just above the alpha-particle density gradient threshold, Alfvènic (TAE/EPM) drive enhances transport in α-particle and background channels. This trend continues as n_α and TAE/EPM microturbulence drive increase. The focus is on conditions for obtaining stationary nonlinearly saturated transport avoiding any subcritical limit on the total beta gradient.

[1] J. Candy and R.E. Waltz, Phys. Rev. Lett. **91**, 045001 (2003).
[2] C. Estrada-Mila, *et al.*, Phys. Plasmas **13**, 112303 (2006).

*Supported by US DOE under DE-FC02-08ER54977 and DE-FG03-95ER54309.

10:30
XI3 3 Energetic Particle Transport by Microturbulence.*
W.L. ZHANG, *UC Irvine*

The confinement of energetic particles is a critical issue in ITER, since ignition relies on self-heating by the energetic alpha particles. Recent DIII-D experiments [1] show significant transport of fast ions produced by neutral beam injection (NBI) in the absence of appreciable MHD activity. We study the diffusion of energetic particles by microscopic ion temperature gradient turbulence in large-scale simulations using a global gyrokinetic toroidal code (GTC). The ion radial excursion is found to be a diffusive process and thus the diffusivity as a function of the energy and pitch angle can be calculated using the random walk model. We find that the diffusivity decreases drastically for high-energy particles due to the averaging effects of the large gyroradius and orbit width, and the fast wave-particle decorrelation [2]. The NBI ion diffusivity is found to decrease rapidly for birth energies up to ten times the plasma temperature and more gradually to a very low level for higher birth energy. Results from GTC simulations explain many features of the fast-ion transport in beam-heated DIII-D plasmas. As predicted by the simulations, the profiles and spectra of fast ions (measured by fast ion D_α diagnostic) deviate more strongly from neoclassical predictions when the plasma temperature is high and when the fast-ion energy is low. TRANSP simulations that use fast-ion diffusion coefficients derived from the GTC simulations improve the agreement with experimental measurements, indicating that the predicted transport by the microturbulence is the correct size to explain the observations.

[1] W.W. Heidbrink, *et al.*, submitted to Phys. Rev.Lett. (2009).
[2] W. Zhang, *et al.*, Phys. Rev. Lett. **101**, 095001 (2008).

*Supported by US DOE under DE-FC02-04ER54698 and SC-G903402. In collaboration with Z. Lin, L. Chen, W.W. Heidbrink, D.C. Pace (UCI), the DIII-D Team and the SciDAC GSEP Center.

11:00
XI3 4 Experiments in DIII-D Toward Achieving Rapid Shutdown with Runaway Electron Suppression.*
E.M. HOLLMANN, *UCSD*

For safe discharge shutdown in future large tokamaks in the event of an unavoidable disruption, it is important to develop rapid ($\sim$ several ms)shutdown methods to avoid large runaway electron currents, which pose a serious threat to plasma facing components. Prevention of runaway current formation has been proposed by either increasing electron-electron collisionality with massive particle injection, or magnetically by using externally applied non-axisymmetric fields to increase radial diffusive losses of a runaway seed population. Experiments studying both approaches have been pursued in the DIII-D tokamak. For collisional suppression, three different rapid shutdown methods are being investigated: massive gas injection, massive shattered cryogenic pellet injection, and polystyrene shell pellet injection. First-of-kind demonstrations of fast shutdowns were produced by 3000 Torr-l (0.8-g) shattered D_2 pellets and large, 10-mm diameter, 0.3-g polystyrene shell pellets filled with boron powder. The application of external magnetic perturbations shows promising preliminary results in suppressing seed runaway electrons, although lack of repeatability in the runaway seed term made these results challenging to interpret. Experiments have been performed to help understand how runaways form and are transported during rapid shutdown. These experiments confirm that the commonly used 0D loop voltage + Dreicer evaporation picture of runaway seed formation is not applicable here, with relativistic $E > 0.5$ MeV electrons forming before any external loop voltage appears. Present applications of 0D, 1D, and 2D models to the rapid shutdown and runaway confinement experiments, as well as preliminary extrapolations to ITER, will be discussed.

*Supported by US DOE under under DE-FC02-04ER54698 and DE-FG02-07ER54917.

11:30
XI3 5 Beam particle distribution modification by low amplitude modes.*
ROSCOE WHITE, *Princeton University*

Modification of a high energy particle distribution by a spectrum of low amplitude modes is investigated using a guiding center code. Only through resonance are modes effective in modifying the distribution. Diagnostics are investigated to illustrate the mode-particle interaction. Effects of pitch angle scattering and drag are included, as well as time dependence of the equilibrium and mode frequencies. A specific example of changes observed in a DIIID neutral beam distribution in the presence of low amplitude Toroidal Alfvèn (TAE) eigenmodes and Reversed Shear Alfvèn (RSAE) eigenmodes is examined in detail. Comparison with experimental data shows that low amplitude modes, properly including sufficient mode harmonics and the polarization potentials, in conjunction with pitch angle scattering and mode frequency chirping, can account for significant modification of high energy beam particle distributions. The existence of these effects make necessary the inclusion of a phase space dependent term for beam evolution in deposition codes, which can be larger than neoclassical diffusion terms. It is found that there is a stochastic threshold for beam profile modification, and that the experimental amplitudes are only slightly above this threshold. Collaborators: N. Gorlenkov, PPPL, W. Heidbrink and M. Van Zeeland, General Atomics

*Supported by the U.S. Department of Energy Grants DE-AC02-09CH11466, SC-6903402 and DE-FC02-04ER54698.

12:00
XI3 6 Observation of a nonaxisymmetric MHD self-organized state.*
CHRISTOPHER COTHRAN,† *Swarthmore College*

A nonaxisymmetric stable magnetohydrodynamic (MHD) equilibrium within a prolate cylindrical conducting boundary has been produced experimentally at SSX (Swarthmore Spheromak Experiment). It has $m = 1$ toroidal symmetry, helical distortion, and flat λ profile. Each of these observed characteristics are in agreement with the magnetically relaxed minimum magnetic energy Taylor state. The Taylor state is computed using the methods described by A. Bondeson *et al.*, Phys. Fluids **24**, 1682 (1981) and by J. M. Finn *et al.*, Phys. Fluids **24**, 1336 (1981) and is compared in detail to the measured internal magnetic structure. The lifetime of this nonaxisymmetric CT is comparable to or greater than that of the axisymmetric CTs produced at SSX, thus suggesting good confinement. Despite varied initial conditions determined by two helicity injectors on the SSX device, this same equilibrium consistently emerges as the final state. These results therefore describe a new example of self-organization in an MHD plasma.

*Work supported by the U.S. Department of Energy and the National Science Foundation Center for Magnetic Self-organization
†Currently with GLOBAL Strategies Group (North America)

SESSION XP8: POSTER SESSION IX: SUPPLEMENTAL AND POST-DEADLINE POSTERS
Friday Morning, 6 November 2009
Grand Hall East at 9:30

XP8 1 SUPPLEMENTARY ABSTRACTS

XP8 2 Neoclassical Toroidal Plasma Viscosity in the Vicinity of an Island in Tokamaks N.T. ISLAND, K.C. SHAING, *Plasma and Space Science Center, National Cheng Kung University* S.A. SABBAGH, *Columbia University* M.S. CHU, *General Atomics* It is known that the broken toroidal symmetry in $|B|$ spectrum caused by the presence of the error fields and magnetohydrodynamic (MHD) activities in tokamaks enhances totoidal flow damping rate through the neoclassical toroidal viscosity. Recent extensions of the theory for the neoclassical toroidal plasma viscosity for non-resonant perturbations are generalized to calculate the symmetry breaking induced plasma viscosity in the vicinity of a rotating island. Specifically, the effects of orbit squeezing, collisional boundary layer, collisionless detrapping-retrapping, drift resonance caused superbananas, and bounce-transit and drift resonance are now included to complete the original theory. The results can be compared with experimental measurements of the flow damping rate in the vicinity of the islands. This extensive theory will form a basis for the further development of the island rotation theory in tokamaks.

XP8 3 EUV Measurements and Analytic Models of a Laboratory Solar Coronal Loop Simulation R.J. PERKINS, P.M. BELLAN, *Caltech* Solar coronal loops typically erupt abruptly after long quiescent periods. Such eruptions might be initiated by interactions between adjacent loops; this was explored in a laboratory experiment where two plasma-filled flux tubes merge in either a co- or counter-helicity arrangement (J.F. Hansen, S.K.P. Tripathi, and P.M. Bellan, Phys. Plasma 2, 3177(2004)). The latter arrangement produces a bright region with enhanced soft x-ray emission. We investigate such mergings with a new array of EUV photodetectors (based on S.J. Zweben, R.J. Taylor, Plasma Physics, Vol. 23, No. 4(1981)), and with analytic studies of particle orbits. The EUV array provides spatially and temporally resolved measurements of radiation between 10 and 120 nm needed to observe the bright regions. Precautions are taken against capacitive coupling, incoming plasma, and noise. We model the orbits of individual particles to understand the merging process. These models suggest two classes of trajectories: those confined to a single flux tube and those that move symmetrically between adjacent flux tubes, and how trajectories transition from these classes.

XP8 4 Dusty Modes in Nano-technological Plasmas STEVEN BEKHOR, *Michigan Plasma Physics Research Institute* An updated set of dispersion relations for dust acoustic, ion-acoustic and magneto-acoustic waves as well as the linear instabilities and dust charge relaxation processes associated with certain electrostatic and electromagnetic waves is presented using typical parameters for nano-technological plasmas based on a multi-fluid treatment. In the future, these may be used in an assessment of the optimal parameters for dynamical self-organization in multi-component plasmas used in the plasma enhanced chemical vapor deposition (PECVD) of self-assembled vertically aligned nanostructures.

XP8 5 H-1NF: The Australian National Plasma Fusion Facility: Results and Upgrade Plans B.D. BLACKWELL, *Australian National University* J. HOWARD, M.J. HOLE, D.G. PRETTY, J.W. READ, H. PUNZMANN, S.T.A. KUMAR, M. McGANN, R.L. DEWAR, *Australian National University* C.A. NUEHRENBERG, *Max-Planck-Institut fur Plasmaphysik, Greifswald* The H-1 National Plasma Fusion Research Facility will be upgraded to support the development of world-class diagnostic systems for application to international facilities in preparation for ITER. The upgrade will include new heating systems and deliver access to new magnetic configurations relevant to development of edge and divertor plasma diagnostics for next generation devices. The Facility plan will be presented, including target parameters and configurations, modelling results and the relation to the strategic plan for Australian fusion research, developed by the Australian ITER Forum. New results from some of the optical imaging and magnetic diagnostics underpinning the upgrade plans will be presented, including a new method of coherence imaging of ion temperatures and flows. Synchronous imaging of MHD mode structure using fast optical emission imaging promises to supplement data from two poloidal arrays of Mirnov coils and a precision step-scanned interferometer to provide detailed information about radial and toroidal mode structure. Comparisons with theory will include a CAS3D study.

XP8 6 Superdiffusion in strongly coupled 2D Yukawa plasmas MICHAEL BONITZ,*TORBEN OTT, *Kiel University, Inst. Theoretical Physics and Astrophysics* Numerical simulation results for the mass transport by diffusion in dusty plasmas are presented and compared to experimental measurements, e.g. [1, 2]. For a wide range of parameters, an anomalous behaviour of the diffusion process, i.e., "superdiffusion," is shown to exist for monolayer systems. In such superdiffusive systems, the mean-squared displacement does not obey the Einstein relation $\langle|\vec{r}(t) - \vec{r}(t_0)|^2\rangle \sim t^\alpha$ with $\alpha = 1$. In contrast, the diffusion exponent is greater than unity on large time scales. The dependence of α on the plasma conditions has been investigated by varying the temperature, the screening and the dissipation in the numerical simulations, thus providing detailed predictions for the superdiffusion process in dusty plasmas [3,4]. In addition, we present results for the persistence of superdiffusion, i.e., we adress the question whether superdiffusion extends to arbitrarily long time scales. [1] B. Liu and J. Goree, *Physical Review Letters* **100**, 055003 (2008) [2] W.-T. Juan and L. I, *Physical Review Letters* **80**, 3073 (1998) [3] T. Ott, M. Bonitz, P. Hartmann, subm. to *Physical Review Letters* [4] T. Ott *et al.*, *Physical Review E* **78**, 026409 (2008)

*Supported by DFG via SFB-TR 24

XP8 7 Progress in the SciDAC FSP Prototype Center for Plasma Edge Simulation (CPES)* C.S. CHANG, *New York University, and the CPES Team* The present status of and the future plans for the SciDAC FSP Prototype Center for Plasma Edge Simulation (CPES) will be reported. The full-f XGC1 gyrokienetic edge turbulence code evaluates 5D edge turbulence in realistic tokamak geometry, with the inner boundary pushed all the way to

the magnetic axis to study edge pedestal effect on core turbulence. Full-f XGC0 is a kinetic-based transport modeling code in realistic 3D magnetic geometry, which is designed to predict plasma transport behavior on experimental time scale, in integration with MHD codes to include large scale instability events (such as ELMs) on plasma profile evolution. DEGAS2 code is integrated into XGC for higher fidelity neutral transport. The code integration is achieved by computer science means on EFFIS framework (End-to-end Framework for Fusion Integrated Simulation).

*This project is supported by US DOE OFES and OASCR

XP8 8 Envelope equation of a plasma jet* CHIPING CHEN, *Massachusetts Institute of Technology* A self-consistent phase-space moment description is developed for high-energy-density plasma jets in the context of plasma jet approaches to high-energy density physics (HEDP). The phase-space moment theory is the truncated moment average of the kinetic equation. Using the phase-space moment theory, the root-mean-square (rms) envelope equations, which describe the orientation and size of the plasma jet, are derived for high-energy-density plasma jets. The envelope equations are demonstrated to agree with the virial theorem. In the regime where the internal field energy density is negligibly small compared with the thermal energy density and the internal flow energy density (Zhou and Chen, 2008), the rms envelope and density profiles for a plasma jet column are determined analytically, and used to predict the characteristics of a plasma jet column under compression.

*Research supported by DOE Grant No. DE-FG02-05ER54836.

XP8 9 Particle-in-cell simulations of the excitation mechanism for fusion-product-driven ion cyclotron emission from tokamaks RICHARD DENDY, *UKAEA Culham* JAMES COOK, SANDRA CHAPMAN, *Warwick University* Suprathermal ion cyclotron emission (ICE) was the first collective radiative instability, driven by fusion products, observed on JET and TFTR. Strong emission occurs at sequential cyclotron harmonics of the energetic ion population at the outer mid-plane. Its intensity scales linearly with fusion reactivity, including its time evolution during a discharge. The emission mechanism is probably the magnetoacoustic cyclotron instability (MCI), involving resonance between: fast Alfvén waves; cyclotron harmonic waves supported by the energetic particle population and by the background thermal plasma; and a subset of the centrally born fusion products, just inside the trapped-passing boundary, whose drift orbits make large radial excursions. The linear growth rate of the MCI has been intensively studied analytically, and yields good agreement with several key observational features of ICE. To address outstanding issues in the nonlinear ICE regime, we have developed a particle-in-cell code which self-consistently evolves electron and multi-species ion macroparticles and the electromagnetic field. We focus on the growth rate of the MCI, as it evolves from the linear into the nonlinear regime for JET-like parameters.

XP8 10 ICF Fast Ignition with Ultra-Relativistic Electrons CLAUDE DEUTSCH, *LPGP UParisXI* JEAN-PIERRE DIDELEZ, *IPN UParis XI* HIGHFIS COLLABORATION, In contradistinction to the main-stream fast ignition scenario based on collisional stopping in the compressed DT-fuel of relativistic electron beams(REB) in the 1-2 Mev energy range(ER) [1], we consider an ultra-relativistic extension of the Malkin- Fisch [2] attempt at using REB in the several tenths of MeV ER, and stopping them in target through strong induced Langmuir turbulence. We stress therefore the additional and substantial contribution to REB stopping of strongly inelastic reactions such as the Trident production of electron-positron pairs as well as the many ways of electro-desintegrating deuterons and tritons, firstly in nucleons and eventually at higher energy with negative pion production included. In the latter case, it seems attactive to consider pion-catalyzed DT-fusion in a very dense and hot plasma with no sticking. This claim is supported by preliminary estimates based on Debyelike diatomic plasma orbitals. [1] C. Deutsch, H. Furukawa, K. Mima, M. Murakami and K. Nishihara Phys.Rev.Lett. 77, 2483 (1996) and also K.V. Starikov and C. Deutsch, Phys.Plasmas 14, 022704 (2007) [2] V.N. Malkin and N.J. Fisch, Phys.Rev.Lett. 89, 125004 (2002)

XP8 11 Diagnostic Systems of the Princeton MRI Experiment E.M. EDLUND, H. JI, K. GAROT, M.D. NORNBERG, A.H. ROACH, E.J. SPENCE, *Center for Magnetic Self-Organization, PPPL* The MRI experiment at the Princeton Plasma Physics Laboratory is a Taylor-Couette device for the study of rotational instabilities in sheared flows of a magnetized liquid metal GaInSn alloy [1]. Four components of the containment vessel (the inner and outer cylinders, and segmented top and bottom plates) may be rotated independent of each other to tailor the fluid rotation profile. External azimuthal coils produce vertical magnetic fields up to 5 kG. The primary signatures of rotational turbulence are found in the fluctuations of the magnetic field and fluid velocity. An array of 72 externally mounted magnetic pick-up coils detects global magnetic perturbations and can distinguish low order axial and azimuthal mode numbers. A proposed additional coil may be mounted in a fin and inserted into the fluid for measurement of local magnetic perturbations. An outer wall mounted transducer, acting as both transmitter and receiver, operates at 4 MHz in a pulse-echo configuration and measures both the equilibrium and fluctuating fluid velocity. We will present plans for a novel diagnostic to measure the torque at the fluid-wall interface, employing strain gauges between the outer wall and a coaxial sleeve. Work supported by the US DOE, NASA and the NSF. [1] E. Schartman, H. Ji and M.J. Burin, RSI 80, 24501 (2009).

XP8 12 Turbulence and magnetic field generation by magnetic electron drift vortex modes in a nonuniform plasma* BENGT ELIASSON, PADMA K. SHUKLA, *Theoretical Physics IV, Ruhr-University Bochum, Germany* VLADIMIR P. PAVLENKO, *Department of Physics and Astronomy, Uppsala University, Sweden* We present a simulation study of the dynamical evolution of nonlinearly interacting two-dimensional magnetic electron drift vortex modes in a nonuniform plasma. Depending on the equilibrium density and temperature gradients, the system can either be stable or unstable. The unstable system reveals spontaneous generation of magnetic fields from noise level, and large-scale magnetic field structures are formed. When the system is linearly stable, one encounters magnetic electron drift vortex (MEDV) mode turbulence in which there is a competition between zonal flows and streamers. For large MEDV mode amplitudes, one encounters the formation of localized and small-scale magnetic vortices and vortex pairs with scale sizes of the order of the electron skin depth. The MEDV turbulence exhibits non-Kolmogorov and anisotropic spectra for different sets of plasma parameters.

*This work was partially supported by the DFG through the Research Unit 1048 and by the Swedish Research Council (VR).

XP8 13 Molecular Dynamics Simulations of Energy Relaxation in Multi-Component Plasmas* FRANK GRAZIANI, LORIN BENEDICT, JAMES GLOSLI, RICHARD MORE, *Lawrence Livermore National Laboratory* MICHAEL MURILLO, *Los Alamos National Laboratory* DAVID RICHARDS, MICHAEL SURH, *Lawrence Livermore National Laboratory* Using the massively parallel molecular dynamics code ddcMD, we simulate the relaxation process of an out of equilibrium fully ionized multi-component plasma consisting of a weakly coupled component (electron + proton) and a strongly coupled component (argon). We compare several theoretical models with the simulations including, modified Landau-Spitzer, the convergent kinetic theory method of Brown-Preston-Singleton and the coupled mode approach of Dharma-wardana and Perrot. Results are also shown of the energy relaxation process when radiation is present.

*The work performed under the auspices of the U.S. Department of Energy by Lawrence Livermore National Laboratory under Contract DE-AC52-07NA27344.

XP8 14 Focusing and neutralization of intense ion beams with a metallic funnel* E. HENESTROZA, F.M. BIENIOSEK, *Lawrence Berkeley National Laboratory* F. HERNANDEZ, *UCLA* The phenomenon of grazing incidence reflection of MeV ion beams from a metallic surface and the production of secondary electrons from this interaction is the basis for a proposal to provide additional focusing and neutralization using a metallic funnel for the ion beams of the Neutralized Drift Compression Experiments (NDCX1 and NDCX2) at LBNL; these beams will be used to heat targets to high temperatures for the study of matter under warm dense matter (WDM) conditions. The present design of the final focus system provides a high-field solenoid and an injected neutralizing plasma to focus the beam onto the target. The addition of a metallic funnel inserted in close proximity to the target will concentrate the ions and provide additional secondary electrons for neutralization in the region of high compression. We will present Particle-in-Cell simulations of the dynamics of the ion beam as it propagates through the funnel and onto the target for cases where the inner bore of the cone may have a straight or curved profile, and compare with initial experiments to focus ion beams with a gold cone in the NDCX1 accelerator.

*This work was supported by the Director, Office of Science, Office of Fusion Energy Sciences, of the U.S. Department of Energy under Contract No. DE-AC02-05CH11231.

XP8 15 Optical Comparison of Single and Double Dielectric barrier plasma actuators* NOAH HERSHKOWITZ, LUTFI OKSUZ, ALAN HOSKINSON, *University of Wisconsin Madison* Time resolved ICCD pictures are taken for double and single surface barrier discharge plasma actuator for thick and thin powered electrodes. The filament and jet propagation minimum speeds are measured for both single and double barrier actuators. Optical emission spectra are measured using a monochromator. In a typical OES spectrum, O_2, O^+, CO, OH, N, N_2, N_2^+ and also optical emission lines from exposed electrodes (stainless steel, copper and tungsten lines) were observed for single barrier actuators. The optical data are fit by SPECAIR code[1]. The translational and rotational temperatures are found to be approximately room temperature while the vibrational temperatures were1700 K and 1200 K, the electron temperatures were 3200 K and 2400 K for thick and thin electrode respectively. The different regimes in a discharge will be discussed.

*This work was supported by NASA under cooperative agreement NNX07AB84A and the Air Force Office of Scientific Research (AFOSR) under grant FA9550-07-1-0025.

XP8 16 Manipulation of Laser-generated Proton Beam Energy Distribution for (p,n) Neutron Production D.P. HIGGINSON, *UCSD* J.M. McNANEY, D.C. SWIFT, *LLNL* T. BARTAL, *UCSD* H. CHEN, D.S. HEY, S. LE PAPE, A.J. MACKINNON, *LLNL* N. NAKANII, *UCSD* H. NAKAMURA, *ILE* F.N. BEG, *UCSD* Laser-accelerated proton beams have many applications including proton fast ignition, oncology, and neutron production. Neutrons can be created from (p,n) type reaction and in many elements this reaction is at relatively low proton energy (e.g. ^{7}Li(p,n)^{7}Be peaks at $\sim$ 0.5 barns at 2-6 MeV). Thus the ability to increase the low energy protons (i.e. decrease the temperature) while keeping the conversion efficiency constant will lead to higher neutron production. In this experiment, the Titan laser ($4x10^{19}$ W/cm^2) was used to accelerate protons from 25 μm thick Cu foils. Laser pulse length (0.7 to 10 ps) and intensity were systematically varied to show a change in the proton energy distribution. These protons then struck various (p,n) converter materials to create neutrons. Experimental results will be discussed. This work performed under the auspices of the U.S. Department of Energy by Lawrence Livermore National Laboratory under Contract DE-AC52-07NA27344.

XP8 17 Short-time behavior of a spherically trapped Yukawa plasma* HANNO KAEHLERT, MICHAEL BONITZ, *ITAP, University of Kiel* The formation of correlations in non-ideal plasmas and the associated heating or cooling effects have attracted considerable attention in recent years [1-4]. These results were obtained for macroscopic plasmas. Here, this question is reconsidered for charged particles confined by a spherical trap. Langevin dynamics simulations are used to study the correlation buildup and the formation of a strongly correlated Coulomb liquid when starting from a completely uncorrelated state. We observe an oscillatory behavior of the potential energy with the signature of a breathing oscillation of the whole cluster and a strong dependence of the maximal heating effect on the initial density profile. Results are also presented for the temperature relaxation to equilibrium. [1] M. Bonitz, D. Semkat and D. Kremp, Phys. Rev. E **56**, 1246 (1997) [2] D. Semkat, D. Kremp, and M. Bonitz, Phys. Rev. E **59**, 1557 (1999) [3] D.O. Gericke, M.S. Murillo, D. Semkat, M. Bonitz, and D. Kremp, J. Phys. A: Math. Gen. **36**, 6087-6093 (2003) [4] D. Semkat et al., Progress in Nonequilibrium Green's functions II, p. 83, M. Bonitz and D. Semkat (Eds.), World Scientific Publ. (2003)

*supported by the DFG via SFB-TR 24

XP8 18 Variational approach for the fully three-dimensional quantum Zakharov system* PADMA KANT SHUKLA, FERNANDO HAAS, *Ruhr University Bochum, Bochum, Germany* The three-dimensional quantum Zakharov system is derived from a two time-scales technique and hydrodynamic equations. The Lagrangian formalism as well as the pertinent conservation laws are identified. In the adiabatic and semiclassical case, the quantum Zakharov system reduces to a quantum modified vector

nonlinear Schrodinger (NLS) equation for the envelope electric field. The variational structure is used to investigate the dynamics of localized, Gaussian shaped solutions, via the Rayleigh-Ritz variational method. The formal classical limit is considered in detail. Quantum corrections are shown to prevent the collapse of localized Langmuir envelope fields, in both two and three-spatial dimensions. Moreover, the quantum terms can produce a breather-like, oscillatory behavior of the width of the approximate Gaussian solutions. The variational method is shown to preserve the essential conservation laws of the quantum modified vector NLS equation. The possibility of laboratory tests in the next generation intense laser-solid plasma compression experiment is discussed.

*This work was partially supported by the Alexander von Humboldt Foundation.

XP8 19 Self-consistent effects and breather mode in semiconductor quantum wells* PADMA KANT SHUKLA, FERNANDO HAAS, *Ruhr University Bochum, Bochum, Germany* GIOVANNI MANFREDI, PAUL-ANTOINE HERVIEUX, *Louis Pasteur University, Strasbourg, France* A novel breather mode in the self-consistent electron dynamics in semiconductor quantum wells is identified and characterized. The breather solution corresponds to coherent oscillations of the size of the electron gas around a self-consistent equilibrium. A non-perturbative time-dependent variational formalism is used to describe the relevant properties of the breather mode, both in the linear and nonlinear regimes, in the context of a quantum hydrodynamic model. The time-dependent Wigner-Poisson or Hartree equations are shown to be in excellent agreement with our analytical results. For asymmetric quantum wells, a signature of the breather mode is observed in the dipole response, which can be detected by standard optical means. The present approach should equally apply to metal nanoparticles and carbon-based systems such as fullerenes.

*This work was partially supported by the Alexander von Humboldt Foundation and by the Agence Nationale de la Recherche.

XP8 20 Negative energy modes and the quantum two-stream instability* PADMA KANT SHUKLA, FERNANDO HAAS, *Ruhr University Bochum, Bochum, Germany* ANTOINE CLAUDE BRET, *ETSI Industriales, Universidad de Castilla-La Mancha, Ciudad Real, Spain* The quantum two-stream instability is a benchmark displaying many of the particularities of quantum plasmas, including a new unstable branch of the dispersion relation for large wave- numbers and almost stationary, quasineutral, nonlinear oscillations without analog in classical plasmas. The unexpected features of the two-stream instability in electrostatic quantum plasmas are interpreted in terms of the coupling of approximate fast and slow waves. This is accomplished thanks to the factorization of the dispersion relation into different sectors carrying positive or negative energy. The concept of negative and positive energy waves, therefore, is shown to be useful not only for classical, but for quantum plasmas as well. The analysis can in principle be carried on in similar problems, like for the quantum beam- plasma instability or the case of parallel propagating quantum beams.

*This research was financially supported by the Alexander von Humboldt Foundation, and by the Spanish Ministerio de Educacion y Ciencia and PAI-05-045 of the Consejeria de Educacion y Ciencia de la Junta de Comunidades de Castilla-la Mancha.

XP8 21 Experimental Investigation of Trigger Problem in Magnetic Reconnection* N. KATZ, J. EGEDAL, W. FOX, A. LE, A. VRUBLEVSKIS, J. BONDE, M. PORKOLAB, *MIT, PSFC* In order for magnetic reconnection to be explosive there must be a sudden transition from slow to fast reconnection. This so- called "trigger mechanism," which is responsible for the spontaneous and explosive release of magnetic energy in solar flares, magnetospheric substorms, and sawtooth crashes in magnetic fusion devices, is not yet well-understood. We use the Versatile Toroidal Facility (VTF) at MIT to study this transition [1], focusing specifically on its 3D nature. To this end, we use multiple arrays of Langmuir probes, magnetic probes, and Rogowski coils to map out the full 3D structure of the reconnecting plasma. The emerging picture is one in which a global plasma mode ($q = 2$ or $q = 3$) plays a key role in the onset of reconnection, by breaking the axi-symmetry of the device and allowing 3D effects to arise. [1] J. Egedal et al., Phys. Rev. Lett. **98**, 015003 (2007).

*Supported by: DOE Junior Faculty Award DE-F602-06ER54878 and NSF/DOE Award PHY-0613734.

XP8 22 Ideal Magnetohydrodynamic Simulations of Low Beta Compact Toroid Injection into a Hot Strongly Magnetized Plasma* WEI LIU, SCOTT HSU, HUI LI, *LANL* We present results from three-dimensional ideal magnetohydrodynamic simulations of low beta compact toroid (CT) injection into a hot strongly magnetized plasma, with the aim of providing insight into CT fueling of a tokamak with parameters relevant for ITER (International Thermonuclear Experimental Reactor). A regime is identified in terms of CT injection speed and CT-to-background magnetic field ratio that appears promising for precise core fueling. Shock-dominated regimes, which are probably unfavorable for tokamak fueling, are also identified. The CT penetration depth is proportional to the CT injection speed and density. The entire CT evolution can be divided into three stages: (1) initial penetration, (2) compression in the direction of propagation, and reconnection with the background magnetic field, and (3) coming to rest and spreading in the direction perpendicular to injection. Tilting of the CT is not observed due to the fast transit time of the CT across the background plasma.

*Supported by LANL-LDRD

XP8 23 Long Term Evolution of Magnetized Bubbles in Galaxy Clusters* WEI LIU, HUI LI, SCOTT HSU, SHENGTAI LI, *LANL* We have performed nonlinear ideal MHD simulations of the long term evolution of a magnetized low-density "bubble" plasma formed by a radio galaxy in a stratified cluster medium. It is found that about 3.5% of the initial magnetic energy remains in the bubble after 8 billion years, and the initial magnetic bubble expansion is adiabatic. The bubble can survive for at least 8 billion years due to the stabilizing effect of the bubble magnetic field on Rayleigh-Taylor and Kelvin-Holmholtz instabilities, possibly accounting for "ghost cavities" as observed in Perseus-A. A filament structure spanning about 500 kpc is formed along the path of bubble motion. The mean value of the magnetic field inside this structure is 0.88 micro Gauss at 8 billion years. Finally, the initial bubble momentum and rotation have limited influence on the long term evolution of the bubble.

*Supported by LANL-LDRD.

XP8 24 Dynamical Screening and Wake Effects in Spherical Dusty Plasmas PATRICK LUDWIG, MICHAEL BONITZ, *University of Kiel* GLENN JOYCE, *University of Maryland, College Park, MD* MARTIN LAMPE, *Naval Research Lab, Washington, DC* Previous investigations have shown that 3D dusty plasma balls [1] can be well described by a one-component model with a static Yukawa-type pair interaction [2]. However, the multi-component plasma environment requires a systematic investigation of collective many-particle effects on the crystal formation. In particular the effect of streaming ions (i.e. a dynamically-screened Coulomb potential) can strongly influence structure and dynamics of a strongly-coupled dusty plasma. In a plasma with ions streaming at a uniform velocity, the dust-dust potential takes the form of a wake structure, which results in attractive forces between the similarly charged dust grains [3]. Of central interest are therefore the remarkable structural and dynamical consequences for 3D plasma crystals due to the non-reciprocal forces of the wakefield.The considered simulation model comprises an accurate representation of all plasma properties, including screening, wake effects, ion and electron thermal effects, Landau damping, as well as collisional damping. [1] Arp et al., Phys. Rev. Lett. 93, 165004 (2004) [2] Bonitz et al., Phys. Rev. Lett. 96, 075001 (2006) [3] Lampe et al., Phys. Plasmas 7, 3851 (2000)

XP8 25 Quest for impact ignition and its future prospect MASAKATSU MURAKAMI, H. AZECHI, T. WATARI, T. SAKAIYA, K. OHTANI, K. TAKEDA, H. SHIRAGA, K. SHIGEMORI, S. FUJIOKA, H. NAGATOMO, T. JOHZAKI, *ILE, Osaka Univ.* J. GARDNER, J. BATES, A. VELIKOVICH, Y. AGLITSKIY, M. KARASIK, J. WEAVER, S. OBENSCHAIN, *NRL* JAPAN-US IMPACT TEAM, Since the impact ignition has been proposed [1], we have achieved such crucial milestones under the operation of Gekko XII (ILE) and NIKE (NRL) laser systems as super-high-velocity acceleration of foils ranging 700-1000 km/s and hundred-fold increase in neutron yield by impact collision [2]. For the latter achievement, the kinetic energy of the impactor was efficiently converted into thermal energy generating a temperature of 1.6 keV. The use of Bromine-doped plastic target are key measure to suppress Rayleigh-Taylor instabilities and thus to achieve effective collisions. Based on these preliminary results, we have done two-dimensional hydrodynamic simulations to demonstrate that ignition occurs when impactor with a velocity beyond 1500 km/s and a density of 50 g/cm3 collides with main fuel with a density of 400 g/cm3, when the maximum impactor kinetic energy is 10 kJ. [1] M. Murakami and H. Nagatomo, Nucl. Inst. & Meth. Phys. Res. A544, 67 (2005). [2] H. Azechi, et al., Phys. Rev. Lett. 102, 235002 (2009).

XP8 26 Quasi-Static Magnetic Filed Generation in Interaction of Circularly Polarized Laser Pulses with Underdense Plasma NEDA NASERI, *Department of Physics-University of Alberta-Edmonton-Canada* VALERY YU. BYCHENKOV, *Lebedev Physics Institute- Moscow, Russia* WOJCIECH ROZMUS, *Department of Physics-University of Alberta, Edmonton, Canada* The excitation of quasi-static axial magnetic field by circularly polarized laser pulses in plasma channels due to inverse Farday effect is studied. The distribution of axial quasi-static magnetic filed is found numerically for different laser intensity and plasma channel distributions. To check that magnetic field changes its sign with change of left to right circular polarization, we performed 3D PIC simulations with right-hand and left-hand circularly polarized laser light and found that the excited magnetic filed due to inverse Faraday effect changes its sign with the change of polarization as predicted from theory. The distribution of quasi-static axial magnetic filed is found numerically by adopting the distribution of the laser intensities and density channels from our 3D simulations and compared with quasi-static magnetic filed calculated from the simulation.

XP8 27 Off-axis stability of intense continuous relativistic beams* RENATO PAKTER, LUCIANO C. MARTINS, FELIPE B. RIZZATO, *Instituto de Fisica - Universidade Federal do Rio Grande do Sul, Brazil* This paper investigates the stability of off-axis continuous intense relativistic beams propagating inside a circular conducting pipe. The equations of motion for the centroid and the envelope of slightly off-axis beams are derived and used to determine equilibrium and stability conditions for the beam transport. It is shown that depending on the parameters of the system, beams propagating along the pipe axis may become unstable due to the presence of the wall, imposing a fundamental limitation in the effective area that an equilibrium beam can occupy inside the conductor. Self-consistent N-particle simulations are used to verify the findings.

*Work supported by CNPq, Brazil and the US-AFOSR under Grant No. FA9550-09-1-0283.

XP8 28 Generation of Langmuir turbulence and stochastic acceleration in laser beat wave process PRERANA SHARMA, R.P. SHARMA, *IIT, Delhi* This paper investigates the filamentation process of two co-axially propagating laser beams in a collisionless plasma. On account of the ponderomotive nonlinearity, two laser beams affect the dynamics of each other and cross-focusing takes place. The initial Gaussian laser beams are found to have non-Gaussian structures in the plasma. Using the laser beam and the plasma parameters, appropriate for beat wave process, the filaments of the laser beams have been studied. Using these results, the Langmuir wave (LW) excitation at the beat wave frequency (when the laser beams are having filamentary structures) has been studied. The excited LW is modeled with the help of a driven oscillator and it is found that the excited LW is not a plane wave; rather it has a turbulent structure. We have obtained the power spectrum of the excited beat wave (Langmuir wave) and calculated the spectral index. The stochastic electron acceleration has been studied in the presence of this Langmuir turbulence and relevance of these results to beat wave process has been pointed out.

XP8 29 Effect of Laser Beam Filamentation on Second Harmonic Spectrum in Laser Plasma Interaction PRERANA SHARMA, R.P. SHARMA, *Indian Institute of Technology, Delhi, India* This paper presents the laser beam filamentation at ultra relativistic laser powers, when the restriction on the beam is relaxed during filamentation process. On account of laser beam intensity gradient and background density gradients in filamentary regions the electron plasma wave (epw) at pump wave frequency is generated, this epw is found to be highly localized on account of the laser beam filaments. Interaction of incident laser beam with these epw leads to second harmonic generation. The second harmonic spectrum has also been studied in detail and its correlation with the filamentation of the laser beam has been established. Starting almost with a monochromatic component of laser beam propagation, the second harmonic spectrum becomes more complicated and broadened as the laser beam propagates further, and

filamentation takes place. For the typical laser beam and plasma parameters: λ_0= 1064 nm, power flux (10^{22} W/cm^2), $\omega_p = 0.03\omega_0$, $v_{th} = 0.1c$, $n_0 = 1.9\times 10^{19}$. We found that conversion efficiency comes out to be $(E_2/E_0) = 8\times 10^{-3}$, and the spectrum is quite broad which depends upon the laser beam propagation distance. The results (specifically, second harmonic spectral feature) presented here may be used for the diagnostics of laser produced plasmas.

XP8 30 Nonlinear Simulations of the inhomogeneous magnetic electron drift vortex mode turbulence P.K. SHUKLA, *Ruhr University Bochum, Germany* DASTGEER SHAIKH, *The University of Alabama in Huntsville* B. ELIASSON, *Ruhr University Bochum, Germany* A simulation study of the magnetic electron drift vortex (MEDV) mode turbulence in a magnetoplasma in the presence of inhomogeneities in the plasma temperature and density, as well as in the external magnetic field, is presented. The study shows that the influence of the magnetic field inhomogeneity is to suppress streamer-like structures observed in previous simulation studies without background magnetic fields. The MEDV mode turbulence exhibits non-universal (non-Kolmogorov type) spectra for different sets of the plasma parameters. In the presence of an inhomogeneous magnetic field, the spectrum changes to a 7/3 power law, which is flatter than without magnetic field gradients. The relevance of this work to laboratory and cosmic plasmas is briefly mentioned.

XP8 31 Dark and grey electromagnetic electron-cyclotron envelope solitons in an electron-positron magnetoplasma P.K. SHUKLA, *Institut für Theoretische Physik IV, Fakultät für Physik und Astronomie, Ruhr-Universität Bochum, D-44780 Bochum* R. BINGHAM, *STFC Rutherford Appleton Laboratory* A.D.R. PHELPS, *Scottish Universities Physics Alliance (SUPA), Department of Physics, University of Strathclyde, Glasgow G4 0NG* L. STENFLO, *Dept. of Physics, Linköping University, SE-58183 Linköping, Sweden* We present an investigation of the amplitude modulation of an external magnetic field-aligned right-hand circularly polarized electromagnetic electron-cyclotron (EMEC) wave in a strongly magnetized electron-positron plasma. It is shown that the dynamics of the modulated EMEC wave packet is governed by a cubic nonlinear Schrödinger equation. The latter reveals that a modulated wave packet can propagate in the form of either a dark or a grey envelope soliton. This result could have relevance to the transport of electromagnetic wave energy over long distances via envelope solitons in the magnetospheres of pulsars and magnetars.

XP8 32 An Interpretation of "Puff & Pump" Radiative Divertor Experiments in DIII-D* W.M. STACEY, *Georgia Tech* T.W. PETRIE, *General Atomics* A series of "puff & pump" experiments in which argon is injected into the private flux region to achieve a radiative divertor, and deuterium is puffed into the chamber to achieve an enhanced gas flow in the scrape-off layer (SOL), intended to entrain and sweep escaping argon into the divertor, have been performed on DIII-D [1]. A calculational model [2] for particle flows and drifts in the SOL has been modified to represent the puff and pump experimental situation. We focus here on the effectiveness of varying the deuterium gas puff rate on argon accumulation in the core plasma, particularly with respect to how the ∇B drift impacts these results. Our analysis will be compared with experimental results.[1] T.W. Petrie, *et al.*, Nucl. Fusion **49**, 065013 (2009).[2] W.M. Stacey, Phys. Plasmas **16**, 042502 (2009).

*Work supported in part by the US DOE under DE-FC02-04ER54698.

XP8 33 Reduced Modeling of Electron Trapping Nonlinearity in Raman Scattering* D.J. STROZZI, R.L. BERGER, *LLNL* H.A. ROSE, *LANL* A.B. LANGDON, E.A. WILLIAMS, *LLNL* The trapping of resonant electrons in Langmuir waves generated by stimulated Raman scattering (SRS) gives rise to several nonlinear effects, which can either increase or decrease the reflectivity. We have implemented a reduced model of these nonlinearities in the paraxial propagation code pF3D [R. L. Berger et al., Phys. Plasmas 5 (1998)], consisting of a Landau damping reduction and Langmuir-wave frequency downshift. Both effects depend on the local wave amplitude, and gradually turn on with amplitude. This model is compared with 1D seeded Vlasov simulations, that include a Krook relaxation operator to mimic, e.g., transverse side-loss out of a multi-D, finite laser speckle. SRS in these runs develops from a counter-propagating seed light wave. Applications to ICF experiments will also be presented.

*Prepared by LLNL under Contract DE-AC52-07NA27344.

XP8 34 EBW Heating in the Pegasus Spherical Experiment* F. VOLPE, R. FONCK, A. REDD, *U. Wisc.* T. BIGELOW, S.J. DIEM, *ORNL* Electron Bernstein Wave (EBW) heating (H) and current drive (CD) are strong candidates for the growth of ST plasmas initiated by helicity injection up to become appropriate targets for neutral beam H&CD. Additionally they can improve beta, help sustaining the plasma current and tailor its profile, possibly in synergy with the high harmonic fast wave system. A 2.45GHz, 1MW EBW H&CD system is presently under consideration for a proposal for Pegasus. It would rapidly and cost-effectively address the applicability and scalability of EBW techniques to larger STs such as NSTX and a future component test facility. Two klystrons and part of the hardware originally deployed for lower hybrid heating in the PLT tokamak could serve for this purpose. It is proposed to explore both the ordinary-extraordinary-Bernstein and extraordinary-Bernstein conversion by means of a new launcher capable of oblique, adjustable launch, probably combined with a local limiter to steepen the density profile and so improve the mode conversion efficiency. A phase shifter would make the polarization elliptical, as required for modal purity.

*Supported by U.S. DoE grant No. DE-FG02-96ER54375

XP8 35 Proposed MHD Control in Pegasus* F. VOLPE, *U. Wisc.* The high beta, high edge-current-density Pegasus spherical experiment is interested by low-order tearing modes in the core and by the peeling mode at the edge. Controlling the two instabilities would further increase beta and tame the plasma edge, thus enabling its coupling with mode-converted electron Bernstein waves and with fast waves, for heating and current drive. Passive stabilizing rings and external or internal coils of various geometries (mid-plane radial field coils, segmented poloidal field coils or divertor coils) are being considered for this purpose. They were modeled with a finite-element code taking into account the image currents in the wall. The feasibility of the magnetic topologies desired for control (toroidal mode number, poloidal spectrum,

Chirikov parameter, radial penetration) was studied for the various designs. Requirements for the strength and frequency of the perturbation in the plasma were translated in power supply requirements. These and other considerations on the ease of installation, or the fact that some designs can simultaneously perform additional tasks such as error field correction or vertical stabilization, will guide the finalization of a conceptual design and proposal.

*Supported by U.S. DoE grant No. DE-FG02-96ER54375

XP8 36 Modeling of turbulent transport and flow generation in the HELCAT experiemnt A.S. WARE, M. OLSEN, M. BREYFOGLE, *University of Montana* M. GILMORE, *University of New Mexico* E. SCHUSTER, *Lehigh University* This work investigates modeling of transport and flow generation in a linear plasma device using a 1-D transport code. The goal is to model the HELCAT experiment including the use of biased concentric rings as control elements for the radial electric field profile. By varying the bias voltages, the local $\mathbf{E}\times\mathbf{B}$ flow can be modified. The effect will be identical to a source of $\mathbf{E}\times\mathbf{B}$ flow in the limit of zero β (i.e., when diamagnetic flows are negligible). By varying the momentum sources a sheared radial electric field can be generated that can suppress turbulent particle and heat transport. Analysis of drift wave turbulence models will be used to derive models for the growth rate and Reynolds stress parameterization in the transport model. We will test the impact of different numerical models for the momentum sources and compare the results with experimental measurements of the radial electric field in the HELCAT experiment.

XP8 37 POST-DEADLINE ABSTRACTS

XP8 38 SVD Techniques Applied to Modulated ECH Data on DIII-D* D.F. MEYERSON, M.E. AUSTIN, K.W. GENTLE, *U. Texas-Austin* T.C. LUCE, C.C. PETTY, *General Atomics* Sawtooth contamination is a serious problem that interferes with modulated electron cyclotron heating (MECH) induced heat pulse propagation analysis. To address this issue we apply system identification SVD techniques (SI-SVD) to separate the effect of sawteeth and MECH. DIII-D ECE data with and without sawtooth contamination is analyzed and compared to assess the validity of the method. While the different sources separated out by this method are assumed to have the ability to excite the same eigenmodes of the linearized energy transport equation, the sources themselves are assumed to be independent of one another. It is well known that the location of MECH deposition can alter the character of sawtooth instability; to quantify to what degree the location of deposition alters the results we consider on-axis as well as off-axis MECH shots. Additionally the technique gives a means of verifying the power deposition profile of the relevant sources. The results are compared with local power balance calculations as well as calculations of absorption profiles.

*Supported by the US Department of Energy under DE-FG03-07ER54415 and DE-FC02-04ER54698.

XP8 39 Relativistic MHD Jets HUI LI, *LANL* We present the formulation of relativistic MHD flows, likely occurring in the environment of accretion onto supermassive black holes. Three-dimensional relativistic MHD simulations will be presented on how the energy outflow will partition among different physical components and on the collimation and stability of such systems. The interaction between such flows with their environment, e.g., the intra-cluster medium, will be discussed.

XP8 40 Application of Hilbert-Huang Transform for the determination of instantaneous low frequency of Plasma waves* EKONG NATHANIEL, NATASHA BELOFF, ANDREW BUCKLEY, Downstream of a quasi-perpendicular bow shock of the Earth, various wave modes associated with the different boundaries have been confirmed and different methods have been used to find frequency and instantaneous frequency of the different modes. We applied Hilbert-Huang Transform in the determination of instantaneous frequency by decomposing the data observed by in-situ spacecraft in certain region in space called the Magnetosheath into intrinsic mode functions (IMFs) using empirical mode decomposition (EMD) technique of Huang et al., 1998. Instantaneous frequencies for the different IMFs were computed using Hilbert transform. The determined instantaneous frequency supports the non-stationary and non-linear nature of the data. The instantaneous wave vector was then computed. The observed data were taken from FGM instrument on Cluster II mission which provides 3-dimensional advantage for this analysis, and the results compared with the instantaneous frequency computed using simple Hilbert transform with electric field measurements of Cluster II mission already carried out.

*I am grateful to the FGM team and ESA Cluster Active Archive for their good work, which provided data for this analysis.

XP8 41 Nero Zero Frequency Sounding in Layered Media* CHASTITY AUTRY, *Physics Department, Georgia State University* ALEXANDRU TAMASAN, JOHANN VERAS, *Mathematics Department, University of Central Florida* We consider the mathematical model of frequency sounding of a continuously layered media. By the means of frequency asymptotic expansion of the wave field, this problem is equivalent to an inverse boundary value problem for the Ricatti equation. We solve the inverse Ricatti problem via a Cauchy problem for a first order quadratic equation for sequence-valued maps. The quadratic equation contains no unknown coefficients. The information of the medium is encoded in the initial value. For specific data, the Cauchy problem has a unique solution. Based on the contraction mapping principle the method of proof provides a stable reconstruction algorithm. The computational feasibility of the proposed approach is demonstrated in a numerical experiment.

*Funding was provided by the National Science Foundation Grants DMS 0649159, DMS 0803059, and DMS 0905799.

XP8 42 Magnetic spectrometry of deuteron spectra in plasma focus device MAHMUD VAHDAT ROSHAN, ALIREZA TALEBITAHER, RAJDEEP SINGH RAWAT, PAUL LEE, STUART VICTOR SPRINGHAM, Magnetic spectrometry using polymer nuclear track detectors is used for high-resolution measurement of the energy spectrum of deuterons emitted from the pinch-column of the NX2 plasma focus (PF). The spectrum is measured for single PF shots. A 25 μm pinhole images the deuteron source

on the spectrometer. Deuteron tracks are measured with an automated scanning system. The recognized and counted tracks are accumulated in a histogram of track displacement in bins representing equal energy stripes on the detector. A very distinct neutrals spot is clearly visible for each spectrum, resulting from uncharged deuterons passing through the spectrometer in straight-line paths and producing a densely tracked zone. The deuteron trajectory in the magnetic field is calculated in order to obtain the deuteron energy as a function of the distance from the neutrals spot on the detector. The deuteron spectrum $d^2N/dEd\Omega$ is derived from the track displacement histogram. The deuteron spectrum is used to estimate the beam-target contribution for fusion neutron production. The number of Nitrogen-13 nuclides in the activation of graphite through $^{12}C(d,n)^{13}N$ is estimated using the deuteron spectra and the thick target yield.

XP8 43 Nonlinear Landau damping and edge electron heating of electron Bernstein waves* JOHN R. CARY, *University of Colorado and Tech-X Corporation* NONG XIANG, *University of Colorado* In 1D simulations, it has been shown that nonlinear wave- particle interactions such as parametric decays and nonlinear Landau damping play an important role in electron Bernstein wave (EBW) propagations and absorptions. In this work, 3D particle-in-cell simulations are conducted with taking the wave antenna structure into account. The wave coupling and propagation around the mode-conversion layer are extensively studied. It is found that for typically experimental EBW heating parameters, if the incident frequency is larger than the second harmonic electron cyclotron frequency near the upper hybrid resonance (UHR), the incident wave may decay to an electron cyclotron wave whose frequency equals the electron gyro-frequency near the UHR, and an EBW at a lower frequency. As a result, a significant portion of the incident wave power will be absorbed at the plasma edge and electrons are strongly heated. This nonlinear Landau damping could much reduce the electron heating efficiency in the core plasma, and significantly affect the edge plasma properties.

*The work was supported by DOE Contract No.DE-FG02-04ER54735.

XP8 44 Plasma instability driven by noise CHANG-BAE KIM, *Soongsil University* Plasma response to an external noise is explored in the long-time and- large-scale limit. External noise is assumed to depend on a particular direction that may simulate the strong magnetic field or the gradient of the density and the temperature. The noise is thought to represent the short-scale background turbulence of certain physical origins whose spectrum is a transverse tensor to the wave vector. It is found that noise generates two effects: One is to enhance the dissipation by the isotropic spectrum and the other is a destabilizing term due to the anisotropic part. Depending on the relative strength of the anisotropic noise to the isotropic part the plasma may be unstable for small k modes. Potential relevance to the large-scale flows like the zonal flow and the streamer will be discussed in the presentation.

XP8 45 Physics validation for design change of KSTAR passive stabilizer* Y.M. JEON, J.Y. KIM, Y.K. OH, H.L. YANG, W.C. KIM, H.K. KIM, *National Fusion Research Institute* S.A. SABBAGH, J.M. BIALEK, *Columbia University* D.A. HUMPHREYS, A.S. WELANDER, M.L. WALKER, *General Atomics* Recently, the design of the passive stabilizer in KSTAR has been changed to improve controllability of the active control system and reduce the possibility of producing an additional error field. Originally the passive stabilizer in KSTAR was designed for RWM and vertical instability (or VDE) stabilizations and plasma startup efficiency, so that current bridges were designed and combined through 3D saddle-loop connections. Since the key design change is removing the current bridges, it's essential to assure satisfactory control performance for these instabilities under the design change. Control capability for n=1 RWM and achievable β_N will be addressed as a primary goal of the passive stabilizer together with vertical instability control and effects on plasma startup. In addition, the changes in electro-magnetic force on conducting structures will be discussed qualitatively as a key engineering issue of the design change.

*This work was supported by Korean Ministry of Education, Science and Technology.

XP8 46 Ion acceleration with a picosecond CO_2 laser* IGOR POGORELSKY, MARCUS BABZIEN, MIKHAIL POLYANSKIY, KARL KUSCHE, *BNL* PETER SHKOLNIKOV, MICHAEL ISPIRIAN, *SUNY Stony Brook* DAVID NEELY, *Rutherford Appleton Lab.* PAUL McKENNA, DAVID CARROLL, *Univ. of Strathclyde* NIZAR NAJMUDIN, JOERG SCHREIBER, CHARLOTTE PALMER, NICHOLAS DOVER, *Imperial college* VITALY YAKIMENKO, *BNL* The ion acceleration experiment at BNL explores the laser wavelength scaling from optical to mid-IR region. 10^{16} W/cm^2 of a CO_2 laser intensity focused on a 8 μm Al foil produced a 1-MeV proton beam. This observation agrees with predicted scaling of the proton energy $E_p \sim I^{1/2}\lambda$. We now initiated new ion acceleration runs where a gas jet is a target. At the CO_2 laser wavelength ($\lambda = 10$ μm), a critical plasma density is 100 times lower (10^{19} cm^{-3}) than for a glass laser. This opens new opportunities for time-resolved interferometric optical diagnostic of over-critical laser/plasma interactions. We present the latest results from both foil and gas jet ion acceleration experiments and give an outlook on possibilities of attaining multi-terawatt femtosecond pulses with CO_2 lasers.

*Supported by US DOE Grant.

XP8 47 Direct measurements of the magnetic field inside the magnetospheric plasma RT-1 YOSHIHISA YANO, ZENSHO YOSHIDA, JUNJI MORIKAWA, HARUHIKO SAITOH, TATSUNORI MIZUSHIMA, *Graduate School of Frontier Sciences, University of Tokyo* The magnetospheric plasma experiment RT-1 (Ring trap -1) has achieved stable confinement of high-beta plasma produced by electron cyclotron resonance heating (ECH). The observed diamagnetic signals ($\sim$ 3mWb) correspond to the maximum local beta values exceeding 40%, according to the MHD equilibrium analysis. (Soft X-ray measurements confirmed the existence of high energy electrons of Te $\sim$ 10 keV, which is consistent to the estimated plasma pressure.) As a diagnostic of internal profile of the plasma pressure, we developed a multi-channel magnetic probe system and carried out direct measurement of the diamagnetic signals inside the plasma. We found that the pressure profile peaks steeply near the ECH resonance surface and has dependence on the fueling gas pressure.

XP8 48 The relativistic virial theorem in plasma EOS calculations* JOSEPH OREG, *Artep Inc. Ellicott City MD 21042* AVRAHAM BARSHALOM, *NRCN, P.O. Box 9001 Beer-Sheva, Israel* A method for enhancing EOS calculations is presented. Our model combines the two pressure representations: the basic definition - as the volume derivative of the free energy F, and the

"virial pressure" $P_v = [E - c^2B] / 3V$ derived from the relativistic virial theorem, where B is the lower component contribution to the electronic density. The model takes into account the deviation δ between the two representations and presents an exact differential equation for F that provides analytic expressions for both F and P, in terms of $M = \delta + c^2B - TS$. Using the LDA approximation for M in these exact expressions, together with a boundary condition at the normal density, improves the EOS LDA results significantly. We present a survey of comparisons with experiments showing excellent agreements with the calculations.

*We acknowledge the encouragement of S. Obenschain, Head of the Laser Plasma Branch of the Naval Research Laboratory, and his support funded by the USDOE.

XP8 49 Spectrally Resolved X-ray Scattering from Implosion Targets ANDREA KRITCHER, *Lawrence Livermore National Laboratory, UC Berkeley* TILO DOEPPNER, *Lawrence Livermore National Laboratory* HAE JA LEE, *UC Berkeley* PAUL DAVIS, *Lawrence Livermore National Laboratory, UC Berkeley* OTTO LANDEN, SIEGFRIED GLENZER, *Lawrence Livermore National Laboratory* LLNL TEAM, UCB TEAM, Spectrally resolved x-ray Thomson scattering has been applied at the Omega Laser Facility to investigate the capsule adiabat of cone-in-shell targets. The technique of scattering from implosion targets was developed and tested for use as a diagnostic at the National Ignition Facility (NIF), LLNL. Measurement of the adiabat is applied to test low-adiabat pulse shaping methods, designed for optimum compressibility and stability. Theoretical equation of state models (EOS) can also be studied for conditions encountered during implosion. In these experiments, the noncollective, or microscopic behavior of the plasma, was probed with a Zn He-alpha x-ray source at a scattering angle of 113°. For these degenerate plasmas, the width of the inelastic scattering peak is proportional to the Fermi energy, and thus the electron density. The electron temperature is obtained from the measured intensities of the elastic and inelastic features. In-flight scattering measurements yielded electron densities of $\sim$ $1.2\text{x}10^{24}\text{cm}^{-3}$, temperatures of $\sim$ 10 eV, and an ionization state of C(+4)H(+1). This work was performed under the auspices of the DOE by LLNL under Contract No. DE-AC52-07NA27344, LDRD 08-ERI-003, and the Nat. Lab. User Fac. Prog.

XP8 50 The effect of the Hall term on Jeans instability in quantum magnetoplasma with resistive effects* ZHENGWEI WU, *City University of Hong Kong* HAIJUN REN, *University of Science and Technology of China* PAUL CHU, *City University of Hong Kong* The Jeans instability in dense quantum plasmas is investigated by taking into account the Hall term and resistive effect in the presence of two dimensional (2-D) magnetic fields. The general dispersion relation is presented. The presence of Hall term is shown to induce a frequency shift and have no effect on the instability criterion. The resistance is shown to introduce both damping and destabilizing effect on the system in different cases. The analytical expressions of the growth/damping rate of Jeans instability are obtained for both the finite and remarkable resistive effects cases in the absence of Hall term.

*This work was supported by Hong Kong Research Grants Council (RGC) General Research Funds (GRF) CityU 112306 and 112307.

XP8 51 Magnetothermal instability of plasmas in a horizontal magnetic field* HAIJUN REN, *University of Science and Technology of China* ZHENGWEI WU, *City University of Hong Kong* JINTAO CAO, *University of Science and Technology of China* PAUL CHU, *City University of Hong Kong* The linear buoyancy instability in a magnetized plasma, generally referred to as magnetothermal instability (MTI), is investigated by considering anisotropic heat conduction. The external magnetic field is assumed to be horizontal and background heat flux is not taken into account. The general dispersion relationship of the convective instability is derived. The growth rate of the MTI in fixed boundary condition is presented and discussed. The effect of density special gradient on the MTI is investigated. The magnetic field is shown to suppress the MTI and even quench the instability when the magnetic field is strong enough. Under the standard Wentzel-Kramaers-Brillouin (WKB) approximation, our results could be simplified to a brief form reported by one previous paper (E.Quataert, Astrophys. J. **673**, 758 (2008)).

*This work was supported by Hong Kong Research Grants Council (RGC) General Research Funds (GRF) CityU 112306 and 112307.

XP8 52 Reply to "Notes on Pioneer Anomaly Explanation by Satellite-Shift Formula of Quaternion Relativity" VIC CHRISITANTO, *Sciprint.org* FLORENTIN SMARANDACHE, *University of New Mexico, Gallup Campus* In the present article we would like to make a few comments on a recent paper by A. Yefremov in Progress in Physics international journal. It is interesting to note here that he concludes his analysis by pointing out that using full machinery of Quaternion Relativity it is possible to explain Pioneer XI anomaly with excellent agreement compared with observed data, and explain around 45% of Pioneer X anomalous acceleration. We argue that perhaps it will be necessary to consider extension of Lorentz transformation to Finsler-Berwald metric, as discussed by a number of authors in the past few years. In this regard, it would be interesting to see if the use of extended Lorentz transformation could also elucidate the long-lasting problem known as Ehrenfest paradox. Further observation is of course recommended in order to refute or verify this proposition.

XP8 53 Towards Recombination Pumped H-Like N X-Ray Laser ITAY GISSIS, ASAF LIFSHITZ, NIR KAMPEL, AVI RIKANATI, ILAN BEERY, URI AVNI, AMIT BEN-KISH, AMNON FISHER, AMIRAM RON, *Physics Department, Technion, Israel* The recombination pumping scheme for soft X-Ray lasers has better energy scaling, in comparison to the collisional pumping scheme. Implementation of an H-like $3 \rightarrow 2$ Nitrogen recombination laser, at $\lambda \sim 13.4$ nm requires initial conditions of 50% fully stripped Nitrogen, Te$\sim$ 140eV and $N_e \sim 10^{20}\text{cm}^{-3}$. The cooling period to below 60eV should be faster than the typical three-body recombination time. Here we study the possibility to achieve the required plasma conditions using a capillary discharge Z-Pinch apparatus. The experimental setup includes a 90mm long ceramic capillary with an inner diameter of 5mm, coupled to a pulsed power generator supplying a peak current of $\sim$ 60 kA, with a quarter-period of 60 ns. We used various diagnostics techniques to measure the plasma dynamics including X-Ray diodes, time-integrated spectrometry and time-resolved pin-hole imaging (using a framing MCP camera). Analysis of the results shows a rapid cooling period to a temperature below 60eV, demonstrating the feasibility of recombination-pumped capillary discharge lasers.

XP8 54 Nonlinear Landau damping, and nonlinear envelope equation, for a driven plasma wave DIDIER BENISTI, OLIVIER MORICE, LAURENT GREMILLET, *CEA/DAM/DIF* DAVID STROZZI, *Lawrence Livermore National Laboratory* A nonlinear envelope equation for a laser-driven electron plasma wave (EPW) is derived in a 3-D geometry, starting from first principles. This equation accounts the nonlinear variations of the EPW Landau damping rate, frequency, and group velocity, as well as for the nonlinear variations of the coupling of the EPW to the electromagnetic waves. All these quantities are moreover shown to be nonlocal because of nonlocal variations of the electron distribution function. Each piece of our model is carefully tested against Vlasov simulations of stimulated Raman scattering (SRS), and very good agreement is found between the numerical and theoretical results. Our envelope equations for both, the electrostatic and electromagnetic waves, are solved numerically, and comparisons with Vlasov simulations regarding the growth of SRS are provided. Finally, from our theory we can straightforwardly deduce a nonlinear gain factor which provides an alternate, simpler and faster method to quantify the SRS reflectivity. First results using this method will be shown.

XP8 55 Lateral Propagation of MeV Electrons Generated by Femtosecond Laser Irradiation JOHN SEELY, *Naval Research Laboratory* CSILLA SZABO, PATRICK AUDEBERT, ERIK BRAMBRINK, EMERIC TABAKHOFF, LAWRENCE HUDSON, Using high-resolution hard x-ray spectroscopy, the propagation of MeV electrons generated by intense ($\approx 10^{19}$ W/cm^2) femtosecond laser irradiation, in the lateral direction perpendicular to the incident laser beam, was studied using targets consisting of irradiated metal wires and neighboring spectator wires embedded in electrically conductive (aluminum) or resistive (teflon) substrates. It was found that electron propagation through teflon was inhibited, compared to aluminum, implying a relatively weak return current and incomplete space-charge neutralization. The energetic electron propagation in the direction parallel to the electric field of the laser beam was larger than perpendicular to the electric field. Such lateral electron propagation to distance up to 1 mm from the focal spot can be detrimental to fast-ignition fusion and hard x-ray backlighter radiography.

XP8 56 Charge dependence of impurity peaking factor SARA MORADI, *Department of Statistical and Plasma Physics, Universite libre de Bruxelles, Brussels, Belgium* M.Z. TOKAR, *Institut für Energieforschung - Plasmaphysik, Forschungszentrum Jülich, Association EURATOM-FZJ, Trilateral Euregio Cluster, Germany* BORIS WEYSSOW, *EFDA-CSU Garching, München Germany* The experimentally found dependence of impurity transport characteristics, such as diffusivity and pinch velocity, on the impurity ion charge Z, remains unexplained both by neoclassical and anomalous theoretical predictions. In this contribution the model for the impurity anomalous transport due to the ITG/TE unstable modes has been developed further by taking into account the effects of impurity ion collisions with the main plasma components becoming more and more important with increasing impurity charge. In linearized transport equations these effects are included as friction and thermal forces and collision energy exchange affecting perturbations of impurity ion parallel velocity and temperature, correspondingly. For the plasma conditions examined here, where the magnetic shear is low, the collisional effects are dominant in the pinch velocity and result in a very strong Z dependence of the impurity peaking factor. The sign and magnitude of the pinch-velocity and p depends essentially on the instability mechanism, i.e., ITG or TE drive. The results of calculations are compared with the experimental observations.

XP8 57 Observation of Neutral Depletion in High Power Helium-Helicon Plasmas SAEID HOUSHMANDYAR, SAIKAT CHAKRABORTY THAKUR, STEPHANIE SEARS, JERRY CARR, EARL SCIME, *West Virginia University* Helicon plasmas are known for their high plasma density. However, the effects of neutral atoms on wave dispersion cannot be neglected, even in the high density core, *e.g.* Alfvén wave propagation in helicon plasmas. Laser Induced Fluorescence (LIF), a noninvasive diagnostic tool, was used to measure the neutral density profile of helium atoms in high-density, helium helicon plasmas. At 578.725 nm (vacuum), the LIF signal of neutral helium atoms resulting from injection of the laser along the magnetic field, exhibits a dip, at the Doppler shifted central wavelength, that results from the finite optical depth of the plasma at that wavelength [51st APS-DPP, GP8.00133]. In a series of experiments performed in WVU HELIX (Hot hELIcon eXperiment), the neutral density profile and optical depth are measured for different ambient magnetic fields, radial positions and driving frequencies of the helicon source. As a result, the optimum plasma performance (*i.e.*, largest neutral depletion cases) for helium-helicon plasmas was determined.

XP8 58 Characterization of Low frequency zonal flow in linear magnetized plasma* JINLIN XIE, RAN CHEN, TAO LAN, ADI LIU, WANDONG LIU, CHANGXUAN YU, *CAS Key Laboratory of Basic Plasma Physics, Department of Modern Physics, University of Science and Technology of China, Hefei, China 230026* A low frequency, poloidally symmetrical potential structure that peaks near zero frequency is observed in a steady linear magnetized plasma device. The complete 3D spectral features of this structure have been identified to have the characteristics expected for the low frequency zonal flow (LFZF). The analysis of the nonlinear interaction between the LFZF and ambient drift turbulence suggests that the LFZF may be generated in energy-conserving nonlinear interactions with the turbulence. The LFZF frequency bandwidth is found to scale inversely with the square root of the ion mass, which implies that the collisional damping mechanism dominates the saturation of the LFZF in our case.

*Supported by National Natural Science Foundation of China (Nos. 10605025).

XP8 59 Observations of geodesic acoustic modes and low-frequency zonal flow in the edge of HL-2A and HT-7 tokamaks* T. LAN, C.X. YU, H.L. ZHAO, D.F. KONG, A.D. LIU, *USTC, China* L.W. YAN, WENYU HONG, K.J. ZHAO, J.Q. DONG, J. QIAN, J. CHENG, D.L. YU, Q.W. YANG, X.R. DUAN, *SWIP, China* B.N. WAN, X. GAO, J.G. LI, *IPP, China* Zonal Flows, including Low-Frequency Zonal Flow (LFZF) and geodesic acoustic mode (GAM), had both been characterized in the HL-2A tokamak and the HT-7 tokamak. The radial spectral features of GAM fluctuations were measured using two radial rake probe arrays separated toroidally. The GAMs with a fixed mode frequency were located within a radial distance inside the LCFS; the amplitude, radial wavenumber, phase velocity and group velocity profiles had all been measured. The radial wavenumber of GAM had been observed to decrease with increasing radial posi-

tion. The group velocity of GAM had also been observed to spread outward with a tuning position from which the GAM propagated inward. The spectral characteristics of density and electron temperature fluctuations of GAM had been studied in detail as well.

*Supported by NBRPC under Grant 2008CB717800 and NSFC under Grants 10875124 and 10335060 and EMC under Grant 20060358059 and CPSF under Grant 20080440104.

XP8 60 First real-time detection of surface dust in a tokamak* C.H. SKINNER, L. ROQUEMORE, H.W. KUGEL, R. MARSALA, T. PROVOST, *P.P.P.L.* Dust accumulating in the vacuum vessel from plasma surface interactions has important consequences for the operation and safety of next-step devices such as ITER. Local measurements of dust are part of the ITER dust strategy, but to date no real time measurements of dust on internal tokamak surfaces have been reported. We will present the first measurements of dust in the NSTX vessel using an novel electrostatic surface dust detector. A fine grid of interlocking circuit traces was biased to 50 v. Impinging dust particles create a temporary short circuit and the resulting current pulse is recorded by counting electronics. Techniques used to increase the sensitivity to match NSTX dust levels while suppressing electrical pickup will be presented. Results from a separate experiment to gauge the mobilization of dust from ITER-scale castellations will also be reported.

*Support is provided by the U.S. DOE Contract Nos. DE AC02-09CH11466.

XP8 61 Self-Similar Decay of Enstrophy in an Electron Plasma DOUGLAS RODGERS, SERGIO SERVIDIO, WILLIAM MATTHAEUS, TRAVIS MITCHELL, *Department of Physics and Astronomy, University of Delaware, Newark, DE 19716* The similarity solution for energy decay in 3D hydrodynamic turbulence, due to Taylor and von Karman [1], based on the self preservation hypothesis for the shape of the two point correlation, implies that the energy E decays as $dE/dt = - a Z^3/L$, where a is a constant, Z is the turbulence amplitude and L is a similarity length scale. Extensions of this idea to MHD [2] have been of great utility in solar wind and coronal heating studies. While the hydrodynamic case is well studied experimentally, we are not aware that similarity decay has been examined in a laboratory plasma. Here we conduct an experimental study of this idea in the context of two dimensional electron plasma turbulence. Specifically, we propose an expression for the decay of enstrophy of a single-signed-vorticity fluid which is analogous to the von Karman decay of energy in 3D turbulence, and compare this to the dynamical relaxation of a pure electron plasma in a Malmberg-Penning (MP) trap [3]. Results show good agreement between the proposed decay law and the MP experiments. [1] G. I. Taylor, Proc. Roy. Soc. Lon. A, 151:421, 1935; T. de Karman and L. Howarth, Proc. Roy. Soc. Lon. A, 164:192, 1938. [2] W. H. Matthaeus, G. P. Zank and S. Oughton. J. Plas. Phys., 56:659, 1996. [3] D. J. Rodgers et al, Phys. Rev. Lett., 102(24):244501, 2009.

XP8 62 Characterization of Meta-Stable Equilibria of a Electron Plasma: Relaxation Towards Minimum Enstrophy and Maximum Entropy States DOUGLAS RODGERS, SERGIO SERVIDIO, WILLIAM MATTHAEUS, *Department of Physics and Astronomy, University of Delaware, Newark, DE 19716* DAVID MONTGOMERY, *Department of Physics and Astronomy, Dartmouth College, Hanover, NH 03755* TRAVIS MITCHELL, *Department of Physics and Astronomy, University of Delaware, Newark, DE 19716* Dynamical relaxation of a pure electron plasma in a Malmberg-Penning trap is studied, comparing experiments and statistical theories of weakly dissipative two-dimensional turbulence [1]. Statistical analysis of many experimental runs favors a theoretical picture of relaxation to a near-maximum entropy state with constrained energy, circulation and angular momentum, rather than to a minimum enstrophy state [2]. However it is possible to vary experimental parameters continuously so that the results move from near-equal accord with the two theories to more strongly favoring maximum entropy. One way to accomplish this is to vary the initial distribution so that more complex electron patches are produced; this generally appears to increase the level of turbulent activity, favoring maximum entropy over minimum enstrophy. Research supported in part by USDOE Grant No. DE-FG02-06ER54853. [1] D. J. Rodgers et al, Phys. Rev. Lett., 102(24):244501, 2009. [2] X. -P. Huang, C. F. Driscoll, Phys. Rev. Lett., 72(14):2187, 1995

XP8 63 Recyclable Solid Blanket for a Fusion Reactor* M.V. UMANSKY, *LLNL* Neutron damage and tritium inventory will limit the lifetime of inner wall components of a fusion reactor, leading to increased operation cost and possibly making it economically unattractive. Thick liquid walls may be a solution to this; however, at present the feasibility of forming and maintaining thick liquid walls remains to be demonstrated for a tokamak configuration. Here it is proposed to construct inner wall components of a reactor using a meltable material. During the normal operation the blanket is maintained in the solid state. After some period of operation, when a critical level of neutron damage and tritium inventory in the blanket is accumulated, the structure is melted and drained out of the reactor chamber. After that, by bringing in fresh liquid blanket material and freezing it to the solid state on the walls, the blanket is rebuilt. Thus the blanket is periodically replaced without opening up the reactor chamber, relatively easily compared to a solid blanket. Preliminary calculations demonstrate that such system can satisfy the basic requirements of thermal transport and tritium breeding in a reactor.

*Work performed for U.S. DOE by LLNL under contract DE-AC52-07NA27344.

XP8 64 Magnetic Reconnection in Electron Magnetohydrodynamics HUISHAN CAI, DING LI, *USTC, China* The dissipation mechanisms of magnetic reconnection, pressure anisotropy effects and guide field gradient effects on magnetic reconnection and tearing mode instability are investigated, respectively. It is found that the conditions either pressure-based dissipation or electron inertia-based dissipation dominant depend on the relative magnitude between electron thermal Larmor radius and electron inertial skin depth.The dissipation mechanisms have a great relation with the magnitude of guide field. The effects of pressure gradient depend on the relative magnitude between the parallel and perpendicular pressure gradients. The guide field gradient can affect significantly on tearing mode. In the small guide field gradient limit, namely the guide field gradient is smaller than the magnetic field shear at the

magnetic null plane, the growth rate of tearing mode instability is enhanced by the guide field gradient. In the large guide field gradient limit, the guide field gradient can destabilize tearing mode instability dramatically and the growth rate is proportional to the guide field gradient.

XP8 65 Study of the heating and expansion of spherical nanoplasmas GIANNI COPPA, ROBERTA MULAS, *Politecnico di Torino, Italy* ELISABETTA BOELLA, GIAN LUCA DELZANNO, *Los Alamos National Laboratory* The present work deals with the analysis of the interaction between a laser pulse and a gas cluster. The phenomenon is characterized by three different phases: 1) electron ionization and heating by the laser radiation; 2) escape of the most energetic electrons; 3) ion acceleration due to the positive charge inside the sphere. Although these three phases have different timescales, for a rigorous analysis they cannot be studied as completely separated. In the poster, results obtained by means of a numerical code developed by the Authors are presented. In the code a three-dimensional particle technique for electrons and positive ions is employed, in which the electric field is calculated considering a perfect spherical symmetry by resorting to the Gauss law. The method has two advantages: 1) it preserves the symmetry of the problem; 2) a grid is not necessary and, consequently, the calculation of the electric field requires little computational effort. In the code, a simplified model for the electron heating is introduced by considering collisions between electrons and fictitious energetic particles.

XP8 66 Diffusion and energization of charged particles in time-dependent chaotic magnetic field* GANG LI, BRAHMANANDA DASGUPTA, ABHAY RAM, Chaotic magnetic field can be obtained from simple steady state current system consisting of straight wires and loops in an asymmetric configuration. Since in solar flares macroscopic and time varying currents in the form of filaments and/or loops commonly exist, the resulting magnetic field must be chaotic. Consequently, to understand solar flare phenomena, studying particle motion in a time-dependent chaotic magnetic field is of fundamental importance. These currents, time-varying, can induce electric fields. Therefore, electrons and ions are subject to potential (2nd order Fermi) acceleration. We report recent results on charged particle motion in a chaotic electric and magnetic fields. Particle trajectories are followed using the Lorentz equation with a 4-th order Runge-Kutta skeme. The running diffusion coefficient, particle spectrum, and the chaotic magnetic field spectrum are obtained. Implications of our result to particle acceleration and heating at a flare site are discussed.

*This work is supported by a NASA grants NNG05GM62G and NAG5-10932 at UAH.

XP8 67 An Empirical Model for the Interaction of Ultra-Intense Laser Pulses with Fully Ionized Plasmas Including Electrostatic Effects J.-H. YANG, R.S. CRAXTON, *Laboratory for Laser Energetics, U. of Rochester* This work investigates the capability of ultrafast lasers with irradiance $I \geqslant 10^{18}$ W cm^{-2} to produce highly energetic electron beams in a Gaussian focus in a low-density plasma. A simple particle simulation code including a physical model of collective electrostatic effects in relativistic plasmas has been developed. Without electrostatic fields, free electrons escape from the Gaussian focal region of a 10-ps petawatt laser pulse very quickly, well before the laser field reaches its maximum amplitude. In this case very small net energy transfer occurs, indicating that free electrons cannot extract enough energy for ignition. However, it has been demonstrated that the electrostatic field generated by the electron flow is able to strongly modify the range and direction of the laser-generated MeV electrons by allowing trapped electrons to experience much higher laser-intensity peaks along their trajectories and, therefore, be accelerated to higher velocities, drifting along the laser direction. This modeling predicts some collimation, but not enough to meet the requirements of fast ignition. This work was supported by the U. S. Department of Energy Office of Inertial Confinement Fusion under Cooperative Agreement No. DE-FC52-08NA28302.

XP8 68 Improving the Dynamic Range of CR39 Detectors for ICF Experiments Through Multiple Track Overlap Detection Algorithms* A. ZYLSTRA, N. SINENIAN, M. MANUEL, H.G. RINDERKNECHT, M.J. ROSENBERG, D.T. CASEY, J.A. FRENJE, C.K. LI, F.H. SEGUIN, R.D. PETRASSO, *MIT* CR39 based nuclear detectors are in widespread use for Inertial Confinement Fusion (ICF) experiments [1,2]. Current analysis methods only count scanned shapes of single tracks, limiting the standard dynamic range of the detector to approximately 100. We present simulations and experimental studies at the MIT accelerator of methods for accurately determining the total particle count when overlapping tracks are a non-negligible fraction of the total. Advancements in analysis algorithms to accurately count at higher track densities through these methods could significantly increase the dynamic range of CR39 based detectors at OMEGA and the NIF. [1] F. H. Seguin et al., Rev. Sci. Instrum 74 (2003) 975. [2] C.K. Li et al, Phys. Rev. Lett. 100, 225001 (2008).

*This work was supported in part by the U.S. DoE, LLE, and LLNL. A. Zylstra is supported by the DoE NNSA Stockpile Stewardship Graduate Fellowship.

XP8 69 Modeling of the Lightning Plasma Channel Stroke to a Spacecraft during Ascent ALFONSO TARDITI, JOHN NORGARD, *ESCG - NASA Johnson Space Center* Lightning protection is an important aspect of modern aerospace design: the increased use of composite materials (*vs.* metals) reduces the shielding and robustness of the conducting path that the outer shell of a vehicle can present to a lightning discharge. A spacecraft during ascent becomes vulnerable to lightning strokes immediately after leaving the launch pad: in addition to natural lightning conditions, there is the possibility of triggered lightning events, caused by a perturbation of the atmospheric electric field [1]. The purpose of this study, in support of the NASA Constellation program, is to determine the evolution of the plasma current and its distribution on the spacecraft surface. Following earlier "gas dynamic" approaches [2], the model considers a plasma channel attached to the ascending spacecraft after a return stroke is established. The conductive exhaust plume [3] is an integral part of the model. The *NIMROD* 3D plasma fluid code [4] is used to model the plasma channel, reproducing the full transient due to the self-consistent magnetic field and the possibility of sweeping of the attachment point along the moving structure [5]. **References**: [1] M.A. Uman, Proc. IEEE, 76, 1548 (1988). [2] V. A. Rakov, M. A. Uman, IEEE Trans. EMC, EMC-2940, 403 (1998). [3] J. D. Norgard, G.S. Smith, IEEE Trans. EMC, EMC-29, 157 (1987) [4] C. R. Sovinec *et al.*, J. Comput. Phys. 195, 355 (2004). [5] Larsson *et al.*, J. Phys. D, 33, 1876 (2000)

XP8 70 FRC Formation and Stability in an Accelerated Plasma Flow ALFONSO G. TARDITI, *University of Houston - Clear Lake* Electric propulsion concepts based on FRC's and acceleration of compact tori (CT) have been considered in the past [*e.g.* 1-5], particularly due to FRC's attractive properties in term of stability and low beta. Unlike previous CT concepts, the present study focuses on the formation of FRC plasmoids in an accelerated plasma column [6]. The 3D fluid code *NIMROD* [7] is used to explore the formation of an FRC from a plasma accelerated through a magnetic nozzle, effectively producing a detachment of the plasma from the guiding magnetic field. The stability of the detached FRC and the energy balance are investigated. **References:** [1] K Miller, APS-DPP Conf. New Orleans (LA) 1998, Bull. APS (1998). [2] M.J. Schaffer, Proc. NASA Advanced Propulsion Workshop in Fusion Propulsion, Huntsville, AL, Nov. 2000. [3] Slough, J., AIAA paper 2001-3674 (2001). [4] S. J. Koelfgen, AIAA paper 2003-4992 (2003). [5] T. Weber, this conference. [6] A. G. Tarditi, Int. Sherwood Fus. Theory Conf., Stateline NV, April 2005. [7] C. R. Sovinec et al., J. Comput. Phys. 195, 355 (2004).

A
Abarr, Miles NP8 60
Abdallah Jr., J. TO6 10
Abdrashitov, G.F. TP8 59
Abdullaev, Sadrilla NO4 5, UP8 76
Abe, K. PP8 98, PP8 99, PP8 100
Abiteboul, J. BP8 26
Abla, G. BO4 5, JP8 86, JP8 87
Abreu, P. JP8 137, NP8 108
Adams, Steven PP8 120
Adamson, P. TP8 143, TP8 144
Adham, N. GP8 89
Afeyan, B. JO5 8, NP8 106
Afeyan, Bedros NP8 32, **TO5 7**
Aglitskiy, Y. CP8 99, **TO7 3**, XP8 25
Agostini, Matteo UP8 68
Agren, Olov **CM9 5**
Ahn, J.W. PP8 45, PP8 46, PP8 71
Ahn, Joon-Wook **JO4 6**
Aiba, N. GP8 92, **UP8 85**, UP8 86
Airoldi, A. **GP8 17**, NO4 16
Akcay, C. UP8 19, UP8 22, **UP8 23**
Akers, Rob JO4 15
Akli, K.U. CP8 53, CP8 103, CP8 104, CP8 105, CP8 106, NO5 1, NO5 2, NO5 8, PO5 2
Albert, Felicie **BO6 5**, BO6 6, BO6 7, NP8 28
Alberto, Bottino BO4 1
Albright, B.J. BP8 45, CP8 88, CP8 89, **CP8 107**, NM9 7, NM9 8, TP8 115, TP8 122
Alessi, David **NP8 33**
Alexander, A.B. JO6 8, JO6 9, JO6 13
Alexeff, Igor **CO7 6**
Alfier, Alberto **TP8 55**
Ali, Halima JP8 8, JP8 9, JP8 10, JP8 11, JP8 70
Ali, S. **GP8 104**, PO6 11
Allain, J.P. JO4 8, PP8 40, PP8 44, PP8 46
Allen, B. JP8 135, **JP8 136**, **NP8 14**, TO4 15
Allen, S.L. **CO4 2**, JP8 101, JP8 112
Almagri, A.F. JM9 7, TP8 42, TP8 45, TP8 56, TP8 62, TP8 64, TP8 68, TP8 69, TP8 70
Almagri, A.R. GP8 129
Almeida, R. NP8 50
Alper, B. NP8 127
Altemara, S.D. NP8 75
Aluie, Hussein **UO6 2**
Amatucci, B. **GP8 124**
Amatucci, William BP8 12, GP8 122, GP8 123, GP8 125
Ambrosiano, J. CP8 65
Amdahl, D.J. NP8 85, TP8 143, TP8 144
Amendt, Peter BO5 11, BO5 12, BO5 14, CP8 100, CP8 113, NO5 4, TO7 4, **TO7 5**
Ampleford, D.J. CP8 45, NP8 59, NP8 61, NP8 77, TO7 11, TO7 13, **UI3 5**
An, B.I. PP8 98
An, Bung Il PP8 96
An, Byung Il PP8 97, PP8 100
An, W.M. JP8 130
An, Weiming GO6 13, **JP8 131**
Andachi, Takehisa BP8 21
Anderegg, F. **BP8 72**
Anderson, D.T. **TP8 102**, TP8 104
Anderson, F.S.B. TP8 104
Anderson, G. BO6 5, NP8 27
Anderson, J. JO6 4
Anderson, J.K. GP8 129, TP8 42, TP8 44, TP8 49, TP8 50, TP8 55, TP8 56, TP8 59, TP8 60, TP8 61, **TP8 65**, TP8 66, TP8 67
Anderson, K.S. NO5 3, NO5 6, TO5 3, TO5 4, **UO5 4**
Anderson, M.W. **BP8 71**
Anderson, S.G. BO6 7, NP8 27
Anderson, Scott BO6 5, BO6 6, NP8 28, TO7 7
Ando, K. GP8 7, **UP8 15**
Andre, R. JP8 102
Andre, Robert GP8 51
Andreason, Samuel **UP8 10**
Andrew, Y. CP8 2
Angelopoulos, V. GM9 4
Angioni, C. TP8 75
Angus, Justin **JP8 146**
Antiochos, Spiro **JM9 1**
Antonsen, Thomas BO6 4, BO6 13, CP8 77
Aoki, H. UP8 143
Appel, L.C. BO4 6
Appel, Lynton JO4 15
Appelbe, B. GO5 3
Apruzese, J.P. NP8 59, TO7 11, TO7 13
Arad, Ron JO6 6
Arai, K. **PP8 9**
Arakawa, H. **GP8 146**
Aramaki, Mitsutoshi GP8 149
Arastoo, Reza **GP8 38**
Archuleta, F. GO6 3, PO5 12
Arefiev, Alexey CP8 73, CP8 74, **PP8 125**
Aristova, Maria JP8 37
Armijo, J. NP8 93
Arnoux, G. UO4 5, UO4 8
Asai, Tomohiko UP8 14
Asakura, Nobuyuki CP8 3
Ascasibar, E. BO4 10
Astanovitskiy, A. NP8 75
Astanovitsky, A. CP8 46
Atanasiu, Calin V. **UP8 88**
Atchison, W. CP8 65, **NP8 56**
Atherton, B.W. JP8 145
Atherton, J. BO5 2, BO5 3
Audebert, P. BP8 69, GO6 5, JP8 144
Audebert, Patrick XP8 55
Auerbach, D.W. GP8 141, GP8 142, **GP8 143**, GP8 144
Auriemma, Fulvio **TP8 84**
Auster, U. GM9 4
Austin, M.E. CO4 3, **CO4 9**, GP8 10, JP8 95, JP8 109, XP8 38
Austin, Travis CP8 18, **CP8 22**
Autry, Chastity **XP8 41**
Avni, Uri XP8 53
Avril, A. **JP8 74**
Avsarkisov, V.S. GP8 152
Awe, T. TP8 144
Awe, Thomas TP8 148, **TP8 160**
Axley, A. **JP8 73**
Aydemir, A.Y. **GP8 30**
Azechi, Hiroshi NP8 91, XP8 25

B
Baalrud, S.D. **BP8 3**, **GI2 3**
Babonneau, D. TO7 9
Babzien, M. JP8 135, JP8 136
Babzien, Marcus TO4 15, XP8 46
Baciero, A. GP8 70
Back, C.A. BO5 14
Bader, A. PP8 27, PP8 28, **PP8 29**
Baek, S.G. **PP8 8**
Baek, Sung-Hyun BP8 67
Baerny, Jennifer CP8 34
Bagaipo, Jupiter **UP8 98**
Bagryansky, Peter CM9 1, UP8 46
Bahr, R.E. JO5 14
Bailey, J.E. CP8 45, **TO6 10**, TO7 11, TO7 14
Baity, F.W. CO4 7, JP8 106, JP8 107, JP8 117, NP8 40
Balandin, Alexander TP8 136, UP8 30
Balasundaram, Arun CO7 6
Balay, S. PP8 117, PP8 118
Bale, Stuart JO6 1
Balzer, Karsten UO6 13
Bandyopadhyay, M. BP8 106
Bandyophadhyay, M. NO4 7
Banerjee, Sudeep TO4 4, TO4 5
Barada, D. PO5 10
Barlis, A. JP8 66
Barnard, Harold **PP8 25**
Barnard, J. TO5 2
Barnard, J.J. **NP8 93**, NP8 94, NP8 95, NP8 96
Barnes, D. CP8 65
Barnes, Michael **DI3 1**
Barnsley, R. UO4 12
Barrios, M.A. CO5 4, **JI2 2**, TO5 3, UO5 1
Barshalom, Avraham XP8 48
Bartal, T. CP8 106, GO6 2, NO5 2, **PO5 12**, XP8 16
Bartell, B. **JP8 44**, UP8 120
Barth, Ido **BP8 88**

Barty, C.P.J. BO6 7, NP8 27
Barty, Chris BO6 5, BO6 6, GP8 90, NP8 28, NP8 29
Baruah, B. NO4 7
Bass, E.M. **XI3 2**
Bastiani-Ceccotti, Serena JP8 14
Basu, Debjyoti GP8 73
Batani, D. CP8 103, CP8 105, CP8 106
Batchelor, Donald **GP8 57**, GP8 59
Bateman, G. **CM9 12**, GP8 11, GP8 36, GP8 51, **GP8 53**, GP8 54, GP8 55, JP8 54, UP8 79
Bates, J. XP8 25
Bates, J.W. CP8 99, TO7 1
Batha, S.H. NP8 82
Batha, Steven UO5 6
Baton, S.D. CP8 106
Battaglia, D.J. GP8 50, JO4 12, PP8 86, PP8 101
Bauch, Sebastian UO6 13
Bauer, Bruno TP8 160
Baumgaertel, J.A. **TP8 100**
Baumgartner, Henning UO6 11
Baver, D.A. GO4 11, **GP8 69**
Baxter, Emily **NP8 17**
Baylor, L.R. GP8 19, **JP8 89**, JP8 90, NO4 15, PP8 94, UO4 4
Bayramian, A. BO6 7
Bayramian, Andy **NP8 29**
Bazouin, G. NP8 3
Beaumont, B. NO4 9
Beck, W. PP8 32
Becker, Richard CO5 10
Beer, Glenn NP8 29
Beery, Ilan XP8 53
Beg, F.N. CP8 53, CP8 66, CP8 80, CP8 103, CP8 104, CP8 105, CP8 106, CP8 108, GO6 2, JP8 52, NO5 1, NO5 2, NO5 8, NO5 9, NO5 12, NP8 60, PO5 9, PO5 12, **UI2 5**, XP8 16
Beidler, C.D. GP8 56
Beiersdorfer, P. BP8 69, CP8 12, CP8 52, JP8 5, JP8 144, NP8 47, NP8 84, PP8 39, TO7 7, UO4 12
Bekhor, Steven **TO6 15**, **XP8 4**
Beklemishev, Alexei **CM9 1**, **UP8 46**
Belknap, Donald **JP8 28**
Bell, Anthony NP8 109
Bell, M. **JO4 2**, JO4 13, PP8 38, PP8 44, PP8 74
Bell, R.E. JO4 2, JO4 3, JO4 9, JO4 10, JO4 11, JP8 67, **NI3 3**, PP8 37, PP8 41, PP8 47, PP8 48, PP8 49, PP8 52, PP8 53, PP8 56, PP8 57, PP8 58, PP8 59, PP8 67, PP8 75, PP8 77, UO4 6
Bellan, Paul **UP8 27**, UP8 28, UP8 29, UP8 128, UP8 129, UP8 130, UP8 131, UP8 132, XP8 3
Belle, Kunegunda NP8 89
Bellei, C. TO4 8
Belli, E.A. TP8 100
Beloff, Natasha XP8 40
Belov, V.P. TP8 59
Belova, E.V. **UP8 17**, UP8 18
Ben-Kish, Amit XP8 53
Benage, John **CP8 38**, NP8 89, NP8 90, UO5 12, UO6 15
Benedict, L. JP8 144, UO5 15, **UO6 15**, XP8 13
Bengtson, Roger D. CP8 75
Benisti, Didier **XP8 54**
Benjamin, Mark **JP8 58**
Benkadda, S. NO4 14, PP8 13
Benkadda, Sadruddin BP8 42
Bennett, G.R. **JP8 145**
Beno, J. GP8 10
Benwell, Andrew NP8 17
Bergen, B. CP8 89
Berger, R. BO5 2, BO5 3, **JO5 2**, XP8 33
Berger, Thomas NM9 5
Bergerson, W.F. TP8 42, TP8 43, **TP8 44**, TP8 45, TP8 62
Bergmann, R.M. UP8 50, UP8 51, UP8 52, UP8 53
Berk, Herbert **CM9 3**, GP8 88, GP8 127, JP8 109, **XI3 1**
Berkery, J. **GI3 5**, JO4 10, PP8 53
Bernhardt, P.A. GP8 89
Bernier, Joel CO5 10
Berninger, Michael NP8 86
Bernshtam, V. CP8 45, NP8 78, TO7 11
Berrill, Mark NP8 33, **UO6 6**
Berry, L.A. CP8 16, CP8 17, CP8 23, GP8 59, JO4 11, **JP8 2**, PP8 77
Berta, S. GP8 18
Bertram, J. BO4 6
Bertsche, William **BP8 79**
Berzak, L. PP8 88, **PP8 89**, PP8 95, UP8 56
Bespamyatnov, I.O. GO4 3, NO4 14, PP8 13, **PP8 14**, PP8 28
Bessho, Naoki **TP8 119**
Betti, R. BO5 13, BO5 14, CP8 56, CP8 106, NO5 3, NO5 6, NO5 7, **PT3 1**, PO5 1, PO5 2, TO5 4, TO7 2, UO5 4, UO5 11, UO7 1, UP8 87
Betts, S.M. BO6 7
Betts, Shawn BO6 5
Beurskens, M.N.A. CO4 13, UO4 8
Bhattacharjee, A. CO6 12, GP8 128, GM9 2, **JM9 3**, TP8 72, TP8 116, TP8 117, TP8 118, TP8 119
Bialek, J.M. JO4 10, PP8 79, XP8 45
Bianchi, A. **GP8 20**, GP8 21
Biener, Juergen UO5 15
Bieniosek, F.M. CP8 57, NP8 2, NP8 93, **NP8 95**, XP8 14
Bienioske, F.M. NP8 96
Biewer, T.M. **CP8 2**
Bigelow, T.S. **GP8 14**, GP8 15, PP8 84, XP8 34
Billing, Jaspreet TP8 160
Biloiu, I.A. GP8 134
Bingham, Derek UP8 149
Bingham, R. **GP8 81**, UP8 110, UP8 139, XP8 31
Bird, T.M. GP8 50, **PP8 101**
Birn, Joachim **GM9 3**
Bishofberger, Kip NP8 30
Bitter, M. **NP8 47**, PP8 39, UO4 12
Black, C. **GP8 128**
Blackman, Eric UP8 136
Blackwell, B.D. BO4 6, **BO4 10**, **XP8 5**
Blackwell, D. **GP8 123**, GP8 124, GP8 125
Blancard, C. TO6 10
Blanchard, P. CP8 10
Bland, S.N. GO5 1, GO5 5, NP8 74, NP8 81, TO6 3
Blasing, D. JP8 30, **JP8 31**, UP8 125
Blaskiewicz, Michael NP8 14
Blesener, I.C. GO5 9, **NP8 72**, NP8 76
Blesener, Kate **NP8 76**
Blobner, Florian GO5 14
Block, Dietma NO6 5
Blokland, J.W.S. **UP8 105**
Blue, B.E. **CO5 8**, UP8 152
Blue, Brent GO5 2
Blumenfeld, I. JP8 130
Boboc, A. NP8 127
Bochkarev, S.G. **CP8 67**
Bodi, K. **NP8 115**
Boedo, J.A. JP8 96, NO4 10, TP8 27, TP8 28, TP8 29, TP8 30
Boeglin, Werner JP8 69
Boehly, T.R. CO5 2, CO5 4, CO5 5, PO5 1, TO5 3, **UO5 1**, UO5 2, UP8 146
Boehmer, Heinrich GP8 76
Boella, Elisabetta XP8 65
Bogatu, I.N. **GP8 8**, NP8 98
Bogdanov, Yevgeny PP8 120
Boldyrev, Stanislav **CO6 10**, CO6 11
Bolser, Diana BP8 103, NO6 8
Bolzonella, T. JP8 84
Bombarda, F. CP8 11, GP8 19, **NO4 15**, NO4 16
Bomgardner, R. TP8 150, UP8 48

Bomgardner, Richard TP8 153, TP8 154
Bond, E. JO5 1
Bonde, J. JM9 8, XP8 21
Bonfiglio, D. TP8 78, **TP8 80**
Bongard, M.W. **JO4 7**, JO4 12, PP8 85, PP8 86, PP8 87
Bonitz, Michael JP8 23, JP8 55, NO6 4, UO6 11, UO6 12, **UO6 13**, XP8 6, XP8 17, XP8 24
Bonli, P.T. PP8 30
Bonnell, J. GM9 4
Bonnin, X. TP8 16
Bonoli, P. CP8 21, JO4 11, PP8 29
Bonoli, P.J. JP8 67
Bonoli, P.T. GO4 8, GP8 6, GP8 59, **PP8 5**, PP8 7, PP8 77
Bonoli, Paul PP8 4, PP8 6, PP8 96
Bonomo, F. TP8 54, TP8 82, **TP8 85**
Booske, John **BO6 1**
Boozer, A.H. BP8 80, TP8 79
Boozer, Allen PP8 51, PP8 61, **PP8 104**, TP8 101
Boozer, Allen H. BP8 82
Borchardt, M.T. TP8 52
Borghesi, M. GO6 4, NO5 11, NO5 13
Borgogno, D. TP8 121
Boris, David UP8 61
Bornath, T. UO6 14
Bortolon, A. GO4 13
Bosco, J. PP8 19
Bose, B. **GO4 4**
Bott, Simon JP8 52, **NP8 60**
Bourdelle, C. UP8 73
Bourgade, J.L. BO5 11, BO5 12, TO7 4
Bowers, K.J. CP8 88, CP8 89, NM9 7, TP8 115, TP8 122
Bowers, Kevin BP8 45, NM9 8
Bowman, Arnesto JP8 152
Bowman, Joel M. UP8 157
Boyer, Daniel **GP8 36**
Boyle, D. PP8 88, PP8 95, **UP8 55**
Boyle, Patrick GP8 36
Bozhenkov, Sergey NO4 5, **UO4 5**, UP8 76
Braams, Bastiaan J. UP8 157
Bradley, P.A. NP8 82
Bradley, Paul UO5 6
Brainerd, Andrew NP8 15
Brambrink, Erik XP8 55
Brandao, B. GP8 81
Brandon, S. UO5 13
Brandt, Christian PO6 2
Brantov, A.V. CP8 67
Braun, D.G. TO5 3
Bravenec, R. **GP8 67**
Bray, B.D. CO4 3, **JP8 113**, TP8 30
Brecht, Stephen UP8 140
Brecht, T. **JP8 67**, PP8 77
Breizman, Boris CP8 73, CP8 74, **GP8 85**, GP8 88
Breneman, Aaron JO6 1
Brennan, D.P. GP8 95, GP8 99, JP8 97, **UP8 100**
Brenner, P.W. BP8 80, **BP8 81**
Brenner, Paul BP8 83, BP8 84
Breslau, J. **GP8 31**, UP8 97, UP8 103, UP8 104
Brewer, Samuel M. BO4 7
Breyfogle, M. XP8 36
Brezinsek, S. UO4 5, UO4 8
Briesemeister, A. **TP8 104**
Bristow, W.A. GP8 89
Brizard, A.J. CP8 31
Brockington, S. TP8 150, TP8 153, **TP8 154**, UP8 39, UP8 48
Bromberg, L. **GP8 6**, TP8 101
Brombin, Matteo TP8 84
Brookhart, M. GP8 96, GP8 97, **GP8 98**
Brooks, A. UP8 89
Brooks, Jeffrey GP8 5
Brooks, N.H. CO4 2, JP8 71, JP8 111, **JP8 115**, TP8 25, TP8 26, TP8 27, TP8 30
Brooks, R.D. UP8 2
Brower, D.C. TP8 62
Brower, D.L. **KI3 4**, PP8 19, TP8 42, TP8 43, TP8 44, TP8 45, TP8 46, TP8 61
Brown, B. **CP8 7**, CP8 8
Brown, C. JO5 8
Brown, D.J. NP8 85
Brown, Greg **CP8 52**, JP8 5, TO7 7
Brown, M. **TP8 141**
Brown, M.R. JP8 48
Brown, P.N. NP8 100
Brown, Thomas **TP8 101**
Bruder, Dan JP8 3, **JP8 4**
Bruhwiler, David JP8 125, **JP8 126**, JP8 129, TO4 12, TO4 14
Bruner, N.L. CO5 6
Brunner, D. PP8 20, **PP8 21**, PP8 22
Buchenauer, C. Jerald NP8 24
Buckley, Andrew XP8 40
Buczek, T. TO7 6
Budny, R.V. GP8 11, GP8 64, GP8 66, JP8 99, **JP8 102**
Buffechoux, S. GO6 1, GO6 5
Bulanov, S.S. JP8 122, TO4 11
Bulanov, Sergei GO6 9
Bulanov, Stepan **GO6 8**, JP8 140
Buratti, P. BO4 12
Burby, J. **JP8 72**
Burdiak, G. GO5 1, GO5 5, NP8 74, NP8 81, TO6 3
Bures, Brian **GO5 14**
Burin, M. **GP8 139**, JP8 46, NP8 57
Burke, B. **NP8 113**
Burke, D.R. TP8 56, TP8 63, **TP8 64**
Burke, M. CP8 59
Burrell, K.H. CO4 14, CO4 15, JP8 111, JP8 114, TP8 3, TP8 5, TP8 6, TP8 12, TP8 13, TP8 14, **TP8 20**
Bursa, M. UP8 153
Bush, C.E. PP8 69
Busquet, Michel NP8 105, **UP8 150**
Bussman, M. GO6 3
Bussmann, M. GO6 1, TO4 1
Buttery, R.J. **PP8 50**
Bychenkov, V. Yu. CP8 67, GO6 6, TO4 3, XP8 26

C

Caflisch, R.E. PP8 121
Cai, Hongbo CP8 102
Cai, Huishan **XP8 64**
Caillaud, T. BO5 11, BO5 12, **TO7 4**
Cairns, Alan UP8 110
Cairns, Iver JO6 2
Caldas, Ibere UP8 66
Califano, Francesco GM9 6
Caligaris, Taylor JP8 40
Callahan, D. BO5 1, BO5 2, BO5 3, **BO5 5**, BO5 6, BO5 7, CP8 84, TO5 1
Callen, J.D. BP8 3, GP8 58, **NI3 1**, TP8 16, **TP8 17**, TP8 96
Camacho, J.F. NP8 85, TP8 143, TP8 144, **TP8 147**
Campanell, Michael JP8 63, **NP8 57**
Campbell, David **UO4 1**
Campbell, R.B. BP8 70
Campbell, Rob NP8 29
Canaud, Benoit CO5 7
Candy, J. BP8 18, BP8 29, **DI3 2**, GP8 67, PP8 10, PP8 66, PP8 117, PP8 118, TP8 11, TP8 12, UP8 81
Canik, J. GP8 4, JO4 2, JO4 5, TP8 17, TP8 26, **UO4 6**
Canton, Alessandra TP8 84
Cao, Jintao XP8 51
Cao, Q.H. PP8 98
Cao, Qinghong PP8 99, PP8 100
Cappello, S. TP8 78, TP8 80
Caravelli, G. CP8 43
Cardinali, A. **CP8 32**, GP8 21
Carlsson, J. CP8 18, **CP8 25**, GP8 58, PP8 117, PP8 118, UP8 80
Carlsten, Bruce NP8 30
Carr, Jerry GP8 132, GP8 133, **GP8 135**, XP8 57
Carraro, L. TP8 85
Carroll, David XP8 46

Carroll, Jeff TO7 8
Carscadden, John UP8 49
Carstensen, Jan NO6 6
Carter, Mark CP8 25
Carter, Stuart UP8 157
Carter, T.A. CO4 8, GP8 111, GP8 141, GP8 142, GP8 143, GP8 144, GP8 152, JP8 18, PO6 3, PP8 63, **TI2 5**, TP8 46
Cartwright, K. NP8 22
Carver, R. CO5 8
Cary, J.R. JP8 125, JP8 126, NP8 122, **PP8 117**, PP8 118, UP8 80, **XP8 43**
Casanova, Michel CP8 114
Case, Andrew TP8 150, **TP8 153**, TP8 154, UP8 39, UP8 48
Casey, D.T. CP8 55, CP8 56, **CP8 59**, CP8 62, XP8 68
Casner, A. BO5 11, BO5 12, TO7 4
Caspary, K.J. **TP8 42**, TP8 43
Casper, T.A. JP8 97, TP8 38
Cassak, Paul PM9 4, TP8 131
Cassibry, Jason TP8 149, TP8 150, **TP8 151**, TP8 152
Castor, John TO7 7
Castro, Enrique **BP8 99**, GP8 28
Catalyurek, U.V. UO6 8
Cater, Troy GP8 76
Cattell, Cynthia **JO6 1**
Catto, Peter TP8 94, UP8 78
Caughman, J.B. CO7 5, GP8 14, GP8 19, JP8 107, NP8 40, **PP8 84**
Cavallo, Robert CO5 10, CO5 11
Cavaloo, Robert CO5 9
Cavazzana, R. **TP8 77**
Cavazzana, Roberto TP8 87, UP8 68
Celeste, J. BO5 3
Celliers, P.M. CO5 4, TO5 3, UO5 1
Cenacchi, G. GP8 17, NO4 16
Cengher, M. JP8 103, JP8 104, **JP8 105**
Cerfon, Antoine **UP8 99**
Cerjan, C.J. BO5 4, TO5 1, UO5 13, UO5 14
Chacon, L. BP8 60, **GP8 65**, PP8 116, TP8 80, TP8 121
Chagelishvili, G.D. GP8 152
Chaikovsky, S.A. NP8 71
Chakrabarti, N. NP8 126
Chakraborty, A. NO4 7
Chakraborty, M. BP8 106
Chakraborty Thakur, Saikat GP8 132, **GP8 133**, GP8 135, XP8 57
Chalenski, David **GO5 7**, GO5 8, NP8 76
Challis, C.D. BO4 12, **CO4 12**, PP8 50
Chaly, O. CP8 46
Chalyy, O. NP8 75
Chamberlain, F. JP8 106
Chan, V.S. **GP8 2**, GP8 3, JP8 87, TP8 2
Chandler-Smith, Nate TO4 4, TO4 5
Chang, B. NP8 100
Chang, C.S. BO4 3, BP8 26, BP8 27, BP8 28, BP8 35, BP8 47, CM9 12, GP8 53, GP8 54, **GP8 55**, NP8 124, NP8 125, **XP8 7**
Chang, J.F. NO4 2
Chang, P. **TO5 4**, UO7 1
Chang, P.Y. UO5 4
Chang, Shen-Wu UP8 112
Chang, Xijiang BP8 13
Chaplin, Vernon **UP8 131**
Chapman, B.E. TP8 42, TP8 43, TP8 44, TP8 47, TP8 51, TP8 54, TP8 56, TP8 59
Chapman, David CP8 78
Chapman, I.T. BO4 12
Chapman, Sandra XP8 9
Chaschin, Maxim CM9 1
Chaudhari, M. BP8 97
Chavez-Alarcon, Esteban **GP8 71**
Chawla, S. CP8 53, CP8 103, CP8 105, GO6 2, NO5 2
Chawla, Sugreev **CP8 104**
Che, Haihong GP8 86, GM9 6, **TP8 132**
Chen, C.D. CP8 53, NO5 1, NO5 2, PO5 13
Chen, Chiping **BO6 9**, NP8 15, NP8 16, **XP8 8**
Chen, Eugene **GP8 88**
Chen, G. NP8 40, PP8 124
Chen, Guangye **CP8 23**
Chen, H. BP8 69, CP8 106, JP8 144, NO5 2, NO6 14, PO5 13, XP8 16
Chen, J. UP8 97
Chen, Kuan-Ren **BP8 14**
Chen, L.J. TP8 123
Chen, Li-Jen **CO6 5**
Chen, Qiang NO6 13
Chen, Ran XP8 58
Chen, S. JP8 144
Chen, S.N. PO5 13
Chen, Sophia **BP8 69**
Chen, X. **TP8 47**, TP8 48, TP8 49
Chen, Y. BP8 36
Chen, Yang BP8 18, BP8 35, GP8 72, **GP8 126**, TP8 135, UP8 72
Cheng, Baolian **UO6 9**
Cheng, C.Z. **BO4 9**, **JM9 2**, UP8 91
Cheng, J. XP8 59
Cheng, Jianhua **TP8 135**
Cheng, Xi **UP8 127**
Chilenski, M.A. **JP8 65**, UP8 19
Chittenden, J.P. GO5 1, **GO5 3**, GO5 5, NP8 81, TO6 3
Cho, M. PP8 68
Cho, Suwon **GP8 80**
Choe, G.S. JM9 2
Choi, M. CO4 7, CP8 16, JP8 72, PP8 76, **TI3 1**
Chong, Y.K. NP8 59, NP8 61
Chou, Jason UP8 149
Choudhury, F. BP8 89, JP8 19
Chowdhury, E.A. CP8 76
Chrisitanto, Vic **XP8 52**
Christlieb, Andrew PP8 112
Chu, M.S. BO4 5, CO4 6, GP8 32, GP8 33, **JP8 80**, JP8 81, JP8 83, JP8 85, JP8 86, JP8 87, TP8 22, XP8 2
Chu, Paul XP8 50, XP8 51
Chu, Sam BO6 6
Chu, T.S. **NP8 27**
Chung, H.K. **NO5 8**, NP8 84
Chung, Kyu-Sun BP8 104
Chung, Moses NP8 9
Chung, Sang-Young **GO6 10**, TO4 7
Chuvatin, A.S. GO5 13
Chvykov, V. JP8 122, JP8 140, TO4 3, TO4 8, TO4 11
Cianciosa, M. **GP8 121**, JP8 38, TP8 107
Ciardi, A. TO6 3
Citrin, Jonatan JO6 6
Clai, G. GP8 17
Clark, D. BO5 4, CP8 76, CP8 84, **CP8 100**, JO5 6, NO5 4, NO5 6, TO5 1, UO5 13, UO5 14
Clark, E. GO6 4
Clark, R. NP8 61, NP8 78
Clark, R.E. BP8 70
Clark, R.W. NP8 59, **NP8 69**, NP8 77, TO7 11
Clarke, Shaun TO4 4, TO4 5
Clary, M.R. UP8 41
Clary, Ryan UP8 39
Classen, I.G.J. UP8 102
Claude Bret, Antoine XP8 20
Clayton, C. JP8 130
Clayton, D.J. TP8 42, **TP8 56**, TP8 64
Clementson, J. **CP8 12**, CP8 52, JP8 5
Clerouin, Jean **CO5 7**
Cobble, J. CP8 39
Cobble, J.A. NP8 82
Cobble, J.C. GO6 2
Cobble, James **CP8 58**, UO5 6
Coffey, S.K. NP8 85, TP8 143, TP8 144
Cohen, B.I. PP8 121, UP8 26
Cohen, Bruce **CP8 64**, NO5 4
Cohen, R. GO4 11, NP8 110, NP8 112, NP8 115, NP8 117, **NP8 118**, NP8 120, NP8 122, PP8 117, PP8 118

Cohen, S.A. CP8 42, CP8 44
Cok, A.M. UO5 7
Colas, L. NO4 9
Cole, A. CO4 15, **TP8 96**, UP8 101
Cole, M. GP8 4, NP8 40, UP8 89
Colella, P. NP8 118
Collette, Andrew NM9 3, **UP8 135**
Collier, A. BO4 5, **JP8 86**, JP8 87, UP8 81
Collins, C. JP8 27, JP8 45, UP8 121
Collins, G.W. CO5 4
Collins, T.J.B. **TO5 3**, UO5 5
Collins IV, Gilbert NP8 60
Colombant, D. JO5 9
Colvin, J.D. CP8 37
Colvin, Jeffrey **TO7 10**
Combs, S.K. GP8 19, JP8 90, PP8 94, TP8 42
Comley, Andrew NP8 89
Commaux, N. JP8 89, JP8 90, JP8 91, JP8 95, JP8 96, JP8 106, JP8 117, TP8 37, **UO4 4**
Compton, Christopher GP8 123
Cone, G.A. **GP8 41**
Constantin, C.G. PO5 8
Constantin, Carmen GP8 140, TO6 1
Conway, Garrard CP8 9
Conway, Neil JO4 15
Cook, Alan GO6 12
Cook, James XP8 9
Cook, Mike BP8 100, BP8 102, NO6 9, NO6 10, NO6 11, NO6 12
Cooper, Chris GP8 145, JP8 18
Cooper, Guy A. **JP8 15**
Cooper, W. Anthony JP8 15, **UP8 95**
Coppa, Gianni **XP8 65**
Coppi, B. BP8 52, BP8 59, CP8 32, GP8 16, GP8 17, GP8 18, GP8 20, **GM9 8**, NO4 15, **NO4 16**, **UI3 4**, UP8 153, UP8 154
Cormier-Michel, E. JP8 125, JP8 129, TO4 12, TO4 13, **TO4 14**
Cormier-Michelle, Estelle JP8 126
Correa, C.E. **GP8 152**, **UP8 116**
Cortez, R.J. TP8 145
Cosse, Ph. TO6 10
Coster, D. JP8 30, JP8 31, UP8 125
Coster, Dylan JP8 43
Cothran, C.D. **BP8 12**, GP8 123, GP8 124, **XI3 6**
Couedel, L. **BP8 93**, BP8 97
Covele, B. UP8 64
Coverdale, C.A. CP8 37, CP8 45, NP8 59, NP8 61, NP8 69, NP8 77, TO7 11, TO7 12, **TO7 13**
Cowan, B. JP8 125, JP8 126, JP8 129, **TO4 12**, TO4 14
Cowan, T.E. GO6 1, GO6 3, TO4 1
Cowley, Stephen CO6 8, TP8 120
Crabtree, C. **BP8 59**
Craig, D. JP8 30, JP8 31, TP8 57, TP8 58, TP8 68, **UP8 125**
Crain, Marlon BO6 10
Crank, Willie **JP8 10**
Craxton, R.S. JO5 10, JO5 14, NO5 3, **PO5 6**, TO7 2, UO5 7, UO5 8, XP8 67
Creel, James **BP8 102**
Crocker, N.A. PP8 55, **PP8 56**, PP8 57, PP8 58, PP8 63, PP8 64
Crombe, K. CP8 2
Cross, Adrian UP8 110
Cross, Rick BO6 6
Cruz, Edward NP8 21, **NP8 23**
Cummings, J. GP8 55
Cummings, P.G. JP8 122
Cummings, Paul **PP8 122**
Cuneo, M.E. CP8 45, GO5 3, NP8 59, NP8 64, NP8 79, TO7 11, TO7 13
Cunningham, G. CO4 11
Cunningham, Nathaniel TO4 4, TO4 5
Cyrin, Bricette **GP8 109**
Czarnocki, C. NP8 57
Czarnocki, Cyprian JP8 43, **JP8 46**, JP8 47
Cziegler, Istvan **BI3 5**, GO4 10

D

D'Humieres, Emmanuel GO6 3, NO5 10, NO5 13, PO5 4
D'Ippolito, D.A. CP8 19, CP8 20, GO4 11, PP8 71, **UP8 65**
Dahlin, J. JP8 30, JP8 31, UP8 125
Dal Bello, S. TP8 77
Daniels, Stephen NP8 37
Danielson, J.R. **BP8 76**
Darrow, D.S. **PP8 55**, PP8 57, PP8 58, PP8 59
Das, Amita CP8 97
Dasgupta, A. NP8 59, **NP8 77**, NP8 78, TO7 11, TO7 13
Dasgupta, B. GP8 94, **GP8 100**
Dasgupta, Brahmananda XP8 66
Daskalova, R.L. CP8 76
Datte, P. JO5 1
Daughthon, W. TP8 123
Daughton, W. CO6 5, **NM9 7**, PM9 3, TP8 111, TP8 112, TP8 115, **TP8 122**, UO6 7
Davidson, Ronald JP8 51, JP8 61, NP8 5, **NP8 6**, NP8 7, NP8 8, NP8 9, UP8 17
Davis, Evan **JP8 64**
Davis, J. JP8 139, NP8 59, NP8 69, NP8 77, NP8 78, TO7 11, TO7 13
Davis, J.F. CP8 37
Davis, J.W. CO4 2
Davis, Jack CP8 70, CP8 72
Davis, M. UP8 50, UP8 51, UP8 52, UP8 53, **UP8 54**
Davis, Paul XP8 49
Davis, William JP8 69
Davydenko, V.I. TP8 59
de la Luna, Elena **PI2 2**
Dearborn, J. TP8 72
Deards, C.L. UP8 2, **UP8 3**
Debayle, Arnaud NO5 10, NO5 13
Debock, Maarten JO4 15
DeBono, B. GP8 22, GP8 23, GP8 24, GP8 25, GP8 26, **GP8 27**
DeBoo, J.C. CO4 5, JP8 98, JP8 101, JP8 105, **KI3 3**, TP8 6, TP8 12, TP8 14, TP8 15, UO4 15
Debus, A. TO4 1
Decamps, H. NO4 7
Decker, Joan JO4 16
Decoster, Alain CO5 7
Decyk, V. BP8 32, BP8 62, CP8 95, **JP8 137**, NP8 108, TO5 6
Deeney, C. GO5 6, NP8 78, TO7 12, TO7 13
DeFriend Obrey, K.A. NP8 82
Degnan, J.H. **TP8 143**, TP8 144
deGrassie, J.S. NO4 11, **TP8 3**, TP8 14
DeHart, T. UP8 4
Deichuli, P.P. TP8 59
del-Castillo-Negrete, Diego BP8 34, **BP8 60**, PP8 124
Delaney, R. TP8 143
Delettrez, J.A. CP8 50, CP8 51, JO5 11, JO5 13, JO5 14, JO5 15, PO5 2, TO7 2, UO5 3, UO5 9, **UO5 10**, UO5 11
Delgado-Aparicio, L. CP8 43, JO4 10, PP8 52, **PP8 53**, PP8 54
DeLooper, John JP8 3, JP8 4, JP8 6
Delzanno, Gian Luca PP8 119, **TP8 86**, XP8 65
Demers, D.R. TP8 47, **TP8 48**, TP8 49
Demidov, Vladimir BP8 110, **CP8 15**, PP8 120
Den Hartog, B. JP8 114
Den Hartog, D.J. CP8 5, CM9 11, JP8 25, TP8 42, TP8 44, TP8 45,

TP8 50, TP8 51, **TP8 52**, TP8 53, TP8 54, TP8 55, TP8 57, TP8 58, TP8 61, UP8 36, UP8 37
Dendy, Richard **BP8 43**, **XP8 9**
Deng, Wenjun **UP8 74**
DenHartog, D. TP8 89
DePasquale, S. JP8 106
Despain, Kate **UP8 115**
Detering, F. BO4 10
Deterly, T.M. JP8 113
Detragiache, P. GP8 17, NO4 16
Deutsch, Claude **BP8 15**, BP8 64, CO5 13, NP8 83, **XP8 10**
Devolder, Barbara NP8 89
Dewald, E. BO5 2, BO5 3, BO5 8, BO5 9
Dewar, R.L. BO4 6, **UO6 4**, XP8 5
Dewhurst, Joseph BP8 43
Diallo, A. GP8 78
Diamond, P.H. BP8 26, BP8 28, BP8 44, BP8 47, BP8 50, **BP8 53**, BP8 54, BP8 55, BP8 61, PO6 8, **TI2 6**, UP8 67, UP8 75, UP8 83
Dickens, James CO7 3
Dickson, Shannon **BP8 8**
Didelez, Jean-Pierre XP8 10
Diem, S.J. GP8 4, PP8 84, **TP8 67**, XP8 34
Dif-Pradalier, Guilhem **BP8 26**
Dimant, Y.S. **CO6 15**
Dimits, A.M. **PP8 121**
Dimits, Andris **DI3 4**
Ding, B.J. NO4 3
Ding, Siye **PP8 47**
Ding, W.X. PP8 19, TP8 42, TP8 43, TP8 44, **TP8 45**, TP8 46, TP8 61, TP8 62
Ditmar, J.R. **JP8 12**
Ditmire, T. CP8 75, JP8 144
Ditmire, Todd JP8 119
Divin, A. CO6 6, GM9 4, GM9 6
Divol, L. BO5 2, BO5 3, JO5 1, NO5 1, PO5 8, TO6 12
Divol, Laurent CP8 47, CP8 64, JO5 2, NO5 4, TO6 13
Dixit, S. BO5 2, BO5 3
Dixon, Alex JP8 5
Dmitruk, Pablo PM9 4
Doane, J.L. JP8 103, JP8 105
Dodd, E.S. **UO5 12**
Dodd, Evan NP8 90, UO5 6
Dodin, I.Y. **GP8 79**
Dodin, Ilya PP8 107
Doeppner, T. CO5 2, CO5 3, CP8 104, **PO5 3**, PO5 8
Doeppner, Tilo XP8 49
Dogariu, A. NP8 39
Dollar, F. JP8 122, TO4 8
Dollar, F.J. TO4 3
Dollar, Franklin **JP8 140**
Domier, C.W. CP8 6, GP8 40, JO4 3, PP8 67, PP8 68, **PP8 82**, UP8 102
Domingue, Scott NP8 33
Dominguez, A. GO4 2, **GO4 12**
Domonkos, M. TP8 143, TP8 144
Dong, J.Q. PO6 6, XP8 59
Dong, P. JP8 119, JP8 120, **TO4 11**
Donne, A.J.H. CP8 6, UP8 102
Donovan, David UP8 60, **UP8 61**
Dorf, M. NP8 6, **NP8 7**, NP8 8
Dorfman, S. JP8 49, **PM9 3**, TP8 110, **TP8 112**, TP8 113, TP8 114, TP8 115
Dorland, Bill PO6 4
Dorland, W. BP8 25, BP8 37, GP8 67, TP8 100, TP8 134, UP8 115
Doron, Ramy **JO6 6**
Dorr, M. NP8 118
Dorris, J.R. TP8 13
Doss, F.W. **TO6 8**, UP8 147, UP8 148
Douglas, M. CO5 8, **UP8 152**
Douglass, Angela **BP8 101**
Dover, Nicholas XP8 46
Downer, M. CP8 73, JP8 119, JP8 120
Downey, Shannan TO5 11
Doyle, E.J. CO4 5, JP8 98, JP8 99, JP8 100, JP8 101, NO4 11, TP8 5, TP8 6, TP8 12, TP8 14, TP8 15, **UO4 15**
Draganic, Ilija N. BO4 7
Drake, J.F. **PM9 8**, PM9 9, **TP8 131**, TP8 132, TP8 133
Drake, Paul TO5 8, UP8 146
Drake, R.P. CP8 49, JP8 12, JP8 13, **TO6 4**, TO6 8, TO6 9, UP8 142, UP8 145, UP8 147, UP8 148, UP8 151
Dremel, M. NO4 7
Drewsen, Michael **UI3 2**
Driscoll, C.F. BP8 72, BP8 74, **BP8 75**, **UI3 1**
Driscoll, M. UO7 5
Droege, Michael TO5 11
Droemer, Darryl BO6 10
Duan, X.R. XP8 59
Dubin, D.H.E. BP8 72, **BP8 73**, BP8 74, BP8 75
DuBois, A. **GP8 119**, GP8 120
DuBois, D.F. JO5 10, JO5 13
Dudnikova, Galina CP8 68, **JP8 143**
Duffy, T. TO7 6
Dufty, James UO6 12
Dumont, R. NO4 9
Dunn, J. JP8 144, UO4 12, UP8 144
Durand de Gevigney, B. BP8 80, **BP8 82**
Durmaz, T. NP8 75
Durodie, Frederic **UO4 13**
Duval, B.P. **GO4 13**
Dux, R. UO4 7
Dyer, G. JP8 144
Dylov, Dmitry V. **PO6 10**, PO6 13
Dymond, K.F. UP8 108
Dymond, Ken UP8 109
Dzenitis, E. BO5 2

E

Eadon, A. GP8 119, **GP8 120**
Ebbers, C. BO6 6, BO6 7, GP8 140
Ebrahimi, F. GP8 58, TP8 42, TP8 50, TP8 61, TP8 73, **UP8 124**
Eckberg, J. TP8 105, TP8 106
Edgell, D.H. JO5 10, JO5 13, **JO5 14**, JO5 15, UO5 9
Edlington, T. UP8 89
Edlund, E. **GO4 5**, PP8 9, PP8 30, **XP8 11**
Edlund, Eric UP8 118
Edwards, J. UO5 13
Edwards, M. BO5 4, BO5 6, BO5 7, BO5 9, TO5 1, UO5 7, UO5 14
Efthimion, P.C. **NP8 5**
Egedal, J. JM9 8, **TP8 123**, TP8 124, TP8 125, TP8 126, XP8 21
Eggert, J.H. CO5 4
Eggert, Jon **UI3 3**
Eggleston, D.L. **BP8 90**
Eich, T. UO4 8
Eidietis, N.W. CO4 11, JP8 91, **JP8 92**, JP8 93, JP8 95
Einav, Tal NO6 14
Ejiri, A. PP8 96, PP8 97, PP8 98, PP8 100, TP8 89
Elberson, Lee **JP8 142**
Elder, J.D. **TP8 30**
Eliasson, B. BP8 92, **CP8 68**, PO6 12, **XP8 12**, XP8 30
Ellis, R. JP8 112, PP8 44
Ellis, Richard **BM9 5**, GP8 10, JP8 20, **UP8 39**, UP8 40, UP8 41, UP8 43, UP8 48, UP8 59
Ellison, C.L. **JP8 42**, UP8 13
Ellsworth, J. UP8 51
Ellsworth, J.E. UP8 52
Ellsworth, J.L. UP8 50, **UP8 53**, UP8 59
Ellsworth, Jennifer UP8 54
Elor, Ronny JP8 5
Elsholz, A. CP8 104, CP8 106
Elton, R. TP8 150, TP8 153, TP8 154, UP8 39, UP8 48
Elwasif, W.R. GP8 58
Emig, J. CP8 52, CP8 104, CP8 106, TO7 7

Emmert, Gilbert **UP8 60**
Endler, Antonio NP8 12, **NP8 13**
Endo, Takashi CO5 1, TO6 14
Endo, Takuma NP8 54
Ennis, D.A. TP8 68, **UP8 19**, UP8 20, UP8 21, UP8 22, UP8 24
Epperly, T. NP8 122, PP8 117, PP8 118
Epstein, R. **UO5 3**, UO5 8
Erickson, Daniel BP8 87
Erler, C. TO4 1
Ernst, D.R. **BP8 29**
Ernst, Darin PP8 15
Esarey, Eric JP8 125, JP8 126, JP8 127, JP8 128, **JP8 129**, TO4 12, TO4 14
Esaulov, A.A. GO5 11, GO5 13, NP8 62, NP8 63, TO7 12
Escande, D.F. TP8 80
Escande, Dominique **TP8 78**
Esirkepov, Timur GO6 9
Esposito, B. UO4 2
Estep, D.J. PP8 117
Estep, Don PP8 118
Ethier, S. JP8 58, JP8 59, **PP8 65**, UP8 83
Evans, Russell UP8 31, UP8 32, UP8 33
Evans, T.E. CO4 3, CO4 4, JP8 70, JP8 80, JP8 88, JP8 89, JP8 91, JP8 95, JP8 96, JP8 101, TP8 8, TP8 21, **TP8 24**, TP8 25, TP8 26, TP8 29, TP8 37, UO4 4, UO4 6, UP8 89
Everson, Erik GP8 140, **TO6 1**
Eyink, Gregory **UO6 1**, UO6 2

F

Faehl, R. CP8 65, **CP8 66**, NP8 30
Faeustlin, R.R. UO6 14
Fahey, M.R. PP8 117
Fahey, Mark PP8 118
Fahlen, J.E. CP8 94
Fahlen, Jay CP8 95, CP8 96, **TO5 6**
Fajans, Joel **BP8 77**
Falcone, R.W. CO5 3
Falk, K. CO5 2
Falkowski, A.F. TP8 42
Faltens, A. NP8 4
Farge, M. PP8 124
Farley, D.R. **CP8 42**, CP8 44
Fasoli, A. CP8 10, GP8 77, **GP8 78**
Fassina, Alessandro TP8 55
Fatenejad, M. **NP8 103**, UO5 4
Faussurier, G. TO6 10
Faust, C.F. TP8 42
Fawley, W.M. TO4 13
Feder, H. PP8 83
Feder, R. PP8 83, UO4 12
Federspiel, L. GP8 78
Fedosejevs, R. CP8 53, CP8 103, CP8 105, NO5 1, PO5 9
Fehling, D. GP8 19
Feibelman, Peter J. **EE1 1**
Feibush, Eliot GP8 51, JP8 60
Feldman, S. JP8 144
Feldman, U. JO5 8
Fenstermacher, M.E. **CO4 1**, CO4 3, JP8 88, JP8 89, JP8 101, TP8 20, TP8 25, TP8 30
Fernsler, R.F. BP8 12
Fernsler, Richard GP8 125
Ferraro, N.M. **TP8 22**, UP8 97
Ferris, Pamella JP8 3, JP8 4
Ferro, A. GP8 92
Ferron, J.E. **JP8 98**
Ferron, J.R. CO4 5, JP8 94, JP8 97, JP8 101, TP8 25, TP8 38, UO4 15
Fetterman, Abraham **CM9 10**, **NP8 53**
Fichtl, Chris **PP8 119**
Field, Anthony JO4 15
Figueroa-Hernandez, Angel Mario **NP8 38**
Fiksel, G. **BI2 5**, TP8 42, TP8 45, TP8 57, TP8 58, **TP8 59**, TP8 60, TP8 62, TP8 68, TP8 69
Filevich, Jorge UP8 144
Fimognari, P.J. TP8 47, TP8 48, **TP8 49**
Finken, Karl Heinz NO4 5, UP8 76
Finkenthal, M. CP8 43, PP8 53, PP8 54
Finn, John PP8 119, TP8 86
Finnegan, S.M. **CP8 88**, CP8 89
Fiore, Catherine **GO4 3**, PP8 13, PP8 14
Fisch, Nathaniel CP8 30, CP8 81, CM9 9, CM9 10, GP8 79, GP8 130, JO5 6, JP8 147, NP8 48, NP8 49, NP8 51, NP8 53, PP8 106, **PP8 107**
Fischer, Wolfram NP8 14
Fisher, A. NP8 78
Fisher, Amnon XP8 53
Fisher, D. UP8 145
Fisher, R. **BP8 95**
Fisher, V. CP8 45, NP8 78, TO7 11
Fitzpatrick, B. CO4 2
Fiuza, F. **CP8 101**, CP8 109, CP8 111, NP8 31, NP8 108
Flanagan, S.M. JP8 93
Flauta, Randolph **CO7 5**
Fleischer, Jason W. PO6 10, PO6 13
Fletcher, K. CP8 59
Flicker, D. BP8 70, NP8 69
Flippo, K. CP8 39, **GO6 2**, GO6 3, PO5 12, UO5 6
Florido, R. CP8 50, CP8 51, **GP8 70**
Floyd, J.P. TP8 34
Fogarty, P.J. GP8 4
Foley, E.L. CP8 4, GP8 9, JP8 66, **NO4 8**
Fonck, R.J. JO4 7, JO4 12, JP8 116, PP8 83, **PP8 85**, PP8 86, PP8 87, TP8 7, TP8 8, XP8 34
Fonseca, R.A. CP8 101, CP8 109, CP8 111, JP8 132, JP8 133, JP8 137, NP8 31, **NP8 108**, TO4 8, UP8 137, UP8 139
Foord, M. CP8 103, CP8 104, CP8 105
Forbes, Terry NM9 2
Forest, C.B. **CT3 1**, GP8 96, GP8 97, GP8 98, GP8 129, JP8 26, JP8 27, TP8 50, TP8 56, TP8 63, TP8 64, TP8 65, TP8 66, TP8 67, UP8 122, UP8 123, UP8 124
Fortmann, C. UO6 14
Fortov, V.E. NO6 7
Foster, J.M. CO5 8, UP8 152
Foster, John CP8 83
Fournier, K.B. **CP8 37**
Fournier, Kevin TO7 7, TO7 10
Foust, C. GP8 19
Fox, M. TO7 6
Fox, W. JM9 8, **TP8 124**, TP8 125, TP8 126, XP8 21
Frank, A. UP8 152
Frank, Anna **JM9 6**
Frank, Klaus CO7 3
Frank, Zoe NM9 5
Frankel, Miriam CP8 52
Franz, P. TP8 42, TP8 53, **TP8 54**, TP8 55, TP8 77
Franzi, M.A. NP8 64
Franzi, Matthew **NP8 21**
Frassinetti, L. CO4 13
Fratanduono, D.E. **CO5 4**, UO5 1
Frater, E. BP8 89, **JP8 19**
Frattolillo, A. **GP8 19**, NO4 15
Fredd, E. JP8 106
Frederick, C. CP8 104
Fredrickson, E.D. PP8 43, PP8 55, PP8 56, PP8 57, **PP8 58**, PP8 59, PP8 61, PP8 73
Freeman, R.R. CP8 53, CP8 76, NO5 1, NO5 2, NO5 12, PO5 9
Freidberg, J.P. UP8 96
Freidberg, Jeffrey UP8 99
Freitas, Barry NP8 29
French, D.M. NP8 18, **NP8 20**, NP8 64, NP8 79, NP8 80
Frenje, J.A. BO5 12, BO5 13, BO5 14, CP8 54, CP8 55, CP8 56, CP8 59, CP8 62, **NI2 4**, NO5 3, TO7 2, UO5 2, UO5 8, UO5 10, UO5 12, XP8 68
Frerichs, H. CO4 3
Frese, M.H. TP8 143, TP8 144

Frese, S.D. TP8 143, TP8 144
Friedland, Lazar GP8 82, **GP8 83**
Friedman, A. **CI2 1**, NP8 4, NP8 93, NP8 95, NP8 110
Friedman, B. **GP8 141**, GP8 142, GP8 143, GP8 144
Friesen, H. **CP8 53**, CP8 103, CP8 105
Friis, Z.W. **TP8 33**
Fromy, Patrice BP8 64
Frosi, P. GP8 20, GP8 21
Froula, D.H. TO6 9, TO6 12
Froula, Dustin CP8 47, JO5 2, **QI3 2**, TO6 13
Fruchtman, Amnon BP8 108, JO6 6, **JO6 7**
Fryxell, B. JP8 13, UP8 147, **UP8 149**
Fu, G.Y. **GP8 66**, GP8 72, GP8 126, JP8 109
Fu, Sean NO4 14, **UP8 66**
Fu, X. PP8 13
Fuchs, J. GO6 1, GO6 5, JP8 42, JP8 144, PO5 4
Fuelling, Stephan TP8 148, TP8 160
Fujii, A. TP8 89
Fujii, Takashi GO6 9
Fujioka, S. XP8 25
Fujisawa, A. GP8 146
Fujita, S. TP8 89, TP8 90, TP8 91, TP8 92
Fuks, Mikhail NP8 24
Fukumoto, N. GP8 7, UP8 15
Fukuyama, A. **BO4 4**, GP8 56
Funaba, H. BM9 4
Fundamenski, Wojciech **BI3 2**, UO4 8
Furman, M.A. TO4 13
Furno, I. **GP8 77**, GP8 78
Furukawa, M. **UP8 94**
Furukawa, Masaru UP8 85
Futatani, S. NO4 14, PP8 13
Fyfe, D.E. TO7 1

G

Gaillard, S.A. CP8 39, CP8 48, **GO6 3**, PO5 12
Gaio, E. GP8 92
Galante, Matthew GP8 132
Gale, D. TP8 143
Gale, D.G. TP8 144
Galkin, Sergei A. GP8 8, **NP8 98**
Gall, B.B. GO6 3
Gallardo, Juan BO6 11
Gamboa, Eliseo **UP8 151**
Gangadhara, S. TP8 68
Ganguli, G. GP8 122, GP8 123, GP8 124
Gao, Peng BO6 1
Gao, W. NO4 2
Gao, X. NO4 2, XP8 59
Gao, Xiaohui **CP8 73**, CP8 74
Garate, Eusebio UP8 11, UP8 12
Garbet, X. BP8 26, BP8 42, BP8 54, PP8 13, UP8 73
Garcia-Munoz, M. GP8 34
Gardner, J. XP8 25
Gardner, J.H. TO7 3
Garg, Vijay **JP8 150**
Gargate, Luis **UP8 139**
Garnier, D.T. CP8 41, JP8 21, JP8 22, **UP8 50**, UP8 51, UP8 52, UP8 53, UP8 54, UP8 55, UP8 59
Garofalo, A.M. CO4 6, **CO4 15**, GP8 2, GP8 3, JP8 75, JP8 76, JP8 81, JP8 83, JP8 84
Garot, K. **JP8 43**, UP8 118, XP8 11
Garrett, M.L. **PP8 32**
Gary, S. Peter PP8 114, PP8 115, **UP8 117**
Gates, D.A. CO4 11, **JO4 4**, JO4 5, JO4 9, PP8 37, PP8 45, PP8 48, PP8 78, PP8 80, UO4 6
Gatling, G. GP8 123, GP8 124
Gaul, Erhard JP8 119
Gauthier, M. JP8 144
Gautier, D.C. CP8 39, GO6 2, GO6 3
Geddes, Cameron **JP8 125**, JP8 126, JP8 129, TO4 6, TO4 12, TO4 13, TO4 14
Geer, R. JP8 112
Geissel, M. GO6 3, JP8 145
Geissler, Michael NO5 13
Gekelman, Walter GP8 116, GP8 117, GP8 118, GP8 145, GP8 150, **NM9 3**, TO6 1, TO6 2, UP8 135
Genoni, T.C. BP8 70
Gentile, Charles JP8 34, JP8 35, JP8 36, JP8 37
Gentile, N. NP8 99
Gentle, Kenneth CO4 9, PP8 13, PP8 14, UP8 63, **UP8 64**, XP8 38
Geoffroy, Ghita UP8 150
George, David BP8 100, BP8 102
George, Miley NP8 107
Gerhardt, S. JO4 2, JO4 4, JO4 5, **JO4 9**, JO4 10, PP8 38, PP8 39, PP8 43, PP8 44, PP8 45, PP8 50, PP8 51, PP8 52, PP8 53, PP8 73, PP8 79, UO4 6, UP8 97
Germaschewski, K. GP8 128, JM9 3, TP8 72, TP8 117
Gerres, J.M. GP8 89
Gershman, S. PP8 88, **PP8 95**
Geyer, Kathleen **NP8 15**
Geyko, V.I. GP8 79
Ghantous, Katy **GP8 12**
Ghendrih, Ph. BP8 26
Ghiaassian, Seyed UO7 8
Gholizadeh, Reza **JP8 134**
Giar, Ryan BP8 10
Gibson, D. BO6 5, BO6 6, BO6 7, NP8 27, **NP8 28**
Gigliotti, A. GP8 116, **GP8 117**, GP8 118
Gil, J.M. GP8 70
Gilgenbach, Ronald NP8 19, NP8 20, NP8 21, NP8 22, NP8 23, NP8 64, NP8 79, NP8 80
Gillaspy, John D. BO4 7
Gilleron, F. TO6 10
Gillespie, Karen UP8 110
Gilligan, Nick JP8 3, JP8 4
Gillis, Chad **JP8 5**
Gilmore, M. **GP8 106**, GP8 107, GP8 108, GP8 109, GP8 111, TP8 149, TP8 150, TP8 151, TP8 152, UP8 133, XP8 36
Gilson, Erik **CI2 3**, JP8 61, NP8 2, NP8 5
Giraldez, E.M. NO5 1
Girard, F. CP8 37, **TO7 9**
Gissis, Itay **XP8 53**
Giudicotti, Leonardo TP8 84
Giuliani, J. NP8 59, NP8 61, NP8 69, NP8 77, **NP8 78**, TO7 11, TO7 13
Giunchi, G. GP8 18
Gizzi, L.A. CP8 106
Gjeci, N. **JP8 13**
Glasser, A.H. **GP8 42**, GP8 47
Glassmeier, K.H. GM9 4
Glazyrin, I.V. TO4 3
Glebov, V.Yu. BO5 11, CP8 59, NO5 3, TO7 2, TO7 4, **TO7 6**, UO5 8, UO5 12
Glenn, Steven BO5 8
Glenzer, S.H. BO5 1, **BO5 2**, BO5 3, BO5 5, BO5 7, CO5 2, CO5 3, CP8 47, CP8 49, GP8 140, JO5 1, JO5 2, PO5 3, PO5 8, PO5 14, TO6 9, TO6 12, TO6 13, UO6 14, XP8 49
Glosi, J. JP8 144
Glosli, James PO5 14, UO6 15, XP8 13
Gobbin, M. **TP8 79**, TP8 81, TP8 83
Goedbloed, Hans **UO6 3**
Goetz, J.A. **TP8 41**, TP8 42, TP8 53, TP8 54, TP8 63, TP8 64
Goetz, Keith JO6 1
Gohil, P. NO4 11, **TP8 4**, TP8 20
Goldman, Martin CO6 6, GP8 86, **GM9 6**
Goldstein, T. **JP8 54**
Goldston, R. **GP8 5**, UO4 6
Golingo, R.P. JP8 25, UP8 7, UP8 36, **UP8 37**, UP8 38
Golovkin, I.E. NP8 104, TO6 10, **TO7 14**
Golubev, Sergey NP8 35
Gomez, M. NP8 64, **NP8 79**, NP8 80
Goncharov, V.N. CO5 2, CO5 5, CP8 110, JO5 14, JO5 15, UO5 1,

UO5 2, UO5 3, UO5 8, UO5 10, UO5 11
Gong, X.Z. NO4 2
Gonsalves, Anthony **UI2 1**
Gonzales, R. GO6 3, PO5 12
Goodman, Jeremy BO4 8
Goodrich, Tasha **TP8 148**, TP8 160
Goodwin, P.M. BP8 68
Gorbachev, Alexey NP8 35
Gordon, Daniel JP8 124, TO4 10
Goree, John **NO6 7**
Gorelenkov, N.N. BO4 9, GP8 12, JP8 109, JP8 110, PP8 55, PP8 56, PP8 57, PP8 58, PP8 59, **PP8 61**
Gorelenkova, M. GP8 51, GP8 66
Gorelov, Y.A. JP8 103, **JP8 104**, JP8 105
Gosling, John **GM9 1**
Gotchev, O. TO7 2, UO7 1
Goto, M. NP8 47
Goulding, R. GP8 13, JP8 106, JP8 107, NO4 9, **NP8 40**
Gourdain, P.A. GO5 9, NP8 65, NP8 66, NP8 67
Grabowski, C. TP8 143, TP8 144
Grabowski, T.C. NP8 85
Granatstein, Victor **BO6 2**, BO6 3
Grandgirard, V. BP8 26
Grando, Luca TP8 83
Granetz, Robert PP8 14, **PP8 26**, PP8 28, PP8 29, UO4 3, UO4 10
Granstedt, E.M. PP8 88, **PP8 93**, PP8 94, PP8 95
Granucci, G. UO4 2
Grasso, D. TP8 121
Grasso, G. **GP8 18**
Grava, Jonathan UP8 144
Graves, Jonathan **GI3 2**, JP8 15
Gray, T. JP8 48, TP8 141
Gray, Tim **BI2 6**
Gray, Travis **NO4 6**
Graziani, Frank JP8 144, PO5 14, **UO6 10**, UO6 15, **XP8 13**
Green, D. **CP8 16**, JO4 11, PP8 76
Greenaugh, N.L. JP8 107
Greenly, John **GO5 8**, GO5 9, NP8 65, NP8 66, NP8 67, NP8 70, NP8 72, NP8 76
Greenough, N.L. JP8 106
Greenwald, Martin GO4 2, GO4 6, **JT3 1**, PP8 10, PP8 11, PP8 15
Greenway, Wayne G. BO6 14
Gregg, C.W. NP8 85
Gregori, G. CO5 2, PO5 13, TO6 9, UO6 14
Gregory, C. UP8 143
Greiner, Franko **NO6 6**
Gremillet, Laurent XP8 54
Gribov, Y. UO4 11
Grierson, B.A. UP8 57, **UP8 58**
Grim, G.P. UO5 14
Grismayer, Thomas CP8 95, **CP8 96**, TO5 6
Griswold, Martin E. **PP8 106**
Groebner, R.J. CO4 13, CO4 14, JP8 111, JP8 114, PP8 117, TP8 3, TP8 16, TP8 17, TP8 18, **TP8 19**, TP8 20, TP8 32, TP8 35
Gronberg, J. PO5 13
Grosskopf, M.J. JP8 12, JP8 13, UP8 145, UP8 146, **UP8 147**, UP8 148, UP8 149
Grosskopt, M.J. TO6 9
Grossnickle, J.A. **UP8 2**, UP8 3
Grote, D.P. NO5 5, NP8 110, TO4 13
Groth, M. TP8 30
Gruber, Ralf JP8 15, UP8 95
Gruener, Florian JP8 127
Grulke, Olaf **PO6 2**
Grun, E. BP8 105
Grun, J. TO7 3
Grunloh, H.J. JP8 103
Gryaznevich, Mikhail **BO4 12**
Gu, M.F. NP8 47
Gu, Ming CP8 52
Guadamuz, Saul **CP8 33**
Guan, Xiaoyin **CP8 30**
Guazzotto, L. BP8 27, **UP8 87**, UP8 96
Gudmundson, Jesse **NP8 42**
Gumerov, N.A. GP8 116
Guo, H.Y. **NO4 2**
Guo, S.C. TP8 75
Guo, W. BO4 5, **JP8 85**, JP8 86
Gupta, Sudip S. CP8 97
Gurcan, O.D. BP8 53, BP8 54, UP8 67
Gustafson, Kyle **BP8 37**
Guterl, Jerome **BP8 5**
Gutierrez, M.S. **JP8 61**
Guy, W. JP8 87
Guzdar, P.N. BP8 29, GM9 4, **GM9 5**, NP8 126, UP8 98

H

Ha, Bao Nguyen Quoc **UP8 132**
Haan, S. BO5 4, CP8 84, **TO5 1**, UO5 13, UO5 15
Haas, Fernando XP8 18, XP8 19, XP8 20
Haasz, A.A. CO4 2
Habara, Hideaki CP8 80, CP8 97, **XI2 3**
Haberberger, D. GO6 12, **JP8 141**
Haboub, A. **NP8 73**, NP8 75
Hafizi, Bahman TO4 10
Hager, J. **CO5 12**, CP8 56
Hagmann, Christian BO6 5
Hagnestal, Anders CM9 5
Hagstrom, George **GP8 153**
Hahm, T.S. BP8 48, BP8 49, **BP8 50**, BP8 54, PP8 64, PP8 65, PP8 70, UP8 67, UP8 83
Hahn, M.S. BP8 80, BP8 81, BP8 83
Hahn, S.H. CO4 11
Haill, T.A. CO5 6
Haines, Malcolm **CP8 108**
Hakel, P. NP8 75, PO5 5
Hakim, A. NP8 122, PP8 117, PP8 118, TP8 157, TP8 158, UP8 81
Hall, G.N. **GO5 1**, GO5 5, NP8 74, NP8 81, TO6 3
Hall, I.M. CP8 48
Hallatschek, Klaus **PO6 9**
Halpern, F.D. GP8 11
Hameiri, Eliezer BP8 27, **GP8 101**
Hammel, B.A. CP8 86, TO5 1, UO5 14
Hammer, D.A. GO5 9, NP8 65, NP8 66, NP8 70, NP8 71, NP8 72, NP8 76
Hammett, G.W. **BP8 23**, BP8 24, PP8 66, PP8 93, PP8 117, TP8 100
Hamp, W.T. UP8 19
Han, Hyunsun GP8 39, NP8 127
Hanashima, Kentaro PP8 96, PP8 97, PP8 100
Hannum, D.A. **GP8 96**, GP8 97, GP8 98
Hansen, Alexander **GP8 134**, GP8 135
Hansen, Chris GP8 45
Hansen, J.F. CO5 8, UP8 152
Hansen, S. **CP8 45**, NP8 84, TO6 10, TO7 11
Hanson, G.R. JP8 106, **JP8 117**, PP8 31
Hanson, J. TP8 105, TP8 107
Hanson, J.D. TP8 106
Hanson, J.M. CO4 6, JP8 81, **JP8 82**
Hanson, James CP8 13
Harada, Takashi NO6 13
Harding, E.C. TO7 3, UP8 145, UP8 151, **XI2 2**
Harris, Brandon NO6 9
Harris, J. TP8 98, UP8 89
Harris, W.S. TP8 52
Harris, Wayne UP8 11, **UP8 12**
Hart, Grant W. BP8 85, **BP8 86**, BP8 87
Hartemann, F.V. BO6 5, **BO6 6**, BO6 7, GP8 90, NP8 27, NP8 28
Hartigan, P. CO5 8, UP8 152
Hartwell, G. GP8 121, TP8 105, **TP8 106**, TP8 107
Hartwig, Zach **PP8 24**
Harvey, R.W. **CP8 26**, GO4 8, GP8 52, GP8 58, GP8 59, JO4 11, PP8 5, PP8 8, PP8 76, PP8 77, TP8 56, TP8 67

Harvey-Thompson, A.J. GO5 1, **NP8 81**, TO6 3
Harvey-Thomson, A. GO5 5
Hashimoto, Hiroki BP8 21
Hassam, Adil BM9 5, GM9 5, JP8 20, UP8 39, UP8 40, UP8 41, UP8 42, UP8 43, **UP8 47**, UP8 77, UP8 98
Hassan, S. GO6 4
Hatakeyama, Rikizo NO6 13, PO6 7
Hatch, D. BP8 31, **BP8 39**
Hatchett, S. UO5 13
Hatchett II, S.P. UO5 14
Hathcett, S.P. TO5 1
Hau-Riege, S. JP8 144, **PO5 14**, UO6 15
Hauschildt, Peter H. UP8 157
Hawes, J. PP8 84
Hawkes, N.C. CP8 2
Hawryluk, R. UP8 89
Hay, M. NP8 93, **NP8 94**, TO5 2
Hayashi, Hiroyuki PP8 96, PP8 97, PP8 100
Hayashi, Nobuhiko **BI3 1**
Hayashi, Yoshinori **TP8 137**, TP8 138
Hayes, Tiffany **GP8 108**, GP8 109
Haynam, C. BO5 3
Hazeltine, R.D. PP8 111, UP8 141
Hazi, A. JP8 144
He, Long BP8 13
Headley, D.I. JP8 145
Hebert, J. **CP8 13**, TP8 107
Heeter, Robert CP8 52, **TO7 7**
Hegna, C.C. BP8 3, GP8 58, GP8 93, GP8 99, NP8 113, TP8 96, **UP8 90**, UP8 92, UP8 101
Heidbrink, W.W. CO4 7, GP8 76, JP8 108, JP8 109, JP8 110, JP8 111, PP8 56, PP8 57, PP8 60, PP8 76, TP8 9, UP8 11, UP8 12
Heim, B. PP8 40
Heinrich, J. **BP8 94**, NO6 1, NO6 2
Heitzeroeder, Phil TP8 101
Held, E.D. GP8 43, GP8 58, GP8 61, GP8 93, GP8 99, **UP8 82**
Helle, Michael JP8 124, **TO4 10**
Hemsworth, R. NO4 7
Hender, T.C. BO4 12
Henderson, Alexander NO6 14
Henderson, D. CP8 65
Henderson, Watson JP8 119
Henestroza, E. NP8 93, NP8 95, **NP8 96**, **XP8 14**
Henning, Christian UO6 13
Hernandez, F. XP8 14
Herrera-Velazquez, Julio GP8 71
Herrmann, H.W. NP8 82, UO5 14
Herrmann, M.C. GO5 3, JP8 145, TP8 156
Herrmann, Mark GO5 2, UO5 15
Herron, Ison **BO4 8**
Hershcovitch, A. **UO7 5**
Hershkowitz, Noah BP8 7, BP8 107, **JO6 5**, NP8 42, NP8 45, **XP8 15**
Hervieux, Paul-Antoine XP8 19
Hess, Mark **BO6 8**
Hesse, Michael GM9 3, **PM9 5**
Hewett, Dennis **PP8 113**, UP8 140
Hey, D. CP8 53, CP8 103, CP8 105, GO6 2, NO5 1, NO5 2, NO5 3, NO5 4, NO5 6, PO5 12, XP8 16
Hibbard, R. JO5 1
Hicks, D.G. CO5 4, UO5 1
Hicks, N.K. **GP8 34**
Higashi, T. GP8 7, UP8 15
Higginson, D.P. CP8 53, CP8 103, **NO5 2**, NO5 8, PO5 12, **XP8 16**
Hihara, R. PP8 98, PP8 99, PP8 100
Hilburn, Guy GM9 7
Hill, D.N. JP8 75
Hill, K.W. NP8 47, **UO4 12**
Hill, Wendell JP8 142
Hillesheim, J.C. **CO4 8**, TP8 5, TP8 6, TP8 12, TP8 14
Hillis, D.L. CP8 2
Himura, H. TP8 89, TP8 90, TP8 91, TP8 92
Hinkel, D. BO5 2, BO5 3, BO5 5, CP8 90, JO5 3, **JO5 4**, JO5 5, TO5 5
Hinson, E.T. JO4 7, PP8 85, **PP8 87**
Hinton, Courtney **JP8 8**
Hinton, F.L. **BO4 3**, PP8 49
Hirano, Y. PP8 98
Hiratsuka, Junichi PP8 96, PP8 97, PP8 100
Hiroi, Masanori UP8 14
Hironaka, Yoichiro CO5 1
Hirota, Makoto **GP8 114**, UP8 85
Hirschman, S.P. TP8 79
Hizanidis, K. BP8 42, CP8 27, **CP8 28**, CP8 29
Hnat, Bogdan BP8 43
Ho, D.D. TO5 1
Ho, Darwin **UO5 15**
Hochstuhl, David UO6 13
Hoff, B. NP8 21, NP8 22, NP8 23
Hoffman, A.L. UP8 2
Hoffman, Nelson **CP8 86**
Hoffmann, Dieter H.H. CO5 13
Hogan, M. GO6 13, JP8 130
Hojo, H. BM9 3, BM9 4
Holcomb, C.T. **CO4 5**, JP8 97, JP8 98, JP8 101, JP8 112, JP8 114
Hole, M.J. **BO4 6**, UO6 4, XP8 5
Holland, C. BP8 40, GP8 67, GP8 138, TP8 6, TP8 7, **TP8 12**, TP8 14
Holland, G. JO5 8
Hollmann, E.M. CO4 10, JP8 90, JP8 91, JP8 92, JP8 95, JP8 96, **TP8 37**, UO4 4, **XI3 4**
Holloway, James TO5 8
Holod, I. **BO4 2**
Holst, B. UO6 14
Homoelle, Doug NO5 4
Hong, Sang Hee GP8 39, NP8 127
Hong, Wenyu XP8 59
Hongbo, Cai CP8 112
Honrubia, Javier **NO5 10**, NO5 13
Hooper, E.B. **UP8 25**, UP8 26
Hoppe, M.L. UO5 7
Hopwood, Jeffrey **GI2 4**
Hora, Heinrich **NP8 92**, UO7 4
Horak, W. UO7 5
Horanyi, M. BP8 105
Hori, Yasunori CO5 1
Horioka, Kazuhiko TO6 7
Hornstein, M. GO6 11
Horovitz, Y. JP8 122
Horton, A.R. JP8 106, JP8 117
Horton, L. UP8 89
Horton, L.D. CO4 13
Horton, Robert **UP8 31**, UP8 32, UP8 33
Horton, W. CM9 12, GP8 152, **NO4 14**, PP8 13, UP8 66, UP8 116
Hosea, J. CO4 7, JO4 3, JO4 11, JP8 67, JP8 106, JP8 107, **PP8 75**, PP8 77
Hoskinson, Alan XP8 15
Hossack, A.C. UP8 19, **UP8 22**
Hou, Lu-Jing NO6 6
Hou, Ya-Wei TP8 127
Houshmandyar, Saeid GP8 135, **GP8 136**, **XP8 57**
Houshmandyar, Saied GP8 132
Houshmyandar, Saied BP8 9
Howard, J. BO4 6, XP8 5
Howard, N. GO4 2, **PP8 11**
Howell, D. BO4 12, UP8 89
Howell, E.C. **UP8 34**
Hoyt, C.L. NP8 65, **NP8 66**, NP8 70, NP8 76
Hsing, W. BO5 3
Hsu, S.C. **TP8 149**, TP8 150
Hsu, Scott TP8 151, TP8 152, UO5 6, UP8 133, XP8 22, XP8 23
Hu, Jing **BO6 12**
Hu, Q. GP8 94

Hu, Q.S. NO4 2
Hu, S.X. **CO5 5**, CO5 12, UO5 1
Huang, C. GO6 13, **JP8 130**, JP8 131, JP8 132, JP8 134, JP8 136
Huang, M.C. JP8 138
Huang, Tian-Sen UP8 8, UP8 9
Huang, Y. PP8 121
Huang, Yi-Min **BI2 1**, JM9 3, **TP8 116**, TP8 117, TP8 118
Hubbard, A. **GO4 1**, GO4 2, GO4 6, GP8 5, GP8 6, PP8 7, PP8 8
Huber, A. UO4 5, **UO4 8**
Hudson, B. JP8 77, NO4 11, **TP8 21**
Hudson, Lawrence XP8 55
Hudson, S.R. UO6 4
Hueller, Stefan JP8 41
Huete Ruiz de Lira, C. **CO5 14**, CO5 15, CP8 87
Hughes, J. **BI3 4**, GO4 2, PP8 7, PP8 15, PP8 16, PP8 20
Hughes, Steve **CP8 78**
Humanik, Peter JP8 46, **JP8 47**
Hummelt, Jason BP8 10
Humphreys, D.A. CO4 11, JP8 90, **JP8 91**, JP8 92, JP8 93, JP8 94, JP8 96, JP8 102, TP8 37, TP8 38, TP8 39, UO4 4, UO4 9, XP8 45
Hund, J.D. CO5 8
Hung, ChingPui **UP8 77**
Huntington, C.M. **CP8 49**, TO4 8, UP8 148, UP8 151
Hurd, L. **JP8 71**
Hurry, T. GO6 3, PO5 12
Huser, Gael CP8 114
Hutchinson, Ian PP8 12, **TI2 1**, UO4 3, UO4 14
Hutchison, C. NP8 74
Hutsel, B.T. **NP8 50**
Hwang, David UP8 31, UP8 32, UP8 33
Hwang, Seok Won GO6 10, **TO4 7**
Hwang, Y.S. PP8 102
Hyatt, A.W. CO4 11, JP8 87, **JP8 93**, JP8 111, TP8 25, UO4 9
Hyde, Truell BP8 100, BP8 101, BP8 102, BP8 103, NO6 8, NO6 9, NO6 10, NO6 11, NO6 12

I

Ibano, Kenzo NP8 130
Ichimura, M. BM9 3, BM9 4, CM9 2
Ide, S. GP8 92
Ide, T. UP8 143
Iglesias, C. BP8 69, TO6 10, TO7 7
Igochine, V. GP8 34
Igumenshchev, I.V. JO5 14, **JO5 15**, UO5 9
Ii, Toru TP8 137, **TP8 138**
Ikeyama, Taeko **UP8 14**
Ikezoe, R. TP8 89, TP8 90, TP8 91, **TP8 92**
Ikoma, Masahiro CO5 1
Imadera, Kenji **BP8 30**, PO6 6
Imai, N. BM9 4
Imai, T. BM9 4
Imai, Tsuyoshi **BM9 3**, CM9 2
Imazawa, R. PP8 98, **PP8 99**, PP8 100
In, Y. **JP8 83**, JP8 84
Inagaki, S. GP8 146
Ince-cushman, A. GO4 6, NP8 47
Indireshkumar, K. GP8 51, **GP8 52**, PP8 117, PP8 118
Innocente, Paolo TP8 84
Inomoto, Michiaki PP8 98, PP8 99, PP8 100, TP8 136, TP8 137, TP8 138, TP8 139
Inoue, Masahiko CP8 77
Intrator, T. **TP8 144**
Intrator, T.F. TP8 143
Intrator, T.P. **CM9 7**, JP8 32, JP8 33, **NM9 6**, TP8 145
Iraji, D. GP8 78
Irby, J. PP8 19, PP8 36, UO4 10
Ishizawa, Akihiro **TP8 130**, UP8 71
Island, N.T. **XP8 2**
Ispirian, Michael XP8 46
Itoh, K. GP8 146, UP8 69
Itoh, S.I. GP8 146
Ivancic, S. PO5 6
Ivanov, A. CP8 17
Ivanov, A.A. **BM9 6**, TP8 59
Ivanov, V.V. CP8 46, NP8 73, **NP8 75**
Ivlev, A. BP8 93, NO6 7
Iwamoto, Akifumi CO5 1
Izumi, N. BO5 7, BO5 12, NO5 4
Izzo, V.A. **CO4 10**, JP8 87, PP8 26, UP8 23

J

Jaanimagi, P.A. PO5 2
Jachmich, S. UO4 5, UO4 8
Jackson, G.L. CO4 6, CO4 11, CO4 15, JP8 81, JP8 83, JP8 84, JP8 102, NO4 10, **TI3 4**, TP8 37, UO4 9
Jackson, J. JO5 1
Jacobson, C.M. PP8 88, **PP8 91**
Jacobson, Craig PP8 95
Jacome, David **JP8 22**
Jacquet, L. TO7 9
Jaeger, E.F. CP8 16, **CP8 17**, CP8 26, GP8 59, PP8 30, PP8 77
Jaeger, F. CP8 23, NO4 9
Jafer, R. CP8 106
Jain, Neeraj **CO6 3**, PM9 7
Jakubowski, M.W. CO4 3
Jakubowski, Marcin NO4 5, UP8 76
Jamer, Michelle **JP8 29**
James, A.N. CO4 10, JP8 91, **JP8 95**, JP8 96, TP8 37, UO4 4
James, D.L. CP8 104
Jansen, K. UP8 97
Janvier, Miho PO6 6, **TP8 129**
Janzer, M.A. UO4 7
Jara-Almonte, J. **JP8 27**
Jarboe, T.R. GP8 49, JO4 13, JP8 65, **PP8 74**, UP8 19, UP8 20, UP8 21, UP8 22, UP8 23, UP8 24
Jardin, S.C. TP8 22, UP8 96, **UP8 97**
Jaspers, R. CP8 6
Jassem, N. UP8 145
Jaworski, M.A. **NP8 131**, PP8 45
Jayakumar, R.J. JP8 97
Jefferson, R.A. **JP8 38**
Jenkins, Thomas G. **GP8 58**
Jenko, F. BP8 31, BP8 39
Jennings, C. CP8 45, **JI2 4**, NP8 59, NP8 61, TO7 11
Jeon, Y.M. **XP8 45**
Jernigan, T.C. JP8 89, **JP8 90**, JP8 91, JP8 92, JP8 95, JP8 96, TP8 37, UO4 4
Ji, H. JP8 43, JP8 44, JP8 45, JP8 46, JP8 47, JP8 49, PM9 3, TP8 110, **TP8 111**, TP8 112, TP8 113, TP8 114, TP8 115, UP8 118, UP8 119, UP8 120, UP8 121, XP8 11
Ji, J.Y. **GP8 43**, GP8 58, GP8 61, UP8 82
Jimenez-Gomez, R. BO4 10
Jitsui, Tatsuya CO5 1, TO6 14
Jochmann, A. TO4 1
Joffrin, E. BO4 12, CO4 12
Johns, H.M. CP8 50
Johnson, B. UO7 5
Johnson, Blake PP8 110
Johnson, D. UO4 12
Johnson, Evan **CO6 4**
Johnson, J.A. JO6 13
Johnson, Jay UP8 111
Johnson, Jeffrey **TP8 140**
Johnson, M. PP8 67
Johnson, Megan NO6 12
Johnson, Micah BO6 5
Johnson, R.D. JP8 94
Johnson, R.P. GO6 3, PO5 12
Johnson, Robert **PP8 109**
Johnson III, J.A. JO6 8, JO6 9, JO6 10, JO6 11, JO6 12
Johnston, Mark **BO6 10**
Johnston, T.W. **CP8 79**
Johnston, Tudor EE1 1
Johzaki, T. **CP8 102**, CP8 112, NP8 91, XP8 25
Jones, A.D. PP8 88, **UP8 56**

Jones, Andrew PP8 95
Jones, B. CP8 45, JP8 65, NP8 59, NP8 61, NP8 77, **TO7 11**, TO7 13
Jones, F. NP8 47
Jones, O. **BO5 4**, BO5 9, BO5 10
Jones, Robert **PP8 90**
Jones, T.G. **GO6 11**
Jongewaard, E. NP8 27
Joseph, I. BP8 18, **NP8 112**, NP8 120
Joshi, C. GO6 12, GO6 13, JO5 6, JP8 130, JP8 141, NP8 31, TO4 2
Joyce, Glenn XP8 24
Jung, J.Y. NP8 4, NP8 95
Juo, J.R. NO4 3

K

Kabantsev, A.A. **BP8 74**, BP8 75
Kabcenell, A.N. JP8 61
Kadono, Toshihiko CO5 1
Kaehlert, Hanno JP8 55, **NO6 4**, UO6 11, UO6 12, **XP8 17**
Kagan, Grigory **UP8 78**
Kaganovich, Dmitri **JP8 124**, TO4 10
Kaganovich, Igor BP8 110, **CI2 2**, CP8 98, NP8 6, NP8 7
Kagei, Yasuhiro UP8 35
Kageiwa, N. GO6 4
Kaita, C. **JP8 45**, UP8 121
Kaita, R. CP8 43, JO4 2, PP8 37, PP8 38, PP8 39, PP8 40, PP8 43, PP8 44, PP8 45, **PP8 46**, PP8 47, PP8 54, PP8 67, PP8 68, PP8 82, PP8 88, PP8 89, PP8 91, PP8 92, PP8 93, PP8 95, UP8 56
Kakati, B. BP8 106
Kakuda, Hidetoshi PP8 96, PP8 97, PP8 100
Kalantar, D. BO5 2, BO5 3
Kalentev, Oleksandr CO7 2
Kalintchenko, G. JP8 122, JP8 140, TO4 3, TO4 8, TO4 11
Kalling, R. JP8 74
Kallman, J. PP8 38, PP8 39, PP8 43, PP8 44, **PP8 45**, PP8 46, PP8 69
Kalmykov, S. JP8 119, JP8 120, **JP8 121**, TO4 11
Kamada, Y. GP8 29, GP8 92
Kamataki, K. GP8 146
Kamdin, K. TP8 105, TP8 106
Kamio, S. PP8 98, PP8 99, PP8 100
Kampel, Nir XP8 53
Kaneko, Toshiro **NO6 13**, PO6 7
Kang, J. PP8 102
Kanki, Takashi **UP8 35**
Kanojia, A. PP8 19
Kant Shukla, Padma **XP8 18**, **XP8 19**, **XP8 20**
Kantsyrev, V.L. GO5 11, **GO5 13**, NP8 62, NP8 63, TO7 12
Kapitonov, V.A. TP8 59
Kaplan, D.H. JP8 114
Kaplan, E.J. JP8 26, UP8 122, **UP8 123**
Karasik, M. CP8 99, **JI2 5**, TO7 3, XP8 25
Karavaev, A. GP8 115, **GP8 116**, GP8 117
Kardon, B. **CP8 41**, UP8 50, UP8 52
Karimabadi, H. GP8 62, NM9 7, TP8 115, TP8 122, **UO6 8**
Karipides, Dan CP8 18
Kariya, T. BM9 3, BM9 4
Karle, Jeffrey **UP8 109**
Karnes, John TO5 10, **TO5 11**
Karni, Smadar TO5 8
Kasdin, Jeremy PP8 78, PP8 80
Kashyn, Dmytro **BO6 4**
Kasuya, N. GP8 146
Katanuma, I. BM9 3, BM9 4, **CM9 2**
Kato, T. UP8 143
Katsouleas, T. JP8 130, NP8 14
Katsouleas, Tom GO6 13, JP8 134
Katsuro-Hopkins, Oksana **PP8 79**
Katz, N. **JM9 8**, TP8 123, TP8 124, TP8 125, TP8 126, **XP8 21**
Kaufman, A.N. CP8 31
Kaufman, M.C. **TP8 63**, TP8 64
Kaufman, Michael CP8 25
Kaur, Sukhdeep **GP8 131**
Kausik, S.S. BP8 106
Kaw, P.K. NP8 126
Kaw, Predhiman CP8 97
Kawahata, K. BM9 4
Kawamura, Tohru TO6 7
Kawata, S. **PO5 10**
Kaye, S. JO4 3, PP8 47, PP8 48, PP8 49, PP8 62, PP8 65, PP8 66, PP8 70, UO4 6, UP8 83
Kazarian, F. NO4 9
Keesee, Amy JP8 16, **UP8 113**
Kehne, D. JO5 7, JO5 8
Keidar, M. BP8 109, **GI2 6**, NP8 39
Keiter, Paul CP8 38, **NP8 89**
Keith, M.R. GP8 89
Kellett, Barry UP8 110
Kellogg, Paul JO6 1
Kelly, Frederick **PP8 73**
Kelly, J.H. PO5 1
Kelly, Ralph GP8 109
Kemp, A. CP8 64, NO5 1, NO5 4, NO5 5, PO5 8, **UI2 6**
Kemp, David NP8 33
Kemp, E. CP8 53
Kendall, Mark **UP8 130**
Kendrick, R. GP8 96, GP8 97, GP8 98, JP8 26, JP8 27, UP8 122, UP8 123
Kerbel, G.D. **NP8 99**, NP8 100, NP8 101
Kersten, Kris JO6 1
Kesner, J. CP8 41, JP8 21, JP8 22, UP8 50, UP8 51, **UP8 52**, UP8 53, UP8 55, UP8 59
Kessel, C. GO4 2, JP8 102, PP8 7, **UO4 14**
Kessler, J. **JP8 70**
Key, M. CP8 105, NO5 4, PO5 9
Key, M.H. CP8 106, NO5 1, NO5 2, NO5 8, NO5 12, PO5 12
Key, M.K. CP8 53, CP8 103
Khalzov, I.V. UP8 124
Khalzov, Ivan **TP8 73**
Khoori, Essa NP8 81
Khoory, E. GO5 5, NP8 74, TO6 3
Khrabrov, Alexander V. **BP8 110**
Khudik, V.N. JP8 121
Khudik, Vladimir **CP8 98**, NP8 10, PP8 125
Kikuchi, Mitsuru **NO4 1**
Kikuchi, Y. GP8 7, UP8 15, **UP8 24**
Kilkenny, J. BO5 3, BO5 12
Kilkenny, J.D. BO5 14, UO5 7
Kim, C.C. GP8 41, GP8 48, GP8 49, GP8 95, NP8 114, UP8 23
Kim, Chang-Bae **XP8 44**
Kim, Charlson C. **GP8 44**
Kim, Deok-Kyu **BP8 67**
Kim, Dong Eon GO6 10
Kim, Doohyun **GP8 39**
Kim, E. BP8 41, CO6 7
Kim, Eun-jin **JO6 4**
Kim, H.K. XP8 45
Kim, Hyunseok **GP8 63**
Kim, Inho BP8 67
Kim, J. PP8 55, **PP8 68**
Kim, J.H. GP8 152
Kim, J.S. JP8 83, JP8 84, NP8 98
Kim, J.Y. XP8 45
Kim, Jason NP8 131
Kim, Jin-Soo GP8 8
Kim, Juhyung **BP8 51**
Kim, Ki Min GP8 39, **NP8 127**
Kim, KyongNam NP8 44
Kim, S.H. NO6 1
Kim, Su-Hyun BP8 94, NO6 2
Kim, Sung-jin UO7 4
Kim, W.C. XP8 45
Kimmel, M.W. JP8 145
Kimura, Tomoaki CO5 1, TO6 14
Kindel, J. CP8 46, GO5 6, **GO5 10**, JO6 3, NP8 75
King, J.D. **JP8 112**
King, Jacob **TP8 71**
Kinsey, J.E. GP8 64, JP8 99, JP8 101, TP8 10, **TP8 11**, TP8 12, UO4 15
Kionka, John CO7 5
Kirby, N. JP8 130
Kirk, Harold PP8 123
Kirkpatrick, A.M. UP8 20

Kirkpatrick, R. CP8 65
Kirkwood, R.K. **JO5 6**
Kirtley, David CO7 1, UO7 2, UO7 3
Kishimoto, Yasuaki BP8 30, **PO6 6**, TP8 129
Kitagawa, Yoneyoshi JP8 123
Kiyama, S. PP8 98
Klapisch, Marcel **NP8 105**
Klasky, S. BP8 35, GP8 55
Klassen, Mikhail UP8 58
Kletzing, Craig GP8 75
Kleva, R.G. **NP8 126**
Klimas, Alex PM9 5
Klimo, O. PO5 10
Kline, J. BO5 1, BO5 2, **BO5 3**, BO5 8, CP8 48, CP8 88, JO5 1, JO5 5
Klinger, Thomas PO6 2
Klir, Daniel CP8 61, **GO5 15**
Kluge, T. GO6 3
Knapp, P.F. GO5 8, GO5 9, NP8 66, NP8 70
Knapp, Patrick **NP8 65**, NP8 76
Knauer, J. BO5 14
Knauer, J.P. CP8 49, UO5 8, UO5 10, **XI2 1**
Knecht, S.D. UP8 36, **UP8 38**
Kneip, S. **TO4 8**
Knoll, Dana PP8 116
Knowlton, S. GP8 121, **TP8 105**, TP8 106, TP8 107
Knudson, Marcus **JI2 1**
Ko, J. PP8 7, **PP8 17**, PP8 18
Kobayashi, H. PP8 96, PP8 97, PP8 98, PP8 100
Kobayashi, Kenichi BP8 21
Kobayashi, Masahiro **PI2 4**
Koch, J. BO5 12, CP8 50
Koch, Norbert CO7 2
Kodama, R. CO5 1, GO6 5, TO6 14, UP8 143
Koenig, M. UP8 143
Koenig, Mihcel TO6 14
Koepke, Mark CP8 15
Koert, P. PP8 9, PP8 32
Koga, James GO6 9
Koguchi, H. PP8 98
Kohno, Haruhiko **CP8 20**
Kolemen, E. JO4 4, PP8 45, PP8 78, **PP8 80**
Kolesnichenko, Ya.I. JP8 108
Kolesnikov, R. BP8 19, **PP8 49**, UP8 83
Koliner, J.J. **GP8 129**
Kolmogorov, V.V. TP8 59
Kominis, Y. **CP8 27**, CP8 28, CP8 29
Kon, A. GO6 5
Kondo, Kiminori JP8 123
Kondo, Kotaro **TO6 7**
Kondo, Tadashi CO5 1
Kong, D.F. XP8 59
Kong, Jie **NO6 9**, NO6 10, NO6 11
Kong, Q. PO5 10
Kong, X. CP8 6
Kong, Xianglong **JP8 138**, UP8 136
Koning, J.M. NP8 100, **NP8 101**
Konishi, Y. TP8 89, TP8 90, TP8 92
Korein, M. **JP8 48**, TP8 141
Koslowski, R. BO4 12, UP8 89
Kostora, M. NP8 85, TP8 143, TP8 144
Kosuga, Y. BP8 54, **BP8 61**
Kotschenreuther, M. GP8 4
Kovaleski, S.D. NP8 50
Kovaleski, Scott BO6 12, NP8 17
Kowal, Grzegorz CO6 9, PM9 1
Kowalski, E.J. GP8 15
Kozub, T. PP8 88, PP8 89, PP8 92, PP8 95
Kozue, Kazuki NP8 54
Kraft, S. GO6 1, **TO4 1**
Kramer, G. GO4 5, GO4 12, JP8 109, **JP8 110**, PP8 27, PP8 56, PP8 58
Krasheninnikov, S. JP8 146, NP8 115, NP8 122, **NP8 128**, PP8 41
Krasheninnikova, Natalia **BI3 6**, BP8 5, BP8 6
Krasny, Robert PP8 112
Krauland, C.M. CP8 49
Krauland, Christine **UP8 146**
Krauter, K. JO5 1
Kravarik, Jozef CP8 61, GO5 15
Krishnan, Mahadevan GO5 14
Kritcher, A.L. PO5 3
Kritcher, Andrea **XP8 49**
Kritz, A.H. CM9 12, **GP8 11**, GP8 36, GP8 51, GP8 53, GP8 54, GP8 55, JP8 54, UP8 79
Kroll, Mattias **NO6 5**
Krommes, J. **BP8 17**, TP8 108
Kroupp, E. NP8 78
Kruer, William **CP8 91**
Kruezi, U. UO4 5
Kruger, S.E. GP8 58, GP8 93, **GP8 99**, NP8 113, NP8 114, NP8 122, PP8 117, PP8 118, UP8 80, UP8 81, UP8 100, UP8 101
Krushelnick, K. CP8 70, **FR1 1**, JP8 122, JP8 139, JP8 140, TO4 3, TO4 8
Krushelnik, K. TO4 11
Krygier, A.G. CP8 76
Ku, S. BP8 26, **BP8 28**, BP8 35, BP8 47, CM9 12, GP8 53, GP8 54, GP8 55, NP8 125
Kubes, Pavel CP8 60, CP8 61, GO5 15
Kubota, S. JP8 17, PP8 55, PP8 56, PP8 57, PP8 58, PP8 63, **PP8 64**, PP8 70
Kudryavtsev, Anatoly **PP8 120**
Kudyakov, Timur **NO4 5**, UP8 76
Kugel, H.W. JO4 2, JO4 6, JO4 8, PP8 36, PP8 37, PP8 38, PP8 40, PP8 41, **PP8 44**, PP8 45, PP8 46, PP8 47, PP8 74, XP8 60
Kugland, N.L. **PO5 8**
Kugland, Nathan GP8 140, TO6 1
Kuhn, Siegbert NP8 123
Kujak-Ford, B.A. PP8 85, PP8 87
Kulcinski, Gerald CM9 4
Kulsrud, R. JP8 50, TP8 110
Kumar, Deepak **UP8 29**, UP8 131
Kumar, G. Ravindra CP8 97
Kumar, Santhosh TP8 42, TP8 57, **TP8 58**, TP8 62, XP8 5
Kung, E. GP8 78
Kuniyoshi, Masaya UP8 108
Kuramitsu, Y. UP8 143
Kuranz, C.C. CP8 49, JP8 12, JP8 13, UP8 145, UP8 146, UP8 147, **UP8 148**
Kurashina, Hiroki PP8 96, PP8 97, PP8 100
Kurita, G. GP8 92
Kuritsyn, A. TP8 68
Kusche, K. JP8 135, JP8 136, TO4 15, XP8 46
Kusse, B.R. GO5 9, NP8 66, NP8 72
Kusse, Bruce GO5 7, NP8 65, NP8 67
Kuwabara, Hajime JP8 123
Kuznetsova, Masha PM9 5
Kwan, J.W. BO6 14, CP8 4, **NP8 4**
Kwan, Thomas **NP8 86**
Kwon, J.W. NP8 50
Kwon, Jae NP8 17
Kyrala, G. BO5 6, **BO5 7**, NP8 90, UO5 12
Kyralla, G. BO5 2

L

La Haye, R.J. CO4 5, CO4 6, **GI3 3**, JP8 81, JP8 83, JP8 84, JP8 87, JP8 95, JP8 98, JP8 101, **JM9 4**, PP8 50, UO4 15, UP8 100
La Plante, Paul **JP8 23**
Labe, K.R. **JP8 49**
Labik, G. PP8 83
Labit, B. GP8 77, GP8 78
LaBombard, B. GO4 2, GO4 7, GO4 9, GO4 10, GO4 11, **PP8 20**, PP8 21, PP8 22, PP8 23, UO4 10
Laffite, Stephane CP8 114
Laity, George **CO7 3**
Lake, P.W. TO6 10

Lamalle, P. CP8 17, **NO4 9**
Lambert, Flavien CO5 7
Lampe, Martin XP8 24
Lan, T. **XP8 59**
Lan, Tao XP8 58
Lancaster, Kate GO6 4
Lanctot, M.J. **CO4 6**, CO4 15, JP8 80, JP8 81, JP8 82, JP8 83, JP8 84
Land, Victor BP8 103, **NO6 8**
Landen, O.L. BO5 2, BO5 3, BO5 7, BO5 8, BO5 9, BO5 12, BO5 14, CO5 2, CO5 3, JO5 6, **NI2 1**, PO5 3, TO5 1, UO5 13, XP8 49
Landes, Arjun **JP8 51**
Landoas, O. BO5 11, BO5 12, TO7 4
Landreman, Matt **TP8 94**
Lang, J. BP8 29, **GP8 72**, GP8 126, UP8 83
Lang, P.T. NP8 127
Langdon, A.B. JO5 4, JO5 5, TO5 5, XP8 33
Langdon, B. **CP8 90**, JP8 144
Langer, S.H. BO5 1, BO5 4
Lanier, Nick CP8 38, NP8 89
Lao, L.L. BO4 5, CO4 10, GP8 64, JP8 80, JP8 85, JP8 86, **JP8 87**, JP8 99, JP8 100
Lapenta, Giovanni CO6 1, **CO6 6**, GM9 6, **PM9 6**
Larson, D. BO5 3, GM9 4, NO5 4, NP8 100, **UP8 140**
Lasinski, Barbara CP8 100
Laskinski, Barbara NO5 4
Lasnier, C.J. CO4 3, JP8 75, JP8 95, NO4 10, TP8 24, TP8 25, **TP8 27**, TP8 28, TP8 29
Lason, D. NO5 1
Lau, Cornwall **PP8 31**
Lau, Y.Y. NP8 18, NP8 19, NP8 20, NP8 21, **NP8 22**, NP8 23, NP8 64, NP8 79, NP8 80
Lauck, R. NO5 3, TO7 6
Laurent, Villard BO4 1
Lawrence, Eric **BI2 2**, NM9 3
Lazarian, Alex **CO6 9**, PM9 1
Lazarus, E.A. JP8 108, **TP8 23**
Le, A. **BI2 4**, JM9 8, TP8 123, TP8 124, **TP8 125**, TP8 126, XP8 21
Le Corre, T. JP8 125
Le Pape, S. BO5 3, CP8 53, CP8 103, CP8 105, GO6 2, NO5 1, NO5 2, NO5 4, PO5 3, PO5 12, XP8 16
Leach, Christopher GP8 109, **GP8 110**
Lebedev, Sergey GO5 1, **GO5 5**, NP8 74, NP8 81, TO6 3
LeBlanc, B.P. JO4 3, JO4 9, JO4 10, **JO4 11**, JP8 67, PP8 37, PP8 46, PP8 47, PP8 48, PP8 53, PP8 56, PP8 57, PP8 58, PP8 59, PP8 67, PP8 75, PP8 77, PP8 88, PP8 91, PP8 95, UO4 6
Leblanc, Philippe **CP8 63**
LeBlanc, S. BP8 105
Leboeuf, J.N. **BP8 32**, BP8 33, BP8 62, GO5 6, JO6 3
Leccacorvi, R. PP8 19
Lecherbourg, L. BP8 69
Lechte, Carsten **CP8 9**
Leckbee, Joshua BO6 10
Lecoanet, Daniel **JP8 50**
Lee, C. **BP8 55**
Lee, E.P. NP8 4
Lee, H.J. **CO5 3**, PO5 3
Lee, Hae Ja XP8 49
Lee, Hae June GO6 10, TO4 7
Lee, Hyunyeong PP8 102
Lee, Jungpyo **PP8 4**
Lee, K.C. PP8 55, **PP8 67**, PP8 68, PP8 82
Lee, K.Y. **UP8 7**
Lee, Kitae GO6 10
Lee, Matt NP8 131
Lee, Myoung-Jae **BP8 104**
Lee, Paul XP8 42
Lee, R.W. CO5 3
Lee, S.G. NP8 47, UO4 12
Lee, W. GP8 40
Lee, W.W. **BP8 19**, PP8 49, PP8 65, UP8 83
Lee, Wei-Li BP8 21, JP8 58
Lee, Wonjae GP8 63
Leemans, Wim JP8 125, JP8 126, JP8 127, JP8 129, TO4 6, TO4 11, TO4 14
Leeper, R.J. TO7 14
Leeper, Ramon TO5 9
Lefebvre, B. TP8 123
Lehmberg, R.H. JO5 7, JO5 8
Lehnen, M. NO4 5, UO4 5, UP8 76
Lehr, F.M. TP8 143
Leitner, M. NP8 4, NP8 110
Leitner, M.A. NP8 95
Lemke, R.W. CO5 6
Lemons, Don PP8 110, PP8 114, **PP8 115**
Leonard, A.W. CO4 13, CO4 14, JP8 105, NO4 10, TP8 18, TP8 19, TP8 21, TP8 27, TP8 28, TP8 29, TP8 30, **TP8 32**, TP8 33
Leonard, Anthony GP8 5
LePape, Sebastien BO5 2, **JI2 3**
LePell, P.D. TO7 13
Leprovost, N. **CO6 7**
Lepson, J.K. **PP8 39**
Lerche, E. NO4 9
Letzring, S. CP8 39, CP8 58, GO6 3, PO5 12
Leuer, J.A. **CO4 11**
Leung, K.N. CP8 4
Levesque, J.P. GP8 22, GP8 23, **GP8 24**, GP8 25, GP8 26, GP8 27
Levin, Yan NP8 11
Levinton, F.M. CP8 4, **GP8 9**, JO4 3, JP8 66, NO4 8, PP8 56, PP8 58
Lewicki, B.T. JO4 7, PP8 85, PP8 87
Li, Bo **UP8 63**, UP8 64
Li, C.K. BO5 11, BO5 12, BO5 13, **BO5 14**, CP8 54, CP8 55, CP8 56, CP8 59, CP8 62, TO7 5, UO5 8, XP8 68
Li, Ding XP8 64
Li, G. BO4 5, **CP8 110**, JP8 85, JP8 86, JP8 87, PO5 6
Li, Gang **XP8 66**
Li, Hui BP8 45, BP8 111, GM9 7, NM9 8, UP8 133, UP8 155, XP8 22, XP8 23, **XP8 39**
Li, J. NO4 2
Li, J.G. XP8 59
Li, Jiangang **BI3 3**
Li, Jiquan BP8 30, PO6 6, TP8 129
Li, Q. NO4 2
Li, Shengtai XP8 23
Li, Xiaoying **BP8 66**
Li, Zebing BP8 13
Liang, Edison **GM9 7**, **NO6 14**, NM9 8
Liang, Rongqing **BP8 13**
Liang, T. CP8 6, **GP8 40**
Liang, Y. UP8 89
Liao, K.T. PP8 13, PP8 14, **PP8 28**, UP8 64
Lidia, S.M. CP8 57, **NP8 2**, NP8 3, NP8 95
Lifshitz, Asaf XP8 53
Light, A. **UP8 13**
Lima, Reinaldo CO6 9
Limbach, S. TP8 42, TP8 59
Limpouch, J. PO5 10
Lin, C. JP8 125
Lin, L. GO4 5, GO4 6, GM9 2, PP8 30, **TP8 43**, TP8 42, TP8 45
Lin, Liang **KI3 2**
Lin, Y. GO4 5, **GO4 6**, GO4 7, PP8 30, PP8 32
Lin, Yijun PP8 12, PP8 31
Lin, Yu **UP8 111**, UP8 112
Lin, Z. BO4 2, PO6 8, TP8 9, UP8 74, UP8 114
Lindemuth, Irvin TP8 161
Lindl, J. BO5 5, TO5 1, UO5 13
Lindon, Michael **BP8 9**
Ling, Zhihong UP8 127
Link, A. CP8 53, CP8 76, **NO5 12**, PO5 9
Linker, Jon NM9 2
Lipaev, A.M. NO6 7
Lipschultz, B. GO4 2, GO4 7, GP8 5, PP8 20, PP8 23, PP8 25, **UO4 10**
Lipscombe, Trevor **PP8 110**
Lisgo, S. TP8 30
Litseva, Ekaterina **CP8 60**
Litvak, Alexander **NP8 35**

Litz, Marc TO7 8
Liu, A.D. XP8 59
Liu, Adi XP8 58
Liu, Bin NO6 7
Liu, C. JP8 113
Liu, Chuan S. CP8 68
Liu, D. PP8 56, PP8 57, **PP8 76**
Liu, Fei UP8 31, UP8 32, **UP8 33**
Liu, H.L. JO6 4
Liu, Kaijun **PP8 114**, PP8 115
Liu, T.C. CP8 68
Liu, Wandong XP8 58
Liu, Wei GM9 7, **NM9 8**, UP8 133, **XP8 22**, **XP8 23**
Liu, Y.Q. BO4 12, CO4 6, JP8 80, JP8 81, JP8 83, JP8 85
Liu, Yi-Hsin PM9 9
Liu, Yue TP8 128
Lloyd, B. PP8 84
Loarte, A. CP8 17, NO4 9
Lobo, Carlos **NP8 46**
Lockard, T. CP8 48, GO6 3
LoDestro, L.L. JP8 97, **UP8 26**
Logan, B.G. NP8 4, NP8 5, NP8 93, NP8 94, NP8 95, TO5 2
Lohr, J. CO4 11, **JP8 103**, JP8 104, JP8 105
Loiseau, Pascal CP8 114
Lomas, P. CO4 13
Lominadze, J.G. GP8 152
Lomonosov, Igor CO5 13
London, R. JO5 1, JO5 2, **JO5 3**, JP8 144, PO5 14, UO6 15
Longcope, Dana **NM9 4**
Loomis, Eric **NI2 6**
Lopez, Frand CP8 58
Lopez, M.R. NP8 64, NP8 79
Lore, J. **NI3 6**, TP8 103, TP8 104
Lorenz, Thomas CO5 10
Lorenzini, R. TP8 77
Lotz, D. CP8 14, UP8 4
Loucks, S.J. PO5 1
Loupias, B. BP8 69, UP8 143
Loureiro, J. GP8 105
Loureiro, Nuno **CO6 8**, PM9 2, TP8 120, TP8 134
Loverich, John TP8 157, **TP8 158**
Loving, A. UP8 89
Lowenstern, M.E. GO6 3, UP8 145
Lowernstern, Mariano UP8 151
Lowrie, Robert TO6 5
Lowrie, Weston **GP8 46**
Lowry, C.G. **UP8 89**
Lu, T. TP8 36
Lu, W. **GO6 13**, JP8 130, JP8 131, TO4 2
Lu, Xing-Qiang TP8 127
Luce, T.C. **AR1 1**, CO4 5, CO4 12, JP8 76, JP8 87, JP8 97, JP8 98, JP8 99, JP8 100, JP8 101, JP8 102, JP8 111, TP8 25, TP8 38, UO4 9, UO4 15, XP8 38
Ludescher-Furth, Christiane GP8 51
Ludwig, Patrick **UO6 11**, XP8 24
Luginsland, J. NP8 18, NP8 20, NP8 22
Luhmann, N.C. JO4 3
Luhmann Jr., N.C. **CP8 6**, GP8 40, PP8 67, PP8 68, PP8 82, UP8 102
Lui, Chuan JP8 143
Lukin, V.S. GP8 42, GP8 46, GP8 47, JP8 48
Lund, S.M. NP8 110
Lundberg, D.P. GO4 11, PP8 71, PP8 88, **PP8 92**
Lundberg, Daniel PP8 95
Luo, G.N. NO4 2
Luo, X. TP8 22, UP8 97
Luther, Brad NP8 33
Lutsenko, V.V. JP8 108
Lynn, A.G. GP8 106, GP8 109, TP8 143, TP8 144, TP8 147, TP8 152, UP8 133, **UP8 134**
Lyons, Brendan C. **JP8 41**
Lyssoivan, A. NO4 9

M

Ma, T. CP8 66, CP8 106, NO5 1, NO5 2, NO5 8
Ma, Y.Y. PO5 10
Ma, Yunxing **PP8 15**, PP8 16
Ma, Zhi-Wei **TP8 127**
Maassberg, H. GP8 56
MacFarlane, J.J. **NP8 104**, TO6 10, TO7 14
Macgearailt, Niall NP8 37
MacGowan, B. BO5 2, BO5 3, JO5 1, TO5 1
Mackinnon, A.J. CP8 53, CP8 103, CP8 104, CP8 105, CP8 106, GO6 2, JP8 142, NO5 1, NO5 2, NO5 4, NO5 12, PO5 2, PO5 9, PO5 12, XP8 16
Maclaren, Stephan TO7 7
Macnab, Angus CP8 34, **CP8 35**
MacPhee, A.G. CP8 53, CP8 103, CP8 104, CP8 105, GO6 2, NO5 1, NO5 2, NO5 4
Madden, Robert GO5 14
Madsen, Niels **BP8 78**
Maeyama, Shinya **UP8 71**
Magee, E.W. CP8 12
Magee, Ed CP8 52, JP8 5
Magee, R.M. TP8 42, TP8 58, TP8 62
Magee, Richard **TP8 57**
Magelssen, G.R. **NP8 82**
Magelssen, Glenn NP8 89, UO5 6
Maggiora, R. CP8 24, CP8 33, NO4 9
Maggs, J.E. GP8 151, **PO6 3**
Mahajan, S.M. UP8 116
Mahajan, Swadesh BP8 111, UP8 141
Mahdavi, M.A. CO4 2
Maingi, Logan **JP8 57**
Maingi, R. GP8 5, JO4 2, JO4 5, JO4 6, JP8 68, **PI2 3**, PP8 36, PP8 37, PP8 41, PP8 43, PP8 44, PP8 45, PP8 46, PP8 70, PP8 72, PP8 73, PP8 75, TP8 26, UO4 6
Majeski, R. PP8 44, **PP8 88**, PP8 89, PP8 91, PP8 92, PP8 93, PP8 94, PP8 95
Majoribanks, R. BP8 69
Majumdar, A. UO6 8
Makhin, V. TP8 143
Makowski, M.A. JP8 74, JP8 75, JP8 112, TP8 12, TP8 27, **TP8 28**
Makrinich, Gennady **BP8 108**, JO6 7
Maksimchuk, A. CP8 70, GO6 8, JP8 122, JP8 139, JP8 140, TO4 3, TO4 11
Maksimchuk, G. TO4 8
Maksimov, Vladimir UP8 46
Maksimovic, Milan JO6 1
Makwana, K.D. **BP8 46**
Malik, Anil Kumar **GO6 7**
Malik, Hitender Kumar GO6 7
Malkin, V. **CP8 81**, JO5 6
Malkov, M. BP8 44, **UP8 75**
Mallick, Bani UP8 149
Maloney, A.D. PP8 117
Malony, Allen PP8 118
Mamun, A.A. **BP8 92**
Manchester, W. UP8 134
Mancini, R.C. CP8 50, **CP8 51**, NP8 75, PO5 5, TO6 10
Manfredi, Giovanni XP8 19
Mangles, S.P.D. TO4 8
Manickam, J. PP8 53
Manka, C. JO5 7, JO5 8
Mansfield, D. JO4 2, JP8 69, PP8 19, **PP8 36**, PP8 43, PP8 44
Mantovani, S. GP8 21
Manuel, M. BO5 13, CP8 41, **CP8 56**, CP8 59, CP8 62, XP8 68
Mao, J.S. **NO4 3**
Maqueda, R. **PP8 69**, PP8 70, PP8 71
Maraschek, M. GP8 34, **UO4 2**
Marchiori, G. TP8 77, TP8 83
Marconi, Mario UP8 144
Marinak, M.M. BO5 4, BO5 9, NO5 6, NP8 99, **NP8 100**, NP8 101, NP8 102, TO5 1, TO5 3
Marine, T. TP8 99
Marion, D.C. **UP8 145**, UP8 148
Markhotok, Anna **GP8 91**
Markidis, S. CO6 6
Marklin, G.J. **GP8 45**, UO7 2, UP8 19, UP8 21

Marleau, Gabriel-Dominique **JP8 55**
Marmar, E. **GO4 2**, GO4 4, GO4 6, GO4 7, GO4 12, PP8 19
Maron, Y. CP8 45, JO6 6, NP8 76, NP8 78, TO7 11
Marozas, J.A. UO5 1, **UO5 5**, UO5 7
Marrelli, L. JP8 83, JP8 84, TP8 79, TP8 81
Marrelli, Lionello **TP8 82**, TP8 83
Marrs, Ross TO7 7
Marsala, R. XP8 60
Marsh, K. JP8 130, TO4 2
Marshall, F.J. BO5 13, NO5 3, TO7 2, TO7 4, UO5 3, **UO5 8**
Marshall, K.L. TO7 6
Martel, P. GP8 70
Martin, D. NP8 118
Martin, Matthew NP8 65
Martin, Michael **JP8 14**
Martin, P. JP8 83, JP8 84
Martin, Pablo BP8 99, **GP8 28**
Martin, Piero **NI3 5**, **TP8 76**
Martin, William TO5 8
Martinell, Julio **BP8 34**
Martines, Emilio TP8 87
Martinez, B.M. NP8 85
Martinez, D. GO5 12, TO6 6
Martinez, Mikael JP8 119
Martins, J. CP8 71, JP8 133, NP8 108, TO4 8, **UP8 137**
Martins, Luciano C. XP8 27
Martins, S.F. JO5 6, NP8 108, TO4 2, TO4 8, UP8 137
Martins, Samuel BP8 66, NP8 31, **UI2 3**
Martz, Dale NP8 33
Masamune, S. **TP8 89**, TP8 90, TP8 91, TP8 92
Mashimo, Tsutomu TO6 14
Mason, R.J. **CP8 65**, CP8 66, NP8 56
Masser, Thomas **TO6 5**
Masson-Laborde, Paul-Edouard **CP8 114**
Mastovsky, I. NP8 26
Matlis, N.H. JP8 125, TO4 11
Matlis, Nicholas **TO4 6**
Matsukawa, M. GP8 92
Matsunaga, G. **GP8 92**
Matsuoka, T. **JP8 122**, JP8 140, TO4 3, TO4 8, TO4 11
Matsuzawa, Haduki PP8 97
Matsuzawa, Hazuki PP8 96
Matthaeus, William PM9 4, XP8 61, XP8 62
Matthews, Lorin BP8 100, BP8 101, BP8 102, BP8 103, NO6 8, NO6 9, NO6 10, NO6 11, NO6 12
Mattsson, T.R. **CO5 6**
Matyash, Konstantin CO7 2
Mauel, M.E. GP8 22, GP8 23, GP8 24, GP8 25, GP8 26, GP8 27, JP8 21, UP8 50, **UP8 51**, UP8 52, UP8 53, UP8 54, UP8 55, UP8 57, UP8 58, UP8 59
Mauk, B. GM9 4
Maurer, D.A. GP8 22, **GP8 23**, GP8 24, GP8 25, GP8 26, GP8 27
Maximov, A.V. CP8 93, JO5 10, **JO5 11**, JO5 13, JO5 14, JO5 15, UO5 10
May, J. CP8 101, CP8 109, **CP8 111**
May, M. CO5 9, CP8 37, **NP8 84**, TO7 10
Maynard, Gilles NP8 83
Mazaheri, Kavous BO6 14
Mazarakis, M.G. NP8 64, NP8 79
Mazevet, Stephane CO5 7
Mazzucato, E. JO4 3, JO4 11, PP8 62, PP8 65
McAlpin, Stuart **CP8 83**
McCollam, K.J. **TP8 61**, TP8 62
McConville, Sandra **UP8 110**
McCormick, M. CP8 75
McCrory, R.L. CO5 2, PO5 1, UO5 2, UO5 7, UO5 9, UO5 11
McCune, D. GP8 11, **GP8 51**, GP8 52, GP8 64, JP8 60, JP8 99, JP8 102, PP8 117, PP8 118
McDermott, R. GO4 2, GO4 13
McDevitt, C. BP8 54, **UP8 67**
McFadden, J. GM9 4
McGahan, Christina JP8 34, **JP8 35**
McGann, M. UO6 4, XP8 5
McGarry, M.B. TP8 42, **TP8 53**, TP8 54, TP8 55
McGraw, Sean **JP8 52**
McGuffey, C. JP8 122, JP8 140, TO4 3, TO4 8, TO4 11
McGuire, Sean **JP8 77**
McInnes, L. PP8 117, PP8 118
McJill, J.M. GP8 19
McKee, G.R. CO4 14, JP8 109, JP8 116, PP8 83, TP8 5, TP8 6, TP8 7, **TP8 8**, TP8 9, TP8 12, TP8 14, TP8 19
McKenna, Paul XP8 46
McKenty, P.W. TO5 3, UO5 3, **UO5 7**, UO5 8, UO5 9
McKinley, Michael S. NP8 102
McLean, Adam **PI2 5**
McLean, E. JO5 7, JO5 8
McLean, H.S. CP8 12, CP8 53, CP8 103, CP8 104, CP8 105, CP8 106, **CM9 11**, NO5 1, NO5 2, NO5 4, NO5 8, PO5 12, UP8 26
McMaster, Brooks BP8 102
McMillan, Ben **BO4 1**
McNabb, D.P. BO6 7
McNabb, Dennis BO6 5, BO6 6, NP8 28
McNaney, J.M. XP8 16
McWilliams, Roger GP8 76, UP8 11, UP8 12
Medley, S.S. PP8 48, PP8 55, PP8 56, PP8 58, **PP8 59**, PP8 76
Medvedev, Mikhail **TO6 11**, UP8 138, UP8 156
Meeker, Don CP8 100, NO5 4
Meezan, N. BO5 1, BO5 2, BO5 3, BO5 5, BO5 6, BO5 7, JO5 1, JO5 2, JO5 6, **QI3 1**
Mehlhorn, T.A. BP8 70, GO5 6, NP8 64
Meier, E.T. **GP8 47**
Meige, A. GP8 134
Meitner, S. GP8 19, JP8 90, NP8 40, PP8 94
Melnik, P.A. UP8 2, UP8 3, **UP8 4**
Melrose, Don JO6 2
Menard, J. JO4 9, **PP8 35**, PP8 37, PP8 51, PP8 53, PP8 73, PP8 81, PP8 89, UO4 6, UP8 56
Mendonca, J.T. GP8 81, GP8 105, **PO6 11**
Mendonca, Jose Tito GP8 104
Meneghini, O. GO4 8, **PP8 3**, PP8 5, PP8 7, PP8 32
Mengin, G. GP8 96, GP8 97, GP8 98
Merali, Aliya **JP8 39**
Merkel, George TO7 8
Merlino, R.L. BP8 94, BP8 96, NO6 1, **NO6 2**
Merritt, Elizabeth **TP8 152**
Mertens, Ph. UO4 8
Merz, F. BP8 39
Messer, S. TP8 150, TP8 153, TP8 154, UP8 39, **UP8 48**
Messerly, M. BO6 5, BO6 6, BO6 7, NP8 28
Messiaen, A. NO4 9
Messmer, Peter TO4 12
Metzkes, J. GO6 1
Metzler, N. CP8 99, TO7 3
Meyer, O. JP8 115
Meyer, W.H. TP8 38
Meyerhofer, D.D. BO5 13, BO5 14, CO5 2, CO5 4, CO5 12, CP8 59, NO5 3, NO5 7, **PO5 1**, PO5 2, PO5 13, TO7 2, UO5 1, UO5 2, UO5 3, UO5 7, UO5 11
Meyerson, D.F. **XP8 38**
Mezonlin, E.D. **JO6 10**, JO6 11, JO6 12
Miah, M. NP8 122, PP8 118
Michael, Clive **JO4 15**
Michael, P. PP8 19, UP8 50, **UP8 59**

Micheau, Samuel NO5 10, **NO5 13**
Michel, P. BO5 2, BO5 5, JO5 1, JO5 6, **QI3 3**, TO5 5
Migliori, S. GP8 19, NO4 15
Miki, Kazuhiro **PO6 8**
Mikic, Zoran NM9 2
Mikkelsen, D. BP8 36, GO4 4, **PP8 10**, PP8 12, PP8 66, TP8 100
Milanesio, D. **CP8 24**, NO4 9
Milchberg, Howard CP8 77
Miles, Aaron **GO5 4**
Miles, C.J. **JP8 75**
Miles, R.B. NP8 39
Miley, George NP8 92, **UO7 4**
Militze, B. CO5 5
Miller, K.E. **CP8 14**, UP8 2, UP8 5, UP8 6
Miller, Ken UP8 49
Miller, M.C. JM9 7, TP8 62, **TP8 68**, TP8 70
Milosavljevic, Vladimir NP8 37
Milovich, J. **BO5 9**, BO5 10, BO5 12, BO5 14
Milovich, Jose BO5 8, TO7 5
Milroy, R.D. CO7 1, GP8 41, **GP8 48**, GP8 49, UO7 2, UP8 2, UP8 3, UP8 6
Mima, Kunioki CO5 1, CP8 69, CP8 102, CP8 112
Minami, R. BM9 3, BM9 4
Minervini, Joseph TP8 101
Ming, T.F. NO4 2
Mingaleev, A.R. NP8 71
Minguez, E. GP8 70
Mirnov, S.V. **NP8 129**
Mirnov, V.V. CP8 5, JM9 7, TP8 70, TP8 71, TP8 73, **UP8 93**
Mirza, Ahmed TP8 88
Mishra, Rohini **PO5 5**
Mitchell, Travis XP8 61, XP8 62
Mithen, J. PO5 13
Mitic, S. BP8 97
Mitrani, J.M. **CP8 44**
Mitteau, R. NO4 9
Miura, H. UP8 116
Miyanishi, Kohei CO5 1, TO6 14
Miyata, Y. BM9 3, BM9 4
Mizuguchi, M. BM9 4
Mizushima, Tatsunori XP8 47
Moeller, C.P. JP8 103, JP8 105
Moiseenko, V.E. CM9 5
Molander, William NP8 29
Molotkov, V.I. NO6 7
Molvik, A.W. **CM9 6**, **UP8 45**
Montgomery, Andrea **UP8 101**
Montgomery, D.S. CP8 39, **CP8 48**, GO6 3, PO5 12
Montgomery, David XP8 62
Monticello, D. TP8 108
Moody, J. BO5 2, **JO5 1**, JO5 3
Moon, Chanho **PO6 7**
Moon, Stephen TO7 10, UP8 144
Morace, A. CP8 103, CP8 105
Moradi, Sara **XP8 56**
Morales, C.H. UP8 48
Morales, Cristina **JP8 78**
Morales, G.J. CP8 96, **GP8 151**, PO6 3
Moran, M.J. TO7 6
Moraru, Augustin UP8 88
Mordijck, S. CO4 3, **CO4 4**, JP8 88, TP8 25
More, R.M. JP8 144, NP8 93, NP8 95, NP8 96, UO6 10, XP8 13
Morfill, G.E. BP8 93, NO6 1, NO6 7
Morgan, James JP8 3, JP8 4, JP8 6
Morgan, P.D. UO4 5
Mori, Warren BP8 66, CP8 94, **CP8 95**, CP8 96, CP8 101, CP8 109, CP8 110, CP8 111, GO6 13, JP8 130, JP8 131, JP8 132, JP8 134, JP8 141, NP8 106, NP8 108, TO4 2, TO5 6
Mori, Wayne D. BP8 66
Mori, Yoshitaka **JP8 123**
Morice, Olivier XP8 54
Morikawa, Junji XP8 47
Morita, S. NP8 47
Morita, T. UP8 143
Moroz, Paul **NP8 36**
Morris, A. PP8 117, PP8 118
Morris, K. UO4 12
Morrison, J.T. **CP8 76**
Morrison, P.J. PP8 108, PP8 111, UP8 66
Morrison, Philip GP8 153
Morse, E.C. JP8 112
Morse, S.F.B. PO5 1
Morton, John NP8 89
Morton, Lucas TO6 1
Moser, A.L. **UP8 28**
Moses, E. BO5 2
Moses, Gregory CP8 85, NP8 103
Moss, James CO7 3
Motoi, H. TP8 89
Motomura, Taisei GP8 112, **GP8 113**
Motta, Brian TO5 10, TO5 11
Moyer, R.A. CO4 3, CO4 4, JP8 88, JP8 89, JP8 101, NO4 10, TP8 8, TP8 29
Mucino, J.E. GO6 3
Mueller, D. CO4 11, **JO4 13**, PP8 37, PP8 74
Muggli, Patric BP8 66, GO6 13, JP8 130, JP8 134, **JP8 135**, JP8 136, NP8 14, **TO4 15**
Mukherjee, A. NO4 9
Mulas, Roberta XP8 65
Muller, S. GP8 78
Muller, S.H. **BP8 40**, GP8 138, GP8 139
Mumgaard, Bob PP8 17
Mumgaard, R. **PP8 18**
Munro, D.H. TO5 1, UO5 7
Munsat, T. BP8 105, CP8 7, CP8 8, PP8 70, UP8 13
Munsat, Tobin **UP8 102**
Murakami, M. CP8 99, JP8 97, **JP8 99**, JP8 100, JP8 101, JP8 106, NO4 11, TP8 9
Murakami, Masakatsu **CP8 69**, NP8 91, **XP8 25**
Murakami, S. BO4 4, GP8 56
Murillo, M. CP8 48, JP8 144, UO6 10, UO6 15, XP8 13
Murphy, C.D. JP8 139, PO5 13
Murray, R. PP8 19
Murtas, F. CP8 11
Muscatello, C.M. **JP8 108**
Musumeci, Pietro GO6 12
Mutzke, Andreas CO7 2
Myatt, J.F. JO5 10, JO5 11, **JO5 13**, JO5 14, JO5 15, NO5 7, NO5 8, PO5 2, PO5 13
Myers, Clayton E. **UP8 18**
Mynick, Harry JP8 57
Myra, Eric NP8 87, **NP8 88**, TO5 8
Myra, J.R. **CP8 19**, CP8 20, CP8 23, GO4 11, GP8 69, PP8 71, UP8 65

N

Na, Yong-su GP8 63, NP8 127
Nagasaki, K. BO4 10
Nagashima, Y. GP8 146, PP8 96, **PP8 97**, PP8 98, PP8 100
Nagata, M. GP8 7, UP8 15, UP8 24, UP8 35
Nagatomo, H. CP8 102, CP8 112, **NP8 91**, XP8 25
Nagayama, T. **CP8 50**, CP8 51
Nagel, S.R. TO4 8
Nagy, A. **JP8 106**, JP8 107, JP8 117
Nahar, S.N. TO6 10
Nair, Vijay UP8 149
Naitou, Hiroshi **BP8 21**
Najmudin, Nizar XP8 46
Najmudin, Z. GO6 4, TO4 8
Nakai, Mitsuo CO5 1
Nakajima, Mitsuo TO6 7
Nakajima, Noriyoshi TP8 130, UP8 71
Nakamura, H. XP8 16
Nakamura, K. JP8 125
Nakamura, Keisuke NP8 54
Nakamura, M. TP8 89

Nakanii, N. CP8 53, CP8 103, CP8 105, XP8 16
Nakanii, Nobuhiko **CP8 80**
Nakashima, Y. BM9 3, BM9 4, CM9 2
Nakata, M. Takeshi **BP8 85**, BP8 86
Nakata, Motoki **BP8 38**
Nakatsu, T. UP8 94
Nakatsuka, M. **GP8 7**, UP8 15
Nakatsutsumi, M. **GO6 5**
Nam, S.K. **NP8 116**
Namba, Shinichi **NP8 54**
Namkung, W. PP8 68
Nardon, E. UP8 89
Naseri, Neda **PO5 7**, **XP8 26**
Nash, Tom **NP8 68**, TO6 10
Nathaniel, Ekong **XP8 40**
Natta, Saswathi **JP8 37**
Naulin, V. NP8 126
Navratil, G.A. CO4 6, **GP8 22**, GP8 23, GP8 24, GP8 25, GP8 26, GP8 27, JP8 82
Nazarov, W. JP8 139
Nazikian, R. CP8 6, GP8 66, JP8 106, **JP8 109**, JP8 110
Neely, David XP8 46
Neff, A. **JP8 76**
Neff, S. GO5 12, **TO6 6**
Neilson, G.H. UP8 89
Neilson, J. NP8 26
Neko, L.T. **BP8 54**
Nelson, A.S. UP8 24
Nelson, B.A. CO7 1, **GP8 49**, JO4 13, JP8 25, JP8 65, PP8 74, UP8 19, UP8 20, UP8 21, UP8 22, UP8 23, UP8 24, UP8 36, UP8 37, UP8 38
Nemoto, Koshichi GO6 9
Neuber, Andreas CO7 3
Neumann, Martin CO7 5, NP8 44, NP8 130, NP8 131
Neumeyer, Charles JP8 56
Nevins, W.M. **BP8 18**, BP8 22, BP8 29, BP8 31, BP8 39
Newman, D.E. **BP8 33**, GP8 68, GP8 106
Newman, David BP8 32, BP8 62, CO6 6
Newman, David L. **GP8 86**, GM9 6
Newton, A. **BP8 41**
Ng, C.S. GP8 128, **GM9 2**
Ng, S.F. NP8 93
Nguyen van yen, R. **PP8 124**
Ni, L. **TP8 117**
Ni, P.A. **CP8 57**, NP8 2, NP8 93, NP8 95, NP8 96
Niasse, N. GO5 1, NP8 74
Nicholas, M. GO6 11
Nichols, Jacob **JP8 69**
Niederriter, Robert **JP8 18**
Nielsen, D.S. TO6 10
Niemann, C. GP8 140, JO5 1, PO5 8, TO6 1
Niemiec, Jacek UP8 139
Nieto, Martin **BP8 2**, NP8 38
Nightingale, M. NO4 9, UO4 13
Nikolic, L. CP8 79, PO5 9
Nikroo, A. BO5 12, BO5 14, UO5 7
Nilson, P.M. GO6 2, JP8 139, NO5 3, NO5 7, PO5 1, **PO5 2**
Nishimura, H. CP8 37
Nishimura, Y. **UP8 91**
Nishino, N. TP8 90
Noack, Klaus CM9 5
Nogami, S.H. **JP8 21**
Nogi, Yasuyuki UP8 14
Noguez, J.A. GP8 139
Nora, R. UO5 4
Norgard, John XP8 69
Norimatsu, T. UP8 143
Nornberg, M. TP8 59
Nornberg, M.D. JP8 43, JP8 44, JP8 46, JP8 47, UP8 118, UP8 119, **UP8 120**, XP8 11
Norreys, P.A. CP8 106, GO6 4, NO5 3, NO5 11, NP8 109
Nosenko, V. BP8 93, **NO6 1**
Nourgostar, Sirous **BP8 107**
Novello, L. GP8 92
Nuehrenberg, C.A. XP8 5
Nuga, H. BO4 4
Numata, Ryusuke **TP8 134**
Nunami, Masanori BP8 20
Nunes, I. CO4 13
Nunes, Roger NP8 12, NP8 13
Nusinovich, Gregory BO6 2, **BO6 3**, BO6 4, BO6 13
Nygren, R.E. PP8 44

O

O'Brien, Matthew NP8 102
O'Bryan, J.B. **GP8 50**, PP8 101
O'Connell, R. TP8 50, TP8 56
O'Mullane, M. UO4 12
O'Neil, T.M. BP8 71, BP8 72, BP8 75
O. Silva, Luis UP8 139
Obenschain, S.P. JO5 7, JO5 8, JO5 9, TO7 1, TO7 3, XP8 25
Oberto, R. TP8 144
Oberto, R.J. CM9 7, **JP8 25**, JP8 32, NM9 6, TP8 145, UP8 36, UP8 37
Obrey, Kimberly UO5 6
Ochoukov, R. GO4 7, **PP8 23**
Offerman, D.T. CP8 48, UO5 6
Offermann, D.T. GO6 2, GO6 3, PO5 12
Ogawa, H. TP8 93
Ogiwara, Kohei **GP8 149**
Oh, J. **JO5 7**, JO5 8, JO5 9, TO7 3
Oh, Y.K. CO4 11, XP8 45
Ohia, O. **BP8 52**
Ohkuma, Yasunori UP8 14
Ohno, Y. BM9 4
Ohsawa, Yukiharu GP8 87
Ohtani, K. XP8 25
Ohtani, S. GM9 4
Okabayashi, Atsunori **CP8 97**
Okabayashi, M. CO4 6, JP8 81, JP8 83, **JP8 84**
Okamoto, T. BO4 4
Okamura, Shoichi **TP8 97**
Oki, K. TP8 89, TP8 90, **TP8 91**, TP8 92
Oksuz, Lutfi XP8 15
Okuchi, Takuo CO5 1
Oliva, S. GP8 129, TP8 42, TP8 59
Oliver, B.V. BO6 10, GO5 6, NP8 64
Olsen, M. XP8 36
Olson, R.E. **BO5 1**, BO5 3, BO5 10, JO5 5
Olson, T.D. CM9 7, NM9 6, TP8 144
Olson, Thiago **JP8 32**
Olynyk, G. CO4 10
Omelchenko, Yuri **GP8 62**, UO6 8
Omran, H. UP8 89
Onchi, T. TP8 89, **TP8 90**, TP8 91, TP8 92
Ong, Benjamin **PP8 112**
Onishchenko, O.G. GO5 6, JO6 3
Ono, Masaayuki **PP8 34**
Ono, Y. JM9 2, PP8 98
Ono, Yashushi PP8 99
Ono, Yasushi **JM9 5**, PP8 100, TP8 136, TP8 137, TP8 138, **TP8 139**, UP8 30
Oosako, T. PP8 96, PP8 97, PP8 98, PP8 100
Opher, M. PM9 8
Oppenheim, M.M. CO6 15
Oreg, Joseph **XP8 48**
Orlov, D.M. **JP8 88**
Osborne, G.C. GO5 11, GO5 13, NP8 62, **NP8 63**, TO7 12
Osborne, T.H. CO4 3, **CO4 13**, CO4 14, JP8 87, JP8 88, JP8 99, JP8 101, NO4 11, TP8 17, TP8 18, TP8 19, TP8 20, TP8 21, UO4 6
Osin, D. NP8 78
Osinski, Jaksa GP8 110
Otani, Kazuto CO5 1
Otmianowska-Mazur, Katarzyna PM9 1
Ott, Torben JP8 23, XP8 6
Ou, J. NO4 2
Ou, Qiongrong BP8 13
Ou, Y. **TP8 38**
Ouart, N.D. NP8 62, TO7 12
Ouroua, A. GP8 10
Ouyang, Zihao **NP8 44**
Ovchinnikov, V.M. CP8 76, JP8 139, NO5 1, PO5 9
Owen, L.W. NP8 40, **TP8 16**, TP8 17
Oyama, N. CP8 3, GP8 29, GP8 92
Oz, E. JP8 49, PM9 3,

TP8 110, TP8 112, TP8 113, **TP8 114**
Ozaki, N. CO5 1, **TO6 14**, UP8 143

P

Pablant, N. JP8 111, **JP8 114**
Paccagnella, R. TP8 87, TP8 89, TP8 91, UP8 103, **UP8 104**
Pace, D.C. PO6 3, **TP8 9**
Pacheco-Sotelo, Joel NP8 38
Paguio, R.R. CO5 8
Pain, J.C. TO6 10
Pak, A. **TO4 2**
Pakter, Renato **NP8 11**, NP8 12, NP8 13, **XP8 27**
Pal, Rabindranath **GP8 73**
Palastro, J.P. CP8 47, **TO6 12**, TO6 13
Palmer, Charlotte TO4 8, XP8 46
Palmer, J. CO5 8
Palmer, James GO5 1
Palmer, Robert BO6 11, PP8 123
Pan, C. BO4 5, JP8 85, JP8 86, JP8 87
Pankin, A.Y. CM9 12, GP8 11, GP8 53, **GP8 54**, JP8 54, PP8 117, PP8 118, TP8 17, UP8 79, UP8 80
Papadopoulos, Dennis GP8 117, JP8 143
Papadopoulos, K. GP8 115, GP8 116
Papp, D. NP8 75
Paradkar, B.S. CP8 80, CP8 103, CP8 105, NO5 8, **NO5 9**
Paraschiv, I. **JO6 3**
Park, Chong Shik BO6 8
Park, G.Y. BP8 27, CM9 12, GP8 53, GP8 54, GP8 55, NP8 124, **NP8 125**
Park, H. BO5 12, PP8 67, PP8 68
Park, H.K. CP8 6, GP8 40, JO4 3, UP8 102
Park, Hye-Sook **BO5 11**, CO5 9, CO5 10, CO5 11, **NI2 5**, TO7 4
Park, J. JP8 135, JP8 136
Park, J.K. UO4 6
Park, J.M. BO4 5, JP8 86, JP8 87, JP8 99, **JP8 100**, TP8 9
Park, Jaehong **UP8 136**
Park, Jangho TO4 15
Park, Jong-Kyu JO4 9, **PP8 51**
Park, P.B. **TP8 36**
Park, W. GP8 31
Park, Y.S. PP8 102
Parke, E. **CP8 5**, TP8 42, TP8 51
Parker, J.V. NP8 85, TP8 143
Parker, Jeffrey B. JP8 64, **NP8 48**, NP8 49
Parker, R. GO4 8, **PP8 2**, PP8 3, PP8 5, PP8 7, PP8 8, PP8 9, PP8 27, PP8 29
Parker, Scott BP8 18, **BP8 35**, BP8 36, GP8 55, GP8 126, TP8 135, UP8 72
Parks, P.B. JP8 89, JP8 91, TP8 37, TP8 144, TP8 162, UO4 4
Parmar, P.R. BP8 9
Parra, Felix I. **DI3 3**
Pasley, J. CP8 103, CP8 105
Patel, M.V. NP8 100, **NP8 102**
Patel, P.K. CP8 53, CP8 103, CP8 105, CP8 106, JP8 142, NO5 1, NO5 2, NO5 3, **NO5 4**, NO5 6, NO5 8, NO5 12, PO5 2, PO5 9, PO5 12
Patel, Rahul JP8 69
Patel, Vikram GP8 137
Pathak, Vishwa Bandhu **JP8 133**
Patterson, Nick **UP8 142**
Paul, Kevin JP8 125, JP8 126, **PP8 123**, TO4 12, TO4 14
Paul, S.F. JO4 2, PP8 37, **PP8 38**, PP8 46, PP8 47
Pautasso, G. UO4 2
Pavlenko, Vladimir P. XP8 12
Pawlowski, R.P. GP8 65
Payne, J. PP8 20, PP8 21, **PP8 22**
Paz-Soldan, C. GP8 96, **GP8 97**, GP8 98
Pearlstein, L.D. JP8 97
Pedersen, T.S. **BP8 80**, BP8 81, BP8 83, BP8 84, GP8 22, GP8 23, GP8 24, GP8 25, GP8 26, GP8 27
Peebles, W.A. CO4 8, JP8 17, PP8 63, PP8 64, TP8 5, TP8 6, TP8 12, TP8 14, TP8 15
Pekker, Leonid **NP8 55**
Pekker, Oksana NP8 55
Penaflor, B.G. JP8 94
Penco, R. GP8 18
Peng, Y.K.M. GP8 4, PP8 84
Pengvanich, Phongphaeth NP8 23
Pereira, Nino **TO7 8**
Pereverzev, G.V. PP8 88, PP8 95
Perez, Jean C. CO6 10, **CO6 11**, GP8 152, **TI2 4**
Perkins, Francis **GP8 84**, UP8 72
Perkins, L.J. NP8 93, NP8 94, **TO5 2**
Perkins, R.J. **XP8 3**
Perkins, Rory **UP8 128**
Peters, David NP8 52
Peterson, Bryan G. BP8 85, **BP8 87**
Peterson, J.L. BP8 23, **PP8 66**
Peterson, K. GO5 2, GO5 3
Peterson, Randolph S. JP8 15
Petrasso, R.D. BO5 11, **BO5 12**, BO5 13, BO5 14, CP8 54, CP8 55, CP8 56, CP8 59, CP8 62, NO5 3, TO7 2, TO7 5, UO5 2, UO5 8, XP8 68
Petrie, T.W. CO4 5, JP8 98, **TP8 25**, XP8 32
Petrov, George **CP8 70**, CP8 72, JP8 139
Petrov, O. NO6 7
Petrov, Yu. **GP8 59**
Petrov, Yuri UP8 8, **UP8 9**
Petrova, Tzvetelina CP8 70, **CP8 72**
Petrovic, Bojan UO7 7
Petta, Nicole TO5 10, TO5 11
Petty, C.C. CO4 5, CO4 9, JP8 77, JP8 97, JP8 98, **JP8 101**, JP8 106, NO4 11, TP8 5, TP8 6, TP8 9, TP8 12, TP8 14, TP8 15, TP8 21, TP8 25, XP8 38
Peysson, Yves JO4 16
Phelps, A.D.R. XP8 31
Phelps, Alan UP8 110
Philippe, F. BO5 11, BO5 12
Philippe, Franck TO7 4
Philipps, V. UO4 8
Phillips, C.K. JO4 11, JP8 67, PP8 5, PP8 6, PP8 68, PP8 75, **PP8 77**
Phillips, L. JO5 7, JO5 8, **JO5 9**
Phillips, Michael W. NP8 97
Phillips, P.E. **GP8 10**
Pickett, Stephen **BP8 103**
Pickworth, L. GO5 1, GO5 5, NP8 74, NP8 81, TO6 3
Piel, Alexander NO6 3, NO6 5, NO6 6
Pigarov, A. **NP8 122**, PP8 37, PP8 41, PP8 117, PP8 118
Piglowski, D.A. JP8 94
Pihl, Chris UO7 2, UO7 3
Pikuz, S.A. GO5 8, NP8 65, NP8 66, **NP8 70**, NP8 71, NP8 72, NP8 76
Pilch, Iris **NO6 3**
Pinches, Simon **JO4 14**, UP8 105
Ping, Y. CP8 53, CP8 105, CP8 106, JO5 6, JP8 142, NO5 4
Pino, Jesse **BP8 111**
Pinsker, R.I. **CO4 7**, JP8 72, JP8 73, JP8 106, JP8 107, JP8 117
Pinsonneault, M. TO6 10
Piovesan, P. TP8 80, TP8 82, **TP8 83**
Piriz, A.R. CO5 13
Piron, Lidia TP8 82, TP8 83
Pitts, R.A. NO4 10, TP8 29, UO4 8
Pizzicaroli, G. CP8 11

Plateau, G.R. JP8 125, TO4 6
Plechaty, C. GO5 12, TO6 6
Pletzer, A. NP8 122, PP8 117, PP8 118, **UP8 80**, UP8 81
Plunk, G.G. BP8 25, **PO6 4**
Plyushchev, G. GP8 78
Podda, S. GP8 19
Podesta, J.J. **CO6 12**
Podesta, M. GP8 78, PP8 55, **PP8 57**, PP8 58, PP8 59, PP8 60, PP8 76
Podhorszki, N. BP8 35
Podpaly, Y. GO4 3, PP8 2, **PP8 12**, PP8 15, UO4 12
Pogorelsky, Igor **XP8 46**
Polevoi, A. CP8 17
Poli, F. GP8 78, PP8 65
Politzer, P.A. CO4 5, CO4 11, CO4 12, JP8 97, JP8 98, JP8 100, JP8 101, JP8 102, TP8 25, **UO4 9**, UO4 15
Pollaine, Stephen CO5 9, CO5 10, **CO5 11**
Pollock, B. TO6 12
Pollock, Bradley **CP8 47**, TO6 13
Polomarov, O. **UO7 1**
Polyanskiy, Mikhail XP8 46
Pomeroy, Joshua M. BO4 7
Pomphrey, N. JP8 57, TP8 79
Ponce, D. JP8 103, JP8 104, JP8 105, JP8 113
Pope, Michael BP8 101
Popoff, Romain BP8 15, **NP8 83**
Popov, Konstantin **GO6 6**
Popovic, Dusan **NP8 37**
Popovic, Svetozar GP8 91
Popovich, P. GP8 76, GP8 141, **GP8 142**, GP8 143, GP8 144, JP8 18
Porazik, Peter **UP8 114**
Porkolab, M. BP8 55, CO4 7, CP8 10, GO4 5, GO4 6, JP8 106, JM9 8, PP8 5, PP8 7, PP8 9, PP8 30, **SR1 1**, TP8 13, TP8 124, TP8 125, TP8 126, XP8 21
Porter, G.D. TP8 25, TP8 32
Porter, J.L. CP8 75, JP8 145
Post, R.F. **CM9 8**
Potashev, Alexander NP8 87, NP8 88
Pothapragada, Sriharsha UP8 138, **UP8 156**
Poulsen, P. NP8 85
Powell, Kenneth **TO5 8**
Powers, Nathan **TO4 4**, TO4 5
Pozzi, Sara TO4 4, TO4 5
Pradhan, A.K. TO6 10
Prager, James NP8 41, **NP8 52**
Prager, Jim UP8 49
Prager, S. TP8 111
Prager, S.C. JM9 7, TP8 45, TP8 68, TP8 69, TP8 70
Prasad, Rahul BO5 8
Prasad, Sarita **NP8 24**
Prater, R. BO4 5, CO4 11, CP8 26, JP8 86, JP8 87, JP8 103, **NO4 11**, TP8 12
Pratt, J. CM9 3, CM9 12
Predebon, I. **TP8 75**
Preinhaelter, Josef JO4 16
Prestwich, Kenneth NP8 24
Presura, R. CP8 63, **GO5 12**, JO6 3, NP8 75, TO6 6
Pretty, D.G. BO4 10, XP8 5
Pribyl, Patrick GP8 117, **GP8 118**, GP8 145
Priest, Eric NM9 2
Prikhodko, Vadim UP8 46
Primout, M. TO7 9
Prisbrey, Shon **CO5 9**, CO5 10, CO5 11
Procassini, R. NP8 100, NP8 102
Proctor, Camron **JP8 53**
Provost, T. XP8 60
Pruyne, A. TO7 6
Pu, Ruifeng BO6 3
Pu, Zuyin NM9 1
Puddu, S. **CP8 11**
Puerta, Julio BP8 99
Puetterich, T. **UO4 7**
Puiatti, M.E. TP8 76, TP8 77, TP8 85
Punjabi, Alkesh JP8 8, JP8 9, JP8 10, JP8 11, JP8 70
Punzmann, H. XP8 5
Purvis, M. JP8 144, **UP8 144**

Q

Qian, J. XP8 59
Qiao, Ke BP8 102, NO6 9, **NO6 10**, NO6 11
Qin, Hong CP8 30, JP8 51, NP8 6, **NP8 9**
Quataert, E. TP8 131
Quevedo, H.J. CP8 75

R

Radha, P.B. CO5 2, CO5 5, CP8 59, UO5 2, UO5 3, UO5 8, UO5 10, **UO5 11**
Raeth, C. **BP8 97**
Raffestin, Didier UP8 150
Rafig, T. TP8 17
Rafiq, T. CM9 12, GP8 11, GP8 53, GP8 54, JP8 54, **UP8 79**
Rahbarnia, Kian PO6 2
Raitses, Yevgeny BP8 109, BP8 110, CP8 15, JP8 64, NP8 48, **NP8 49**
Ralchenko, Yuri **BO4 7**
Ralph, Joseph **UI2 2**
Ram, A.K. CP8 27, CP8 28, **CP8 29**
Ram, Abhay XP8 66
Raman, R. **JO4 1**, JO4 13, JP8 65, PP8 37, PP8 74
Ramanathan, Vidya TO4 4, **TO4 5**
Rambo, P.K. JP8 145
Ramos, Gonzalo BP8 2, NP8 38
Ramos, J.J. **GP8 60**
Randerson, Lew GP8 51
Ranjbar, Vahid CP8 22
Rapp, Steve NO6 9
Rappaport, H.L. **BP8 4**
Rasmus, A.M. **JP8 26**, UP8 122, UP8 123
Rasmussen, D.A. GP8 13, GP8 14, GP8 15, JP8 106, JP8 107, NO4 9, PP8 84, PP8 94
Rasmussen, J.J. NP8 126
Rassuchine, J.M. GO6 3
Rath, N. BP8 84, GP8 22, GP8 23, GP8 24, GP8 25, **GP8 26**, GP8 27
Raubenheimer, T. GO6 13, JP8 130
Rawat, Rajdeep Singh XP8 42
Raynor, C.T. **JO6 8**, JO6 9, JO6 10, JO6 11, JO6 12, JO6 13
Read, J.W. XP8 5
Reader, Joseph BO4 7
Rebusco, P. **UP8 153**
Recoules, Vanina CO5 7
Redd, A.J. JO4 7, **JO4 12**, PP8 85, PP8 86, PP8 87, XP8 34
Redmer, R. UO6 14
Ree, Francis TO6 14
Reed, K. NP8 84
Reed, S.A. JP8 120, TO4 11
Reed, Stephen **JP8 119**
Regan, S.P. **CO5 2**, CP8 50, CP8 51, PO5 1, UO5 3, UO5 11
Rehman, A. GO6 4
Reich, M. GP8 34
Reichstein, Torben NO6 3
Reid, R. **UP8 42**
Reid, S. GO6 3, PO5 12
Reiman, A. **TP8 108**
Reimerdes, H. CO4 3, CO4 6, CO4 15, JP8 80, **JP8 81**, JP8 82, JP8 83, JP8 84, JP8 101
Reinke, M. GO4 2, GO4 3, GO4 6, GO4 7, GO4 13, NP8 47, PP8 12, PP8 20, **UO4 3**, UO4 12
Remington, Bruce CO5 9, **CO5 10**, CO5 11
Remington, T.P. UP8 145
Ren, C. CP8 93, CP8 101, CP8 109, CP8 110, CP8 111, JP8 138, PO5 6, UP8 136
Ren, Haijun XP8 50, **XP8 51**
Ren, He BP8 11
Ren, Q. **BO4 5**, JP8 85, JP8 86, JP8 87
Ren, Y. **TP8 69**
Renaudin, P. BP8 69
Rendell, D. UP8 89
Rensink, M.E. PP8 41
Rensink, M.R. TP8 33
Reusch, J.A. TP8 42,

TP8 44, TP8 45, TP8 49, **TP8 50**, TP8 51, TP8 52, TP8 55, TP8 61
Rewoldt, G. BP8 18, **BP8 36**, PP8 65, UP8 83
Reyes, Jorge Carmona **BP8 100**, BP8 102, NO6 10, NO6 11
Reynolds, Sarah **UP8 138**, UP8 156
Rezac, Karel CP8 60, **CP8 61**, GO5 15
Rhoads, J.R. JP8 44, UP8 120
Rhoads, John **PP8 72**
Rhodes, T.L. CO4 5, CO4 8, CO4 9, CO4 14, JP8 98, TP8 5, **TP8 6**, TP8 12, TP8 14, TP8 15, TP8 19
Ricci, P. GP8 77, GP8 78, UP8 63
Rice, J.E. GO4 3, GO4 6, GO4 13, NP8 47, PP8 2, PP8 7, PP8 11, PP8 12, PP8 15, UO4 12
Richards, David PO5 14, UO6 15, XP8 13
Richardson, A.S. **CP8 21**, CP8 31
Richter, T. GO6 1
Rikanati, Avi XP8 53
Rinderknecht, H.G. BO5 12, **CP8 55**, CP8 59, CP8 62, XP8 68
Rittershofer, Wolf JP8 127
Rizzato, Felipe **NP8 12**, NP8 13, XP8 27
Roach, Austin JP8 43, JP8 46, JP8 47, UP8 118, **UP8 119**, XP8 11
Roberson, Race **NP8 41**
Roberts, S. CP8 59
Robertson, Craig UP8 110
Robertson, S. BP8 8, BP8 105
Robey, H.F. **BO5 10**, BO5 11, BO5 12, CP8 113, TO5 1, TO6 8, TO7 4, **XI2 4**
Robey, R. BO5 12
Robinson, A.P.L. **PO5 11**
Robinson, J. PP8 38, PP8 45, PP8 52
Robinson, M. JO6 8, **JO6 9**
Robinson, Peter JO6 2
Rocca, J. JP8 144, NP8 33, UO6 6, UP8 144
Rochau, G.A. CP8 45, TO6 10, TO7 11, TO7 14
Rochau, Gregory **WR1 1**
Roche, Thomas **UP8 11**, UP8 12
Roderick, N.F. TP8 143, TP8 144
Rodgers, Douglas **XP8 61**, **XP8 62**
Rodgers, J.C. UP8 42
Rodriguez, R. GP8 70
Rogers, Barrett GP8 77, JM9 3, TP8 116, TP8 134, UP8 63
Rogers, Garrett CO7 3
Rogers, J.A. UP8 22
Rognlien, T.D. NP8 115, NP8 116, **NP8 117**, NP8 118, NP8 120, NP8 122, PP8 41, PP8 117, TP8 17
Rognlien, Tom PP8 118
Rohrbach, J.L. UP8 36
Rohringer, N. JP8 144
Rokhman, Y. PP8 19
Romero-Talamas, C.A. JP8 20, UP8 39, UP8 40, UP8 41, **UP8 43**
Ron, Amiram XP8 53
Ronald, Kevin UP8 110
Root, S. CO5 6
Ropokis, George BP8 42
Roquemore, A.L. CP8 43, JO4 6, JO4 8, JO4 11, JO4 13, JP8 65, JP8 69, PP8 36, PP8 37, PP8 39, PP8 40, PP8 44, PP8 45, PP8 46, PP8 53, PP8 54, PP8 59, PP8 70, PP8 74, PP8 75, XP8 60
Rose, B.C. **JP8 17**, PP8 64
Rose, David **BP8 70**, TO5 9
Rose, H.A. BP8 45, CP8 89, **UO6 7**, XP8 33
Rosen, Mordecai **CP8 82**
Rosen, P.A. CO5 8, UP8 152
Rosenberg, M. BO5 11, BO5 12, BO5 14, BP8 96, **CP8 54**, CP8 62, XP8 68
Rosenzweig, James GO6 12
Roser, T. UO7 5
Ross, J.S. TO6 12
Ross, James CP8 47, **TO6 13**
Ross, P.W. **PP8 48**
Rossmanith, James **UO6 5**
Rost, J.C. **TP8 13**
Roth, Ilan JO6 1
Rothermel, R. NO6 7
Rotti, C. NO4 7
Rousseau, P. JP8 122, JP8 140
Rousseaux, Christophe CP8 114
Rovang, D.C. CP8 75
Roveta, G. GP8 19
Rovey, Joshua L. BO6 12
Rowan, W.L. GO4 3, GP8 10, NO4 14, **PP8 13**, PP8 14, PP8 28, UP8 64
Rowley, Clarence PP8 78, PP8 80
Roy, P.K. **BO6 14**, NP8 2, NP8 3, NP8 95
Roybal, Marvin NP8 24
Roytershteyn, V. **BI2 3**, BP8 5, BP8 6, NM9 7, PM9 3, TP8 111, TP8 112, **TP8 115**, TP8 122
Rozmus, Wojciech CP8 67, GO6 6, PO5 7, XP8 26
Rubiano, J.G. GP8 70
Rubinstein, Boaz JO6 6
Rudakov, D.L. **NO4 10**, TP8 29, TP8 30
Rudakov, L.I. GO5 13
Rudd, Robert CO5 10
Ruden, E.L. **NP8 85**, TP8 143, TP8 144, TP8 147
Runov, A. GM9 4
Ruskov, E. PP8 56, PP8 57, **PP8 60**
Russell, D.A. GO4 11, JO5 10, JO5 13, **PP8 71**, UP8 65
Rutter, E.M. JP8 13
Ruzic, David CO7 5, NO4 6, NP8 44, NP8 130, NP8 131
Ryan, Duncan UP8 144
Ryan, P.M. JO4 11, JP8 67, JP8 106, **JP8 107**, PP8 75, PP8 77
Rygg, J.R. BO5 13, BO5 14
Ryu, Duchwan UP8 149
Ryutov, D.D. **BM9 2**, CM9 6, NP8 112, NP8 119, **NP8 120**, UP8 45
Ryutova, Margarita **NM9 5**

S

Saarelma, S. CO4 13
Sabbagh, S.A. GP8 32, GP8 33, JO4 9, **JO4 10**, PP8 51, PP8 52, PP8 53, PP8 67, PP8 73, PP8 79, UO4 6, XP8 2, XP8 45
Safira, Arthur **JP8 40**
Safronova, A.S. GO5 13, NP8 62, NP8 63, **TO7 12**
Safronova, Alla GO5 11
Sagdeev, Roald CP8 68, JP8 143
Saikia, B.K. **BP8 106**
Sainct, Florent PP8 25
Saitoh, Haruhiko XP8 47
Sakagami, Hitoshi CP8 102
Sakai, Osamu **GI2 1**
Sakaiya, T. CO5 1, XP8 25
Sakakibara, S. BO4 10
Sakakita, H. PP8 98
Sakamoto, Takuya PP8 96, PP8 97, PP8 100
Sakamoto, Yoshiteru GP8 29
Sakasai, S. GP8 92
Sakawa, Youichi **UP8 143**
Sakumura, M. PP8 98, PP8 99, PP8 100
Sakurai, S. GP8 92
Salmonson, J.D. BO5 4, **CP8 84**, TO5 1, UO5 13, UO5 14, UO5 15
Salvetti, Matteo **GP8 16**
Samaddar, Debasmita BP8 33, **GP8 68**
Samm, U. UO4 8
Sammadar, D. GP8 106
Sammuli, B.S. JP8 94
Samokhvalova, Ksenia BO6 9
Samtaney, Ravi **TP8 120**
Samulyak, R. TP8 36
Samulyak, Roman **TP8 162**
Sanchez, Andrew GP8 109
Sanchez, R. BP8 32, BP8 33, **BP8 62**, GP8 68
Sandberg, Ingmar **BP8 42**
Sangster, Craig TO7 4
Sangster, T.C. CO5 2, CO5 12, CP8 59,

JO5 14, JP8 139, **NI2 2**, NO5 3, PO5 1, PO5 2, TO7 2, TO7 6, UO5 1, UO5 2, UO5 3, UO5 11
Sano, T. **CO5 1**, TO6 14, UP8 143
Sanpei, A. TP8 89, TP8 90, TP8 91, TP8 92
Santarius, John **CM9 4**, **TP8 155**, UP8 60
Santner, J. JP8 48, TP8 141
Santos, J.J. GP8 81
Sarasola, X. BP8 80, BP8 81, **BP8 83**, BP8 84
Sarazin, Y. BP8 26
Sarff, J.S. GP8 129, JM9 7, **MR1 1**, TP8 42, TP8 43, TP8 44, TP8 45, TP8 59, TP8 61, TP8 62, TP8 69, TP8 70, TP8 86
Sarkisov, G.S. **CP8 46**, NP8 73
Sarri, G. **GO6 4**, NO5 11
Sartori, R. NO4 9
Sassi, M. **GP8 21**
Sato, Kuninori NP8 54
Sato, M. GP8 56
Satoh, D. PO5 10
Sattin, Fabio UP8 68
Satyanarayan, K. BP8 9
Sauerbrey, R. GO6 1, TO4 1
Saule, E. UO6 8
Savage, M. CP8 75
Sawada, H. CP8 53, CP8 80, CP8 103, **CP8 105**, CP8 106
Sawheny, Rapinder CO7 6
Scannapieco, Anthony UO6 9
Scarin, Paolo **UP8 68**
Schablinski, Jan NO6 5
Schaeffer, Derek **GP8 140**, TO6 1
Schaffer, M.J. CO4 6, JP8 80, JP8 81, JP8 83, **NO4 13**, PP8 51, TP8 25, UP8 89
Schaffner, D. GP8 141, GP8 142, GP8 143, **GP8 144**
Schamiloglu, Edl GP8 110, NP8 24
Scharer, John **BP8 10**, BP8 11
Schartman, Ethan **CP8 4**, JP8 43, UP8 118
Scheffel, Jan **TP8 88**
Schekochihin, Alexander BP8 25, CO6 8, PM9 2, TP8 120, TP8 134
Schilling, Oleg CP8 86, **CP8 113**
Schirra, Martin CO7 2
Schissel, D.P. JP8 74
Schlossberg, D.J. JO4 12, JP8 116, PP8 85, **PP8 86**, TP8 7, TP8 8
Schlutt, Mark **GP8 93**
Schmidt, A.E. GO4 8, PP8 2, PP8 7
Schmidt, M. UP8 13
Schmidt, Ruediger CO5 13
Schmit, Paul **JP8 147**
Schmitt, A.J. CP8 99, JO5 8, JO5 9, **TO7 1**, TO7 3
Schmitt, J.C. **TP8 103**
Schmitt, M.J. GO6 2, NP8 82
Schmitt, Mark NP8 86, **UO5 6**
Schmitt, Ronald **BP8 27**
Schmitz, L. CO4 8, CO4 9, TP8 5, TP8 6, TP8 12, **TP8 14**
Schmitz, O. **CO4 3**, JP8 71, JP8 81, TP8 26
Schmoke, Jimmy BP8 100, BP8 102, NO6 9, NO6 10, NO6 11, NO6 12
Schnack, D.D. GP8 58, **NP8 114**, TP8 50, TP8 73, UP8 124
Schneck, K. **UP8 154**
Schneider, H. JP8 69, PP8 44
Schneider, K. PP8 124
Schneider, M. BO5 3, CP8 104, NP8 84, TO7 7
Schneider, Ralf **CO7 2**, NP8 123, UP8 157
Schoch, P.M. TP8 47, TP8 48
Schoeffler, K. PM9 8, **TP8 133**
Schollmeier, M. GO6 3, JP8 145
Schrafel, Peter GO5 9, **NP8 67**
Schramm, U. GO6 1, TO4 1
Schreiber, J. TO4 8, XP8 46
Schroeder, C.B. JP8 125, JP8 126, **JP8 127**, JP8 128, JP8 129, TO4 6, TO4 14
Schueller, C. NO4 9
Schultz, David TO4 4
Schulz, J. GP8 6
Schumacher, D.W. CP8 53, CP8 76, NO5 12, **PO5 9**
Schumaker, William **TO4 3**
Schumer, Joseph TO7 8
Schunke, B. **NO4 7**
Schuster, E. GP8 35, GP8 36, GP8 37, GP8 38, TP8 38, TP8 39, XP8 36
Schwarz, M. JP8 145
Schwarz, V. UO6 14
Schweer, B. UO4 8
Scime, Earl BP8 9, GP8 132, GP8 133, GP8 134, GP8 135, GP8 136, JP8 16, **TI2 3**, UP8 113, XP8 57
Scofield, J. NP8 84
Scott, B.D. PP8 70
Scott, H.A. PP8 42
Scott, Howard TO7 10
Scott, M. JO6 13
Scott, R. GO6 4
Scott, S. NP8 47, PP8 7, PP8 17, PP8 18
Scotti, F. **PP8 42**
Sears, J. **PP8 27**, PP8 29
Sears, Stephanie **GP8 132**, GP8 135, XP8 57
Sebastien, Jolliet BO4 1
Sechrest, Y. CP8 7, **CP8 8**
Sedita, Paul **JP8 34**
Seely, J. JO5 8, TO7 8, **XP8 55**
Sefkow, A.B. JP8 145, **TP8 156**
Seguin, F.H. BO5 11, BO5 12, **BO5 13**, BO5 14, CP8 54, CP8 55, CP8 56, CP8 59, CP8 62, TO7 5, UO5 8, XP8 68
Seidl, P.A. BO6 14, CP8 57, NP8 2, **NP8 3**, NP8 5, NP8 95
Seka, W. **JO5 10**, JO5 11, JO5 13, JO5 14, JO5 15, PO5 6, TO7 2, UO5 1, UO5 11, UO5 12
Selcher, C.A. GP8 89
Selivanov, A.N. TP8 59
Seltzman, A. TP8 65, **TP8 66**, TP8 67
Semenov, Vlad BO6 6
Sen, Amiya K. GP8 147, GP8 148
Sen, N. CP8 7, CP8 8, GP8 86
Sennikov, Petr NP8 35
Senter, A. BP8 80, **BP8 84**
Sentoku, Yasuhiko CP8 63, GO6 3, **PO5 4**, PO5 5
Sepke, S.M. BO5 10, NP8 100, NP8 102
Sergeev, V. GM9 4
Sergienko, G. UO4 8
Serianni, Gianluigi TP8 87, UP8 68
Serlin, V. JO5 7, JO5 8, TO7 3
Servidio, Sergio **PM9 4**, XP8 61, XP8 62
Seryi, A. GO6 13, JP8 130
Sestero, A. NO4 16
Severn, Greg JO6 5, JP8 53
Shadid, J.N. GP8 65
Shadwick, B.A. **JP8 128**, JP8 129
Shadwick, Bradley JP8 127
Shafer, M.W. CO4 14, JP8 109, JP8 116, **TP8 7**, TP8 8, TP8 12
Shah, G. UP8 36
Shah, S. NO4 7
Shaikh, Dastgeer **GP8 94**, GP8 100, PO6 12, XP8 30
Shaing, K.C. **GP8 32**, GP8 33, XP8 2
Shamrai, Konstantin P. GP8 113
Shao, X. CP8 68, **GP8 115**, GP8 116, GP8 117
Shapiro, M.A. GP8 14, **GP8 15**, NP8 26
Sharma, A.K. **CP8 40**, GP8 131, JP8 148, JP8 151
Sharma, A.S. GP8 115, GP8 116
Sharma, Amit R. UP8 157
Sharma, Mukta **GP8 61**, UP8 82
Sharma, P.K. BP8 9
Sharma, Prerana **CP8 92**, **XP8 28**, **XP8 29**

Sharma, R.P. XP8 28, XP8 29
Sharma, Rampal CP8 92
Sharma, Surjalal CO6 3, **PM9 7**
Sharp, W.M. **NP8 110**
Shasharina, S. NP8 122, PP8 117, **PP8 118**
Shashurin, Alexey BP8 109, **NP8 39**
Shay, H. CP8 100, NO5 4, NO5 6
Shay, M.A. TP8 131
Shay, Michael PM9 4
Sheehan, J.P. **NP8 45**
Sheerin, J.P. **GP8 89**
Shelkovenko, T.A. GO5 8, NP8 65, NP8 66, NP8 70, NP8 71, NP8 72, NP8 76
Shende, S. PP8 117, PP8 118
Sheng, Z.M. PO5 10
Shephard, M. UP8 97
Shepherd, R. BP8 69, JP8 142, **JP8 144**
Sherlock, M. CP8 67
Sherrill, M.E. TO6 10
Shetler, Gary NO6 9
Shevchenko, V. PP8 84
Shevelko, A.P. NP8 75
Shi, M. **NP8 25**, PO6 3
Shi, Y.J. NO4 2
Shibata, S. UP8 143
Shidara, H. BM9 3, BM9 4
Shiffler, Don **NP8 18**, NP8 20
Shigemori, K. CO5 1, UP8 143, XP8 25
Shim, Bonggu CP8 73
Shima, Y. BM9 4
Shimada, T. GO6 3, PO5 12
Shimizu, Katsuya CO5 1
Shimizu, S. TP8 93
Shinohara, Shunjiro GP8 112, GP8 113, GP8 137
Shinohara, T. TP8 93
Shiraga, H. XP8 25
Shiraishi, Junya **UP8 86**
Shiraiwa, S. GO4 8, PP8 3, PP8 5, PP8 7, PP8 17, PP8 18, PP8 32, **TI3 3**
Shiraki, D. GP8 22, GP8 23, GP8 24, **GP8 25**, GP8 26, GP8 27
Shiroshita, A. CO5 1, UP8 143
Shivamoggi, Bhimsen **CO6 2**
Shkolnikov, Peter XP8 46
Shlyaptsev, Vyacheslav UP8 144
Shlyaptseva, V. GO5 11, GO5 13, TO7 12
Shneider, M.N. NP8 39
Short, R.W. JO5 10, JO5 11, **JO5 12**, JO5 13, JO5 14
Shoucri, Magdi **NP8 32**
Shoup III, M.J. TO7 6
Shrauner, Barbara **BP8 65**
Shrestha, I. GO5 11, GO5 13, NP8 62, NP8 63, TO7 12
Shu, Anthony **BP8 105**
Shukla, Nitin GP8 105
Shukla, P.K. BP8 92, CP8 68, GP8 81, GP8 104, GP8 105, **PO6 12**, XP8 12, **XP8 30**, **XP8 31**
Shumlak, U. GP8 46, GP8 47, GP8 102, JP8 24, JP8 25, **UP8 36**, UP8 37, UP8 38
Shurter, R.P. BP8 68
Shutov, Alexander CO5 13
Shvarts, D. UO5 4, UO5 10, UO5 11
Shverdin, M. BO6 5, BO6 6, **BO6 7**, NP8 28
Shvets, G. CP8 98, JP8 119, JP8 120, JP8 121, NP8 10, TO4 11
Shvydky, A. JO5 15, UO5 8, **UO5 9**
Shylaptseva, V. NP8 62
Siders, Craig BO6 5, BO6 6, BO6 7, GP8 90, NP8 28
Sieck, P.E. TP8 144, **TP8 145**
Siemon, Carl **NP8 10**
Siemon, Richard TP8 143, TP8 144, TP8 148, TP8 160, **TP8 161**
Silva, L.O. CP8 71, CP8 101, CP8 109, CP8 111, GP8 81, JP8 132, JP8 133, JP8 137, **NP8 31**, NP8 108, UP8 137
Silva, S.O. TO4 8
Simakov, A.N. **TP8 121**
Simonen, T.C. CM9 6
Simonen, Thomas **BM9 1**, **UP8 44**, UP8 45
Sinars, D.B. GO5 3
Sinars, Daniel **GO5 2**
Sinenian, N. CP8 54, CP8 55, CP8 56, CP8 59, **CP8 62**, XP8 68
Singh, Amrita **JP8 151**
Singh, Divyaprakash BP8 103
Singh, M. NO4 7
Singh, N. NO4 7
Singh, R. NP8 126
Singh, T.V. JP8 137
Sinitsyn, Oleksandr BO6 3, **BO6 13**
Sips, A.C.C. UO4 14
Sirigiri, J.R. GP8 14, GP8 15, NP8 26
Sitnov, M. **GM9 4**, GM9 5
Skender, Marina **CO6 1**
Skiff, Fred GP8 75, **GP8 137**
Skinner, C.H. **JO4 8**, JP8 69, PP8 40, PP8 41, PP8 46, **XP8 60**
Skoric, Milos UP8 71
Skovorodin, Dmitriy UP8 46
Skupsky, S. CO5 5, UO5 2, UO5 9, UO5 11
Slough, John CO7 1, **UO7 2**, UO7 3, UP8 10
Slutz, S.A. GO5 2, GO5 3, **JI2 6**, TP8 156
Smalyuk, V.A. CO5 2, CO5 12, CP8 50, CP8 51, CP8 56, PO5 1, UO5 2, UO5 3, UO5 11
Smarandache, Florentin XP8 52
Smick, Noah **GO4 9**
Smirnov, A.P. GO4 8, GP8 52, GP8 58
Smirnov, R. NP8 128, PP8 37, **PP8 41**
Smith, Bernard BP8 101, **NO6 12**
Smith, Cosmo CP8 34
Smith, D.R. JO4 3, PP8 62, **PP8 83**
Smith, J.P. GP8 2, GP8 3
Smith, Kurt **UP8 126**
Smith, M. CP8 6, PP8 17, PP8 18
Smith, R. CO5 4
Smith, R.J. **TP8 146**, UP8 19, UP8 20, UP8 21, UP8 22
Smith, S.P. **UP8 96**
Smithe, David **CP8 18**, CP8 22, CP8 25
Smolyakov, A.I. **UP8 73**
Smolyakov, Andrei **TI3 5**
Smoniewski, J. **BP8 89**
Snieckus, K. PP8 88
Snieckus, Kurt PP8 95
Snipes, J.A. NO4 13, **UO4 11**
Snyder, P.B. CO4 13, CO4 14, GP8 54, GP8 64, JP8 88, JP8 99, JP8 100, NP8 113, **TP8 18**, TP8 19, TP8 20, TP8 21, TP8 22
Soe, Min BP8 58
Sokolov, Igor **NP8 87**, NP8 88, TO5 8
Sokolov, Vladimir GP8 147, **GP8 148**
Soldatkina, Elena CM9 1
Solodov, A.A. NO5 3, **NO5 7**
Solomon, W.M. CO4 6, CO4 15, JP8 81, JP8 111, **NI3 2**, TP8 3, TP8 5, TP8 15, TP8 20, UP8 83
Somers, William **JP8 62**
Sommars, W. TP8 143, TP8 144
Sommer, Chris **UO7 7**
Sontag, A. GP8 4, **JO4 5**, UO4 6
Soppelsa, Anton TP8 83
Sorce, C.M. CP8 37, TO7 7
Sorokin, A.V. TP8 59
Sotnikov, V.I. CP8 46, **GO5 6**, JO6 3
Soukhanovskii, V. JO4 5, JO4 6, JO4 8, **PP8 37**, PP8 41, PP8 42, PP8 44, PP8 45, PP8 46, PP8 74, PP8 88, PP8 92, PP8 95
Soures, J.M. BO5 14
Souza, Everton NP8 12, NP8 13
Sovinec, C.R. GP8 48, GP8 50, GP8 58, GP8 99, NP8 113, PP8 101, TP8 71, UP8 34, UP8 92

Spagnolo, Silvia TP8 87
Spatschek, K.H. TP8 24
Spears, B.K. BO5 6, TO5 1, **UO5 13**, UO5 14
Speirs, David **UI3 6**, UP8 110
Spence, Erik JP8 43, JP8 46, JP8 47, **UP8 118**, UP8 119, XP8 11
Spencer, Ross L. BP8 85, BP8 86
Spindloe, C. CP8 106
Spizzo, G. TP8 77, **TP8 81**, TP8 82
Spolaore, M. TP8 77
Spolaore, Monica TP8 87, UP8 68
Spong, D. GP8 129, **TP8 98**, TP8 99
Springer, P. UO5 13, UO5 14
Springham, Stuart Victor XP8 42
Srama, R. BP8 105
Srinivasan, Bhuvana **GP8 102**
Srinivasan, R. BO4 5, JP8 86, JP8 87
Srivastava, Nimisha **CO7 4**, NP8 43
St. John, H.E. BO4 5, **GP8 64**, JP8 86, JP8 99, JP8 100
Stacey, W.M. TP8 16, TP8 17, TP8 33, TP8 34, **TP8 35**, **UO7 6**, UO7 7, UO7 8, **XP8 32**
Staebler, G.M. GP8 64, JP8 99, JP8 100, **TP8 10**, TP8 11, TP8 12
Stambaugh, R.D. GP8 2, **GP8 3**
Stambulchik, E. NP8 78
Stangeby, P.C. NO4 10, TP8 29, TP8 30, **TP8 31**
Stapleton, D. **JP8 30**, JP8 31, UP8 125
Stark, Casey **JP8 60**
Starobinets, A. CP8 45, TO7 11
Starobintes, A. NP8 78
Starrett, Charles CO5 7
Startsev, E. BP8 19, NP8 6, NP8 7, **NP8 8**
Stefan, V. Alexander **NO4 12**
Stehle, C. TO6 3
Stein, S. GO5 12, TO6 6
Steiner, Adam **JP8 66**
Steinhauer, L.C. UP8 3, **UP8 16**
Stemmler, Ph. TO7 9
Stenflo, L. XP8 31
Stenson, Eve **UP8 129**
Stepanov, Anton **NP8 51**
Stephens, H.D. **GI3 4**, TP8 42, TP8 44, TP8 50, TP8 51, TP8 55, TP8 61
Stephens, R.B. CP8 53, CP8 66, CP8 80, CP8 103, CP8 104, CP8 105, CP8 106, CP8 108, **NO5 1**, NO5 2, NO5 3, NO5 8, NO5 9, NO5 12, PO5 12
Stepp, M.A. NP8 39
Sternovsky, Z. BP8 105
Stevenson, B.A. CP8 13, GP8 121, TP8 105, **TP8 107**
Stevenson, Richard CP8 83
Still, Bert CP8 90
Still, C.H. JO5 4, JO5 5, **TO5 5**
Stober, J. GP8 34, UO4 2
Stoeckl, C. JO5 11, JP8 139, NO5 3, NO5 7, PO5 1, PO5 2, PO5 3, **TO7 2**, TO7 6, UO5 10, UO5 11
Stoltz, Peter CP8 18, TP8 157
Stone, D. TP8 61, **TP8 62**, TP8 68
Stoneking, M.R. BP8 89
Stoneking, Matthew JP8 19
Storm, M. NO5 7
Stotler, D.P. GO4 11, GP8 55, **NP8 124**, PP8 37, PP8 41, PP8 71
Stout, Quentin TO5 8
Strachan, J. UP8 89
Strait, E.J. CO4 6, JP8 80, JP8 81, JP8 82, JP8 83, JP8 84, JP8 87, JP8 91, JP8 92, JP8 94, JP8 95, JP8 96, JP8 109, TP8 37
Stratakis, Diktys **BO6 11**, **CI2 4**, PP8 123
Stratton, B.C. PP8 83
Strauss, H.R. BP8 27, GP8 55, **UP8 103**, UP8 104
Streit, Jon **TO5 10**, TO5 11
Streitz, F. JP8 144, UO6 15
Strickler, T. PP8 88, PP8 91, PP8 95
Stroth, Ulrich CP8 9, **PO6 1**
Strozzi, D.J. CP8 90, NO5 4, **NO5 5**, **XP8 33**, XP8 54
Strugarek, A. BP8 26
Struve, K.W. CP8 75
Stupishin, N.V. TP8 59
Stutman, D. **CP8 43**, PP8 53, PP8 54, PP8 61
Stygar, W.A. BP8 70, TO5 9
Suarez, D. GP8 70
Sugama, Hideo **BP8 20**, BP8 38, UP8 70
Sugihara, M. TP8 89, TP8 90, TP8 92
Sugita, S. GP8 146
Sugiyama, L. GP8 55, **PI2 1**
Sullivan, B.P. **TP8 118**
Summers, H.P. JP8 114
Sumner, Tyler **UO7 8**
Sun, Can **PO6 13**
Sun, Xuan JP8 32
Sun, Y. GP8 32, UP8 89
Sun, Y.W. NO4 3
Sunahara, Atsushi CP8 102, **CP8 112**
Sung, Chieh GO6 12
Sung, Choongki **PP8 102**
Sunn Pedersen, Thomas BP8 82
Surany, Jonathan **JP8 68**
Surh, Michael XP8 13
Surko, C.M. BP8 76
Surla, Vijay NO4 6, NP8 44, **NP8 130**, NP8 131
Suter, L.J. BO5 1, BO5 2, BO5 3, BO5 5, BO5 7, JO5 2, JO5 3, JO5 6, TO5 1
Sutherland, D. TP8 144
Sutherland, D.A. **JP8 33**
Sutter, L. JO5 1
Sutton, Steve NP8 29
Suttrop, W. GP8 34
Suzuki, Takahiro **CP8 3**
Suzuki-Vidal, F. GO5 1, GO5 5, NP8 74, **TO6 3**
Suzuki-Vidal, Fransisco NP8 81
Svensson, J. BO4 6
Svidzinski, Vladimir **BP8 45**
Svimonishvili, Tengiz NP8 30
Swadling, George GO5 1, GO5 5, **NP8 74**, NP8 81, TO6 3
Swain, D. **GP8 13**, NO4 9
Swan, G. UP8 41
Swiatlowski, Maximilian **JP8 56**
Swift, D.C. XP8 16
Swisdak, M. GM9 4, GM9 5, PM9 8, **PM9 9**, TP8 131, TP8 132, TP8 133
Sydora, Richard GO6 6
Sydorenko, Dmytro BP8 110, **GI2 2**
Szabo, Csilla XP8 55

T

Ta Phuoc, K. TO4 8
Tabak, M. CP8 100, NO5 4, NO5 5, NO5 6
Tabakhoff, Emeric XP8 55
Taccetti, J.M. **BP8 68**
Taccogna, Francesco CO7 2
Taguchi, Toshihiro **CP8 77**
Tahir, Naeem A. **CO5 13**
Taira, Kunihiko **PP8 78**
Taitano, William **PP8 116**
Takabe, H. UP8 143
Takahashi, Hideki CO5 1
Takahashi, Hiro **PP8 43**, PP8 73
Takahashi, K. PO5 10
Takahashi, R. **GP8 95**
Takahashi, Seiichi **GP8 87**
Takahashi, Tsutomu UP8 14
Takase, Y. **PP8 96**, PP8 97, PP8 98, PP8 99, PP8 100
Takechi, M. GP8 92
Takeda, K. XP8 25
Takenaga, Hidenobu GP8 29
Takiyama, Ken NP8 54
Tala, T. TP8 15
Talebitaher, Alireza XP8 42
Tallaksen, Katharine **JP8 16**
Tallaksen, Katherine GP8 132
Talmadge, J.N. TP8 103, TP8 104

Tamasan, Alexandru XP8 41
Tamura, Shuichi PO6 7
Tan, Joseph N. BO4 7
Tanabe, Hiroshi **TP8 136**, UP8 30
Tanabe, M. CP8 37
Tanaka, K. CP8 80, CP8 97, GO6 4
Tanaka, Masayoshi Y. GP8 149
Tang, W. NP8 22, **NP8 80**
Tang, W.M. PP8 49, PP8 65, UP8 83
Tang, W.W. NP8 64
Tang, Xianzhu BP8 5, **BP8 6**
Tanga, A. NO4 7
Tangri, Varun **TP8 74**
Tanikawa, Takao **GP8 112**, GP8 113
Tanimoto, T. GO6 4
Tanji, H. UP8 143
Tankut, A. UP8 2, **UP8 5**
Tantawi, S. BO6 6, NP8 27
Tarditi, Alfonso **XP8 69**
Tarditi, Alfonso G. **XP8 70**
Tarman, Lisa **JP8 3**, JP8 4
Tashev, Bekbolat **BP8 64**
Tatineni, M. UO6 8
Tatsuno, T. **BP8 25**, PO6 4, TP8 134
Taverniers, Soren PP8 105
Tax, D.S. GP8 15, **NP8 26**
Taylor, C. JO4 8, **PP8 40**, PP8 46
Taylor, G. JO4 11, JP8 67, PP8 75, PP8 77, UP8 43
Taylor, Gary JO4 16, **TI3 2**
Taylor, Graham **JP8 20**
Taylor, Mark NP8 89
Taylor, N.Z. JP8 26, **UP8 122**, UP8 123
Taylor, P.T. CO4 11
Tejero, Erik **GP8 122**, GP8 123
Teles, Tarcisio N. NP8 11
Telford, Steve NP8 29
Temkin, R.J. GP8 14, GP8 15, NP8 26
TenBarge, Jason **UP8 141**
Teodorescu, C. JP8 20, UP8 39, **UP8 40**, UP8 41, UP8 43, UP8 48
Tercas, Hugo **GP8 105**
Terranova, D. TP8 77, TP8 79, TP8 83
Terry, J.L. **GO4 10**, PP8 20, PP8 22
Terry, James GO4 11
Terry, Jim PP8 11
Terry, Matthew **CP8 85**
Terry, P.W. **BP8 31**, BP8 39, BP8 46, TP8 69, TP8 74, UP8 126
Terry, Paul T. BP8 51
Teychenne, Denis CP8 114
Thais, Frederic UP8 150
Thakur, Arvind BP8 9
Tharp, T.D. **JM9 7**, TP8 68, **TP8 70**
Theiler, C. GP8 77, GP8 78
Then, H. PO6 11
Theoald, W. PO5 6
Theobald, W. CP8 106, **NO5 3**, NO5 6, NO5 7, PO5 1, PO5 2, PO5 3, TO7 2, TO7 6, UO5 3
Thfoin, Isabelle TO7 4
Thide, Bo PO6 11
Thiele, R. **UO6 14**
Thiem, Hoang CO6 9
Thoma, Carsten **TP8 159**
Thoma, Carston NP8 104
Thoma, M. BP8 97
Thomas, A.G.R. JP8 122, TO4 3, TO4 8, TO4 11
Thomas, Alec JP8 140, PP8 122, **TO4 9**, **UI2 4**
Thomas, C.E. PP8 88, PP8 93, PP8 95
Thomas, Cliff BO5 8
Thomas, D.M. JP8 77
Thomas, Dan PP8 14
Thomas, E. BP8 95, **BP8 96**, BP8 97, BP8 105, GP8 119, GP8 120, GP8 121, GP8 122, JP8 38
Thomas, H. BP8 97
Thomas, H.M. BP8 93, NO6 7
Thomas, R.D. TO6 10
Thomas Jr., C.E. (Tommy) **PP8 94**
Thompson, Paul **JP8 59**
Thomsen, Hauke UO6 11
Thorn, D.B. JP8 125
Thorn, Daniel CP8 52
Thornhill, J.W. **NP8 59**, NP8 77, NP8 78, TO7 11, TO7 13
Thornhill, W. NP8 61
Thornton, Katsuyo UP8 142
Thuecks, Derek **GP8 75**
Tiedje, H. CP8 103, CP8 105
Tikhonchuk, Vladimir NO5 10
Tilikin, I.N. NP8 71
Timberlake, J. PP8 44, PP8 88, PP8 95
Ting, A. GO6 11, JP8 124, TO4 10
Title, Alan NM9 5
Titov, Viacheslav **NM9 2**
Titus, J.B. JO6 10, **JO6 11**, JO6 13
Tobias, B. UP8 102
Tobias, B.J. CP8 6, GP8 40
Tochitsky, S. **GO6 12**, JP8 141
Toda, S. **UP8 69**
Todd, T.N. UP8 89
Todosow, M. UO7 5
Tokar, M.Z. XP8 56
Tokuda, Shinji BP8 21, GP8 114, UP8 85, UP8 86
Tommasini, R. CP8 50, CP8 51
Tonge, J. CP8 101, **CP8 109**, CP8 110, CP8 111, NP8 108
Torrey, Jon BP8 109
Torrezan, A.C. NP8 26
Toth, Csaba TO4 6
Toth, G. TO5 8
Totsuji, Hiroo **BP8 91**
Town, J.P. CP8 56
Town, R. BO5 5, BO5 12, BO5 14, CP8 100, NO5 4, NO5 5, **NO5 6**, TO5 1
Trabert, Elmar JP8 5
Tracy, E.R. **CP8 31**
Tran, Trach-Minh BO4 1
Trans, B.C. **GP8 33**
Trask, Erik UP8 11, UP8 12
Tregillis, I.L. NP8 82, UO5 12
Tregillis, Ian UO5 6
Treutterer, W. GP8 34, UO4 2
Trines, R. GO6 4, GP8 81, **NO5 11**, NP8 109
Tripathi, Deepak **JP8 149**
Tripathi, Shreekrishna GP8 76, **TO6 2**
Tripathi, Vipin Kumar JP8 149
Tritz, K. CP8 43, JO4 10, PP8 53, PP8 54, PP8 55, PP8 61, PP8 62, PP8 75
Tsai, W.C. PP8 67, PP8 82
Tschentscher, T. UO6 14
Tsidulko, Yu.A. BP8 73, BP8 74, BP8 75
Tskhakaya, David **NP8 123**
Tsui, Y.Y. CP8 53, CP8 103, CP8 105, NO5 1, PO5 9
Tsuji-Iio, Shunji UP8 71
Tsujii, N. GO4 5, GO4 6, PP8 9, **PP8 30**
Tsung, F. CP8 93, CP8 94, CP8 96, JP8 141, **NP8 106**, NP8 108, NP8 109
Tsutsui, Hiroaki UP8 71
Tucker, W. TP8 143
Turchi, P.J. TP8 143
Turco, F. CO4 5, **JP8 97**, JP8 98
Turnbull, A.D. **GI3 1**, JP8 87, JP8 97, NP8 114
Tushentsov, Mikhail CP8 73, CP8 74
Tynan, G.R. BP8 40, CP8 47, GP8 138, GP8 139, JP8 95, TO6 13, TP8 12
Tyshetskiy, Y. CP8 79
Tzoufras, Michail **NP8 109**

U

Ullrich, Stefan PO6 2
Ulreich, J. CP8 59
Ulrickson, Michael GP8 5
Ulvestad, A. **BP8 44**
Uma, R. JP8 149
Umansky, M. GO4 11, GP8 69, GP8 142, JP8 74, NP8 117, **NP8 119**, NP8 120, **XP8 63**
Umstadter, Donald TO4 4, TO4 5
Unterberg, E.A. CO4 2, CO4 3, CO4 4, JP8 71, JP8 88, **TP8 26**, TP8 30, UO4 6

Urano, Hajime GP8 29
Urban, Jakub **JO4 16**
Utsumi, Takayuki BP8 30
Uzdensky, Dmitri CO6 8, **CO6 14**, **PM9 2**, TP8 110, TP8 120
Uzun-Kaymak, I. **JP8 116**, PP8 83, UP8 39, UP8 41, UP8 48

V
Vadlamani, S. PP8 117, PP8 118, UP8 80, **UP8 81**
Vahala, George BP8 56, BP8 57, **BP8 58**, JO4 16
Vahala, Linda BP8 56, BP8 57, BP8 58, JO4 16
Vahdat Roshan, Mahmud **XP8 42**
Vainionpaa, H. CP8 4
Valanju, P. GP8 4
Valeo, E. GO4 12, JO5 6, JP8 67, PP8 5, PP8 6, PP8 7, PP8 77
Valisa, M. TP8 85
Van Compernolle, Bart **GP8 145**
Van Dam, J.W. UP8 84
van den Bogert, K. NP8 2
Van der Holst, Bart TO5 8
Van Eester, D. NO4 9
Van Keuren, Edward JP8 124
Van Maren, R.D. CP8 106
van Mourik, R.A. JP8 125
van Tilborg, Jeroen TO4 6
Van Woerkom, L.D. CP8 53, CP8 76, NO5 1, NO5 2, NO5 12, PO5 9
Van Zeeland, M.A. JP8 90, JP8 96, JP8 108, JP8 109, JP8 110, **JP8 111**, TP8 9, UO4 4
Vane, Randy TO4 4
Vasquez, S. **JP8 63**, NP8 57
Vaughan, Kelly CP8 83, **NI2 3**
Vay, J.L. NP8 110, TO4 13
Vazquez, Justin **JP8 9**
Veitzer, S.A. NP8 93
Veitzer, Seth PP8 123
Velas, K.M. CP8 14, UP8 2, **UP8 6**
Velikovich, A.L. CO5 14, **CO5 15**, CP8 87, CP8 99, GO5 13, NP8 69, NP8 78, TO7 3, XP8 25
Veranda, M. TP8 80
Veras, Johann XP8 41
Verboncoeur, John **PP8 105**
Verdon, Alix **JO6 2**
Verma, Updesh CP8 40, JP8 148
Vernon, S. JO5 1
Vesey, R.A. GO5 2, GO5 3, TP8 156
Vianello, N. TP8 77, TP8 87, UP8 68
Victor, B.S. UP8 19, **UP8 20**, UP8 22
Vidal, F. CP8 79
Vieira, J. **JP8 132**, NP8 108
Vieira, R. PP8 19
Vikharev, Anatoly NP8 35
Villette, B. CP8 37, TO7 9
Vincena, S. GP8 75, GP8 76, GP8 142, GP8 143, GP8 144, **GP8 150**, GP8 151, NM9 3
Vinci, Tommaso TO6 14
Vinko, Sam **GO6 15**
Viola, M. PP8 44
Virani, Chetan BP8 9
Visco, A. **TO6 9**, UP8 147, UP8 148
Vishniac, Ethan CO6 9, **PM9 1**
Vishniakou, S. NP8 72
Vlases, G.C. UP8 2, UP8 5
Vlasov, Alexander **CI2 5**
Vlieks, A. BO6 6, NP8 27
Vogman, G.V. **JP8 24**, UP8 36
Volotskova, Olga **BP8 109**
Volpe, F. JP8 70, **PP8 52**, PP8 85, **XP8 34**, **XP8 35**
von Nessi, G. BO4 6
Vorgul, Irena UP8 110
Voskoboinikov, R.V. TP8 59
Votroubek, George UO7 2, **UO7 3**
Vranic, Marija **CP8 71**
Vrublevskis, A. JM9 8, TP8 125, **TP8 126**, XP8 21
Vu, H.X. JO5 10, JO5 13, UO6 8

W
Wacharasindhu, T. NP8 17, NP8 50
Wade, M.R. JP8 111
Wade-Stein, David PP8 118
Waelbroeck, F.L. **PP8 111**
Waganaar, W.J. TP8 144, TP8 145
Wagner, M. BP8 105
Wakasa, A. BO4 4, GP8 56
Wakatsuki, T. PP8 96, PP8 97, PP8 98, **PP8 100**
Waksman, J. TP8 59, **TP8 60**
Waldron, W.L. BO6 14, CP8 57, NP8 2, NP8 3, NP8 4, NP8 5, NP8 95, NP8 110
Walker, D. GP8 123, GP8 124, **GP8 125**
Walker, M.D. JP8 93
Walker, M.L. CO4 11, GP8 38, **JP8 94**, TP8 38, TP8 39, XP8 45
Wallace, G.M. **GO4 8**, PP8 5, PP8 7
Wallace, R. BO5 2
Walsh, Mike JO4 15
Walton, S.G. BP8 12
Waltz, R.E. BP8 29, PP8 10, PP8 66, TP8 10, TP8 11, TP8 12, TP8 74, **UP8 106**
Wan, B.N. NO4 2, PP8 47, XP8 59
Wan, Weigang BP8 35, **UP8 72**
Wang, C.M. PP8 121
Wang, Chuji CO7 4, **NP8 43**
Wang, D.S. NO4 2
Wang, Eric BP8 18, **BP8 22**
Wang, G. CO4 9, **TP8 5**, TP8 6, TP8 12, TP8 14
Wang, H. NO4 3
Wang, Hua **PP8 81**
Wang, J. NO4 2
Wang, Lu **BP8 48**, BP8 50
Wang, P. TO6 10
Wang, P.X. PO5 10
Wang, T.L. JO5 6
Wang, Tao **BP8 57**
Wang, W.X. PP8 49, PP8 65, **UP8 83**
Wang, X.G. BP8 47
Wang, Xiaogang NM9 1, **TP8 128**
Wang, Xiaoming CP8 73, JP8 119
Wang, Xueyi UP8 111, **UP8 112**
Wang, Yi-Ming UO5 6
Wang, Yong NP8 33
Wang, Yuhou GP8 117
Wang, Z. PP8 36
Wang, Z.H. **BP8 47**
Wang, Z.X. PO6 6
Wang, Zhengxiong TP8 128
Ware, A.S. **TP8 99**, **XP8 36**
Wark, Justin **GO6 14**
Warmbier, Robert **UP8 157**
Warrick, A. BO5 3
Watanabe, Masayuki **TP8 93**
Watanabe, Osamu PP8 96, PP8 97, PP8 100
Watanabe, Tomo-Hiko BP8 20, BP8 38, **UP8 70**, UP8 71
Watari, T. XP8 25
Watkins, B.J. GP8 89
Watkins, J.G. NO4 10, TP8 25, TP8 27, **TP8 29**, TP8 30
Watrous, Jack NP8 18
Watt, Robert UO5 6
Watts, Christopher GP8 106, GP8 107, GP8 108, GP8 109, GP8 110, GP8 111, **UP8 108**, UP8 109, UP8 133, UP8 134
Waugh, J. UP8 143
Waxer, L.J. PO5 1
Way, Jesse BP8 10
Weatherford, C.A. JO6 10
Weaver, J.L. JO5 7, **JO5 8**, JO5 9, TO7 3, XP8 25
Weber, S.V. **BO5 6**, BO5 7, BO5 9, TO5 1, UO5 13, UO5 14
Weber, T.R. BP8 76, **GI2 5**
Weber, Thomas **CO7 1**
Wehner, William **GP8 35**
Wei, Haofei **NP8 16**
Wei, M.S. CP8 53, CP8 66, CP8 80, **CP8 103**, CP8 105, CP8 106, CP8 108,

NO5 1, NO5 2, NO5 8, NO5 9, NO5 12, PO5 9, PO5 12
Wei, Xiao **GP8 147**
Weiner, D. PO5 6
Weingarten, L. CP8 45, TO7 11
Weinhold, D. JP8 48, TP8 141
Weisheit, J. JP8 144
Weisheit, Jon PO5 14
Weitzner, Harold BP8 27, NP8 25, **TP8 95**
Welander, A.S. XP8 45
Welch, Dale BO6 10, BP8 70, NP8 97, NP8 104, PO5 13, **TO5 9**, TP8 159
Weller, M.E. GO5 11, GO5 13, **NP8 62**, NP8 63, TO7 12
Werner, Gregory **CI2 6**
Wesley, J.C. JP8 90, JP8 91, JP8 92, JP8 93, JP8 95, JP8 96, UO4 4
West, W.P. TP8 27
Westover, B. NO5 2, NO5 8
Weynants, R. NO4 9
Weyssow, Boris XP8 56
White, A.E. CO4 5, JP8 98, **KI3 1**, TP8 5, TP8 6, TP8 7, TP8 12, TP8 14
White, D.G. CO4 2
White, R.B. JP8 110, PP8 48, PP8 56, PP8 58, PP8 61, TP8 81, **XI3 5**
White, W. TP8 143
Whitney, K.G. CP8 70, CP8 72, NP8 59, TO7 11, TO7 13
Whittle, T.E. GP8 14
Whyte, Colin G. UP8 110
Whyte, Dennis CO4 10, GO4 2, GO4 7, GO4 8, GP8 5, GP8 6, **PI2 6**, PP8 20, PP8 23, PP8 24, PP8 25, PP8 26, UO4 3, UO4 10
Widmann, K. BO5 1, BO5 2, BO5 3, CP8 52, JO5 1, **QI3 4**
Wiebold, Matt **BP8 11**
Wiewior, P. CP8 46, NP8 75
Wiggins, D.L. **JO6 12**
Wilde, B.H. CO5 8, UP8 152
Wilgen, J. JP8 117, PP8 46, PP8 75
Wilgen, John PP8 31
Wilhelm, H. NP8 70
Wilke, M.D. NP8 82, UO5 14
Wilke, Mark UO5 6
Wilks, S.C. JO5 6, JP8 142, NO5 1, NO5 4, NO6 14, **PO5 13**, TO7 5
Willams, K.M. **JO6 13**
Willi, Oswald NO4 5, **UP8 76**
Williams, E. BO5 3
Williams, E.A. BO5 1, CP8 90, JO5 3, JO5 4, **JO5 5**, JO5 6, TO5 5, TO6 12, XP8 33
Williams, J. BP8 97, **BP8 98**
Williams, K.M. JO6 10, JO6 11
Williams, Oliver GO6 12
Williams, R.J.R. CO5 8, UP8 152
Williams, Ronald **JP8 152**
Williamson, K.M. **GO5 11**, GO5 13, NP8 62, NP8 63, TO7 12
Willingale, Louise CP8 70, **JP8 139**, JP8 140
Willis, C.R. CP8 76
Wilson, B. BP8 69, NP8 84, TO7 7
Wilson, D.C. BO5 6, NP8 90, NP8 102, TO5 1, UO5 12, UO5 13, **UO5 14**
Wilson, H.R. TP8 18
Wilson, J.R. GO4 8, JO4 11, JP8 67, JP8 106, JP8 107, PP8 5, **PP8 7**, PP8 75, PP8 77
Wilson III, Lynn JO6 1
Wilson-Elliot, Kristi GO5 14
Wingen, A. TP8 24
Wingfield, T. BP8 105
Winglee, Robert NP8 41, NP8 52
Winjum, Benjamin **CP8 94**, CP8 95, CP8 96, TO5 6
Winske, Dan PP8 114, PP8 115
Winter, A. UO4 11
Winz, G. JP8 116, PP8 83, PP8 85, PP8 87
Wisher, M. **CP8 75**
Wisse, Marco JO4 15
Witherspoon, Douglas NP8 97, NP8 104, TP8 149, **TP8 150**, TP8 151, TP8 152, TP8 153, TP8 154, UP8 39, UP8 48
Wittbrodt, A. GP8 89
Wohlbier, John TO6 5
Wolf, R.C. UO4 5
Wolfe, S.M. UO4 14
Wolfe, Stephen PP8 51
Wong, Alfred **TI2 2**
Wong, C.P.C. GP8 2, GP8 3
Wong, K. NP8 84
Wong, K.L. **PP8 62**
Wong, S.K. **TP8 2**
Wood, R.D. CP8 12, UP8 26
Woodruff, Pamela NP8 104, TO7 14
Woodruff, Simon **CP8 34**, CP8 35
Woolsey, N. UP8 143
Workman, J.B. GO6 3
Workman, Jonathan **CP8 39**
Worrall, M. BO4 5, JP8 86
Worstell, M.W. **UP8 57**, UP8 58
Woskov, P. **CP8 10**, CP8 41, JP8 21, JP8 22, PP8 9, UP8 50, UP8 51, UP8 52, UP8 59
Wouchuk, J.G. CO5 14, CO5 15, **CP8 87**
Wright, J.C. CP8 21, GO4 6, GO4 8, GP8 52, GP8 59, JO4 11, JP8 67, PP8 4, PP8 5, **PP8 6**, PP8 7, PP8 30, PP8 77, PP8 96
Wrighton, Jeffrey **UO6 12**
Wrobel, J.S. UP8 19, **UP8 21**, UP8 22, UP8 24
Wrobel, Matt CP8 22
Wu, James K. BO6 14
Wu, L. TP8 150
Wu, Linchun **NP8 97**, TP8 154
Wu, Lingling TP8 162
Wu, Sheldon **GP8 90**
Wu, W. TP8 37
Wu, Y. CP8 4
Wu, Z.W. NO4 2
Wu, Zhengwei **XP8 50**, XP8 51
Wukitch, S.J. GO4 5, GO4 6, **GO4 7**, GO4 8, PP8 9, PP8 29, PP8 30, PP8 31, PP8 32
Wurden, G.A. JP8 33, **NO4 4**, TP8 143, TP8 144, TP8 145, TP8 146
Wurm, Alexander **PP8 108**
Wurtele, J. JO5 6, NP8 93, PP8 106
Wygant, John JO6 1
Wysocki, Fred **NP8 90**, UO5 6, UO5 12

X

Xiang, Nong XP8 43
Xiao, B.J. NO4 2
Xiao, Chijie **NM9 1**
Xiao, Yong **PO6 5**
Xie, F. **TP8 39**
Xie, J. JP8 49
Xie, Jinlin **XP8 58**
Xie, S. GP8 106
Xie, Shuangwei **GP8 107**, GP8 108, GP8 109
Xu, Chao **GP8 37**
Xu, Hao **UP8 155**
Xu, M. BP8 40, **GP8 138**, GP8 139
Xu, P. **PP8 19**
Xu, Q. NO4 2
Xu, Wenbin TP8 128
Xu, Wenyu NP8 131
Xu, X. CP8 8
Xu, X.Q. NP8 117, NP8 118, NP8 121
Xu, Yuhong NO4 5, UP8 76

Y

Yaakobi, Oded **GP8 82**, GP8 83
Yabuuchi, T. CP8 80, CP8 97, CP8 103, CP8 105, **CP8 106**, NO5 1, NO5 9
Yadykin, D. JP8 85
Yagi, Kotaro CM9 2
Yagi, M. BP8 21, GP8 146
Yaguchi, F BM9 4
Yakimenko, V. JP8 135, JP8 136, TO4 15, XP8 46

Yakovenko, Yu.V. JP8 108
Yamada, I. BM9 4
Yamada, Kotaro PP8 96, PP8 97, PP8 100
Yamada, M. JP8 49, JP8 50, PM9 3, **TP8 110**, TP8 111, TP8 112, TP8 113, TP8 114, TP8 115
Yamada, T. GP8 146, **PP8 98**, PP8 99, PP8 100, TP8 139
Yamaguchi, Takashi PP8 96, PP8 97, PP8 100
Yamaguchi, Y. BM9 3, BM9 4
Yamamoto, S. BO4 10
Yampolsky, Nikolai **NP8 30**
Yan, L.W. XP8 59
Yan, Lincan GP8 106, GP8 107, GP8 108, GP8 109, **GP8 111**
Yan, R. **CP8 93**, CP8 110
Yan, Z. **CO4 14**, GP8 138, JP8 116, TP8 7, TP8 8, TP8 12, TP8 19
Yang, H. JM9 3, TP8 117
Yang, H.L. XP8 45
Yang, Hongang TP8 116
Yang, J.H. XP8 67
Yang, Q.W. XP8 59
Yang, Xiaokang **UP8 8**, UP8 9
Yang, Xiaoling **NP8 107**, UO7 4
Yang, Y.H. JM9 2
Yang, Y.M. CP8 5, **TP8 51**, TP8 52
Yano, Yoshihisa **XP8 47**
Yanovsky, V. JP8 122, JP8 140, TO4 3, TO4 8, TO4 11
Yashio, Noriyasu NP8 54
Yasin, E. CP8 46, GO5 6, JO6 3
Yates, K. CP8 46
Yates, T. TP8 42
Yates, T.F. TP8 43, TP8 45, **TP8 46**
Yepes, Pablo NO6 14
Yepez, Jeffrey BP8 58
Yi, S. **JP8 120**, JP8 121, TO4 11
Yilmaz, M.F. GO5 13, NP8 62, NP8 63, TO7 12
Yin, L. CP8 88, **CP8 89**, NM9 7, NM9 8, TP8 115, TP8 122
Yip, Chi-Shung **BP8 7**, JO6 5
Yokoyama, M. GP8 56
Yoo, J. JP8 49, PM9 3, TP8 110, TP8 112, **TP8 113**, TP8 114
Yoon, E.S. BO4 3, **BP8 49**
Yoon, Peter H. TP8 132
Yoon, S.W. CO4 11
Yoshida, Maiko **GP8 29**
Yoshida, Z. UO6 4, XP8 47
Yoshikawa, M. BM9 3, **BM9 4**, CM9 2
Yoshimura, Shinji GP8 149
You, Setthivoine TP8 136, **UP8 30**
Young, W. JP8 20, UP8 39, UP8 40, **UP8 41**, UP8 43, UP8 48
Yousef, Tarek CO6 8
Yu, C.X. XP8 59
Yu, Changxuan XP8 58
Yu, D.L. XP8 59
Yu, J.H. BP8 40, CO4 11, GP8 138, JP8 89, JP8 91, JP8 95, **JP8 96**, JP8 108, JP8 111, TP8 37, UO4 4
Yu, Jiao BO6 3
Yu, S.S. NP8 93
Yu, Y.H. JP8 90
Yuh, H. GP8 9, **JO4 3**, JO4 9, JO4 11, NO4 8, PP8 55, PP8 58
Yun, G.S. GP8 40

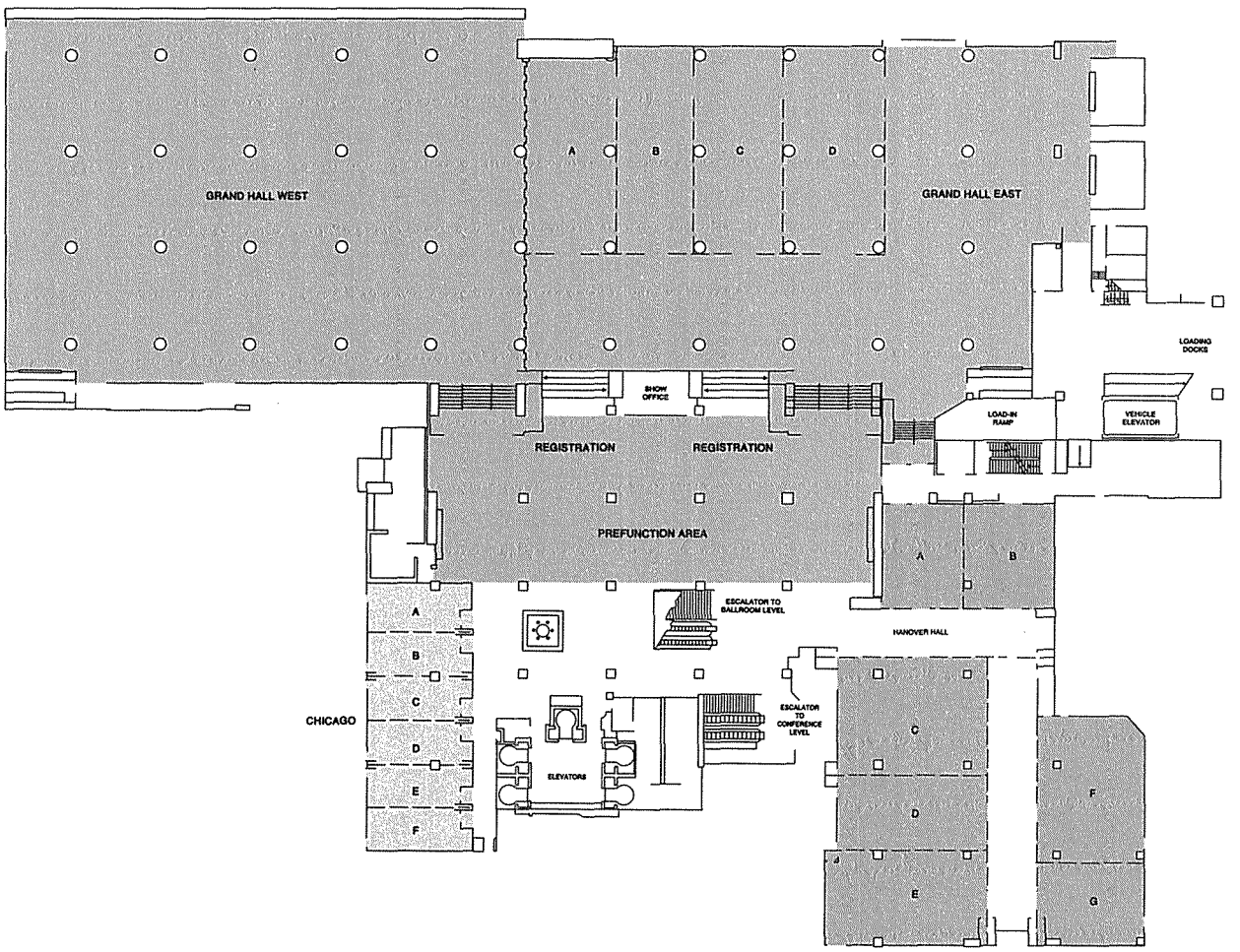
Z

Zaharia, S. BO4 9
Zakharov, L. **BO4 11**, PP8 44, PP8 88, PP8 89, PP8 95, UP8 88
Zalesak, S.T. TO7 1, TO7 3
Zalesak, Steven **CP8 99**
Zanca, P. TP8 78, TP8 82
Zaniol, B. TP8 82, TP8 85
Zank, G.P. GP8 94, GP8 100
Zanotto, L. TP8 77
Zarnstorff, M. GP8 12, **NI3 4**, TP8 101, TP8 108
Zastrow, K.D. CP8 2
Zatz, I. UP8 89
Zeil, K. **GO6 1**
Zekic, Andrijana NP8 37
Zelenty, Jennifer **JP8 36**
Zeng, L. CO4 5, CO4 14, JP8 98, NO4 10, TP8 5, TP8 6, TP8 12, TP8 14, **TP8 15**, TP8 19
Zenitani, Seiji PM9 5
Zhai, K. TP8 104
Zhang, Bo **BP8 56**
Zhang, H. PP8 117
Zhang, Hong PP8 118
Zhang, J. **PP8 63**
Zhang, Jiexi **PP8 16**
Zhang, L. NO4 2
Zhang, P. NP8 80
Zhang, Peng **NP8 19**
Zhang, Shuyu BP8 13
Zhang, W. NO4 2, TP8 9
Zhang, W.L. **XI3 3**
Zhang, Yue GP8 109, **UP8 133**
Zhang, Zach UP8 149
Zhang, Zhuanhao NO6 9, NO6 10, **NO6 11**
Zhao, H.L. XP8 59
Zhao, K.J. XP8 59
Zhao, Kun TO4 5
Zhao, Michael **JP8 11**
Zhdanov, S.K. BP8 93, NO6 1
Zheng, L.J. **GI3 6**, **UP8 84**
Zheng, Linjin GP8 88
Zhidkov, Alexei GO6 8, **GO6 9**
Zhmoginov, Andrey **CM9 9**, **GP8 130**
Zhou, C.D. TO7 2
Zhou, Chuandong **TP8 157**
Zhou, Jing BO6 9
Zhou, Sean TP8 158
Zhou, Shu **GP8 76**
Zhou, Tianchun **GP8 127**
Zhou, Ye **CO6 13**
Zhu, Ben UP8 31, **UP8 32**, UP8 33
Zhu, Jian-Zhou **BP8 24**
Zhu, P. NP8 113, **UP8 92**
Zhu, S. NO4 2
Zhu, Y. CO4 7
Ziemba, Tim CP8 34, NP8 41
Ziemba, Timothy NP8 52, **UP8 49**
Zier, J.C. **NP8 64**, NP8 79, NP8 80
Zigler, Ari JP8 143
Zilli, Enrico TP8 84
Zimmer, G. PP8 39
Zinn, J. NP8 56
Zobin, N. CP8 31
Zocco, A. TP8 121
Zuegel, J.D. PO5 2, UO5 5
Zuin, Matteo **TP8 87**
Zurro, B. GP8 70
Zweben, S.J. CP8 8, GO4 10, **GO4 11**, JP8 63, NP8 57, PP8 64, PP8 69, PP8 70, PP8 71
Zweben, Stuart PP8 43
Zwicker, Andrew JP8 4, **JP8 6**, JP8 39, JP8 40, JP8 62
Zylstra, A. NP8 93, **XP8 68**

NOTES

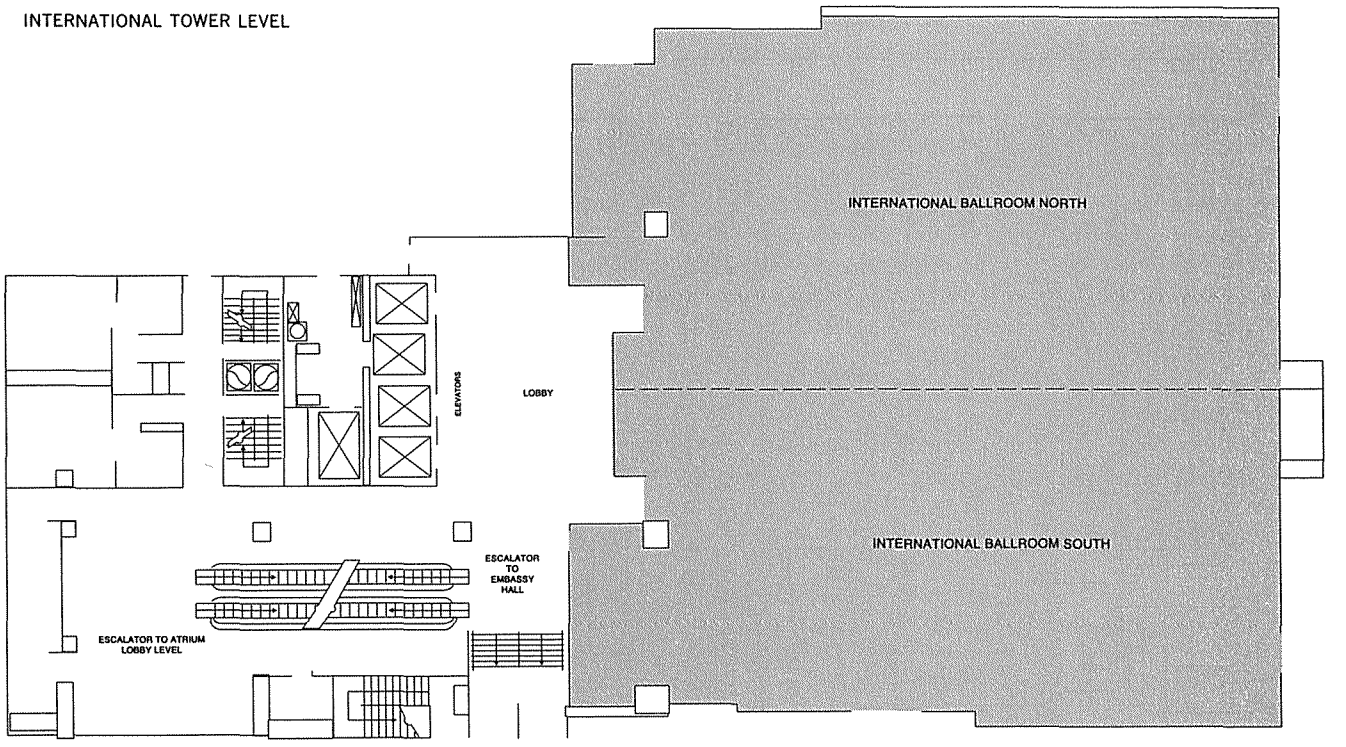
Hyatt Regency Atlanta

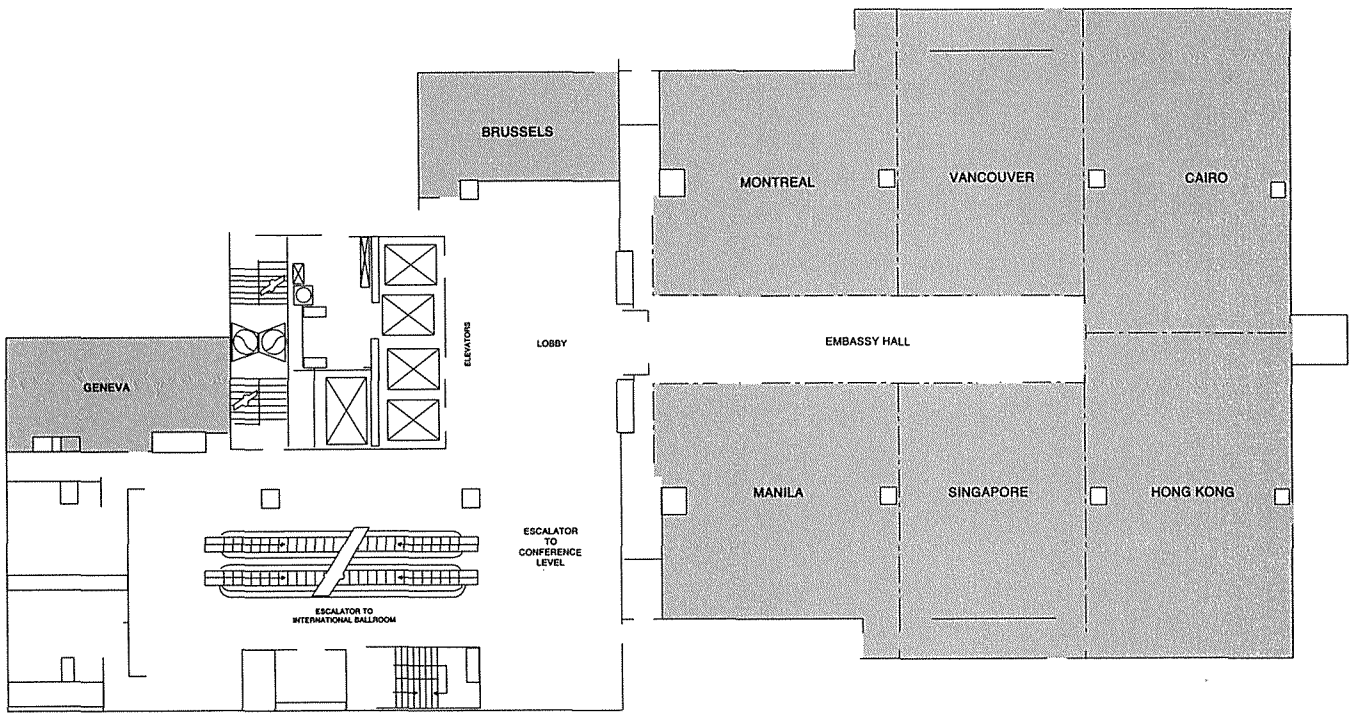
EXHIBIT LEVEL



Hyatt Regency Atlanta

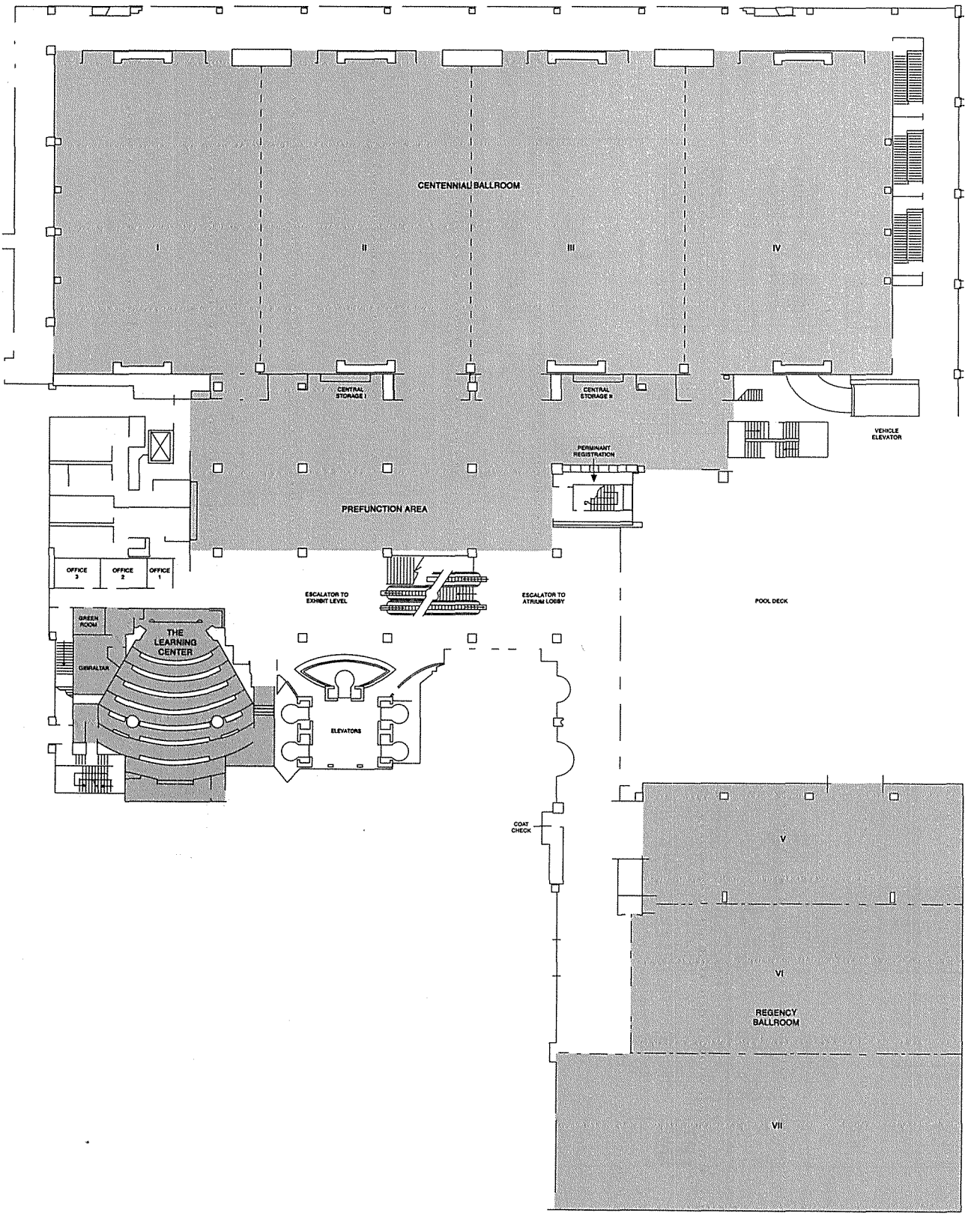
INTERNATIONAL TOWER LEVEL





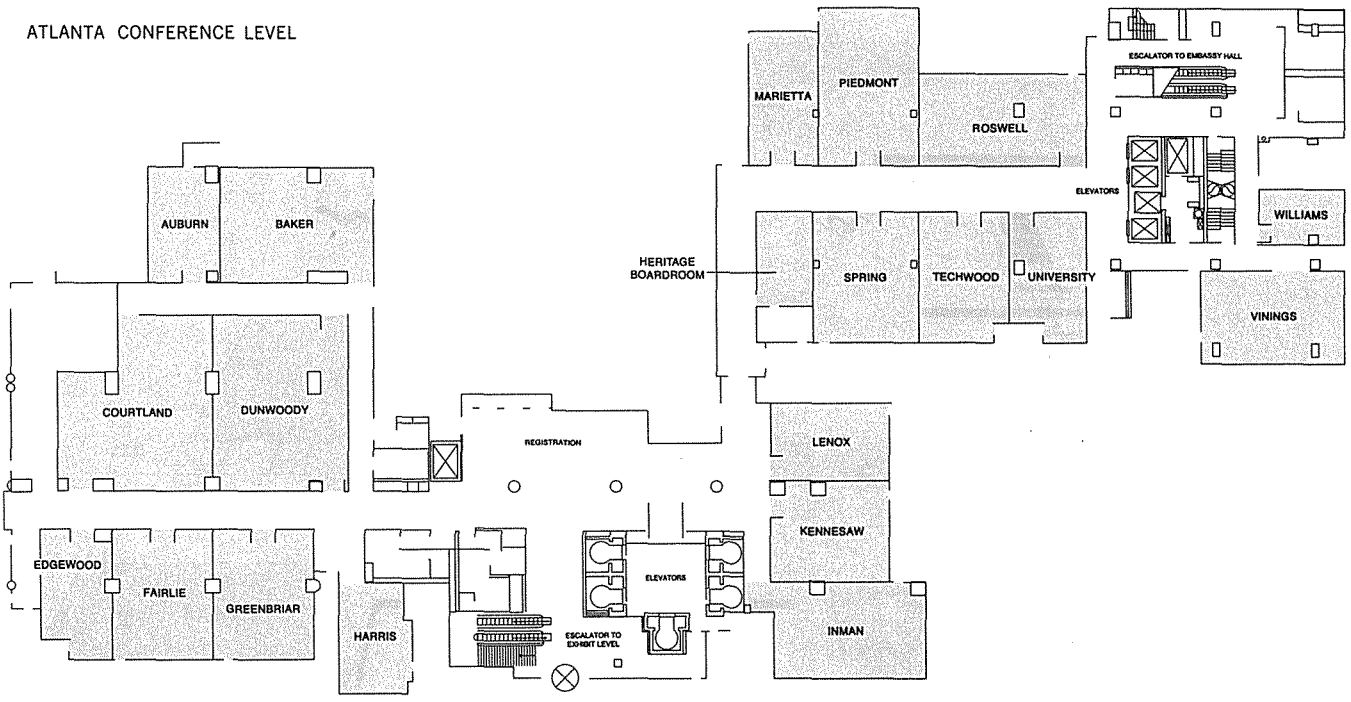
Hyatt Regency Atlanta

BALLROOM LEVEL

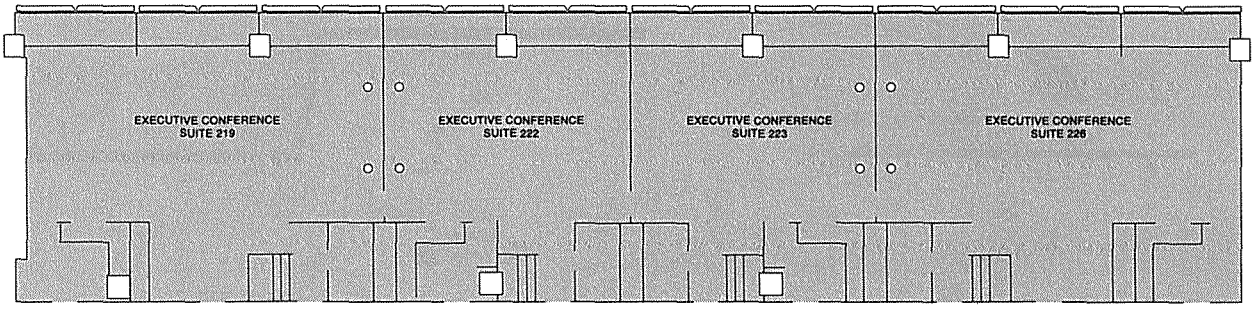


Hyatt Regency Atlanta

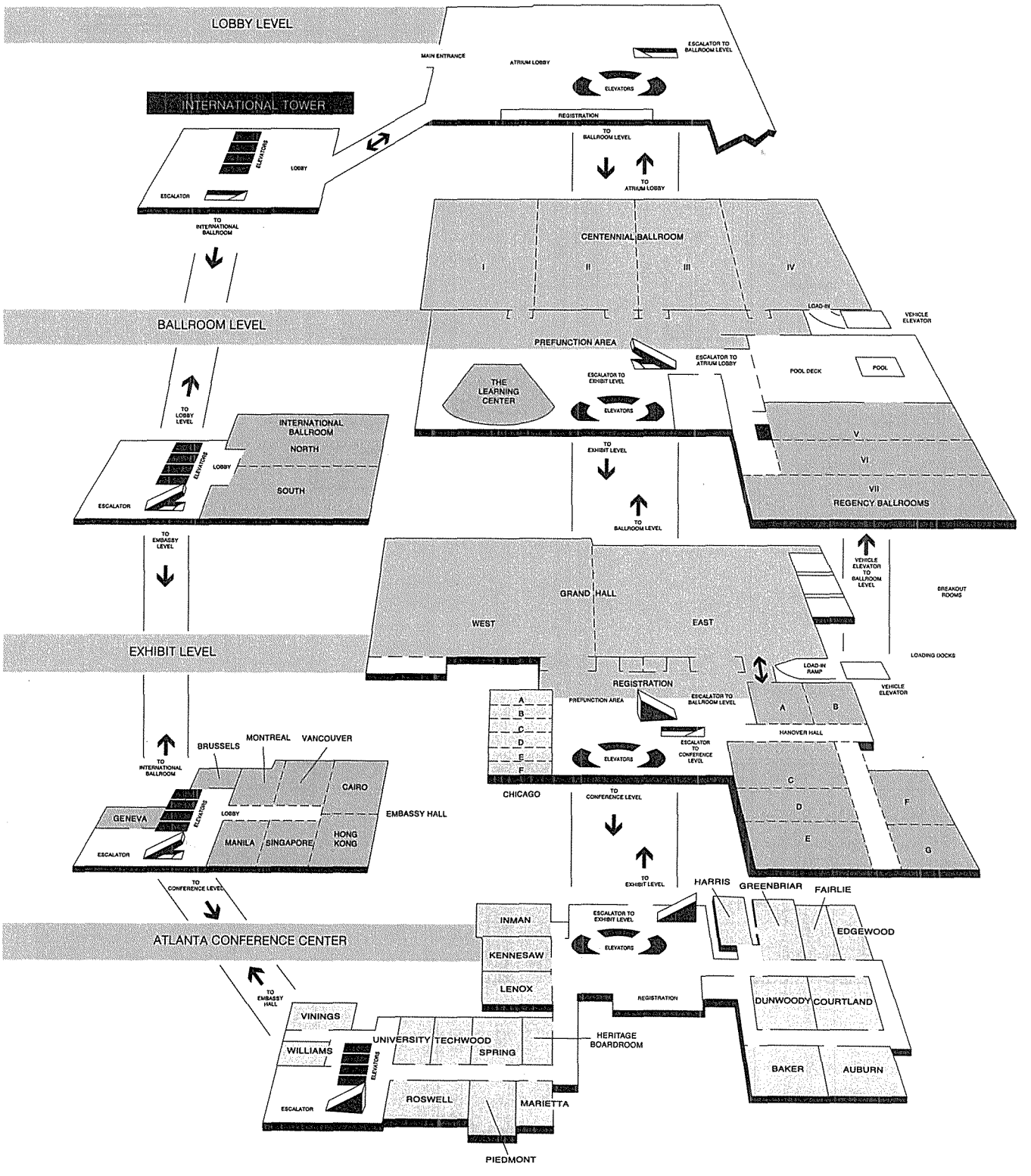
ATLANTA CONFERENCE LEVEL



EXECUTIVE SUITES



Hyatt Regency Atlanta



8:00 WEDNESDAY MORNING
4 NOVEMBER 2009

MR1 **Review: Physics Progress of Reversed Field Pinch Magnetic Confinement**
John S. Sarff
Centennial I-II

9:30 WEDNESDAY MORNING
4 NOVEMBER 2009

NI2 **ICF Capsules and Rayleigh-Taylor Instability**
Otto Landen, T.C. Sangster, Kelly Vaughan, Johan Frenje, Hye-Sook Park, Eric Loomis
Centennial I

NI3 **Plasma Rotation and Helical Equilibria**
J.D. Callen, W.M. Solomon, R.E. Bell, Michael Zarnstorff, Piero Martin, Jeremy Lore
Centennial II

NO4 **International Tokamak Research and ITER**
Regency VI

NO5 **Fast Ignition**
Hanover CDE

NO6 **Complex Plasmas**
Hanover FG

NP8 **Poster Session V: Electron and Ion Beams and Radiation Generation; Low Temperature Plasmas; Pinches, Equations of State, and Simulations; Edge**
Grand Hall East

NM9 **Mini-Conference on Unsteady Reconnection in Laboratory and Nature III: 3D Reconnection and Diffusion Region**
Regency V

14:00 WEDNESDAY AFTERNOON
4 NOVEMBER 2009

PI2 **Tokamak Physics: Edge, Scrape-off Layer and Wall**
Linda E. Sugiyama, Elena de la Luna, Rajesh Maingi, Masahiro Kobayashi, Adam McLean, Dennis Whyte
Centennial I

PT3 **Tutorial: ICF Ignition: The Lawson Criterion, and Comparison with MFE Ignition**
R. Betti
Centennial II

PO5 **High-intensity Short-pulse Laser Plasma Interactions**
Hanover CDE

PO6 **Waves, Turbulence, and Boundary Effects in Laboratory and Space Plasmas II**
Hanover FG

PP8 **Poster Session VI: C-Mod; NSTX and General Spherical Torus; Simulation and Modeling of Basic Plasma Phenomena**
Grand Hall East

PM9 **Mini-Conference on Unsteady Reconnection in Laboratory and Nature IV: Turbulence and Multiple Reconnections**
Regency V

15:00 WEDNESDAY AFTERNOON
4 NOVEMBER 2009

QI3 **ICF and Ignition**
Nathan Meezan, Dustin Froula, Pierre Michel, Klaus Widmann
Centennial II

17:15 WEDNESDAY EVENING
4 NOVEMBER 2009

RE1 **DPP Business Meeting**
Hanover FG

18:30 WEDNESDAY EVENING
4 NOVEMBER 2009

RE2 **Reception and Banquet**
Centennial III/IV

8:00 THURSDAY MORNING
5 NOVEMBER 2009

SR1 **Maxwell Prize Address: Taming Magnetically Confined Plasmas with RF Waves: A Historical Perspective**
Miklos Porkolab
Centennial I-II

9:30 THURSDAY MORNING
5 NOVEMBER 2009

TI2 **Flows and Turbulence in Laboratory and Space**
Ian H. Hutchinson, Alfred Wong, Earl Scime, Jean C. Perez, Troy Carter, P.H. Diamond
Centennial I

TI3 **RF in Tokamaks and ITER**
M. Choi, Gary Taylor, Syun'ichi Shiraiwa, G.L. Jackson, Andrei Smolyakov
Centennial II

TO4 **Laser Wakefield Accelerators and Radiation Sources**
Regency VI

TO5 **ICF Simulations and Target Fabrications**
Hanover CDE

TO6 **Laboratory Astrophysics**
Hanover FG

TO7 **Shock Ignition, Diagnostics, and X-ray Sources**
Regency VII

TP8 **Poster Session VII: DIII-D Tokamak III; MST, RFP, and Stellarator; Magnetic Reconnection; Magneto-Inertial-Fusion**
Grand Hall East

14:00 THURSDAY AFTERNOON
5 NOVEMBER 2009

UI2 **Laser Wakefield Acceleration and Solid Target Interactions**
Anthony Gonsalves, Joseph Ralph, Samuel Martins, Alec Thomas, Farhat Beg, Andreas Kemp
Centennial I

UI3 **Basic Plasmas: Novel Plasmas in Laboratory and Space**
C. Fred Driscoll, Michael Drewsen, Jon Eggert, Bruno Coppi, David Ampleford, David Speirs
Centennial II

UO4 **Research In Support of ITER**
Regency VI

UO5 **Compression and Burn**
Hanover CDE

UO6 **Basic Plasma Phenomena: Theory and Simulation**
Hanover FG

UO7 **Magneto Inertial Fusion and Neutron Generation**
Regency VII

UP8 **Poster Session VIII: Alternates; Turbulence, Transport, and Stability; Space and Astrophysical Plasmas**
Grand Hall East

8:00 FRIDAY MORNING
6 NOVEMBER 2009

WR1 **Review: Applied Spectroscopy in Pulsed Power Plasmas**
Gregory Rochau
Centennial I-II

9:30 FRIDAY MORNING
6 NOVEMBER 2009

XI2 **High Energy Density Physics and High Performance Capsule Implosions**
J.P. Knauer, E.C. Harding, Hideaki Habara, Harry F. Robey
Centennial I

XI3 **Energetic Particles**
Herbert Berk, E.M. Bass, W.L. Zhang, E.M. Hollmann, Roscoe White, Christopher Cothran
Centennial II

XP8 **Poster Session IX: Supplemental and Post-Deadline Posters**
Grand Hall East

12:35 FRIDAY AFTERNOON
6 NOVEMBER 2009

YR1 **Door Prize Drawing**
Centennial I

On the Cover: This image shows the x-ray emission at 8 keV from one of the first capsule implosion shots on the National Ignition Facility. The 1.8 mm diameter plastic capsule was filled with propane and placed in the center of a 8.4 mm long gas filled hohlraum. The hohlraum was heated with 192 smoothed laser beams and total energy of 506 kJ in a 10.7 ns shaped pulse. The soft x-radiation of the hohlraum compresses the capsules more than 10x in radius at 12.4 ns after the beginning of the laser pulse. The diameter of the circle in the image is 60 micrometers. The first experiments mark the start of the National Ignition Campaign on NIF with the goal to produce a burning fusion plasma.
Image courtesy of Siegfried Glenzer LLNL.

Epitome of the 2009 Annual Meeting of the Division of Plasma Physics of the American Physical Society

8:00 MONDAY MORNING
2 NOVEMBER 2009

AR1 **Review: Realizing Steady State Tokamak Operation for Fusion Energy**
T.C. Luce
Centennial I-II

9:30 MONDAY MORNING
2 NOVEMBER 2009

BI2 **Reconnection in Laboratory and Space**
Yi-Min Huang, Eric Lawrence, Vadim Roytershteyn, Ari Le, Gennady Fiksel, Tim Gray
Centennial I

BI3 **Advances in Tokamaks: Core and Edge Physics**
Nobuhiko Hayashi, Wojciech Fundamenski, Jiangang Li, Jerry Hughes, Istvan Cziegler, Natalia Krasheninnikova
Centennial II

BO4 **Magnetic Confinement Theory, Simulation and Modeling**
Regency VI

BO5 **Hohlraum Physics**
Hanover CDE

BO6 **Microwaves, Compton Scattering and Accelerator Physics**
Hanover FG

BP8 **Poster Session I: Plasma Sources and Boundaries; Gyrokinetics and Turbulence; Complex, Non-neutral and Other Novel Plasmas**
Grand Hall East

BM9 **Mini-Conference on Innovative Magnetic Mirror Concepts and Applications I**
The Learning Center

14:00 MONDAY AFTERNOON
2 NOVEMBER 2009

CI2 **Accelerators, Beam Dynamics and Radiation**
Alex Friedman, Igor Kaganovich, Erik Gilson, Diktys Stratakis, Alexander Vlasov, Gregory Werner
Centennial I

CT3 **Tutorial: Flow driven MHD Instabilities in Weakly Magnetized Laboratory Experiments: Dynamos and MRI**
Cary Forest
Centennial II

CO4 **DIII-D Tokamak**
Regency VI

CO5 **Equation of State, Strength, and Hydrodynamics**
Hanover CDE

CO6 **Magnetic Reconnection and Turbulence**
Hanover FG

CO7 **Low Temperature Plasmas I**
Regency VII

CP8 **Poster Session II: Diagnostics, Heating, Current Drive; Diagnostics, Laser Plasma Interactions, and Fast Ignition**
Grand Hall East

CM9 **Mini-Conference on Innovative Magnetic Mirror Concepts and Applications II**
The Learning Center

15:00 MONDAY AFTERNOON
2 NOVEMBER 2009

DI3 **Gyrokinetic Theory and Simulation**
Michael Barnes, J. Candy, Felix I. Parra, Andris Dimits
Centennial II

17:30 MONDAY EVENING
2 NOVEMBER 2009

EE1 **Panel Discussion: Tools Needed to Survive in Science**
Regency VI

19:00 MONDAY EVENING
2 NOVEMBER 2009

EE2 **University Fusion Association General Meeting, including Town Meeting on DOE Research Needs Workshops**
Hanover CDE

21:00 MONDAY EVENING
2 NOVEMBER 2009

EE3 **Town Hall Meeting on the High Energy Density Laboratory Plasma Research Needs Workshop**
Hanover FG

8:00 TUESDAY MORNING
3 NOVEMBER 2009

FR1 **Review: Ion Acceleration using Ultra-high Intensity Lasers**
Karl Krushelnick
Centennial I-II

9:30 TUESDAY MORNING
3 NOVEMBER 2009

GI2 **Micro and Low-temperature Plasmas**
Osamu Sakai, Dmytro Sydorenko, Scott D. Baalrud, Jeffrey Hopwood, T.R. Weber, Michael Keidar
Centennial I

GI3 **Islands, Kinks and Sawteeth**
A.D. Turnbull, Jonathan Graves, R.J. La Haye, Hillary Stephens, John W. Berkery, L.J. Zheng
Centennial II

GO4 **C MOD Tokamak**
Regency VI

GO5 **Z-pinches, X-pinches, and Dense Plasma Focus**
Hanover CDE

GO6 **Laser Acceleration and Transport; Radiation and FELs**
Hanover FG

GP8 **Poster Session III: ITER, General Tokamak, Simulation and Modeling; MHD, Linear and Nonlinear Phenomena; Waves and Instabilities in Basic Plasmas**
Grand Hall East

GM9 **Mini-Conference on Unsteady Reconnection in Laboratory and Nature I: Reconnection Rate and Dynamics**
Regency V

13:00 TUESDAY AFTERNOON
3 NOVEMBER 2009

HE1 **Town Meeting on Concerns of Junior Scientists**
The Learning Center

14:00 TUESDAY AFTERNOON
3 NOVEMBER 2009

JI2 **ICF Compression, Equations of State and Z-pinches**
Marcus Knudson, M.A. Barrios, Sebastien Lepape, Christopher Jennings, Max Karasik, Stephen Slutz
Centennial I

JT3 **Tutorial: Verification and Validation for Magnetic Fusion: Moving Toward Predictive Capability**
Martin Greenwald
Centennial II

JO4 **NSTX Spherical Torus**
Regency VI

JO5 **Laser-plasma Coupling at Long Scale Lengths**
Hanover CDE

JO6 **Waves, Turbulence, and Boundary Effects in Laboratory and Space Plasmas I**
Hanover FG

JP8 **Poster Session IV: Education and Outreach; Undergraduate and High School Research; DIII-D Tokamak II; Laser and Plasma Based Accelerators**
Grand Hall East

JM9 **Mini-Conference on Unsteady Reconnection in Laboratory and Nature II: Impulsive Reconnection and Onset**
Regency V

15:00 TUESDAY AFTERNOON
3 NOVEMBER 2009

KI3 **Turbulent Transport Measurement and Modeling**
A.E. White, Liang Lin, J.C. DeBoo, David L. Brower
Centennial II

19:30 TUESDAY EVENING
3 NOVEMBER 2009

LE2 **Town Meeting: A Conversation with Dr. Steven Koonin, Undersecretary for Science, Department of Energy**
Centennial I

0003-0503(200911)54:15;1-G